Stony Brook University

The design, synthesis and biological evaluation of novel taxoid anticancer agents and their tumor-targeted drug conjugates

A Dissertation Presented

by

Joshua Seitz

to

The Graduate School

in Partial Fulfillment of the

Requirements

for the Degree of

Doctor of Philosophy

in

Chemistry

Stony Brook University

August 2013

Stony Brook University

The Graduate School

Joshua Seitz

We, the dissertation committee for the above candidate for the

Doctor of Philosophy degree, hereby recommend

acceptance of this dissertation.

Iwao Ojima – Dissertation Advisor
Distinguished Professor, Department of Chemistry

Orlando Schärer – Chairperson of Defense
Professor, Department of Chemistry

Nancy Goroff – Third Member
Associate Professor, Department of Chemistry

Susan B. Horwitz – Outside Member
Distinguished Professor, Department of Molecular Pharmacology
Albert Einstein College of Medicine, Bronx, New York

This dissertation is accepted by the Graduate School

Charles Taber
Interim Dean of the Graduate School

Abstract of the Dissertation

The design, synthesis and biological evaluation of novel taxoid anticancer agents and their tumor-targeted drug conjugates

by

Joshua Seitz

Doctor of Philosophy

in

Chemistry

Stony Brook University

2013

Cancer is the second leading cause of death in the United States and is responsible for one in eight deaths worldwide. Traditional chemotherapeutics target the processes involved in cell division and consequently produce dangerous and dose-limiting side effects. In an effort to identify the therapeutic windown of these drugs, tumor targeted drug conjugates (TTDCs) are currenly under development.

The Ojima lab has developed and extensive panel of next-generation taxoids that possess the requisite sub-nanomolar potency for incorporation into effective conjugates. A small library of 17 taxoids was synthesized and their cytotoxicity investigated. Selected taxoids were synthesized on the half-gram to multi-gram scales for use in TTDCs.

Polyunsaturated fatty acids (PUFAs) have been widely used as tumor-tageting moieties (TTMs), due to their high binding affinity for human serum albumin. These strategies are best exemplified by Taxoprexin® and Abraxane®. Selected taxoids were conjugated to the PUFAs DHA and/or LNA and were evaluated in vitro and in vivo, demonstrating promising results. The PK profile for DHA-1214 was also investigated. In addition, a novel conjugate bearing a cytotoxic DHA-Propofol moiety was synthesized and evaluated in vitro.

Vitamins have also been successfully applied to TTDCs. The most notable example is folic acid and the folate-drug conjugate Vintafolide®. A novel synthetic route to a solubilized folate-taxoid conjugate was developed via solid phase pepetide synthesis and Cu-free click chemistry.

Biotin is also under investigation in our lab as a promising new TTM. Biotin conjugates were synthesized and their efficacy evaluated in vivo, demonstrating clear evidence for tumor-targeting.

To facilitate the preclinical development of the various taxoid-based TTDCs in our lab, an efficient route to radio-labeled next-generation taxoids was developed through a vinylstannyl taxoid intermediate. Using a Cu/Pd catalyzed Stille coupling, we can efficiently indroduce a methyl group in the last step of the synthesis, amenable for labeling with 11C for PET, and tritium or 14C for liquid scintigraphy. This tool has the potential to greatly enhance our understanding of the protein binding kinetics and biodistribution of our taxoids and their respective drug conjugates.

This thesis is dedicated to the memory of my grandfather, James Leamy

Table of Contents

Chapter 3: Drug Conjugates Based on Polyunsaturated Fatty Acids

List of Figures

Figure Page

Chapter 1

Chapter 2

Chapter 3

Chapter 4

Chapter 5

Chapter 6

List of Schemes

Scheme Page

Chapter 1

Chapter 2

Chapter 3

Chapter 4

Chapter 5

Chapter 6

List of Tables

Table Page

Chapter 1

Chapter 2

Chapter 3

Chapter 4

Chapter 6

List of Abbreviations

5-FU 5-Fluorouracil
10-DAB III 10-Deacetylbaccatin III
°C Degrees Celsius
μM Micromolar
ABC ATP-binding cassette
Ac Acetyl
ADC Antibody-drug conjugate
AIDS Acquired immune deficiency syndrome
ALL Acute lymphoblastic leukemia
Alloc Allyloxycarbonyl
Arg Arginine
Asp Asparagine
ATP Adenosine triphosphate
BOC tert-Butyl carbonate
Bu Butyl
BuLi Butyl lithium
CAN Ceric ammonium nitrate
Cbz Carboxybenzyl
CD Cluster of differentiation
CDC Complement-dependent cytotoxicity
CFM Confocal microscopy
CMF Cyclophosphamide, methotrexate and 5-fluorouracil
CML Chronic myelogenous leukemia
COSY Correlation spectroscopy
CSC Cancer stem cell
d Day
DCC N,N'-Dicyclohexylcabodiimide
DHA Docosahexaenoic acid
DIC Diisopropylcarbodiimide
DIPEA N,N-Diisopropylethylamine
DMAc Dimethylacetamide
DMAP 4-Dimethylaminopyridine
DMF Dimethylformamide
DMSO Dimethyl sulfoxide
DNA Deoxyribonucleic acid
DPC Di-2-pyridyl carbonate DPBS Dulbecco's Phosphate buffered saline
EDC 1-Ethyl-3-(3-dimethylaminopropyl)carbodiimide
ee Enantiomeric excess
EGFR Epidermal growth factor receptor
EPA Eicosapentaenoic acid
Et Ethyl
EtOH Ethanol
eV Electonvolt

FA Folic acid
FACS Fluorescence-activated cell sorting
FBS Fetal Bovine Serum
FDA Food and drug administration
FITC Fluorescein isothiocyanate
Fmoc Fluorenylmethyloxycarbonyl
FR Folate receptor
g Gram
GABA γ-Aminobutyric acid
Glu Glutamic acid
Gly Glycine
gp60 glycoprotein 60
GSH Glutathione
GSH-OEt Glutathione ethyl ester
GTP Guanosine-5'-triphosphate
h Hours
HBTU O-Benzotriazole-N,N,N’,N’-tetramethyluroniumhexafluorophosphate
HL Hodgkin lymphoma
HOAc Acetic acid
HObt Hydroxybenzotriazole
HOSu N-Hydroxysuccinimide
HPLC High-performance liquid chromatography
HSA Human serum albumin
Hz Hertz
IC_{50} Half maximal inhibitory concentration
Ig Immunoglobin
IPA Isopropanol
k Kilo
L Liter
Leu Leucine
LiHMDS Lithium bis(trimethylsilyl)amide and lithium hexamethyldisilazide
LNA Linolenic acid
Lys Lysine
m Meter
mAbs Monoclonal antibodies
MACS Magnetic activated cell sorting
MALDI Matrix-assisted laser desoprtion/ionization
MDR Multidrug resistance
Me Methyl
mg Milligram
MHz Megahertz
min Minutes
mL Milliliter
MMAE Monomethylauristatin E
mmol Millimole
m.p. Melting point

MSCBM Mesenchymal stem cell basal medium
Ms Mesyl
MsCl Mesyl chloride
MTT 3-(4,5-Dimethylthiazol-2-yl)-2,5-diphenyltetrazolium bromide
NCI National Cancer Institute
nM Nanomolar
NMR Nuclear magnetic resonance
NPC Nuclear pore complex
NSCLC Non-small-cell lung carcinoma
PBS Phosphate buffer solution
PEG Polyethylene glycol
PET Positron emission tomography
Pgp P-glycoprotein
Ph Phenyl
Phe Phenylalanine
pM Picomolar
PMA Phosphomolybdic acid
PMP p-Methoxyphenyl
Pr Propyl
PUFA Polyunsaturated fatty acid
py Pyridine
r.t. Room temperature
RME Receptor-mediated endocytosis
RPMI Roswell Park Memorial Institute medium
s Seconds
SAR Structure-activity relationship
SB-T Stony Brook taxoid
scFv Single-chain variable fragment
SCID Severe combined immune deficiency
SCLC Small-cell lung carcinoma
SET Single electron transfer
SPARC Secreted protein acidic and rich in cysteine
SPECT Single-photon emission tomography
TBDMS tert-Butyldimethylsilyl
TES Triethylsilyl
TESCl Triethylsilyl chloride
TFA Trifluoroacetic acid
THF Tetrahydrofuran
TIPS Triisopropyl
TLC Thin layer chromatography
topo I Topoisomerase I
TIPS Triisopropylsilyl
TIPSCl Triisopropylsilyl chloride
TPPO Triphenyphosphineoxide
TTM Tumor-targeting module
Val Valine

Acknowledgments

First, I would like to thank my advisor, Professor Ojima for the opportunity to work with him on this project. I would especially like to thank him for his patience with me during this process and for always pushing me to stretch to the edge of my capabilities. It is this constant challenge that provides a lifetime of learning and discovery. In addtition, I would like to thank Mrs. Yoko Ojima for all the hospitality that she has shown over the years.

Also, I would like to thank my committee, Professors Schärer and Goroff, for their helpful insights and understading. In this way you have helped to mold me as a scientist and as a person. I would like to thank Professor Horwitz for agreeing to be my outside member. I am genuinely grateful for this honor.

I would also like to thank all of the Stony Brook faculty, staff, students and custodial crew who have helped to enrich my time here.

In addition, I would like to thank Professor Krapcho for taking the time to screw my head on straight and introducing me to the fascinating world of science.

Ah yes, and my friends and family. They have been quite patient with me too.

So, thank you all again. I really do appreciate all that you have done for me

Vita

Education:

2007	B.S.	University of Vermont
2013	Ph.D.	Stony Brook University

Selected Publications & Reviews:

Seitz, J. D.; Vineberg, J.; Zuniga, E. S.; Ojima, I. Fluorine-Containing Taxoid Anticancer Agents and Their Tumor-targeted Drug Delivery. *J. Fluor. Chem.* **2013**, *152*, 157-165.

Ojima, I.; Kamath, A.; **Seitz, J. D.** Taxol, Taxoids and Related Taxanes. In Hanessian, S. (Ed.) *Natural Products in Medicinal Chemistry.* Wiley-VCH. Weinheim, Germany. In press.

Ojima, I.; Zuniga, E. S.; **Seitz, J. D.** Advances in the Use of Enantiopure β-Lactams for the Synthesis of Biologically Active Compounds of Medicinal Interest. *Top. Heterocycl. Chem*. **2013**, *30*, 1-64.

Kuznetsova, L.; Sun, L; Chen, J.; Zhao, X.; **Seitz, J. D.**; Das, M. Li, Y.; Veith, J. M.; Pera, P.; Bernacki, R. J.; Xia, X.; Horwitz, S. B.; Ojima, I. Synthesis an Biological Evaluation of Novel C3'-difluorovinyl Taxoids. *J. Fluor. Chem.* **2012**, *143*, 177-188.

Seitz, J. D.; Ojima, I. Chapter V.9. Drug Conjugates with Polyunsaturated Fatty Acids. In Kratz, F.; Senter, P.; Steinhagen, H. (Eds.) *Drug Delivery in Oncology – From Research Concepts to Cancer Therapy*. **2011**, Wiley-VCH. Weinheim, Germany.

Krapcho, A. P.; Sparapani, S.; Leenstra, A.; **Seitz, J. D.** Displacement reactions of 2-chloro- and 2,9-dichloro-1,10-phenanthroline: synthesis of a sulfur-bridged bis-1,10-phenanthroline macrocycle and a 2,2'-amino-substituted-bis-1,10-phananthroline. *Tetrahedron Lett.* **2009**, *26*, 3195-3197.

Selected Presentations:

Seitz, J. D.; Ojima, I. *Design and Synthesis of a Novel Taxoid for Radiolabeling Studies of Tumor-Targeted Drug Conjugates*. 245th ACS National Meeting and Exposition. **2013**, New Orleans, LA.

Seitz, J. D.; Zuniga, E. S.; Ojima, I. *Synthesis and Biological Evaluation of a Novel Drug Conjugate Bearing DHA-Propofol and a Next-Generation Taxoid.* 242nd ACS National Meeting and Exposition. **2011**, Denver, CO.

Seitz, J. D.; Zuniga, E. S.; Ojima, I. *Synthesis and Biological Evaluation of Novel and Highly Potent Next-Generation Taxoids for Tumor-Targeted Drug Delivery*. 240th ACS National Meeting and Exposition. **2010**, Boston, MA.

Chapter 1

β-Lactam Synthon Method & Application towards Taxoid Synthesis

Content

§ 1.0 The β-Lactam Synthon Method

The β-lactam initially became a structure of immense interest for synthetic chemists due to widespread application of β-lactam antibiotics such as penicillin. However, β-lactams are versatile synthetic intermediates and can be readily prepared in a highly enantio-enriched fashion.[1] Due to the highly strained 4-membered ring and amide functionality, the β-lactam exhibits a unique reactivity profile and is optimally suited for use as a synthetic building block. Depending on the reaction conditions employed, the ring can be opened at any of the four bonds as shown in **Figure 1-1**. The recognition of this structure as a unique and powerful tool in synthetic chemistry was first described by Ojima as the "β-lactam synthon method" in the late 1970's.[2, 3] Since then, major advances have been made in ring-opening reactions of β-lactams as well as their application to the synthesis of complex natural products and medicinally active compounds.[2-4]

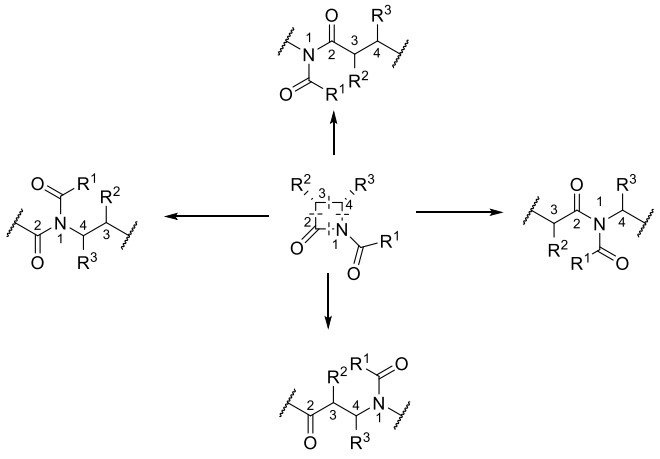

Figure 1-1: Ring opening transformations of β-lactams (adapted from [4])

The most widely employed ring-opening reaction is through breakage of the N1-C2 bond via nucleophilic acyl substitution of the N1 carbonyl group. Intermolecular reactions of the β-lactam with water, alcohols, amines, and amino acid esters produce the respective β-amino acids, β-amino esters/amides, and dipeptides.[5] In addition, intramolecular reactions results in the formation of functionalized cyclic products such as amino-γ-lactones, 5-membered enaminolactones,[6] γ-lactams and macrocycles.[7] Reductive N1-C2 bond cleavage can be employed for the synthesis of γ-amino alcohols.[8] A more subtle, but still extensively developed tranformation is the N1-C4 bond cleavage, either through reduction or catalytic ring expansion or contraction processes.[1, 9, 10] This reductive ring opening was first used to produce amino acids, and provided a foundation for the early development of the β-lactam synthon method. It has been applied to the synthesis of aromatic α-amino acids, α-hydroxy acids, dipeptides, and oligopeptides.[11, 12] Reduction of enantiopure β-lactams leads to the formation of azetidines, which can be further converted to polyamines, polyamino alcohols and polyamino ethers.[13] Ring opening via the C3-C4 bond is possible through

pericyclic reactions,[14] catalytic ring expansions[15] and radical processes.[16] These reactions have been utilized to produce a variety of heterocyclic compounds with well-defined stereochemistry. Although breakage of the C2-C3 bond is rare, it has been applied to the synthesis of various α-amino acids,[17] *N*-carboxy anhydrides,[18]and spirobicyclic compounds.[19]

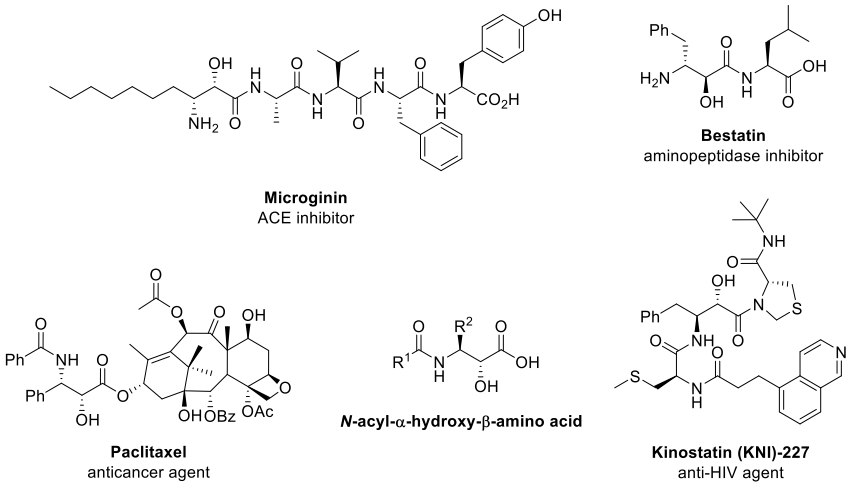

Figure 1-2: Isoserine-containing compounds of medicinal interest (adapted from [4])

The β-lactam synthon method has found widespread applications, including the stereospecific synthesis of biologically active oligopeptides and peptidomimetics, the stereoselective labeling of dipeptides, as well as the synthesis of antimicrobial agents and complex natural products, such as paclitaxel.[20, 21] Isoserines, a common β-amino acid found in numerous biologically active compounds (**Figure 1-2**), can be obtained through the N1-C2 cleavage of 3-hydroxy-β-lactams. Therefore, despite their vastly different biological applications, all of these compounds may be accessed through the appropriate β-lactam intermediates. Other noteworthy applications of the β-lactam synthon method can be found in recent syntheses of ezetimbe (an ACAT inhibitor), (-)-Lankacindin C (a macrocyclic antimicrobial agent), cryptophycins (macrocyclic cytotoxins), and combretostatin analogues(cytotoxic antitumor agents).[22, 23]

§ 1.0.1 The Semisynthesis of Paclitaxel via the β–Lactam Synthon Method

Although the β-lactam synthon method has demonstrated substantial value across a vast array of synthetic applications, the primary focus of this work was centered on the synthesis of highly potent taxoids.[24] Paclitaxel and docetaxel, two highly potent anticancer agents, contain phenylisoserine side chains, which can be accessed *via* the β-lactam synthon method (**Figure 1-3**).

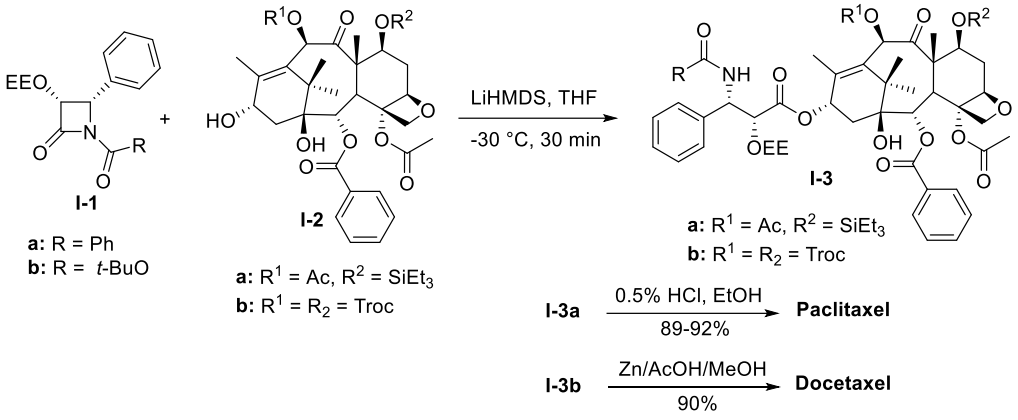

Figure 1-3: The semi-synthesis of paclitaxel and docetaxel (adapted from [4])

The Ojima-Holton coupling was originally developed in the early 1990's for the semisynthetic production of paclitaxel and docetaxel. (3*S*,4*R*)-1-Benzoyl-3-EEO-4-phenyl-β-lactam **I-1a** (EE = 1-ethoxylethyl) was prepared from (3*S*,4*R*)-3-TIPSO-4-phenyl-β-lactam (98% ee), which was synthesized through the chiral ester enolate – *N*-TMS-imine cyclocondensation.[21, 25, 26] β-lactam **I-1a** was then reacted with 7-TES-baccatin III (**I-2a**) using a base (DMAP, pyridine at 25 ºC for 12 h or LiHMDS at -30 ºC for 30 min) in THF, to afford the coupled product **I-3a**. As shown in **Figure 1-3**, this intermediate was then deprotected with 0.5% HCl in ethanol at 0 ºC to afford enantiopure paclitaxel in 89-92% yield.[21] There is a kinetic resolution during the ring-opening coupling with the baccatin derivative, so **I-3a** was isolated enantiomerically and diastereomerically pure.[27] Utilizing the same synthetic strategy, docetaxel was synthesized in 90% yield through the ring-opening coupling of (3*S*,4*R*)-1-Boc-3-TIPSO-4-phenyl-β-lactam **1b** (98% ee) with 7,10-diTroc-10-deacetylbaccatin III (**2b**) (Troc = 2,2,2-trichloroethoxycarbonyl). Enantiopure docetaxel was obtained after deprotection of the Troc and EE groups with Zn/AcOH/MeOH.[26]

This highly efficient coupling method has become known as the Ojima-Holton coupling. Once it was successfully applied to the semisynthesis of paclitaxel and docetaxel, it facilitated the synthesis and biological studies of a myriad of paclitaxel congeners, or "taxoids". [28, 29] The standard procedure for these couplings has since evolved to the use of 1-acyl- or 1-carbalkoxy-3-TIPSO-β-lactams and LiHMDS as the base (**Figure 1-4**).[30]

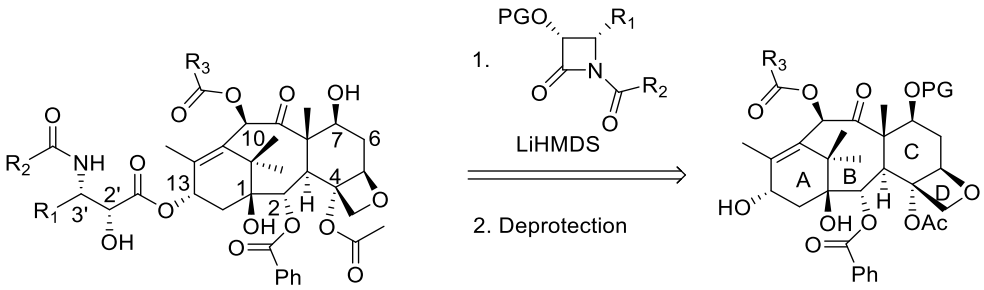

Figure 1-4: The Ojima-Holton Coupling

The development of the Ojima-Holton coupling provided an avenue to the rapid synthesis of hundreds of taxoids and facilitated the development of a detailed understanding of the structure-activity relationship (SAR) for the anticancer properties of these taxoids.[29, 30] Based on these previous SAR studies, β-lactam **(+)-1-6** with an isobutenyl group at C4 and a *t*-Boc protected N1 positions was synthesized.[24, 29, 30] Enantioselective synthesis of the valuable intermediate was carried out utilizing two different methods: (1) the Staudinger [2+2] cycloaddition followed by enzymatic resolution or (2) the chiral ester-enolate cyclocondensation.

§ 1.1 Staudinger [2+2] Cycloaddition

The 1907, Staudinger reported the first synthesis of a β-lactam, whereby 1,3,3,4-tetraphenylazetidin-2-one was synthesized via a thermal [2+2] cycloaddition between diphenylketene and the Schiff base derived from aniline and benzaldehyde.[31] The Staudinger ketene-imine cycloaddition has become regarded as the most versatile methods for the synthesis of β-lactams.

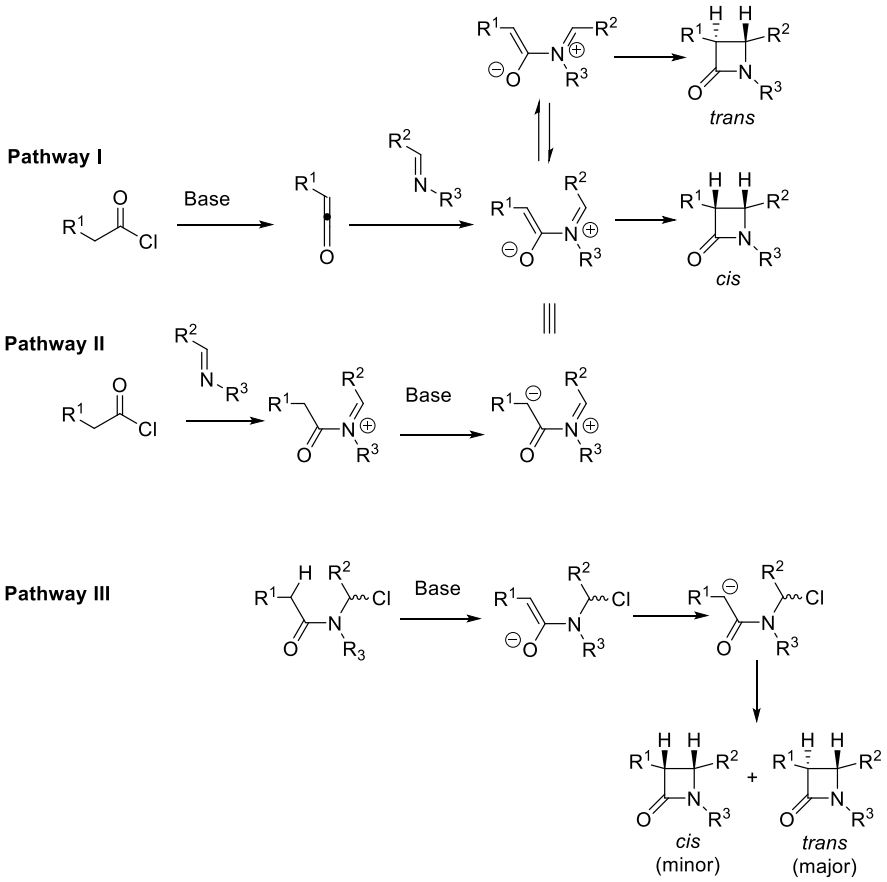

Figure 1-5: Mechanistic pathways of the Staudinger [2+2] cycloaddition (adapted from [4])

Although the Staudinger reaction was discovered over a century ago, some mechanistic details of the [2+2] cycloaddition are still unknown. This subject has been the focus of two recent reviews.[32, 33] Currently, the most commonly accepted model is that the reaction proceeds in a 2-step process through the nucleophilic attack of an imine nitrogen to the electrophilic central carbon of a ketene, forming a zwitterionic intermediate. This intermediate then may undergo conrotatory ring closure to give the 4-membered ring, as shown in **Figure 1-5** (pathway I). When both *cis*- and/or *trans*-β-lactam products can be obtained, the ratio of the products depends on the substrate structures and reaction conditions.[32, 33] The *cis*-β-lactam is exclusively formed when *Z* to *E* isomerization of the zwitterionic intermediate is not possible in the reaction. It has been demonstrated that *E*-imines preferentially form *cis*-β-lactams, while *Z*-imines predominately afford *trans*-β-lactams.[34, 35] However, when isomerization is possible in the zwitterionic intermediate, the relative rate difference between ring closure and *Z* to *E* isomerization will influence the stereochemical outcome of the reaction.

Two other pathways, also shown in **Figure 1-5** (Pathways II and III), have also been proposed for Staudinger reaction performed by simultaneously mixing an acid chloride, a base and an imine. This mechanism involves the initial acylation of the imine nitrogen, followed by deprotonation at the α-carbon by a base to generate the same zwitterinonic intermediate as that in the pathway I (pathway II). Alternatively, another mechanism has been proposed in which the chloride ion that is generated in the first step adds to the iminium bond, forming an *N*-α-chloroalkylamide anion that can undergo cyclization through an intramolecular SN_2 reaction (pathway III). This proposed mechanism has been used to explain the formation of *trans*-β-lactam as the major product under certain conditions.[32, 33]

Although asymmetric versions of the Staudinger reaction have been developed, chiral β-lactams are also frequently obtained from racemic mixtures *via* enzymatic kinetic resolution.[36]

§ 1.1.1 Synthesis of (+)-1-6 via Staudinger [2+2] and Enzymatic Resolution

The first route employed for the synthesis of β-lactam **(+)1-6** was through a Staudinger [2+2] cycloaddition followed by a kinetic enzymatic resolution with PS Amano Lipase. Using this method, multi-gram quantities of **(+)1-6** were prepared, but this route proved to be slow, unreliable and labor intensive.

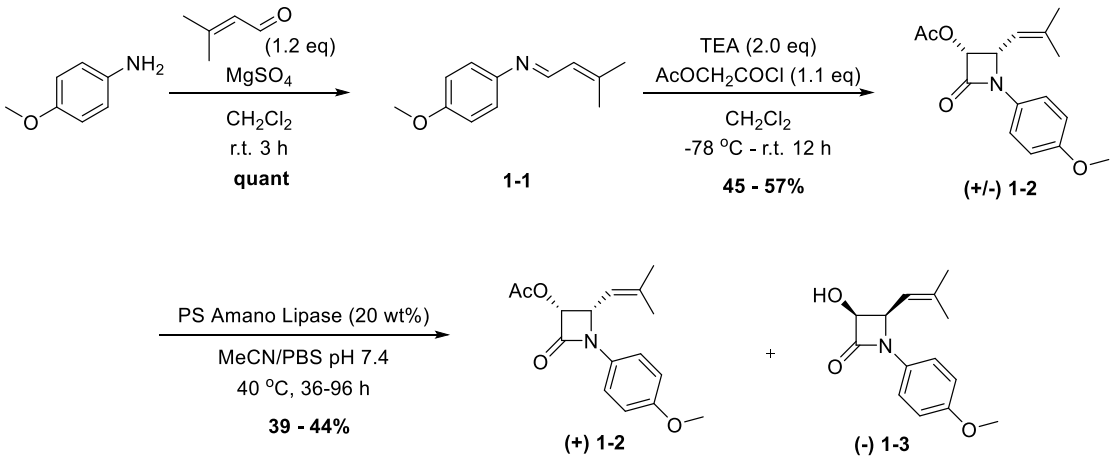

Scheme 1-1: Synthesis of β-lactam **(+)1-2** via Staudinger cycloaddition and enzymatic resolution

The synthesis of the desired β-lactam **(+)-1-6** (**Scheme 1-1**) commenced with the imine formation between *p*-anisidine and 3-methylbut-2-enal, the product of which was used directly in the next step. It was reacted with the ketene generated in situ from acetoxyacetyl chloride and TEA to afford the racemic β-lactam **1-2**. Although care was taken to maintain anhydrous conditions and low temperature, the yields at this step were modest and a significant amount of side product formation was observed (Section 1.1.2). The racemic material was then subjected to hydrolysis by PS Amano Lipase, selectively cleaving the acetoxy from the (-) enantiomer and allowing selective isolation of the desired **(+)-1-2** in >99% ee

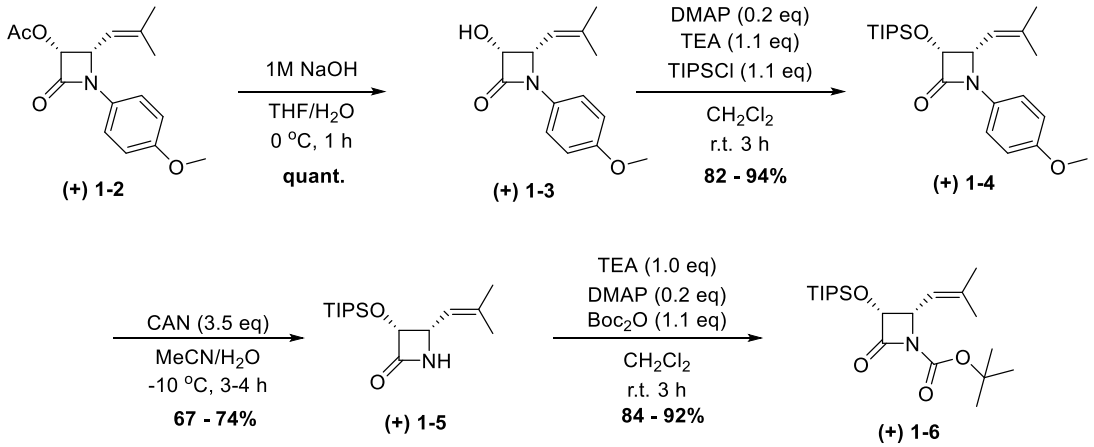

Scheme 1-2: Conversion of β-lactam **(+) 1-2** to **(+) 1-6**

Hydrolysis of the acetyl group and subsequent TIPS protection of the resulting alcohol produced (+) **1-4** in good yield. The *p*-methoxyphenyl (PMP) group was removed *via* oxidative cleavage with cerium (IV) ammonium nitratre (CAN) in decent yield. Treatment of the free amine with *t*-Boc anyhydride and TEA afforded **(+) 1-6**, which was used for taxoid synthesis (Section 2.1).

§ 1.1.2 Characterization of the Byproduct from the Staudinger Reaction

An unexpected byproduct was isolated from the [2+2] cycloaddition. Due to its similarity in R_f to the desired β-lactam, it was originally assumed to be the unwanted *trans* isomer. However, NMR analysis suggested that the correct structure was that of **1-7** (**Figure 1-6**). After recystallization from hexanes and ethyl ether, the structure was confirmed by single crystal X-ray diffraction.

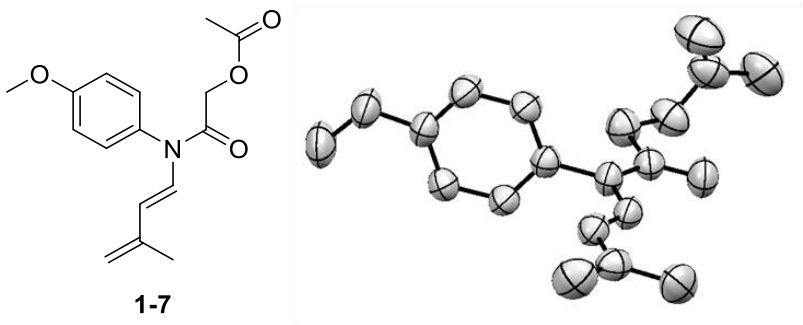

Figure 1-6: Structure of byproduct **1-7** and ORTEP diagram

The proposed mechanism for the formation of **1-7** is given in **Figure 7**. Intermediate **1-8** can be formed by direct displacement of the chloride by the imine, followed by an unexpected deprotonation of the charged intermediate **1-8**. The proton on the methyl group is activated due to its proximity to the conjugated electrophillic pi system, and deprotonation occurs to neutralize the positive charge. The resulting byproduct possesses extended conjugation through the diene and the amide, as seen in the ORTEP diagram in **Figure 1-6**.

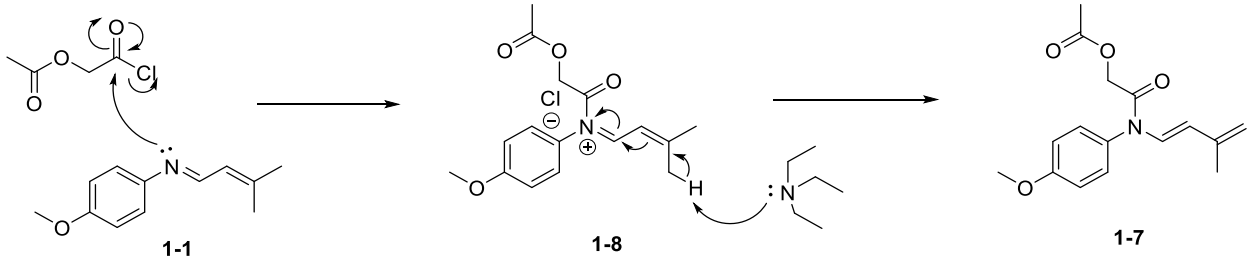

Figure 1-7: Proposed mechanism for the formation of byproduct **1-7**

This information may be of use to those attempting to optimize this reaction; however, the overall yield of this synthetic route is severely limited by the necessity for enzymatic resolution. Therefore, it is advantageous to avoid this low-yielding and unpredictable reaction by utilizing an alternative method for chiral induction in the synthesis of β-lactam **(+)-1-6**.

§ 1.2 The Chiral Ester-Enolate Cyclocondensation

Another effective method for the synthesis of highly enantio-enriched β-lactams is the chiral ester enolate-imine cyclocondensaiton. It has been successfully applied to the synthesis of 3-amino and 3-hydroxy-β-lactams with high enantio-purity.[25, 37] As shown in **Figure 1-8**, treatment of a chiral ester with LDA results in the formation of a chiral enolate, which can readily attack the desired imine, producing an uncyclized amide intermediate. Subsequent ring closure produces the desired enantio-enriched β-lactam and regenerates the chrial auxiliary in the process.

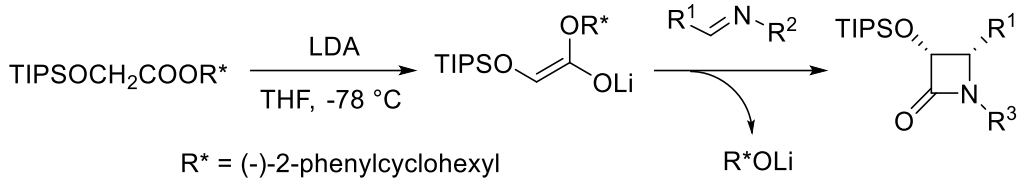

Figure 1-8: Synthesis of β-lactams *via* the asymmetric chiral ester enolate-imine cyclocondensation

Entry	R*	R^1	R^2	Yield (%)	% *trans* (% ee)	% *cis* (% ee)
1	(-)-menthyl	Ph	PMP	68	100 (>99)	
2	(-)-2-Ph-cyclohexyl	Ph	PMP	58	100 (>99)	
3	(-)-menthyl	4-F-C_6H_4	PMP	55	100 (>99)	
4	(-)-menthyl	4-CF_3-C_6H_4	PMP	59	100 (>99)	
5	(-)-menthyl	4-MeO-C_6H_4	PMP	70	89 (>99)	11 (38)
6	(-)-menthyl	3,4-$(MeO)_2C_6H_4$	PMP	70	91 (>99)	9 (38)
7	(-)-2-Ph-cyclohexyl	(*E*)-PhCH=CH_2	TMS	46		100 (78)

Table 1-1: Optimization of conditions for the cyclocondensation (adapted from [12])

As both the chiral auxiliary and *O*-protecting groups provide steric influence in the transition state of the chiral ester enolate-imine cyclocondensation, each of these moieties was screened to find the optimal chiral ester for this process.[12] During the optimization process, benzyl, TBS and TIPS groups as well as (-)-menthyl, (+)-*N*-methylephedrinyl, (-)- and (+)-*trans*-2-phenylcyclohexyl groups were investigated, and the combination of TIPS and (-)-2- or (+)-2-phenylcyclohexyl (Whitesell's chiral auxiliary) groups was found to give the best results for the

formation of 3-hydroxy-4-substituted β-lactams.[12] Furthermore, it was found that *cis*-β-lactams were formed exclusively in this process.

Later, a screening of chiral esters and protecting groups demonstrated that the use of TIPS-protected glycolic ester derived from Whitesell's chiral auxiliary also provides optimal yield and enantioselectivity for the synthesis of **(+)-1-4**.

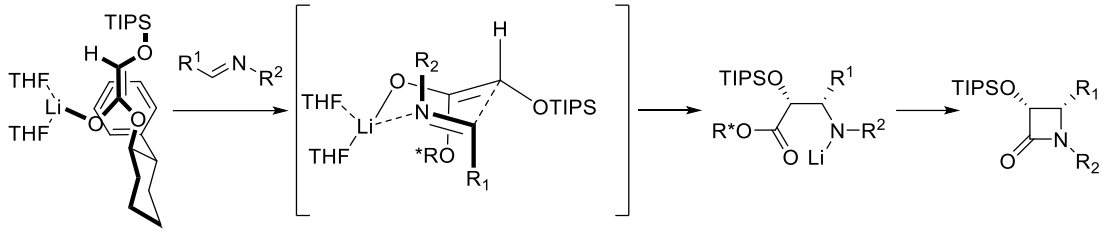

Figure 1-9: Mechanism of the chiral ester enolate-imine cyclocondensation (adapted from [4])

The origin of the excellent enantioselectivity can be understood by examining the mechanism outlined in **Figure 1-9**. Formation of the *E*-enolate is favored due to the kinetically controlled deprotonation conditions. The approach of the imine is blocked by one face of the enolate by the phenyl moiety in Whitesell's chiral auxiliary, setting the first level of chiral induction. The six-membered chair transition state is formed due to coordination of both the enolate oxygen and the imine nitrogen to the lithium counter ion, which stabilizes the system throughout the initial nucleophilic attack and counter ion transfer. The combined bulk of the TIPS protecting group and the chiral auxiliary force the imine to adopt the orientation shown in the transition state in **Figure 1-9**, leading to *cis*-β-lactam formation.

§ 1.2.1 Synthesis of Whitesell's Chiral Auxiliary (1-10)

In order to produce the amount of **(+) 1-6** necessary for taxoid synthesis and drug conjugate development, an easy and high yielding procedure for the synthesis of Whitesell's chiral auxiliary (**1-10**) is necessary. The previous method to synthesize **1-10** relied on an enzymatic chiral resolution using pig liver acetone powder (PLAP), and was therefore subject to the same low yield and high labor associated with enzymatic resolution of **(+/-) 1-2.** Fortunately, a facile synthesis was developed on the industrial scale, starting from 1-phenylcyclohexane and utilizing a Sharpless asymmetric dihydroxylation to set the two stereocenters (**Scheme 1-3**).

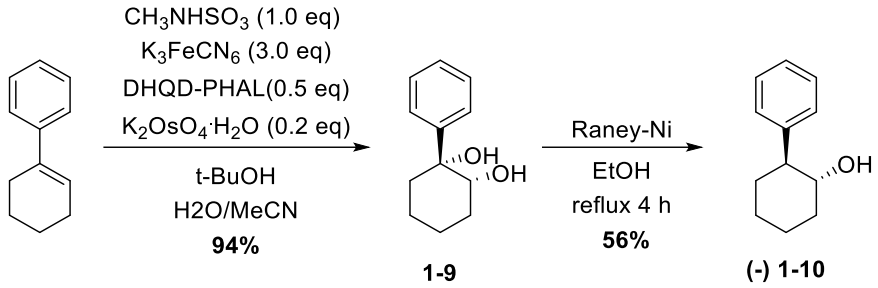

Scheme 1-3: Synthesis of Whitesell's chiral auxiliary

The Sharpless dihydroxylation proceeded smoothly according to the literature procedure when run on a >20g scale. The crude diol **1-9** was treated with Raney Nickel in ethanol to remove the benzylic hydroxyl group. Direct recrystallization of the crude from pentane afforded pure Whitesell's chiral auxiliary **1-10** in 50 % overall yield and >98% ee.

§ 1.2.2 Synthesis of Chiral Ester (-) 1-14

The previous method for synthesizing chiral ester (-) **1-14** involved the use of harsh conditions. Therefore an easy, scalable and reliable method was sought to procure the necessary TIPS protected glycolic acid for chiral ester synthesis.

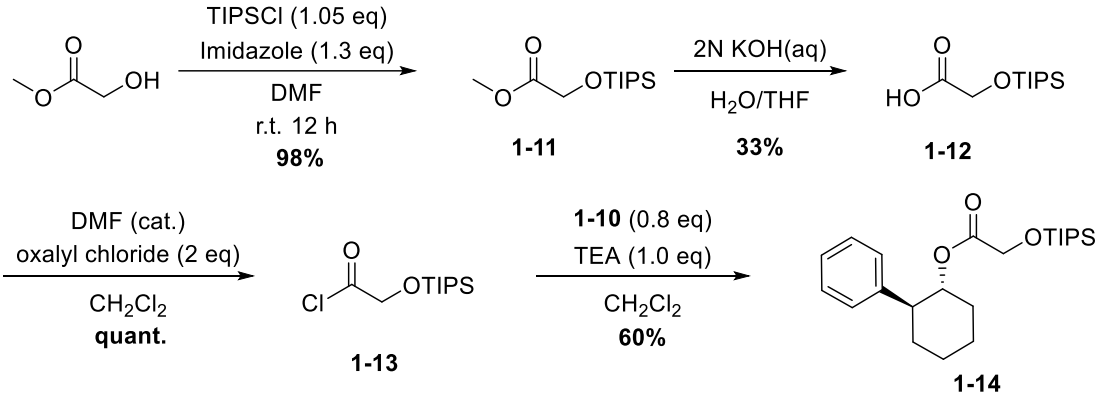

Scheme 1-4: Synthesis of chiral ester (-) **1-14** from methyl glycolate

The first method developed started from the TIPS protection of methyl glyocolate (**Scheme 5**), which proceeded in excellent yield. Hydrolysis of the methyl ester however did not prove to be as reliable. A significant amount of hexaisopropyldisiloxane, identified by proton NMR, was generated during the hydrolysis, as well as during the acid-base work up. This seemingly innocuous byproduct interfered with the cyclocondensation, and therefore had to be removed completely before the chiral ester was used. Purification of the chiral ester was painstaking using this method, as the two compounds have quite similar R_f values. Therefore, an easier way to produce clean chiral ester was desirable.

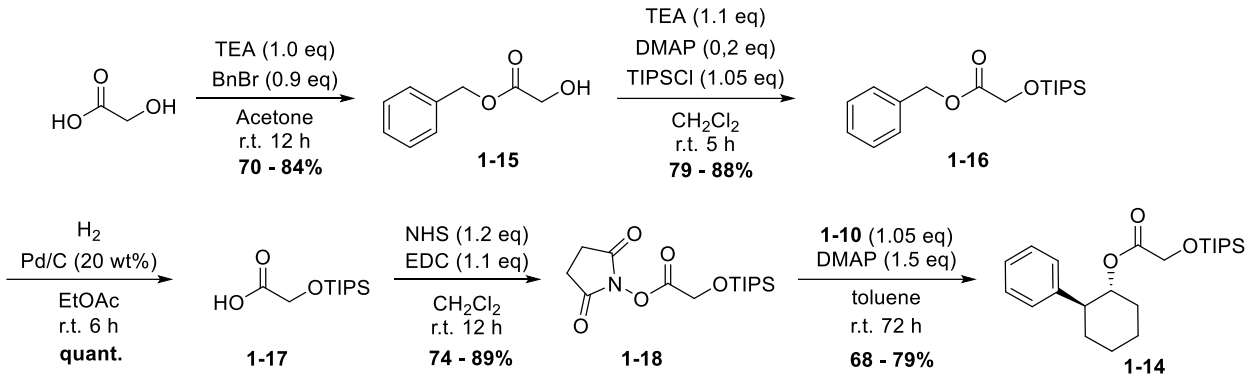

Scheme 1-5: Synthesis of chiral ester **(-) 1-14** from glycolic acid

An alternative method for the preparation of the chiral ester is outlined in **Scheme 1-5**. Starting from glycolic acid, selective benzylation of the carboxylic acid proceeded smoothly in decent and reproducible yield. After TIPS protection of the alcohol, this product was purified by column chromatography and pure **1-16** was obtained. Hydrogenation and formation of the activated ester both proceed in excellent yield. Furthermore, as compound **1-18** is a solid, it can be recrystallized at this step, if desired. Coupling to the Whitesell's chiral auxiliary is slow at room temperature, but the mixture likely can be heated to increase both the speed and yield of this reaction. Also, it may be worth using the acid chloride at this stage to investigate the effects on the overall yield of this process. While this scheme has not been completely optimized, it almost entirely avoids generation of the disiloxane and affords cleaner material in a better overall yield.

§ 1.2.3 Synthesis of (+) 1-4 *via* Cyclocondensation

With a route secured to reproducibly synthesize the chiral ester on a >10g scale, relatively larger scale synthesis of **(+) 1-4** is possible via the chiral ester enolate-imine cyclocondensation (**Scheme 7**). Compound **(+) 1-4** can be produced in a much shorter and more reliable time frame, when compared to the enzymatic resolution method outlined in **Scheme 1-1**.

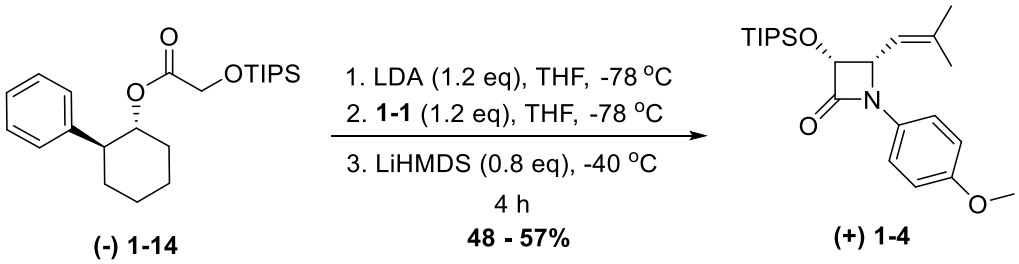

Scheme 1-6: Cyclocondensation to produce **(+) 1-4**

This reaction was carried out on 3.5 g and 10.0 g scales, producing spectroscopically pure, highly enantiomerically enriched product **(+) 1-4** in 57% and 48% yields, respectively after recrystallization. To recrystallize, the material was dissolved in hexanes and cooled gradually in a dry ice/acetone bath. Most of this material was used to synthesize **(+) 1-6** (as shown in **Scheme 1-2)**, which was used for taxoid synthesis described in later chapters.

§ 1.3.0 Conclusions and Perspectives

The β-lactam synthon is a versatile tool for the synthesis of biologically active molecules. One of the most impressive examples of this is the Ojima-Holton coupling for the synthesis of taxoid anticancer agents. For that reason, β-lactam **(+)-1-6** was synthesized utilizing two methods: the Staudinger [2+2] cycloaddition and the chiral ester enolate-imine cyclocondensation. The primary impurity of the Staudinger [2+2] cycloaddition has been isolated and its structure unambiguously assigned by NMR and X-ray crystallography, allowing the optimization of this key step. However, this method still requires a highly variable enzymatic resolution that wastes half of the material and suffers from unreliable reaction efficiency. However, to make the chiral ester enolate-imine cyclocondensation an effective method for the multi-gram scale production of **(+)-1-6**, a reliable and high yielding route to **(-)-1-14** was required. As the TIPS group on the glycolate is metastable, care must be taken to avoid acidic or basic conditions. Therefore, the route outlined in **Scheme 1-5** was developed. It can be reliably performed by a student of modest training on a decagram scale to produce clean **(-)-1-14**. Using this methodology, many grams of **(+)-1-6** can be produced quickly and reliably.

§ 1.4.0 Experimental

§ 1.4.1 General Methods

^{1}H and ^{13}C NMR spectra were measured on a Varian 300, 400, 500 or 600 MHz NMR spectrometer. Melting points were measured on a Thomas Hoover Capillary melting point apparatus and are uncorrected. Mass to charge values were measured by flow injection analysis on an Agilent Technologies LC/MSD VL. TLC was performed on Merck DC-alufolien with Kieselgel 60F-254 and column chromatography was carried out on silica gel 60 (Merck; 230-400 mesh ASTM). In determining enantiopurity (% ee), a Chiracel OD-H chiral column was used, with an isocratic mixture of 85:15 hexanes:ethyl acetate at a flow rate of 0.6 mL/min.

§ 1.4.2 Materials

The chemicals were purchased from Aldrich Co. and Sigma and purified before use by standard methods. Tetrahydrofuran was freshly distilled from sodium metal and benzophenone. Dichloromethane was also distilled immediately prior to use under nitrogen from calcium hydride.

In addition, various dry solvents were degassed and dried using PureSolv™ solvent purification system (Innovative Technologies, Newburyport, MA).

§ 1.4.3 – Experimental Procedures

N-(4-Methoxyphenyl)-3-methyl-2-butenaldimine [1-1][38]

p-Anisidine (8.00 g (65 mmol), recrystallized from hexanes, was dissolved in CH_2Cl_2 (125mL) with anhydrous Na_2SO_4 (10 g). To this mixture, 3-methylbut-2-enal (6.6 mL, 87 mmol), was added dropwise under inert conditions. The mixture was stirred at room temperature and monitored *via* TLC. After 3 h, the solvent was evaporated and concentrated *in vacuo* to afford **(±) 1-1** as red oil (12.7 g, 100% yield), and was used immediately in the subsequent step: ^{1}H NMR (300 MHz, $CDCl_3$) δ) 1.89 (s, 3H), 1.94 (s, 3H), 3.73 (s, 3H), 6.16 (d, J = 7.2 Hz, 1H), 6.84 (d, J = 5.2 Hz, 2 H), 7.07 (d, J = 5.1 Hz, 2H), 8.33 (d, J = 7.2 Hz, 1H). All data were found to be in agreement with literature values.[38]

(±)-1-(4-Methoxyphenyl)-3-acetoxyl-4-(2-methylprop-1-enyl)azetidin-2-one [(±) 1-2] [38]

An aliquot of **(±) 1-1** (12.7 g, 67 mmol) was dissolved in CH_2Cl_2 (120 mL), cooled to -78 ˚C with 4.5 Å molecular sieves, and TEA (14 mL, 100 mmol) was added under inert conditions. Acetoxyacetyl chloride (9.3 mL, 87 mmol) was added to the solution dropwise *via* syringe. The solution was maintained at -78 ˚C under N_2 atmosphere overnight. Then the mixture was then allowed to warm slowly to room temperature. The reaction was quenched with saturated NH_4Cl (10 mL) and the product was extracted with CH_2Cl_2 (3 x 100 mL). The organic layer was washed with brine (3 x 100 mL), dried over $MgSO_4$, the filtrate collected, evaporated and concentrated *in vacuo* producing dark red black oil. Purification by column chromatography on silica gel (hexanes:ethyl actetate = 2:1) was done to afford **(±) 1-2** (8.2 g, 45% yield) as a pale yellow solid, which could be easily recrystallized from hexanes, producing a white crystalline material: m.p 108-109 ^{o}C (lit.[42] 107-108 ^{o}C); ^{1}H NMR (300 MHz, $CDCl_3$) δ 1.80 (s, 3H), 1.83 (s, 3H), 2.13 (s, 3H), 3.78 (s, 3H), 4.98 (dd, J = 9.0, 5.1 Hz, 1H), 5.14 (m, 1H), 5.81 (d, J = 5.1 Hz, 1H), 6.87 (d, J = 9.0 Hz, 2H) 7.33 (d, J = 9.0 Hz, 2H). All data were found to be in agreement with literature values.[38]

N-(4-Methoxyphenyl)-*N*-acetoxyacetyl-1-aminobutyl-1,3-diene [1-7]

This compound eluted directly before **(±) 1-2** and was collected as an orange oil that could be solidified from cold hexanes. This sample was then recrystallized by slow evaporation of ether from a hexanes/ether mixture to afford **1-7** as pale yellow crystals: ^{1}H NMR (400 MHz, $CDCl_3$) δ 1.85 (s, 3H), 2.12 (s, 3H), 3.85 (s, 3H), 4.32 (s, 2H), 4.65 (s, 1H), 4.77 (s, 1H), 5.20 (d, J = 14.4 Hz, 1H), 7.00 (d, J = 6.4 Hz, 2H), 7.15 (d, J = 6.4 Hz, 2H), 7.60 (d, J = 14.4 Hz, 1H); ^{13}C NMR

(100 MHz, $CDCl_3$) δ 18.08, 20.50, 55.55, 61.94, 115.05, 115.53, 117.37, 128.19, 129.17, 129. 96, 140.39, 160.15, 165.47. MS (ESI) calcd for $C_{16}H_{20}NO_4$ $(M+H)^+$: 290.13, found 290.1.

(+)-1-(4-Methoxyphenyl)-3-acetoxyl-4-(2-methylprop-1-enyl)azetidin-2-one [(+) 1-2][36]

A racemic mixture of **(+/-) 1-2** (10.0 g, 34.6 mmol) was dissolved in 0.2 M sodium phosphate buffer (pH 7.4) with 10 volume % acetonitrile and heated to 50 °C. To the solution PS-Amano Lipase (2.0 g) was added and the mixture was stirred vigorously at 50 °C with a mechanical stirrer for 5 days. The reaction was monitored *via* HPLC and ^{1}H-NMR, and upon completion, the remaining Lipase was vacuum filtered and washed with CH_2Cl_2 (3 x 150 mL). The organic layer was collected, washed with brine (3 x 200 mL), dried over anhydrous $MgSO_4$, suction-filtered and the filtrate concentrated *in vacuo*. Purification was done by column chromatography on silica gel with increasing amounts of ethyl acetate in hexanes (hexanes:ethyl acetate = 1:0 - 4:1) to afford enantioenriched beta-lactam **(+) 1-2** (3.62 g, 36%) as a white solid. The enantiopurity was determined to be > 99% via HPLC by analysis with a chiracel OD-H column in hexanes: isopropanol 85:15: ^{1}H NMR (300 MHz, $CDCl_3$) δ 1.80 (s, 3H), 1.83 (s, 3H), 2.13 (s, 3H), 3.78 (s, 3H), 4.88 (dd, J = 9.0, 5.1 Hz, 1H), 5.03 (d, J = 5.1 Hz, 1H), 5.29 (m, 1H), 7.33 (d, J = 9.0 Hz, 2H), 6.87 (d, J = 9.0 Hz, 2H). All data were found to be in agreement with literature values.[36]

(3*R*,4*S*)-1-(4-Methoxyphenyl)-3-hydroxy-4-(2-methylprop-1-enyl)azetidin-2-one [(+) 1-3] [39]

The enantiomerically pure **(+) 1-2** (3.6 g, 12.4 mmol) was dissolved in THF (50 mL) and cooled to 0 °C. To this mixture was added, chilled, 1 M KOH (50 mL). The reaction was stirred and monitored by TLC. Upon completion, the reaction was quenched with saturated NH_4Cl (5 mL) and extracted with ethyl acetate (2 x 30 mL). The organic layer was collected, washed with brine, dried over anhydrous $MgSO_4$, and concentrated *in vacuo* to afford **(+) 1-3** (3.4 g, 100% yield) as a white solid: ^{1}H NMR (300 MHz, $CDCl_3$) δ 7.33 (d, J = 9.0 Hz, 2H), 6.87 (d, J = 9.0 Hz, 2H) 5.29 (d, J = 9.0 Hz, 1H), 5.81 (d, J = 5.1 Hz, 1H), 4.98 (dd, J = 9.0, 5.1 Hz, 1H) 3.78 (s, 3H), 2.13 (s, 3H), 1.83 (s, 3H), 1.80 (s, 3H). All data were found to be in agreement with literature values.[39]

(3*R*,4*S*)-1-4-Methoxyphenyl-3-triisopropylsiloxy-4-(2-methylpropen-2-yl)azetidin-2-one [**(+) 1-4**][40]

Compound **(+) 1-3 (**3.4 g, 12.4 mmol) and DMAP (540 mg, 4.4 mmol) were dissolved in CH_2Cl_2 (65 mL). The solution will was cooled to 0 °C under inert conditions. To this solution was added TEA (4.1 mL, 29 mmol), followed by the dropwise addition of TIPSCl (5.5 mL, 22 mmol). The reaction mixture was stirred at room temperature and monitored by TLC. Upon completion the reaction was quenched with saturated NH_4Cl (5 mL) and extracted with CH_2Cl_2 (1 x 70 mL). The organic layer was collected, washed with brine (3 x 35 mL), dried over anhydrous $MgSO_4$, and concentrated *in vacuo*. Purification was done by column chromatography on silica gel

(hexanes:ethyl acetate = 19:1) to afford **(+) 1-4** (4.8 g, 96% yield) as a white solid: ^{1}H NMR (300 MHz, $CDCl_3$) δ 1.07 (m, 21H), 1.79 (s, 3H), 1.84 (s, 3H), 3.77 (s, 3H), 4.80 (dd, J = 9.9, 5.1 Hz, 1H), 5.05 (d J = 4.8 Hz, 1H), 5.32 (d, J = 9.9 Hz, 1H), 6.83 (d, J = 9.0 Hz, 2H), 7.32 (d, J = 9.0 Hz, 2H). All data were found to be in agreement with literature values.[40]

(3*R*,4*S*)-3-Triisopropylsilyloxy-4-(2-methylpropen-2-yl)azetidin-2-one [(+) 1-5] [29]

An aliquot of **(+) 1-4** (1.3 g, 3.2 mmol) was dissolved in acetonitrile (125 mL) and cooled to -10 °C. To this solution was added CAN (7.0 g, 12.8 mmol) dissolved in H_2O (125 mL) and added dropwise *via* an addition funnel. The reaction temperature of -10 °C was maintained throughout the reaction. The reaction was monitored by TLC and upon completion the mixture was extracted with ethyl acetate (80 mL). The organic layer was washed with aqueous Na_2SO_3 (4 x 60 mL), brine (3 x 50 mL), dried over $MgSO_4$ and concentrated *in vacuo*. Purification was done by column chromatography on silica gel with increasing amounts of ethyl acetate in hexanes (hexanes:ethyl acetate 1:0 – 2:1) to afford **(+) 1-5** (600 mg, 64% yield) as a pale yellow solid: ^{1}H NMR (300 MHz, $CDCl_3$) δ 1.07 (m, 21H), 1.67 (s, 3H), 1.75 (s, 3H) 4.43 (dd, J = 9.6, 4.8 Hz, 1H), 4.98 (m, 1H), 5.29 (m, 1H), 6.24 (s, 1H). All data were found to be in agreement with literature values.[29]

(3*R*,4*S*)-1-(*t*-Butoxycarbonyl)-3-triisopropylsiloxy-4-(2-methylpropen-2-yl)azetidin-2-one [(+)1-6][29]

Compound **(+) 1-5 (**600 mg, 2.0 mmol), DMAP (80 mg, 0.7 mmol) and di-*tert*-butyl dicarbonate (580 mg, 26 mmol) was dissolved in CH_2Cl_2 (10 mL) and cooled to 0 °C under inert conditions. To the mixture, TEA (0.6 mL, 40 mmol) was added dropwise. The reaction was stirred at room temperature and monitored *via* TLC. Upon completion the reaction was quenched with saturated NH_4Cl (1 mL) and extracted with CH_2Cl_2 (20 mL). The organic layer was collected, washed with brine (3 x 30 mL), dried over anhydrous $MgSO_4$, and concentrated *in vacuo*. Purification was done by column chromatography on silica gel (hexanes:ethyl acetate = 9:1) to afford **(+) 1-6** (772 mg, 96% yield) of as a colorless oil: ^{1}H NMR (300 MHz, $CDCl_3$) δ 1.04 (m, 21H), 1.48 (s, 9H), 1.76 (s, 3H), 1.79 (s, 3H), 4.75 (dd, J = 9.9, 5.7 Hz), 4.96 (d, J = 5.7 Hz), 5.28 (m, 1H). All data were found to be in agreement with literature values.[29]

(1R,2R)-1-1-Phenylcyclohexane-1,2-diol [1-9][41]

To 1 L round bottom flask containing hexapotassium ferrocyanide (125 g, 381 mmol), potassium carbonate (53 g, 381 mmol), and methanesulfonamide (12 g, 127 mmol) was added *t*-butanol (140 ml) and distilled water (200 mL). The mixture was cooloed to 0 ^oC in an ice bath while stirring. After few minutes of stirring, potassium osmate dihydrate (0.122 g, 0.333 mmol) and the $(DHQD)_2$-PHAL ligand (0.94 g, 1.21 mmol) were added. After stirring for 15 minutes, 1-phenyl-1-cyclohexene (20 mL, 127 mmol) of was added dropwise to the mixture. The reaction equilibrated

to room temperature and was stirred for 2 days. Upon completion, the reaction appeared two layers: yellow and orange color. The reaction was monitored via TLC (9:1 hexanes/ethyl acetate, stain-vanillin). Ethyl acetate was added to the solution while it was stirring. After 10 minutes, the yellow compound dissolved. The solution was filtered through 2 cm celite to remove the insoluble material. The organic layer was washed with 2M KOH (2 x 400 mL), and dried over $MgSO_4$. The dried organic layer was suction filtered the filtrate was concentrated *in vacuo* to afford **1-9** (21.8 g, 89.7%) as a white solid. ^{1}H NMR (300 MHz, $CDCl_3$) δ: 1.40-1.95 (m, 10H), 4.0 (dt, *J* = 4.0, 11.0 Hz, 1H), 7.33 (t, *J* = 7.5 Hz, 2H), 7.40 (t, *J* = 7.5 Hz, 1H), 7.56 (d, *J* = 8.5 Hz, 2H). All data were found to be in agreement with literature values.[41]

(-)-*trans*-2-Phenylcyclohexanol [1-10][41]

To a 1000 mL round bottom flask containing **1-9** (4.7 g, 24.5 mmol) was added ethanol (48 mL). Raney nickel was allowed to settle out of suspension in a 250 mL cylinder, the water was decanted and washed with ethanol (3 x 100 mL). The Raney nickel was transferred into the RBF and an additional 100 mL of ethanol was used to wash it completely into the reaction vessel. The reaction was kept under reflux for 3 hours at 100 ^{o}C. The reaction was monitored via TLC (4:1 hexanes/ethyl acetate, stain-vanillin). Upon completion, the solution was cooled to about 40 ^{o}C. The mixture was filtered through 2 cm Celite while being constantly washed with ethanol. The ethanol was then concentrated *in vacuo*, and the resulting residue was dissolved in ethyl acetate (100 mL) The organic layer was washed with brine (3 x 25 mL), dried over $MgSO_4$, and suction filtered. The filtrate was concentrated *in vacuo* to give a slightly yellow liquid. Recrystallization from cold pentane was obtained to afford **1-10** (2.4 g, 56%) as a white crystal. The enantiopurity was assessed *via* Normal Phase HPLC (ChiralCel OD-H column with 98% hexanes/IPA mobile phase with a flow rate of 0.4 mL/min). The % ee was determined to be 98%. ^{1}H NMR (300 MHz, $CDCl_3$) δ: 1.31-1.57 (m, 6H), 1.78-1.80 (m, 1H), 1.96 (m, 2H), 2.12-2.14 (m, 1H), 2.42-2.47 (m, 1H), 3.70-3.80 (m, 1H), 7.34-7.38 (m, 3H), 7.41 (t, J=7.5 Hz, 2H). All data were found to be in agreement with literature values.[41]

Trisopropylsilyl-methyglycolate [1-11][42]

To a 100 mL round bottom flask containing methylglycolate (5.6 g, 62.2 mmol) was added imidazole (12.9 g, 190 mmol) and the reaction vessel was purged with N_2. To this was added DMF (30 mL) via syring, and the solution was cooled to 0 ^{o}C in an ice bath with stirring. After 10 minutes, triisopropylsilyl chloride (16.2 mL) was added dropwise. The temperature warmed back to room temperature overnight. Upon completion, saturated ammonium chloride was added to quench reaction. After the extraction with ethyl acetate, organic layer was washed with brine three times. The organic layer then dried with $MgSO_4$, and filtered. Solvent was removed using a rotary

evaporator to afford **1-11** a crude as a slight yellow oil. ^{1}H NMR (300 MHz, $CDCl_3$) δ: 1.05-1.10 (m, 21H), 3.73 (s, 3H), 4.31 (s, 2H). All data were found to be in agreement with literature values.[42]

Triisopropylsilyloxyacetic acid [1-12][43]

To a 500 mL round bottom flask containing **1-11** (15.3 g, 62.2 mmol) was added THF (100 mL). The solution was cooled to 0 ^{o}C in an ice bath To the solution was added $LiOH{\cdot}H_2O$ (4.4 g of in 105 mL distilled water) dropwise with an addition funnel over 20 minutes. The reaction was stirred at room temperature for 16 hours. After the addition of CH_2Cl_2, the solution was cloudy. The solution was added 1 N HCl. After the extraction with CH_2Cl_2, the organic layer was washed with brine three times and dried over with $MgSO_4$. pH was 5. More concentrated HCl was added into aqueous layer to adjust pH to 2. After the extraction with CH_2Cl_2, organic layer was washed with brine and dried with $MgSO_4$, and filtered. Solvent was removed using a rotary evaporator to give a yellow liquid. Purification was done via column chromatography on alumina gel (hexanes: ethyl acetate=9:1) to afford **1-12** (4.8 g, 33.3 %) as a clear liquid. ^{1}H NMR (300 MHz, $CDCl_3$) δ: 1.0-1.1 (m, 21H), 4.35 (s, 2H). All data were in agreement with literature values. However, there was a significant amount of disiloxane present in the product.[43]

Triisopropylsilyloxyacetyl chloride [1-13]

In a 100 mL round bottom flask, **1-12** (4.6 g, 19.8 mmol) of was dissolved in CH_2Cl_2 (58 mL). The solution was cooled to 0 ^{o}C in an ice bath. Oxalyl chloride (2.19 mL, 25.7 mmol) was added dropwise over the course of 5 minutes. After ten minutes, 5 drops of DMF was added. The reaction was allowed to stir from 0 ^{o}C to room temperature overnight. The reaction was monitored by ^{13}C-NMR of small aliquots of the crude reaction mixture after concentration *in vacuo*. The solvent was removed using *in vacuo* to afford **1-13** (3.84 g, 78%) as a light yellow oil. ^{1}H NMR (300 MHz, $CDCl_3$) δ:1.0-1.2 (m, 21H), 4.75 (s, 2H).

(1R, 2S)-(-)-2-Phenylcyclohexyl-triisopropylsilyloxyacetate [1-14][20]

In a 250 mL round bottom flask, **1-10** (2.37 g, 13.5 mmol) and DMAP (800 mg, 6.6 mmol) were dissolved in CH_2Cl_2 (32 mL). To this solution, pyridine (1.56 g, 19.7 mmol) was added slowly, followed by the dropwise addition of **1-13** (3.8 g, 15.2 mmol) dissolved in CH_2Cl_2 (10 mL). The reaction was allowed to proceed at room temperature for 24 hours. The reaction was monitored by TLC (9:1 hexanes/ethyl acetate, stain- PMA). Upon completion, the reaction was quenched with saturated sodium bicarbonate (10 mL). Water was used to dilute the solution. The diluted solution was washed with saturated $CuSO_4$ (2 x 20 mL) and H_2O (2 x 20 mL). The organic layer was washed with brine (3 x 20 mL), dried over $MgSO_4$, suction filtered and the filtrate concentrated *in vacuo*. Purification was done by column chromatography on silica gel (hexanes:EtOAc 200:1). The product was collected and solvent was removed *in vacuo* to afford **1-14** (2.265 g, 43%) as a

colorless liquid. ^{1}H NMR (300 MHz, $CDCl_3$) δ: 1.03-1.04 (m, 21H), 1.40-1.60 (m, 6H), 1.80-2.0 (m, 2H), 2.18 (s, 1H), 2.70-2.80 (t, *J* = 15 Hz, 1H), 4.09 (d, *J* = 15 Hz, 2H), 5.10-5.20 (m, 1H), 7.25-7.30 (m, 5H). All data were found to be in agreement with literature values.[20]

Benzyl glycolate [1-15][44]

In a 250 mL round bottom flask, glycolic acid (5.00 g, 65.8 mmol) and triethylamine (10.0 mL, 71. mmol) were dissolved in acetone (65 mL). After two minutes of stirring, benzyl bromide (10 g, 59 mmol) was added dropwise. White solid began to precipitate after 30 minutes and the reaction was stirred overnight. The reaction was monitored by TLC (2:1 hexanes/ethyl acetate). The white solid was removed by suction filtration, and filtrate was concentrated *in vacuo* to afford a colorless oil which was dissolved in EtOAc (150 mL) and washed with H_2O (100 mL) and brine (3 x 50 mL). The organic layer was dried with $MgSO_4$, filtered and the filtrate was concentrated *in vacuo* to afford **1-15** (760 mg, 79%) as a colorless oil: ^{1}H NMR (300 MHz, $CDCl_3$) δ: 2.20 (s, 1H), 4.0-4.10 (s, 2H), 5.1-5.2 (s, 2H), 7.2 (s, 5H). All data were found to be in agreement with literature values.[44]

Benzyl-(triisopropylsilyloxy)-acetate [1-16][43]

In a 100 mL of round bottom flask, **1-15** (7.86 mg, 47.35 mmol) and DMAP (580 mg, 4.74 mmol) were dissolved in 100 mL of CH_2Cl_2 in an ice bath. While stirring, triethylamine (8.6 mL, 61.6 mmol) was added, followed by the dropwise addition of triisopropylsilyl chloride (10.0 g, 52.1 mmol). The reaction was allowed to warm to room temperature for 3 hours. The reaction was monitored by TLC (3:1 hexanes/ethyl acetate). Upon completion, the reaction was quenched with 20 mL of NH_4Cl. The solution was diluted with H_2O (200 mL) and CH_2Cl_2 (100 mL). The organic layer was washed with brine (3 x 100mL), dried with $MgSO_4$, filtered and the filtrate was concentrated *in vacuo*. Purification was done by column chromatography using silica gel (1% ethyl acetate in hexanes) to afford **1-16** (13.17 g, 85%) as colorless oil. ^{1}H NMR (300 MHz, $CDCl_3$) δ: 1.0-1.1 (m, 21H), 4.20 (s, 2H), 5.15 (s, 2H), 7.1-7.2 (m, 5 H). All data were found to be in agreement with literature values.[43]

Triisopropylsilyloxyacetic acid [1-17][43]

To a solution of **1-16** (13.16 g, 40.9 mmol) in EtOAc (200mL), $Pd(OH)_2$ (300 mg, 2.14 mmol) was added. The flask was evacuated and flushed with H_2 three times. The mixture was stirred for 4.5 hours. The reaction was monitored by TLC (9:1 hexanes/ethyl acetate). Upon completion, 20 wt% $Pd(OH)_2$/C was filtered through 2.5 cm of Celite. The Celite was washed with CH_2Cl_2. The filtrate was concentrated *in vacuo* to afford **1-17** (9.48 g, quant.) as colorless oil. ^{1}H NMR (300 MHz, $CDCl_3$) δ: 1.0-1.1 (m, 21H), 4.15 (s, 2 H). All data were found to be in agreement with literature values.[43]

Triisopropylsilyloxyacetic acid *N*-hydroxysuccinimide ester [1-18]

To a solution of **1-17** (9.48 g, 40.9 mmol) and NHS (5.64 g, 49.1 mmol) in CH_2Cl_2 (100 mL) was added a suspension of EDC·HCl (11.8 g, 61.4 mmol in CH_2Cl_2 (100 mL). The reaction mixture was stirred overnight at room temperature and monitored by TLC (2:1 Hx:EtOAc). The organic layer was then washed with bring (3 x 75 mL), dried over $MgSO_4$, filtered and the filtrate was concentrated *in vacuo* to afford a colorless oil which could be triturated with hexanes and filtered to afford **1-15** (12.02 g, 89%) as a white solid: ^{1}H NMR (300 MHz, $CDCl_3$) δ 1.08 (m, 21H), 2.84 (s, br, 4H), 4.67 (s, 2H). HRMS calcd for $C_{15}H_{28}NO_5Si$ $(M+H)^+$: 370.1737, found: 310.1730 (Δ -2.1 ppm, -0.7 mDa).

(1R, 2S)-(-)-2-Phenylcyclohexyl-triisopropylsilyloxyacetate[1-14][20]

To a solution of **(-) 1-10** (6.0 g, 33.5 mmol) and DMAP (6.17 g, 50.6 mmol) in toluene (50 mL) was added **1-15** (13.3 g, 40.5 mmol) dissolved in toluene (50 mL) using an addition funnel. The reaction was stirred at room temperature for 72 hours, during which time a white precipitate formed. After observing the completion of the reaction by TLC (9:1 Hx:EtOAc), the white solid was filtered off and filtrate was condensed *in vacuo*. The yellow oil was then dissolved in EtOAc (200 mL) and washed with brine (3 x 75 mL). The organic layer was then dried over $MgSO_4$, filtered and the filtrate was concentrated *in vacuo* to afford a pale yellow oil. Purification was done by column chromatography using silica gel (hexanes:EtOAc = 1:0 to 1:50) to afford **1-14** (13.17 g, 85%) as colorless oil. ^{1}H NMR (300 $CDCl_3$) δ 0.94-1.06 (m, 2H), 1.33-1.55 (m, 5H), 2.20 (m, 1H), 2.73 (dd, J = 11.7, 3.6 Hz, 1H), 3.96 (d, J = 16.5 Hz, 1H), 4.14 (d, J = 16.5 Hz, 1H), 5.15 (m, 1H), 7.23 (m, 3H), 7.31 (m, 2H). All data were found to be in agreement with literature values.[20]

(3*R*,4*S*)-1-4-Methoxyphenyl-3-triisopropylsiloxy-4-(2-methylpropen-2-yl)azetidin-2-one [(+) 1-4][24]

Diisopropyl amine (1.19 g, 11.8 mmol) was dissolved in anhydrous THF (10 mL) under inert atmosphere and cooled to -30 °C in an acetone bath with dry ice. To this was added *n*-BuLi (1.6 M in hexanes, 6.7 mL) dropwise and allowed to up to room temperature for 1 hour before being cooled to -78 °C. To this solution was added a pre-cooled solution of **1-14** (3.5 g, 8.92 mmol) in THF (10 mL) *via* cannula over 30 minutes at -78 °C, over which time the color of the solution turned to a pale yellow. To this was added a pre-cooled solution of **1-1** (1.49 g, 10.7 mmol) dissolved in THF (10 mL) at -78 °C over the course of 2 hours *via* cannula. During the addition, the reaction mixture turned a deep orange color and was stirred for 2 hours at -78 °C, at which time LiHMDS (1 M in THF, 7 mL) was added dropwise and the reaction was allowed to warm to -40 °C over 1 hour. The reaction was quenched with NH_4Cl (aq) (5 mL), H_2O was added (40 mL) and the aqueous layer was extracted with EtOAc (3 x 40 mL). The combined organic layer was then washed with brine (3 x 40 mL), collected, dried over MgSO4, filtered and the filtrate evaporated *in vacuo* to afford an orange oil. Purification was done by column chromatography on silica gel

with increasing amounts of ethyl acetate in hexanes (hexanes:ethyl acetate 1:0 – 25:1) to afford a pale yellow solid, which could be precipitated from pure hexanes at -78 °C to afford **(+) 1-4** (2.01 g, 57 %) as a white solid: ^{1}H NMR (300 MHz, $CDCl_3$) δ 1.07 (m, 21H), 1.79 (s, 3H), 1.84 (s, 3H), 3.77 (s, 3H), 4.80 (dd, J = 9.9, 5.1 Hz, 1H), 5.05 (d J = 4.8 Hz, 1H), 5.32 (d, J = 9.9 Hz, 1H), 6.83 (d, J = 9.0 Hz, 2H), 7.32 (d, J = 9.0 Hz, 2H). All data were found to be in agreement with literature values.[24]

§ 1.5.0 References

1. Ojima, I., Asymmetric Syntheses by Means of β-Lactam Synthon Method. In *Advances in Asymmetric Synthesis*, Hassner, A., Ed. JAI Press, Inc.: Greenwich, CT, 1995; Vol. 1, pp 95-146.
2. Hatanaka, N.; Abe, R.; Ojima, I., β-Lactam as Synthetic Intermediate: Synthesis of Leucine-Enkephalin. *Chem. Lett.* **1981,** *10*, 1297-1298.
3. Ojima, I.; Inaba, S.; Yoshida, K., New and effective Route to β-Lactams. The Reaction of Ketene Silyl Acetals with Schiff Bases Promoted by Titanium Tetrachloride. *Tetrahedron Lett.* **1977,** *18*, 3643-3646.
4. Ojima, I.; Zuniga, E.; Seitz, J., Advances in the Use of Enantiopure B-lactams for the Synthesis of Bioligcally Active Compounds of Medicinal Interest. *Top. Heterocycl. Chem.* **2013,** *30*, 1-64.
5. Ojima, I.; Kuznetsova, L.; Ungureanu, I. M.; Pepe, A.; Zanardi, I.; Chen, J., Fluoro-β-lactams as Useful Building Blocks for the Synthesis of Fluorinated Amino Acids, Dipeptides, and Taxoids. In *Fluorine-containing Synthons*, Soloshonok, V., Ed. American Chemical Society/Oxford University Press: Washington, D.C., 2005; pp 544-561.
6. Alcaide, B.; Aly, M.; Rodriguez, C.; Rodriguez-Vicente, A., Base-Promoted Isomerization of cis-4-Formyl-2-azetidinones: Chemoselective C4-Epimerization vs Rearrangement to Cyclic Enaminones. *J. Org. Chem.* **2000,** *65*, 3453-3459.
7. Romo, D.; Rzasa, R. M.; Shea, H. A.; Park, K.; Langenhan, J. M.; Sun, L.; Akhiezer, A.; Liu, J. O., Total Synthesis and Immunosuppressive Activity of (−)-Pateamine A and Related Compounds: Implementation of a β-Lactam-Based Macrocyclization. *J. Am. Chem. Soc.* **1998,** *120*, 12237-12254.
8. Del Buttero, P.; Molteni, G.; Roncoroni, M., Reductive ring opening of 2-azetidinones promoted by sodium borohydride. *Tetrahedron Lett.* **2006,** *47*, 2209-2211.
9. Alcaide, B.; Almendros, P.; Cabrero, G.; Ruiz, M., Organocatalytic Ring Expansion of β-Lactams to γ-Lactams through a Novel N1−C4 Bond Cleavage. Direct Synthesis of Enantiopure Succinimide Derivatives. *Org. Lett.* **2005,** *7*, 3981-3984.
10. Dejaegher, Y.; Mangelinckx, S.; De Kimpe, N., Rearrangement of 2-Aryl-3,3-dichloroazetidines: Intermediacy of 2-Azetines. *J. Org. Chem.* **2002,** *67*, 2075-2081.
11. Ojima, I.; Chen, H.-J. C., Novel and Effective Routes to Optically Pure Amino Acids, Dipeptides, and Their Derivatives via β-Lactams obtained through Asymmetric Cycloaddition. *J. Chem. Soc. Chem. Commun.* **1987,** *1987*, 625-626.
12. Ojima, I., Recent Advances in the β-Lactam Synthon Method. *Acc. Chem. Res.* **1995,** *28*, 383-389.
13. Ojima, I.; Zhao, M.; Yamato, T.; Nakahashi, K.; Abe, R., Azetidines and bisazetidines. Their synthesis and use as the key intermediates to enantiomerically pure diamines, amino alcohols, and polyamines. *J. Org. Chem.* **1991,** *56*, 5263-5277.

14. Saito, T.; Kobayashi, S.; Ohgaki, M.; Wada, M.; Nagahiro, C., Diene-transmissive hetero Diels–Alder reaction of cross-conjugated azatrienes with ketenes: a novel and efficient, stereo-controlled synthetic method for hexahydroquinolinones *Tetrahedron Lett.* **2002,** *43*, 2627-2631.
15. Alcaide, B.; Almendros, P.; Cabrero, G.; Callejo, R.; Ruiz, M.; Arno, M.; Domingo, L., Ring Expansion versus Cyclization in 4-Oxoazetidine-2-carbaldehydes Catalyzed by Molecular Iodine: Experimental and Theoretical Study in Concert. *Adv. Synth. Catal.* **2010,** *352*, 1688-1700.
16. Alcaide, B.; Rodriguez-Campos, I. M.; Rodriguez-Lopez, J.; Rodriguez-Vicente, A., Stereoselective Synthesis of Fused Bicyclic β-Lactams through Radical Cyclization of Enyne-2-azetidinones. *J. Org. Chem.* **1999,** *64*, 5377-5387.
17. Alcaide, B.; Almendros, P.; Aragoncillo, C., A Novel One-Step Approach for the Preparation of α-Amino Acids, α-Amino Amides, and Dipeptides from Azetidine-2,3-diones. *Chem. Eur. J.* **2002,** *8*, 3646-3652.
18. Palomo, C.; Aizpurua, J. M.; Gracenea, J. J., Diastereoselective Conjugate Reduction and Enolate Trapping with Glyoxylate Imines. A Concise Approach to β-Lactams that Involves a Ternary Combination of Components. *J. Org. Chem.* **1999,** *64*, 1693-1698.
19. Paquette, L. A.; Behrens, C., A Ring-Expansion Route to Analogues of Dideoxyhydantocidin. *Heterocycles* **1997,** *46*, 31-35.
20. Ojima, I.; Park, Y. H.; Sun, C. M.; Zhao, M.; Brigaud, T., New and Efficient Routes to Norstatine and Its Analogs with High Enantiomeric Purity by β-Lactam Synthon Method. *Tetrahedron Lett.* **1992,** *33*, 5739-5742.
21. Ojima, I.; Habus, I.; Zhao, M.; Zucco, M.; Park, Y. H.; Sun, C.-M.; Brigaud, T., New and Efficient Approaches to the Semisynthesis of Taxol and Its C-13 Side Chain Analogs by Means of b-Lactam Synthon Method. *Tetrahedron* **1992,** *48*, 6985-7012.
22. Vidya, R.; Eggen, M. J.; Nair, S. K.; Georg, G. I.; Himes, R. H., Synthesis of Cryptophycins via an N-Acyl-β-lactam Macrolactonization. *J. Org. Chem.* **2003,** *68*, 9687-9693.
23. O'Boyle, N.; Carr, M.; Greene, L.; Bergin, O.; Nathwani, S.; McCabe, T.; Lloyd, D.; Zisterer, D.; Meegan, M., Synthesis and Evaluation of Azetidinone Analogues of Combretastatin A-4 as Tubulin Targeting Agents. *J. Med. Chem.* **2010,** *53*, 8569-8584.
24. Ojima, I. C., J.; Sun, L.; Borell, C. P.; Wang, T.; Miller, M. L.; Lin, S.; Geng, X.; Kuznetsova, L.; Qu, C.; Gallager, D.; Zhao, X.; Zanardi, I.; Xia, S.; Horwitz, S. B.; Mallen-St. Clair, J.; Guerriero, J. L.; Bar-Sagi, D.; Veith, J. M.; Pera, P.; Bernacki, R. J. , Design, Synthesis, and Biological Evaluation of New-Generation Taxoids. *J. Med. Chem.* **2008,** *51*, 3203-3221.
25. Ojima, I.; Habus, I.; Zhao, M.; Georg, G. I.; Jayasinghe, R., Efficient and Practical Asymmetric Synthesis of the Taxol C-13 Side Chain, N-Benzoyl-(2*R*,3*S*)-3-Phenylisoserine, and Its Analogs via Chiral 3-Hydroxy-4-aryl-β-lactams Through Chiral Ester Enolate-Imine Cyclocondensation. *J. Org. Chem.* **1991,** *56*, 1681.
26. Ojima, I.; Sun, C. M.; Zucco, M.; Park, Y. H.; Duclos, O.; Kuduk, S. D., New and Efficient Route to Taxotere by the β-Lactam Synthon Method. *Tetrahedron* **1992,** *48*, 6985-7012.
27. Lin, S.; Fang, K.; Hashimoto, M.; Nakanishi, K.; Ojima, I., Design and Synthesis of A Novel Photoaffinity Taxoid as Probe for The Study of Paclitaxel-Microtubule Interactions. *Tetrahedron Lett.* **2000,** *41*, 4287-4290.
28. Georg, G. I.; Harriman, G. C. B.; Vander Velde, D. G.; Boge, T. C.; Cheruvallath, Z. S.; Datta, A.; Hepperle, M.; Park, H.; Himes, R. H.; Jayasinghe, L., Medicinal Chemistry of Paclitaxel: Chemistry, Structure-Activity Relationships, and Conformational Analysis. In *Taxane Anticancer Agents: Basic Science and Current Status*, Georg, G. I.; Chen, T. T.; Ojima, I.; Vyas, D. M., Eds. American Chemical Society: Washington D.C., 1995; pp 217-232.

29. Ojima, I.; Slater, J. C.; Michaud, E.; Kuduk, S. D.; Bounaud, P.-Y.; Vrignaud, P.; Bissery, M. C.; Veith, J. M.; Pera, P.; J., B. R., Syntheses and Structure-Activity Relationships of the Second-Generation Antitumor Taxoids: Exceptional Activity against Drug-Resistant Cancer Cells. *J. Med. Chem.* **1996,** *39*, 3889-3896.
30. Ojima, I.; Park, Y. H.; Fenoglio, I.; Duclos, O.; Sun, C.-M.; Kuduk, S. D.; Zucco, M.; Appendino, G.; Pera, P.; Veith, J. M.; Bernacki, R. J.; Bissery, M.-C.; Combeau, C.; Vrignaud, P.; Riou, J. F.; Lavelle, F., Syntheses and Structure-Activity Relationships of New Taxoids. In *Taxane Anticancer Agents: Basic Science and Current Status, ACS Symp. Series 583*, Georg, G. I.; Chen, T. T.; Ojima, I.; Vyas, D. M., Eds. American Chemical Society: Washington, D. C., 1995; pp 262-275.
31. Staudinger, H., Zur Kenntniss der Ketene. Diphenylketen. *Justus Liebigs Ann. Chem.* **1907,** *356*, 51-123.
32. Cossio, F. P.; Arrieta, A.; Sierra, M. A., The Mechanism of the Ketene-Imine (Staudinger) Reaction in its Centennial: Still an Unsolved Problem? *Acc. Chem. Res.* **2008,** *41*, 925-936.
33. Venturini, A.; Gonzalez, J., Mechanistic Aspects of the Ketene-Imine Cycloaddition Reactions. *Mini Rev. Med. Chem.* **2006,** *3*, 185-194.
34. Dumas, S.; Hegedus, L. S., Electronic Effects on the Stereochemical Outcome of the Photochemical Reaction of Chromium Carbene Compleses with Imines to Form β-Lactams. *J. Org. Chem.* **1994,** *59*, 4967-4971.
35. Georg, G. I.; Ravikumar, V. T., Stereocontrolled ketene-imine cycloaddition reactions. In *Organic Chemistry β-lactams*, G.I., G., Ed. VCH Publishing: New York, NY, 1993; pp 295-368.
36. Brieva, R.; Crich, J. Z.; Sih, C. J., Chemoenzymic synthesis of the C-13 side chain of taxol: optically active 3-hydroxy-4-phenyl β-lactam derivatives. *J. Org. Chem.* **1993,** *58*, 1068-1075.
37. Ojima, I.; Habus, I., Asymmetric Synthesis of β-Lactams by Chiral Ester Enolate – Imine Condensation. *Tetrahedron Lett.* **1990,** *31*, 4289-4292.
38. Ojima, I.; Slater, J. C.; Kuduk, S. D.; Takeuchi, C. S.; Gimi, R. H.; Sun, C.-M.; Park, Y. H.; Pera, P.; Veith, J. M.; Bernacki, R. J., Syntheses and Structure-Activity Relationships of Taxoids Derived from 14β-Hydroxy-10-deacetylbaccatin III. *J. Med. Chem.* **1997,** *40*, 267-278.
39. Wang, T., Doctoral Dissertation. *SUNY at Stony Brook, Stony Brook* **1999**.
40. Ojima, I.; Slater, J.; Kuduk, S.; Takeuchi, C.; Gimi, R.; Sun, C.; Park, Y.; Pera, P.; Veith, J.; Bernacki, R., Syntheses and Structure-Activity Relationships of Taxoids Derived from 14-beta-Hydroxy-10-deacetylbaccatin III. *J. Med. Chem.* **1997,** *40*, 267-278.
41. Gonzalez, J.; Aurigemma, C.; Truesdale, L., Synthesis of (+)-(1S,2R)- and (-)-(1R,2S)-trans-2-phenylcyclohexanol via Sharpless Asymmetric Dihydroxylation. *Org. Synth.* **2002,** *79*.
42. Bai, X.; Eliel, E., 2. Convenient synthesis of α-heterosubstituted acyloxathianes. *J. Org. Chem.* **1992,** *57*, 5162-5166.
43. Yu, H.; Ballard, C.; Boyle, P.; Wang, B., An inexpensive carbohydrate derivative used as a chiral auxiliary in the synthesis of a-hydroxy carboxylic acids. *Tetrahedron* **2002,** *58*, 7663-7679.
44. Macrae, M.; Blake, S.; Mayer, M.; Yang, J., Nanoscale ionic diodes with tunable and switchable rectifying behavior. *J. Am. Chem. Soc.* **2010,** *132*, 1766-1767.

Chapter 2

Synthesis and Biological Evaluation of Next-Generation Taxoids

Content

§ 2.0.0 Cancer Development and Progression

Cancer is the leading cause of death in most developed countries and is the second leading cause in developing countries.[1] As life styles change in these developing countries, it is likely that the prevalence of certain cancers will also rise. One out of every four deaths in the United States can be attributed to cancer, and it has been estimated that there were 1.6 million new cancer cases and over half a million deaths from cancer in 2011 in the United States alone.[2] Because cancer originates from cells with the same genetic composition as the host and uses the same biochemical machinery, it is significantly more difficult to treat than most pathogenic infections.

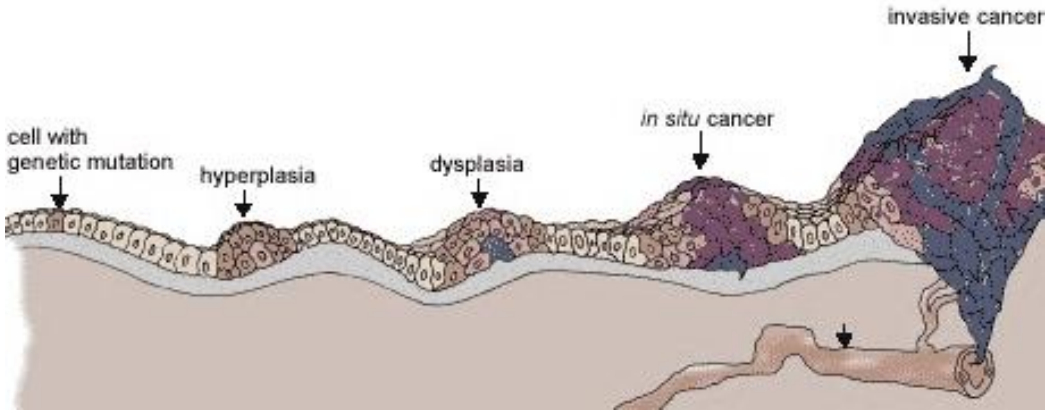

Figure 2-1: Cancer development and disease progression (adapted from [2])

Cancer begins with oncogenic mutations in a somatic cell, causing the cell to increase its rate of division and the formation of hyperplasia (**Figure 2-1**). The disease progresses to form a dysplasia, a mass with an abnormal amount of immature and dedifferentiated cells. At this stage, the disease is still confined, but if it continues to progress into a malignant mass, it will begin to break down the basement membrane and invade the surrounding tissue until it eventually becomes a systemic disease. This is an extremely simplified model of carcinogenesis and cancer progression, and there are many factors at the genetic, epigenetic and microenvironmental levels that contribute to the amazing complexity of this process.

§ 2.0.1 The Hallmarks of Cancer

In the past 5 decades, an immense body of knowledge has been discovered pertaining to the biological and chemical mechanisms that contribute to the regulation, development and progression of cancer. Although cancer describes over 200 different diseases, there are many common characteristics that can be used in defining carcinogenesis. These “hallmarks of cancer” are shown in **Figure 2-2**.[3, 4]

Inherent to the development of cancer is genomic instability and mutation. Mutations in genes result in the production of mutant proteins that may have altered catalytic activity, or different sub-cellular localization. Mutations that occur in regulatory sequences can cause to the

altered expression levels of downstream proteins. These mutations are passed from each cell to its daughter cells after mitosis, allowing these mutations to accumulate over the generations, if not corrected. As a result, the careful homeostasis within a cell may eventually be disrupted, causing systemic alterations that lead to the development of other cancer hallmarks.[3]

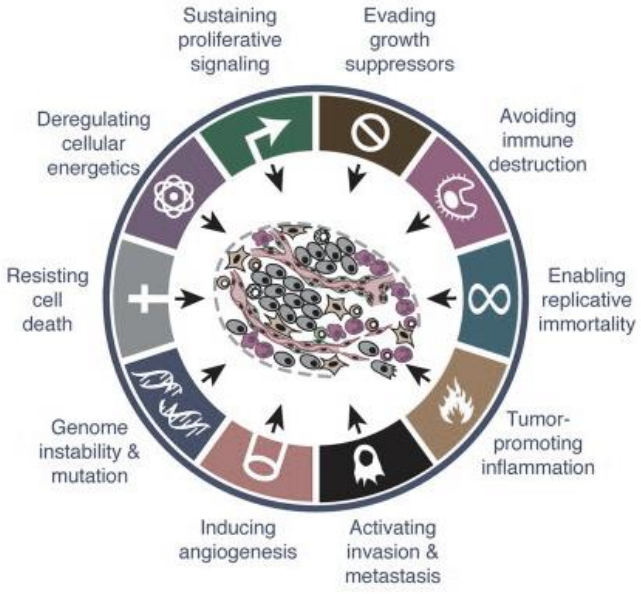

Figure 2-2: The hallmarks of cancer (adapted from [3])

The enhanced proliferation common among tumors serves not only to grow the tumor, but also to augment the rate at which somatic mutations occur, leading to further genomic instability. In healthy cells, endless replication results in the loss of telomeres and the eventual degradation of the DNA. The enzyme telomerase, which replaces these lost telomeres, is highly expressed in most cancers, contributing to the replicative immortality that is characteristic of the disease.[5] To fuel its enhanced growth, the disease develops a deregulated cellular metabolism and becomes unresponsive to host growth-suppressing hormones.[6] This disconnect from the host regulatory systems is paralleled by its ability to evade the immune system, allowing the disease to grow essentially undetected in the early stages.[7]

The growth of a tumor is inevitably contained by its inability to obtain the requisite nutrients and as a result, it can remain static for prolonged periods of time. However, once the disease acquires the ability to begin angiogenesis, the newly formed blood vessels provide the sustenance required for prolonged and sustained growth. In this way, the angiogenic switch acts as a checkpoint for solid tumors, allowing them to continue beyond their initial growth phase.[8] Eventually, the surrounding microenvironment is broken down, and the disease can invade the surrounding tissue until a sub-population of cells escapes into the blood stream or the lymphatic system in a process known as metastasis. These metastases form microscopic tumors in remote

organs and they begin the processes over again. If left untreated, most cancers inevitably lead to organ failure and death.

§ 2.0.2 Strategies of Cancer Treatment: Chemotherapy

Cancer is usually treated with a combination of surgery, radiation therapy and/or chemotherapy. Whereas surgery and radiation are both localized treatments, chemotherapy, the use of chemical and biochemical agents to control or kill the disease, is a systemic therapy capable of treating even micrometastases that would otherwise escape detection. For that reason, chemotherapy is often administered after surgical resection of the tumor mass in a process called adjuvant therapy. In other cases, the chemotherapeutic regimen is given before surgery to reduce the size of the tumor, facilitating its removal. This strategy is known as neoadjuvant therapy. As each patient and therefore affliction is unique, this practice of combined modality treatment is custom-tailored to every case in an effort to minimize toxicity and risk to the patient, while maximizing the therapeutic benefit.

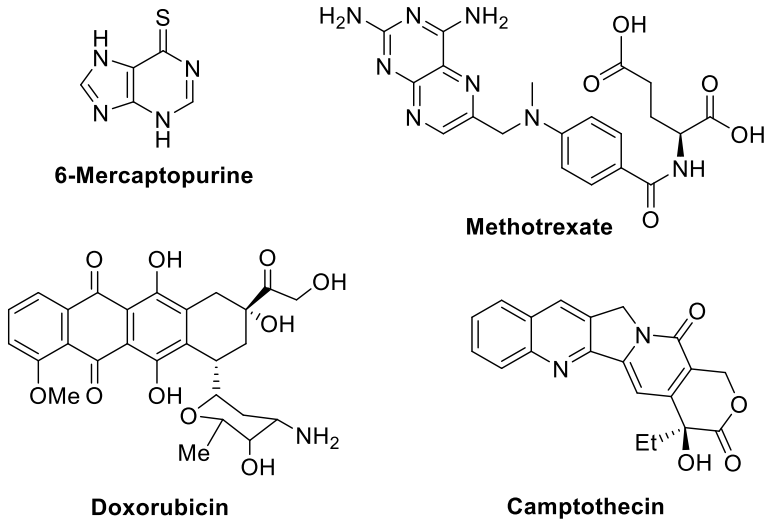

Figure 2-3: Examples of traditional chemotherapeutics

Nitrogen mustards, which were originally used as war gas, were the first chemical agents to be recognized for their antineoplastic properties, and by the early to mid 1940's, they were being used for the treatment of lymphomas.[9] These compounds are DNA alkylators, and can form crosslinks on DNA, leading to the death of the treated cells. Shortly after, in the late 1940's, it was found that the administration of folic acid enhanced the rate of leukemia growth in children. This observation led to the discovery and development of methotrexate (**Figure 2-3**), an anti-folate, as a potent anti-cancer agent.[10] By 1951, 6-mercaptopurine had been developed and chemotherapy was emerging as an important tool for the management and cure of cancer.[11]

Since these early discoveries, a vast arsenal of chemotherapeutic agents have been discovered, and most indications are treated by regimens that include a cocktail of different

chemical agents administered at different dosing schedules.[11] These 'traditional chemotherapeutics' are chemical compounds that act on biomolecular processes that are required for cell division such as DNA synthesis (anti-metabolites), DNA repair (intercalators, alkylating agents), RNA transcription (intercalators, cytotoxic antibiotics) and microtubule dynamics (taxanes, vinca alkaloids). The underlying premise of this strategy is the fact that cancerous cells divide significantly faster than most healthy tissues, so compounds that interfere with processes required for cell division should exhibit preferential toxicity to these rapidly multiplying cells. However, there are many important cells in the human body that also rapidly divide, including those in the gastrointestinal tract, hair follicles, reproductive system and bone marrow. Therefore, these cytotoxic chemotherapeutics produce severe, dose-limiting and often life-threatening side effects such as myelosuppression, neutropenia, anemia, neuropathy as well as damage to the heart, liver and kidneys.

§2.1.0 Paclitaxel and Taxanes

Paclitaxel **1**, is one of the most successful FDA-approved chemotherapeutic agents, and is currently used for the treatment of ovarian, breast, non-small-cell lung cancer (NSCLC) and Karposi's sarcoma.[12-14] It is a member of the Taxane diterpenoid family, composed of a baccatin III core structure and an N-benzoyl-phenylisoserine sidechain at C13 (**Figure 2-4**). Two other synthetic paclitaxel derivative (taxoids), docetaxel and cabazitaxel are also FDA-approved chemotherapeutics.[14]

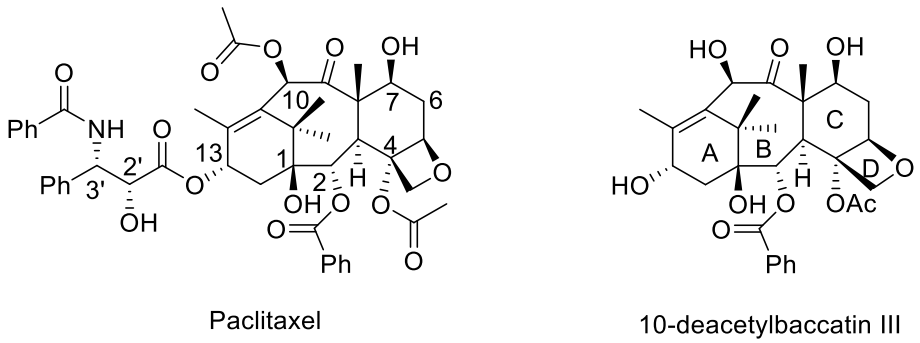

Figure 2-4: The structure of paclitaxel and 10-DAB-III

After immensely successful Phase II trials in 1988, the NCI began to look for pharmaceutical companies interested in further development of paclitaxel, as the financial requirement for clinical development was beyond the score of the Institute. Through the Cooperative Research and Development Agreement (CRADA), Bristol-Myers Squibb (BMS) was selected as the partner in 1989. In 1990, BMS filed an application to trademark the original name of the compound, taxol, as "Taxol®". This was approved in 1992 after extensive dispute in journals and courts, and the common name of taxol was changed to paclitaxel.

Paclitaxel was originally isolated from the bark of the Pacific yew (*Taxus brevifolia* Nutt), and its extraction required harvesting of the bark and the tedious extraction of the active agent. Paclitaxel entered clinical trials in 1983, resulting in an increase in demand for the bark of the slow-growing yew trees.[15, 16] The extraction process was low yielding, as 10,000 kg of bark produces only 1 kg of paclitaxel, and the trees had to be sacrificed in order to harvest the bark.[17] Therefore, extensive work was done to find alternative sources of the compound as well as synthetic and semi-synthetic approaches to its production. At this time, the semi-synthesis of paclitaxel using the Ojima-Holton coupling (Chapter 1) became a valuable method for the commercial production of this compound.[18] Currently, paclitaxel is primarily produced using a plant cell fermentation method followed by extraction from the culture.[19]

§2.1.1 Discovery and Clinical Development of Paclitaxel (Taxol®)

Paclitaxel is a diterpenoid natural product first isolated by Wall and Wani in 1966 during a screening program initiated by the National Cancer Institute (NCI) to discover potential anti-cancer compounds from plant sources.[20] It was discovered as the primary active component in extracts from the bark of the Pacific yew (*Taxus brevifolia* Nutt) that exhibited cytotoxicity towards a panel of cancer cell lines.[20] The chemical structure of paclitaxel was subsequently elucidated and published in 1971 (**Figure 2-4**).[21] It was found to demonstrate impressive efficacy *in vivo* against LX1 (lung), MX1 (breast) and CX1 (colon) carcinoma xenografts in murine tumor models.[22, 23] In 1979, Horwitz discovered its unique mechanism of action, accelerating the formation of microtubules and stabilizing them against depolymerization.[24] As all other known microtubule-binding agents at that time, such as colchicine and vinblastin, induced microtubule depolymerization, this finding spurred intense research interested in paclitaxel and helped to fuel its development to the clinic.[25]

Following these promising preclinical results, paclitaxel began Phase I clinical trials in 1983 as a Cremaphor-based formulation (Taxol®). Although Cremophor is known to cause histamine release and is associated with acute hypersensitivity reactions (HSR), the low aqueous solubility of paclitaxel left the developers with few options for formulation.[26] The clinical dosing regimen was initially a 24-hour infusion schedule to minimize HSR, but alternative schedules in combination with prophylaxis with antihistamines also proved effective. Major side-effects of paclitaxel treatment were found to be peripheral neuropathy, neutropenia and cardiac arrhythmia.[14, 27]

Taxol® was first approved for the treatment of epithelial ovarian cancer in 1992, based on the results of single-agent trials utilizing a 24-hour infusion schedule every 3 weeks. For the clinical treatment of ovarian and breast cancers, it was administered every three weeks at a dose of 175 mg/m^2 or 135–175 mg/m^2 as a 3-hour or 24-hour infusion, respectively. A phase II study revealed severe neutropenia to be the main dose-limiting side effect at higher dosing levels of 250 mg/m^2.[13] When used in combination therapy with *cis*platin, Taxol® showed appreciable efficacy in lung, ovarian and breast cancers.[28, 29] In contrast, Taxol® did not demonstrate efficacy against gastric, brain, colorectal, renal or prostate cancers.[30] Eventually, Taxol® went on to become one of

the most successful FDA-approved chemotherapeutic agents, and has been clinically effective in the treatment of ovarian, breast and non-small cell lung cancer (NSCLC), AIDS-related Karposi's sarcoma and other solid tumors.[30, 31]

§2.1.1 Mechanism of Action of Taxane Anticancer Agents

Paclitaxel binds to the β-tubulin subunit of the tubulin heterodimer,[32] altering microtubule morphology and leading to a reduced number of protofilaments in microtubules.[33] Changes in protofilament number we observed within seconds of paclitaxel incubation, even in preformed microtubules,[34] and paclitaxel exhibits a binding preference to microtubules over individual tubulin heterodimers.[35] Exposure of tubulin to paclitaxel results in enhanced rate of polymerization and hyperstabilization of the resulting microtubule.[36] This effect can commonly be observed *in vitro* as microtubule bundling and the inhibition of cell cycle progression at the G2/M phase of mitosis (**Figure 2-5**).[36]

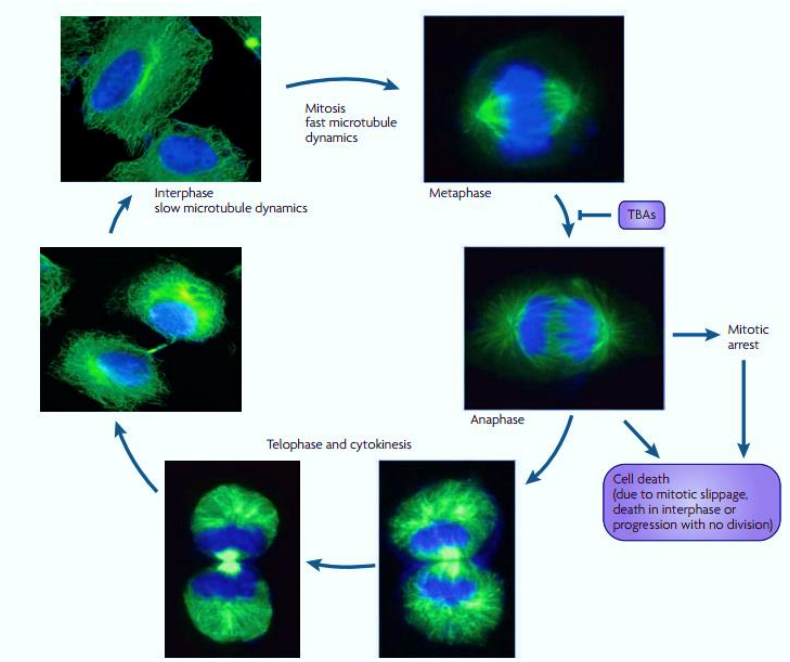

Figure 2-5: Microtubule dynamics during mitosis (adapted from [36])

At clinically relevant concentrations of 1-10 nM,[37] paclitaxel exerts its cytotoxic effects through the suppression of microtubule dynamics, a process which is especially important during the process of cell division.[38] Paclitaxel interferes with the assembly of the mitotic spindle and inhibits the ability of chromosomes to separate during mitosis.[39] This leads to mitotic arrest and has been correlated with the cytotoxicity of paclitaxel.[39] Furthermore, cells undergoing mitosis are more sensitive to the drug, which is likely why Taxol® has been successful as a chemotherapeutic agent.[40] Treatment with paclitaxel *in vitro* has been shown to destabilize the microtubule-kinetochore attachment point, causing activation of signaling pathways that delay the progression through the cell cycle.[41] Depending on the cell lines treated, paclitaxel can induce apoptosis

through caspase-independent and dependent mechanisms.[42, 43] Caspases 3, 8 and 10 are known to be frequently activated by treatment with paclitaxel.[42]

Following mitotic arrest, intracellular signaling pathways send the signal for the affected cell to enter apoptosis. Signaling pathways that have been found to be involved in apoptosis induced by paclitaxel treatment include JNK, p38 MAPK and ERK.[44, 45] However, the clinical relevance of these pathways to Taxol® treatment is still not fully understood.[46] Treatment with paclitaxel results in the hyperphosporylation of Bcl-2, and anti-apoptotic protein, an event that coincides with the initiation of apoptosis.[47, 48] Hyperphosphorylation of Bcl-2 is a found in cells treated with all microtubule-targeted drugs, but it is not found with common DNA-damaging agents.[47] Alterations in the expression and phosphorylation of Bcl-2 and related Bcl-xL proteins have been implicated in resistance to paclitaxel-induced apoptosis.[49-51] In addition, expression levels of Bcl-2 is a prognostic marker for clinical response to taxane treatment for breast cancer and hormone-refractory prostate cancer.[52, 53]

It is very likely that the kinase responsible for the phosphorylation of Bcl-2 and its subsequent degradation may be cell-type specific. Hyperphosphorylation of Bcl-2 following paclitaxel treatment may be caused by JNK,[54] Raf-1,[55] and the Ras/MEK/ERK pathway.[56] Recently, it was discovered that paclitaxel binds directly to Bcl-2, and this binding may influence its phosphorylation and degradation.[57]

§ 2.1.2 Drug Resistance to Paclitaxel

Resistance to paclitaxel is commonly associated with the multi-drug resistanant (MDR) phenotype, and many paclitaxel-resistant MDR cell lines have been identified.[58] MDR is commonly caused by the overexpression of ATP-binding cassettes, most notably P-glycoprotein (Pgp), a transmembrane glycoprotein. Pgp acts as an efflux pump and binds to and removes hydrophobic molecules from the cell.[59] The expression levels of Pgp, which is coded for by the *mdr1* gene, have demonstrated predictive value for anticipating tumor response to Taxol® treatment in NSCLC and ovarian cancer.[60, 61] Furthermore, the expression levels of different Pgp polymorphisms was shown to affect the progression-free survival in patients with ovarian cancer patients.[62] However, the clinical relevance of Pgp expression has been debated due to difficulties in quantifiying MDR in a clinical setting.[58, 63]

Other mechanisms of paclitaxel resistance are directly related to the structure or function of microtubules.[64] For examples, paclitaxel resistance has been demonstrated in ovarian and cervical cancer cell lines that contain point mutations in the paclitaxel binding pocket.[64, 65] Tubulin mutations have been correlated with poor prognosis in NCSLC tumor samples from patients undergoing Taxol®-based therapy.[66] Paclitaxel resistance has been observed in leukemia, lung carcinoma and prostate cancer cell lines that exhibit increased expression of the β-tubulin isoforms, class III and class IV tubulins.[67] Clinically, overexpression of the class III β-tubulin isoform has been shown to be predictive of poor response to paclitaxel treatment in NSCLC and ovarian cancer patients.[68, 69] Other microtubule-targeted agents are not as sensitive to β-tubulin isoform

expression as paclitaxel *in vitro*.[70] Paclitaxel resistance has also been correlated with differential expression of α-tubulin isoforms.

§ 2.2.0 Taxoid Structure-Activity Relationships

Initially, the early structure-activity relationships (SAR) studies of paclitaxel were primarily conducted in the 1980's – early 1990's in the laboratories of Kingston and Potier.[71-73] The major findings of early SAR studies are as follows:

- The baccatin scaffold itself is not sufficient to induce the stabilization of microtubules and resulting cytotoxicity.
- The C13 phenylisoserine side is necessary for biological activities, but replacement of C3'*N*-phenyl group with a *t*-Boc group is permitted.
- The free hydroxyl group at C2' is essential for biological activity.
- The A-ring is required to maintain cytotoxicity.
- The C2-benzoyl group is required for high potency.
- Removal of the C-4 acetyl group diminishes biological activity.
- The epimerization or acetylation at C7 has little effect on potency.
- Removal of the acetate at C10, or replacement with other esters is permitted
- An intact oxetane ring is essential for maximal potency.

During early work on the semisynthesis of paclitaxel, the *t*-Boc group was used to protect the amine on the phenylisoserine side chain. This key synthetic intermediate was tested for its biological activity, and it was found to exhibit higher potency than paclitaxel.[74] As a result, docetaxel (**Figure 2-7**) became the first synthetic paclitaxel analog and the term "taxoid" (i.e. taxol like compound) was introduced to describe this new class of synthetic taxanes. Docetaxel was approved by FDA in 1996, and eventually went on to become a top-selling anti-cancer drug (Taxotere®), with success equivalent to that of Taxol®.[14]

Although paclitaxel and docetaxel were found to be efficacious in controlling a variety of indications, both compounds were also ineffective against cancers originate from tissues with high expression levels of the *mdr1* gene such as colon and renal carcinoma.[75, 76] In addition, the significant hypersensitivity problem caused by the use of Chremophor as a surfactant led many to pursue compounds with greater solubility than paclitaxel. As a means to overcome these problems, hundreds of new taxoids have been synthesized, many of which possess improved solubility and were found to be highly potent against MDR cancer cells and tumors. In the course of developing this next-generation of taxoid chemotherapuetics, extensive work has been done to elucidate a detailed structure-activity relationship for the taxane skeleton, as well as the effects of substitutions at each position on potency and susceptibility to drug resistance.

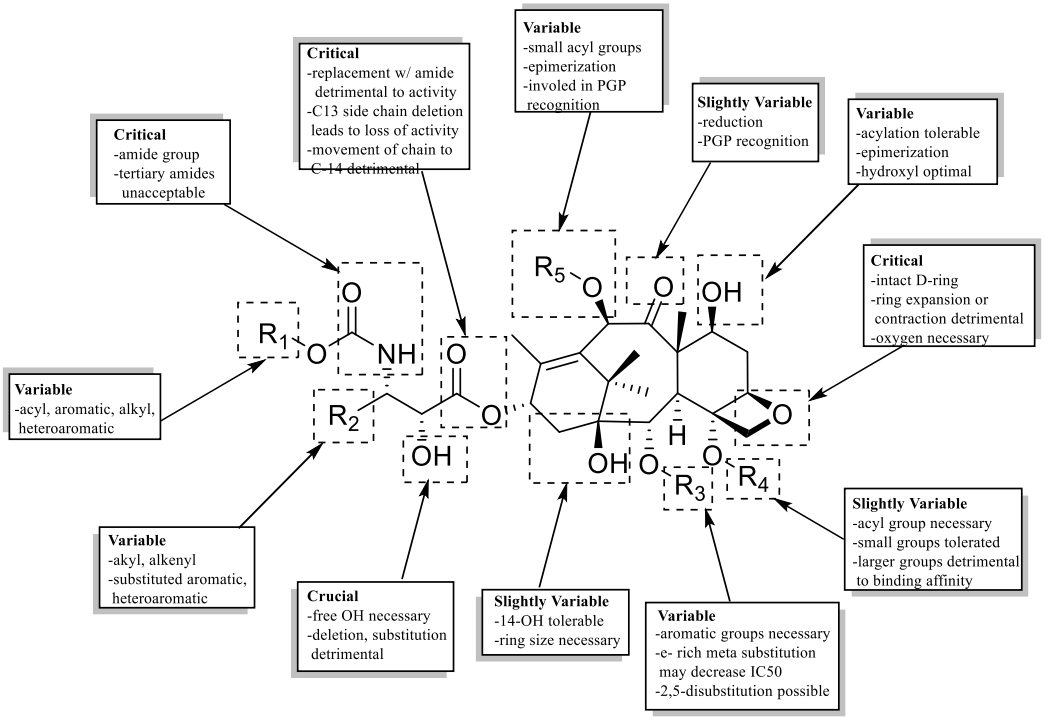

Figure 2-6 – Current Understanding of taxane SAR

In the past two decades, numerous advances in the selective chemical modification of the components of the baccatin skeleton, its substituents and the composition of the C-13 side chain have led to an extensive SAR study of the taxane family (**Figure 2-6**).

In most cases, the baccatin core of the taxoids cannot be manipulated much without significant loss in anticancer activity. Early SAR studies demonstrated the importance of an intact A ring to biological activity.[77] Although the C ring is a central component of the baccatin skeleton, novel C-seco taxoids have been synthesized that possess potent cytotoxicity towards paclitaxel-resistant cell lines.[78] Larotaxel, a clinical candidate (**Figure 2-7**), possesses a unique cyclopropane methylene bridging the C7 and C8 positions on the C ring.[79] The oxetane D ring is optimal for activity, important for maintaining the correct conformation of the taxoid skeleton and may be involved in hydrogen bonding to β-tubulin. Replacement of the oxetane oxygen atom with nitrogen, sulfur or selenium, exhibited markedly reduced activity, while replacement of the D ring with a cyclopropane resulted in only a two-fold reduction of activity.[80-82] As a result of these optimization studies, six semi-synthetic taxoids are currently undergoing clinical evaluation.

The C13 side chain provides a good handle for variation at the 3' position in both its direct (**Figure 2-6** - R_1) and the N-acyl (**Figure 2-6** - R_2) substituent, resulting in improved potency and reduced Pgp recognition.[83, 84] The amide bond has been shown to be optimal in this position, and both primary and secondary R1 substituents have been shown to be detrimental to activity, whereas tertiary and aromatic groups at this position tend to improve efficacy. At the other variable region (R_2), larger alkyl, alkenyl and aromatic groups were found to be tolerable and tunable for optimization, while replacement with smaller alkyl substitutents, such as methyl, resulted in

diminished activity.[85-88] For example, ortataxel **(Figure 2-7**), a clinical candidate derived from 14β-hydoxybaccatin possesses an isobutyl group at C3' and is active in MDR cell lines.[89] The chirality at 2' and 3' positions have been shown to be necessary for full activity of these compounds, and furthermore, the 2' free hydroxyl moiety is needed for target binding, and deletion or acylation at this position has been shown to significantly hinder the *in vitro* efficacy of these compounds. The ester functionality at C13 has been shown to be optimal, and replacement for an amide bond leads to almost complete loss of activity.

The northern half of the baccatin scaffold has been shown to be quite variable without causing as serious loss the binding energy. Small acyl groups at the C-10 position are optimal, and because this position is involved in recognition by the PGP efflux pump, alterations in this position can seriously alter the efficacy of the compound against MDR cell lines.[84, 90, 91] The carbonyl at C9 can be reduced to an alcohol without significant loss of activity.[92] A series of highly active 9-β-dihydro-9,10-diacetyl taxoids have been developed from 9-dihydrobaccatin, leading to the development of the clinical candidate tesetaxel (**Figure 2-7**).[93] The C7 position is also amenable to alterations, including acylation and alkylation.[94] Alkylation and acetylation at C7 can be found in the FDA-approved cabazitaxel and the clinical candidate milataxel.(**Figure 2**-7)

The southern half is slightly variable, and although substitutents at the C2 and C4 positions can be changed, the basic substitution pattern of aromatic acylation at C2 and small group acylation at C4 is optimal for biological activity. Benzoyl groups at C2 bearing methoxy, azido and halogen groups in the *meta* position have been shown to greatly increase the binding affinity of the taxane to β-tubulin.[84] The C4 can be changed to small acyl groups such as trifluoroacetyl and propionyl, but substitution with larger groups, such as aromatics, result in dimished activity. However, no compounds to date have been advanced to clinical trials with alterations at the C2 or C4 positions.

§ 2.2.1 Taxoids under Clinical Development

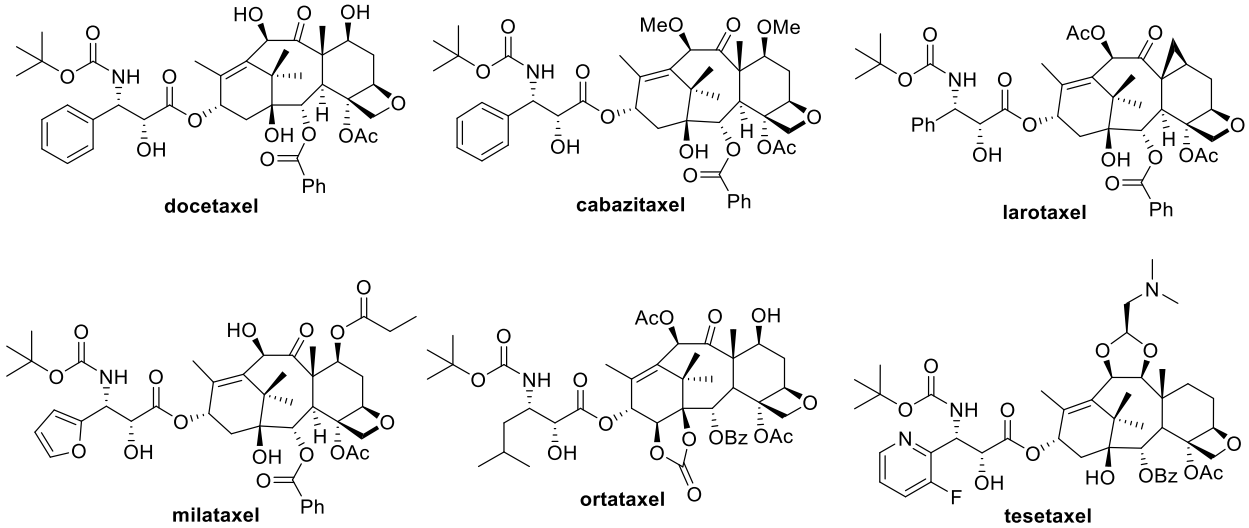

Figure 2-7: Taxoids under clinical development

Currently, there are two semi-synthetic taxoids on the market: docetaxel and cabazitaxel, which are active against a number of solid tumors. Docetaxel was first approved in 1996 for the treatment of metatastatic breast cancer resistant to treatment with anthracyclines.[95] Since then, it has been approved for locally advanced breast cancer,[96] advanced gastric cancer,[97] locally advanced or metastatic NSCLC,[98] hormone-refractory prostate cancer[99] and locally advanced head and neck cancer.[100] In most cases, docetaxel is administered as part of a combination therapy with other cytotoxic agents, although the drug has been approved as a single agent second-line therapy for locally advanced and metastatic breast cancer and advanced NSCLC.[101] For the treatment of squamous cell carcinoma of the head and neck, docetaxel is combined with cisplatin and 5-FU, a combination that is also administered to patients with unresectable gastric carcinoma. Docetaxel is used in combination with prednisone as a second line treatment of hormone-refractory prostate cancer.[102] The combination of docetaxel with doxorubicin-cyclophosphamide (TAC) is used as an adjuvant therapy in node-positive breast cancer. Docetaxel has been approved in combination with cisplatin as a frontline therapy for advanced and metastatic NSCLC. Cabazitaxel, the second semi-synthetic taxane to pass phase III evaluation, was approved by the FDA in combination with prednisone as a second-line treatment of hormone-refractory prostate cancer resistant to treatment with docetaxel.[103] Both docetaxel and cabazitaxel are still currently under active clinical evaluation as single agents and in combination studies for numerous incidations.

Other taxoids are currently undergoing clinical evaluation including Larotaxel, Mirataxel, Ortataxel and Tesetaxel. Larotaxel is under clinical evaluation as a single agent or in combination therapy for urethral blatter cancer, advanced pancreatic cancer, advanced NSCLC and metastatic breast cancer.[104-107] Ortataxel is currently under phase II evaluation for taxane-refractory NSCLC and metastatic breast cancer.[108] After failing to demonstrate improved efficacy in a phase II evaluation in metastatic colorectal cancer, Tesetaxel has recently completed phase I and phase I/II trials in solid tumors.[109-111] Milataxel failed to demonstrate efficacy in a phase II study for advanced previously-treated colorectal cancer, but proved to be effective in a separate study in patients with platinum-refractory NSCLC.[112]

§ 2.2.2 Next-Generation Taxoids

SAR studies on the C3'N and C3' positions with non-aromatic substituents led to the development of "second generation" taxoids **(Figure 2-8).** Second generation taxoids bearing a *t*-Boc group at C3'N, an isobutenyl or isobutyl group at C3', and small acyl, carbamoyl or alkoxycarbonyl groups at C10 exhibited increased potency of 1-2 orders of magnitude compared to that of paclitaxel against drug-sensitive and drug-resistant (MDR) cancer cell lines, respectively.[84, 113] Taxoids bear meta-substitution on the C2-benzoate moiety were found to have up to 3 orders of magnitude higher potency than paclitaxel or docetaxel against a panel of drug-resistant cell lines.[84, 114] The "resistance factor" (R/S), defined as [IC_{50} for drug-resistant cell line (R)] / [IC_{50} for drug-sensitive cell line (S)], was developed as an indicator for the susceptibility of a compound to MDR. Some C2-modified next-generation taxoids, such as SB-T-121303 (**2-10, g**), possess a resistance factor of 1 or less than 1, indicating that they are completely immune to Pgp-

mediated efflux.[84] These highly potent next-generation taxoids, with little or no susceptibility to MDR, have been defined as the "third generation" taxoids.

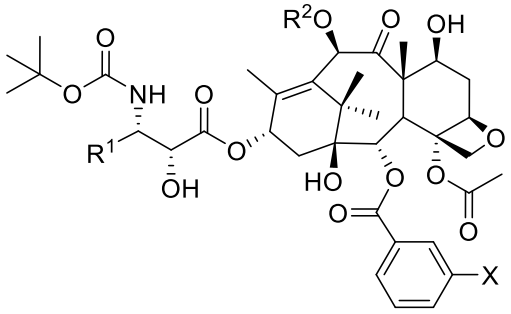

R^1= Me_2C=CH-, R^2 = EtO, X = H (SB-T-1213)
R^1= Me_2C=CH-, R^2 = *c*-PrCO, X = H (SB-T-1214)
R^1= Me_2C=CH-, R^2 = Me_2NCO, X = H (SB-T-1216)
R^1= Me_2C=CH-, R^2 = MeOCO, X = H (SB-T-1217)
R^1= Me_2C=CH-, R^2 = EtO, X = OMe (SB-T-121303)
R^1= Me_2CHCH_2-, R^2 = EtO, X = H (SB-T-1103)
R^1= Me_2CHCH_2-, R^2 = EtO, X = OMe (SB-T-11033)

Figure 2-8: Selected examples of new generation taxoids

A typical second generation taxoid, SB-T-1213 (**Figure 2-8**), was found to bind to Pgp, inhibiting its function as an efflux pump.[115] Next-generation taxoids were also found to accelerate tubulin polymerization much faster than paclitaxel or docetaxel, strongly stabilizing the resulting microtubules.[84] Three next-generation taxoids, SB-T-1214, SB-T-121303 and SB-T-11033, exhibited 2 orders of magnitude higher potency than paclitaxel against paclitaxel-resistant ovarian cancer cell lines, 1A9PTX10 and IA9PTX22 that have point mutations in the paclitaxel binding site in β-tubulin.[84] These data indicate that these next-generation taxoids can bind tightly to β–tubulin in spite of the presence of point mutations that disrupt paclitaxel binding.

Next-generation taxoid SB-T-1214 demonstrated promising efficacy *in vivo* against human tumor xenografts in mice.[84] In a CFPAC-1 pancreatic tumor xenograft, treatment with SB-T-1214 (q3d x3; 60 mg/kg total dose) caused complete tumor eradication with no trace of cancer cells by histopathological analysis 8 weeks post-treatment. In a MDR colon cancer DLD-1 xenograft, treatment with SB-T-1214 (q3d x3; 60 mg/kg total dose) achieved total regression with no detectable tumor tissue for more than 150 days, while paclitaxel at its optimal dose (q3d x3; 60 mg/kg total dose) was found to be totally ineffective.[84]

§ 2.3.0 Synthesis of Next-Generation Taxoids

To facilitate the work of ongoing collaborations and to expand upon the current SAR study of next-generation taxoids, a small library of 15 taxoids was synthesized according to known literature procedure. The focus of the study was on the relationship between different combinations of taxoids with modifications at the C10 and C2 position. To compare with previously synthesized compounds, the C10 was acylated with propanoyl, cyclobutane carbonyl and *N,N*-dimethylcarbamyl groups. The C2 benzoate was substituted with methyl and methoxy groups at the meta position as well as 2,5-disubstituted rings for comparison.

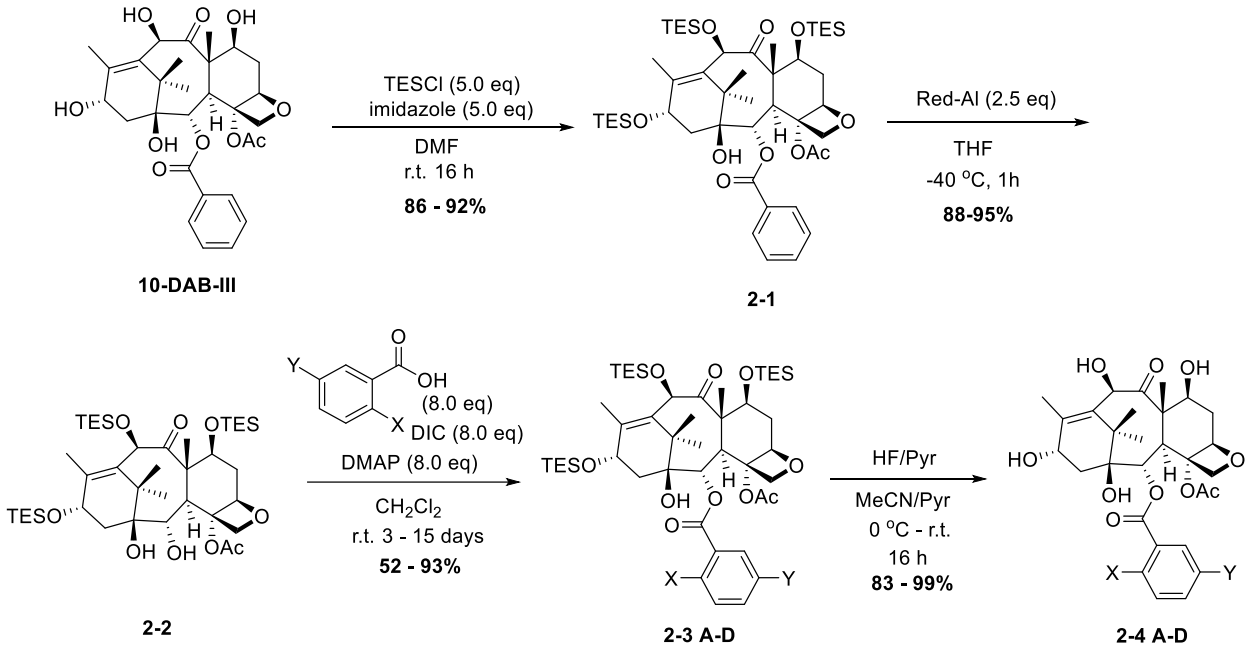

Scheme 2-1: Modification of the C2 position

The synthesis of C2-modified baccatins (**Scheme 2-1**) commenced with exhaustive TES protection. Due to the sterically encumbered position of the C1 hydroxyl, this position cannot be protected with a large silyl group. The free C1 hydroxyl group allows selective cleavage of the C2 benzoate *via* treatment with Red-Al (sodium bis-(methoxyethoxy) aluminum hydride). This reaction is quite selective, as the free C1 OH can coordinate to the reducing agent, allowing specific hydride delivery to the C2 ester affording compound 2-2 in good yield. DIC coupling to attach the desired modified benzoyl group was followed by silyl deprotection to afford the desired C2-modified baccatins (**2-4 (A-D)**).

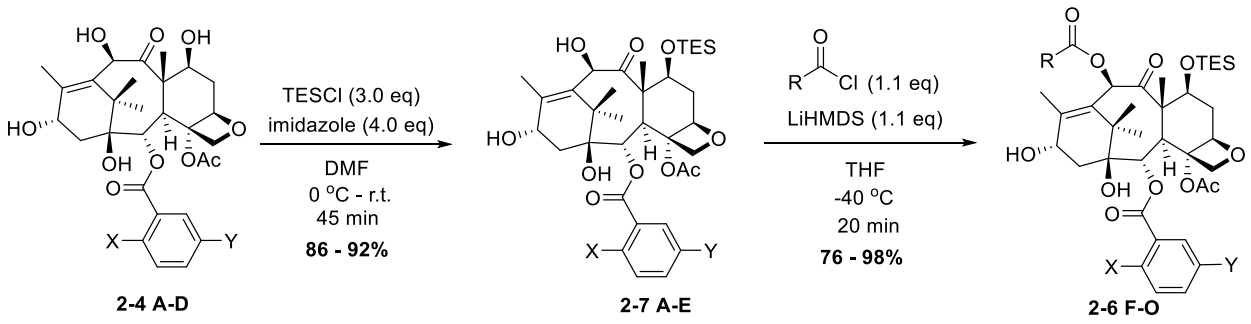

Scheme 2-2: Modification of C10 *via* alkoxide acylation

Modification of the C10 position was performed using two methods. In the first method, the C7 position was protected with TES and subsequent treatment of the mono-protected baccatin with LiHMDS and the appropriate acyl chloride afforded the desired C10 acylated intermediate

(**Scheme 2-2**). This was used to produce taxoids with cyclopropanecarbonyl, *N*,*N*-dimethylcarbamoyl and *p*-methoxyphenylacetyl groups at C10.

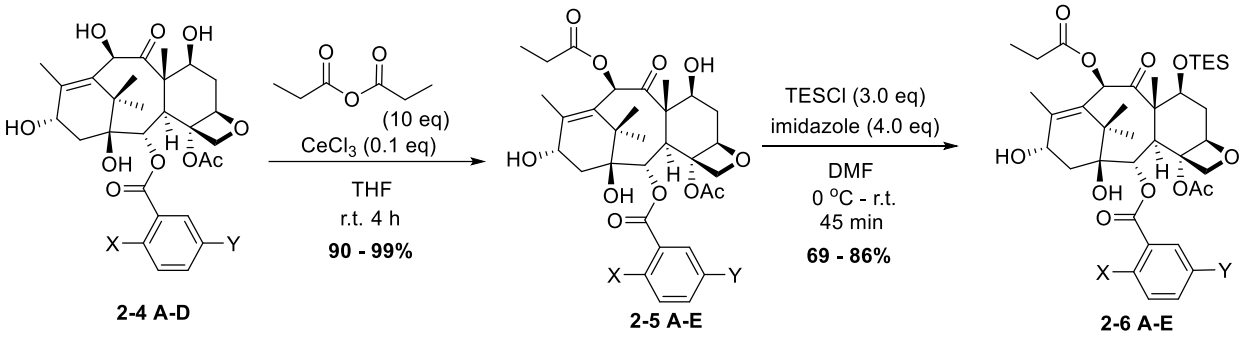

Scheme 2-3: Modification of C10 *via* $CeCl_3$ catalyzed acylation

Alternatively, direct acylation of the C10 hydroxyl was achieved utilizing a site-selective cerium (III)-catalyzed reaction between the appropriate baccatin **2-4** and propionic anhydride (**Scheme 2-3**). Subsequent protection of the C7 position was then performed using TESCl to afford the 7-TES-10-propanyl baccatin intermediate.

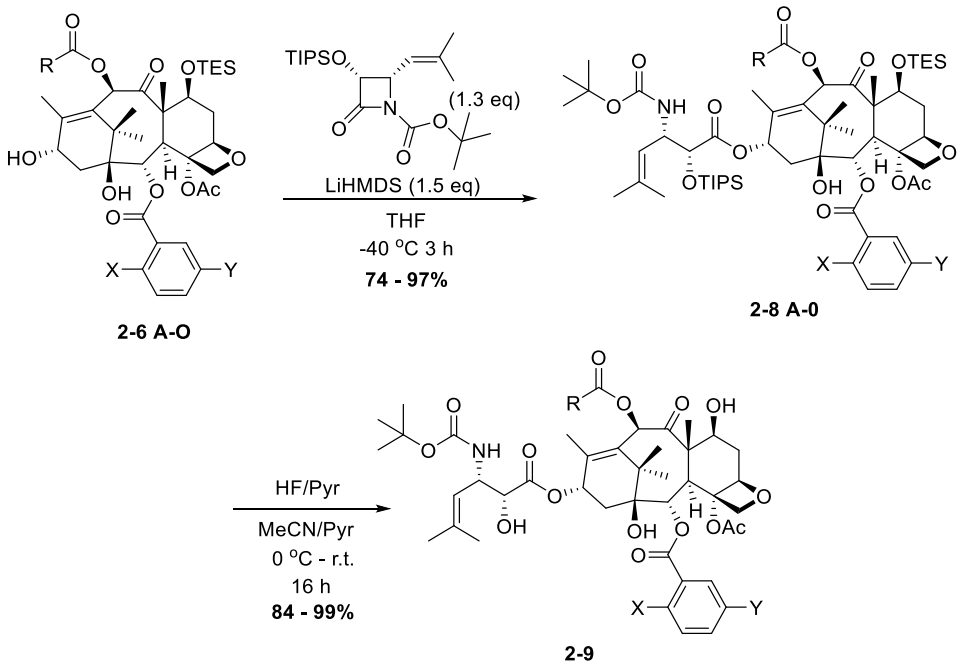

Scheme 2-4: Ojima-Holton coupling and deprotection

Attachment of the C13 side chain was performed via the Ojima-Holton coupling with β-lactam **1-6** and was followed by silyl deprotection affored the next-generation taxoids **(Table 2-1)** in moderate to good yields. The structures of the 16 taxoids produced utilizing this methodology is given in **Table 2-1**. The taxoids prepared on a ~100-300 mg scale and were purified to >97% (as measured by HPLC) by column chromatography and recrystalization. Selected samples of

taxoids were sent to the following collaborators: Dr. Agnieszka Bialkowska (Department of Medicine, SBU), Dr. Alfred Zippelius (Universitat Basel, Switzerland), Dr. Emily Chen (Department of Medicine, SBU), Dr. Galina Botchkina (Department of Chemistry, SBU), Dr. Ivan Gut (NIPH, Czech Republic), Dr. Howard Crawford (Department of Medicine, SBU), Dr. Rainer Jordan (Technische Universität Dresden, Germany). These studies are currently ongoing, and the material that has been produced will provide the basis for continued collaboration.

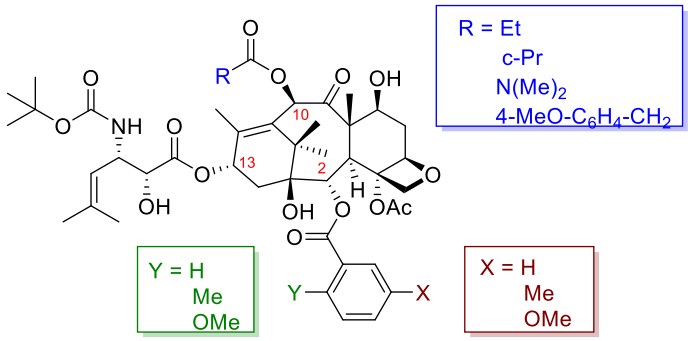

Compound	R	X	Y
1213	Et	H	H
1214	*c*-Pr	H	H
1216	$N(Me)_2$	H	H
121302	Et	H	Me
121402	*c*-Pr	H	Me
121602	$N(Me)_2$	H	Me
121303	Et	H	OMe
121403	*c*-Pr	H	OMe
121603	$N(Me)_2$	H	OMe
121312	Et	Me	Me
121612	$N(Me)_2$	Me	Me
121313	Et	OMe	OMe
121413	*c*-Pr	OMe	OMe
121613	$N(Me)_2$	OMe	OMe
12130301	4-OMe-Bn	H	OMe

Table 2-1: Structures of synthesized next-generation taxoids

§ 2.3.1 Preliminary Biological Evaluation of Taxoid "Mini-Library"

Preliminary screening of selected taxoids was done by Dr. Edison Zuniga, utilizing the standard MTT cytotoxicity assay. Selected results are given in **Table 2-2**. The compounds were screened against a panel of seven different cancer cell lines. As seen in **Table 2-2**, **SB-T-1214**, a known next-generation taxoid and our current lead compound exhibited consistently high potency, with IC_{50} values in the sub-nanomolar range.

Taxane	CFPac-1 (pancreatic cancer)	Panc-1 (pancreatic cancer)	HT-29 (colon cancer)	DLD-1 (colon cancer)
Paclitaxel	**68.0 ± 22.9**	**1.97 ± 0.76**	**11.6 ± 3.57**	**29.5 ± 10.8**
SB-T-1213	4.58 ± 2.58	1.11 ± 0.52	0.37 ± 0.22	0.39 ± 0.24
SB-T-121312	3.09 ± 1.39	49.8 ± 10.2	52.9 ± 19.1	-
SB-T-121313	**0.025 ± 0.001**	**0.56 ± 0.39**	**3.60 ± 1.35**	**13.2 ± 0.64**
SB-T-1214	**0.38 ± 0.14**	**0.35 ± 0.14**	**0.73 ± 0.30**	**0.38 ± 0.21**
SB-T-121402	3.36 ± 0.10	0.27 ± 0.14	2.11 ± 0.94	1.19 ± 0.12
SB-T-121403	1.79 ± 0.59	0.34 ± 0.14	19.0 ± 3.00	14.3 ± 4.86
SB-T-121413	1.88 ± 0.14	0.31 ± 0.14	45.5 ± 7.26	-
SB-T-1216	0.66 ± 0.46	3.29 ± 2.12	0.052 ± 0.012	0.54 ± 0.19
SB-T-121602	**0.31 ± 0.10**	**2.82 ± 1.58**	**0.003 ± 0.002**	**0.046 ± 0.011**
SB-T-121603	3.74 ± 1.21	3.70 ± 0.83	0.003 ± 0.002	4.50 ± 1.32
SB-T-121613	58.1 ± 20.0	-	34.1 ± 10.1	-

Table 2-2: Cytotoxicity of next-generation taxoids (pancreatic and colon cancer cells)

Taxane	A2780 (ovarian cancer)	ID8 (ovarian cancer)	MCF-7 (breast cancer)
Paclitaxel	**16.2 ± 8.28**	**14.5 ± 5.88**	**6.25 ± 0.76**
SB-T-1213	0.041 ± 0.020	8.92 ± 1.61	0.20 ± 0.11
SB-T-121312	8.97 ± 3.44	82.8 ± 14.6	37.7 ± 2.06
SB-T-121313	**1.46 ± 0.32**	**0.016 ± 0.003**	**0.30 ± 0.01**
SB-T-1214	**0.36 ± 0.03**	**2.51 ± 1.24**	**0.35 ± 0.11**
SB-T-121402	0.40 ± 0.01	0.53 ± 0.01	0.54 ± 0.25
SB-T-121403	0.41 ± 0.03	0.071 ± 0.01	6.05 ± 0.78
SB-T-121413	0.14 ± 0.03	0.66 ± 0.24	3.76 ± 2.81
SB-T-1216	0.96 ± 0.46	5.49 ± 2.51	0.34 ± 0.20
SB-T-121602	**0.29 ± 0.17**	**3.79 ± 2.10**	**0.08 ± 0.05**
SB-T-121603	0.25 ± 0.11	4.02 ± 2.71	0.18 ± 0.09
SB-T-121613	39.6 ± 7.38	40.6 ± 24.3	3.29 ± 1.47

Table 2-3: Cytotoxicity of next-generation taxoids (ovarian and breast cancer cells)

Two other novel standout compounds from this library were **SB-T-121313** and **SB-T-121602**. Interestingly, **SB-T-121313** was found to be significantly more potent against the pancreatic cancer cell lines tested than the two colon cancer cell lines. On the other hand, **SB-T-121602** appeared to be extremely potent against colon cancer cells, while still retaining reasonable toxicity towards pancreatic cancer. Taxoids with the dimethyl benzoyl substituent at C2 (exemplified by **SB-T-121312**) had modest activity against most cell lines tested whereas the dimethoxy analogues retained potency, and observation consistent with the known literature. Additional results are given in **Table 2-3**.

Based on the results outlined in **Tables 2-2 and 2-3**, **SB-T-121602** (**Figure 2-9**) was chosen for resynthesis on a larger scale. The picomolar IC_{50} of this compound against breast and colon cancer cell lines makes it a good candidate for use in tumor-targeting drug conjugates.

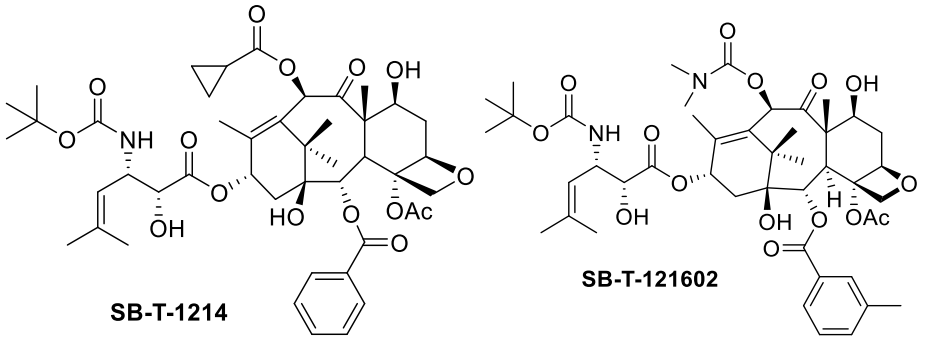

Figure 2-9: Highly potent next-generation taxoids **SB-T-1214** and **SB-T-121602**

SB-T-121602 was therefore resynthesized, following the procedures outlined in **Schemes 8 and 9** on a >300 mg scale for conjugate synthesis and further biological evaluation. In addition, **SB-T-1214** was synthesized in multi-gram batches for use in conjugate synthesis.

§ 2.3.2 POx Formulation Studies

Poly(2-oxazoline) (POx) block copolymers (**Figure 2-10**) have been demonstrated to be efficient solubilizing agents for drugs with poor aqueous solubility such as paclitaxel, cyclosporin A and amphotericin B1. The best results achieved for paclitaxel utilized a triblock copolymer with a butyl-2-oxazoline core. At 45 wt% paclitaxel (nearly 1 to 1 mixture of drug and polymer) full activity of the drug was maintained and its solubility was greatly enhanced. Therefore, 7 selected next-generation taxoids (**Figure 2-10**) were used to investigate if these advanced cancer agents could be solubilized, without the changes in chemical structure altering the loading capacity (LC) of the drug. This work was conducted by Anita Schultz in Dr. Rainer Jordan's lab.

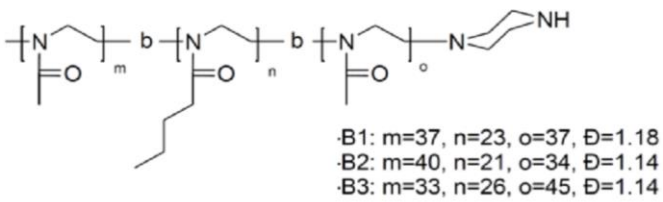

Figure 2-10: Structure of the POx block copolymers

All samples were found to readily dissolve in ethanol allowing stock solutions of 20 g/l, except SB-T-1216, which needed to be diluted down to 10 g/L. In general it is best to use a minimal amount of ethanol to enhance the formation of the polymer-drug films.

Drug ID	5 g/L			10g/L		
	DC* (g/L)	LE [%]	LC [%wt]	DC* (g/L)	LE [%]	LC [%wt]
SB-T-1213	4.9±0.1	98	33	8.4±0.4	84	46
SB-T-1214	4.2±0.2	84	30	8.6±0.3	86	46
SB-T-1216	4.8±0.1	96	32	8.2±1.0	82	45
SB-T-121302	4.3±0.1	86	30	8.6±0.2	86	46
SB-T-121303	4.2±0.3	84	30	7.3±0.4	73	42
SB-T-121402	4.5±0.1	90	31	7.5±0.6	75	43
SB-T-121602	4.1±0.3	82	29	9.0±0.2	90	47
Docetaxel	4.5±0.3	88	31	9.0±0.3	90	47

DC: Drug Concentration, **LE**: Loading Efficiency, **LC**: Loading Capacity

Table 2-5: Solubility of taxoids at lower concentrations

All samples were found to be well solubilized at starting concentration of 5 g/L (**Table 2-5**). At increased concentrations of up to 10 g/L, similar loading capacities to those for paclitaxel and docetaxel were obtained.

Drug ID	12 g/L			15 g/L		
	DC* (g/L)	LE [%]	LC [%wt]	DC* (g/L)	LE [%]	LC [%wt]
SB-T-1213	8.2±0.4	68	45	8.3±1.0	55	45
SB-T-1214	9.2±0.7	77	48	9.1±0.9	61	48
SB-T-1216	8.3±0.6	69	45			
SB-T-121302	8.9±0.9	74	47			
SB-T-121303	10.4±1.0	87	51	5.6±0.7	37	36
SB-T-121402	9.9±0.5	83	50	9.2±0.4	61	48
SB-T-121602	9.2±1.0	77	48	9.6±0.2	64	49
Docetaxel	9.8±0.2	82	49	3.1±3.2	21	24

DC: Drug Concentration, **LE**: Loading Efficiency, **LC**: Loading Capacity

Table 2-6: Solubility of taxoids at higher concentrations

As shown in **Table 2-6**, loading capacities could be even further increased close to 50 wt% when the taxoid was used in higher amounts (12 g/L). However, in spite of this slightly increased LC, there is a considerable drop in loading efficiency most samples at 12g/L. Only SB-T-121303

and SB-T-121402 display an increase of both LC and LE when the drug concentration was increased from 10 g/L to 12 g/L (**Table 2-6**). Considering that both are only moderately solubilized at 10 g/L in comparison to the other samples, this observation seems reasonable. The maximum of LC appears to be reached at just under 50 %wt. When increasing the starting drug concentration even higher (15 g/L), drug uptake appears to plateu, except in the case of SB-T-121303 and docetaxel, where such high starting concentration seems to impede solubility in the polymer.

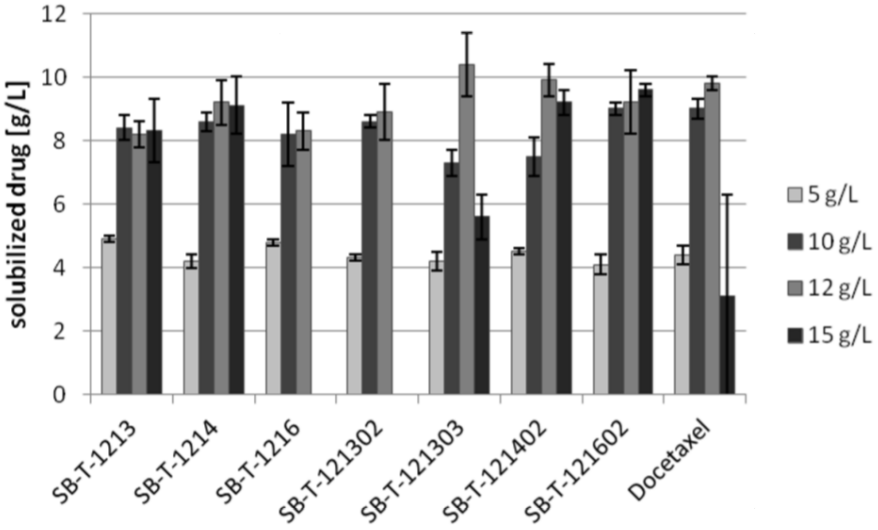

Figure 2-11: Loading capacity of taxoids in POx copolymers

These results are summarized in **Figure 2-11**. All taxoids were able to be solubilized up to very high concentrations. The substituents at C3' and C2 do not seem to influence the peak solubility capacity of the poly(2-oxazoline) triblock copolymer. However, interesting results were obtained with the *meta*-methoxy compound **SB-T-121303**, demonstrating a unique solublity profile. In general, the maximum loading capacity was found to be reached at 50 wt%.

To assess the *in vivo* efficacy of the POx-copolymer solubilized taxoid, 400 mg of **SB-T-1214** was sent to UNC Chapel Hill for evaluation in human tumor xenograft mouse models.

§ 2.4.0 Difluorovinyl Taxoids

The incorporation of fluorine into compounds of medicinal interest offers numerous advantages. The high electronegativity of fluorine can polarize bonds allowing the formation of unique electrostatic topologies that are able to facilitate ligand binding. Additionally, the strength of the C-F bond prevents oxidative metabolism and can therefore greatly alter the pharmacokinetics of a compound.

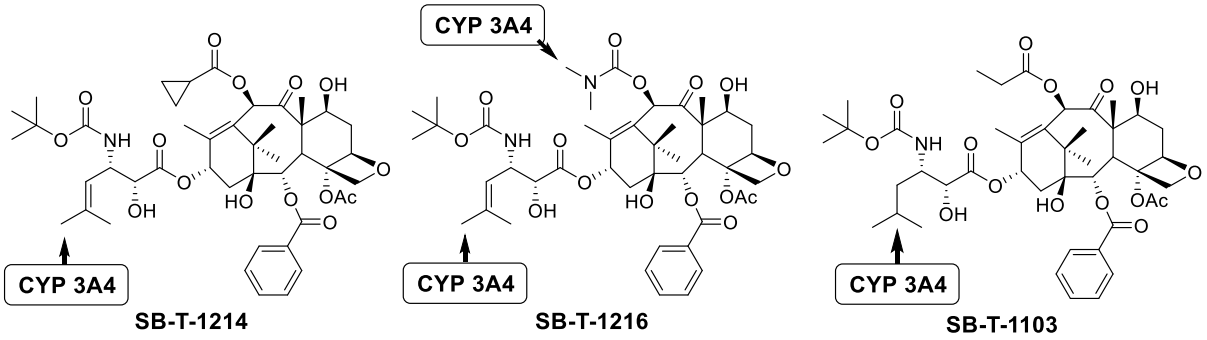

Figure 2-12: Metabolic hydroxylation of next-generation taxoids[116]

Metabolic studies on the next generation taxoids revealed interesting patterns of CYP 3A4 hydroxylation. Whereas the primary metabolic sites for docetaxel reside on the *t*-butoxy group at the C3'N position, next-generation taxoids are hydoxylated at the positions illustrated in Figure 2-14. For those taxoids possessing an isobutenyl C3' substitution, hydroxylation occurs predominantly at the primary allylic position of the side chain.[116] In order to block this particular metabolic pathway, difluorovinyl taxoids were prepared.

§ 2.4.1 Synthesis of Difluorovinyl β-lactam (2-13)

In order to prepare the desired difluorovinyl taxoid **SB-T-12854**, the corresponding difluorovinyl β-lactam must be synthesized. The synthesis of this compound starting from intermediate **(+) 1-4** is shown in **Scheme 2-5**.

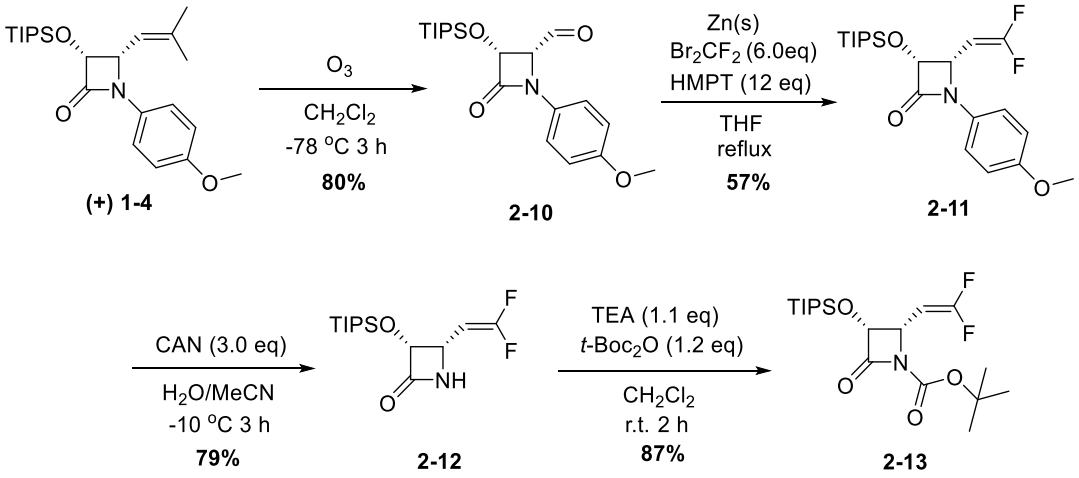

Scheme 2-5: Synthesis of difluorovinyl β-lactam **2-13**

Cleavage of the double bond via ozonolysis proceeded in modest yield, and purification was performed on alumina gel to prevent degradation of the product. The difluorovinyl group was installed via a Wittig-type reaction between aldehyde **2-10** and CBr_2F_2, producing the desired difluorovinyl β-lactam **2-11**. CAN deprotection followed by *t*-Boc protection afforded **2-13** in good yield.

§ 2.4.2 Synthesis of SB-T-12854

The difluorovinyl taxoid **SB-T-12854** was synthesized due to its efficacy in previous cell-based assays. Due to it extremely high potency, investigations of **SB-T-12854** as both a single agent as well as incorporated into novel drug delivery platforms was warranted. Therefore, it was synthesized according the route laid out in **Scheme 2-6**. TES protection followed by acylation with *N*,*N*-dimethylcarbamoyl chloride proceeded smoothly to provide intermediate **2-8 K**. Ojima-Holton coupling with β-lactam **2-13** and subsequent deprotection afforded **SB-T-12854** on a ~200 mg scale.

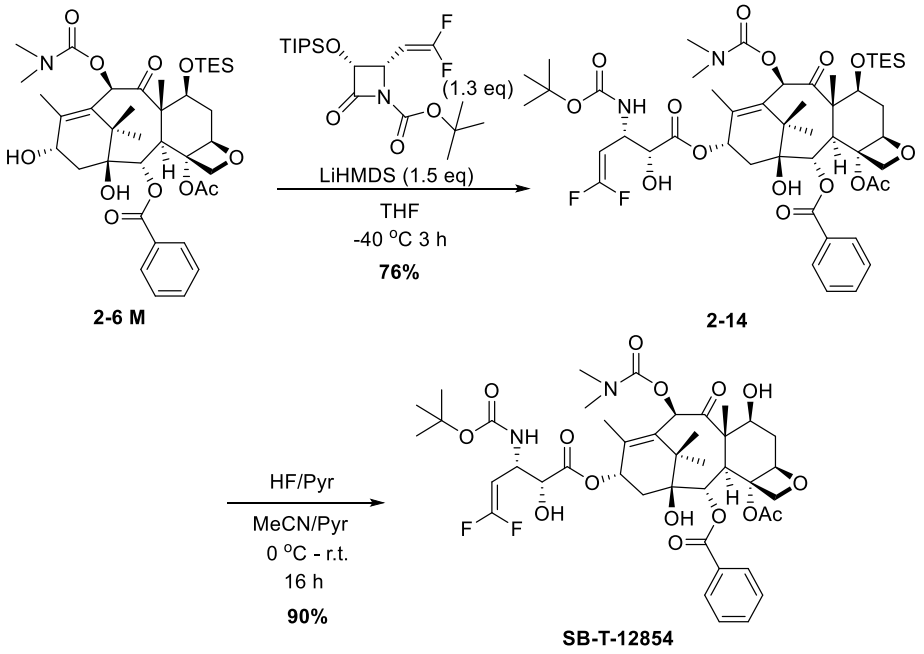

Scheme 2-6: Synthesis of **SB-T-12854**

This material was used for biological testing by our collaborators, as well as the synthesis of Polyunsaturated Fatty Acid (PUFA) drug conjugates (Section 3.1.2).

§ 2.4.3 Biological Evaluation of Taxoids in CSC-Enriched Populations

Recently, SB-T-1214 was shown to possess outstanding activity against highly drug-resistant cancer stem cell (CSC)-derived tumor spheroids.[117] The surviving cells exhibited compromised clonogenic capacity and significantly impaired ability to generate secondary spheroids. In addition, colon CSC treated with SB-T-1214 showed down-regulation of stem cell-related genes.[117] As CSCs are believed to be responsible for tumor reoccurrence and metastasis,[118] the ability of next generation taxoids such as SB-T-1214 to critically damage CSC populations *in vitro* and *in vivo* strongly supports the use of these compounds as efficacious anticancer agents. To assess the potency of selected next-generation taxoids against CSC-enriched cell populations, they were compared to standard chemotherapeutic agents in an *in vitro* MTT assay by Dr. Edison Zuniga. The results of this screen are shown in **Table 2-7**.

Anticancer agent	IC_{50} (nM)
cisplatin	4,540±276
doxorubicin	78.0±28.2
methotrexate	32.7±11.2
paclitaxel	33.8±3.33
topotecan	451±12
SB-T-1214	0.28±0.10
SB-T-121602	0.24±0.13
SB-T-12854	0.14±0.05

Table 2-7: IC_{50} values of taxanes and chemotheraputics against CSC-enriched populations

Next-generation taxoids clearly retain their high potency when tested against this CSC-enriched cell population. These next-generation taxoids are two orders of magnitude more active than paclitaxel, methotrexate and doxorubicin, which are some of the most potent clinically used anti-cancer agents. These results are encouraging and support the further development of these taxoid anti-cancer agents.

§ 2.5.0 Conclusions and Perspective

The taxane family of compounds possess some of the most potent cytotoxic agents known to man, and have produced 3 FDA-approved chemotherapeutics. Next generation taxoids have demonstrated superior potency in MDR cancer cell lines *in vitro* and improved efficacy in human cancer xenografts *in vivo*. These agents have also demonstrated activity against CSC-enriched cell populations and have been shown to cause a downregulation of stemness genes. Therefore, next generation taxoids warrant further research and development. A small library of taxoids was synthesized to study the effect of modifications at the C2 and C10 positions. It revealed that 2,5-disubstituted benzoates at C2 can either provide a strong enhancement or detriment to the potency of the compound, depending on the substituent. Also, novel highly potent taxoids were discovered and their biological activity was assessed by numerous collaborators. However, these agents are highly cytotoxic and are dangerous when administered systemically and would benefit from conjugation to tumor-targeting moieties to reduce systemic exposure. As certain next-generation taxoids possess the requisite sub-nanomolar potency required for use in targeted drug conjugates, selected compounds taxoids were used for the synthesis of novel tumor-targeted drug conjugates.

§ 2.6.0 Experimental

§ 2.6.1 General Methods

^{1}H and ^{13}C NMR spectra were measured on a Varian 300, 400, 500 or 600 MHz NMR spectrometer. Melting points were measured on a Thomas Hoover Capillary melting point apparatus and are uncorrected. Mass to charge values were measured by flow injection analysis on an Agilent Technologies LC/MSD VL. TLC was performed on Merck DC-alufolien with Kieselgel 60F-254 and column chromatography was carried out on silica gel 60 (Merck; 230-400

mesh ASTM). Compound purity was verified by reverse phase HPLC on a Shimadzu LC-2010A with a Curosil-B 5 column (250 x 4.6 nm). The mobile phase was acetonitrile-water. The analyses were performed at a flow rate of 1 ml/min with the UV detector set at 254 and 227 nm. The gradient was run from 20% to 95% acetonitrile in water over a 40 minute period.

§ 2.6.2 Materials

The chemicals were purchased from Aldrich Co. and Sigma and purified before use by standard methods. Tetrahydrofuran was freshly distilled from sodium metal and benzophenone. Dichloromethane was also distilled immediately prior to use under nitrogen from calcium hydride. In addition, various dry solvents were degassed and dried using PureSolv™ solvent purification system (Innovative Technologies, Newburyport, MA).

§ 2.6.3 – Experimental Procedures

7,10,13-Tris(triethylsilyl)-10-deacetylbaccatin III (2-1) [84]

An aliquot of **10-DAB III** (1.5 g, 2.75 mmol) and imidazole (938 mg) was dissolved in DMF (3.8 mL) and cooled to 0 °C under inert conditions. To the mixture TESCl (3.8 mL, 13.8 mmol) was added dropwise. The mixture was stirred, allowed to warm to room temperature and monitored by TLC. Upon completion, the reaction was quenched with saturated NH_4Cl (2 mL) and extracted with ethyl acetate (2 x 75 mL). The organic layer was collected, washed with brine (3x 50 ml), dried over anhydrous $MgSO_4$, and concentrated *in vacuo*. Purification was be done by column chromatography on silica gel with increasing amounts of ethyl acetate in hexanes (hexanes:ethyl acetate = 1:0 – 3:1) to afford **2-1** (2.048 g, 84% yield) as a white solid: mp 202-203 ^oC; ^1H NMR (300 MHz, $CDCl_3$) δ 0.70 (m, 18H), 1.05 (m, 27H), 1.12 (s, 3H), 1.26 (s, 3H), 1.26 (m, 1H), 1.72 (s, 3H), 1.93 (m, 1H), 2.05 (s, 3H), 2.19 (m, 1H), 2.35 (s, 3H), 2.60 (m, 1H), 3.92 (d, J = 7.8 Hz, 1H), 4.20 (d, J = 8.1 Hz, 1H), 4.35 (d, J = 8.1 Hz, 1H), 4.48 (dd, J = 10.5, 6.6 Hz, 1H), 5.00 (m, 2H), 5.26 (s, 1H), 5.69 (d, J = 7.2 Hz, 1H), 7.53 (t, 7.2 Hz, 2H), 7.66 (t, 7.2 Hz, 1H), 8.15 (d, 6.9 Hz, 2H). MS (ESI) calcd for $C_{47}H_{79}O_{10}Si_3$ $(M+H)^+$: 887.49, found 887.5. All data were found to be in agreement with literature values.[84]

7,10,13-Tris(triethylsilyl)-2-debenzoyl-10-deacetylbaccatin III (2-2) [84]

An aliquot of **2-1** (1.10 g, 1.127 mmol) was dissolved in dry THF (22 mL), and cooled to -30^{o}C under inert conditions. To the solution was added sodium bis(2-methoxyethyoxy) aluminum hydride, 65 wt% in toluene (0.9 mL, 12.6 mmol), dropwise. The temperature was maintained at -30^{o}C and the progress of the reaction was monitored by TLC. Upon completion, the reaction was quenched with saturated NH_4Cl (5 mL), diluted with H_20 (100 mL) and extracted with ethyl acetate (2 x 75 mL). The organic layers were collected, washed with brine (3 x 75 mL), dried over anhydrous $MgSO_4$, and concentrated *in vacuo*. Purification was be done by column chromatography on silica gel (hexanes:ethyl acetate = 4:1) to afford **2-2** (946 mg, 96% yield) as a white solid: mp 69-70 ^oC; ^1H NMR (300 MHz, $CDCl_3$) δ 0.61 (m, 18H), 0.97 (m, 27H), 1.08 (s, 3H), 1.16 (s, 3H), 1.25 (m, 1H), 1.62 (s, 3H), 1.89 (m, 1H), 1.91 (s, 3H), 2.03 (m, 1H), 2.17 (s, 3H), 2.29 (m, 1H), 2.45 (d, J = 6.3 Hz, 1H), 2.61 (m, 1H), 3.45 (d, J = 6.6 Hz, 1H), 3.87, (t, J =

6.6 Hz, 1H), 4.35 (dd, (J = 10.2, 6.3 Hz, 1H), 4.54 (d, J = 9.0 Hz, 1H), 4.95 (m, 2H), 5.12 (s, 1H). MS (ESI) calcd for $C_{40}H_{75}O_9Si_3$ $(M+H)^+$: 783.47, found 783.4. All data were found to be in agreement with literature values.[84]

7,10,13-Tris(triethylsilyl)-2-debenzoyl-2-(3-methoxybenzoyl)-10-deacetylbaccatin III (2-3 A) [84]

Compound **2-2** (450 mg, 0.575 mmol), DMAP (625 mg, 5.12 mmol) and meta-methoxybenzoic acid (696 mg, 5.12 mmol) were dissolved in CH_2Cl_2 (6 mL), and purged with nitrogen. To the mixture DIC (0.8 mL, 5.12 mmol) was added dropwise under inert conditions. The mixture was allowed at room temperature and the reaction progress was monitored by TLC. Upon completion, the reaction was quenched with saturated NH_4Cl (1 mL), diluted with H_20 (70 mL) and extracted with ethyl acetate (2 x 65 mL). The organic layers were collected, washed with brine (3 x 75 mL), dried over anhydrous $MgSO_4$, and concentrated *in vacuo*. Purification was be done by column chromatography on silica gel (hexanes:ethyl acetate = 4:1) to afford **2-3 A** (462 mg, 88% yield) as a white solid: ^{1}H NMR (300 MHz, $CDCl_3$) δ 0.62 (m, 18H), 0.98 (m, 27H), 1.13 (s, 3H), 1.23 (s, 3H), 1.31 (m, 1H), 1.65 (s, 3H), 1.88 (m, 1H), 1.98 (s, 3H), 2.18 (m, 2H), 2.27 (s, 3H), 2.52 (m, 1H), 3.85 (s, 3H), 3.87 (m, 1H), 4.14 (d, J = 9.0, 1H), 4.31 (d, J = 8.4, 1H), 4.41 (dd, J = 10.5, 6.9, 1H), 4.93 (m, 2H), 5.19 (s, 1H), 5.61 (d, J = 7.2 Hz, 1H), 7.12 (m, 1H), 7.37 (t, J = 7.5 Hz, 1H), 7.62 (m, 1H), 7.68 (d, 7.5, 1H). MS (ESI) calcd for $C_{48}H_{81}O_{11}Si_3$ $(M+H)^+$: 917.51, found 917.5. All data were found to be in agreement with literature values.[84]

7,10,13-Tris(triethylsilyl)-2-debenzoyl-2-(3-methylbenzoyl)-10-deacetylbaccatin III (2-3 B)

According to the procedure previously listed for **2-3 A**, compound **2-2** was used to produce **2-3 B** (533 mg, 93%) as a white solid: ^{1}H NMR (300 MHz, $CDCl_3$) δ 0.56-0.70 (m, 19H), 0.93-1.04 (m, 28H), 1.12 (s, 3H), 1.18 (s, 3H), 1.22 (m, 1H), 1.57 (s, 1H), 1.65 (s, 3H), 1.84 (m, 1H), 1.98 (s, 3H), 2.11 (m, 1H), 2.20 (m, 1H), 2.28 (s, 3H), 2.40 (s, 3H), 2.51 (m, 1H), 3.85 (d, J = 7.2 Hz, 1H), 4.14 (d, J = 8.1 Hz, 1H),, 4.28 (d, J = 8.1, 1H), 4.41 (dd, J = 10.5, 6.3, 1H), 4.93 (m, 2H), 5.19 (s, 1H), 5.61 (d, J = 7.2 Hz, 1H), 7.31-7.41 (m, 2H), 7.88 (d, 7.2, 1H), 7.92 (s, 1H). MS (ESI) calcd for $C_{48}H_{81}O_{10}Si_3$ $(M+H)^+$: 900.51, found 900.5.

7,10,13-Tris(triethylsilyl)-2-debenzoyl-2-(2,5-dimethoxybenzoyl)-10-deacetylbaccatin III (2-3 C)

According to the procedure previously listed for **2-3 A**, compound **2-2** (1.70 g, 2.17 mmol) was used to produce **2-3 C** (1.36 g, 66%) as a white solid: ^{1}H NMR (300 MHz, $CDCl_3$) δ 0.50 – 0.76 (m, 18H), 0.90-1.06 (m, 27H), 1.16 (s, 3H), 1.19 (s, 3H), 1.67 (s, 3H), 1.82-1.96 (m, 1H), 1.97 (s, 3H), 2.13-2.21 (m, 2H), 2.17 (s, 3H), 2.42-2.57 (m, 1H), 3.80 (s, 3H), 3.81 (m, 1H), 4.2-4.32 (m, 2H), 4.39 (dd, J = 6.9, 10.5 Hz, 1H), 4.88-5.02 (m, 2H), 5.18 (s, 1H), 5.64 (d, J = 6.9 Hz, 1H), 6.93 (d, J = 9.0 Hz, 1H), 7.07 (dd, J = 3.0, 9.0 Hz, 1H), 7.43 (d, J = 3.0 Hz, 1H). All data were found to be in agreement with literature values.

7,10,13-Tris(triethylsilyl)- 2-debenzoyl-2-(2,5-dimethylbenzoyl)-10-deacetylbaccatin III (2-3 D)

According to the procedure previously listed for **2-3 A**, compound **2-2** 1.40 g, 1.79 mmol) was used to produce **2-3 D (**1.11 g, 52% yield)as a white solid: ^{1}H NMR (300 MHz, $CDCl_3$) δ 0.52–0.78 (m, 18H), 0.90-1.08 (m, 27H), 1.14 (s, 3H), 1.19 (s, 3H), 1.65 (s, 3H), 1.80-1.94 (m, 1H), 1.97 (s, 3H), 2.10-2.26 (m, 2H), 2.24 (s, 3H), 2.34 (s, 3H), 2.42-2.56 (m, 1H), 2.58 (s, 3H), 3.84 (d, J = 6.6 Hz, 1H), 4.14 (d, J = 8.4 Hz, 1H), 4.20 (d, J = 8.4 Hz, 1H), 4.40 (dd, J = 6.0, 10.5 Hz, 1H), 4.86-4.98 (m, 2H), 5.19 (s, 1H), 5.59 (d, J = 7.2 Hz, 1H), 7.13 (d, J = 7.8 Hz, 1H), 7.23 (d, J = 7.8 Hz, 1H), 7.88 (s, 1H). MS (ESI) calcd for $C_{49}H_{83}O_{10}Si_3$ $(M+H)^+$: 915.52, found 915.5.

2-Debenzoyl-2-(3-methoxybenzoyl)-10-deacetylbaccatin III (2-4 A) [84]

Compound **2-3 A** (700 mg, 0.76 mmol) was dissolved in a 1:1 mixture of acetonitrile:pyridine (32 mL total) and cooled to 0 °C under inert conditions. To the mixture excess HF, 70% in pyridine (7.0 mL), was added dropwise. The reaction was stirred at room temperature and monitored by TLC. Upon completion, the reaction was quenched with 10% aqueous citric acid (15 mL), diluted with H_2O (150) neutralized with $NaHCO_3$(s) and extracted with ethyl acetate (2 x 100 mL). The organic layer was collected, washed with saturated $CuSO_4$ solution (2 x 50 mL), water (2 x 70 mL) and brine (3 x 75 mL). The extract was then dried over anhydrous $MgSO_4$, suction filtered and the filtrate concentrated *in vacuo*. Purification was done *via* column chromatography on silica gel (hexanes:ethyl acetate = 2:1) to afford **2-4 A** (426 mg, 97% yield) as a white solid: ^{1}H NMR (300 MHz, DMSO-d_6) δ 0.92 (s, 6H), 1.01 (m, 1H), 1.52 (s, 1H), 1.64 (m, 1H), 1.87 (s, 3H), 2.14 (m, 1H), 2.17 (s, 3H), 2.28 (m, 1H), 3.83 (s, 3H), (4.08 (m, 1H), 4.34 (s, 1H), 4.62 (m, 1H), 4.77 (d, J = 2.7 Hz, 1H), 4.92 (d, J = 8.7, 1H), 5.00 (d, J = 7.2, 1H), 5.13 (d, J = 2.4 Hz, 1H), 5.21 (d, J = 4.5 Hz, 1H), 5.38 (d, J = 6.9 Hz, 1H), 7.24 (m, 1H), 7.47 (t, J = 7.8 Hz, 1H), 7.61 (m, 2H). MS (ESI) calcd for $C_{30}H_{39}O_{11}$ $(M+H)^+$: 574.24, found 574.3. All data were found to be in agreement with literature values.[84]

2-Debenzoyl-2-(3-methylbenzoyl)-10-deacetylbaccatin III (2-4 B)

According to the procedure previously listed for **2-4 A**, compound **2-3 B** (1.05g, 1.16 mmol) was used to produce **2-4 B** (645 mg, 99%) as a white solid: mp 186-188 ºC; ^{1}H NMR (300 MHz, DMSO-d_6) δ 0.93 (s, 6H), 1.52 (s, 3H), 1.62 (m, 1H), 1.89 (s, 3H), 2.14 (m, 2H), 2.27 (m, 1H), 2.39 (s, 1H), 3.80 (d, J = 6.6 Hz, 1H), 4.02- 4.14 (m, 2H), 4.33 (s, 1H), 4.61 (m, 1H), 4.79 (d, 2.1 Hz, 1H), 4.92 (d, J = 8.7 Hz, 1H), 5.00 (d, J = 6.9 Hz, 1H), 5.12 (s, 1H), 5.23 (d, J = 4.5 Hz, 1H), 5.37 (d, J = 6.9 Hz, 1H), 7.41 – 7.50 (m, 2H), 7.81 (d, J = 7.2 H), 7.85 (s, 1H). MS (ESI) calcd for $C_{30}H_{39}O_{10}$ $(M+1)^+$: 559.25, found: 559.2.

2-Debenzoyl-2-(2,5-dimethoxybenzoyl)-10-deacetylbaccatin III (2-4 C)

According to the procedure previously listed for **2-4 A**, compound **2-3 C** (750 mg, 0.79 mmol) was used to produce **2-4 C.** The exception being that after workup, purification was done *via* column chromatography on silica gel (hexanes:ethyl acetate = 2:1) to afford **2-4 C** (450 mg, 95%

yield) as a white solid: ^{1}H NMR (300 MHz, DMSO-d_6) δ 0.94 (s, 6H), 1.52 (s, 3H), 1.56-1.72 (m, 1H), 1.87 (s, 3H), 2.07 (s, 3H), 2.12-2.20 (m, 2H), 2.21-2.36 (m, 1H), 3.76 (s, 6H), 3.75 (m, 1H), 4.09 (m, 2H), 4.28 (s, 1H), 4.56-4.70 (m, 1H), 4.75 (d, J = 2.1 Hz, 1H), 4.88 (d, J = 8.1 Hz, 1H), 4.97 (d, J = 6.9 Hz, 1H), 5.11 (d, J = 2.4 Hz, 1H), 5.18 (d, J = 4.2 Hz, 1H), 5.34 (d, J = 6.9 Hz, 1H), 7.07 (d, J = 9.3 Hz, 1H), 7.14 (dd, J = 3.0, 9,3 Hz, 1H), 7.45 (d, J = 3.0 Hz, 1H). All data were found to be in agreement with literature values.

2-Debenzoyl-2-(2,5-dimethylbenzoyl)-10-deacetylbaccatin III (2-4 D)

According to the procedure previously listed for **2-4 A**, compound **2-4 D** (800 mg, 0.88 mmol) was used to produce **2-4 D** (413 mg, 85% yield) as a white solid: ^{1}H NMR (300 MHz, DMSO-d_6) δ 0.95 (s, 16H), 1.54 (s, 3H), 1.60-1.68 (m, 1H), 1.90 (s, 3H), 2.12-2.19 (m, 2H), 2.14 (s, 3H), 2.24 – 2.32 (m, 1H), 2.34 (s, 3H), 2.53 (s, 3H), 3.79 (d, J = 7.2 Hz, 1H), 4.02 (d, J= 8.4 Hz, 1H), 4.07 (d, J = 8.4 Hz, 1H), 4.09 (m, 1H), 4.28 (s, 1H), 4.63 (m, 1H), 4.74 (d, J = 1.8 Hz, 1H), 4.91 (d, J = 9.6 Hz, 1H), 4.97 (d, J = 7.2 Hz, 1H), 5.13 (d, J = 1.8 Hz, 1H), 5.20 (d, J = 4.2 Hz, 1H), 5.40 (d, J = 7.2 Hz, 1H), 7.20 (d, J = 7.8 Hz, 1H), 7.30 (d, J = 7.8, 1H), 7.89 (s, 1H). MS (ESI) calcd for $C_{31}H_{41}O_{10}$ $(M+H)^+$: 572.26, found 573.3.

10-Propanoyl-10-deacetylbaccatin III (2-5 A) [84]

An aliquot of **10-DAB-III** (500 mg, 0.95 mmol) was dissolved in THF (40 mL), and to the mixture was added cerium chloride hexahydrate (53.5 mg, 0.095 mmol). The solution was then cooled in an ice bath and propionic anhydride (1.23 mL, 9.45 mmol) was added dropwise. The reaction mix was allowed to warm to room temperature and monitored by TLC. Upon completion, the THF was removed under vacuum and ethyl acetate (40 mL) was added. The organic layer was washed with H_2O (40 mL), saturated $NaHCO_3$ solution (3 x 30 mL), brine (3 x 30 mL), dried over $MgSO_4$, and concentrated *in vacuo* to afford **2-5 A** (489 mg, 92%) as a white solid: ^{1}H NMR ($CDCl_3$, 300 MHz) δ 1.11 (s, 6H), 1.18 (t, 3H), 1.64 (s, broad, 1H), 1.67 (s, 3H), 1.87 (m, 1H), 2.05 (s, 3H), 2.28 (s, 3H), 2.31 (s, 1H), 2.46 (q, 2H), 2.53 (m, 2H), 3.87, (d, J = 8.4 Hz, 1H), 4.17 (d, J = 7.8 Hz, 1H), 4.30 (d, J = 8.4 Hz, 1H), 4.47 (m, 1H), 4.89 (t, 1H), 4.98 (d, J = 7.8 Hz, 1H), 5.02 (d, J = 7.8 Hz, 1H), 6.34 (s, 1H), 7.47 (t, J = 7.2 Hz, 2H), 7.59 (t, J = 7.2 Hz, 1H), 8.10 (d, J = 7.2 Hz, 2H); MS (ESI) calcd for $C_{32}H_{41}O_{11}$ $(M+H)^+$: 600.26, found 600.3. All data were found to be in agreement with literature values.[84]

2-Debenzoyl-2-(3-methoxybenzoyl)-10-(propanoyl)-10-deacetylbaccatin III (2-5 B) [84]

According to the procedure previously listed for **2-5 A**, compound **2-4 A** (220 mg, 0.29 mmol) was used to produce **2-4 B** (240 mg, 99%) as a white solid: ^{1}H NMR ($CDCl_3$, 300 MHz) δ 0.81 – 0.92 (m, 1H), 1.10 (s, 6H), 1.26 (t, 3H), 1.66 (s, 3H), 1.86 (m, 1H), 2.04 (s, 3H), 2.28 (s, 3H), 2.31 (s, 1H), 2.43 – 2.61 (m, 3H), 3.87, (d, J = 9.0 Hz, 1H), 4.15 (d, J = 8.1 Hz, 1H), 4.34 (d, J = 8.1 Hz, 1H), 4.47 (m, 1H), 4.88 (t, 1H), 4.98 (d, J = 8.1Hz, 1H), 4.98 (d, J = 8.1 Hz, 1H), 5.60 (d, J = 7.5 Hz, 1H), 6.33 (s, 1H), 7.14 (m, 1H), 7.38 (t, J = 7.8 Hz, 1H), 7.63 (s, 1H), 7.69 (d, J = 7.8 Hz, 2H); All data were found to be in agreement with literature values.[84]

2-Debenzoyl-2-(3-methylbenzoyl)-10-(propanoyl)-10-deacetylbaccatin III (2-5 C)

According to the procedure previously listed for **2-5 A**, compound **2-4 B** (220 mg, 0.29 mmol) was used to produce **2-5 C** (233 mg, 96%) as a white solid: mp 186-188 ^{o}C; ^{1}H NMR ($CDCl_3$, 300 MHz) δ 1.26 (t, J = 7.8 Hz, 3 H), 1.63 (s, 1H), 1.66 (s, 3H), 1.86 (m, 1H), 2.04 (s, 3H), 2.05 (s, 1H), 2.11 (m, 1H), 2.43 (s, 3H), 2.54 (q, J = 7.8 Hz, 2H), 2.59 (m, 1H), 3.88 (d, J = 7.2 Hz, 1H), 4.14 (d, 7.5 Hz, 1H), 4.31 (d, J = 8.1 Hz, 1H), 4.47 (m, 1H), 4.89 (m, 1H), 4.99 (d, J = 6.6 Hz, 1H), 5.60 (d, J = 7.8 Hz, 1H), 6.33 (s, 1H), 7.33 – 7.44 (m, 2H), 7.90 (d, J = 7.5 Hz, 1H), 7.93 (s, 1H). MS (ESI) calcd for $C_{33}H_{43}O_{11}$ $(M+H)^+$: 615.27, found 615.3.

2-Debenzoyl-2-(2,5-dimethoxybenzoyl)-10-(propanoyl)-10-deacetylbaccatin III (2-5 D)

According to the procedure previously listed for **2-5 A**, compound **2-4 C** (230 mg, 0.38 mmol) was used to produce **2-5 D** (225 mg, 90%) as a white solid: ^{1}H NMR ($CDCl_3$, 300 MHz) δ 1.10 (s, 3H), 1.13 (s, 3H), 1.23 (t, J = 7.5 Hz, 3H), 1.70 (s, 3H), 1.80-1.94 (m, 1H), 2.05 (s, 3H), 2.16 (s, 3H), 2.26-2.32 (m, 2H), 2.40-2.62 (m, 3H), 3.78-3.84 (m, 1H), 3.82 (s, 3H), 3.90 (s, 3H), 4.32 (m, 2H), 4.45 (dd, J = 6.9, 11.1 Hz, 1H), 4.93 (m, 2H), 5.62 (d, J = 6.6 Hz, 1H), 6.33 (s, 1H), 6.95 (d, J = 9.0 Hz, 1H), 7.08 (dd, J = 3.3, 9.0 Hz, 1H), 7.40 (d, J = 3.3 Hz, 1H). MS (ESI) calcd for $C_{34}H_{45}O_{13}$ $(M+H)^+$: 661.28, found 661.3 (M+H).

2-Debenzoyl-2-(2,5-dimethylbenzoyl)-10-(propanoyl)-10-deacetylbaccatin III (2-5 E)

According to the procedure previously listed for **2-5 A**, compound **2-4 D** (130 mg, 0.23 mmol) was used to produce **2-5 E** (152 mg, 99%) as a white solid: ^{1}H NMR ($CDCl_3$, 300 MHz) δ 1.11 (s, 6H), 1.23 (t, J = 7.2 Hz, 3H), 1.66 (s, 3H), 1.80-1.93 (m, 1H), 2.04 (s, 3H), 2.24 (s, 3H), 2.28-2.36 (m, 2H), 2.38 (s, 3H), 2.42-2.64 (m, 1H) 2.55 (q, J = 7.2 Hz, 2H), 3.86 (d, J = 6.9 Hz, 1H), 4.14 (d, J = 8.4, 1H), 4.25 (d, J = 8.4 Hz, 1H), 4.46 (m, 1H), 4.89 (m, 1H), 4.97 (d, J = 7.8 Hz, 1H), 5.60 (d, J = 6.9 Hz, 1H), 6.33 (s, 1H), 7.15 (d, J = 7.8 Hz, 1H), 7.26 (d, J = 7.8 Hz, 1H), 7.92 (s, 1H). MS (ESI) calcd for $C_{34}H_{45}O_{11}$ $(M+H)^+$: 629.29, found 629.3 (M+H).

7-Triethylsilyl-10-(propanoyl)-10-deacetylbaccatin III (2-6 A) [84]

Compound **2-5 A** (520 mg, 0.89 mmol) and imidazole (240 mg, 3.55 mg) was dissolved in DMF (10 mL) and cooled to 0 °C under inert conditions. To the mixture TESCl (0.38 mL, 2.67) was added dropwise. The mixture was stirred, allowed to warm to room temperature and monitored by TLC. Upon completion the reaction was quenched with saturated NH_4Cl (3 mL) and extracted with ethyl acetate (2 x 30 mL). The organic layer was collected, washed with brine (3 x 30 mL), dried over anhydrous $MgSO_4$, and concentrated *in vacuo*. Purification was done by column chromatography on silica gel with increasing amounts of ethyl acetate in hexanes (hexanes:ethyl acetate) to afford (489 mg, 77% yield) of **2-6 A** as a white solid: ^{1}H NMR ($CDCl_3$, 300 MHz) δ 0.58 (m, 6H), 0.92 (t, 9H), 1.03 (s, 3H), 1.16 (s, 3H), 1.20 (t, 3H), 1.62 (s, br, 1H), 1.68 (s, 3H), 1.86 (m, 1H), 2.04 (m, 1H), 2.20 (s, 3H), 2.28 (s, 3H), 2. 47 (q, 2H), 2.45 (m, 1H), 3.89 (d, J = 8.4 Hz, 1H), 4.14 (d, J = 8.1 Hz, 1H), 4.30 (d, J = 8.4 Hz, 1H), 4.49 (dd, J = 10.5, 6.6 Hz, 1H), 4.83 (m, 1H), 4.95 (d, J = 7.8, 1H), 5.63 (d, J = 7.2, 1H), 6.48 (s, 1H), 7.47 (t, J = 7.2 Hz, 2H), 7.60 (t,

J = 7.2 Hz, 1H), 8.10 (d, J = 7.2 Hz, 2H). MS (ESI) calcd for $C_{38}H_{55}O_{11}Si$ $(M+H)^+$: 715.35, found 715.4. All data were found to be in agreement with literature values.[84]

2-Debenzoyl-2-(3-methoxybenzoyl)-7-triethylsilyl-10-(propanoyl)-10-deacetylbaccatin III (2-6 B) [84]

According to the procedure previously listed for **2-6 A**, compound **2-5 B** (220 mg, 0.35 mmol) was used to produce **2-6 B** (175 mg, 69% yield) as a white solid: ^{1}H NMR ($CDCl_3$, 300 MHz) δ 0.53–0.62 (m, 6H), 0.92 (m, 9H), 1.03 (s, 3H), 1.19 (s, 3H), 1.21 (t, 3H), 1.25 (s, 1H), 1.68 (s, 3H), 1.87 (m, 1H), 2.20 (s, 3H), 2.25 (s, 1H), 2.27 (s, 3H), 2.39-2.59 (m, 3H), 3.87 (s, 3H), 3.88 (d, J = 8.1 Hz, 1H), 4.14 (d, J = 8.1 Hz, 1H), 4.34 (d, J = 7.8 Hz, 1H), 4.49 (dd, J = 10.5, 6.9 Hz, 1H), 4.83 (t, J = 7.8 Hz, 1H), 4.96 (d, J = 8.1, 1H), 5.62 (d, J = 7.5, 1H), 6.48 (s, 1H), 7.13 (m, 1H), 7.38 (t, J = 8.1 Hz, 1H), 7.64 (s, 1H), 7.70 (d, J = 7.8 Hz, 1H). All data were found to be in agreement with literature values.[84]

2-Debenzoyl-2-(3-methylbenzoyl)-7-triethylsilyl-10-(propanoyl)-10-deacetylbaccatin III (2-6 C)

According to the procedure previously listed for **2-6 A**, compound **2-5 C** (210 mg, 0.34 mmol) was used to produce **2-6 C** (203 mg, 82%) as a white solid: ^{1}H NMR ($CDCl_3$, 300 MHz) δ 0.53-0.62 (m, 6H), 0.92 (m, 9H), 1.03 (s, 1H), 1.19 (s, 3H), 1.21 (t, J = 7.8 Hz, 3 H), 1.25 (s, 3H), 1.63 (s, 1H), 1.67 (s, 3H), 1.87 (m, 1H), 2.05 (m, 1H), 2.20 (s, 3H), 2.25 (s, 1H), 2.28 (s, 3H), 2.42 (s, 3H), 2.43-2.58 (m, 3H), 3.88 (d, J = 6.9 Hz, 1H), 4.13 (d, 8.7 Hz, 1H), 4.31 (d, J = 8.7 Hz, 1H), 4.49 (dd, J = 10.2, 6.9 Hz, 1H), 4.96 (d, J = 8.4 Hz, 1H), 5.61 (d, J = 6.9 Hz, 1H), 6.48 (s, 1H), 7.33 – 7.42 (m, 2H), 7.90 (d, J = 7.5 Hz, 1H), 7.93 (s, 1H). MS (ESI) calcd for $C_{39}H_{57}O_{11}Si$ $(M+H)^+$: 729.36, found 729.4.

2-Debenzoyl-2-(2,5-dimethoxybenzoyl)-7-triethylsilyl-10-(propanoyl)-10-deacetylbaccatin III (2-6 D)

According to the procedure previously listed for **2-6 A**, compound **2-5 D** (215 mg, 0.33 mmol) was used to produce **2-6 D** (211 mg, 84%) as a white solid: ^{1}H NMR ($CDCl_3$, 300 MHz) δ 0.50-0.63 (m, 6H), 0.85-0.99 (m, 9H), 1.06 (s, 3H), 1.20 (t, J = 7.2 Hz, 3H), 1.20 (s, 3H), 1.71 (s, 3H), 1.81-1.94 (m, 1H), 2.16 (s, 3H), 2.20 (s, 3H), 2.23-2.34 (m, 2H), 2.34-2.58 (m, 3H), 3.78-3.83 (m, 1H), 3.81 (s, 3H), 3.90 (s, 3H), 4.31 (m, 1H), 4.46 (dd, J = 6.6, 10.5 Hz, 1H), 4.86 (m, 1H) 4.92 (d, J = 7.8 Hz, 1H), 5.63 (d, J = 6.9 Hz, 1H), 6.46 (s, 1H), 6.94 (d, J = 9.0 Hz, 1H), 7.07 (dd, J = 3.3, 9.0 Hz, 1H), 7.41 (d, J = 3.3 Hz, 1H). MS (ESI) calcd for $C_{40}H_{59}O_{13}Si$ $(M+H)^+$: 775.37, found: 775.4 (M+H).

2-Debenzoyl-2-(2,5-dimethylbenzoyl)-7-triethylsilyl-10-(propanoyl)-10-deacetylbaccatin III (2-6 E)

According to the procedure previously listed for **2-6 A**, compound **2-5 E** (135 mg, 0.322mmol) was used to produce **2-6 E** (131 mg, 82% yield) as a white solid: ^{1}H NMR ($CDCl_3$, 300 MHz) δ 0.49-0.64 (m, 6H), 0.84-0.96 (m, 9H), 1.04 (s, 3H), 1.21 (t, J = 7.6 Hz, 1H), 1.22 (s, 3H), 1.68 (s,

3H), 1.81-1.93 (m, 1H), 2.21 (s, 3H), 2.25 (s, 3H), 2.27-2.31 (m, 2H), 2.36 (s, 3H), 2.40-2.60 (m, 3H), 2.60 (s, 3H), 3.87 (d, J = 7.2 Hz, 1H), 4.13 (d, J = 8.4 Hz, 1H), 4.24 (d, J = 8.4 Hz, 1H), 4.48 (dd, J = 6.9, 10.8 Hz, 1H), 4.84 (m, 1H), 4.95 (d, J = 7.8 Hz, 1H), 5.61 (d, J = 6.9 Hz, 1H), 6.47 (s, 1H), 7.14 (f, J = 7.8 Hz, 1H), 7.25 (d, J = 7.8 Hz, 1H), 7.93 (s, 1H). MS (ESI) calcd for $C_{40}H_{59}O_{11}Si$ $(M+H)^+$: 743.38, found 743.4.

7-Triethylsilyl-10-deacetylbaccatin III (2-7 A) [84]

An aliquot of **10-DAB III** (650 mg**,** 1.23 mmol) and imidazole (340 mg, 4.9 mmol) was dissolved in DMF (12 mL) and cooled to 0 °C under inert conditions. To the mixture TESCl (0.62 mL, 2.7 mmol) was added dropwise. The mixture was stirred and allowed to warm to room temperature while being monitored by TLC. Upon completion the reaction was quenched with saturated NH_4Cl (1 mL) and extracted with ethyl acetate (3 x 15 mL). The organic layer was collected, washed with brine (3 x 30 mL), dried over anhydrous $MgSO_4$, and concentrated *in vacuo*. Purification was be done *via* column chromatography on silica gel (hexanes:ethyl acetate = 9:1) to afford **2-7 A** (733 mg, 90% yield) as a white solid: ^{1}H NMR ($CDCl_3$, 300 MHz) δ 0.58 (m, 6 H), 0.93 (m, 9 H), 1.06 (s, 6H), 1.78 (m, 1H), 1.89 (m, 1H), 2.09 (s, 3H), 2.21 (s, 3 H), 2.29 (s, 1H), 2.31 (s, 3H), 2.54 (m, 1H), 3.89 (d, J = 6.8 Hz, 1H), 4.15 (d, J = 8.4 Hz, 1H), 4.32 (d, J = 8.4 Hz, 1H), 4.49 (dd, J = 10.4, 6.8 Hz, 1H), 4.88 (t, J = 8.0 Hz, 1H), 4.97 (d, J = 9.2 Hz, 1H), 5.19 (s, 1H), 5.64 (d, J = 6.8, 1H), 7.48 (t, J = 7.6 Hz, 2H), 7.61 (t, J = 7.6, 1H), 8.12 (d, J = 7.6 Hz, 2H). MS (ESI) calcd for $C_{35}H_{51}O_{10}Si$ $(M+H)^+$: 659.33, found 659.3. All data were found to be in agreement with literature values.[84]

2-Debenzoyl-2-(3-methoxybenzoyl)-7-triethylsilyl-10-deacetylbaccatin III (2-7 B) [84]

According to the procedure previously listed for **2-7 A**, compound **2-4 A** (104 mg, 1.53 mmol) was used to produce **2-7 B** (188 mg, 72% yield) as a white solid: ^{1}H NMR ($CDCl_3$, 300 MHz) δ 0.56 (m, 6H), 0.96 (m, 9H), 1.08 (s, 6H), 1.15 (m, 1H), 1.72 (s, 3H), 1.93 (m, 1H), 2.08 (s, 3H), 2.24 (m, 1H), 2.27 (s, 3H), 2.48 (m, 1H), 3.86 (s, 3H), 3.94 (d, J = 7.2 Hz, 1H), 4.16 (d, J = 8.1 Hz, 1H), 4.26 (d, J = 1.8 Hz, 1H), 4.35 (d, J = 8.7 Hz, 1H), 4.39 (dd, J = 10.5, 6.6 Hz, 1H), 4.87 (m, 1H), 4.98 (d, J = 8.1 Hz), 5.17 (d, J = 1.8 Hz, 1H), 5.58 (d, J = 6.9 Hz, 1H), 7.13 (m, 1H), 7.38 (t, J = 7.8 Hz, 1H), 7.63 (m, 1H), 7.70 (d, 7.8, 1H). MS (ESI) calcd for $C_{36}H_{53}O_{11}S$ $(M+H)^+$: 689.34, found 689.3. All data were found to be in agreement with literature values.[84]

2-Debenzoyl-2-(3-methylbenzoyl)-7-triethylsilyl-10-deacetylbaccatin III (2-7 C)

According to the procedure previously listed for **2-7 A**, compound **2-4 B** (420 mg, 0.75 mmol) was used to produce **2-7 C** (328 mg, 65%) as a white solid: ^{1}H NMR ($CDCl_3$, 300 MHz) δ 0.50-0.66 (m, 7H), 0.93 (m, 9H), 1.07 (s, 6 H), 1.19 (s, 3H), 1.25 (s, 1H), 1.61 (s, 1H), 1.72 (s, 3H), 1.89 (m, 1H), 2.04 (s, 1H), 2.07 (s, 3H), 2.11 (m, 1H), 2.24 (s, 1H), 2.25 (s, 3 H), 2.41 (s, 3H), 2.47 (m, 1H), 3.93 (d, J = 7.2 Hz, 1H), 4.14 (d, 8.7 Hz, 1H), 4.26 (s, 1H), 4.38 (d, J = 8.7 Hz, 1H), 4.40 (dd, J = 10.2, 7.2 Hz, 1H), 4.85 (m, 1H), 5.16 (s, 1H), 5.57 (d, J = 6.9 Hz, 1H), 7.33 – 7.42 (m, 2H), 7.90 (d, J = 7.8 Hz, 1H), 7.93 (s, 1H). Calc for $C_{36}H_{52}O_{10}Si$: 672.33, found 672.3 (M+H).

2-Debenzoyl-2-(2,5-dimethoxybenzoyl)-7-triethylsilyl-10-deacetylbaccatin III (2-7 D)

According to the procedure previously listed for **2-7 A**, compound **2-7 C** (460 mg, 0.76 mmol) was used to produce **2-7 D** (503 mg, 92%) as a white solid: ^{1}H NMR ($CDCl_3$, 300 MHz) δ 0.44-0.65 (m, 6H), 0.84-0.98 (m, 9H), 1.07 (s, 3H), 1.11 (s, 3H), 1.76 (s, 3H), 1.86-1.96 (m, 1H), 2.07 (s, 3H), 2.17 (s, 3H), 2.20-2.31 (m, 2H), 2.40-2.52 (m, 1H), 3.81 (s, 3H), 3.86-3.90 (m, 1H), 3.90 (s, 3H), 4.24-4.42 (m, 4H), 4.84-4.93 (m, 2H), 5.16 (s, 1H), 5.59 (d, J = 7.2 Hz, 1H), 6.94 (d, J = 9.0 Hz, 1H), 7.07 (dd, J = 3.3, 9.0 Hz, 1H), 7.40 (d, J = 3.3 Hz, 1H). Calc for $C_{37}H_{54}O_{12}Si$: 718.34, found 719.4 (M+H). All data were found to be in agreement with literature values.[84]

2-Debenzoyl-2-(2,5-dimethylbenzoyl)-7-triethylsilyl-10-deacetylbaccatin III (2-7 E)

According to the procedure previously listed for **2-7**, compound **2-4 D** (260 mg, 0.46 mmol) was used to produce **2-7 E** (268 mg, 86% yield) as a white solid: ^{1}H NMR ($CDCl_3$, 300 MHz) δ 0.46-0.64 (m, 6H), 0.82-0.98 (m, 9H), 1.09 (s, 6H), 1.73 (s, 3H), 1.84-1.96 (m, 1H), 2.08 (s, 3H), 2.25 (s, 3H), 2.24-2.31 (m, 2H), 2.37 (s, 3H), 2.40-2.56 (m, 1H), 2.59 (s, 3H), 3.93 (d, J = 7.2 Hz, 1H), 4.14 (d, J = 8.4 Hz, 1H), 4.25 (d, J = 8.4 Hz, 1H), 4.39 (dd, J = 6.9, 10.8 Hz, 1H), 4.88 (m, 1H), 4.94 (d, J = 7.8 Hz, 1H), 5.17 (s, 1H), 5.57 (d, J = 7.2 Hz, 1H), 7.14 (d, J = 8.1 Hz, 1H), 7.26 (d, J = 8.1, 1H), 7.92 (s, 1H). Calc for $C_{37}H_{54}O_{10}Si$ 686.34, found 687.3 (M+H).

7-Triethylsilyl-10-(cyclopropanecarbonyl)-10-deacetylbaccatin III (2-6 F)[84]

Compound **2-7 A** (720 mg, 1.06 mmol) was dissolved in THF (21 mL) and cooled to -40 °C under inert conditions. To the mixture LiHMDS, 1.0 M in *tert*-butyl methyl ether (1.2 mL), was added dropwise, followed by the dropwise addition of cyclopropanecarboxylic acid chloride. (0.11 mL, 1.31 mmol). The mixture was stirred and monitored by TLC. Upon completion, the reaction was quenched with saturated NH_4Cl (2 mL) and extracted with ethyl acetate (2 x 25 mL). The organic layer was collected, washed with brine (3 x 30 mL), dried over anhydrous $MgSO_4$, and concentrated *in vacuo*. Purification was done by column chromatography on silica gel with increasing amounts of ethyl acetate in hexanes (hexanes:ethyl acetate = 1:0 - 4:1) to afford **2-6 F** (739 mg, 92% yield) as a white solid: ^{1}H NMR ($CDCl_3$, 300 MHz) δ 0.60 (m, 6H), 0.91 (m, 11 H), 1.05 (s, 3 H), 1.20 (s, 3H), 1.68 (s, 3H), 1.76 (m, 1H), 1.97 (m, 1H), 2.05 (m, 2 H), 2.19 (s, 3 H), 2.26 (s, 1H), 2.28) s, 3H), 2.52 (m, 1H), 3.89 (d, J = 7.1 Hz, 1H), 4.15 (d, J = 8.7 Hz, 1H), 4.31 (d, J = 8.7 Hz, 1H), 4.48 (dd, J= 6.3, 10.5 Hz, 1H), 4.85 (t, J = 7.8 Hz 1H), 4.97 (d, J = 9.0 Hz, 1H), 5. 64 (d, J = 6.8 Hz, 1H), 6.47 (s, 1H), 7.48 (t, J = 7.6 Hz, 2H), 7.61 (t, J = 7.6, 1H), 8.12 (d, J = 7.6 Hz, 2H). MS (ESI) calcd for $C_{39}H_{55}O_{11}Si$ $(M+H)^+$: 727.35, found 727.3. All data were found to be in agreement with literature values.[84]

2-Debenzoyl-2-(3-methoxybenzoy)-7-triethylsilyl-10-(cyclopropanecarbonyl)-10-deacetylbaccatin III (2-6 G) [84]

According to the procedure previously listed for **2-6 F**, compound **2-7 A** (170 mg, 0.23 mmol) was used to produce **2-6 G** (242 mg, 97% yield) as a white solid: ^{1}H NMR ($CDCl_3$, 300 MHz) δ 0.51 – 0.60 (m, 6H), 0.83 – 0.97 (m, 11 H), 1.05 (s, 3 H), 1.16 – 1.19 (m, 2H), 1.20 (s, 3H), 1.25 (s,

1H), 1.68 (s, 3H), 1.74 (m, 1H), 2.19 (s, 3 H), 2.25 (s, 1H), 2.26 (s, 3H), 2.51 (m, 1H), 3.87 (s, 3H), 3.88 (d, J = 6.3 Hz, 1H), 4.15 (d, J = 8.7 Hz, 1H), 4.34 (d, J = 8.7 Hz, 1H), 4.48 (dd, J= 10.5 Hz, 6.6 1H), 4.83 (t, J = 7.5 Hz 1H), 4.97 (d, J = 8.1 Hz, 1H), 5. 62 (d, J = 7.2 Hz, 1H), 6.47 (s, 1H), 7.14 (m, 1H), 7.38 (t, J = 7.5 Hz, 1H), 7,64 (s, 1H), 7.70 (d, J = 7.8 Hz, 1H). All data were found to be in agreement with the literature values.[84]

2-Debenzoyl-2-(3-methylbenzoyl)-7-triethylsilyl-10-(cyclopropanecarbonyl)-10-deacetylbaccatin III (2-6 H)

According to the procedure previously listed for **2-6 F**, compound **2-7 B** (170 mg, 0.23 mmol) was used to produce **2-6 H** (164 mg, 88%) as a white solid: ^{1}H NMR ($CDCl_3$, 300 MHz) δ 0.50-0.66 (m, 6H), 0.93 (m, 9H), 1.05 (s, 3H), 1.19 (s, 3H), 1.18 (m, 2H), 1.25 (s, 1H), 1.65 (s, 1H), 1.67 (s, 3H), 1.76 (m, 1H), 1.87 (m, 1H), 2.14 (m, 2H), 2.19 (s, 3H), 2.25 (s, 1H), 2.28 (s, 3 H), 2.42 (s, 3H), 2.51 (m, 1H), 3.87 (d, J = 6.9 Hz, 1H), 4.14 (d, 8.4 Hz, 1H), 4.30 (d, J = 8.4 Hz, 1H), 4.47 (dd, J = 10.2, 6.6 Hz, 1H), 4.83 (m, 1H), 4.93 (d, J = 8.4 Hz, 1H), 5.61 (d, J = 6.9 Hz, 1H), 6.46 (s, 1H), 7.33 – 7.42 (m, 2H), 7.90 (d, J = 7.5 Hz, 1H), 7.93 (s, 1H). MS (ESI) calcd for $C_{40}H_{57}O_{11}Si$ $(M+H)^+$: 741.36, found 741.4.

2-Debenzoyl-2-(2,5-dimethoxybenzoyl)-7-triethylsilyl-10-(cyclopropanecarbonyl)-10-deacetylbaccatin III (2-6 I)

According to the procedure previously listed for **2-6 F**, compound **2-7 C** (200 mg, 0.28 mmol) was used to produce **2-6 I** (214 mg, 98%) as a white solid: ^{1}H NMR ($CDCl_3$, 300 MHz) δ 0.51-0.62 (m, 6H), 0.84-0.94 (m, 9H), 1.00-1.12 (m, 2H), 1.08 (s, 3H), 1.14-1.22 (m, 2H), 1.20 (s, 3H), 1.71 (s, 3H), 1.76 (m, 1H), 1.82-1.93 (m, 1H), 2.16 (s, 3H), 2.19 (s, 3H), 2.23-2.31 (m, 2H), 2.41-2.56 (m, 1H), 3.79-3.83 (m, 1H), 3.81 (s, 3H), 3.90 (s, 3H), 4.31 (m, 2H), 4.44 (dd, J = 6.6, 10.2 Hz, 1H), 4.86 (m, 1H), 4.92 (d, J = 8.1 Hz, 1H), 5.63 (d, J = 6.6 Hz, 1H), 6.45 (s, 1H), 6.95 (d, J = 9.0 Hz, 1H), 7.07 (dd, J = 3.0, 9.0 Hz, 1H), 7.41 (d, J = 3.0 Hz, 1H). MS (ESI) calcd for $C_{41}H_{59}O_{13}Si$ $(M+H)^+$: 777.37, found 777.4.

7-Triethylsilyl-10-(*N,N*-dimethylcarbamoyl)-10-deacetylbaccatin III (2-6 J) [84]

Compound **2-7 A** (160 mg, 0.23 mmol) was dissolved in THF (4.6 mL) and cooled to -40 °C under inert conditions. To the mixture LiHMDS, 1.0 M in *tert*-butyl methyl ether (0.26 mL) was added dropwise, followed by the dropwise addition of N,N-dimethylcarbamoyl chloride (0.026, 0.28 mmol). The mixture was stirred and monitored by TLC. Upon completion, the reaction was quenched with saturated NH_4Cl (1 mL), diluted with water (30 mL) and extracted with ethyl acetate (50 mL). The organic layer was collected, washed with brine (2 x 40 mL), dried over anhydrous $MgSO_4$, and concentrated *in vacuo*. Purification was done by column chromatography on silica gel (hexanes:ethyl acetate = 2:1) to afford **2-6 J** (152 mg, 87% yield) as a white solid: ^{1}H NMR ($CDCl_3$, 300 MHz) δ 0.53-0.64 (m, 6H), 0.86-0.94 (m, 9H), 1.04 (s, 3H), 1.19 (s, 3H), 1.62 (s, 3H), 1.68 (s, 3H), 1.85-1.92 (m, 1H), 2.11 (m, 1H), 2.25 (m, 1H), 2.24 (s, 3H), 2.46-2.52 (m, 1H), 2.92 (s, 3H), 3.07 (s, 3H), 3.90 (d, J = 7.2 Hz, 1H), 4.14 (d, J = 8.1 Hz, 1H), 4.30 (d, J = 8.1 Hz, 1H), 4.50 (m, 1H), 4.82 (m, 1H), 4.95 (d, J = 8.7 Hz, 1H), 5.63 (d, J = 7.2 Hz, 1H), 6.38 (s,

1H), 7.47 (t, J = 7.5 Hz, 2H), 7.59 (t, J = 7.5 Hz, 1H), 8.11 (d, J = 7.2 Hz, 2H). All data were found to be in agreement with literature values.[84]

2-Debenzoyl-2-(3-methoxylbenzoyl)-7-triethylsilyl-10-(*N,N*-dimethylcarbamoyl)-10-deacetylbaccatin III (2-6 K) [84]

According to the procedure previously listed for **2-6 J**, compound **2-7 B** (160 mg, 0.22 mmol) was used to produce **2-6 K** (176 mg, 90% yield) as a white solid: ^{1}H NMR ($CDCl_3$, 300 MHz) δ 0.55-0.64 (m, 6H), 0.86-0.94 (m, 9 H), 1.05 (s, 3H), 1.19 (s, 3H), 1.26 (s, 3H), 1.60 (s, 3H), 1.61 (s, 3H), 1.68 (s, 3H), 1.86 (m, 1H), 2.06 (m, 1H), 2.24 (s, 3 H), 2.26 (m, 1H), 2.56 (m, 1H), 2.93 (s, 3H), 3.07 (s, 3H), 3.86 (s, 3H), 3.89 (s, J = 6.6 Hz, 1H), 4.14 (d, J = 8.4 Hz, 1H) 4.34 (d, J = 8.4 Hz, 1H), 4.48 (dd, 10.2, 6.6 Hz, 1H), 4.83 (m, 1H), 4.96 (d, J = 9.9 Hz, 1H), 5.36 (d, J = 6.9 Hz, 1H), 6.38 (s, 1H), 7.14 (dd, J = 8.4, 2.7 Hz, 1H), 7.38 (t, J = 7.8 Hz, 1H), 7.65 (m, 1H), 7.71 (d, J = 8.1, 1H). All data were found to be in agreement with literature values.[84]

2-Debenzoyl-2-(3-methylbenzoyl)-7-triethylsilyl-10-(*N,N*-dimethylcarbamoyl)-10-deacetylbaccatin III (2-6 L)

According to the procedure previously listed for **2-6 J**, compound **2-7 C** (160 mg, 0.22 mmol) was used to produce **2-6 L** (176 mg, 90% yield) as a white solid: ^{1}H NMR ($CDCl_3$, 300 MHz) δ 0.54-0.66 (m, 7H), 0.93 (m, 9H), 1.04 (s, 3H), 1.18 (s, 3H), 1.25 (s, 1H), 1.67 (s, 3H), 1.87 (m, 1H), 2.09 (m, 1H), 2.24 (s, 3H), 2.42 (s, 1H), 2.51 (m, 1H), 2.93 (s ,3H) 3.07 (s, 3H), 3.90 (d, J = 6.9 Hz, 1H), 4.13 (d, 7.8 Hz, 1H), 4.30 (d, J = 7.8 Hz, 1H), 4.48 (dd, J = 10.2, 6.6 Hz, 1H), 4.83 (m, 1H), 4.97 (d, J = 8.7 Hz, 1H), 5.61 (d, J = 6.9 Hz, 1H), 6.37 (s, 1H), 7.33 – 7.42 (m, 2H), 7.90 (d, J = 7.5 Hz, 1H), 7.93 (s, 1H). MS (ESI) calcd for $C_{39}H_{58}NO_{11}Si$ $(M+H)^+$: 744.37, found 744.4.

2-Debenzoyl-2-(2,5-dimethoxybenzoyl)-7-triethylsilyl-10-(*N,N*-dimethylcarbamoyl)-10-deacetylbaccatin III (2-6 M)

According to the procedure previously listed for **2-6 J**, compound **2-7 D** (200 mg, 0.28 mmol) was used to produce **2-6 M** (166 mg, 76%) as a white solid: ^{1}H NMR ($CDCl_3$, 300 MHz) δ 0.48-062 (m, 6H), 0.81- 1.00 (m, 9H), 1.08 (s, 3H), 1.19 (s, 3H), 1.71 (s, 3H), 1.81-2.03 (m, 1H), 2.16 (s, 3H), 2.24 (s, 3H), 2.25-2.29 (m, 2H), 2.42-2.55 (m, 1H), 2.93 (s, 3H), 3.07 (s, 3H), 3.79-3.85 (m, 1H), 3.81 (s, 3H), 3.90 (s, 3H), 4.31 (m, 2H), 2.43 (dd, J = 6.9, 10.8 Hz, 1H), 4.80-4.91 (m, 1H), 4.92 (d, J = 6.3 Hz, 1H), 5.63 (d, J = 6.3 Hz, 1H), 6.40 (s, 1H), 6.94 (d, J = 9.0 Hz, 1H), 7.07 (dd, J = 3.3, 9.3 Hz, 1H), 7.41 (d, J = 3.3 Hz, 1H). MS (ESI) calcd for $C_{40}H_{60}NO_{13}Si$ $(M+H)^+$: 790.38, found 790.4.

2-Debenzoyl-2-(2,5-dimethylbenzoyl)-7-triethylsilyl-10-(*N,N*-dimethylcarbamoyl)-10-deacetylbaccatin III (2-6 N)

According to the procedure previously listed for **2-6 J**, compound **2-7 E** (120 mg, 0.18 mmol) was used to produce **2-6 N** (124 mg, 94% yield) as a white solid: ^{1}H NMR ($CDCl_3$, 300 MHz) δ 0.52-0.67 (m, 6H), 0.88-0.98 (m, 9H), 1.06 (s, 3H), 1.20 (s, 3H), 1.68 (s, 3H), 1.81-1.92 (m, 1H), 2.24 (s, 3H), 2.25 – 2.30 (m, 2H), 2.37 (s, 3H), 2.46-2.58 (m, 1H), 2.59 (s, 3H), 2.93 (s, 3H), 3.08 (s,

3H), 3.88 (d, J = 6.9 Hz, 1H), 4.13 (d, J = 8.4 Hz, 1H), 4.24 (d, J = 8.4 Hz, 1H), 4.48 (dd, J = 7.2, 10.8 Hz, 1H), 4.84 (m, 1H), 4.95 (d, J = 7.8 Hz, 1H), 5.61 (d, J = 7.2 Hz, 1H), 6.38 (s, 1H), 7.14 (d, J = 7.8 Hz, 1H), 7.25 (d, J = 7.8 Hz, 1H), 7.93 (s, 1H). MS (ESI) calcd for $C_{40}H_{60}NO_{11}Si$ $(M+H)^+$: 758.39, found 758.4.

2-Debenzoyl-2-(3-methoxybenzoyl)-7-triethylsilyl-10-(*p*-methoxyphenylacetyl)-10-deacetylbaccatin III (2-6 O)[84]

According to the procedure previously listed for **2-6 J**, compound **2-7 B** (100 mg, 0.15 mmol) was used to produce **2-6 O** (80 mg, 60% yield) as a white solid: ^{1}H NMR ($CDCl_3$, 300 MHz) δ 0.48-0.61 (m, 6H), 0.82-0.94 (m, 9H), 0.92 (s, 3H), 1.09 (s, 3H), 1.68 (s, 3H), 1.80-1.92 (m, 1H), 2.17 (s, 3H), 2.20-2.28 (m, 2H), 2.26 (s, 3H), 2.49-2.59 (m, 1H), 3.69 (d, J = 2.1 Hz, 1H), 3.78 (s, 3H), 3.84 (m, 1H), 3.86 (s, 3H), 4.13 (d, J = 7.8 Hz, 1H), 4.33 (d, J = 7.8 Hz, 1H), 4.46 (dd, J = 6.9, 11.1 Hz, 1H), 4.79 (m, 1H), 4.95 (d, J = 8.4 Hz, 1H), 5.30 (s, 1H), 5.60 (d, J = 6.9 Hz, 1H), 6.44 (s, 1H), 6.86 (m, J = 8.4 Hz, 2H), 7.14 (d, J = 7.8 Hz, 1H), 7.24 (m, J = 8.4 Hz, 2H), 7.37 (t, J = 7.8 Hz, 1H), 7.63 (s, 1H), 7.69 (d, J = 7.8 Hz, 1H). All data were found to be in agreement with literature values.[84]

2'-Triisopropylsilyl-3'-dephenyl-3'-(2-methyl-2-propenyl)-7-triethylsilyl-10-(propanoyl)-docetaxel (2-8 A) [84]

Compound **2-6 A** (480 mg, 0.67 mmol) and **(+) 1-6** (320 mg, 0.81 mmol) were dissolved in THF (33 mL), and cooled to -40 ^oC under inert conditions. To the mixture was added LiHMDS, 1M in tert-butyl methyl ether (0.75 mL), dropwise. The reaction was monitored at low temperature by TLC, and upon completion was quenched with sat. NH_4Cl solution (5 mL). The mixture was then allowed to warm to room temperature, diluted with H_2O (30 mL) and extracted with ethyl acetate (2 x 30 mL). The organic layer was then washed with brine (3 x 30 mL), dried over $MgSO_4$, and concentrated *in vacuo*. Purification was done by column chromatography on silica gel (hexanes:ethyl acetate = 4:1) to afford **2-8 A (**575 mg, 78% yield) as a white solid: ^{1}H NMR ($CDCl_3$, 300 MHz) δ 0.58 (m, 6H), 0.91 (m, 9H), 1.12 (m, 21H), 1.10 (s, 3H), 1.17 (s, 3H), 1.21 (t, 3H), 1.33 (s, 9H), 1.68 (s, 3H), 1.73 (s, 1H), 1.75 (s, 3H), 1.90, m, 1H), 2.01 (s, 3H), 2.36 (s, 3H), 2.48 (m, 3H), 3.84 (d, J = 6.9 Hz, 1H), 4.20 (d, J = 8.4 Hz, 1H), 4.30 (d, 8.4 Hz, 1H), 4.47, (m, 2H), 4.79 (m, 2H), 4.95 (d, J = 8.7 Hz, 1H), 5.33 (d, J = 8,4 Hz, 1H), 5.68 (d, 7.2 Hz, 1H), 5.33 (d, J = 8.4 Hz, 1H), 5.68 (d, J = 7.2 Hz, 1H), 6.08 (t, 1H), 6.49 (s, 1H), 7.46 (t, J = 7.5 Hz, 2H), 7.60 (t, J = 7.5 Hz, 1H), 8.10 (d, J = 7.2 Hz, 2H); MS (ESI) calcd for $C_{59}H_{94}O_{15}NSi_2$ $(M+H)^+$: 1112.62, found 1112.4. All data were found to be in agreement with literature values.[84]

2'-Triisopropylsilyl-3'-dephenyl-3'-(2-methyl-2-propenyl)-7-triethylsilyl-10-(cyclopropanecarbonyl)docetaxel (2-8 B) [84]

According to the procedure previously listed for **2-8 A**, compound **2-6 F** (860 mg, 1.18 mmol) was used to produce **2-8 B** (1.011 g, 76%) as a white solid: ^{1}H NMR ($CDCl_3$, 300 MHz) δ 0.60 (m, 6H), 0.91 (m, 11 H), 1.05 (s, 3 H), 1.21 (s, 3 H), 1.40 (s, 9H), 1.68 (s, 3H), 1.76 (m, 1H), 1.82 (s, 3H), 1.85 (s, 3H),1.97 (m, 1H), 2.05 (m, 2 H), 2.19 (s, 3 H), 2.26 (s, 1H), 2.28 (s, 3H), 2.52 (m,

1H), 3.91 (d, J = 6.9 Hz, 1H), 4.19 (m, 1H), 4.26 (d, J = 8.7 Hz, 1H), 4.37 (d, J = 8.7 Hz, 1H), 4.52 (m, 2H), 4.88 (m, 2H), 5.00 (d, J = 8.4 Hz, 1H), 5.40 (d, J = 8.7 Hz, 1H), 5.75 (d, J = 6.9 Hz, 1H), 6.16 (t, J = 8.0 Hz, 1H), 6.55 (s, 1H), 7.53 (t, J = 7.5, 2H), 7.67 (t, J = 7.5 Hz, 1H), 8.17 (d, J = 7.5 Hz, 2H); MS (ESI) calcd for $C_{60}H_{94}O_{15}NSi_2$ $(M+H)^+$: 1124.62, found 1124.6. All data were found to be in agreement with literature values.[84]

2'-Triisopropylsilyl-3'-dephenyl-3'-(2-methyl-2-propenyl)-7-triethylsilyl-10-(*N*,*N*-dimethylcarbamoyl)docetaxel (2-8 C) [84]

According to the procedure previously listed for **2-8 A**, compound **2-6 J** (420 mg, 0.60mmol) was used to produce **2-8 C** (480 mg, 76%) as a white solid: ^{1}H NMR ($CDCl_3$, 300 MHz) δ 0.66 (m, 6H), 0.98 (m, 9H), 1.20 (m, 25 H), 1.26 (s, 3H), 1.37 (m, 1H), 1.42 (s, 9H), 1.60 (m, 1H), 1.72 (s, 3H), 1.82 (s, 6H), 1.92 (m, 1H), 2.11 (s, 3H), 2.42 (s, 3H), 2.60, (m, 1H), 3.00 (s, 3H), 3.13 (s, 3H), 3.81 (m, 3H), 3.93 (d, J = 7.2 Hz, 1H), 4.37 (d, J = 9.0 Hz, 1H), 4.47 (d, J = 9.0 Hz, 1H), 4.54 (m, 2H), 4.88 (m, 2H), 5.01 (d, J = 8.1 Hz, 1H), 5.40 (d, J = 8.7, 1H) 5.76 (d, J = 6.9 Hz, 1H), 6.17 (m, 1H), 6.35 (s, 1H), 7.53 (t, J = 7.5 Hz, 2H), 7.67 (t, J = 7.5 Hz, 1H), 8.18 (d, J = 7.2 Hz, 2H). MS (ESI) calcd for $C_{59}H_{95}O_{15}N_2Si_2$ $(M+H)^+$: 1127.63, found 1127.6. All data were in agreement with literature values[84]

2'-Triisopropylsilyl-3'-dephenyl-3'-(2-methyl-2-propenyl)-2-debenzoyl-2-(3-methoxybenzoyl)-7-triethylsilyl-10-(propanoyl)docetaxel (2-8 D) [84]

According to the procedure previously listed for **2-8 A**, compound **2-6 B** (120 mg, 0.28 mmol) was used to produce **2-8 D** (242 g, 97%) as a white solid: ^{1}H NMR ($CDCl_3$, 300 MHz) δ 0.53 – 0.61 (m, 6H), 0.91 (m, 9H), 1.08 – 1.18 (m, 21 H), 1.17 (s, 3 H), 1.21 (t, J = 7.8 Hz, 3H), 1.23 (s, 3H), 1.25 (s, 1H), 1.33 (s, 9H), 1.68 (s, 3H), 1.75 (s, 3H), 1.77 (s, 3H), 1.88 (m, 1H), 2.02 (s, 3H), 2.35 (m, 1H), 2.36 (s, 3 H), 2.41 – 2.57 (m, 3H), 3.84 (d, J = 6.6 Hz, 1H), 3.87 (s, 3H), 4.18 (d, J = 8.7 Hz, 1H), 4.32 (d, J = 8.7 Hz, 1H), 4.42 (d, J = 4.5 Hz, 1H), 4.47 (dd, J = 10.2, 6.6 Hz, 1H), 4.72 – 4.85 (m, 2H), 4.94 (d, J = 7.5 Hz, 1H), 5.33 (d, J = 8.4 Hz, 1H), 5.67 (d, J = 7.2 Hz, 1H), 6.08 (t, J = 9.6 Hz, 1H), 6.49 (s, 1H), 7.14 (m, 1H), 7.38 (t, J = 7.5 Hz, 1H), 7,64 (s, 1H), 7.70 (d, J = 7.8 Hz, 1H). All data were found to be in agreement with literature values.[84]

2'-Triisopropylsilyl-3'-dephenyl-3'-(2-methyl-2-propenyl)-2-debenzoyl-2-(3-methoxybenzoyl)-7-triethylsilyl-10-(cyclopropanelcarbonyl)docetaxel (2-8 E) [84]

According to the procedure previously listed for **2-8 A**, compound **2-6 G** (170 mg, 0.22 mmol) was used to produce **2-8 E** (194 mg, 76%) as a white solid: ^{1}H NMR ($CDCl_3$, 300 MHz) δ 0.53 – 0.61 (m, 6H), 0.82 – 0.93 (m, 11H), 1.08 – 1.18 (m, 23 H), 1.19 (s, 3 H), 1.23 (s, 3H), 1.25 (s, 1H), 1.33 (s, 9H), 1.68 (s, 3H), 1.73 – 1.78 (m, 1H), 1.75 (s, 3H), 1.77 (s, 3H), 1.76 (s,s 3H), 1.88 (m, 1H), 2.00 (s, 3H), 2.35 (s, 3 H) 2.51 (m, 1H), 3.83 (s, 3H), 3.84 (d, J = 9.0 Hz, 1H), 3.87 (s, 3H), 4.18 (d, J = 8.7 Hz, 1H), 4.34 (d, J = 9.0 Hz, 1H), 4.42 (d, J = 3.0 Hz, 1H), 4.47 (dd, J = 10.2, 6.9 Hz, 1H), 4.72 – 4.86 (m, 2H), 4.94 (d, J = 8.4 Hz, 1H), 5.33 (d, J = 8.4 Hz, 1H), 5.67 (d, J = 7.2 Hz, 1H), 6.08 (t, J = 7.5 Hz, 1H), 6.49 (s, 1H), 7.14 (m, 1H), 7.36 (t, J = 8.1Hz, 1H), 7,64 (s, 1H), 7.70 (d, J = 7.5 Hz, 1H). All data were found to be in agreement with literature values.[84]

2'-Triisopropylsilyl-3'-dephenyl-3'-(2-methyl-2-propenyl)-2-debenzoyl-2-(3-methoxybenzoyl)-7-triethylsilyl-10-(*N,N*-dimethylcarbamoyl)docetaxel (2-8 F)[84]

According to the procedure previously listed for **2-8 A**, compound **2-6 K** (165 mg, 0.18 mmol) was used to produce **2-8 F** (192 mg, 82%) as a white solid: ^{1}H NMR ($CDCl_3$, 300 MHz) δ 0.55-0.63 (m, 6H), 0.89-0.95 (m, 9H), 1.09 (m, 21H), 1.11 (s, 3H), 1.25 (s, 3H), 1.33 (s, 9H), 1.68 (s, 3H), 1.73 (s, 3H), 1.76 (s, 3H), 1.87 (m, 1H), 2.35 (s, 3H), 2.30-2.48 (m, 2H), 2.53 (m, 1H), 2.94 (s, 3H), 3.06 (s, 3H), 3.86 (d, J = 6.9 Hz, 1H), 3.87 (s, 3H), 4.19 (d, J = 8.5 Hz, 1H), 4.35 (d, J =8.5 Hz, 1H), 4.42 (m, 1H), 4.46 (m, 1H), 4.74 (m, 1H), 4.82 (m, 1H), 4.95 (m, 1H), 5.33 (d, J = 8.7 Hz, 1H), 5.68 (d, J = 6.9 Hz, 1H), 6.09 (t, J = 7.2 Hz, 1H), 6.40 (s, 1H), 7.13 (dd, J = 8.4, 2.7 Hz, 1H), 7.36 (t, J = 8.1 Hz, 1H), 7.65 (s, 1H), 7.70 (d, J = 7.8 Hz, 1H). All data were found to be in agreement with literature values.[84]

2'-Triisopropylsilyl-3'-dephenyl-3'-(2-methyl-2-propenyl)-2-debenzoyl-2-(3-methoxybenzoyl)-7-triethylsilyl-10-(*p*-methoxyphenylacetyl)docetaxel (2-8 G)[84]

According to the procedure previously listed for **2-8 A**, compound **2-6 O** (75 mg, 0.09 mmol) was used to produce **2-8G** (93 mg, 79%) as a white solid: ^{1}H NMR ($CDCl_3$, 300 MHz) δ 0.52-0.69 (m, 6H), 0.82-0.96 (m, 9H), 1.018 (s, 3H), 1.06-1.15 (m, 21H), 1.122 (s, 3H), 1.329 (s, 9H), 1.678 (s, 3H), 1.738 (s, 3H), 1.754 (s, 3H), 1.80-1.94 (m, 1H), 1.981 (s, 3H), 2.24-2.40 (m, 2H), 2.341 (s, 3H), 2.43-2/58 (m, 1H), 3.691 (d, J = 5.4 Hz, 1H), 3.75-3.82 m, 1H), 3.788 (s, 3H), 3.860 (s, 3H), 4.173 (d, J = 8.4 Hz, 1H), 4.336 (d, J = 8.4 Hz, 1H), 4.40-4.43 (m, 1H), 4.444 (dd, J = 6.6, 10.5 Hz, 1H), 4.69-4.79 (m, 1H), 4.80-4.87 (m, 1H), 4.933(d, J = 8.4 Hz, 1H), 5.656 (d, J = 6.9 Hz, 1H), 6.029 (m, 1H), 6.448 (s, 1H), 6.869 (d, J = 8.7 Hz, 2H), 7.129 (dd, J = 7.8, 2.7 Hz, 1H), 7.244 (d, J = 8.7 Hz, 1H), 7.353 (t, J = 7.8 Hz, 1H), 7.631 (d, J = 2.7 Hz, 1H), 7.688 (d, J = 7.8 Hz, 1H). All data were found to be in agreement with literature values.[84]

2'-Triisopropylsilyl-3'-dephenyl-3'-(2-methyl-2-propenyl)-2-debenzoyl-2-(3-methylbenzoyl)-7-triethylsilyl-10-(propanoyl)docetaxel (2-8 H)

According to the procedure previously listed for **2-8 A**, compound **2-6 C** (180 mg, 0.31 mmol) was used to produce **2-6 H** (253 mg, 91%) as a white solid: ^{1}H NMR ($CDCl_3$, 300 MHz) δ 0.53-0.62 (m, 6H), 0.81 – 0.92 (m, 9H), 1.06 – 1.16 (m, 21H), 1.26 – 1.33 (m, 10 H),1.33 (s, 9 H), 1.68 (s, 3H), 1.72 (s, 1H), 1.74 (s, 3 H), 1.77 (s, 3H), 1.87 (m, 1H), 2.01 (s, 3H), 2.36 (s, 3H), 2.40 (m, 3H), 2. 41 (s, 3H), 2.48 (m, 1H), 3.85 (d, J = 7.5 Hz, 1H), 4.17 (d, 8.4 Hz, 1H), 4.31 (d, J = 8.4 Hz, 1H), 4.42 – 4.50 (m, 2H), 4.78 – 4.87 (m, 2H), 4.94 (d, J = 8.4 Hz, 1H), 5.33 (d, J = 8.4 Hz, 1H), 5.67 (d, J = 7.2 Hz, 1H), 6.07 (t, J = 8.4 Hz), 6.49 (s, 1H), 7.30 – 7.42 (m, 2H), 7.90 (d, J = 8.1 Hz, 1H), 7.93 (s, 1H). MS (ESI) calcd for $C_{60}H_{96}NO_{15}Si_2$ $(M+H)^+$: 1126.62, found 1126.6.

2'-Triisopropylsilyl-3'-dephenyl-3'-(2-methyl-2-propenyl)-2-debenzoyl-2-(3-methylbenzoyl)-7-triethylsilyl-10-(cyclopropanecarbonyl)docetaxel (2-8 I)

According to the procedure previously listed for **2-8 A**, compound **2-6 H** (160 mg, 0.22 mmol) was used to produce **2-8 I** (235 mg, 95%) as a white solid: ^{1}H NMR ($CDCl_3$, 300 MHz) δ 0.54-0.63 (m, 6H), 0.84-0.95 (m, 11H), 1.04 – 1.10 (m, 23H), 1.19 (s, 3H), 1.23 (s, 3H), 1.25 (s, 1H),

1.33 (s, 9H), 1.67 (s, 3H), 1.74 (s, 3H), 1.76 (m, 1H), 1.77 (s, 3H), 1.88 (m, 1H), 2.00 (s, 3H), 2.36 (s, 3H), 2.35- 2.40 (m , 3H), 2.41 (s, 3H), 2.49 (m, 1H), 3.83 (d, J = 6.9 Hz, 1H), 4.18 (d, 8.4 Hz, 1H), 4.32 (d, J = 8.4Hz, 1H), 4.42 – 4.50 (m, 2H), 4.72 – 4.86 (m, 2H), 4.94 (d, J = 8.1 Hz, 1H), 5.33 (d, J = 8.1 Hz, 1H), 5.67 (d, J = 6.9 Hz, 1H), 6.07 (t, J = 7.8 Hz), 6.48 (s, 1H), 7.33 – 7.42 (m, 2H), 7.90 (d, J = 7.8 Hz, 1H), 7.93 (s, 1H). MS (ESI) calcd for $C_{61}H_{96}NO_{15}Si_2$ $(M+H)^+$: 1138.62, found 1138.6.

2'-Triisopropylsilyl-3'-dephenyl-3'-(2-methyl-2-propenyl)-2-debenzoyl-2-(3-methylbenzoyl)-7-triethylsilyl-10-(*N*,*N*-dimethylcarbamoyl)docetaxel (2-8 J)

According to the procedure previously listed for **2-8 A**, compound **2-6 L** (165 mg, 0.22 mmol) was used to produce **2-8 J** (229 mg, 90%) as a white solid: ^{1}H NMR ($CDCl_3$, 300 MHz) δ 0.54-0.63 (m, 6H), 0.93 (m, 9H), 1.10 (m, 21H), 1.18 (s, 3H), 1.21 (s, 3H), 1.33 (s, 9H), 1.67 (s, 3H), 1.74 (s, 3H), 1.77 (s, 3H), 1.87 (m, 1H), 2.05 (s, 3H), 2.36 (s, 3H), 2.41 (s, 3H), 2.49 (m, 1H), 2.93 (s ,3H) 3.05 (s, 3H), 3.85 (d, J = 7.2 Hz, 1H), 4.18 (d, 7.8 Hz, 1H), 4.33 (d, J = 7.8 Hz, 1H), 4.42 – 4.50 (m, 2H), 4.75 – 4.85 (m, 2H), 4.94 (d, J = 8.1 Hz, 1H), 5.33 (d, J = 8.4 Hz, 1H), 5.67 (d, J = 7.2 Hz, 1H), 6.09 (t, J = 8.1 Hz), 6.40 (s, 1H), 7.33 – 7.42 (m, 2H), 7.90 (d, J = 7.8 Hz, 1H), 7.93 (s, 1H). MS (ESI) calcd for $C_{60}H_{97}N_2O_{15}Si_2$ $(M+H)^+$: 1141.63, found: 1141.6.

2'-Triisopropylsilyl-3'-dephenyl-3'-(2-methyl-2-propenyl)-2-debenzoyl-2-(2,5-dimethoxybenzoyl)-7-Triethylsilyl-10-(propanoyl)docetaxel (2-8 K)

According to the procedure previously listed for **2-8 A**, compound **2-6 D** (200 mg, 0.28 mmol) was used to produce **2-8 K** (278 mg, 92%) as a white solid: ^{1}H NMR ($CDCl_3$, 300 MHz) δ 0.49-0.64 (m, 6H), (0.84-0.97 (m, 9H), 1.05-1.16 (m, 21H), 1.199 (s, 3H), 1.224 (s, 3H), 1.16-1.30 (m, 2H), 1.373 (s, 9H), 1.685 (s, 3H), 1.722 (s, 6H), 1.84-1.96 (m, 1H), 2.005 (s, 3H), 2.169 (s, 3H), 2.28-2.58 (m, 5H), 3.223 (s, br, 1H), 3.759, (d, J = 6.3 Hz, 1H), 3.804 (s, 3H), 3.966 (s, 3H), 4.283 (d, J = 8.1 Hz, 1H), 4.441 (d, J = 8.1 Hz, 1H), 4.36-4.49 (m, 2H), 4.758 (t, J = 9.9 Hz, 1H), 4.89 (m, 2H), 5.342 (d, J = 8.7 Hz, 1H), 5.677 (d, J = 6.6 Hz, 1H), 6.063 (m, 1H), 6.674 (s, 1H), 6.945 (d, J = 9.0 Hz, 1H), 7.061 (dd, J = 9.0, 3.0 Hz, 1H), 7.301 (d, 3.0 Hz, 1H). MS (ESI) calcd for $C_{61}H_{98}NO_{17}Si_2$ $(M+H)^+$: 1172.63, found 1172.6.

2'-Triisopropylsilyl-3'-dephenyl-3'-(2-methyl-2-propenyl)-2-debenzoyl-2-(2,5-dimethoxybenzoyl)-7-triethylsilyl-10-(cyclopropanecarbonyl)docetaxel (2-8 L)

According to the procedure previously listed for **2-8 A**, compound **2-6 I** (200 mg, 0.28 mmol) was used to produce **2-8 L** (155 mg, 74% yield based on 70% conversion) as a white solid: ^{1}H NMR ($CDCl_3$, 300 MHz) δ 0.50-0.65 (m, 6H), 0.83-0.97 (m, 9H), 1.00-1.04 (m, 2H), 1.05-1.13 (m, 21H), 1.18-1.31 (m, 2H), 1.218 (s, 3H), 1.234 (s, 3H), 1.377 (s, 9H), 1.686 (s, 3H), 1.723 (s, 6H), 1.82-1.96 (m, 1H), 1.997 (s, 3H), 2.165 (s, 3H), 2.29-2.41 (m, 2H), 2.42-2.56 (m, 1H), 3.20 (s, br, 1H), 3.757 (d, J = 6.6 Hz,1H), 3.807 (s, 3H), 3.969 (s, 3H), 4.283 (d, J = 7.8 Hz, 1H), 4.36-4.48 (m, 3H), 4.71-4.80 (m, 1H), 4.81-4.92 (m, 2H), 5.347 (d, J = 9.9 Hz, 1H), 5.681 (d, J = 6.3 Hz, 1H), 6.608 (m, 1H), 6.047 (s, 1H), 6.946 (d, J = 9.0 Hz, 1H), 7.031 (J = 9.0, 3.0 Hz, 1H), 7.308 (d, J = 3.0 Hz, 1H). MS (ESI) calcd for $C_{62}H_{98}NO_{17}Si_2$ $(M+H)^+$: 1184.63, found 1184.6.

2'-Triisopropylsilyl-3'-dephenyl-3'-(2-methyl-2-propenyl)-2-debenzoyl-2-(2,5-dimethoxybenzoyl)-7-triethylsilyl-10-(*N*,*N*-dimethylcarbamoyl)docetaxel (2-8 M)

According to the procedure previously listed for **2-8 A**, compound **2-6 M** (150 mg, 0.19 mmol) was used to produce **2-8 M** (160 mg, 94% based on 75% conversion) as a white solid: ^{1}H NMR ($CDCl_3$, 300 MHz) δ 0.52-0.69 (m, 6H), 0.82-1.00 (m, 9H), 1.04-1.15 (m, 21H), 1.219 (s, 6H), 1.375 (s, 9H), 1.685 (s, 3H), 1.721 (s, 3H), 1.727 (s, 3H), 1.81-1.96 (m, 1H), 2.043 (s, 3H), 2.168 (s, 3H), 2.168 (s, 3H), 2.30-2.42 (m, 2H), 2.43-2.57 (m, 1H), 2.929 (s, 3H), 3.056 (s, 3H), 3.19 (s, br, 1H), 3.77-3.81 (m, 1H), 3.806 (s, 3H,), 3.969 (s, 3H), 4.284 (d, J = 8.4 Hz, 1H), 4.34-4.44 (m, 2H), 4.754 (t, J = 9.0 Hz, 1H), 5.347 (d, J = 9.0 Hz, 1H), 5.685 (d, J = 6.6 Hz, 1H), 6.084 (m, 1H), 6.393 (s, 1H), 6.946 (d, J = 9.0 Hz, 1H), 7.060 (dd, J = 9.0, 3.0 Hz, 1H), 7.308 (d, J = 3.0 Hz, 1H). MS (ESI) calcd for $C_{61}H_{99}N_2O_{17}Si_2$ $(M+H)^+$: 1187.64, found 1187.5.

2'-Triisopropylsilyl-3'-dephenyl-3'-(2-methyl-2-propenyl)-2-debenzoyl-2-(2,5-dimethylbenzoyl)-7-triethylsilyl-10-(propanoyl)docetaxel (2-8 N)

According to the procedure previously listed for **2-8 A**, compound **2-6 F** (120 mg, 0.16 mmol) was used to produce **2-8 N** (174 g, 95%) as a white solid: ^{1}H NMR ($CDCl_3$, 300 MHz) δ 0.51-0.63 (m, 6H), 0.83-0.98 (m, 9H), 1.04-1.16 (m, 21H), 1.178 (s, 3H), 1.19-1.28 (m, 2H), 1.232 (s, 3H), 1.347 (s, 9H), 1.684 (s, 3H), 1.735 (s, 3H), 1.752 (s, 3H), 1.81-1.94 (m, 1H), 2.012 (s, 3H), 2.330 (s, 3H), 2.364 (s, 3H), 2.37-2.41 (m, 2H), 2.42-2.58 (m, 4H), 2.594 (s, 3H), 3.823 (d, J = 6.3 Hz, 1H), 4.177 (d, J = 8.1 Hz, 1H), 4.267 (d, J = 81 Hz, 1H), 4.416 (d, J = 2.6 Hz, 1H), 4.42-4.50 (m, 1H), 4.70-4.87 (m, 2H), 4.943 (d, J = 7.2 Hz, 1H), 5.329 (d, J = 8.1 Hz, 1H), 5.667 (d, J = 7.5 Hz, 1H), 6.073 (m, 1H), 6.489 (s, 1H), 7.148 (d, J = 7.8 Hz, 1H), 7.248 (d, J = 7.8 Hz, 1H), 7.930 (s, 1H). MS (ESI) calcd for $C_{61}H_{98}NO_{15}Si_2$ $(M+H)^+$: 1140.64, found: 1140.7.

2'-Triisopropylsilyl-3'-dephenyl-3'-(2-methyl-2-propenyl)-2-debenzoyl-2-(2,5-dimethylbenzoyl)-7-triethylsilyl-10-(*N*,*N*-dimethylcarbamoyl)docetaxel (2-8 O)

According to the procedure previously listed for **2-8 A**, compound **2-6 N** (110 mg, 0.15 mmol) was used to produce **2-8 O** (163 mg, 97%) as a white solid: ^{1}H NMR ($CDCl_3$, 300 MHz) δ 0.55-0.68 (m, 6H), 0.82-1.01 (m, 9H), 1.02-1.13 (m, 24H), 1.22 (s, 3H), 1.38 (s, 9H), 1.61 (s, 3H), 1.69 (s, 3H), 1.73 (s, 3H), 1.89 (m, 1H), 2.04 (s, 3H), 2.17 (s, 3H), 2.30-2.52 (m, 3H), 2.93 (s, 3H), 3.06 (s, 3H), 3.18 (s, br, 1H), 3.78 (d, J = 6.3 Hz, 1H), 3.81 (s, 3H), 3.97 (s, 3H), 4.29 (d, J = 6.3 Hz, 1H), 4.40 (m, 2H), 4.44 (d, J = 8.4 Hz, 1H), 4.75 (m, 1H), 4.89 (m, 2H), 5.34 (d, 1H), 5.68 (d, J = 6.6 Hz, 1H), 6.08 (t, J = 9.6 Hz, 1H), 6.39 (s, 1H), 6.95 (d, J = 9.3 Hz, 1H), 7.06 (dd, J = 9.0, 3.0 Hz, 1H), 7.31 (m, 1H). MS (ESI) calcd for $C_{61}H_{97}N_2O_{15}Si_2$ $(M+H)^+$: 1155.65, found 1155.7.

3'-Dephenyl-3'-(2-methyl-2-propenyl)-10-(propanoyl)docetaxel [SB-T-1213] [84]

Compound **2-8 A** (560 mg, 0.50 mmol) of was dissolved in a 1:1 mixture of acetonitrile:pyridine (34 mL total) and cooled to 0 °C under inert conditions. To the mixture excess HF, 70% in pyridine (5.6 mL), was added dropwise. The reaction was stirred at room temperature and monitored by TLC. Upon completion the reaction was quenched with 10% aqueous citric acid (5 mL), neutralized with saturated $NaHCO_3$ (30 mL) and extracted with ethyl acetate (2 x 30 mL). The

organic layer was collected, washed with saturated $CuSO_4$ solution (3 x 30 mL), water (2 x 30 mL) and brine (3 x 30 mL). The extract was then dried over anhydrous $MgSO_4$, and concentrated *in vacuo*. Purification was done by column chromatography on silica gel with increasing amounts of ethyl acetate in hexanes (hexanes:ethyl acetate = 1:0 – 2:1) to afford **SB-T-1213 (**335 mg, 84% yield) as a crystalline white solid. The purity of this compound was determined to be >97% by HPLC, using conditions detailed in **Section 3.1.0**: (m.p. = 153-154). ^{1}H NMR (500 MHz, $CDCl_3$) δ 0.91 (m, 1H), 1.15 (s, 3H), 1.23 (t, J = 7.5 Hz, 3H), 1.35 (s, 9H), 1.65 (m, 1H), 1.68 (s, 3H), 1.75 (s, 1H), 1.77 (s, 6H), 1.88 (m, 1H), 1.90 (s, 3H), 2.04 (s, 1H), 2.36 (s, 1H), 2.38 (m, 1H), 2.53 (m, 2H), 2.54 (q, J = 7.5 Hz, 2H), 3.39 (m, 1H), 3.82 (d, J = 6.5 Hz, 1H), 4.20 (m, 2H), 4.30 (d, J = 8.0 Hz, 1H), 4.48 (t, J = 8.0 Hz, 1H), 4.74, (m, 2H), 4.96 (d, J = 8.0 Hz, 1H), 5.51 (d, J = 7.5 Hz, 1H), 5.67 (d, J = 7.0 Hz, 1H), 6.17 (t, J = 9.0 Hz, 1H), 6.32 (s, 1H), 7.47 (t, J = 8.0 Hz, 2H), 7.60 (t, J = 8.0 Hz, 1H), 8.10 (d, J = 7.5 Hz, 1H). ^{13}C NMR (400 MHz, $CDCl_3$) δ 9.05, 9.57, 14.96, 18.58, 21.88, 22.42, 25.73, 26.67, 27.59, 28.52, 29.73, 35.60, 35.64, 43.22, 45.70, 51.63, 58.61, 72.22, 72.36, 73.79, 75.12, 75.48, 76.47, 79.19, 79.99, 81.11, 84.47, 120.67, 128.66, 129.27, 130.17, 132.78, 133.69, 137.95, 142.25, 166.97, 170.12, 174.64, 203.85. MS (ESI) calcd for $C_{44}H_{60}O_{15}N$ $(M+H)^+$: 842.40, found 842.3. All data were found to be in agreement with literature values.[84]

3'-Dephenyl-3'-(2-methyl-2-propenyl)-10-(cyclopropanecarbonyl)docetaxel [SB-T-1214][84]

According to the procedure previously listed for **SB-T-1213**, compound **2-8 B** (1.01 g, 0.90 mmol) was used to produce **SB-T-1214** (617 mg, 81% yield) as a crystalline white solid. The purity of this compound was determined to be >96% by HPLC, using conditions detailed in **Section 3.1.0**: mp 155-156 ^{o}C (lit.158-160 ^{o}C); ^{1}H NMR (300 MHz, $CDCl_3$) δ 1.08 (m, 2H), 1.20 (m, 1H), 1.23 (s, 3H), 1.33 (s, 3H), 1.42 (s, 9H), 1.74 (s, 3H), 1.79 (s, 1H), 1.83 (s, 6H), 1.90 (m, 1H), 1.97 (s, 3H), 2.11 (s, 1H), 2.42 (s, 3H), 2.45 (m, 1H), 2.60 (m, 1H), 2.65 (m, 1H), 3.45 (d, J = 6.6 Hz, 1H), 3.88 (d, J = 6.9 Hz, 1H), 4.24 (m, 2H), 4.38 (d, 8.4 Hz, 1H) 4.48 (m, 1H), 4.83 (m, 2H), 5.03 (d, 7.8 H), 5.38 (m, 1H), 5.74 (d, 7.2 Hz, 1H), 6.24 (t, 1H), 6.37 (s, 1H), 7.54 (t, 7.2, 2H), 7.68 (t, 7.5 Hz, 1H), 8.17 (d, 7.2 Hz, 2H). MS (ESI) calcd for $C_{45}H_{60}O_{15}N$ $(M+H)^+$: 854.40, found 854.4. All data were found to be in agreement with literature values.[84]

3'-Dephenyl-3'-(2-methyl-2-propenyl)-10-(*N*,*N*-dimethylcarbamoyl)docetaxel (SB-T-1216) [84]

According to the procedure previously listed for **SB-T-1213**, compound **2-8 C** (460 mg, 0.41 mmol) was used to produce **SB-T-1216** (319 mg, 92% yield) as a white solid: m.p. = 161 – 162^{o}C. ^{1}H NMR (400 MHz, $CDCl_3$) δ 1.23 (s, 3H), 1.30 (s, 3H), 1.36 (m, 1H), 1.42 (s, 9H), 1.74 (s, 3H), 1.79 (m, 1H), 1.81 (s, 6H), 1.96 (m, 1H), 2.11 (s, 3H), 2.43 (s, 3H), 2.46 (m, 1H), 2.60 (m, 1H), 3.03 (s, 3H), 3.11 (s, 3H), 3.28 (d, J = 3.6 Hz, 1H), 3.43 (m, 1H), 2.88 (d, J = 6.9 Hz, 1H), 4.20 (m, 2H), 4.27 (d, J = 8.4 Hz, 1H), 4.38 (d, J = 8.4 Hz, 1H), 4.53 (m, 1H), 4.81 (m, 1H), 5.05 (d, J = 7.8 Hz, 1H), 5.73 (d, J = 6.9 Hz, 1H), 5.25 (t, 1H), 6.33 (s, 1H), 7.54 (t, J = 7.2 Hz, 2H), 7.68 (t, J = 7.2, 1H), 8.18 (d, J = 7.2 Hz, 2H). ^{13}C NMR (125 MHz, $CDCl_3$) δ 9.33, 10.14, 14.28, 18.64, 21.31, 22.40, 25.78, 26.92, 28.30, 35.46, 35.75, 36.01, 36.68, 43.27, 45.68, 58.50, 59.31, 72.46, 72.52, 73.85, 75.28, 76.51, 79.34, 80.02, 81.21, 84.73, 120.76, 128.59, 129.36, 130.22, 133.70,

133.59, 156.21, 166.93, 130.02, 205.76. MS (ESI) calcd for $C_{44}H_{62}O_{15}N_2$ $(M+H)^+$: 857.41, found 857.3. All data were found to be in agreement with literature values.[84]

3'-Dephenyl-3'-(2-methyl-2-propenyl)-2-debenzoyl-2-(3-methoxybenzoyl)-10-(propanoyl)-docetaxel [SB-T-121303][84]

According to the procedure previously listed for **SB-T-1213**, compound **2-8 D** (220 mg, 0.19 mmol) was used to produce **SB-T-121303 (**164 mg, 98% yield) as a white solid. ^{1}H NMR (500 MHz, $CDCl_3$) δ 1.16 (s, 3H), 1.22 (t, J = 7.5 Hz, 3H), 1.26 (s, 3H), 1.35 (s, 9H), 1.68 (s, 3H), 1.74 (s, 3H), 1.77 (s, 3H), 1.88 (m, 1H), 1.90 (s, 3H), 2.34-2.41 (m, 2H), 2.36 (s, 3H), 2.46-2.60 (m, 4H), 3.49 (s, br, 1H), 3.83 (d, J = 7.0 Hz, 1H), 3.88 (s, 3H), 4.20 (m, 2H), 4.35 (d, J = 8.5 Hz, 1H), 4.44 (m, 1H), 4.74 (m, 1H), 4.78 (m, 1H), 4.98 (d, J = 8.5 Hz, 1H), 5.33 (m, 1H), 5.67 (d, J = 7.0 Hz, 1H), 6.18 (t, J = 9.0 Hz, 1H), 6.32 (s, 1H), 7.15 (dd, J = 8.0, 2.0 Hz, 1H), 7.38 (t, J = 8.0 HZ, 1H), 7.65 (s, 1H), 7.71 (d, J = 7.5 Hz, 1H); ^{13}C NMR (125 MHz, $CDCl_3$) δ 9.06, 9.56, 14.97, 18.55, 21.88, 22.43, 25.73, 26.64, 27.60, 28.22, 29.72, 35.54, 43.20, 45.66, 51.53, 55.38, 58.56, 72.19, 72.38, 73.71, 73.13, 75.46, 76.47, 79.08, 79.99, 81.12, 84.45, 114.62, 120.14, 120.64, 122.55, 129.67, 130.45, 132.93, 137.90, 142.50, 155.44, 159.63, 166.81, 170.09, 173.19, 174.67, 203.86. All data were found to be in agreement with literature values.[84]

3'-Dephenyl-3'-(2-methyl-2-propenyl)-2-debenzoyl-2-(3-methoxybenzoyl)-10-(cyclopropanecarbonyl)docetaxel [SB-T-121403][84]

According to the procedure previously listed for **SB-T-1213**, compound **2-8 E** (180 mg, 0.156 mmol) was used to produce **SB-T-121403** (132 mg, 95%) as a white solid: ^{1}H NMR (500 MHz, $CDCl_3$) δ 1.03 (m, 2H), 1.17 (m, 2H), 1.19 (s, 3H), 1.29 (s, 3H), 1.38 (s, 9H), 1.70 (s, 3H), 1.77 (s, 3H), 1.81 (s, 3H), 1.83 (m, 1H), 1.90 (m, 1H), 1.93 (s, 3H), 2.37 (s, 3H), 2.38-2.43 (m, 2H), 2.59 (m, 1H), 2.63 (s, br, 1H), 3.84 (d, J = 7.0 Hz, 1H), 3.90 (s, 3H), 4.22 (m, 2H), 4.38 (d, J = 8.5 Hz, 1H), 4.76 (m, 1H), 4.80 (m, 1H), 5.00 (d, J = 8.0, 1H), 5.35 (m, 1H), 5.69 (d, J = 7.0 Hz, 1H), 6.21 (t, J = 8.0 Hz, 1H), 6.33 (s, 1H), 7.18 (dd, J = 8.0, 2.0 Hz, 1H), 7.41 (t, J = 8.0 Hz, 1H), 7.67 (s, 1H), 7.73 (d, J = 7.5 Hz, 1H); ^{13}C NMR (125 MHz, $CDCl_3$) δ 9.24, 9.49, 9.53, 13.06, 15.02, 18.56, 21.98, 22.44, 23.74, 26.72, 28.23, 35.56, 35.58, 43.21, 45.63, 51.52, 55.34, 58.58, 72.24, 72.40, 73.71, 75.14, 75.47, 76.47, 79.14, 80.05, 81.12, 84.44, 114.61, 120.16, 120.64, 122.56, 129.67, 130.49, 132.90, 137.93, 142.70, 155.42, 159.65, 166.83, 170.05, 173.18, 175.18, 203.96. All data were found to be in agreement with literature values.[84]

3'-Dephenyl-3'-(2-methyl-2-propenyl)-2-debenzoyl-2-(3-methoxybenzoyl)-10-(*N*,*N*-dimethylcarbamoyl)docetaxel [SB-T-121603][84]

According to the procedure previously listed for **SB-T-1213**, compound **2-8 F** (175 mg, 0.15 mmol) was used to produce **SB-T-121603** (124 mg, 91%) as a white solid: ^{1}H NMR (500 MHz, $CDCl_3$) δ 1.17 (s, 3H), 1.26 (s, 3H), 1.41. (s, 9H), 1.68 (s, 3H), 1.75 (s, 3H), 1.79 (s, 3H), 1.89 (m, 1H), 1.93 s, 3H), 2.36 (s, 3H), 2.38 (m, 2H), 2.54(m, 1H), 2.97 (s, 3H), 3.06 (s, 3H), 3.41 (s, br, 1H), 3.82 (d, J = 6.5 Hz, 1H), 3.88 (s, 3H), 4.21 (m, 2H), 4.36 (d, J = 8.5 Hz, 1H), 4.46 (m, 1H), 4.75 (m, 1H), 4.79 (m, 1H), 5.00 (d, J = 8.5 Hz, 1H), 5.33 (m, 1H), 5.67 (d, J = 6.5 Hz, 1H), 6.20

(t, J = 9.0 Hz, 1H), 6.27 (s, 1H), 7.16 (m, 1H), 7.34 (t, J = 8.0 Hz, 1H), 7.65 (s, 1H), 7.71 (d, J = 8.5 Hz, 1H). All data were found to be in agreement with literature values.[84]

3'-Dephenyl-3'-(2-methyl-2-propenyl)-2-debenzoyl-2-(3-methoxybenzoyl)-10-(*p*-methoxyphenylacetyl)docetaxel [SB-T-12130301][84]

According to the procedure previously listed for **SB-T-1213**, compound **2-8 G** (85 mg, 0.05 mmol) was used to produce **SB-T-12130301** (68 mg, 97 %) as a white solid: ^{1}H NMR (500 MHz, $CDCl_3$) δ 1.10 (s, 3H), 1.21 (s, 3H), 1.37 (s, 9H), 1.71 (s, 3H), 1.77 (s, 3H), 1.79 (s, 3H), 1.90 (m, 1H), 1.93 (s, 1H), 2.37-2.50 (m, 2H), 2.38 (s, 3H), 2.58 (m, 1H), 3.40 (s, br, 1H), 3.81 (s, 2H), 3.83 (s, 3H), 3.90 (s, 3H), 4.20 (d, J = 8.5 Hz, 1H), 4.21 (m, 1H), 4.39 (d, J = 8.5 Hz, 1H), 4.42 (m, 1H), 4.77 (m, 2H), 4.99 (d, J = 8.0 Hz, 1H), 5.36 (m, 1H), 5.68 (d, J = 7.0 Hz, 1H), 6.16 (t, J = 8.5 Hz, 1H), 6.35 (s, 1H) 6.91 (d, J = 8.5 Hz, 2H), 7.17 (m, 1H), 7.25 (d, J = 8.5 Hz, 2H), 7.41 (t, J = 8.0 Hz, 1H), 7.66 (s, 1H), 7.72 (d, J = 7.5 Hz, 1H); ^{13}C NMR (125 MHz, $CDCl_3$) δ 9.61, 14.95, 18.55, 21.69, 22.42, 22.73, 26.48, 28.23, 29.72, 35.55, 35.66, 40.14, 43.14, 45.72, 55.30, 55.38, 58.56, 72.07, 72.07, 73.71, 75.09, 75.91, 76.45, 79.03, 79.98, 81.09, 84.42, 114.02, 114.62, 120.14, 122.55, 125.37, 129.66, 130.49, 130.59, 132.76, 137.88, 142.48, 155.43, 158.79, 159.65, 166.79. 170.08, 172.85, 173.16, 203.46. All data were found to be in agreement with literature values.[84]

3'-Dephenyl-3'-(2-methyl-2-propenyl)-2-debenzoyl-2-(3-methylbenzoyl)-10-(propanoyl)-docetaxel [SB-T-121302]

According to the procedure previously listed for **SB-T-1213**, compound **2-8 H** (230 mg, 0.20 mmol) was used to produce **SB-T-121302** (153 mg, 87%) as a white solid: m.p. = 165-167 ^{o}C; ^{1}H NMR (500 MHz, $CDCl_3$) δ 0.82 – 0.98 (m, 2H), 1.14 (s, 3H), 1.23 (t, J = 7.8 Hz, 3H), 1.25 (s, 3H), 1.34 (s, 9 H), 1.65 (s, 1H), 1.67 (s, 3H), 1.73 (s, 1H), 1.75 (s, 3 H), 1.76 (s, 3H), 1.87 (m, 1H), 1.89 (s, 3H), 2.36 (s, 3H), 2.40 (m, 1H), 2.42 (s, 3H), 2.48 – 2.62 (m, 4H), 3.38 (d, J = 6.9 Hz, 1H), 3.81 (d, J = 7.2 Hz, 1H), 4.13 – 4.22 (m, 2H), 4.31 (d, J = 7.8 Hz, 1H), 4.42 (m, 1H), 4.73 – 4.80 (m, 2H), 4.97 (d, J = 9.6 Hz, 1H), 5.33 (d, J = 8.1 Hz, 1H), 5.65 (d, J = 6.6 Hz, 1H), 6.16 (t, J = 8.7 Hz), 6.31 (s, 1H), 7.30 – 7.42 (m, 2H), 7.90 (d, J = 7.5 Hz, 1H), 7.93 (s, 1H); ^{13}C NMR (125 MHz, $CDCl_3$) δ 9.06, 9.56, 14.99, 18.59, 21.38, 21.88, 22.38, 25.74, 26.64, 27.60, 28.23, 35.58, 43.20, 45.68, 51.57, 58.57, 72.25, 72.45, 73.75, 74.92, 75.47, 76.49, 79.16, 79.97, 91.10, 84.43, 120.65, 127.32, 128.54, 129.12, 130.83, 132.93, 134.48, 137.89, 138.36, 142.51, 153.43, 167.08, 170.04, 173.17, 174.68, 203.86. HRMS (ESI) calcd for $C_{45}H_{62}NO_{15}$ $(M+H)^+$: 856.4119, found 856.4101 (Δ -2.1 ppm, -1.8 mDa).

3'-Dephenyl-3'-(2-methyl-2-propenyl)-2-debenzoyl-2-(3-methylbenzoyl)-10-(cyclopropanecarbonyl)docetaxel [SB-T-121402]

According to the procedure previously listed for **SB-T-1213**, compound **2-8 I** (220 mg, 0.19 mmol) was used to produce **SB-T-121402** (98mg, 59%) as a white solid: m.p. = 172-174 ^{o}C; ^{1}H NMR (400 MHz, $CDCl_3$) δ 1.02 (m, 2H), 1.61 (m, 2H), 1.18 (s, 3H), 1.28 (s, 3H), 1.38 s, 9H), 1.67 (s,

3H), 1.77 (s, 3H), 1.81 (s, 3H), 1.85 (m, 1H), 1.89 (m, 1H), 1.92 (s, 3H), 2.37 (s, 3H), 2.42 (m, 1H), 2.45 (s, 3H), 2.52-2.61 (m, 2H), 3.82 (d, J = 6.8 Hz, 1H), 3.90 (s, br, 1H), 4.22 (d, J = 8.4 Hz, 1H), 4.24 (m, 1H), 4.33 (d, J = 8.4 Hz, 1H), 4.75-4.83 (m, 2H), 4.78 (m, 1H), 4.99 (d, J = 8.0 Hz, 1H), 5.34 (d, J = 8.0 Hz, 1H), 5.66 (d, J = 6.8 Hz, 1H), 6.19 (t, J = 8.4 Hz, 1H), 6.32 (s, 1H), 7.37 (t, J = 7.6 Hz, 1H), 7.43 (d, J = 7.6 Hz, 1H), 7.92 (d, J = 7.6 Hz, 1H), 7.95 (s, 1H); ^{13}C NMR (125 MHz, $CDCl_3$) δ 9.19, 9.43, 9.51, 13.04, 14.98, 18.56, 21.35, 21.45, 22.35, 25.71, 26.69, 28.2 2, 35.54, 43.19, 45.66, 51.56, 58.56, 72.24, 72.41, 73.73, 74.95, 75.44, 79.17, 79.95, 81.11, 84.44, 120.67, 127.31, 128.57, 129.14, 139.81, 132.94, 134.45, 137.56, 138.34, 142.64, 155.41, 167.07, 170.01, 173.14, 175.14, 203.93. HRMS (ESI) calcd for $C_{46}H_{62}NO_{15}$: $(M+H)^+$: 858.4119, found 858.4111 (Δ -0.9 ppm, -0.8 mDa).

3'-Dephenyl-3'-(2-methyl-2-propenyl)-2-debenzoyl-2-(3-methylbenzoyl)-10-(*N*,*N*-dimethylcarbamoyl)docetaxel [SB-T-121602]

According to the procedure previously listed for **SB-T-1213**, compound **2-8 J** (220 mg, 0.19 mmol) was used to produce **SB-T-121602** (153 mg, 91%) as a white solid: m.p = 175-176 ^{o}C; ^{1}H NMR (500 MHz, $CDCl_3$) δ 1.19 (s, 3H), 1.29 (s, 3H), 1.38 (s, 9H), 1.70 (s, 3H), 1.79 (s, 3H), 1.80 (s, 3H), 1.94 (m, 1H), 1.95 (s, 3H), 2.32-2.45 (m, 2H), 2.39 (s, 3H), 2.46 (s, 3H), 2.58 (m, 1H), 3.00 (s, 3H), 3.08 (s, 3H), 3.40 (m, 1H), 3.84 (d, J = 6.5, 1H), 4.21 (d, J = 8.5 Hz, 1H), 4.25 (m, 1H), 4.35 (d, J = 8.5 Hz, 1H), 4.48 (m, 1H), 4.79 (m, 2H), 5.02 (d, J = 8.0 Hz, 1H), 5.36 (m, 1H), 5.36 (d, J = 6.5 Hz, 1H), 6.22 (t, J = 6.0 Hz, 1H), 6.29 (s, 1H), 7.39 (t, J = 7.5 Hz, 1H), 7.45 (d, J = 7.5 Hz, 1H), 7.93 (d, J = 7.5 Hz, 1H), 7.97 (s, 1H); ^{13}C NMR (125 MHz, $CDCl_3$) δ 9.36, 14.12, 15.03, 18.57, 21.35, 22.24, 22.35, 22.65, 25.71, 26.82, 28.22, 31.59, 35.41, 35.62, 36.03, 36.64, 43.20, 45.62, 51.56, 58.50, 72.47, 73.75, 75.05, 76.24, 76.48, 79.26, 79.93, 81.17, 84.63, 120.68, 127.31, 128.51, 129.16, 130.81, 133.23, 134.43, 137.86, 138.33, 142.89, 155.42, 156.16, 167.08, 169.97, 173.14, 205.71. HRMS (ESI) calcd for $C_{45}H_{63}N2O_{15}$ $(M+H)^+$: 871.4228, found 871.4237 (Δ 1.0 ppm, 0.9 mDa).

3'-Dephenyl-3'-(2-methyl-2-propenyl)-2-debenzoyl-2-(2,5-dimethoxybenzoyl)-10-(propanoyl)docetaxel [SB-T-121313]

According to the procedure previously listed for **SB-T-1213**, compound **2-8 K** (260 mg, 0.22 mmol) was used to produce **SB-T-121313** (189 mg, 96%) as a white solid: m.p. = 166-168 ^{o}C ^{1}H NMR (500 MHz, $CDCl_3$) δ 1.14 (s, 3H), 1.22 (t, J = 7.5 Hz, 3H), 1.27 (s, 3H), 1.37 (s, 9 H), 1.68 (s, 3H), 1.72 (s, 3H), 1.74 (s, 3 H), 1.87 (m, 1H), 1.88 (s, 3H), 2.17 (s, 3H), 2.36 -2.40(m, 1H), 2.46 – 2.60 (m, 5H), 3.17 (s, br), 3.74 (d, J = 6.5 Hz, 1H), 3.80 (s, 3H), 3.93 (s, 3H), 4.15 (s, 1H) 4.28 (d, J = 8.0 Hz, 2H), 4.38 (m, 1H), 4.41 (d, J = 8.0 Hz, 1H), 4.71, (t, J = 9.0 Hz, 1H), 4.79 (d, J = 9.0 Hz, 1H), 4.93 (d, J = 8.0 Hz, 1H), 5.35 (m, 1H), 5.65 (d, J = 6.5 Hz, 1H), 6.15 (t, J = 9.0

Hz, 1H), 6.31 (s, 1H), 6.94 (d, J = 9.0 Hz, 1H), 7.06 (dd, J = 9.0, 3.0 Hz, 1H), 7.30 (d, J = 3.0 Hz, 1H); ^{13}C NMR (125 MHz, $CDCl_3$) δ 11.70, 12.21, 17.62, 21.06, 24.43, 25.06, 28.25, 29.36, 30.26, 30.86, 38.40, 39.23, 45.51, 48.30, 54.10, 58.53, 59.16, 61.47, 74.82, 75.42, 76.03, 78.27, 79.09, 80.30, 82.45, 83.73, 87.22, 116.122, 118.54, 122.77, 123.44, 135.96, 140.31, 145.03, 155.47, 156.13, 157.89, 169.47, 172.62, 176.06, 177.24, 206.67. HRMS (ESI) calcd for $C_{46}H_{64}NO_{17}$ $(M+H)^+$: 902.4174, found 902.4166 (Δ -0.9 ppm, -0.8 mDa).

3'-Dephenyl-3'-(2-methyl-2-propenyl)-2-debenzoyl-2-(2,5-dimethoxybenzoyl)-10-(cyclopropanecarbonyl)docetaxel [SB-T-121413]

According to the procedure previously listed for **SB-T-1213**, compound **2-8 L** (145 mg, 0.12 mmol) was used to produce **SB-T-121413** (106 mg, 95%) as a white solid: m.p. = 165 – 168 ºC; ^{1}H NMR (500 MHz, $CDCl_3$) δ 0.92-1.04 (m, 4H), 1.15 (s, 3H), 1.24 (s, br, 1H), 1.28 (s, 3H), 1.37 (s, 9 H), 1.67 (s, 3H), 1.71 (s, 3H), 1.74 (s, 3 H), 1.87 (s, 3H), 1.88 (m, 1H), 2.17 (s, 3H), 2.36-2.40(m, 1H), 2.46 – 2.60 (m, 3H), 3.07 (s, br, 1H), 3.36 (s, br, 1H), 3.73 (d, J = 6.5 Hz, 1H), 3.80 (s, 3H), 3.93 (s, 3H), 4.15 (s, 1H) 4.28 (d, J = 8.0 Hz, 2H), 4.38 (m, 1H), 4.40 (d, J = 8.0 Hz, 1H), 4.71, (t, J = 8.0 Hz, 1H), 4.80 (d, J = 8.0 Hz, 1H), 4.92 (d, J = 9.0 Hz, 1H), 5.34 (m, 1H), 5.65 (d, J = 6.0 Hz, 1H), 6.15 (t, J = 8.0 Hz, 1H), 6.30 (s, 1H), 6.94 (d, J = 9.0 Hz, 1H), 7.06 (dd, J = 9.0, 3.0 Hz, 1H), 7.30 (d, J = 3.0 Hz, 1H); ^{13}C NMR (125 MHz, $CDCl_3$) δ 9.07, 9.27, 9.49, 13.03, 14.92, 18.36, 21.81, 22.34, 25.55, 26.71, 28.16, 35.66, 36.52, 42.81, 45.59, 51.39, 55.81, 56.45, 58.76, 72.11, 72.72, 73.33, 75.54, 76.39, 77.63, 79.75, 81.04, 84.54, 113.43, 115.85, 120.08, 120.74, 133.24, 137.60, 142.46, 152.79, 153.42, 155.19, 166.75, 169.92, 173.36, 175.01, 204.07. MS (ESI) calcd for $C_{47}H_{64}NO_{17}$ $(M+H)^+$: 914.41, found: 914.4.

3'-Dephenyl-3'-(2-methyl-2-propenyl)-2-debenzoyl-2-(2,5-dimethoxybenzoyl)-10-(*N,N*-dimethylcarbamoyl)docetaxel [SB-T-121613]

According to the procedure previously listed for **SB-T-1213**, compound **2-8 M** (150 mg, 0.13 mmol) was used to produce **SB-T-121613** (103 mg, 89%) as a white solid: m.p. = 153-156 ºC; ^{1}H NMR (500 MHz, $CDCl_3$) δ 1.17 (s, 3H), 1.26 (s, 3H), 1.39 (s, 9H), 1.69 (s, 3H), 1.72 (s, 3H), 178 (s, 3H), 1.81 (m, 1H), 1.91 (s, 3H), 1.94 (m, 1H), 2.19 (s, 3H), 2.37 (m, 1H), 2.53 (m, 2H), 2.97, (s, 3H), 3.05 (s, 3H), 3.16 (s, br, 1H), 3.28 (m, 1H), 3.75 (d, J = 6.5 Hz, 1H), 3.82 (s, 3H), 3.95 (s, 3H), 4.17 (m, 1H), 4.17 (d, J = 8.5 Hz, 1H), 4.43 (m, 2H), 4.75 (m, 2H), 4.96 (d, J = 8.0 Hz, 1H), 5.36 (m, 1H), 5.67 (d, J = 6.5 Hz, 1H), 6.18 (t, J = 9.0 Hz, 1H), 6.27 (s, 1H), 6.96 (d, J = 9.0 z, 1H), 7.08 (dd, J = 9.0, 3.0 Hz, 1H), 7.32 (s, 1H); ^{13}C NMR (500 MHz, $CDCl_3$) δ 9.37, 15.10, 15.45, 18.45, 22.17, 22.43, 25.63, 26.90, 28.21, 28.44, 29.72, 35.55, 36.05, 36.60, 36.64, 42.85, 45.55, 51.42, 55.87, 56.49, 58.77, 72.47, 72.88, 73.38, 77.75, 81.12, 84.78, 113.42, 115.80, 120.12, 120.73, 133.56, 137.73, 142.84, 152.79, 153.44, 155.22, 156.19, 166.89, 169.92, 173.44, 205.95. HRMS (ESI) calcd for $C_{46}H_{64}N_2O_{17}$ $(M+H)^+$: 917.4283, found 917.4274 (Δ -1.0 ppm, -0.9 mDa).

3'-Dephenyl-3'-(2-methyl-2-propenyl)-2-debenzoyl-2-(2,5-dimethylbenzoyl)-10-(propanoyl)docetaxel [SB-T-121312]

According to the procedure previously listed for **SB-T-1213**, compound **2-8 N** (165 mg, 0.15 mmol) was used to produce **SB-T-121312** (108 mg, 86%) as a white solid: m.p. = 159-162 ^{o}C; ^{1}H NMR (500 MHz, $CDCl_3$) δ 0.82 – 0.98 (m, 2H), 1.15 (s, 3H), 1.23 (t, J = 7.8 Hz, 3H), 1.25 (s, 3H), 1.35 (s, 9 H), 1.68 (s, 3H), 1.74 (s, 3H), 1.76 (s, 3 H), 1.87 (m, 1H), 1.89 (s, 3H), 2.31 (s, 3H), 2.36 (m, 1H), 2.37 (s, 3H), 2.48 – 2.62 (m, 4H), 2.59 (s, 3H), 3.28 (s, br), 3.80 (d, J = 7.0 Hz, 1H), 4.18 (d, J = 8.5 Hz, 1H), 4.19 (s, 1H), 4.26 (d, J = 8.5 Hz, 1H), 4.42 (m, 1H), 4.74 – 4.79 (m, 2H), 4.95 (d, J = 8.0 Hz, 1H), 5.34 (m, 1H), 5.65 (d, J = 7.0 Hz, 1H), 6.18 (t, J = 10.0 Hz, 1H), 6.31 (s, 1H), 7.15 (d, J = 7.0 Hz, 1H), 7.26 (d, J = 7.0 Hz, 1H), 7.93 (s, 1H); ^{13}C NMR (125 MHz, $CDCl_3$) δ 9.01, 9.58, 14.94, 18.52, 20.88, 21.56, 21.81, 22.29, 25.66, 26.67, 27.56, 28.20, 35.59, 35.66, 43.23, 45.74, 51.49, 58.61, 72.22, 72.49, 73.66, 74.51, 75.47, 76.55, 79.14, 79.87, 81.03, 84.40, 120.70, 127.83, 131.76, 131.98, 132.99, 133.59, 135.31, 137.81, 138.55, 142.52, 155.29, 167.67, 169.91, 174.63, 203.86. HRMS (ESI) calcd for $C_{46}H_{64}N_2O_{15}$ $(M+H)^+$: 870.4276, found 870.4271 (Δ -0.6 ppm, -0.5 mDa).

3'-Dephenyl-3'-(2-methyl-2-propenyl)-2-debenzoyl-2-(2,5-dimethylbenzoyl)-10-(*N*,*N*-dimethylcarbamoyl)docetaxel [SB-T-121612]

According to the procedure previously listed for **SB-T-1213**, compound **2-8 O** (155 mg, 0.13 mmol) was used to produce **SB-T-121612** (113 mg, 95%) as a white solid: m.p. = 158-160 ^{o}C; ^{1}H NMR (500 MHz, $CDCl_3$) δ 1.16 (s, 3H), 1.24 (m, 1H), 1.25 (s, 3H), 1.35 (s, 9 H), 1.67 (s, 3H), 1.73 (s, 3H), 1.75 (s, 3 H), 1.88 (m, 1H), 1.91 (s, 3H), 2.30 (s, 3H), 2.36 (s, 3H), 2.42-2.56 (m, 2H), 2.58 (s, 3H), 2.95 (s, 3H), 3.04 (s, 3H), 3.39 (s, br, 1H), 3.79 (d, J = 7.5 Hz, 1H), 4.18 (d, J = 8.5 Hz, 1H), 4.19 (s, 1H) 4.25 (d, J = 8.5 Hz, 2H), 4.44 (m, 1H), 4.73-4.81 (m, 2H), 4.96 (d, J = 8.5 Hz, 1H), 5.33 (m, 1H), 5.63 (d, J = 7.5 Hz, 1H), 6.18 (t, J = 9.0 Hz, 1H), 6.25 (s, 1H), 7.14 (d, J = 8.0 Hz, 1H), 7.25 (d, J = 8.0 Hz, 1H), 7.92 (s, 1H); ^{13}C NMR (125 MHz, $CDCl_3$) δ 12.07, 16.86, 17.69, 21.20, 23.55, 23.70, 24.23, 24.87, 24.96, 25.31, 28.33, 29.54, 30.88, 34.24, 38.09, 38.39, 38.69, 39.30, 45.91, 48.36, 54.16, 61.21, 63.05, 75.15, 76.35, 77.32, 78.92, 79.22, 81.91, 82.49, 83.76, 87.29,123.43, 130.54, 134.45, 134.63, 135.93, 136.24, 137.97, 140.42, 141.19, 145.63, 157.96, 158.83, 170.35, 172.53, 173.82, 175.86, 208.41. HRMS (ESI) calcd for $C_{46}H_{65}N_2O_{15}$ $(M+H)^+$: 885.4385, found 885.4380 (Δ -0.6 ppm, -0.5 mDa).

1-(4-Methoxyphenyl)-3-triisopropylsiloxy-4-(formyl)-azetidin-2-one [2-10][119]

A solution of **(+) 1-4** (500 mg, 1.23 mmol) in CH_2Cl_2 (100 mL) was cooled to -78 ^{o}C and purged with O_2. Ozone was then bubbled through the solution and the reaction progress was monitored by TLC (alumina plates). After 4 hours, the solution had turned a faint blue color and the vessel was purged with N_2. Dimethylsulfide (2 mL,) was then added and the reaction mixture was stirred 2 hours at room temperature. The mixture was then concentrated in vacuo and purified by column chromatography on alumina gel using increasing amounts of ethyl acetate in hexanes (hexanes:EtOAc = 1:0 to 1:1) to afford **2-10** (376 mg, 80%) as a clear oil: 300 MHz, 1.08 (m, 21H), 4.46 (dd, J = 5.4, 4.2 Hz, 1H), 5.30 (d, J = 5.4 Hz, 1H), 6.87 (d, J = 4.5 Hz, 2H), 7.28 (d, J

= 4.5 Hz, 2H), 9.77 (d, J = 4.2 Hz, 1H). All data were found to be in agreement with literature values.

1-(4-Methoxyphenyl)-3-triisopropylsiloxy-4-(2,2-difluorovinyl)-azetidin-2-one [2-11][119]

To a solution of **2-10** (350 mg, 0.92 mmol) in THF (45 mL) was added zinc (258 mg, 3.98 mmol) and the reaction vessel was purged with N_2 and cooled to 0 ^oC. Dibromodifluoromethane (1.05 g mg, 3.18 mmol) was dissolved in THF (25 mL) under N_2 and cooled to 0 ^oC and to this solution HMPT (1.54 g, 9.48 mmol) was added, forming a white precipitate in a brown solution. This suspension was then added to the reaction mixture and heated to 70 ^oC for one hour during which time the reaction was monitored by TLC (6:1 Hx:EA). Upon completion, the reaction mixture was filtered through celite, washed with EtOAc and the filtrate was concentrated *in vacuo* to afford a red oil. This oil was then dissolved in EtOAc (50 mL), washed with H_2O (3 x 50 mL), brine (3 x 50 mL). The organic layer was collected, dried over MgSO4, suction filtered, filtrate collected and concentrated in vacuo to afford a red oil that was purified by column chromatography on silica gel with increasing amounts of ethyl acetate in hexanes (hexanes:ethyl acetate 1:0 – 5:1) to afford **2-11** (217 mg, 57%) as a colorless oil: ^1H NMR ($CDCl_3$, 300 MHz): δ 1.08-1.15 (m, 21 H), 3.79 (s, 3 H), 4.54 (ddd, *J* = 1.5 Hz, 6.3 Hz, 16.5 Hz, 1 H), 4.83 (m, 1 H), 5.14 (d, *J* = 5.1 Hz, 1 H), 6.87 (d, *J* = 9.0 Hz,2H), 7.32 (d, *J* = 9.0 Hz, 2H); ^{19}F NMR (282 MHz, $CDCl_3$): δ -80.80 (d, *J* = 32.7 Hz, 1F), -86.34 (dd, *J* = 2.8 Hz, 28.2 Hz, 1F). All data were found to be in agreement with literature values.

3-Triisopropylsilanyloxy-4-(2,2-difluorovinyl)-azetidin-2-one [2-12][119]

To a solution of **2-11** (217 mg, 0.53 mmol) in acetonitrile (20 mL) and H_2O (5 mL), was added dropwise a solution of ceric ammonium nitrate (1.24 g, 2.15 mmol) in water (15 mL). The reaction mixture was stirred for 3 hours and the reaction temperature of -10 °C was maintained throughout the reaction. The reaction was monitored by TLC and upon completion the mixture was extracted with ethyl acetate (40 mL). The organic layer was washed with aqueous Na_2SO_3 (4 x 20 mL), brine (3 x 25 mL), dried over $MgSO_4$, filtered and the filtrate concentrated *in vacuo*. Purification was done by column chromatography on silica gel with increasing amounts of ethyl acetate in hexanes (hexanes:ethyl acetate 1:0 – 2:1) to afford **2-12** (126 mg, 79%) as a pale yellow oil: ^1H NMR ($CDCl_3$, 400 MHz): δ 1.03-1.18 (m, 21 H), 4.44-4.54 (m, 2 H), 5.04 (dd, *J* = 1.6 Hz, 2.4 Hz, 1 H), 6.59 (bs, 1 H); ^{19}F NMR (282 MHz, $CDCl_3$): δ -82.33 (d, *J* = 34.7 Hz, 1F), -87.50 (dd, *J* = 9.3 Hz, 25.7Hz, 1 F). All data were found to be in agreement with literature values.

1-(*tert*-Butoxycarbonyl)-3-triisopropylsiloxy-4-(2,2-difluorovinyl)-azetidin-2-one [2-13][119]

To a solution of **2-12** (126 mg, 0.41 mmol), TEA (0.07 mL, 0.51 mmol), and DMAP (15 mg, 0.12 mmol) in CH_2Cl_2 (9 mL), was added Boc_2O (134 mg, 0.59 mmol). The reaction was stirred for 3 hour at room temperature and reaction progress was monitored by TLC. The reaction mixture was diluted with EtOAc (30 mL) and the organic layer was washed with brine (3 x 20 mL), dried over $MgSO_4$, filtered and the filtrate concentrated *in vacuo* affording a brown oil. Purification was done by column chromatography on silica gel with increasing amounts of ethyl acetate in hexanes

(hexanes:ethyl acetate 1:0 – 9:1) to afford **2-13** (146 mg, 79%) as a pale yellow oil: ^{1}H NMR ($CDCl_3$, 300 MHz): δ 1.04-1.17 (m, 21 H), 1.49 (s, 9 H), 4.49 (ddd, *J* = 1.6 Hz, 13.8 Hz, 23.7 Hz, 1 H), 4.75 (m, 1 H), 5.04 (d, *J* = 5.7 Hz, 1 H), 6.59 (bs, 1 H); ^{19}F NMR (282 MHz, $CDCl_3$): δ -81.20 (d, *J* = 31.0 Hz, 1 F), -85.83 (dd, *J* = 5.6 Hz, 29.3 Hz, 1F). All data were found to be in agreement with literature values.

2'-Triisopropylsilyl-3'-dephenyl-3'-(2,2-difluorovinyl)-7-triethylsilyl-10-(*N*,*N*-dimethylcarbamoyl)-docetaxel[119] [2-14]

According to the procedure previously listed for **2-8 A**, compound **2-6 J** (300 mg, 0.25 mmol) was used to produce **2-14)** (353 mg, 76%) as a white solid: ^{1}H NMR ($CDCl_3$, 300 MHz) δ 0.55-0.63 (m, 6H), 0.86-0.94 (m, 9H), 1.12 (m, 21H), 1.19 (s, 3H), 1.30 (s, 3H), 1.46 (s, 9H), 1.68 (s, 3H), 1.88 (m, 1H), 2.06 (s, 3H), 2.31-2.38 (m, 2H), 2.33 (s, 3H), 2.45 (m, 1H), 2.51 (m, 1H), 2.93 (s, 3H), 3.06 (s, 3H), 3.84 (d, J = 6.9 Hz, 1H), 4.18 (d, J = 8.4 Hz, 1H), 4.32 (d, J = 8.4 Hz, 1H), 4.45-4.51 (m, 3H), 4.83-4.96 (m, 3H), 5.69 (d, J = 6.0 Hz, 1H), 6.18 (t, J = 9.3 Hz, 1H), 6.39 (s, 1H), 7.49 (t, J = 7.5 Hz, 2H), 7.61 (t, J = 7.5 Hz, 1H), 8.12 (d, J = 7.2 Hz, 2H). All data were found to be in agreement with literature values.

3'-Dephenyl-3'-(2,2-difluorovinyl)-10-(N,N-dimethylcarbamoyl)-docetaxel, [SB-T-12854] [119]

According to the procedure previously listed for **SB-T-1213**, compound **2-14** (350 mg, 0.19 mmol) was used to produce **SB-T-12854** (242 mg, 90%) as a white solid: white solid; mp 166-170 °C; ^{1}H NMR ($CDCl_3$, 400 MHz) δ 1.15 (s, 3 H), 1.25 (s, 3 H), 1.30 (s, 9 H), 1.67 (s, 3 H), 1.84 (m, 1 H), 1.89 (m, 4 H), 2.31 (m, 2 H), 2.38 (s, 3 H), 2.53 (m, 1 H), 2.96 (s, 3 H), 3.05 (s, 3 H), 3.24 (bs, 1 H), 3.64 (d, *J* = 5.6 Hz, 1 H), 3.80 (d, *J* = 6.8 Hz, 1 H), 4.17 (d, *J* = 8.4 Hz, 1 H), 4.29 (m, 2 H), 4.44 (m, 1 H), 4.57 (dd, *J* = 10.0 Hz, 25.2 Hz, 1 H), 4.86 (t, *J* = 8.8 Hz, 1 H), 4.97 (d, *J* = 9.2 Hz, 1 H), 5.02 (d, *J* = 9.6 Hz, 1 H), 5.66 (d, *J* = 7.2 Hz, 1 H), 6.24 (m, 2 H), 7.49 (t, *J* = 7.6 Hz, 2H), 7.59 (t, *J* = 7.2 Hz, 1 H), 8.10 (d, *J* = 7.6 Hz, 2 H); ^{19}F NMR, ($CDCl_3$, 282 MHz) δ –84.31 (dd, *J* = 25.7 Hz, 37.2 Hz, 1 F), –86.23 (d, *J*= 36.4 Hz, 1 F). All data were found to be in agreement with literature values.

§ 2.4.0 References

1. Jemal, A.; Bray, F.; Center, M.; Ferlay, J.; Ward, E.; Forman, D., Global Cancer Statistics. *CA Cancer J. Clin.* **2011,** *61*, 69-90.
2. Siegel, R.; Ward, E.; Brawley, O.; Jemal, A., Cancer Statistics, 2011. *CA Cancer J. Clin.* **2011,** *61*, 212-236.
3. Hanahan, D.; Weinberg, R. A., Hallmarks of Cancer: The Next Generation. *Cell* **2011,** *144*, 646-674.
4. Hanahan, D.; Weinberg, R. A., The hallmarks of cancer. *Cell* **2000,** *100*, 57-70.
5. Del Buttero, P.; Molteni, G.; Roncoroni, M., Reductive ring opening of 2-azetidinones promoted by sodium borohydride. *Tetrahedron Lett.* **2006,** *47*, 2209-2211.
6. Hsu, P. P.; Sabatini, D. M., Cancer cell metabolism: Warburg and beyond. *Cell* **2008,** *134*, 703-707.

7. Kim, R.; Emi, M.; Tanabe, K., Cancer immunoediting from immune surveillance to immune escape. *Immunol.* **2007,** *121*, 1-14.
8. Hanahan, D.; Folkman, J., Patterns and emerging mechanisms of the angiogenic switch during tumorigenesis. *Cell* **1996,** *86*, 353-364.
9. Goodman, L. S.; Wintrobe, M. M.; Dameshek, W.; Goodman, M. J.; Gilman, A.; McLennan, M. T., Nitrogen mustard therapy: use of methyl-bis (b-chloroethyl}) amine hydrochloride and tris (b-chloroethyl)amine hydrochloride for Hodgkin's disease, lymphosarcoma, leukemia and certain allied and miscellaneous disorders. *J. Am. Med. Assoc.* **1446,** *103*, 409-415.
10. Farber, S.; Diamond, L. K.; Mercer, R. D., Temporary remissions in acute leukemia in children produced by folic acid antagonist, 4-aminopteroyl-glutamic acid (aminopterin). *N. Eng. J. Med.* **1948,** *238*, 787-793.
11. DeVita, V. T.; Chu, E., A History of Cancer Chemotherapy. *Cancer Res.* **2008,** *68*, 8643-8653.
12. Suffness, M., *Taxol: Science and Applications; CRC Press: New York*. 1995.
13. Rowinsky, E. K.; Onetto, N.; Canetta, R. M.; Arbuck, S. G., Taxol: the first of the taxanes, an important new class of anti-cancer agents. *Semin. Oncol.* **1992,** *19*, 646-662.
14. Rowinsky, E. K., The development and clinical utility of the taxane class of antimicrotubule chemotherapy agents *Ann. Rev. Med.* **1997,** *48*, 353–374.
15. Cragg, G. M., Schepartz, S.A., Suffness, M., Grever, M. R., The taxol supply crisis: New NCI policies for handling the large-scale production of novel natural product anticancer and anti-HIV agents. *J. Nat. Prod.* **1993,** *56*, 1657-1668.
16. Blume, E., Government Moves To Increase Taxol Supply. *J. Natl. Cancer Inst.* **1991,** *83*, 1054-1056.
17. Chauvière, G.; Guénard, D.; Picot, F.; Sénilh, V.; Potier, P., Structural Analysis and Biochemical Study of Isolated Products of the Yew: *Taxus Baccata* L. (Taxaceae). *C. R. Seances Acad. Sci., Ser 2* **1981,** *293*, 501-503.
18. Holton, R. A. 15599, 1995.
19. Agency, U. E. P., Greener Synthetic Pathways Award: Bristol-Myers Squibb Company: Development of a Green Synthesis for TAXOL Manufacture via Plant Cell Fermentation and Extraction. 2004; p http://www.epa.gov/greenchemistry/pubs/pgcc/winners/gspa04.html.
20. Wall, M. E.; Wani, M. C.; Cook, C. E.; Palmer, C. E.; McPhail, A. T., Plant antitumor agents. I: The isolation and structure of camptothecin, a novel alkaloidal leukemia and tumor inhibitor from Camptotheca acuminata. *J. Am. Chem. Soc.* **1966,** *88*, 3888-3894.
21. Wani, M. C.; Taylor, H. L.; Wall, M. E.; Coggan, P.; McPhail, A. T., Plant antitumor agents. VI. The isolation and structure of taxol, a novel antileukemic and antitumor agent from *Taxus brevifolia*. *J. Am. Chem. Soc.* **1971,** *93*, 2325-2327.
22. Patel, R. N., Tour De Paclitaxel: Biocatalysis for Semisynthesis. *Ann. Rev. Microbiol.* **1998,** *98*, 361.
23. Fuchs, D. A.; Johnson, R. K., Cytologic evidence that taxol, an antineoplastic agent from Taxus brevifolia, acts as a mitotic spindle poison. *Cancer Treat. Rep.* **1978,** *62*, 1219-1222.
24. Horwitz, S. B.; Fant, J.; Schiff, P. B., Promotion of microtubule assembly in vitro by taxol. *Nature* **1979,** *277*, 665-667.
25. Horwitz, S. B., Personal Recollections on the Early Development of Taxol. *J. Nat. Prod.* **2004,** *67*, 136-138.
26. Weiss, R.; Donehower, R. C.; Wiernik, P. H., Hypersenstivity reactions from taxol. *J. Clin. Oncol.* **1990,** *8*, 1263-68.

27. Rowinsky, E. K.; A., E. E.; Chaudhry V., Clinical toxicities encountered with taxol. *Sem. Oncol. 20(Suppl.3)* **1993**, 1–15.
28. McGuire, W. P.; Hoskins, W. J.; Brady, M. F., Cyclophosphamide and cisplatin compared with paclitaxel and cisplatin in patients with stage III and stage IV ovarian cancer *N. Engl. J. Med.* **1996,** *334*, 1–6.
29. Rowinsky, E. K.; Gilbert, M.; McGuire, W. P., Sequences of taxol and cisplatin: a phase I and pharmacologic study. *J. Clin. Oncol.* **1991,** *9*, 1692–703.
30. Rowinsky, E. K.; Donehower, R. C., Paclitaxel (taxol). *N. Engl. J. Med.* **1995,** *332*, 1004-1014.
31. Suffness, M., Taxol, Science and Applications. *CRC Press, New York* **1995**.
32. Nogales, E.; Wolf, S.; Khan, I.; Luduena, R.; Downing, K., Structure of tubulin at 6.5 A and location of the taxol-binding stie *Nature* **1995,** *375*, 424-427.
33. Andreu, J.; Bordas, J.; Diaz, J.; Ancos, J. d.; Gil, R.; Medrano, F.; Nogales, E.; Pantos, E.; Towns-Andrews, E., Low resolution structure of micrtubules in solution: Synchrotron X-ray scattering and electron microscopy of taxol-induced microtubules assembled from purified tubulin in comparison with glycerol and MAP-induced microtubules. *J. Mol. Biol.* **1992,** *226*, 169-184.
34. Diaz, J.; Valpuesta, J.; Chacon, P.; Diakun, G.; Andreu, J., Changes in Microtubule Protofilament Number Induced by Taxol Binding to an Easily Accessible Site. *J. Biol. Chem.* **1998** *272*, 33803-33810.
35. Sackett, D.; Fojo, T., Taxanes. *Cancer Chemother. Biol. Response Modifiers* **1997,** *17*, 59-79.
36. Schiff, P. B., Fant, J., Horwitz, S. B., Taxol stabilizes microtubules in mouse fibroblast cells. *Proc. Natl. Acad. Sci.* **1980,** *77*, 1561-1565.
37. Huizing, M.; Keung, A.; Rosing, H.; Kuij, V. v. d.; Huinink, W. t. B.; Mandjes, I.; Dubbelman, A.; Pinedo, H.; Beijen, J., Pharmacokinetics of paclitaxel and metabolites in a randomized compartive study in platinum-pretreated ovarian cancer patients. *J. Clin. Oncol.* **1993,** *11*, 2127-2135.
38. Jordan, M.; Wilson, L., Microtubules and actin filaments: dynamic targets for cancer chemotherapy. *Curr. Opin. Cell Biol.* **1998,** *10*, 123-130.
39. Long, B.; Fairchild, C., Paclitaxel inhibits progression of mitotic cells to G1 phase by interference with spindle formation without affecting other microtubule functions during anaphase and telephase. *Cancer Res.* **1994,** *54*, 4355-4361.
40. Donaldson, K.; Goolsby, G.; Wahl, A., Cytotoxicity of the anti-cancer agents cisplatin and Taxol during cell proliferation and the cell cycle. *Int. J. Cancer* **1994,** *57*, 847-855.
41. Sorger, P.; Dobles, M.; Tournebize, R.; Hyman, A., Coupling cell division and cell death to microtubule dynamics. *Curr. Opin. Cell Biol.* **1997,** *9*, 807-814.
42. Oyaizu, H.; Adachi, Y.; Taketani, S.; Tokunaga, R.; Fukuhara, S.; Ikehara, S., A crucial role of caspase 3 and caspase 8 in paclitaxel-induced apoptosis. *Mol. Cell. Biol. Res. Commun.* **1999,** *2*, 36-41.
43. Huisman, C.; Ferreira, C.; Broker, L.; Rodriguez, J.; Smit, E.; Postmus, P.; Kruyt, F.; Giaccone, G., Paclitaxel Triggers Cell Death Primarily via Caspase-independent Routes in the Non-Small Cell Lung Cancer Cell Line NCI-H460. *Clin. Cancer Res.* **2002,** *8*, 596-606.
44. Subbaramaiah, K.; Hart, J.; Norton, L.; Dannenberg, A., Microtubule-interfering Agents Stimulate the Transcription of Cyclooxygenase-2 Evidence for involvement of ERK1/2 and p38 mitogen-activated protein kinase pathways. *J. Biol. Chem.* **2000,** *275*, 14838-14845.

45. Shtil, A.; Madlekar, S.; Yu, R.; Walter, R.; Hagen, K.; Tan, T.; Roninson, I.; Kong, A., Differential regulation of mitogen-activated protein kinases by microtubule-binding agents in human breast cancer cells. *Oncogene* **1999,** *18*, 377-384.
46. Blagosklonny, M.; Fojo, T., Molecular effects of paclitaxel: myths and reality (a critical review). *Int. J. Cancer* **1999,** *83*, 151-156.
47. Blagosklonny, M.; Giannakakou, P.; El-Deiry, W.; Kingston, D.; Higgs, P.; Neckers, L.; Fojo, T., Raf1/bcl2 phosphorylation: a step from microtubule damage to cell death. *Cancer Res.* **1997,** *57*, 130-135.
48. Haldar, S.; Chintapalli, J.; Croce, C., Taxol Induces bcl-2 Phosphorylation and Death of Prostate Cancer Cells. *Cancer Res.* **1996,** *56*, 1253-1255.
49. Chun, E.; Lee, K.-Y., Bcl-2 and Bcl-xL are important for the induction of paclitaxel resistance in human hepatocellular carcinoma cells. *Biochem. Biophys. Res. Comm.* **2004,** *315*, 771-779.
50. Gazitt, Y.; Rothenberg, M.; Hilsenback, S.; Fey, V.; Thomas, C.; Montegomrey, W., Bcl-2 overexpression is associated with resistance to paclitaxel, but not gemcitabine, in multiple myeloma cells. *Int. J. Oncol.* **1998,** *13*, 839-848.
51. Ibrado, A.; Liu, L.; Bhalla, K., Bcl-xL overexpression inhibits progression of molecular evens leading to paclitaxel-induced apoptosis of human AML HL-60 cells. *Cancer Res.* **1997,** *57*, 1109-1115.
52. Callagy, G.; Pharoah, P.; Pinder, S., Bcl-2 is a prognostic marker in breast cancer independently of the Nottingham Prognostic Index. *Clin. Cancer Res.* **2006,** *12*, 2468-2475.
53. Yoshino, T.; Shiina, H.; Urakami, S., Bcl-2 expressin as a predictive marker of hormone-refractory prostate cancer treated with taxane-based chemotherapy. *Clin. Cancer Res.* **2006,** *12*, 6116-6125.
54. Pushkarev, V.; Starenki, D.; Saenko, V.; Namba, H.; Kurebayashi, J.; Tronko, M.; Yamashita, S., Molecular Mechanisms of the Effects of Low Concentrations of Taxol in Anaplastic Thyroid Cancer Cells. *Endocrinol.* **2004,** *145*, 3143-3152.
55. Blagosklonny, M.; Schulte, T.; Nguyen, P.; Trepel, J.; Neckers, L., Taxol-induced Apoptosis and Phosphorylation of Bcl-2 Protein involves c-Raf-1 and Prepresents a Novel C-Raf-1 Signal Transduction Pathway. *Cancer Res.* **1996,** *56*, 1851-1854.
56. Okano, J.-I.; Rustgi, A., Paclitaxel Induces Prolonged Activation of the Ras/MEK/ERK Pathway Independently of Activating the Programmed Cell Death Machinery. *J. Biol. Chem.* **2001,** *276*, 19555-19564.
57. Ferlini, C.; Cicchillitti, L.; Raspaglio, G.; Bartollino, S.; Cimitan, S.; Bertucci, C.; Mozzetti, S.; Gallo, D.; Persico, M.; Fattorusso, C.; Campiani, G.; Scambia, G., Paclitaxel Directly Binds to Bcl-2 and Functionally Mimics Activity of Nur77. *Cancer Res.* **2009,** *69*, 6906-6914.
58. Szakacs, G.; Paterson, J.; Ludwig, J.; Booth-Genthe, C.; Gottesman, M., Targeting multidrug resistance in cancer. *Nature Rev. Drug Discov.* **2006,** *5*, 219-234.
59. Gottesman, M.; Pastan, I., Biochemistry of multidrug resistance mediated by the multidrug transporter. *Ann. Rev. Biochem.* **1993,** *62*, 385-427.
60. Yeh, J.; Hsu, W.; Wang, J.; Ho, S.; Kao, A., Predicting Chemotherapy Response to Paclitaxel-Based Therapy in Advanced Non-Small-Cell Lung Cancer with P-Glycoprotein Expression. *Respiration* **2003,** *70*, 32-35.
61. Penson, R.; Oliva, E.; Skates, S.; Glyptis, T.; Fuller, A. J.; Goodman, A.; Selden, M., Expression of multidrug resistance-1 protein inversely correlates with paclitaxel response and survival in ovarian cancer patients: a study in serial samples. *Gynecol. Oncol.* **2004,** *93*, 98-106.

62. Johnatty, S.; Beesley, J.; Paul, J.; Fereday, S.; Spurdle, A.; Webb, P.; Byth, K.; Marsh, S.; McLeod, H.; Harnett, P.; Brown, R.; deFazio, A.; Chenevix-Trench, G., ABCB (MDR 1) Polymorphisms and Progression-Free Survival among Women with Ovarian Cancer following Paclitaxel/Carboplatin Chemotherapy. *Clin. Cancer Res.* **2008,** *14*, 5594-5601.
63. Leonard, G.; Fojo, T.; Bates, S., The Role of ABC Transporters in Clinical Practice. *Oncologist* **2003,** *8*, 411-424.
64. Orr, G.; Verdier-Pinard, P.; McDaid, H.; Horwitz, S., Mechanisms of Taxol resistance related to microtubules. *Oncogene* **2003,** *22*, 7280-7295.
65. Giannakakou, P.; Gussio, R.; Nogales, E.; Downing, K.; Zaharevitz, D.; Bollbuck, B.; Poy, G.; Sackett, D.; Nicolaou, K.; Fojo, T., A common pharmacophore for epothiolone and taxanes: Molecular basis for drug resistance conferred by tubulin mutations in human cancer cells. *Proc. Nat. Acad. Sci.* **2000,** *97*, 2904-2909.
66. Monzo, M.; Rosell, R.; Sanchez, J.; Lee, J.; O'Brate, A.; Gonzalez-Larriba, J.; Alberola, V.; Lorenzo, J.; Nunez, L.; Ro, J.; Martin, C., Paclitaxel Resistance in Non-Small-Cell Lung Cancer Associated With Beta-Tubulin Gene Mutations. *J. Clin. Oncol.* **1999,** *17*, 1786-1793.
67. Ranganathan, S.; Benetatos, C.; Colarusso, P.; Dexter, D.; Hudes, G., Altered beta-tubulin isotype expression in paclitaxel-resistant human prostate carcinoma cells. *Br. J. Cancer* **1998,** *77*, 562-566.
68. Seve, P.; Isaaac, S.; Tredan, O.; Souquet, P.-J.; Pacheco, Y.; Perol, M.; Lafanechere, L.; Penet, A.; Peiller, E.-L.; Dumontet, C., Expression of Class III B-Tubulin Is Predictive of Patient Outcome in Patients with Non-Small Cell Lung Cancer Receiving Vinorelbine-Based Chemoterapy. *Clin. Cancer Res.* **2005,** *11*, 5481-5486.
69. Mozzetti, S.; Ferlini, C.; Concolino, P.; Filippetti, F.; Raspaglio, G.; Prislei, S.; Gallo, D.; Martinelli, E.; Ranelletti, F. O.; Ferrandina, G.; Scambia, G., Class III β-Tubulin Overexpression Is a Prominent Mechanism of Paclitaxel Resistance in Ovarian Cancer Patients. *Clin. Cancer Res.* **2005,** *11*, 298-305.
70. Nicoletti, M.; Valoti, G.; Giannakakou, P.; Zhan, Z.; Kim, J.; Lucchini, V.; Landoni, F.; Mayo, J.; Giavazzi, R.; Fojo, T., Expression of b-Tubulin Isotypes in Human Ovarian Carcinoma Xenografts and in a Sub-Panel of Human Cancer Cell Lines from the NCI-Anticancer Drug Screen Correlation with Sensitivity to Microtubule Active Agents. *Clin. Cancer Res.* **2001,** *7*, 2912-2922.
71. Potier, P., Search and Discovery of New Antitumour Compounds. *Chem. Soc. Rev.* **1992**, 113-119.
72. Kingston, D. G.; Hawkins, D. R.; Ovington, L., New Taxanes from *Taxus Brevifolia*. *J. Nat. Prod.* **1982,** *45*, 466-470.
73. Parness, J.; Kingston, D. G. I.; Powell, R. G.; Harracksingh, C.; Horwitz, S. B., Structure-activity study of cytotoxicity and microtubule assembly by taxol and related taxanes. *Biochem. Biophys. Res. Commun.* **1982,** *105*, 1082–1089.
74. Guenard, D.; Gueritte-Voegelein, F.; Potier, P., Taxol and Taxotere: Discovery, Chemistry, and Structure-Activity Relationships. *Acc. Chem. Res.* **1993,** *26*, 160-167.
75. Lage, H.; Dietel, M. J., Multiple mechanisms confer different drug-resistant phenotypes in pancreatic carcinoma cells. *Cancer Res. Clin. Oncol.* **2002**, 349-357.
76. O'Driscoll, L.; Walsh, N.; Larkin, A.; Ballot, J.; Ooi, W. S.; Gullo, G.; O'Connor, R.; Clynes, M.; Crown, J.; Kennedy, S., MDR1/P-glycoprotein and MRP-1 Drug Efflux Pumps in Pancreatic Carcinoma. *Anticancer Res.* **2007**, 2115–2120.

77. Ojima, I.; Fenoglio, I.; Park, Y. H.; Sun, C.-M.; Appendino, G.; Pera, P.; Bernacki, R. J., Synthesis and Structure-Activity Relationships of Novel Nor-Seco Analogs of Taxol® and Taxotere®. *J. Org. Chem.* **1994,** *59*, 515-517.
78. Pepe, A.; Sun, L.; Zanardi, I.; Wu, X.; Ferlini, C.; Fontana, G.; Bombardelli, E.; Ojima, I., Novel C-seco-taxoids possessing high potency against paclitaxel-resistant cancer cell lines overexpressing class III β-tubulin. *Bioorg. Med. Chem. Lett.* **2009,** *19*, 3300-3304.
79. Sessa, C.; Cuvier, C.; Caldiera, S.; Bauer, J.; Bosch, S. V. D.; Monnerat, C.; Semiond, D.; Perard, D.; Lebecq, A.; Besenval, M.; Marty, M., Phase I clinical and pharmacokinetic studies of the taxoid derivative RPR 109881A administered as a 1-hour or a 3-hour infusion in patients with advanced solid tumors. *Ann. Oncol.* **2002,** *13*, 1140-1150.
80. Marder-Karsenti, R.; Dubois, J.; Bricard, L.; Guenard, D.; Gueritte-Voegelein, F., Synthesis and Biological Evaluation of D-Ring-Modified Taxanes: 5(20)-Azadocetaxel Analogs. *J. Org. Chem.* **1997,** *62*, 6631-6637.
81. Gunatilaka, A. A. L.; Ramdayal, F. D.; Sarragiotto, M. H.; Kingston, D. G. I., Synthesis and Biological Evaluation of Novel Paclitaxel (Taxol) D-Ring Modified Analogues. *J. Org. Chem.* **1999,** *64*, 2694-2703.
82. Dubois, J.; Thoret, S.; Gueritte, F.; Guenard, D., Synthesis of 5(20)deoxydocetaxel, a New Active Docetaxel Analogue. *Tetrahedron Lett.* **2000,** *41*, 3331-3334.
83. Ojima, I.; Wang, T.; Miller, M. L.; Lin, S.; Bollera, C. P.; Geng, X.; Pera, P.; Bernacki, R. J., Synthesis and Structure–Activity Relationships of New Second-Generation Taxoids. *Bioorg. Med. Chem. Lett.* **1999,** *9*, 3423-3428.
84. Ojima, I. C., J.; Sun, L.; Borell, C. P.; Wang, T.; Miller, M. L.; Lin, S.; Geng, X.; Kuznetsova, L.; Qu, C.; Gallager, D.; Zhao, X.; Zanardi, I.; Xia, S.; Horwitz, S. B.; Mallen-St. Clair, J.; Guerriero, J. L.; Bar-Sagi, D.; Veith, J. M.; Pera, P.; Bernacki, R. J. , Design, Synthesis, and Biological Evaluation of New-Generation Taxoids. *J. Med. Chem.* **2008,** *51*, 3203-3221.
85. Ojima, I.; Lin, S.; Wang, T., Recent Advances in the Medicinal Chemistry of Taxoids with Novel β-Amino Acid Side Chians. *Curr. Med. Chem.* **1999,** *6*, 519-534.
86. Ali, S. M.; Hoemann, M. Z.; Aube, J.; Mitscher, L. A.; Georg, G. I.; McCall, R.; Jayasinghe, L. R., Novel Cytotoxic 3'-(*tert*-Butyl) 3-Dephenyl Analogs of Paclitaxel and Docetaxel. *J. Med. Chem.* **1995,** *38*, 3821-3828.
87. Gueritte-Voegelein, F.; Guenard, D.; Lavelle, F.; Le Goff, M.-T.; Mangatal, L.; Potier, P., Relationships between the Structure of Taxol Analogues and Their Antimitotic Activity. *J. Med. Chem.* **1991,** *34*, 992-998.
88. Ojima, I., Kuduk, S. D., Pera, P., Veith, J. M., Bernacki, R. J., Synthesis of and Structure-Activity Relationships of Non-Aromatic Taxoids. Effects of Alkyl and Alkenyl Ester Groups on Cytotoxicity. *J. Med. Chem.* **1997,** *40*, 279-285.
89. Ojima, I.; Fenoglio, I.; Park, Y. H.; Pera, P.; Bernacki, R. J., Synthesis and Biological Activity of 14β-Hydroxydocetaxel *Bioorg. Med. Chem. Lett.* **1994,** *4*, 1571-1574
90. Georg, G. I.; Boge, T. C.; Cheruvallath, Z. S.; Clowers, J. S.; Harriman, G. C. B.; Hepperle, M.; Park, H., The Medicinal Chemistry of Taxol. In *Taxol®: Science and Applications*, Suffness, M., Ed. CRC Press: New York, 1995; pp 317-375.
91. Chen, S.-H.; Fairchild, C.; Mamber, S. W.; Farina, V., Taxol Structure-Activity Relationships: Synthesis and Biological Evaluation of 10-Deoxytaxol. *J. Org. Chem.* **1993,** *58*, 2927-2928.
92. Klein, L. L., Synthesis of 9-Dihydrotaxol: A Novel Bioactive Taxane. *Tetrahedron Lett.* **1993,** *34*, 2047-2050.

93. Ishiyama, T.; Iimura, S.; Ohsuki, S.; Uoto, K.; Terasawa, H.; Soga, T., New Highly Active Taxoids from 9β-Dihydrobaccatin-9,10-acetals. *Bioorg. Med. Chem. Lett.* **2002,** *12*, 1083-1086.
94. Chen, R.; Kingston, D. G. I., Isolation and structure elucidation of new taxoids from Taxus Brevifolia. *J. Nat. Prod.* **1994,** *57*, 1017-1021.
95. Ravdin, R.; III, H. B.; Cook, G.; Eisenberg, P.; Kane, M.; Bierman, W.; Mortimer, J.; Genevois, E.; Bellet, R., Phase II trial of docetaxel in advanced anthracycline-resistant or anthracenedione-resistant breast cancer. *J. Clin. Oncol.* **1995,** *13*, 2879-2885.
96. Martin, M.; Pienkowski, T.; Mackey, J.; Pawlicki, M.; Guastalla, J.; Weaver, C.; Tomiak, E.; Al-Tweigeri, T.; Chap, L.; Juhos, E.; Guevin, R.; Howell, A.; Fornadnder, T.; Hainsworth, J.; Coleman, R.; Winholes, J.; Modiano, M.; Pinter, T.; Tang, S.; Colwell, B.; Prady, C.; Provencher, L.; Walde, D.; Rodriguez-Lescure, A.; Hugh, J.; Loret, C.; Rupin, M.; Blitz, S.; Jacovs, P.; Murawsky, M.; Riva, A.; Vogel, C., Adjuvant docetaxel for node-positive breast cancer. *N. Engl. J. Med.* **2005,** *352*, 2302-2312.
97. Cutsem, E. V.; Moiseyenko, V.; Tjulandin, S.; Majlis, A.; Constenla, M.; Boni, B.; Rodrigues, A.; Fodor, M.; Chao, Y.; Voznyi, E.; Risse, M.-L.; Ajani, J., Phase III Study of Docetaxel and Cisplatin Plus Fluorouracil Compared with Cisplatin and Fluorouracil As First-Line Therapy for Advanced Gastic Cancer: A Report of the V325 Study Group. *J. Clin. Oncol.* **2006,** *24*, 4991-4997.
98. Fossella, F.; Pereira, J.; Pawel, J. v.; Pluzanska, A.; Gorbounova, V.; Kaukel, E.; Mattson, K.; Ramlau, R.; Szczesna, A.; Fidias, P.; Millward, M.; Belani, C., Randomized, Multinational, Phase III Study of Docetaxel Plus Platinum Combinations Versus Vinorelbine Plus Cisplatin for Advanced Non-Small-Cell Lung Cancer: The TAX 326 Study Group. *J. Clin. Oncol.* **2003,** *21*, 3016-3024.
99. Dagher, R.; Li, N.; Abraham, S.; Rahman, A.; Sridhara, R.; Pazdur, R., Approval Summary: Docetaxel in Combination with Prednisone for the Treatment of Androgen-Independent Hormone-Refractory Prostate Cancer. *Clin. Cancer Res.* **2004,** *10*, 8147-8151.
100. Vermorken, J.; Remenar, E.; Herpen, C. v.; Gorila, T.; Mesia, R.; Degardin, M.; Stewart, J.; Jelic, S.; Betka, J.; Preiss, J.; Weyndaert, D. v. d.; Awada, A.; Cupissol, D.; Kienzer, H.; Rey, A.; Desaunois, I.; Bernier, J.; Lefebvre, J.-L., Cisplatin, Fluorouracil, and Docetaxel in Unresectable Head and Neck Cancer. *N. Engl. J. Med.* **2007,** *357*, 1695-1704.
101. Fossella, R.; DeVore, R.; Kerr, R.; Crawford, J.; Natale, R.; Dunphy, F.; Kalman, L.; Miller, V.; Lee, J.; Moore, M.; Gandara, D.; Karp, D.; Vokes, E.; Kris, M.; Kim, Y.; Gamza, F.; Hammershaimb, L., Randomized Phase III Trial of Docetaxel Versus Vinorelbine or Ifosfamide in Patients With Advanced Non-Small-Cell Lung Cancer Previously Treated With Platinum-Containing Chemotherapy Regimens. *J. Clin. Oncol.* **2000,** *18*, 2354-2362.
102. Tannock, I.; Wit, R. d.; Berry, W.; Horti, J.; Pluzanska, A.; Chi, K.; Oudard, S.; Theodore, C.; James, N.; Turesson, I.; Rosenthal, M.; Eisenberger, M., Docetaxel plus Prednisone or Mitoxantrone plus Prednisone for Advanced Prostate Cancer. *N. Engl. J. Med.* **2004,** *351*, 1502-1512.
103. Galsky, M.; Dritselis, A.; Kirkpatrick, P.; Oh, W., Cabazitaxel. *Nature Rev. Drug Discov.* **2010,** *9*, 677-678.
104. Robert, F.; Harper, K.; Ackerman, J.; Gupta, S., A phase I study of larotaxel (XRP9881) administered in combination with carboplatin in chemotherapy-naïve patients with stage IIIB or stage IV non-small cell lung cancer. *Cancer Chemother. Pharmacol.* **2010,** *65*, 227-234.
105. Metzger-Filho, O.; Moulin, C.; Azambuja, E. d.; Ahmad, A., Larotaxel: broadening the road with new taxanes. *Exp. Op. Invest. Drugs* **2009,** *18*, 1183-1189.

106. Dieras, V.; Viens, P.; Veyret, C.; Romieu, G.; Awada, A.; Lidbrink, E.; Bonnefoi, H.; Mery-Mignard, D.; Dalenc, F.; Roche, H., Larotaxel (L) in combination with trastuzumab in patients with HER2+ metastatic breast cancer (MBC): Interim analysis of an open phase II label study. *J. Clin. Oncol.* **2008,** *26*, 1070.
107. Dieras, V.; Limentani, S.; Romieu, G.; Tubiana-Huli, M.; Lortholary, A.; Kaufman, P.; Girre, V.; Besenval, M.; Valero, V., Phase II multicenter study of larotaxel (XRP9881), a novel taxoid, in patients with metastatic breast cancer who previously received taxane-based therapy. *Ann. Oncol.* **2008,** *19*, 1255-1260.
108. Beer, M.; Lenaz, L.; Amadori, D., Phase II study of ortataxel in taxane-resistant breast cancer. *Journal of Clinical Oncology* **2008,** *26*, a1066.
109. Moore, M.; Jones, C.; Harker, G.; Lee, F.; Ardalan, B.; Saif, M.; Hoff, P.; Coomes, J.; Rollins, C.; Felt, K., Phase II trial of DJ-927, an oral tubulin depolymerization inhibitor, in the treatment of metastatic colorectal cancer. *J. Clin. Oncol.* **2006,** *24*, s3591.
110. Roche, M.; Kyriakou, H.; Seiden, M., Drug evaluation: tesetaxel--an oral semisynthetic taxane derivative. *Curr. Opin. Invest. Drugs* **2006,** *7*, 1092-1099.
111. Beeram, M.; Papadopoulos, K.; Patnaik, A.; Qureshi, A.; Tolcher, A., Phase I dose-ranging, pharmacokinetic (PK) study of tesetaxel, a novel orally active tubulin-binding agent. *J. Clin. Oncol.* **2010,** *28*, ae13075.
112. Ramanathan, R.; Picus, J.; Raftopoulos, H.; Bernard, S.; Lockhart, A.; Frenette, G.; Macdonald, J.; Melin, S.; Berg, D.; Brescia, F.; Hochster, H.; Cohn, A., A phase II study of milataxel: a novel taxane analogue in previously treated patients with advanced colorectal cancer. *Cancer Chemother. Pharmacol.* **2008,** *61*, 435-438.
113. Ojima, I.; Slater, J. C.; Michaud, E.; Kuduk, S. D.; Bounaud, P.-Y.; Vrignaud, P.; Bissery, M. C.; Veith, J. M.; Pera, P.; J., B. R., Syntheses and Structure-Activity Relationships of the Second-Generation Antitumor Taxoids: Exceptional Activity against Drug-Resistant Cancer Cells. *J. Med. Chem.* **1996,** *39*, 3889-3896.
114. Ojima, I.; Wang, T.; Miller, M. L.; Lin, S.; Borella, C. P.; Geng, X.; Pera, P.; Bernacki, R. J., Synthesis and Structure-Activity Relationships of New Second-Generation Taxoids. *Bioorg. Med. Chem. Lett.* **1999,** *9*, 3423-3428.
115. Ferlini, C.; Distefano, M.; Pignatelli, F.; Lin, S.; Riva, A.; Bombardelli, E.; Mancuso, S.; Ojima, I.; Scambia, G., Antitumor Activity of Novel Taxanes That Act as Cytotoxic Agents and P-Glycoprotein Inhibitors at the Same Time. *Br. J. Cancer* **2000,** *83*, 1762-1768.
116. Gut, I.; Ojima, I.; Vaclavikova, R.; Simek, P.; Horsky, S.; Linhart, I.; Soucek, P.; Knodrova, E.; Kuzetsova, L.; Chen, J., Metabolism of new-generation taxanes in human, pig, minipig and rat liver microsomes. *Xenobiotica* **2006,** *36*, 772-792.
117. Botchkina, G.; Zuniga, E.; Das, M.; Wang, Y.; Wang, H.; Zhu, S.; Savitt, A.; Rowehl, R.; Leyfman, Y.; Ju, J.; Shroyer, K.; Ojima, I., New-generation taxoid SB-T-1214 inhibits stem cell-related gene expression in 3D cancer spheriods induced by purified colon tumor-initiating cells. *Mol. Cancer* **2010,** *9*, 192-204.
118. Li, F.; Tiede, B.; Massague, J.; Kang, Y., Beyond tumorigenesis: cancer stem cells. *Cell Res.* **2007,** *17*, 3-14.
119. Kuznetsova, L.; Sun, L.; Chen, J.; Zhao, X.; Seitz, J.; Das, M.; Li, Y.; Veith, J.; Pera, P.; Bernacki, R.; Xia, S.; Horwitz, S.; Ojima, I., Synthesis and Biological Evaluation of Novel 3'-Difluorovinyl Taxoids. *J. Fluor. Chem.* **2012,** *143*, 177-188.

Chapter 3

Drug Conjugates Based on Polyunsaturated Fatty Acids

Content

§ 3.0.0 Drug Conjugates of Polyunsaturated Fatty Acids

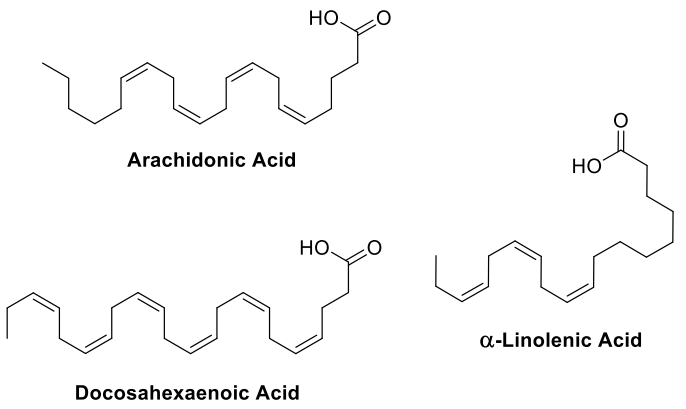

Figure 3-1: Chemical structures of selected polyunsaturated fatty acids

Polyunsaturated fatty acids (PUFAs) are a major class of biochemicals that are utilized as cellular membrane components, catabolized as energy sources and metabolized into intracellular signaling molecules. These PUFAs affect a number of cellular processes involved in human disease, such as inflammation and metabolic regulation. As tumors are fast-growing tissues, they require a relatively high intake of vital nutrients to feed their rapidly proliferating cell population. In a single arterial tissue perfusion study, it was demonstrated that the uptake of certain PUFAs was significantly increased in tumor tissue compared to healthy tissue.[1] Based on this phenomenon of elevated PUFA uptake in malignant tissues, numerous PUFA-drug conjugates have been synthesized and are currently in various of stages of drug development.[2] Compared to the parent compound, PUFA conjugates have been found to possess drastically altered pharmacokinetic and biodistribution profiles, resulting in tumor-specific accumulation of the drugs.

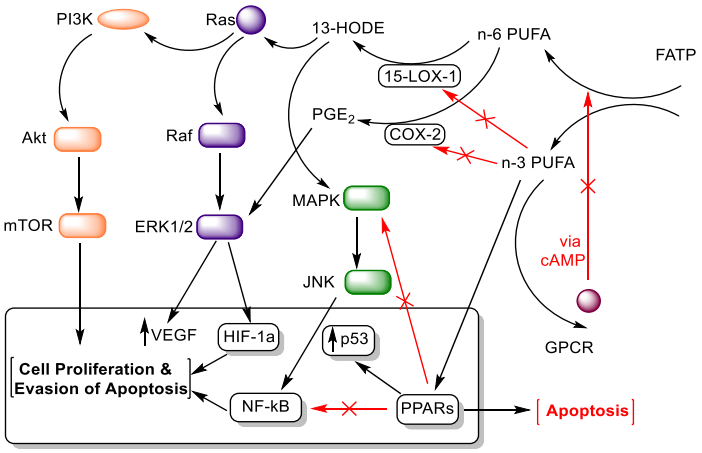

Figure 3-2: Intracellular signaling pathways affected by PUFAs (adapted from [2])

Pronounced effects of dietary intake of PUFAs have been demonstrated on cancer development and progression. Specifically, the ratio of certain PUFAs present in the diet can lead to either a stimulation or inhibition of cancer growth *in vitro* and *in vivo*.[3] For instance, populations that consume significant amounts of n-3 PUFAs, such as docosahexaenoic acid (DHA) and eicosapentaenoic acid (EPA), have significantly reduced incidence rates of cancer compared to populations with a diet rich in n-6 PUFAs, such as linoleic acid (LA) and arachidonic acid (AA).[4] The structures of these PUFAs are shown in **Figure 3-1**. Fish and fish oil are typically contain high levels of n-3 PUFAs, whereas n-6 PUFAs are present in terrestrial plants such as corn, as well as the animals fed from these plants. The physiological reasons for these trends in cancer incident rates are rapidly emerging at the biochemical level (**Figure 3-2**). Detailed information pertaining to the PUFA transport, internalization, and metabolism and their effects on cellular signaling has recently been discovered that helps to tie together these epidemiological trends with alterations in metabolism and inflammatory response.[3, 5-8]

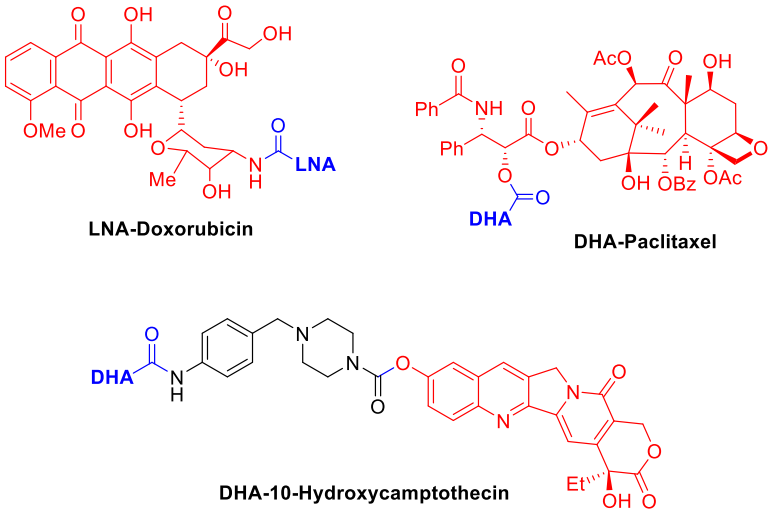

Figure 3-3: Structures of selected PUFA-drug conjugates

The conjugation of cytotoxic drugs with PUFAs, such as the structures shown in **Figure 3-3**, is an attractive strategy for novel drug development for several reasons. PUFAs are non-toxic, FDA-approved food additives and some PUFAs possess cancer-specific toxicity via a myriad of signaling pathways overexpressed in various cancers.[9, 10] Synergy has been observed with a variety of cytotoxic drugs against various cancer cell lines *in vitro* and human tumors *in vivo*.[11, 12] In addition, PUFAs appear to have protective effects on healthy cells by preventing drug-induced apoptosis, and conjugation to PUFAs may limit systemic toxicity by reducing the exposure of healthy tissues to cytotoxic drugs. Currently PUFA conjugates have been synthesized for the following drugs: Camptothecin (topoisomerase I inhibitor),[13] doxorubicin (topoisomerase II inhibitor),[14, 15] illudin M (dna alkylator),[16] chlorambucil (dna alkylator),[17] mytomycin C (dna alkylator),[18] 2'-deoxy-5-flurouridine (dna synthesis inhbititor),[19] and methoxtrexane (antifolate).[20] Currently, the most successful PUFA-drug conjugate is DHA-paclitaxel (Taxoprexin), which is currently in phase III clinical trials for the treatment of malignant melanoma.[21]

§ 3.0.1 DHA-Paclitaxel (Taxoprexin®)

Most chemotherapeutic agents act on processes involved in cell division, poisening actively dividing cells at either the S or G2/M phases of mitosis. This includes paclitaxel, which targets the G2/M phase, making it an excellent choice for the treatment of rapidly dividing tumors.[22] However, many cancers and certain subpopulations of cells within solid tumors, divide much more slowly and may not be affected by paclitaxel treatment during traditional dosing regimens. Accordingly, it may be advantageous to maintain constant levels of anticancer drugs in the tumor tissue for prolonged periods of time, so that they may affect even the slowly dividing cancer cell populations. This premise, combined with the observation that PUFAs are rapidly taken up by tumors from the bloodstream, was the rationale behind the development of DHA-paclitaxel (Taxoprexin®) (TXP).[23] In TXP, DHA was covalently linked to paclitaxel at its 2'-position through an ester linkage, as it has been shown that the esterification of the 2'-hydroxyl group substantially decrease the cytotoxicity of paclitaxel.[23] The resulting prodrug possesses a drastically altered pharmacokinetic (PK) profile compared to that of paclitaxel and is well suited for the prolonged treatment of solid tumors.[23]

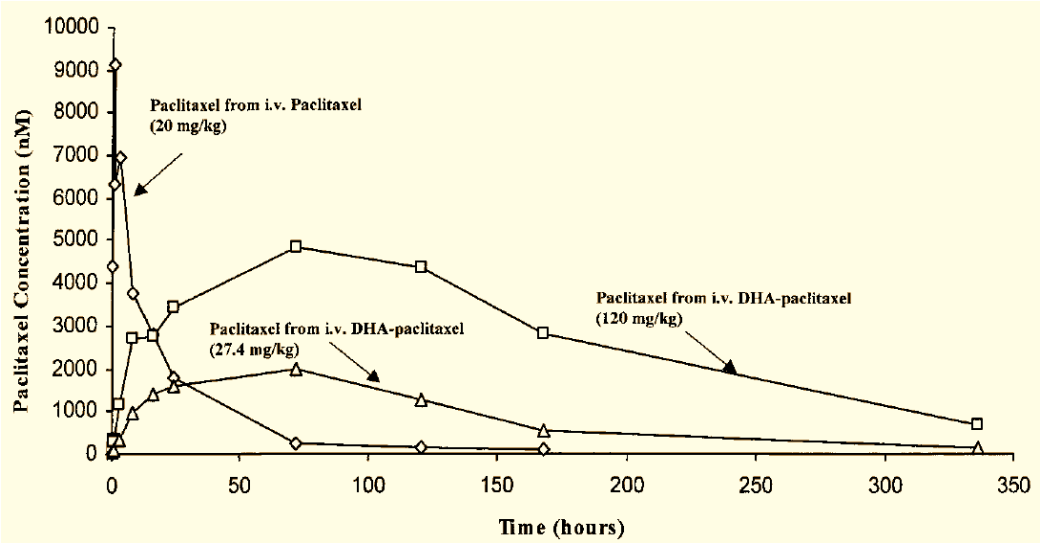

Figure 3-4: Plasma concentration of free and TXP-derived paclitaxel in blood (adapted from [23])

In order to elucidate the factors responsible for the improved efficacy of TXP, a detailed PK study was conducted.[23] Three major parameters investigated were maximal concentration (Cmax), time of maximal concentration (Tmax) and the area under the curve (AUC) on the drug concentration vs. time plot. To investigate the biodistribution of the conjugate, data for each of the three parameters were taken from the blood plasma, muscle tissue and tumor tissue. For example, **Figure 3-4** shows the plot for blood plasma concentration with respect to time.

When paclitaxel was administered intravenously, the plasma Cmax of 42 µM was quickly reached at a Tmax of ~5 min, and was rapidly cleared to the surrounding tissue with a tissue half-life of ~12 hours (**Figure 3-4**). The Cmax for muscle and tumor tissues occurred 30 minutes after injection and were found to be 7.6 and 9.2 µM, respectively, indicating little tumor specificity.[23] In stark contrast, the plasma Cmax of ~2.5 mM for DHA-paclitaxel was reached in 30 minutes after injection. After 8 hours the conjugate had reached Cmax levels of 14.9 and 107.4 µM in the muscular and tumor tissues, respectively. Free paclitaxel levels derived from TXP reached a Cmax of only 340 nM in muscle tissues compared to 4.8 µM in tumor tissues, with half-lives of 120 hours and 72 hours, respectively, In contrast to free paclitaxel injection, with a plasma AUC value of 34 µM x h indicative of rapid and indiscriminant clearance, TXP showed a marked increase in plasma distribution, with AUC values of 12.8 mM x h, demonstrating prolonged retention in the plasma compartment. Later studies, identified binding to the plasma proteins human serum albumin (HAS) and α1-acid glycoprotein (AAG) as the major factor for TXP's extended half-life and slow release from the plasma compartment.[24] These two proteins were found to contribute equally to the plasma drug binding level of >99.6%, compared to 89.1% measured for paclitaxel.[24, 25]

In phase I, the maximum dose for TXP was found to be 1100 mg/m^2, which is substantially higher than that of 175 mg/m^2 for free paclitaxel. Although no patients developed alopecia, peripheral neuropathy or musculoskeletal toxicity > grade 1, myelosuppression and neutropenia were found to be serious and dose-limiting toxicities. In contrast to paclitaxel treatment, no neurotoxicity was observed in TXP-treated patients.[26] Taxoprexin was advanced to phase II clinical trials for eight different indications including NSCLC, metastatic melanoma, as well as prostate, breast and gastric cancers.[27-29] Hematological side effects were found to be dose-limiting in all phase II trials. Out of all indications in which TXP was evaluated, it was advanced to phase III only in malignant melanoma.[21]

§ 3.0.2 Tumor Targeting by PUFA Conjugation

Although the mechanism of tumor-selective accumulation for PUFA-drug conjugates is not entirely clear, pharmacokinetic studies on Taxoprexin have clearly demonstrated three facts: (1) DHA-paclitaxel accumulates in solid tumors preferentially compared to paclitaxel (2) plasma protein binding of DHA-paclitaxel is >99%, significantly higher than for paclitaxel (3) DHA-paclitaxel has a smaller volume of distribution and a larger plasma AUC than paclitaxel.[24, 30] These facts lend themselves to a hypothesis in which the tumor-specific accumulation of PUFA-drug conjugates *in vivo* is mediated by blood plasma proteins such as HSA.

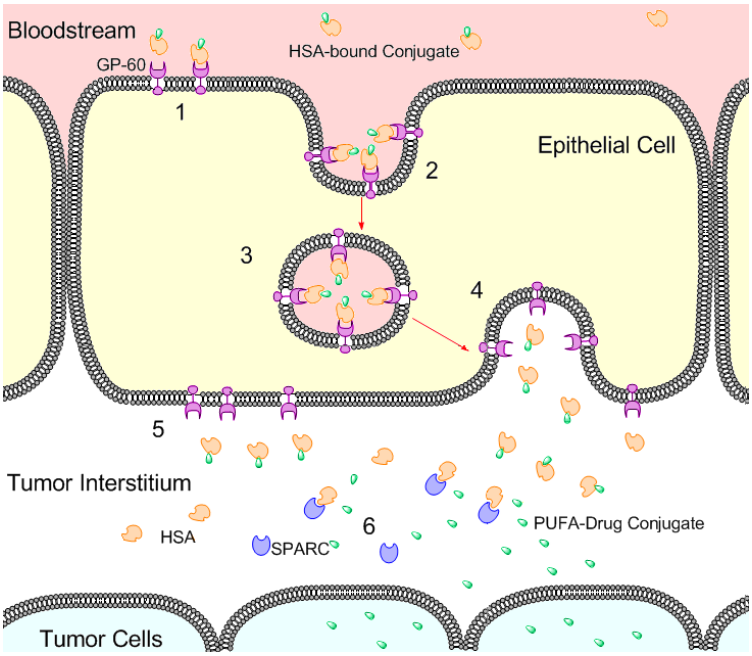

Figure 3-5: Tumor-selective accumulation *via* enhanced trans-epithelial transport (adapted from [2])

There is a large body of evidence suggesting that tumors exhibit an enhanced uptake of plasma proteins, and that these proteins are catabolized as an energy source.[31] Furthermore, according to the early studies that elucidated the enhanced permeability and retention (EPR) effect in solid tumors, HSA does accumulate in the tumor interstitial space due to the highly degraded vasculature and poorly developed lymphatic system of the tumor.[32] In addition to the EPR effect, epithelial transcytosis mediated by gp60 (**Figure 3-5**) has been implicated in the tumor-selective accumulation of HSA. Albumin has been shown to bind gp60, also known as albondin, resulting in the transcytosis of HSA across the epithelial cells. It has not been demonstrated that albondin internalizes HSA and transports it to the lysosome for degradation. Secreted Protein Acidic and Rich in Cystein (SPARC) has been shown to bind albumin and other albondin substrates. SPARC is a homologue of α-feto protein that binds to fatty acid-albumin complexes and causes the release of the cargo prior to degradation of the albumin. Thus, it has been proposed that SPARC binds the albumin-conjugate complex, releasing the conjugate for internalization following gp60-mediated transcytosis.[33] This mechanism has been used to explain the tumor selectivity of the FDA-approved Abraxane®, an HSA nanoparticle formulation of paclitaxel.[34] Increased expression levels of SPARC in patients with solid tumors has been correlated to improved efficacy of Abraxane® treatment, providing a solid clinical basis for this model of albumin-mediated drug delivery.[34]

§ 3.0.3 PUFA–2nd-Generation Taxoid Conjugates

Although Taxoprexin® has not demonstrated sufficient clinical efficacy to warrant FDA approval, its clinical development has provided evidence for the profound effect that PUFA conjugation has on the pharmacokinetics of the parent drug. Furthermore, as paclitaxel is a well-known substrate for Pgp-mediated efflux, it was hypothesized that the efficacy of TXP might be further limited in MDR tumors. To test this hypothesis, PUFA conjugates of six second-generation taxanes were synthesized and tested alongside DHA-paclitaxel and DHA-docetaxel *in vivo*.[35] Conjugates were administed to SCID mice bearing drug-sensitive A121 (ovarian cancer, Pgp-) and drug resistant DLD-1 (drug resistant, Pgp+) tumor xenografts. In the drug sensitive A121 tumor xenografts, DHA-paclitaxel showed improved efficacy compared to free paclitaxel, curing 2/5 mice for >186 days, with minimal toxicity. However, in the drug-resistant DLD-1 tumor xenografts, DHA-paclitaxel was ineffective even at the dose of 240 mg/kg. The next-generation taxoid conjugate, DHA-1214 (**Figure 3-6**), achieved complete regression at the same dose in all five mice for over 187 days (**Figure 3-6**, bottom left). These data clearly indicate that the efficacy of DHA-paclitaxel is severely limited by Pgp expression *in vivo*.

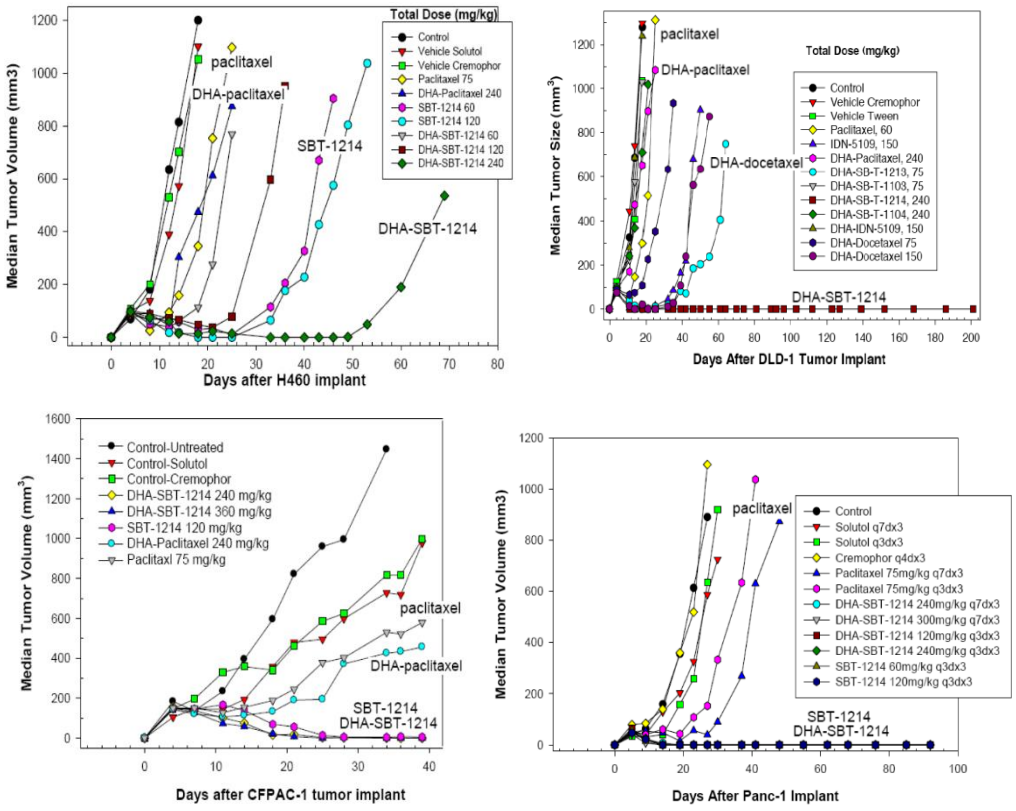

Figure 3-6: Tumor volumes of mice bearing tumor xenografts treated with PUFA conjugates (Adapted from [2])

To compare the efficacy of n-3 and n-6 PUFAs, LNA and LA conjugates of the next-generation taxoid SB-T-1213 were synthesized and tested against the A121 tumor models. While DHA-1213 treatment resulted in tumor growth delays of only 54 days and no cured animals, LNA-1213 treatments provided growth delays of 104 days and produced cures in 2/5 mice.[35] Treatment with the n-6 PUFA conjugate LA-1213 showed very little efficacy, with growth inhibition of only 21 days and no long-term survivors. This study clearly illustrated the difference between taxane conjugates of n-3 and n-6 PUFAs and suggested the possible advantage of utilizing LNA in drug conjugates.

Figure 3-6 shows the results of four drug-resistant tumor xenograft mouse models treated with PUFA conjugates of next generation taxoids. For comparison, mice were also treated with paclitaxel, DHA-paclitaxel and/or a free next-generation taxoid.[35] In the CFPAC-1 pancreatic tumor model in Swiss Webster nude mice, paclitaxel caused only short term growth delay, SB-T-1214 provided prolonged growth delays and one cure, while DHA-1214 caused complete remissions and cures in all mice treated (**Figure 3-6**, top right). Treatment of the highly aggressive H460 human NSCLC xenograft in an RPCI SCID mouse model (**Figure 3-6**, top left) with DHA-1214 resulted in tumor growth delays of 50 days while paclitaxel treatment was virtually ineffective. When RPCI SCID mice bearing Panc-1 pancreatic tumor xenografts were treated with DHA-1214, complete remissions with growth delays of >90 days were observed (**Figure 3-6**, bottom right), while paclitaxel treatment provided only growth delays of 25 days. These *in vivo* results demonstrated the superiority of next-generation taxoid-based PUFA drug conjugates against MDR tumors, and provided strong support to further the evaluation of these PUFA-taxoid conjugates.

§ 3.1.1 Synthesis of DHA-Taxoid Conjugates

DHA conjugates of selected next-generation taxoids were performed according to modified literature procedures.[35]

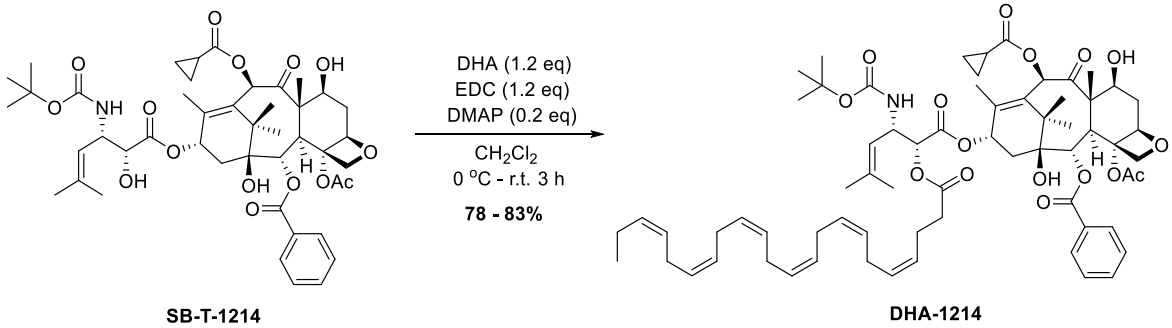

Scheme 3-1: Synthesis of DHA-Taxoid conjugates

DIC coupling of **SB-T-1214** proceeded in decent yield. Care must be taken when working with DHA, as it is very susceptible to allylic oxidation due to its 7 allylic positions and the all *cis*

configuration of its double bonds. This particular batch of **DHA-1214** was used for *in vitro* analysis and comparison to a novel DHA-based taxoid conjugate (Section 3.3.6). With **SB-T-121602** in hand, the synthesis of **DHA-121602** is planned for preliminary *in vivo* evaluation of the novel conjugate. Due to the instability of these conjugates, this reaction will be performed when the appropriate amount of mice are available for the pilot study.

§ 3.1.2 Synthesis of LNA-Taxoid Conjugates

Due to the successful application of DHA to the development of tumor-targeted drug conjugates, other PUFAs were tested for their ability for enhance tumor specific drug accumulation *in vivo*. Of those tested, α-linoleic acid (LNA) proved to be effective. LNA is much cheaper than DHA and has greater chemical stability. Therefore, **LNA-1214** has also undergone preclinical pharmacokinetic evaluation.

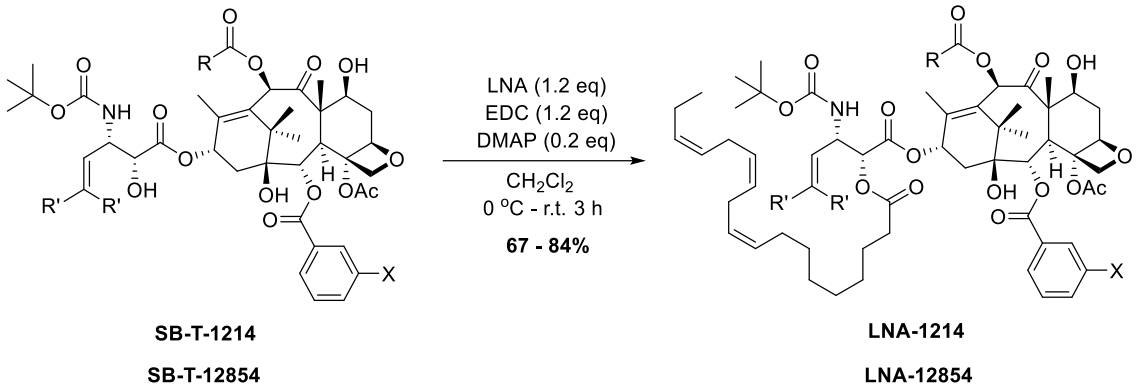

Scheme 3-2: Synthesis of LNA-Taxoid conjugates

Similar to the conjugation of DHA, DIC coupling afforded the desired **LNA-1214** in good yield. Interestingly, **LNA-1214** has very limited activity *in vitro*, yet retains activity *in vivo*. This material will be used to analyze the source of this apparent discrepancy. **LNA-12854** was also synthesized for *in vivo* evaluation. Although this study is currently underway, preliminary results indicate that this compound is quite toxic, limiting the dose that can be administered *in vivo*. Pilot *in vivo* studies on **LNA-121602** have been planned, and the compound will be synthesized when the animals are ready.

§ 3.2.1 Design of the Isotopically-labeled Internal Standard d5-Bz-SB-T-1214

To facilitate the preclinical pharmacokinetic profiling of **DHA-1214** and **LNA-1214**, an isotopically-labeled SB-T-1214 was designed. Due to the relatively high molecular weight of **DHA-1214** (MW = 1164 Da), labeling the structure with only M+1 would not be sufficient to resolve the internal standard from the isotopic distribution of the parent compound. In fact, only a standard with a MW 5 or above would have overlap with a natural isotope of < 1% intensity than

the parent compound. In addition, **Figure 3-7** shows the two most commonly observed fragments during analysis of SB-T-1214 by mass spectroscopy.

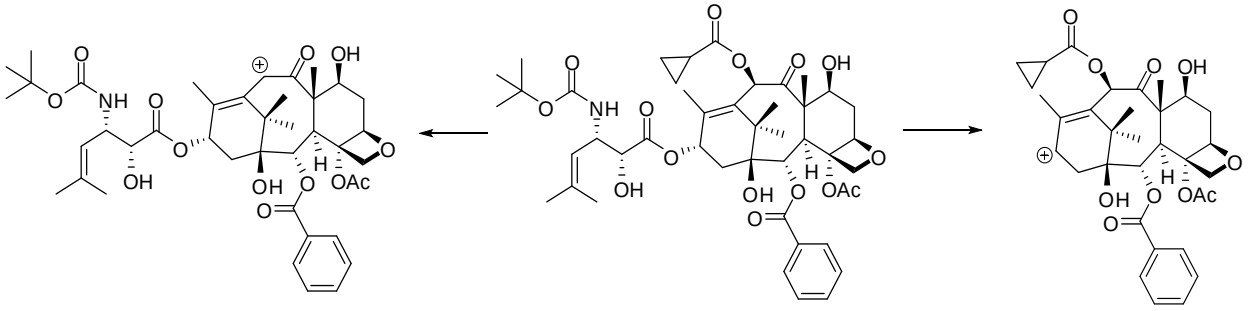

Figure 3-7: MS fragmentation pattern for SB-T-1214

Fragmentation commonly occurs at the C10 or C13 positions, with loss of the hydroxyl group and any moieties attached. This is due to the stability of the allylic cation that is formed upon ionization and fragmentation. As it is desirable to have a unique fragmentation pattern for the internal standard, these two positions were not considered appropriate for isotopic labeling. Thus, the C2 position was chosen and due to the requirement for resolution from the isotopic distribution of the parent compound, a pentadeuterated (M+5) benzoyl group was chosen as the label.

§ 3.2.2 Sythesis Towards d5-Bz-SB-T-1214

Starting from the 1,2 diol intermediate **2-2**, straightforward DIC coupling using standard conditions resulted in two products which were quite difficult to purify by column chromatography (ΔR_f = ~0.03). Partial separation was achieved via painstaking chromatography to afford samples of the two pure products. After NMR and MS analysis of the products, their structures appeared to correspond to compounds **3-1** and **3-2**. Although it was possible to acquire the desired product using this method, the reaction was slow, low yielding, and required multiple rounds of chromatography to fully separate the two products. Therefore, alternative methods for the production of **3-2** were investigated.

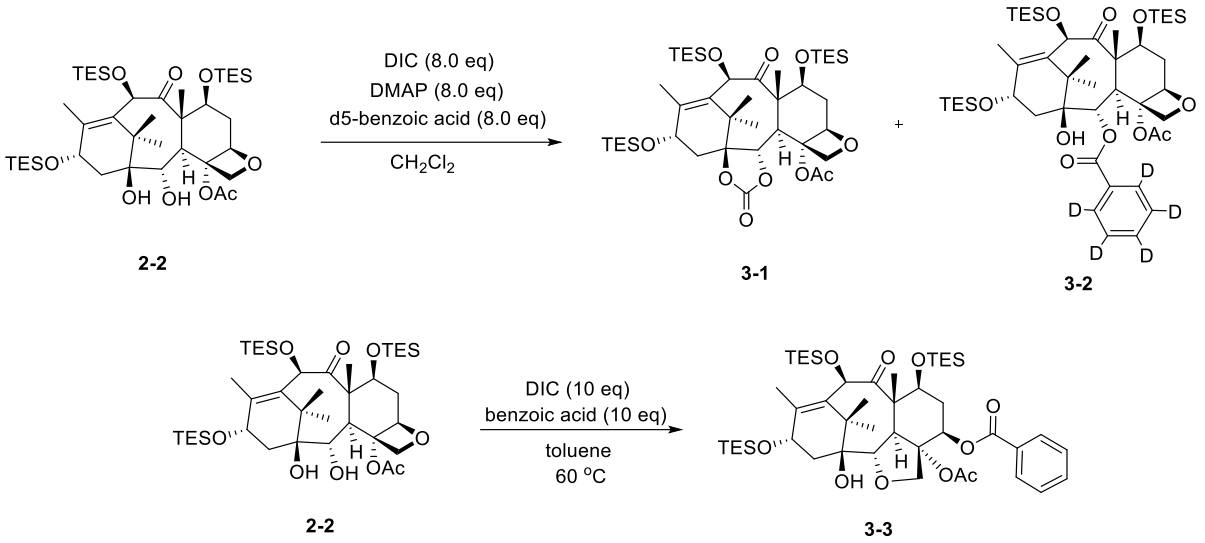

Scheme 3-3: Initial route to C2-d_5-Bz-modified 10-DAB-III

Treatment of **2-2** using catalytic DMAP with heating resulted in the exclusive formation of the D-ring opened compound **3-3**. This rearrangement is known to occur in relatively harsh acidic conditions and the structure was confirmed by comparison of the NMR spectra to that reported in the literature. In order to confirm structure **3-1**, diol **2-2** was treated with triphosgene and **3-1** was isolated after column chromatography, according to a known procedure. Spectra obtained from the byproduct of the DIC coupling matched that of carbonate **3-1**, confirming the structure.

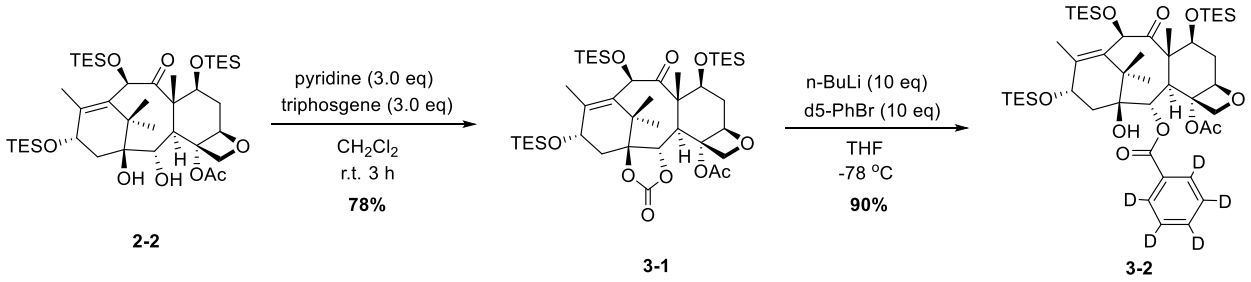

Scheme 3-4: Improved synthetic route to C2-d_5-Bz-modified 10-DAB-III

With pure 1,2 carbonate **3-1** in hand, a selective ring opening was attempted according to Holton's method. Generation of the d_5-phenyl lithium was performed via the treatment of d5-bromobenzene with n-BuLi in THF. On a small scale, these conditions resulted in the exclusive formation of the desired product **3-2**; however this procedure proved to be too harsh for scale up. Concomitant with this development, the synthesis of the desired internal standard **d_5-Bz-1214** and **DHA-d_5-Bz-1214** were achieved by Radha Bonala (Chem Masters Int.) using the first procedure, although in low overall yield.

§ 3.3.0 Formulation and Stability Study

To assist *in vivo* experiments, a stability study on DHA-1214 in the stock formulation was performed. This was an HPLC-based procedure, and as such required extraction before injection into the HPLC. Therefore, the extraction procedure was validated to ascertain the reliability and error inherent in this method.

At each calibration time point, 1.0 mg of solid DHA-1214 was dissolved in 1 mL of HPLC grade methanol. The HPLC trace was taken and the peak area was used as the "Before Extraction" value. To get the "After Extraction" value, 1.0 mg of solid DHA-1214 was dissolved in 20 uL of 1:1 Solutol:ethanol, dissolved in 2.0 mL EtOAc, washed with brine (3 x 2.0 mL), and the organic solvents removed by vacuum pump. The resulting solid was dissolved in 1.0 mL of methanol for HPLC analysis.

Calibration point 1 – Day 0 directly from the -78 ^{o}C freezer
Calibration point 2 – 2 hours room temperature as a solid
Calibration point 3 – 7 days at room temperature as a solid

Values before correction for impurity at 19.3 min

Calibration Point	Before Ext 220 nm	After Ext 220 nm	Error 220 nm	Before Ext 254 nm	After Ext 254 nm	Error 254 nm
1	96.64	94.78	1.86	96.71	96.25	0.46
2	96.80	91.76	5.01	94.98	91.95	2.14
3	74.60	59.35	15.25	53.21	47.39	5.82

Values after correction for impurity at 19.3 min

Calibration Point	Before Ext 220 nm	After Ext 220 nm	Error 220 nm	Before Ext 254 nm	After Ext 254 nm	Error 254 nm
1	96.64	94.78	1.86	96.71	96.25	0.46
2	96.80	94.89	1.91	94.98	92.84	2.14
3	74.60	67.88	6.92	53.21	48.89	4.32

Table 3-1: Calibration of extraction for stability test

Although this method of performing liquid-liquid extraction is not quantitative, it has been shown that the values obtained after extraction are reasonable estimates of the sample's purity. As seen on the next page, the UV traces from the HPLC data show that there is no appreciable amount of impurity lost during extraction (i.e. the impurity profile of the traces before and after extraction match). However, the procedure does introduce new impurities, (e.g. the impurity at 19.3 min – see next page), and therefore it appears the values from the study may underestimate the actual purity of the sample. When the impurity artifact at 19.3 is corrected for, the "After Extraction" values appear to follow the "Before Extraction" values, and the discrepancy between the two increases as the compound decomposes.

Major Impurity at 19.2 – 19.4 min appears to be an artifact of the extraction

Calibration point 2: 254 nm

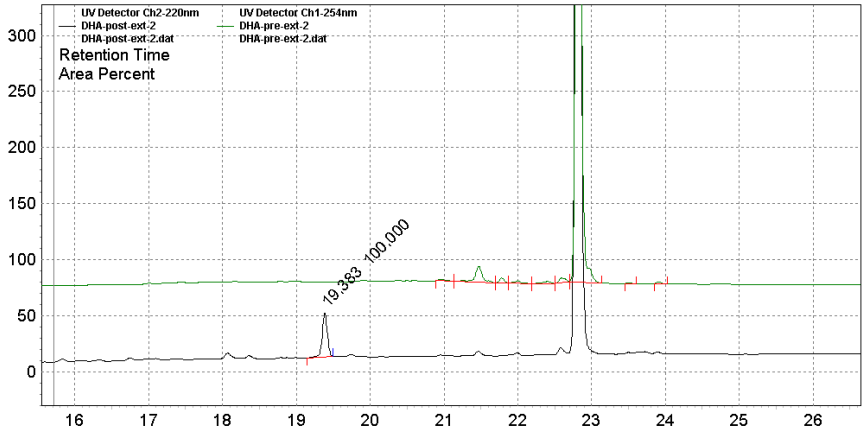

Calibration point 3: 254 nm

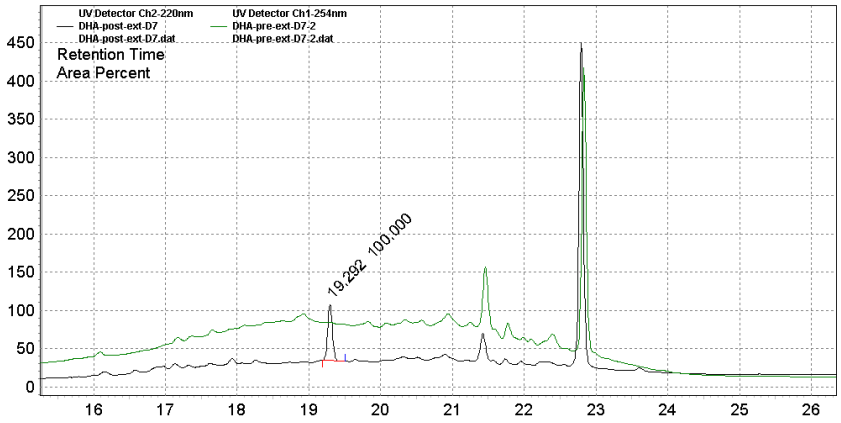

Figure 3-8: Sample HPLC traces used in the validation of the stability study

Clearly this impurity is a result of the extraction process, and variable from one batch to another. In the actual experiment, it shows up as an impurity (2 - 4 %) mostly at 254 nm with almost a random pattern. Perhaps it was a contaminant in the EtOAc, but at any rate is not likely to be a result of decomposition in the surfactant mixture.

All values and error are approximations based on the calibration data

Room Temperature

Days in Storage	254 nm	220 nm
0	96.7 ± 1.9	96.3 ± 2.1
4	96.7 ± 1.9	94.1 ± 2.1
7	96.1 ± 1.9	94.3 ± 2.1
14	94.6* ± 1.9	92.2* ± 2.1
28	94.7 ± 1.9	93.7 ± 2.1

Four Degrees Celsius

Days in Storage	254 nm	220 nm
0	96.71 ± 1.9	96.25 ± 2.1
4	97.12 ± 1.9	94.96 ± 2.1
7	96.43 ± 1.9	93.50 ± 2.1
14	95.14* ± 1.9	94.84* ± 2.1
28	95.56 ± 1.9	95.66 ± 2.1

*Values corrected for erroneous impurity around 19.3 min

Table 3-2: Purity values based on HPLC analysis of DHA-1214 stock solutions

In the degassed Solutol:ethanol formulation, DHA-1214 appears to be degrading to a detectable level by about 2 weeks. Any improvement in stability from storage at 4 ^{o}C cannot be concluded within error of this experiment as of 2 weeks. The two compounds analyzed upon their return from DLAR showed varying levels of decomposition, with the older and more frequently used vial exhibiting a greater level of deterioration.

§ 3.3.1 Biological Evaluation of PUFA-1214 Conjugates Against MX-1 Xenografts

To further assess the efficacy of the PUFA conjugates DHA and LNA-1214, they were tested in SCID mice bearing MX-1 breast cancer xenografts. Both conjugates were formulated in 1:1 Ethanol:Solutol H-15 1:1at stock solution concentrations of 50 mg/mL and diluted to 200 µL total volume with saline for injections. Paclitaxel was also formulated using stock concentrations of 50 mg/mL in 1:1 Chremophor:Ethanol, which is significantly more concentrated than the standard stock concentration of 7.5 mg/mL. The work for this study was conducted by Jean Rooney and Dr. Tom Zimmerman at the Division of Laboratory Animal Resources (DLAR) at Stony Brook University.

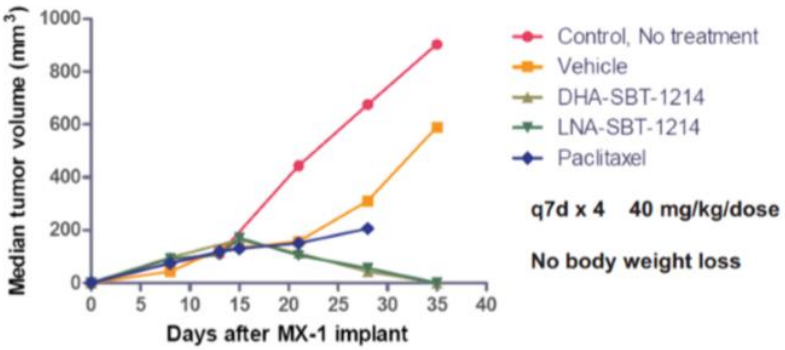

Figure 3-9: Median tumor volume in MX-1 xenograft study

The MX-1 xenografts grew rapidly, as seen in **Figure 3-9**, and the mice were euthanized at day 35 with large tumors. The control vehicle, a mix of 1:1 Ethanol:Solutol H-15, had some minor tumor-suppressing effects, but ultimately these mice also had to be euthanized at 35 days. Paclitaxel did significantly slow the rate of tumor growth, but proved to be highly toxic, killing the mice on the fourth dose. Therefore, the concentration of the stock solution for paclitaxel must be kept at 7.5 mg/mL and higher concentrations are significantly deleterious to the efficacy of the treatment. The PUFA-1214 conjugates were found to be highly effective in this breast cancer model and produced complete tumor regressions in 5 out of 5 mice for both compounds.

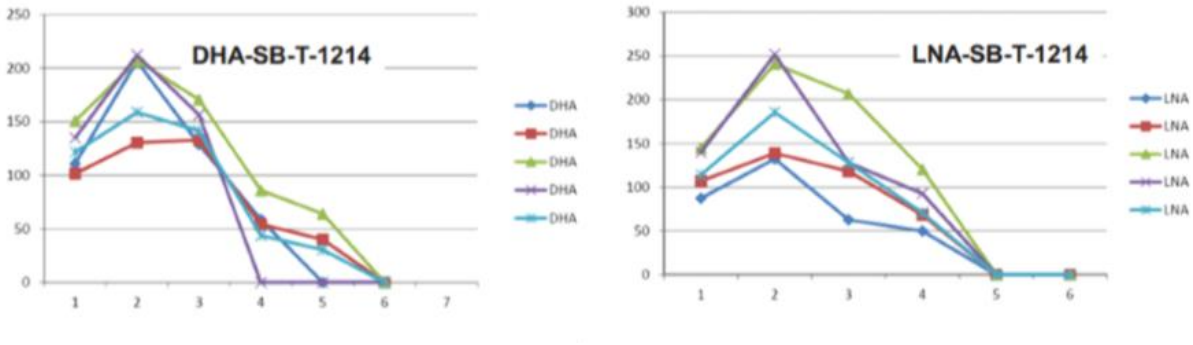

Figure 3-10: Tumor volumes of individual mice treated with PUFA-1214 conjugates

PUFA conjugates for this experiment were provided by ChemMaster Int. Both DHA-1214 and LNA-1214 succeeded in effectively curing all mice tested in this study. Looking at the tumor burden of the individual mice (Figure 3-11), it appears as though LNA-1214 was actually faster at reducing the tumor mass than DHA-1214, as evidence by the fact that all 5 mice had no discernable tumors before those treated with DHA-1214. Impressively, LNA-1214 was successful in treating mice whose tumors had grown to ~250 mm3 before dosing. This result prompted an investigation into the *in vivo* efficacy of another LNA-taxoid conjugate, **LNA-12854**.

§ 3.3.2 Biological Evaluation of LNA-12854 Conjugates Against MX-1 Xenografts

As LNA-1214 was found to exhibit comparable efficacy to DHA-1214 against MX-1 breast cancer xenografts, another LNA conjugate, LNA-12854 was tested in the same model. It was compared against a control, the vehicle (1:1 Ethanol:Solutol H:15) and SB-T-1214. The results are shown in **Figure 3-11**. This study was also conducted by Jean Rooney and Dr. Tom Zimmerman at the Stony Brook DLAR.

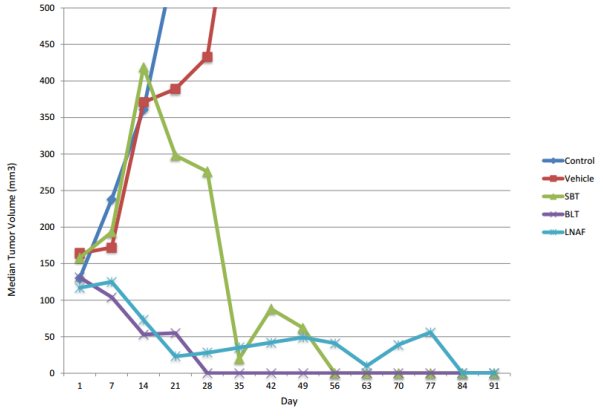

Figure 3-11: Median tumor volume of SCID mice bearing MX-1 xenografts

As seen by both the control and the vehicle-treated populations, the MX-1 tumors grew extremely fast, producing large tumors in just a few weeks post-injection. The rapid and erratic growth rate of these tumors when the cells were introduced by tail vein injection posed a logistical difficulty in working with this cell line. Even in these rapidly growing tumors, free SB-T-1214 was able to control the mass of these tumors and eventually lead to full remission in all surviving mice (**Figure 3-11**, *green*). For mice treated with LNA-12854, complete tumor regression was observed in 5 out of 5 mice tested at the higher dose (**Figure 3-12**).

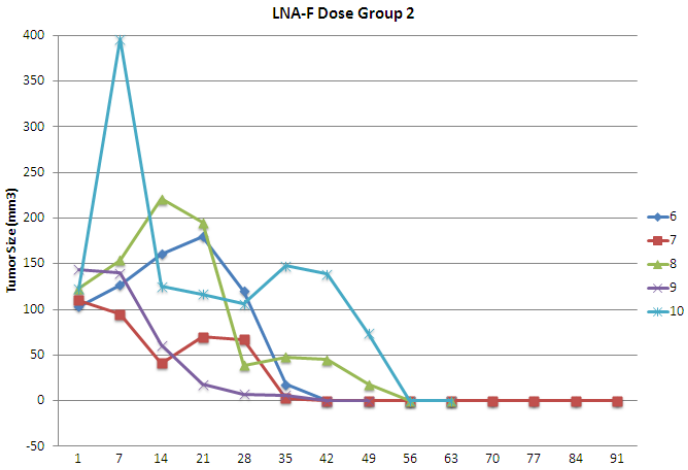

Figure 3-12: MX-1 Tumor volume for SCID mice treated with LNA-12854

Treatment of SCID mice bearing MX-1 tumor xenografts with LNA-12854 resulted in a total tumor regression in all mice, with survival up to 90 days. Impressively, even tumors that had grown up to 400 mm^3 before treatment were completely gone following treatment with LNA-12854. However, weight loss was observed in mice in this treatment group. Therefore, it appears that this compound, although highly potent, may be difficult to develop in a safe therapeutic window and dosing regimen. This increased toxicity may be a result of the fact that SB-T-12854 is completely impervious to metabolic hydroxylation by CYP enzymes in the liver.

§ 3.3.3 Biological Evaluation of DHA-1214 against Met-CSC Derived Tumors

Following the results of the MX-1 experiment, DHA-1214 was tested against tumor xenografts derived from a metastatic CSC-enriched population of breast cancer cells. This highly aggressive and drug-resistant cell line was used as a model for tumors that are refractory to standard chemotherapies. These cells were grown by Dr. Emily Chen at the Stony Brook Department of Pathology and the animal studies were done by Dr. Chen in conjunction with Stony Brook DLAR.

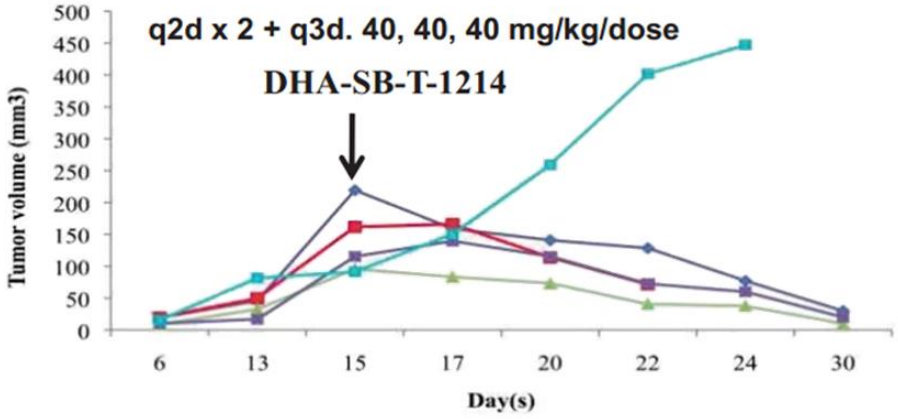

Figure 3-13: Tumor volume of mice bearing Met-CSC tumors treated with DHA-1214

Treatment of a small group of mice bearing these Met-CSC derived tumors with three 40 mg/kg doses of DHA-1214 on a q2dx2 + q3d schedule led to significant reduction in tumor burden and almost complete regression. Although these tumors eventually returned, DHA-1214 demonstrated the impressive ability to control the tumor burden of even this highly drug-resistant tumor model.

To assess the efficacy of an altered dosing regimen, a single tumor-bearing mouse was treated with a 60, 20, 20 mg/kg q7dx3. In this dosing schedule an initial higher dose was administered and two smaller doses were given to maintain the therapeutic window over the course of the study. The result of this experiment is shown in **Figure 3-14**.

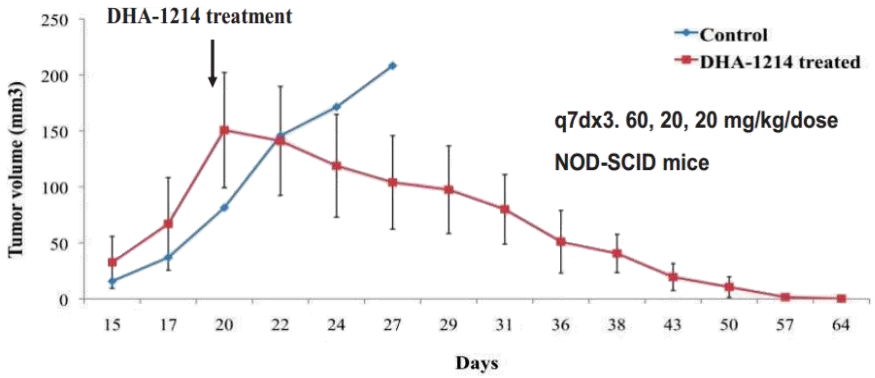

Figure 3-14: Tumor volume of mouse treated with a 60, 20, 20 dosing regimen

Using this dosing regimen, the tumor burden was controlled and a full regression was achieved. This dosing strategy is consistent with a pharmacokinetic model of an active agent with an extended half-life. It may be worthwhile to repeat analogous dosing schedules in other tumor models to see if cures can be obtained with a safer therapeutic window and reduced toxicity.

§ 3.4.0 DHA-Propofol

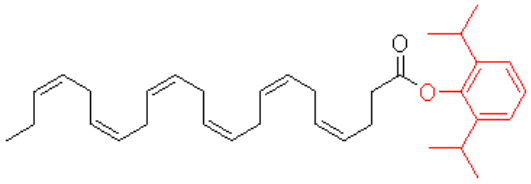

Figure 3-15: The structure of DHA-propofol

Propofol (2,6 diisoproplyphenol) is a widely used general anesthetic that has been found to confer some survival advantage when used during surgical removal of solid tumors. Interestingly, when it was conjugated to DHA via an ester bond (**Figure 3-15**), it exhibited selective toxicity against breast cancer cells *in vitro* with single digit micromolar IC_{50} values (**Figure 3-16**).[36] The DHA-propofol (DHA-PPF) conjugate caused these cells to commit to apoptosis as confirmed by a Caspase 3 assay and it was hypothesized that it might exert its pro-apoptotic effects via inhibition of histone deacetlyase (HDAC) activity.[37]

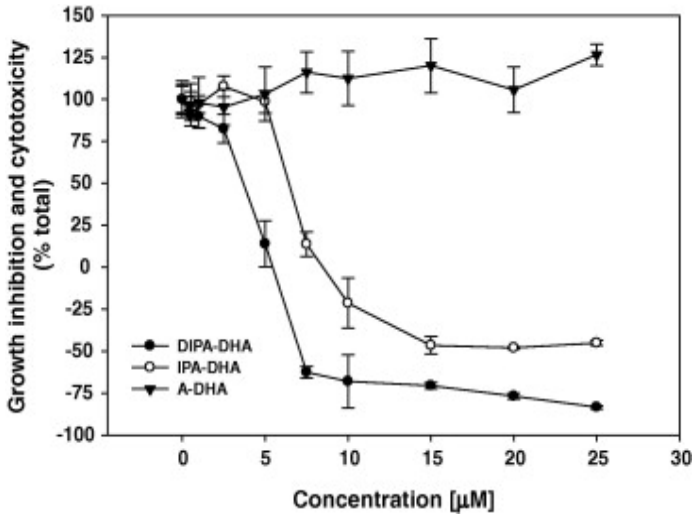

Figure 3-16: Growth inhibition in MBA-MD-231 breast cancer cells by DHA-PPF analogues (adapted from [37])

Due to the preclinical success of DHA-1214, and the apparent tumor-selective toxicity of DHA-PPF, it was hypothesized that a conjugate of SB-T-1214 and DHA-PPF (DHA-PPF-1214) may possess some advantageous properties. The presence of the diisopropylphenyl group near C2' ester bond may slow non-specific cleavage of the prodrug *in vivo*, thereby suppressing off-target toxicity. In addition, the release of an active agent in place of inactive DHA may enhance the therapeutic benefit of the conjugate. The incorporation of the DHA-PPF moiety may also augment the selectivity for internalization of the resulting conjugates. In order to test these hypotheses, three novel conjugates were synthesized.

§ 3.3.1 Synthesis of *N*-Boc-Protected *p*-Amino-DHA-PPF and FITC Conjugate

To enable conjugation to the *para* position of the diisopropylphenyl ring, an amine functionality was introduced. Propofol was subjected to nitration according to the literature procedure using cyclohexane as a solvent. Under these conditions, the product precipitated out cleanly as a solid and could be easily crystallized to afford yellow needles in 30% yield. It is worth mentioning that attempts to reproduce other literature procedures that claimed much higher yields failed, and complicated mixtures were obtained. After laborious chromatography, the best yield obtained using this procedure was 14%. The primary byproduct of this reaction appeared to be a dimeric hemi-quinone derived from a radical dimerization of propofol under these conditions. As propofol is a known antioxidant, this result was not surprising. Use of antioxidants such as BHT may improve the yield of this reaction.

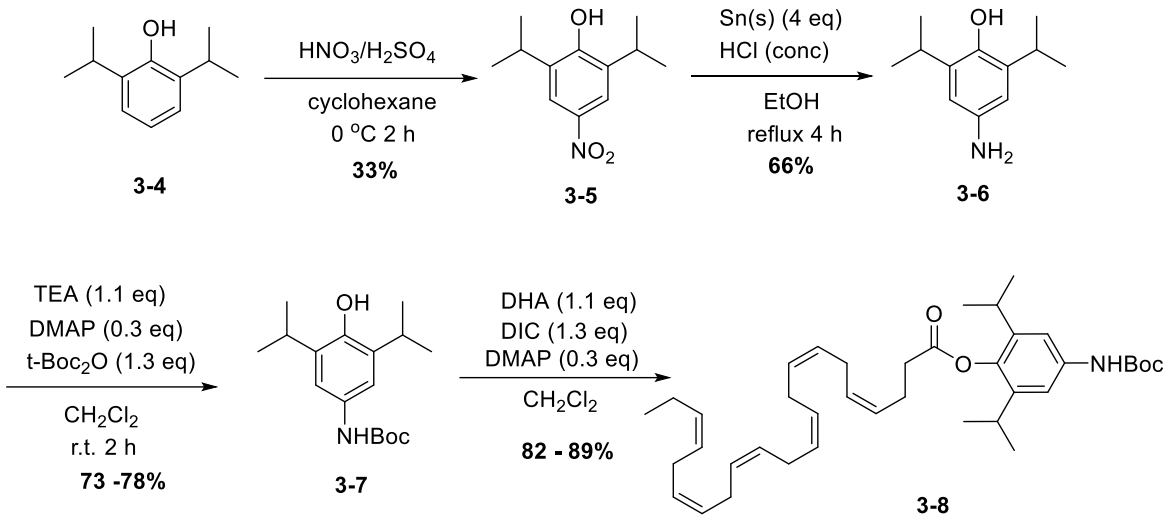

Scheme 3-5: Synthesis of *N*-Boc-protected *p*-amino-DHA-PPF **3-8**

Reduction of the nitro group by tin chloride, generated *in situ* by the reaction of tin and hydrochloric acid according to the literature procedure, proceeded in decent yield. The resulting aniline appeared to be meta-stable, and the best results were obtained when the material was taken directly to the next step. Protection of the free amine with *t*-Boc afforded compound **3-7**, which was benchtop stable, and could be triturated with cold hexanes, producing a white solid. Although the overall yield for these three steps was low, chromatographic purification was not needed and gram quantities of this material could be produced with minimal labor. Conjugation of the protected aniline to DHA afforded the versatile intermediate **3-8** in decent yield.

§ 3.3.2 Synthesis and FACS Analysis of DHA-PPF-FITC

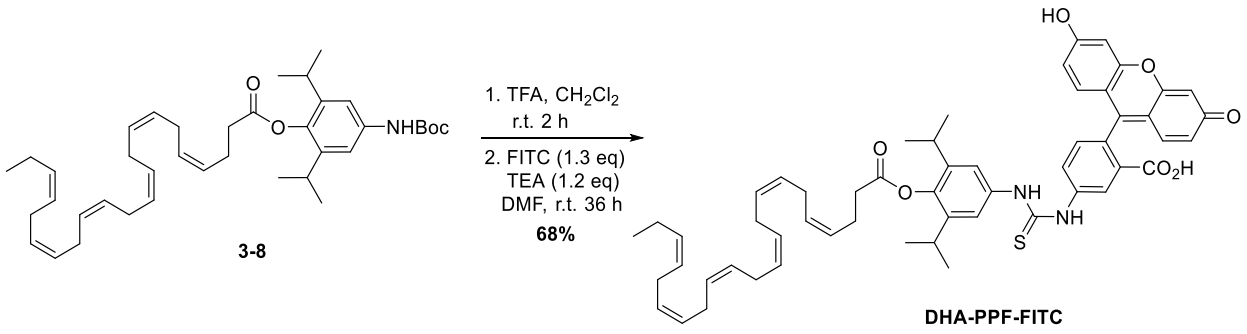

Scheme 3-6: Synthesis of fluorescent probe **DHA-PPF-FITC**

Intermediate **3-8** was deprotected with TFA, neutralized with pyridine and coupled to FITC in decent yield of the desired product **DHA-PPF-FITC**, following purification by column chromatography. This material was used to compare internalization rates between healthy cells and breast cancer cells *in vitro* by fluorescence activated cell sorting (FACS) analysis.

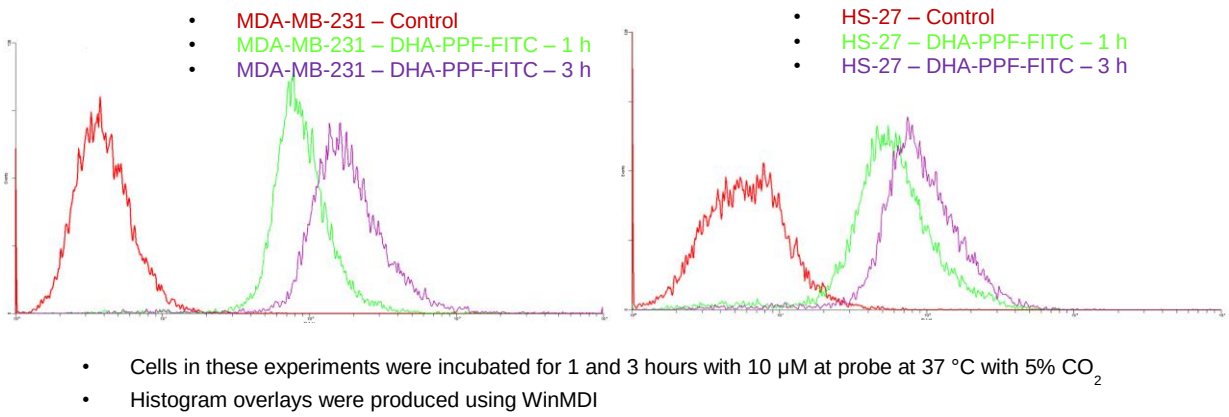

Figure 3-17: FACS analysis of **DHA-PPF-FITC** in MDA-MB-231 (*left*) and HS-27 (*right*) cells

Cells were incubated with **DHA-PPF-FITC** at 1, 3 and 24 hours and the internalization of the probe was quantified by FACS. Internalization of the probe in the breast cancer cell line MDA-MB-231 (**Figure 3-17**, *left*) was compared to the healthy human foreskin cell line HS-27 (**Figure 3-17**, *right*). The intensity of the fluorescent signal is given on the X axis, while the Y axis is a measurement of the number of cells that exhibited that intensity. Values for 24 hour incubation are not given on the graph, as the geometric mean value was too high in both samples to permit analysis. Autofluorescence of cells not incubated with **DHA-PPF-FITC** are given as the controls.

These data indicate that both the healthy cells and the breast cancer internalized the probe, although to different extents. The geometric mean (X axis value at the peak of the statistical bell curve) can be used as an indicator of the average internalization level for a given population of cells. When these values are normalized to the autofluorescence of the control population, the relative level of internalization can be discerned. It was found that the **DHA-PPF-FITC** probe was internalized 2.5 – 3 fold more in the cancerous cells than the healthy cells. For comparison, a fluorescently-tagged DHA-PPF-Taxoid probe was synthesized.

§ 3.3.3 Synthesis and FACS Evaluation of DHA-PPF-7'-fluorescein-1214

It has been demonstrated that large groups may be appended to the C7 hydroxyl group of taxoids without abolishing their microtubule binding capacity. Therefore, the C7 has been exploited as a position to attach fluorescent markers to taxanes, allowing their intracellular positioning *in vitro* to be observed *via* confocal microscopy. Therefore, a fluorescein moiety bearing a butanoic acid was prepared and coupled to **SB-T-1214** at the C7 position. This probe has previously been used to monitor the internalization of taxoid based conjugates.

The synthesis of the fluorescein tether is outlined in **Scheme 3-7**. Reduction of *t*-butyl succinic acid afforded the tether component **3-9**. In order to selectively couple this tether to fluorescein, the carboxylic acid was protected as a methyl ester in decent yield. The limited

solubility of the product **3-10** during aqueous workup resulted in some lost product. Precipitation of the product from the reaction mixture may provide compound **3-10** with improved yield.

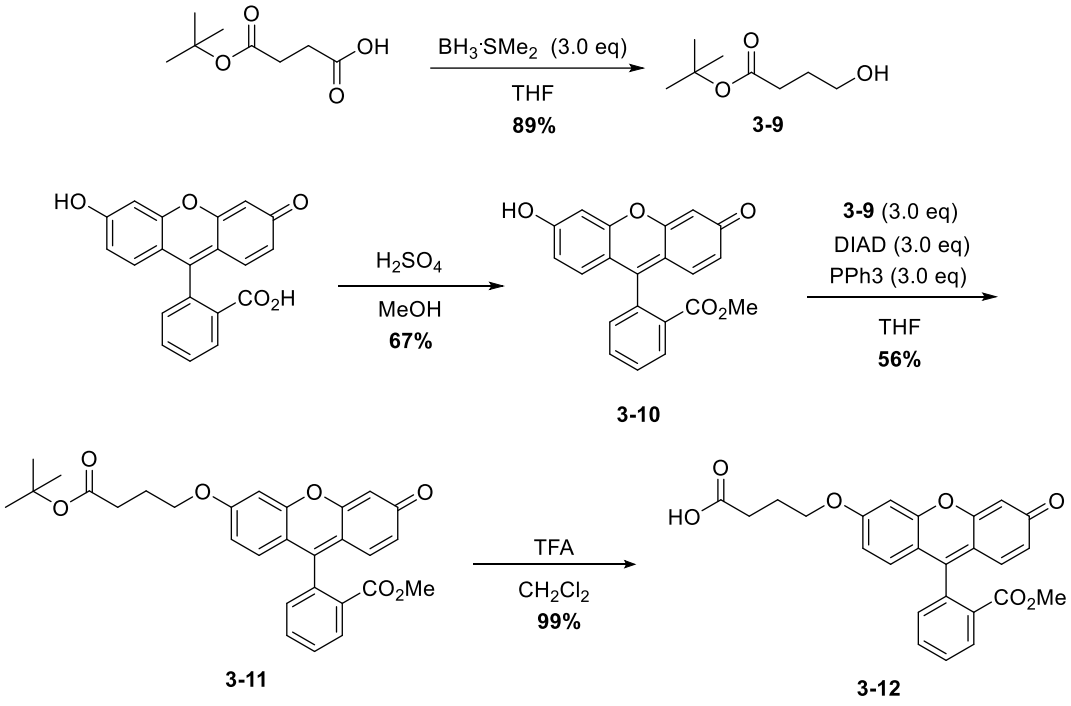

Scheme 3-7: Synthesis of the fluorescein-tether **3-12**[38]

Tether **3-9** was coupled to fluorescein methyl ester *via* a Mitsunobu reaction. Separation of the product from triphenylphosphine oxide was difficult, and incomplete separation was obtained after careful chromatography. Pure material was deprotected in excellent yield. Impure product was subjected to deprotection conditions and the free acid **3-12** was obtained cleanly after an acid/base work up. Alternatively, column chromatography may be carried out on the free acid, and it is significantly easier to purify than the protected intermediate. As triphenylphosphine oxide does not appear to affect the deprotection, it may be advantageous use the protected intermediate crude and purify the free acid after deprotection.

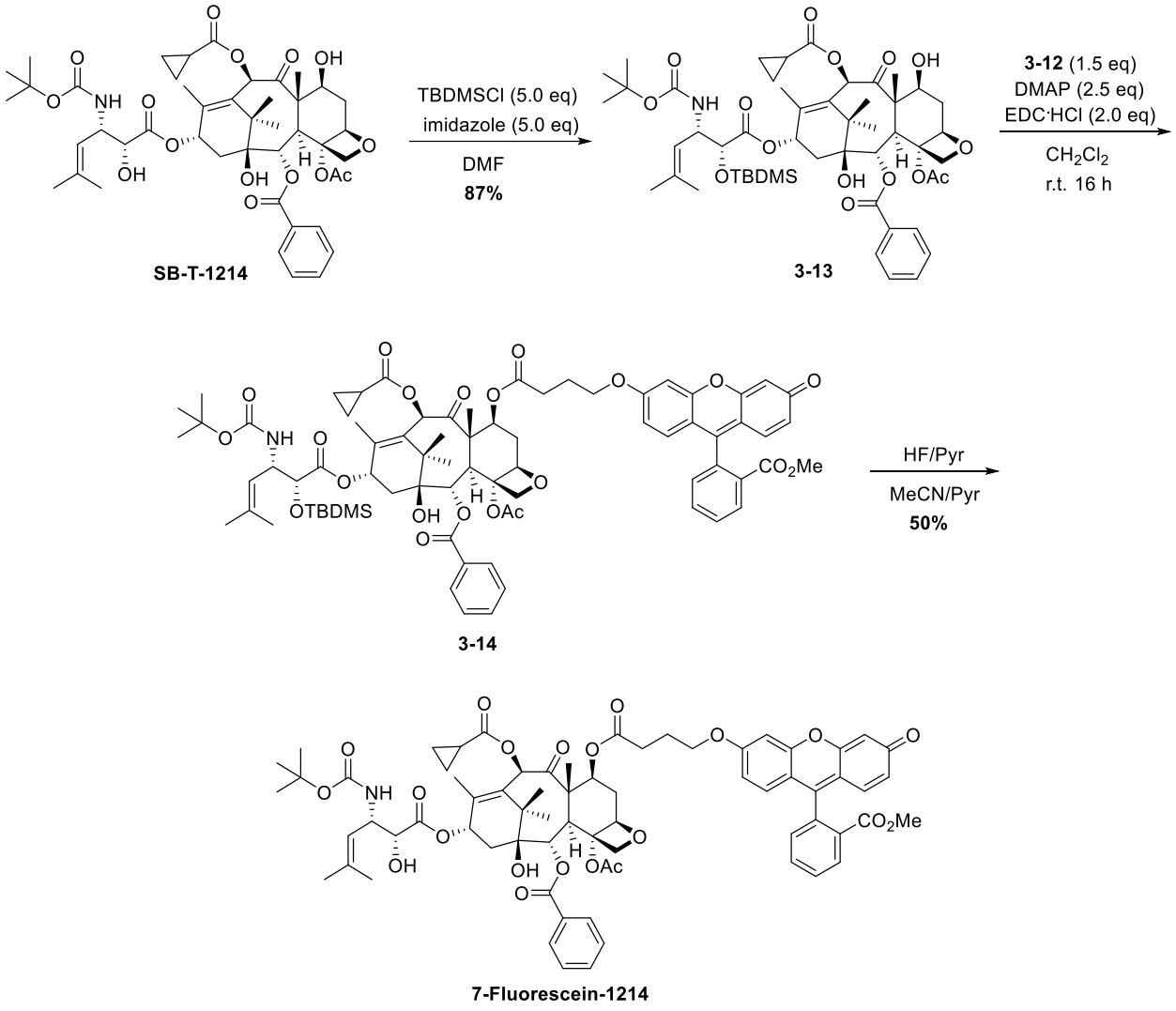

Scheme 3-8: Synthesis of **7-fluorescein-1214**[38]

Selective TBDMS protection of the C2' position on SB-T-1214 proceeded in good yield after purification. EDC coupling of 2'-TBDMS-1214 to the fluorescent tag **3-12** followed by silyl deprotection with HF/Pyridine afforded the desired fluorescent probe in modest yield. The yield for the deprotection was low because a small amount of byproduct was generated during the course of the synthesis which had a very similar R_f to the desired product. A substantial amount of slightly impure material was collected but not counted in the calculated yield for this reaction.

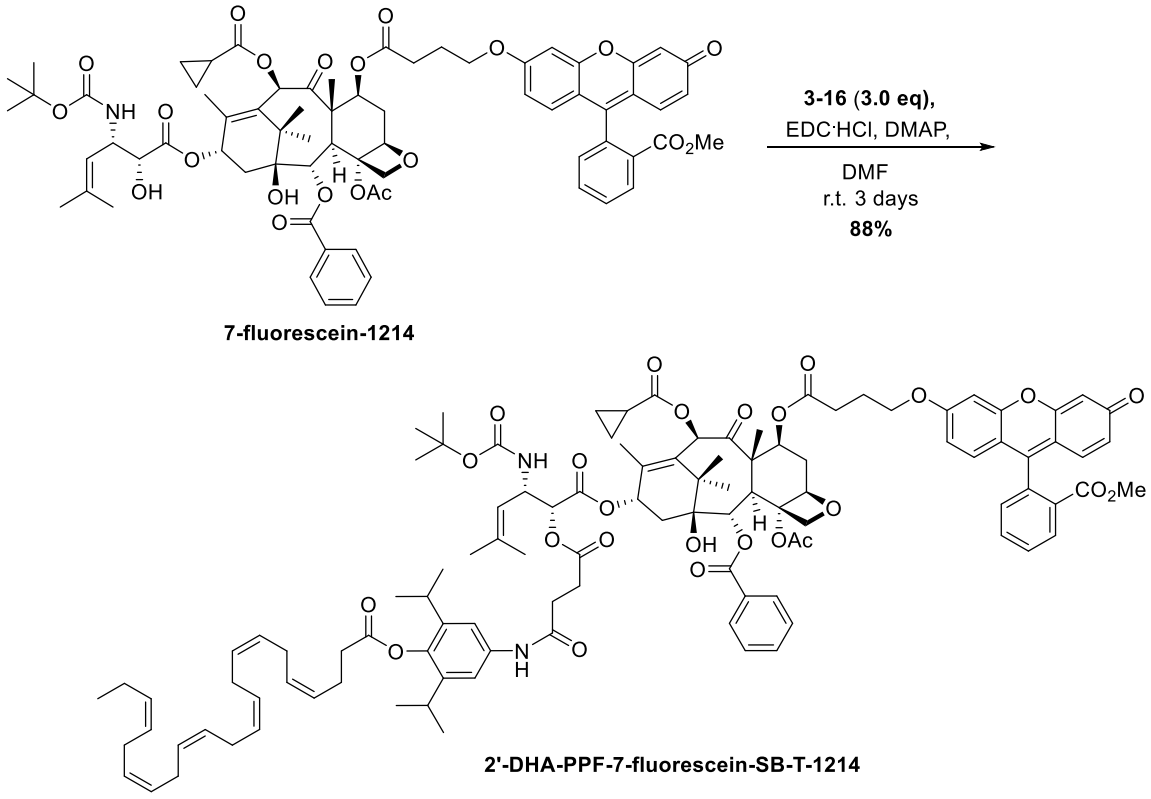

Scheme 3-9: Synthesis of **7-fluorescein-DHA-PPF-1214**

To complete the synthesis of the 'active' conjugate DHA-PPF-1214 and fluorescent probe 7-fluorescein-DHA-PPF-1214, intermediate **3-8** was deprotected and the product was neutralized and reacted with succinic anhydride in THF. Attempts to use CH_2Cl_2 as a solvent were unsuccessful, as succinic anhydride possesses only limited solubility. This material was purified by column chromatography before coupling to the desired taxoids. Coupling to SB-T-1214 proceeded in decent yield, although the reaction was stopped before all of the starting material was consumed due to the formation of a C2',C7-*bis*-substituted byproduct. As there was no possibility for the formation of this byproduct during the synthesis of 7-fluorescein-DHA-PPF-1214, higher yield was achieved using more forcing conditions.

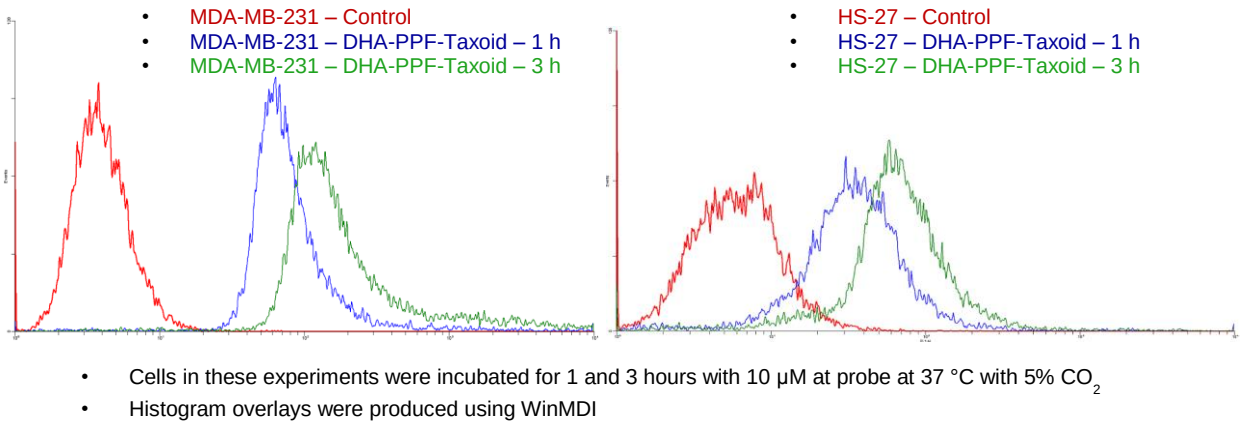

Figure 3-18: FACS analysis of **2'-DHA-PPF-SB-T-1214-7-fluorescein** in MDA-MB-231 (*left*) and HS-27 (*right*) cells

The internalization of **7'-fluorescein-DHA-PPF-1214** was examined using FACS analysis as previously described in section 3.3.2. For the fluorescent probe bearing a taxoid, the increased accumulation in the breast cancer cells was 5-6 times greater than the normal human cells. This effect was slightly more pronounced than that observed for the **DHA-PPF-FITC** probe, indicating that the cancer cells are more prone to internalize larger organic molecules than healthy cells. When comparing these data to results from similar experiments run on fluorescent DHA conjugates (data not shown), it appears as though the incorporation of the 2,6-diisopropylphenyl moiety does not greatly affect internalization trends *in vitro*.

§ 3.3.4 Synthesis and Biological Evaluation of DHA-PPF-1214 *in vitro*

The synthesis of **DHA-PPF-1214** is outlined in **Scheme 3-10**. TFA deprotection followed by coupling to succinic anhydride to afford **3-16**. This intermediate was then coupled to **SB-T-1214** *via* EDC coupling to afford the desired **DHA-PPF-1214** in good yield.

Preliminary cytotoxicity analysis was performed for the **DHA-PPF-1214** conjugate and the synthetic intermediate **3-16**, which would be released after cleavage of the C2' ester bond. The results are given in **Table 4**. The compounds were tested against the cell lines LCC6-MDR (drug resistant breast cancer overexpressing Pgp), MDA-MB-231 (drug sensitive breast cancer) and HT-29 (drug sensitive colon cancer). **Paclitaxel, SB-T-1214**, **DHA** and **DHA-1214** were tested as controls.

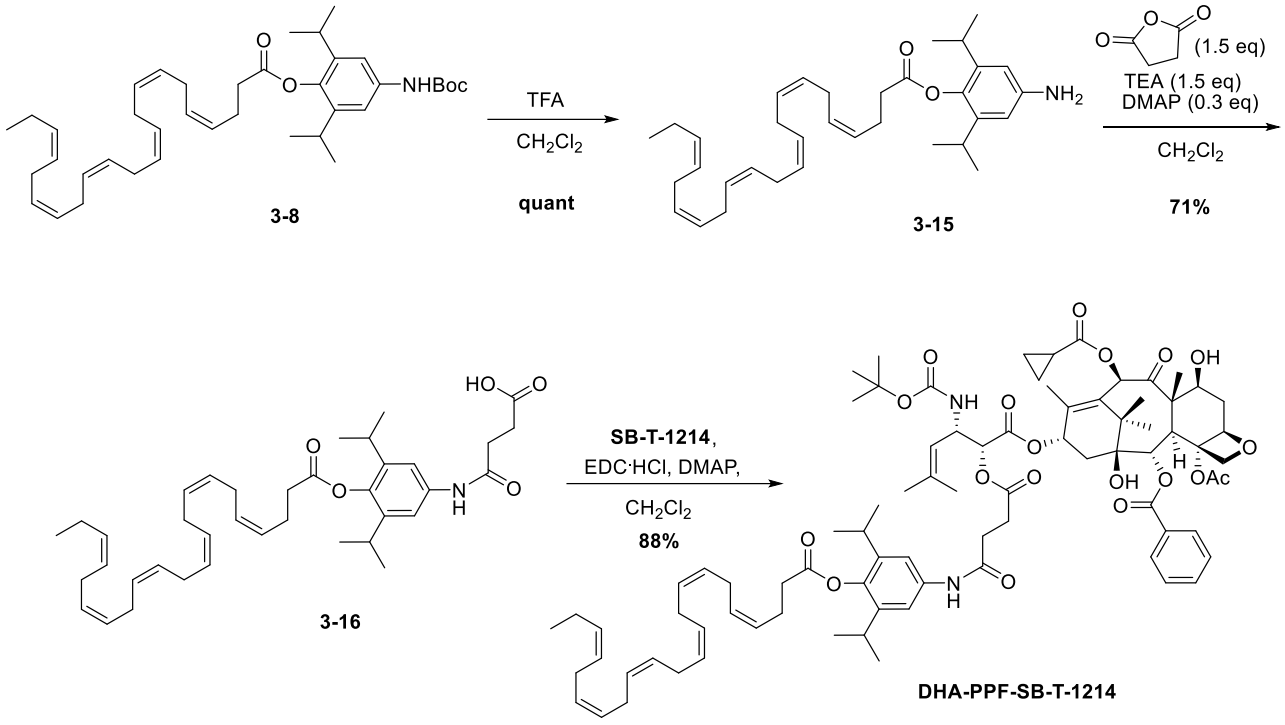

Scheme 3-10: Synthesis of **DHA-PPF-1214**

	LCC6-MDR	MDA-MB-231	HT-29
Taxol	560 nM ± 10.3	8.8 nM ± 1.1	7.0 nM ± 0.3
SB-T-1214	5.7 nM ± 0.2	3.7 nM ± 1.3	4.1 nM ± 2.0
DHA-1214	19.2 nM ± 1.2	86.1 nM ± 35.1	74.3 nM ± 17.9
DHA-PPF-1214	18.6 nM ± 1.0	30.7 nM ± 6.8	19.7 nM ± 4.2
DHA + 1214	5.5 nM ± 0.1	11.1 nM ± 4.7	12.2 nM ± 3.2
DHA	-	>200 uM	>200 uM
DHA-PPF-Boc	58.2 uM ± 3.7	-	-
DHA-PPF-CO_2H	-	35.7 uM ± 10.6	-

- The reported values are a calculated average of IC_{50} values determined from three individual experiments
- IC_{50} values were calculated using SigmaPlot v10.0
- Cells used in these experiments were incubated for 48 hours at 37 °C with 5% CO_2 after treatment

Table 3-3: Cytotoxicity analysis of **DHA-PPF-1214** and synthetic intermediates

The resistance of LCC6-MDR to paclitaxel is evident when compared to the two Pgp-negative cell lines. Equally apparent is the high potency of **SB-T-1214**, and the lack of susceptibility of this compound to Pgp-mediated MDR. **DHA-1214** has an IC50 value that is 5 to 20 fold greater than the parent compound, which is consistent with previous results. Interestingly, **DHA-PPF-1214** is significantly more cytotoxic than **DHA-1214** in MDA-MB-231 and HT-29 and

equipotent in LCC6-MDR cell lines. As previously reported, DHA appeared non-toxic to the cells tested, whereas the DHA-PPF analogues were cytotoxic in the micromolar range, as expected. The combination of **DHA** and **SB-T-1214** in a 1:1 ratio appeared to be slightly antagonistic in MDA-MB-231 and HT-29 cells when compared to the values obtained for **SB-T-1214** in the same cells. However, it is not likely that this antagonism is responsible for the apparent 3-4 fold increase in cytotoxicity between **DHA-PPF-1214** and **DHA-1214**. Likely rates of hydrolysis (either enzymatic or chemical) are higher for **DHA-PPF-1214**, causing the apparent increase in toxicity.

Further studies on the chemical stabilities of the ester bonds as well as antagonism/synergism between DHA-PPF and 1214 and DHA and 1214 are warranted. Also, the HSA binding of this compound should be evaluated, and preliminary efficacy studies *in vivo* should be done.

§ 3.4.0 Experimental

§ 3.4.1 General Methods

^{1}H and ^{13}C NMR spectra were measured on a Varian 300, 400, 500 or 600 MHz NMR spectrometer. Melting points were measured on a Thomas Hoover Capillary melting point apparatus and are uncorrected. Mass to charge values were measured by flow injection analysis on an Agilent Technologies LC/MSD VL. TLC was performed on Merck DC-alufolien with Kieselgel 60F-254 and column chromatography was carried out on silica gel 60 (Merck; 230-400 mesh ASTM). Compound purity was verified by reverse phase HPLC on a Shimadzu LC-2010A with a Curosil-B 5 column (250 x 4.6 nm). The mobile phase was acetonitrile-water. The analysese were performed at a flow rate of 1ml/min with the UV detector set at 254 and 227 nm. The gradient was run from 20% to 95% acetonitrile in water over a 40 minute period.

§ 3.4.2 Materials

The chemicals were purchased from Aldrich Co. and Sigma and purified before use by standard methods. Tetrahydrofuran was freshly distilled from sodium metal and benzophenone. Dichloromethane was also distilled immediately prior to use under nitrogen from calcium hydride. In addition, various dry solvents were degassed and dried using PureSolv™ solvent purification system (Innovative Technologies, Newburyport, MA).

§ 3.4.3 Experimental Procedures

SB-T-1214-2'-Docosahexaenoate (DHA-1214)[35]

To a solution of **SB-T-1214** (200 mg, 0.23 mmol), DHA (120 mg, 0.25 mmol) and DMAP (30 mg, 0.26 mmol) in CH_2Cl_2 (6 mL), was added EDC hydrochloride (56 mg, 0.26 mmol) suspended in CH_2Cl_2 (2 mL). The solution was stirred at room temperature for 4 hours and the solvent was

removed *in vacuo* to afford light brown oil. Purification by column chromatography afforded **DHA-1214** (192 mg, 74% yield) as a white solid: ^{1}H NMR (300 MHz, $CDCl_3$) δ 0.98 (t, J = 7.5 Hz, 3H), 1.08 (m, 2H), 1.20 (m, 1H), 1.23 (s, 3H), 1.33 (s, 3H), 1.42 (s, 9H), 1.74 (s, 3H), 1.79 (s, 1H), 1.83 (s, 6H), 1.90 (m, 1H), 1.97 (s, 3H), 2.05-2.14 (m, 3H), 2.42 (s, 3H), 2.45 (m, 1H), 2.60-2.78 (m, 14 H), 3.45 (d, J = 6.6 Hz, 1H), 3.88 (d, J = 6.9 Hz, 1H), 4.24 (m, 2H), 4.38 (d, 8.4 Hz, 1H) 4.48 (m, 1H), 4.83 (m, 2H), 5.03 (d, 7.8 H), 5.27-5.45 (m, 13 H), 5.74 (d, 7.2 Hz, 1H), 6.24 (t, 1H), 6.37 (s, 1H), 7.54 (t, 7.2, 2H), 7.68 (t, 7.5 Hz, 1H), 8.17 (d, 7.2 Hz, 2H). All data were found to be in agreement with literature values.[35]

SB-T-12854-2'-linolenoate (LNA-12854)

According to the procedure to synthesize DHA-1214, **SB-T-12854** (200 mg, 0.23 mmol) and LNA (58 mg, 0.21 mmol) were used to produce **LNA-12854** (165 mg, 67% yield) as a white solid: ^{1}H NMR (500 MHz, $CDCl_3$) δ 0.98 (t, J = 7.5 Hz, 2H), 1.15 (s, 3H), 1.24 (s, 3H), 1.26-1.34 (m, 17H), 1.78 (m, 1H), 1.85 (m, 1H), 1.95 (s, 3H), 2.05-2.10 (m, 2H), 2.22 (m, 1H), 2.30 (m, 1H), 2.35 (s, 3H), 2.45-2.56 (m, 3H), 2.82 (m, 2H), 2.95 (s, 3H), 3.03 (s, 3H), 3.81 (d, J = 7.0 Hz, 1H), 4.18 (d, J = 8.5 Hz, 1H), 4.31 (d, J = 8.5 Hz, 1H), 4.37-4.50 (m, 2H), 4.95-5.04 (m, 3H), 5.30-5.41 (m, 3H), 5.66 (d, J = 7.0 Hz, 1H), 6.27 (m, 2H), 7.50 (t, J = 7.0 Hz, 2H), 7.61 (t, J = 7.0 Hz, 1H), 8.12 (d, J = 7.0 Hz, 2H); ^{13}C NMR (125 MHz, $CDCl_3$) δ 9.41, 14.31, 14.85, 20.57, 22.27, 22.52, 24.70, 25.54, 25.63, 26.89, 27.20, 28.12, 29.02, 29.09, 29.17, 29.59, 33.66, 35.34, 35.46, 36.02, 36.64, 43.22, 45.58, 45.65, 58.44, 71.81, 72.43, 73.88, 75.26, 76.17, 76.42, 79.36, 80.58, 81.01, 84.69, 127.11, 127.79, 128.24, 128.73, 129.17, 130.22, 131.98, 133.00, 133.66, 143.28, 154.62, 156.13, 156.57, 167.15, 167.43, 169.84, 172.57, 205.43. HRMS (ESI) calcd for $C_{60}H_{83}F_2N_2O_{16}$ $(M+H)^+$: 1125.5711, found 1125.5681 (Δ-2.7 ppm, -3.0 mDa).

7,10,13-Tris(triethylsilyl)-2-debenzoyl-10-deacetylbaccatin III 1,2 carbonate (3-1)[39]

A solution of **2-2** (110 g, 0.14 mmol) in CH_2Cl_2 (3 mL) was added to a flask containing triphosgene (146 mg, 0.44 mmol) under inert conditions. To the resulting solution was added pyridine (3 mL) dropwise at 0 ^oC, during which time the solution turned dark red and gas evolution was observed. The mixture was stirred for 45 minutes and quenched with concentrated NH_4Cl (1 mL) and Na_2CO_3 (1 mL). It was then diluted with H_2O (20 mL), extracted with EtOAc (3 x 20 mL), the organic layer washed with $CuSO_4$ (aq) (3 x 15 mL), H_2O, (2 x 20 mL), brine (3 x 20 mL) and was dried over $MgSO_4$. The organic layer was then suction filtered, the filtrate concentrated in vacuo, and the residue purified by column chromatography to afford **3-1** (98 mg, 86% yield) as a white solid: ^{1}H NMR (300 MHz, $CDCl_3$) δ 0.51-0.73 (m, 18H), 0.90-1.05 (m, 27H), 1.18 (s, 3H), 1.27 (s, 3H), 1.70 (s, 3H), 1.83-1.95 (m, 1H), 1.98 (s, 3H), 2.06-2.15 (m, 1H), 2.17 (s, 3H), 2.27-2.43 (m, 1H), 2.50-2.64 (m, 1H), 3.43 (d, J = 6.0 Hz, 1H), 4.37 (dd, J = 7.2, 9.6 Hz, 1H), 4.42-4.50 (m, 1H), 4.45 (d, J = 9.3 Hz, 1H), 4.60 (d, J = 9.3 Hz, 1H), 4.90-5.05 (m, 2H), 5.15 (s, 1H); ^{13}C NMR

(100 MHz, $CDCl_3$) δ 4.83, 5.11, 5.84, 6.78, 6.85, 6.91, 10.44, 15.09, 20.88, 22.40, 25.23, 37.08, 37.91, 41.23, 43.83, 59.86, 67.40, 71.96, 76.47, 79.61, 81.82, 83.92, 90.86, 133.81, 142.40, 153.38, 170.07, 206.02. All data were found to be in agreement with literature values.[39]

7,10,13-Tris(triethylsilyl)-2-debenzoyl-(2-d5-benzoyl)-10-deacetylbaccatin III (3-2)

To a cooled solution of d-5 bromobenzene (100 mg, 0.62 mmol) in THF (2.5 mL), was added *n*-BuLi (1.6 M in hexanes) (0.38 mL, 0.62 mmol) at -78 ^oC. The mixture was allowed to warm to -45 ^oC and stir for 30 minutes. The aryl lithium solution was then added to a solution of **3-1** (60 mg, 74 nmol) in THF (2.5 mL) at -45 ^oC. The reaction mixture was stirred at this temperature for 30 minutes before being quenched with concentrated NH_4Cl (2 mL). It was then diluted with H_2O (10 mL), extracted with EtOAc (3 x 15 mL), the organic layer washed with brine (3 x 15 mL), dried over $MgSO_4$, suction filtered, and the filtrate concentrated *in vacuo* leaving pale yellow oil. The residue was purified by column chromatography to afford **3-2** (62 mg, 94% yield as a white solid: ^1H NMR (300 MHz, $CDCl_3$) δ 0.62 (m, 18H), 0.98 (m, 27H), 1.13 (s, 3H), 1.23 (s, 3H), 1.31 (m, 1H), 1.65 (s, 3H), 1.88 (m, 1H), 1.98 (s, 3H), 2.18 (m, 2H), 2.27 (s, 3H), 2.52 (m, 1H), 3.85 (s, 3H), 3.87 (m, 1H), 4.14 (d, J = 9.0, 1H), 4.31 (d, J = 8.4, 1H), 4.41 (dd, J = 10.5, 6.9, 1H), 4.93 (m, 2H), 5.19 (s, 1H), 5.61 (d, J = 7.2 Hz, 1H).

4-Nitro-2,6-diisopropylphenol (3-5)[40]

A mixture of nitric acid (0.7 mL) and sulfuric acid (0.8 mL) was added dropwise to a round bottom flask containing propofol (1.00 g, 5.61 mmol) at 0 ^oC. During the course of addition, the color changed from yellow to orange to black, producing a tar. The reaction was stirred at room temperature for 2 hours. To this was added H_2O (50 mL) and extracted with CH_2Cl_2 (50 mL). The organic layer was then washed with brine (3 x 20 mL), dried over $MgSO_4$, filtered and the filtrate was concentrated *in vacuo*. The resulting black residue was purified by column chromatography with increasing amounts of ethyl acetate in hexanes (final eluent: 8% ethyl acetate in hexanes). The resulting orange brown solid was recrystallized from hexanes to afford 4-nitropropfol (**3-5**) (160 mg, 13% yield) as pale yellow needles: ^1H NMR (300 MHz, $CDCl_3$) δ 1.31 (d, J = 6.9 Hz, 12H), 3.17 (m, 2H), 5.48 (S, 1H), 8.00 (s, 2H). All data were found to be in agreement with literature values.[40]

4-Amino-2,6-diisopropylphenol hydrochloride (3-6)[41]

To a round bottom flask containing 4-nitropropofol (**3-5**) (140 mg, 0.63 mmol) and tin (500 mg), ethanol (1 mL) was added followed by the dropwise addition of concentrated HCl (2.5 mL). The flask was equipped with a condenser and allowed to reflux for 1 hour, during which time all of the tin had dissolved. The resulting solution was suction filtered to remove any insoluble and the filtrate was condensed to 1 mL *in vacuo* and cooled to -20 ^oC. A solid precipitated during cooling,

which was collected by suction filtration and washed with ether (5 mL), affording **3-6** (139 mg, 97% yield) as a white solid: ^{1}H NMR (300 MHz, DMSO-d6) δ 1.12 (d, J = 9.6 Hz, 12H), 3.31 (m, 2H), 6.98 (s, 2H), 8.46 (s, 1H), 9.6-10.2 (br s, 3H). All data were found to be in agreement with literature values.[41]

***N-tert*butoxycarbonyl-4-amino-2,6-diisopropylphenol (3-7)**[42]

To a round bottom flask containing di-*tert*-butyl dicarbonate (110 mg, 0.51 mmol) and **3-6** (90 mg, 0.39 mmol) was added CH_2Cl_2 (3 mL).The resulting white suspension was cooled to 0 ^{o}C in an ice bath, and triethylamine (0.11 mL, 0.78 mmol) was added dropwise. During the addition, the liquid portion of the suspension turned pale yellow, and the reaction was allowed to stir over night at room temperature. The reaction was monitored by TLC (eluent 3:1 hexanes:ethyl acetate), and upon completion was quenched with saturated NH_4Cl (1 mL). The reaction mixture was then diluted with water (10 mL) and extracted with EtOAc (2 x 10 mL). The combined organic layers were washed with brine (3 x 10 mL), dried over $MgSO_4$, suction filtered and the filtrate concentrated *in vacuo* to afford **3-6 (**115 mg, 39% yield) as an off white solid: ^{1}H NMR (300 MHz, $CDCl_3$) δ 1.25 (d, J = 6.9 Hz, 12H), 1.51 (s, 9H), 3.13 (m, 2H), 4.57 (s, 1H) 6.31 (br s, 1H), 7.02 (s, 2H). MS (ESI) calcd for $C_{17}H_{27}NO_3$: 294.2, found 294.2. All data were found to be in agreement with literature values.[42]

***N-tert*butoxycarbonyl-4-amino-2,6-diisopropylphenoxydocosahexaenoate (3-8)**

Docosahexaenoic acid (45 mg, 0.15 mmol) and dimethylaminopyridine (10 mg, 0.08 mmol) were weighed into a round bottom flask, vacuum dried and placed under an atmosphere of N_2. To this was added a solution of **3-7** (45 mg, 0.15 mmol) in CH_2Cl_2 (3 mL) via syringe. The resulting solution was cooled in an ice bath and to it was added diisopropylcarbodiimide (29 mg, 0.23 mmol) dropwise. The reaction was allowed to warm to room temperature and stir for 3 hours while monitored by TLC (eluent: 10:1 hexanes: EtOAc). Upon completion, the reaction mixture was concentrated in vacuo to a volume of 1 mL and loaded directly onto a silica gel column. The material was purified by column chromatography (eluent: 1:50 EtOAc:hexanes) to afford **3-8** as a waxy white solid: ^{1}H NMR (300 MHz, $CDCl_3$) δ 0.97 (t, J = 7.5 Hz, 3H), 1.17 (d, J = 6.9 Hz, 12H), 1.51 (s, 9H), 2.07 (m, 2H), 2.55 (m, 2H), 2.67 (t, J = 6.0 Hz, 2H), 2.77-2.91 (m, 12H), 5.27-5.42 (m, 10H), 5.46 (d, J = 4.8 Hz, 2H), 6.44 (br s, 1H), 7.13 (s, 2H). MS (ESI) calcd for $C_{39}H_{58}NO_4$ $(M+H)^+$: 604.43, found 604.4.

4-(Fluoresceinylthiourea)-2,6-diisopropylphenoxydocosahexaenoate (DHA-PPF-FITC)

Trifluoroacetic acid (0.3 mL) was added to a solution of **3-7** (25 mg, 0.04 mmol) in CH_2Cl_2 (1.2 mL) at 0 ^{o}C. Care was taken throughout the course of this reaction to avoid prolonged exposure of any of the compounds to light. The brown solution was allowed to warm to room temperature and

stir for 3 hours, during which time it was monitored by TLC (eluent: 3:7 EtOAc:hexanes). Upon completion, the solvent was removed *in vacuo*, forming a tacky brown solid. To the crude TFA salt was added fluorescein isothiocyanate (15 mg, 0.04 mmol), and the two compounds were dissolved in DMF (1 mL). Triethylamine was added dropwise to neutralize the excess TFA, and addition was continued until a change was noticed on TLC (eluent: 3:2 EtOAc:hexanes), with a final addition volume of 0.3 mL. The reaction was then allowed to stir for 16 hours at room temperature and upon completion; the solvent was concentrated *in vacuo*, forming red oil. The product was purified by chromatography on silica gel with increasing amounts of ethyl acetate in hexanes (pure hexanes to 3:1 EtOAc:hexanes) to afford **DHA-PFF-FITC** as a yellow solid: ^{1}H NMR (300 MHz, $CDCl_3$) δ 0.95 (t, J = 7.5 Hz, 3H), 1.15 (d, J = 6.9 Hz, 12H), 2.06 (m, 2H), 2.55 (m, 2H), 2.54 (m, 2H), 2.70-2.95 (m, 14H), 5.24-5.40 (m, 10H), 5.47 (d, J = 5.4 Hz, 2H), 6.55 (d, J = 8.7 Hz, 2H), 6.61 (d, J = 8.7 Hz, 2H), 6.67 (s, 2H), 7.10 (d, J = 8.1 Hz), 7.22 (s, 2H), 7.72 (d, J = 8.1 Hz, 1H), 8.04 (s, 1H). MS (ESI) calcd for $C_{55}H_{61}N_2O_7S$ $(M+H)^+$: 893.41, found: 893.4.

***Tert*-butyl-4-hydroxy-butanoate (3-9)**[38]

Tert-butylsuccinate (1.00 g, 5.75 mmol) was weighed into a round bottom flask, and dissolved in THF (8mL) under inert conditions. The solution was cooled to 0 ^{o}C, and to it was added a 2.0 M solution of borohydride dimethylsulfide complex (3.1 mL, 6.2 mmol) in THF. Gas evolution was observed during addition. The reaction mixture was allowed to warm to room temperature and stir overnight. After stirring for 20 hours, EtOAc (30 mL) was added and washed with water (30 mL). The aqueous layer was extracted with EtOAc (20 mL) and the combined organic layers were washed with brine (3 x 20 mL), dried over $MgSO_4$, suction filtered and the filtrate concentrated *in vacuo*, producing a yellow liquid. Purification was performed by column chromatography on silica gel with hexanes and EtOAc (1:6 EtOAc:hexanes) to afford **3-9** (820 mg, 89% yield) as a pale yellow oil: ^{1}H NMR (300 MHz, $CDCl_3$) δ 1.41 (s, 9H), 1.80 (m, 2H), 2.31 (t, J = 7.2 Hz, 2H), 3.63 (t, J = 6.3 Hz, 2H). All data are in agreement with literature values.[38]

Fluorescein methyl ester (3-10)[38]

To a suspension of fluorescein (500 mg, 1.5 mmol) in MeOH (1.5 mL) was added H_2SO_4 (0.4 mL) dropwise. The round bottom flask was fit with a condenser and refluxed for 14 hours. The contents of the flask were diluted with EtOAc (200 mL), producing a red solution and red insoluble material. The solid was collected by suction filtration, and the organic layer was washed with saturated sodium $NaHCO_3$ (3 x 50 mL), dried over $MgSO_4$, suction filtered and the filtrate concentrated *in vacuo*. The resulting residue was combined with the previously collected solid to afford **3-10** (346 mg, 67% yield) as a red solid: ^{1}H NMR (300 MHz, $CDCl_3$) δ 3.57 (s, 3H), 6.27-6.66 (m, 4H), 6.75 (s, 1H), 6.78 (s, 1H), 7.47 (d, J = 7.5 Hz, 1H), 7.76 (t, J = 7.5 Hz, 1H), 7.85 (t, J = 7.5 Hz, 1H), 8.19 (d, 7.5 Hz, 1H). All data are in agreement with literature values.[38]

***tert*-Butyl 4-[9-(2-methoxycarbonylphenyl)-3-oxo-3H-xanthen-6-yloxy]butanoate (3-11)**[38]

Triphenylphospine (186 mg, 1.08 mmol), **3-9** (172 mg, 1.08 mmol) and **3-10** (120 mg, 0.36 mmol), were weighed in a round bottom flask and flushed with nitrogen. Acetonitrile (2.5 mL) and THF(2.5 mL) were added, resulting in a red suspension. Diisopropyl azodicarboxylate (DIAD) was added dropwise, forming a red solution that was stirred at room temperature overnight. Upon confirmation of completion by TLC (eluent: 9:1 CH_2Cl_2:MeOH), the solvent was removed *in vacuo*, and the resulting mixture was dissolved in CH_2Cl_2. The crude was purified by column chromatography on silica gel (eluent: 49:1 CH_2Cl_2:MeOH), producing impure **3-11** as a red solid (93 mg) and pure **3-11** (62 mg, 37% yield) was isolated as an orange solid: ^{1}H NMR (300 MHz, $CDCl_3$) δ 1.41(s, 9H), 1.80 (m, 2H), 2.31 (t, J = 7.2 Hz, 2H), 3.57 (s, 3H), 3.63 (t, J = 6.3 Hz, 2H), 6.27-6.66 (m, 4H), 6.75 (s, 1H), 6.78 (s, 1H), 7.47 (d, J = 7.5 Hz, 1H), 7.76 (t, J = 7.5 Hz, 1H), 7.85 (t, J = 7.5 Hz, 1H), 8.19 (d, 7.5 Hz, 1H). All data are in agreement with literature values.[38]

4-[9-(2-Methoxycarbonylphenyl)-3-oxo-3H-xanthen-6-yloxy]butanoic acid (3-12)[38]

To a solution of **3-11** (62 mg, 0.13 mmol) in CH_2Cl_2 (2 mL) was added trifluoroacetic acid (0.6 mL) dropwise. The resulting solution was allowed to stir at room temperature, during which time the color turned from orange to brown. The reaction was monitored by TLC (eluent: 9:1 CH_2Cl_2:MeOH) and after 3 hours, the solvent was removed in vacuo, producing a tacky yellowish brown residue. This residue was dissolved in CH_2Cl_2 and purified by column chromatography on silica gel using increasing amount of MeOH in CH_2Cl_2 (final eluent: 9:1 CH_2Cl_2:MeOH). Purification afforded **3-12** (56 mg, 99% yield) as an orange solid: ^{1}H NMR (300 MHz, $CDCl_3$) δ 1.80 (m, 2H), 2.31 (t, J = 7.2 Hz, 2H), 3.57 (s, 3H), 3.63 (t, J = 6.3 Hz, 2H), 6.27-6.66 (m, 4H), 6.75 (s, 1H), 6.78 (s, 1H), 7.47 (d, J = 7.5 Hz, 1H), 7.76 (t, J = 7.5 Hz, 1H), 7.85 (t, J = 7.5 Hz, 1H), 8.19 (d, 7.5 Hz, 1H). All data are in agreement with literature values.[38]

2'-Tertbutyldimethylsilyl-SB-T-1214 (3-13)[38]

To a mixture of **SB-T-1214** (300 mg, 0.40 mmol), TBDMSCl (302 mg, 2.0 mmol) and imidazole (273 mg, 4.0 mmol) was added dry DMF (0.54 mL). After stirring the mixture at room temperature for 4 h, the reaction was quenched by adding NH_4Cl (aq) (2mL) and EtOAc (90 mL). The resulting solution was washed by water and brine, dried over MgSO4, and concentrated. The crude product was purified by column chromatography to afford **3-13** (330 mg, 82% yield) as a white solid: ^{1}H NMR (300 MHz, $CDCl_3$) δ 0.07 (s, 3 H), 0.10 (s, 3H), 0.92 (s, 9 H), 1.08 (m, 2H), 1.20 (m, 1H), 1.23 (s, 3H), 1.33 (s, 3H), 1.42 (s, 9H), 1.74 (s, 3H), 1.79 (s, 1H), 1.83 (s, 6H), 1.90 (m, 1H), 1.97 (s, 3H), 2.11 (s, 1H), 2.42 (s, 3H), 2.45 (m, 1H), 2.60 (m, 1H), 2.65 (m, 1H), 3.45 (d, J = 6.6 Hz, 1H), 3.88 (d, J = 6.9 Hz, 1H), 4.24 (m, 2H), 4.38 (d, 8.4 Hz, 1H) 4.48 (m, 1H), 4.83 (m, 2H), 5.03

(d, 7.8 H), 5.38 (m, 1H), 5.74 (d, 7.2 Hz, 1H), 6.24 (t, 1H), 6.37 (s, 1H), 7.54 (t, 7.2, 2H), 7.68 (t, 7.5 Hz, 1H), 8.17 (d, 7.2 Hz, 2H); All data were found to be in agreement with literature values.[38]

2'-*tert*-butyldimethylsilyl -7-(4-Fluorescein-butanoyl)-SB-T-1214 (3-14)[38]

To a solution of **3-13** (120 mg, 0.12 mmol), DMAP (18 mg, 0.124 mmol) and **3-12** (107 mg, 0.25 mmol) in DCM (5 mL) and DMF (2 mL) was added DIC (40 uL, 0.25 mmol) at room temperature with stirring. The mixture was stirred overnight at room temperature. The white precipitate was filtered off through Celite, and rinsed with DCM. The DCM filtrates were combined and concentrated under reduced pressure. The crude product was purified on a silica gel column (eluent: 2% MeOH in DCM) to afford 2 to afford **3-14** (115 mg, 70 % yield) as an orange solid: ^{1}H NMR (300 MHz, $CDCl_3$) δ 0.07 (s, 3H), 0.10 (s, 3H), 0.92 (s, 9H), 0.99 (m, 2H), 1.06 (m, 2H), 1.16 (s, H), 1.22 (s, 3H), 1.34 (s, 9H), 1.66 (m, 1H), 1.73 (s, 3H), 1.77 (s, 3 H), 1.79 (s, 3H), 1.93 (s, 3H), 2.09 (m, 2H), 2.15 (m, 1H), 2.29 (m, 1H), 2.40 (s, 3H), 2.46 (m, 2H), 2.57 (m, 2H), 3.61 (s, 3H), 3.69 (s, 1H), 3.95 (d, J = 6.8 Hz, 1H), 4.10 (m, 2H), 4.17 (d, J = 8.4 Hz, 1H), 4.23 (d, J = 3.2 Hz, 1H), 4.30 (d, J = 8.4 Hz, 1H), 4.74 (m, 1 H), 4.80 (m, 1H), 4.93 (d, J= 8.8 Hz, 1H), 5.22 (d, J = 8.0 Hz, 1H), 5.60 (dd, J = 10.8, 7.2 Hz, 1H), 5.66 (d, J = 6.8 Hz, 1H), 6.13 (t, J = 8.8 Hz, 1H), 6.29 (s, 1H), 6.49 (s, 1H), 6.54 (d, J = 10 Hz, 1H), 6.73 (m, 1H), 6.86 (m, 2H), 6.96 (t, J = 2.4 Hz, 1H), 7.28 (d, J = 7.2 Hz, 1H), 7.46 (t, J = 8.0 Hz, 2H), 7.64 (m, 3H), 8.08 (d, J = 8.8 Hz, 2H), 8.22 (m, 1H). All data were found to be in agreement with literature values.[38]

7-(4-Fluorescein-butanoyl)-SB-T-1214 (7-Fluorescein-1214)[38]

According to the procedure to synthesize **SB-T-1213**, **3-14** (100 mg, 0.09 mmol) was used to produce **7-Fluorescein-1214** (58 mg, 50% yield) as an orange solid: ^{1}H NMR (400 MHz, $CDCl_3$) δ 0.99 (m, 2 H), 1.06 (m, 2 H), 1.16 (s, 3 H), 1.22 (s, 3 H), 1.34 (s, 9 H), 1.66 (m, 1 H), 1.73 (s, 3 H), 1.77 (s, 3 H), 1.79 (s, 3 H), 1.93 (s, 3 H), 2.09 (m, 2 H), 2.15 (m, 1 H), 2.29 (m, 1 H), 2.40 (s, 3 H), 2.46 (m, 2 H), 2.57 (m, 2 H), 3.61 (s, 3 H), 3.69 (s, 1 H), 3.95 (d, J = 6.8 Hz, 1 H), 4.10 (m, 2 H), 4.17 (d, J = 8.4 Hz, 1 H), 4.23 (d, J = 3.2 Hz, 1 H), 4.30 (d, J = 8.4 Hz, 1H), 4.74 (m, 1H), 4.80 (m, 1H), 4.93 (d, J= 8.8 Hz, 1H), 5.22 (d, J = 8.0 Hz, 1H), 5.60 (dd, J = 10.8, 7.2 Hz, 1H), 5.66 (d, J = 6.8 Hz, 1H), 6.13 (t, J = 8.8 Hz, 1H), 6.29 (s, 1H), 6.49 (s, 1H), 6.54 (d, J = 10 Hz, 1H), 6.73 (m, 1H), 6.86 (m, 2H), 6.96 (t, J = 2.4 Hz, 1H), 7.28 (d, J = 7.2 Hz, 1H), 7.46 (t, J = 8.0 Hz, 2H), 7.64 (m, 3H), 8.08 (d, J = 8.8 Hz, 2H), 8.22 (m, 1H). All data were found the be consistent with literature values.[38]

***N*-(succinic acid*)*-4-amido-2,6-diisopropylphenoxydocosahexaenoate (3-16)**

Trifluoroacetic acid (1.0 mL) was added dropwise to a stirred solution of 3-14 (400 mg, 0.66 mmol) in CH_2Cl_2 (10 mL) and was allowed to stir at room temperature for 4 hours. Pyridine (1.0 mL) was added, concentrated *in vacuo* to afford a brown solid which was dissolved in THF (10

mL). To this solution, succinic anhydride (100 mL) and TEA (0.14 mL, 1.0 mmol) were added and the mixture was stirred for 18 hours. The reaction mixture was concentrated *in vacuo* and purified directly by column chromatography to yield **3-16** (383 mg, 92% yield) as a waxy yellow solid: ^{1}H NMR (300 MHz, $CDCl_3$) δ 0.77 (t, J = 7.5 Hz, 3H), 1.16 (d, J = 6.9 Hz, 12H), 2.07 (m, J = 6.9 Hz, 2H), 2.49-2.59 (m, 2H), 2.59-2.72 (m, 4H), 2.72-2.96 (m, 14 H), 5.23-5.43 (m, 10H), 5.46 (t, J = 5.4 Hz, 2H), 7.30 (s, 2H), 7.59 (br s, 1H). MS (ESI) calcd for $C_{38}H_{52}NO_5$ $(M-H)^-$: 602.39, found 602.4.

DHA-PPF-1214

To a solution of **SB-T-1214** (250 mg, 0.30 mmol), **3-16** (200 mg, 0.33 mmol) and DMAP (50 mg, 0.41 mmol) in CH_2Cl_2 (9 mL) was added EDC hydrochloride (80 mg, 0.42 mmol) suspended in CH_2Cl_2 (3 mL). The mixture was stirred at room temperature for 6 hours and upon completion, was quenched with conc. NH_4Cl (2 mL). Water (20 mL) was added, and the mixture was extracted with EtOAc (3 x 20 mL), the organic layer washed with brine (3 x 20 mL), dried over $MgSO_4$, suction filtered and the filtrate concentrated *in vacuo* to obtain a yellow solid. Purification was done by column chromatography to afford **DHA-PPF-1214** (376 mg, 76% yield) as a white solid: ^{1}H NMR (300 MHz, $CDCl_3$) δ 0.77 (t, J = 7.5 Hz, 3H), 0.89-1.20 (m, 5H), 1.16 (d, J = 6.9 Hz, 12H), 1.23 (s, 3H), 1.33 (s, 3H), 1.42 (s, 9H), 1.74 (s, 3H), 1.79 (s, 1H), 1.83 (s, 6H), 1.90 (m, 1H), 1.97 (s, 3H), 2.04-2.15 (m, 3H), 2.42 (s, 3H δ2.49-2.59 (m, 3H), 2.60 (m, 1H), 2.65 (m, 1H), 2.72-2.96 (m, 14 H), 3.45 (d, J = 6.6 Hz, 1H), 3.88 (d, J = 6.9 Hz, 1H), 4.24 (m, 2H), 4.38 (d, 8.4 Hz, 1H) 4.48 (m, 1H), 4.83 (m, 2H), 5.03 (d, 7.8 H), 5.23-5.43 (m, 11H), 5.46 (t, J = 5.4 Hz, 2H), 5.74 (d, 7.2 Hz, 1H), 6.24 (t, 1H), 6.37 (s, 1H), 7.54 (t, 7.2, 2H), 7.68 (t, 7.5 Hz, 1H), 8.17 (d, 7.2 Hz, 2H); 7.30 (s, 2H). MS (ESI) calcd for $C_{83}H_{111}N_2O_{19}$ $(M+H)^+$: 1439.77, found: 1439.8 (M+H).

DHA-PPF-7-Fluorescein-1214

According to the procedure to synthesize **DHA-PPF-1214**, **7-Fluorescein-1214** (30 mg, 19 nmol) was used to produce **DHA-PPF-7-Fluorescein-1214** (32 mg, 97% yield) as an orange solid: ^{1}H NMR (300 MHz, $CDCl_3$) δ 0.97 (t, J = 7.5 Hz, 3H), 0.89-1.20 (m, 5H), 1.16 (d, J = 6.9 Hz, 12H), 1.23 (s, 3H), 1.33 (s, 3H), 1.42 (s, 9H), 1.74 (s, 3H), 1.79 (s, 1H), 1.80 (m, 2H), 1.75 (s, 3H), 1.80 (3H), 1.90-2.08 (m, 1H), 1.97 (s, 3H), 2.04-2.15 (m, 3H), 2.07 (t, J = 7.2 Hz, 2H), 2.39 (s, 3H), 2.42 (s, 3H) 2.32-2.59 (m, 3H), 2.60 (m, 1H), 2.65 (m, 1H), 2.72-2.96 (m, 14 H), 3.45 (d, J = 6.6 Hz, 1H), 3.63 (s, 3H), 3.88 (d, J = 6.9 Hz, 1H), 4.12 (m, 1H), 4.24 (m, 2H), 4.38 (d, 8.4 Hz, 1H) 4.48 (m, 1H), 4.96 (m, 2H), 5.03 (d, 7.8 H), 5.32-5.50 (m, 13H), 5.46 (t, J = 5.4 Hz, 2H), 5.74 (d, 7.2 Hz, 1H), 6.24 (t, 1H), 6.37 (s, 1H), 6.63 (m, 2H), 6.79 (m, 1H), 6.89 (t, 2H), 7.25 (s, 2H), 7.30 (d, J = 4.2 Hz, 1H), 7.49 (t, 2H), 7.60 (t, 1H), 7.68 (t, 4.5 Hz, 1H), 7.73 (t, J = 4.5 Hz 1H), 8.17 (d, 7.2 Hz, 2H), 8.24 (d, J = 4.2 Hz, 1H). ^{13}C NMR (125 MHz $CDCl_3$) δ 8.74, 18.88, 12.83, 14.25, 14.48, 20.55, 21.40, 22.51, 22.60, 23.71, 25.54, 25.63, 28.21, 29.68, 33.58, 33.68, 35.38, 43.25, 46.88, 52.40, 56.02, 68.03, 71.52, 74.99, 74.55, 74.12, 78.85, 79.88, 80.74, 83.97, 100.84, 114.74,

117.43, 119.98, 127.02, 128.09, 128.27, 128.57, 129.21, 129.57, 130.16, 130.37, 131.12, 132.04, 132.19, 132.63, 133.10, 134.60, 138.04, 141.88, 154.75, 154.96 159.10, 165.57, 166.94, 168.40, 169.49, 171.70, 172.13, 172.79, 202.49. MS (ESI) calcd for $C_{108}H_{129}N_2O_{25}$ $(M+H)^+$: 1853.88, found:1853.9.

§ 3.5.0 References

1. Sauer, L. A.; Dauchy, R. T., The effect of omega-6 and omega-3 fatty acids on 3H-thymidine incorporation in hepatoma 7288CTC perfused in situ. *Br. J. Cancer* **1992,** *66*, 297-303.
2. Seitz, J.; Ojima, I., Chapter V.9. Drug Conjugates with Polyunsaturated Fatty Acids. In *Drug Delivery in Oncology - From Research Concepts to Cancer Therapy*, Kratz, F.; Senter, P.; Steinhagen, H., Eds. Wiley-VCH: Weinheim, Germany, 2011.
3. Berquin, I. M.; Edwards, I. J.; Chen, Y. Q., Multi-targeted therapy of cancer by omega-3 fatty acids. *Cancer Lett.* **2008,** *269*, 363-367.
4. Colquhoun, A.; Miyake, J. A.; Benadiba, M., Fatty acids, eicosanoids and cancer. *Nutr. Ther. Metabol.* **2009,** *27*, 105-112.
5. Pownall, H. J.; Hamilton, J. A., Energy translocation across cell membranes and membrane models. *Acta Physiologica Scandanavia* **2003,** *178*, 357-365.
6. Rose, D. P.; Connolly, J. M., Regulation of tumor angiogenesis by dietary fatty acids and eicosanoids. *Nutr. Cancer* **2000,** *2*, 879-890.
7. Hardman, W. E., (n-3) Fatty Acids and Cancer Therapy. *J. Nutr.* **2004,** *134*, 3427S-3430S.
8. Brown, M. D.; Hart, C. A.; Gazi, E.; Bagley, S.; Clarke, N. W., Promotion of prostatic metastatic migration towards human bone marrow stoma by Omega 6 and its inhibition by Omega 3 PUFAs. *Br. J. Cancer* **2006,** *94*, 842-853.
9. Calviello, G.; Niculolo, F. D.; Gragnoli, S.; Piccioni, E.; Serini, S.; Maggiano, N.; Tringali, G.; Navarra, P.; O'Ranelletti, F.; Palozza, P., n-3 PUFAs reduce VEGF expression in human colon cancer cells modulating the COX-2/PGE2 induced ERK -1 and -2 and HIF-1α induction pathway. *Carcinogenesis* **2004,** *25*, 2303-2320.
10. Novak, T. E.; Babcock, T. A.; Jho, D. H.; Helton, W. S.; Espat, N. J., NF-kappa B inhibition by omega-3 fatty acids modulates LPS-stimulated macrophage TNF-alpha transcription. *Am. J. Physiol.* **2003,** *284*, L84-L85.
11. Tuller, E. R.; Brock, A. L.; Yu, H.; Lou, J. R.; Benbrook, D. M.; Ding, W.-Q., PPARα signaling mediates the synergistic cytotoxicity of clioquinol and docosahexaenoic acid in human cancer cells. *Biochem. Pharmacol.* **2009,** *77*, 1480-1486.
12. Zhuo, Z.; Zhang, L.; Mu, Q.; Lou, Y.; Gong, Z.; Shi, Y.; Ouyang, G.; Zhang, Y., The effect of combination treatment with docoahexaenoic acid and 5-fluorouracil on the mRNA expression of apoptosis-related genes, including the novel gene BCL2L12, in gastric cancer cells. *In Vitro Cellular Developmental Biology - Animal* **2009,** *45*, 69-74.
13. Wang, Y.; Li, L.; Jiang, W.; Larrick, J. W., Synthesis and evaluation of a DHA and 10-hydroxycamptotecin conjugate. *Bioorg. Med. Chem.* **2005,** *13*, 5592-5599.
14. Wang, Y.; Li, L.; Jiang, W.; Yang, Z.; Zhang, Z., Synthesis and preliminary antitumor activity evaluation of a DHA and doxorubicin conjugate. *Bioorg. Med. Chem. Lett.* **2006,** *16*, 2974-2977.
15. Huan, M.-I.; Zhou, S.-Y.; Teng, Z.-H.; Zhang, B.-I.; Liu, X.-Y.; Wang, J.-P.; Mei, Q.-B., Conjugation with a-linolenic acid improves cancer cell uptake and cytotoxicity of doxorubicin. *Bioorg. Med. Chem. Lett.* **2009,** *19*, 2579-2584.

16. Schobert, R.; Biersack, B.; Knauer, S.; Ocker, M., Conjugates of the fungal cytotoxin illudin M with improved tumour specificity. *Bioorg. Med. Chem. Lett.* **2008,** *16*, 8592-8597.
17. Anel, A.; Halmos, T.; Torres, J. M.; Pineiro, A.; Antonakis, K.; Uriel, J., Cytotoxicity of chlorambucil and chlorambucil-fatty acid conjugates against human lymphomas and normal human peripheral blood lymphocytes. *Biochem. Pharmacol.* **1990,** *40*, 1193-1200.
18. Shikano, M.; Onimura, K.; Fukai, Y.; Hori, M.; Fukazawa, H.; Mizuno, S.; Yazawa, K.; Uehara, Y., 1a-Docosahexaenoyl Mitomycin C: A Novel Inhibitor of Protein Tyrosine Kinase. *Biochm. Biophys.Res. Comm.* **1998,** *248*, 858-863.
19. Halmos, T. M. P.; Antonakis, K.; Uriel, J., Fatty acid conjugates of 2'-dexoy-5-fluorouridine as prodrugs for the selective delivery of 5-fluorouracil to tumor cells. *Biochem. Pharmacol.* **1999,** *44*, 149-155.
20. Zerouga, M.; Stillwell, W.; Jenski, L. J., Synthesis of a novel phosphatidylcholine conjugated to docosahexaenoic acid and methotrexate that inhibits cell proliferation. *Anti-Cancer Drugs* **2002,** *13*, 301-311.
21. Hennenfent, K. L.; Govindan, R., Novel formulations of taxanes: a review. Old wine in a new bottle? *Ann. Oncol.* **2006,** *17*, 735-749.
22. Tannock, I. F., Principles of cell proliferation: cell kinetics. In *Cancer: Principle and Practice of Oncology*, 3 ed.; DeVita Jr., V. T.; Hellman, S.; Rosenberg, S. A., Eds. J. P. Lippincott: Philadelphia, PA, 1989; pp 3-13.
23. Bradley, M. O.; Webb, N. L.; Anthony, F. H.; Devanesan, P.; Witman, P. A.; Hemamali, S.; Chander, M. C.; Baker, S. D.; He, L.; Horwitz, S. B.; Swindell, C. S., Tumor Targeting by Covalent Conjugation of a Natural Fatty Acid to Paclitaxel. *Clin. Cancer Res.* **2001,** *7*, 3229-3258.
24. Sparreboom, A.; Wolff, A. C.; Verweig, J.; Zabelina, Y.; Zomeren, D. M. v.; McIntire, G. L.; Swindell, C. S.; Donehower, R. C.; Baker, S. D., Disposition of Docosahexaenoic Acid-Paclitaxel, a Novel Taxane, in Blood: In Vitro and Clinical Pharmacokinetic Studies. *Clin. Cancer Res.* **2003,** *9*, 151-159.
25. Sparreboom, A.; van-Zuylen, L.; Brouwer, E.; Loos, W. J.; de-Bruijn, P.; Gelderblom, H.; Pillay, M.; Nooter, K.; Stoter, G.; Verweig, J., Cremophor EL-mediated alteration of paclitaxel distribution in human blood: clinical pharmacokinetic implications. *Cancer Res.* **1999,** *59*, 1454-1457.
26. Wolff, A. C.; Donehower, R. C.; Carducci, M. K.; Carducci, M. A.; Brahmer, J. R.; Zabelina, Y.; Bradley, M. O.; Anthony, F. H.; Swindell, C. S.; Witman, P. A.; Webb, N. L.; Baker, S. D., Phase I Study of Docosahexaenoic Acid-Paclitaxel: a Taxane-Fatty Acid Conjugate with a Unique Pharmacology and Toxicity Profile. *Clin. Cancer Res.* **2003,** *9*, 3589-3597.
27. Johnston, S. R. D.; Houston, S.; Jones, A.; Evans, T. R.; Schacter, L., Efficacy of DHA-paclitaxel (TXP) for the second-line treatment of breast cancer. *Proc. Am. Soc. Oncol.* **2003,** *22*, 17.
28. Modiano, M. R.; Houston, S.; Savage, P.; Price, C.; Schacter, L.; Gilby, E., Efficacy of DHA-paclitaxel (TXP) in malignant melanoma. *Proc. Am. Soc. Oncol.* **2003,** *22*, 713.
29. Harries, M.; O'Donnell, A.; Scurr, M.; Reade, S.; Cole, C.; Judson, I.; Greystoke, A.; Twelves, C.; Kaye, S., Phase I/II study of DHA-paclitaxel in combination with carboplatin in patients with advanced malignant solid tumors. *Br. J. Cancer* **2004,** *91*, 1651-1655.
30. Bradley, M. O.; Swindell, C. S.; Anthony, F. H.; Witman, P. A.; Pevanesan, P.; Webb, N. L.; Baker, S. D.; Wolff, A. C.; Donehower, R. C., Tumor targeting by conjugation of DHA to paclitaxel. *J. Controlled Release* **2001,** *74*, 233-236.

31. Stehle, G., Plasma protein (albumin) catabolism by the tumor itself - implications for tumor metabolism and the genesis of cachexia. *Crit. Rev. Oncol. Hematol.* **1997,** *26*, 77-100.
32. Deher, M.; Liu, W.; Michelich, C.; Dewhirst, M.; Yuan, F.; Chilkoti, A., Tumor Vascular Permeability, Accumulation and Penetration of Macromolecular Drug Carriers. *J. Nat. Cancer Inst.* **2006,** *98*, 335-344.
33. Desai, N.; Yao, Z.; Trieu, V.; Soon-Shoing, P.; Dykes, D.; Noker, P., Evidence of greater tumor and red cell partitioning and superior antitumor activity of cremophor free nanoparticle paclitaxel (ABI-007) compared to taxol. *Breast Cancer Res. Treat.* **2003,** *82(suppl 1):S83*, Abstract 348.
34. Ibrahim, N. K.; Desai, N.; Legha, S.; Soon-Shiong, P.; Theriault, R.; Rivera, E.; Esmaeli, B.; Ring, S. E.; Bedikian, A.; Hortobagyi, G. N.; Ellerhorst, J. A., Phase I and Pharmacokinetic Study of ABI-007, a Cremophor-free, Protein-stabilized Nanparticle Formulation of Paclitaxel. *Clin. Cancer Res.* **2002,** *8*, 1038-1044.
35. Kuznetsova, L.; Chen, J.; Sun, L.; Wu, X.; Pepe, A.; Veith, J. M.; Pera, P.; Bernacki, R. J.; Ojima, I., Synthesis and evaluation of novel fatty acid-second-generation taxoid conjugates as promising anticancer agents. *Bioorg. Med. Chem. Lett.* **2006,** *16*, 974-977.
36. Siddiqui, R. A.; Zerouga, M.; Wu, M.; Castillo, A.; Harvey, K.; Zaloga, G. P.; Stillwell, W., Anticancer properties of propofol-docosahexaenoate and propofol-eicosapentaenoate of breast cancer cells. *Breast Cancer Res.* **2005,** *7*, R645-R654.
37. Harvey, K. A.; Xu, Z.; Whitley, P.; Davisson, V. J.; Siddiqui, R. A., Characterization of anticancer properties of 2,6-diisopropylphenol-docasahexaenoate and analogues in breast cancer cells. *Biorg. Med. Chem* **2010,** *10*, 1866-1874.
38. Chen, S.; Zhao, X.; Chen, J.; Chen, J.; Kuznetsova, L.; Wong, S.; Ojima, I., Mechanism-based tumor-targeting drug delivery system. Validation of efficient vitamin receptor-mediated endocytosis and drug release. *Bioconjugate Chem.* **2010,** *21*, 979-987.
39. Marder-Karsenti, R.; Dubois, J.; Bricard, L.; Guenard, D.; Gueritte-Voegelein, F., 1. Synthesis an Biological Evaluation of D-Ring-Modified Taxanes:5(20)-Azadocetaxel Analogs. *J. Org. Chem.* **1997,** *62*, 6631-6637.
40. Meek, J.; Fowler, J.; Monroe, P.; Clark, T., The Reaction of Hindered Phenols with Diazomethane. *J. Org. Chem.* **1968,** *33*, 223-226.
41. Trapani, G.; Latrofa, A.; Franco, M.; Altomare, C.; Sanna, E.; Usala, M.; Biggo, G.; Liso, G., 2. Propofol Analogs. Synthesis, Relationships between Structure and Affinity at GABAA Receptor in Rat Brain. andDifferential Electrophysiological Profile at Recombinant Human GABAA Receptors. *J. Med. Chem.* **1998,** *41*, 1846-1854.
42. Kimura, K.; Masuda, T.; Yamada, K.; Mitani, M.; Kubota, N.; Kawakatsu, N.; Kishii, K.; Inazu, M.; Kiuchi, Y.; Oguchi, K.; Namiki, T., 2. Novel diphenylalkyl piperazine derivatives with high affinities for the dopamine transporter. *Bioorg. Med. Chem.* **2003,** *11*, 3953-3963.

Chapter 4

Synthesis and Biological Evaluation of Biotin-Taxoid Conjugates

Content

§ 4.0.0 Biotin as a Tumor-Targeting Moiety

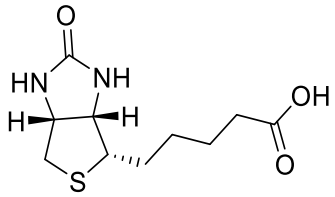

Figure 4-1: The chemical structure of Biotin

Vitamins are essential nutrients, many of which (e.g. vitamin B_{12}, folic acid, biotin and riboflavin) act as cofactors for a number of processes involved in cell division such as beta-oxidation of fatty acids and the synthesis of proteins and nucleic acids. Therefore, the need for certain vitamins in rapidly dividing cancer cells is elevated compared to that of most healthy somatic cells. The receptors for these vitamins have been found to be overexpressed in many cancer cell lines to facilitate the increased uptake. As many cancers have shown to have higher expression levels of these receptors on their cell surfaces with respect to cells in healthy tissue, these vitamin receptors serve as useful targets for tumor-targeted drug delivery.[1-3] Furthermore, their increased expression levels can be exploited as biomarkers for the identification and imaging of tumor cells. To date, the folate receptor has been most extensively studied and the biotin receptor is emerging as a potential target.[2, 4, 5]

Tumour	Mouse	Type	Folate	Cbl	Biotin
O157	Balb/C	Bcell lymph	+/–	+/–	+/–
BW5147	AKR/J	Lymphoma	+/–	+/–	+/–
B16	C57/Bl	Melanoma	–	–	–
LL-2	C57/Bl	Lung	–	–	–
HCT-116	Balb/C-Nu	Colon	–	–	–
L1210	DBA/2	Leukemia	+/–	+/–	–
L1210FR	DBA/2	Leukemia	++	+	+++
Ov 2008	Balb/C-Nu	Ovarian	+++	–	++
ID8	C57/Bl	Ovarian	+++	–	++
Ovcar-3		Ovarian	+++	–	++
Colo-26	Balb/C	Colon	+/–	++	+++
P815	DBA/2	Mastocytoma	+/–	++	+++
M109	Balb/C	Lung	+	+++	+++
RENCA	Balb/C	Renal cell	+	+++	+++
RD995	C3H/HeJ	Renal cell	+	++	+++
4T1	Balb/C	Breast	+	++	+++
JC	Balb/C	Breast	+	++	+++
MMT060562	Balb/C	Breast	+	++	+++

Table 4-1: The relative expression levels of vitamin receptors in cancer cells (adapted from [3])

Biotin (vitamin B_7, vitamin H, or coenzyme R), shown in **Figure 4-1**, serves as a coenzyme for five biotin-dependent carboxylases, and is responsible for the transfer of single carbon units at their highest oxidation state.[6, 7] As such, it is intimately involved in the processes of epigenetic

regulation, fatty acid biosynthesis, energy production and the catabolism of fats and amino acids.[8, 9] Little was known about the expression levels of biotin receptors until it was discovered in 2004 that the receptors for biotin were even more overexpressed on the surface of some cancer cells than those for folic acid and vitamin B_{12} (**Table 4-1**).[3] Accordingly, the biotin receptor has emerged as a potential new target for tumor-targeted drug delivery.[10]

§ 4.0.1 Receptor-Mediated Endocytosis

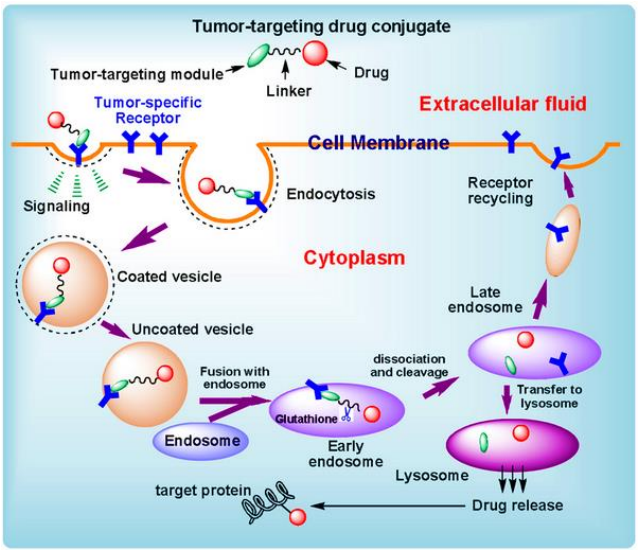

Figure 4-2: Receptor mediated endocytosis and drug release[2]

Vitamins are recognized by receptors on the cell surface, and internalized via the process of receptor-mediated endocytosis (RME), illustrated in **Figure 4-2**.[11-13] After binding to the receptor, a signaling cascade is initiated leading to the formation and internalization of a coated vesicle that then fuses with an endosome. The conjugate is then transferred from the endosome to the lysosome, and during this process the linker is cleaved releasing the free drug. Depending on the type of linker chosen for a given conjugate, drug release can occur in the extracellular matrix, endosome or lysosome. In the case of disulfide linkers, drug release begins in the early endosome, and cleaves fully in the lysosome, where there is a high reducing potential and elevated glutathione (GSH) concentration.[14, 15] This process of cellular internalization and drug release has been validated for biotin conjugates using CFM, and conjugate internalization was quantified *via* fluorescence activated cell sorting (FACS) flow cytometry.[13, 16]

§ 4.0.2 Disulfide Linkers

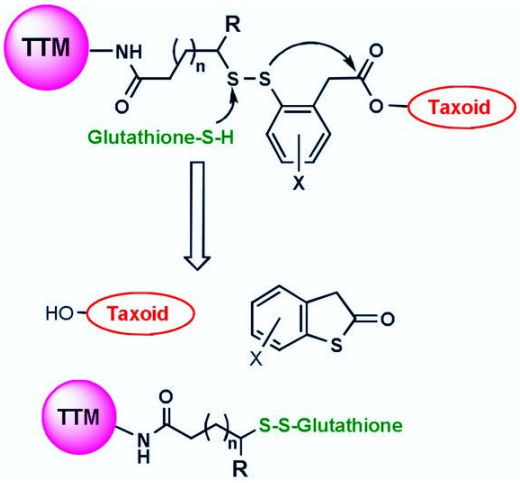

Figure 4-3: Glutathione-Triggered Drug Release (adapted from [2])

Disulfide bonds are quite stable under oxidizing conditions, yet rapidly cleave via reduction, or through disulfide exchange. As the glutathione concentration is 3 orders of magnitude higher in intracellular compartments than in the blood stream, disulfide linkers are good candidates for the development of tumor-targeted drug conjugates.[17-19] Our lab has developed a self-immolative disulfide linker, specifically designed to release the unmodified taxoid upon linker cleavage (**Figure 4-3**), to prevent loss of potency of the active agent.[2, 20] Following disulfide exchange, the resulting thiolate is positioned by the aromatic ring to rapidly react with the C2' ester bond. After thiolactonization, the free drug is released.

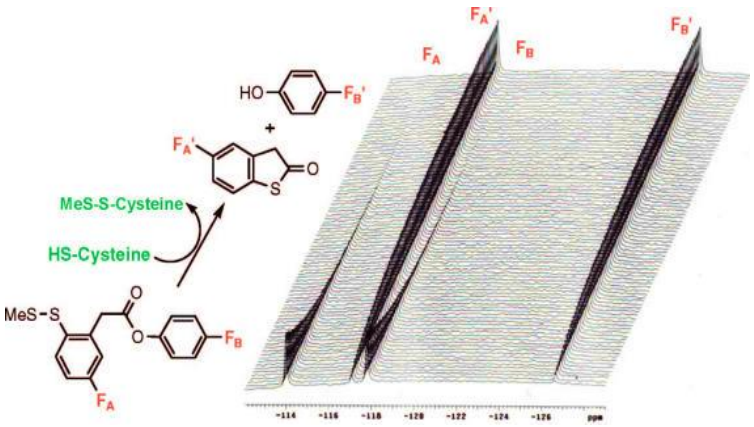

Figure 4-4: ^{19}F NMR Validation of linker release mechanism (adapted from [21])

Using a simplified model system, this drug-release mechanism was observed using fluorine-labeling and monitoring by ^{19}F NMR spectroscopy.[21] Upon addition of the free thiol-containing cysteine, disulfide cleavage and subsequent thiolactonization can be seen clearly by the

change in chemical shifts over time (**Figure 4-4**). This result was corroborated with *in vitro* studies with cancer cells using fluorescence-labeling and CFM.[13] These second-generation disulfide linkers have been successfully incorporated into various tumor-targeting drug conjugates and their efficacy has been evaluated *in vitro*.[10]

§ 4.0.3 Biotin-Linker Taxoid *In Vitro* Studies

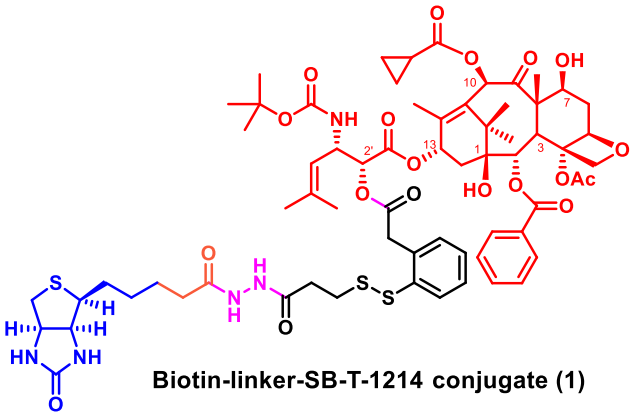

Figure 4-5: The structure of the first biotin-linker-taxoid conjugate (adapted from [13])

The structure of the first generation biotin-linker-taxoid conjugate is shown in **Figure 4-5**, SB-T-1214 was chosen as the active agent, coupled to biotin *via* a self-immolative disulfide linker.[13] This conjugate was evaluated against three cell lines: L1210FR (murine leukemia cell line, overexpressing folate- and biotin-receptors), L1210 (parent murine leukemia cell line) and WI-38 (normal human lung fibroblast cell line).[13] The conjugate (**Figure 4-5**) exhibited high potency (IC_{50} 8.8 nM) against the biotin receptor overexpressing L1210FR cell lines, but the values against L1210 and WI38 cell lines were 59 times (522 nM) and 65 times (570 nM) larger, respectively. This result shows a marked selectivity of the conjugate for the cell line that has been shown to overexpress biotin receptors. In contrast, SB-T-1214 was also assayed against those three cell lines and was not able to distinguish these cell lines, resulting in very similar IC_{50} values.

Three fluorescent probes, shown in **Figure 4-6**, were used to quantify the cellular uptake of the biotin conjugate *via* RME, as well as validate the drug-release process and intracellular drug distribution using confocal microscopy.[13] The biotin-FITC (probe A) was used to establish the RME of biotin conjugates through competition and temperature-dependence studies. The biotin-linker-coumarin conjugate (Probe B) was designed to observe linker cleavage and Probe C was used to test the selective internalization of a biotin-taxoid conjugate.

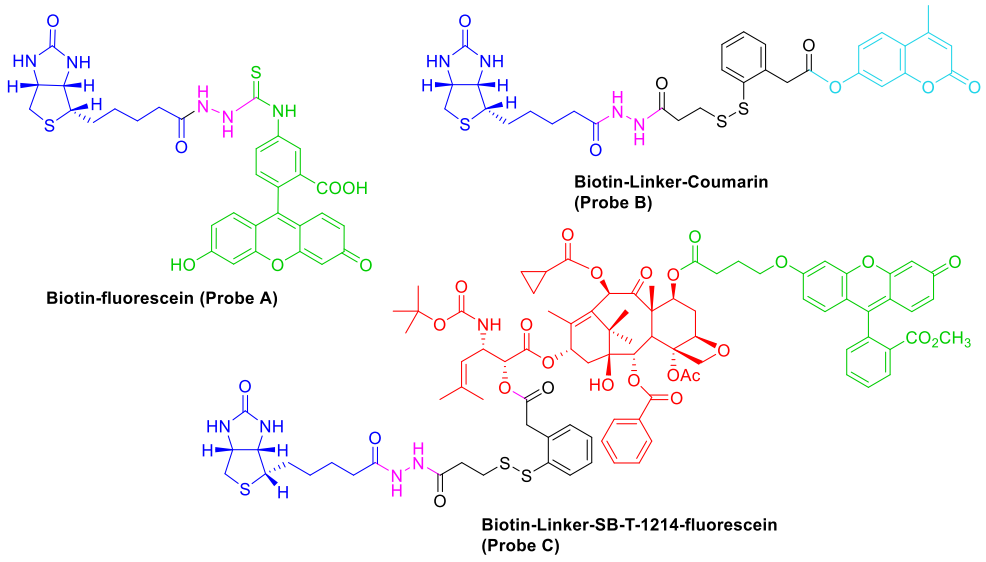

Figure 4-6: Structures of probes used to validate RME of biotin conjugates (adapted from [13])

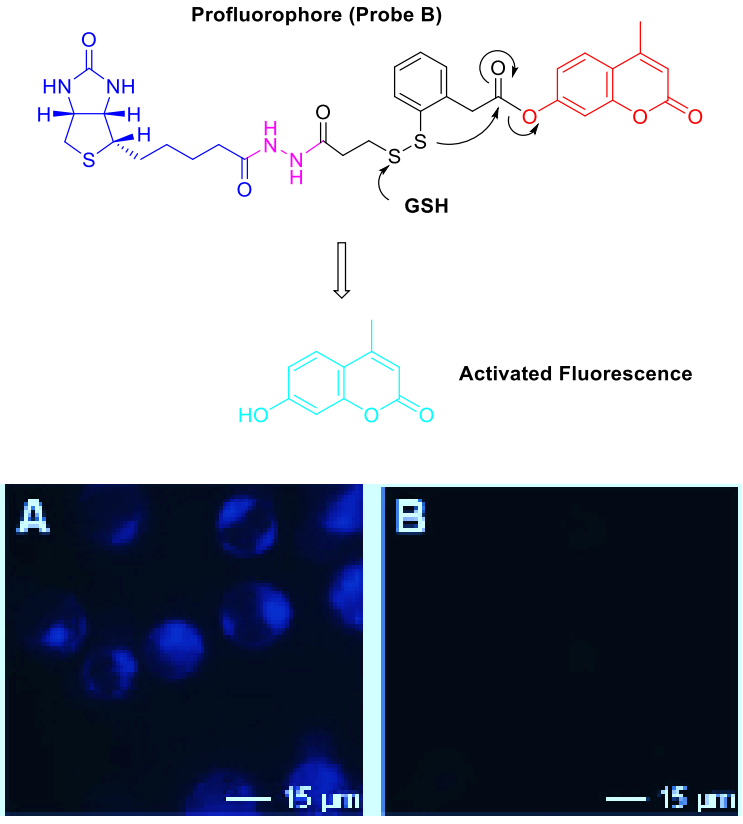

Figure 4-7: Activation of Probe B (*top*) in BR+ cells (*left*) and BR- cells (*right*)

(adapted from [13])

In order to investigate the cellular uptake of these probes, their internalization was monitored by confocal fluorescence microscopy (CFM) and fluorescence-activated cell sorting (FACS) flow cytometry. The biotin-fluorescein (Probe A) was shown to be selectively internalized by the L1210FR cells in a temperature- and time-dependent process that was found to be inhibited by biotin in a concentration dependent manner. The taxoid probe (Probe C) also demonstrated the same internalization trends and selectivity as Probe A, showing that the conjugate was internalized via RME. Probe B, a coumarin pro-fluorophore linked to biotin *via* a disulfide linker, was found to be selectively internalized and activated in biotin-overexpressing cells. The activation mechanism of the coumerin pro-fluorophore is shown in **Figure 4-7**. Only after disulfide cleavage by glutathione and subsequent thiolactonization is the fluorescence of the system activated. Therefore, CFM images clearly show this fluorescence activated selectively in the L1210FR cell line, which overexpresses the biotin receptor. These experiments validated both the model of cellular internalization as well as the linker cleavage and subsequent drug release.

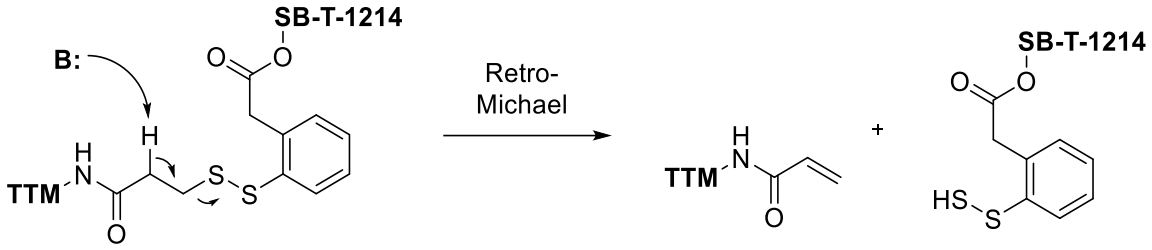

Figure 4-8: Proposed decomposition of 3-carbon linker *via* retro-Michael addition

The original biotin conjugate possessed a 3-carbon disulfide linker, and was found to be unstable in aqueous media for extended periods of time. The slow decomposition of the linker was attributed to a retro-Michael reaction, shown in **Figure 4-8**. In this linker system the disulfide can be eliminated under basic conditions forming an α,β-unsaturated ketone and the free disulfide. By extending the linker one carbon, this reaction is not possible and subsequent HPLC studies confirmed that the half-life of the 4-carbon linker was longer by about an order of magnitude compared to the original design.[22] Increasing the steric bulk at the α-position of a disulfide bond has been shown to increase the stability of the linker. Therefore, a 5-carbon branched linker was synthesized for use in taxoid-based tumor-targeted drug conjugates.

§ 4.1.0 Synthesis of the Disulfide Linker and Coupling-Ready Construct

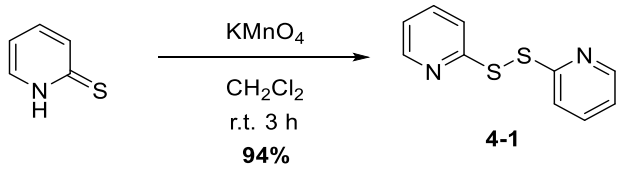

Scheme 4-1: Oxidative dimerization of 2-mercaptopyridine[31]

The synthesis of the disulfide linker begins with the oxidative dimerization of 2-mercaptopyridine to form **4-1** in excellent yield (**Scheme 4-1**).

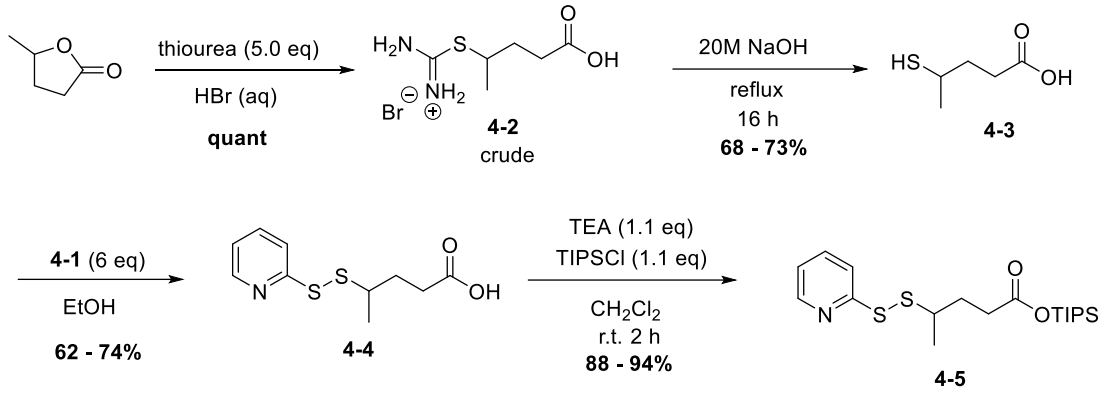

Scheme 4-2: Synthesis of disulfide intermediate **4-5**[13, 33]

The 5-carbon tether of the linker is prepared by ring opening of γ-valerolactone with thiourea followed by basic hydrolysis to afford 4-mercaptophenylacetic acid **4-3**. Following disulfide exchange of **4-3** with 6 equivalents of **4-1,** TIPS protection of activated disulfide **4-4** affords the desired linker component **4-5** (**Scheme 4-2**).

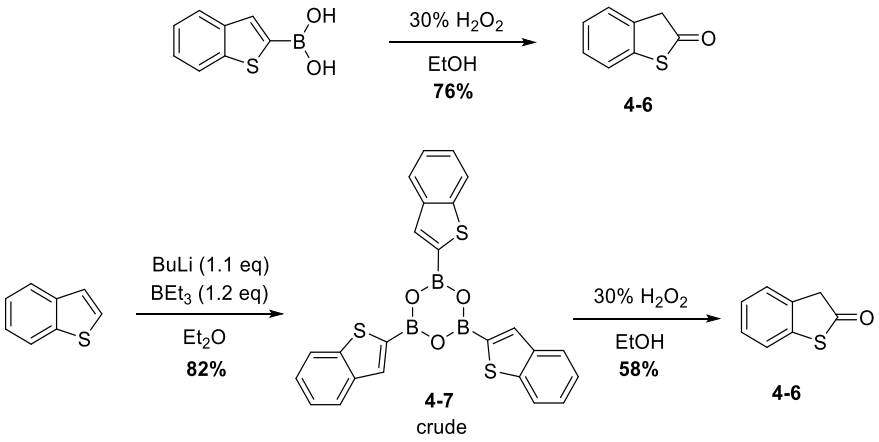

Scheme 4-3: Synthesis of thiolactone **4-6**[23]

Synthesis of the phenyl acetic acid component of the linker begins with the oxidation of thionapthene-2-boronic acid with peroxide, yielding thiolactone **4-6**. Alternatively, treatment of thianapthene with butyl lithium and tributyl borate affords the cyclotrioxaborane **4-7** following acid/base workup. Oxidation of this intermediate using peroxides affords the thiolactone in modest yield (**Scheme 4-3**).[23]

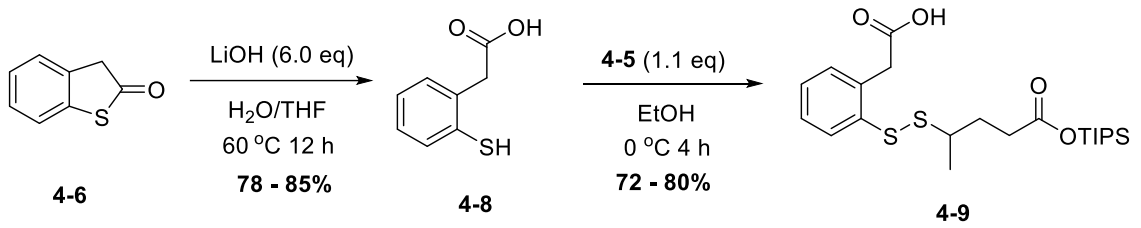

Scheme 4-4: Hydrolysis of **4-6** and second disulfide exchange[24]

Basic hydrolysis of thiolactone **4-6** and subsequent disulfide exchange affords the desired TIPS-protected linker **4-9** (**Scheme 4-4**). The mono-protected di-carboxylic acid was isolated by column chromatography and should be stored at low temperature, as deprotection may occur on standing at higher temperatures.

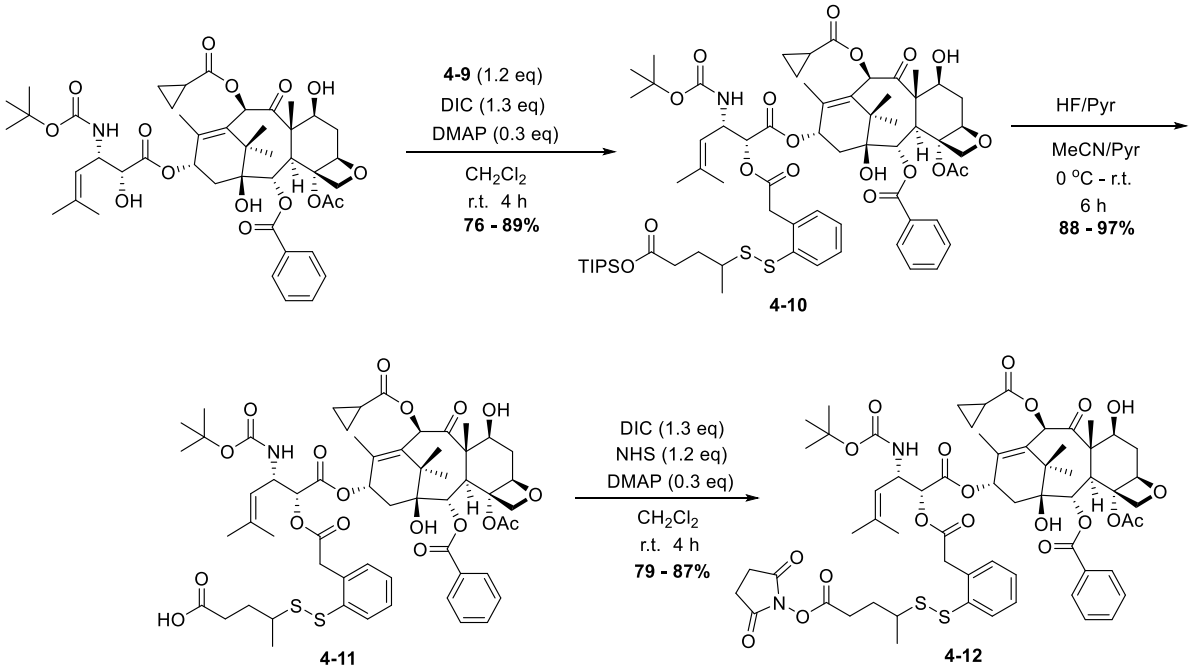

Scheme 4-5: Synthesis of coupling-ready SB-T-1214-linker construct **4-12**

With the mono-protected linker intermediate **4-9** in hand, the drug was coupled to the phenyl acetic acid moiety followed by silyl deprotection and DIC coupling to afford the active ester **4-12** (**Scheme 4-5**).This 'coupling-ready' construct can be applied to the synthesis of different conjugates *via* standard peptide coupling procedures.

§ 4.1.1 Synthesis of Biotin-Linker-Taxoid (BLT)

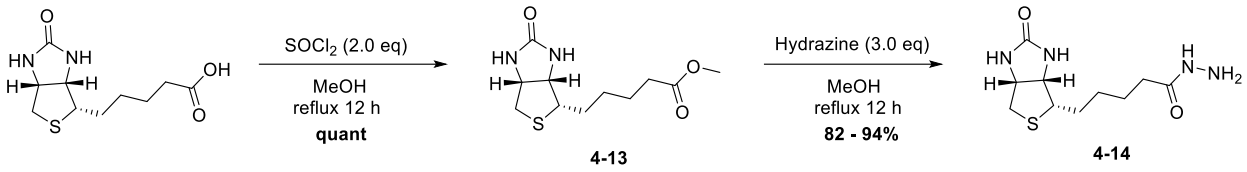

Scheme 4-6: Synthesis of biotin hydrazide[13]

Biotin was converted to the methyl ester via acid chloride formation in methanol. Reflux of the methyl ester with excess hydrazine in methanol afforded biotin hydazide **4-14** (**Scheme 4-6**), which could be triturated to a white solid from ether and hexanes.

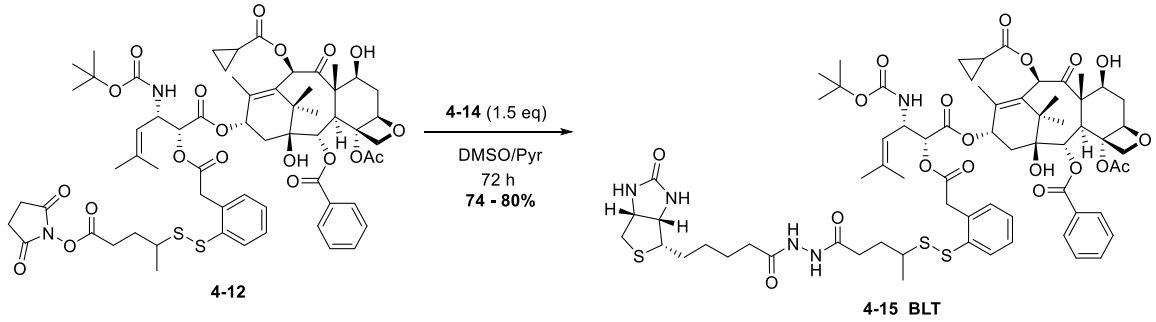

Scheme 4-7: Biotin coupling to form biotin-linker-taxoid (BLT) conjugate **4-15**

Coupling of biotin hydrazide to the coupling-ready construct **4-12** proceeds slowly at room temperature, but the desired conjugate **4-15** was obtained in decent yield after column purification (**Scheme 4-7**). This material was used for *in vivo* testing in an MX-1 breast cancer tumor model, the results of which is described in the next section.

§ 4.1.2 Biological Evaluation of BLT *in Vivo* in Mice Bearing MX-1 Xenografts

The efficacy of the BLT conjugate was investigated *in vivo* using SCID mice bearing MX-1 tumor xenografts. It was later corroborated that MX-1 cells have an increased expression level of biotin receptors as assessed by in vitro FACS studies conducted by Jacob Vineberg. A side by side comparison of the tumor volumes of mice treated with the BLT conjugate and free SB-T-1214 is shown in **Figure 4-9**.

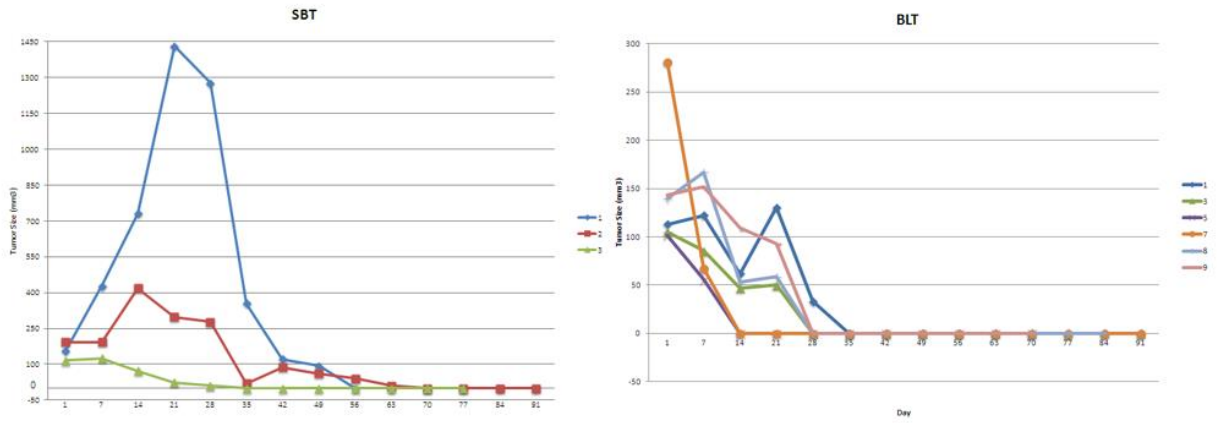

Figure 4-9: Tumor volumes for surviving mice treated with **SB-T-1214** (*left*) and **BLT** (*right*)

Complete tumor regressions were obtained in 3 out of 5 mice treated with SB-T-1214 (**Figure 4-9**, *left*), whereas all mice receiving treatment with the biotin conjugate achieve full regression. However, looking at the surviving mice treated with SB-T-1214, tumor growth rates were highly variable due to the direct injection of MX-1 cells. Impressively, one tumor in the SB-T-1214 treated group that had grown to over 1200 mm^3 before treatment had fully regressed by the time that the mouse was euthanized. Response to treatment with the biotin conjugate appeared to be substantially faster and more consistent, as evidenced by complete cures in all treated mice by 35 days following treatment. These responses were found to be lasting, and mice were found to survive tumor-free for up to 91 days following the treatment.

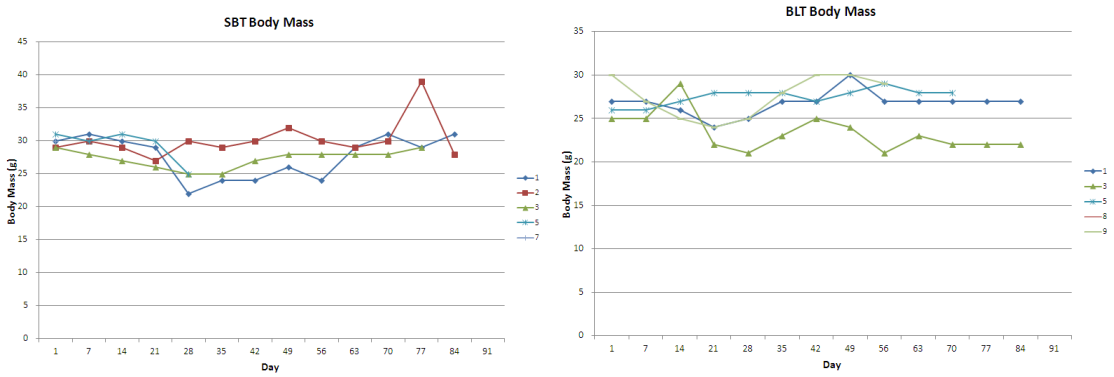

Figure 4-10: Body mass of SCID mice treated with **SB-T-1214** (*left*) and **BLT** (*Right*)

To assess the relative toxicity of the BLT conjugate, the body mass of all treated mice was also measured throughout the course of the study. Although two mice in the SB-T-1214 treated group had to be euthanized early in the study due to erratic and rapid tumor growth as a result of the xenograft protocol, those that survived long enough for treatment were found to experience only moderate weight loss. None of the mice from either group (SBT or BLT) had to be euthanized

due to excessive weight loss. The biotin conjugate was not without toxicity and one of the treated mice experienced some statistically significant weight loss (**Figure 4-10**). However, it must be noticed that this study was not performed using an optimized formulation or dosing regimen, and the erratic tumor growth rates complicate the analysis of the data. Regardless of these shortcomings, these data provide strong evidence of biotin-mediated tumor targeting *in vivo*. A repeat study is currently underway.

§ 4.2.1 Design of a Fluorinated BLT-F Probe for Stability Studies in Complex Media

Specific labeling of biologically active substances with fluorine can be useful, as fluorine is not found in natural substances. Therefore, the fluorine nucleus can be specifically observed via ^{19}F NMR in complex organic and biological mixtures.[25-27] During the validation of the self-immolative disulfide linker, ^{19}F NMR was used to monitor cleavage of a model system in real time (**Figure 4-4**).[21]

As the stability of the linker is of the utmost importance, effort has been made to estimate its stability in blood plasma using different analytical methods. Analysis of the conjugate in phosphate buffered (PBS) saline and acetonitrile (MeCN) has been performed using HPLC, but this model system has little relevance to *in vivo* applications.[22] HPLC was also used to investigate the blood plasma stability of the conjugate following extraction into organic solvent. Even after extraction into MeCN, the chromatogram was quite messy and difficult to read. Nevertheless, a rough estimate of the half-life based on the available data was 4 hours in blood plasma.[22] In order to obtain a better understanding of the conjugate's stability to disulfide cleavage in complex media, a probe was synthesized with two fluorine residues strategically built into the BLT conjugate. This fluorinated biotin conjugate, **BLT-F**, was designed bearing fluorine on the phenyl acetic acid moiety of the linker and on the *meta*-position of the C2 benzoyl group to act as a cleavage signal and internal standard, respectively during NMR analysis. The purpose of this probe was to directly observe disulfide cleavage in biologically relevant systems that could not otherwise be analyzed by HPLC.

§ 4.2.2 Synthesis of Fluorine-Labeled BLT-F Conjugate

The synthesis of the fluorine-labeled taxoid was executed using standard conditions for modification of the C2 position starting from intermediate **2-2**. DIC coupling followed by deprotection afforded the C2-modified baccatin **4-17** in decent yield. The purified baccatin products were combined for the subsequent steps. Protection of the C7 position with TES followed by C10 acylation proceeded smoothly, and intermediate **4-19** was obtained in good yield. Ojima-Holton coupling followed by deprotection afforded the fluorine labeled taxoid **SB-T-121405**.[16]

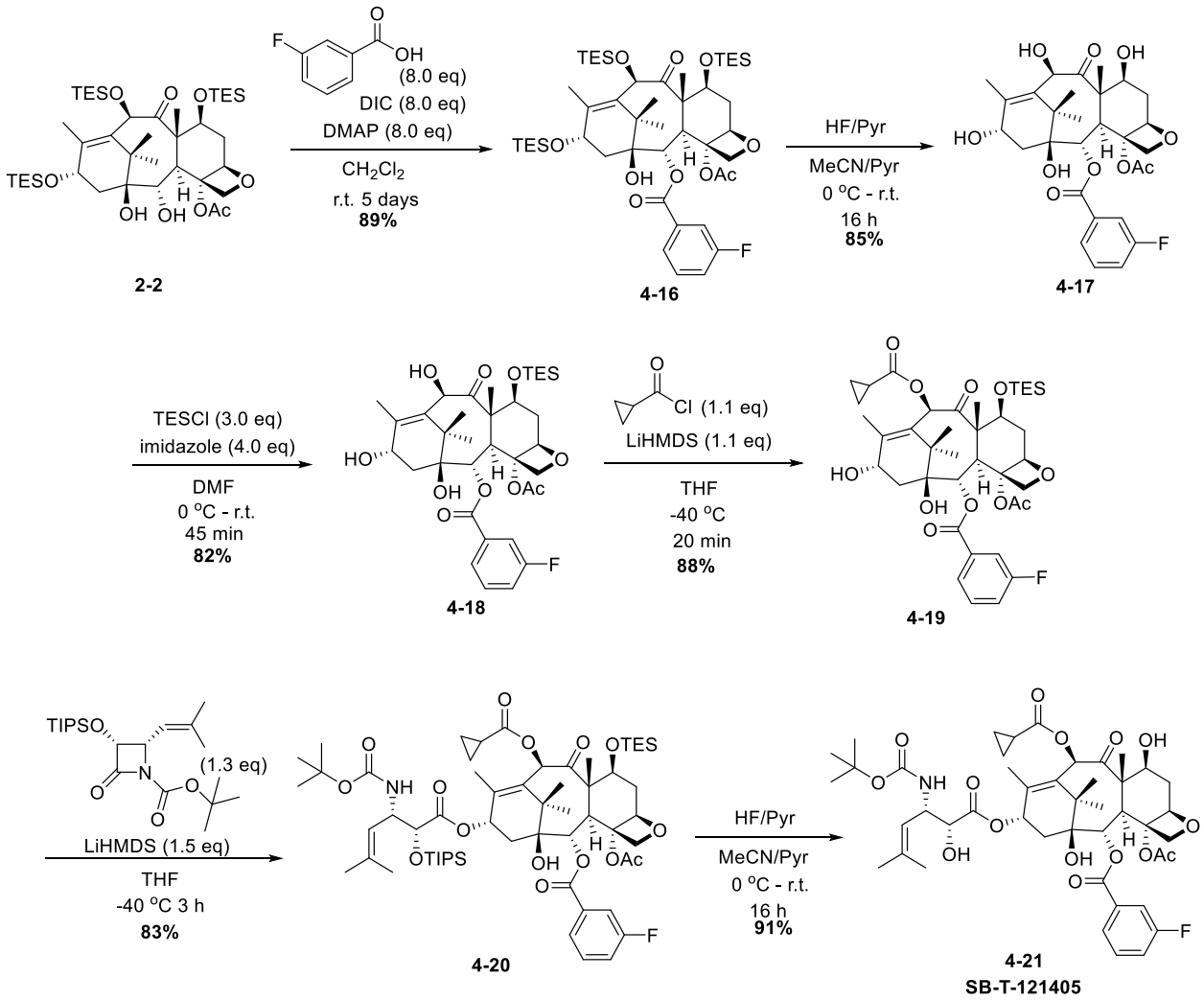

Scheme 4-8: Synthesis of **SB-T-121405**[16]

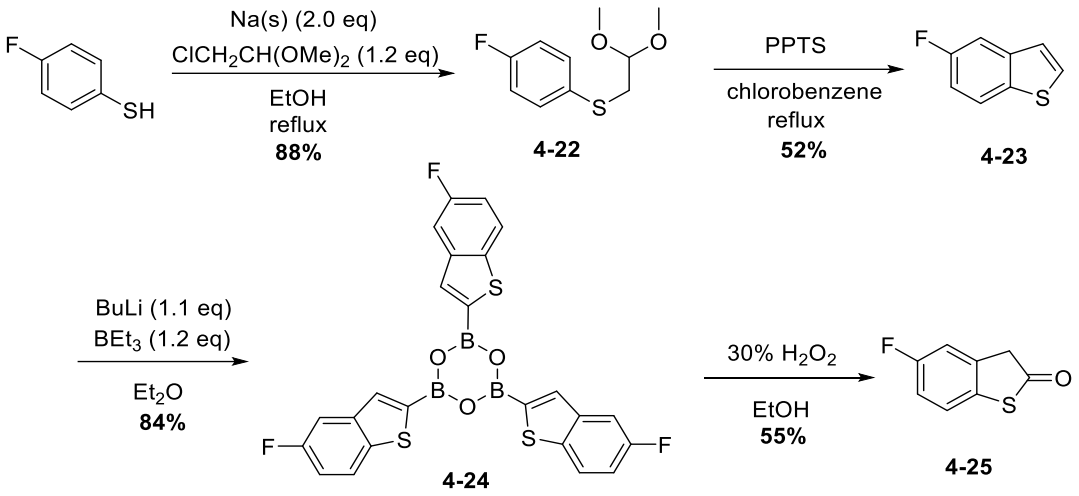

Scheme 4-9: Synthesis of fluorinated thiolactone **4-25**[23, 28]

Thiolactone **4-25** was synthesized according to known literature methods. Alkylation of the thiol in the presence of ethoxide proceeded in good yield and acid catalyzed ring closure produced the desired fluoro-benzothiophene **4-23**.[28] This reaction was low yielding, partly due to difficulties purifying the desired compound. As this compound is surprisingly volatile, some of it may have been lost during evaporation of chlorobenzene following aqueous workup. Formation of cyclotrioxaborane **4-24** and subsequent oxidation with hydrogen peroxide afforded the desired thiolactone in modest yield.[23]

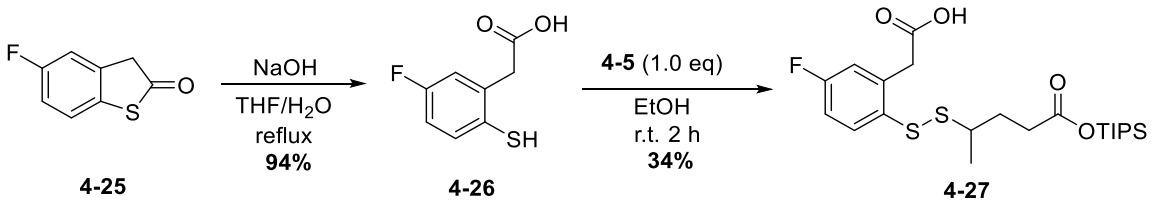

Scheme 4-10: Synthesis of fluorine-labeled linker intermediate **4-27**

Hydrolysis followed by disulfide exchange between **4-26** and **4-5** gave the desired fluorinated linker component **4-27** in low yield. Low yield of this reaction was due to impurities in **4-5** and incomplete conversion. Further optimization can doubtlessly result in dramatic improvement in the yield for this step.

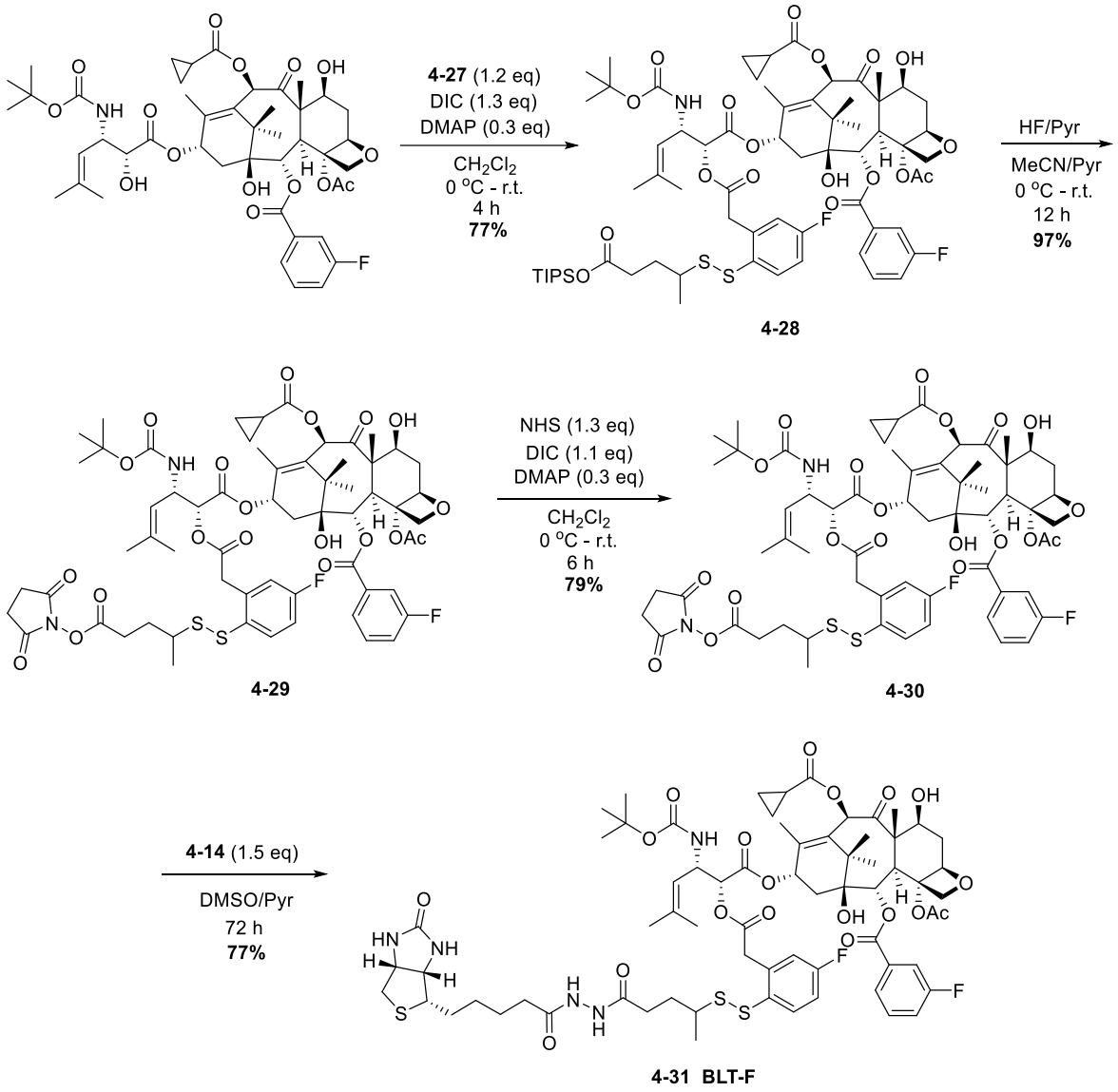

Scheme 4-11: Synthesis of fluoro-BLT '1st Generation Probe' **BLT-F**

Coupling of **SB-121405** to **4-23** proceeded in decent yield to afford TIPS protected conjugate **4-24**. Silyl deprotection with HF/Pyridine followed by DIC coupling produced the bis-fluorine labeled coupling ready conjugate **4-26**. Coupling to biotin hydrazide **4-13** and purification gave the desired **BLT-F** first generation ^{19}F NMR probe in good yield. This conjugate was used to investigate the effects of formulation on linker stability.

§ 4.2.3 ^{19}F NMR Evaluation of First Generation BLT-F

Before evaluating the probe in complex media, it was first necessary to ascertain where the signals from each fluorine nucleus would show up during the cleavage process. Therefore, the probe was dissolved in 30% DMSO in D_2O, and 5 equivalents of GSH in D_2O was added.

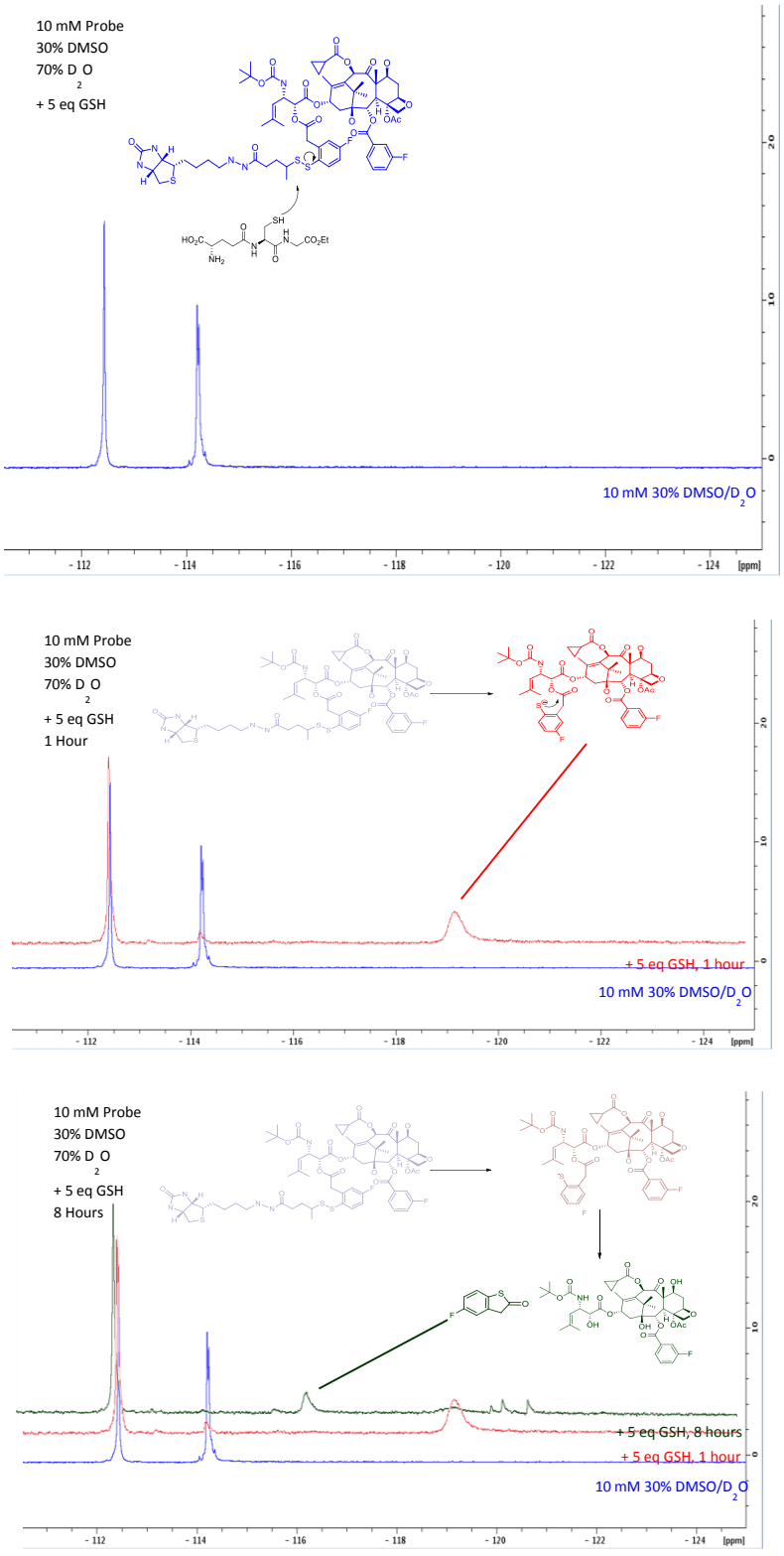

Figure 4-11: Observation of ^{19}F NMR Signals during Disulfide Cleavage of **BLT-F**

As seen in **Figure 4-11**, before addition of GSH, the two signals for the fluorine atoms can clearly be seen. Within 1 hour of GSH addition, the signal from the fluorine on the linker at -114 ppm is completely gone, demonstrating rapid disulfide exchange. Interestingly, a new peak appears at -119 ppm that has been attributed to the stabilized thiolate or corresponding thiol before ring closure. After 8 hours, the thiolactonization has almost been completed, and the thiolactone can be observed as the new signal at -116 ppm. The stabilization of the thiolate/thiol and slow rate of drug release is likely an artifact of two effects: (1) stabilization of the thiolate due to the electron-withdrawing capacity of the *p*-fluorine group and (2) the presence of 30% DMSO may stabilize this intermediate and slow down the drug release process. It is clear from the initial data that there is baseline separation between all signals from the linker and that thiolactonization of the conjugate can be observed using ^{19}F NMR.

Due to the low aqueous solubility of taxoids and small-molecule taxoid conjugates, a 1:1 mixture of Solutol H-15 and ethanol is used to solubilize the active agents. The effect of this formulation on the cleavage rate of the disulfide bond in the BLT conjugate has not been investigated. This information will be useful when designing formulations for this compound as it progresses through preclinical evaluation. We therefore used the BLT-F probe to ascertain what, if any, effect the surfactant has on the stability of the linker to disulfide exchange.

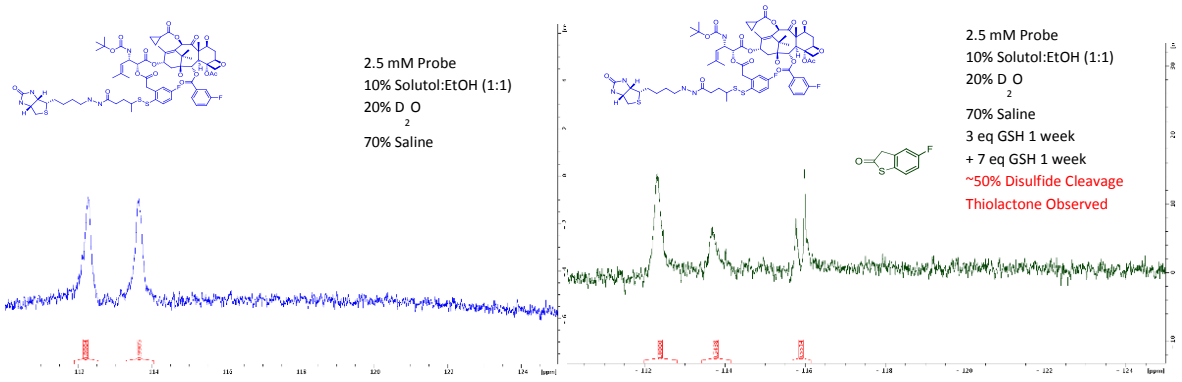

Figure 4-12: Stability of **BLT-F** in injectable formulation with 10 eq GSH

Figure 4-12 shows the NMR spectra in a standard "injectable formulation" of BLT-F, composed of a 50 mg/mL stock solution diluted 10 fold in saline. D_2O was included for the lock signal. Originally, 3 eq of GSH was added. No change was noticed after 8 hours and only ~20% cleavage was apparent after one week (data not shown). After the addition of an additional 7 eq of GSH and another week of standing, ~50% disulfide cleavage was observed and two signals can be seen corresponding at -116, corresponding to the chemical shift for the thiolactone. At the moment, the cause for the extra signal can only be speculated, and this experiment will be repeated. Although not quantitative, these data confirm the hypothesis that the surfactant in the injectable formulation can play a substantial role in the stabilization of the linker to disulfide exchange.

§ 4.2.4 Proposed Design for 2nd Generation BLT-F Probe

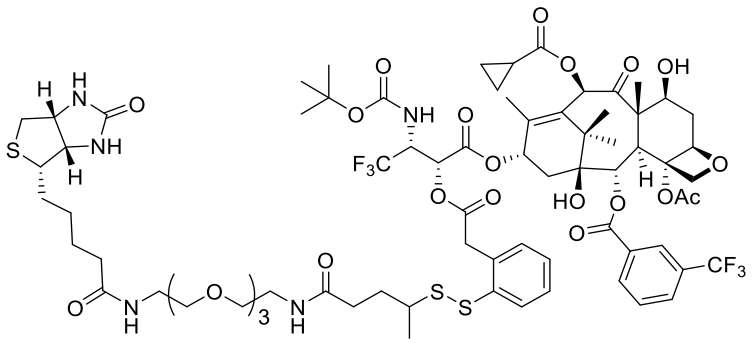

Figure 4-13: Design of the '2nd Generation **BLT-CF₃** Probe'

Although effective as a 'proof of concept' and useful for simple experiments, the first generation BLT-F was greatly hindered by two main drawbacks: (1) aqueous solubility and (2) low signal intensity. For more advanced studies in live cell culture, the conjugate in **Figure 4-14** has been designed for improved solubility and heightened sensitivity. This conjugate should be synthesized for future, more in depth NMR studies.

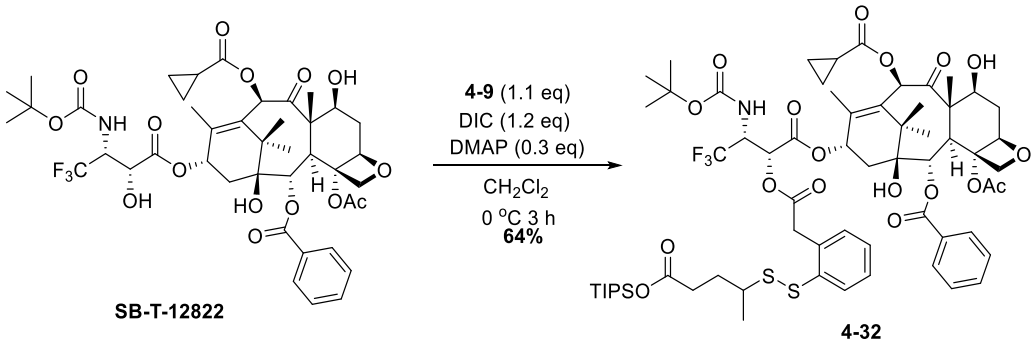

Scheme 4-12: Synthesis of model CF_3 conjugate **4-32** for NMR feasibility study

The success of the BLT-CF_3 probe is contingent on a difference in chemical shift between the CF_3 group on C3' before and after linker cleavage. Ideally, the two peaks should be baseline resolved so that they might be integrated for quantitative assessment of linker stability. To assess the feasibility of this approach, **SB-T-12822**, synthesized by Dr. Chi Feng Lin, was coupled to the mono-protected linker intermediate **4-9** (**Scheme 4-12**). Prototype compound **4-32** was mixed in a 1:1 ratio with SB-T-12822. On a 400 MHz machine, there is baseline resolution of the two peaks. Therefore it is likely that the C3' trifluoromethyl groups can be used as quantitative indicators of linker cleavage *via* ^{19}F NMR, offering significant improvements in sensitivity compared to the first-generation **BLT-F**.

§ 4.3.0 Improving the Pharmacokinetic Properties of the Biotin-Taxoid Conjugate

The original design of the BLT was sufficient for the early *in vitro* proof of concept studies but it was not designed with solubility and pharmacokinetics in consideration. During the course of the preliminary *in vivo* study and the NMR stability studies, the limited aqueous solubility of original conjugate became quite apparent and a considerable limitation. Hydrophobicity may be a problem for efficacy of the conjugate *in vivo*, because hydrophobic molecules readily bind to blood plasma proteins and this binding could interfere with the tumor-targeting potential mediated by the vitamin. In addition, the current biotin conjugate can only be solubilized in aqueous solution with a substantial amount of surfactant. The surfactant may also interfere with the recognition of the tumor-targeting moiety by the target receptor. Therefore, increasing the hydrophilicity of the compound is important to balancing the clearance rates and tumor-targeting properties of the conjugate in a way that will maximize its therapeutic efficacy.

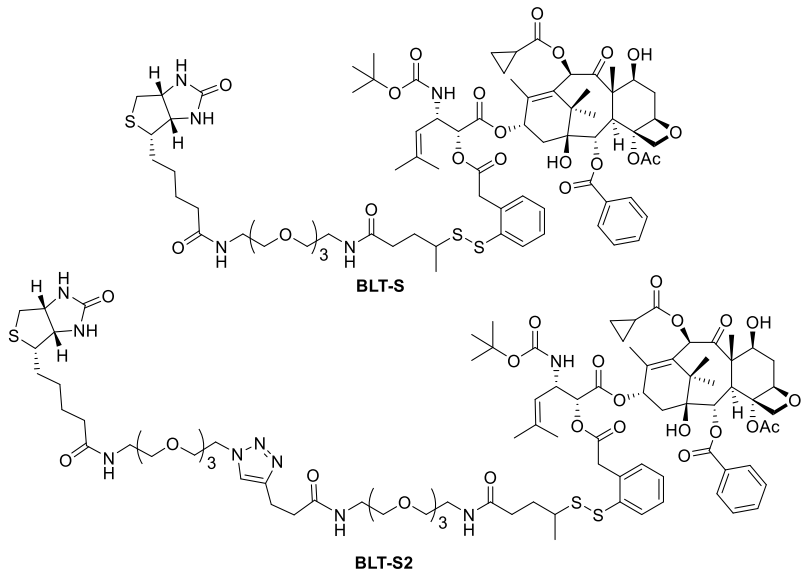

Figure 4-14: Structures of PEGylated conjugates **BLT-S** and **BLT-S2**

A strategy to increase the solubility of these conjugates is to build into the structure solubilizing moieties that do not interfere with the potency of the released drug. Polyethylene glycol (PEG) units of discrete length were introduced to the linker portion of the conjugate to assess its effect on aqueous solubility in injectable solutions. The structures of the two conjugates are shown in **Figure 4-16**. These PEG units effectively act as intramolecular surfactants, covering the most hydrophobic portions of the molecule, aiding in solubility and preventing the aggregation that leads to precipitation from the solution.

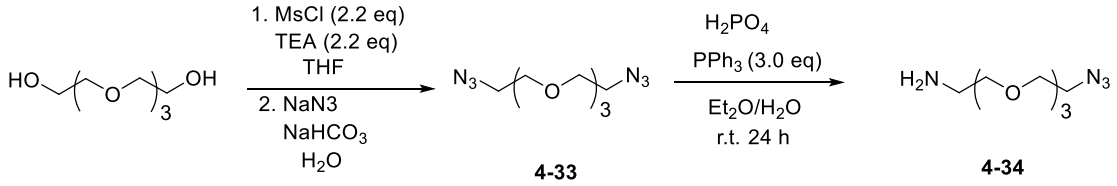

Scheme 4-13: Synthesis of amino-PEG$_3$-azide **4-34**[29]

Amino-PEG-azide 4-34 was syntheisized according to the literature procedure.[29] Dimesylation of tetraethylene glycol was followed by displacement with sodium azide to afford diazide **4-33**. Subsequent 2-phase selective mono-reduction was performed to produce **4-34** on the multi-gram scale.

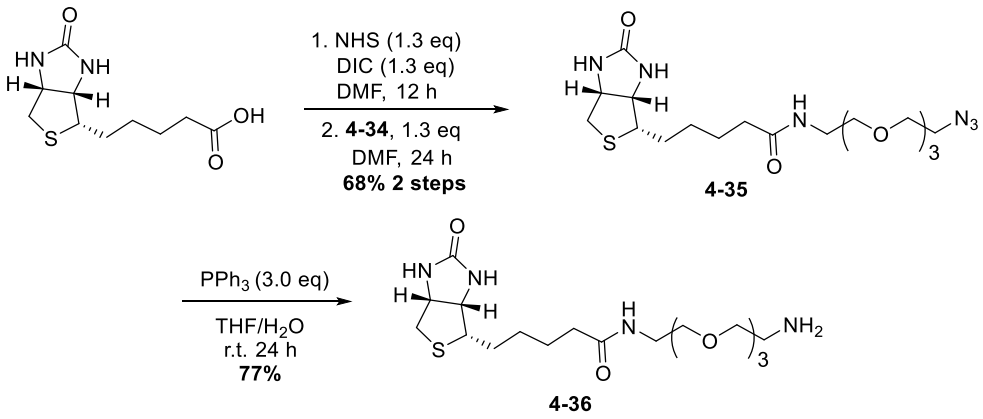

Scheme 4-14: Synthesis of biotin-PEG-azide **(4-35)** and amine **(4-36)**[30]

Biotin was activated by DIC coupling of NHS in DMF, and the activated ester was reacted *in situ* with amino-PEG-azide to afford **4-35**, which was purified by column chromatography. Staudinger reduction afforded the free amine **4-36** in good yield.

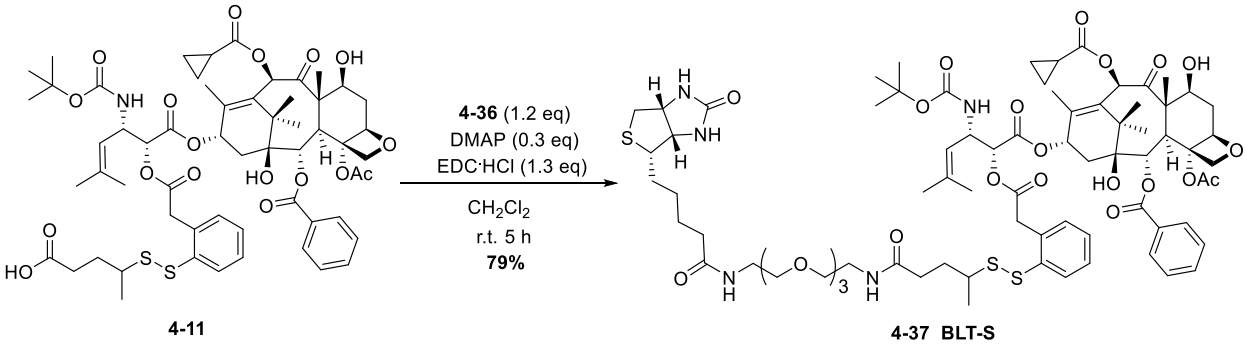

Scheme 4-15: Synthesis of **BLT-S** for *in vivo* evaluation

Biotin-PEG-amine **4-36** was directly coupled to free acid **4-11** with EDC and DMAP, as shown in **Scheme 4-15**. PEGylated **BLT-S** was used for a comparative *in vivo* study to effect of drug:surfactant ratio on tumor targeting.

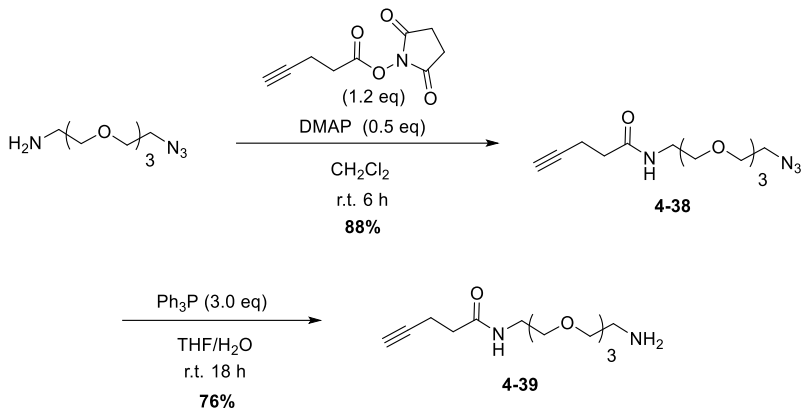

Scheme 4-16: Synthesis of amino-PEG-alkyne **4-39**

Direct EDC coupling of amino-PEG_3-azide to 4-pentynoic acid resulted in reproducibly low yields of ~30% following purification. Therefore, the activated ester of 4-pentynoic acid was used, and good yields could be obtained in a consistent and reproducible manner. Staudinger reduction of the azide afforeded the desired compound **4-39** in good overall yield.

Amino-PEG-alkyne **4-39** was conjugated to free acid **4-11** to afford 1214-linker-PEG-alkyne **4-40**. This will be used in a click reaction with **4-38** to afford the PEG6 biotin conjugate **BLT-S2** (**Scheme 4-17**), used in a comparative solubility study.

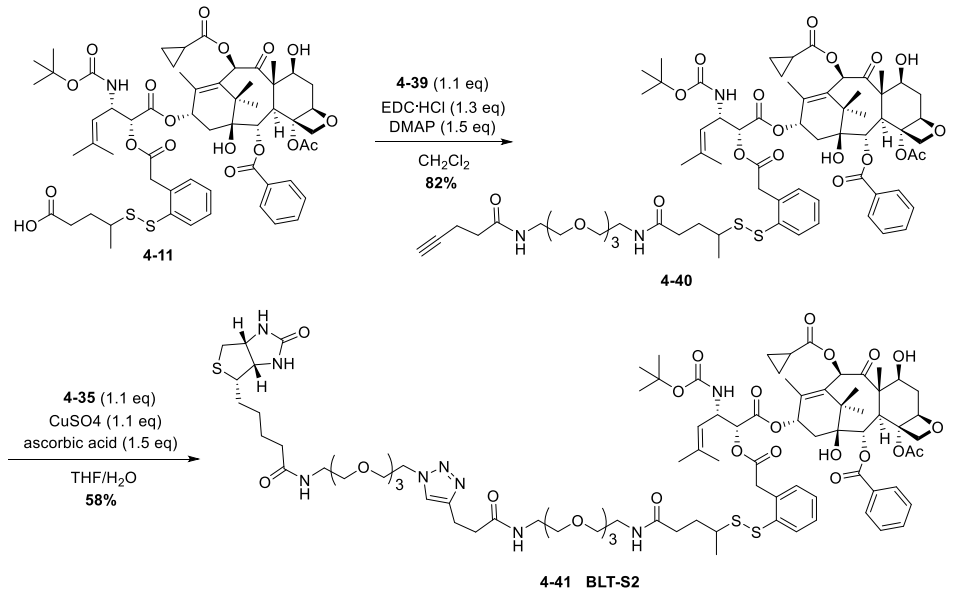

Scheme 4-17: Synthesis of **BLT-S2** for systematic solubility comparison

Compound	MW	MW/SB-T-1214	Max. Stock Conc.
SB-T-1214	853	1.00	7.5 mg/mL
BLT	1376	1.61	15 mg/mL
BLT-S	1537	1.80	30 mg/mL
BLT-S2	1834	2.15	50 mg/mL

Table 4-1: Comparative solubility of Biotin-1214 conjugates in injectable formulation

Table 4-1 shows the maximum drug concentration in the surfactant that can be diluted with saline without precipitation. The stock solutions were made using 1:1 Ethanol:Solutol H15 and diluted with saline to the requisite concentration for injectable dosing. A clear correlation can be seen between the incorporation of PEG units into the linker and the loading capacity of the formulation. This trend will be confirmed with the synthesis and solubility evaluation of **BLT-S2**. These data show that introduction of intramolecular surfactants into the linker region of the biotin conjugate is an effective and simple way to increase the ratio of drug to surfactant in the injectable formulation. The effect of this ratio on conjugate efficacy *in vivo* is currently under investigation.

§ 4.4.0 Conclusions and Perspective

Increased expression levels of biotin receptors have been observed on the cell surface of certain cancer cell lines, and this expression has been correlated with an increased uptake of biotin conjugates *via* RME. A first generation biotin-linker-taxoid conjugate was synthesized and tested against MX-1 xenografts in SCID mice, demonstrating what may be the first example of biotin-mediated tumor targeting *in vivo*. However, this conjugate possesses poor aqueous solubility and this may have a deleterious effect on its tumor-targeting capacity. Therefore, PEGylation between the biotin and linker moieties was shown to improve the aqueous solubility of the conjugate and increase the drug to surfactant ratio in the injectable formulation. In addition to PEGylation, the introduction of charged residues into the spacer region between the linker and biotin may further increase the tumor-selective uptake of the conjugate and further improve its pharmacokinetic profile. This strategy will be explored in the next chapter.

Fluorine NMR has been shown to be an effective method for investigating dynamic processes in complex biological media. To evaluate variables that may affect the rate of linker cleavage, a ^{19}F-labeled BLT conjugate was synthesized. Unfortunately, this conjugate did not possess high enough aqueous solubility to be investigated in cell culture experiments. Furthermore, its utility was limited by the high concentrations needed for the machine to detect the single fluorine nuclei. In spite of these limitations, a strong protecting effect by the surfactant was discovered when the injectable formulation was exposed to GSH. A second-generation probe has been designed with specific improvements to solubility and sensitivity. The CF_3 group at C3' was shown to have a significant change in chemical shift upon esterification by the linker at C2, and therefore can be used as a signal to indicate linker cleavage with increased sensitivity. As

PEGylation can improve the overall aqueous solubility of the conjugate, the incorporation of discreet PEG units into the linker region will help to keep the conjugate in solution at concentrations required for detection by NMR.

§ 4.5.0 Experimental Section

§ 4.5.1 General Methods

^{1}H and ^{13}C NMR spectra were measured on a Bruker or Varian model 300, 400, 500 MHz NMR spectrometer. Melting points were measured on a Thomas Hoover Capillary melting point apparatus and are uncorrected. Mass to charge values were measured by flow injection analysis on an Agilent Technologies LC/MSD VL. TLC was performed on Merck DC-alufolien with Kieselgel 60F-254 and column chromatography was carried out on silica gel 60 (Merck; 230-400 mesh ASTM). Compound purity was verified by reverse phase HPLC on a Shimadzu LC-2010A machine with a 2.6 angstrom Phenomenex polyfluorophenyl (PFP) column. The mobile phase was methanol-water. The analyses were performed at a flow rate of 1ml/min with the UV detector set at 254 and 227 nm. The gradient was run from 40% to 95% methanol in water over a 40 minute period.

§ 4.5.2 Materials

The chemicals were purchased from Aldrich Co. and Sigma and purified before use by standard methods. Tetrahydrofuran was freshly distilled from sodium metal and benzophenone. Dichloromethane was also distilled immediately prior to use under nitrogen from calcium hydride. In addition, various dry solvents were degassed and dried using PureSolv™ solvent purification system (Innovative Technologies, Newburyport, MA).

§ 4.5.3 Experimental Procedures

1,2-Di(pyridine-2-yl)disulfane [4-1][31]

Pyridine-2(*1H*)-thione (12.5 g, 112 mmol) was dissolved in CH_2Cl_2 (110 mL). To the mixture $KMnO_4$ (52 g, 336 mmol) was added slowly over a period of fifteen minutes. The solution was stirred vigorously and the reaction progress was monitored by TLC. Upon completion, the solution will be filtered over celite and concentrated *in vacuo* to afford **4-I (**11.2 g, 92% yield) as colorless needle crystals: mp 55–56 ^{o}C (lit.[31] 56-57 ^{o}C). ^{1}H NMR ($CDCl_3$) δ 8.45 (m, 2H), 7.60 (m, 4H), 7.10 (m, 2H). All data were found to be in agreement with literature values.[31]

3*H*-Benzo[b]thiophen-2-one [4-2][32]

Thianaphthene-2-boronic acid (3.64 g, 20 mmol) of was dissolved in EtOH (40 mL). To the solution was added 30% hydrogen peroxide (7.2 mL, 40 mmol) dropwise. The mixture was stirred

at room temperature, open to the atmosphere and monitored by TLC. Upon completion, the mixture was diluted with water (50 mL) and extracted with CH_2Cl_2 (4 x 40 mL). The organic layer was combined, washed with brine (2 x 30 mL), dried over $MgSO_4$, and concentrated *in vacuo*. Purification was done *via* column chromatography on silica gel with increasing amounts of ethyl acetate in hexanes (hexanes:ethyl acetate) to afford **4-2 (**2.34 g, 76% yield) as a pale yellow solid: mp 44-46 ºC (lit.[54] 43-44 ºC). ^{1}H NMR δ 7.40 - 7.28 (m, 4H), 4.04 (s, 2H). All data were found to be in agreement with literature values.[32]

2-Sulfhydrylphenyl acetic acid [4-3][13]

An aliquot of **4-2** (2.00 g, 12 mmol) was dissolved in THF (65 mL) and warmed to 60 °C under inert conditions. To the mixture was added LiOH monohydrate (3.3, 78 mmol) was dissolved in H_2O (65 mL) dropwise. The mixture was stirred at 60 °C and the reaction progress was monitored by TLC. Upon completion, the reaction was allowed to cool to room temperature. The mixture was acidified to pH 2 using 1 M HCl and extracted with ethyl acetate (3 x 75 mL). The organic layers were combined, washed with brine (2 x 50 mL) dried over $MgSO_4$, and concentrated *in vacuo*. Purification was done by column chromatography on silica gel (hexanes:ethyl acetate = 3:1) to yield **4-3 (**1.952 g, 85% yield) of as a pale yellow solid: ^{1}H NMR ($CDCl_3$) δ 3.49 (s, 1H), 3.82 (s, 2H), 7.16 – 7.26 (m, 3H), 7.40 (m, 1H). All data were found to be in agreement with literature values.[13]

4-Sulfhydrylpentanoic acid [4-4][33]

γ-Valerolactone (1.0g, 10.0 mmol) was dissolved in HBr (7.5 mL, 62 mmol) was heated to 70°C. At 70°C, thiourea (4.0 g, 50 mmol) was added slowly and the mixture was allowed to reflux overnight. The reaction was allowed to cool slowly and diluted with ice-water (25 mL). The aqueous solution was washed with ether (15 mL) and then CH_2Cl_2 (15 mL). The pH was adjusted to pH 13 with 20 M NaOH. The aqueous layer was then collected, and stirred vigorously under reflux. Upon completion, the reaction mixture was allowed to cool to room temperature and diluted with H_2O (20 mL). The pH was adjusted to 2 with 1 N HCl. The aqueous layer was extracted with CH_2Cl_2 (3 x 25 mL). The combined organic layers was washed with H_2O (30 mL), brine (2 x 20 mL), dried over $MgSO_4$ and concentrated *in vacuo* to afford **4-4 (**1.04 g, 77% yield) as a colorless oil: ^{1}H NMR δ 11.2 (s, broad, 1H), 2.91 (m, 1H), 2.49 (m, 2H) 1.94 (m, 1H), 1.73 (m, 1H), 1.47 (d, J = 6.8 Hz, 1H), 1.32 (d, 6.8 Hz, 3H). All data were found to be in agreement with literature values.[33]

4-(Pyridin-2-yldisulfanyl)pentanoic acid [4-5][33]

An aliquot of **4-1 (**11.2 g, 50 mmol) was dissolved in EtOH (210 mL) under inert conditions, and heated to reflux. To this mixture was added **4-4** (1.0 g, 8 mmol) dissolved in EtOH (75mL) dropwise and the reaction progress was monitored by TLC. Upon completion, the mixture was

allowed to cool to room temperature, the solvent was evaporated and the residual mixture was purified by column chromatography on silica gel with increasing amounts of ethyl acetate in hexanes (hexanes:ethyl acetate = 1:0 – 2:1) to afford **4-5** (1.235 g, 69% yield) as a yellow oil: ^{1}H NMR δ 1.31 (d, J = 6.9 Hz, 3H), 1.92 (m, 1 H), 1.97 (m, 1H), 2.5 (t, J = 8.1 Hz, 2H), 3.0 (m, 1H), 7.08 (m, 1H), 7.22 (m, 1H), 7.63 (m, 1H), 8.44 (m, 1H), 9.6 (s, br, 1H). All data were found to be in agreement with literature values.[33]

Triisopropylsilyl 4-(pyridin-2-yldisulfanyl)pentanoate [4-6][24]

An aliquot of **4-5** (320 mg, 1.32 mmol) and TEA (0.28 mL, 2.0 mmol) were dissolved in CH_2Cl_2 (7 mL) and cooled to 0 °C under inert conditions. To the mixture was added TIPSCl (0.5 mL, 2.0 mmol) dropwise and was stirred at room temperature while the reaction progress was monitored by TLC. Upon completion, the reaction was quenched with NH_4Cl (1 mL), diluted with water (20 mL) and extracted with CH_2Cl_2 (30 mL). The organic layers were collected, washed with brine (3 x 25 mL) dried over $MgSO_4$ and concentrated *in vacuo*. Purification was done by column chromatography on silica gel with increasing amounts of ethyl acetate in hexanes (hexanes:ethyl acetate = 1:0 – 3:1) to afford **4-6** (520 mg, 99% yield) as a colorless oil: ^{1}H NMR δ 1.25 (m, 21H), 1.31 (d, J = 6.9 Hz, 3H), 1.81 (m, 1 H), 1.97 (m, 1H), 2.51 (t, J = 8.1 Hz, 2H), 3.04 (m, 1H), 7.08 (m, 1H), 7.63 (m, 1H), 7.2 (m, 1H), 8.45 (m, 1H). All data were found to be in agreement with literature values.[24]

2-(1-methyl-4-oxo-5-triisopropylsilyloxybutyldisulfanyl)-phenylacetic acid [4-8][24]

Compound **4-6** (525 mg, 1.32 mmol) was dissolved in THF (2.5 mL) and cooled to 0 °C under inert conditions. To this mixture was added **4-3** (220 mg, 1.32 mmol) dissolved in THF (1.5 mL), previously cooled to 0 °C. The mixture was stirred at 0 °C for 30 minutes and allowed to warm to room temperature. The reaction was monitored by TLC. Upon completion, the solvent was evaporated and the residual was purified by column chromatography on silica gel with increasing amounts of ethyl acetate in hexanes (hexanes:ethyl acetate = 1:0 – 3:1) to afford **4-8** (212 mg, 35% yield) as a colorless oil: ^{1}H NMR ($CDCl_3$) δ 1.03 (m, 21H), 1.80 (m, 1H), 1.96 (m, 1H), 2.02 (s, 3H), 2.41 (m, 2H), 2.90 (m, 1H), 3.99 (s, 2H), 7.20 (m, 2H), 7.59 (m, 1H), 7.81 (d, J = 7.8, 1H); 11.88, 17.71, 17.79, 20.30, 31.03, 33.13, 38.95, 45.85, 127.53, 128.34, 130.16, 130.84, 133.16, 137.78, 173.49, 176.11. All data were found to be in agreement with literature values.[24]

SB-T-1214-Linker-CO_2TIPS [4-9][24]

SB-T-1214 (260 mg, 0.30 mmol) and DMAP (8 mg, 0.06 mmol) was dissolved in CH_2Cl_2 (6 mL), and cooled to -10 °C under inert conditions. To this mixture was added DIC (0.043 mL, 0.28 mmol) dropwise, followed by the dropwise addition of **4-8** (115 mg, 0.30 mmol) dissolved in CH_2Cl_2 (4 mL). The solution was stirred at -10 °C and the reaction was monitored by TLC. Upon completion, the organic layer was evaporated and the residual was purified by column

chromatography on silica gel with increasing amounts of ethyl acetate in hexanes (hexanes:ethyl acetate = 1:0 – 3:1) to afford **4-9** (271 mg, 83% yield) as a white solid: ^{1}H NMR ($CDCl_3$) δ 0.94 (m, 2H), 1.06 (m, 21H), 1.13 (s, 3H), 1.16 (s, 3H), 1.21 (m, 2H), 1.33 (s, 9H), 1.66 (s, 3H), 1.69 (s, 3H), 1.72 (s, 3H), 1.74-1.86 (m, 2H), 1.90 (s, 3H), 2.04 (s, 3H), 2.35 (s, 3H), 2.42 (m, 2H), 2.53 (m, 1H), 2.60 (m, 1H), 2.90 (m, 1H), 3.45 (m, 1H), 3.83 (m, 2H), 3.96 (m, 2H), 4.10 (m, 2H), 4.18 (d, J = 8.4 Hz, 1H), 4.30 (d, J = 8.4, 1H), 4.42 (m, 1H), 4.79 (d J = 8.8, 1H), 4.93 (m, 3H), 5.07 (d, J = 8.4 Hz, 1H), 5.67 (d, J = 7.2 Hz, 1H), 6.19 (t, J = 9.2 Hz, 1H), 6.28 (s, 1H), 7.22 (m, 2H), 7.28 (m, 1H), 7.47 (t, J = 7.6 Hz, 2H), 7.59 (t, J = 7.6 Hz, 1H), 7.80 (d, J = 8.0 Hz, 1H), 8.11 (d, J = 7.6 Hz, 2H); 9.18, 9.39, 9.57, 11.88, 13.03, 14.85, 17.81, 18.51, 20.53, 20.58, 22.27, 22.43, 25.72, 26.70, 28.23, 30.95, 32.97, 33.01, 35.43, 35.52, 38.81, 43.18, 45.60, 46.00, 48.99, 58.36, 71.83, 72.17, 74.98, 75.25, 75.47, 76.39, 79.27, 79.81, 80.94, 84.51, 120.00, 127.70, 128.33, 128.64, 129.29, 130.10, 130.18, 130.87, 132.42, 133.13, 133.61, 137.39, 137.65, 143.53, 154.94, 166.98, 168.09, 169.63, 170.15, 173.03, 175.12, 204.13; MS (ESI) calcd for $C_{70}H_{100}NO_{18}S_2S$ $(M+H)^+$: 1333.62, found 1334.7. All data were found to be in agreement with literature values.[24]

SB-T-1214-Linker-CO_2H [4-10][24]

Compound **4-9** (260 mg, 0.20 mmol) was dissolved in a 1:1 mixture of acetonitrile:pyridine (10 mL total) and cooled to 0 °C under inert conditions. To the mixture excess HF, 70% in pyridine (2.6 mL), was added dropwise. The reaction was stirred at room temperature and monitored by TLC. Upon completion the reaction was quenched with 10% aqueous citric acid (5 mL), neutralized with saturated $NaHCO_3$ (20 mL) and extracted with ethyl acetate (2 x 40 mL). The organic layer was collected, washed with saturated $CuSO_4$ solution (2 x 50 mL), water (50 mL) and brine (3 x 50mL). The extract was then dried over anhydrous $MgSO_4$, suction filtered and the filtrate concentrated *in vacuo*. Purification was done by column chromatography on silica gel with increasing amounts of ethyl acetate in hexanes (hexanes:ethyl acetate = 1:0 – 1:1) to afford **4-10 (**215 mg, 94% yield) as a white solid: ^{1}H NMR ($CDCl_3$) δ 0.94 (m, 1H), 0.95 (m, 1H), 1.15 (s, 6H), 1.37 (s, 9H), 1.60 (m, 1H), 1.62 (s, 3H), 1.72 (s, 3H), 1.77 (m, 1H), 1.87 (m, 1H), 1.91 (s, 3H), 2.04 (s, 3H), 2.34 (m, 1H), 2.39 (s, 3H), 2.43 (m, 1H), 2.53 (m, 1H), 3.10 (m, 1H), 3.79 (m, 1H), 3.93 (m, 1H), 4.06 (m, 1H), 4.11 (m, 1H), 4.18 (d, J = 8.4, 1H), 4.31 (d, J = 8.4, 1H), 4.41 (m, 1H), 4.86 – 5.08 (m, 3H), 5.15 (m, 1H), 5.68 (d, J = 6.6, 1H), 6.21 (m, 1H), 6.29 (s, 1H), 7.23 (m, 2H), 7.31 (m, 1H), 7.48 (t, J = 7.2 Hz, 2H), 7.61 (t, J = 7.2 Hz, 1H), 7.80 (m, 1H), 8.10 (d, J = 7.2 Hz, 2H); 9.23, 9.43, 9.58, 13.05, 14.84, 18.52, 20.21, 20.37, 22.15, 22.19, 22.42, 25.80, 26.70, 30.54, 30.65, 35.48, 38.75, 43.17, 45.74, 45.77, 48.98, 58.45, 71.62, 72.10, 72.14, 74.92, 75.17, 75.49, 75.53, 76.57, 79.27, 79.92, 81.14, 84.46, 119.92, 127.70, 127.80, 128.36, 128.43, 128.67, 129.23, 130.16, 131.04, 132.46, 133.11, 133.21, 133.69, 137.86, 143.41, 155.04, 167.02, 168.31, 170.29, 170.61, 175.19, 175.22, 176.33, 204.02; MS (ESI) calcd for $C_{58}H_{72}NO_{18}S_2$ $(M-H)^-$: 1134.42, found 1134.3. All data were found to be in agreement with literature values.[24]

SB-T-1214-Linker-OSu [4-11]

Compound **4-10** (200 mg, 0.18 mmol) and N-hydroxysuccinimde (61 mg, 0.53 mmol) was dissolved in a 1:1 mixture of THF and pyridine (4 mL total) and cooled to 0^{o}C under inert conditions. To the mixture was added DIC (0.33 mL, 0.21 mmol) dropwise under inert conditions. The reaction chamber was allowed to warm to room temperature, and the progress of the reaction was monitored by TLC. Upon completion, the solvent was evaporated, and purification was done by column chromatography on silica gel with increasing amounts of ethyl acetate in hexanes (hexanes:ethyl acetate) to afford **4-11 (**201 mg, 87% yield) as a white solid: ^{1}H NMR ($CDCl_3$) δ 0.89(s, 3H), 0.99 (m, 2H), 1.13 (m, 1H), 1.17 (m, 1H), 1.27 (s, 6H), 1.28 (m, 1H), 1.35 (s, 9H), 1.67 (s, 3H), 1.73 (s, 3H), 1.76 (s, 3H), 1.78 (m, 1H), 1.87 (m, 1H), 1.92 (s, 3H), 1.98 (m, 1H), 2.06 (s, 1H), 2.07 (m, 1H), 2.19 (s, 1H), 2.36 (s, 3H), 2.41 (m, 1H), 2.55 (m, 1H), 2.65 (m, 1H), 2.85 (s, 4H), 3.02 (m, 1H), 3.81 (d, J = 6.5 Hz, 1H), 4.00 (dd, J = 2.0, 16.5 Hz, 1H), 4.13 (m, 1H), 4.20 (d, J = 8.0 Hz, 1H), 4.31 (d, J = 8.0 Hz, 1H), 4.43 (dd, J = 7.0, 15.0 Hz, 1H), 4.99 (d, J = 9.5, 1H), 5.12 (d, J = 8.5 Hz, 1H), 5.69 (d, J = 7.5 Hz, 1H), 6.21 (t, J = 10 Hz, 1H), 6.30 (s, 1H), 7.24-7.35 (m, 3H), 7.47 (t. J = 8.0 Hz, 2H), 7.60 (t, J = 7.5 Hz, 1H), 7.81 (d, J = 7.5 Hz, 1H), 8.13 (d, J = 7.5 Hz, 2H). ^{13}C NMR ($CDCl_3$) δ 9.11, 9.29, 9.54, 13.01, 14.76, 18.48, 20.33, 22.39, 25.29, 25.57, 25.71, 26.67, 28.17, 28.26, 29.69, 30.27, 35.47, 35.63, 38.75, 43.16, 45.60, 45.64, 58.42, 71.80, 72.08, 74.97, 75.28, 75.97, 76.41, 79.01, 80.98, 84.54, 119.74, 128.02, 128.45, 128.53, 129.44, 130.20, 120.62, 130.96, 132.54, 133.43, 137.17, 143.28, 166.79, 168.04, 168.14, 169.10, 169.60, 170.13, 171.43, 175.04, 204.09. MS (ESI) calcd for $C_{62}H_{79}N_2O_{20}S_2$ $(M+H)^+$: 1233.45, found 1234.1.

Biotin methyl ester [4-12][13]

Biotin (300 mg, 1.20 mmol) was suspended in methanol (3 mL) and cooled to 0 ºC. Thionyl chloride (0.3 mL) was added dropwise and allowed to stir at room temperature overnight. The solution was concentrated in vacuo, and the residue was triturated with hexanes and suction filtered to afford biotin methyl ester (253 mg, 80% yield) as a white solid: ^{1}H NMR (CD_3OD) δ 1.45 (q, J = 7.2 Hz, 2H), 1.53-1.70 (m, 4H), 2.70 (d, 12.6 Hz, 1H), 2.34 (t, J = 7.2 Hz, 2H), 2.92 (dd, J = 4.8, 12.6, 1H), 3.20 (m, 1H), 3.65 (s, 3H), 4.30 (m, 1H), 4.48, (m, 1H). All data were found to be in agreement with literature values.[13]

Biotin hydrazide [4-13][13]

Biotin methyl ester (150 mg, 0.58 mmol) was suspended in methanol (2 mL) and hydrazine (0.2 mL) was added dropwise. The mixture was refluxed for 8 hours and upon completion, was cooled to room temperature. Methanol was removed *in vacuo*, and hexanes were added to the crude. Trituration with hexanes and ether afforded (135 mg 90% yield) as a white solid: ^{1}H NMR (CD_3OD)δ 1.30 (q, J = 7.2 Hz, 2H), 1.38-1.70 (m, 4H), 2.11 (t, J = 7.2 Hz, 2H), 2.67 (d, 12.6 Hz,

1H), 2.87 (dd, J = 4.5, 12.6 Hz, 1H), 3.22 (m, 1H), 4.32 (m, 1H), 4.49 (m, 1H). All data were found to be in agreement with literature values.[13]

Biotin-Linker-Taxoid [BLT]

Biotin hydrazide (66 mg, 0.25 mmol) and **4-11** (210 mg, 0.17 mmol were dissolved in DMSO (1 mL) under N_2. The solution was cooled to 0 ºC and pyridine (0.15 mL) was added dropwise. The reaction was allowed to stir at room temperature for 72 hours, and upon completion, the reaction mixture was purified directly by column chromatography (CH_2Cl_2:MeOH 1:0 – 13:1) to afford **BLT** (169 mg, 72%) as a white solid: m.p. = 160-162 ºC; ^{1}H NMR (500 MHz, CD_3OD) δ 0.89(s, 3H), 0.99 (m, 2H), 1.13 (m, 1H), 1.17 (m, 1H), 1.27 (s, 6H), 1.28 (m, 1H), 1.35 (s, 9H), 1.35 (q, J = 7.2 Hz, 2H), 1.38-1.70 (m, 4H), 1.67 (s, 3H), 1.73 (s, 3H), 1.76 (s, 3H), 1.78 (m, 1H), 1.87 (m, 1H), 1.92 (s, 3H), 1.98 (m, 1H), 2.06 (s, 1H), 2.07 (m, 1H), 2.11 (t, J = 7.2 Hz, 2H), 2.19 (s, 1H), 2.36 (s, 3H), 2.41 (m, 1H), 2.55 (m, 1H), 2.65 (m, 1H), 2.67 (d, 12.6 Hz, 1H), 2.87 (dd, J = 4.5, 12.6 Hz, 1H), 3.02 (m, 1H), 3.22 (m, 1H), 3.81 (d, J = 6.5 Hz, 1H), 4.00 (dd, J = 2.0, 16.5 Hz, 1H), 4.13 (m, 1H), 4.20 (d, J = 8.0 Hz, 1H), 4.35 (m, 2H), 4.43 (dd, J = 7.0, 15.0 Hz, 1H), 4.49 (m, 1H), 4.99 (d, J = 9.5, 1H), 5.12 (d, J = 8.5 Hz, 1H), 5.69 (d, J = 7.5 Hz, 1H), 6.21 (t, J = 10 Hz, 1H), 6.30 (s, 1H), 7.24-7.35 (m, 3H), 7.47 (t. J = 8.0 Hz, 2H), 7.60 (t, J = 7.5 Hz, 1H), 7.81 (d, J = 7.5 Hz, 1H), 8.13 (d, J = 7.5 Hz, 2H); ^{13}C NMR (125 MHz, CD_3OD) δ 7.80, 9.04, 12.40, 13.63, 19.45, 19.56, 20.99, 21.88, 24.77, 24.98, 25.59, 27.40, 27.96, 28.13, 30.51, 30.60, 30.90, 32.97, 35.35, 36.14, 38.11, 39.02, 39.66, 43.20, 45.78, 45.89, 48.24, 49.31, 55.53, 57.87, 60.26, 61.84, 70.92, 71.58, 74.92, 75.17, 75.33, 76.06, 77.70, 79.10, 80.93, 84.48, 119.84, 127.50, 128.05, 128.29, 129.75, 130.02, 130.11, 133.17, 133.37, 133.54, 137.26, 137.41, 137.46, 141.25, 156.09, 164.75, 166.20, 168.90, 170.08, 170.88, 172.67, 173.46, 173.71, 203.75. HRMS (ESI) calcd for $C_{68}H_{90}N_5O_{19}S_3$ $(M+H)^+$: 1376.5392 Found: 1376.5343, (Δ -3.6 ppm, -4.9 mDa).

7,10,13-Tris(triethylsilyl)-2-debenzoyl-2-(3-fluorobenzoyl)-10-deacetylbaccatin III [4-14][16]

According to the procedure previously listed for **2-3**, (Section 2.3) compound **2-2** (400 mg, 0.64 mmol) was used to produce **4-14** (414 mg, 89% yield) as a white solid: ^{1}H NMR (300 MHz, $CDCl_3$) δ 0.53-0.71 (m, 18H), 0.94-1.04 (m, 27H), 1.13 (s, 3H), 1.19 (s, 3H), 1.65 (s, 3H), 1.81-1.93 (m, 1H), 1.981 (s, 3H), 2.02-2.23 (m, 2H), 2.9 (s, 3H), 2.43-2.60 (m, 1H), 3.85 (d, J = 7.5 Hz, 1H), 4.13 (d, J = 8.4 Hz, 1H), 4.27 (d, J = 8.4 Hz, 1H), 4.41 (dd, J = 6.3, 11.1 Hz, 1H), 4.89-4.96 (m, 2H), 5.19 (s, 1H), 5.58 (d, J = 7.2 Hz, 1H), 7.31 (dd, J = 3.0, 8.4, 1H), 7.45 (dt, J = 3.0, 7.8 Hz, 1H), 7.77 (d, J = 8.4 Hz, 1H), 7.88 (d, J = 7.8 Hz, 1H). All data were found to be in agreement with literature values.[16]

2-Debenzoyl-2-(3-fluorobenzoyl)-10-deacetylbaccatin III [4-15][16]

According to the procedure previously listed for **2-4 A**, (Section 2.3) compound **4-14** (400 mg, 0.45 mmol) was used to produce **4-15** (211 mg, 85% yield) as a white solid: ^{1}H NMR (300 MHz,

CD_3OD) δ 1.14 (br s, 6H), 1.75 (s, 3H), 1.81-1.96 (m, 1H), 2.11 (s, 3H), 2.30-2.42 (m, 2H), 2.33 (s, 3H), 2.46-2.58 (m, 1H), 4.05 (d, J = 6.9 Hz, 1H), 4.22-4.31 (m, 3H), 4.34 (dd, J = 6.6, 11.1 Hz, 1H), 4.83-4.91 (m, 2H), 5.09 (d, J = 8.7 Hz, 1H), 5.38 (s, 1H), 5.66 (d, J = 7.2 Hz, 1H), 7.46 (t, J = 8.1 Hz, 1H), 7.62 (m, 1H), 7.87 (d, J = 9.6 Hz, 1H), 8.01 (d, J = 7.8 Hz, 1H). All data were found to be in agreement with literature values.[16]

2-Debenzoyl-2-(3-fluorobenzoyl)- 7-triethylsilyl-10-deacetylbaccatin III [4-16][16]

According to the procedure previously listed for **2-7** , (Section 2.3) compound **4-15** (205 mg, 0.53 mmol) was used to produce **4-16** (203 mg, 82% yield) as a white solid: ^{1}H NMR (300 MHz, $CDCl_3$) δ 0.51-0.62 (m, 6H), 0.89-0.98 (m, 9H), 1.08 (s, 6H), 1.50 (s, 1H), 1.57 (s, 3H), 1.73 (s, 3H), 1.84-1.96 (m, 1H), 2.08 (s, 3H), 2.23-2.30 (m, 2H), 2.29 (s, 3H), 2.42-2.56 (m, 1H), 3.95 (d, J = 6.9 Hz, 1H), 4.14 (d, J = 8.4 Hz, 1H), 4.26 (d, J = 2.1 Hz, 1H), 4.31 (d, J = 8.4 Hz, 1H), 4.40 (dd, J = 6.9, 10.2 Hz, 1H), 4.86 (m, 1H), 4.96 (d, J = 7.8 Hz, 1H), 5.17 (d, J = 2.1 Hz, 1H), 5.57 (d, J = 7.2 Hz, 1H), 7.31 (t, J = 9.0 Hz, 1H), 7.46 (m, 1H), 7.78 (d, J = 9.6 Hz, 1H), 7.89 (d, J = 7.5 Hz, 1H). All data were found to be in agreement with literature values.[16]

2-Debenzoyl-2-(3-fluorobenzoyl)-7-Triethylsilyl-10-(cyclopropylcarbonyl)-10-deacetylbaccatin III [4-17][16]

According to the procedure previously listed for **2-6 F**, (Section 2.3) compound **4-16** (200 mg, 0.29 mmol) was used to produce **4-17** (191 mg, 88%) as a white solid: ^{1}H NMR (300 MHz, $CDCl_3$) δ 0.48-0.64 (m, 6H), 0.82-0.96 (m, 13H), 1.05 (s, 3H), 1.19 (s, 3H), 1.56 (s, 3H), 1.68 (s, 3H), 1.80-1.94 (m, 1H), 2.19 (s, 3H), 2.23-2.30 (m, 2H), 2.42-2.60 (m, 1H), 3.88 (d, J = 6.9 Hz, 1H), 4.13 (d, J = 8.4 Hz, 1H), 4.29 (d, J = 8.4 Hz, 1H), 4.47 (dd, J = 6.9, 10.2 Hz, 1H), 4.83 (m, 1H), 4.97 (d, J = 8.7 Hz, 1H), 5.60 (d, J = 6.9 Hz, 1H), 6.46 (s, 1H), 7.31 (m, 1H), 7.46 (m, 1H), 7.79 (d, J = 9.0 Hz, 1H), 7.90 (d, J = 8.1 Hz, 1H). All data were found to be in agreement with literature values.[16]

2-Debenzoyl-2-(3-fluorobenzoyl)-2'-Triisopropylsilane-3'-dephenyl)-3'-(2-methyl-2-propenyl)-7-triethylsilyl-10-(cyclopropylcarbonyl)docetaxel [4-18][16]

According to the procedure previously listed for **2-8 A**, (Section 2.3) compound **2-6 F** (185 mg, 0.25 mmol) was used to produce **4-18** (236 mg, 83% yield) as a white solid: ^{1}H NMR (300 MHz, $CDCl_3$) δ 0.46-0.64 (m, 6H), 0.82-0.98 (m, 13 H), 1.04-1.14 (m, 21H), 1.19 (s, 3H), 1.27 (s, 3H), 1.34 (s, 9H), 1.68 (s, 3H), 1.75 (s, 3H), 1.78 (s, 3H), 1.82-1.96 (m, 1H), 2.01 (s, 3H), 2.20-2.32 (m, 2H), 2.36 (s, 3H), 2.42-2.58 (m, 1H), 3.85 (d, J = 7.2 Hz, 1H), 4.17 (d, J = 8.4 Hz, 1H), 4.30 (d, J = 8.4 Hz, 1H), 4.40-4.52 (m, 2H), 4.70-4.86 (m, 2H), 4.95 (d, J = 8.1 Hz, 1H), 5.33 (d, J = 8.7 Hz, 1H), 5.65 (d, J = 7.5 Hz, 1H), 6.06 (t, 1H), 6.48 (s, 1H), 7.31 (m, 1H), 7.45 (m, 1H), 7.79 (d, J = 10.2 Hz, 1H), 7.90 (d, J = 7.8 Hz, 1H). All data were found to be in agreement with literature values.[16]

2-Debenzoyl-2-(3-fluorobenzoyl)-3'-dephenyl)-3'-(2-methyl-2-propenyl)-10-(cyclopropylcarbonyl)docetaxel [SB-T-121405][16]

According to the procedure previously listed for **SB-T-1213**, (Section 2.3) compound **4-18** (230 mg, 0.20 mmol) was used to produce **SB-T-121405** (159 mg, 91% yield) as a white solid: ^{1}H NMR (300 MHz, $CDCl_3$) δ 1.02-1.20 (m, 4H), 1.22 (s, 3H), 1.33 (s, 3H), 1.42 (s, 9H), 1.60-1.72 (m, 1H), 1.74 (s, 3H), 1.83 (s, 3H), 1.833 (s, 3H), 1.97 (s, 3H), 2.11 (s, 1H), 2.28-2.50 (m, 2H), 2.42 (s, 3H), 2.54-2.72 (m, 1H), 3.88 (d, J = 7.2 Hz), 1H), 4.21 (d, J = 8.4 Hz, 1H), 4.27 (d, J = 8.4 Hz, 1H), 4.48 (dd, J = 6.6, 10.5 Hz, 1H), 4.74-4.88 (m, 2H), 5.04 (d, J = 8.1 Hz, 1H), 5.39 (d, J = 6.0 Hz, 1H), 5.70 (d, J = 7.2 Hz, 1H), 6.23 (t, J = 9.0 Hz, 1H), 6.37 (s, 1H), 7.381 (t, J = 8.4 Hz, 1H), 7.53 (m, 1H), 7.86 (d, J = 9.0 Hz, 1H), 7.97 (d, J = 7.8 Hz); ^{13}C NMR (100 MHz, $CDCl_3$) δ 9.25, 9.51, 13.05, 15.03, 18.54, 21.97, 22.35, 25.73, 26.66, 28.22, 35.49, 35.55, 43.15, 45.65, 51.60, 58.52, 72.23, 72.39, 73.71, 75.42, 75.52, 76.31, 79.25, 81.04, 84.49, 116.85, 117.05, 120.54, 120.72, 120.89, 126.01, 130.34, 130.40, 131.42 (d, J = 7.5 Hz), 132.78, 142.80, 155.46, 161.56, 163.51, 165.70, 170.03, 175.17, 202.87. All data were found to be in agreement with literature values.[16]

1-(2-Dimethoxyethylthio)-4-fluorobenzene [4-19][12]

A solution of of sodium ethoxide in ethanol was prepared by the addition of sodium (1.25 g, 54 mmol) to anhydrous ethanol (25 mL) at -10 ^{o}C. The mixture was stirred, and slowly warmed to 60 ^{o}C until all sodium had dissolved. To this was added 4-Fluorothiophenol (5.0 g, 39 mmol) dropwise and the mixture was heated to reflux. At reflux, chloroacetaldehyde was added dropwise and the solution was allowed to reflux for 16 hours. Upon completion, the ethanol was removed *in vacuo*, and the residue was dissolved in ether and water (100 mL each). The organic phase was separated, washed with water (2 x 100 mL), dried over MgSO4, suction filtered and the filtrate was condensed *in vacuo* to produce **4-19** (8.7 g, 92% yield) as a yellow oil: ^{1}H NMR ($CDCl_3$) δ 3.05 (d, J = 5.7 Hz, 2H), 3.34 (s, 6H), 4.49 (t, J = 5.7 Hz, 1H), 6.99 (t, J = 8.7 Hz, 2H), 7.40 (m, 2H). All data were found to be in agreement with literature values.[12]

5-Fluorobenzo[*b*]thiophene [4-20][12]

Anhydrous chlorobenzene (80 mL) was added to polyphosphoric acid (9.2 g), and the mixture was heated to reflux and stirred vigorously. To the reaction, **4-19** (2.5 g, 11 mmol) was added dropwise and reflux was maintained for 24 hours. After cooling to room temperature, water (200 mL) was added, stirred vigorously for an hour and , extracted with CH_2Cl_2 (2 x 300 mL). The organic was separated and washed with brine (3 x 200 mL), dried over $MgSO_4$, suction filtered and the filtrate condensed *in vauco*, resulting in crude dark red oil. Purification by column chromatography on silica gel afforded **4-20** (2.52 g, 52% yield) as a clear oil: ^{1}H NMR ($CDCl_3$) δ 7.11 (dt, J = 2.4, 8.7 Hz, 1H), 7.29 (d, J = 5.4 Hz, 1H), 7.48 (dd, J = 2.4 Hz, 9.3 Hz, 1H), 7.53 (d, J = 5.7 Hz, 1H), 7.80 (dd, J = 5.4, 8.7 Hz, 1H). All data were found to be in agreement with literature values.[12]

5-Fluoro-3H-benzo[*b*]thiophene-2-boronic acid [4-21] [12]

To a solution of **4-20** (350 mg, 2.3 mmol) in ether (5 mL) was added *n*-BuLi (1.4 mL, 1.6 M in hexanes) dropwise at -40 ºC. The mixture was allowed to stir at this temperature for 45 min, after which time tributyl borate (635 mg, 2.76 mmol) in ether (1 mL) was added. The reaction was warmed to 0 ºC for 1 hour and quenched with 2 N HCl (10 mL), diluted with water (20 mL), and extracted with ether (3 x 30 mL). The organic layer was extracted with 2 M NaOH (3 x 30 mL), acidified to pH of 1 with concentrated HCl, extracted again with ether (3 x 25 mL), and the organic was dried over $MgSO_4$. Suction filtration and evaporation of the filtrate in vacuo afforded **4-21** (343 mg, 84% yield) as an off white solid, which was used directly for the next step.[12]

5-Fluoro-3*H*-benzo[*b*]thiophen-2-one [4-22][34, 35]

Cyclooxyborate **4-21** (330 g, 0.62 mmol) of was dissolved in EtOH (4 mL). To the solution was added 30% hydrogen peroxide (1.3 mL, 10 mmol) dropwise. The mixture was stirred at room temperature, open to the atmosphere and monitored by TLC. Upon completion, the mixture was diluted with water (10 mL) and extracted with CH_2Cl_2 (2 x 20 mL). The organic layer was combined, washed with brine (2 x 30 mL), dried over $MgSO_4$, and concentrated *in vacuo*. Purification was done *via* column chromatography on silica gel with increasing amounts of ethyl acetate in hexanes (hexanes:ethyl acetate) to afford **4-22 (**172 mg, 55% yield) as a pale yellow solid: ^{1}H NMR ($CDCl_3$) δ 3.98 (s, 2H), 7.01-7.07 (m, 1H), 7.05 (d, J = 8.7 Hz, 1H), 7.29 (dd, J = 4.8, 9.6 Hz, 1H). All data were found to be in agreement with literature values.[34]

2-Sulfhydryl-5-fluoro-phenyl acetic acid [4-23][12]

An aliquot of **4-23** (165 mg, 0.98 mmol) was dissolved in THF (2 mL) and warmed to 60 °C under inert conditions. To the mixture was added LiOH monohydrate (300 mg, 7.8 mmol) was dissolved in H_2O (2 mL) dropwise. The mixture was stirred at 60 °C and the reaction progress was monitored by TLC. Upon completion, the reaction was allowed to cool to room temperature. The mixture was acidified to pH 2 using 1 M HCl and extracted with ethyl acetate (3 x 15 mL). The organic layers were combined, washed with brine (2 x 15 mL) dried over $MgSO_4$, and concentrated *in vacuo*. Purification was done by column chromatography on silica gel (hexanes:ethyl acetate = 3:1) to yield **4-24 (**171 mg, 94% yield) as an off-white solid: ^{1}H NMR ($CDCl_3$) δ 3.40 (br s, 1H), 3.84 (s, 2H), 6.92 (dt, J = 2.7, 8.4 Hz, 1H), 7.01 (dd, J = 2.7, 9.0 Hz, 1H), 7.43 (dd, J = 5.4, 8.4 Hz, 1H). All data were found to be in agreement with literature values.[12]

2-(1-methyl-4-oxo-5-triisopropylsilyloxybutyldisulfanyl)-5-fluoro-phenylacetic acid [4-24]

Compound **4-24** (165 mg, 0.89 mmol) was dissolved in THF (2.0 mL) and cooled to 0 °C under inert conditions. To this mixture was added **4-5** (354 mg, 0.89 mmol) dissolved in THF (2.0 mL), previously cooled to 0 °C. The mixture was stirred at 0 °C for 30 minutes and allowed to warm to

room temperature. The reaction was monitored by TLC. Upon completion, the solvent was evaporated and the residual was purified by column chromatography on silica gel with increasing amounts of ethyl acetate in hexanes (hexanes:ethyl acetate = 1:0 – 3:1) to afford **4-24** (142 mg, 34% yield) as a colorless oil: ^{1}H NMR ($CDCl_3$) δ 1.00-1.10 (m, 18H), 1.20-1.32 (m, 3H), 1.26 (d, J = 6.9 Hz, 3H), 1.81 (m, J = 8.1 Hz, 1H), 1.94 (m, J=8.1 Hz, 1H), 2.39 (dt, J = 2.7, 7.8 Hz, 2H), 2.89 (m, J = 6.9 Hz, 1H), 3.89 (s, 2H), 6.94 -7.02 (m, 1H), 6.97 (d, J = 8.4 Hz, 1H), 7.74 (dd, J = 6.0, 8.4 Hz, 1H). MS (ESI) calcd for $C_{21}H_{32}FO_4S_2Si$ $(M-H)^-$: 459.16, found: 459.2.

SB-T-121405-F-Linker-CO_2TIPS [4-25]

SB-T-121405 (140 mg, 0.16 mmol) and DMAP (4 mg, 0.03 mmol) was dissolved in CH_2Cl_2 (4 mL), and cooled to -10 °C under inert conditions. To this mixture was added DIC (0.024 mL, 0.13 mmol) dropwise, followed by the dropwise addition of **4-24** (61 mg, 0.13 mmol) dissolved in CH_2Cl_2 (4 mL). The solution was stirred at -10 °C and the reaction was monitored by TLC. Upon completion, the organic layer was evaporated and the residual was purified by column chromatography on silica gel with increasing amounts of ethyl acetate in hexanes (hexanes:ethyl acetate = 1:0 – 3:1) to afford **4-25** (132 mg, 77% yield) as a white solid: ^{1}H NMR ($CDCl_3$) δ 1.02-1.20 (m, 22H), 1.20-1.32 (m, 3H), 1.23 (s, 3H), 1.24-1.28 (m, 3H), 1.33 (s, 3H), 1.42 (s, 9H), 1.60-1.72 (m, 1H), 1.74 (s, 3H), 1.81 (m, 1H), 1.83 (s, 3H), 1.84 (s, 3H), 1.92 (m, 1H), 1.97 (s, 3H), 2.11 (s, 1H), 2.24-2.52 (m, 4H), 2.42 (s, 3H), 2.54-2.72 (m, 1H), 2.87 (m, 1H), 3.88 (d, J = 7.2 Hz, 1H), 3.93 (s, 2H), 4.21 (d, J = 8.4 Hz, 1H), 4.27 (d, J = 8.4 Hz, 1H), 4.48 (dd, J = 6.6, 10.5 Hz, 1H), 4.74-4.88 (m, 2H), 5.04 (d, J = 8.1 Hz, 1H), 5.39 (d, J = 6.0 Hz, 1H), 5.70 (d, J = 7.2 Hz, 1H), 6.23 (t, J = 9.0 Hz, 1H), 6.37 (s, 1H), 6.94 -7.02 (m, 2H), 7.381 (t, J = 8.4 Hz, 1H), 7.53 (m, 1H), 7.75 (dd, J = 6.0, 8.4 Hz, 1H), 7.86 (d, J = 9.0 Hz, 1H), 7.97 (d, J = 7.8 Hz). ^{19}F NMR (CDCl3) δ -112.87 (s, 1F), -111.93 (s, 1F). MS (ESI) calcd for $C_{67}H_{92}F_2NO_{18}S_2Si$ $(M+H)^+$: 1328.54, found: 1328.5.

SB-T-121405-F-Linker-CO_2H [4-26]

Compound **4-25** (132 mg, 0.10 mmol) was dissolved in a 1:1 mixture of acetonitrile:pyridine (8 mL total) and cooled to 0 °C under inert conditions. To the mixture excess HF, 70% in pyridine (1.3 mL), was added dropwise. The reaction was stirred at room temperature and monitored by TLC. Upon completion the reaction was quenched with 10% aqueous citric acid (5 mL), neutralized with saturated $NaHCO_3$ (20 mL) and extracted with ethyl acetate (2 x 40 mL). The organic layer was collected, washed with saturated $CuSO_4$ solution (2 x 50 mL), water (50 mL) and brine (3 x 50mL). The extract was then dried over anhydrous $MgSO_4$, suction filtered and the filtrate concentrated *in vacuo*. Purification was done by column chromatography on silica gel with increasing amounts of ethyl acetate in hexanes (hexanes:ethyl acetate = 1:0 – 1:1) to afford **4-26 (**113 mg, 97% yield) as a white solid: ^{1}H NMR ($CDCl_3$) δ 1.03-1.24 (m, 4H), 1.23 (s, 3H), 1.24-1.28 (m, 3H), 1.33 (s, 3H), 1.42 (s, 9H), 1.60-1.72 (m, 1H), 1.74 (s, 3H), 1.81 (m, 1H), 1.83 (s, 3H), 1.84 (s, 3H), 1.92 (m, 1H), 1.97 (s, 3H), 2.11 (s, 1H), 2.24-2.52 (m, 4H), 2.42 (s, 3H),

2.54-2.72 (m, 1H), 2.87 (m, 1H), 3.88 (d, J = 7.2 Hz, 1H), 3.93 (s, 2H), 4.21 (d, J = 8.4 Hz, 1H), 4.27 (d, J = 8.4 Hz, 1H), 4.48 (dd, J = 6.6, 10.5 Hz, 1H), 4.74-4.88 (m, 2H), 5.05 (d, J = 8.1 Hz, 1H), 5.39 (d, J = 6.0 Hz, 1H), 5.70 (d, J = 7.2 Hz, 1H), 6.23 (t, J = 9.0 Hz, 1H), 6.37 (s, 1H), 6.94 -7.02 (m, 2H), 7.381 (t, J = 8.4 Hz, 1H), 7.53 (m, 1H), 7.75 (dd, J = 6.0, 8.4 Hz, 1H), 7.86 (d, J = 9.0 Hz, 1H), 7.97 (d, J = 7.8 Hz). ^{19}F NMR ($CDCl_3$) δ -113.41 (d, 1F), -111.86 (s, 1F). MS (ESI) calcd for $C_{58}H_{71}F_2NO_{18}S_2$ $(M+H)^+$: 1172.41, found 1172.4.

SB-T-121405-F-Linker-OSu [4-27]

Compound **4-26** (113 mg, 0.097 mmol) and *N*-hydroxysuccinimde (33 mg, 0.53 mmol) was dissolved in a 1:1 mixture of THF and pyridine (3 mL total) and cooled to 0ºC under inert conditions. To the mixture was added DIC (0.016 mL, 0.104 mmol) dropwise under inert conditions. The reaction chamber was allowed to warm to room temperature, and the progress of the reaction was monitored by TLC. Upon completion, the solvent was evaporated, and purification was done by column chromatography on silica gel with increasing amounts of ethyl acetate in hexanes (hexanes:ethyl acetate) to afford **4-27 (**91 mg, 79% yield) as a white solid: ^{1}H NMR ($CDCl_3$) δ All data were found to be in agreement with literature values. 1.03-1.24 (m, 4H), 1.23 (s, 3H), 1.24-1.28 (m, 3H), 1.33 (s, 3H), 1.42 (s, 9H), 1.60-1.72 (m, 1H), 1.74 (s, 3H), 1.81 (m, 1H), 1.83 (s, 3H), 1.84 (s, 3H), 1.92 (m, 1H), 1.97 (s, 3H), 2.11 (s, 1H), 2.24-2.52 (m, 4H), 2.42 (s, 3H), 2.54-2.72 (m, 1H), 2.83 (br s, 4H), 2.87 (m, 1H), 3.88 (d, J = 7.2 Hz, 1H), 3.93 (s, 2H), 4.21 (d, J = 8.4 Hz, 1H), 4.27 (d, J = 8.4 Hz, 1H), 4.48 (dd, J = 6.6, 10.5 Hz, 1H), 4.74-4.88 (m, 2H), 5.05 (d, J = 8.1 Hz, 1H), 5.39 (d, J = 6.0 Hz, 1H), 5.70 (d, J = 7.2 Hz, 1H), 6.23 (t, J = 9.0 Hz, 1H), 6.37 (s, 1H), 6.94 -7.02 (m, 2H), 7.381 (t, J = 8.4 Hz, 1H), 7.53 (m, 1H), 7.75 (dd, J = 6.0, 8.4 Hz, 1H), 7.86 (d, J = 9.0 Hz, 1H), 7.97 (d, J = 7.8 Hz). ^{19}F NMR ($CDCl_3$) δ -112.87 (s, 1F), -111.93 (s, 1F). MS (ESI) calcd for $C_{62}H_{75}F_2N_2O_{20}S_2$ $(M+H)^+$: 1269.42, found 1269.4.

Biotin-*p*-fluoro-Linker-SB-T-121405 [BLT-F]

Biotin hydrazide (28 mg, 0.11 mmol) and **4-27** (87 mg, 0.069 mmol) were dissolved in DMSO (0.5 mL) under N_2. The solution was cooled to 0 ºC and pyridine (0.15 mL) was added dropwise. The reaction was allowed to stir at room temperature for 72 hours, and upon completion, the reaction mixture was purified directly by column chromatography (CH_2Cl_2:MeOH 1:0 – 13:1) to afford **BLT-F** (62 mg, 77%) as a white solid: ^{1}H NMR ($CDCl_3$) δ 1.03-1.24 (m, 4H), 1.23 (s, 3H), 1.24-1.32 (m, 5H), 1.38-1.70 (m, 4H), 1.33 (s, 3H), 1.42 (s, 9H), 1.60-1.72 (m, 1H), 1.74 (s, 3H), 1.81 (m, 1H), 1.83 (s, 3H), 1.84 (s, 3H), 1.92 (m, 1H), 1.97 (s, 3H), 2.11 (m, 3H), 2.24-2.52 (m, 4H), 2.42 (s, 3H), 2.54-2.72 (m, 2H), 2.83 (br s, 4H), 2.87 (m, 2H), 3.22 (m, 1H), 3.88 (d, J = 7.2 Hz, 1H), 3.93 (s, 2H), 4.21 (d, J = 8.4 Hz, 1H), 4.27 (d, J = 8.4 Hz, 1H), 4.48 (dd, J = 6.6, 10.5 Hz, 1H), 4.74-4.32 (m, 1H), 4.49 (m, 1H), 4.88 (m, 2H), 5.05 (d, J = 8.1 Hz, 1H), 5.39 (d, J = 6.0 Hz, 1H), 5.70 (d, J = 7.2 Hz, 1H), 6.23 (t, J = 9.0 Hz, 1H), 6.37 (s, 1H), 6.94 -7.02 (m, 2H), 7.381 (t, J = 8.4 Hz, 1H), 7.53 (m, 1H), 7.75 (dd, J = 6.0, 8.4 Hz, 1H), 7.86 (d, J = 9.0 Hz, 1H), 7.97 (d, J = 7.8 Hz). ^{13}C NMR (CD_3OD) δ 7.78, 8.99, 12.38, 13.59, 17.22, 19.41, 19.49, 20.93, 21.81, 24.88,

24.96, 25.55, 27.36, 27.94, 28.11, 29.35, 30.45, 30.53, 30.90, 32.96, 35.35, 36.11, 38.15, 39.03, 39.64, 43.16, 45.72, 45.81, 46.67, 49.30, 55.51, 57. 86, 60.26, 61.84, 70.15, 70.91, 71.59, 75.32, 75.44, 75.94, 77.69, 79.11 80.96, 84.45, 114.87, 115.09, 116.11, 116.34, 117.68, 117.91, 119.78, 119.93, 120.15, 125.68, 130.29, 130.37, 132.32, 132.39, 132.97, 133.36, 133.45, 136.67, 137.30, 141.25, 156.09, 161.16, 161.37, 163.60, 163.81, 164.74, 164.88, 168.82, 169.98. ^{19}F NMR (CDCl3) δ -112.95, -111.88. HRMS (ESI) calcd for $C_{68}H_{88}F_2N_5O_{19}S_3$ $(M+H)^+$: 1412.5204, Found: 1412.5159 (Δ -3.2 ppm, -4.5 mDa).

Biotin PEG azide [4-35][30]

Biotin (500 mg, 2.05 mmol), DMAP (75 mg, 0.6 mmol) and NHS (280 mg, 2.45 mmol) were dissolved in DMF (2 mL), and let stir at room temperature. To this solution was added DIC (0.27 mL, 2.67 mmol) dropwise, and the solution was stirred overnight. The next day, a solution of **4-34** (585 mg, 2.67 mmol) in DMF (1 mL) was added dropwise, and the solution stirred at room temperature overnight. The reaction mixture was diluted with H_2O (30 mL) and extracted with CH_2Cl_2 (3 x 25 mL). The combined organic layer was washed with brine (2 x 20 mL), dried over $MgSO_4$, filtered and the filtrate was concentrated *in vacuo*. Purification was done by column chromatography using silica gel with increasing amount of methanol in CH_2Cl_2 (CH_2Cl_2:MeOH 1:0 – 9:1) to afford **4-35** (623 mg, 68%) as an off-white solid: ^{1}H NMR (300 MHz, $CDCl_3$) δ 1.40-1.42 (m, 2H), 1.62-1.74 (m, 4H), 2.21 (t, J = 7.5 Hz, 2H), 2.71 (d, J = 13.0 Hz, 1H), 2.88 (m, 1H), 3.12 (q, J = 4.5 Hz, 1H), 3.36-3.42 (m, 4H), 3.54 (m, 2H), 3.60-3.66 (m, 10H), 4.29 (m, 1H), 4.48 (m, 1H), 5.81 (s, 1H), 6.69 (s, 1H), 6.78 (s, 1H). MS (ESI) calcd for $C_{18}H_{32}N_6O_5S$ $(M+H)^+$: 445.22, found 445.2.[30]

Biotin-PEG-Amine [4-36][30]

Triphenylphosphine (930 mg, 3.54 mmol) and **4-35** (500 mg, 1.18 mmol) were weighed into a round bottom flask and dissolved in a THF (14 mL) and water (4 mL). The reaction mixture was allowed to stir at room temperature overnight. The THF was then removed *in vacuo*, and the resulting residue dissolved in water (30 mL) and benzene (10 mL). The aqueous layer was separated and washed with benzene (5 x 15 mL), and the water layer was collected and evaporated *in vacuo* to afford the product (373 mg, 77%) as an off-white solid: ^{1}H NMR (300 MHz, $CDCl_3$) δ 1.40-1.46 (m, 2H), 1.61-1.76 (m, 4H), 2.22 (t, J = 7.5 Hz, 2H), 2.73 (d, J = 13.0 Hz, 1H), 2.88 (m, 3H), 3.13 (dd, J = 13.0, 5.0 Hz, 1H), 3.41 (m 2H), 3.55 (m, 4H), 3.62 (m, 8H), 4.31 (m, 1H), 4.49 (m, 1H), 5.65 (s, 1H), 6.60 (s, 1H), 7.32 (s, 1H). MS (ESI) calcd for $C_{18}H_{34}N_4O_5S$ $(M+H)^+$: 419.22, found 419.2.[30]

Biotin-PEG3-Linker-SB-T-1214 [BLT-S]

To a solution of **4-11** (300 mg, 0.26 mmol), **4-36** (135 mg, 0.32 mmol) and DMAP (14 mg, 0.11 mmol) in CH_2Cl_2 (7 mL) was added a suspension of EDC·HCl (81 mg, 0.32 mmol) in CH_2Cl_2 (3

mL) dropwise. The mixture was stirred at room temperature for 5 hours and monitored by TLC. Upon completion of the reaction, the reaction mixture was purified directly by column chromatography with silica using increasing amounts of methanol in CH_2Cl_2 (CH_2Cl_2:MeOH 1:0 – 15:1) to afford **BLT-S** (313 mg, 79%) as a white solid: m.p. = 118-122 ^oC; ^1H NMR (500 MHz, $CDCl_3$) δ 0.99-1.03 (m, 2H), 1.18)s, 3H), 1.13 (s, 3H), 1.27 (s, 3H), 1.31 (d, J = 7.0 Hz, 3H), 1.38 (s, 9H), 1.45 (m, 2H), 1.62-1.80 (m, 6H), 1.69 (s, 3H), 1.72 (s, 3H), 1.75 (s, 3H), 1.80-2.05 (m, 8H), 1.93 (s, 3H), 2.23 (m, 4H), 2.30-2.41 (m 2H), 2.39 (s, 3H), 2.55 (m, 1H), 2.74 (d, J = 13.0 Hz, 1H), 2.93 (m, 2H), 3.04 (m, 1H), 3.16 (m, 1H), 3.40-3.46 (m, 4H), 3.55-3.66 (m, 4H), 3.66 (m, 8H), 3.83 (d, J = 6.5 Hz), 4.01 (d, J = 15.5 Hz, 1H), 4.13 (d, J = 15.5, 1H), 4.32 (d, J = 8.5 Hz, 1H), 4.48 (m, 2H), 4.43 (m, 1H), 4.50 (m 1H), 4.92-5.02 (m, 3H), 5.05-5.15 (m, 2H), 5.28 (m, 1H), 5.70 (d, J = 7.0 Hz, 1H), 6.15 (m, 1H), 6.20 (t, J = 8.0 Hz, 1H), 6.34 (s, 1H), 6.50 (s, br, 1H), 6.68 (s, br, 1H), 7.25-730 (m 3H), 7.50 (t, J = 7.5 Hz, 2H), 7.63 (t, J = 7.5 Hz, 1H), 7.83 (m, 1H), 8.14 (d, J = 7.5 Hz, 2H). 9.17, 9.33, 9.64, 13.06, 14.81, 18.54, 20.67, 20.72, 22.14, 22.49, 25.54, 25.78, 26.65, 28.12, 31.32, 33.40, 33.51, 35.48, 35.68, 35.87, 38.78, 39.13, 40.53, 43.22, 45.82, 46.31, 49.06, 55.47, 58.40, 60.15, 61.79, 69.93, 70.03, 70.10, 70.38, 71.84, 71.98, 75.10, 75.16, 75.45, 76.41, 79.15, 79.79, 81.01, 84.51, 119.96, 127.80, 128.34, 128.65, 129.31, 130.18, 130.48, 131.01, 131.06, 132.58, 133.34, 133.63, 137.48, 137.60, 137.83, 143.07, 155.03, 163.66, 166.95, 168.28, 169.68, 170.44, 172.42, 173.25, 174.90, 204.06. HRMS (ESI) calcd for $C_{76}H_{106}N_5O_{22}S_3$ $(M+H)^+$: 1536.6492, found: 1536.6454 (Δ -2.5 ppm, -3.8 mDa).

Alkyne-PEG-Azide [4-38][36]

To a round bottom flask containing 4-pentynoic acid NHS ester (700 mg, 3.57 mmol), dissolved in CH_2Cl_2 (10 mL), was added a solution of amino-PEG3-azide (600 mg, 2.75 mmol) in CH_2Cl_2 (5 mL). The reaction mixture was stirred at room temperature overnight and monitored by TLC (10% MeOH in CH_2Cl_2.). Upon completion, the reaction mixture was purified directly by column chromatography (CH_2Cl_2:MeOH 1:0 – 50:1) to afford the desired product (647 mg, 79%) as a clear oil: ^1H NMR (300 MHz, $CDCl_3$) δ 2.01 (t, J = 2.7 Hz, 1H), 2.43 (t, J = 6.9 Hz, 2H), 2.50 (m, 2H), 3.40 (t, J = 5 .1 Hz, 2H), 3.46 (q, J = 6.3 Hz, 2H), 3.60 (m, 2H), 3.60-3.71 (m, 10H), 6.32 (s, br, 1H). MS (ESI) calcd for $C_{13}H_{23}N_4O_4$ $(M+H)^+$: 299.16, found: 299.2. All data were found to be in agreement with literature values[36]

Alkyne-PEG-Amine [4-39][36]

Alkyne-PEG-azide (630 mg, 2.28 mmol) and triphenylphosphine (1.78 g, 6.84 mmol) were weighed into a round bottom flask and dissolved in a THF (21 mL) and water (6 mL). The reaction mixture was allowed to stir at room temperature overnight. The THF was then removed in vacuo, and the resulting residue dissolved in water (30 mL) and benzene (10 mL). The aqueous layer was separated and washed with benzene (5 x 15 mL), and the water layer was collected and evaporated *in vacuo* to afford the product (430 mg, 68%) as a pale yellow oil: ^1H NMR (300 MHz, $CDCl_3$) δ 2.00 (t, 2.7 Hz, 1H), 2.31 (s, br, 2H), 2.39 (t, 7.8 Hz, 2H), 3.38 (t, J = 4.8 Hz, 2H), 2.44 (q, J = 5.4

Hz, 2H), 3.50-3.68 (m, 10H), 6.43 (s, br, 1H). MS (ESI) calcd for $C_{13}H_{25}N_2O_4$ $(M+H)^+$: 272.17, found: 273.2. All data were found to be in agreement with literature values.[36]

SB-T-1214-Linker-PEG-alkyne [4-40]

To a solution of **4-11** (400 mg, 0.35 mmol), **4-39** (120 mg, 0.46 mmol) and DMAP (20 mg, 0.16 mmol) in CH_2Cl_2 (8 mL) was added a suspension of EDC·HCl (90 mg, 0.46 mmol) in CH_2Cl_2 (3 mL) dropwise. The mixture was stirred at room temperature for 5 hours and monitored by TLC. Upon completion of the reaction, the reaction mixture was purified directly by column chromatography with silica using increasing amounts of methanol in CH_2Cl_2 (CH_2Cl_2:MeOH 1:0 – 15:1) to afford **4-40** as a white solid: ^{1}H NMR (300 MHz, $CDCl_3$) δ 0.84-1.02 (m, 2H), 1.08-1.14 (m, 2H), 1.23 (s, 3H), 1.28 (d, 3H), 1.34 (s, 9H), 1.66 (S, 3H), 1.70 (s, 3H), 1.72 (s, 3H), 1.81-1.94 (m, 2H), 1.92 (s, 3H), 2.02 (t, J = 3.0 Hz, 1H), 2.16-2.21 (m, 1H), 2.26-2.34 (m, 1H), 2.32 (s, 3H), 2.38-2.45 (m, 2H), 2.48-2.55 (m, 3H), 2.67 (m, 1H), 2.91 (m, 1H), 3.38-3.43 (m, 2H), 3.46 (m, 2H), 3.51 (dd, J = 8.0 5.2 Hz, 2H), 3.56 (t, J = 5.2 Hz, 2H), 3.60-3.66 (m, 8H), 3.79 (d, J = 6.8 Hz, 1H), 3.96 (d, J = 16.4 Hz, 1H), 4.10 (d, J = 16.4 Hz, 1H), 4.17 (d, J = 8.4 Hz, 1H), 4.30 (d, J = 8.4 Hz, 1H), 4.41 (m, 1H), 4.89-5.00 (m 4H), 5.10 (m, 1H), 5.67 (d, J = 7.2 Hz, 1H), 6.04 (s, br, 1H), 6.18 (t, J = 8.8 Hz, 1H), 6.29 (s, 1H), 6.30 (s, br, 1H), 7.21-7.35 (m, 3H), 7.47 (t, J = 7.6 Hz, 2H), 7.79 (d, J = 7.6 Hz, 1H), 8.11 (d, J = 7.6 Hz, 2H). 9.13, 9.33, 9.57, 13.01, 14.81, 14.88, 18.52, 20.70, 20.75, 22.19, 22.44, 25.74, 26.68, 28.24, 31.25, 33.44, 33.54, 35.26, 35.51, 38.78, 39.19, 39.28, 43.19, 45.68, 46.31, 46.41, 49.06, 58.46, 69.39, 69.90, 70.20, 70.47, 71.80, 72.09, 75.04, 75.19, 75.43, 79.26, 79.79, 80.98, 83.10, 84.49, 119.99, 127.85, 128.31, 128.64, 129.29, 130.17, 130.59, 130.99, 131.03, 132.51, 133.42, 133.61, 137.44, 137.57, 137.61, 137.81, 143.91, 154.95, 166.98, 168.14, 169.65, 170.34, 171.01, 172.13, 175.00, 204.07. HRMS (ESI) calcd for $C_{71}H_{96}N_3O_{21}S_2$ $(M+H)^+$: 1390.5978, found: 1390.5947 (Δ -2.2 ppm, -3.1 mDa).

Biotin-PEG6-Linker-SB-T-1214 [BLT-S2]

A solution of **4-40** (60 mg, 43 µmol) in CH_2Cl_2 (1 mL) was added to a solution of $CuSO_4$ (12 mg, 60 µmol) and ascorbic acid (8 mg, 60 µmol) in H_2O (1 mL) followed by the addition of 4-38 (18 mg, 60 µmol) in methanol (1 mL). The reaction mixture was stirred at room temperature for 3 hours and the reaction progress was monitored by TLC. Upon comp letion of the reaction, CH_2Cl_2 (10 mL) was added, the organic layer was washed with brine (3 x 5 mL) dried over $MgSO_4$, suction filtered and concentrated in vacuo. The crude product was purified by column chromatography using increasing amounts of methanol in CH_2Cl_2 (CH_2Cl_2:MeOH 1:0 – 1:7) to afford BLT-S2 (46 mg, 58%) as a white solid: m.p. = 86-90 ^{o}C; ^{1}H NMR (500MHz, $CDCl_3$) 0.96-1.04 (m 2H), 1.08-1.15 (m, 2H), 1.13 (s, 3H), 1.24-1.31 (m, 5H), 1.26 (s, 3H), 1.36 (s, 9H), 1.58-1.63 (m, 2H), 1.68 (s, 3H), 1.72 (s, 3H), 1.73 (s, 3H), 1.78 (m, 1H), 1.82-1.98 (m, 4H), 1.92 (s, 3H), 2.09-2.20 (m, 6H), 2.24 (m, 2H), 2.30-2.44 (m, 2H), 2.38 (s, 3H), 2.54 (m, 1H), 2.64 (t, J = 8.0 Hz, 2H), 2.73 (d, J = 15.5 Hz, 1H), 2.90 (dd, J = 6.0, 15.5 Hz, 1H), 3.04 (t, J = 9.5 Hz, 2H), 3.14 (m, 1H), 3.33-3.48 (m, 6H), 3.48-3.72 (m, 18 H), 3.81 (d, J = 8.5 Hz, 1H), 3.87 (t, J = 6.0 Hz, 2H), 4.19 (d, J = 10.5

Hz, 1H), 4.31 (d, J = 10.5 Hz, 1H), 4.32 (m, 1H), 4.43 (m, 1H), 4.48 (m, 2H), 4.92-5.04 (m, 3H), 5.05-5.22 (m, 2H), 5.68 (d, J = 8.5 Hz, 1H), 6.12 (s, br, 1H), 6.19 (t, J = 10.5 Hz, 1H), 6.33 (s, 1H), 6.69 (s, br, 1H), 6.82 (s, br, 1H), 7.01 (s, br, 1H), 7.23-7.36 (m, 3H), 7.48 (t, J = 9.5 Hz, 2H), 7.60 (m, 1H), 7.61 (s, 1H), 7.80 (d, J = 8.5 Hz, 1H), 8.12 (d, J = 9.5 Hz, 2H); ^{13}C NMR (125 MHz, $CDCl_3$) 9.16, 9.32, 9.64, 11.46, 13.06, 14.15, 14.81, 18.54, 20.59, 20.64, 20.72, 21.55, 22.16, 22.48, 22.68, 25.30, 25.490, 25.78, 26.65, 28.09, 28.18, 28.27, 29. 72, 31.34, 31.61, 33.37, 33.48, 34.68, 35.53, 35.71, 38.77, 39.16, 40.52, 43.22, 45.81, 46.28, 46.36, 49.07, 50.09, 53.47, 55.57, 58.41, 60.14, 61.86,69.48, 69.90, 70.08, 70.43, 70.50, 71.83, 72.00, 75.08, 75.18, 75.46, 76.42, 79.16, 79.78, 81.01, 84.52, 120.00, 122.75, 127.74, 128.36, 128.66, 129.34, 130.19, 130.34, 130.39. 131.02, 132.57, 133.26, 133.64, 137.50, 137.61, 137.78, 143.12, 146.51, 155.05, 163.64, 166.96, 168.28, 169.70, 170.42, 172.41, 172.49, 173.32, 174.90, 204.10; HRMS calcd for $C_{89}H_{128}N_9O_{26}S_3$ $(M+H)^+$: 1834.8133, found: 1834.8065 (Δ -3.7 ppm, -6.8 mDa).

§ 4.6.0 References

1. Low, P. S.; Henne, W. A.; Doorneweerd, D. D., Discovery and Development of Folic-Acid-Based Receptor Targeting for Imaging and Therapy of Cancer and Inflammatory Diseases. *Acc. Chem. Res.* **2008,** *41*, 120-129.
2. Ojima, I., Guided Molecular Missiles for Tumor-Targeting Chemotherapy-Case Studies Using the Second-Generation Taxoid as Warheads. *Acc. Chem. Res.* **2008,** *41*, 108-119.
3. Russell-Jones, G.; McTavish, K.; McEwan, J.; Rice, J.; Nowotnik, D., Vitamin-mediated targeting as a potential mechanism to increase drug uptake by tumours. *J. Inorg. Biochem.* **2004,** *98*, 1625-1633.
4. Leamon, C.; Reddy, J.; Betzel, M.; Dorton, R.; Westrick, E.; Parker, N.; Wang, Y.; Vlahov, I., Folate targeting enables durable and specific antitumor responses from a therapeutically null tubulysin B analogue. *Cancer Res.* **2008,** *68*, 9839-9844.
5. Xia, W.; Low, P., Folate-targeted therapies for cancer. *J. Med. Chem.* **2010,** *53*, 6811-6824.
6. Waldrop, G.; Holden, H.; Maurice, M. S., The enzymes of biotin dependent CO2 metabolism: what structures reveal about their mechanisms. *Protein Sci.* **2012,** *21*, 1597-1619.
7. McMahon, J., Biotin in metabolism and molecular biology. *Ann. Rev. Nutr.* **2002,** *22*, 221-239.
8. Zempleni, J., Uptake, Localization, and Noncarboxylate Roles of Biotin. *Ann. Rev. Nutr.* **2005,** *25*, 175-196.
9. Zempleni, J.; Wijeratne, S.; Hassan, Y., Biotin. *Biofactors* **2009,** *35*, 36-46.
10. Ojima, I.; Zuniga, E.; Berger, W.; Seitz, J., Tumor-targeting drug delivery of new-generation taxoids. *Future Med. Chem.* **2012,** *4*, 33-50.
11. Seetharam, B., Receptor-mediated endocytosis of cobalamin (vitamin B12). *Ann. Rev. Nutr.* **1999,** *19*, 173-195.
12. Lee, R.; Low, P., Delivery of liposomes into cultured KB cells via folate receptor-mediated endocytosis. *J. Biol. Chem.* **1994,** *269*, 3198-3204.

13. Chen, S.; Zhao, X.; Chen, J.; Chen, J.; Kuznetsova, L.; Wong, S.; Ojima, I., Mechanism-based tumor-targeting drug delivery system. Validation of efficient vitamin receptor-mediated endocytosis and drug release. *Bioconjugate Chem.* **2010,** *21*, 979-987.
14. Kigawa, J.; Minagawa, Y.; Kanamori, Y.; Itamochi, H.; Cheng, X.; Okada, M.; Oisho, T.; Terakawa, N., Glutathione concentration may be a useful predictor of response to second-line chemotherapy in patients with ovarian cancer. *Cancer* **1998,** *82*, 697-702.
15. Saito, G.; Swanson, J.; Lee, K.-D., Drug delivery strategy utilizing conjugation via reversible disulfide linkages: role and site of cellular reducing activities. *Adv. Drug Delivery Rev.* **2003,** *55*, 199-215.
16. Ojima, I. C., J.; Sun, L.; Borell, C. P.; Wang, T.; Miller, M. L.; Lin, S.; Geng, X.; Kuznetsova, L.; Qu, C.; Gallager, D.; Zhao, X.; Zanardi, I.; Xia, S.; Horwitz, S. B.; Mallen-St. Clair, J.; Guerriero, J. L.; Bar-Sagi, D.; Veith, J. M.; Pera, P.; Bernacki, R. J. , Design, Synthesis, and Biological Evaluation of New-Generation Taxoids. *J. Med. Chem.* **2008,** *51*, 3203-3221.
17. Erickson, H.; Park, P.; Widdison, W.; Kovtun, Y.; Garrett, L.; Hoffman, K.; Lutz, R.; Goldmacher, V.; Blattler, W., Antibody-Maytansinoid Conjugates Are Activated in Targeted Cancer Cells by Lysosomal Degredation and Linker-Dependent Intracellular Processing. *Cancer Res.* **2006,** *66*, 4426-4435.
18. Chari, R., Targeted delivery of chemotherapuetics: tumor-activated prodrug therapy. *Adv. Drug Delivery Rev.* **1998,** *31*, 89-104.
19. Vlahov, I. R.; Santhapuram, H. K. R.; Wang, Y.; Kleindl, P. J.; You, F.; Howard, S. J.; Westrick, E.; Reddy, J. A.; Leamon, C. P., An Assembly Concept for the Consecutive Introduction of Unsymmetrical Disulfide Bonds: Synthesis of a Resleasable Multidrug Conjugate of Folic Acid. *J. Org. Chem.* **2007,** *72*, 5968-5967.
20. Wu, X.; Ojima, I., Tumor specific novel taxoid-monoclonal antibody conjugates. *Curr. Med. Chem.* **2004,** *11*, 429-438.
21. Ojima, I., Use of Fluorine in the Medicinal Chemistry and Chemical Biology of Bioactive Compounds - A Case Study on Fluorinated Taxane Anticancer Agents. *ChemBioChem* **2004,** *5*, 628-635.
22. Das, M. Design, Synthesis and Biological Evaluation of Novel Tumor-targeting Taxane-based Drug Delivery Systems. Doctoral Dissertation. Stony Brook University. **2011**.
23. Bordwell, F.; Fried, H., Heterocyclic aromatic anions with 4n-2pi- electrons. *J. Org. Chem.* **1991,** *56*, 4218-4223.
24. Bannerjee, P. S.; Zuniga, E. S.; Ojima, I.; Carrico, I. S., Targeted and armed oncolytic adenovirus via chemoselective modification. *Bioorg. Med. Chem. Lett.* **2011,** *21*, 4985-4988.
25. Li, C.; Wang, G.-F.; Wang, Y.; Creager-Allen, R.; Lutz, E.; Scronce, H.; Slade, K.; Ruf, R.; Mehl, R.; Pielak, G., Protein 19F NMR in Escherichia coli. *J. Am. Chem. Soc.* **2010,** *132*, 321-327.
26. Wolf, W.; Presant, C.; Servis, K.; el-Tahtawy, A.; Albright, M.; Barker, P.; Ring, R.; Atkinson, D.; Ong, R.; King, M., Tumor trapping of 5-fluorouracil: in vivo 19F NMR spectroscopic pharmacokinetics in tumor-bearing humans and rabbits. *Proc. Natl. Acad. Sci.* **1990,** *87*, 492-496.
27. Martino, R.; Gilard, V.; Desmoulin, F.; Malet-Martino, M., Fluorin-19 or phophorus-31 NMR spectroscopy: A suitable analytical technique for quantitative in vitro metabolic studies of fluorinated or phosphorylated drugs. *J. Pharm. Biomed. Anal.* **2005,** *38*, 871-891.
28. Fevrier, B.; Dupas, G.; Bourguignon, J.; Queguiner, G., Synthesis of new 4-quinolone-type compounds in the benzo[b]thiophene series. *J. Heterocycl. Chem.* **1993,** *30*, 1085-1088.

29. Schwabacher, A.; Lane, J.; Sciesher, M.; Leigh, K.; Johnson, C., Desymmetrization Reactions: Efficient Preparation of Unsymmetrically Substituted Linker Molecules. *J. Org. Chem.* **1998,** *63*, 1727-1729.
30. Borcard, F.; Godinat, A.; Staedler, D.; Blanco, H.; Dumont, A.; Chapuis-Bernasconi, C.; Scaleta, C.; Applegate, L.; Juillerat, F.; Gonzenbach, U.; Gerber-Lemaire, S.; Juillerat-Jeanneret, L., Covalent cell surface functionalization of human fetal osteoblasts for tissue engineering. *Bioconjugate Chem.* **2011,** *22*, 1422-1432.
31. Shaabani, A.; Tavasoli-Rad, F.; Lee, D., Potassium Permanganate Oxidation of Organic Compounds. *Syn. Comm.* **2005,** *35*, 571-580.
32. Kamila, S.; Biehl, E. R., New synthesis of 3H-benzo[b]thiophen-2-ones. *Heterocycles* **2004,** *63*, 1813-1819.
33. Widdison, W. C.; Wilhelm, S. D.; Cavanagh, E. E.; Whileman, K. R.; Leece, B. A.; Kovtun, Y.; Goldmacher, V. S.; Xie, H.; Steeves, R. M.; Lutz, R. J.; Zhao, R.; Wang, L.; Blaettler, W. A.; Chari, R. V. J., Semisynthetic Maytansine Analogs for the Targeted Treatment of Cancer. *J. Med. Chem.* **2006,** *49*, 4392-4408.
34. Dickinson, R. P., Iddon, B., Condensed Thiophen Ring Systems. Part III. A New Synthesis of Benzo[b]thiophen-2(3H)- and - 3(2H)-ones and Some Reactions of Benzo[b]thiophen-2(3H)-one with Dimethyl Sulphate in the Presence of Base. *J. Chem. Soc.* **1970,** *14*, 1926-1928.
35. Bordwell, F. G., Fried, H.E., Heterocyclic aromatic anions with 4n + 2 pi-electrons. *J. Org. Chem.* **1991,** *56*, 4218-4223.
36. Ban, H.; Nagano, M.; Gavrilyuk, J.; Hakamata, W.; Inokuma, T.; Barbas, C., Facile and Stabile Linkages through Tyrosine: Bioconjugation Strategies with the Tyrosine-Click Reaction. *Bioconjugate Chem.* **2013,** *24*, 520-532.

Chapter 5

Synthesis of a Taxoid-Folate Conjugate via Cu-Free Click Chemistry

Content

§ 5.0.0 Folic Acid as a Tumor-Targeting Moiety

Folic acid, also known as vitamin B9, is an essential dietary nutrient and is utilized as a cofactor for many enzymes where it mediates the transfer of single carbon units at oxidation states of I, II and III. The biologically active form of folic acid is tetrahydrofolate, which is synthesized from folic acid *via* two reductase enzymes: folic acid reductase and dihydrofolate reductase. It is required for many biochemical process including the synthesis and repair of DNA, making it especially important for populations of actively dividing cells.[1] Therefore, cancer cells have an increased need for tetrahydrofolate, and antifolates, such as the dihydrofolate reductase inhibitor methotrexate, are a clinically used and highly potent class of antineoplastic agents.[2]

Folic acid is transported across cellular membranes by the folate receptor (FR) and the reduced folate carrier (RFC), and each of these proteins has different affinities for folate, tetrahydrofolate, antifolates and folic acid conjugates.[3, 4] Unlike the RFC, which is ubiquitously expressed throughout the body, the folate receptor has very low expression level in almost all healthy tissues. The exception is in the proximal tubules of the kidneys, where the FR is used for folate recycling *via* a receptor-mediated trancytosis pathway. The folate receptor has been shown to be overexpressed in numerous cancer cell lines in vitro[5-7] and heightened expression levels of the FR has been detected in many solid tumors including ovarian cancer.[8] Owing its heightened expression in cancerous tissue and relatively low basal expression in the host, the FR is therefore considered a reliable biomarker for the tumor detection.

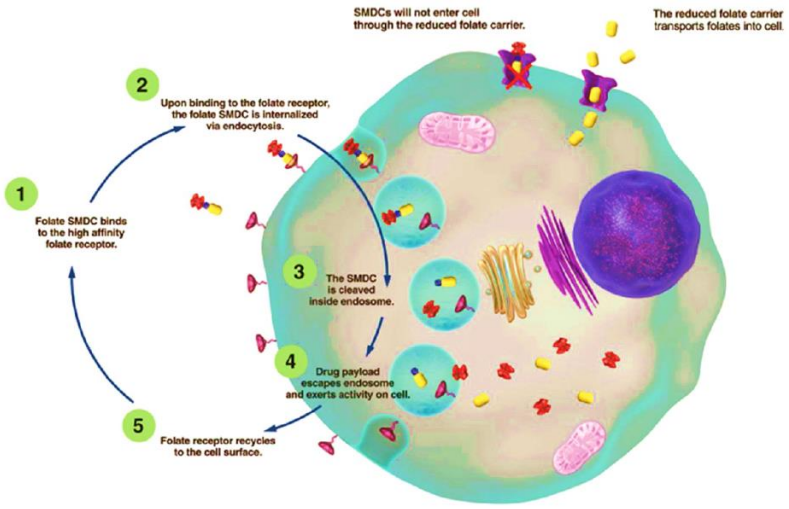

Figure 5-1: Selective internalization of folate-drug conjugates *via* folate receptor (adapted from [9])

Oxidized folates such as folic acid have high affinity for the FR and this affinity is retained even after conjugation to a cytotoxic agent.[9, 10] On the contrary, the RFC has very low affinity for

folate-drug conjugates, and is not significantly involved in their transport.[11] This concept is demonstrated in **Figure 5-1**, wherein the drug conjugates are blocked from entering cells *via* the ubiquitously-expressed RFC and is therefore selectively internalized by cells overexpressing the FR. In this way, drug conjugates of folic acid exhibit excellent tumor specificity and folic acid has been one of the most clinically successful small molecule tumor-targeting moieties to date.

§ 5.0.1 Drug Conjugates of Folic Acid

Early work on constructing folic acid-drug conjugates consisted of simple designs, with little attention paid to drug release, solubility or other pharmacokinetic considerations.[12] Active agents used in these early conjugates include paclitaxel, maytansinoids, PEG-carboplatin and bis(haloethyl) phosphoramidites.[13-16] However, because these simple conjugates lacked an effective drug release mechanism and proper solubilizing moieties, the development was met with limited success.

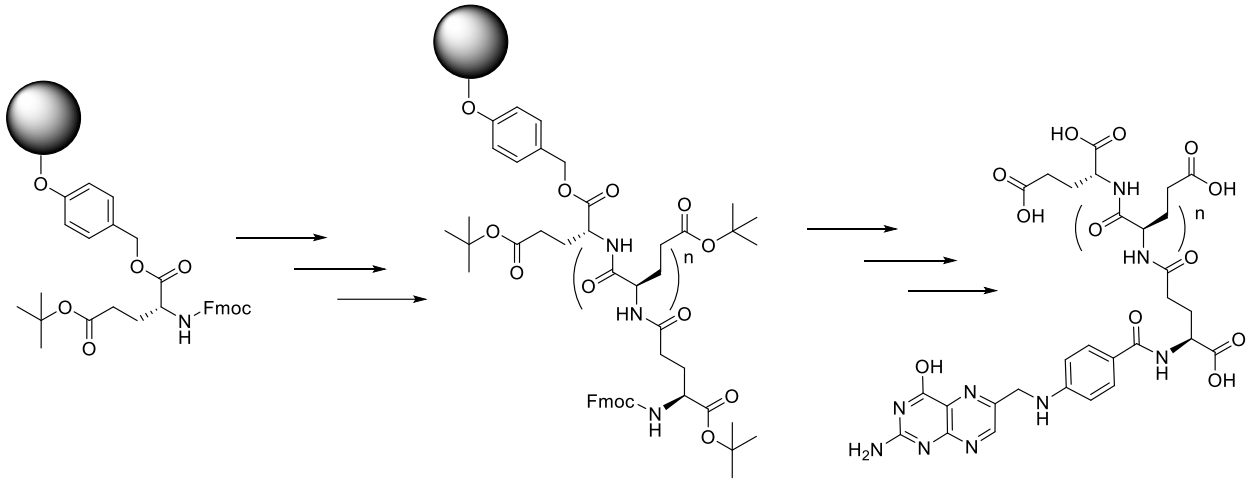

Figure 5-2: Solid-phase assembly strategy for folate-polyglutamate synthesis

Later strategies, developed primarily by Endocyte Inc., focused on the use of solid phase peptide synthesis for the construction of folate-drug conjugates.[12] This method was not only effective in adding charged solubilizing moieties to the final conjugate, but provided a way to overcome the poor solubility of folic acid and the associated troubles of conducting multi-step synthesis with it. This solid phase approach to working with folate has been documented for almost 50 years, when it was first used to produce folate polyglutamates from pteroic acid.[17] The general strategy is shown in **Figure 5-2**.

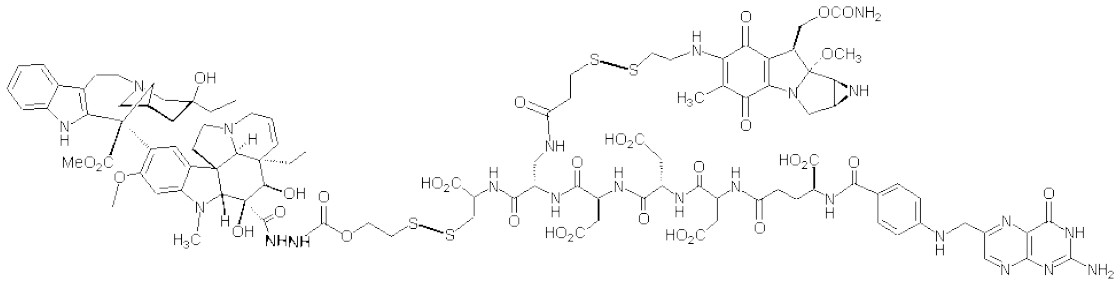

Figure 5-3: A folate-peptide drug conjugate bearing desacetylvinblastin and mytomycin C

Endocyte has produced a number of folic acid drug conjugates featuring cleavable disulfide linkers and solubilizing polypeptide spacers. In collaboration with Bristol-Myers Squibb or ImmunoGen, derivatives of epothilone A, maytansine, camptothecin, tubulysin B and vinblastine have all been incorporated into folate conjugates utilizing this methodology.[18-20] Furthermore, they have successfully produced a novel folate conjugate EC0225 bearing both mytomycin C and desacetylvinblastine monohydrazide, the structure of which is shown in **Figure 5-3**.[21] These conjugates are currently under various staged of preclinical and clinical evaluation.

§ 5.0.2 Clinical Development of Folate Conjugates

The first folate receptor-targeted drug conjugate to enter clinical evaluation was Vintafolide (EC145, a folate-desacetylvinblastine monohydrazide conjugate). After a promising preclinical results and a successful phase I trial, EC145 was advanced to phase II evaluation in NSCLC and platinum-resistant ovarian cancer.[22, 23] Patient selection for these trials was guided using the imaging agent EC40, a ^{99}Tc-chelated folate derivative, used for selecting patients with tumors that highly overexpressed the FR. Progression-free survival was found to be 4 months in patients with NSCLC, while those with platinum refractory ovarian cancer receiving a combination of EC145 and Doxil®, experience increases in PFS of up to 4 months, a 260% increase compared to Doxil® alone.[24] The major side effects were found to be neutropenia, intestinal problems, constipation and palmar-plantar erythrodysesthesia.[24] Vintafolide is currently under phase III evaluation in platinum-resistant ovarian cancer and was recently liscensed to Merck & Co. for development with milestone payments up to one billion dollars.

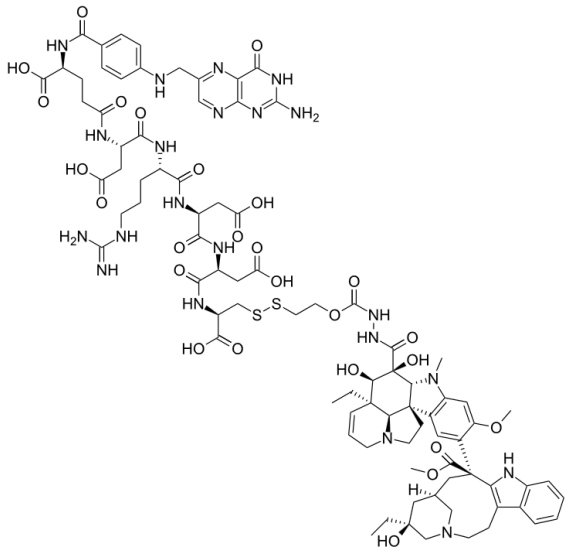

Figure 5-4: The chemical structure of EC145 (Vintafolide®)

Other folate-drug conjugates undergoing clinical evaluation include EC0225 (a folate conjugate containing both desacetylvinblastine monohydrazide and mytomycin C) and EC0489 (a derivative of EC145 with a carbohydrate-based spacer for enhanced PK properties). The spacer region of EC0489 was engineered to reduce hepatobiliary uptake of the conjugate in an attempt to reduce the associated gastrointestinal toxicity.[25] In preclinical evaluation, a 70% reduction in biliary clearance was observed in rats, effectively doubling the MTD and therapeutic index.[25] Currently, EC0489 is under phase I evaluation in patients with metastatic cancer who have exhausted standard treatment options. EC0225 was evaluated in phase I and an MTD of 2.3 mg/m2 was found, with common side effects including anemia, constipation, leukopenia and fatigue. The folate-epothilone conjugate BMS-753493 (Epofolate) was designed and synthesized analogous to Vintafolide and a paper describing the process of scale up and purification of BMS-753493 has recently been published. Epofolate is currently in phase I/II trials for patients with advanced solid tumors.

§ 5.2.0 Logistical Considerations for the Design of a Folate-Drug Conjugate

The success of a folate-drug conjugate depends on its efficacy in treating disease *in vivo*, and guidelines for developing successful folate-drug conjugates were recently outlined by some of the key scientists at Endocyte Inc.[12] First, they found that highly potent drugs are needed, with IC50 values in the low nanomolar to sub-nanomolar range being a prerequisite for producing efficacious conjugates. This trend is due to the limited number of folate receptors on a cell surface (roughtly 1-10 million/cell) and a recycling time of 8-12 hours, effectively limiting the amount conjugate that can be internalized by any given tumor cell. Augmentation of the hydrophilicity through charged residues was also a key feature of successful drug conjugates, as this not only enhanced the aqueous solubility of the conjugate but also prevented the conjugate from entering cells through the non-specific process of passive diffusion. Furthermore, site-specific linkage of a stable yet cleavable linker to the drug is necessary and the drug must be released with retention of

full potency. Finally, the molecular weight must not get too far above 2000, to ensure deeper tissue penetration and rapid systemic clearance. These points, in conjunction with the logistical difficulties in working with folic acid in synthetic chemistry, guided the design of the solubilized folate-taxoid conjugate.

§ 5.2.1 Retrosynthetic Strategy for Solublized Folate-Linker-Taxoid

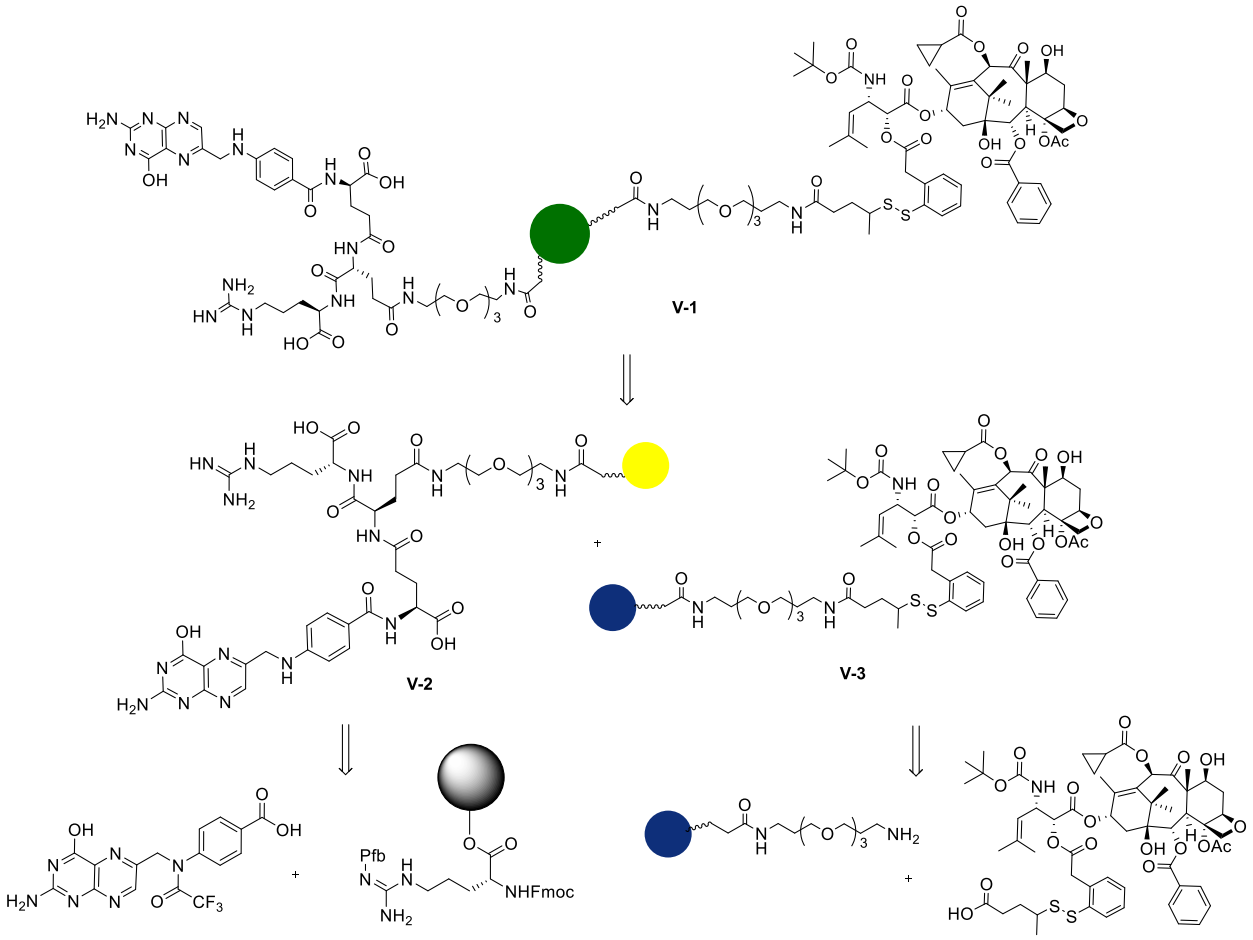

Figure 5-5: Retrosynthetic analysis of solubilized folate conjugate

The desired folate-taxoid conjugate **V-1** (**Figure 5-5**) has been designed to possess greatly improved solubility and to be constructed from two smaller units using bioorthoganal chemistry. The conjugate has been designed to possess multiple charges around the folate moiety to improve aqueous solubility, as well as two triethylene glycol groups to act as intramolecular surfactants, solubilizing the taxoid-linker section. In theory, this design should help to bury the taxoid-linker within the center of the molecule, while maximizing the exposure of the folic acid to the aqueous media, enhancing the recognition by folate receptors on the surface of the tumor cells. Furthermore, the incorporation of polar and amphiphillic residues will help to maximize the active

agent concentration in the injectable solution and minimize the need for surfactants during formulation.

The retrosynthetic analysis for the construction of folate-taxoid conjugate **V-1** is shown in **Figure 5-5**. This route has been designed to minimize linear steps utilizing the taxoid linker construct and to avoid solution phase chemistry with folic acid, due to its poor solubility in almost any solvent. The folate moiety **2** can be constructed using solid phase peptide synthesis and a modified amino acid bearing a group for bioorthogonal chemistry. By building in zwitterionic amino acids and a triethylene glycol group into the folate moiety, the solubility in solvents such as methanol and water will be increased, facilitating the final conjugation reaction. For the final conjugation, the alkyne-azide cycloaddition, or "click" reaction was chosen to conjugate the two pieces and an azide was built into the final design of the folate moiety, while a PEG alkyne was built into the taxoid linker section, again to facilitate solubility in the reaction solvent. This PEGylated taxoid-linker construct **3** can be synthesized in one step from free acid **4-11**, thereby minimizing the number of linear steps in the synthesis.

§ 5.3.0 Synthesis of Solubilized Folate Moiety 5-4

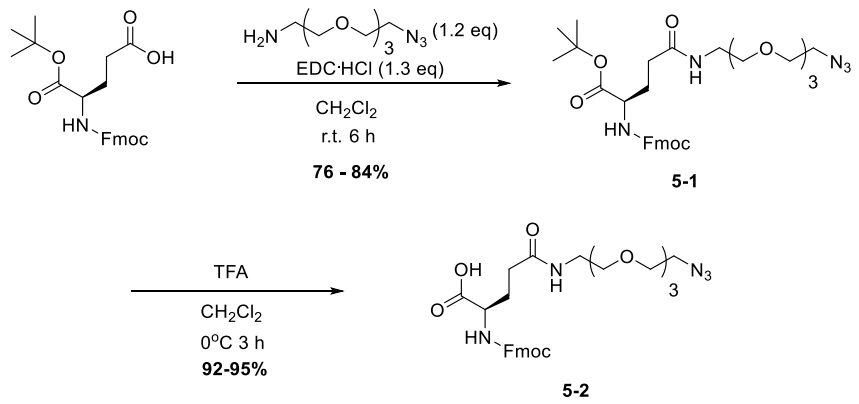

Scheme 5-1: Glutamic acid modification for installation of PEG azide handle

Synthesis of the desired Fmoc-Glu(PEG_3N_3)-OH (**5-2**) was performed in a straightforward manner as delineated in Scheme **5-1**. EDC coupling of the amino-PEG3-azide went in good yield to afford **5-1**. It is worth noting that DMAP should not be used in this reaction. The use of DMAP resulted in the deprotection of the Fmoc group, and the desired product was recovered in only ~30% yield. Following TFA deprotection of the *t*-butyl group, **5-2** was obtained after an aqueous work up to remove any residual TFA.

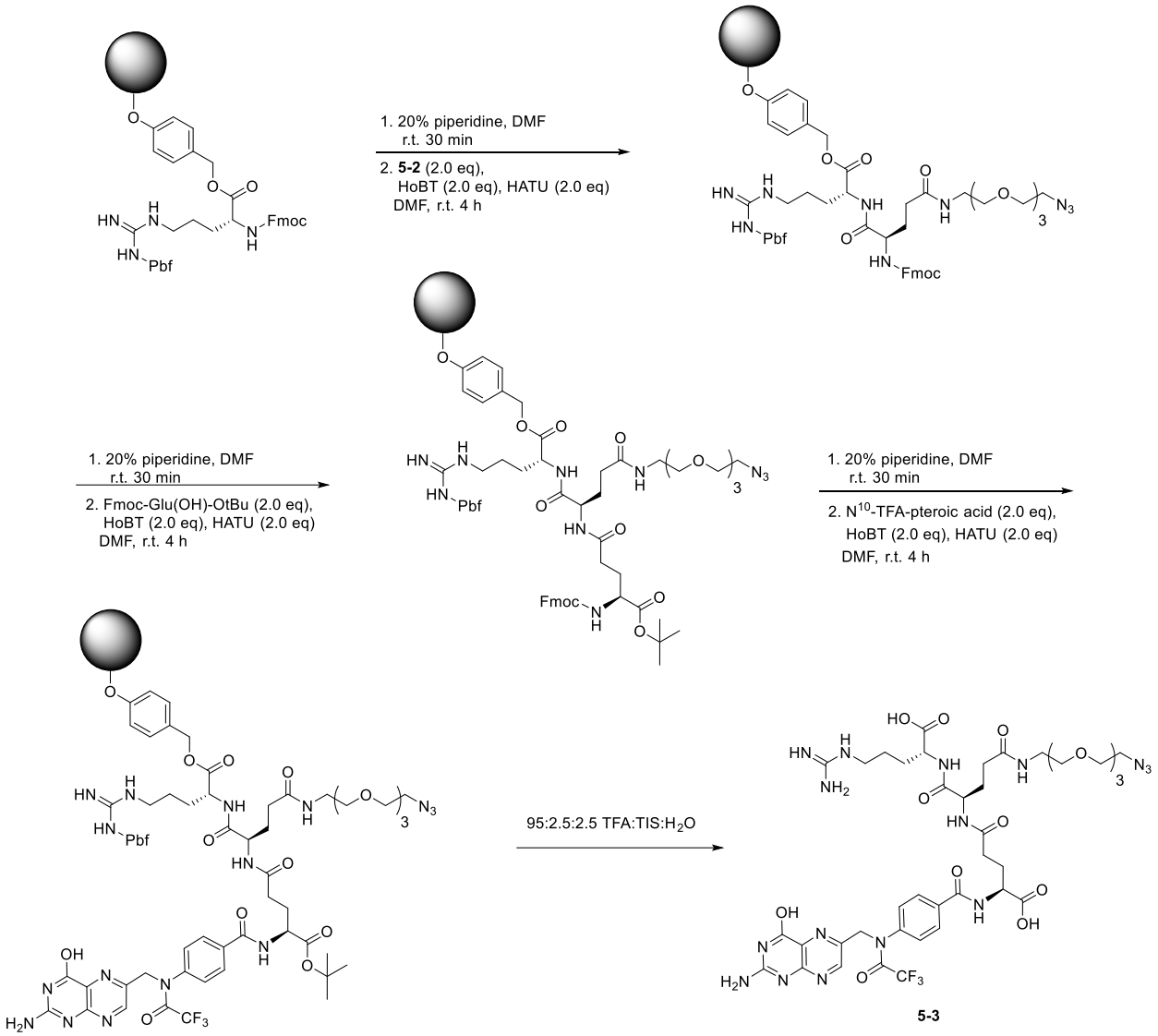

Scheme 5-2: Solid phase construction of solubilized folate moiety **5-3**

The folate moiety **5-3** was synthesized using solid-phase chemistry on a Wang resin, and the progress of each reaction was monitored by qualitative ninhydrin test and quantification of deprotected Fmoc via UV/Vis absorption. Starting with the commercially available Fmoc-Arg(Pbf)-Wang, the Fmoc was deprotected, and the modified amino acid **5-2** was coupled to the resin. Following another round of deprotection, the Fmoc-Glu(OH)-tBu was coupled to the resin through the side chain carboxylic acid to afford the tripepetide. After the last Fmoc deprotection, N^{10}-trifluoroacetyl-pteroic acid was coupled to the resin, and subsequent cleavage from the resin and deprotection of the acid-labile protecting groups in one step with TFA afforded the desired compound **5-3**. The structure of this compound was verified using HRMS and ^{1}H NMR. Furthermore, it is soluble in methanol and H_2O at room temperatures, albeit only at low concentrations.

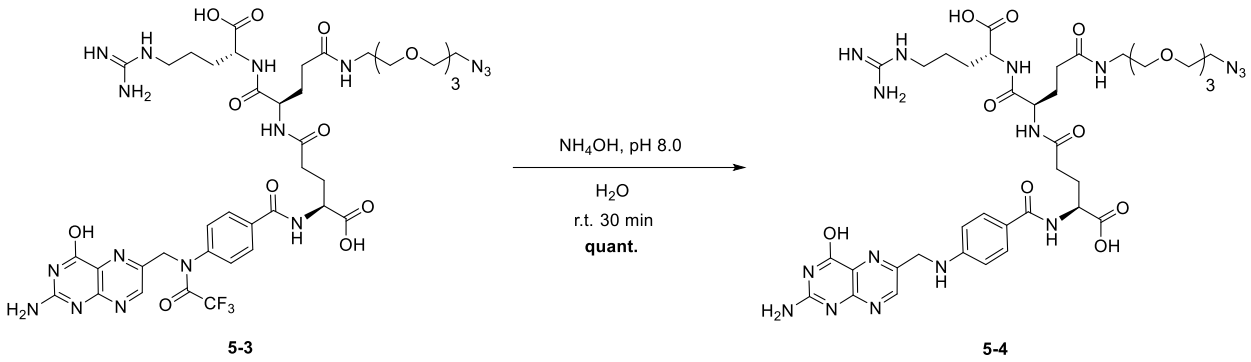

Scheme 5-3: TFA deprotection under mild conditions

Deprotection of the TFA group was achieved using basic aqueous solution. The reaction progress was monitored by FIA and following completion of the reaction, **5-4** was obtained after the solvent was removed *via* lyophilization.

§ 5.3.1 Attempted synthesis of SB-T-1214-Linker-PEG$_6$-Folate (5-5)

With the solubilized folate moiety **5-4** in hand, attention was turned to the synthesis of the PEGylated taxoid-linker construct bearing an alkyne.

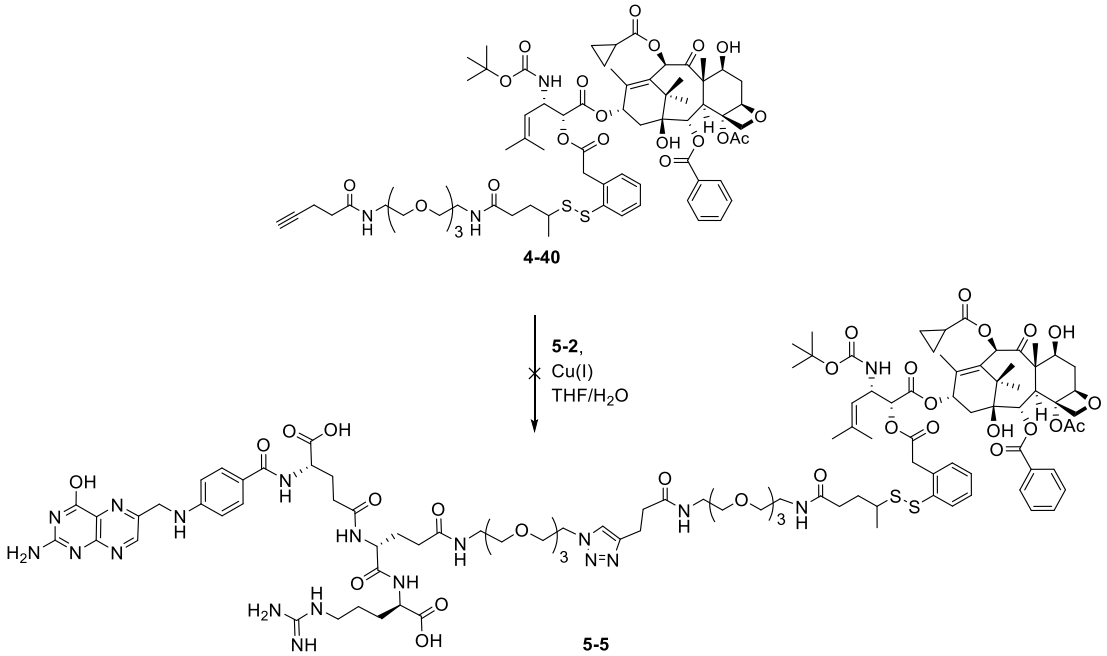

Scheme 5-4: Attempted use of Cu(I)-mediated click chemistry for conjugation

Unfortunately, the copper-catalyzed "click" reaction between **4-40** and **5-4** did not work. Instead, a brown precipitate was formed following the mixing of **5-4** with the Cu(I) salt. Analysis

of the supernatant by LCMS showed no presence of the folate moiety **5-4**. Therefore, it was deduced that chelation of the Cu(I) ion by the terminal arginine residue formed an insoluble complex that precipitated from the solution. Arginine residues have been demonstrated to effectively chelate copper ions. Both copper(I) bromide and the mixture of copper(II) sulfate and ascorbic acid were ineffective in promoting this reaction, and both conditions resulted in the formation of precipitate with no detectable product. Therefore, the use of a copper-catalyzed click reaction was abandoned and the synthetic route was redesigned to feature the use of a strained cyclooctyne moiety capable of undergoing a [3+2] cycloaddition without the need of a copper catalyst.

§ 5.3.2 Synthesis of SB-T-1214-Linker-PEG$_3$-Cyclooctyne (5-15)

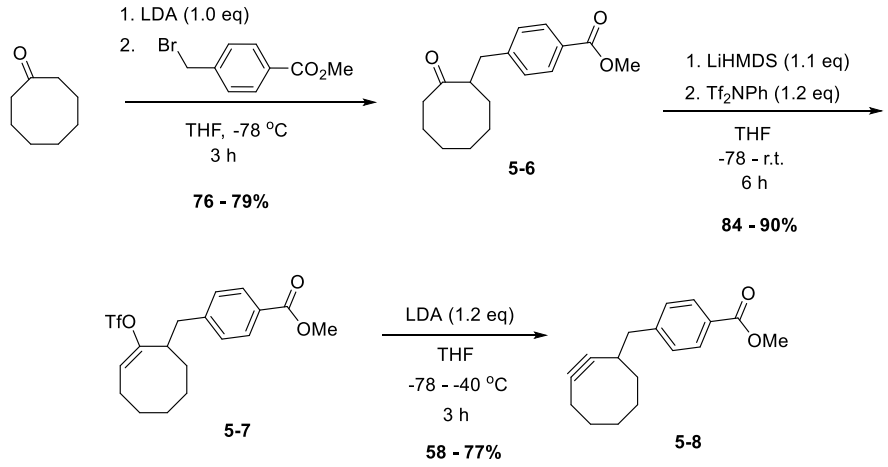

Scheme 5-5: Cyclooctyne synthesis

The synthesis of **5-8** was modified from the original published method to provide significantly increased yields for both the triflate formation and elimination reactions. To the cyclooctanone enolate was added 4-methylbromo-benzoic acid methyl ester to afford **5-6** in modest yield. Careful control of kinetic enolate formation was obtained by the slow addition of **5-6** to a solution of excess LiHMDS followed by trapping with *N*,*N*-ditriflylaniline. Slow addition of LDA to a solution of **5-7** at -78 °C afforded the desired cyclooctyne **5-8** in moderate yield. It is worth noting that the yield for these two steps was improved from the reported 16% to 53% by these slight alterations in the procedure.

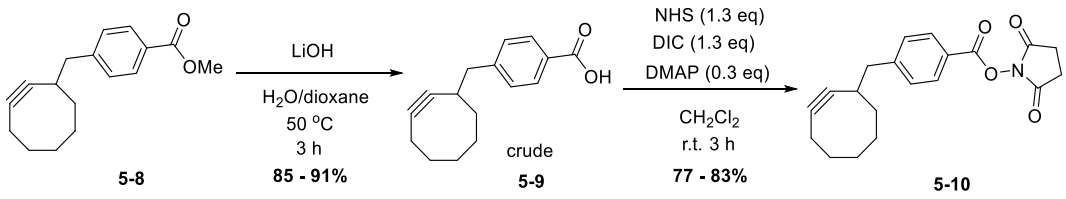

Scheme 5-6: Synthesis of activated ester **5-10**

Hydrolysis of the methyl ester using LiOH in water and dioxane was conducted according to the literature procedure, and produced the free acid **5-9** in good yield. Attempts to perform this hydrolysis using NaOH in water and THF at room temperature were unsuccessful, and starting material was recovered. With free acid in hand, coupling directly to mono-protected PEG diamines was attempted using **5-9** purified by column chromatography, but it only provided the desired product in low yields (**Scheme 5-7**). Therefore, the activated ester **5-10** was synthesized by DIC coupling.

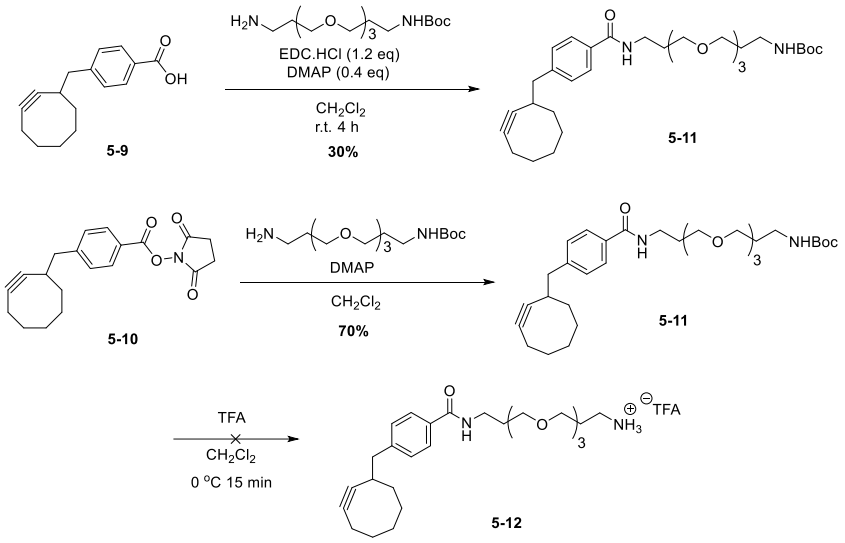

Scheme 5-7: Attempted synthesis of **5-14** via mono-Boc-protected diamine **5-11**

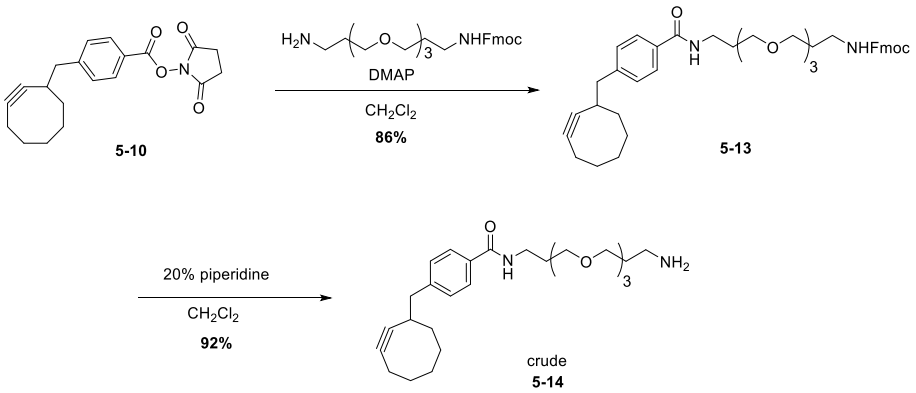

Scheme 5-8: Synthesis of **5-14** via mono-Fmoc-protected diamine **5-13**

Coupling of the N-*t*-Boc-diamino-PEG_3 using activated ester **5-10** in the presence of DMAP produced the desired product in good yield. However, deprotection of the *t*-Boc was unsuccessful and resulted in the degradation of the product. It is likely that the strained cyclooctyne is unstable in strong acidic conditions, and neither TFA nor HCl were successful in producing deprotected intermediate **5-12**. As the cyclooctyne moiety is not stable under *t*-Boc deprotection

conditions, Fmoc was used as the protecting group. Coupling of the activated ester **5-10** to the mono-Fmoc-protected diamino PEG group proceeded in good yield. Deprotection of the Fmoc group readily produced the free amine **5-14**, which was used directly for the next step.

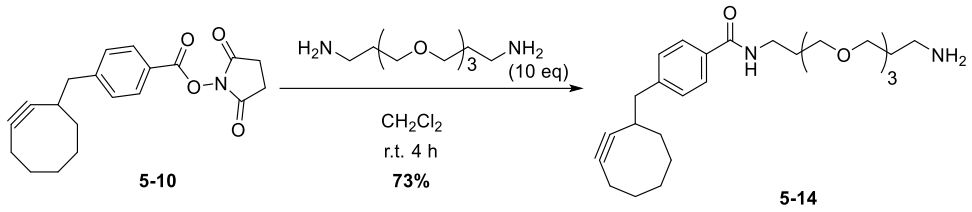

Scheme 5-9: Direct synthesis of amino-PEG-cyclooctyne **5-14**

Slow addition of the activated ester **5-10** to an excess of the diamine provided direct access to the required mono-substituted compound **5-14**. As it affords the desired compound in one step, free from chromatography, this is the method of choice for producing mono-substituted PEG diamines.

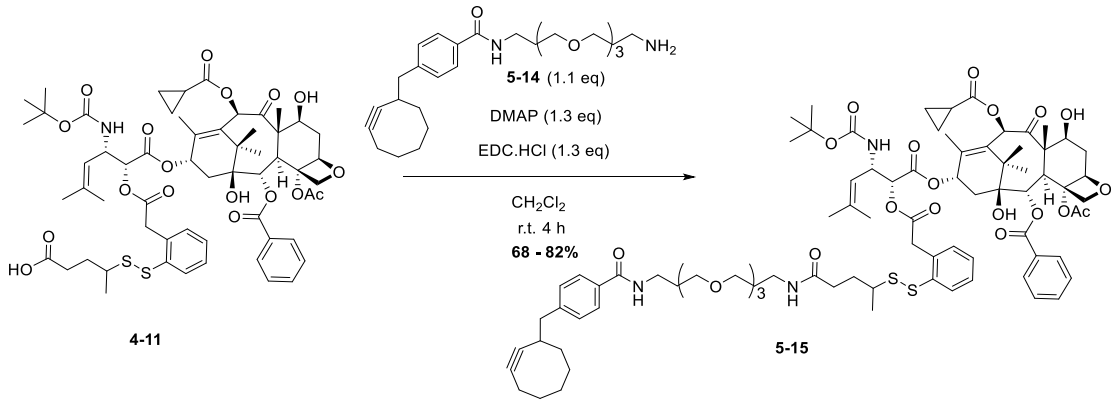

Scheme 5-10: Coupling to form 1214-linker-PEG-cyclooctyne **5-15**

With crude free amine **5-14** in hand, it was directly coupled to the carboxylic acid on **4-11** to provide SB-T-1214-linker-PEG3-cyclooctyne **5-15** in good yield. This compound was then used in a model reaction with N^{10}-TFA protected folate moiety **5-3**.

§ 5.3.3 Synthesis of Folate-Taxoid Conjugate (5-17)

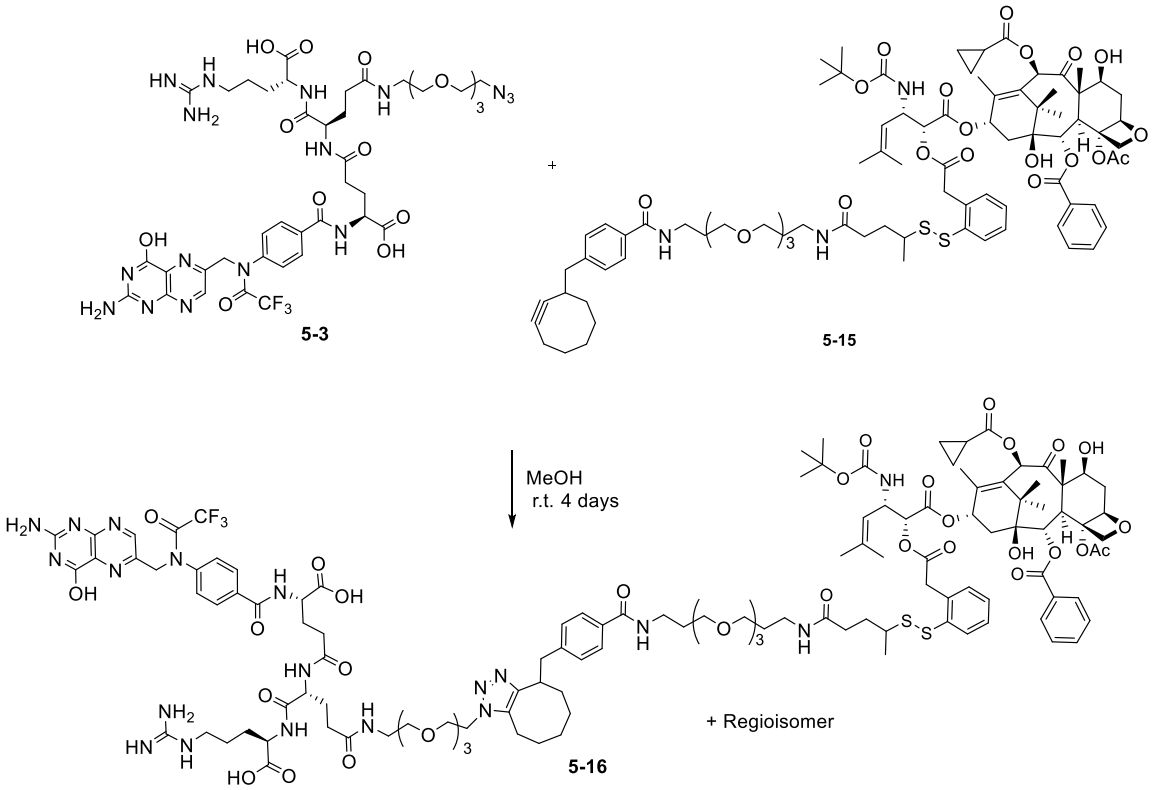

Scheme 5-11: Model reaction for formation of folate conjugate

Coupling of the cyclooctyne to the azide was monitored by LCMS. The successful formation of the product was observed as shown in **Figure 5-6**. The peak at 21 minutes is the starting material **5-15**, while the highly polar folate moiety **5-3** elutes with the solvent front under these LC condiditons (peak at 1 minute).

Formation of the product can clearly be observed at 5.5-6 minutes. The top trace is the reaction mixture after 24 hours, showing substantial product formation at this time. The next trace was taken after 48 hours and the ratio of **5-15** to **5-16** appears to be almost 1:1. The third trace is the same time point taken at 335 nm, clearly showing the presence of the folate moiety on the newly formed peak at 5.5 minutes. The mass spectrum of this peak is shown in **Figure 5-7**. According the LC/MS analysis, the ratio of product to starting material was approaching 1:1 (uncorrected for extinction coefficient) after 2 days of reaction. Therefore, the reaction should be run for at least 4 days at room temperature to ensure significant formation of the desired taxoid-folate conjugate.

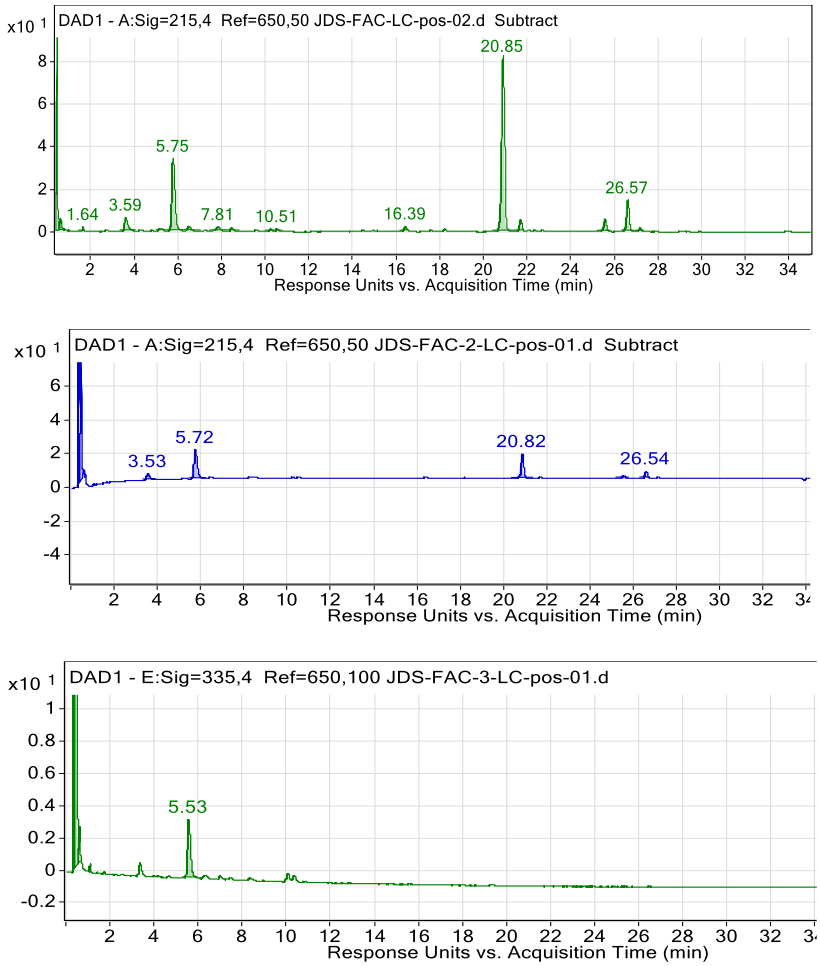

Figure 5-6: Reaction progress monitoring by LC/HRMS

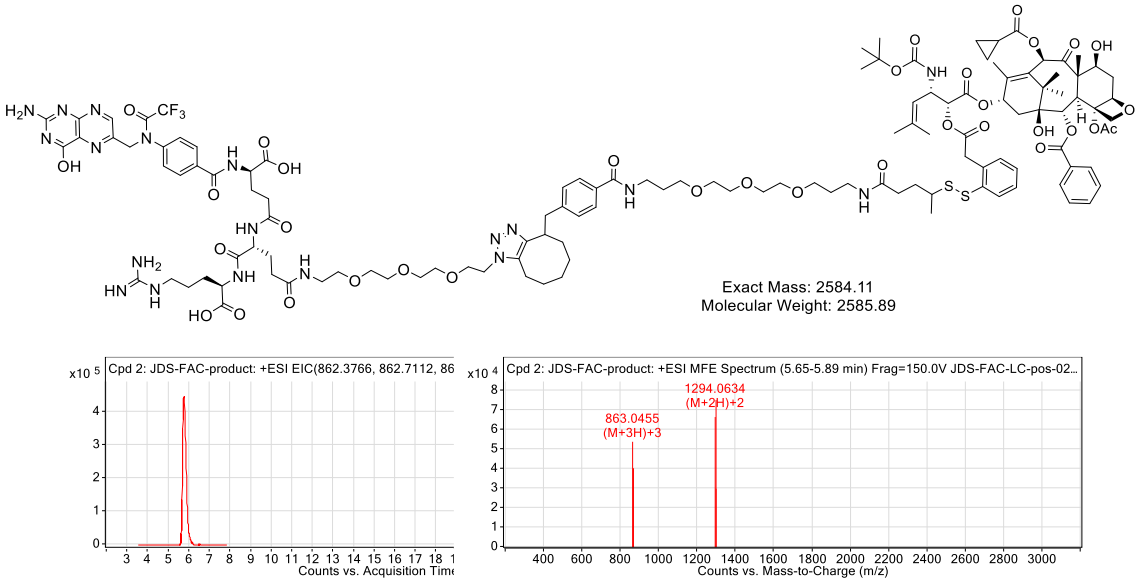

Figure 5-7: Confirmation of desired product formation by LC/HRMS

The complete structure of the desired conjugate is given in **Figure 5-7** (top), along with its monoisotopic mass and molecular weight. The LC/HRMS result for the newly formed peak is also shown in **Figure 5-7** (bottom). The only m/z values obtained from this peak are 863 and 1294, which correspond to the triply charged [M+3H] and doubly charged [M+2H] ions, respectively. Deconvolution of these values gives us a parent ion mass of 2586, consistent with the major isotope peak of the desired product. Therefore this model reaction confirmed that this is an effective synthetic route for the synthesis of solubilized folate-taxoid conjugates.

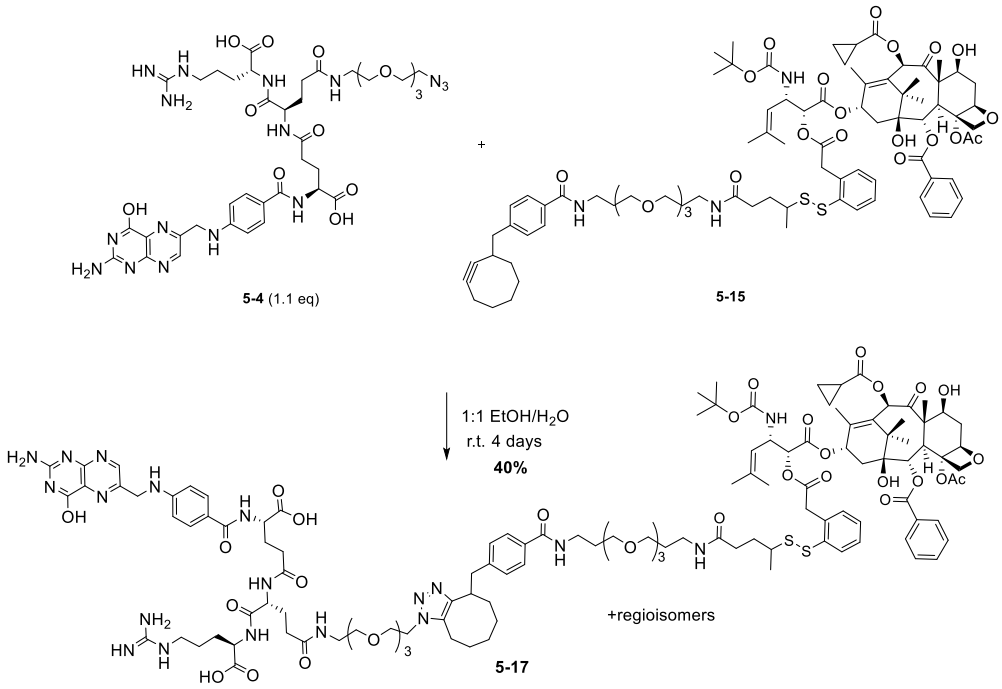

Scheme 5-12: Synthesis of the desired folate-taxoid conjugate **5-17**

A synthesis of **5-17** was performed by dissolving the folate moiety **5-4** in water and the taxoid conjugate **5-15** in ethanol and mixing the two to a final ratio of 1:1 ethanol to water. In this solvent system, both the taxoid and the folate moieties were dissolved in a yellow solution. During the course of 4 days at room temperature, a substantial amount of yellow precipitate had formed, and the solution was considerably less clear. The yellow solid was isolated by centrifugation, washing and lyophilization to afford a yellow solid that was soluble in neither water nor ethanol. NMR analysis of this solid confirmed the structure as shown in **5-17**. A 1:1 ratio of key folate and taxoid protons in the ^{1}H NMR as well as the disappearance of the strained alkyne carbon peaks at 94.9 and 96.3 in the ^{13}C NMR provide strong evidence that the isolated solid is indeed compound **5-17**. This route does not require HPLC purification and therefore can be considered scalable for the production of this conjugate for *in vivo* testing. Although the yield is low of this reaction, the isolation process has not been optimized and it is highly likely that it can be significantly improved.

§ 5.4.0 Modified Polypepdites as Versatile Scaffolds for Tumor-Targeted Drug Conjugates

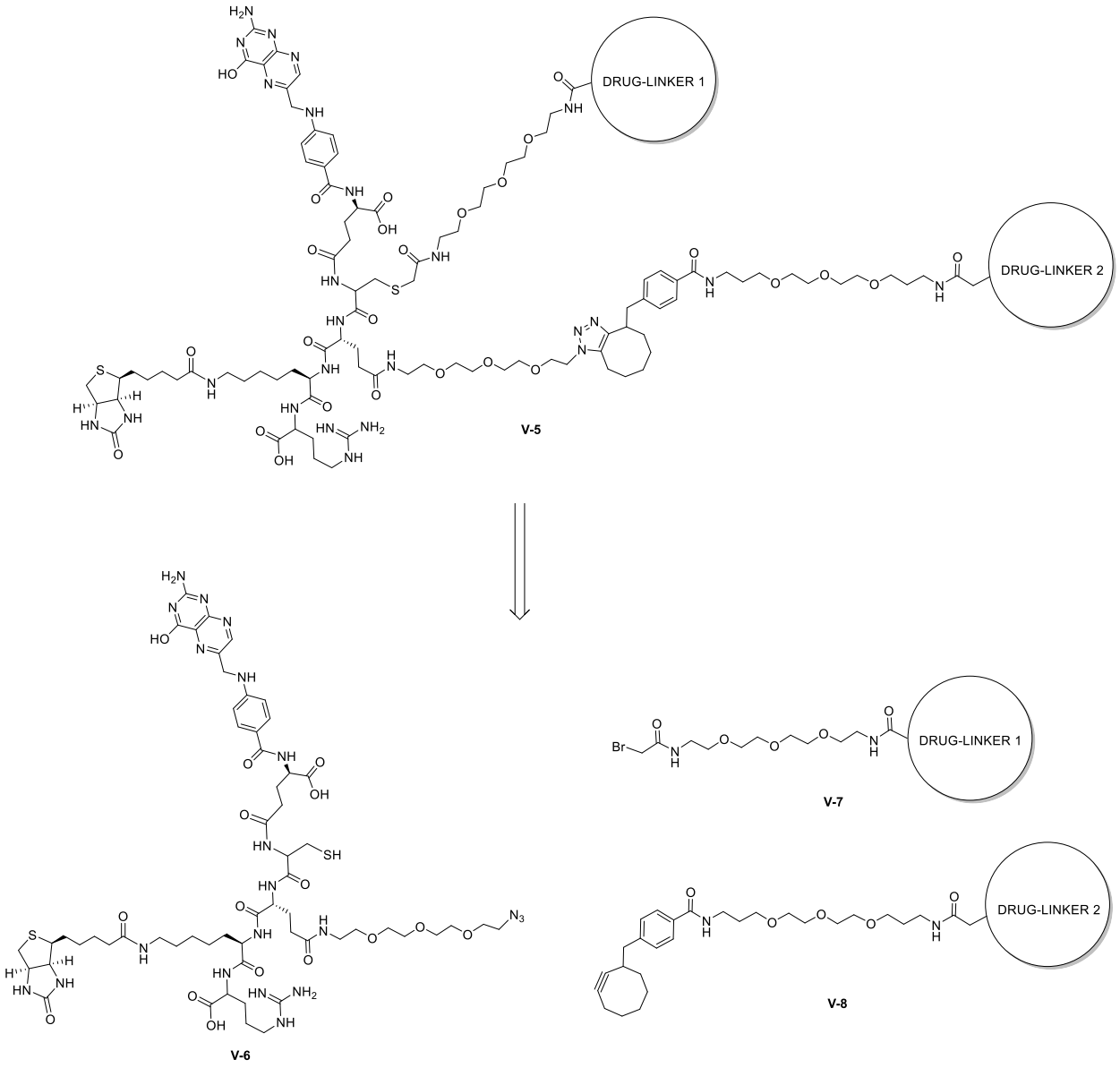

Figure 5-8: Potential drug conjugate utilizing the peptide-scaffold design strategy

A natural extension of the preliminary work described in this chapter is the use of modified and unnatural polypeptides as modular scaffolds for tumor-targeted drug conjugates. Some advantages of using peptides are low cost, increased water solubility, easy and fast synthesis, and all moieties that are stable to deprotection conditions can be installed to the scaffold via modified amino acids that can be synthesized in three or less steps. For example, **Figure 5-8** shows a simple

conjugate design of a peptide scaffold bearing folic acid, biotin and two different drug-linker systems attached *via* orthogonal reactions that create no reaction byproducts.

Drug conjugate **V-5** can be synthesized in 2 steps in one pot from components **V-6, V-7** and **V-8**. First, **V-6** and **V-7** can be attached through a thioether formation between the free thiol on the cysteine residue and the bromoacetamide moiety on **V-7**. At the completion of this reaction, **V-8** can be added, and conjugated to the modified glutamic acid residue via copper free click chemistry affording the desired dual-vitamin dual-warhead conjugate **V-5**. Furthermore, **V-6** can be synthesized directly using solid phase peptide synthesis with pre-functionalized amino acids. It is envisioned that this strategy can allow the rapid synthesis of scaffolds for the rapid modular construction of novel tumor-targeted drug conjugates.

§ 5.5.0 Experimental

§ 5.5.1 General Methods

^{1}H and ^{13}C NMR spectra were measured on a Varian 300, 400, 500 or 600 MHz NMR spectrometer. Melting points were measured on a Thomas Hoover Capillary melting point apparatus and are uncorrected. Mass to charge values were measured by flow injection analysis on an Agilent Technologies LC/MSD VL. TLC was performed on Merck DC-alufolien with Kieselgel 60F-254 and column chromatography was carried out on silica gel 60 (Merck; 230-400 mesh ASTM). Compound purity was verified by reverse phase HPLC on a Shimadzu LC-2010A with a Curosil-B 5 column (250 x 4.6 nm). The mobile phase was acetonitrile-water. The analyses were performed at a flow rate of 1ml/min with the UV detector set at 254 and 227 nm. The gradient was run from 20% to 95% acetonitrile in water over a 40 minute period.

§ 5.5.2 Materials

The chemicals were purchased from Aldrich Co. and Sigma and purified before use by standard methods. Tetrahydrofuran was freshly distilled from sodium metal and benzophenone. Dichloromethane was also distilled immediately prior to use under nitrogen from calcium hydride. In addition, various dry solvents were degassed and dried using PureSolv™ solvent purification system (Innovative Technologies, Newburyport, MA).

§ 5.5.3 Experimental Procedures

Fmoc-Glu(PEG$_3$N$_3$)-OtBu [5-1][26]

To a solution of Fmoc-Glu-OtBu (200 mg, 0.47 mmol) and **4-34** (120 mg, 0.56 mmol) in CH_2Cl_2 (10 mL) was added a suspension of EDC·HCl (135 mg, 0.71 mmol) in CH_2Cl_2 (5 mL). The solution was stirred for at room temperature for 4 hours and the reaction progress was monitored by TLC. Upon completion of the reaction, the reaction was diluted with H_2O, extracted with CH_2Cl_2 (3 x

20 mL), washed with brine (3 x 15 mL), dried over $MgSO_4$, filtered and the filtrate concentrated *in vacuo*. Purification was performed by column chromatography on silica gel with increasing amounts of ethyl acetate in hexanes (hexanes:ethyl acetate 1:0 – 1:3) to afford **5-1** (234 mg, 83%) as a white solid: ^{1}H NMR (400 MHz, $CDCl_3$) δ 1.46 (s, 9H), 1.95 (m, 1H), 2.16-2.27 (m, 3H), 3.34 (m, 2H), 3.44 (m, 2H), 3.55 (m, 2H), 3.63 (m, 10H), 4.21 (m, 2H), 4.39 (m, 2H), 5.69 (d, J = 8.0 Hz, 1H), 6.27 (s, br, 1H), 7.30 (t, J = 7.6 Hz, 2H), 7.39 (t, J = 7.2 Hz, 2H), 7.60 (m, 2H), 7.75 (d, J = 7.6 Hz, 2H); ^{13}C NMR (100 MHz, $CDCl_3$) δ 28.01, 28.73, 32.51, 39.33, 47.21, 50.67, 54.11, 60.39, 66.94, 69.75, 70.01, 70.27, 70.53, 70.60, 70.66, 82.37, 119.97, 125.15, 127.08, 127.71, 141.31, 143.75, 143.96, 156.25, 171.16, 171.97. HRMS (ESI) calcd for $C_{32}H_{44}N_5O_8$ $(M+H)^+$: 626.3190, found: 626.3188 (Δ -0.3 ppm, -0.2 mDa). All data were found to be in agreement with literature values.[26]

Fmoc-Glu(PEG$_3$N$_3$)-OH [5-2][26]

A solution of **5-1** (170 mg, 0.15 mmol) in CH_2Cl_2 (8 mL) was cooled to 0 °C and TFA (2 mL) was added dropwise. The reaction mixture was stirred at 0 °C for 3 hours and the reaction progress was monitored by TLC. Upon completion of the reaction, the mixture was diluted with CH_2Cl_2 (30 mL) washed with H_2O (4 x 20 mL) until the pH of the aqueous was no longer acidic. The organic layer was then dried over $MgSO_4$, filtered and the filtrate concentrated *in vacuo* to afford **5-2** (155 mg, 98%) as a yellow oil that could be triturated an off-white solid in ether/hexanes: ^{1}H NMR (400 MHz, $CDCl_3$) δ 2.11 (m, 1H), 2.19 (m, 1H), 2.39 (m, 1H), 2.48 (m, 1H), 3.35 (m, 2H), 3.46 (m, 2H), 3.55 (m, 2H), 3.63 (m, 10H), 4.21 (t, J = 7.2 Hz, 1H), 4.37 (m, 2H), 6.01 (d, J = 6.8 Hz, 1H), 6.69 (s, br, 1H), 7.30 (t, J = 7.2 Hz, 2H), 7.39 (t, J = 7.2 Hz, 2H), 7.59 (m, 2H), 7.75 (d, J = 7.6 Hz, 2H); ^{13}C NMR (100 MHz, $CDCl_3$) δ 28.62, 32.30, 39.60, 47.12, 50.61, 53.40, 67.04, 69.45, 69.93, 70.11, 70.40, 70.54, 119.96, 125.14, 125.20, 127.12, 127.73, 141.28, 143.70, 143.93, 156.27, 173.56, 173.62. HRMS (ESI) calcd for $C_{28}H_{36}N_5O_8$ $(M+H)^+$: 570.2564, found 570.2560 (Δ -0.7 ppm, -0.4 mDa). All data was found to be in agreement with literature values.[26]

***N^{10}*-TFA-Folate-Glu(PEG$_3$N$_3$)-Arg-OH [5-3]**

Fmoc-Arg(Pbf)-Wang Resin (150 mg, 75 µmol) was suspended in 2 mL DMF, shaken 1 hour, and the solvent was filtered off. To the beads was added a 20% solution of piperidine in DMF (2 mL) and the mixture was shaken for 30 minutes. The solvent was filtered off, the beads were washed with DMF (2 x 2 mL), and each wash was kept for UV analysis. A solution of **5-2** (130 mg, 225 µmol), DIPEA (165 µL), HOBt (35 mg, 225 µmol) and HBTU (85 mg, 225 µmol) in DMF (1.835 mL) was added to the beads and the reaction mixture was shaken for 4 hours. The solvent was filtered off and the beads were washed with DMF (3 x 2 mL).

To the beads was added a 20% solution of piperidine in DMF (2 mL) and the mixture was shaken for 30 minutes. The solvent was filtered off, the beads were washed with DMF (2 x 2 mL), and each wash was kept for UV analysis. A solution of **Fmoc-Glu-OtBu** (95 mg, 225 µmol), DIPEA (165 µL), HOBt (35 mg, 225 µmol) and HBTU (85 mg, 225 µmol) in DMF (1.835 mL)

was added to the beads and the reaction mixture was shaken for 4 hours. The solvent was filtered off and the beads were washed with DMF (3 x 2 mL).

To the beads was added a 20% solution of piperidine in DMF (2 mL) and the mixture was shaken for 30 minutes. The solvent was filtered off, the beads were washed with DMF (2 x 2 mL), and each wash was kept for UV analysis. A small aliquot was dried, cleaved from the resin with 50 µL of 95:2.5:2.5 mixture of TFA:TIS:H_2O, and the solution evaporated by N_2 stream before being dissolved in methanol for FIA analysis (m/z = 633.3, M+1).

A solution of ***N*^{10}-TFA-Pteroic Acid** (90 mg, 225 µmol), DIPEA (165 µL), HOBt (35 mg, 225 µmol) and HBTU (85 mg, 150 µmol) in DMF (1.835 mL) was added to the beads and the reaction mixture was shaken for 4 hours. The solvent was filtered off and the beads were washed with DMF (3 x 2 mL). A small aliquot was dried, cleaved from the resin with 50 µL of a 95:2.5:2.5 mixture of TFA:TIS:H_2O, and the solution evaporated by N_2 stream before being dissolved in methanol for FIA analysis (m/z = 1023.4, M+1).

Upon confirmation of the product by FIA, the beads were transferred into a conical vial and a 95:2.5:2.5 mixture of TFA:TIS:H_2O was added shaken lightly for 1 hour. The yellow solution was separated from the beads by pipette and the liquid was concentrated *in vacuo*. Upon the addition of ether (5 mL), the yellow oil was triturated to a pale yellow solid, which was dissolved in H_2O (20 mL), washed with ether (3 x 10 mL), and lyophilized to afford **5-3** (43 mg, 56%) as a pale yellow solid: ^{1}H NMR (400 MHz, CD_3OD) δ 162-1.80 (m, 4H), 1.83-1.98 (m, 3H), 2.06-2.18 (m, 2H), 2.28-2.40 (m, 1H), 2.36 (t, J = 7.6 Hz, 2H), 2.45 (t, J = 8.4 Hz, 2H), 3.24 (m, 2H), 3.37 (m, 2H), 3.55 (t, J = 5.6 Hz, 2H), 3.60-3.71 (m, 10H), 4.31 (dd, J = 8.8, 5.6 Hz, 1H), 4.44 (m, 1H), 4.61 (dd, J = 9.6, 4.8 Hz, 1H), 5.20 (s, 2H), 7.58 (d, J = 8.4 Hz, 2H), 7.95 (d, J = 8.4 Hz, 2H), 8.73 (s, br, 1H). MS (ESI) calcd for $C_{40}H_{54}F_3N_{16}O_{13}$ $(M+H)^+$: 1023.40, found 1023.4.

Folate-Glu(PEG$_3$N$_3$)-Arg-OH [5-4]

To a round bottom flask containing **5-3** (20 mg, 20 µmol), was added a pH 8 solution of NH_4OH in H_2O (2 mL). Deprotection of the *N*^{10}-TFA moiety was monitored by FIA, and after 30 minutes, the sample was lyophilized to afford **5-4** (20 mg, 100%) as a pale yellow solid, which was used directly for conjugation: MS (ESI) calcd for $C_{38}H_{55}N_{16}O_{12}$ $(M+H)^+$: 927.41, found 927.4.

2-(4-carbomethoxy)benzylcyclohexanone [5-6][27]

A solution of diisopropyl amine (1.56 g, 15.4 mmol) in THF (10 mL) was cooled to -78 ^{o}C under N_2 and *n*-BuLi (1.6 M in hexanes, 9.6 mL) was added dropwise. The mixture was allowed to warm to 0 ^{o}C and stir for 30 minutes before it was cooled to -78 ^{o}C again and added dropwise to a solution of cyclooctanone (1.76 g, 14.0 mmol) in THF (20 mL) *via* cannula. The reaction mixture was allowed to warm to -40 ^{o}C for 30 minutes, cooled back down to -78 ^{o}C, and a solution of methyl 4-bromomethylbenzoate (3.53 g, 15.4 mmol) in THF (10 mL) was added dropwise *via* cannula. The reaction was allowed to warm to room temperature and stirred for 2 hours. The reaction

progress was monitored by TLC and upon completion, it was quenched with saturated NH_4Cl (5 mL), diluted with H_2O (30 mL) and extracted with ethyl acetate (3 x 40 mL). The organic layer was washed with brine (3 x 30 mL), dried over $MgSO_4$ and concentrated *in vacuo*. Purification was done by column chromatography on silica gel with increasing amounts of ethyl acetate in hexanes (hexanes:ethyl acetate 1:0 – 9:1) to afford **5-6** (2.91 g , 79%) as a colorless oil: ^{1}H NMR ($CDCl_3$, 300 MHz): δ 1.10-1.28 (m, 1H), 1.28-1.42 (m, 1H), 1.42-1.80 (m, 6H), 1.80-1.90 (m, 1H), 1.90-2.08 (m, 1H), 2.08-2.18 (m, 1H), 2.22-2.35 (m, 1H), 2.64 (dd, 1H, *J* = 12.6, 6.0 Hz), 3.01 (m, 2H), 3.89 (s, 3H), 7.20 (d, 2H, *J* = 8.1 Hz), 7.93 (d, 2H, *J* = 8.4 Hz). All data were found to be in agreement with the literature values.[27]

3-(4-carbomethoxy)benzyl-2-trifyloxycyclohex-1-ene [5-7][27]

A solution of LiHMDS (8.60 mmol) in THF (10 mL) was cooled to -78 ^{o}C under N_2, and to it was added a solution of **5-6** (2.30 g, 7.82 mmol) in THF (20 mL) dropwise *via* cannula. The reaction mixture was allowed to warm to -40 ^{o}C and stirred for 30 minutes, at which point it was cooled again to -78 ^{o}C. To this was added a solution of Tf_2NPh (3.07 g, 8.60 mmol) in THF (10 mL) dropwise *via* cannula, and upon completion of addition, the reaction mixture was allowed to warm to room temperature and stir for 2 hours. The reaction progress was monitored by TLC and upon completion, it was quenched with saturated NH_4Cl (5 mL), diluted with H_2O (30 mL) and extracted with ethyl acetate (3 x 40 mL). The combined organic layer was washed with brine (3 x 40 mL), dried over $MgSO_4$ and concentrated *in vacuo*. Purification was done by column chromatography on silica gel with increasing amounts of ethyl acetate in hexanes (hexanes:ethyl acetate 1:0 – 9:1) to afford **5-7** (3.04 g, 90%) contaminated with 7-10% regioisomer as a colorless oil: ^{1}H NMR (300 MHz, $CDCl_3$) δ 1.35-1.59 (m, 2H), 1.60-1.77 (m, 4H), 1.80-1.89 (m, 2H), 2.05-2.15 (m 1H), 2.25 (m, 1H), 2.79 (dd, J = 6.6, 13.0 Hz, 1H), 3.05 (dd, J = 8.1, 13.8 Hz 1H), 3.19 (m, 1H), 3.97 (s, 3H), 5.82 (t, J = 8.4 Hz, 1H), 7.32 (d, J = 8.4 Hz, 2H), 8.03 (d, J = 8.4 Hz, 2H). All data were found to be in agreement with the literature values. [27]

2-(4-carbomethoxy)benzylcyclohex-1-yne [5-8][27]

To a solution of diisopropyl amine (745 mg, 7.38 mmol) in THF (10 mL), cooled to -78 ^{o}C under N_2, was added *n*-BuLi (1.6 M in hexanes,4.6 mL) dropwise, and the solution was allowed to warm to room temperature for 30 minutes before being cooled back to -78 ^{o}C. A solution of **5-8** (1.50 g, 3.69 mmol) was cooled to -78 ^{o}C, and the LDA solution was added dropwise *via* cannula until the disappearance of the starting material was determined by TLC analysis. In total, ~1.3-1.5 equivalents of LDA was added. The reaction was then quenched with saturated NH_4Cl (5 mL), diluted with H_2O (40 mL) and extracted with ethyl acetate (3 x 30 mL). The combined organic layer was washed with brine (3 x 30 mL), dried over $MgSO_4$, filtered, and the filtrate concentrated *in vacuo*. Purification was done by column chromatography on silica gel with increasing amounts of ethyl acetate in hexanes (hexanes:ethyl acetate 1:0 – 9:1) to afford **5-8** (668 mg, 70%) as a colorless oil: ^{1}H NMR (500 MHz, $CDCl_3$) δ 1.38-1.46 (m, 2H), 1.58-1.65 (m, 1H), 1.72-1.87 (m,

3H), 1.90-1.95 (m, 1H), 2.72-2.77 (m, 2H), 3.89 (s, 3H), 7.27 (d, J = 8.5 Hz, 2H), 7.95 (d, J = 8.5 Hz, 2H). All data were found to be in agreement with the literature values. [27]

2-(4-carbohydroxy)benzyl-cyclohex-1-yne [5-9][27]

To a solution of **5-8** (600 mg, 2.34 mmol) in dioxane (25mL) was added H_2O (6 mL) and LiOH (1.10 g, 45 mmol). The suspension was then heated to 50 ^oC for 4 hours, and the reaction progress was monitored by TLC. Upon completion of the reaction, the dioxane was removed under vacuum, H_2O (20 mL) was added and the reaction was acidified to pH 2 with HCl (conc.). EtOAc (50 mL) was added, and the organic layer was washed with H_2O (2 x 30 mL), brine (3 x 30 mL), dried over $MgSO_4$, filtered, and the filtrate concentrated *in vacuo* to afford **5-9** (514 mg, 91%) with trace acetic acid as a white solid: ^1H NMR (500 MHz, $CDCl_3$) δ 1.36-1.47 (m, 2H), 1.58-1.66 (m, 1H), 1.66-1.89 (m, 3H), 1.90-1.96 (m, 1H), 2.72-2.78 (m, 2H), 7.27 (d, J = 8.5 Hz, 2H), 7.95 (d, J = 8.5 Hz, 2H); ^{13}C NMR (125 MHz, $CDCl_3$) δ 20.89, 28.49, 29.97, 34.49, 36.49, 40.31, 41.71, 51.98, 94.97, 96.17, 128.10, 128.94, 129.60, 145.69. All data were found to be in agreement with the literature values. [27]

Cyclooctyne-OSu [5-10][28]

To a solution of **5-9** (242 mg, 1.00 mmol), NHS (150 mg, 1.30 mmol) and DMAP (160 mg, 1.30 mmol) in CH_2Cl_2 (10 mL) was added a suspension of DIC (150 mg, 1.30 mmol) CH_2Cl_2 (5 mL) dropwise at room temperature. The resulting solution was stirred for 2 hours and the reaction progress was monitored by TLC. Upon completion of the reaction, H_2O was added (10 mL) and extracted with CH_2Cl_2 (3 x 15 mL). The combined organic layer was washed with brine (3 x 20 mL), dried over $MgSO_4$, filtered, and the filtrate concentrated *in vacuo*. Purification was done by column chromatography on silica gel with increasing amounts of ethyl acetate in hexanes (hexanes:ethyl acetate 1:0 – 2:3) to afford **5-10** (282 mg, 83%) as a white solid: m.p. = 114-115 ^oC; ^1H NMR (500 MHz, $CDCl_3$) δ 1.45 (m, 2H), 1.66 (m, 1H), 1.72-1.91 (m, 3H), 1.98 (m, 1H), 2.10 (m, 1H), 2.15-2.22 (m, 2H), 2.71-2.82 (m, 3H), 2.93 (s, br, 4H), 7.39 (d, J = 8.0 Hz, 2H), 8.09 (d, J = 8.0 Hz, 2H); ^{13}C NMR (125 MHz, $CDCl_3$) δ 20.87, 25.71, 28.50, 29.95, 34.78, 36.45, 40.43, 41.71, 95.40, 95.73, 122.96, 129.52, 130.65, 148.16, 161.86, 169.31. HRMS (ESI) calcd for $C_{20}H_{22}NO_4$ $(M+H)^+$: 340.1549, found 340.1565 (Δ 4.7 ppm, 1.6 mDa). All data were found to be in agreement with literature values.[28]

***N*-*t*-Boc-*N'*-cyclooctyne-PEG3-diamine [5-11]**

To a solution of **5-10** (260 mg, 0.77 mmol) and DMAP (28 mg, 0.23 mmol) in CH_2Cl_2 (5 mL) was added *N*-Boc-PEG3diamine (200 mg, 0.64 mmol) dissolved in CH_2Cl_2 (5 mL). The mixture was stirred at room temperature for 5 hours and the reaction progress was monitored by TLC. Upon completion of the reaction, H_2O was added (10 mL) and extracted with CH_2Cl_2 (3 x 10 mL). The combined organic layer was washed with brine (3 x 10 mL), dried over $MgSO_4$, filtered, and the filtrate concentrated *in vacuo*. Purification was done by column chromatography on silica gel with increasing amounts of ethyl acetate in hexanes (hexanes:ethyl acetate 1:0 – 2:3) to afford **5-11**

(310 mg, 91%) as a colorless oil: 1.40 (m, 2H), 1.42 (s, 9H), 1.58 (m, 1H), 1.65 (m, 2H), 1.66-1.82 (m, 4H), 1.87 (m, 2H), 1.93 (m, 1H), 2.12 (m, 2H), 2.68 (m, 1H), 2.72 (m, 2H), 3.18 (m, 2H), 3.43-3.51 (m, 4H), 3.55-3.63 (m, 4H), 3.66 (m, 6H), 4.93 (s, br, 1H), 7.03 (s, br, 1H), 7.24 (d, J = 8.0 Hz, 2H), 7.71 (d, J = 8.0 Hz, 2H).

***N*-Fmoc-N'-cyclooctyne-PEG3-diamine [5-13]**

To a solution of **5-10** (110 mg, 0.32 mmol) and DMAP (40 mg, 0.32 mmol) in CH_2Cl_2 (5 mL) was added *N*-Boc-PEG3diamineN'TFA (263 mg, 0.29 mmol) dissolved in CH_2Cl_2 (5 mL). The mixture was stirred at room temperature for 5 hours and the reaction progress was monitored by TLC. Upon completion of the reaction, H_2O was added (10 mL) and extracted with CH_2Cl_2 (3 x 10 mL). The combined organic layer was washed with brine (3 x 10 mL), dried over $MgSO_4$, filtered, and the filtrate concentrated *in vacuo*. Purification was done by column chromatography on silica gel with increasing amounts of ethyl acetate in hexanes (hexanes:ethyl acetate 1:0 – 2:3) to afford **5-13** (277 mg, 86 %) as a colorless oil: 1.40 (m, 2H), 1.62 (m, 2H), 1.67-1.78 (m, 3H), 1.79-1.91 (m, 3H), 1.93 (m, 1H), 2.05 (m, 1H), 2.14 (m, 2H), 2.63 (m, 1H), 2.71 (m, 2H), 3.29 (m, 2H), 3.50 (m, 4H), 3.54-3.62 (m, 8H), 4.20 (t, J = 7.0 Hz, 1H), 4.38 (d, J = 6.5 Hz, 2H), 5.37 (s, br, 1H), 6.98 (s, br, 1H), 7.23 (d, J = 7.5 Hz, 2H) 7.30 (t, J = 7.0 Hz, 2H), 7.39 (t, J = 7.0 Hz, 2H), 7.59 (d, J = 7.0 Hz, 2H), 7.68 (d, J = 7.5 Hz, 2H), 7.75 (d, J = 7.5 Hz, 2H).

N-Cyclooctyne-PEG3-diamine [5-14]

To a solution of **5-13** (100 mg, 0.15 mmol) in CH_2Cl_2 (5mL) was added piperidine (1.2 mL) and let stir at room temperature for 2 hours. The reaction progress was monitored by TLC. Upon completion of the reaction, H_2O was added (10 mL) and extracted with CH_2Cl_2 (3 x 10 mL). The combined organic layer was washed with brine (3 x 10 mL), dried over $MgSO_4$, filtered, and the filtrate concentrated *in vacuo* resulting in a yellow oil and a white crystalline solid. The solid was dissolved in hexanes and decanted from the solution (3 x 10 mL) and the resulting residue was dried *in vacuo* to afford crude **5-14** (62 mg, 94%) as a yellow oil and was used directly for the next step: MS (ESI) calcd for $C_{26}H_{41}N_2O_4$, $(M+H)^+$: 445.30, found: 445.3 (M+H).

Alternatively, a solution of **5-10** (100 mg, 0.30 mmol) in CH_2Cl_2 (10 mL) was added dropwise to a solution of PEG3-diamine (650 mg, 3.0 mmol) in CH_2Cl_2 (5 mL) and was allowed to stir at room temperature for 3 hours following completion of addition. The resulting solution was washed with H_2O (3 x 20 mL) and brine (3 x 15 mL), dried over MgSO4, filtered and the filtrate condensed *in vacuo*, resulting in a yellow oil and trace white solid. The oil was dissolved in Et_2O (20 mL), filtered to remove any solid and concentrated to afford **5-14** as a yellow oil (114 mg, 73%): ^{1}H NMR (500 MHz, $CDCl_3$) 1.42 (m, 2H), 1.58 (m, 1H), 1.62 (t, J = 7.0 Hz, 2H), 1.63-2.03 (m, 9H), 2.06 (m, 1H), 2.18 (m, 2H), 2.66 (m, 1H), 2.70-2.81 (m, 4H), 3.45-3.72 (m, 14H), 7.24 (d, J = 7.5 Hz, 2H), 7.35 (S, br, 1H), 7.74 (d, J = 7.5 Hz, 2H); ^{13}C NMR (125 MHz, $CDCl_3$) 20.90, 28.49, 28.90, 29.97, 33.07, 34.81, 36.61, 38.56, 39.62, 40.13, 41.68, 69.50, 70.09, 70.31, 70.41, 70.49,

70.54, 94.83, 96.36, 127.03, 128.93, 132.76, 143.65, 167.31. MS (ESI) calcd for $C_{26}H_{41}N_2O_4$, $(M+H)^+$: 445.30, found: 445.3 (M+H).

SB-T-1214-Linker-PEG3-cyclooctyne [5-15]

To a solution of **4-11** (80 mg, 70 µmol), **5-14** (38 mg, 84 µmol) and DMAP (11 mg, 91 µmol) in in CH_2Cl_2 (3 mL) was added a suspension of EDC·HCl (16 mg, 84 mmol) CH_2Cl_2 (0.5 mL) dropwise at room temperature. The resulting solution was stirred for 5 hours and the reaction progress was monitored by TLC. Upon completion of the reaction, H_2O was added (10 mL) and extracted with CH_2Cl_2 (3 x 10 mL). The combined organic layer was washed with brine (3 x 10 mL), dried over $MgSO_4$, filtered, and the filtrate concentrated *in vacuo*. Purification was done by column chromatography on silica gel with increasing amounts of methanol in CH_2Cl_2 (CH_2Cl_2:methanol 1:0 – 20:1) to afford **5-10** (68 mg, 62%) as a white solid: m.p. = 108-111 ºC; ^{1}H NMR (500 MHz, $CDCl_3$) δ 0.86-0.99 (m, 2H), 1.06-1.15 (m, 2H), 1.14 (s, 3H), 1.23 (s, 3H), 1.28 (d, 3H), 1.34 (s, 9H), 1.36-1.45 (m, 2H), 1.54-1.61 (m, 2H), 1.66 (s, 3H), 1.70-1.97 (m, 5H), 1.72 (s, 3H), 1.74 (s, 3H), 1.90 (s, 3H), 1.99-2.08 (m, 1H), 2.04 (s, 3H), 2.10-2.20 (m, 3H), 2.24-2.42 (m, 2H), 2.35 (s, 1H), 2.48-2.56 (m, 1H), 2.60-2.75 (m, 3H), 2.88 (q, J = 6.5 Hz, 1H), 3.16-3.32 (m, 2H), 3.45 (m, 2H), 3.50 (m, 2H), 3.55 (dd, J = 11.5, 6.0 Hz, 2H), 3.55-3.75 (m, 8H), 3.79 (d, J = 7.0 Hz, 1H), 3.97 (d, J = 21.0 Hz, 1H), 4.05 (m, 2H), 4.17 (d, J = 8.5 Hz, 1H), 7.29 (d, J = 8.5 Hz, 1H), 4.91 (dd, J = 7.0, 10.0 Hz, 1H), 4.87-5.03 (m, 4H), 5.11 (d, J = 7.0 Hz, 1H), 5.66 (d, 7.0 Hz, 1H), 6.11 (s, br, 1H), 6.18 (t, J = 9.0 Hz, 1H), 6.29 (s, 1H), 7.03 (s, br, 1H), 7.20-7.35 (m, 3H), 7.22 (d, J = 8.0 Hz, 2H), 7.47 (t, J = 7.5 Hz, 2H), 7.60 (t, J = 7.5 Hz, 1H), 7.71 (d, J = 8.0 Hz, 2H), 7.78 (m, 1H), 8.11 (d, J = 7.5 Hz, 2H); ^{13}C NMR (125 MHz, CD_3OD) δ 9.17, 9.37, 9.59, 11.47, 13.04, 14.16, 14.84, 18.54, 20.67, 20.72, 20.91, 22.22, 22.47, 22.68, 28.26, 28.51, 29.04, 29.09, 29.99, 31.34, 31.62, 33.53, 33.67, 34.69, 34.83, 35.51, 36.66, 37.63, 37.67, 38.75, 38.79, 40.15, 41.74, 43.21, 45.68, 46.27, 46.42, 58.47, 69.76, 70.04, 70.29, 70.45, 70.51, 71.84, 72.12, 75.08, 75.20, 75.46, 76.42, 79.26, 80.98, 84.52, 94.91, 96.35, 127.02, 127.79. 127.86, 128.32, 128.66, 129.01, 129.30, 130.20, 130.52, 130.58, 131.01, 131.08, 132.64, 133.64, 137.59, 143.84, 167.00, 167.27, 168.19, 172.06, 175.07, 204.13. HRMS (ESI) calcd for $C_{84}H_{112}N_3O_{21}S_2$ $(M+H)^+$: 1562.7230, found: 1562.7192 (Δ -2.4 ppm, -3.8 mDa).

SB-T-1214-Linker-PEG-Arg-N^{10}-TFA-Folate [5-16]

To a solution of **5-3** (3.0 mg, 5 µmol) in methanol (0.5 mL) was added a solution of **5-15** (5.0 mg, 3.5 µmol) in methanol (0.5 mL). The reaction was stirred in the dark at room temperature, and the progress was monitored by LCMS. MS (ESI) cald for $C_{124}H_{165}F_3N_{19}O_{34}S_2$ $(M+H)^+$: 2585.12, found: 863.0466 [(M+3)/3], 1294.0634 [(M+2)/2].

SB-T-1214-Linker-PEG-Arg-Folate [5-17]

To a solution of **5-4** (80 mg, 86.3 µmol) in water (10 mL) was added a solution of **5-15** (120 mg, 76.9 µmol) in ethanol (10 mL) and the resulting yellow solution was stirred at room temperature in the dark for 4 days. During the course of the reaction, a yellow precipitate formed and the

solution became increasingly colorless. After 4 days, the suspension was centrifuged, the supernatant decanted and the solid washed with water and lyophilized to afford **5-17** (80 mg, 40%) as a pale yellow solid: ^{1}H NMR (DMSO-d6, 500 MHz) δ 0.82-1.11 (m, 4 h), 1.06 (s, 3H), 1.12-1.37 (m, 2H), 1.20 (d, J = 6.5 Hz, 3H), 1.24 (S, 3H), 1.39 (s, 9H), 1.43-1.90 (m, 14H), 1.53 (s, 3H), 1.61 (s, 3H), 1.67 (s, 3H), 1.72 (s, 3H), 1.82 (s, 3H), 1.92-2.12 (m, 5H), 2.13-2.30 (m, 4H), 2.34 (s, 3H), 2.66 (m, 1H), 2.72-2.94 (m, 3H), 2.95-3.21 (m, 8H), 3.40-3.52 (m, 20H, overlaps with H_2O), 5.58 (d, J = 7.0 Hz, 1H), 3.76 (m, 1H), 5.89-4.10 (m, 4H), 4.11-4.31 (m, 3H), 4.37 (m, 1H), 4.49 (s, 2H), 7.72 (m, 1H), 4.83 (d, J = 8.0 Hz, 1H), 4.89-5.10 (m, 3H), 5.17 (m, 1H), 5.49 (d, J = 7.0 Hz, 1H), 6.01 (t, 1H), 6.33 (s, 1H), 6.65 (d, J = 6.5 Hz, 2H), 6.95 (m, 2H), 7.22-7.37 (m, 5H), 7.37n (t, J = 7.5 Hz, 1H), 7.55 (t, J = 7.5 HZ, 2H), 7.58-7.72 (m, 4H), 7.75 (t, J = 7.5 Hz, 1H), 7.77 (s, br, 1H), 7.89 (s, br, 1H), 8.02 (d, J = 7.5 Hz, 2H), 8.07 (s, br, 1H), 8.32-8.45 (m, 2H) 8.41-8.49 (m, 1H), 8.65 (s, 1H); ^{13}C NMR (125 MHz, DMSO-d6) δ 8.76, 8.84, 10.24, 13.15, 14.21, 18.36, 20.38, 20.76, 21.51, 21.91, 22.99, 23.96, 24.80, 25.13, 25.96, 26.08, 26.81, 27.73, 27.92, 28.23, 28.39, 29.19, 29.50, 81, 30.03, 31.28, 31.64, 32.06, 32.39, 32.95, 33.06, 35.24, 35.41, 35.89, 36.26, 36.40, 37.05, 37.09, 38.27, 43.49, 45.96, 46.11, 46.40, 46.69, 47.42, 47.69, 49.74, 52.45, 53.03, 53.49, 57.95, 68.52, 68.76, 69.52, 69.82, 70.01, 70.03, 70.14, 70.25, 70.34, 70.88, 71.02, 74.99, 75.12, 75.78, 77.21, 78.59, 80.87, 84.06, 111.75, 120.72, 121.90, 122.44, 127.39, 127.90, 128.40, 128.84, 129.99, 130.40, 131.66, 132.64, 132.85, 133.30, 133.89, 134.57, 136.25, 136.45, 137.31, 139.99, 142.79, 143.35, 143.73, 144.87, 145.55, 149.05, 151.03, 154.36, 155.40, 157.58, 165.60, 166.53, 169.27, 170.07, 170.68, 171.64, 171.94, 172.16, 172.66, 203.03.

§ 5.6.0 References

1. Wagner, C., Biochemical role of folate in cellular metabolism. In *Folate in health and disease*, Bailey, L. B., Ed. CRC Press1995; pp 23-42.
2. Kamen, B., Folate and antifolate pharmacology. *Semin. Oncol.* **1997,** *24*, S18-30-S18-38.
3. Maziarz, K. M.; Monaco, H. L.; Shen, F.; Ratnam, M., Complete mapping of divergent amino acids responsible for differential ligand binding of folate receptors alpha and beta. *J . Biol. Chem.* **1999,** *274*, 11086-11091.
4. Wang, X.; Shen, F.; Freisheim, J. H.; Gentry, L. E.; Ratnam, M., Differential stereospecificities and affinities of folate receptor isoforms for folate compounds and antifolates. *Biochem. Pharmacol.* **1992,** *44*, 1898-1901.
5. Holm, J.; Hansen, S. I.; Hoier-Madsen, M.; Sondergaard, K.; Bzorek, M., Folate receptor of human mammary adenocarcinoma. *APMIS* **1994,** *102*, 413-419.
6. Weitman, R. H.; Coney, L. R.; Fort, D. W.; Frasca, V.; Zurawski, V. R.; Kamen, B. A., Distribution of the Folate Receptor GP38 in Normal and Malignant Cell Lines and Tissues. *Cancer Res.* **1992,** *52*, 3396-3401.
7. Rettig, W.; Garin-Chesa, P.; Beresford, H.; Oettgen, H.; Melamed, M.; Old, L., CEll-surface glycoproteins of human sarcomas: differential expression in normal and malignant tissues and cultured cells. *Proc. Nat. Acad. Sci.* **1988,** *85*, 3110-3114.
8. Toffoli, G.; Cernigio, C.; Russo, A.; Gallo, A.; Bagnoli, M.; Boicchi, M., Overexpression of folate binding protein in ovarian cancers. *Int. J. Cancer* **1997,** *74*, 193-198.

9. Leamon, C. P.; You, F.; Santhapuram, H. K.; Fan, M.; Vlahov, I. R., Properties influencing the relative binding affinity of pteroate derivatives and drug conjugates thereof to the folate receptor. *Pharm. Res.* **2009,** *26*, 1315-1323.
10. Westerhof, G. R.; Schornagel, J. H.; Kathmann, I.; Jackman, A. L.; Rosowsky, A.; Forsch, R. A.; Hynes, J.; Boyl, F. T.; Peters, G. J.; Pinedo, H. M.; JAnsen, G., Carrier- and receptor-mediated transport of folate antagonists targeting folate-dependent enzymes: Correlates of molecular structure and biological activitiy. *Mol. Pharmacol.* **1995,** *48*, 459-471.
11. Leamon, C. P.; Jackman, A. L., Exploitation of the Folate Receptor in the Management of Cancer and Inflammatory Disease. In *Vitamins and Hormones*, Litwack, G., Ed.2008; pp 203-233.
12. Vlahov, I. R.; Leamon, C. P., Engineering Folate-Drug Conjugates to Target Cancer: From Chemistry to Clinic. *Bioconjugate Chem.* **2012,** *23*, 1357-1369.
13. Ladino, C. A.; Chari, R. V. J.; Bourret, L. A.; Kedersha, N. L.; Goldmacher, V. S., Folate-maytansinoids: Target-selective drugs of low molecular weight. *Int. J. Cancer* **1997,** *73*, 859-864.
14. Steinberg, G.; Borch, R. F., Synthesis and evaluation of pteroic acid-conjugated nitroheterocyclic phosphoramidates as folate receptor-targeted alkylating agents. *J. Med. Chem.* **2001,** *44*, 69-73.
15. Lee, J. W.; Lu, J. Y.; Low, P. S.; Fuchs, P. L., Synthesis and evaluatoin of taxol-folic acid conjugates as targeted antineoplastics. *Bioorg. Med. Chem. Lett.* **2002,** *10*, 2397-2414.
16. Aronov, O.; Horowitz, A. T.; Gabizon, A.; Gibson, D., Folate-targeted PEG as a potential carrier for Carboplatin analogs. Synthesis and in vitro studies. *Bioconjugate Chem.* **2003,** *14*, 563-574.
17. Butterworth, C. E.; Baugh, C. M.; Krumdieck, C., A study of folate absorption and metabolism in man utilizing carbon-14-labeled polyglutamates synthesized by the solid phase method. *J. Clin. Invest.* **1969,** *48*, 1131-1142.
18. Vlahov, I. R.; Santhapuram, H. K.; Kleindl, P. J.; Howard, S. J.; Stanford, K. M.; Leamon, C. P., Design and regioselective synthesis of a new generation of targeted chemotherapeutics. Part 1: EC145, a folic acid conjugate of desacetylvinblastine monohydrazide. *Bioorg. Med. Chem. Lett.* **2006,** *16*, 5093-5096.
19. Vlahov, I. R.; Vite, G. D.; Kleindl, P. J.; Wang, Y.; Santhapuram, H. K.; You, F.; Howard, S. J.; Kim, S.; Lee, F. F.; Leamon, C. P., Regioselective synthesis of folate receptor-targeted agents derived from epothilone analogs and folic acid. *Bioorg. Med. Chem. Lett.* **2010,** *20*, 4578-4581.
20. Vlahov, I. R.; Wang, Y.; Kleindl, P. J.; Leamon, C. P., Design and regioselective synthesis of a new generation of targeted chemotherapeutics. Part II: Folic acid conjugates of tubulysins and their hydrazides. *Bioorg. Med. Chem. Lett.* **2008,** *18*, 4558-4561.
21. Vlahov, I. R.; Santhapuram, H. K. R.; Wang, Y.; Kleindl, P. J.; You, F.; Howard, S. J.; Westrick, E.; Reddy, J. A.; Leamon, C. P., An Assembly Concept for the Consecutive Introduction of Unsymmetrical Disulfide Bonds: Synthesis of a Resleasable Multidrug Conjugate of Folic Acid. *J. Org. Chem.* **2007,** *72*, 5968-5967.
22. Sausville, E.; LaRusso, P.; Quinn, M.; Forman, K.; Leamon, C.; Morganstern, D.; Bever, S.; MEssmann, R., A phase I study of EC145 administered weeks 1 and 3 of a 4-week cycle in patients with refractory solid tumors. *Proc. Am. Soc. Clin. Oncol* **2007,** *25*, 2577.
23. Reddy, J. A.; Dorton, R.; Westrick, E.; Dawson, A.; Smith, T.; Xu, L. C.; Vetzel, M.; Kleindl, P.; Vlahov, I. R.; LEamon, C. P., Preclinical evaluation of EC145, a folate-vinca alkaloid conjugate. *Cancer Res.* **2007,** *67*, 4434-4442.
24. Nauman, R.; Coleman, R.; Burger, R.; Herzog, T.; Morris, R.; Sausville, E.; Kutarska, E.; Ghamande, S.; Gabrail, N.; Pasquale, S. D.; Nowara, E.; Gilbert, L.; Caton, J.; Gersh, R.;

Teneriello, M.; Harb, W.; Konstantinopoulos, P.; Symanowski, J.; Lovejoy, C.; Messmann, R., Precedent: a randomized phase II trial comparing EC145 and pegylated liposomal doxorubicin (PLD) in combination, versus PLS alone, in subjects with platinum-resistant ovarian cancer. *Am. Soc. Clin. Oncol. Ann. Meeting* **2010**, abstract 5045.
25. Leamon, C. P.; Reddy, J. A.; Klein, P. J.; Vlahov, I. R.; Dorton, R.; Bloomfield, A.; Nelson, M.; Westrick, E.; Parker, N.; Bruna, K.; Betzel, M.; Gehrke, J. S.; Messmann, R. A.; LoRusso, P. M.; Sausville, E. A., Reducing undesiralbe hepatic clearance of a tumor-targeted vinca alkaloid via novel saccharopeptidic modifications. *J . Pharmacol. Exp. Therp.* **2011,** *336*, 336-343.
26. Willibald, J.; Harder, J.; Sparrer, K.; Conzelmann, K.-K.; Carell, T., Click-Modified Anandamide siRNA Enables Delivery and Gene Silencing in Neuronal and Immune Cells. *J. Am. Chem. Soc.* **2012,** *134*, 12330-12333.
27. Agard, N. J.; Baskin, J. M.; Prescher, J. A.; Lo, A.; Bertozzi, C. R., A comparative study of bioorthogonal reactions with azides. *ACS Chem. Biol.* **2006,** *1*, 644-648.
28. Shelbourne, M.; Chen, X.; Brown, T.; Afaf, A., Fast copper-free click DNA ligation by the ring-strain promoted alkyne-azide cycloaddition reaction. *Chem. Comm.* **2011,** *47*, 6257-6259.

Chapter 6

Towards the Radiolabeling of SB-T-1214

Content

§ 6.0.0 Isotopic Labeling in Pharmaceutical Development

During preclinical development of tumor-targeting drug conjugates, it is important to map the biodistribution of the conjugate *in vivo*. An accurate understanding of where a conjugate accumulates in the body can facilitate the development of improved targeting strategies by predicting off-target side effects before potential drugs enter costly preclinical and clinical evaluation. Furthermore, every potential pharmaceutical agent must undergo extensive preclinical testing before an investigation new drug (IND) application is filed with the FDA. As part of this process, an extensive review of the pharmacokinetic parameters in mammalian systems must be presented including the ADME profile of the active agent. Isotopic labeling of pharmaceuticals is a powerful tool to facilitate preclinical and clinical development of drug candidates.[1] Stable isotope labeling, commonly done through the incorporation of ^{13}C or ^{2}H, has been widely employed to study the metabolism of drug candidates *in vivo* and can be used to provide standards for the quantification of drug concentration using mass spectrometry. Metastable isotopes with long half-lives, such as ^{14}C or ^{3}H, are useful for assessing protein binding *in vitro* and the ADME properties of the compound *in vivo*.[2] Many meta-stable radioisotopes undergo β+ decay, and can be used in positron emission tomography (PET), a powerful tool that is able to image the *in vivo* biodistribution of chemicals in real time.[3]

§ 6.0.1 Positron Emission Tomograpy

Positron emission, also known as β+ decay, describes the process through which a proton in a meta-stable nucleus is converted to a neutron by releasing a positron and an electron neutrino. As positrons and electrons are antiparticles, an annihilation event occurs upon the collision of both particles and two 511 -keV γ-rays are released in opposite directions. In the case of PET, positron-emitting nuclei are built into organic compounds and administered into living systems. The ubiquitous presence of water and other electron-rich biological molecules facilitates the annihilation process, and γ-rays are emitted from a close proximity to the decay event. Detection of these γ-photons pairs and calculation of the time differential between the two antiparallel detection events allows the position of annihilation event to be inferred. In this way, the radiolabeled chemical can be traced throughout the body, and images constructed in areas of high compound concentration. As there is little absorption of γ-radiation in living tissue, there is essential no depth limitation for constructing PET images, which is a major advantage compared to optical imaging techniques.[3]

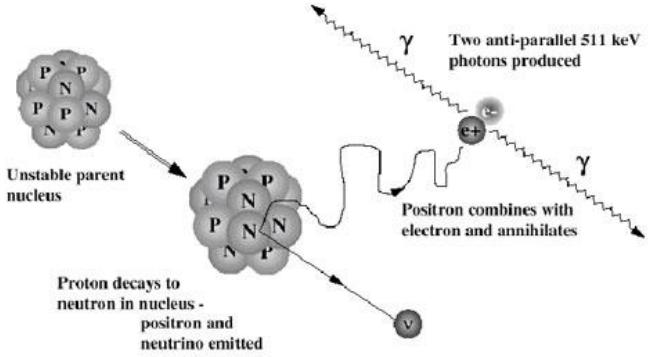

Figure 6-1: β+ decay and positron/electron annihilation (adapted from [3])

The half-lives of positron-emitting radionucleotides vary greatly. Two commonly used nuclei are ^{11}C and ^{18}F, with decay half-lives of ~20 minutes and ~180 minutes respectively. Recently ^{124}I, with a half-life of 4.2 days, has become increasingly utilized in quantitative pharmacological PET studies. Ideally, the decay rate of the radionucleotide should be suited for the scope of the study.[1, 3]

§ 6.0.2 Electron Emission Decay and Liquid Scintillation Counting

The other form of beta decay, β- decay, results from the conversion of a neutron to a proton within a metastable nucleus and is accompanied by the emission of an electron and an electron antineutrino. This process is usually lower in energy than a β+ decay and the decay process has a substantially longer half-life. For example, ^{14}C and ^{3}H (tritium) emit β particles with average energies of 49 keV and 5.7 keV through decay processes with half-lives of 5730 and 12.3 years, respectively. The low-energy radiation has very little tissue penetration, barely penetrating a layer of dead skin. Therefore, the preferred method of detection for these experiments is liquid scintillation counting.

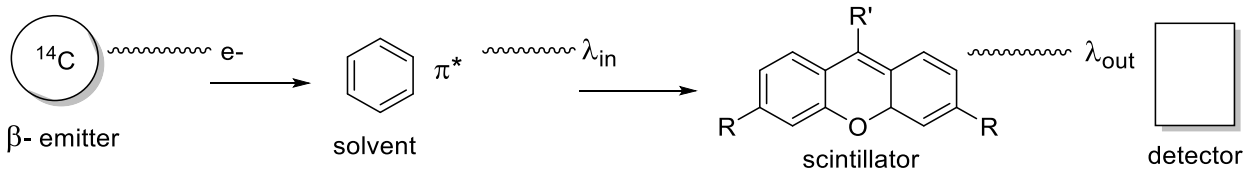

Figure 6-2: β- decay, solvent excitation and scintillation

In liquid scintillation counting, the sample is dispersed in an organic solvent containing surfactants and scintillators. Scintillators are fluorescent compounds which can absorb the energy emitted by the radiation and emit a photon of a specific wavelength. These photons are typically amplified by the counting machine, allowing for quantitative determination of the concentration

of analyte in the sample. This technique is frequently employed to assess the binding of organic compounds to biologically relevant proteins such as P-gp or HSA.[1, 4] Using compounds labeled with β- emitting nuclei, a variety of pharmacokinetic properties can be quantified *in vivo* including tissue distribution, clearance rate, plasma concentration and routes of excretion.[4] Therefore, labeling with ^{14}C is an excellent tool that can greatly streamline the preclinical and early clinical analysis of pharmaceuticals.

§ 6.0.3 Radiolabeling of Taxanes in Clinical Use

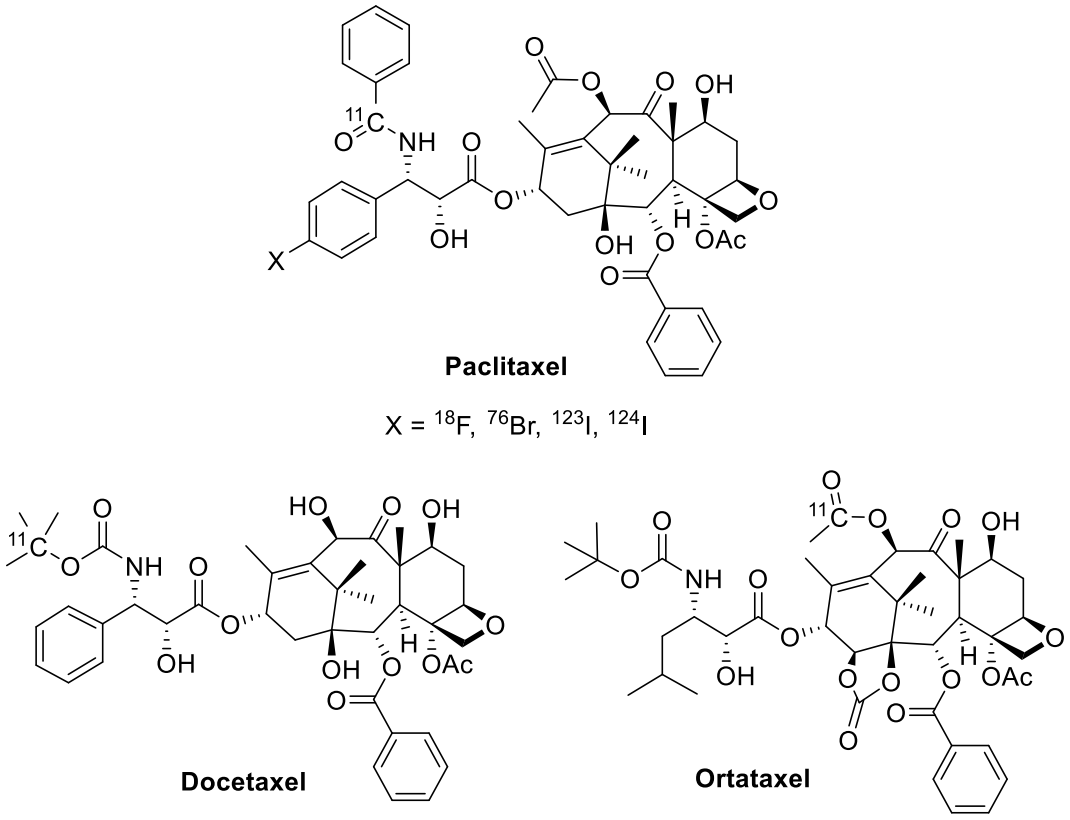

Figure 6-3: Clinical taxanes labeled with β+ emitting nuclei

Of the seven taxanes in clinical use as anticancer agents, five have been labeled with radioactive nuclei and of those five, paclitaxel, docetaxel and ortataxel have been labeled with β+ emitting nuclei for PET (**Figure 6-3**). Paclitaxel has been labeling using ^{11}C at the C3'N- carbonyl[5] as well as with ^{18}F, ^{76}Br and ^{124}I at the para position of the C3' phenyl ring.[6] In addition, ^{123}I, used for SPECT imaging, has been introduced at this position.[7] As paclitaxel is a known Pgp substrate, this fluorinated paclitaxel analogue has been used to visualize MDR *in vivo* in mice and non-human primates.[8, 9] Docetaxel has been labeled with ^{11}C at the quaternary carbon of the C3'N-*t*-Boc group, and this compound was used to assess the biodistribution of docetaxel in patients with advanced solid tumors.[10, 11] Ortataxel was labeled with ^{11}C at the C10 acetyl carbonyl carbon.[12] Both

cabazitaxel and mirataxel have been labeled with ^{14}C to study Pgp-mediated efflux at the blood brain barrier and ADME properties, respectively.[13, 14] All of these compounds were labeled using standard nucelophillic substitution and acylation chemistry. However, with the advent of transition metal-mediated cross coupling reactions, powerful new methods for carbon-carbon bond formation have emerged and many of them are currently being refined for applications to the radiolabeling of pharmaceuticals.[15]

§ 6.0.4 Applications of the Stille Coupling for ^{11}C Labeling

The palladium-mediated cross coupling of organohalides and organotin, known as the Stille coupling, was first discovered in the late 1970's[16] Since then, it has become one of the most widely used cross coupling reactions in organic synthesis and continues to be commonly employed in medicinal chemistry. Out of all of the cross coupling reactions, it is among the most versatile and permits the use of sp2 and sp3 organohalides with sp, sp2 and sp3 organostannanes. A variant of the Stille coupling first developed by Farina uses a copper(I) co-catalyst to enhance the rate of the reaction.[17, 18] The basic mechanism for the Stille Coupling is shown in **Figure 6-4**.

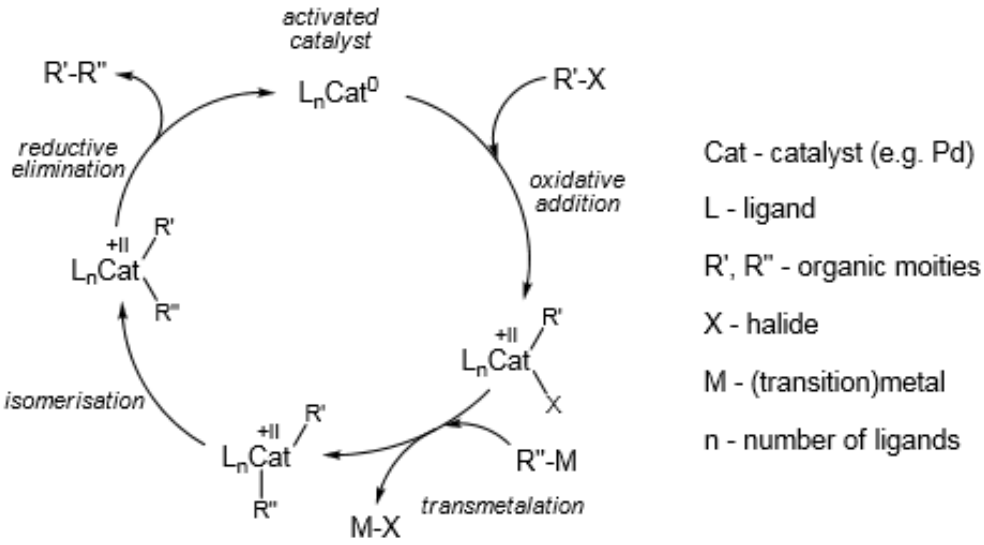

Figure 6-4: Mechanism of the Pd-catalyzed Stille coupling (adapted from [15])

The first step in the Still coupling is an oxidative addition of the organohalide to the Pd(0) species, forming the Pd(II) complex (**Figure 6-4**). Although it was originally hypothesized that the Cu(I) acted solely as a scavenger for excess ligand, later studies suggested in some systems it was also involved in an initial transmetalation step from Sn to Cu, forming an organocuprate. This intermediate then rapidly undergoes a second transmetalation step from Cu to Pd to afford the *trans*-bis-alkyl palladium complex. As transmetalation from Sn to Pd is the rate-limiting step in the Stille coupling, the formation of the organocuprate intermediate can greatly increase the speed

of overall reaction.[18] The *trans*-Pd complex then undergoes a *cis/trans* isomerization to give **the** *cis*-Pd complex, which can then go through reductive elimination to afford the cross-coupled product and regenerate the Pd(0) catalyst. Due to the versatility, speed and robustness of the reaction, as well as the availability of ^{11}C methyl iodide, the Stille coupling has become the most commonly applied cross coupling reaction in the radiolabeling of organic molecules.

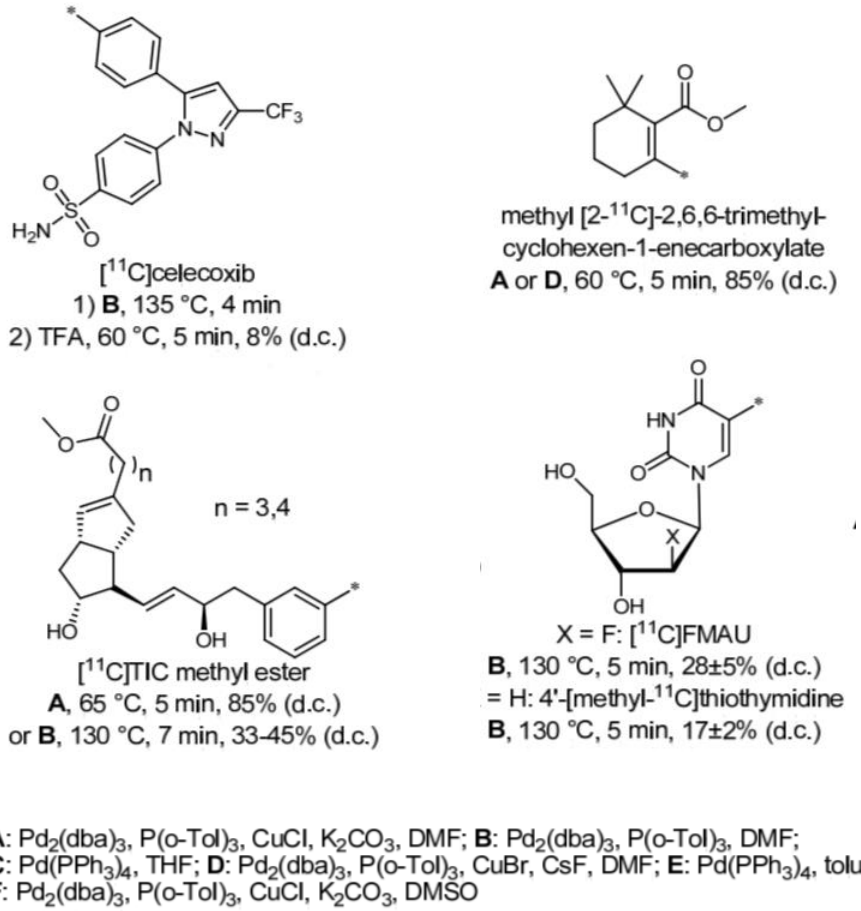

A: $Pd_2(dba)_3$, P(o-Tol)$_3$, CuCl, K_2CO_3, DMF; **B**: $Pd_2(dba)_3$, P(o-Tol)$_3$, DMF;
C: $Pd(PPh_3)_4$, THF; **D**: $Pd_2(dba)_3$, P(o-Tol)$_3$, CuBr, CsF, DMF; **E**: $Pd(PPh_3)_4$, toluene;
F: $Pd_2(dba)_3$, P(o-Tol)$_3$, CuCl, K_2CO_3, DMSO

Figure 6-5: Selected compounds radiolabeled by Stille couplings with methyl iodide (adapted from [15])

The first application of the Stille coupling to ^{11}C labeling was reported in 1995 when simple aryl and vinyl organostannanes were radiolabeled with methyl iodide with decay-corrected radiochemical yields (RCY) that varied from 30 to 85%.[19, 20] Since then, many biologically active small molecules have been labeled with ^{11}C using modified Stille couplings, a few examples of which are shown in **Figure 6-5**.[15] Celecoxib®, a non-steroidal anti-inflammatory drug (NSAID) and selective COX-2 inhibitor, was labeled by using the conditions shown in **Figure 6-5**, albeit in only 8% RCY, due to the required TFA deprotection step after coupling.[21] Utilizing a vinyl stannane, 2,6,6-trimethylcyclohexenyl carboxylic methyl ester, a potential ligand for the nicotinic

acetylcholine receptor, was radiolabeled with ^{11}C.[22] A modified prostacyclin, tetranorisocyclin (TIC) methyl ester, is among the most structurally complex compounds to have been radiolabeled by a Stille coupling.[23-25] In addition, the nucleoside (2'-deoxy-2'-fluoro-β-d-arabinofuranosyl)-thiothymidine (FMAU) has been labeled using a Stille coupling with the corresponding vinyl stannane.[26] Radiolabeled nucleosides, such as FMAU, have been used to the imaging of cell proliferation.[27]

§ 6.1.0 Design of a 3'-Vinylstannyl SB-T-1214 Derivative for Site-Specific Radiolabeling

To directly visualize the effect of conjugation on tumor specificity *in vivo*, PET imaging studies of both free drug and drug conjugates should be done, and the tumor accumulation of the two compared. As SB-T-1214, currently the leading cytotoxin in our lab, does not possess any fluorine atoms, the only realistic option for obtaining its biodistribution profile by radiolabeling is to use ^{11}C labeling.

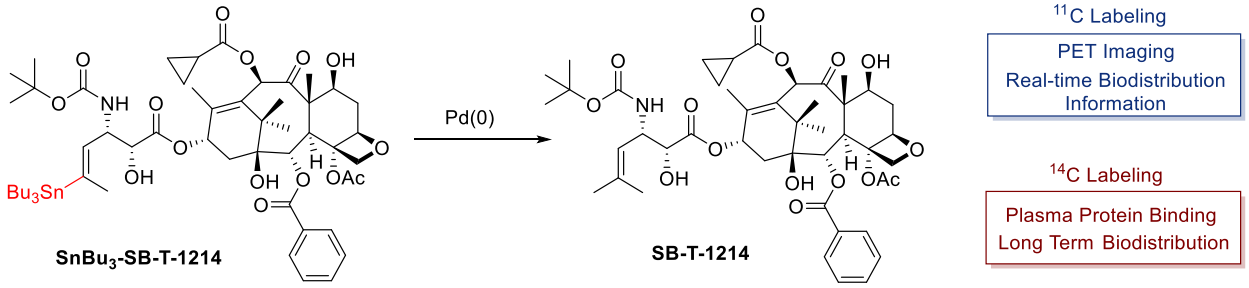

Figure 6-6: 3'-Vinylstannyl-SB-T-1214 as an Intermediate for Radiolabeling

To provide access to site-specific radiolabeling of SB-T-1214, an intermediate is necessary that can be quickly reacted to yield the unmodified SB-T-1214. The speed of the reaction is especially important with respect to ^{11}C labeling, due to the relatively short half-life to the radionucleotide. For these reasons, a Stille coupling was envisioned as an ideal reaction for the introduction of the radiolabeled group. Therefore, 3'-vinylstannyl-SB-T-1214 was designed as the final intermediate for a Stille coupling with the appropriate radiolabeled methyl iodide. Using this synthetic intermediate, facile access may be granted to both ^{11}C- and ^{14}C-labeled SB-T-1214 without changing the native structure of the taxoid. As both β+ and β- emitting radionucleotides can be incorporated into the structure using this intermediate, both sets of complementary PK data can be obtained without redesign and resynthesis of the compound. This methodology may be extended to the radiolabeling of tumor-targeted drug conjugates to expedite their advancement through preclinical evaluation.

§ 6.1.1 Retrosynthetic Analysis of 3'-Vinylstannyl SB-T-1214

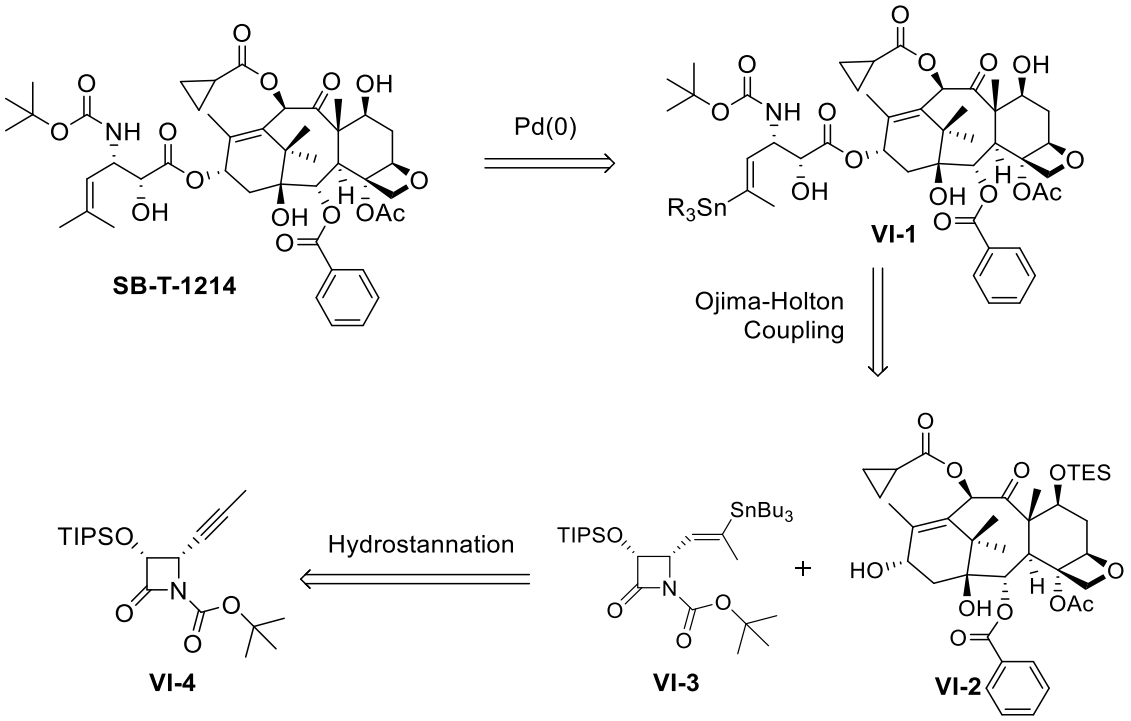

Figure 6-7: Retrosynthetic analysis for the ^{11}C labeling of SB-T-1214

The retrosynthetic analysis for the radiolabeling of **SB-T-1214** is given in **Figure 6-7**. It was envisioned that SB-T-1214 can be labeled at the last synthetic step by methylation at the C3' position of the respective vinyltrialkyltin taxoid **VI-1** through a Pd-catalyzed Stille coupling. This trialkyltin taxoid can be synthesized *via* the Ojima-Holton coupling of the modified baccatin component **VI-2** with the vinylstannyl β-lactam **VI-3**. As there are many known examples of the synthesis of vinylstannanes from alkynes, attention was turned to the synthesis of enantiopure 4-propargyl β-lactam **VI-4**.

§ 6.2.0 Attempted Synthesis of 6-2 from 4-Formyl β-Lactam 2-10

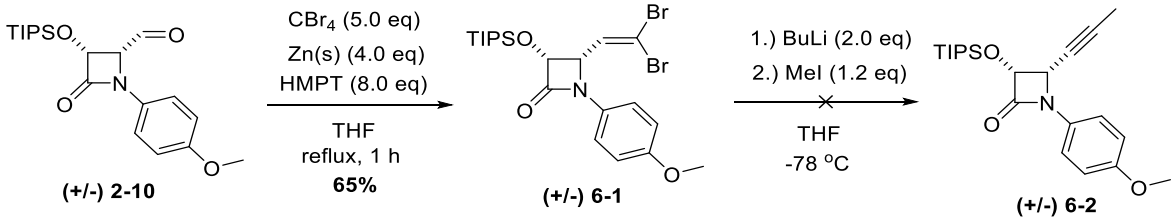

Scheme 6-1: Attempted formation of **6-2** using the Corey-Fuchs reaction

As 4-formyl β-lactam **2-10** was already in hand, racemic **2-10** was used to test direct conversion of the aldehyde to the alkyne *via* a Corey-Fuchs reaction (**Scheme 6-1**). Traditional

Corey-Fuchs conditions utilizing triphenylphosphine produced the desired product in only 8% isolated yield. However, using analogous conditions that were employed in the synthesis of difluorovinyl β-lactam, dibromovinyl β-lactam **6-1** was synthesized in good yield. Conversion of **6-1** did not prove to be successful, and both attempts to generate the alkyne resulted the exclusive formation of byproducts derived from the addition of the butane anion to the β-lactam. Therefore, attention was turned to the more direct route of synthesizing the desired 4-propargyl β-lactam from the corresponding imine.

§ 6.2.1 Synthesis of Racemic Vinylstannyl-β-lactam

Therefore, a racemic β-lactam with a propargyl substitution at C4 was prepared to test reaction conditions for the hydrostannation. The synthesis of this intermediate is outlined in **Scheme 6-2**.

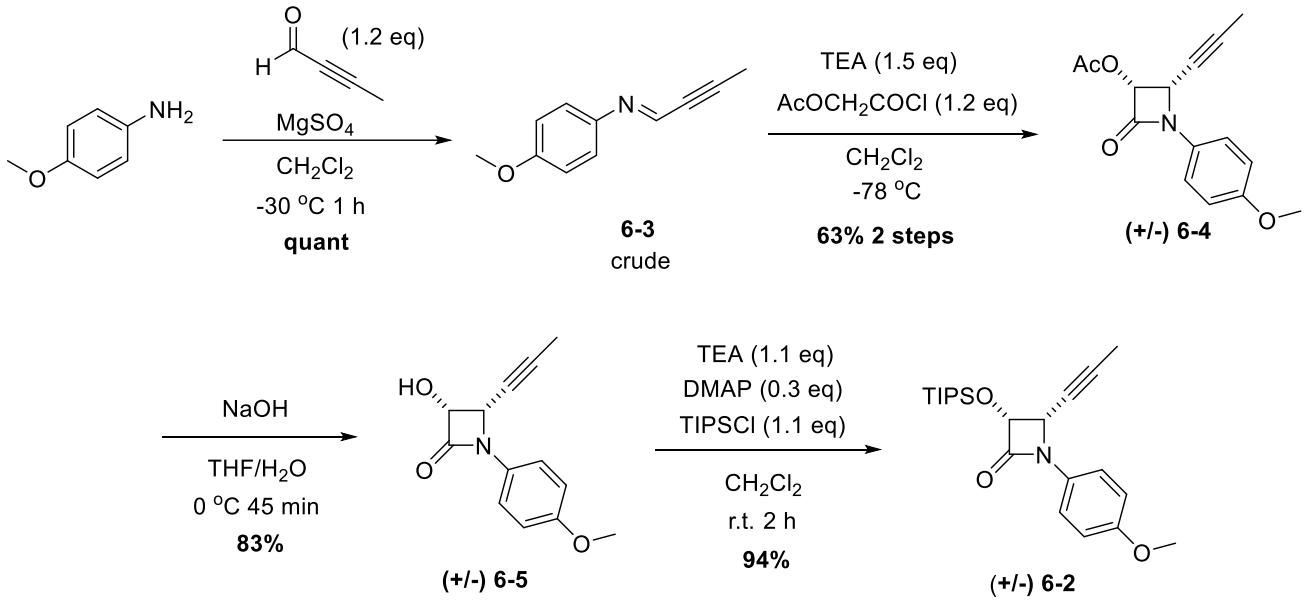

Scheme 6-2: Synthesis of **(+/-) 6-2** via a Staudinger [2+2] cycloaddition

Oxidation of but-2-ynol with $KMnO_4$ gave 2-butynal in low yield after distillation, although this low yield is likely due to loss of the volatile material during distillation. Imine formation proceeded quite rapidly as compared to the isobutenyl aldehyde, and cooling was necessary to avoid degradation of the product. Formation of β-lactam **6-4** via the Staudinger reaction proceeded in good yield after purification. Hydrolysis and TIPS protection afforded the racemic intermediate **6-2**.

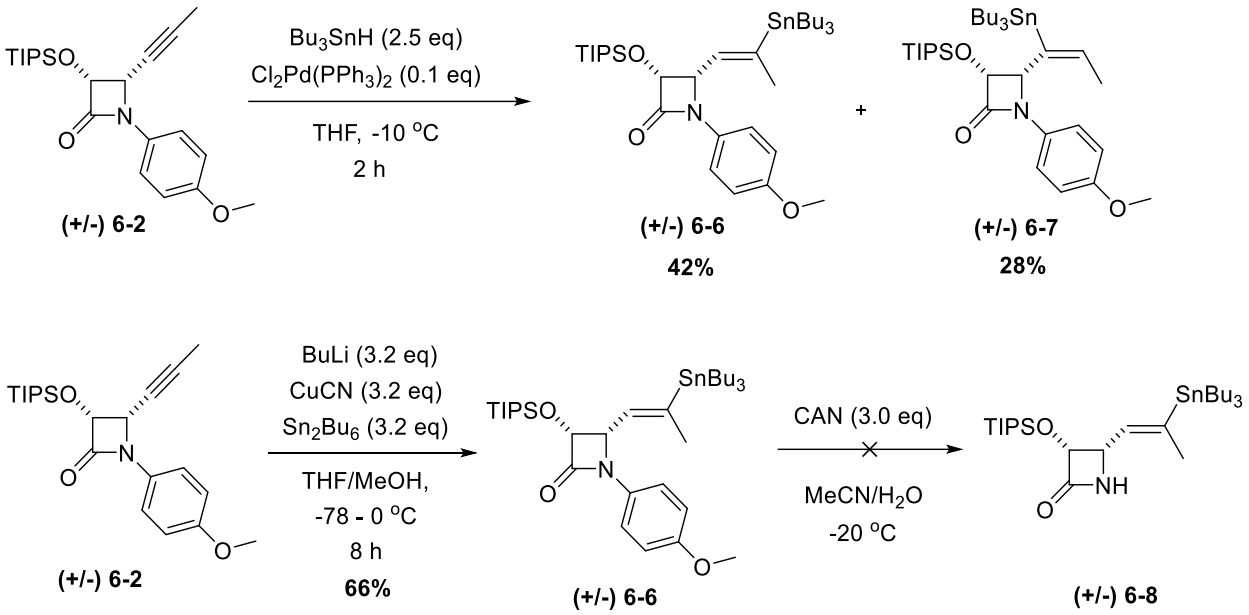

Scheme 6-3: Hydrostannation of alkynyl β-lactam **6-2**

With **6-2** in hand, conditions were tested for the addition of the tributyl tin group to the alkyne (**Scheme 6-3**). Palladium catalyzed hydrostannation produced a mixture of regioisomers that could be partially separated by column chromatography. Cooling of the reaction mixture to -40 °C resulted in a slight increase in the ratio of desired product. Using a stannylcupration method, exclusive formation of the desired regioisomer was achieved and it could be isolated cleanly in decent yield. Unfortunately, the vinyl stannyl β-lactam did not survive CAN deprotection, and rapid degradation of the product was observed.

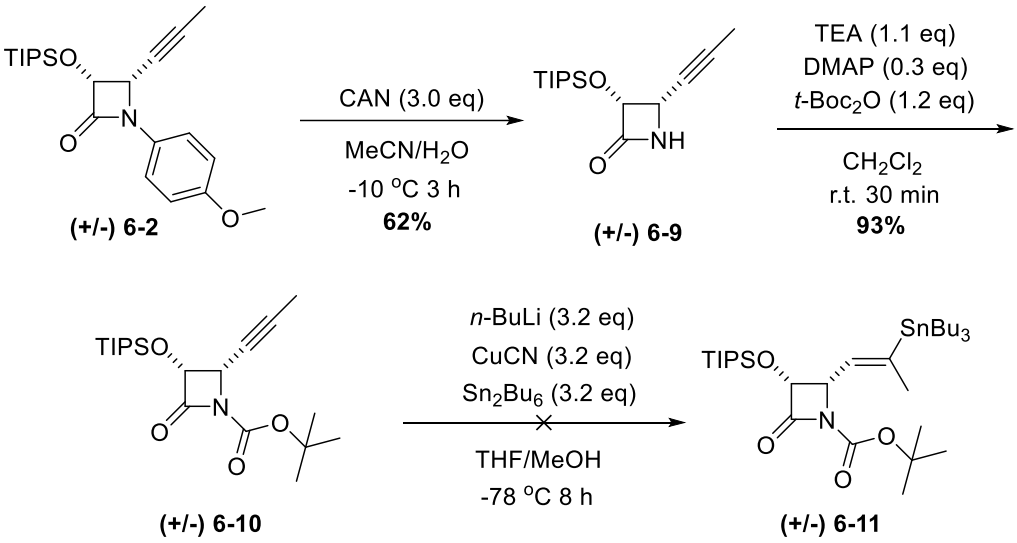

Scheme 6-4: Synthesis towards β-lactam **6-11**

As expected, PMP deprotection of the alkynyl β-lactam **6-2** proceeded and **6-9** was obtained in good yield. Subsequent Boc protection produced intermediate **6-10**. Unfortunately, stannylcuptration of this intermediate resulted in the ring-opened methyl ester, formed by methoxide at C2. It may be possible, however, to run the reaction in the absence of methanol. With the chemistry worked out up to this point, attention was shifted to enantioselective synthesis of the desired β-lactam.

§ 6.2.2 Synthesis of Enantioenriched β-lactam (+) 6-2

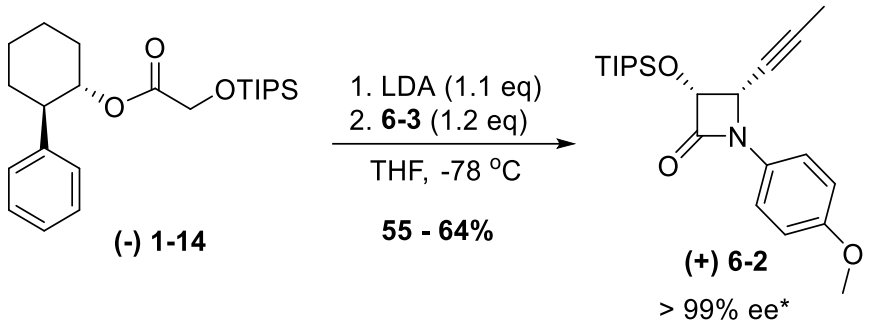

Scheme 6-5: Chiral Ester Enolate-Imine Cyclocondensation to form **(+) 6-2**

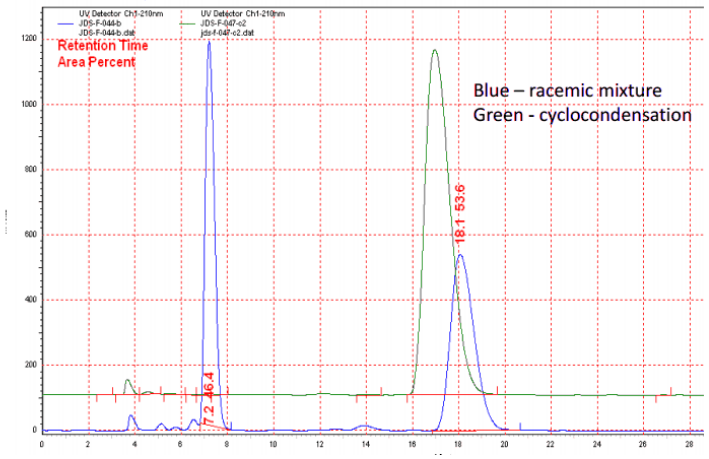

Figure 6-8: Chiral HPLC trace of **(+) 6-2** from cyclocondensation compared to **(+/-) 6-2**

As the chiral ester enolate-imine cyclocondensation was shown to be sensitive to the bulk of the chiral auxiliary component and hydroxyl protecting group and less susceptible to influence by the alkyl moiety on the imine, it was theorized that β-lactam **(+) 6-2** could be synthesized in good enaniomeric excess using this method. The enolate derived from chiral ester **1-14** (Synthesis outlined in Section 1.2) was condensed with **6-3** to form highly enantioenriched β-lactam **5-5**. Following recrystallization from cold hexanes, HPLC analysis revealed no presence of the undesired enantiomer. Thus, this reaction can be employed to reproducibly produce enantiopure β-lactam **(+) 6-2**.

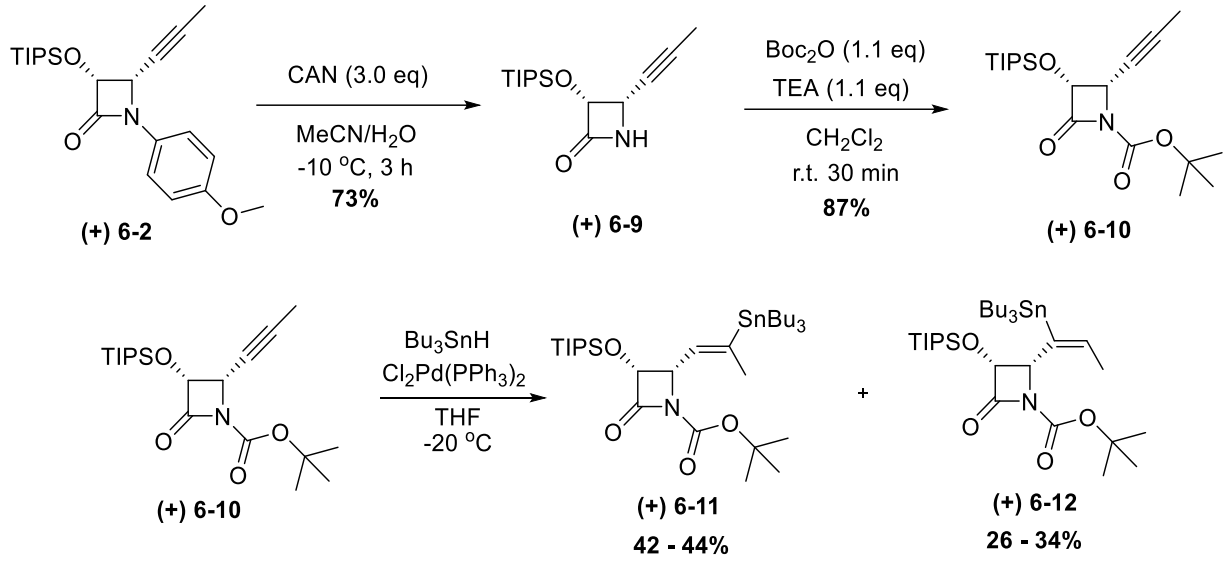

Scheme 6-6: Synthesis of key vinylstannyl β-lactam **(+)-6-11**

CAN deprotection of **(+) 6-2** afforded the free amide **(+) 6-9** in good yield, and subsequent *t*-Boc protection afforded the desired 4-propargyl β-lactam **(+) 6-10**. As stannylcupration did not work on the racemic material, radical hydrostannation was employed, and the desired product in modest yield following stringent column purification. The regiochemistry of these two vinylstannanes was confirmed using NMR coupling constants and COSY analysis.

§ 6.2.3 Synthesis of Vinylstannyl Taxoids 6-14 and 6-16

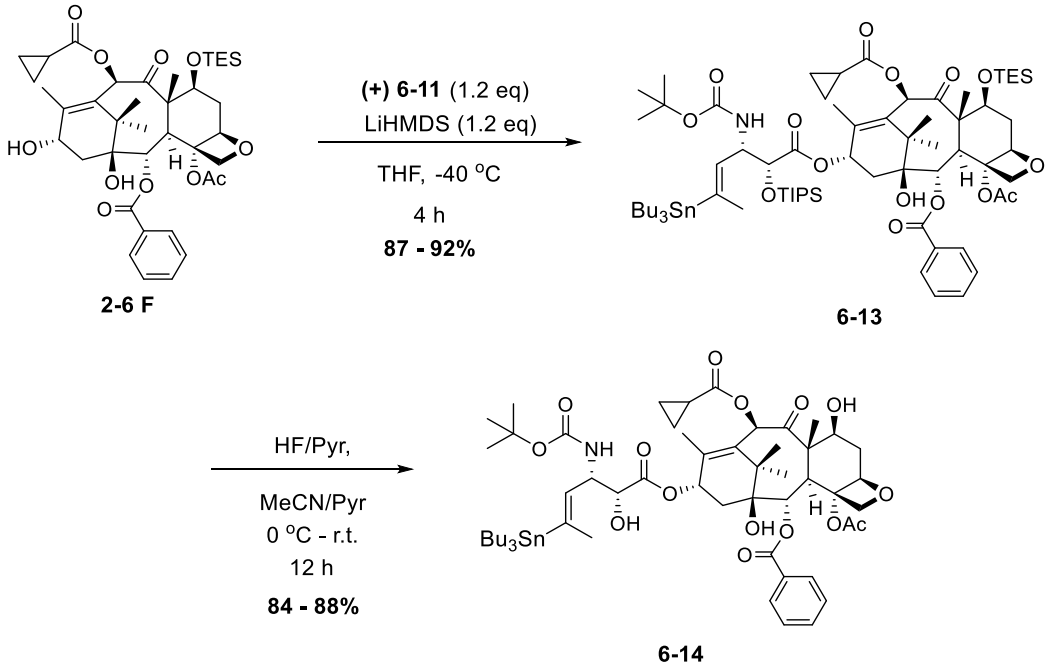

Scheme 6-7: Synthesis of target compound **6-14**

Ojima-Holton coupling of β-lactam **(+) 6-11** to baccatin **2-6 F** proceeded in good isolated yield and deprotection of the silyl groups afforded the vinyltributylstannyl taxoid **6-14**. This compound was synthesized on the >600 mg scale.

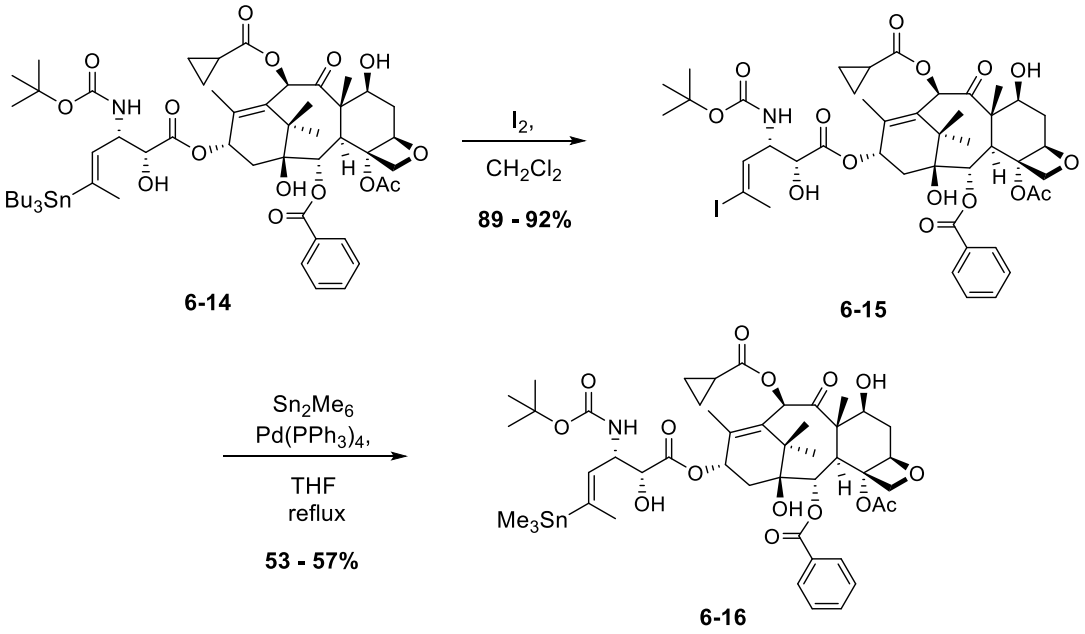

Scheme 6-8: Conversion of **6-14** to **6-16** *via* vinyliodo-taxoid **6-15**

A trimethyltin group was also introduced at the C3' vinyl position as shown in **Scheme 6-8**. Treatment of **6-14** with iodine rapidly formed the desired vinyl iodide **6-15** in excellent isolated yield. Using a Pd-catalyzed coupling, the trimethyl tin group was introduced in modest yield. When toluene was used as the solvent, only the formation of a byproduct was observed. The success of this reaction to form **6-16** was important, as it showed that the vinyl-palladium complex was stable and capable of undergoing reductive elimination. However, in the Stille coupling, the transmetalation step is rate limited, not the oxidative addition, so this precedent did not necessarily ensure the success of the reaction for radiolabeling. With both vinyltrialkylstannanes in hand, reaction conditions for the Stille coupling were screened.

§ 6.3.0 Reaction Condition Screening on Model Compound 6-11

A preliminary screen for Stille coupling conditions on taxoid **6-14** had failed using conditions that had previously been optimized for vinylstannanes. These conditions, utilizing tri-(o-toyl)-phosphine, $PdCl_4$, a copper (I) salt and a base resulted in degradation of the material. LCMS analysis of one of these conditions showed that one of the degradation products showed eluted in the region of the chromatogram where the product should elute. After iterations of these conditions proved to be futile, resulting in either no reaction (without copper) or degredation.

Therefore, a screen of conditions was performed on the β-lactam **6-11** to find any product formation.

The results obtained from this screen are presented in **Table 6-1**. One equivalent of methyl iodide was used and the reaction was allowed to run for 24 hours. Reaction mixtures were analyzed by TLC and HPLC and compared to an authentic sample of isobutenyl β-lactam **1-6**. Because no reaction was observed in the absence of copper (I), different combinations of copper salts and palladium catalysts were screened.

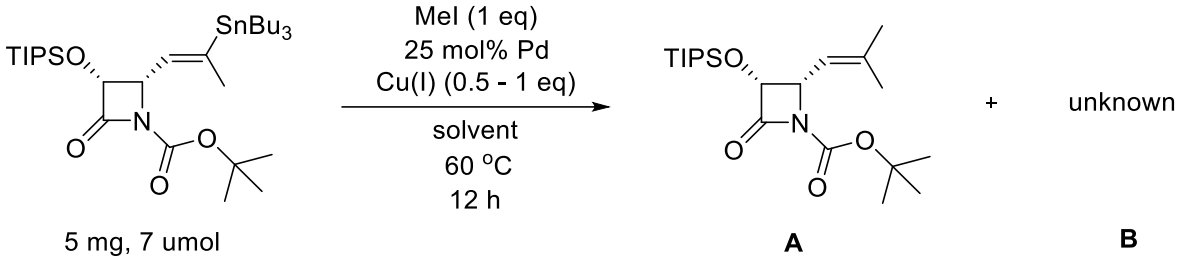

5 mg, 7 umol

A

B

Entry	Solvent	Pd	Ligand	Cu	Conversion*	Result**
1	THF	$Pd(PPh_3)_4$	-	CuCl	~50%	messy
2	THF	$Pd(PPh_3)_4$	-	CuBr	~50%	messy
3	THF	$Pd(PPh_3)_4$	-	CuI	~50%	messy
4	THF	$Pd(PPh_3)_4$	-	CuTC	~50%	messy
5	DMF	$Pd(PPh_3)_4$	-	CuCl	>90%	B only
6	DMF	$Pd(PPh_3)_4$	-	CuBr	>90%	B only
7	DMF	$Pd(PPh_3)_4$	-	CuI	>90%	B only
8	DMF	$Pd(PPh_3)_4$	-	CuTC	>90%	1:1 A:B
9	DMF	$Pd_2(dba)_3$	P(*o*-tol)$_3$	CuCl	~40%	messy
10	DMF	$Pd_2(dba)_3$	P(*o*-tol)$_3$	CuBr	~40%	messy
11	DMF	$Pd_2(dba)_3$	P(*o*-tol)$_3$	CuI	>80%	messy
12	DMF	$Pd_2(dba)_3$	P(*o*-tol)$_3$	CuTC	>80%	messy

Table 6-1: Initial screening for methylation of model compound **6-11**

When THF was used as the solvent with palladium tetrakis, all conditions were messy, with no peak corresponding to the desired product (**Table 6-1**, Entries 1-4). As DMF is a better trap for methyl iodide, it was used as a solvent and the reactions were found to be significantly cleaner than THF using the same conditions. However, only the combination of palladium tetrakis

and copper thiophenecarboxylate (CuTC) appeared to contain product in addition to a single byproduct that was observed exclusively using other copper salts (**Table 6-1**, Entries 5-8). As the combination of $Pd_2(dba)_3$ and $P(o\text{-}tol)_3$ was reported to be effective in promoting these couplings, it was also tested on this system. No base was used, as conditions utilizing fluoride or carbonate had led to degradation of the taxoid. However, only degradation products were observed with these conditions, even on the model system (**Table 6-1**, Entries 9-12). With one condition showing promising results (**Table 6-1**, Entry 8), attempts were made to translate this information into a successful coupling on the taxoid system.

§ 6.3.1 Reaction Condition Screening on Vinylstannyl Taxoids

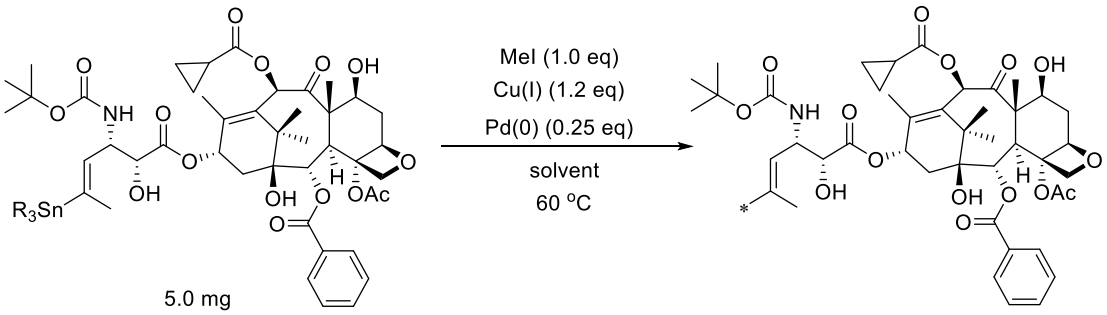

Entry	R	Solvent	Pd	Cu	Conversion	Result
1	Bu	DMF	$Pd(PPh_3)_4$	--	0	N/A
2	Bu	THF	$Pd(PPh_3)_4$	-	0	N/A
3	Bu	DMF	$Pd(PPh_3)_4$	CuCl	~10%	messy
4	Bu	DMF	$Pd(PPh_3)_4$	CuBr	~10%	messy
5	Bu	DMF	$Pd(PPh_3)_4$	CuI	~10%	messy
6	Bu	DMF	$Pd(PPh_3)_4$	CuTC	~30%	m/z = 854
7	Me	DMF	$Pd(PPh_3)_4$	CuTC	~30%	messy

Table 6-2: Screening of Stille coupling conditions on vinylstannyl taxoids **6-14** and **6-16**

As the previous screen on β-lactam had shown the cleanest results were obtained for mixtures of $Pd(PPh_3)_4$ with copper (I) salts in DMF, these conditions were screened on vinylstannyl taxoid **6-14** using a 24 hour reaction time. Each reaction was analyzed by TLC and LCMS with comparison to an authentic sample of SB-T-1214. First, the reaction was run in the absence of copper in both DMF and THF (**Table 6-2**, Entries 1 and 2). In both of these conditions, there was absolutely no conversion, even after 24 hours. Therefore, it was deduced that copper (I) was required to facilitate the transmetalation to palladium in this system. The combination of $Pd(PPh_3)_4$ with four copper (I) salts was tested (**Table 6-2**, Entries 3-6) but the results paralleled

those obtained with β-lactam **6-12**, and the desired product was only obtained using $Pd(PPh_3)_4$ and CuTC. To compare the reactivity profile of the different alkyltin taxoids, the trimethyltin taxoid **6-16** was subjected to the same conditions, but the reaction mixture was complicated and no product appeared to be formed (**Table 6**-2, Entry 7).

§ 6.3.0 First Attempt at Cold Labeling of SB-T-1214

With a working combination of palladium catalyst and copper co-catalyst, a model reaction was done using 1.0 equivalent of methyl iodide for 30 minutes to assess conversion and product formation by LCMS. Although in the hot labeling conditions, the reaction time will only be 5 minutes, a 10-40 fold excess of vinylstannane will be used, which should significantly enhance the reaction rate.

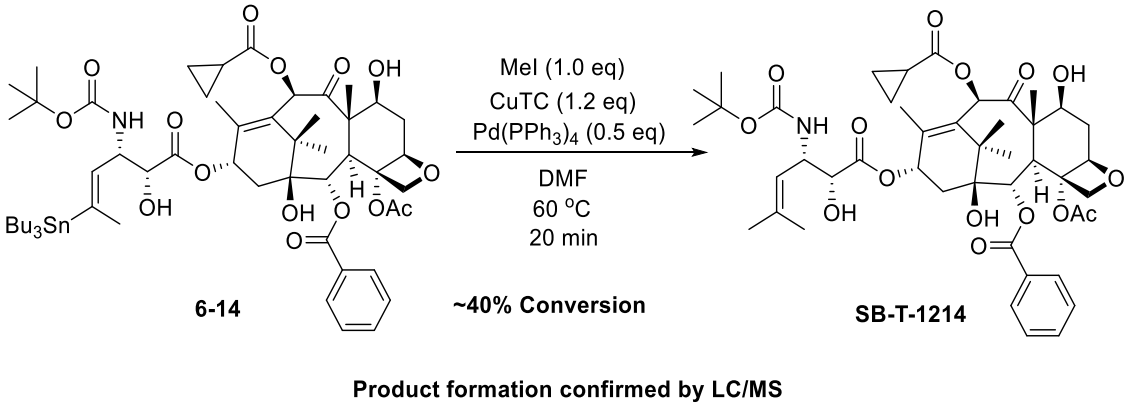

Scheme 6-9: Cold methylation to form SB-T-1214

The conditions for the cold labeling model reaction are shown in **Scheme 6-9**. The CuTC co-catalyst was used stoichiometrically, at 1.2 equivalents and 50 mol% of palladium tetrakis was employed. The reaction was conducted in DMF at 60 °C and after 20 minutes, the reaction mixture was diluted directly with an equal volume of methanol, subjected to solid phase extraction and injected directly into the LCMS for analysis. The results of the LCMS analysis are shown in **Figures 6-9** and **6-10**.

The entire chromatogram is given in **Figure 6-19**. The first peak out is the solvent front, with the DMF being washed out rapidly from the column. Just after that is peak at 2 minutes with a strong absorbance at 215 nm. In control experiments run in the absence of methyl iodide, this peak was not present, and it does not have a mass spectrum that correlates to any taxoid species. Therefore, it is likely to be the result of the excess methyl iodide, and does not interfere with the isolation of the desired product. Smaller peaks appear later in the chromatogram at around 13 min, 20 min, 22.5 min, 30.5 min and 38 min. **Figure 6-10** shows a magnification of this region for the ease of analysis. The peak at 38 min is remaining starting material, vinylstannane **6-14**.

The first peak to elute from this region has an m/z value of 854.4, corresponding to the m/z value of SB-T-1214 (**Figure 6-10**). It possesses the characteristic fragmentation pattern observed with this taxoid, and the isotopic ratio matches that of SB-T-1214 with no evidence for the presence of tin. When compared to an authentic sample of SB-T-1214, the elution times under the exact same HPLC conditions were essentially the same and only differed only by a fraction of a minute. Therefore, it is logical to conclude that this peak, eluting at 13 minutes is SB-T-1214 formed by the Stille coupling. Although 13 minutes is too long of an elution time for HPLC purification in a hot ^{11}C reaction, there are no closely eluting impurities, and it is likely that the HPLC conditions can be optimized cleanly elute the material in the time frame necessary for the hot chemistry (~4-6 min).

Figure 6-9: Full HPLC trace of first methylation

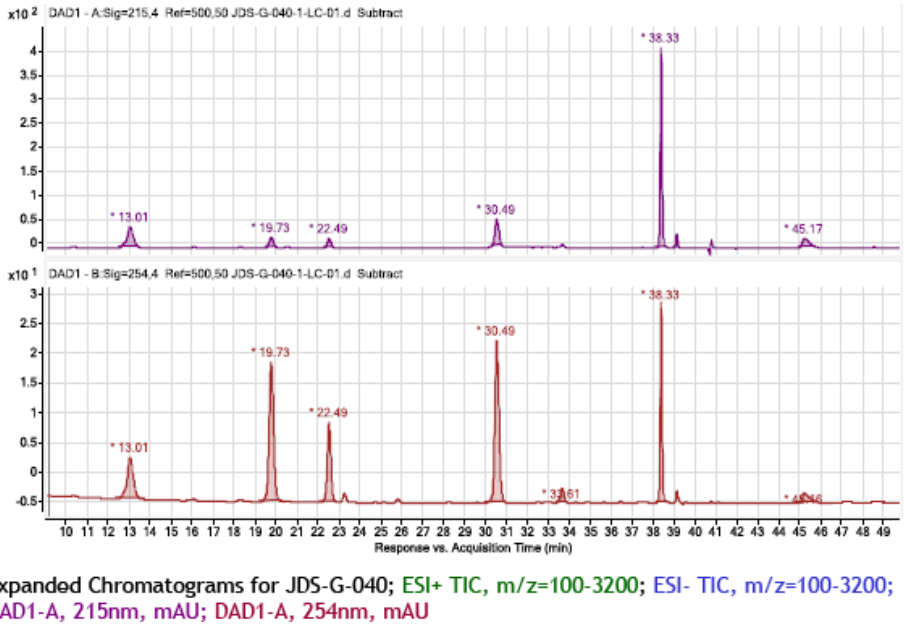

Figure 6-10: Close up on LC region containing taxoid reaction components

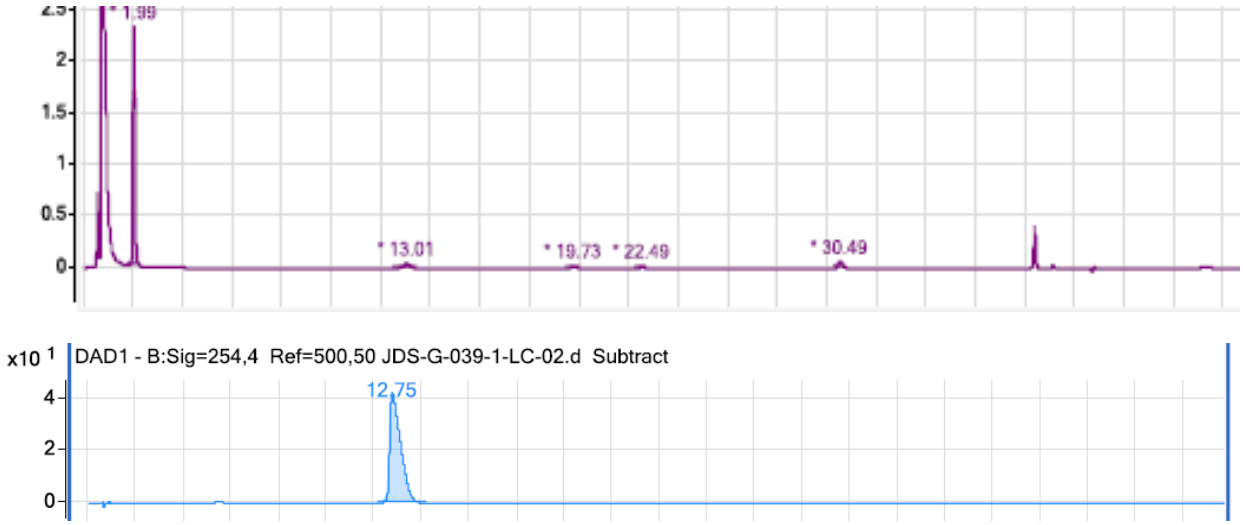

Figure 6-11: Comparison of reaction mixture (*top*) LC trace with standard sample of SB-T-1214 (*bottom*)

Analysis of the mass spectrum of the peak eluting at 20 minutes revealed that it too was a taxoid with no modification to the baccatin core, as evidenced by the same fragmentation pattern of SB-T-1214. However, the parent ion did not have an isotope pattern corresponding to a tin-containing species, and the m/z of the parent ion was found to be 966.3, explained by the formation of vinyl iodo taxoid **6-15**. The proposed mechanism for the formation of both **SB-T-1214** and **6-15** is outlined in **Figure 6-12**.

The formation of the desired product is easily explained by a copper co-catalyzed Stille coupling mechanism in which the copper catalyzes the rate-limiting transmetalation step by the formation of the vinylcuprate intermediate (**Figure 6-12**). This can then undergo a second transmetalation step from the copper to the Pd(II) complex to form the vinyl-palladium species, which can then undergo reductive elimination in the standard manner to afford SB-T-1214. However, during the copper to palladium transmetalation, iodide is released from the Pd(II) complex either as the free anion or as copper(I) iodide. Oxidation of the iodide leads to the formation of iodine radical, which can then react with another equivalent of the vinylstannane **6-14** to afford the vinyliodo taxoid **6-15**. This is plausible as the reaction to form the vinyliodo taxoid from the vinylstannane and I_2 proceeded rapidly and completely (**Scheme 6-8**). This impurity does not interfere with the formation or isolation of labeled SB-T-1214, so efforts have not been made to suppress the formation of this byproduct.

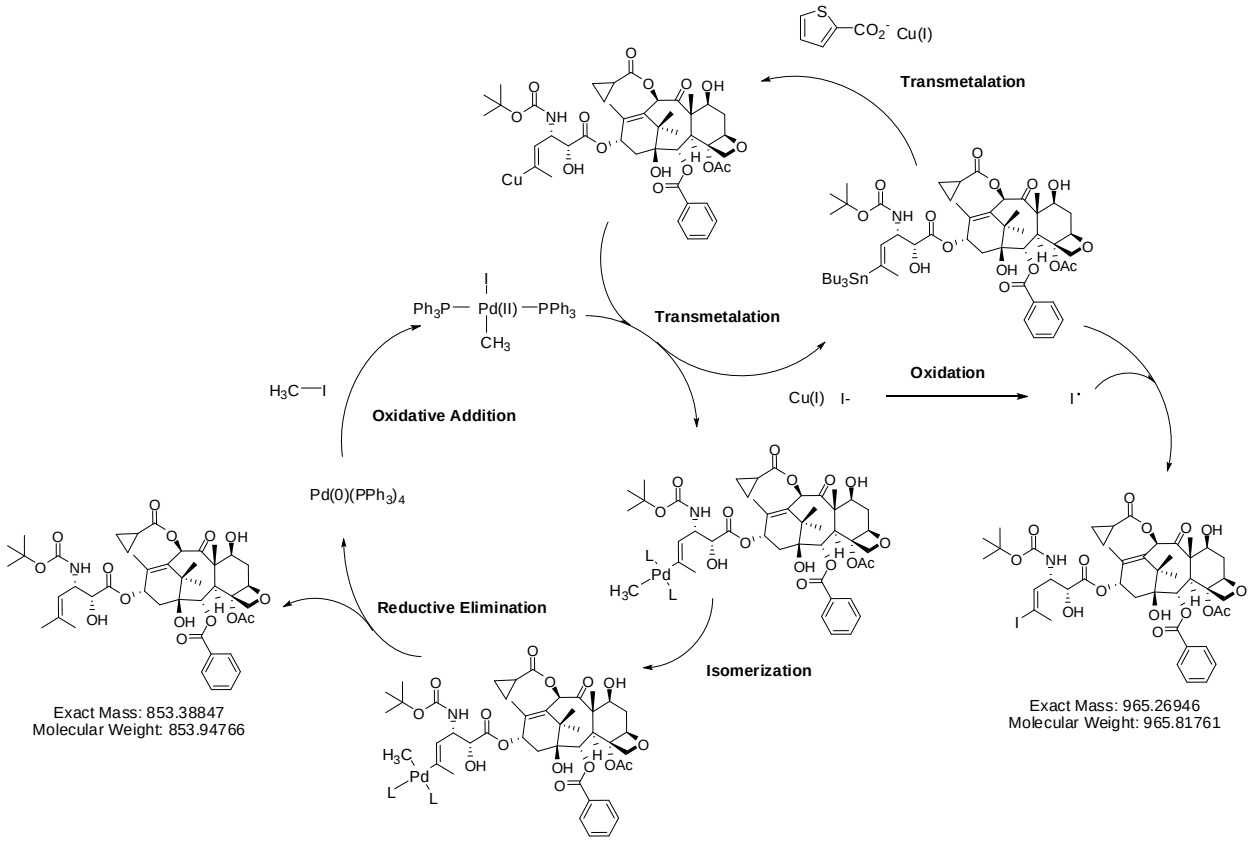

Figure 6-12: Proposed Mechanism for Formation of **SB-T-1214** and **6-15**

The third peak, eluting at 22.5 minutes, can be identified as a taxoid with an unmodified baccatin core due to the characteristic fragmentation pattern observed in the mass spectrum. In addition to the allylic cation fragmentation, the major ions in the positive ionization mode have m/z values of 860.4 and 916.4, while the major m/z values found in negative ionization were 974.4 and 1028.4. These can be explained by a parent compound with a molecular mass of 915.6, with acetate and TFA adducts appearing in the negative mode. The m/z value appearing at 860.4 may be a fragmentation of the parent ion. However, at the moment, not enough evidence is available for the accurate determination of a plausible structure for this impurity.

§ 6.3.1 Second Attempt at Cold Labeling of SB-T-1214

With evidence that the Stille coupling was capable of producing SB-T-1214 from one equivalent of methyl iodide, the reactants were scaled back by a factor of ten. This reaction was run to investigate if the product could be formed in a 5 minute time frame using the conditions shown in **Scheme 6-10**. The work up and analysis by LCMS was performed in a similar fashion to the previous reaction

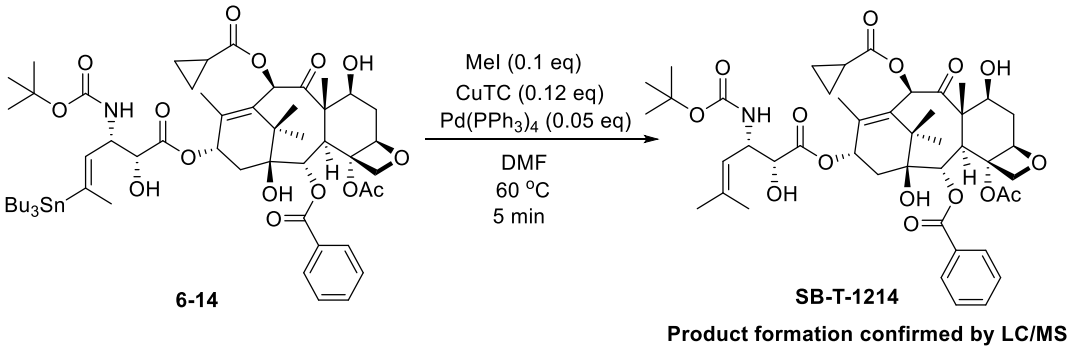

Scheme 6-10: Second cold methylation conditions

The LC chromatogram for this reaction is shown in **Figure 6-13**. A similar, albeit slightly more complex, trace was obtained from this crude reaction, with the four characteristic taxoid peaks appearing at 13.2 min, 20.1 min, 22.8 min and 30.7 min. As expected, the ratio of product to starting material is much smaller for this run, but a discernable peak at 13.16 minutes can be seen.

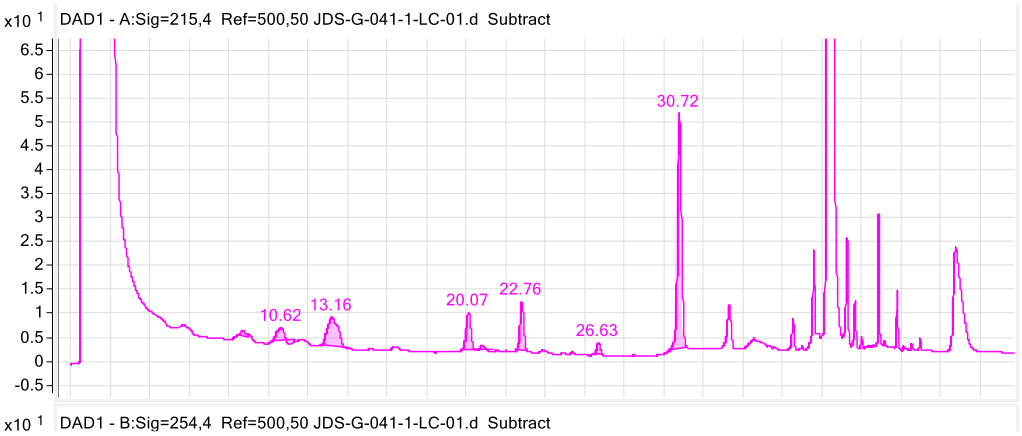

Figure 6-13: LC trace from second cold methylation

Although this result was promising in that it demonstrated product formation in a short time frame acceptable for radiolabeling with ^{11}C, analysis of the product peak by mass spectrometry uncovered an unexpected problem. In addition to the characteristic mass peaks for SB-T-1214, m/z values of 838.4, 855.4, 860.4 and 876.4 were found in the mass spectrum of the peak at 13.16 min. These values correspond to a parent ion with a molecular mass of 837.4, as well as its ammonium, sodium and potassium adducts, respectively. This compound, which did not appear in the mass spectrum of the previous cold labeling experiment, is possibly the C3' allenyl taxoid. This impurity can be generated by a β-hydride elimination of the vinyl palladium complex, competing with the reductive elimination that produces SB-T-1214 (**Figure 6-14**). Although unexpected in this system, vinyl palladium complexes are known to undergo β-hydride elimination leading to the formation of allenes.[28]

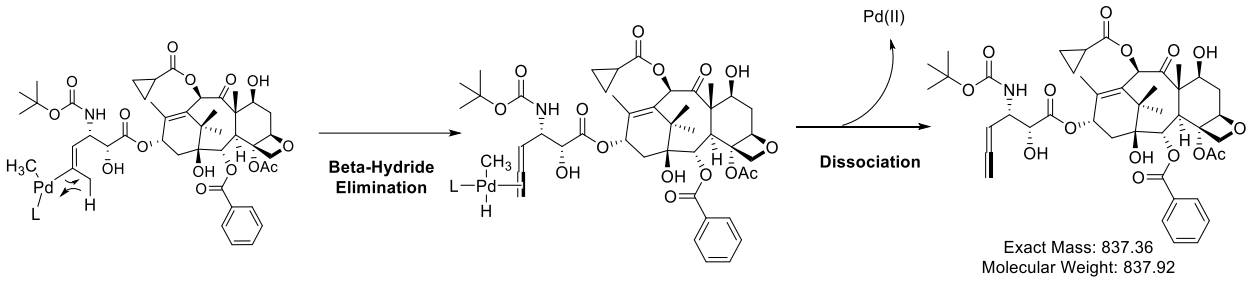

Figure 6-14: Proposed allenyl impurity and mechanism of formation

As the C3'-allenyl taxoid differs only slightly in structure from the desired SB-T-1214, it is not surprising that co-elutes with the product if it is formed during the course of the reaction. It does not, however, incorporate the labeled carbon into the structure and as a result it not only decreases the purity of the product, its formation would decrease the radiochemical yield of the reaction. Therefore, conditions must be developed that avoid its formation and consequently improving the purity and yield of the desired product.

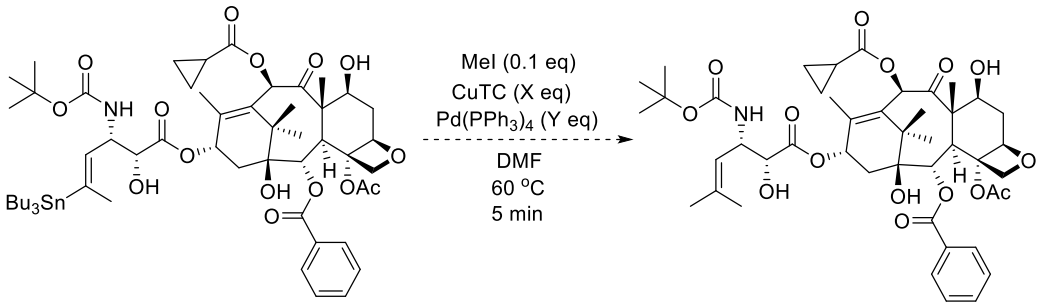

Scheme 6-11: Proposed reaction optimization by adjusting Cu and Pd ratio

Copper (I) salts have been shown not only to act as cocatylsts through formation of organocuprates, they are also well known ligand scavengers. Also, β-hydride eliminations generally require a free coordination site on the palladium and typically occur from three-coordinate palladium complexes. It is likely that this reaction is sensitive to the ratio between the CuTC and the $Pd(PPh_3)_4$, as an excessively high concentration of copper (I) salts may sequester free triphenylphosphine, shifting the equilibrium towards three-coordinate palladium species. Therefore, reactions using 0.1 equivalents of methyl iodide with different ratios of $Pd(PPh_3)_4$ to CuTC will be analyzed by LCMS to find the optimal ratio of Pd to Cu that will suppress the formation of this byproduct and maximize the radiochemical yield of ^{11}C-SB-T-1214.

§ 6.4.0 Vinyliodo taxoids for PET- and SPECT-Based Theranostics

Iodine has been widely employed as an imaging agent for the labeling of proteins and peptides. The two most common metastable isotopes are ^{123}I ad ^{124}I, which can be used for SPECT and PET imaging, respectively.[29, 30] As both isotopes possess long half lives of 13 hours for ^{123}I

and 4.2 days for ^{124}I, they can be used for long-term biodistribution studies of pharmaceuticals.[30] Therefore, a versatile method for the site-specific iodine labeling of taxoid conjugates would be highly desirable and could potentially be of great use in preclinical and clinical evaluation of taxoid-based tumor-targeting drug conjugates.

Iodine is commonly used to label sp2-hybridized carbons via nucleaophillic or electrophilic substitution reactions.[29] In addition, methods have been worked out for the specific labeling of peptides and proteins at tyrosine residues.[29] Electrophillic iodine reacts rapidly with organostannanes in a high yielding and highly regioselective manner, and as such, as become one of the preferred methods for the radiolabeling of organic compounds. Using this methodology, a variety of complex organic molecules have been labeled including a modified morphine (analgesic), purpurinimide (a porpherine derivative) and IML06-08 (EGFR inhibitors).[31-33] As electrophilic substitution of **6-14** (**Scheme 6-8**) occurred almost instantaneously to produce vinyl-iodo taxoid **6-15**, it is envisioned that this reaction could be employed for the labeling of different taxoid conjugates bearing vinylstannyl taxoid **6-14**. As a prototype system, a biotin conjugate, **6-19**, was synthesized.

§ 6.4.1 Synthesis of Labeling-Ready BLT-S Conjugate

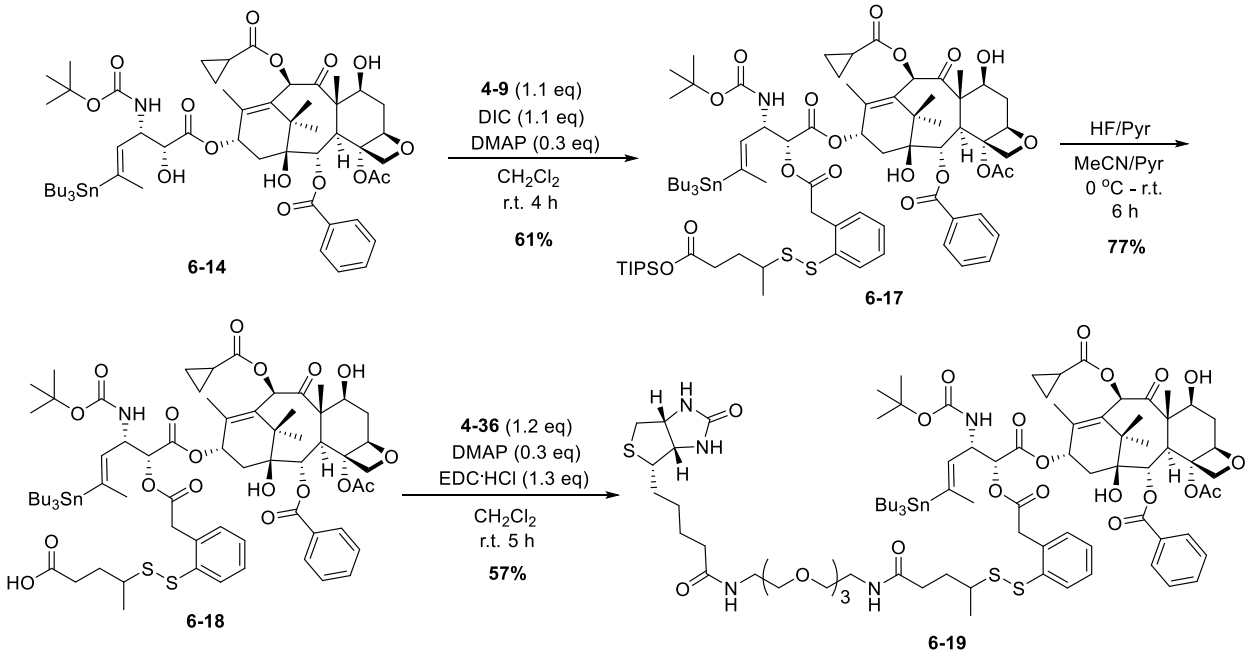

Scheme 6-12: Synthesis of vinyl-stannyl BLT-S conjugate **6-19**

The synthesis of the labeling-ready bearing biotin-PEG-linker-vinylstannyl-taxoid conjugate, **6-19**, is outlined in **Scheme 6-12**. Vinylstannyl taxoid **6-14** was coupled to the methyl

branched linker **4-9** using standard DIC coupling conditions. Following HF/pyridine deprotection, the free acid, **6-18**, was coupled to biotin-PEG3-amine in modest yield to afford the desired conjugate **6-19**. The synthesis of this conjugate is easily scalable to produce material for in vivo tests, as was done with the production of the **BLT-S** conjugate in Section 4.3.0.

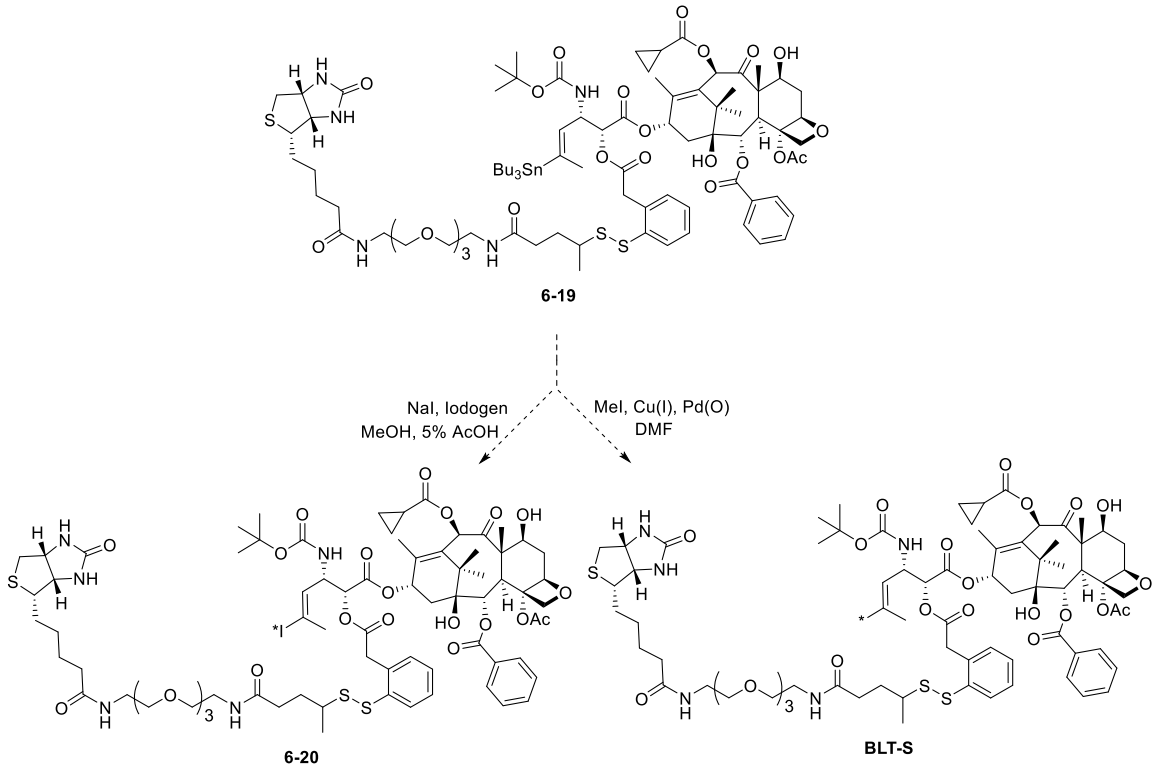

Scheme 6-13: Proposed methods for the labeling of **6-19**

Biotin conjugate **6-19** is potentially a versatile intermediate for radiolabeling. First, it is possible that the conditions for the Stille coupling of **6-14** can be adoped to afford the labeled BLT-S conjugate. Alternatively, using the standard conditions for the electrophilic iodination of organic molecules, the vinyliodo-taxoid conjugate **6-20** can be synthesized. In this system, electrophilic iodine is generated in situ using Iodogen® beads as an oxidizing agent. Preliminary *in vitro* studies against VERO cells showed that **6-15** possesses cytotoxicity within the same order of magnitude as SB-T-1214. Therefore, it would be worthwhile to test the potency of **6-15** against a small panel of cancer cell lines to assess its potential as a theranostic agent.

§ 6.5.0 Conclusions and Perspective

Radiolabeling of pharmaceuticals is a widely used strategy to develop a better understanding of their biodistribution and PK profiles. The radioactive isotopes of carbon ^{11}C and ^{14}C can be used for PET studies and liquid scintilography, respectively and each of these methods offers unique insights into the interactions of the pharmaceutical agent with complex biological systems. Novel taxoids **6-14** and **6-16**, bearing vinyltrialkylstannanes at C3', have been

synthesized using a process that is amenable to gram-scale synthesis. It relies on the production of the key enantiopure β-lactam intermediate **(+) 6-12** through the chiral ester enolate-imine cyclo-condensation. Conditions for a Stille coupling have been successfully developed that allow the formation of SB-T-1214 from taxoid **6-14**, and the reaction parameters are currently being refined to permit the synthesis of ^{11}C-labeled SB-T-1214 suitable for a PET study in mice. This may prove to be among the most complex chemical structures ever to be radiolabeled using a Stille coupling with methyl iodide. In addition, labeling of conjugates bearing these vinylstannyl taxoids via electrophilic iodine is possible and may provide an excellent clinical theranostic tool for tumor-targeted chemotherapy.

§ 6.6.0 Experimental

§ 6.6.1 General Methods

^{1}H and ^{13}C NMR spectra were measured on a Varian 300, 400, 500 or 600 MHz NMR spectrometer. Melting points were measured on a Thomas Hoover Capillary melting point apparatus and are uncorrected. Mass to charge values were measured by flow injection analysis on an Agilent Technologies LC/MSD VL. TLC was performed on Merck DC-alufolien with Kieselgel 60F-254 and column chromatography was carried out on silica gel 60 (Merck; 230-400 mesh ASTM). Compound purity was verified by reverse phase HPLC on a Shimadzu LC-2010A with a Curosil-B 5 column (250 x 4.6 nm). The mobile phase was acetonitrile-water. The analysese were performed at a flow rate of 1ml/min with the UV detector set at 254 and 227 nm. The gradient was run from 20% to 95% acetonitrile in water over a 40 minute period.

§ 6.6.2 Materials

The chemicals were purchased from Aldrich Co. and Sigma and purified before use by standard methods. Tetrahydrofuran was freshly distilled from sodium metal and benzophenone. Dichloromethane was also distilled immediately prior to use under nitrogen from calcium hydride. In addition, various dry solvents were degassed and dried using PureSolv™ solvent purification system (Innovative Technologies, Newburyport, MA).

§ 6.6.3 Experimental Procedures

(±)-3-Triisopropylsilyloxy-4-(2,2-dibromovinyl)azetidin-2-one [(±) 6-1]

To a solution of **2-10** (200 mg, 0.53 mmol) in THF (30 mL) was added zinc (172 mg, 2.65 mmol) and the reaction vessel was purged with N_2 and cooled to 0 ^{o}C. Carbontetrabromide (700 mg, 2.12 mmol) was dissolved in THF (15 mL) under N_2 and cooled to 0 ^{o}C and to this solution HMPT (1.04 g, 6.36 mmol) was added, forming a white precipitate in a brown solution. This suspension was then added to the reaction mixture and heated to 70 ^{o}C for one hour during which time the reaction was monitored by TLC (6:1 Hx:EA). Upon completion, the reaction mixture was filtered through celite, washed with EtOAc and the filtrate was concentrated *in vacuo* to afford a red oil.

This oil was then dissolved in EtOAc (50 mL), washed with H_2O (3 x 50 mL), brine (3 x 50 mL). The organic layer was collected, dried over MgSO4, suction filtered, filtrate collected and concentrated in vacuo to afford a red oil that was purified by column chromatography on silica gel with increasing amounts of ethyl acetate in hexanes (hexanes:ethyl acetate 1:0 – 9:1) to afford **6-1** (185 mg, 65%) as a white solid: ^{1}H NMR (300 MHz, $CHCl_3$) δ 1.18 (m, 21H), 3.86 (s, 3H), 4.90 (dd, J = 5.1, 9.3 Hz, 1H), 5.25 (d, J = 5.1 Hz, 1H), 6.70 (d, J = 9.3 Hz, 1H), 6.95 (d, J = 6.9 Hz, 2H), 7.38 (J = 6.9 Hz, 2H).

***N*-(4-Methoxyphenyl)but-2-ynimine [6-3]**

p-Anisidine (2.00 g, 16 mmol), recrystallized from hexanes, was dissolved in CH_2Cl_2 (25 mL) with anhydrous Na_2SO_4 (1.0 g) and cooled to -20 ºC in an acetone bath with dry ice. To this mixture, but-2-ynal (1.40 g, 21 mmol), was added dropwise under inert conditions. The mixture was stirred at -20 ºC and monitored *via* TLC (2:1 Hx:EA). After 1 hour, the reaction mixture was filtered, washed with CH_2Cl_2 (20 mL) the filtrate was concentrated *in vacuo* to afford **(±) 6-1** (2.81 g, 100% yield) as red oil and was used immediately in the subsequent step: ^{1}H NMR (300 MHz, $CHCl_3$) δ 2.08 (d, J = 1.5 Hz, 3H), 3.81 (s, 3H), 6.89 (m, J = 8.7 Hz, 2H), 7.16 (m, J = 8.7 Hz, 2H), 7.67 (m, J = 1.5 Hz, 1H). MS (ESI) calcd for $C_{11}H_{12}NO$ $(M+H)^+$: 174.08, found: 174.1.

(±)-1-(4-Methoxyphenyl)-3-acetoxyl-4-(propargyl)azetidin-2-one [(±) 6-4]

An aliquot of **6-3** (2.81 g, 16 mmol) was dissolved in CH_2Cl_2 (25 mL), cooled to -78 ˚C, and TEA (3.5 mL, 26 mmol) was added dropwise under inert conditions. Acetoxyacetyl chloride (2.2 mL, 21 mmol) was added to the solution dropwise *via* syringe. The solution was maintained at -78 ˚C under N_2 atmosphere overnight. Then the mixture was then allowed to warm slowly to room temperature. The reaction was quenched with saturated NH_4Cl (2 mL), diluted with H_2O (20 mL) and the product was extracted with CH_2Cl_2 (3 x 20 mL). The organic layer was washed with brine (3 x 20 mL), dried over $MgSO_4$, filtered and the filtrate collected and concentrated *in vacuo* producing dark brown solid. Purification was done by column chromatography on silica gel with increasing amounts of ethyl acetate in hexanes (hexanes:ethyl acetate 1:0 – 1:1) to afford as a pale yellow solid, which could be recrystallized from hot hexanes, producing **(±) 6-4** (2.43 g, 56%) as a white solid: m.p. = 137-138 ºC; ^{1}H NMR (300 MHz, $CHCl_3$) δ 1.84 (d, J = 2.4 Hz, 3H), 2.30 (s, 3H), 4.93 (m, 1H), 5.82 (d, J = 4.5 Hz, 1H), 6.97 (m, J = 8.7 Hz, 2H), 7.53 (m, J = 8.7 Hz, 2H); ^{13}C NMR (100 MHz, $CDCl_3$) δ 3.71, 20.45, 49.69, 55.51, 70.55, 75.35, 85.83, 114.44, 118.69, 130.13, 156.84, 160.32, 169.69. HRMS calcd for $C_{15}H_{16}NO_4$ $(M+H)^+$: 274.1075, found: 274.1079 (Δ -1.5 ppm, -0.4 mDa).

(±)-1-(4-Methoxyphenyl)-3-hydroxy-4-(propargyl)azetidin-2-one [(±) 6-5]

The racemic **(±) 6-4** (1.20 g, 4.42 mmol) was dissolved in THF (12 mL) and cooled to 0 °C. To this mixture was added, chilled, 2 M KOH (12 mL). The reaction was stirred and monitored by TLC. Upon completion, the reaction was quenched with saturated NH_4Cl (5 mL) and extracted with CH_2Cl_2 (2 x 30 mL). The organic layer was collected, washed with brine (3 x 15 mL) dried over anhydrous $MgSO_4$, filtered and concentrated *in vacuo* to afford **(±) 6-5** (876 mg, 85% yield) as a white solid: m.p. = 150-151 ^oC; ^1H NMR (300 MHz, $CHCl_3$) δ 1.83 (d, J = 1.2 Hz, 3H), 3.48 (s, br, 1H), 3.63 (s, 3H), 4.63 (m, 1H), 4.83 (dd, 1H), 6.71 (m, J = 8.7 Hz, 2H), 7.28 (m, 8.7 Hz, 2H). ^{13}C NMR (100 MHZ, $CDCl_3$) δ 3.88, 51.08, 55.52, 71.33, 75.99, 86.99, 114.41, 118.67, 130.28, 156.65, 164.57. HRMS (ESI) calcd for $C_{13}H_{15}NO_3$ $(M+H)^+$: 232.0974, found: 232.0972 (Δ -0.9 ppm, -0.2 mDa).

(±)-1-(4-Methoxy)phenyl-3-triisopropylsiloxy-4-(propargyl)azetidin-2-one [**(±) 6-2**]

Compound (**±) 6-5** (860 g, 3.74 mmol) and DMAP (163 mg, 1.34 mmol) were dissolved in CH_2Cl_2 (15 mL). The solution will was cooled to 0 °C under inert conditions. To this solution was added TEA (0.8 mL, 6.69 mmol), followed by the dropwise addition of TIPSCl (1.08 g, 5.61 mmol). The reaction mixture was stirred at room temperature and monitored by TLC. Upon completion the reaction was quenched with saturated NH_4Cl (3 mL), diluted with H_2O (15 mL) and extracted with CH_2Cl_2 (1 x 40 mL). The organic layer was collected, washed with brine (3 x 20 mL), dried over anhydrous $MgSO_4$, filtered, and concentrated *in vacuo*. Purification was done by column chromatography on silica gel (hexanes:ethyl acetate = 19:1) to afford **(±) 6-2** (1.39 g, 92% yield) as a white solid: m.p. = 105-106 ^oC; ^1H NMR (300 MHz, $CHCl_3$) δ 1.09-1.21 (m, 21H), 1.85 (d, J = 2.1 Hz, 3H), 3.79 (s, 3H), 4.69 m, 1H), 5.05 (d, J = 4.5 Hz, 1H), 6.88 (m, J = 8.7 Hz, 2H), 7.46 (m, J = 8.7 Hz, 2H). MS (ESI) calcd for $C_{22}H_{34}NO_3Si$ $(M+H)^+$: 388.22 Found: 388.2.

(±)-1-(4-Methoxy)phenyl-3-triisopropylsiloxy-4-(2-methyl-2-vinytributylstannyl)azetidin-2-one [6-6]

To a solution of Sn_2Bu_6 (1.10 g, 1.9 mmol) in THF (1.5 mL) cooled at -78 ^oC, was added *n*-BuLi (1.2 mL, 1.6 M in hexanes) dropwise, and the mixture was allowed to warm to -40 ^oC for 20 min before being cooled back to -78 ^oC. This mixture was added to a suspension of CuCN (85 mg, 0.95 mmol) in THF (1.5 mL) at -78 ^oC *via* cannula during which time the solution color changed to a deep orange. The mixture was allowed to stir at -40 ^oC for 20 minutes and cooled to -78 ^oC, at which time methanol (0.5 mL) was added dropwise, forming a red gel that turned to a solution upon warming to -10 ^oC for 20 minutes. The reaction mixture was then cooled to -78 ^oC and a solution of **(+/-) 6-2** (100 mg, 0.25 mmol) in THF (1.5 mL) was added dropwise. The reaction was then warmed to -10 ^oC and stirred at this temperature for 16 hours at which time methanol (0.5

mL) was added. The mixture was then diluted with H_2O (10 mL), extracted with Et_2O (2 x 15 mL) and the organic layer was washed with brine (3 x 15 mL), dried over $MgSO_4$, filtered and evaporated in vacuo to afford a brown oil. Purification was done by column chromatography on silica gel with increasing amounts of ethyl acetate in hexanes (hexanes:ethyl acetate 1:0 – 99:1) to afford **(+/-) 6-6** (114 mg, 66%) as a white solid: m.p = 67-68 ^oC; ^1H NMR (300 MHz, $CHCl_3$) δ 0.79-1.01 (m, 15H), 1.04-1.20 (m, 21H), 1.22-1.33 (m, 6H), 1.34-1.55 (m, 6H), 2.12 (s, J = 22.8 Hz [Sn Split], 3H), 3.79 (s, 3H), 5.02 (dd, J = 9.2, 5.2 Hz, 1H), 5.09 (d, J = 5.2 Hz, 1H), 5.70 (m, J = 9.2 Hz, 1H), 6.84 (d, J = 9.2 Hz, 2H), 7.35 (d, J = 9.2 Hz, 2H); ^{13}C NMR (125 MHz, $CDCl_3$) δ 9.09, 11.94, 13.67, 17.77, 17.80, 19.84, 27.37, 29.11, 55.45, 55.59, 77.34, 114.20, 118.32, 131.56, 134.51, 148.23, 156.02, 165.78. HRMS (ESI) calcd for $C_{34}H_{6e}NO_3SiSn$ $(M+H)^+$: 680.3521, found : 680.3532 (Δ 1.6 ppm, 1.1 mDa).

Alternatively, **(+/-) 6-2** (100 mg, 0.25 mmol) was weighed into an RBF with $PdCl_2(PPh_3)_2$ (4.0 mg, 5 µmol), purged with N_2 and dissolved in THF (3 mL). To this solution was added $SnBu_3H$ (155 mg, 0.53 mmol) dropwise and allowed to stir for 1 hour. The crude reaction was loaded directly onto a silica gel column and purified using increasing amounts of ethyl acetate in hexanes (hexanes:ethyl acetate 1:0 – 50:1) to afford **(+/-) 6-6** (69 mg, 39%) as a white solid, spectroscopically identical to the product of the previously listed method.

(±)-1-(4-Methoxy)phenyl-3-triisopropylsiloxy-4-(2-methyl-1-vinytributylstannyl)azetidin-2-one [6-7]

Compound **(+/-) 6-7** eluted directly before **(+/-) 6-6**, to afford **(+/-) 6-7** (466 mg, 27%) as a white solid: ^1H NMR (300 MHz, $CHCl_3$) δ 0.58-0.97 (m, 15H), 1.10-1.23 (m, 21H), 1.25-1.46 (m, 12H), 1.97 (d, J = 6.3 Hz, 3H), 3.83 (s, 3H), 6.08 (d, J = 6.3 Hz, 1H), 5.12 (d, J = 5.1 Hz, 1H), 5.28 (d, J = 5.1 Hz, 1H), 7.34 (d, J = 9.6 Hz, 2H), 6.89, d, J = 9.6 Hz, 2H); ^{13}C NMR (125 MHz, $CDCl_3$) δ 10.47, 12.04, 13.67, 15.92, 17.69, 17.81, 27.47, 28.98, 55.46, 60.74, 77.92, 114.24, 118.12, 131.62, 140.11, 142.64, 156.09, 165.69. HRMS (ESI) calcd for $C_{34}H_{62}NO_3SiSn$ $(M+H)^+$: 680.3521 found: 680.3546 (Δ 3.7 ppm, 2.5 mDa).

(+)-1-(4-Methoxy)phenyl-3-triisopropylsiloxy-4-(propargyl)azetidin-2-one [(+) 6-2]

Diisopropyl amine (1.86 g, 18.46 mmol) was dissolved in anhydrous THF (20 mL) under inert atmosphere and cooled to -30 ^oC in an acetone bath with dry ice. Butyl lithium (10.5 mL, 1.6 M in hexanes) was added dropwise and allowed to warm up to room temperature for 1 hour and cooled to -78 ^oC. To this solution was added a pre-cooled solution of **1-14** (6.00 g, 15.38 mmol) dissolved in THF (30 mL) *via* cannula over 30 minutes at -78 ^oC, over which time the color of the solution turned to a pale yellow. To this was added a pre-cooled solution of **6-3** (3.20 g, 18.46 mmol) dissolved in THF (40 mL) at -78 ^oC over the course of 2 hours *via* cannula. During the addition, the reaction mixture turned a deep orange color, and was stirred for 2 hours at -78 ^oC at which time

LiHMDS (12.3 mL, 12.32 mmol) was added dropwise and the reaction was allowed to warm to -40 °C over 1 hour. The reaction was quenched with NH_4Cl (aq) (5 mL), H_2O was added (50 mL) and the aqueous layer was extracted with EtOAc (3 x 50 mL). The organic layer was then washed with brine (3 x 60 mL), collected, dried over $MgSO_4$, filtered and the filtrate evaporated in vacuo to afford an orange oil. Purification was done by column chromatography on silica gel with increasing amounts of ethyl acetate in hexanes (hexanes:ethyl acetate 1:0 – 25:1) to afford a yellow solid, which could be crystalized from pure hexanes at -40 °C to afford **(+) 6-2** (3.42 g, 57%) as white crystals: m.p. = 106-107 °C; α_D (22 °C, CH_2Cl_2) = 135°; ^{1}H NMR (300 MHz, $CHCl_3$) δ 1.09-1.21 (m, 21H), 1.85 (d, J = 2.1 Hz, 3H), 3.79 (s, 3H), 4.69 (m, 1H), 5.05 (d, J = 4.5 Hz, 1H), 6.88 (m, J = 8.7 Hz, 2H), 7.46 (m, J = 8.7 Hz, 2H). ^{13}C NMR (100 MHz, $CHCl_3$) δ 3.81, 12.02, 17.67, 51.45, 55.48, 72.32, 85.05, 114.31, 118.52, 130.87, 156.32, 164.54. HRMS (ESI) calcd for $C_{22}H_{34}NO_3Si$ $(M+H)^+$: 388.2308, found: 388.2313 (Δ 1.3 ppm, 0.5 mDa).

(3*R*,4*S*)-3-Triisopropylsilyloxy-4-(propargyl)-azetidin-2-one [(+) 6-9]

An aliquot of **(+) 6-2** (2.80 g, 7.23 mmol) was dissolved in acetonitrile (250 mL) and cooled to -10 °C. To this solution was added CAN (15.08 g, 25.3 mmol) dissolved in H_2O (250 mL) and added dropwise *via* an addition funnel. The reaction temperature of -10 °C was maintained throughout the reaction. The reaction was monitored by TLC and upon completion the mixture was extracted with ethyl acetate (150 mL). The organic layer was washed with aqueous Na_2SO_3 (4 x 60 mL), brine (3 x 50 mL), dried over $MgSO_4$ and concentrated *in vacuo*. Purification was done by column chromatography on silica gel with increasing amounts of ethyl acetate in hexanes (hexanes:ethyl acetate 1:0 – 2:1) to afford **(+) 6-10** (1.48 g, 73% yield) as a pale yellow solid: m.p = 58-62 °C; ^{1}H NMR (300 MHz, $CHCl_3$) δ 1.02-1.23 (m, 21H), 1.85 (d, J = 2.1 Hz, 3H), 4.36 (m, J = 2.1 Hz, 1H), 5.00 (dd, J = 2.1, 4.5 Hz, 1H), 6.01 (s, br, 1H); ^{13}C NMR (125 MHz $CDCl_3$) δ 3.72, 11.96, 17.70, 47.81, 74.34, 79.28, 83.82, 169.21; HRMS (ESI) calcd for $C_{15}H_{27}NO_2Si$ $(M+H)^+$: 282.1889, found: 282.1881 (Δ -2.8 ppm, -0.8 mDa).

(3*R*,4*S*)-1-(*t*-Butoxycarbonyl)-3-triisopropylsiloxy-4-(propargyl)azetidin-2-one [(+) 6-10]

Compound **(+) 6-9 (**1.48 g, 5.27 mmol), DMAP (160 mg, 1.4 mmol) and di-*tert*-butyl dicarbonate (1.38 mg, 6.4 mmol) was dissolved in CH_2Cl_2 (20 mL) and cooled to 0 °C under inert conditions. To the mixture, TEA (1.2 mL, 80 mmol) was added dropwise. The reaction was stirred at room temperature and monitored *via* TLC. Upon completion the reaction was quenched with saturated NH_4Cl (5 mL) and extracted with CH_2Cl_2 (40 mL). The organic layer was collected, washed with brine (3 x 60 mL), dried over anhydrous $MgSO_4$, and concentrated *in vacuo*. Purification was done by column chromatography on silica gel (hexanes:ethyl acetate = 9:1) to afford **(+) 6-10** (1.74 g, 87% yield) of as a colorless oil: ^{1}H NMR (300 MHz, $CHCl_3$) δ 1.03-1.22 (m, 21 H), 1.52 (s, 9H), 1.86 (d, J = 1.6 Hz, 3 H), 4.65 (m, 1H), 4.95 (d, J = 5.6 Hz, 1H); ^{13}C NMR (100 MHz

$CDCl_3$) δ 3.81, 11.89, 17.55, 17.61, 28.05, 50.81, 71.75, 76.70, 83.66, 84.45, 147.78, 165.00. MS (ESI) calcd for $C_{20}H_{36}NO_4Si$ $(M+H)^+$: 382.23, Found: 382.2.

(3*R*,4*S*)-1-(*t*-Butoxycarbonyl)-3-triisopropylsiloxy-4-(2-methyl-2-vinyltributyl-stannyl)azetidin-2- [(+) 6-11]

A round bottom flask containing **(+) 6-10** (1.00 g, 2.62 mmol) and $PdCl_2(PPh_3)_2$ (40 mg, 50 µmol), was purged with N_2 and the contents dissolved in THF (20 mL). To this solution was added $SnBu_3H$ (1.52 g, 5.3 mmol) dropwise and allowed to stir for 2 hour. The crude reaction was loaded directly onto a silica gel column and purified using increasing amounts of ethyl acetate in hexanes (hexanes:ethyl acetate 1:0 – 50:1) to afford **(+) 6-11** (746 mg, 43%) as a colorless oil: ^{1}H NMR (400 MHz, $CHCl_3$) δ 0.76-0.94 (m, 15H) 0.98-1.16 (m, 21H), 1.29 (m, J = 7.5 Hz, 6H), 1.40 – 1.58 (m, 6H), 1.47 (s, 9H), 2.00 (dt, J = 1.5, 44.1 Hz [Sn], 3H), 4.90-5.00 (m, 2H), 5.61 (ddd, J = 1.5, 8.7, 66.9 [Sn], 1H), ^{13}C NMR (100 MHz, $CDCl_3$) δ 9.05, 11.94, 13.62, 17.64 19.59, 27.38 (Sn split), 27.98, 29.07 (Sn split), 54.78 (Sn split), 82.77, 132.44 (Sn split), 147.78, 148.28, 166.76. HRMS (ESI) calc. for $C_{32}H_{63}NO_4SiSn$ $(M+H)^+$: 674.3627, found: 674.3624 (Δ -0.4 ppm, -0.3 mDa).

(3*R*,4*S*)-1-(*t*-Butoxycarbonyl)-3-triisopropylsiloxy-4-(2-methyl-1-vinyltributyl-stannyl)azetidin-2- [(+) 6-12]

Compound **(+/-) 6-12** eluted directly before **(+/-) 6-11**, to afford **(+/-) 6-12** as a colorless oil (466 mg, 27%): ^{1}H NMR (300 MHz, $CHCl_3$) δ 0.82-0.96 (m, 15H), 1.03-1.22 (m, 21H), 1.30-1.39 (m, 6H), 1.40-1.51 (m, 6H), 1.52 (s, 9H), 1.82 (d, J = 6.8 Hz, 3H), 5.00 (d, J = 6.0 HZ, 1H), 5.19 (d, J = 6.0 Hz, 1H), 5.94 (q, J = 6.8 Hz, 1H); ^{13}C NMR (125 MHz $CDCl_3$) δ 10.35, 11.83, 12.29, 13.72, 15.89, 17.72, 27.52, 28.96, 29.12, 60.60, 77.61, 83.15, 139.48, 140.98, 148.57, 166.20. MS (ESI) calcd for $C_{32}H_{64}NO_4SiSn$ $(M+H)^+$: 674.35 Found: 674.4.

Tributyltin-taxoid-TIPS-TES [6-13]

Compound **2-6 F** (700 mg, 0.96 mmol) and **(+) 6-12** (775 mg, 1.15 mmol) were dissolved in THF (30 mL), and cooled to -40 ^{o}C under inert conditions. To the mixture was added LiHMDS, 1M in tert-butyl methyl ether (1.3 mL), dropwise. The reaction was monitored at low temperature by TLC, and upon completion was quenched with sat. NH_4Cl solution (5 mL). The mixture was then allowed to warm to room temperature, diluted with H_2O (30 mL) and extracted with ethyl acetate (3 x 30 mL). The organic layer was then washed with brine (3 x 30 mL), dried over $MgSO_4$, and concentrated *in vacuo*. Purification was done by column chromatography on silica gel (hexanes:ethyl acetate 1:0 - 4:1) to afford **6-13 (**1.152 g, 85% yield) as a white solid: ^{1}H NMR (300 MHz, $CHCl_3$) δ 0.52-0.61 (m, 6H), 0.81-1.07 (m, 32H), 1.09 (m, 21H), 1.19 (s, 3H), 1.23 (s, 3H), 1.25-1.34 (m, 6H), 1.36 (s, 9H), 1.45-1.64 (m, 9H), 1.74 (s, 3H), 1.84 (m, 1H), 1.90-1.96 (m, 1H), 2.04 (s, 3H), 2.20-2.13 (m, 2H), 2.30 (s, 3H), 2.38-2.53 (m, 3H), 3.83 (d, J = 6.6 Hz, 1H), 4.20 (d, J = 8.4 Hz, 1H), 4.30 (d, J = 8.4 Hz, 1H), 4.42-4.47 (m, 2H), 4.90-4.98 (m, 3H), 5.63-5.75

(m, 2H), 6.04 (t, J = 8.7 Hz, 1H), 6.49 (s, 1H), 7.45 (t, J = 7.5 Hz, 2H), 7.60 (t, J = 7.5 Hz, 1H), 8.10 (d, J = 7.5 Hz, 2H). HRMS (ESI) calcd for $C_{71}H_{118}NO_{15}Si_2Sn$ $(M+H)^+$: 1400.7062, found: 1400.7045 (Δ -1.2 ppm, -1.7 mDa).

3'-Tributyltin-taxoid [6-14]

Compound **6-13** (1.14 g, 0.83 mmol) of was dissolved in a 1:1 mixture of acetonitrile:pyridine (50 mL total) and cooled to 0 °C under inert conditions. To the mixture excess HF, 70% in pyridine (11.4 mL), was added dropwise. The reaction was stirred at room temperature and monitored by TLC. Upon completion the reaction was quenched with 10% aqueous citric acid (5 mL), neutralized with saturated $NaHCO_3$ (30 mL) and extracted with ethyl acetate (3 x 40 mL). The organic layer was collected, washed with saturated $CuSO_4$ solution (3 x 30 mL), water (2 x 30 mL) and brine (3 x 30 mL). The extract was then dried over anhydrous $MgSO_4$, and concentrated *in vacuo*. Purification was done by column chromatography on silica gel with increasing amounts of ethyl acetate in hexanes (hexanes:ethyl acetate = 1:0 – 1:1) to afford **6-14 (**725 mg, 77% yield) as a white solid: m.p = 137 – 139; ^{1}H NMR (500 MHz, $CDCl_3$) δ 0.80-0.95 (m, 15H), 0.96-1.10 (m, 4H), 1.15 (s, 3H), 1.26 (s, 3H), 1.27-1.39 (m, 6H), 1.35 (s, 9H), 1.40-1.54 (m, 6H), 1.56-1.64 (m, 1H), 1.70-1.78 (m, 1H), 1.90 (s, 3H), 1.98 (s, Sn split, 3H), 2.34 (s, 3H), 2.36-2.42 (m, 1H), 2.44-2.60 (m, 2H), 3.31 (s, br, 1H), 3.84 (d, J = 6.6 Hz, 1H), 4.20 (d, J = 8.7 Hz, 1H), 4.30 (d, J = 8.7 Hz, 1H), 4.46 (m, 2H), 4.84-5.06 (m, 4H), 5.70 (m, 2H), 6.04 (t, 1H), 6.49 (s, 1H), 7.45 (t, J = 7.2 Hz, 2H), 7.60 (t, J = 7.2 Hz, 8.10 (d, J = 7.5 Hz, 2H); ^{13}C NMR (125 MHz, $CDCl_3$) δ 9.27, 9.50 (m, 7.7, 324 Hz), 13.05, 13.76, 15.06, 20.03, 22.01, 22.38, 26.71, 27.35 (m, J = 28), 28.25, 29.11 (m, J = 10 Hz), 43.22, 45.65, 50.33, 58.61, 72.28, 72.62, 73.47, 75.10, 75.46, 76.47, 79.22, 79.99, 81.09, 84.49, 128.68, 129.24, 130.20, 132.89, 132.71, 135.02, 142.81, 145.56, 155.35, 166.99, 170.06, 173.37, 175.19, 204.02. HRMS (ESI) calcd for $C_{56}H_{84}NO_{15}Sn$ $(M+H)^+$: 1130.4863, found: 1130.4874 (Δ 1.0 ppm, 1.1 mDa).

3'-Vinyliodo-taxoid [6-15]

To a solution of **6-14** (250 mg, 0.22 mmol) in CH_2Cl_2 (3 mL), was added a solution of I_2 (62 mg, 0.24 mmol) in CH_2Cl_2 dropwise and the reaction was monitored by TLC. Upon completion of addition, the reaction mixture was diluted with CH_2Cl_2, washed with sodium thiosulfate solution (3 x 10 mL), brine (3 x 10 mL), dried over MgSO4, filtered and the filtrate concentrated *in vacuo*. Purification was done by column chromatography on silica gel (hexanes:ethyl acetate = 1:1) to afford **6-15 (**197 mg, 92% yield) as a white solid: m.p. = 135 – 138 ^{o}C; ^{1}H NMR (400 MHz, $CDCl_3$) δ 0.83-0.92 (m, 2H), 0.96-1.07 (m, 2H), 1.16 (s, 3H), 1.25 (s, 3H), 1.35 (s, 9H), 1.67 (s, 3H), 1.73-1.81 (m, 1H), 1.81-1.92 (m, 1H), 1.90 (s, 3H), 2.28-2.40 (m, 2H), 2.35 (s, 3H), 2.48-2.60 (m, 2H), 2.58 (s, 3H), 3.45 (s, br, 1H), 3.80 (d, J = 6.8 Hz), 4.17 (d, J = 8.4 Hz, 1H), 4.26 (m, 1H), 4.29 (d, J = 8.4 Hz, 1H), 4.40 (m, 1H), 4.76 (m, 1H), 4.92-4.99 (m, 2H), 5.65 (d, J = 7.2 Hz, 1H), 6.20 (t, J = 8.4 Hz, 1H), 6.30 (s, 1H), 6.35 (d, J = 8.8 Hz, 1H), 7.45 (t, J = 7.6 Hz, 2H), 7.60 (t, J = 7.2 Hz, 1H), 8.09 (d, J = 8.10 Hz, 2H); ^{13}C NMR (125 MHz, $CDCl_3$) δ 9.22, 9.47, 9.52, 13.03, 15.12, 21.80, 22.45, 26.83, 28.20, 28.70, 35.58, 43.18, 45.70, 52.37, 58.64, 72.26, 72.68, 74.99, 75.40,

76.48, 79.10, 80.42, 81.25, 84.43, 100.69, 128.67, 129.15, 130.18, 133.28, 133.74, 136.43, 142.17, 155.01, 167.01, 170.12, 175.11, 203.80. HRMS (ESI) calcd for $C_{44}H_{57}INO_{15}$ $(M+H)^+$: 966.2773, found: 966.2767 (Δ -0.6 ppm, -0.5 mDa).

3'-Trimethyltin-taxoid [6-16]

Palladium tetrakis (19 mg, 16 µmol) and **6-15** (150 mg, 0.16 mmol) were weighed into a RBF, purged with N_2 and dissolved in THF. The solution was warmed to 50 °C and Sn_2Me_6 (110 mg, 0.32 mmol) was added dropwise via syringe. The reaction was stirred at 50 °C for 20 minutes and monitored by TLC. After 20 minutes, the THF was removed *in vacuo* and the reaction mixture was dissolved in CH_2Cl_2 (2 mL). Purification was done directly by column chromatography on silica gel with increasing amounts of ethyl acetate in hexanes (hexanes:ethyl acetate = 1:0 – 1:3) to afford **6-16 (**84 mg, 57% yield) as a white solid: m.p. = 127 – 130 °C; ^{1}H NMR (400 MHz, $CDCl_3$) δ 0.15 (s, J = 54.9 Hz [Sn], 9H), 0.92-1.05 (m, 2H), 1.08-1.17 (m, 2H), 1.16 (s, 3H), 1.31 (s, 3H), 1.35 (s, 9H), 1.72-1.80 (m, 1H), 1.82-1.88 (m, 1H), 1.89 (s, 3H), 1.98 (s, 3H), 2.34 (s, 3H), 2.35-2.46 (m, 1H), 2.48-2.60 (m, 2H), 3.32 (s, br, 1H), 3.80 (d, J=7.2 Hz), 4.18 (d, J = 8.4 Hz, 1H), 4.24 (dd, J = 2.0, 6.8 Hz, 1H), 4.30 (d, J = 8.4 Hz, 1H), 4.42 (m, 1H), 4.78 (d, J = 8.8 Hz, 1H), 4.87-4.97 (m, 2H), 5.60-5.73 (m, 2H), 6.17 (t, J = 8.8 Hz, 1H), 6.30 (s, 1H), 7.47 (t, J = 7.6 Hz, 2H), 7.61 (t, J = 7.2 Hz, 1H), 8.10 (d, J = 8.10 Hz, 2H); ^{13}C NMR (125 MHz $CDCl_3$) δ -9.96, 9.23, 9.48, 9.54, 13.05, 14.16, 15.03, 17.72, 19.07, 19.25, 19.43, 22.01, 22.43, 25.30, 26.74, 28.25, 29.74, 35.51, 35.51, 43.22, 45.65, 50.39, 58.61, 72.28, 72.60, 73.44, 75.08, 75.43, 76.47, 79.22, 80.05, 81.09, 84.49, 128.68, 129.22, 130.20, 132.91, 133.72 134.51, 142.76, 145.64, 155.33, 167.00, 170.07, 173.33, 175.20, 204.00. HRMS (ESI) calcd for $C_{47}H_{66}NO_{15}Sn$ $(M+H)^+$: 1004.3454, found: 1004.3467 (Δ 1.3 ppm, 1.3 mDa).

Stille Coupling to form SB-T-1214 (Cold Methylation 1)

Methyl iodide (0.6 mg, 4 µmol) in DMF (100 µL) was added to a vial containing palladium(0)tetrakis (2.2 mg, 2 µmol in DMF (100 µL). This solution was added to a suspension of CuTC (0.2 mg, 5 µmol) and **6-14** (5 mg, 4 µmol) in DMF (100 uL) in a vial and the reaction mixture was heated to 60 °C for 20 minutes. At this time, the reaction was quenched by the addition of methanol (300 µL), the reaction mixture was passed through a SPE filter and the filtrate was analyzed by LCMS.

Stille Coupling to form SB-T-1214 (Cold Methylation 2)

Methyl iodide (0.06 mg, 0.4 µmol) in DMF (100 µL) was added to a vial containing palladium(0)tetrakis (0.2 mg, 0.2 µmol in DMF (100 µL). This solution was added to a suspension of CuTC (0.02 mg,0.5 µmol) and **6-14** (5 mg, 4 µmol) in DMF (100 uL) in a vial and the reaction mixture was heated to 60 °C for 5 minutes. At this time, the reaction was quenched by the addition of methanol (300 µL), the reaction mixture was passed through a SPE filter and the filtrate was analyzed by LCMS.

SnBu3-Taxoid-Linker-TIPS [6-17]

According to the procedure previously listed for **4-9**, (Section 4.3) compounds **6-14** (50 mg, 44 µmol) and **4-8** (24 mg, 52 µmol) were used to produce **6-17** (42 mg, 61% yield) as a white solid: ^{1}H NMR ($CDCl_3$, 500 MHz) δ 0.93-0.99 (m, 15H), 1.01-1.10 (m, 21H), 1.12-1.20 (m, 2H), 1.17 (s, 3H), 1.28 (s, 3H), 1.29-1.35 (m, 9H), 1.36 (s, 9H), 1.47-1.54 (m, 6H), 1.69 (s, 3H), 1.75 (m, 1H), 1.88 (m, 1H), 1.94 (s, 3H) , 1.99 (s, 3H [Sn split]), 2.36 (s, 3H), 2.37-2.46 (m, 3H), 2.56 (m, 1H), 2.64 (s, br, 1H) 2.96 (m, 1H), 3.83 (d, J = 7.0 Hz, 1H), 4.00-4.13 (m, 2H), 4.22 (d, J = 8.5 Hz, 1H), 4.33 (d, J = 8.5 Hz, 1H),4.46 (m, 1H), 4.86 (d, J = 10.0 Hz, 1H), 4.94 (s, br, 1H), 4.99 (d, J = 8.5 Hz, 1H), 5.16 (m, 1H), 5.46 (m, 1H [Sn split]), 5.70 (d, J = 7.5 Hz, 1H), 6.21 (t, J = 8.5 Hz, 1H), 6.31 (s, 1H), 7.24-7.35 (m, 3H), 7.50 (t, J = 7.5 Hz, 2H), 7.63 (t, J = 7.5 Hz, 1H), 7.84 (d, J = 8.0 Hz, 1H), 8.14 (d, J = 7.5 Hz, 2H); ^{13}C NMR ($CDCl_3$, 125 MHz) δ 9.16 [Sn split], 9.27, 9.57, 11.88, 13.02, 13.80, 14.86, 17.71, 19.99, 20.56, 22.29, 22.35, 26.69, 27.34 [Sn split] 28.22, 29.02, 30.96, 33.02, 35.42, 38.68, 43.19, 45.60, 45.99, 46.02, 47.72, 58.48, 71.94, 72.18, 75.03, 75.23, 75.48, 79.28, 79.86, 80.99, 84.51, 127.67, 127.71, 128.32, 128.65, 129.30, 130.20, 130.65, 133.60, 133..93, 137.46, 143.61, 145.62, 154.95, 166.98, 168.00, 169.61, 170.14, 172.96, 175.14, 204.17. HRMS (ESI) cacd. For $C_{78}H_{117}NO_{18}S_2SiSn$ $(M+H)^+$: 1568.6581, found: 1568.6469 (Δ -7.1 ppm, -11.2 mDa).

SnBu3-Taxoid-Linker-CO2H [6-18]

According to the procedure previously listed for **4-10**, (Section 4.3) compound **6-17** (41 mg, 26 µmol) was used to produce **6-18** (24 mg, 77% yield) as a white solid:: ^{1}H NMR ($CDCl_3$, 500 MHz) δ 0.83-0.92 (m, 15H), 1.04, m, 2H), 1.08 (m, 2H), 1.12 (m, 2H), 1.18 (s, 3H), 1.29 (s, 3H), 1.28-1.36 (m, 9H), 1.36 (s, 9H), 1.37-1.42 (m, 4H), 1.45 -1.59 (m, 4H), 1.69 (s, 3H), 1.82 (m, 2H), 1.86-2.07 (m, 6H), 2.04 (s, 3H [Sn split]), 2.23-2.46 (m, 7H), 2.54 (m, 1H), 2.85-3.04 (m, 1H), 3.82 (m, 1H), 4.02 (m, 1H), 4.10 (m, 1H), 4.26 (d, J = 8.5 Hz, 1H), 4.33 (d, J = 8.5 Hz, 1H), 4.43 (m, 1H), 4.95-5.03 (m, 2H), 5.15 (m, 1H), 5.53 (m, 1H), 5.70 (d, J = 7.0 Hz, 1H), 6.24 (m, 1H), 6.47 (d, 1H), 7.25 (m, 2H), 7.34 (m, 1H), 7.50 (t, J = 7.0 Hz, 2H), 7.63 (t, J = 7.0 Hz, 1H), 7.84 (t, J = 8.0 Hz, 1H), 8.14 (d, J = 7.0 Hz, 2H); ^{13}C NMR ($CDCl_3$, 125 MHz) δ 9.23, 9.41, 9.58, 11.47, 13.04, 14.16, 14.81, 17.77, 20.01, 22.11, 22.30, 22.30, 22.72, 25.30, 26.68, 27.35 [Sn split], 28.23, 29.18, 29.76, 30.57, 34.68, 35.45, 38.64, 43.18, 45.28, 45.78, 45.88, 47.77, 56.00, 58.45, 71.64, 72.07, 74.94, 75.06, 75.54, 79.22, 79.91, 81.21, 84.39, 127.59, 128.35, 128.66, 129.26, 129.72, 130.19, 130.93, 132.38, 132.84, 133.64, 137.08, 137.61, 143.40, 145.87, 154.99, 167.00, 168.32, 170.27, 170.91, 175.18, 175.74, 204.02 (doubling of some peaks due to presence of 2 diastereomers). HRMS (ESI) calcd for $C_{69}H_{98}NO_{18}S_2Sn$ $(M+H)^+$: 1412.5247, found: 1412.5232 (Δ -1.1 ppm, -1.5 mDa).

SnBu3-Taxoid-Linker-PEG3-Biotin [6-19]

According to the procedure previously listed for **BLT-S**, (Section 4.3) compounds **6-18** (23 mg, 20 µmol) and **4-36** (10 mg, 25 µmol) were used to produce **6-19** (16 mg, 57% yield) as a white solid: mp 87-89 ºC; ^{1}H NMR ($CDCl_3$, 500 MHz) δ 0.84-0.97 (m, 15H), 0.93 (t, J = 7.5 Hz, 9H), 1.01 (m, 2H), 1.14 (m, 2H), 1.19 (s, 3H), 1.28 (m, 6H), 1.29-1.35 (m, 6H), 1.38 (s, 9H), 1.43-1.57 (m, 6H), 1.61-1.75 (m, 3H), 1.70 (s, 3H), 1.77 (m, 1H), 1.82-1.97 (m, 6H), 1.93 (s, 3H), 1.99 s, 3H, Sn Split), 2.17-2.28 (m, 1H), 2.23 (t, J = 7.0 Hz, 2H), 2.36 (s, 3H), 2.30-2.49 (m, 2H), 2.51-2.58 (m, 1H), 2.74 (d, J = 12.5 Hz, 1H), 2.92 (m, 1H), 3.15 (m, 1H), 3.32-3.43 (m, 2H), 3.46 (t, J = 5.0 Hz, 2H), 3.54 (m, J = 5.0 Hz, 2H), 3.58 (t, J = 5.0 Hz, 2H), 3.60-3.72 (m, 8H), 3.83 (d, J = 7.0 Hz, 1H), 4.07 (d, J = 10.5 Hz, 1H), 4.12 (d, J = 10.5 Hz, 1H), 4.21 (d, J = 8.5 Hz, 1H), 4.32 (m, 1H), 4.33 (d, J = 8.5 Hz, 1H), 4.43 (m, 1H), 4.97 (m, 1H), 4.93-5.08 (m, 2H), 5.09 - 5.20 (m, 2H), 5.51 (m, 1H), 5.70 (d, J = 7.0 Hz, 1H), 5.91 (m, 1H), 6.19 (t, J = 8.5 Hz, 1H), 6.35 (s, 1H), 6.51 (s, br, 1H), 6.68 (s, br, 1H), 7.25 (m, 2H), 7.33 (m, 1H), 7.50 (t, J = 7.5 Hz, 2H), 7.63 (t, J = 7.5 Hz, 1H), 7.83 (t, J = 8.0 Hz, 1H), 8.14 (d, J = 7.5 Hz, 2H); ^{13}C NMR ($CDCl_3$, 125 MHz) δ 9.16, 9.32, 9.66, 13.07, 13.80, 14.15, 14.81, 20.03, 20.68, 22.11, 22.39, 22.68, 25.48, 26.62, 27.34, 28.05, 28.26, 29.10, 29.72, 31.25, 31.35, 33.47, 35.48, 35.78, 38.67, 39.11, 40.53, 43.24, 45.89, 46.27, 46.39, 47.76, 55.38, 58.39, 60.12, 69.99, 70.02, 70.07, 70.38, 71.91, 72.00, 75.15, 75.48, 76.43, 79.10, 79.90, 81.09, 84.52, 127.82, 128.36, 128.67, 129.34, 130.20, 130.64, 130.64, 130.90, 132.60, 133.23, 133.62, 133.83, 137.57, 137.71, 143.01, 145.96, 155.03, 163.49, 166.95, 168.18, 169.65, 170.51, 172.48, 173.26, 174.87, 204.06. HRMS (ESI) cacd.for $C_{87}H_{130}N_5O_{22}S_3Sn$ $(M+H)^+$: 1812.7392, found: 1812.7380 (Δ -0.7 ppm, -1.2 mDa).

§ 6.7.0 References

1. Langer, O.; Muller, M., Methods to Assess Tissue-Specific Distribution and Metabilism of Drugs. *Curr. Drug. Metabol.* **2005,** *5*, 463-481.
2. Dalvie, D., Recent advances in the applicaitons of radioisotopes in drug metabolism, toxicology and pharmacokinetics. *Curr. Pharm. Des.* **2000,** *6*, 1009-1028.
3. Bergstrom, M.; Grahnen, A.; Langstrom, B., Positron emission tomography microdosing: a new concept with application in tracer and early clinical drug development. *Eur. J. Clin. Pharm.* **2003,** *59*, 357-366.
4. Sparreboom, A.; Wolff, A. C.; Verweig, J.; Zabelina, Y.; Zomeren, D. M. v.; McIntire, G. L.; Swindell, C. S.; Donehower, R. C.; Baker, S. D., Disposition of Docosahexaenoic Acid-Paclitaxel, a Novel Taxane, in Blood: In Vitro and Clinical Pharmacokinetic Studies. *Clin. Cancer Res.* **2003,** *9*, 151-159.
5. Ravert, H. T.; Klecker, R. W.; J M Collins; Mathews, W. B.; Pomper, M. G.; Wahl, R. L.; Dannals, R. F., Radiosynthesis of [11C]paclitaxel. *J. Label. Comp. Radiopharm.* **2002,** *45*, 471-477.
6. Kiesewetter, D. O.; Jagoda, E. M.; Kao, K.; Ma, Y.; Ravasi, L.; Shimoji, K.; Szajek, L. P.; Eckelman, W. C., Fluro-, bromo-, and iodopaclitaxel derivatives: synthesis and biological evaluation. *Nucl. Med. Biol.* **2003,** *30*, 11-24.

7. Roh, E. J.; Park, Y. H.; Song, C. E.; Oh, S.-J.; Choe, Y. S.; Kim, B.-T.; Chi, D. Y.; Kim, D., Radiolabeling of Paclitaxel with Electrophilic 123I. *Bioorg. Med. Chem. Lett.* **2000,** *8*, 65-68.
8. Kurdziel, K. A.; Kalen, J. D.; Hirsch, J. I.; Wilson, J. D.; Agarwal, R.; Barrett, D.; Bear, H. D.; McCumiskey, J. F., Imaging multidrug resistance with 4-[18F]fluoropaclitaxel. *Nucl. Med. Biol.* **2007,** *34*, 823-831.
9. Kurdziel, K. A.; Kiesewetter, D. O.; Carson, R. E.; Eckelman, W. C.; Herscovitch, P., Biodistribution, radiation dose estimates and in vivo pgp modulation studies of 18F-paclitaxel in nonhuman primates. *J. Nucl. Med.* **2003,** *44*, 1330-1339.
10. Tilbug, E. W. v.; Franssen, E. J. F.; Hoevaen, J. J. M. v. d.; Meij, M. v. d.; Elshove, D.; Lammertsma, A. A.; Windhorst, A. D., Radiosynthesis of [11C]docetaxel. *J. Label. Comp. Radiopharm.* **2004,** *47*, 763-777.
11. Van Der Veldt, A. A. M.; Hendrikse, N. H.; Smit, E. F.; Mooijer, M. P. J.; Rijnders, A. Y.; Gerritsen, W. R.; Hoeven, J. J. M. v. d.; Wiindhorst, A. D.; Lammertsma, A. A.; Lubberink, M., Biodistribution and radiation dosimetry of 11C-labelled docetaxel in cancer patients. *Eur. J. Nucl. Med. Mol. Imaging* **2010,** *37*, 1950-1958.
12. Mading, P.; Zessin, J.; Pleib, U.; Fuchtner, F.; Wust, F., Synthesis of a 11C-labelled taxane derivative by [1-11C]acetylation. *J. Label. Comp. Radiopharm.* **2006,** *49*, 357-365.
13. Cisternino, S.; Bourasset, F.; Archimbaud, Y.; Semiond, D.; Sanderink, G.; Scherrmann, J.-M., Nonlinear accumulation in the brain of the new taxoid TXD258 following saturation of P-glycoprotein at the blood-brain barrier in mice and rats. *Br. J. Pharmacol.* **2003,** *138*, 1367-1375.
14. Ono, C.; Takao, A.; Atsumi, R., Absorption, Distribution, and Excretion of DJ-927, a Novel Orally Effective Taxane, in Mice, Dogs, and Monkeys. *Biol. Pharm. Bull.* **2004,** *27*, 345-351.
15. Prezte, M.; Grobe-Gehling, P.; Mamat, C., Cross-Coupling Reactions as Valuable Tool for the Preparation of PET Radiotracers. *Molecules* **2011,** *16*, 1129-1165.
16. Milstein, D.; Stille, J. K., Palladium-catalyzed coupling of tetraorganotin compounds with aryl and benyl halides. Synthetic utility and mechanism. *J. Am. Chem. Soc.* **1979,** *101*, 4992-4998.
17. Mee, S. P. H.; Lee, V.; Baldwin, J. E., Stille Coupling Made Easy - The Synergic Effect of Copper(I) Salts and the Fluoride Ion. *Angew. Chem. Int. Ed. Engl.* **2004,** *43*, 1132-1135.
18. Farina, V.; Kapadia, S.; Krishnan, B.; Wang, C.; Liebeskind, L. S., On the Nature of the "Copper Effect" in the Stille Cross-Coupling. *J. Org. Chem.* **1994,** *59*, 5905-5911.
19. Andersson, Y.; Cheng, A.; Langstrom, B., Pappadium-promoted coupling reactions of [11C]methyl iodide with organotin and arganoboron compounds. *Acta Chem. Scand.* **1995,** *49*, 683-688.
20. Suzuki, M.; Doi, H.; Bjorkman, M.; Andersson, Y.; Langstrom, B.; Watanabe, Y.; Noyori, R., Rapid coupling of methyl iodide with aryltributylstannanes mediated by palladium(0) complexes: a general protocol for the synthesis of 11CH3-labeled PET tracers. *Chem. Eur. J.* **1997,** *3*, 2039-2042.
21. Aamdal, S.; Wolff, I.; Kaplan, S.; Paridaens, R.; Kerger, J.; Schachter, J.; Wanders, J.; Franklin, H.; Verweij, J., Docetaxel (Taxotere) in advanced malignant melanoma: a phase II study of the EORTC early clinical trials group. *Eur. J. Cancer* **1994,** *30*, 1061-1064.
22. Hosoya, T.; Sumi, K.; Doi, H.; Wakao, M.; Suzuki, M., Rapid methylation on carbon frameworks useful for the synthesis of $^{11}CH_3$-incorporated PET tracers: Pd(0)-mediated rapid coupling of methyl iodide with an alkenyltributylstannane leading to a 1-methylalkene. *Org. Biomol. Chem.* **2006,** *4*, 410-415.

23. Bjorkman, M.; Andersson, Y.; Doi, H.; Kato, K.; Suzuki, M.; Noyori, R.; Watanabe, Y.; Langstrom, B., Synthesis of 11C/13C-labelled prostacyclins. *Acta Chem. Scand.* **1998,** *53*, 635-640.
24. Suzuki, M.; Doi, H.; Kao, K.; Bjorkman, M.; Langstrom, B.; Watanabe, Y.; Noyori, R., Rapid methylation for the synthesis of a 11C-labeled tolylisocarbacyclin imaging the IP2 receptor in a living human brain. *Tetrahedron* **2000,** *56*, 8263-8273.
25. Suzuki, M.; Doi, H.; Hosoya, T.; Langstrom, B.; Watanabe, Y., Rapid methylation on carbon framworks leading to the synthesis of a PET tracer capable of imaging a novel CNS-type prostacyclin receptor in living human brain. *Trends Anal. Chem.* **2004,** *23*, 595-607.
26. Samuelsson, L.; Langstrom, B., Synthesis of 1-(2'-deoxy-2'-fluoro-β-d-arabinofuranosyl)-[methyl]-thymine ([11C]FMAU) via a Stille cross-coupling reaction with [11C]methyl iodide. *J. Label. Comp. Radiopharm.* **2003,** *46*, 263-272.
27. Toyohara, J.; Okada, M.; Toramatsu, C.; Suzuki, K.; Irie, T., Freasibility studies of 4'-[methyl-11C]thiothymidine as a tumor proliferation imaging agent in mice. *Nucl. Med. Biol.* **2008,** *35*, 67-74.
28. Crouch, I.; Neff, R.; Frantz, D., Pd-Catalyzed Asymmetric β-Hydride Elimination en Route to Chiral Allenes. *J. Am. Chem. Soc.* **2013,** *135*, 4970-4973.
29. Koehler, L.; Gagnon, K.; McQuarrie, S.; Wuest, F. Iodine-124: A Promising Positron Emitter for Organic PET Chemistry. *Molecules*. **2010**, *15*, 2686-2718.
30. Bevlov, V. V.; Bonab, A. A.; Fischman, A. J.; Heartlein, M.; Calias, P.; Papisov, M. I. Iodine-124 as a Label for Pharmacolical PEG Imaging. *Mol. Pharm*. **2011,** *8*, 736-747.
31. Akgun, E.; Portoghese, P. S.; Sajjad, M.; Nabi, H. A. Synthesis and I-124-labeling of m-iodophenylpyrrolomorphanan as a potential PET imaging agent for delta opiod (DOP) receptors. *J .Label. Compd. Radiopharm*. **2007**, *50*, 165-170.
32. Pandey, S. K.; Sajjad, M.; Chen, Y. H.; Pandey, A. Missert, J. R.; Batt, C. Yao, R. T.; Nabi, H. A.; Oseroff, A. R.; Pandey, R. K. Compared to purpurinimides, the pyropheophorbide containing an iodobenzyl group showed enhanced PDT efficacy and tumor imaging (I-124 PET) ability. *Bioconjug. Chem.* **2009**, *20*, 274-282.
33. Shaul, M.; Abourbeh, G.; Jacobson, O.; Rozen, Y.; Laky, D.; Levitzki, A.; Mishani, E. Novel iodine-124 labeled EGFR inhibitors as potential PET agents for molecular imaging in cancer. *Bioorg. Med. Chem*. **2004**, *12*, 3421-3429.

References

References for Chapter 1:

1. Ojima, I., Asymmetric Syntheses by Means of β-Lactam Synthon Method. In *Advances in Asymmetric Synthesis*, Hassner, A., Ed. JAI Press, Inc.: Greenwich, CT, 1995; Vol. 1, pp 95-146.
2. Hatanaka, N.; Abe, R.; Ojima, I., β-Lactam as Synthetic Intermediate: Synthesis of Leucine-Enkephalin. *Chem Lett* **1981,** *10*, 1297-1298.
3. Ojima, I.; Inaba, S.; Yoshida, K., New and effective Route to β-Lactams. The Reaction of Ketene Silyl Acetals with Schiff Bases Promoted by Titanium Tetrachloride. *Tetrahedron Lett.* **1977,** *18*, 3643-3646.
4. Ojima, I.; Kuznetsova, L.; Ungureanu, I. M.; Pepe, A.; Zanardi, I.; Chen, J., Fluoro-β-lactams as Useful Building Blocks for the Synthesis of Fluorinated Amino Acids, Dipeptides, and Taxoids. In *Fluorine-containing Synthons*, Soloshonok, V., Ed. American Chemical Society/Oxford University Press: Washington, D.C., 2005; pp 544-561.
5. Alcaide, B.; Aly, M.; Rodriguez, C.; Rodriguez-Vicente, A., Base-Promoted Isomerization of cis-4-Formyl-2-azetidinones: Chemoselective C4-Epimerization vs Rearrangement to Cyclic Enaminones. *J. Org. Chem.* **2000,** *65*, 3453-3459.
6. Romo, D.; Rzasa, R. M.; Shea, H. A.; Park, K.; Langenhan, J. M.; Sun, L.; Akhiezer, A.; Liu, J. O., Total Synthesis and Immunosuppressive Activity of (−)-Pateamine A and Related Compounds: Implementation of a β-Lactam-Based Macrocyclization. *J. Am. Chem. Soc.* **1998,** *120*, 12237-12254.
7. Del Buttero, P.; Molteni, G.; Roncoroni, M., Reductive ring opening of 2-azetidinones promoted by sodium borohydride. *Tetrahedron Lett* **2006,** *47*, 2209-2211.
8. Alcaide, B.; Almendros, P.; Cabrero, G.; Ruiz, M., Organocatalytic Ring Expansion of β-Lactams to γ-Lactams through a Novel N1−C4 Bond Cleavage. Direct Synthesis of Enantiopure Succinimide Derivatives. *Org Lett* **2005,** *7*, 3981-3984.
9. Dejaegher, Y.; Mangelinckx, S.; De Kimpe, N., Rearrangement of 2-Aryl-3,3-dichloroazetidines: Intermediacy of 2-Azetines. *J. Org. Chem.* **2002,** *67*, 2075-2081.
10. Ojima, I.; Chen, H.-J. C., Novel and Effective Routes to Optically Pure Amino Acids, Dipeptides, and Their Derivatives via β-Lactams obtained through Asymmetric Cycloaddition. *J. Chem. Soc. Chem. Commun.* **1987,** *1987*, 625-626.
11. Ojima, I., Recent Advances in the β-Lactam Synthon Method. *Acc. Chem. Res.* **1995,** *28*, 383-389.
12. Ojima, I.; Zhao, M.; Yamato, T.; Nakahashi, K.; Abe, R., Azetidines and bisazetidines. Their synthesis and use as the key intermediates to enantiomerically pure diamines, amino alcohols, and polyamines. *J. Org. Chem.* **1991,** *56*, 5263-5277.
13. Saito, T.; Kobayashi, S.; Ohgaki, M.; Wada, M.; Nagahiro, C., Diene-transmissive hetero Diels–Alder reaction of cross-conjugated azatrienes with ketenes: a novel and efficient, stereo-controlled synthetic method for hexahydroquinolinones *Tetrahedron Lett.* **2002,** *43*, 2627-2631.

14. Alcaide, B.; Almendros, P.; Cabrero, G.; Callejo, R.; Ruiz, M.; Arno, M.; Domingo, L., Ring Expansion versus Cyclization in 4-Oxoazetidine-2-carbaldehydes Catalyzed by Molecular Iodine: Experimental and Theoretical Study in Concert. *Adv Synth Catal* **2010,** *352*, 1688-1700.
15. Alcaide, B.; Rodriguez-Campos, I. M.; Rodriguez-Lopez, J.; Rodriguez-Vicente, A., Stereoselective Synthesis of Fused Bicyclic β-Lactams through Radical Cyclization of Enyne-2-azetidinones. *J. Org. Chem.* **1999,** *64*, 5377-5387.
16. Alcaide, B.; Almendros, P.; Aragoncillo, C., A Novel One-Step Approach for the Preparation of α-Amino Acids, α-Amino Amides, and Dipeptides from Azetidine-2,3-diones. *Chem Eur J* **2002,** *8*, 3646-3652.
17. Palomo, C.; Aizpurua, J. M.; Gracenea, J. J., Diastereoselective Conjugate Reduction and Enolate Trapping with Glyoxylate Imines. A Concise Approach to β-Lactams that Involves a Ternary Combination of Components. *J. Org. Chem.* **1999,** *64*, 1693-1698.
18. Paquette, L. A.; Behrens, C., A Ring-Expansion Route to Analogues of Dideoxyhydantocidin. *Heterocycles* **1997,** *46*, 31-35.
19. Ojima, I.; Park, Y. H.; Sun, C. M.; Zhao, M.; Brigaud, T., New and Efficient Routes to Norstatine and Its Analogs with High Enantiomeric Purity by β-Lactam Synthon Method. *Tetrahedron Lett.* **1992,** *33*, 5739-5742.
20. Ojima, I.; Habus, I.; Zhao, M.; Zucco, M.; Park, Y. H.; Sun, C.-M.; Brigaud, T., New and Efficient Approaches to the Semisynthesis of Taxol and Its C-13 Side Chain Analogs by Means of b-Lactam Synthon Method. *Tetrahedron* **1992,** *48*, 6985-7012.
21. Vidya, R.; Eggen, M. J.; Nair, S. K.; Georg, G. I.; Himes, R. H., Synthesis of Cryptophycins via an N-Acyl-β-lactam Macrolactonization. *J. Org. Chem.* **2003,** *68*, 9687-9693.
22. O'Boyle, N.; Carr, M.; Greene, L.; Bergin, O.; Nathwani, S.; McCabe, T.; Lloyd, D.; Zisterer, D.; Meegan, M., Synthesis and Evaluation of Azetidinone Analogues of Combretastatin A-4 as Tubulin Targeting Agents. *J Med Chem* **2010,** *53*, 8569-8584.
23. Ojima, I. C., J.; Sun, L.; Borell, C. P.; Wang, T.; Miller, M. L.; Lin, S.; Geng, X.; Kuznetsova, L.; Qu, C.; Gallager, D.; Zhao, X.; Zanardi, I.; Xia, S.; Horwitz, S. B.; Mallen-St. Clair, J.; Guerriero, J. L.; Bar-Sagi, D.; Veith, J. M.; Pera, P.; Bernacki, R. J. , Design, Synthesis, and Biological Evaluation of New-Generation Taxoids. *J. Med. Chem.* **2008,** *51*, 3203-3221.
24. Ojima, I.; Habus, I.; Zhao, M.; Georg, G. I.; Jayasinghe, R., Efficient and Practical Asymmetric Synthesis of the Taxol C-13 Side Chain, N-Benzoyl-(2*R*,3*S*)-3-Phenylisoserine, and Its Analogs via Chiral 3-Hydroxy-4-aryl-β-lactams Through Chiral Ester Enolate-Imine Cyclocondensation. *J. Org. Chem.* **1991,** *56*, 1681.
25. Ojima, I.; Sun, C. M.; Zucco, M.; Park, Y. H.; Duclos, O.; Kuduk, S. D., New and Efficient Route to Taxotere by the β-Lactam Synthon Method. *Tetrahedron* **1992,** *48*, 6985-7012.
26. Lin, S.; Fang, K.; Hashimoto, M.; Nakanishi, K.; Ojima, I., Design and Synthesis of A Novel Photoaffinity Taxoid as Probe for The Study of Paclitaxel-Microtubule Interactions. *Tetrahedron Lett.* **2000,** *41*, 4287-4290.
27. Georg, G. I.; Harriman, G. C. B.; Vander Velde, D. G.; Boge, T. C.; Cheruvallath, Z. S.; Datta, A.; Hepperle, M.; Park, H.; Himes, R. H.; Jayasinghe, L., Medicinal Chemistry of

Paclitaxel: Chemistry, Structure-Activity Relationships, and Conformational Analysis. In *Taxane Anticancer Agents: Basic Science and Current Status*, Georg, G. I.; Chen, T. T.; Ojima, I.; Vyas, D. M., Eds. American Chemical Society: Washington D.C., 1995; pp 217-232.
28. Ojima, I.; Slater, J. C.; Michaud, E.; Kuduk, S. D.; Bounaud, P.-Y.; Vrignaud, P.; Bissery, M. C.; Veith, J. M.; Pera, P.; J., B. R., Syntheses and Structure-Activity Relationships of the Second-Generation Antitumor Taxoids: Exceptional Activity against Drug-Resistant Cancer Cells. *J. Med. Chem.* **1996,** *39*, 3889-3896.
29. Ojima, I.; Park, Y. H.; Fenoglio, I.; Duclos, O.; Sun, C.-M.; Kuduk, S. D.; Zucco, M.; Appendino, G.; Pera, P.; Veith, J. M.; Bernacki, R. J.; Bissery, M.-C.; Combeau, C.; Vrignaud, P.; Riou, J. F.; Lavelle, F., Syntheses and Structure-Activity Relationships of New Taxoids. In *Taxane Anticancer Agents: Basic Science and Current Status, ACS Symp. Series 583*, Georg, G. I.; Chen, T. T.; Ojima, I.; Vyas, D. M., Eds. American Chemical Society: Washington, D. C., 1995; pp 262-275.
30. Staudinger, H., Zur Kenntniss der Ketene. Diphenylketen. *Justus Liebigs Ann. Chem.* **1907,** *356*, 51-123.
31. Cossio, F. P.; Arrieta, A.; Sierra, M. A., The Mechanism of the Ketene-Imine (Staudinger) Reaction in its Centennial: Still an Unsolved Problem? *Acc. Chem. Res.* **2008,** *41*, 925-936.
32. Venturini, A.; Gonzalez, J., Mechanistic Aspects of the Ketene-Imine Cycloaddition Reactions. *Mini Rev. Med. Chem.* **2006,** *3*, 185-194.
33. Dumas, S.; Hegedus, L. S., Electronic Effects on the Stereochemical Outcome of the Photochemical Reaction of Chromium Carbene Compleses with Imines to Form β-Lactams. *J. Org. Chem.* **1994,** *59*, 4967-4971.
34. Georg, G. I.; Ravikumar, V. T., Stereocontrolled ketene-imine cycloaddition reactions. In *Organic Chemistry β-lactams*, G.I., G., Ed. VCH Publishing: New York, NY, 1993; pp 295-368.
35. Brieva, R.; Crich, J. Z.; Sih, C. J., Chemoenzymic synthesis of the C-13 side chain of taxol: optically active 3-hydroxy-4-phenyl β-lactam derivatives. *J. Org. Chem.* **1993,** *58*, 1068-1075.
36. Ojima, I.; Habus, I., Asymmetric Synthesis of β-Lactams by Chiral Ester Enolate – Imine Condensation. *Tetrahedron Lett.* **1990,** *31*, 4289-4292.

References for Chapter 2:

1. Jemal, A.; Bray, F.; Center, M.; Ferlay, J.; Ward, E.; Forman, D., Global Cancer Statistics. *CA: A Cancer Journal for Clinicians* **2011,** *61*, 69-90.
2. Siegel, R.; Ward, E.; Brawley, O.; Jemal, A., Cancer Statistics, 2011. *CA: A Cancer Journal for Clinicians* **2011,** *61*, 212-236.
3. Hanahan, D.; Weinberg, R. A., Hallmarks of Cancer: The Next Generation. *Cell* **2011,** *144*, 646-674.
4. Hanahan, D.; Weinberg, R. A., The hallmarks of cancer. *Cell* **2000,** *100*, 57-70.
5. Del Buttero, P.; Molteni, G.; Roncoroni, M., Reductive ring opening of 2-azetidinones promoted by sodium borohydride. *Tetrahedron Lett* **2006,** *47*, 2209-2211.

6. Hsu, P. P.; Sabatini, D. M., Cancer cell metabolism: Warburg and beyond. *Cell* **2008,** *134*, 703-707.
7. Kim, R.; Emi, M.; Tanabe, K., Cancer immunoediting from immune surveillance to immune escape. *Immunol.* **2007,** *121*, 1-14.
8. Hanahan, D.; Folkman, J., Patterns and emerging mechanisms of the angiogenic switch during tumorigenesis. *Cell* **1996,** *86*, 353-364.
9. Goodman, L. S.; Wintrobe, M. M.; Dameshek, W.; Goodman, M. J.; Gilman, A.; McLennan, M. T., Nitrogen mustard therapy: use of methyl-bis (b-chloroethyl}) amine hydrochloride and tris (b-chloroethyl)amine hydrochloride for Hodgkin's disease, lymphosarcoma, leukemia and certain allied and miscellaneous disorders. *J. Am. Med. Assoc.* **1446,** *103*, 409-415.
10. Farber, S.; Diamond, L. K.; Mercer, R. D., Temporary remissions in acute leukemia in children produced by folic acid antagonist, 4-aminopteroyl-glutamic acid (aminopterin). *N. Eng. J. Med.* **1948,** *238*, 787-793.
11. DeVita, V. T.; Chu, E., A History of Cancer Chemotherapy. *Cancer Res.* **2008,** *68*, 8643-8653.
12. Suffness, M., *Taxol: Science and Applications; CRC Press: New York*. 1995.
13. Rowinsky, E. K.; Onetto, N.; Canetta, R. M.; Arbuck, S. G., Taxol: the first of the taxanes, an important new class of anti-cancer agents. *Semin. Oncol.* **1992,** *19*, 646-662.
14. Rowinsky, E. K., The development and clinical utility of the taxane class of antimicrotubule chemotherapy agents *Annual Review of Medicine* **1997,** *48*, 353–374.
15. Cragg, G. M., Schepartz, S.A., Suffness, M., Grever, M. R., The taxol supply crisis: New NCI policies for handling the large-scale production of novel natural product anticancer and anti-HIV agents. *J. Nat. Prod.* **1993,** *56*, 1657-1668.
16. Blume, E., Government Moves To Increase Taxol Supply. *J. Natl. Cancer Inst.* **1991,** *83*, 1054-1056.
17. Chauvière, G.; Guénard, D.; Picot, F.; Sénilh, V.; Potier, P., Structural Analysis and Biochemical Study of Isolated Products of the Yew: *Taxus Baccata* L. (Taxaceae). *C. R. Seances Acad. Sci., Ser 2* **1981,** *293*, 501-503.
18. Holton, R. A. 15599, 1995.
19. Agency, U. E. P., Greener Synthetic Pathways Award: Bristol-Myers Squibb Company: Development of a Green Synthesis for TAXOL Manufacture via Plant Cell Fermentation and Extraction. 2004; p http://www.epa.gov/greenchemistry/pubs/pgcc/winners/gspa04.html.
20. Wall, M. E.; Wani, M. C.; Cook, C. E.; Palmer, C. E.; McPhail, A. T., Plant antitumor agents. I: The isolation and structure of camptothecin, a novel alkaloidal leukemia and tumor inhibitor from Camptotheca acuminata. . *J. Am. Chem. Soc.* **1966,** *88*, 3888-3894.
21. Wani, M. C.; Taylor, H. L.; Wall, M. E.; Coggan, P.; McPhail, A. T., Plant antitumor agents. VI. The isolation and structure of taxol, a novel antileukemic and antitumor agent from *Taxus brevifolia*. *J. Am. Chem. Soc.* **1971,** *93*, 2325-2327.
22. Patel, R. N., Tour De Paclitaxel: Biocatalysis for Semisynthesis. *Ann. Rev. Microbiol.* **1998,** *98*, 361.

23. Fuchs, D. A.; Johnson, R. K., Cytologic evidence that taxol, an antineoplastic agent from Taxus brevifolia, acts as a mitotic spindle poison. *Cancer Treat. Rep.* **1978,** *62*, 1219-1222.
24. Horwitz, S. B.; Fant, J.; Schiff, P. B., Promotion of microtubule assembly in vitro by taxol. *Nature* **1979,** *277*, 665-667.
25. Horwitz, S. B., Personal Recollections on the Early Development of Taxol. *J. Nat. Prod.* **2004,** *67*, 136-138.
26. Weiss, R.; Donehower, R. C.; Wiernik, P. H., Hypersenstivity reactions from taxol. *J. Clin. Oncol.* **1990,** *8*, 1263-68.
27. Rowinsky, E. K.; A., E. E.; Chaudhry V., Clinical toxicities encountered with taxol. *Sem. Oncol. 20(Suppl.3)* **1993**, 1–15.
28. McGuire, W. P.; Hoskins, W. J.; Brady, M. F., Cyclophosphamide and cisplatin compared with paclitaxel and cisplatin in patients with stage III and stage IV ovarian cancer *N. Engl. J. Med.* **1996,** *334*, 1–6.
29. Rowinsky, E. K.; Gilbert, M.; McGuire, W. P., Sequences of taxol and cisplatin: a phase I and pharmacologic study. *J. Clin. Oncol.* **1991,** *9*, 1692–703.
30. Rowinsky, E. K.; Donehower, R. C., Paclitaxel (taxol). *N. Engl. J. Med.* **1995,** *332*, 1004-1014.
31. Suffness, M., Taxol, Science and Applications. *CRC Press, New York* **1995**.
32. Nogales, E.; Wolf, S.; Khan, I.; Luduena, R.; Downing, K., Structure of tubulin at 6.5 A and location of the taxol-binding stie *Nature* **1995,** *375*, 424-427.
33. Andreu, J.; Bordas, J.; Diaz, J.; Ancos, J. d.; Gil, R.; Medrano, F.; Nogales, E.; Pantos, E.; Towns-Andrews, E., Low resolution structure of micrtubules in solution: Synchrotron X-ray scattering and electron microscopy of taxol-induced microtubules assembled from purified tubulin in comparison with glycerol and MAP-induced microtubules. *J. Mol. Biol.* **1992,** *226*, 169-184.
34. Diaz, J.; Valpuesta, J.; Chacon, P.; Diakun, G.; Andreu, J., Changes in Microtubule Protofilament Number Induced by Taxol Binding to an Easily Accessible Site. *J. Biol. Chem.* **1998** *272*, 33803-33810.
35. Sackett, D.; Fojo, T., Taxanes. *Cancer Chemother. Biol. Response Modifiers* **1997,** *17*, 59-79.
36. Schiff, P. B., Fant, J., Horwitz, S. B., Taxol stabilizes microtubules in mouse fibroblast cells. *Proc Natl Acad Sci* **1980,** *77*, 1561-1565.
37. Huizing, M.; Keung, A.; Rosing, H.; Kuij, V. v. d.; Huinink, W. t. B.; Mandjes, I.; Dubbelman, A.; Pinedo, H.; Beijen, J., Pharmacokinetics of paclitaxel and metabolites in a randomized compartive study in platinum-pretreated ovarian cancer patients. *J. Clin. Oncol.* **1993,** *11*, 2127-2135.
38. Jordan, M.; Wilson, L., Microtubules and actin filaments: dynamic targets for cancer chemotherapy. *Curr. Opin. Cell Biol.* **1998,** *10*, 123-130.
39. Long, B.; Fairchild, C., Paclitaxel inhibits progression of mitotic cells to G1 phase by interference with spindle formation without affecting other microtubule functions during anaphase and telephase. *Cancer Res.* **1994,** *54*, 4355-4361.

40. Donaldson, K.; Goolsby, G.; Wahl, A., Cytotoxicity of the anti-cancer agents cisplatin and Taxol during cell proliferation and the cell cycle. *Int. J. Cancer* **1994,** *57*, 847-855.
41. Sorger, P.; Dobles, M.; Tournebize, R.; Hyman, A., Coupling cell division and cell death to microtubule dynamics. *Curr. Opin. Cell Biol.* **1997,** *9*, 807-814.
42. Oyaizu, H.; Adachi, Y.; Taketani, S.; Tokunaga, R.; Fukuhara, S.; Ikehara, S., A crucial role of caspase 3 and caspase 8 in paclitaxel-induced apoptosis. *Mol. Cell. Biol. Res. Commun.* **1999,** *2*, 36-41.
43. Huisman, C.; Ferreira, C.; Broker, L.; Rodriguez, J.; Smit, E.; Postmus, P.; Kruyt, F.; Giaccone, G., Paclitaxel Triggers Cell Death Primarily via Caspase-independent Routes in the Non-Small Cell Lung Cancer Cell Line NCI-H460. *Clin. Cancer Res.* **2002,** *8*, 596-606.
44. Subbaramaiah, K.; Hart, J.; Norton, L.; Dannenberg, A., Microtubule-interfering Agents Stimulate the Transcription of Cyclooxygenase-2 Evidence for involvement of ERK1/2 and p38 mitogen-activated protein kinase pathways. *J. Biol. Chem.* **2000,** *275*, 14838-14845.
45. Shtil, A.; Madlekar, S.; Yu, R.; Walter, R.; Hagen, K.; Tan, T.; Roninson, I.; Kong, A., Differential regulation of mitogen-activated protein kinases by microtubule-binding agents in human breast cancer cells. *Oncogene* **1999,** *18*, 377-384.
46. Blagosklonny, M.; Fojo, T., Molecular effects of paclitaxel: myths and reality (a critical review). *Int. J. Cancer* **1999,** *83*, 151-156.
47. Blagosklonny, M.; Giannakakou, P.; El-Deiry, W.; Kingston, D.; Higgs, P.; Neckers, L.; Fojo, T., Raf1/bcl2 phosphorylation: a step from microtubule damage to cell death. *Cancer Res.* **1997,** *57*, 130-135.
48. Haldar, S.; Chintapalli, J.; Croce, C., Taxol Induces bcl-2 Phosphorylation and Death of Prostate Cancer Cells. *Cancer Res.* **1996,** *56*, 1253-1255.
49. Chun, E.; Lee, K.-Y., Bcl-2 and Bcl-xL are important for the induction of paclitaxel resistance in human hepatocellular carcinoma cells. *Biochem. Biophys. Res. Comm.* **2004,** *315*, 771-779.
50. Gazitt, Y.; Rothenberg, M.; Hilsenback, S.; Fey, V.; Thomas, C.; Montegomrey, W., Bcl-2 overexpression is associated with resistance to paclitaxel, but not gemcitabine, in multiple myeloma cells. *Int. J. Oncol.* **1998,** *13*, 839-848.
51. Ibrado, A.; Liu, L.; Bhalla, K., Bcl-xL overexpression inhibits progression of molecular evens leading to paclitaxel-induced apoptosis of human AML HL-60 cells. *Cancer Res.* **1997,** *57*, 1109-1115.
52. Callagy, G.; Pharoah, P.; Pinder, S., Bcl-2 is a prognostic marker in breast cancer independently of the Nottingham Prognostic Index. *Clin. Cancer Res.* **2006,** *12*, 2468-2475.
53. Yoshino, T.; Shiina, H.; Urakami, S., Bcl-2 expressin as a predictive marker of hormone-refractory prostate cancer treated with taxane-based chemotherapy. *Clin. Cancer Res.* **2006,** *12*, 6116-6125.
54. Pushkarev, V.; Starenki, D.; Saenko, V.; Namba, H.; Kurebayashi, J.; Tronko, M.; Yamashita, S., Molecular Mechanisms of the Effects of Low Concentrations of Taxol in Anaplastic Thyroid Cancer Cells. *Endocrinol.* **2004,** *145*, 3143-3152.

55. Blagosklonny, M.; Schulte, T.; Nguyen, P.; Trepel, J.; Neckers, L., Taxol-induced Apoptosis and Phosphorylation of Bcl-2 Protein involves c-Raf-1 and Prepresents a Novel C-Raf-1 Signal Transduction Pathway. *Cancer Res.* **1996,** *56*, 1851-1854.
56. Okano, J.-I.; Rustgi, A., Paclitaxel Induces Prolonged Activation of the Ras/MEK/ERK Pathway Independently of Activating the Programmed Cell Death Machinery. *J. Biol. Chem.* **2001,** *276*, 19555-19564.
57. Ferlini, C.; Cicchillitti, L.; Raspaglio, G.; Bartollino, S.; Cimitan, S.; Bertucci, C.; Mozzetti, S.; Gallo, D.; Persico, M.; Fattorusso, C.; Campiani, G.; Scambia, G., Paclitaxel Directly Binds to Bcl-2 and Functionally Mimics Activity of Nur77. *Cancer Res.* **2009,** *69*, 6906-6914.
58. Szakacs, G.; Paterson, J.; Ludwig, J.; Booth-Genthe, C.; Gottesman, M., Targeting multidrug resistance in cancer. *Nature Rev. Drug Discov.* **2006,** *5*, 219-234.
59. Gottesman, M.; Pastan, I., Biochemistry of multidrug resistance mediated by the multidrug transporter. *Ann. Rev. Biochem.* **1993,** *62*, 385-427.
60. Yeh, J.; Hsu, W.; Wang, J.; Ho, S.; Kao, A., Predicting Chemotherapy Response to Paclitaxel-Based Therapy in Advanced Non-Small-Cell Lung Cancer with P-Glycoprotein Expression. *Respiration* **2003,** *70*, 32-35.
61. Penson, R.; Oliva, E.; Skates, S.; Glyptis, T.; Fuller, A. J.; Goodman, A.; Selden, M., Expression of multidrug resistance-1 protein inversely correlates with paclitaxel response and survival in ovarian cancer patients: a study in serial samples. *Gynecol. Oncol.* **2004,** *93*, 98-106.
62. Johnatty, S.; Beesley, J.; Paul, J.; Fereday, S.; Spurdle, A.; Webb, P.; Byth, K.; Marsh, S.; McLeod, H.; Harnett, P.; Brown, R.; deFazio, A.; Chenevix-Trench, G., ABCB (MDR 1) Polymorphisms and Progression-Free Survival among Women with Ovarian Cancer following Paclitaxel/Carboplatin Chemotherapy. *Clin. Cancer Res.* **2008,** *14*, 5594-5601.
63. Leonard, G.; Fojo, T.; Bates, S., The Role of ABC Transporters in Clinical Practice. *Oncologist* **2003,** *8*, 411-424.
64. Orr, G.; Verdier-Pinard, P.; McDaid, H.; Horwitz, S., Mechanisms of Taxol resistance related to microtubules. *Oncogene* **2003,** *22*, 7280-7295.
65. Giannakakou, P.; Gussio, R.; Nogales, E.; Downing, K.; Zaharevitz, D.; Bollbuck, B.; Poy, G.; Sackett, D.; Nicolaou, K.; Fojo, T., A common pharmacophore for epothiolone and taxanes: Molecular basis for drug resistance conferred by tubulin mutations in human cancer cells. *Proc. Nat. Acad. Sci.* **2000,** *97*, 2904-2909.
66. Monzo, M.; Rosell, R.; Sanchez, J.; Lee, J.; O'Brate, A.; Gonzalez-Larriba, J.; Alberola, V.; Lorenzo, J.; Nunez, L.; Ro, J.; Martin, C., Paclitaxel Resistance in Non-Small-Cell Lung Cancer Associated With Beta-Tubulin Gene Mutations. *J. Clin. Oncol.* **1999,** *17*, 1786-1793.
67. Ranganathan, S.; Benetatos, C.; Colarusso, P.; Dexter, D.; Hudes, G., Altered beta-tubulin isotype expression in paclitaxel-resistant human prostate carcinoma cells. *Br. J. Cancer* **1998,** *77*, 562-566.
68. Seve, P.; Isaaac, S.; Tredan, O.; Souquet, P.-J.; Pacheco, Y.; Perol, M.; Lafanechere, L.; Penet, A.; Peiller, E.-L.; Dumontet, C., Expression of Class III B-Tubulin Is Predictive of Patient

Outcome in Patients with Non-Small Cell Lung Cancer Receiving Vinorelbine-Based Chemoterapy. *Clin. Cancer Res.* **2005,** *11*, 5481-5486.
69. Mozzetti, S.; Ferlini, C.; Concolino, P.; Filippetti, F.; Raspaglio, G.; Prislei, S.; Gallo, D.; Martinelli, E.; Ranelletti, F. O.; Ferrandina, G.; Scambia, G., Class III β-Tubulin Overexpression Is a Prominent Mechanism of Paclitaxel Resistance in Ovarian Cancer Patients. *Clin Cancer Res* **2005,** *11*, 298-305.
70. Nicoletti, M.; Valoti, G.; Giannakakou, P.; Zhan, Z.; Kim, J.; Lucchini, V.; Landoni, F.; Mayo, J.; Giavazzi, R.; Fojo, T., Expression of b-Tubulin Isotypes in Human Ovarian Carcinoma Xenografts and in a Sub-Panel of Human Cancer Cell Lines from the NCI-Anticancer Drug Screen Correlation with Sensitivity to Microtubule Active Agents. *Clin. Cancer Res.* **2001,** *7*, 2912-2922.
71. Potier, P., Search and Discovery of New Antitumour Compounds. *Chem. Soc. Rev.* **1992**, 113-119.
72. Kingston, D. G.; Hawkins, D. R.; Ovington, L., New Taxanes from *Taxus Brevifolia*. *J. Nat. Prod.* **1982,** *45*, 466-470.
73. Parness, J.; Kingston, D. G. I.; Powell, R. G.; Harracksingh, C.; Horwitz, S. B., Structure-activity study of cytotoxicity and microtubule assembly by taxol and related taxanes. *Biochem. Biophys. Res. Commun.* **1982,** *105*, 1082–1089.
74. Guenard, D.; Gueritte-Voegelein, F.; Potier, P., Taxol and Taxotere: Discovery, Chemistry, and Structure-Activity Relationships. *Acc. Chem. Res.* **1993,** *26*, 160-167.
75. Lage, H.; Dietel, M. J., Multiple mechanisms confer different drug-resistant phenotypes in pancreatic carcinoma cells. *Cancer Res. Clin. Oncol.* **2002**, 349-357.
76. O'Driscoll, L.; Walsh, N.; Larkin, A.; Ballot, J.; Ooi, W. S.; Gullo, G.; O'Connor, R.; Clynes, M.; Crown, J.; Kennedy, S., MDR1/P-glycoprotein and MRP-1 Drug Efflux Pumps in Pancreatic Carcinoma. *Anticancer Res.* **2007**, 2115–2120.
77. Ojima, I.; Fenoglio, I.; Park, Y. H.; Sun, C.-M.; Appendino, G.; Pera, P.; Bernacki, R. J., Synthesis and Structure-Activity Relationships of Novel Nor-Seco Analogs of Taxol® and Taxotere®. *J. Org. Chem.* **1994,** *59*, 515-517.
78. Pepe, A.; Sun, L.; Zanardi, I.; Wu, X.; Ferlini, C.; Fontana, G.; Bombardelli, E.; Ojima, I., Novel C-seco-taxoids possessing high potency against paclitaxel-resistant cancer cell lines overexpressing class III β-tubulin. *Bioorg. Med. Chem. Lett.* **2009,** *19*, 3300-3304.
79. Sessa, C.; Cuvier, C.; Caldiera, S.; Bauer, J.; Bosch, S. V. D.; Monnerat, C.; Semiond, D.; Perard, D.; Lebecq, A.; Besenval, M.; Marty, M., Phase I clinical and pharmacokinetic studies of the taxoid derivative RPR 109881A administered as a 1-hour or a 3-hour infusion in patients with advanced solid tumors. *Ann. Oncol.* **2002,** *13*, 1140-1150.
80. Marder-Karsenti, R.; Dubois, J.; Bricard, L.; Guenard, D.; Gueritte-Voegelein, F., Synthesis and Biological Evaluation of D-Ring-Modified Taxanes: 5(20)-Azadocetaxel Analogs. *J. Org. Chem.* **1997,** *62*, 6631-6637.
81. Gunatilaka, A. A. L.; Ramdayal, F. D.; Sarragiotto, M. H.; Kingston, D. G. I., Synthesis and Biological Evaluation of Novel Paclitaxel (Taxol) D-Ring Modified Analogues. *J. Org. Chem.* **1999,** *64*, 2694-2703.

82. Dubois, J.; Thoret, S.; Gueritte, F.; Guenard, D., Synthesis of 5(20)deoxydocetaxel, a New Active Docetaxel Analogue. *Tetrahedron Lett.* **2000,** *41*, 3331-3334.
83. Ojima, I.; Wang, T.; Miller, M. L.; Lin, S.; Bollera, C. P.; Geng, X.; Pera, P.; Bernacki, R. J., Synthesis and Structure–Activity Relationships of New Second-Generation Taxoids. *Bioorg. Med. Chem. Lett.* **1999,** *9*, 3423-3428.
84. Ojima, I. C., J.; Sun, L.; Borell, C. P.; Wang, T.; Miller, M. L.; Lin, S.; Geng, X.; Kuznetsova, L.; Qu, C.; Gallager, D.; Zhao, X.; Zanardi, I.; Xia, S.; Horwitz, S. B.; Mallen-St. Clair, J.; Guerriero, J. L.; Bar-Sagi, D.; Veith, J. M.; Pera, P.; Bernacki, R. J. , Design, Synthesis, and Biological Evaluation of New-Generation Taxoids. *J. Med. Chem.* **2008,** *51*, 3203-3221.
85. Ojima, I.; Lin, S.; Wang, T., Recent Advances in the Medicinal Chemistry of Taxoids with Novel β-Amino Acid Side Chians. *Curr Med Chem* **1999,** *6*, 519-534.
86. Ali, S. M.; Hoemann, M. Z.; Aube, J.; Mitscher, L. A.; Georg, G. I.; McCall, R.; Jayasinghe, L. R., Novel Cytotoxic 3'-(*tert*-Butyl) 3-Dephenyl Analogs of Paclitaxel and Docetaxel. *J. Med. Chem.* **1995,** *38*, 3821-3828.
87. Gueritte-Voegelein, F.; Guenard, D.; Lavelle, F.; Le Goff, M.-T.; Mangatal, L.; Potier, P., Relationships between the Structure of Taxol Analogues and Their Antimitotic Activity. *J. Med. Chem.* **1991,** *34*, 992-998.
88. Ojima, I., Kuduk, S. D., Pera, P., Veith, J. M., Bernacki, R. J., Synthesis of and Structure-Activity Relationships of Non-Aromatic Taxoids. Effects of Alkyl and Alkenyl Ester Groups on Cytotoxicity. *J. Med. Chem.* **1997,** *40*, 279-285.
89. Ojima, I.; Fenoglio, I.; Park, Y. H.; Pera, P.; Bernacki, R. J., Synthesis and Biological Activity of 14β-Hydroxydocetaxel *Bioorg. Med. Chem. Lett.* **1994,** *4*, 1571-1574
90. Georg, G. I.; Boge, T. C.; Cheruvallath, Z. S.; Clowers, J. S.; Harriman, G. C. B.; Hepperle, M.; Park, H., The Medicinal Chemistry of Taxol. In *Taxol®: Science and Applications*, Suffness, M., Ed. CRC Press: New York, 1995; pp 317-375.
91. Chen, S.-H.; Fairchild, C.; Mamber, S. W.; Farina, V., Taxol Structure-Activity Relationships: Synthesis and Biological Evaluation of 10-Deoxytaxol. *J. Org. Chem.* **1993,** *58*, 2927-2928.
92. Klein, L. L., Synthesis of 9-Dihydrotaxol: A Novel Bioactive Taxane. *Tetrahedron Lett.* **1993,** *34*, 2047-2050.
93. Ishiyama, T.; Iimura, S.; Ohsuki, S.; Uoto, K.; Terasawa, H.; Soga, T., New Highly Active Taxoids from 9β-Dihydrobaccatin-9,10-acetals. *Bioorg. & Med. Chem. Lett.* **2002,** *12*, 1083-1086.
94. Chen, R.; Kingston, D. G. I., Isolation and structure elucidation of new taxoids from Taxus Brevifolia. *J. Nat. Prod.* **1994,** *57*, 1017-1021.
95. Ravdin, R.; III, H. B.; Cook, G.; Eisenberg, P.; Kane, M.; Bierman, W.; Mortimer, J.; Genevois, E.; Bellet, R., Phase II trial of docetaxel in advanced anthracycline-resistant or anthracenedione-resistant breast cancer. *J. Clin. Oncol.* **1995,** *13*, 2879-2885.
96. Martin, M.; Pienkowski, T.; Mackey, J.; Pawlicki, M.; Guastalla, J.; Weaver, C.; Tomiak, E.; Al-Tweigeri, T.; Chap, L.; Juhos, E.; Guevin, R.; Howell, A.; Fornadnder, T.; Hainsworth, J.; Coleman, R.; Winholes, J.; Modiano, M.; Pinter, T.; Tang, S.; Colwell, B.; Prady, C.; Provencher,

L.; Walde, D.; Rodriguez-Lescure, A.; Hugh, J.; Loret, C.; Rupin, M.; Blitz, S.; Jacovs, P.; Murawsky, M.; Riva, A.; Vogel, C., Adjuvant docetaxel for node-positive breast cancer. *N. Engl. J. Med.* **2005,** *352*, 2302-2312.
97. Cutsem, E. V.; Moiseyenko, V.; Tjulandin, S.; Majlis, A.; Constenla, M.; Boni, B.; Rodrigues, A.; Fodor, M.; Chao, Y.; Voznyi, E.; Risse, M.-L.; Ajani, J., Phase III Study of Docetaxel and Cisplatin Plus Fluorouracil Compared with Cisplatin and Fluorouracil As First-Line Therapy for Advanced Gastic Cancer: A Report of the V325 Study Group. *J. Clin. Oncol.* **2006,** *24*, 4991-4997.
98. Fossella, F.; Pereira, J.; Pawel, J. v.; Pluzanska, A.; Gorbounova, V.; Kaukel, E.; Mattson, K.; Ramlau, R.; Szczesna, A.; Fidias, P.; Millward, M.; Belani, C., Randomized, Multinational, Phase III Study of Docetaxel Plus Platinum Combinations Versus Vinorelbine Plus Cisplatin for Advanced Non-Small-Cell Lung Cancer: The TAX 326 Study Group. *J. Clin. Oncol.* **2003,** *21*, 3016-3024.
99. Dagher, R.; Li, N.; Abraham, S.; Rahman, A.; Sridhara, R.; Pazdur, R., Approval Summary: Docetaxel in Combination with Prednisone for the Treatment of Androgen-Independent Hormone-Refractory Prostate Cancer. *Clin. Cancer Res.* **2004,** *10*, 8147-8151.
100. Vermorken, J.; Remenar, E.; Herpen, C. v.; Gorila, T.; Mesia, R.; Degardin, M.; Stewart, J.; Jelic, S.; Betka, J.; Preiss, J.; Weyndaert, D. v. d.; Awada, A.; Cupissol, D.; Kienzer, H.; Rey, A.; Desaunois, I.; Bernier, J.; Lefebvre, J.-L., Cisplatin, Fluorouracil, and Docetaxel in Unresectable Head and Neck Cancer. *N. Engl. J. Med.* **2007,** *357*, 1695-1704.
101. Fossella, R.; DeVore, R.; Kerr, R.; Crawford, J.; Natale, R.; Dunphy, F.; Kalman, L.; Miller, V.; Lee, J.; Moore, M.; Gandara, D.; Karp, D.; Vokes, E.; Kris, M.; Kim, Y.; Gamza, F.; Hammershaimb, L., Randomized Phase III Trial of Docetaxel Versus Vinorelbine or Ifosfamide in Patients With Advanced Non-Small-Cell Lung Cancer Previously Treated With Platinum-Containing Chemotherapy Regimens. *J. Clin. Oncol.* **2000,** *18*, 2354-2362.
102. Tannock, I.; Wit, R. d.; Berry, W.; Horti, J.; Pluzanska, A.; Chi, K.; Oudard, S.; Theodore, C.; James, N.; Turesson, I.; Rosenthal, M.; Eisenberger, M., Docetaxel plus Prednisone or Mitoxantrone plus Prednisone for Advanced Prostate Cancer. *N. Engl. J. Med.* **2004,** *351*, 1502-1512.
103. Galsky, M.; Dritselis, A.; Kirkpatrick, P.; Oh, W., Cabazitaxel. *Nature Rev. Drug Discov.* **2010,** *9*, 677-678.
104. Robert, F.; Harper, K.; Ackerman, J.; Gupta, S., A phase I study of larotaxel (XRP9881) administered in combination with carboplatin in chemotherapy-naïve patients with stage IIIB or stage IV non-small cell lung cancer. *Cancer Chemother. Pharmacol.* **2010,** *65*, 227-234.
105. Metzger-Filho, O.; Moulin, C.; Azambuja, E. d.; Ahmad, A., Larotaxel: broadening the road with new taxanes. *Exp. Op. Invest. Drugs* **2009,** *18*, 1183-1189.
106. Dieras, V.; Viens, P.; Veyret, C.; Romieu, G.; Awada, A.; Lidbrink, E.; Bonnefoi, H.; Mery-Mignard, D.; Dalenc, F.; Roche, H., Larotaxel (L) in combination with trastuzumab in patients with HER2+ metastatic breast cancer (MBC): Interim analysis of an open phase II label study. *J. Clin. Oncol.* **2008,** *26*, 1070.

107. Dieras, V.; Limentani, S.; Romieu, G.; Tubiana-Huli, M.; Lortholary, A.; Kaufman, P.; Girre, V.; Besenval, M.; Valero, V., Phase II multicenter study of larotaxel (XRP9881), a novel taxoid, in patients with metastatic breast cancer who previously received taxane-based therapy. *Ann. Oncol.* **2008,** *19*, 1255-1260.
108. Beer, M.; Lenaz, L.; Amadori, D., Phase II study of ortataxel in taxane-resistant breast cancer. *Journal of Clinical Oncology* **2008,** *26*, a1066.
109. Moore, M.; Jones, C.; Harker, G.; Lee, F.; Ardalan, B.; Saif, M.; Hoff, P.; Coomes, J.; Rollins, C.; Felt, K., Phase II trial of DJ-927, an oral tubulin depolymerization inhibitor, in the treatment of metastatic colorectal cancer. *J. Clin. Oncol.* **2006,** *24*, s3591.
110. Roche, M.; Kyriakou, H.; Seiden, M., Drug evaluation: tesetaxel--an oral semisynthetic taxane derivative. *Curr. Opin. Invest. Drugs* **2006,** *7*, 1092-1099.
111. Beeram, M.; Papadopoulos, K.; Patnaik, A.; Qureshi, A.; Tolcher, A., Phase I dose-ranging, pharmacokinetic (PK) study of tesetaxel, a novel orally active tubulin-binding agent. *J. Clin. Oncol.* **2010,** *28*, ae13075.
112. Ramanathan, R.; Picus, J.; Raftopoulos, H.; Bernard, S.; Lockhart, A.; Frenette, G.; Macdonald, J.; Melin, S.; Berg, D.; Brescia, F.; Hochster, H.; Cohn, A., A phase II study of milataxel: a novel taxane analogue in previously treated patients with advanced colorectal cancer. *Cancer Chemother. Pharmacol.* **2008,** *61*, 435-438.
113. Ojima, I.; Slater, J. C.; Michaud, E.; Kuduk, S. D.; Bounaud, P.-Y.; Vrignaud, P.; Bissery, M. C.; Veith, J. M.; Pera, P.; J., B. R., Syntheses and Structure-Activity Relationships of the Second-Generation Antitumor Taxoids: Exceptional Activity against Drug-Resistant Cancer Cells. *J. Med. Chem.* **1996,** *39*, 3889-3896.
114. Ojima, I.; Wang, T.; Miller, M. L.; Lin, S.; Borella, C. P.; Geng, X.; Pera, P.; Bernacki, R. J., Synthesis and Structure-Activity Relationships of New Second-Generation Taxoids. *Bioorg Med Chem Lett* **1999,** *9*, 3423-3428.
115. Ferlini, C.; Distefano, M.; Pignatelli, F.; Lin, S.; Riva, A.; Bombardelli, E.; Mancuso, S.; Ojima, I.; Scambia, G., Antitumor Activity of Novel Taxanes That Act as Cytotoxic Agents and P-Glycoprotein Inhibitors at the Same Time. *Br. J. Cancer* **2000,** *83*, 1762-1768.
116. Gut, I.; Ojima, I.; Vaclavikova, R.; Simek, P.; Horsky, S.; Linhart, I.; Soucek, P.; Knodrova, E.; Kuzetsova, L.; Chen, J., Metabolism of new-generation taxanes in human, pig, minipig and rat liver microsomes. *Xenobiotica* **2006,** *36*, 772-792.
117. Botchkina, G.; Zuniga, E.; Das, M.; Wang, Y.; Wang, H.; Zhu, S.; Savitt, A.; Rowehl, R.; Leyfman, Y.; Ju, J.; Shroyer, K.; Ojima, I., New-generation taxoid SB-T-1214 inhibits stem cell-related gene expression in 3D cancer spheriods induced by purified colon tumor-initiating cells. *Molecular Cancer* **2010,** *9*, 192-204.
118. Li, F.; Tiede, B.; Massague, J.; Kang, Y., Beyond tumorigenesis: cancer stem cells. *Cell Research* **2007,** *17*, 3-14.
119. Kuznetsova, L.; Sun, L.; Chen, J.; Zhao, X.; Seitz, J.; Das, M.; Li, Y.; Veith, J.; Pera, P.; Bernacki, R.; Xia, S.; Horwitz, S.; Ojima, I., Synthesis and Biological Evaluation of Novel 3'-Difluorovinyl Taxoids. *Journal of Fluorine Chemistry* **2012,** *143*, 177-188.

References for Chapter 3:

1. Sauer, L. A.; Dauchy, R. T., The effect of omega-6 and omega-3 fatty acids on 3H-thymidine incorporation in hepatoma 7288CTC perfused in situ. *British Journal of Cancer* **1992,** *66*, 297-303.
2. Seitz, J.; Ojima, I., Chapter V.9. Drug Conjugates with Polyunsaturated Fatty Acids. In *Drug Delivery in Oncology - From Research Concepts to Cancer Therapy*, Kratz, F.; Senter, P.; Steinhagen, H., Eds. Wiley-VCH: Weinheim, Germany, 2011.
3. Berquin, I. M.; Edwards, I. J.; Chen, Y. Q., Multi-targeted therapy of cancer by omega-3 fatty acids. *Cancer Letters* **2008,** *269*, 363-367.
4. Colquhoun, A.; Miyake, J. A.; Benadiba, M., Fatty acids, eicosanoids and cancer. *Nutritional Therapy & Metabolism.* **2009,** *27*, 105-112.
5. Pownall, H. J.; Hamilton, J. A., Energy translocation across cell membranes and membrane models. . *Acta Physiologica Scandanavia* **2003,** *178*, 357-365.
6. Rose, D. P.; Connolly, J. M., Regulation of tumor angiogenesis by dietary fatty acids and eicosanoids. . *Nutr. Cancer* **2000,** *2*, 879-890.
7. Hardman, W. E., (n-3) Fatty Acids and Cancer Therapy. . *Journal of Nutrition* **2004,** *134*, 3427S-3430S.
8. Brown, M. D.; Hart, C. A.; Gazi, E.; Bagley, S.; Clarke, N. W., Promotion of prostatic metastatic migration towards human bone marrow stoma by Omega 6 and its inhibition by Omega 3 PUFAs. *British Journal of Cancer* **2006,** *94*, 842-853.
9. Calviello, G.; Niculolo, F. D.; Gragnoli, S.; Piccioni, E.; Serini, S.; Maggiano, N.; Tringali, G.; Navarra, P.; O'Ranelletti, F.; Palozza, P., n-3 PUFAs reduce VEGF expression in human colon cancer cells modulating the COX-2/PGE2 induced ERK -1 and -2 and HIF-1α induction pathway. *Carcinogenesis* **2004,** *25*, 2303-2320.
10. Novak, T. E.; Babcock, T. A.; Jho, D. H.; Helton, W. S.; Espat, N. J., NF-kappa B inhibition by omega-3 fatty acids modulates LPS-stimulated macrophage TNF-alpha transcription. *Am. J. Physiol.* **2003,** *284*, L84-L85.
11. Tuller, E. R.; Brock, A. L.; Yu, H.; Lou, J. R.; Benbrook, D. M.; Ding, W.-Q., PPARα signaling mediates the synergistic cytotoxicity of clioquinol and docosahexaenoic acid in human cancer cells. . *Biochem. Pharmacol.* **2009,** *77*, 1480-1486.
12. Zhuo, Z.; Zhang, L.; Mu, Q.; Lou, Y.; Gong, Z.; Shi, Y.; Ouyang, G.; Zhang, Y., The effect of combination treatment with docoahexaenoic acid and 5-fluorouracil on the mRNA expression of apoptosis-related genes, including the novel gene BCL2L12, in gastric cancer cells. . *In Vitro Cellular Developmental Biology - Animal* **2009,** *45*, 69-74.
13. Wang, Y.; Li, L.; Jiang, W.; Larrick, J. W., Synthesis and evaluation of a DHA and 10-hydroxycamptotecin conjugate. *Bioorganic & Medicinal Chemistry* **2005,** *13*, 5592-5599.

14. Wang, Y.; Li, L.; Jiang, W.; Yang, Z.; Zhang, Z., Synthesis and preliminary antitumor activity evaluation of a DHA and doxorubicin conjugate. *Bioorganic & Medicinal Chemistry Letters* **2006,** *16*, 2974-2977.
15. Huan, M.-I.; Zhou, S.-Y.; Teng, Z.-H.; Zhang, B.-I.; Liu, X.-Y.; Wang, J.-P.; Mei, Q.-B., Conjugation with a-linolenic acid improves cancer cell uptake and cytotoxicity of doxorubicin. *Bioorganic & Medicinal Chemistry Letters* **2009,** *19*, 2579-2584.
16. Schobert, R.; Biersack, B.; Knauer, S.; Ocker, M., Conjugates of the fungal cytotoxin illudin M with improved tumour specificity. . *Bioorganic & Medicinal Chemistry Letters* **2008,** *16*, 8592-8597.
17. Anel, A.; Halmos, T.; Torres, J. M.; Pineiro, A.; Antonakis, K.; Uriel, J., Cytotoxicity of chlorambucil and chlorambucil-fatty acid conjugates against human lymphomas and normal human peripheral blood lymphocytes. . *1990* **Biochem. Pharmacol. ,** *40*, 1193-1200.
18. Shikano, M.; Onimura, K.; Fukai, Y.; Hori, M.; Fukazawa, H.; Mizuno, S.; Yazawa, K.; Uehara, Y., 1a-Docosahexaenoyl Mitomycin C: A Novel Inhibitor of Protein Tyrosine Kinase. *Biochm. Biophys.Res. Comm.* **1998,** *248*, 858-863.
19. Halmos, T. M. P.; Antonakis, K.; Uriel, J., Fatty acid conjugates of 2'-dexoy-5-fluorouridine as prodrugs for the selective delivery of 5-fluorouracil to tumor cells. *Biochem. Pharmacol.* **1999,** *44*, 149-155.
20. Zerouga, M.; Stillwell, W.; Jenski, L. J., Synthesis of a novel phosphatidylcholine conjugated to docosahexaenoic acid and methotrexate that inhibits cell proliferation. . *Anti-Cancer Drugs* **2002,** *13*, 301-311.
21. Hennenfent, K. L.; Govindan, R., Novel formulations of taxanes: a review. Old wine in a new bottle? . *Annals of Oncology* **2006,** *17*, 735-749.
22. Tannock, I. F., Principles of cell proliferation: cell kinetics. In *Cancer: Principle and Practice of Oncology*, 3 ed.; DeVita Jr., V. T.; Hellman, S.; Rosenberg, S. A., Eds. J. P. Lippincott: Philadelphia, PA, 1989; pp 3-13.
23. Bradley, M. O.; Webb, N. L.; Anthony, F. H.; Devanesan, P.; Witman, P. A.; Hemamali, S.; Chander, M. C.; Baker, S. D.; He, L.; Horwitz, S. B.; Swindell, C. S., Tumor Targeting by Covalent Conjugation of a Natural Fatty Acid to Paclitaxel. *Clinical Cancer Research* **2001,** *7*, 3229-3258.
24. Sparreboom, A.; Wolff, A. C.; Verweig, J.; Zabelina, Y.; Zomeren, D. M. v.; McIntire, G. L.; Swindell, C. S.; Donehower, R. C.; Baker, S. D., Disposition of Docosahexaenoic Acid-Paclitaxel, a Novel Taxane, in Blood: In Vitro and Clinical Pharmacokinetic Studies. . *Clinical Cancer Research* **2003,** *9*, 151-159.
25. Sparreboom, A.; van-Zuylen, L.; Brouwer, E.; Loos, W. J.; de-Bruijn, P.; Gelderblom, H.; Pillay, M.; Nooter, K.; Stoter, G.; Verweig, J., Cremophor EL-mediated alteration of paclitaxel distribution in human blood: clinical pharmacokinetic implications. *Cancer Res.* **1999,** *59*, 1454-1457.
26. Wolff, A. C.; Donehower, R. C.; Carducci, M. K.; Carducci, M. A.; Brahmer, J. R.; Zabelina, Y.; Bradley, M. O.; Anthony, F. H.; Swindell, C. S.; Witman, P. A.; Webb, N. L.; Baker,

S. D., Phase I Study of Docosahexaenoic Acid-Paclitaxel: a Taxane-Fatty Acid Conjugate with a Unique Pharmacology and Toxicity Profile. *Clinical Cancer Research* **2003,** *9*, 3589-3597.
27. Johnston, S. R. D.; Houston, S.; Jones, A.; Evans, T. R.; Schacter, L., Efficacy of DHA-paclitaxel (TXP) for the second-line treatment of breast cancer. *Proc. Am. Soc. Oncol.* **2003,** *22*, 17.
28. Modiano, M. R.; Houston, S.; Savage, P.; Price, C.; Schacter, L.; Gilby, E., Efficacy of DHA-paclitaxel (TXP) in malignant melanoma. *Proc. Am. Soc. Oncol.* **2003,** *22*, 713.
29. Harries, M.; O'Donnell, A.; Scurr, M.; Reade, S.; Cole, C.; Judson, I.; Greystoke, A.; Twelves, C.; Kaye, S., Phase I/II study of DHA-paclitaxel in combination with carboplatin in patients with advanced malignant solid tumors. *British Journal of Cancer* **2004,** *91*, 1651-1655.
30. Bradley, M. O.; Swindell, C. S.; Anthony, F. H.; Witman, P. A.; Pevanesan, P.; Webb, N. L.; Baker, S. D.; Wolff, A. C.; Donehower, R. C., Tumor targeting by conjugation of DHA to paclitaxel. *Journal of Controlled Release* **2001,** *74*, 233-236.
31. Stehle, G., Plasma protein (albumin) catabolism by the tumor itself - implications for tumor metabolism and the genesis of cachexia. *Crit. Rev. Oncol. Hematol.* **1997,** *26*, 77-100.
32. Deher, M.; Liu, W.; Michelich, C.; Dewhirst, M.; Yuan, F.; Chilkoti, A., Tumor Vascular Permeability, Accumulation and Penetration of Macromolecular Drug Carriers. *J. Nat. Cancer Inst.* **2006,** *98*, 335-344.
33. Desai, N.; Yao, Z.; Trieu, V.; Soon-Shoing, P.; Dykes, D.; Noker, P., Evidence of greater tumor and red cell partitioning and superior antitumor activity of cremophor free nanoparticle paclitaxel (ABI-007) compared to taxol. *Breast Cancer Res. Treat,* **2003,** *82(suppl 1):S83*, Abstract 348.
34. Ibrahim, N. K.; Desai, N.; Legha, S.; Soon-Shiong, P.; Theriault, R.; Rivera, E.; Esmaeli, B.; Ring, S. E.; Bedikian, A.; Hortobagyi, G. N.; Ellerhorst, J. A., Phase I and Pharmacokinetic Study of ABI-007, a Cremophor-free, Protein-stabilized Nanparticle Formulation of Paclitaxel. *Clin Cancer Res* **2002,** *8*, 1038-1044.
35. Kuznetsova, L.; Chen, J.; Sun, L.; Wu, X.; Pepe, A.; Veith, J. M.; Pera, P.; Bernacki, R. J.; Ojima, I., Synthesis and evaluation of novel fatty acid-second-generation taxoid conjugates as promising anticancer agents. . *Bioorganic & Medicinal Chemistry Letters* **2006,** *16*, 974-977.
36. Siddiqui, R. A.; Zerouga, M.; Wu, M.; Castillo, A.; Harvey, K.; Zaloga, G. P.; Stillwell, W., Anticancer properties of propofol-docosahexaenoate and propofol-eicosapentaenoate of breast cancer cells. *Breast Cancer Research* **2005,** *7*, R645-R654.
37. Harvey, K. A.; Xu, Z.; Whitley, P.; Davisson, V. J.; Siddiqui, R. A., Characterization of anticancer properties of 2,6-diisopropylphenol-docasahexaenoate and analogues in breast cancer cells. *Biorg. Med. Chem* **2010,** *10*, 1866-1874.

References for Chapter 4:

1. Low, P. S.; Henne, W. A.; Doorneweerd, D. D., Discovery and Development of Folic-Acid-Based Receptor Targeting for Imaging and Therapy of Cancer and Inflammatory Diseases. *Acc. Chem. Res.* **2008,** *41*, 120-129.
2. Ojima, I., Guided Molecular Missiles for Tumor-Targeting Chemotherapy-Case Studies Using the Second-Generation Taxoid as Warheads. *Accounts of Chemical Reseach* **2008,** *41*, 108-119.
3. Russell-Jones, G.; McTavish, K.; McEwan, J.; Rice, J.; Nowotnik, D., Vitamin-mediated targeting as a potential mechanism to increase drug uptake by tumours. *Journal of Inorganic Biochemistry* **2004,** *98*, 1625-1633.
4. Leamon, C.; Reddy, J.; Betzel, M.; Dorton, R.; Westrick, E.; Parker, N.; Wang, Y.; Vlahov, I., Folate targeting enables durable and specific antitumor responses from a therapeutically null tubulysin B analogue. *Cancer Res.* **2008,** *68*, 9839-9844.
5. Xia, W.; Low, P., Folate-targeted therapies for cancer. *Journal of Medicinal Chemistry* **2010,** *53*, 6811-6824.
6. Waldrop, G.; Holden, H.; Maurice, M. S., The enzymes of biotin dependent CO2 metabolism: what structures reveal about their mechanisms. *Protein Sci.* **2012,** *21*, 1597-1619.
7. McMahon, J., Biotin in metabolism and molecular biology. *Ann. Rev. Nutr.* **2002,** *22*, 221-239.
8. Zempleni, J., Uptake, Localization, and Noncarboxylate Roles of Biotin. *Annual Reviews in Nutrition* **2005,** *25*, 175-196.
9. Zempleni, J.; Wijeratne, S.; Hassan, Y., Biotin. *Biofactors* **2009,** *35*, 36-46.
10. Ojima, I.; Zuniga, E.; Berger, W.; Seitz, J., Tumor-targeting drug delivery of new-generation taxoids. *Future Medicinal Chemistry* **2012,** *4*, 33-50.
11. Seetharam, B., Receptor-mediated endocytosis of cobalamin (vitamin B12). *Ann. Rev. Nutr.* **1999,** *19*, 173-195.
12. Lee, R.; Low, P., Delivery of liposomes into cultured KB cells via folate receptor-mediated endocytosis. *J. Biol. Chem.* **1994,** *269*, 3198-3204.
13. Chen, S.; Zhao, X.; Chen, J.; Chen, J.; Kuznetsova, L.; Wong, S.; Ojima, I., Mechanism-based tumor-targeting drug delivery system. Validation of efficient vitamin receptor-mediated endocytosis and drug release. *Bioconjugate Chemistry* **2010,** *21*, 979-987.
14. Kigawa, J.; Minagawa, Y.; Kanamori, Y.; Itamochi, H.; Cheng, X.; Okada, M.; Oisho, T.; Terakawa, N., Glutathione concentration may be a useful predictor of response to second-line chemotherapy in patients with ovarian cancer. *Cancer* **1998,** *82*, 697-702.
15. Saito, G.; Swanson, J.; Lee, K.-D., Drug delivery strategy utilizing conjugation via reversible disulfide linkages: role and site of cellular reducing activities. *Adv. Drug Delivery Rev.* **2003,** *55*, 199-215.
16. Ojima, I. C., J.; Sun, L.; Borell, C. P.; Wang, T.; Miller, M. L.; Lin, S.; Geng, X.; Kuznetsova, L.; Qu, C.; Gallager, D.; Zhao, X.; Zanardi, I.; Xia, S.; Horwitz, S. B.; Mallen-St. Clair, J.; Guerriero, J. L.; Bar-Sagi, D.; Veith, J. M.; Pera, P.; Bernacki, R. J. , Design, Synthesis, and Biological Evaluation of New-Generation Taxoids. *J. Med. Chem.* **2008,** *51*, 3203-3221.
17. Erickson, H.; Park, P.; Widdison, W.; Kovtun, Y.; Garrett, L.; Hoffman, K.; Lutz, R.; Goldmacher, V.; Blattler, W., Antibody-Maytansinoid Conjugates Are Activated in Targeted Cancer Cells by Lysosomal Degredation and Linker-Dependent Intracellular Processing. *Cancer Res.* **2006,** *66*, 4426-4435.
18. Chari, R., Targeted delivery of chemotherapuetics: tumor-activated prodrug therapy. *Adv. Drug Delivery Rev.* **1998,** *31*, 89-104.

19. Vlahov, I. R.; Santhapuram, H. K. R.; Wang, Y.; Kleindl, P. J.; You, F.; Howard, S. J.; Westrick, E.; Reddy, J. A.; Leamon, C. P., An Assembly Concept for the Consecutive Introduction of Unsymmetrical Disulfide Bonds: Synthesis of a Resleasable Multidrug Conjugate of Folic Acid. *J. Org. Chem.* **2007,** *72*, 5968-5967.
20. Wu, X.; Ojima, I., Tumor specific novel taxoid-monoclonal antibody conjugates. *Curr. MEd. Chem.* **2004,** *11*, 429-438.
21. Ojima, I., Use of Fluorine in the Medicinal Chemistry and Chemical Biology of Bioactive Compounds - A Case STudy on Fluorinated Taxane Anticancer Agents. *ChemBioChem* **2004,** *5*, 628-635.
22. Das, M. Design, Synthesis and Biological Evaluation of Novel Tumor-targeting Taxane-based Drug Delivery Systems. Stony Brook University2011.
23. Li, C.; Wang, G.-F.; Wang, Y.; Creager-Allen, R.; Lutz, E.; Scronce, H.; Slade, K.; Ruf, R.; Mehl, R.; Pielak, G., Protein 19F NMR in Escherichia coli. *J. Am. Chem. Soc.* **2010,** *132*, 321-327.
24. Wolf, W.; Presant, C.; Servis, K.; el-Tahtawy, A.; Albright, M.; Barker, P.; Ring, R.; Atkinson, D.; Ong, R.; King, M., Tumor trapping of 5-fluorouracil: in vivo 19F NMR spectroscopic pharmacokinetics in tumor-bearing humans and rabbits. *Proc. Natl. Acad. Sci.* **1990,** *87*, 492-496.
25. Martino, R.; Gilard, V.; Desmoulin, F.; Malet-Martino, M., Fluorin-19 or phophorus-31 NMR spectroscopy: A suitable analytical technique for quantitative in vitro metabolic studies of fluorinated or phosphorylated drugs. *J. Pharm. Biomed. Anal.* **2005,** *38*, 871-891.
26. Kamila, S.; Biehl, E. R., New synthesis of 3H-benzo[b]thiophen-2-ones. *Heterocycles* **2004,** *63*, 1813-1819.
27. Widdison, W. C.; Wilhelm, S. D.; Cavanagh, E. E.; Whileman, K. R.; Leece, B. A.; Kovtun, Y.; Goldmacher, V. S.; Xie, H.; Steeves, R. M.; Lutz, R. J.; Zhao, R.; Wang, L.; Blaettler, W. A.; Chari, R. V. J., Semisynthetic Maytansine Analogs for the Targeted Treatment of Cancer. *J. Med. Chem.* **2006,** *49*, 4392-4408.
28. Bannerjee, P. S.; Zuniga, E. S.; Ojima, I.; Carrico, I. S., Targeted and armed oncolytic adenovirus via chemoselective modification. *Bioorg. Med. Chem. Lett.* **2011,** *21*, 4985-4988.
29. Dickinson, R. P., Iddon, B., Condensed Thiophen Ring Systems. Part III. A New Synthesis of Benzo[b]thiophen-2(3H)- and - 3(2H)-ones and Some Reactions of Benzo[b]thiophen-2(3H)-one with Dimethyl Sulphate in the Presence of Base. *J. Chem. Soc.* **1970,** *14*, 1926-1928.
30. Bordwell, F. G., Fried, H.E., Heterocyclic aromatic anions with 4n + 2 pi-electrons. *Journal of Organic Chemistry* **1991,** *56*, 4218-4223.

References for Chapter 5:

1. Wagner, C., Biochemical role of folate in cellular metabolism. In *Folate in health and disease*, Bailey, L. B., Ed. CRC Press1995; pp 23-42.
2. Kamen, B., Folate and antifolate pharmacology. *Semin. Oncol.* **1997,** *24*, S18-30-S18-38.
3. Maziarz, K. M.; Monaco, H. L.; Shen, F.; Ratnam, M., Complete mapping of divergent amino acids responsible for differential ligand binding of folate receptors alpha and beta. *J . Biol. Chem.* **1999,** *274*, 11086-11091.
4. Wang, X.; Shen, F.; Freisheim, J. H.; Gentry, L. E.; Ratnam, M., Differential stereospecificities and affinities of folate receptor isoforms for folate compounds and antifolates. *Biochem. Pharmacol.* **1992,** *44*, 1898-1901.
5. Holm, J.; Hansen, S. I.; Hoier-Madsen, M.; Sondergaard, K.; Bzorek, M., Folate receptor of human mammary adenocarcinoma. *APMIS* **1994,** *102*, 413-419.
6. S D Weitman, R. H. L.; Coney, L. R.; Fort, D. W.; Frasca, V.; Zurawski, V. R.; Kamen, B. A., Distribution of the Folat eREceptor GP38 in Normal and Malignant Cell Lines and Tissues. *Cancer Res.* **1992,** *52*, 3396-3401.
7. Rettig, W.; Garin-Chesa, P.; Beresford, H.; Oettgen, H.; Melamed, M.; Old, L., CEll-surface glycoproteins of human sarcomas: differential expression in normal and malignant tissues and cultured cells. *Proc. Nat. Acad. Sci.* **1988,** *85*, 3110-3114.
8. Toffoli, G.; Cernigio, C.; Russo, A.; Gallo, A.; Bagnoli, M.; Boicchi, M., Overexpression of folate binding protein in ovarian cancers. *Int. J. Cancer* **1997,** *74*, 193-198.
9. Vlahov, I. R.; Leamon, C. P., Engineering Folate-Drug Conjugates to Target Cancer: From Chemistry to Clinic. *Bioconjugate Chem.* **2012,** *23*, 1357-1369.
10. Leamon, C. P.; You, F.; Santhapuram, H. K.; Fan, M.; Vlahov, I. R., Properties influencing the relative binding affinity of pteroate derivatives and drug conjugates thereof to the folate receptor. *Pharm. Res.* **2009,** *26*, 1315-1323.
11. Westerhof, G. R.; Schornagel, J. H.; Kathmann, I.; JAckman, A. L.; Rosowsky, A.; Forsch, R. A.; Hynes, J.; Boyl, F. T.; Peters, G. J.; Pinedo, H. M.; JAnsen, G., Carrier- and receptor-mediated transport of folate antagonists targeting folate-dependent enzymes: Correlates of molecular structure and biological activitiy. *Mol. Pharmacol.* **1995,** *48*, 459-471.
12. Leamon, C. P.; Jackman, A. L., Exploitation of the Folate Receptor in the Management of Cancer and Inflammatory Disease. In *Vitamins and Hormones*, Litwack, G., Ed.2008; pp 203-233.
13. Ladino, C. A.; Chari, R. V. J.; Bourret, L. A.; Kedersha, N. L.; Goldmacher, V. S., Folate-maytansinoids: Target-selective drugs of low molecular weight. *Int. J. Cancer* **1997,** *73*, 859-864.
14. Steinberg, G.; Borch, R. F., Synthesis and evaluation of pteroic acid-conjugated nitroheterocyclic phosphoramidates as folate receptor-targeted alkylating agents. *J. Med. Chem.* **2001,** *44*, 69-73.
15. Lee, J. W.; Lu, J. Y.; Low, P. S.; Fuchs, P. L., Synthesis and evaluatoin of taxol-folic acid conjugates as targeted antineoplastics. *Bioorg. Med. Chem. Lett.* **2002,** *10*, 2397-2414.

16. Aronov, O.; Horowitz, A. T.; Gabizon, A.; Gibson, D., Folate-targeted PEG as a potential carrier for Carboplatin analogs. Synthesis and in vitro studies. *Bioconjugate Chem.* **2003,** *14*, 563-574.
17. Butterworth, C. E.; Baugh, C. M.; Krumdieck, C., A study of folate absorption and metabolism in man utilizing carbon-14-labeled polyglutamates synthesized by the solid phase method. *J. Clin. Invest.* **1969,** *48*, 1131-1142.
18. Vlahov, I. R.; Santhapuram, H. K.; Kleindl, P. J.; Howard, S. J.; Stanford, K. M.; Leamon, C. P., Design and regioselective synthesis of a new generation of targeted chemotherapeutics. Part 1: EC145, a folic acid conjugate of desacetylvinblastine monohydrazide. *Bioorg. Med. Chem. Lett.* **2006,** *16*, 5093-5096.
19. Vlahov, I. R.; Vite, G. D.; Kleindl, P. J.; Wang, Y.; Santhapuram, H. K.; You, F.; Howard, S. J.; Kim, S.; Lee, F. F.; Leamon, C. P., Regioselective synthesis of folate receptor-targeted agents derived from epothilone analogs and folic acid. *Bioorg. Med. Chem. Lett.* **2010,** *20*, 4578-4581.
20. Vlahov, I. R.; Wang, Y.; Kleindl, P. J.; Leamon, C. P., Design and regioselective synthesis of a new generation of targeted chemotherapeutics. Part II: Folic acid conjugates of tubulysins and their hydrazides. *Bioorg. Med. Chem. Lett.* **2008,** *18*, 4558-4561.
21. Vlahov, I. R.; Santhapuram, H. K. R.; Wang, Y.; Kleindl, P. J.; You, F.; Howard, S. J.; Westrick, E.; Reddy, J. A.; Leamon, C. P., An Assembly Concept for the Consecutive Introduction of Unsymmetrical Disulfide Bonds: Synthesis of a Resleasable Multidrug Conjugate of Folic Acid. *J. Org. Chem.* **2007,** *72*, 5968-5967.
22. Sausville, E.; LaRusso, P.; Quinn, M.; Forman, K.; Leamon, C.; Morganstern, D.; Bever, S.; MEssmann, R., A phase I study of EC145 administered weeks 1 and 3 of a 4-week cycle in patients with refractory solid tumors. *Proc. Am. Soc. Clin. Oncol* **2007,** *25*, 2577.
23. Reddy, J. A.; Dorton, R.; Westrick, E.; Dawson, A.; Smith, T.; Xu, L. C.; Vetzel, M.; Kleindl, P.; Vlahov, I. R.; LEamon, C. P., Preclinical evaluation of EC145, a folate-vinca alkaloid conjugate. *Cancer Res.* **2007,** *67*, 4434-4442.
24. Nauman, R.; Coleman, R.; Burger, R.; Herzog, T.; Morris, R.; Sausville, E.; Kutarska, E.; Ghamande, S.; Gabrail, N.; Pasquale, S. D.; Nowara, E.; Gilbert, L.; Caton, J.; Gersh, R.; Teneriello, M.; Harb, W.; Konstantinopoulos, P.; Symanowski, J.; Lovejoy, C.; Messmann, R., Precedent: a randomized phase II trial comparing EC145 and pegylated liposomal doxorubicin (PLD) in combination, versus PLS alone, in subjects with platinum-resistant ovarian cancer. *Am. Soc. Clin. Oncol. Ann. Meeting* **2010**, abstract 5045.
25. Leamon, C. P.; Reddy, J. A.; Klein, P. J.; Vlahov, I. R.; Dorton, R.; Bloomfield, A.; Nelson, M.; Westrick, E.; Parker, N.; Bruna, K.; Betzel, M.; Gehrke, J. S.; Messmann, R. A.; LoRusso, P. M.; Sausville, E. A., Reducing undesiralbe hepatic clearance of a tumor0targeted vinca alkaloid via novel saccharopeptidic modifications. *J . Pharmacol. Exp. Therp.* **2011,** *336*, 336-343.
26. Agard, N. J.; Baskin, J. M.; Prescher, J. A.; Lo, A.; Bertozzi, C. R., A comparative study of bioorthogonal reactions with azides. *ACS Chem. Biol.* **2006,** *1*, 644-648.

References for Chapter 6:

1. Langer, O.; Muller, M., Methods to Assess Tissue-Specific Distribution and Metabilism of Drugs. *Curr. Drug. Metabol.* **2005,** *5*, 463-481.
2. Dalvie, D., Recent advances in the applicaitons of radioisotopes in drug metabolism, toxicology and pharmacokinetics. *Curr. Pharm. Des.* **2000,** *6*, 1009-1028.
3. Bergstrom, M.; Grahnen, A.; Langstrom, B., Positron emission tomography microdosing: a new concept with application in tracer and early clinical drug development. *Eur. J. Clin. Pharm.* **2003,** *59*, 357-366.
4. Sparreboom, A.; Wolff, A. C.; Verweig, J.; Zabelina, Y.; Zomeren, D. M. v.; McIntire, G. L.; Swindell, C. S.; Donehower, R. C.; Baker, S. D., Disposition of Docosahexaenoic Acid-Paclitaxel, a Novel Taxane, in Blood: In Vitro and Clinical Pharmacokinetic Studies. . *Clinical Cancer Research* **2003,** *9*, 151-159.
5. Ravert, H. T.; Klecker, R. W.; J M Collins; Mathews, W. B.; Pomper, M. G.; Wahl, R. L.; Dannals, R. F., Radiosynthesis of [11C]paclitaxel. *J. Label. Comp. Radiopharm.* **2002,** *45*, 471-477.
6. Kiesewetter, D. O.; Jagoda, E. M.; Kao, K.; Ma, Y.; Ravasi, L.; Shimoji, K.; Szajek, L. P.; Eckelman, W. C., Fluro-, bromo-, and iodopaclitaxel derivatives: synthesis and biological evaluation. *Nucl. Med. Biol.* **2003,** *30*, 11-24.
7. Roh, E. J.; Park, Y. H.; Song, C. E.; Oh, S.-J.; Choe, Y. S.; Kim, B.-T.; Chi, D. Y.; Kim, D., Radiolabeling of Paclitaxel with Electrophilic 123I. *Bioorg. Med. Chem. Lett.* **2000,** *8*, 65-68.
8. Kurdziel, K. A.; Kalen, J. D.; Hirsch, J. I.; Wilson, J. D.; Agarwal, R.; Barrett, D.; Bear, H. D.; McCumiskey, J. F., Imaging multidrug resistance with 4-[18F]fluoropaclitaxel. *Nucl. Med. Biol.* **2007,** *34*, 823-831.
9. Kurdziel, K. A.; Kiesewetter, D. O.; Carson, R. E.; Eckelman, W. C.; Herscovitch, P., Biodistribution, radiation dose estimates and in vivo pgp modulation studies of 18F-paclitaxel in nonhuman primates. *J. Nucl. Med.* **2003,** *44*, 1330-1339.
10. Tilbug, E. W. v.; Franssen, E. J. F.; Hoevaen, J. J. M. v. d.; Meij, M. v. d.; Elshove, D.; Lammertsma, A. A.; Windhorst, A. D., Radiosynthesis of [11C]docetaxel. *J. Label. Comp. Radiopharm.* **2004,** *47*, 763-777.
11. vsn der Veldt, A. A. M.; Hendrikse, N. H.; Smit, E. F.; Mooijer, M. P. J.; Rijnders, A. Y.; Gerritsen, W. R.; Hoeven, J. J. M. v. d.; Wiindhorst, A. D.; Lammertsma, A. A.; Lubberink, M., Biodistribution and radiation dosimetry of 11C-labelled docetaxel in cancer patients. *Eur. J. Nucl. Med. Mol. Imaging* **2010,** *37*, 1950-1958.
12. Mading, P.; Zessin, J.; Pleib, U.; Fuchtner, F.; Wust, F., Synthesis of a 11C-labelled taxane derivative by [1-11C]acetylation. *J. Label. Comp. Radiopharm.* **2006,** *49*, 357-365.
13. Cisternino, S.; Bourasset, F.; Archimbaud, Y.; Semiond, D.; Sanderink, G.; Scherrmann, J.-M., Nonlinear accumulation in the brain of the new taxoid TXD258 following saturation of P-glycoprotein at the blood-brain barrier in mice and rats. *Br. J. Pharmacol.* **2003,** *138*, 1367-1375.

14. Ono, C.; Takao, A.; Atsumi, R., Absorption, Distribution, and Excretion of DJ-927, a Novel Orally Effective Taxane, in Mice, Dogs, and Monkeys. *Biol. Pharm. Bull.* **2004,** *27*, 345-351.
15. Prezte, M.; Grobe-Gehling, P.; Mamat, C., Cross-Coupling Reactions as Valuable Tool for the Preparation of PET Radiotracers. *Molecules* **2011,** *16*, 1129-1165.
16. Milstein, D.; Stille, J. K., Palladium-catalyzed coupling of tetraorganotin compounds with aryl and benyl halides. Synthetic utility and mechanism. *J. Am. Chem. Soc.* **1979,** *101*, 4992-4998.
17. Mee, S. P. H.; Lee, V.; Baldwin, J. E., Stille Coupling Made Easy - The Synergic Effect of Copper(I) Salts and the Fluoride Ion. *Angew. Chem. Int. Ed. Engl.* **2004,** *43*, 1132-1135.
18. Farina, V.; Kapadia, S.; Krishnan, B.; Wang, C.; Liebeskind, L. S., On the Nature of the "Copper Effect" in the Stille Cross-Coupling. *J. Org. Chem.* **1994,** *59*, 5905-5911.
19. Andersson, Y.; Cheng, A.; Langstrom, B., Pappadium-promoted coupling reactions of [11C]methyl iodide with organotin and arganoboron compounds. *Acta Chem. Scand.* **1995,** *49*, 683-688.
20. Suzuki, M.; Doi, H.; Bjorkman, M.; Andersson, Y.; Langstrom, B.; Watanabe, Y.; Noyori, R., Rapid coupling of methyl iodide with aryltributylstannanes mediated by palladium(0) complexes: a general protocol for the synthesis of 11CH3-labeled PET tracers. *Chem. Eur. J.* **1997,** *3*, 2039-2042.
21. Aamdal, S.; Wolff, I.; Kaplan, S.; Paridaens, R.; Kerger, J.; Schachter, J.; Wanders, J.; Franklin, H.; Verweij, J., Docetaxel (Taxotere) in advanced malignant melanoma: a phase II study of the EORTC early clinical trials group. *Eur. J. Cancer* **1994,** *30*, 1061-1064.
22. Hosoya, T.; Sumi, K.; Doi, H.; Wakao, M.; Suzuki, M., Rapid methylation on carbon frameworks useful for the synthesis of 11CH3-incorporated PET tracers: Pd(0)-mediated rapid coupling of methyl iodide with an alkenyltributylstannane leading to a 1-methylalkene. *Org. & Biomol. Chem.* **2006,** *4*, 410-415.
23. Bjorkman, M.; Andersson, Y.; Doi, H.; Kato, K.; Suzuki, M.; Noyori, R.; Watanabe, Y.; Langstrom, B., Synthesis of 11C/13C-labelled prostacyclins. *Acta Chem. Scand.* **1998,** *53*, 635-640.
24. Suzuki, M.; Doi, H.; Kao, K.; Bjorkman, M.; Langstrom, B.; Watanabe, Y.; Noyori, R., Rapid methylation for the synthesis of a 11C-labeled tolylisocarbacyclin imaging the IP2 receptor in a living human brain. *Tetrahedron* **2000,** *56*, 8263-8273.
25. Suzuki, M.; Doi, H.; Hosoya, T.; Langstrom, B.; Watanabe, Y., Rapid methylation on carbon framworks leading to the synthesis of a PET tracer capable of imaging a novel CNS-type prostacyclin receptor in living human brain. *Trends Anal. Chem.* **2004,** *23*, 595-607.
26. Samuelsson, L.; Langstrom, B., Synthesis of 1-(2'-deoxy-2'-fluoro-β-d-arabinofuranosyl)-[methyl]-thymine ([11C]FMAU) via a Stille cross-coupling reaction with [11C]methyl iodide. *J. Label. Comp. Radiopharm.* **2003,** *46*, 263-272.
27. Toyohara, J.; Okada, M.; Toramatsu, C.; Suzuki, K.; Irie, T., Freasibility studies of 4'-[methyl-11C]thiothymidine as a tumor proliferation imaging agent in mice. *Nucl. Med. Biol.* **2008,** *35*, 67-74.

Appendix Chapter 1

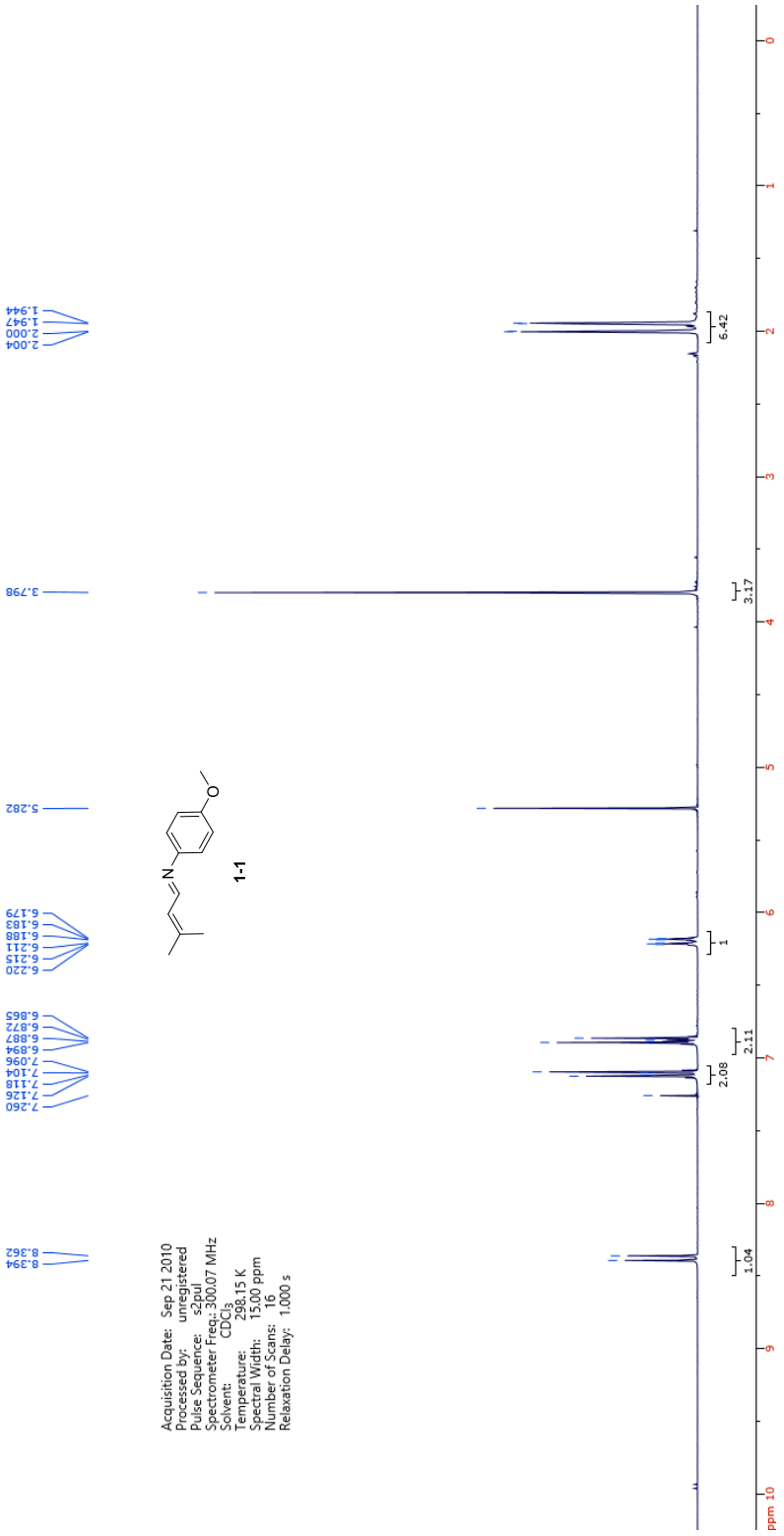
8.394
8.362
7.260
7.126
7.118
7.104
7.096
6.894
6.887
6.872
6.865
6.220
6.215
6.211
6.188
6.183
6.179
5.282
3.798
2.004
2.000
1.947
1.944
1-1
Acquisition Date: Sep 21 2010
Processed by: unregistered
Pulse Sequence: s2pul
Spectrometer Freq.: 300.07 MHz
Solvent: CDCl3
Temperature: 298.15 K
Spectral Width: 15.00 ppm
Number of Scans: 16
Relaxation Delay: 1.000 s
1.04
2.08
2.11
1
3.17
6.42
ppm 10

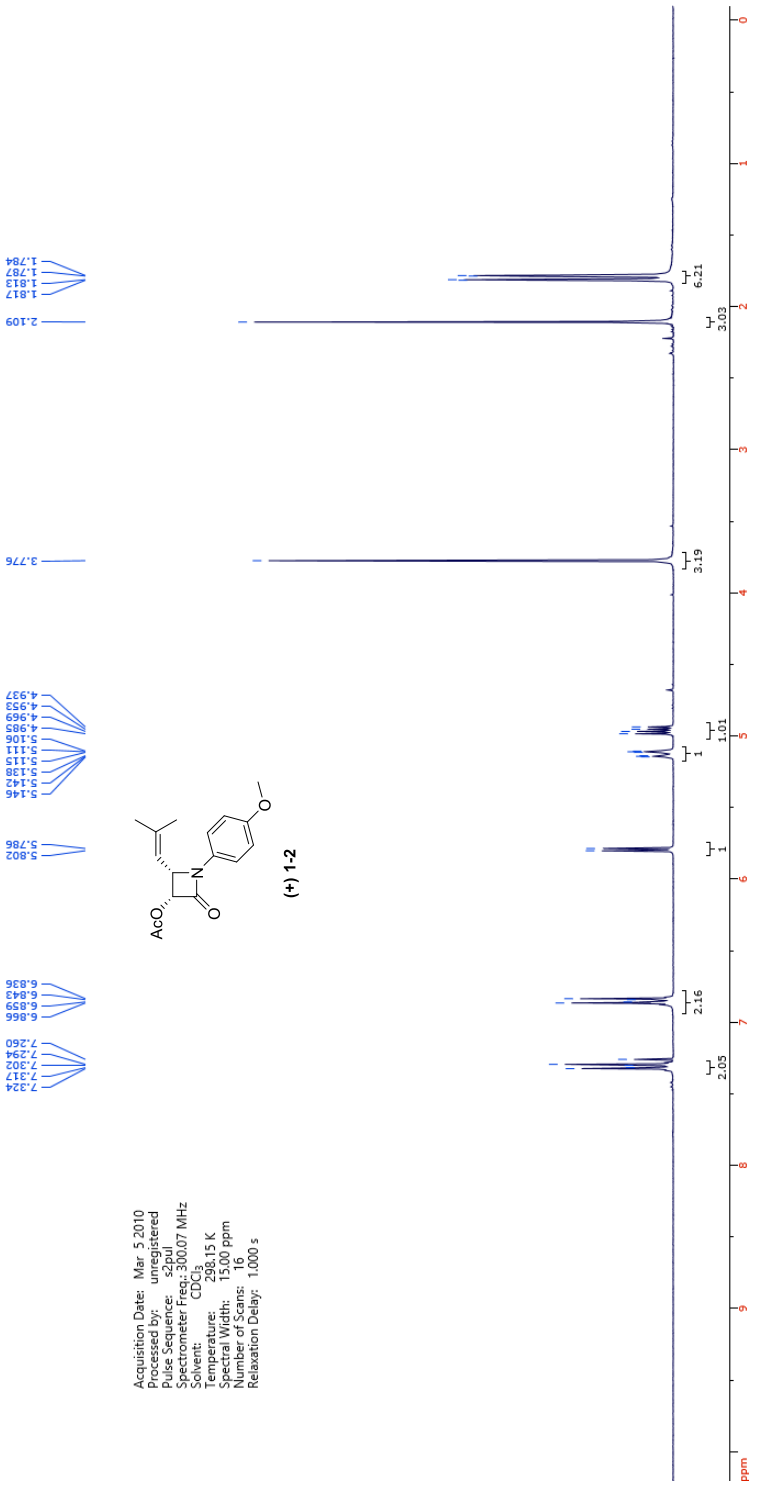
1.784
1.787
1.813
1.817
2.109
3.776
4.937
4.953
4.969
4.985
5.106
5.111
5.115
5.138
5.142
5.146
5.786
5.802
6.836
6.843
6.859
6.866
7.260
7.294
7.302
7.317
7.324
6.21
3.03
3.19
1.01
1
1
2.16
2.05
AcO
O
N
O
(+) 1-2
Acquisition Date: Mar 5 2010
Processed by: unregistered
Pulse Sequence: s2pul
Spectrometer Freq.: 300.07 MHz
Solvent: CDCl3
Temperature: 298.15 K
Spectral Width: 15.00 ppm
Number of Scans: 16
Relaxation Delay: 1.000 s
ppm

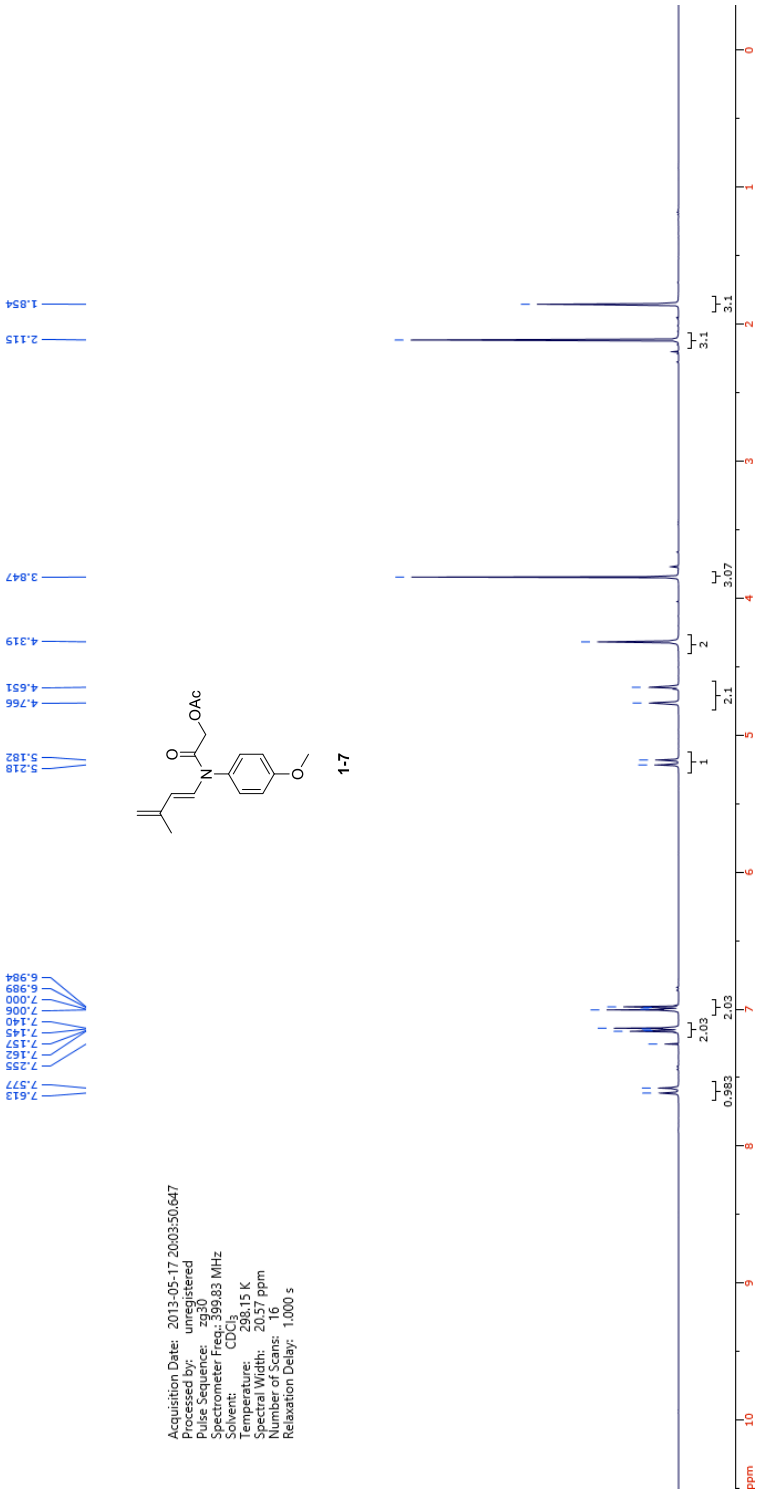
1.854
2.115
3.847
4.319
4.651
4.766
5.182
5.218
6.984
6.989
7.000
7.006
7.140
7.145
7.157
7.162
7.255
7.577
7.613
OAc
O
N
O
1-7
Acquisition Date: 2013-05-17 20:03:50.647
Processed by: unregistered
Pulse Sequence: zg30
Spectrometer Freq.: 399.83 MHz
Solvent: CDCl3
Temperature: 298.15 K
Spectral Width: 20.57 ppm
Number of Scans: 16
Relaxation Delay: 1.000 s
3.1
3.1
3.07
2
2.1
1
2.03
2.03
0.983
ppm

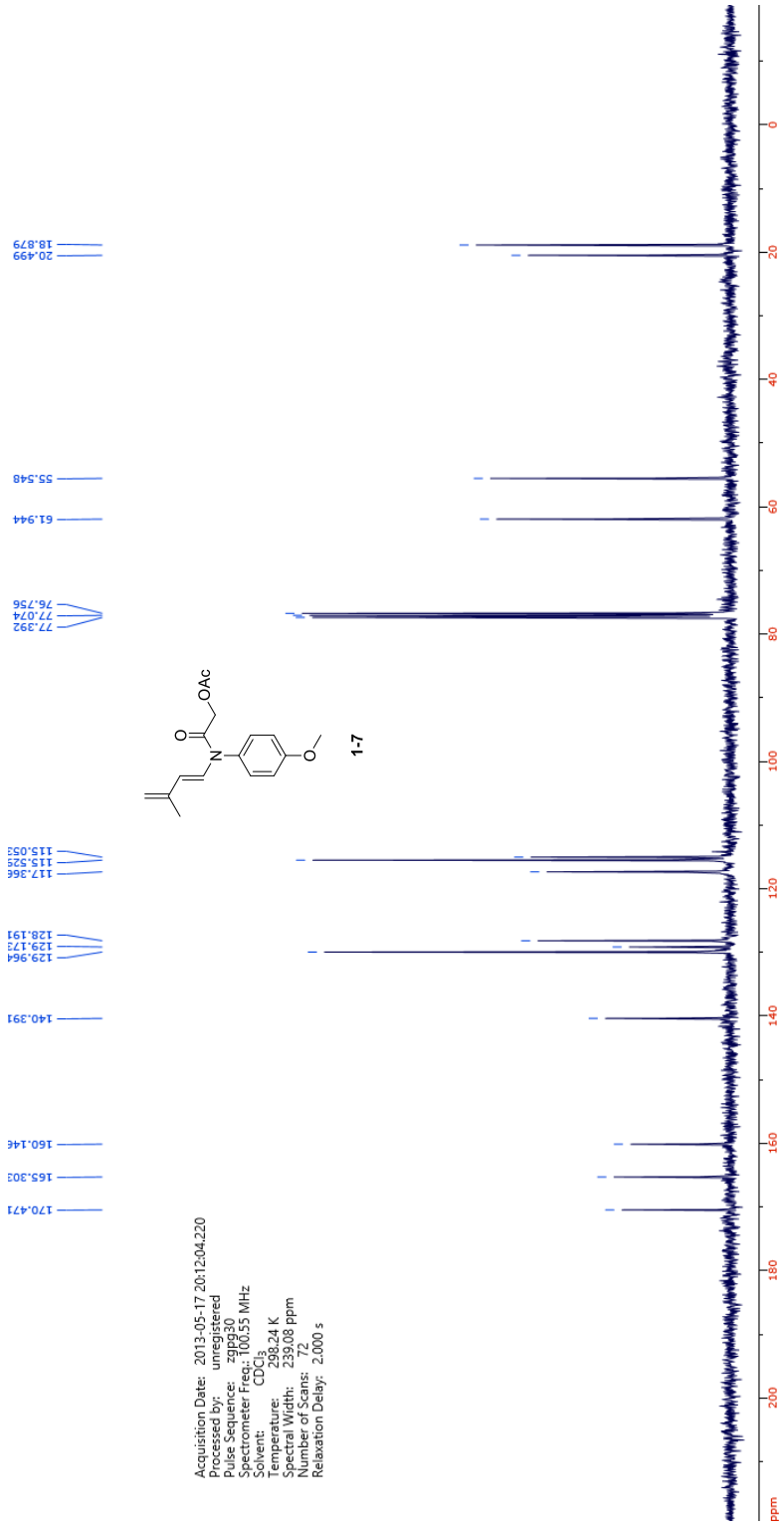
20.499
18.879
55.548
61.944
76.756
77.074
77.392
115.053
115.529
117.366
128.191
129.172
129.964
140.391
160.146
165.303
170.471
OAc
O
N
O
1-7
Acquisition Date: 2013-05-17 20:12:04.220
Processed by: unregistered
Pulse Sequence: zgpg30
Spectrometer Freq.: 100.55 MHz
Solvent: CDCl3
Temperature: 298.24 K
Spectral Width: 239.08 ppm
Number of Scans: 72
Relaxation Delay: 2.000 s
ppm

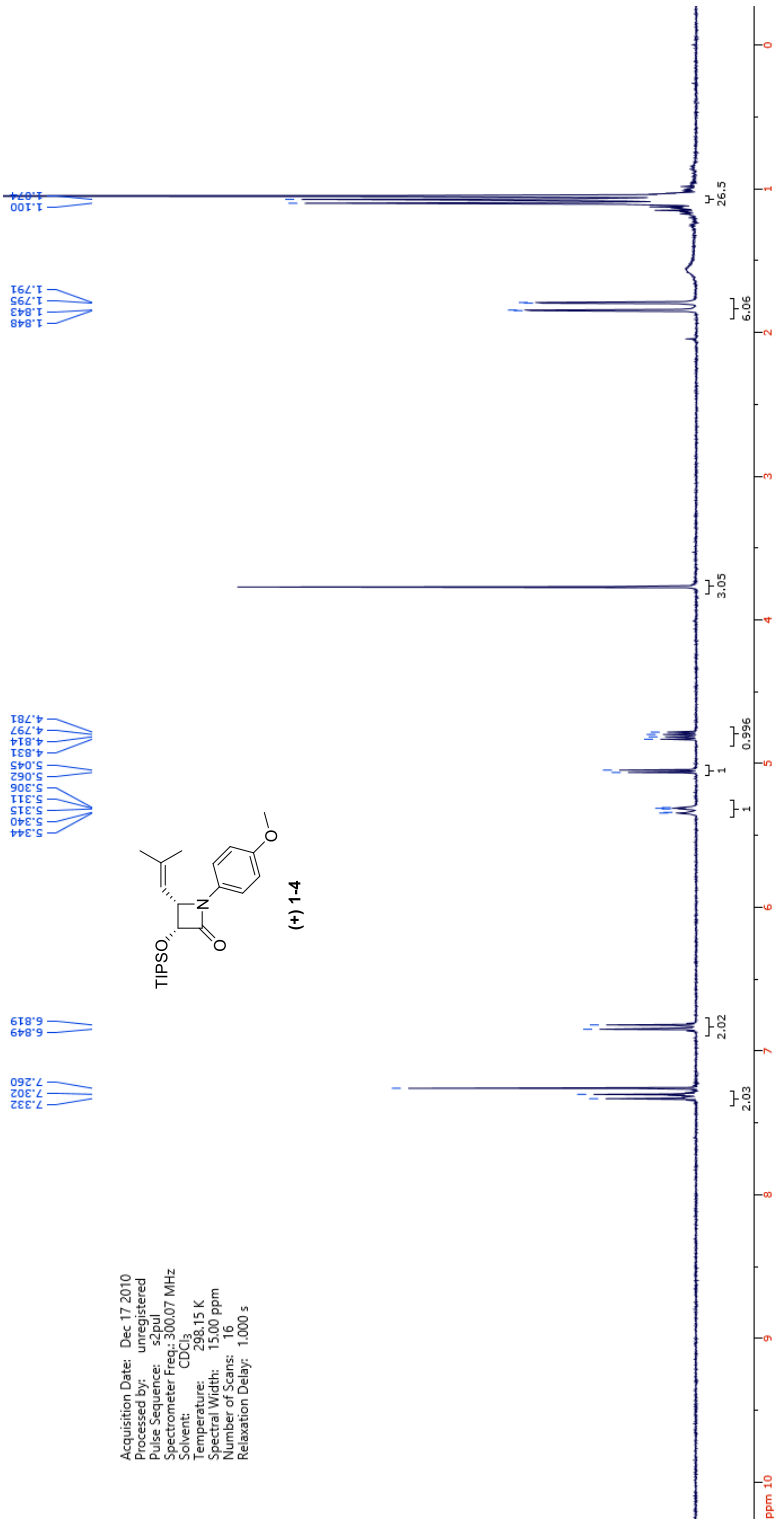
1.074
1.100
1.791
1.795
1.843
1.848
4.781
4.797
4.814
4.831
5.045
5.062
5.306
5.311
5.315
5.340
5.344
6.819
6.849
7.260
7.302
7.332
26.5
6.06
3.05
0.996
1
1
2.02
2.03
TIPSO
O
N
O
(+) 1-4
Acquisition Date: Dec 17 2010
Processed by: unregistered
Pulse Sequence: s2pul
Spectrometer Freq.: 300.07 MHz
Solvent: $CDCl_3$
Temperature: 298.15 K
Spectral Width: 15.00 ppm
Number of Scans: 16
Relaxation Delay: 1.000 s
ppm 10

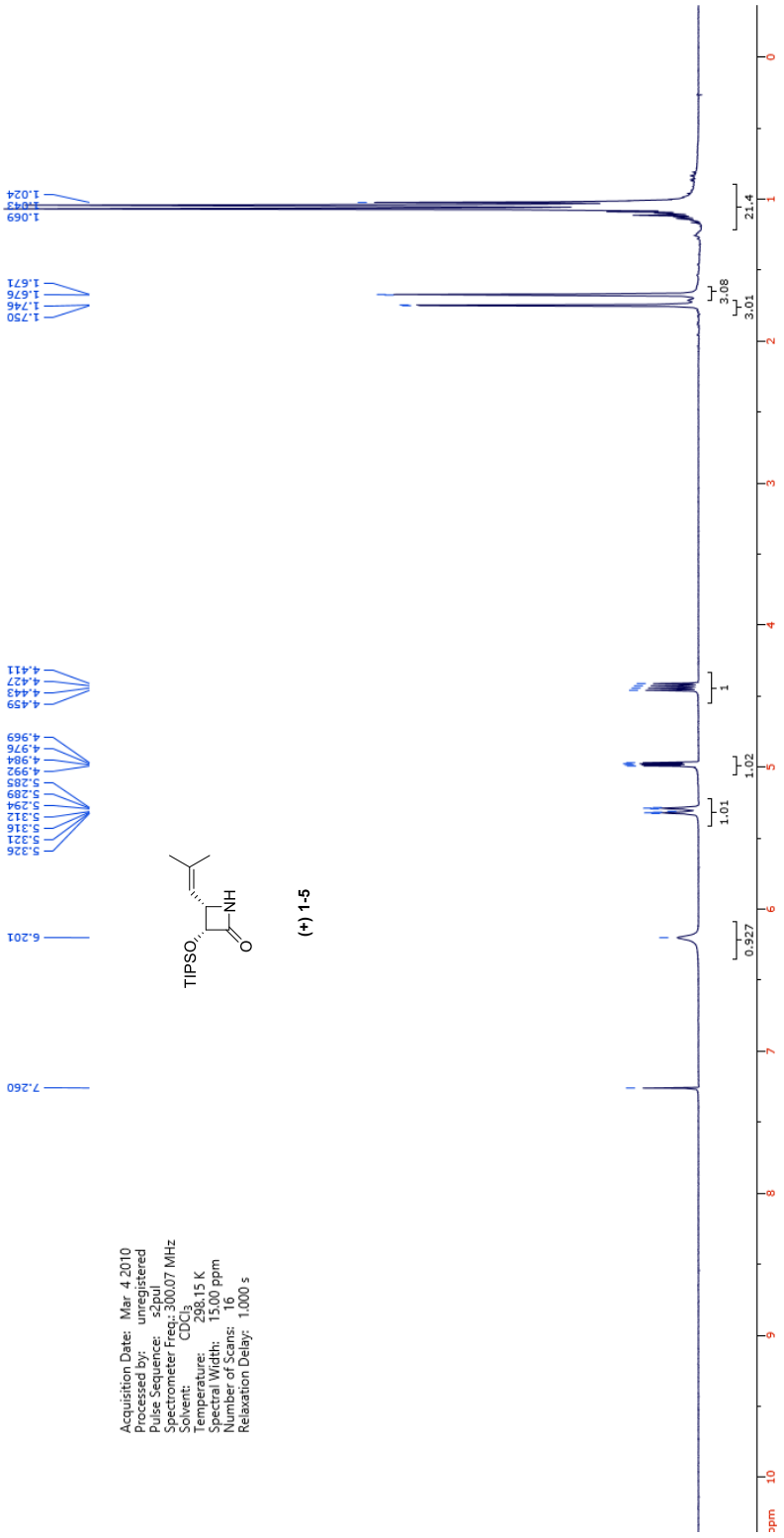
1.024
1.069
1.671
1.676
1.746
1.750
4.411
4.427
4.443
4.459
4.969
4.976
4.984
4.992
5.285
5.289
5.294
5.312
5.316
5.321
5.326
6.201
7.260
21.4
3.08
3.01
1
1.02
1.01
0.927
TIPSO
NH
O
(+) 1-5
Acquisition Date: Mar 4 2010
Processed by: unregistered
Pulse Sequence: s2pul
Spectrometer Freq.: 300.07 MHz
Solvent: $CDCl_3$
Temperature: 298.15 K
Spectral Width: 15.00 ppm
Number of Scans: 16
Relaxation Delay: 1.000 s
ppm

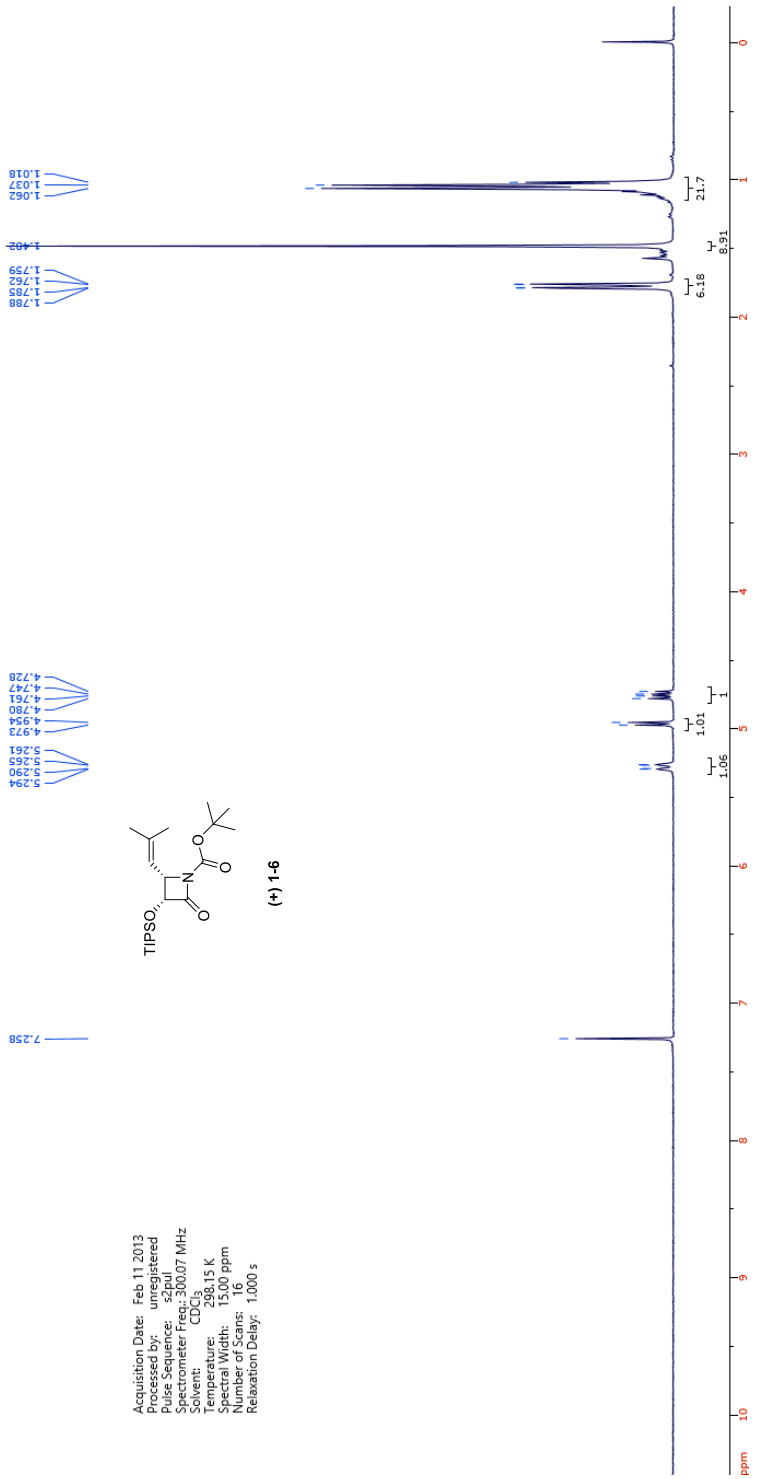
7.258
5.294
5.290
5.265
5.261
4.973
4.954
4.780
4.761
4.747
4.728
1.788
1.785
1.762
1.759
1.402
1.062
1.037
1.018
21.7
8.91
6.18
1.01
1.06
1
ppm
TIPSO
(+) 1-6
Acquisition Date: Feb 11 2013
Processed by: unregistered
Pulse Sequence: s2pul
Spectrometer Freq.: 300.07 MHz
Solvent: CDCl3
Temperature: 298.15 K
Spectral Width: 15.00 ppm
Number of Scans: 16
Relaxation Delay: 1.000 s

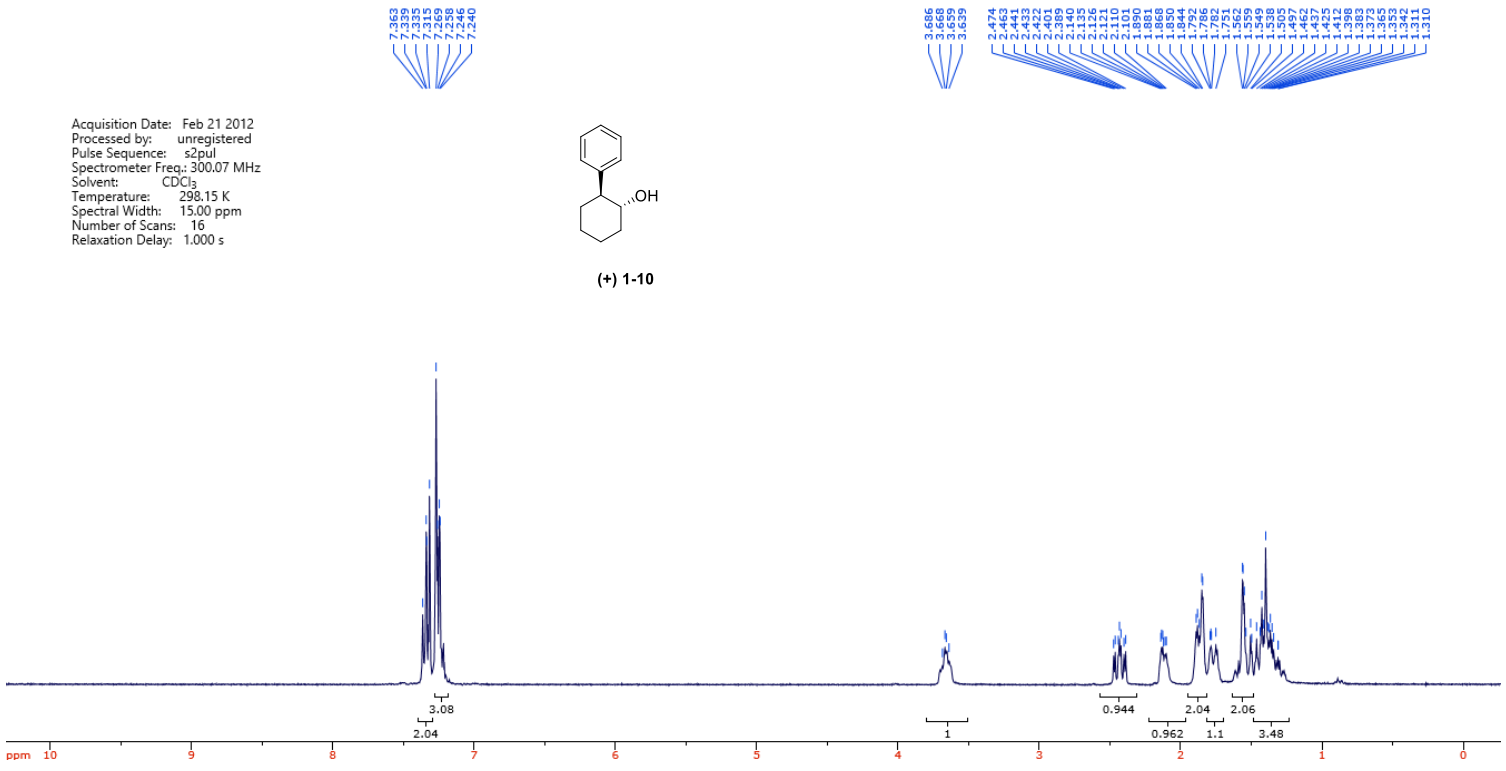
7.363
7.339
7.335
7.315
7.269
7.258
7.246
7.240
3.686
3.666
3.659
3.639
2.474
2.463
2.441
2.433
2.422
2.401
2.389
2.140
2.135
2.125
2.121
2.110
2.101
1.891
1.880
1.868
1.850
1.944
1.792
1.786
1.782
1.751
1.562
1.559
1.549
1.538
1.505
1.497
1.467
1.437
1.425
1.412
1.398
1.383
1.373
1.365
1.353
1.342
1.331
1.310
Acquisition Date: Feb 21 2012
Processed by: unregistered
Pulse Sequence: s2pul
Spectrometer Freq.: 300.07 MHz
Solvent: CDCl3
Temperature: 298.15 K
Spectral Width: 15.00 ppm
Number of Scans: 16
Relaxation Delay: 1.000 s
OH
(+) 1-10
3.08
2.04
1
0.944
0.962
2.04
1.1
2.06
3.48
ppm 10
9
8
7
6
5
4
3
2
1
0

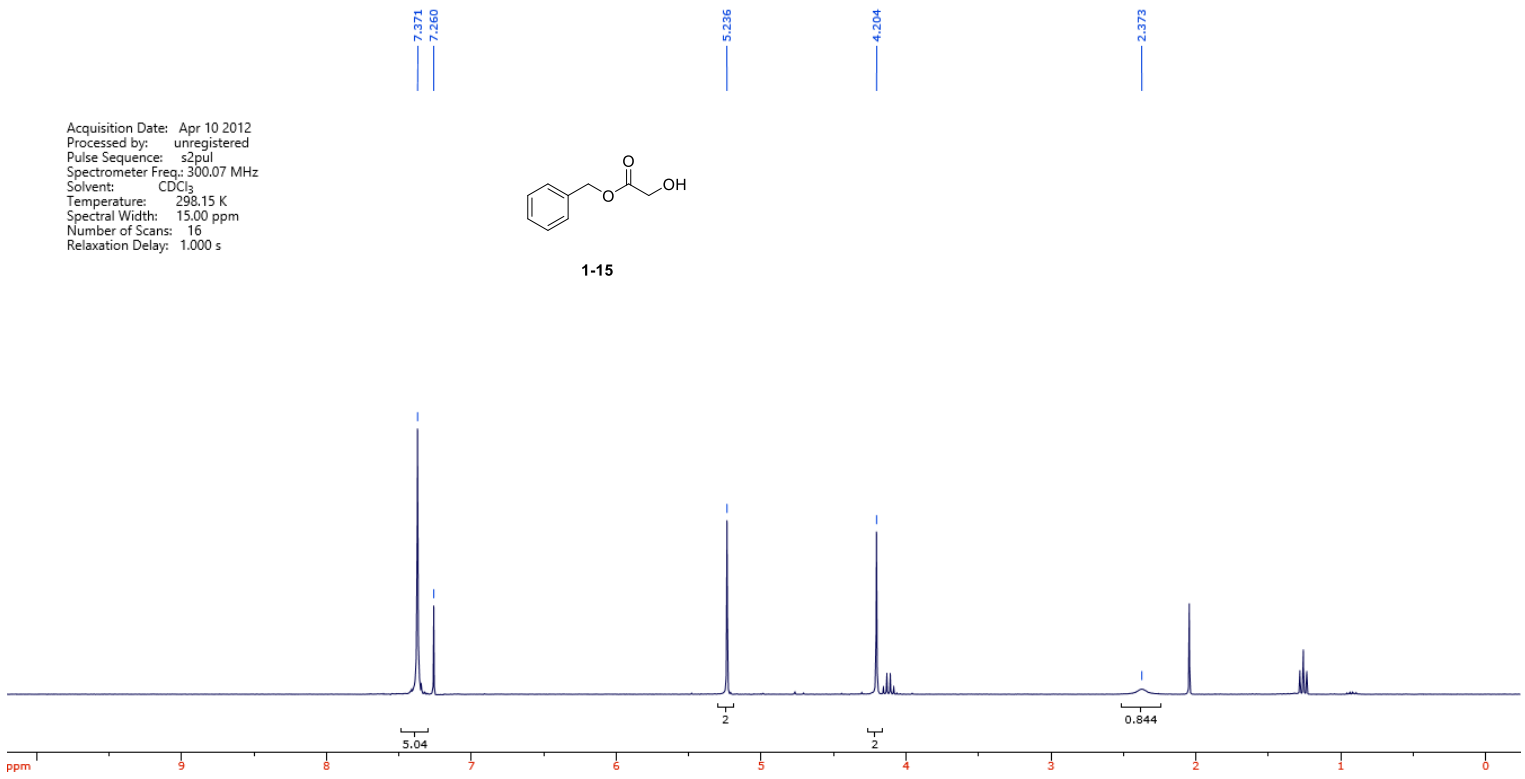
7.371
7.260
5.236
4.204
2.373
Acquisition Date: Apr 10 2012
Processed by: unregistered
Pulse Sequence: s2pul
Spectrometer Freq.: 300.07 MHz
Solvent: CDCl3
Temperature: 298.15 K
Spectral Width: 15.00 ppm
Number of Scans: 16
Relaxation Delay: 1.000 s
O
OH
O
5.04
2
2
0.844
ppm
9
8
7
6
5
4
3
2
1
0

1-15

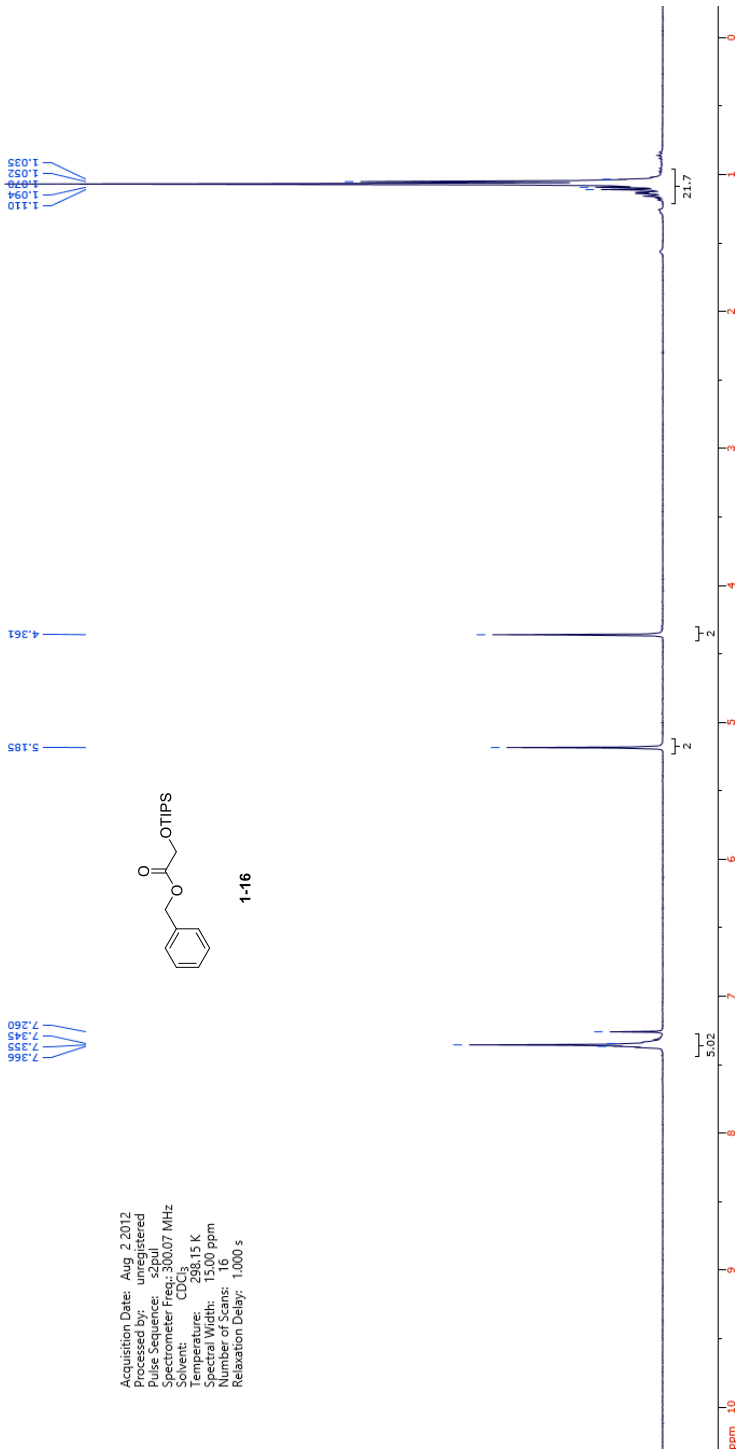
1.035
1.032
1.078
1.094
1.110
4.361
5.185
7.260
7.345
7.355
7.366
21.7
2
2
5.02
ppm
OTIPS
O
O
1-16
Acquisition Date: Aug 2 2012
Processed by: unregistered
Pulse Sequence: s2pul
Spectrometer Freq.: 300.07 MHz
Solvent: CDCl3
Temperature: 298.15 K
Spectral Width: 15.00 ppm
Number of Scans: 16
Relaxation Delay: 1.000 s

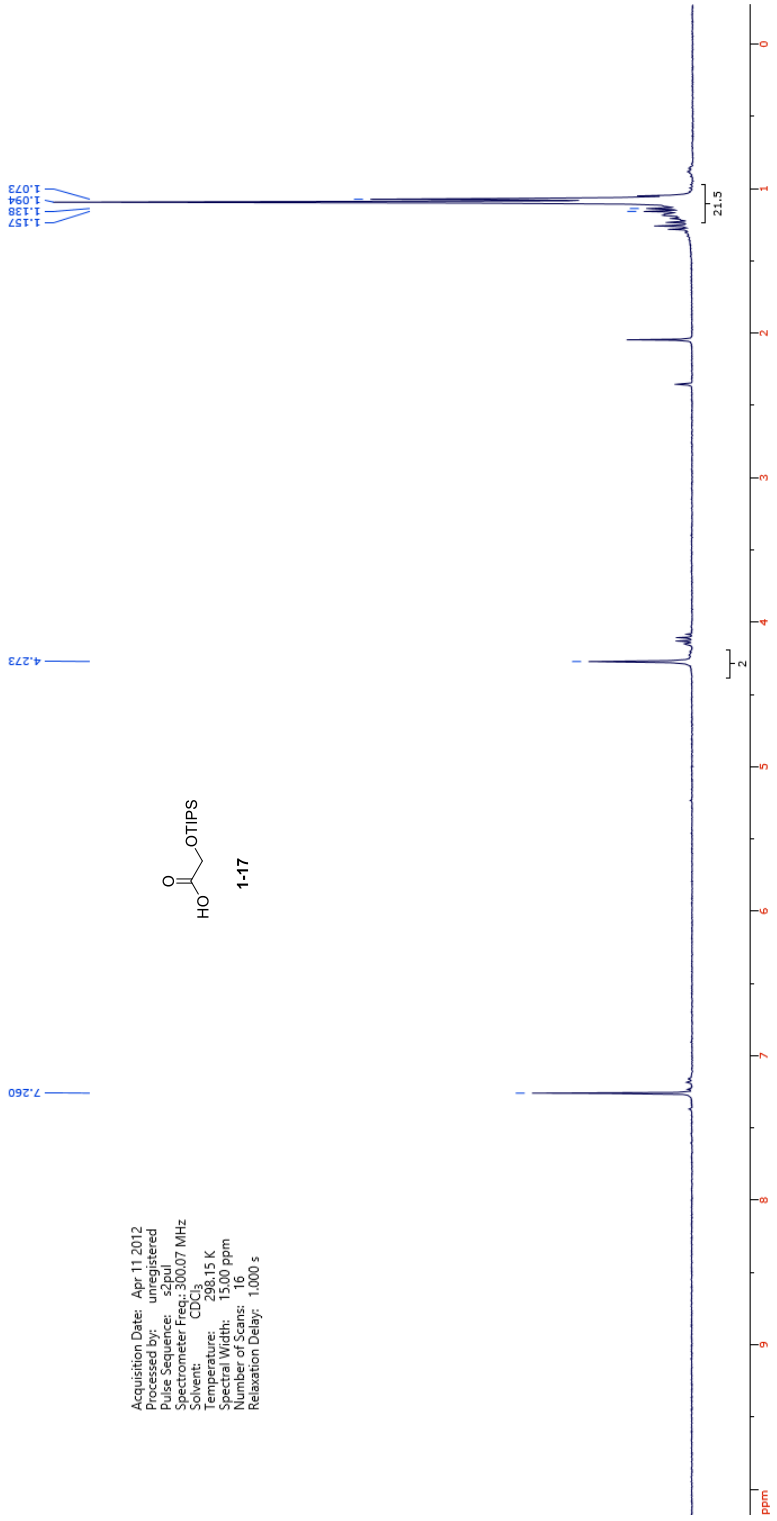
1.157
1.138
1.094
1.073
4.273
7.260
21.5
2
ppm
0
1
2
3
4
5
6
7
8
9
OTIPS
O
HO
1-17
Acquisition Date: Apr 11 2012
Processed by: unregistered
Pulse Sequence: s2pul
Spectrometer Freq.: 300.07 MHz
Solvent: $CDCl_3$
Temperature: 298.15 K
Spectral Width: 15.00 ppm
Number of Scans: 16
Relaxation Delay: 1.000 s

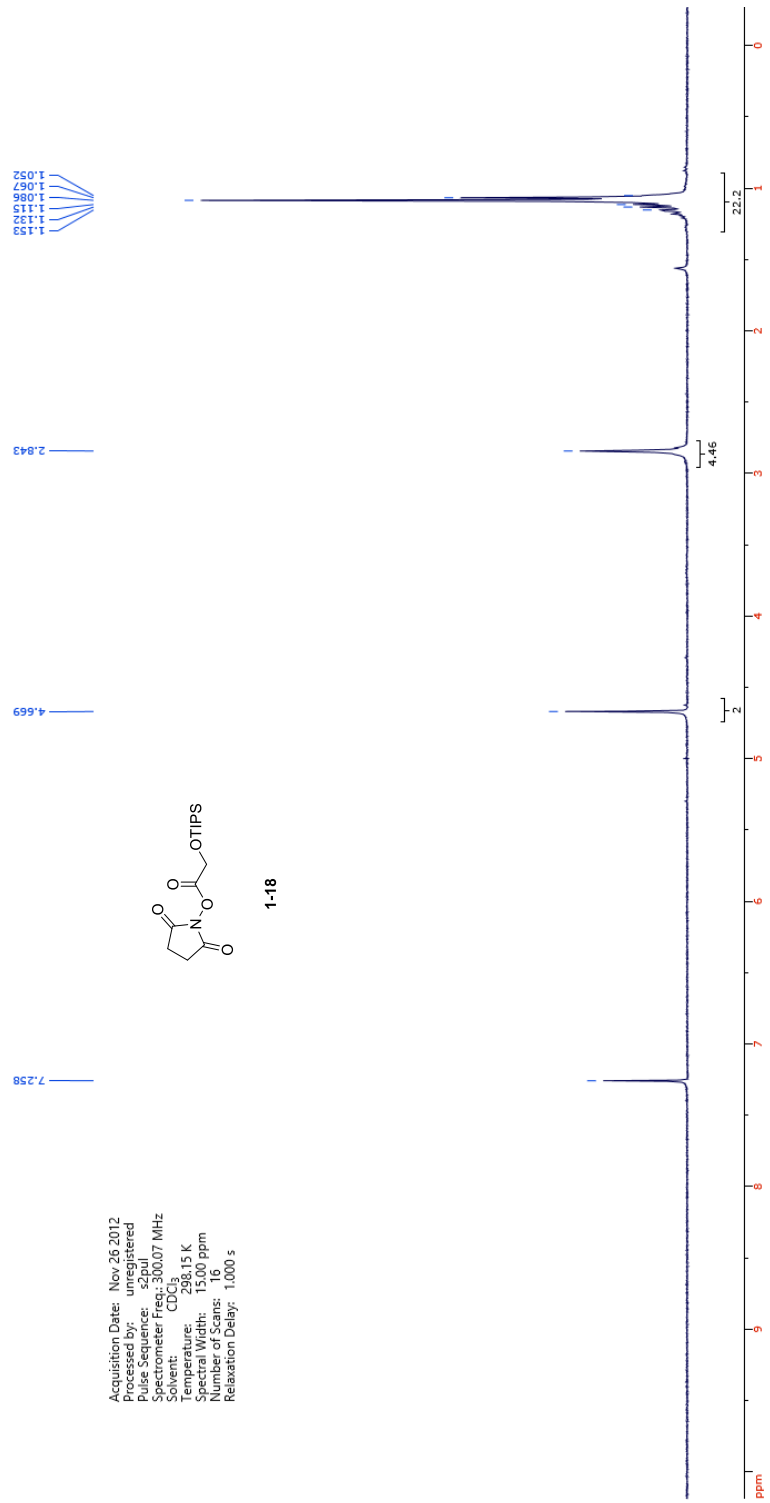
7.258
4.669
2.843
1.153
1.132
1.115
1.086
1.067
1.052
2
4.46
22.2
ppm
OTIPS
1-18
Acquisition Date: Nov 26 2012
Processed by: unregistered
Pulse Sequence: s2pul
Spectrometer Freq.: 300.07 MHz
Solvent: CDCl3
Temperature: 298.15 K
Spectral Width: 15.00 ppm
Number of Scans: 16
Relaxation Delay: 1.000 s

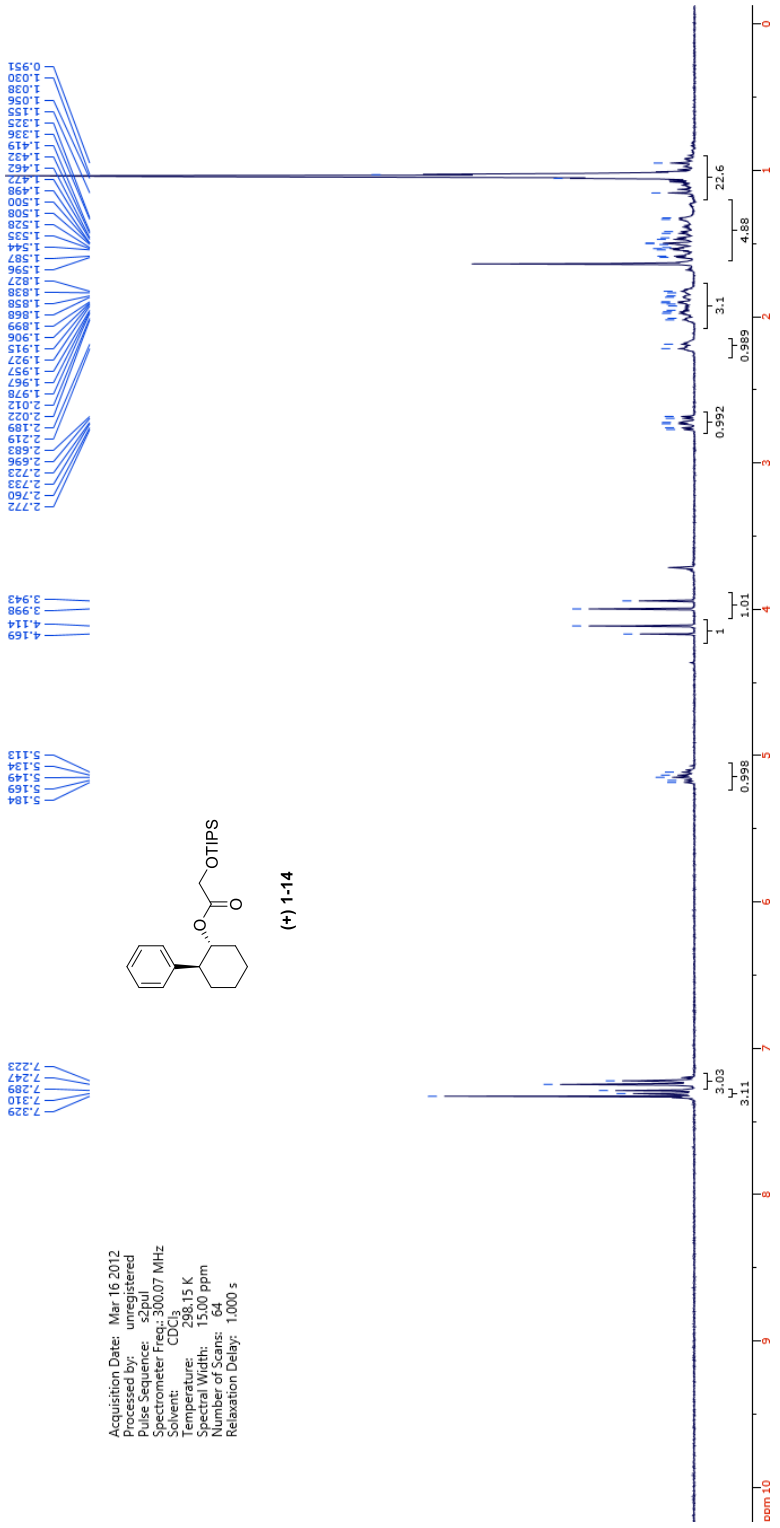
Acquisition Date: Mar 16 2012
Processed by: unregistered
Pulse Sequence: s2pul
Spectrometer Freq.: 300.07 MHz
Solvent: CDCl3
Temperature: 298.15 K
Spectral Width: 15.00 ppm
Number of Scans: 64
Relaxation Delay: 1.000 s
OTIPS
O
O
(+) 1-14

Appendix Chapter 2

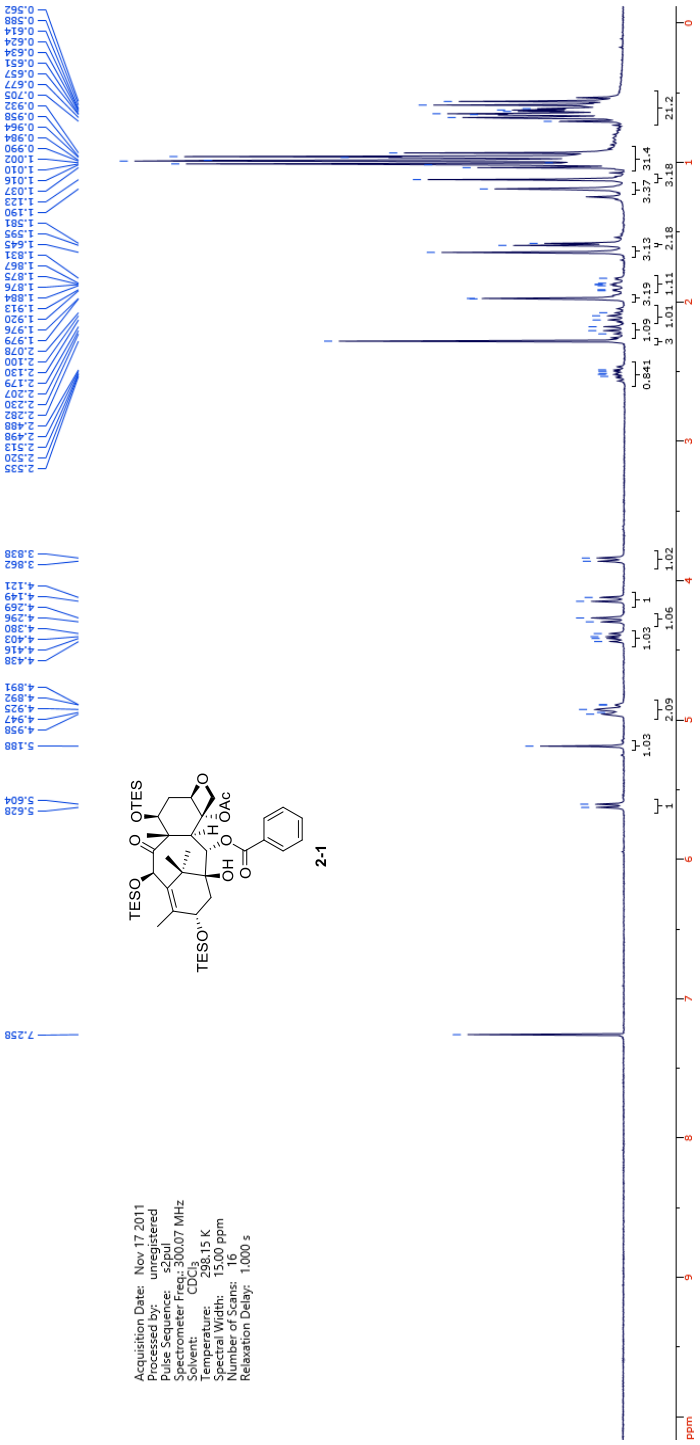
Acquisition Date: Nov 17 2011
Processed by: unregistered
Pulse Sequence: s2pul
Spectrometer Freq.: 300.07 MHz
Solvent: CDCl3
Temperature: 298.15 K
Spectral Width: 15.00 ppm
Number of Scans: 16
Relaxation Delay: 1.000 s
TESO
OTES
OAc
OH
TESO
2-1
ppm

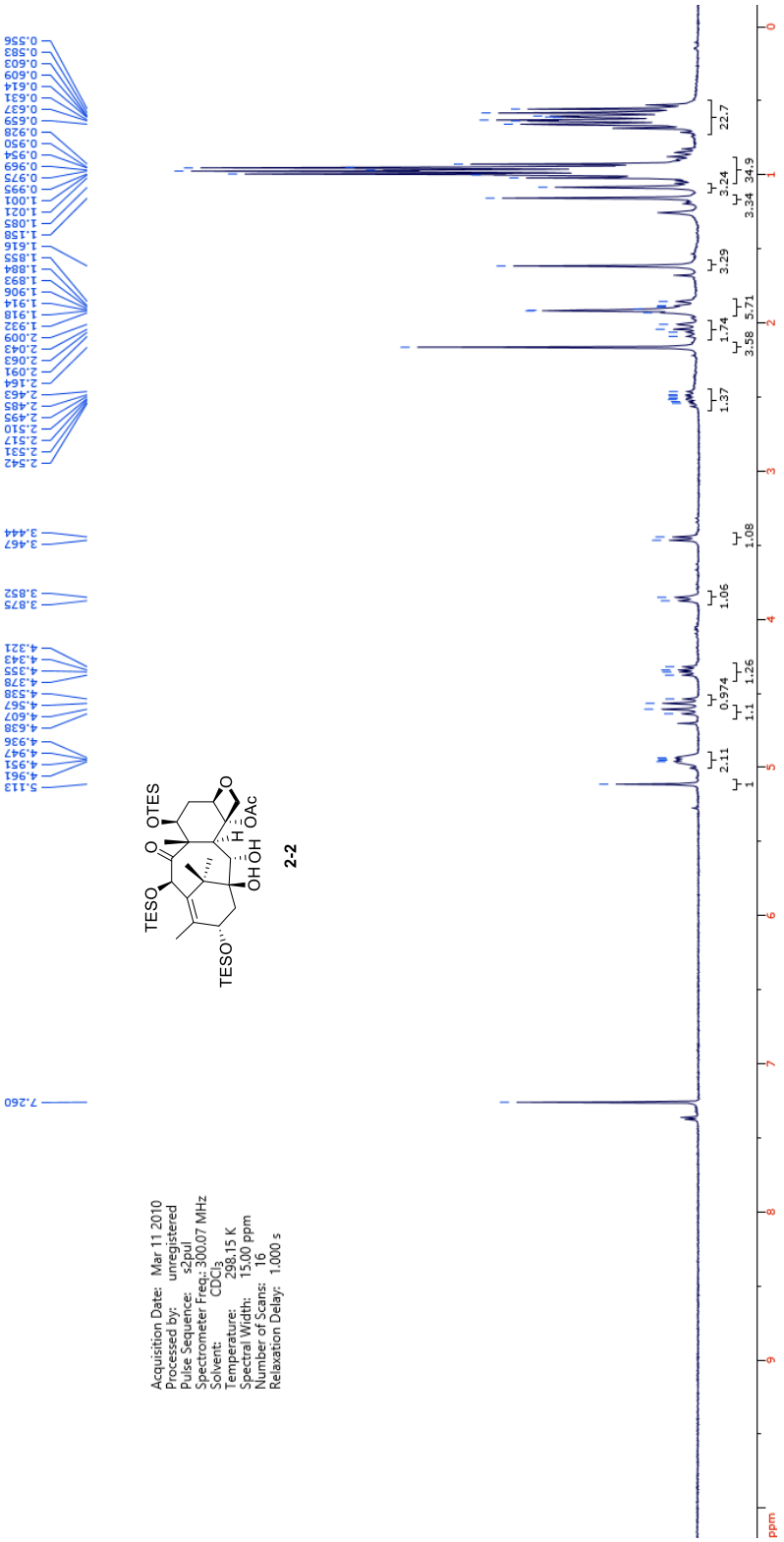
Acquisition Date: Mar 11 2010
Processed by: unregistered
Pulse Sequence: s2pul
Spectrometer Freq.: 300.07 MHz
Solvent: $CDCl_3$
Temperature: 298.15 K
Spectral Width: 15.00 ppm
Number of Scans: 16
Relaxation Delay: 1.000 s
TESO
OTES
O
H
OAc
OH
OH
TESO
2-2
ppm

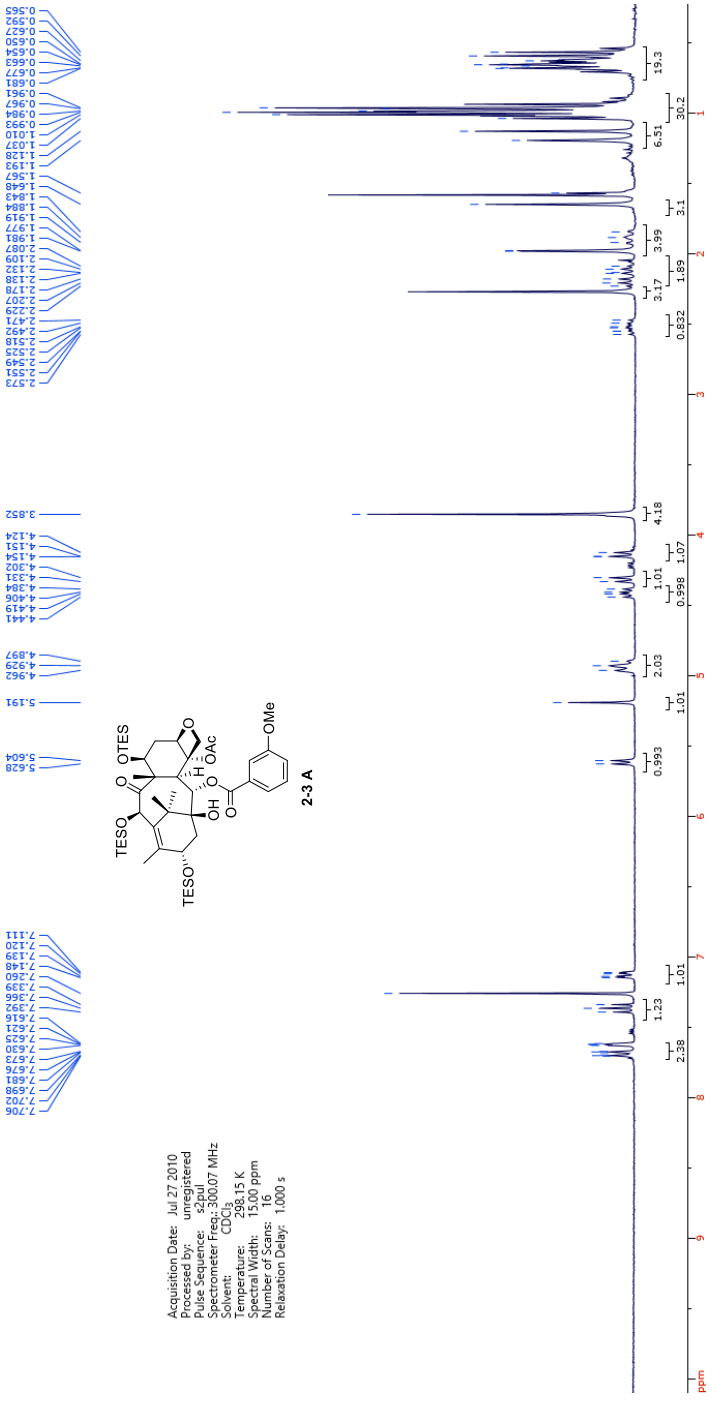
TESO
OTES
O
H
OAc
OH
O
OMe
TESO
2-3 A
Acquisition Date: Jul 27 2010
Processed by: unregistered
Pulse Sequence: s2pul
Spectrometer Freq.: 300.07 MHz
Solvent: CDCl3
Temperature: 298.15 K
Spectral Width: 15.00 ppm
Number of Scans: 16
Relaxation Delay: 1.000 s
ppm

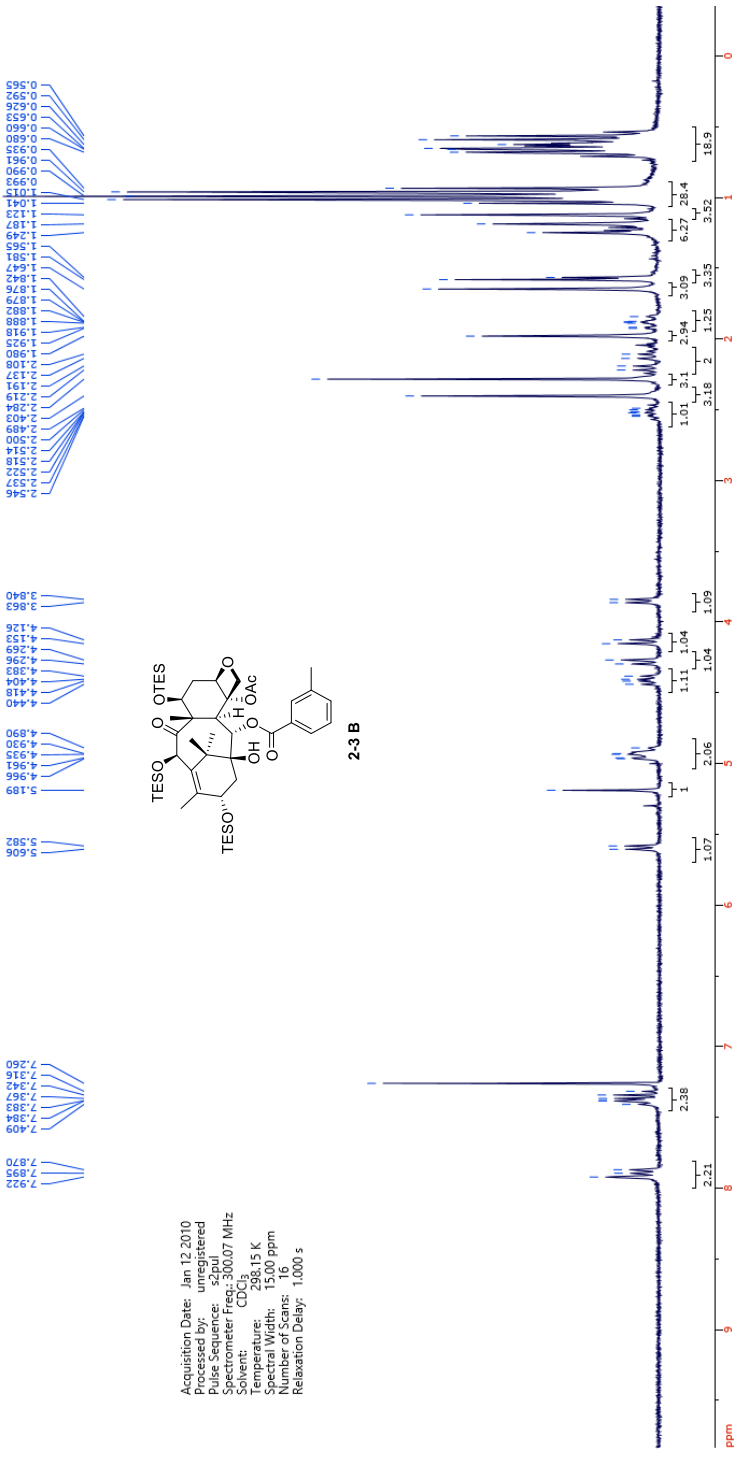
TESO
OTES
O
OAc
H
OH
TESO
O
2-3 B
Acquisition Date: Jan 12 2010
Processed by: unregistered
Pulse Sequence: s2pul
Spectrometer Freq.: 300.07 MHz
Solvent: CDCl3
Temperature: 298.15 K
Spectral Width: 15.00 ppm
Number of Scans: 16
Relaxation Delay: 1.000 s
ppm

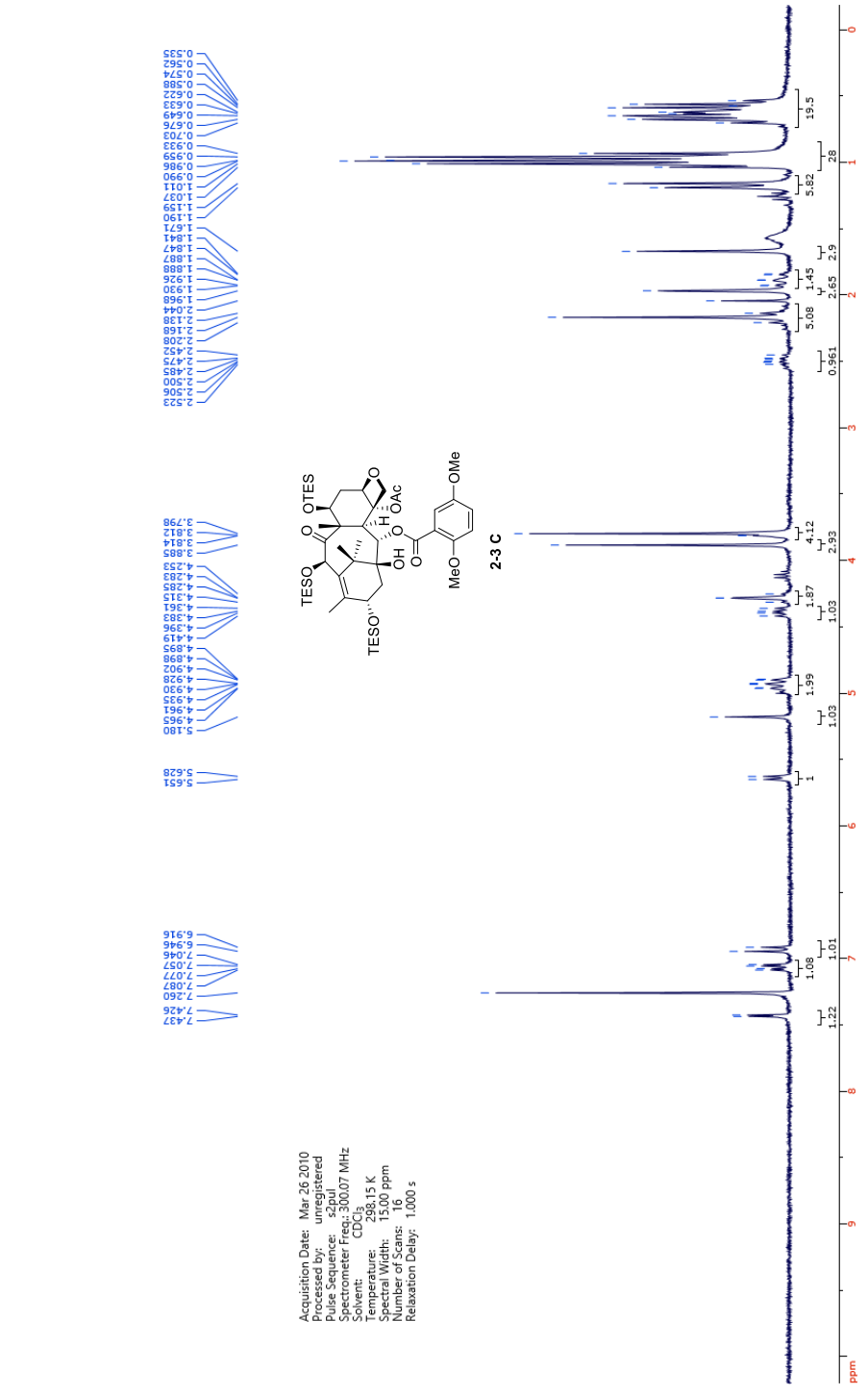
Acquisition Date: Mar 26 2010
Processed by: unregistered
Pulse Sequence: s2pul
Spectrometer Freq.: 300.07 MHz
Solvent: CDCl3
Temperature: 298.15 K
Spectral Width: 15.00 ppm
Number of Scans: 16
Relaxation Delay: 1.000 s
TESO
OTES
OAc
OH
MeO
OMe
2-3 C
ppm

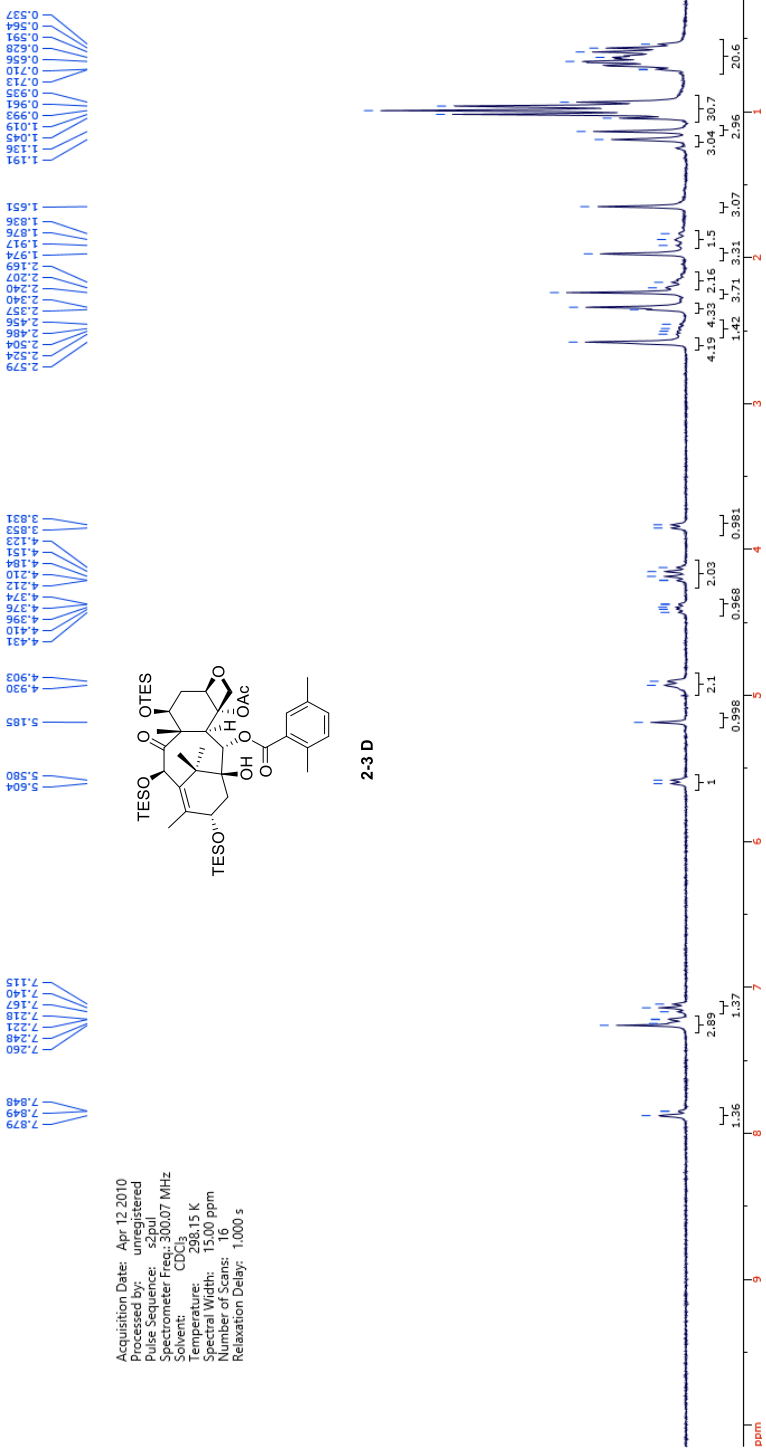
Acquisition Date: Apr 12 2010
Processed by: unregistered
Pulse Sequence: s2pul
Spectrometer Freq.: 300.07 MHz
Solvent: $CDCl_3$
Temperature: 298.15 K
Spectral Width: 15.00 ppm
Number of Scans: 16
Relaxation Delay: 1.000 s
TESO
OTES
OAc
OH
TESO
2-3 D
ppm

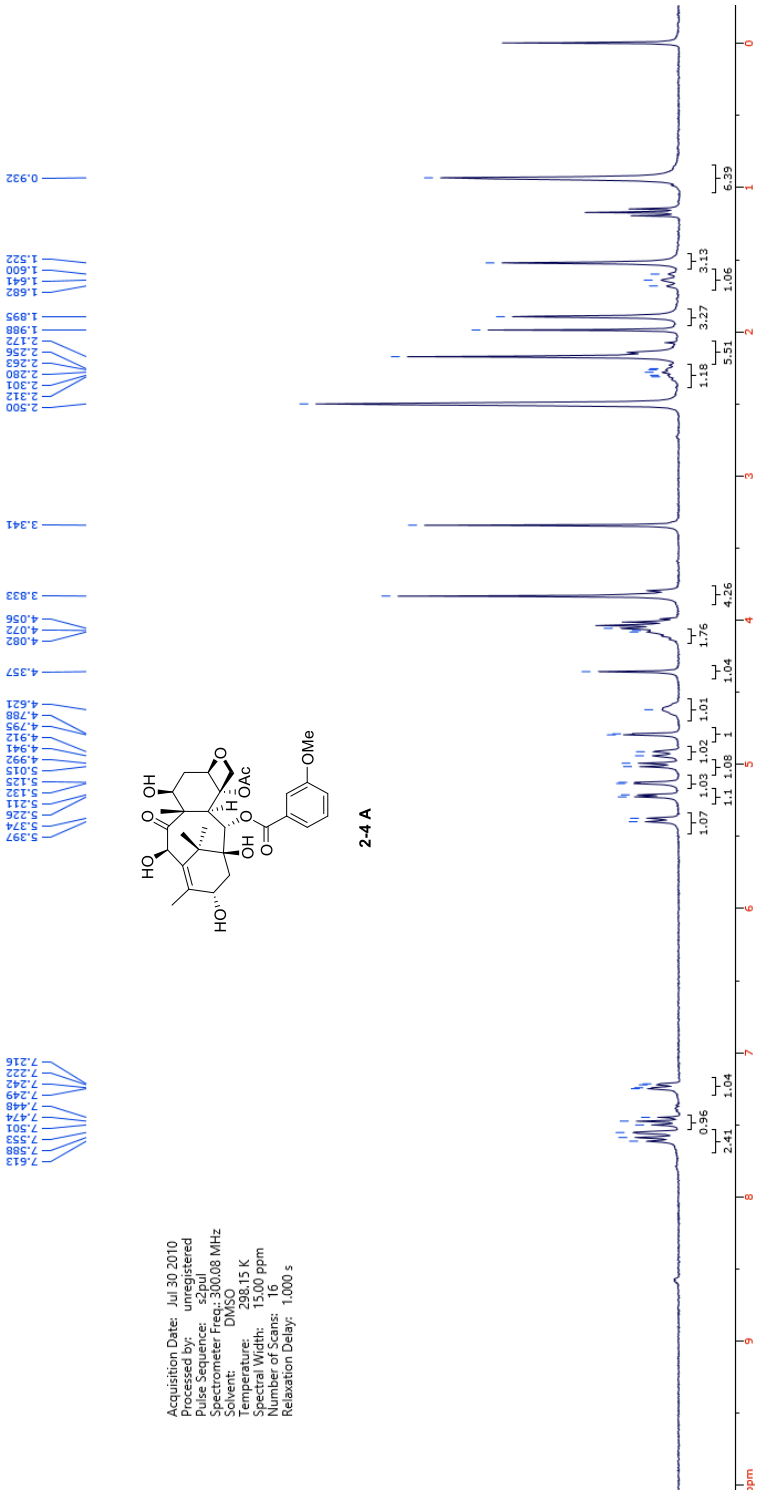
Acquisition Date: Jul 30 2010
Processed by: unregistered
Pulse Sequence: s2pul
Spectrometer Freq.: 300.08 MHz
Solvent: DMSO
Temperature: 298.15 K
Spectral Width: 15.00 ppm
Number of Scans: 16
Relaxation Delay: 1.000 s
2-4 A
OMe
OAc
OH
HO
ppm

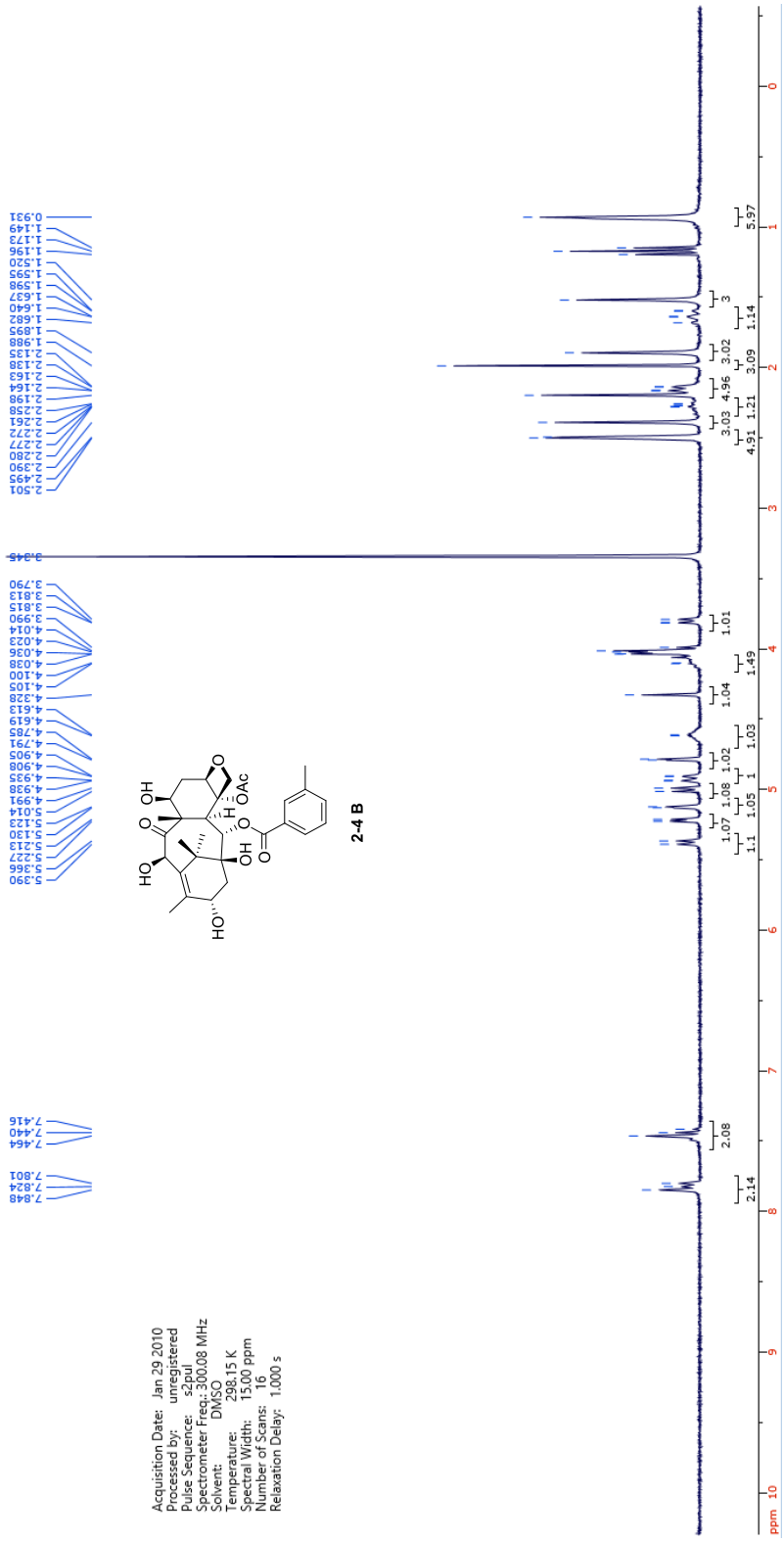
Acquisition Date: Jan 29 2010
Processed by: unregistered
Pulse Sequence: s2pul
Spectrometer Freq.: 300.08 MHz
Solvent: DMSO
Temperature: 298.15 K
Spectral Width: 15.00 ppm
Number of Scans: 16
Relaxation Delay: 1.000 s
2-4 B
ppm

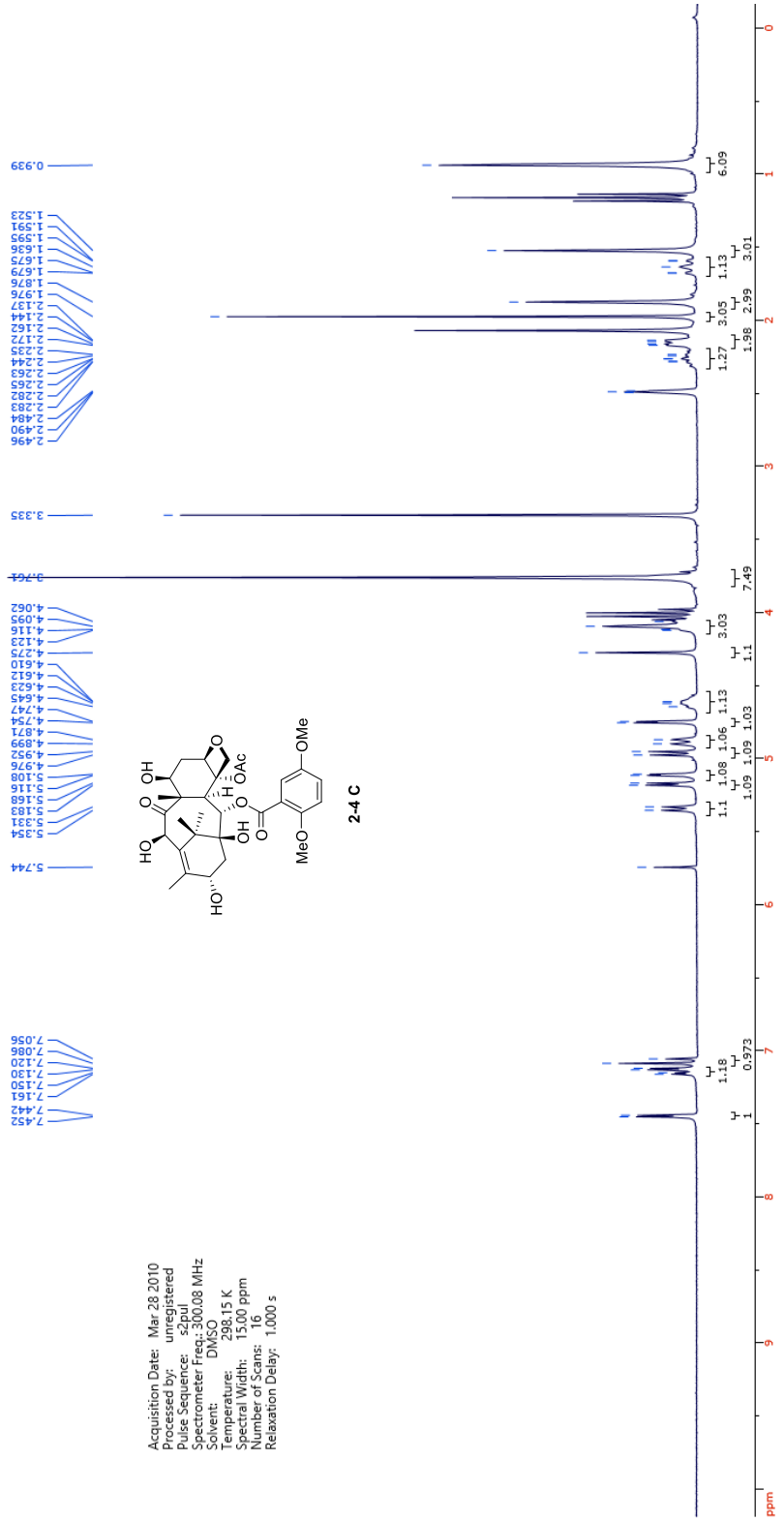
Acquisition Date: Mar 28 2010
Processed by: unregistered
Pulse Sequence: s2pul
Spectrometer Freq.: 300.08 MHz
Solvent: DMSO
Temperature: 298.15 K
Spectral Width: 15.00 ppm
Number of Scans: 16
Relaxation Delay: 1.000 s
2-4 C
ppm

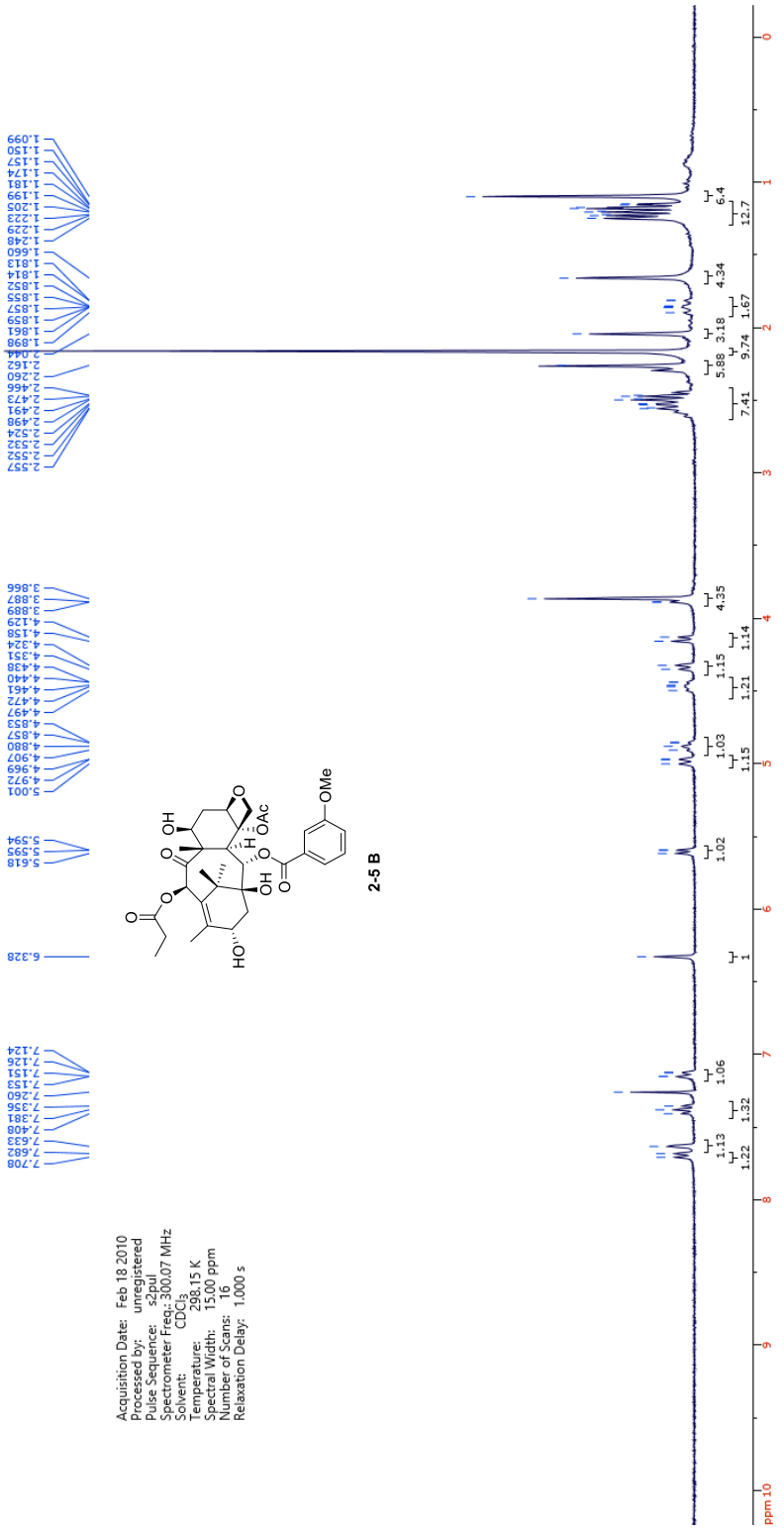
Acquisition Date: Feb 18 2010
Processed by: unregistered
Pulse Sequence: s2pul
Spectrometer Freq.: 300.07 MHz
Solvent: $CDCl_3$
Temperature: 298.15 K
Spectral Width: 15.00 ppm
Number of Scans: 16
Relaxation Delay: 1.000 s
2-5 B
ppm

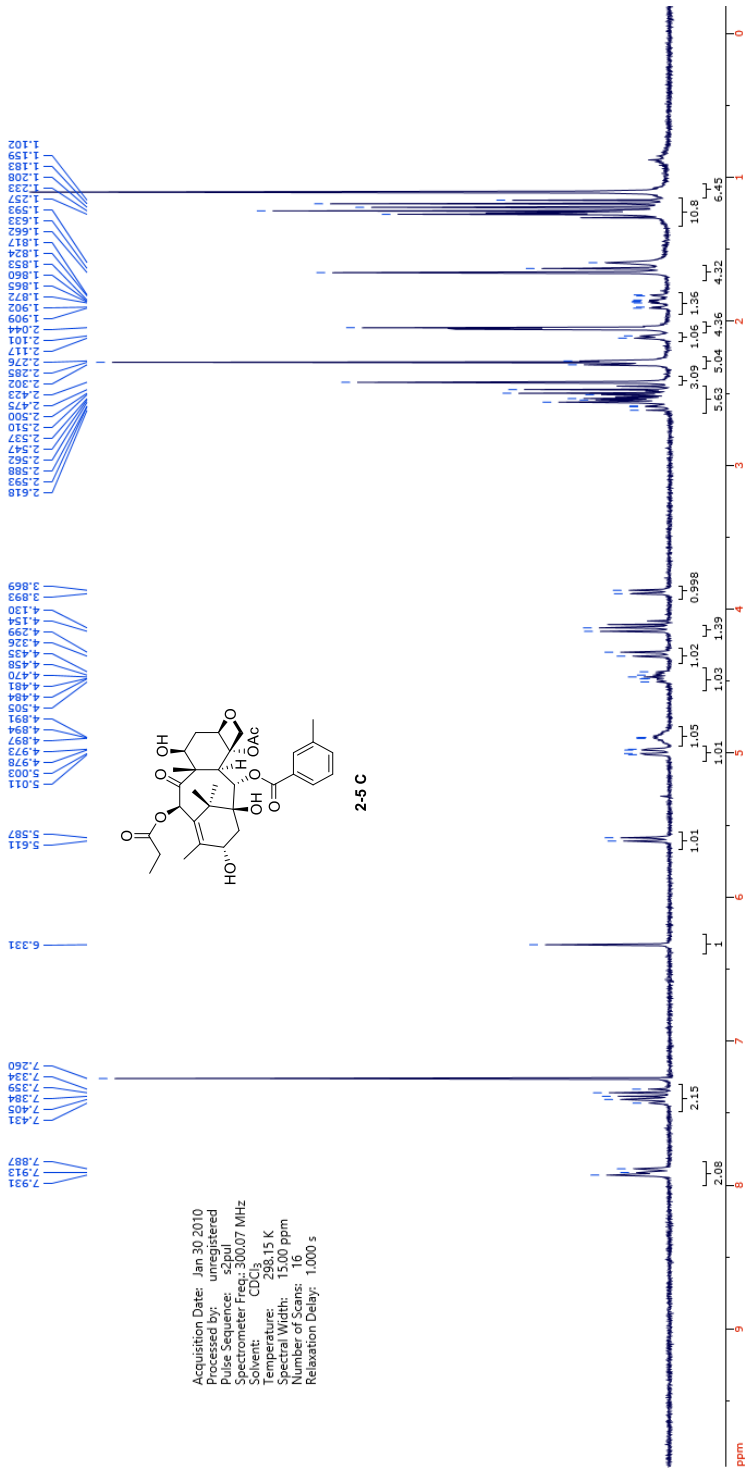
Acquisition Date: Jan 30 2010
Processed by: unregistered
Pulse Sequence: s2pul
Spectrometer Freq.: 300.07 MHz
Solvent: CDCl3
Temperature: 298.15 K
Spectral Width: 15.00 ppm
Number of Scans: 16
Relaxation Delay: 1.000 s
2-5 C
ppm

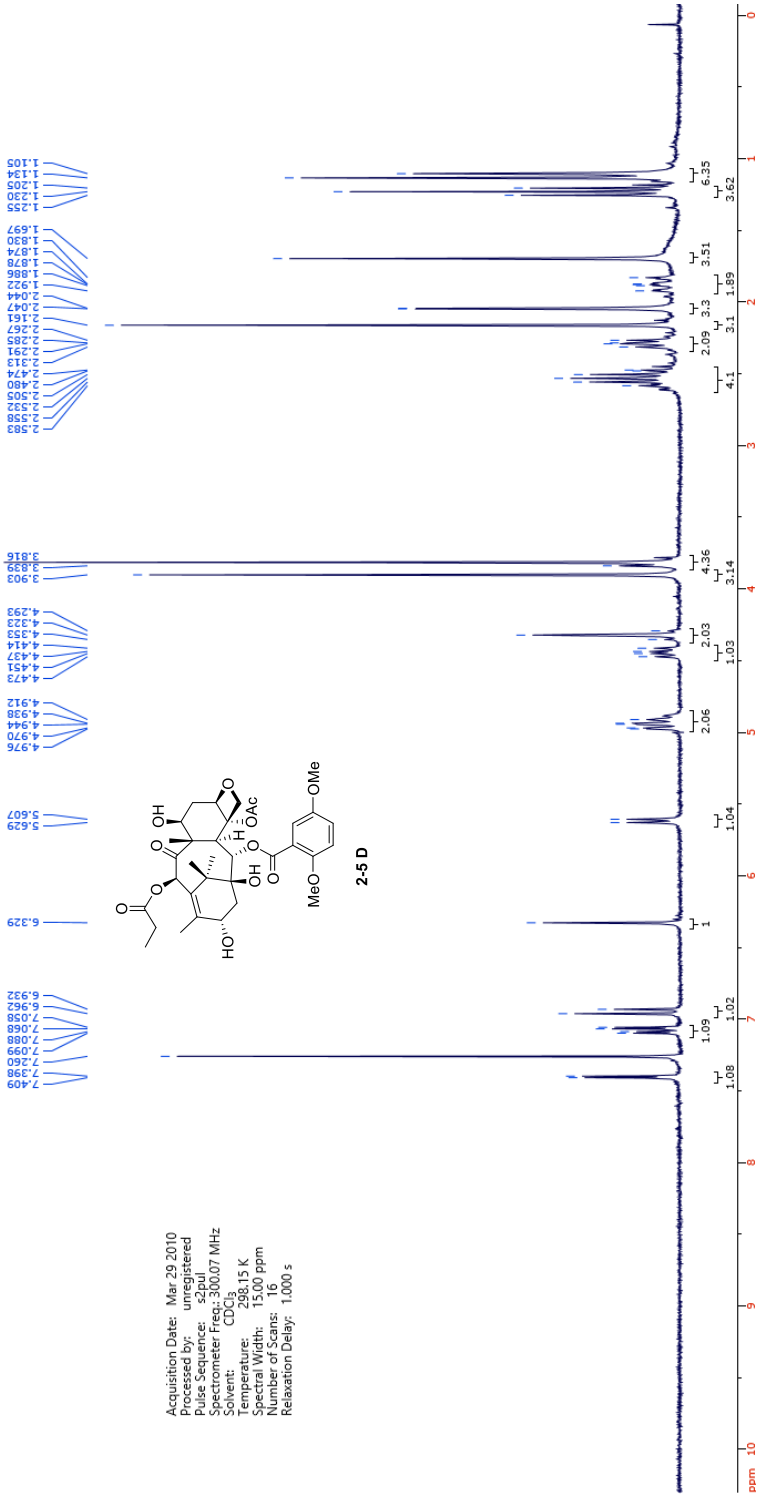
Acquisition Date: Mar 29 2010
Processed by: unregistered
Pulse Sequence: s2pul
Spectrometer Freq.: 300.07 MHz
Solvent: $CDCl_3$
Temperature: 298.15 K
Spectral Width: 15.00 ppm
Number of Scans: 16
Relaxation Delay: 1.000 s
2-5 D
ppm

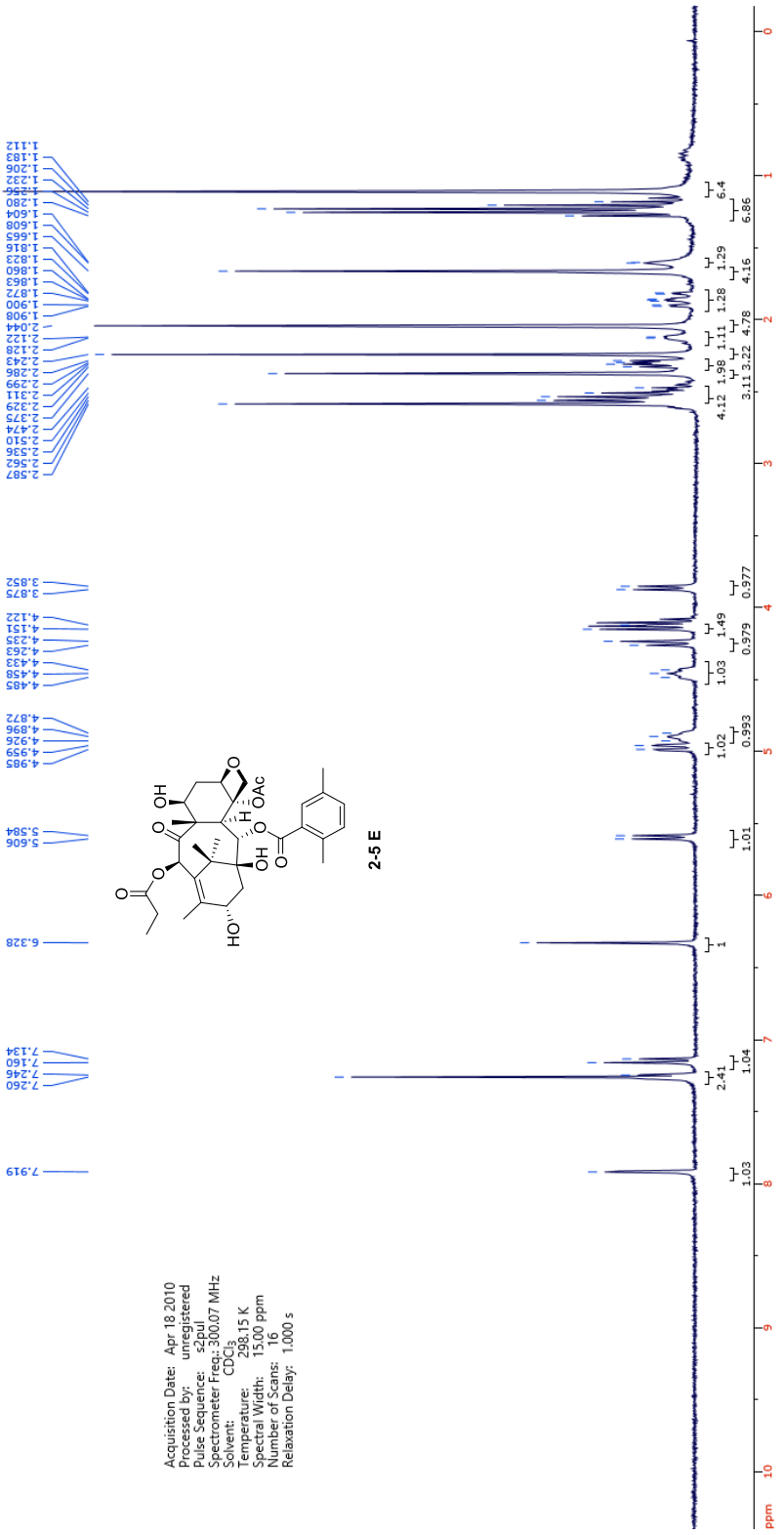
Acquisition Date: Apr 18 2010
Processed by: unregistered
Pulse Sequence: s2pul
Spectrometer Freq.: 300.07 MHz
Solvent: $CDCl_3$
Temperature: 298.15 K
Spectral Width: 15.00 ppm
Number of Scans: 16
Relaxation Delay: 1.000 s
2-5 E
ppm

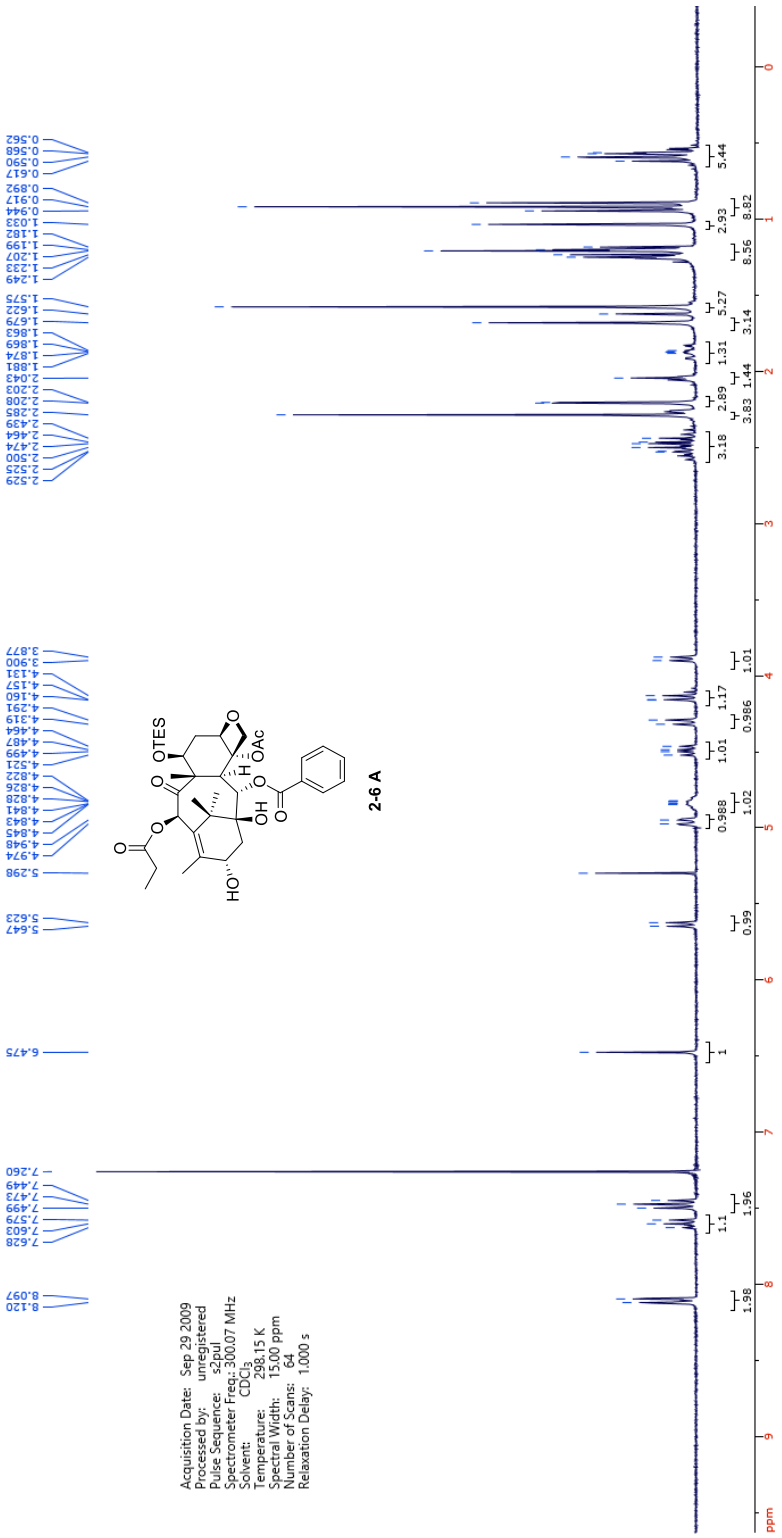
Acquisition Date: Sep 29 2009
Processed by: unregistered
Pulse Sequence: s2pul
Spectrometer Freq.: 300.07 MHz
Solvent: CDCl3
Temperature: 298.15 K
Spectral Width: 15.00 ppm
Number of Scans: 64
Relaxation Delay: 1.000 s
OTES
OAc
OH
HO
2-6 A
ppm

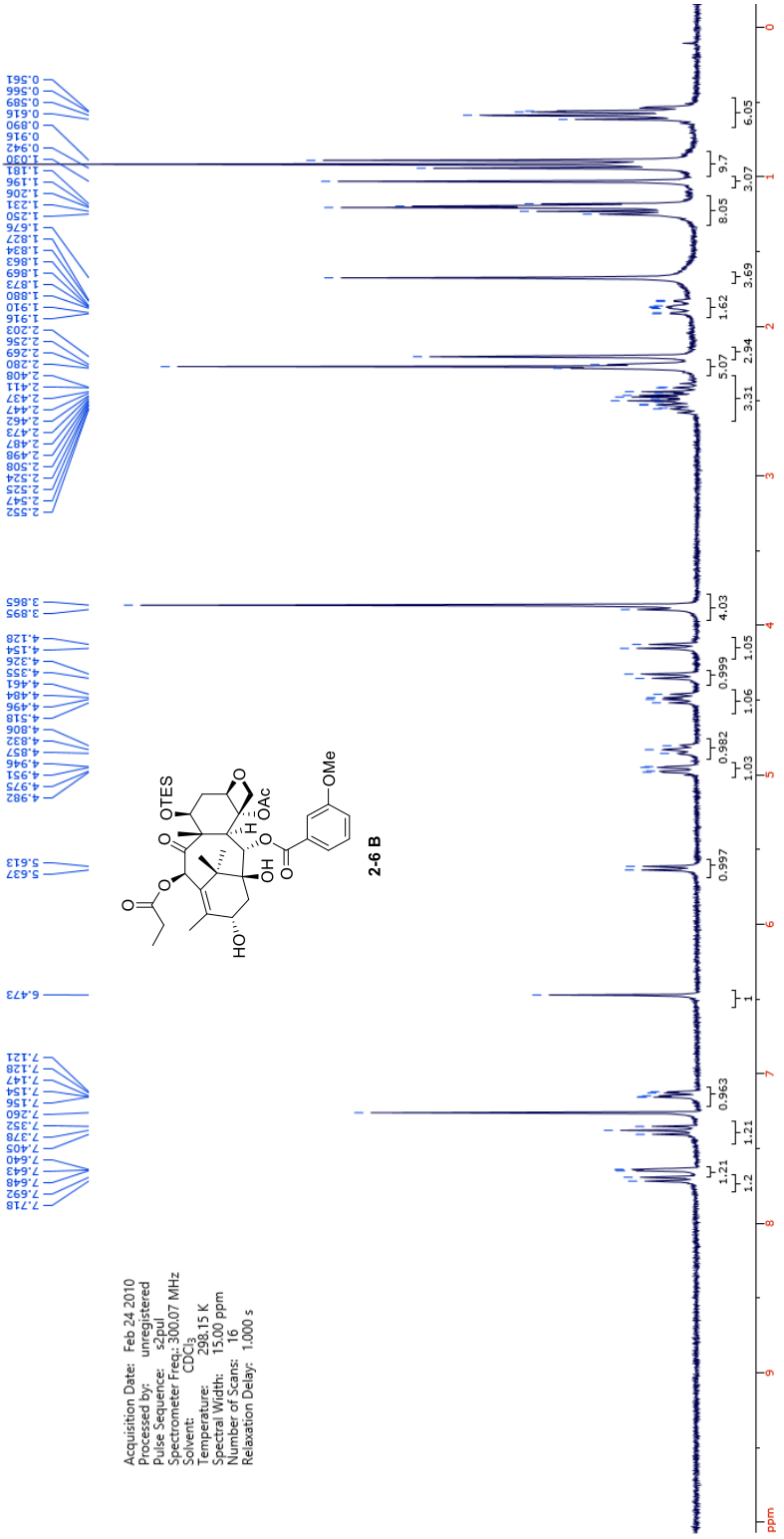
Acquisition Date: Feb 24 2010
Processed by: unregistered
Pulse Sequence: s2pul
Spectrometer Freq.: 300.07 MHz
Solvent: $CDCl_3$
Temperature: 298.15 K
Spectral Width: 15.00 ppm
Number of Scans: 16
Relaxation Delay: 1.000 s
OTES
OAc
OH
OMe
HO
2-6 B
ppm

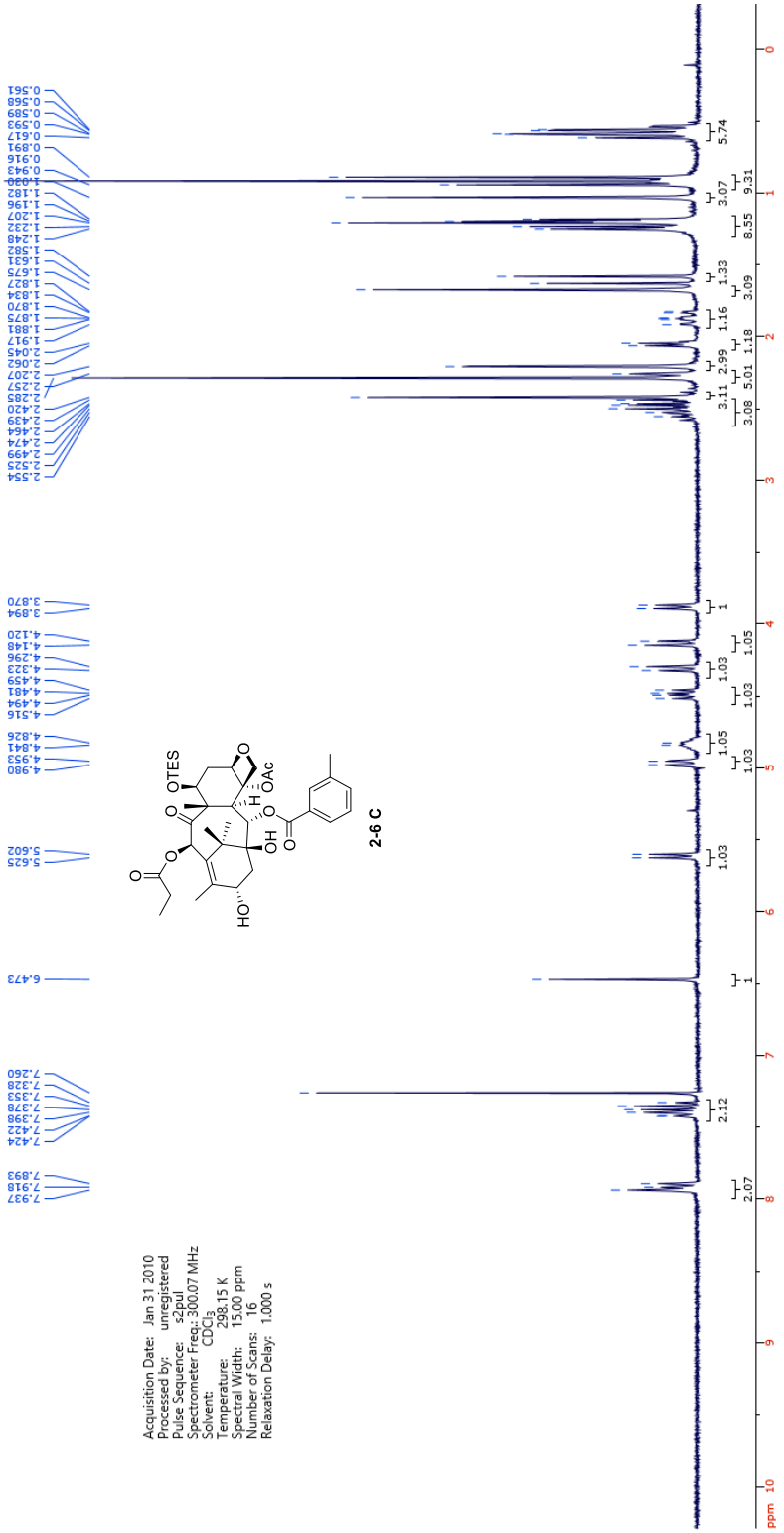
Acquisition Date: Jan 31 2010
Processed by: unregistered
Pulse Sequence: s2pul
Spectrometer Freq.: 300.07 MHz
Solvent: CDCl3
Temperature: 298.15 K
Spectral Width: 15.00 ppm
Number of Scans: 16
Relaxation Delay: 1.000 s
OTES
OAc
OH
HO
2-6 C
ppm

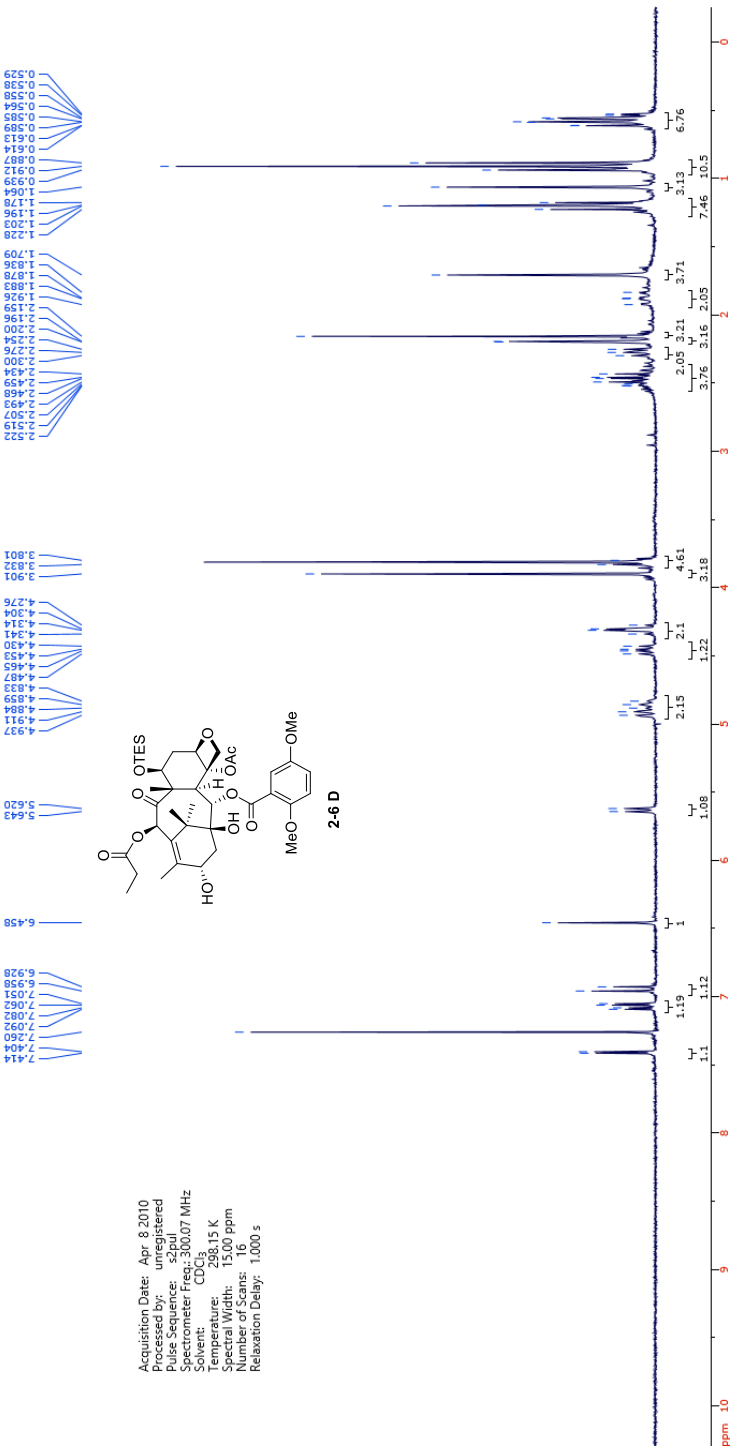
Acquisition Date: Apr 8 2010
Processed by: unregistered
Pulse Sequence: s2pul
Spectrometer Freq.: 300.07 MHz
Solvent: $CDCl_3$
Temperature: 298.15 K
Spectral Width: 15.00 ppm
Number of Scans: 16
Relaxation Delay: 1.000 s
OTES
OAc
OH
HO
MeO
OMe
2-6 D
ppm

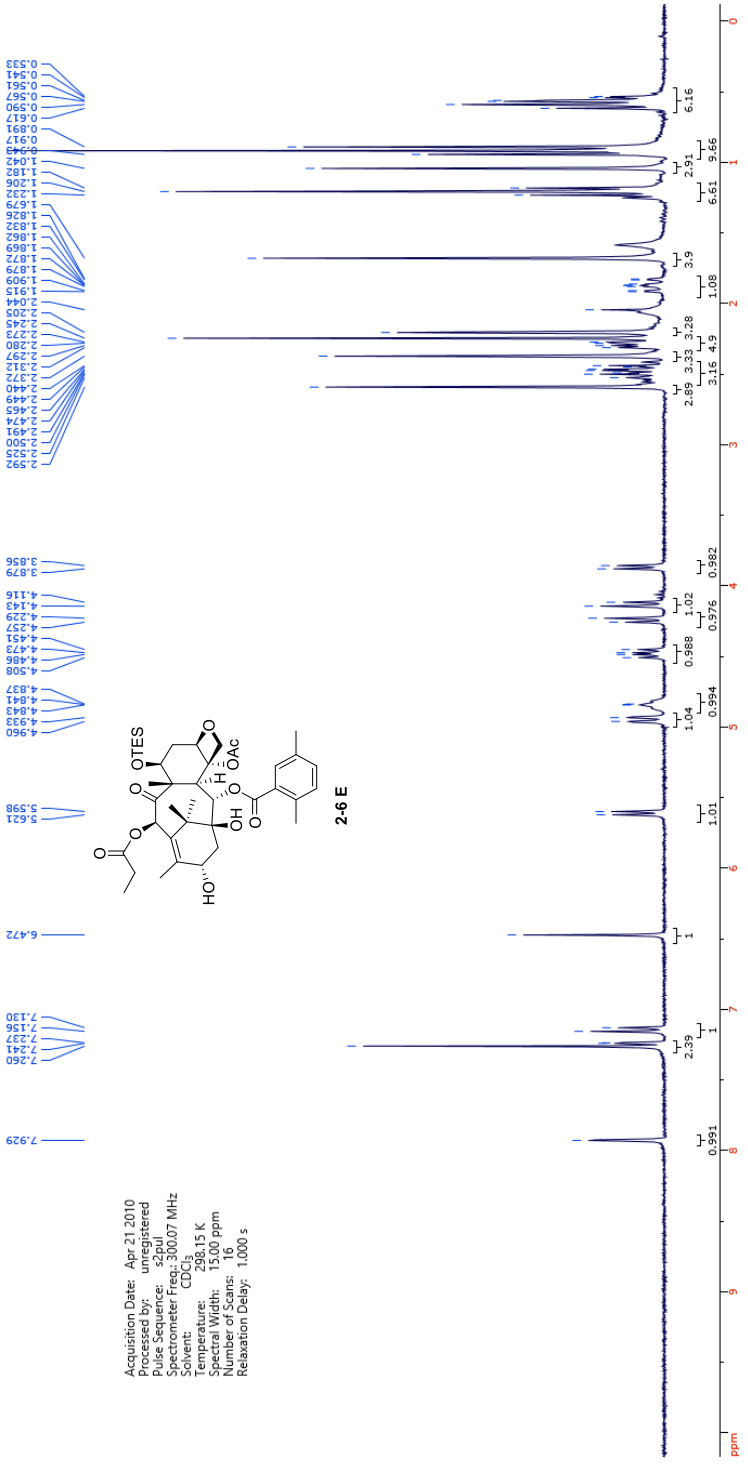
Acquisition Date: Apr 21 2010
Processed by: unregistered
Pulse Sequence: s2pul
Spectrometer Freq.: 300.07 MHz
Solvent: CDCl3
Temperature: 298.15 K
Spectral Width: 15.00 ppm
Number of Scans: 16
Relaxation Delay: 1.000 s
OTES
OAc
OH
HO
2-6 E
ppm

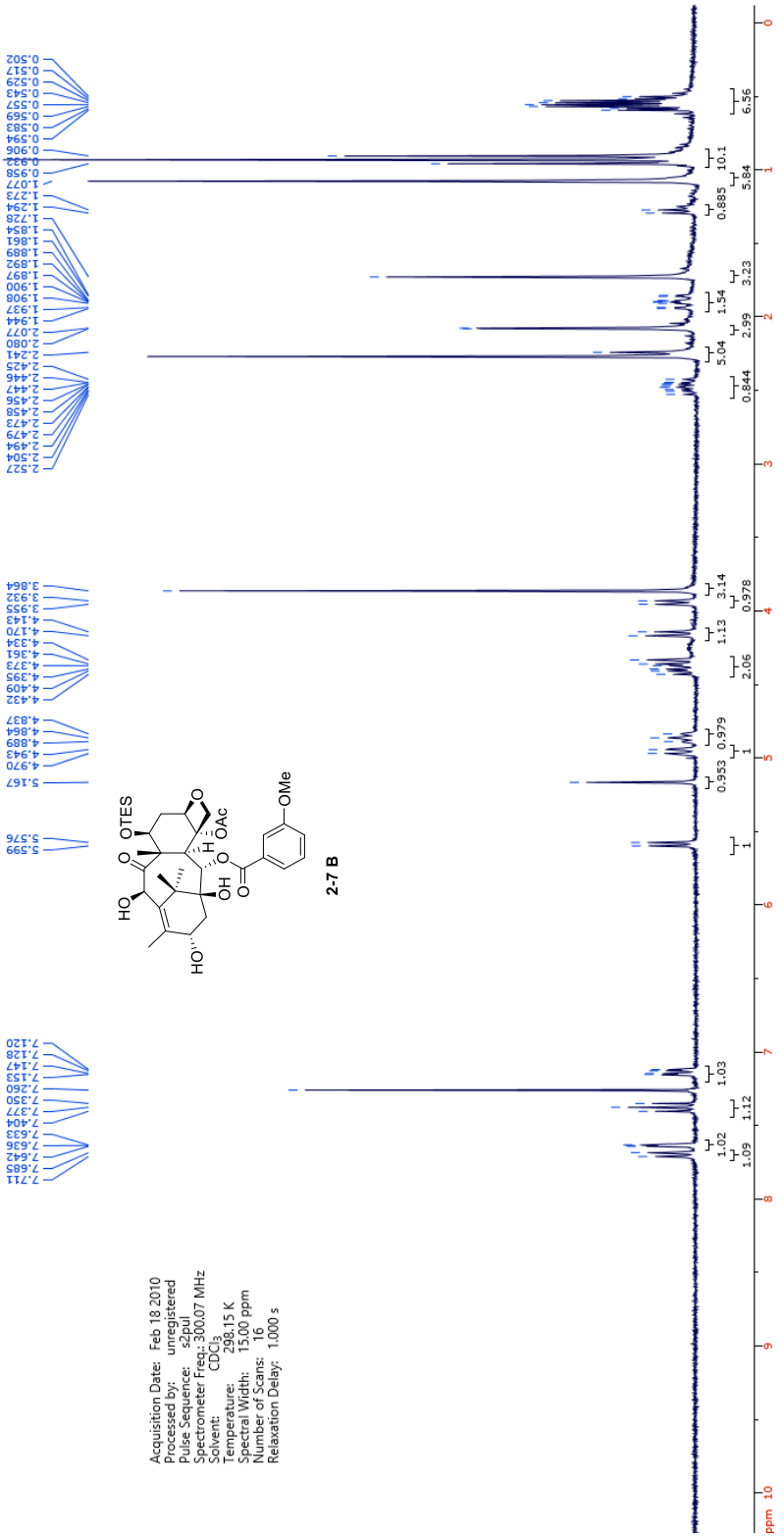
Acquisition Date: Feb 18 2010
Processed by: unregistered
Pulse Sequence: s2pul
Spectrometer Freq.: 300.07 MHz
Solvent: $CDCl_3$
Temperature: 298.15 K
Spectral Width: 15.00 ppm
Number of Scans: 16
Relaxation Delay: 1.000 s
2-7 B
ppm

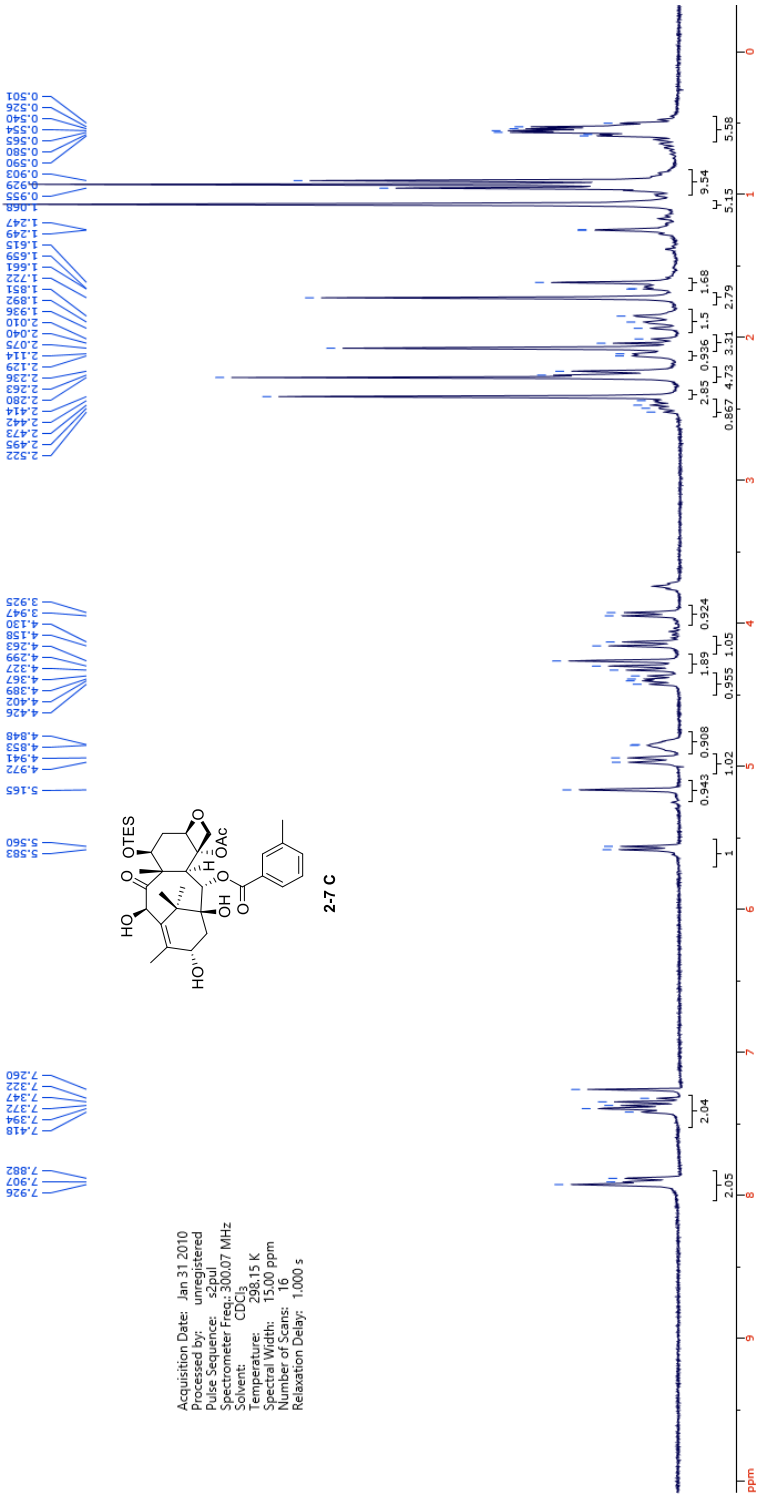
Acquisition Date: Jan 31 2010
Processed by: unregistered
Pulse Sequence: s2pul
Spectrometer Freq.: 300.07 MHz
Solvent: $CDCl_3$
Temperature: 298.15 K
Spectral Width: 15.00 ppm
Number of Scans: 16
Relaxation Delay: 1.000 s
OTES
OAc
HO
OH
2-7 C
ppm

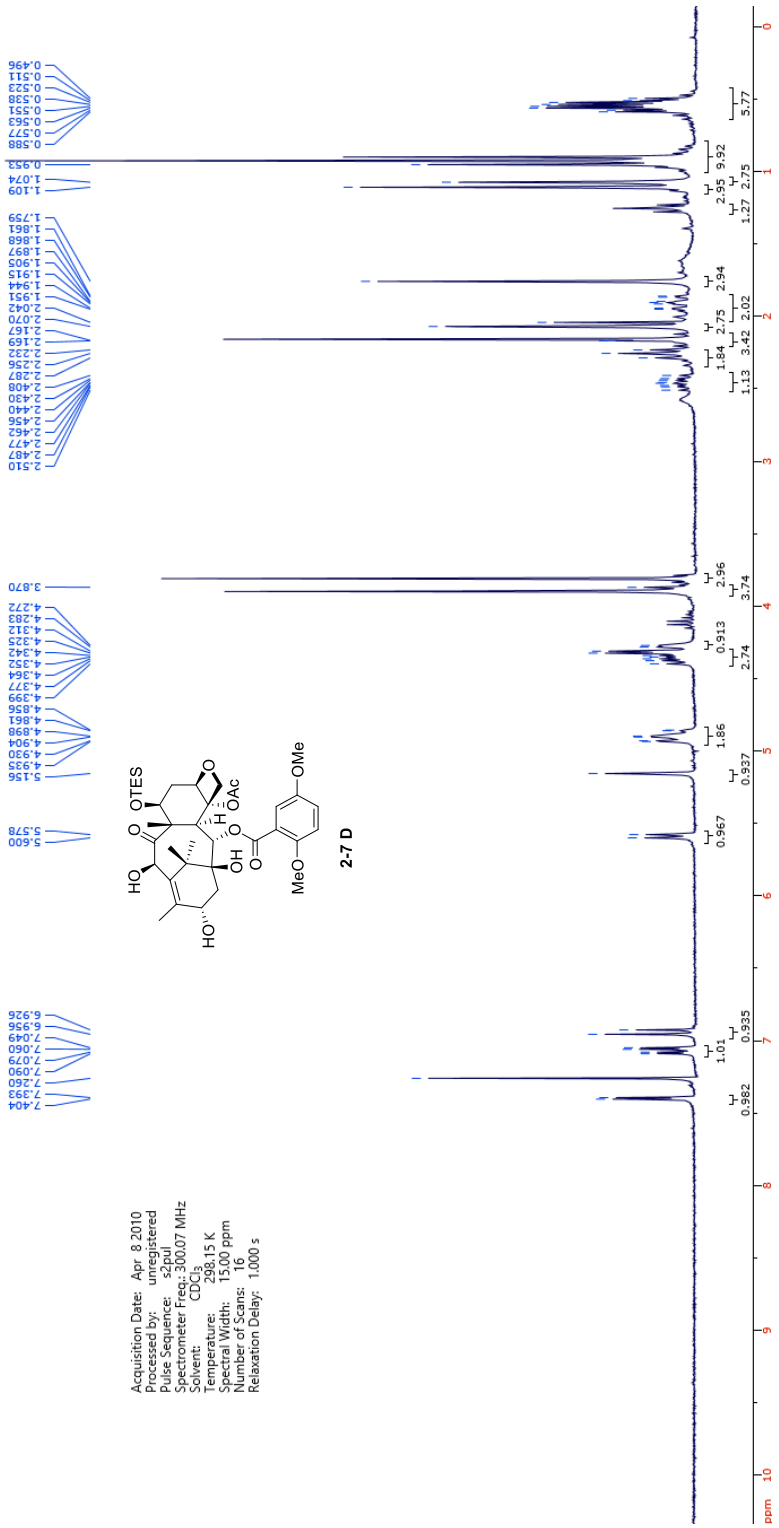
Acquisition Date: Apr 8 2010
Processed by: unregistered
Pulse Sequence: s2pul
Spectrometer Freq.: 300.07 MHz
Solvent: $CDCl_3$
Temperature: 298.15 K
Spectral Width: 15.00 ppm
Number of Scans: 16
Relaxation Delay: 1.000 s
HO
OTES
O
OAc
H
OH
O
O
HO
MeO
OMe
2-7 D
ppm

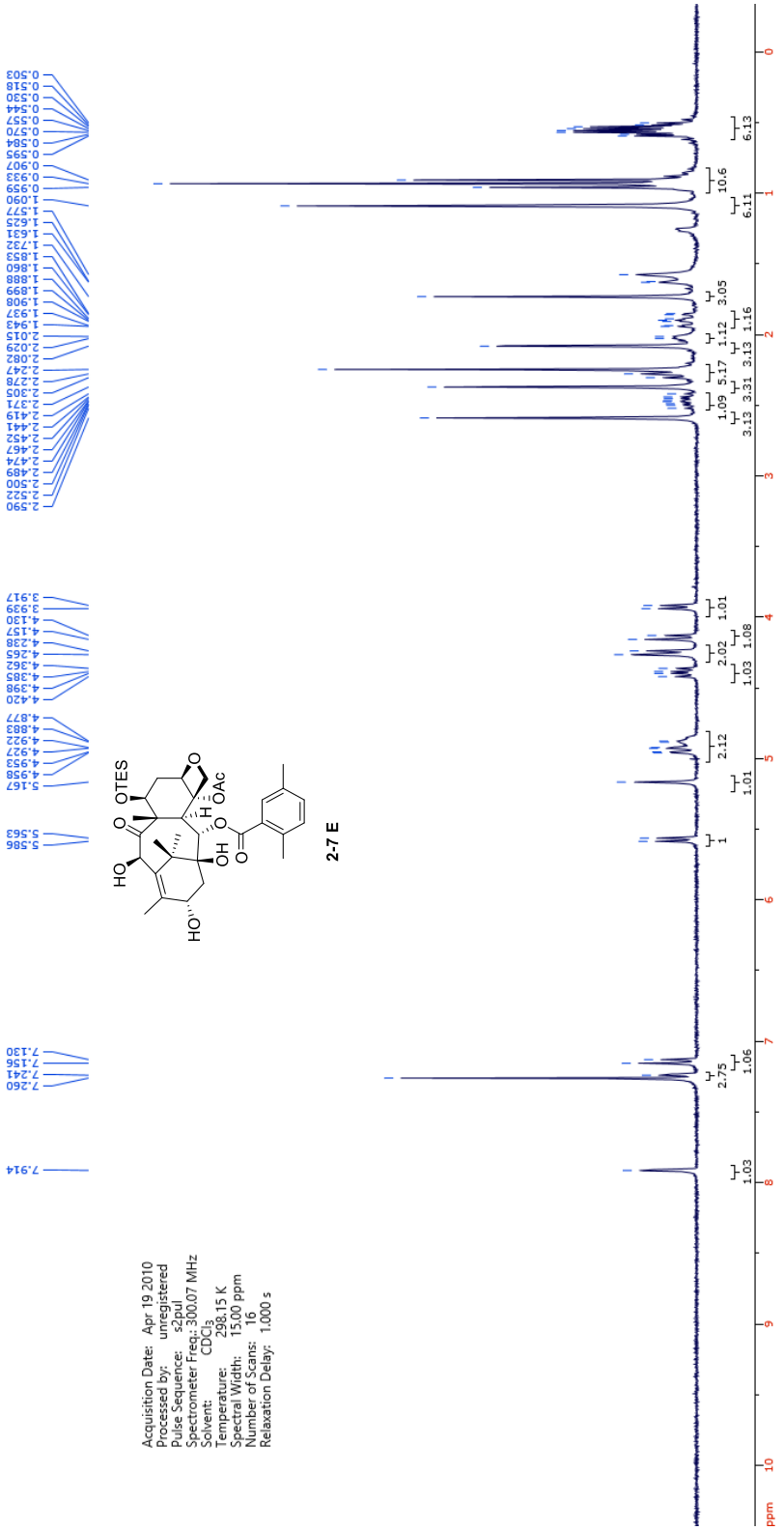
Acquisition Date: Apr 19 2010
Processed by: unregistered
Pulse Sequence: s2pul
Spectrometer Freq.: 300.07 MHz
Solvent: $CDCl_3$
Temperature: 298.15 K
Spectral Width: 15.00 ppm
Number of Scans: 16
Relaxation Delay: 1.000 s
OTES
OAc
HO
OH
HO
2-7 E
ppm

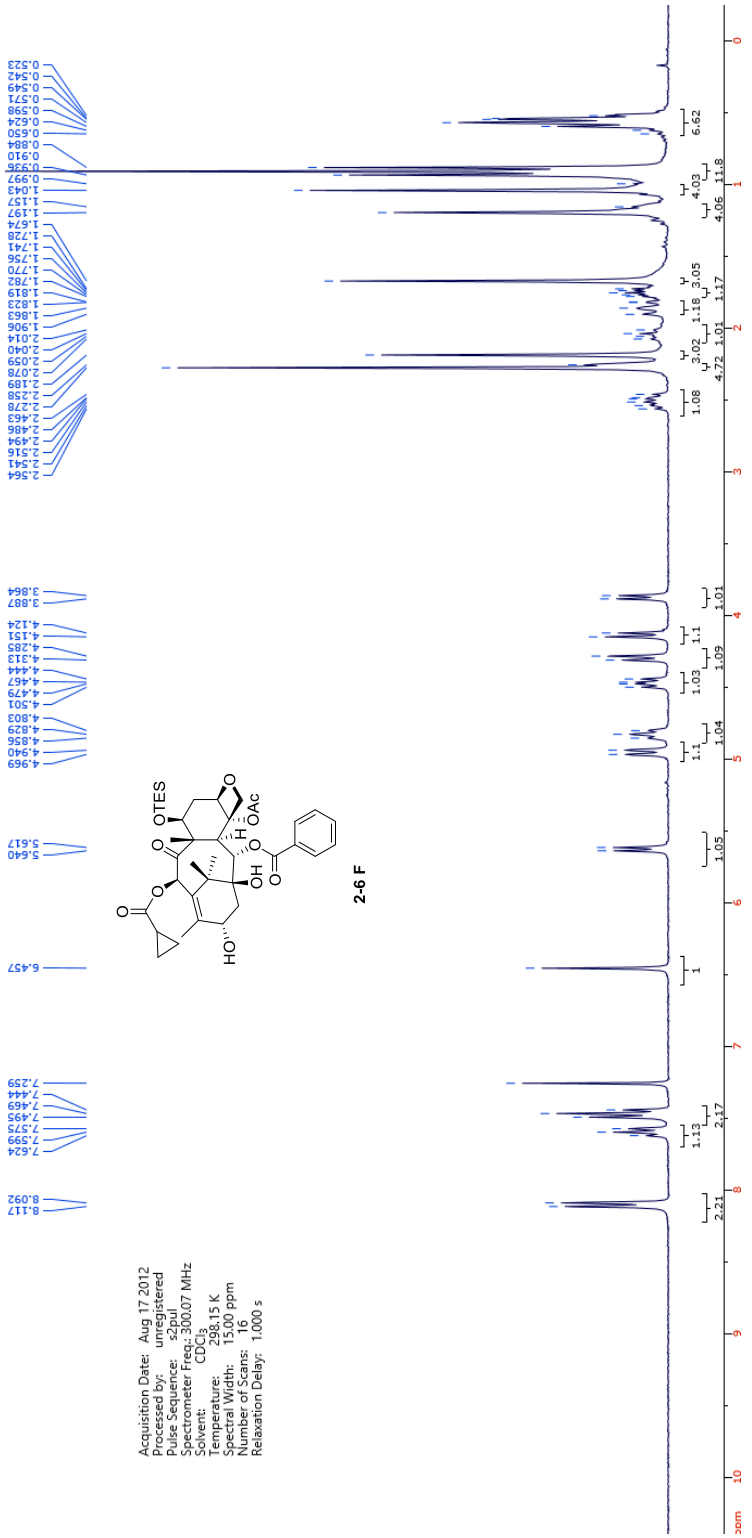
Acquisition Date: Aug 17 2012
Processed by: unregistered
Pulse Sequence: s2pul
Spectrometer Freq.: 300.07 MHz
Solvent: CDCl3
Temperature: 298.15 K
Spectral Width: 15.00 ppm
Number of Scans: 16
Relaxation Delay: 1.000 s
OTES
OAc
OH
HO
2-6 F

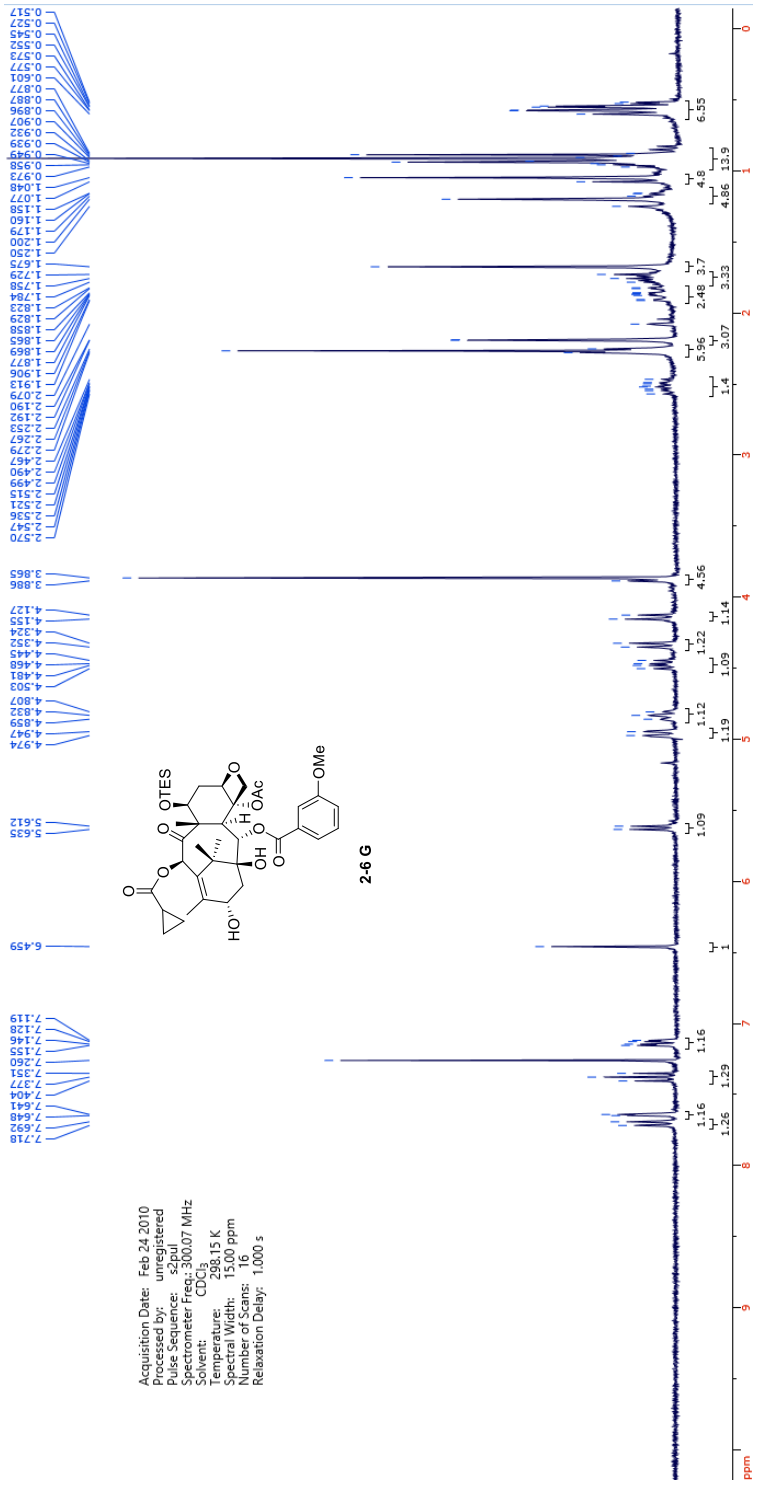
Acquisition Date: Feb 24 2010
Processed by: unregistered
Pulse Sequence: s2pul
Spectrometer Freq.: 300.07 MHz
Solvent: CDCl3
Temperature: 298.15 K
Spectral Width: 15.00 ppm
Number of Scans: 16
Relaxation Delay: 1.000 s
OTES
OAc
OH
HO
OMe
2-6 G
ppm

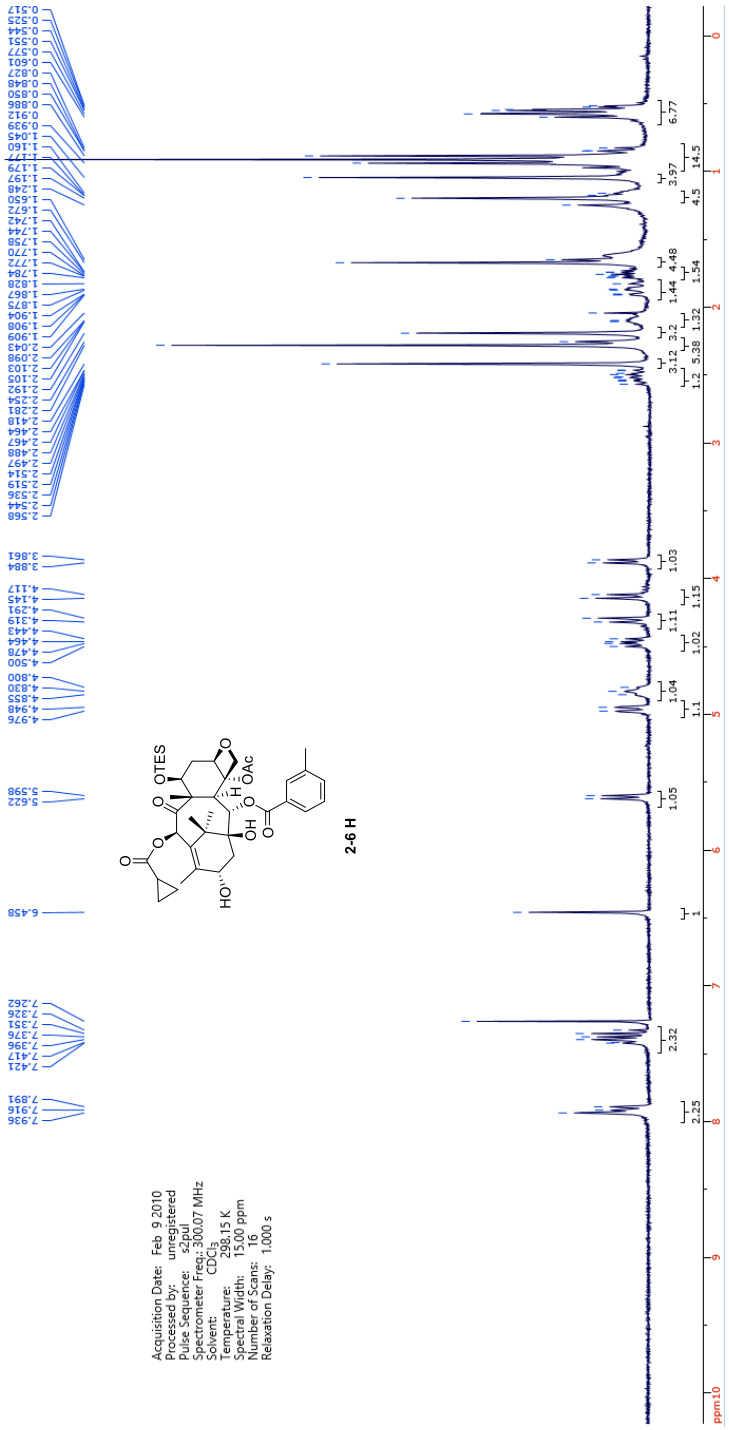
Acquisition Date: Feb 9 2010
Processed by: unregistered
Pulse Sequence: s2pul
Spectrometer Freq.: 300.07 MHz
Solvent: CDCl3
Temperature: 298.15 K
Spectral Width: 15.00 ppm
Number of Scans: 16
Relaxation Delay: 1.000 s
OTES
OAc
OH
HO
2-6 H

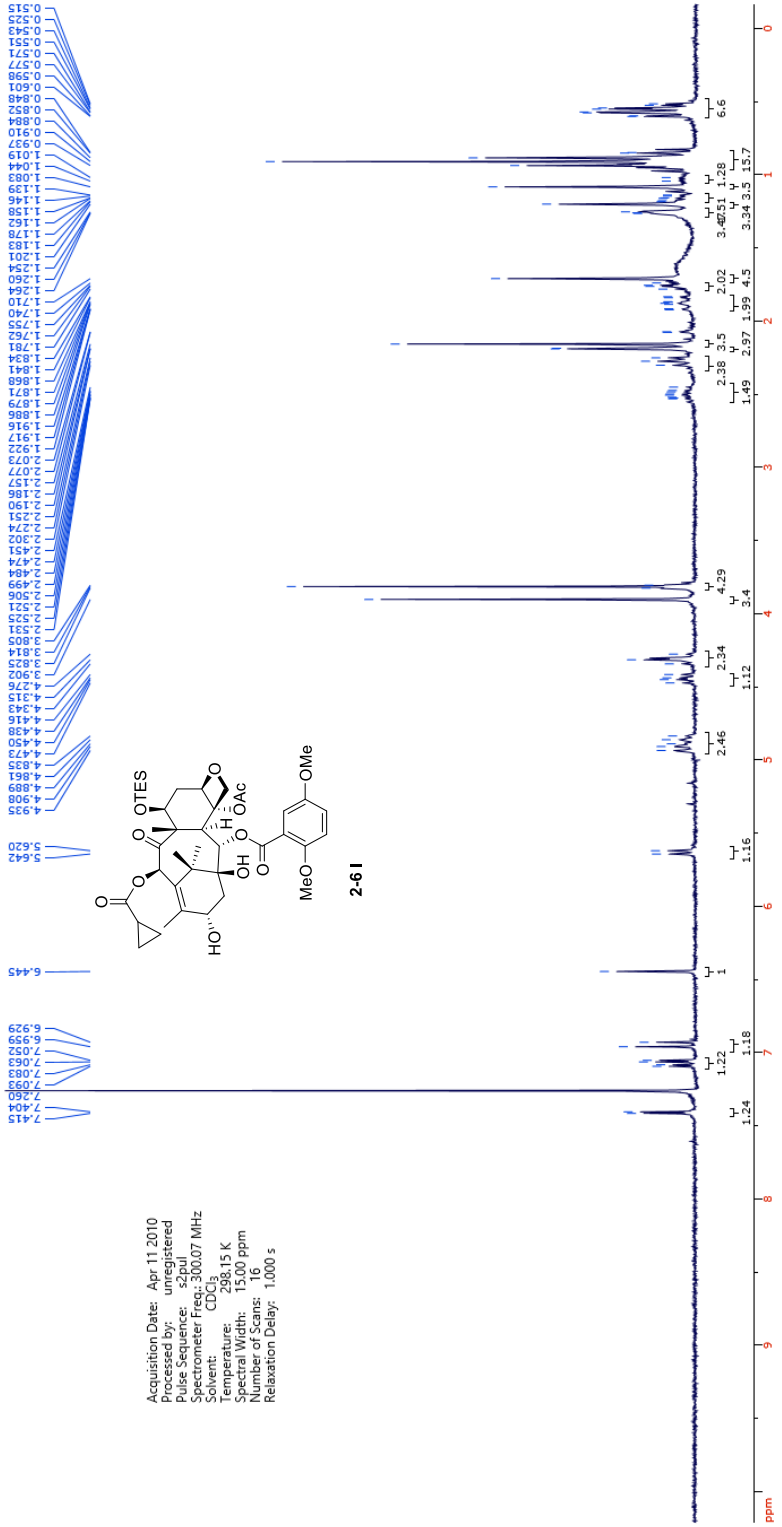
Acquisition Date: Apr 11 2010
Processed by: unregistered
Pulse Sequence: s2pul
Spectrometer Freq.: 300.07 MHz
Solvent: $CDCl_3$
Temperature: 298.15 K
Spectral Width: 15.00 ppm
Number of Scans: 16
Relaxation Delay: 1.000 s
OTES
OAc
OH
HO
MeO
OMe
2-6 l
ppm

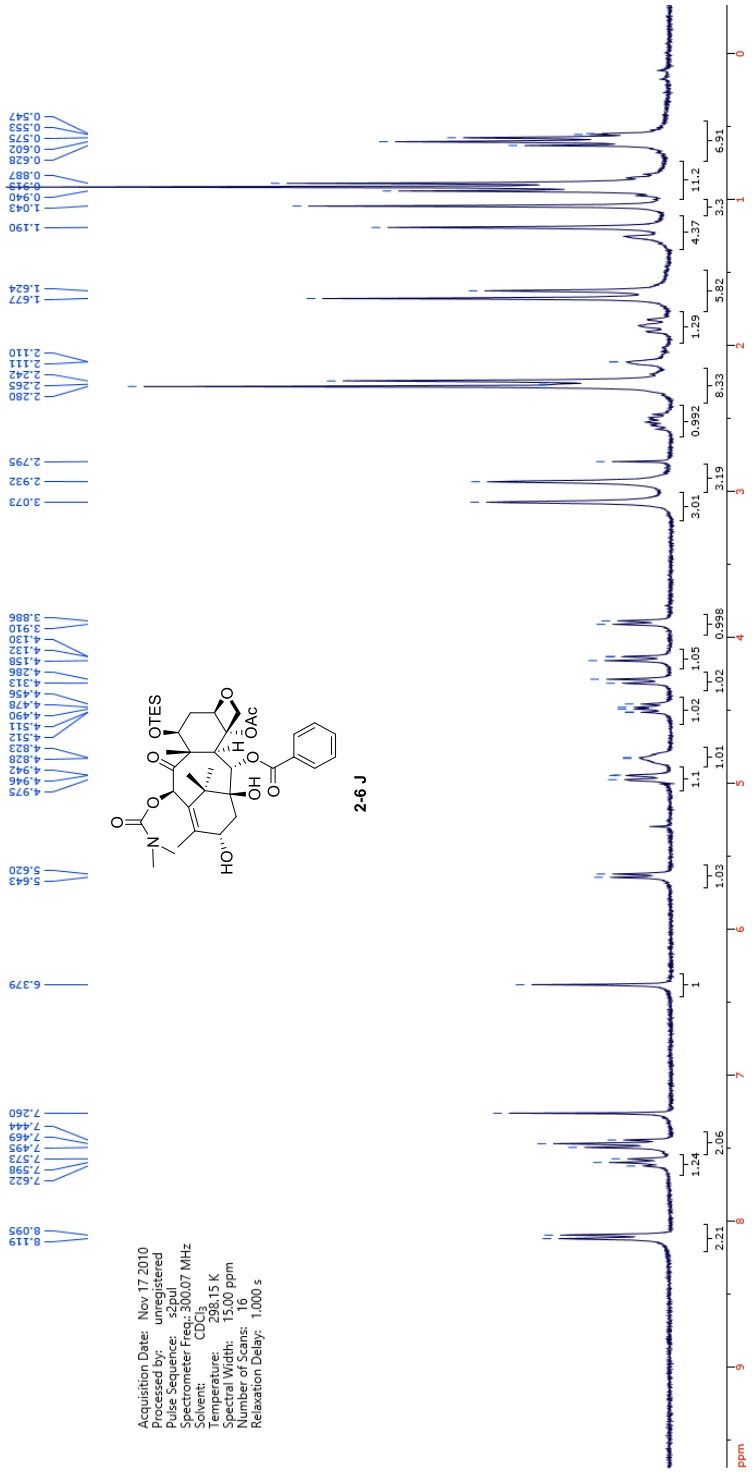
Acquisition Date: Nov 17 2010
Processed by: unregistered
Pulse Sequence: s2pul
Spectrometer Freq.: 300.07 MHz
Solvent: CDCl3
Temperature: 298.15 K
Spectral Width: 15.00 ppm
Number of Scans: 16
Relaxation Delay: 1.000 s
OTES
OAc
OH
HO
2-6 J
ppm

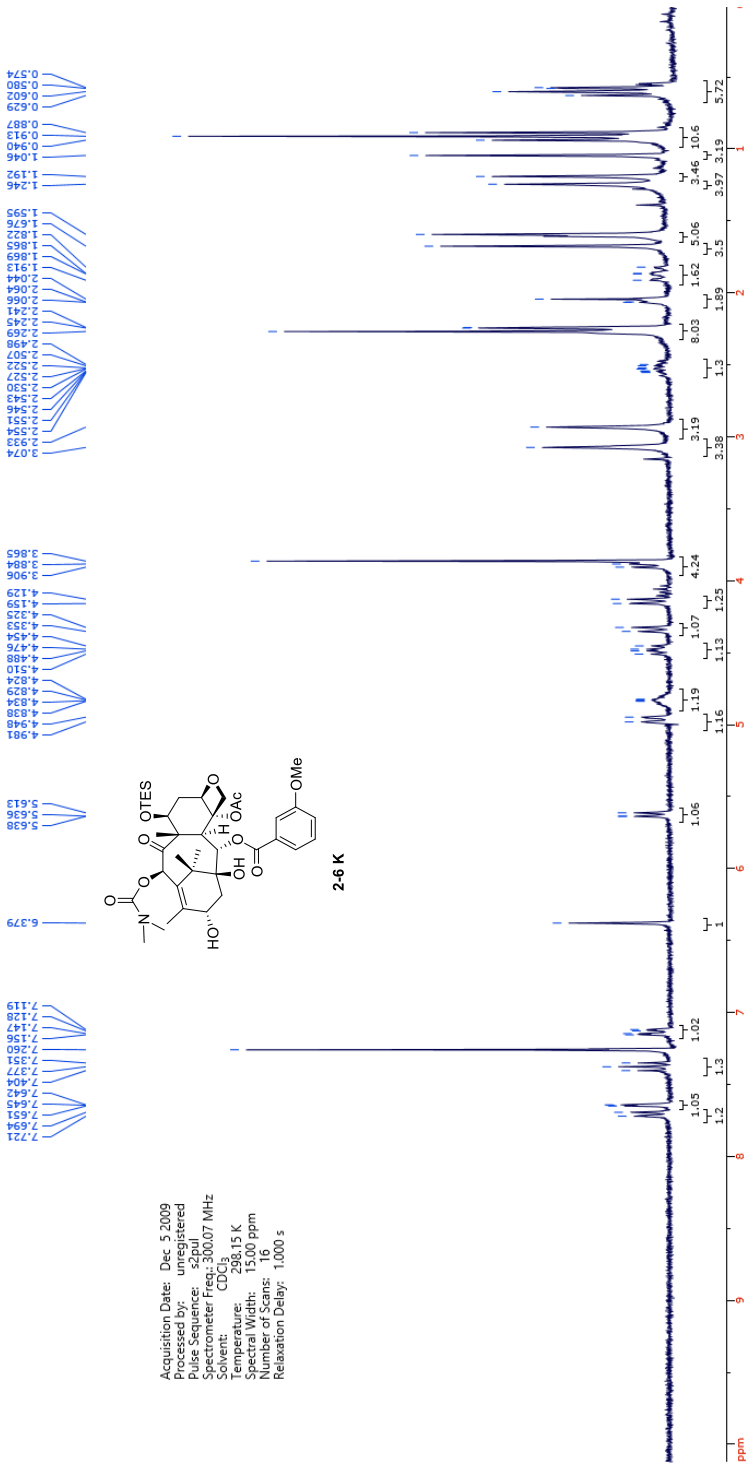
Acquisition Date: Dec 5 2009
Processed by: unregistered
Pulse Sequence: s2pul
Spectrometer Freq.: 300.07 MHz
Solvent: CDCl3
Temperature: 298.15 K
Spectral Width: 15.00 ppm
Number of Scans: 16
Relaxation Delay: 1.000 s
OTES
OAc
OMe
OH
HO
2-6 K

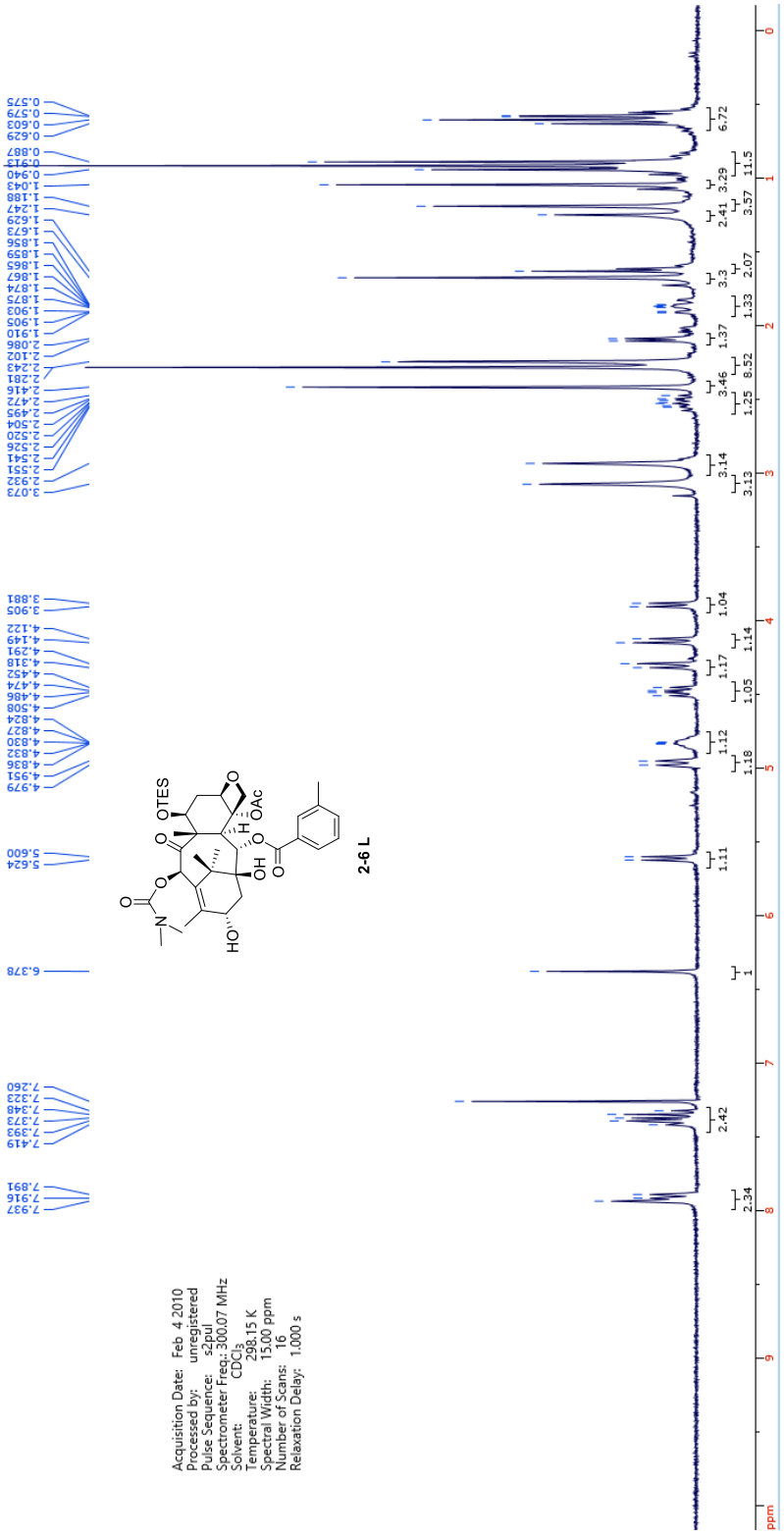
Acquisition Date: Feb 4 2010
Processed by: unregistered
Pulse Sequence: s2pul
Spectrometer Freq.: 300.07 MHz
Solvent: $CDCl_3$
Temperature: 298.15 K
Spectral Width: 15.00 ppm
Number of Scans: 16
Relaxation Delay: 1.000 s
OTES
OAc
OH
HO
2-6 L
ppm

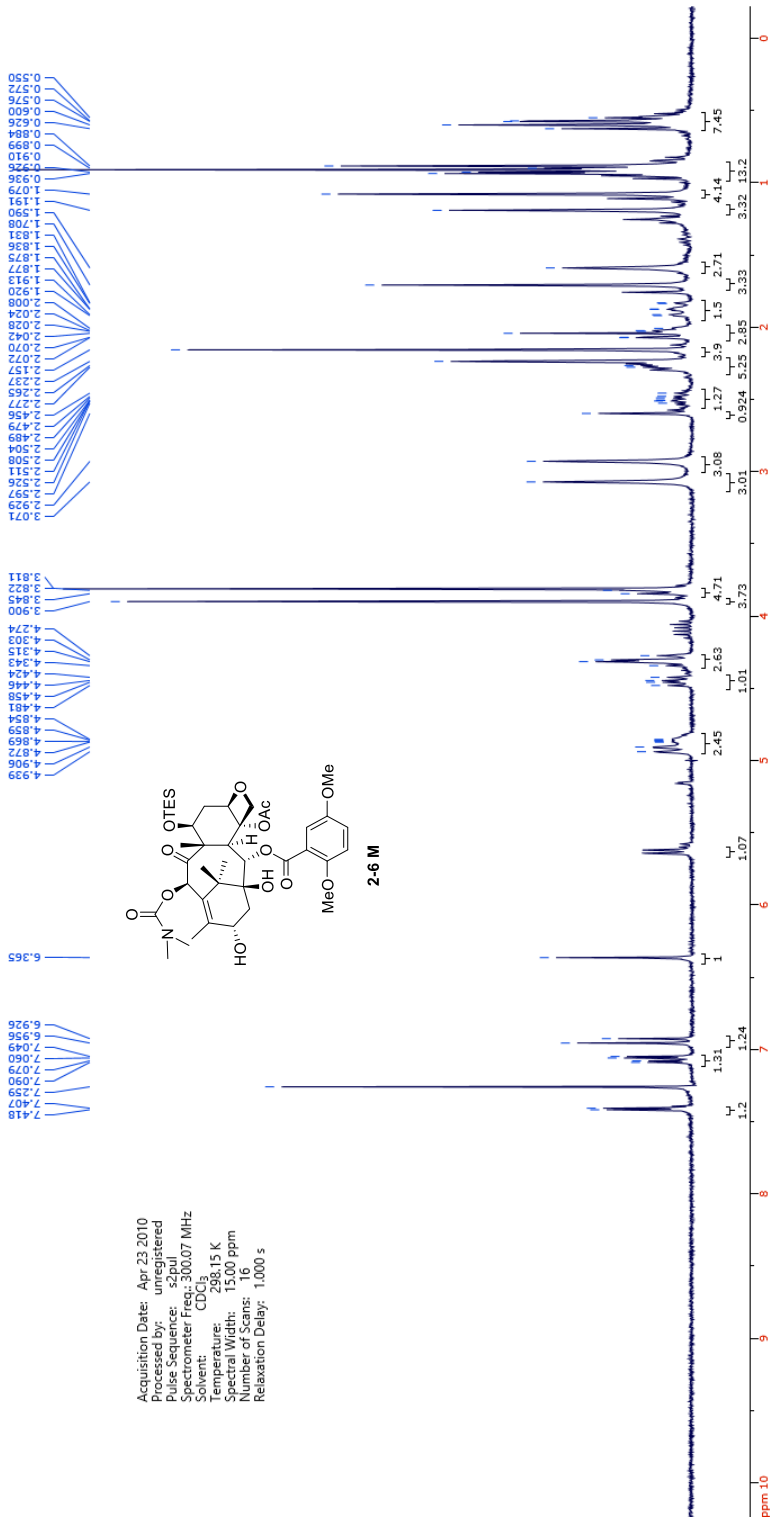
Acquisition Date: Apr 23 2010
Processed by: unregistered
Pulse Sequence: s2pul
Spectrometer Freq.: 300.07 MHz
Solvent: CDCl3
Temperature: 298.15 K
Spectral Width: 15.00 ppm
Number of Scans: 16
Relaxation Delay: 1.000 s
OTES
OAc
OH
HO
MeO
OMe
2-6 M

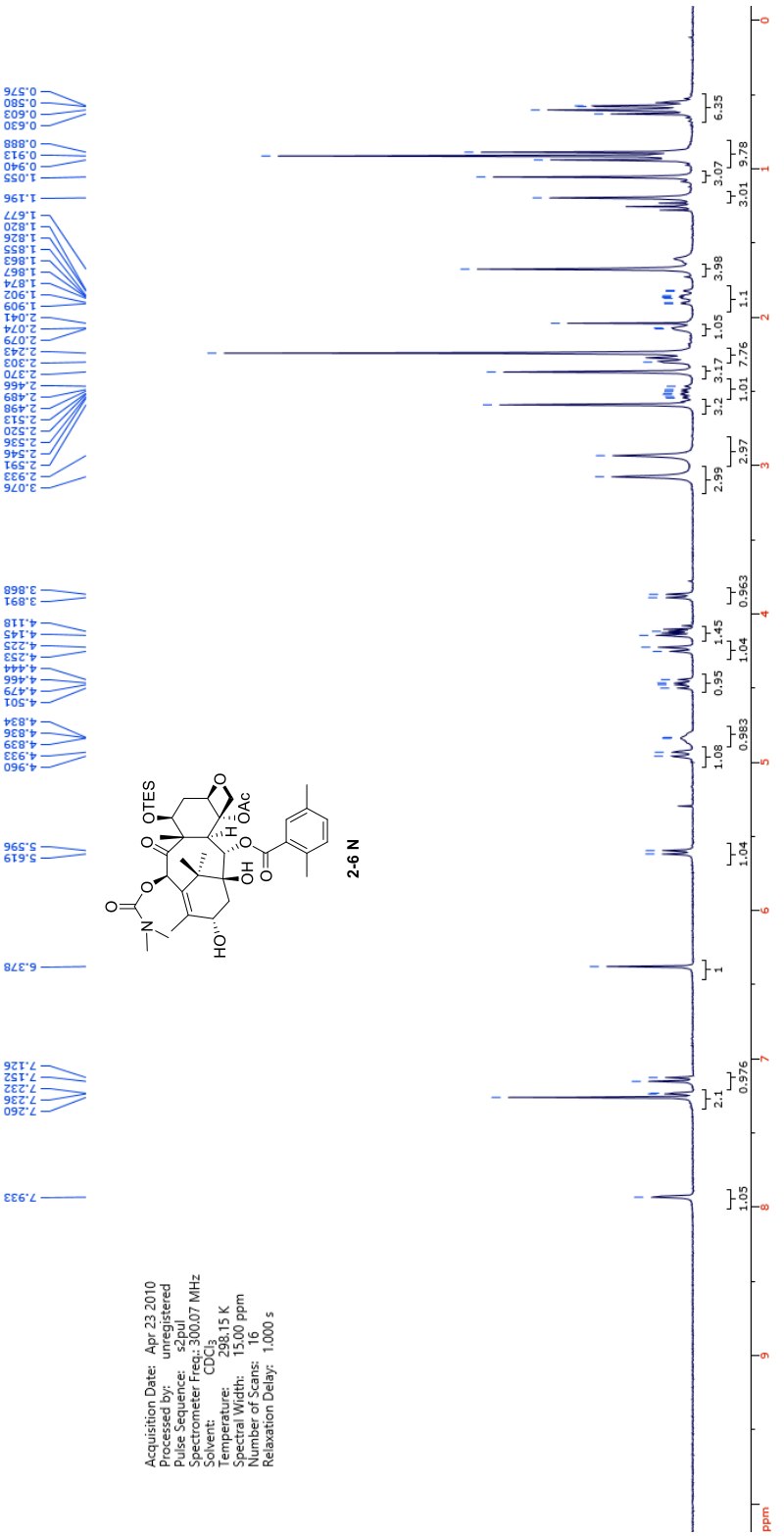
Acquisition Date: Apr 23 2010
Processed by: unregistered
Pulse Sequence: s2pul
Spectrometer Freq.: 300.07 MHz
Solvent: CDCl3
Temperature: 298.15 K
Spectral Width: 15.00 ppm
Number of Scans: 16
Relaxation Delay: 1.000 s
OTES
OAc
OH
HO
2-6 N
ppm

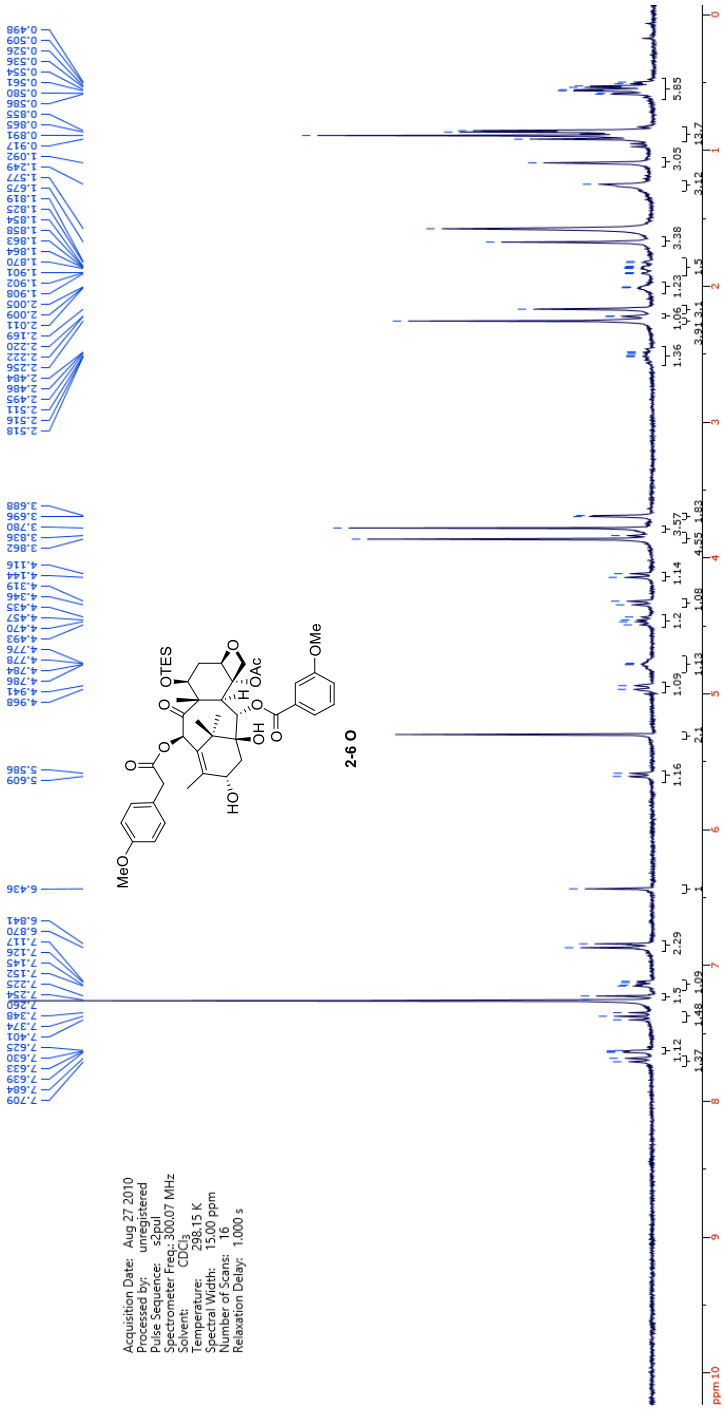
Acquisition Date: Aug 27 2010
Processed by: unregistered
Pulse Sequence: s2pul
Spectrometer Freq.: 300.07 MHz
Solvent: $CDCl_3$
Temperature: 298.15 K
Spectral Width: 15.00 ppm
Number of Scans: 16
Relaxation Delay: 1.000 s
2-6 O
MeO
OTES
OAc
OH
HO
OMe
ppm

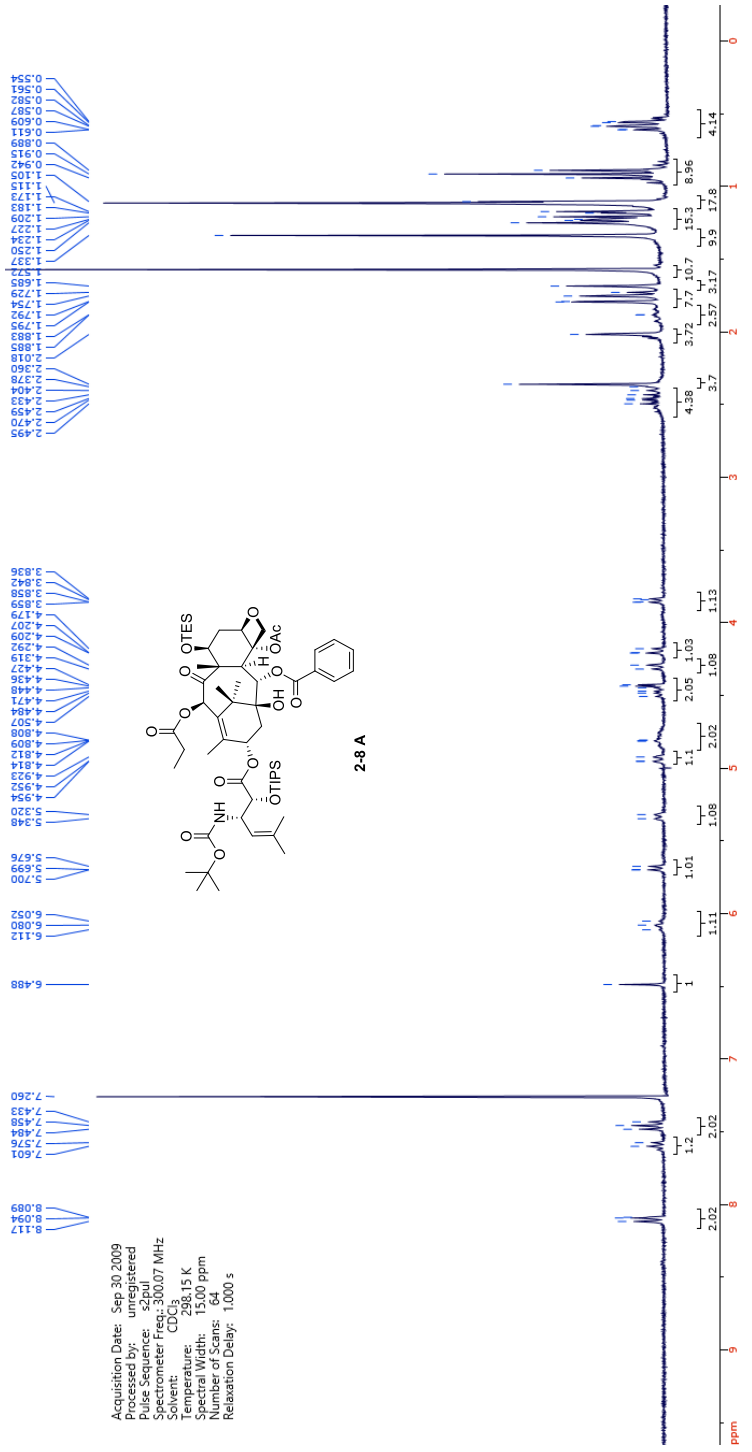
2-8 A
Acquisition Date: Sep 30 2009
Processed by: unregistered
Pulse Sequence: s2pul
Spectrometer Freq.: 300.07 MHz
Solvent: CDCl3
Temperature: 298.15 K
Spectral Width: 15.00 ppm
Number of Scans: 64
Relaxation Delay: 1.000 s
ppm

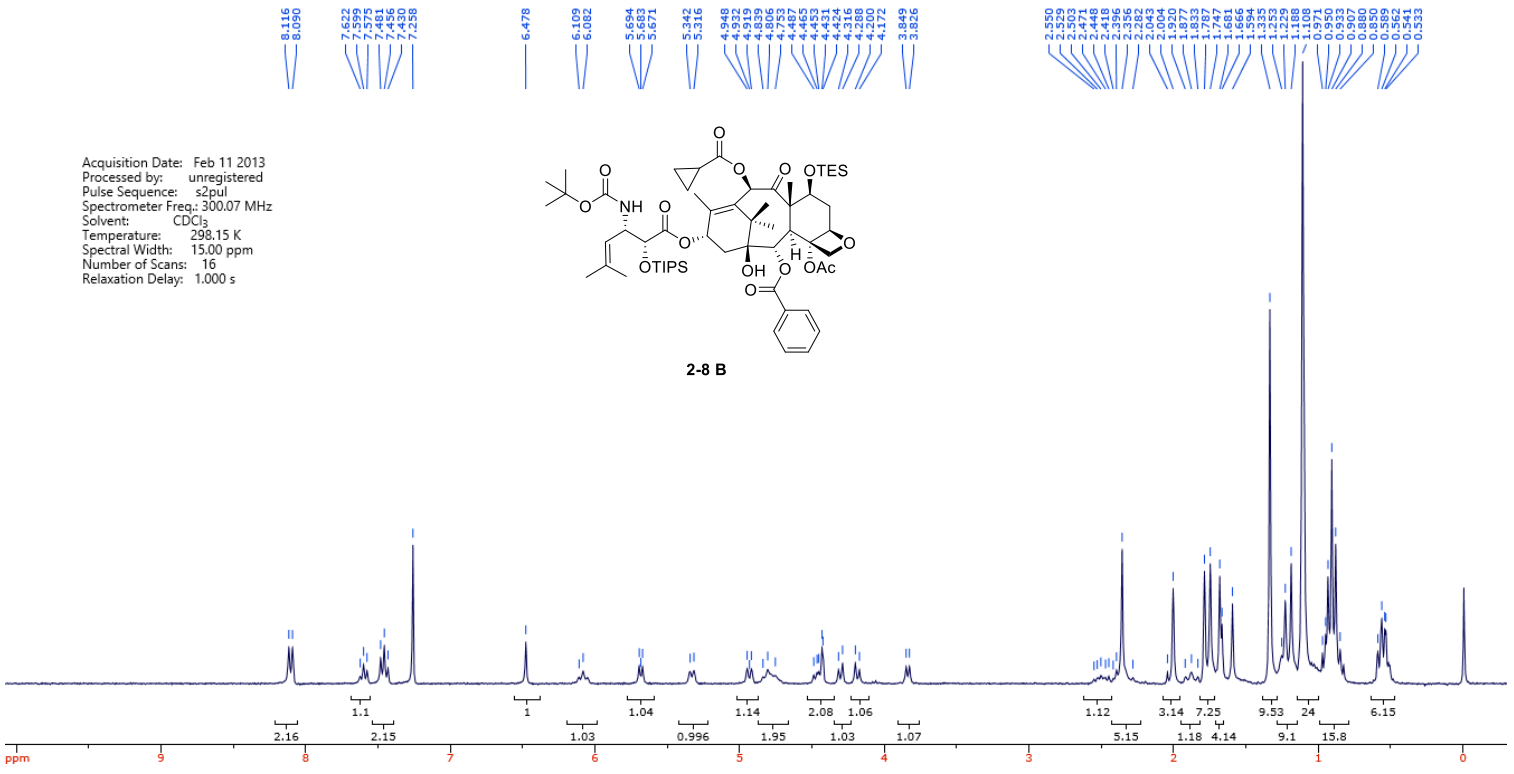
8.116
8.090
7.622
7.599
7.575
7.481
7.456
7.430
7.258
6.478
6.109
6.082
5.694
5.683
5.671
5.342
5.316
4.948
4.932
4.919
4.839
4.806
4.753
4.487
4.465
4.453
4.431
4.424
4.316
4.308
4.200
4.172
3.849
3.826
2.550
2.529
2.503
2.471
2.448
2.418
2.396
2.356
2.282
2.043
2.004
1.920
1.877
1.833
1.787
1.747
1.681
1.666
1.654
1.335
1.253
1.229
1.188
1.168
0.971
0.950
0.933
0.907
0.880
0.850
0.589
0.562
0.541
0.533
Acquisition Date: Feb 11 2013
Processed by: unregistered
Pulse Sequence: s2pul
Spectrometer Freq.: 300.07 MHz
Solvent: CDCl3
Temperature: 298.15 K
Spectral Width: 15.00 ppm
Number of Scans: 16
Relaxation Delay: 1.000 s
OTES
OTIPS
OAc
OH
NH
1.1
1
1.04
1.14
2.08
1.06
1.12
3.14
7.25
9.53
24
6.15
2.16
2.15
1.03
0.996
1.95
1.03
1.07
5.15
1.18
4.14
9.1
15.8
ppm
9
8
7
6
5
4
3
2
1
0

2-8 B

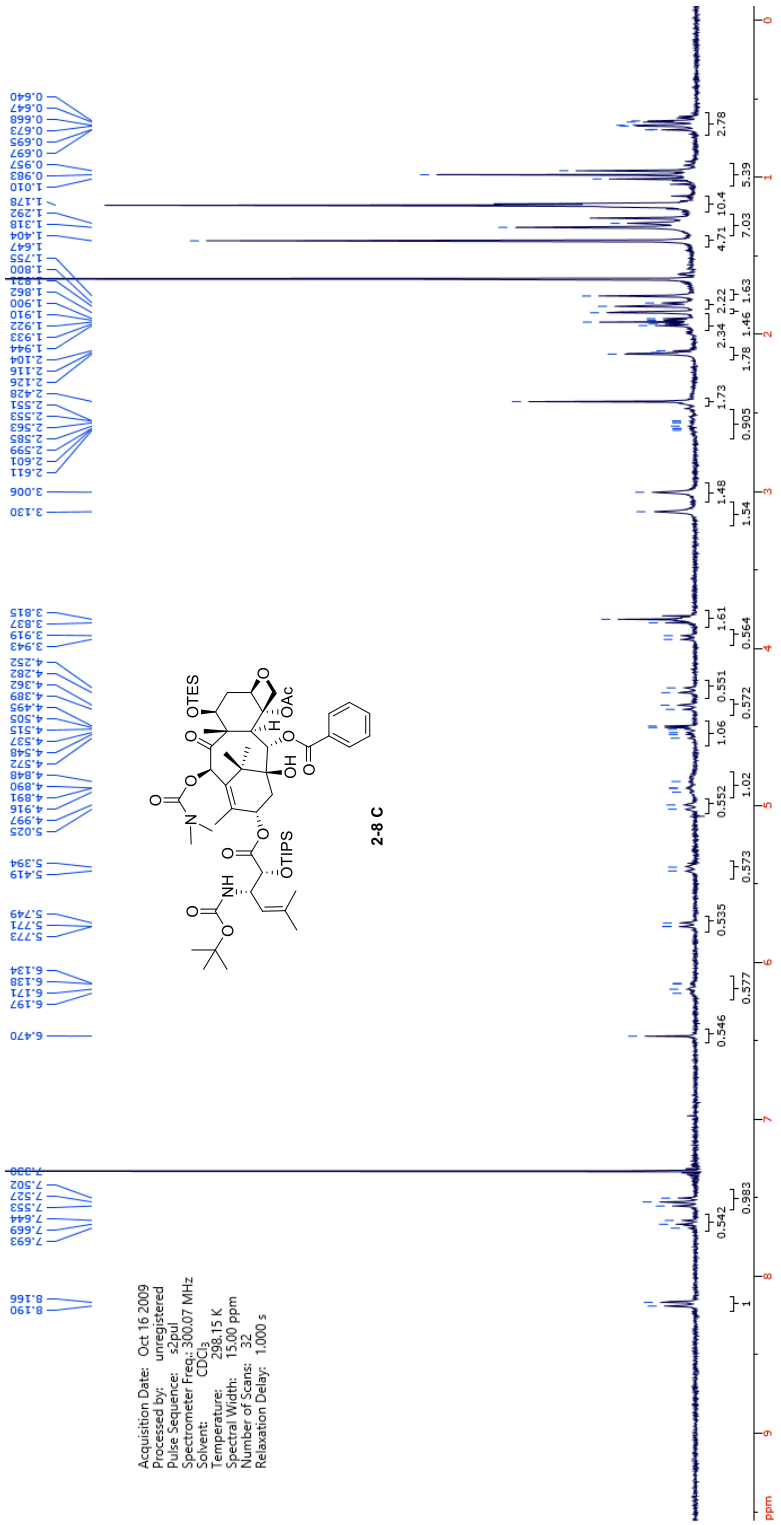
Acquisition Date: Oct 16 2009
Processed by: unregistered
Pulse Sequence: s2pul
Spectrometer Freq.: 300.07 MHz
Solvent: $CDCl_3$
Temperature: 298.15 K
Spectral Width: 15.00 ppm
Number of Scans: 32
Relaxation Delay: 1.000 s
OTES
OAc
OTIPS
NH
OH
2-8 C
ppm

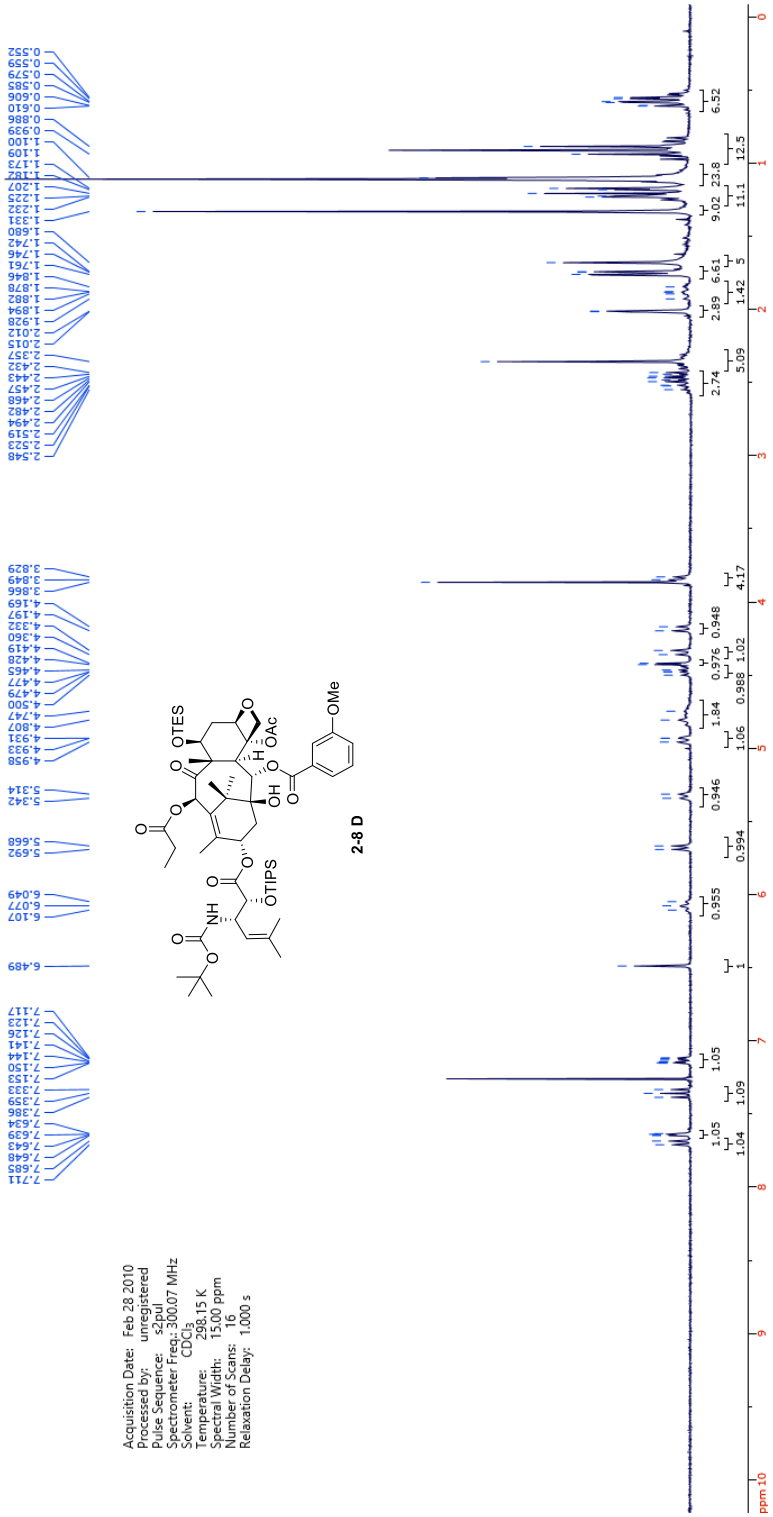
Acquisition Date: Feb 28 2010
Processed by: unregistered
Pulse Sequence: s2pul
Spectrometer Freq.: 300.07 MHz
Solvent: CDCl3
Temperature: 298.15 K
Spectral Width: 15.00 ppm
Number of Scans: 16
Relaxation Delay: 1.000 s
OTES
OAc
OMe
OTIPS
NH
OH
2-8 D
ppm

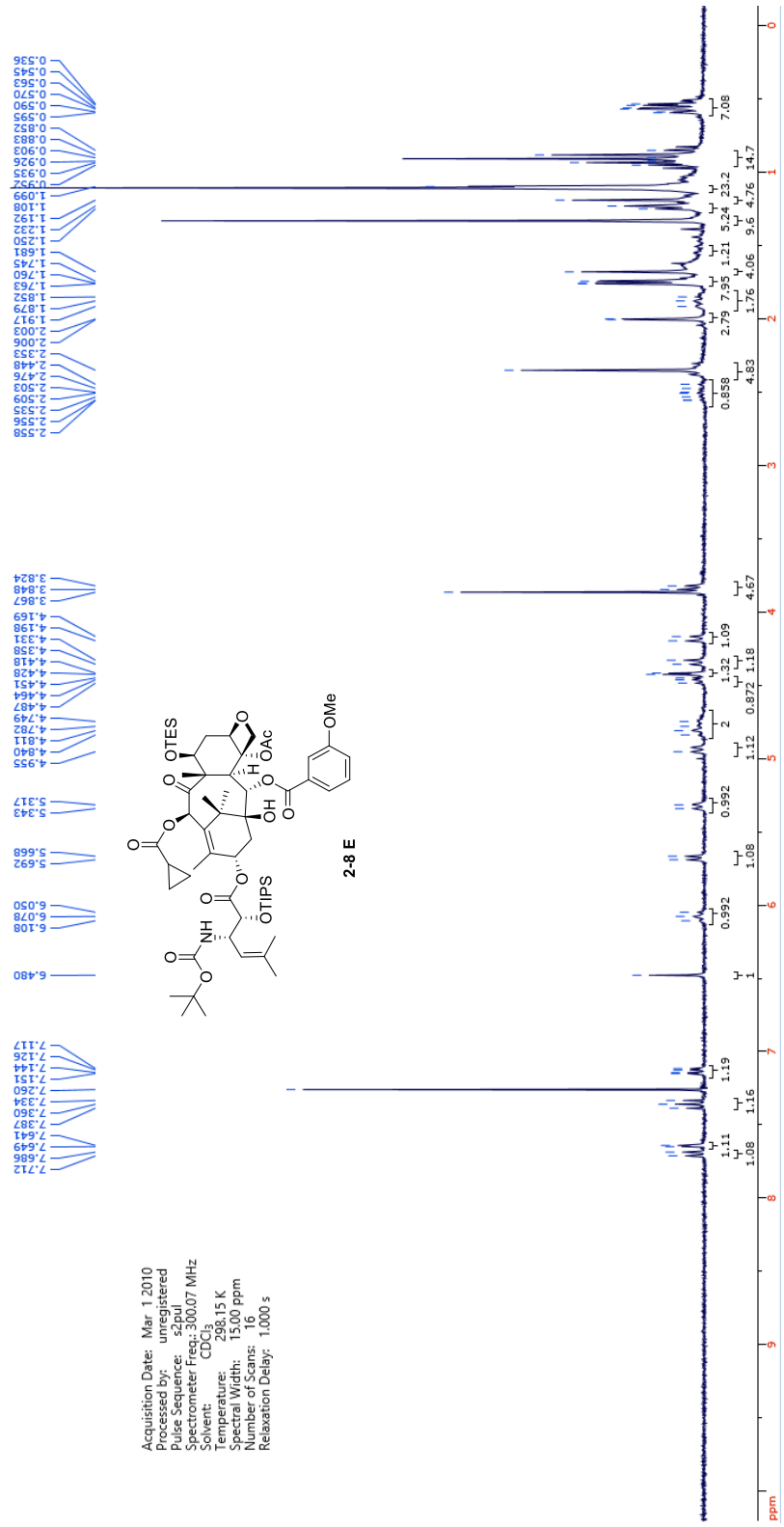
Acquisition Date: Mar 1 2010
Processed by: unregistered
Pulse Sequence: s2pul
Spectrometer Freq.: 300.07 MHz
Solvent: $CDCl_3$
Temperature: 298.15 K
Spectral Width: 15.00 ppm
Number of Scans: 16
Relaxation Delay: 1.000 s
OTES
OAc
OMe
OTIPS
2-8 E
ppm

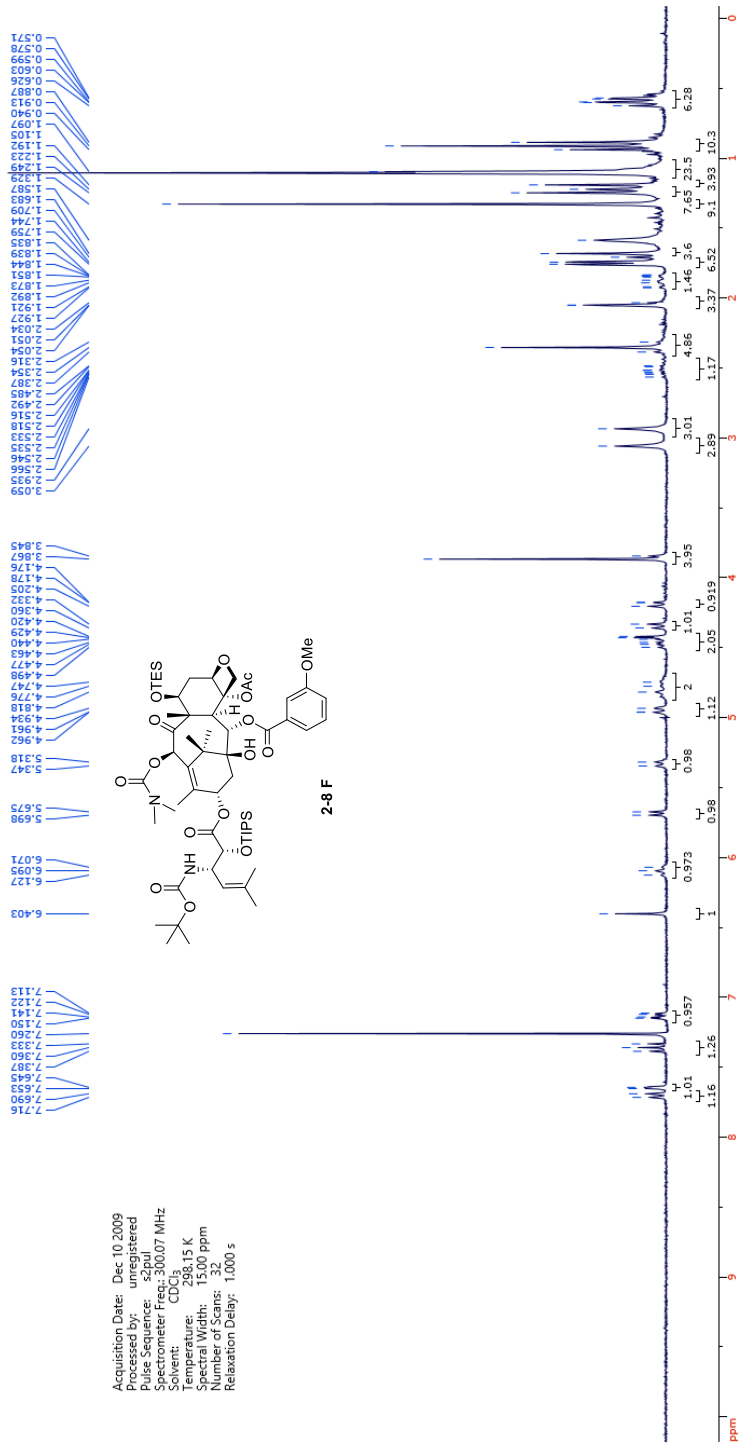
Acquisition Date: Dec 10 2009
Processed by: unregistered
Pulse Sequence: s2pul
Spectrometer Freq: 300.07 MHz
Solvent: CDCl3
Temperature: 298.15 K
Spectral Width: 15.00 ppm
Number of Scans: 32
Relaxation Delay: 1.000 s
OTES
OAc
OH
OTIPS
NH
OMe
2-8 F
ppm

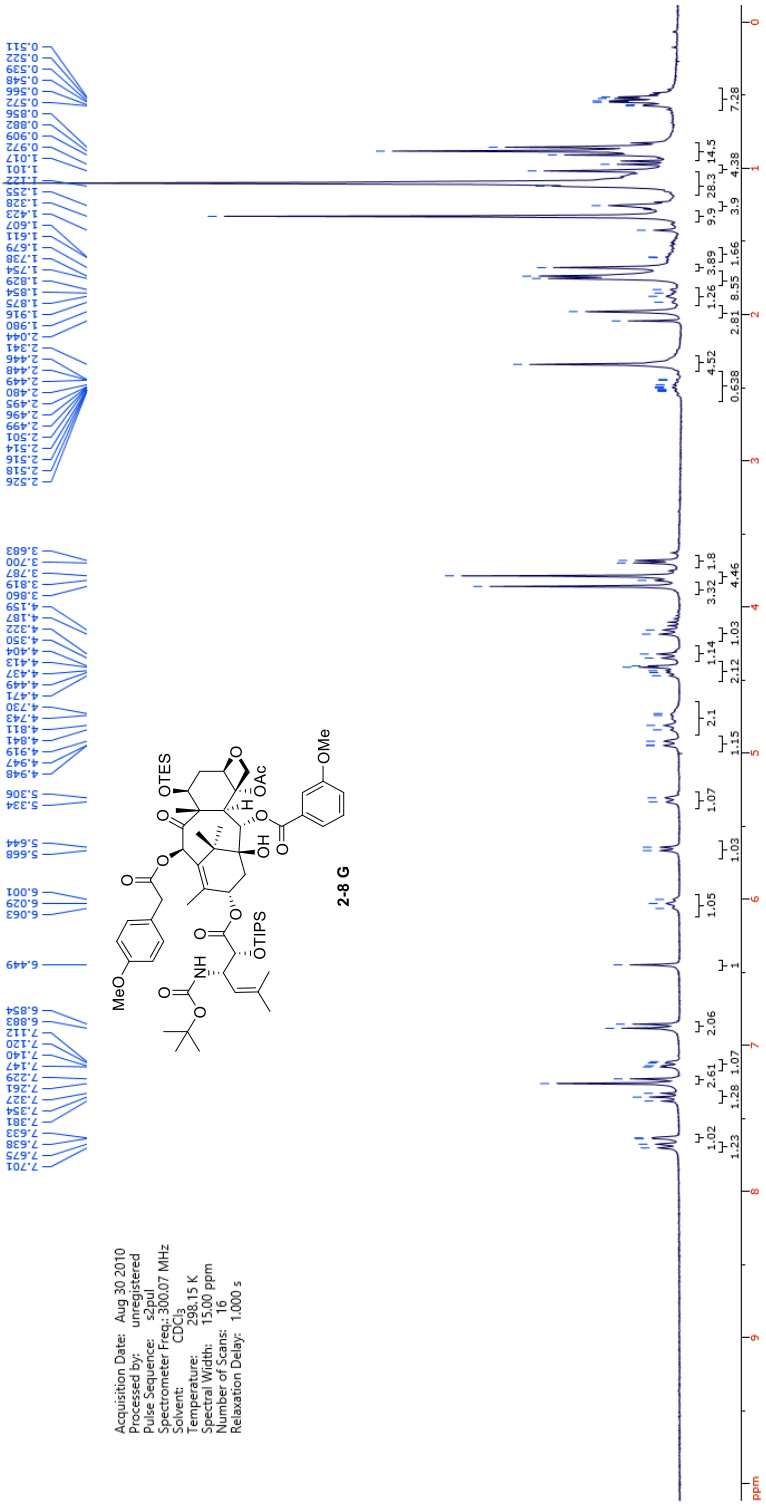
Acquisition Date: Aug 30 2010
Processed by: unregistered
Pulse Sequence: s2pul
Spectrometer Freq.: 300.07 MHz
Solvent: $CDCl_3$
Temperature: 298.15 K
Spectral Width: 15.00 ppm
Number of Scans: 16
Relaxation Delay: 1.000 s
2-8 G
ppm

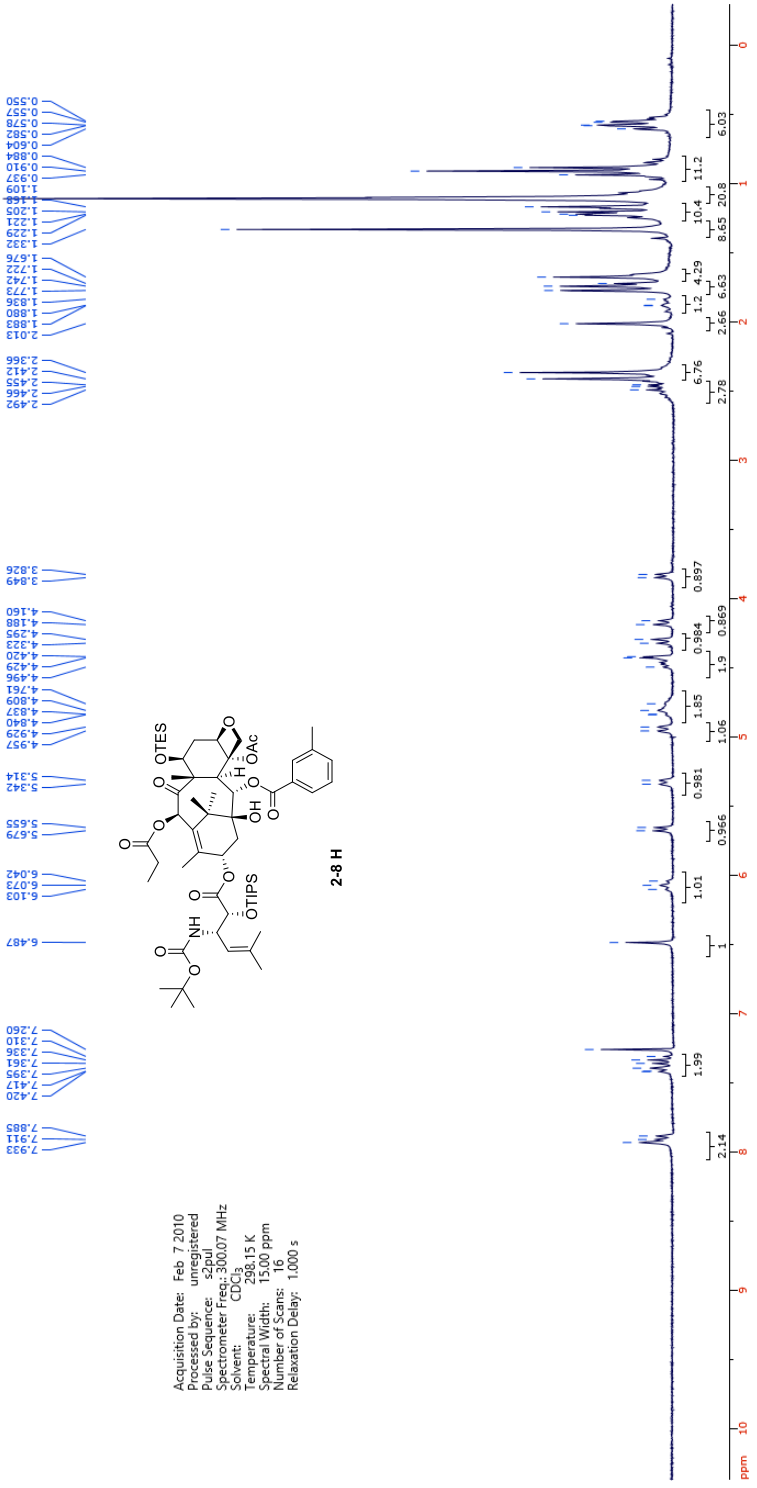
Acquisition Date: Feb 7 2010
Processed by: unregistered
Pulse Sequence: s2pul
Spectrometer Freq.: 300.07 MHz
Solvent: CDCl3
Temperature: 298.15 K
Spectral Width: 15.00 ppm
Number of Scans: 16
Relaxation Delay: 1.000 s
OTES
OAc
OH
OTIPS
NH
2-8 H
ppm

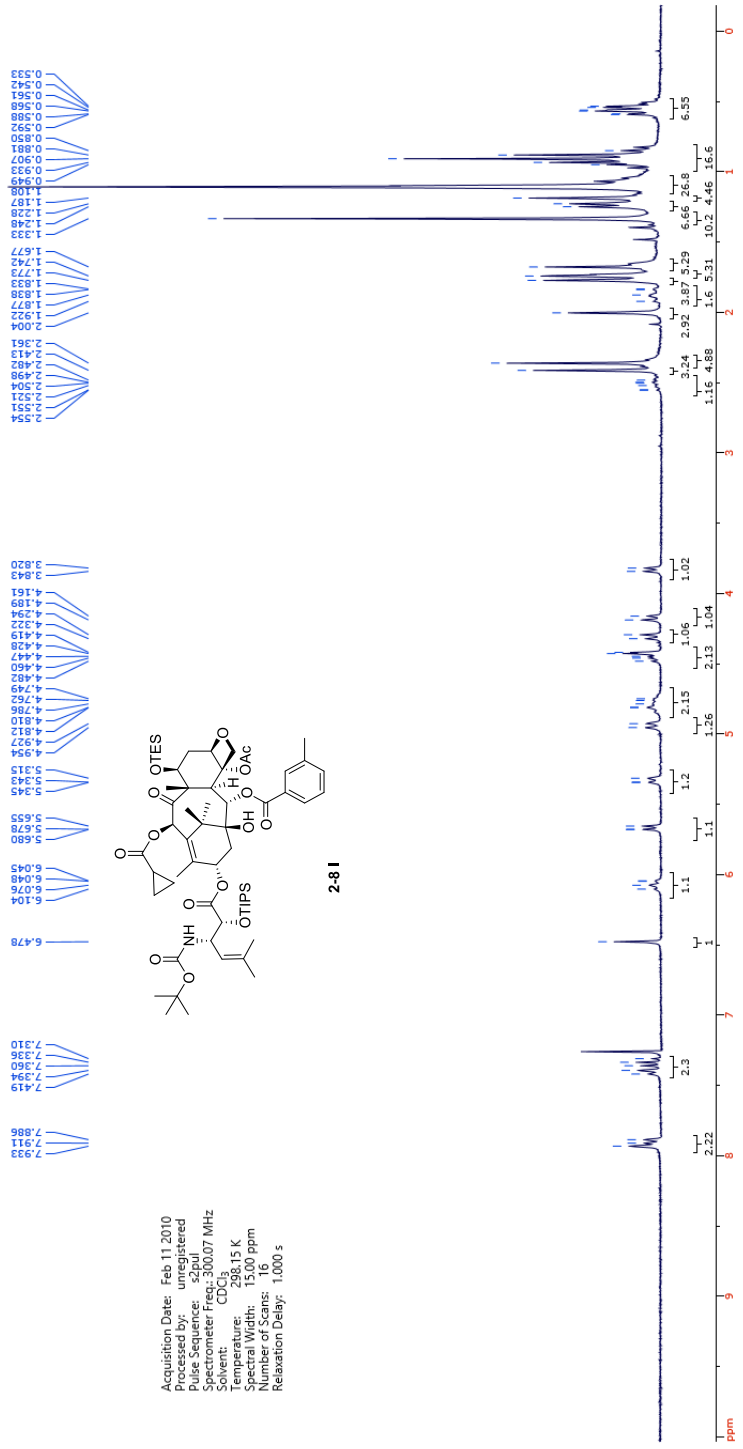
Acquisition Date: Feb 11 2010
Processed by: unregistered
Pulse Sequence: s2pul
Spectrometer Freq.: 300.07 MHz
Solvent: $CDCl_3$
Temperature: 298.15 K
Spectral Width: 15.00 ppm
Number of Scans: 16
Relaxation Delay: 1.000 s
OTES
OAc
OH
OTIPS
NH
2-8 I
ppm

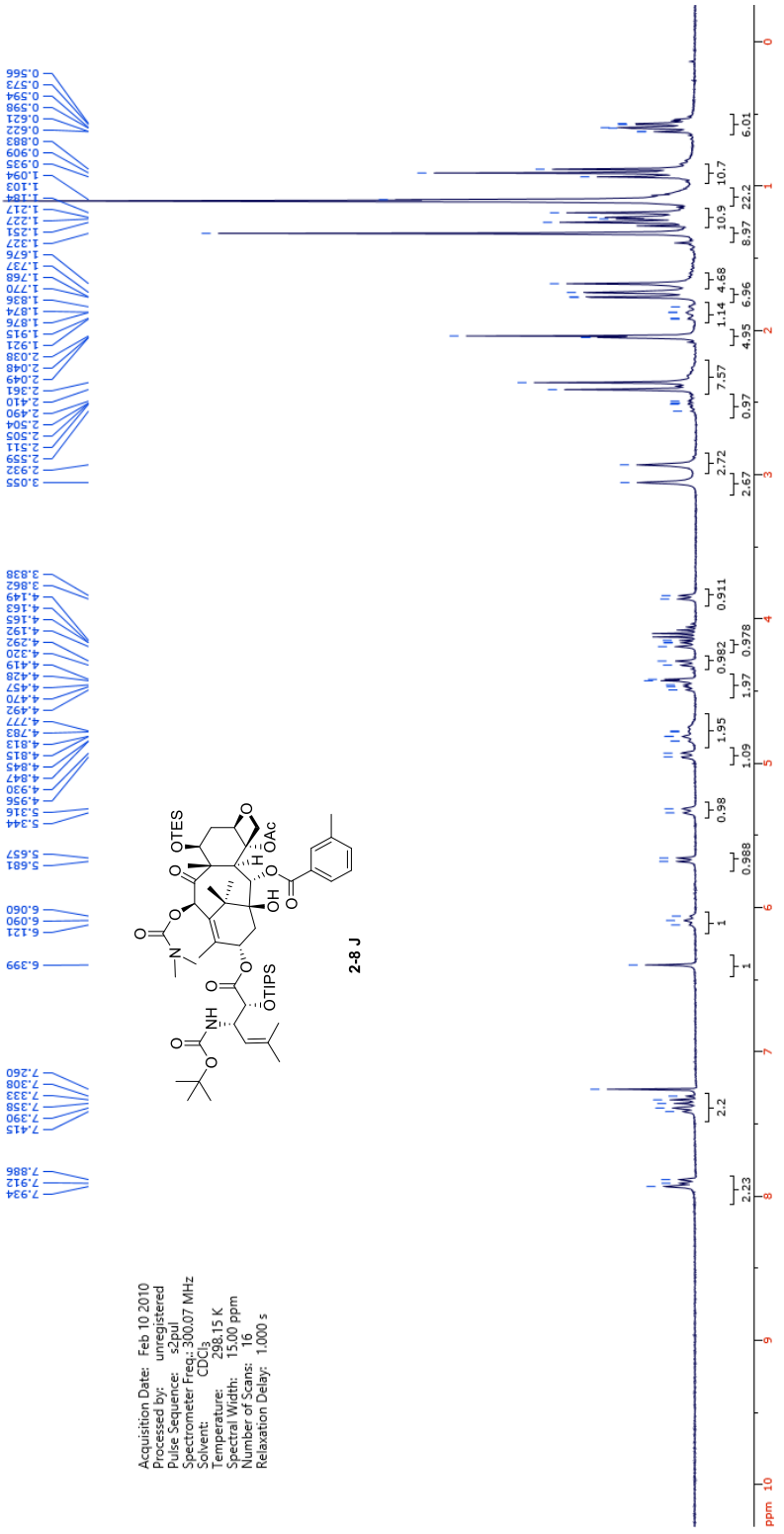
Acquisition Date: Feb 10 2010
Processed by: unregistered
Pulse Sequence: s2pul
Spectrometer Freq.: 300.07 MHz
Solvent: CDCl3
Temperature: 298.15 K
Spectral Width: 15.00 ppm
Number of Scans: 16
Relaxation Delay: 1.000 s
OTES
OAc
OH
OTIPS
NH
2-8 J

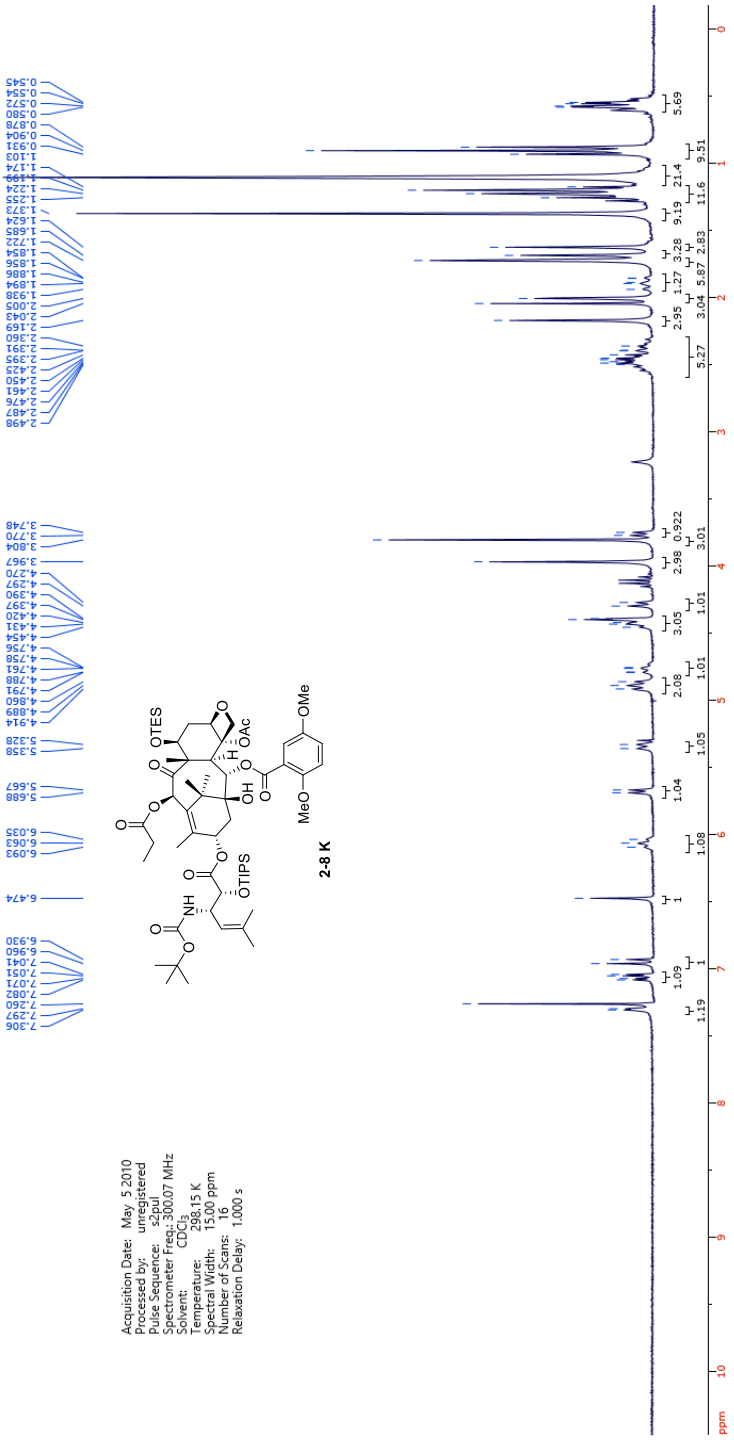
Acquisition Date: May 5 2010
Processed by: unregistered
Pulse Sequence: s2pul
Spectrometer Freq.: 300.07 MHz
Solvent: CDCl3
Temperature: 298.15 K
Spectral Width: 15.00 ppm
Number of Scans: 16
Relaxation Delay: 1.000 s
OTES
OAc
OH
OTIPS
NH
MeO
OMe
2-8 K
ppm

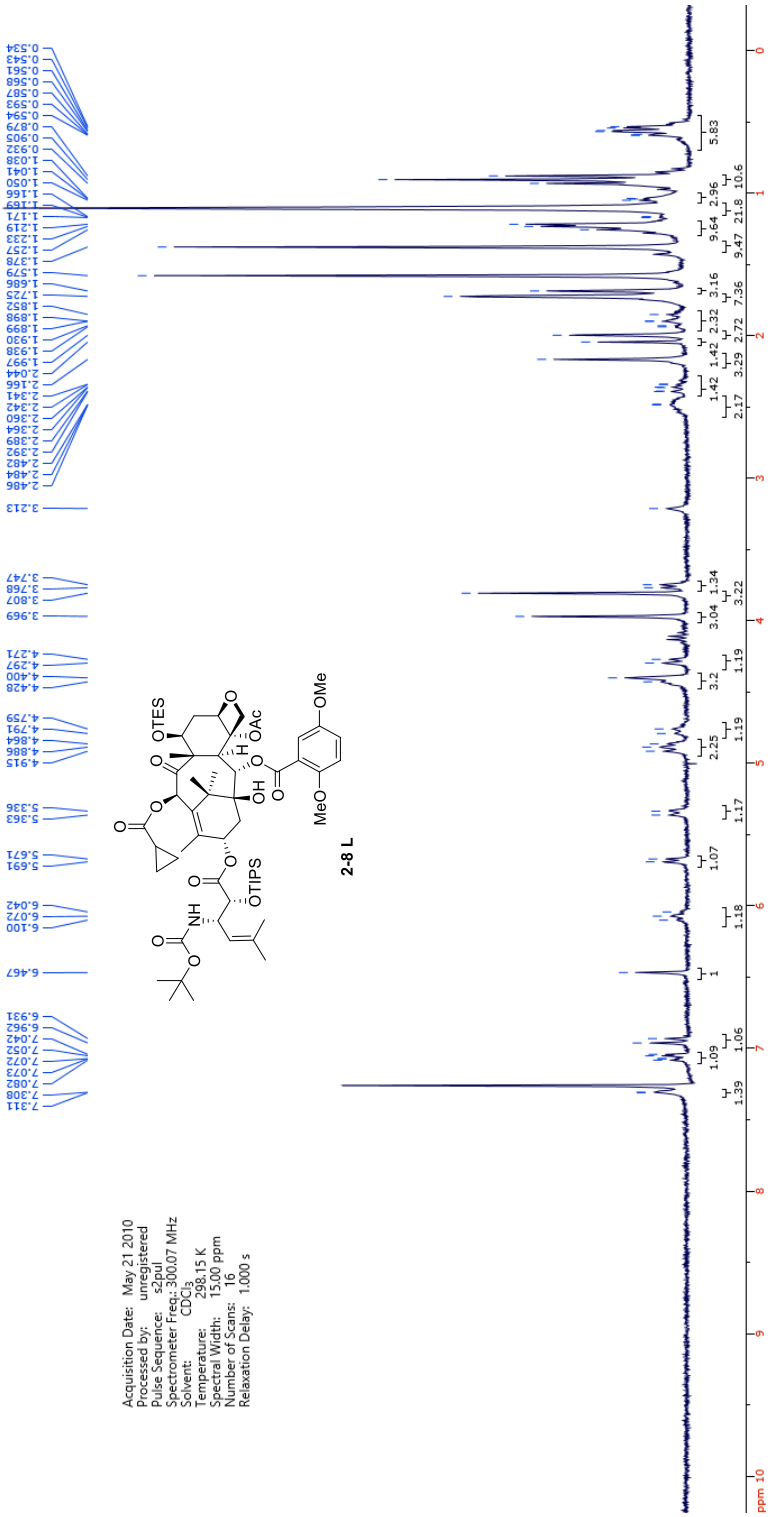
Acquisition Date: May 21 2010
Processed by: unregistered
Pulse Sequence: s2pul
Spectrometer Freq.: 300.07 MHz
Solvent: CDCl3
Temperature: 298.15 K
Spectral Width: 15.00 ppm
Number of Scans: 16
Relaxation Delay: 1.000 s
OTES
OAc
OH
OTIPS
OMe
MeO
2-8 L
ppm

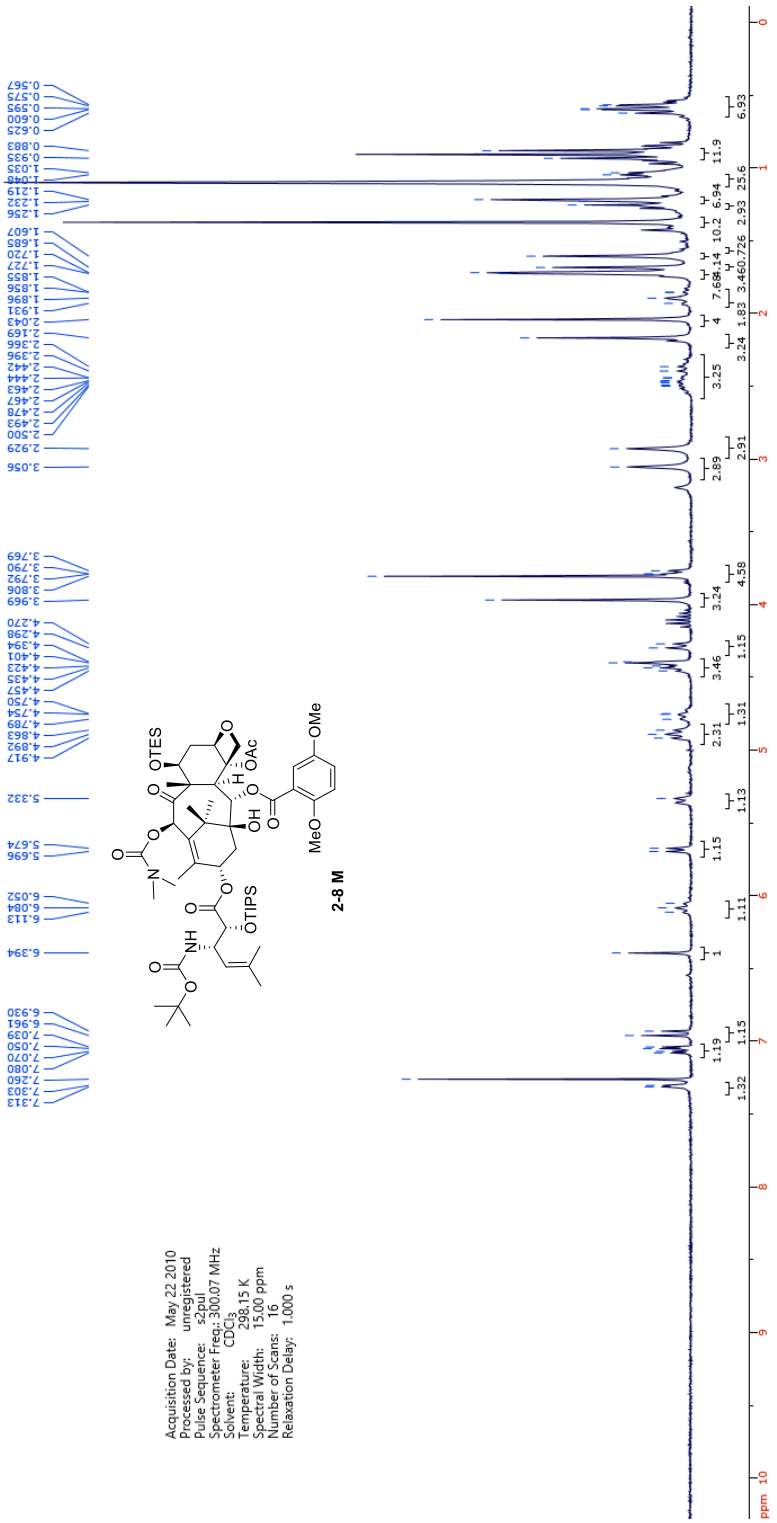
Acquisition Date: May 22 2010
Processed by: unregistered
Pulse Sequence: s2pul
Spectrometer Freq.: 300.07 MHz
Solvent: CDCl3
Temperature: 298.15 K
Spectral Width: 15.00 ppm
Number of Scans: 16
Relaxation Delay: 1.000 s
OTES
OAc
OTIPS
OMe
MeO
2-8 M
ppm

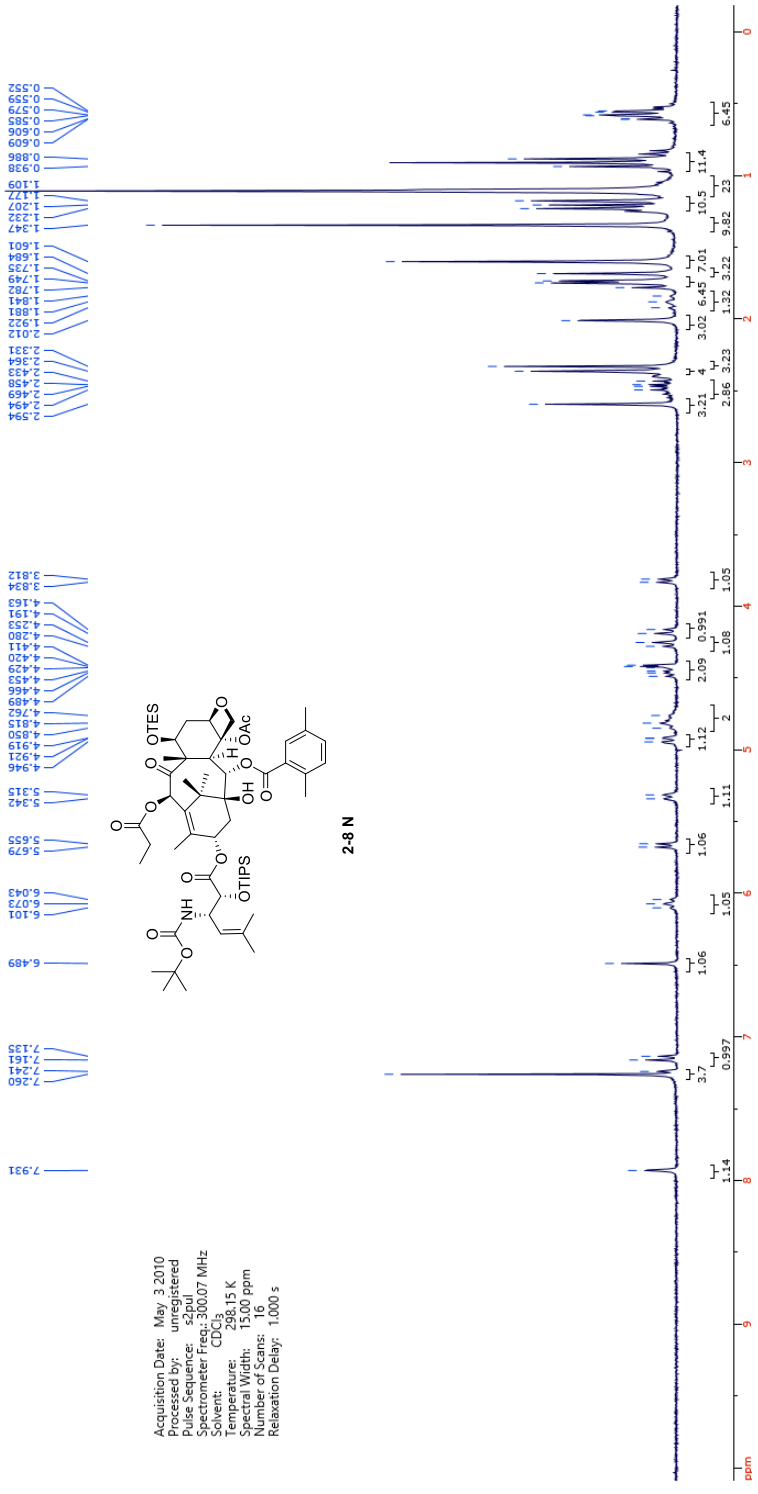
Acquisition Date: May 3 2010
Processed by: unregistered
Pulse Sequence: s2pul
Spectrometer Freq.: 300.07 MHz
Solvent: $CDCl_3$
Temperature: 298.15 K
Spectral Width: 15.00 ppm
Number of Scans: 16
Relaxation Delay: 1.000 s
OTES
OAc
OH
OTIPS
NH
2-8 N
ppm

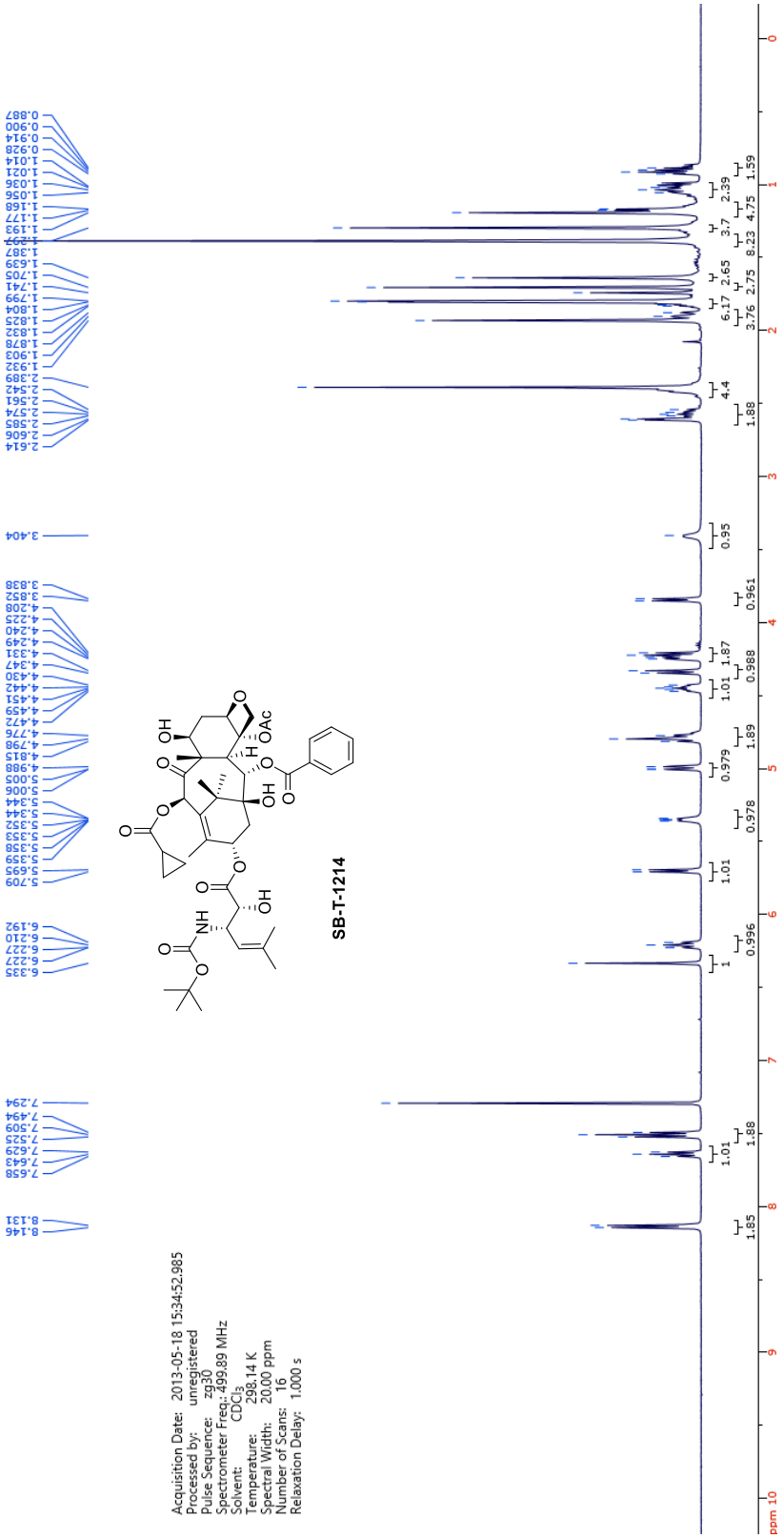
SB-T-1214
Acquisition Date: 2013-05-18 15:34:52.985
Processed by: unregistered
Pulse Sequence: zg30
Spectrometer Freq.: 499.89 MHz
Solvent: CDCl3
Temperature: 298.14 K
Spectral Width: 20.00 ppm
Number of Scans: 16
Relaxation Delay: 1.000 s
ppm

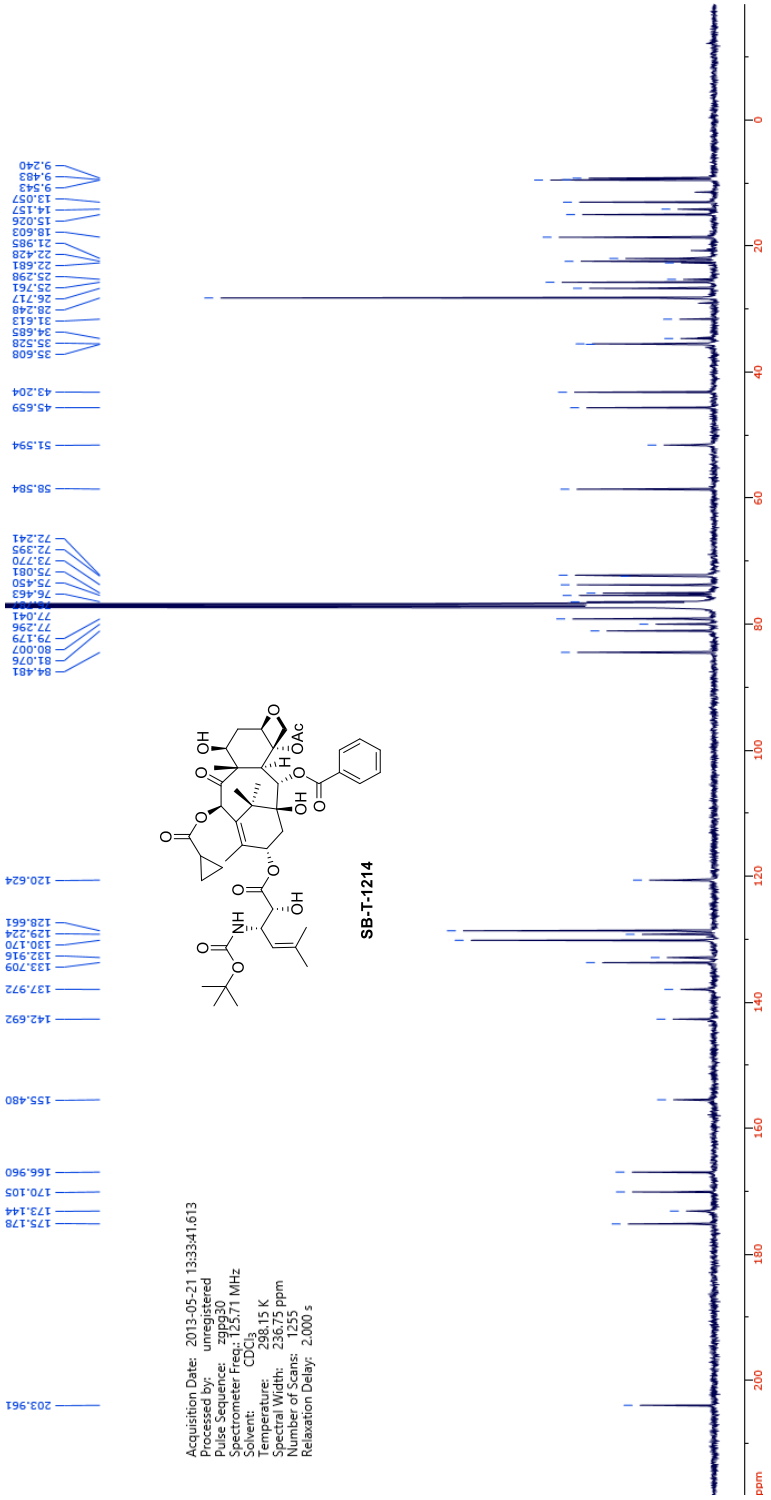
9.240
9.483
9.543
13.057
14.157
15.026
18.603
21.985
22.428
22.681
25.298
25.761
26.717
28.248
31.613
34.685
35.528
35.608
43.204
45.659
51.594
58.584
72.241
72.395
73.770
75.081
75.450
76.463
77.296
79.179
80.007
81.076
84.481
120.624
128.661
129.224
130.170
132.916
133.709
137.972
142.692
155.480
166.960
170.105
173.144
175.178
203.961
SB-T-1214
Acquisition Date: 2013-05-21 13:33:41.613
Processed by: unregistered
Pulse Sequence: zgpg30
Spectrometer Freq.: 125.71 MHz
Solvent: CDCl3
Temperature: 298.15 K
Spectral Width: 236.75 ppm
Number of Scans: 1255
Relaxation Delay: 2.000 s
ppm

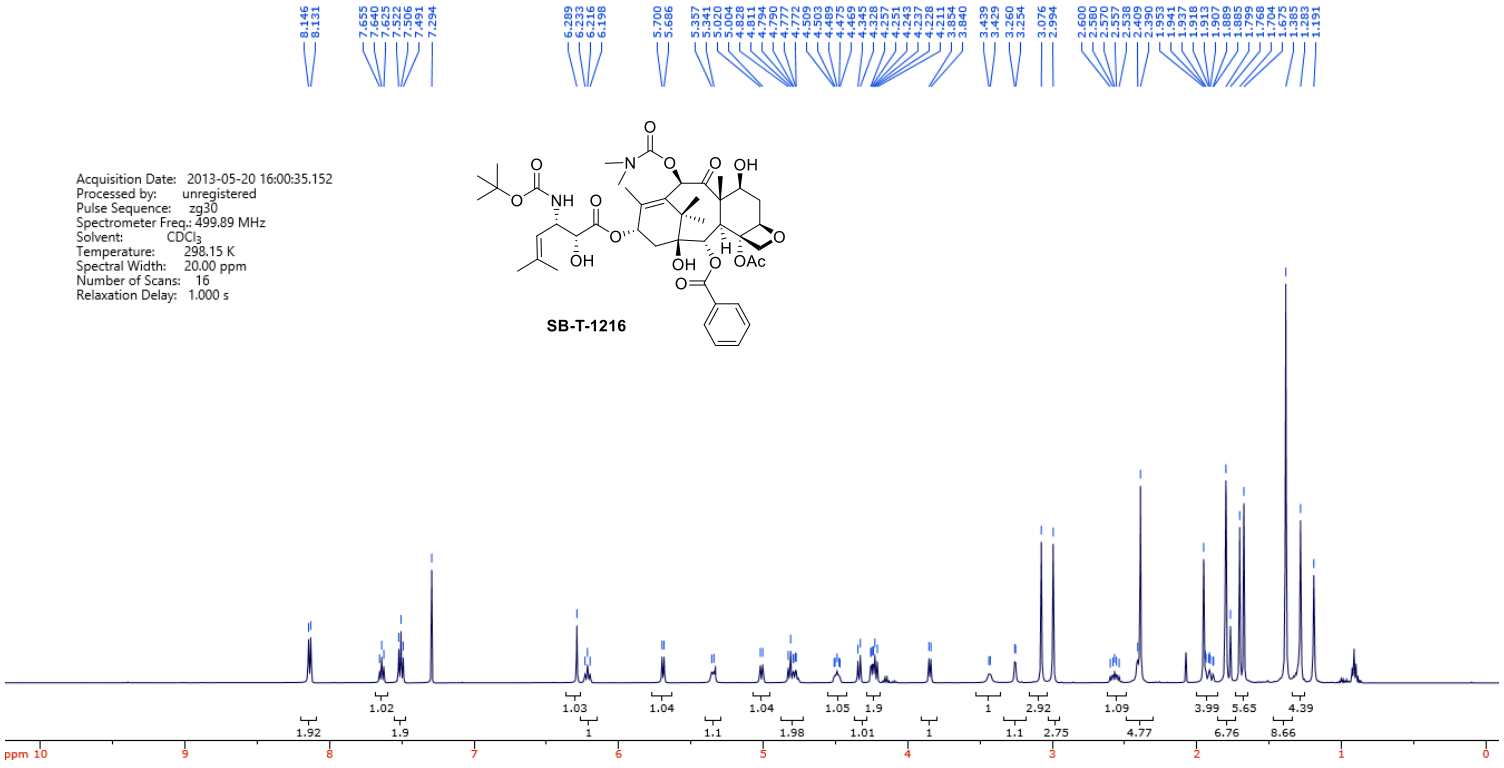
8.146
8.131
7.655
7.640
7.625
7.522
7.506
7.491
7.294
6.289
6.233
6.215
6.198
5.700
5.686
5.357
5.341
5.320
5.004
4.828
4.811
4.794
4.790
4.777
4.772
4.509
4.503
4.489
4.475
4.469
4.345
4.328
4.307
4.251
4.243
4.237
4.228
4.211
3.854
3.840
3.439
3.429
3.260
3.254
3.076
2.994
2.600
2.580
2.570
2.557
2.538
2.409
2.390
1.953
1.941
1.937
1.918
1.913
1.907
1.889
1.885
1.789
1.768
1.704
1.675
1.385
1.383
1.191
Acquisition Date: 2013-05-20 16:00:35.152
Processed by: unregistered
Pulse Sequence: zg30
Spectrometer Freq.: 499.89 MHz
Solvent: CDCl3
Temperature: 298.15 K
Spectral Width: 20.00 ppm
Number of Scans: 16
Relaxation Delay: 1.000 s
SB-T-1216
1.92
1.02
1.9
1.03
1
1.04
1.1
1.04
1.98
1.05
1.01
1.9
1
1
1.1
2.92
2.75
1.09
4.77
3.99
6.76
5.65
4.39
8.66
ppm 10
9
8
7
6
5
4
3
2
1
0

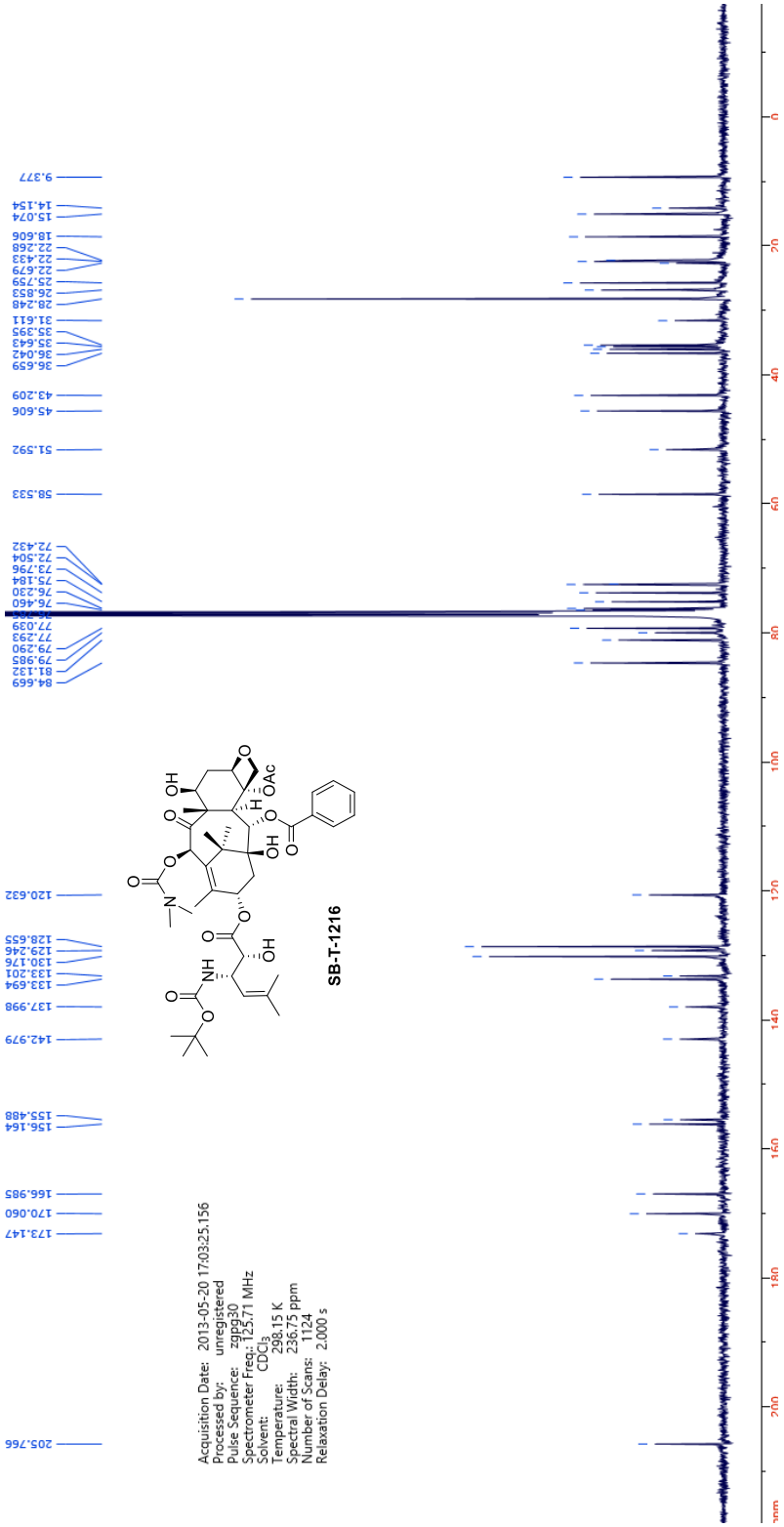
9.377
14.154
15.074
18.606
22.268
22.433
22.679
25.759
26.853
28.248
31.611
35.395
35.643
36.042
36.659
43.209
45.606
51.592
58.533
72.432
72.504
73.796
75.184
76.230
76.460
77.039
77.293
79.290
79.985
81.132
84.669
120.632
128.655
129.246
130.176
133.201
133.694
137.998
142.979
155.488
156.164
166.985
170.060
173.147
205.766
SB-T-1216
Acquisition Date: 2013-05-20 17:03:25.156
Processed by: unregistered
Pulse Sequence: zgpg30
Spectrometer Freq.: 125.71 MHz
Solvent: CDCl3
Temperature: 298.15 K
Spectral Width: 236.75 ppm
Number of Scans: 1124
Relaxation Delay: 2.000 s
ppm

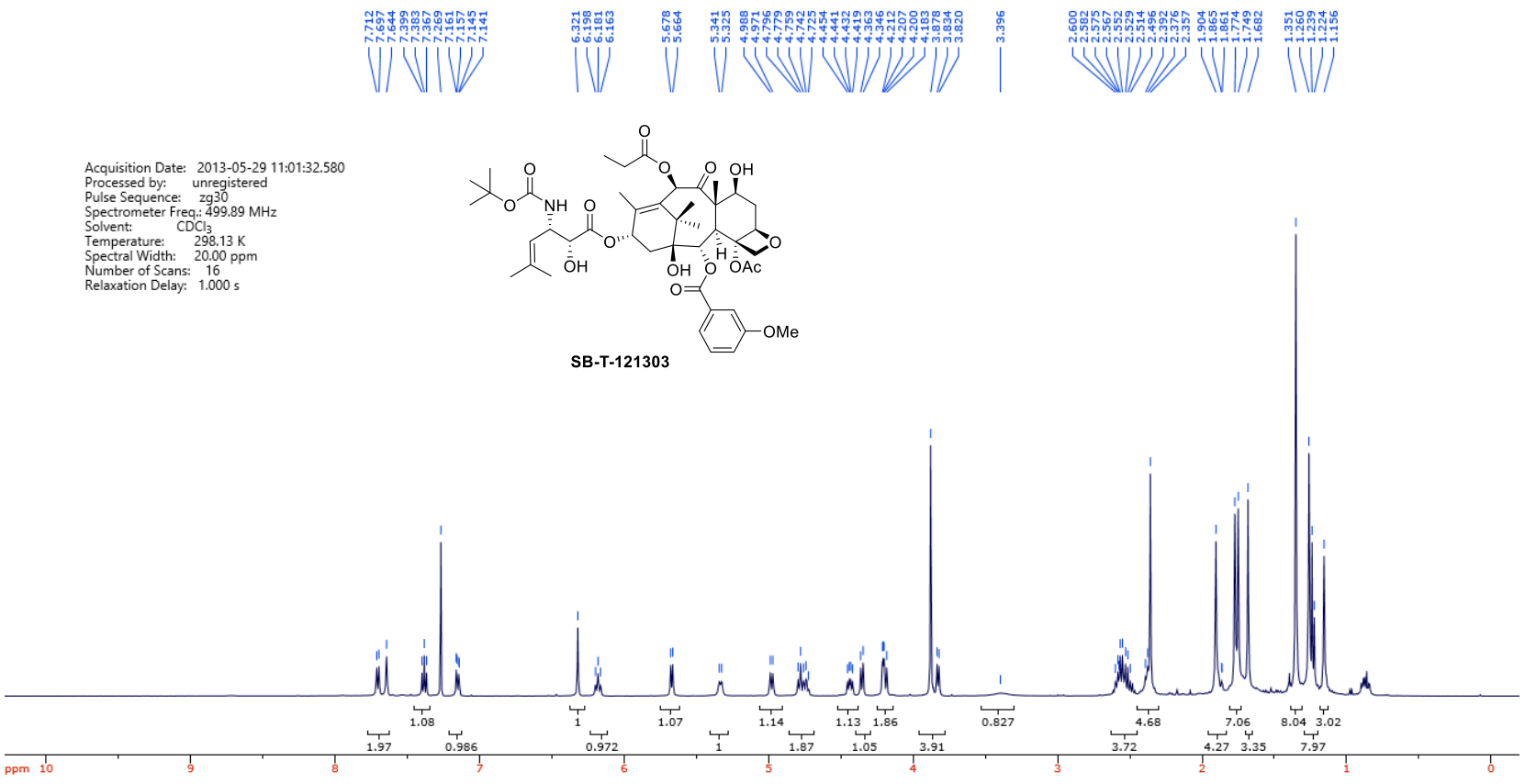
7.712
7.697
7.644
7.399
7.383
7.367
7.169
7.161
7.157
7.145
7.141
6.321
6.198
6.181
6.163
5.678
5.664
5.341
5.325
4.988
4.971
4.796
4.779
4.759
4.742
4.725
4.454
4.441
4.432
4.419
4.363
4.346
4.212
4.207
4.200
4.183
3.878
3.834
3.820
3.396
2.600
2.582
2.575
2.567
2.552
2.529
2.514
2.496
2.392
2.376
2.357
1.904
1.865
1.861
1.744
1.741
1.682
1.351
1.260
1.239
1.224
1.156
Acquisition Date: 2013-05-29 11:01:32.580
Processed by: unregistered
Pulse Sequence: zg30
Spectrometer Freq.: 499.89 MHz
Solvent: CDCl3
Temperature: 298.13 K
Spectral Width: 20.00 ppm
Number of Scans: 16
Relaxation Delay: 1.000 s
SB-T-121303
1.08
1
1.07
1.14
1.13
1.86
0.827
4.68
7.06
8.04
3.02
1.97
0.986
0.972
1
1.87
1.05
3.91
3.72
4.27
3.35
7.97
ppm 10
9
8
7
6
5
4
3
2
1
0

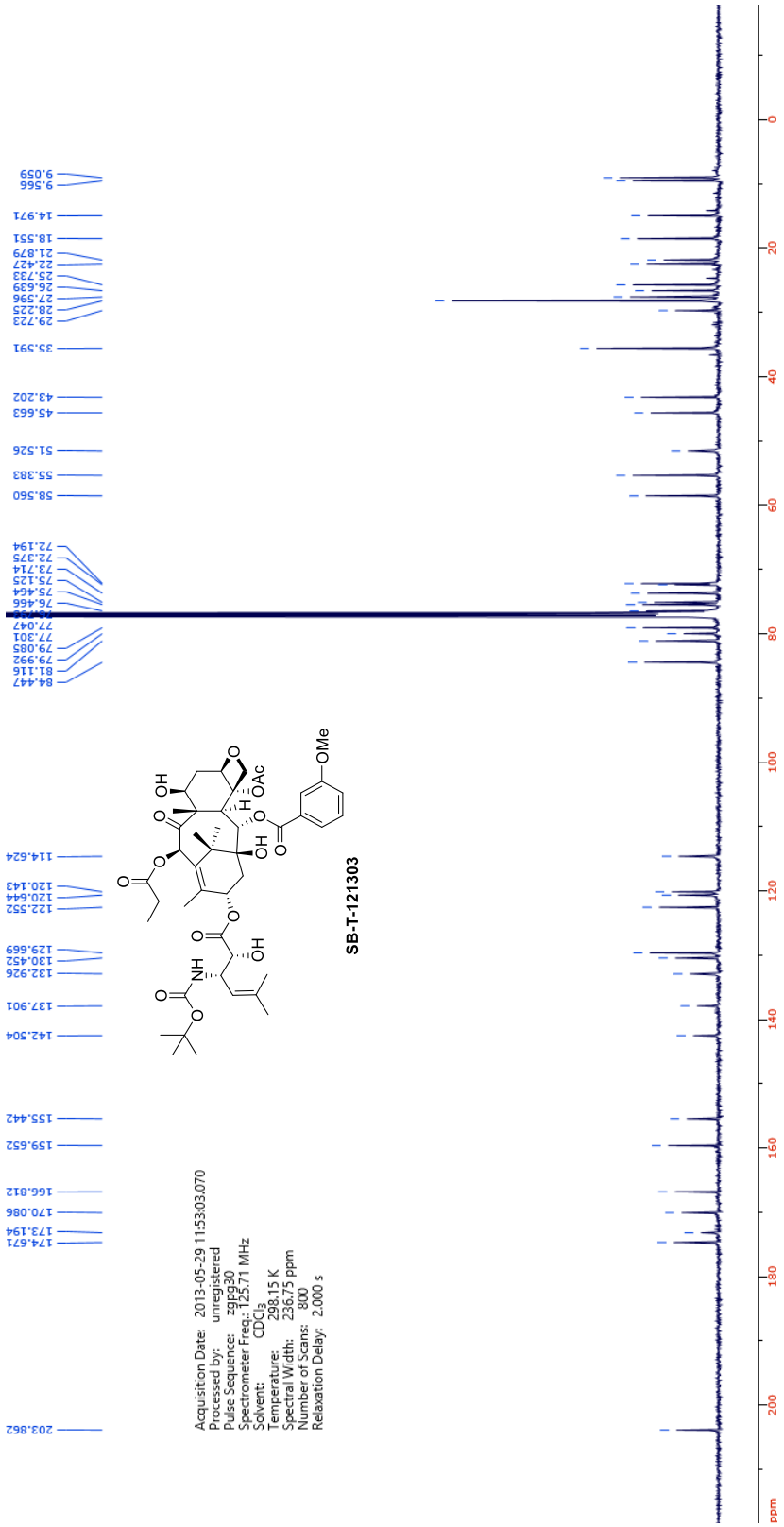
9.059
9.566
14.971
18.551
21.879
22.427
25.733
26.639
27.596
28.225
29.723
35.591
43.202
45.663
51.526
55.383
58.560
72.194
72.375
73.714
75.125
75.464
76.466
77.047
77.301
79.085
79.992
81.116
84.447
114.624
120.143
120.644
122.552
129.669
130.452
132.926
137.901
142.504
155.442
159.652
166.812
170.086
173.194
174.671
203.862
OMe
OAc
OH
NH
SB-T-121303
Acquisition Date: 2013-05-29 11:53:03.070
Processed by: unregistered
Pulse Sequence: zgpg30
Spectrometer Freq.: 125.71 MHz
Solvent: CDCl3
Temperature: 298.15 K
Spectral Width: 236.75 ppm
Number of Scans: 800
Relaxation Delay: 2.000 s
ppm

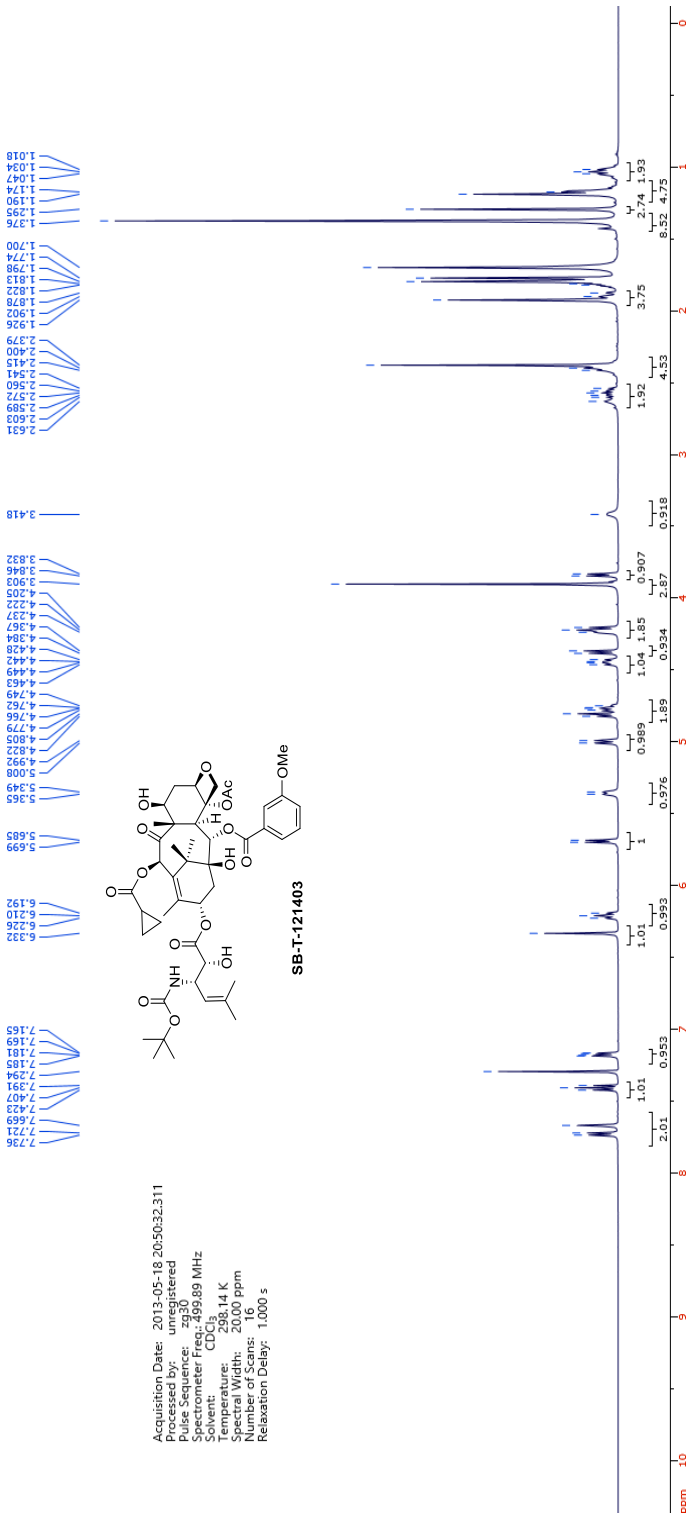
Acquisition Date: 2013-05-18 20:50:32.311
Processed by: unregistered
Pulse Sequence: zg30
Spectrometer Freq.: 499.89 MHz
Solvent: $CDCl_3$
Temperature: 298.14 K
Spectral Width: 20.00 ppm
Number of Scans: 16
Relaxation Delay: 1.000 s
SB-T-121403
ppm

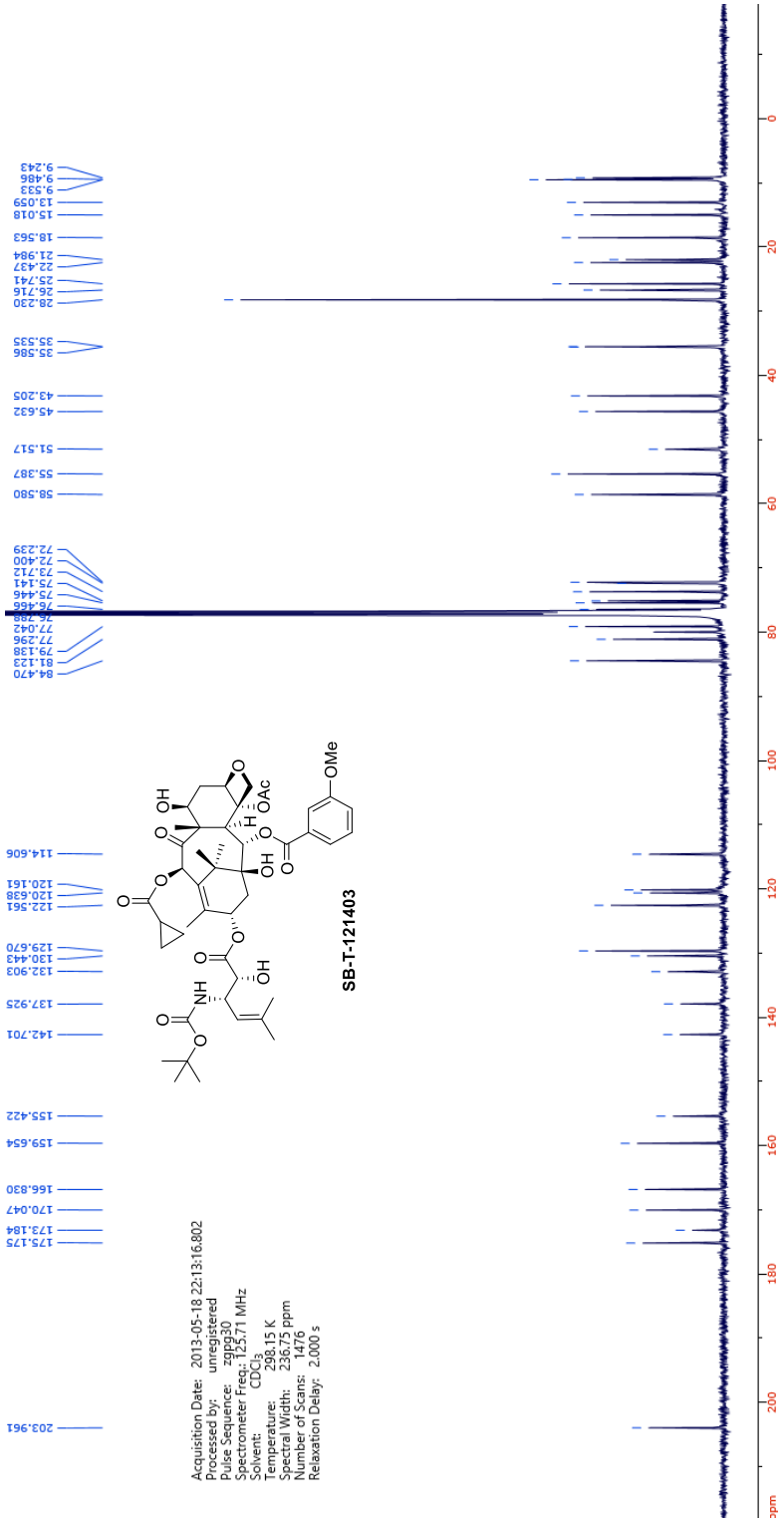
SB-T-121403
Acquisition Date: 2013-05-18 22:13:16.802
Processed by: unregistered
Pulse Sequence: zgpg30
Spectrometer Freq.: 125.71 MHz
Solvent: $CDCl_3$
Temperature: 298.15 K
Spectral Width: 236.75 ppm
Number of Scans: 1476
Relaxation Delay: 2.000 s

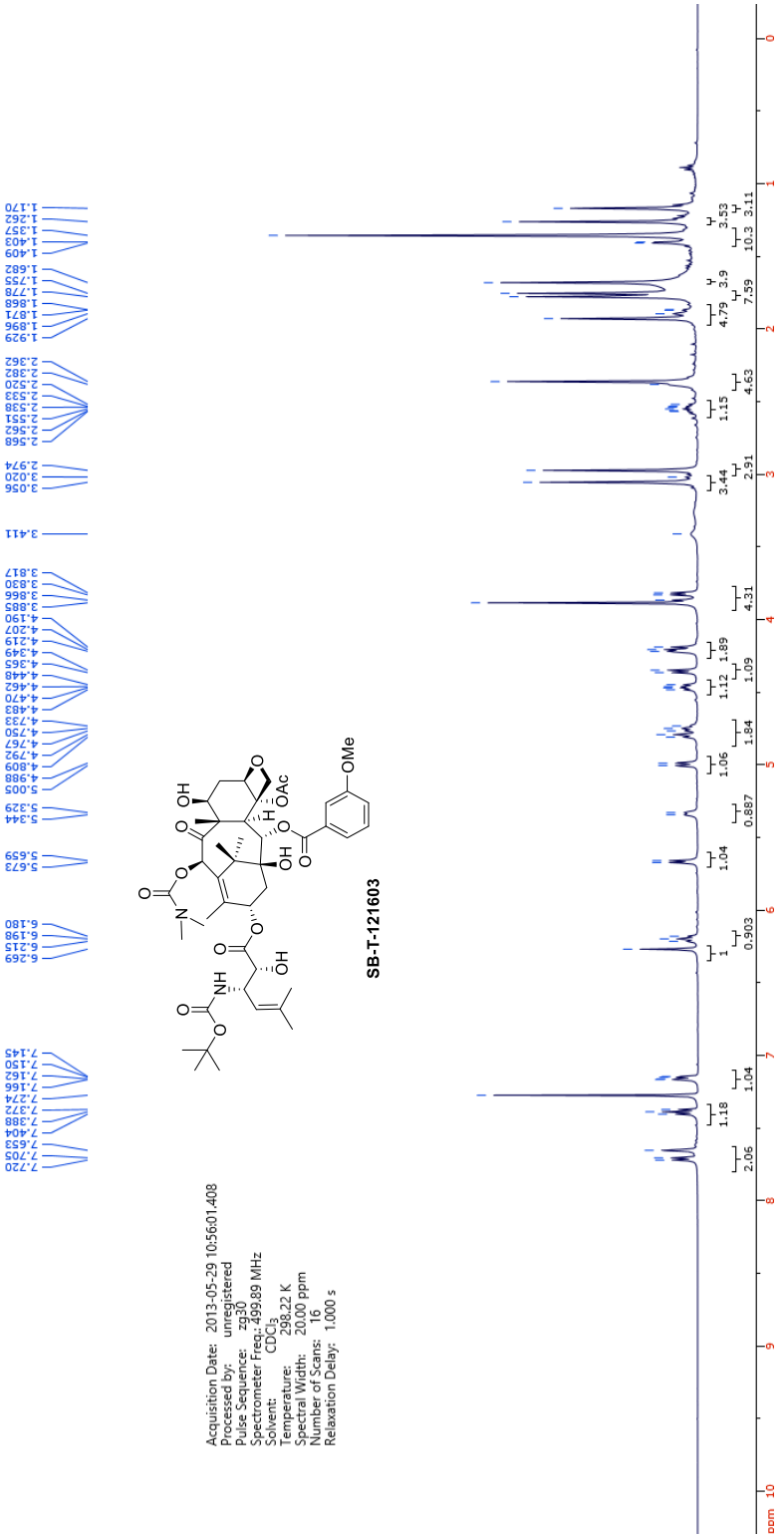
Acquisition Date: 2013-05-29 10:56:01.408
Processed by: unregistered
Pulse Sequence: zg30
Spectrometer Freq.: 499.89 MHz
Solvent: CDCl3
Temperature: 298.22 K
Spectral Width: 20.00 ppm
Number of Scans: 16
Relaxation Delay: 1.000 s
SB-T-121603
OMe
OAc
OH
NH
ppm

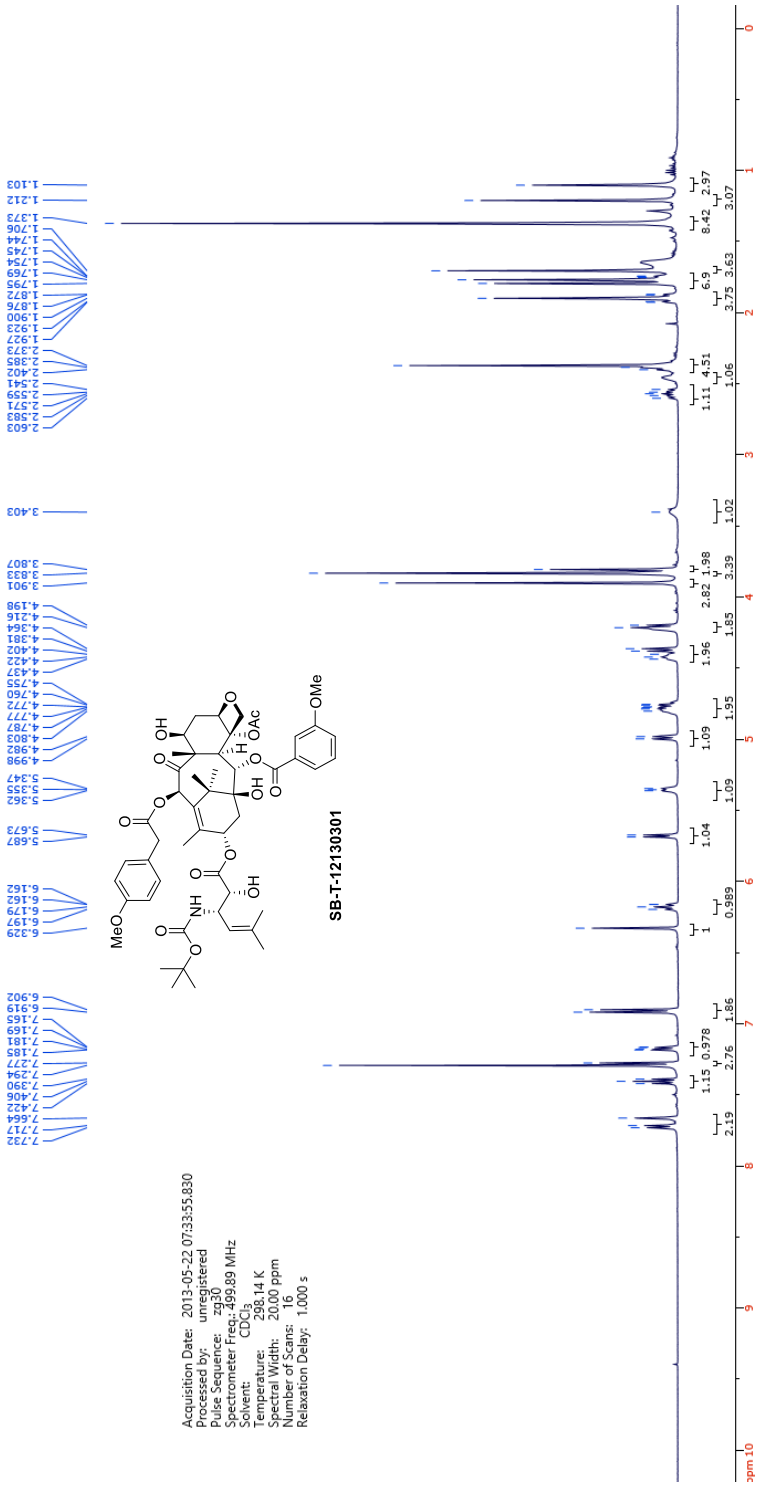
SB-T-12130301
Acquisition Date: 2013-05-22 07:33:55.830
Processed by: unregistered
Pulse Sequence: zg30
Spectrometer Freq.: 499.89 MHz
Solvent: $CDCl_3$
Temperature: 298.14 K
Spectral Width: 20.00 ppm
Number of Scans: 16
Relaxation Delay: 1.000 s

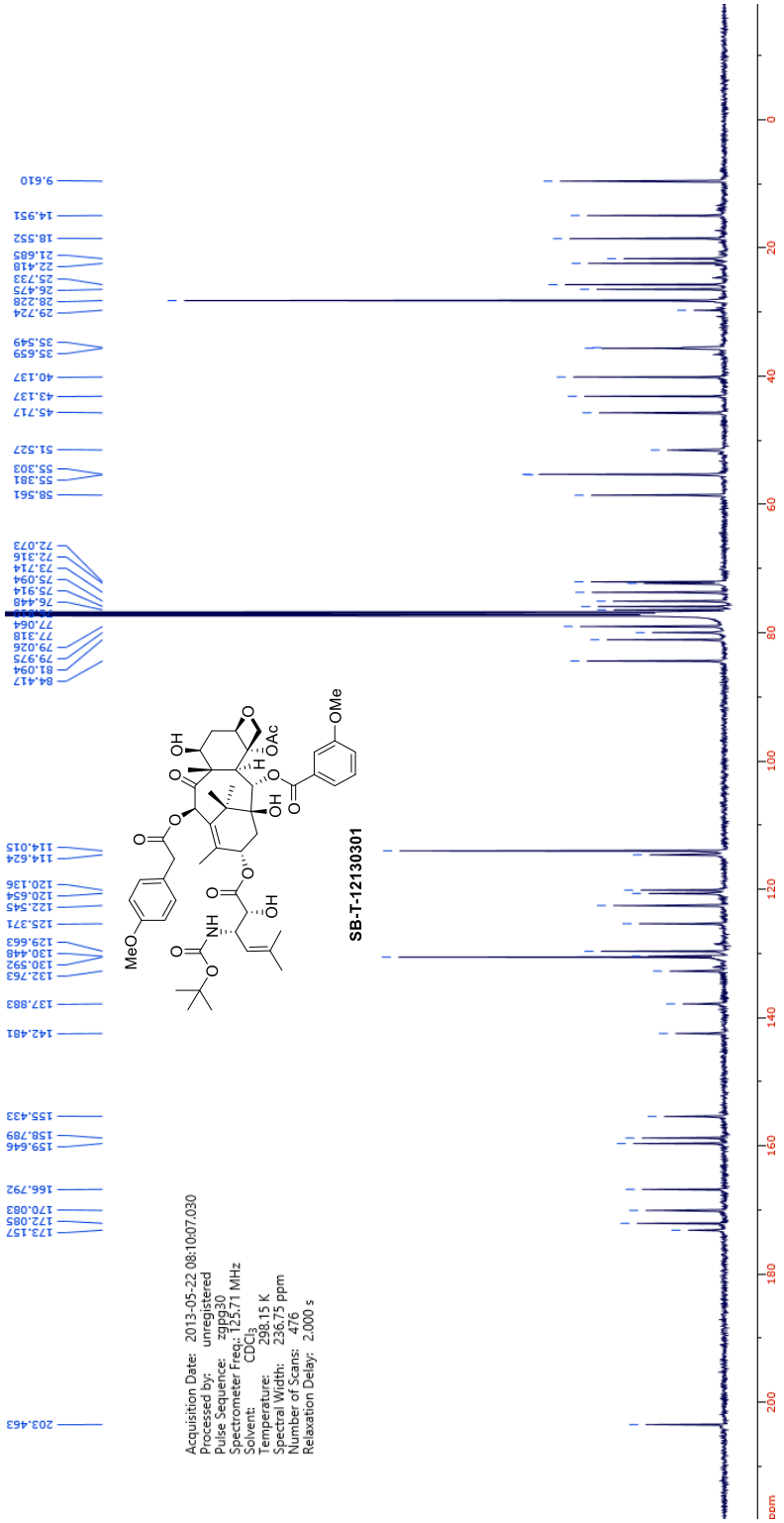
SB-T-12130301
Acquisition Date: 2013-05-22 08:10:07.030
Processed by: unregistered
Pulse Sequence: zgpg30
Spectrometer Freq.: 125.71 MHz
Solvent: $CDCl_3$
Temperature: 298.15 K
Spectral Width: 236.75 ppm
Number of Scans: 476
Relaxation Delay: 2.000 s

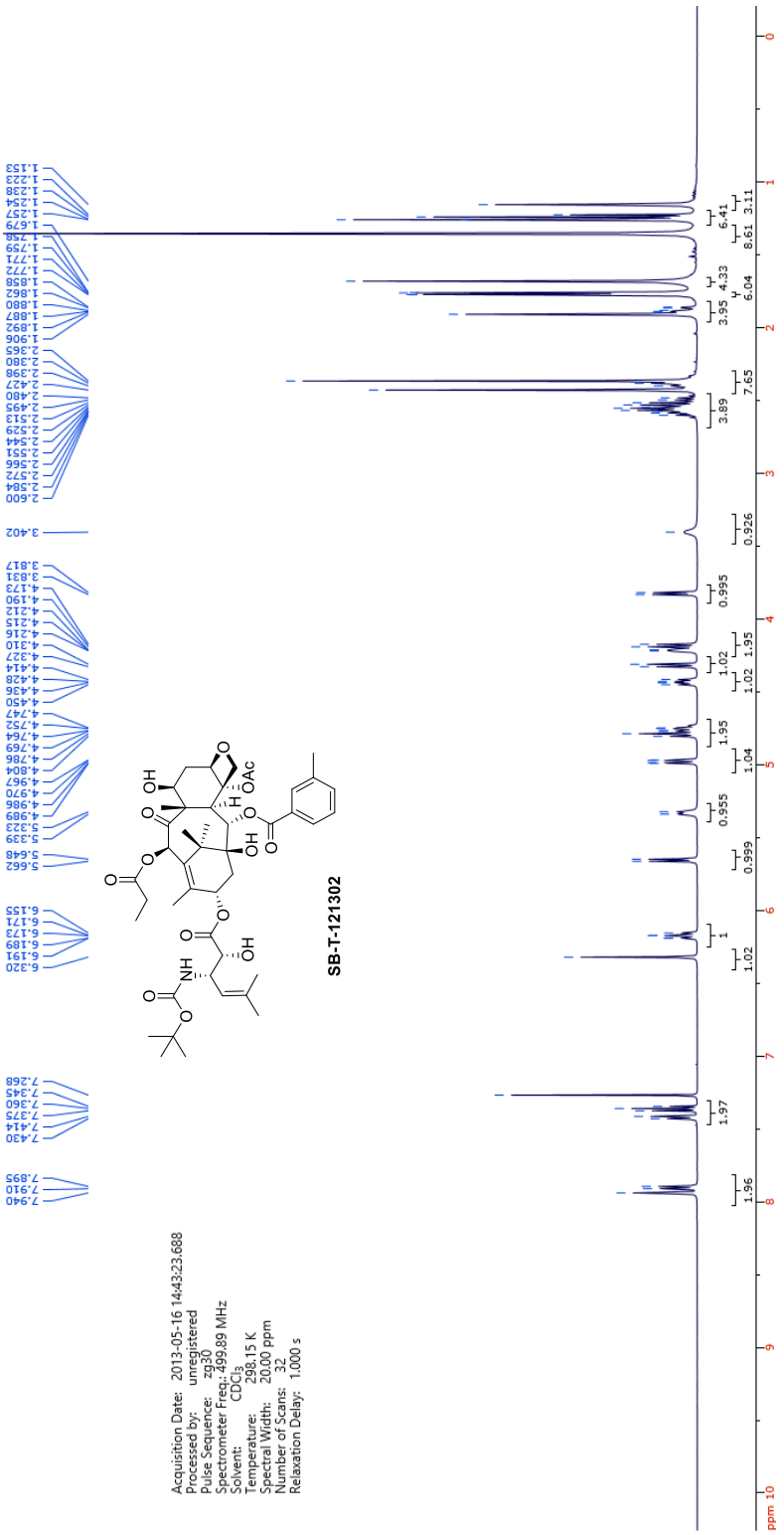
SB-T-121302
Acquisition Date: 2013-05-16 14:43:23.688
Processed by: unregistered
Pulse Sequence: zg30
Spectrometer Freq.: 499.89 MHz
Solvent: $CDCl_3$
Temperature: 298.15 K
Spectral Width: 20.00 ppm
Number of Scans: 32
Relaxation Delay: 1.000 s
ppm 10

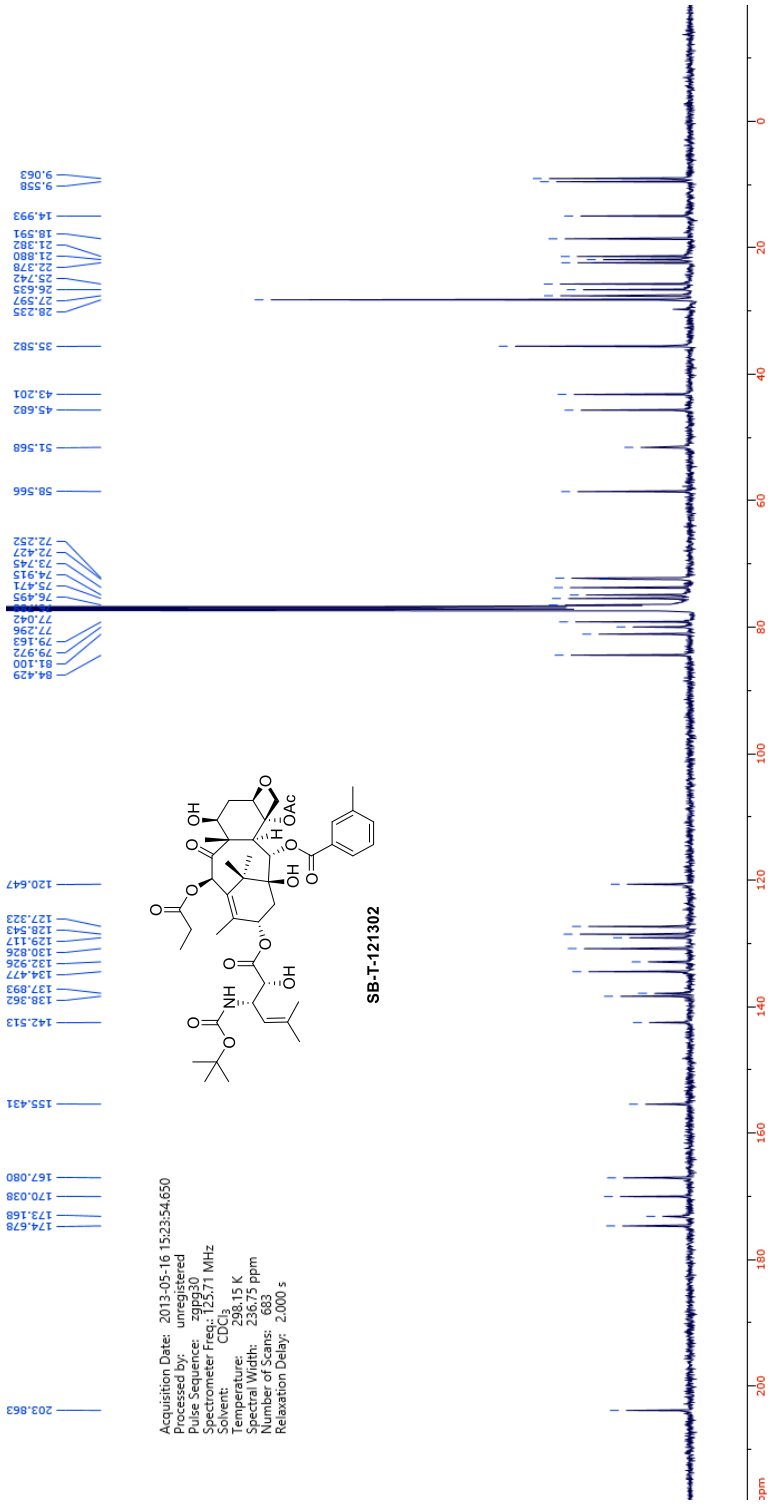
9.063
9.558
14.993
18.591
21.382
21.880
22.378
25.742
26.635
27.597
28.235
35.582
43.201
45.682
51.568
58.566
72.252
72.427
73.745
74.915
75.471
76.495
77.042
77.296
79.163
79.972
81.100
84.429
120.647
127.323
128.543
129.117
130.826
132.926
134.477
137.893
138.362
142.513
155.431
167.080
170.038
173.168
174.678
203.863
OH
O
OAc
H
O
OH
O
O
O
NH
O
O
OH
SB-T-121302
Acquisition Date: 2013-05-16 15:23:54.650
Processed by: unregistered
Pulse Sequence: zgpg30
Spectrometer Freq.: 125.71 MHz
Solvent: CDCl3
Temperature: 298.15 K
Spectral Width: 236.75 ppm
Number of Scans: 683
Relaxation Delay: 2.000 s
0
20
40
60
80
100
120
140
160
180
200
ppm

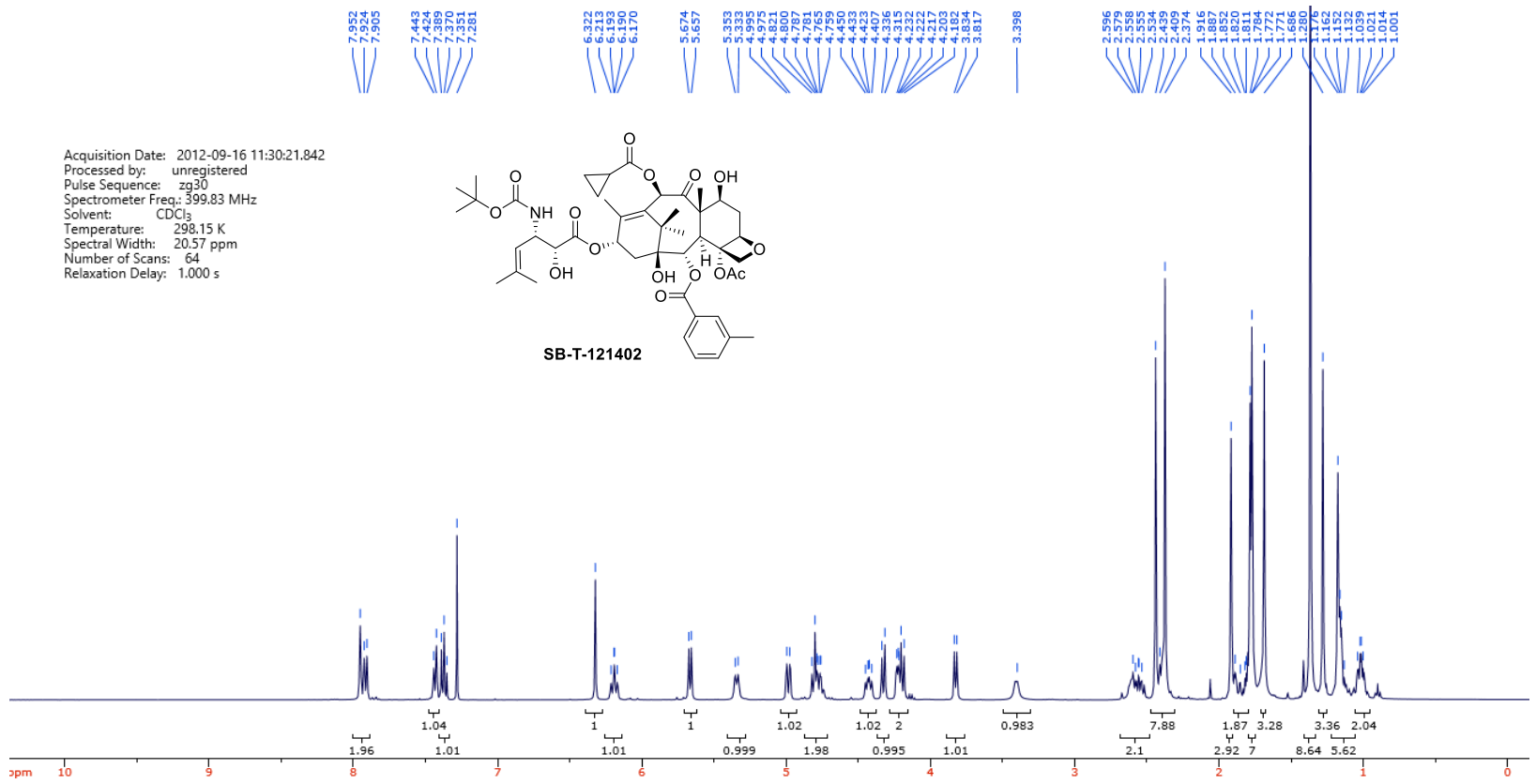
Acquisition Date: 2012-09-16 11:30:21.842
Processed by: unregistered
Pulse Sequence: zg30
Spectrometer Freq.: 399.83 MHz
Solvent: CDCl3
Temperature: 298.15 K
Spectral Width: 20.57 ppm
Number of Scans: 64
Relaxation Delay: 1.000 s
SB-T-121402
7.952 7.924 7.905 7.443 7.424 7.389 7.370 7.351 7.281 6.322 6.213 6.193 6.190 6.170 5.674 5.657 5.353 5.333 4.995 4.975 4.821 4.800 4.787 4.781 4.765 4.759 4.450 4.433 4.423 4.407 4.336 4.315 4.232 4.222 4.217 4.203 4.182 3.834 3.817 3.398 2.596 2.579 2.558 2.555 2.534 2.439 2.409 2.374 1.916 1.887 1.852 1.810 1.811 1.784 1.772 1.771 1.686 1.280 1.176 1.162 1.152 1.132 1.039 1.021 1.014 1.001
1.96 1.04 1.01 1 1.01 1 0.999 1.02 1.98 1.02 2 0.995 1.01 0.983 2.1 7.88 1.87 2.92 3.28 7 3.36 8.64 2.04 5.62
ppm 10 9 8 7 6 5 4 3 2 1 0

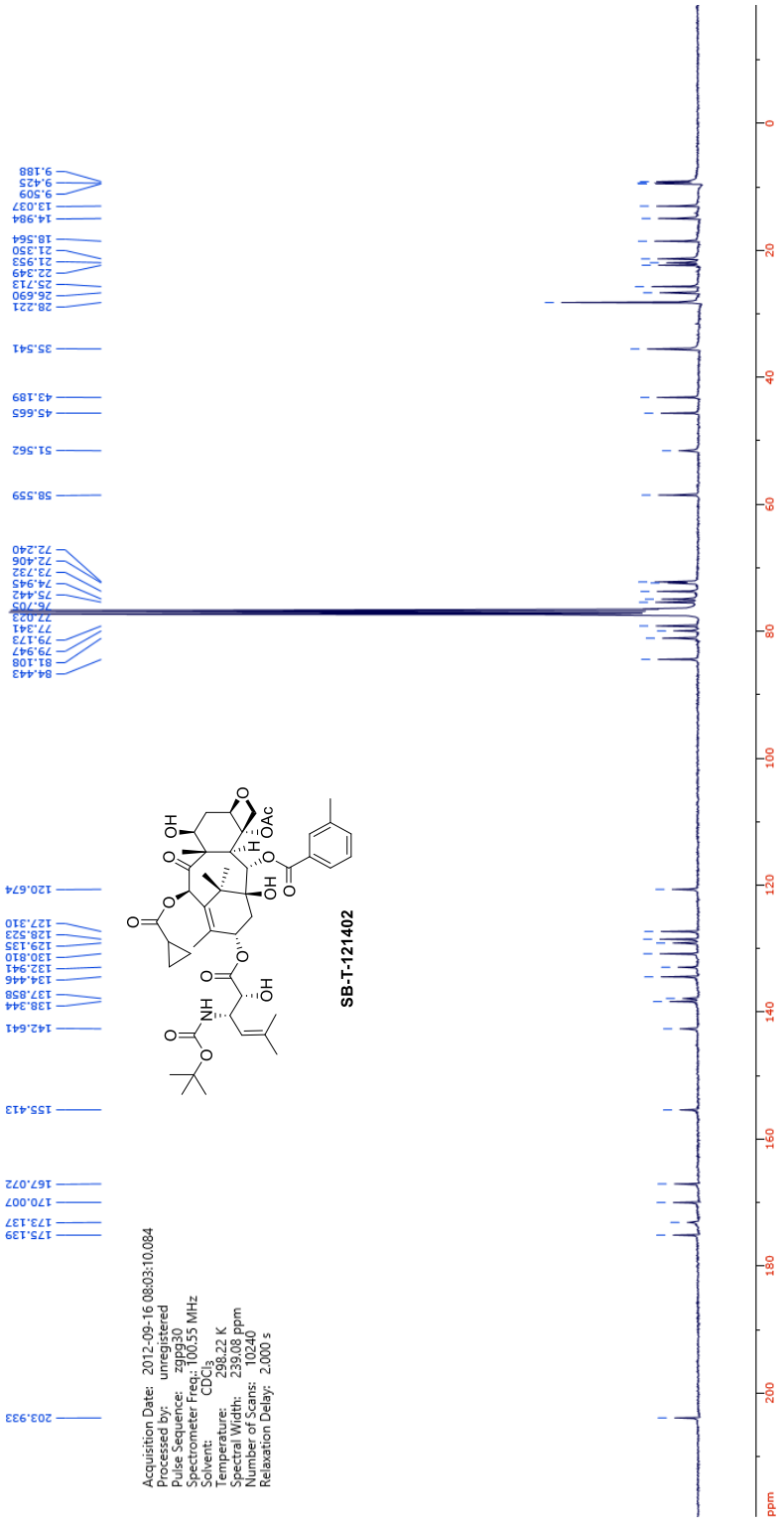
SB-T-121402
Acquisition Date: 2012-09-16 08:03:10.084
Processed by: unregistered
Pulse Sequence: zgpg30
Spectrometer Freq.: 100.55 MHz
Solvent: CDCl3
Temperature: 298.22 K
Spectral Width: 239.08 ppm
Number of Scans: 10240
Relaxation Delay: 2.000 s
ppm

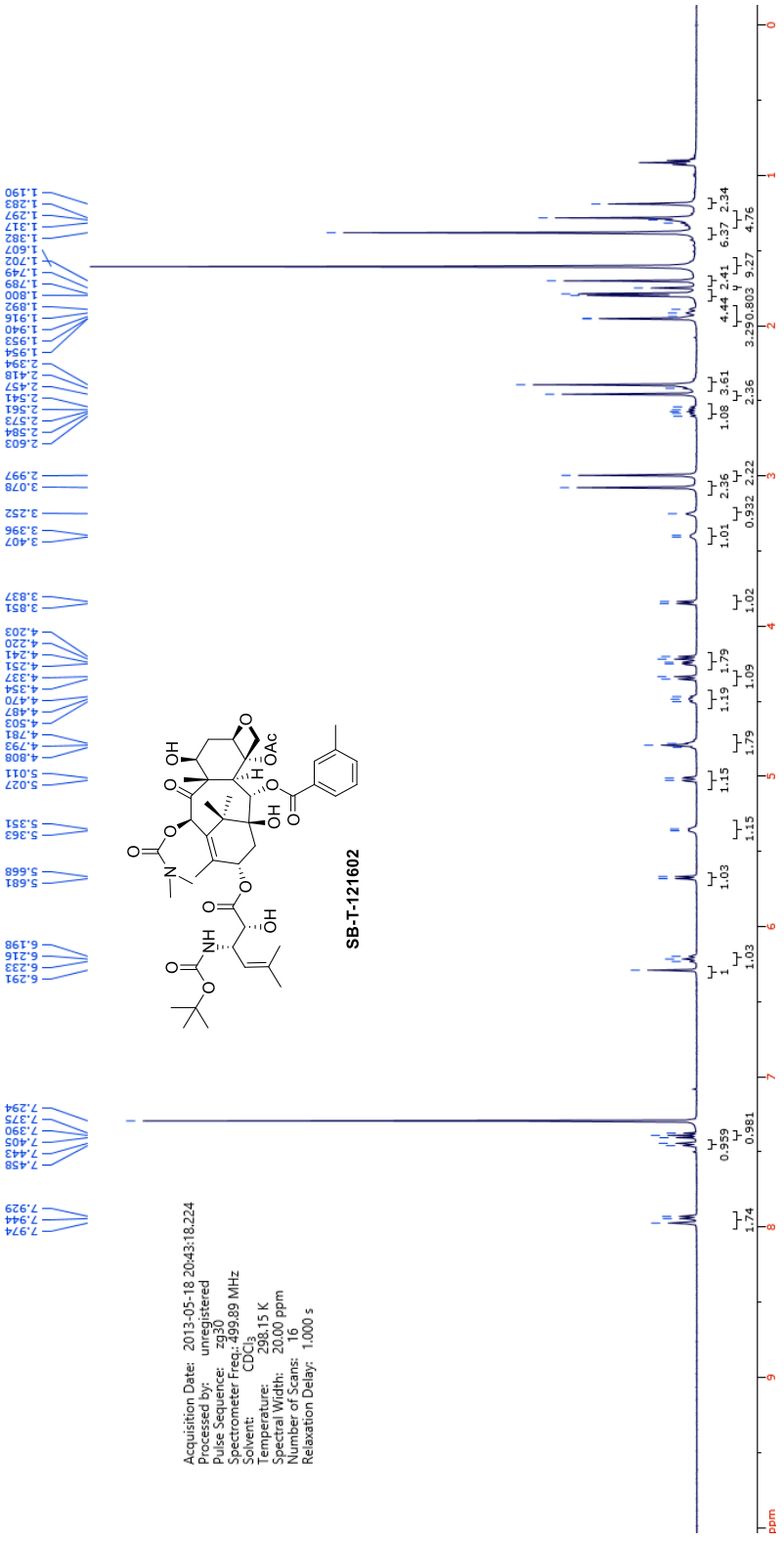
SB-T-121602
Acquisition Date: 2013-05-18 20:43:18.224
Processed by: unregistered
Pulse Sequence: zg30
Spectrometer Freq.: 499.89 MHz
Solvent: CDCl3
Temperature: 298.15 K
Spectral Width: 20.00 ppm
Number of Scans: 16
Relaxation Delay: 1.000 s
ppm

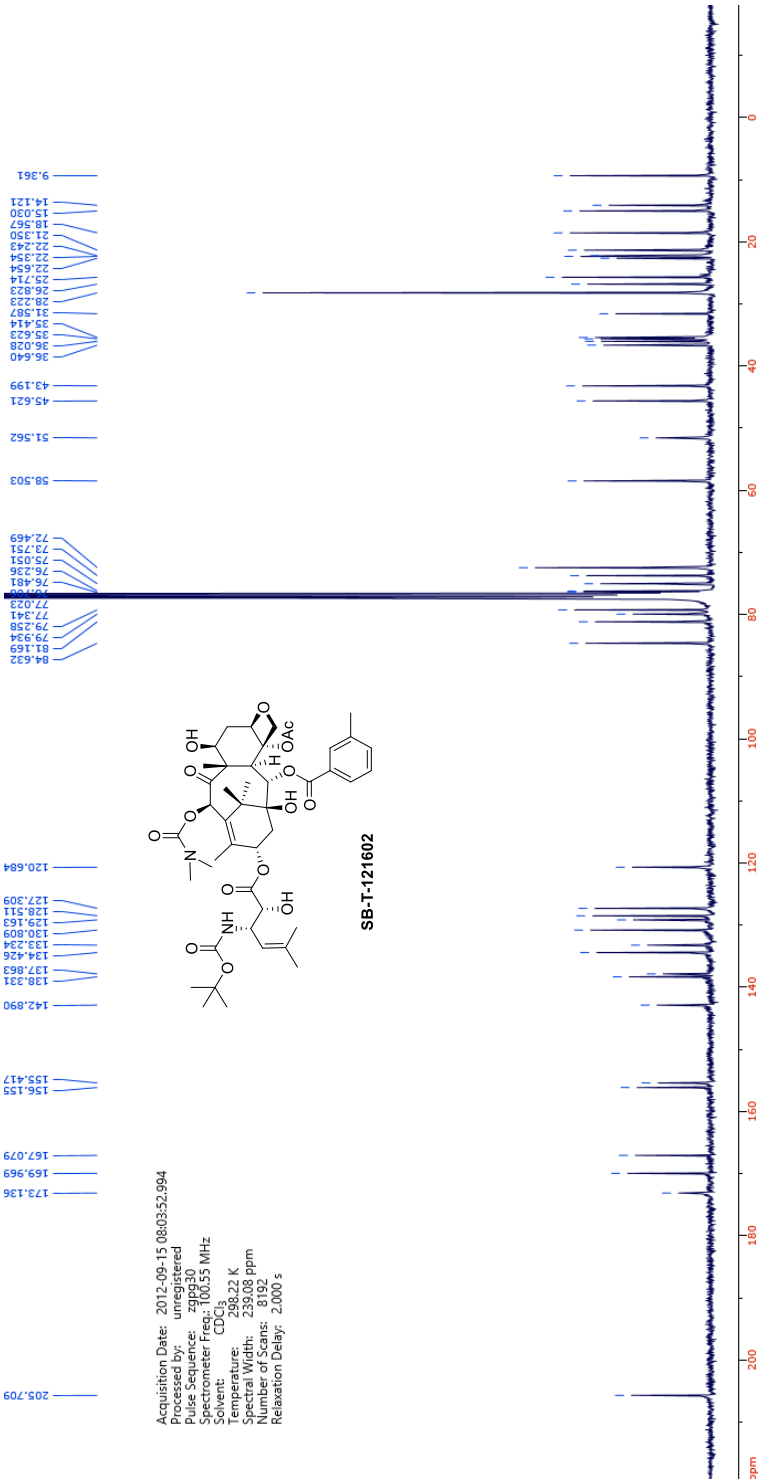
SB-T-121602
Acquisition Date: 2012-09-15 08:03:52.994
Processed by: unregistered
Pulse Sequence: zgpg30
Spectrometer Freq.: 100.55 MHz
Solvent: $CDCl_3$
Temperature: 298.22 K
Spectral Width: 239.08 ppm
Number of Scans: 8192
Relaxation Delay: 2.000 s

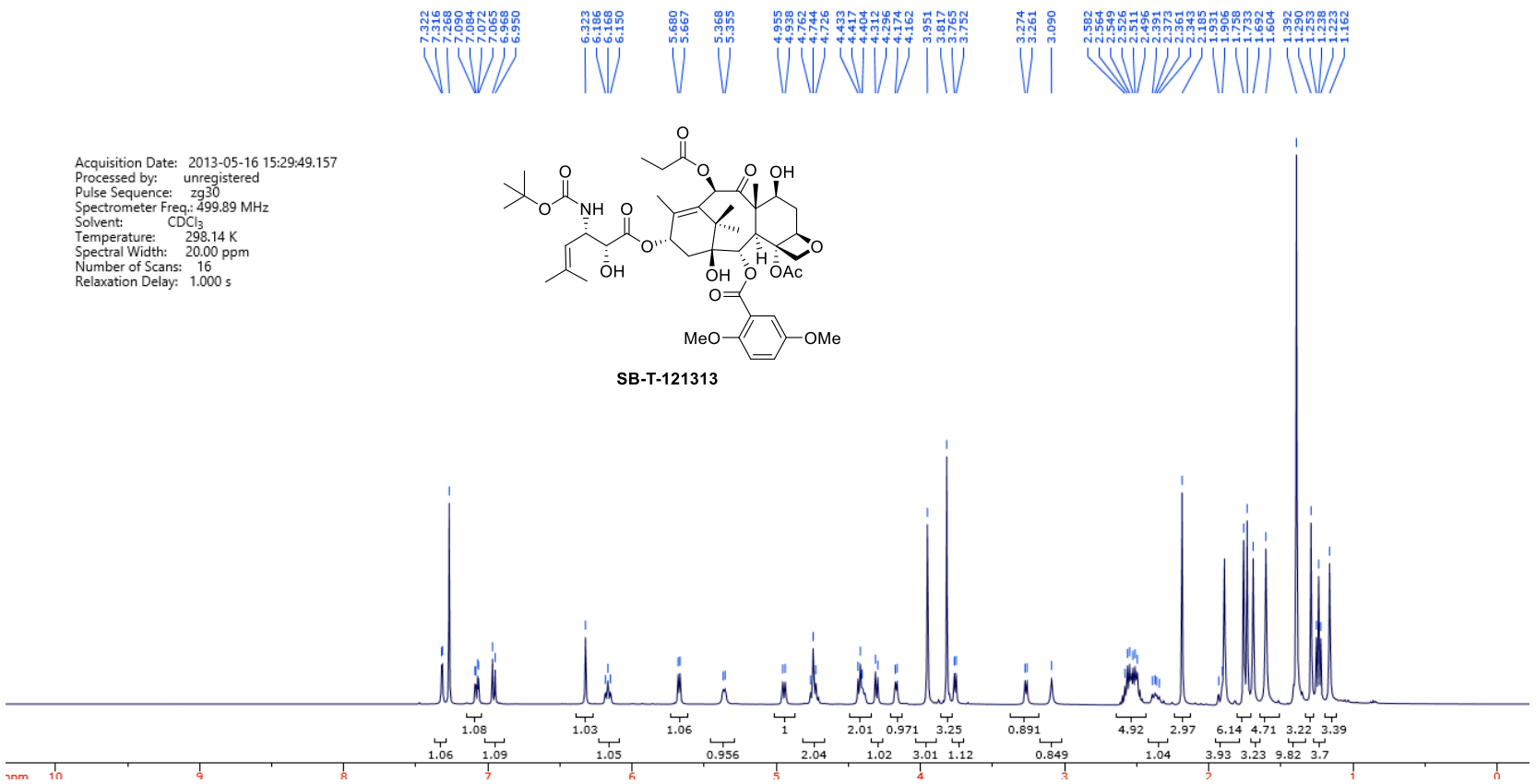
7.322
7.316
7.268
7.090
7.084
7.072
7.065
6.968
6.950
6.323
6.186
6.168
6.150
5.680
5.667
5.368
5.355
4.955
4.938
4.762
4.744
4.726
4.433
4.417
4.404
4.312
4.296
4.174
4.162
3.951
3.817
3.765
3.752
3.274
3.261
3.090
2.582
2.564
2.549
2.526
2.511
2.496
2.391
2.373
2.361
2.343
2.185
1.931
1.906
1.758
1.733
1.692
1.604
1.392
1.290
1.253
1.238
1.223
1.162
Acquisition Date: 2013-05-16 15:29:49.157
Processed by: unregistered
Pulse Sequence: zg30
Spectrometer Freq.: 499.89 MHz
Solvent: CDCl3
Temperature: 298.14 K
Spectral Width: 20.00 ppm
Number of Scans: 16
Relaxation Delay: 1.000 s
SB-T-121313
1.06
1.08
1.09
1.03
1.05
1.06
0.956
1
2.04
2.01
1.02
0.971
3.01
3.25
1.12
0.891
0.849
4.92
1.04
2.97
6.14
3.93
4.71
3.23
3.22
9.82
3.39
3.7
ppm

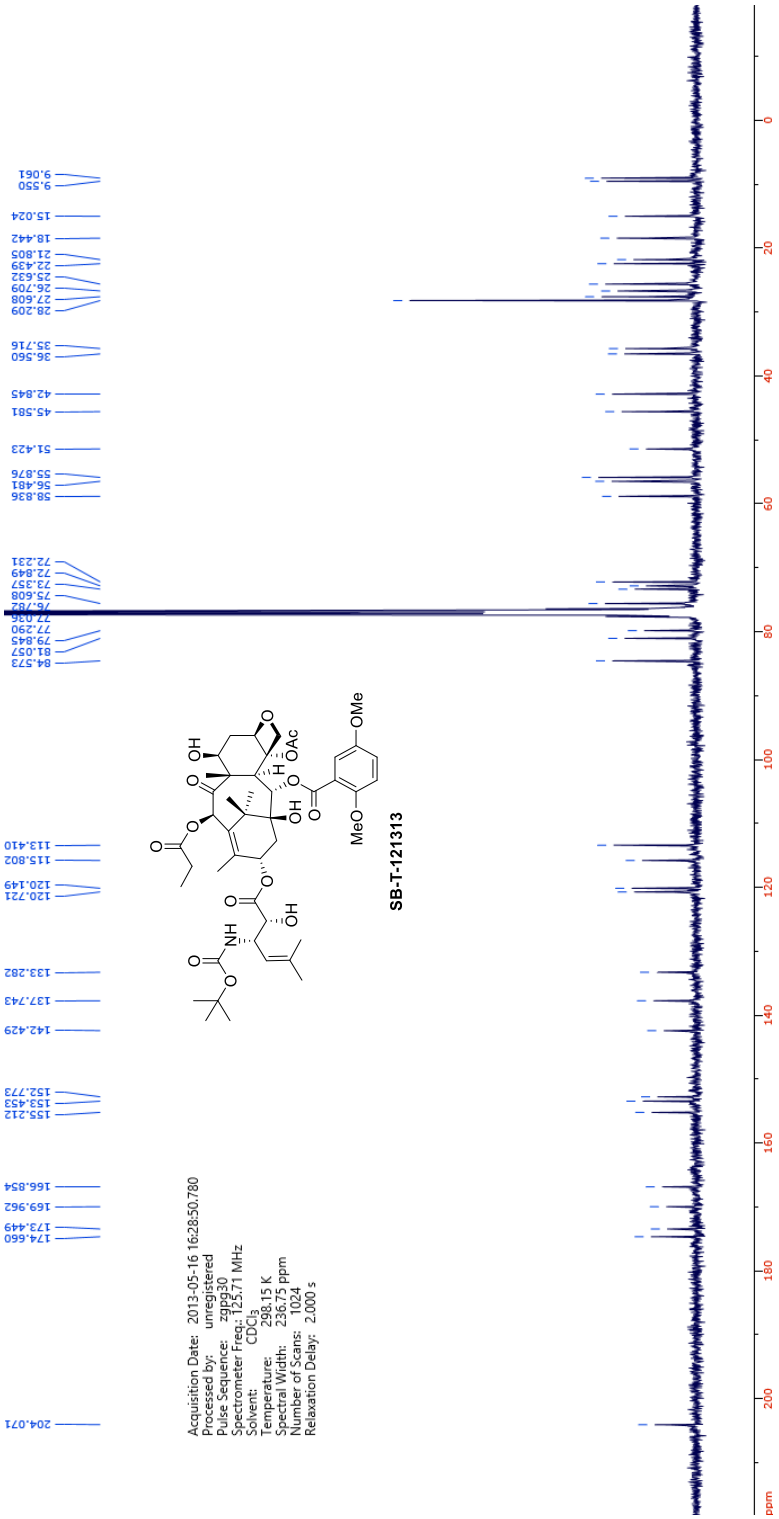
9.061
9.550
15.024
18.442
21.805
22.439
25.632
26.709
27.608
28.209
35.716
36.560
42.845
45.581
51.423
55.876
56.481
58.836
72.231
73.357
73.849
75.608
76.782
77.036
77.290
79.845
81.057
84.573
113.410
115.802
120.149
120.721
133.282
137.743
142.429
152.773
153.453
155.212
166.854
169.962
173.449
174.660
204.071
Acquisition Date: 2013-05-16 16:28:50.780
Processed by: unregistered
Pulse Sequence: zgpg30
Spectrometer Freq.: 125.71 MHz
Solvent: $CDCl_3$
Temperature: 298.15 K
Spectral Width: 236.75 ppm
Number of Scans: 1024
Relaxation Delay: 2.000 s
SB-T-121313
ppm

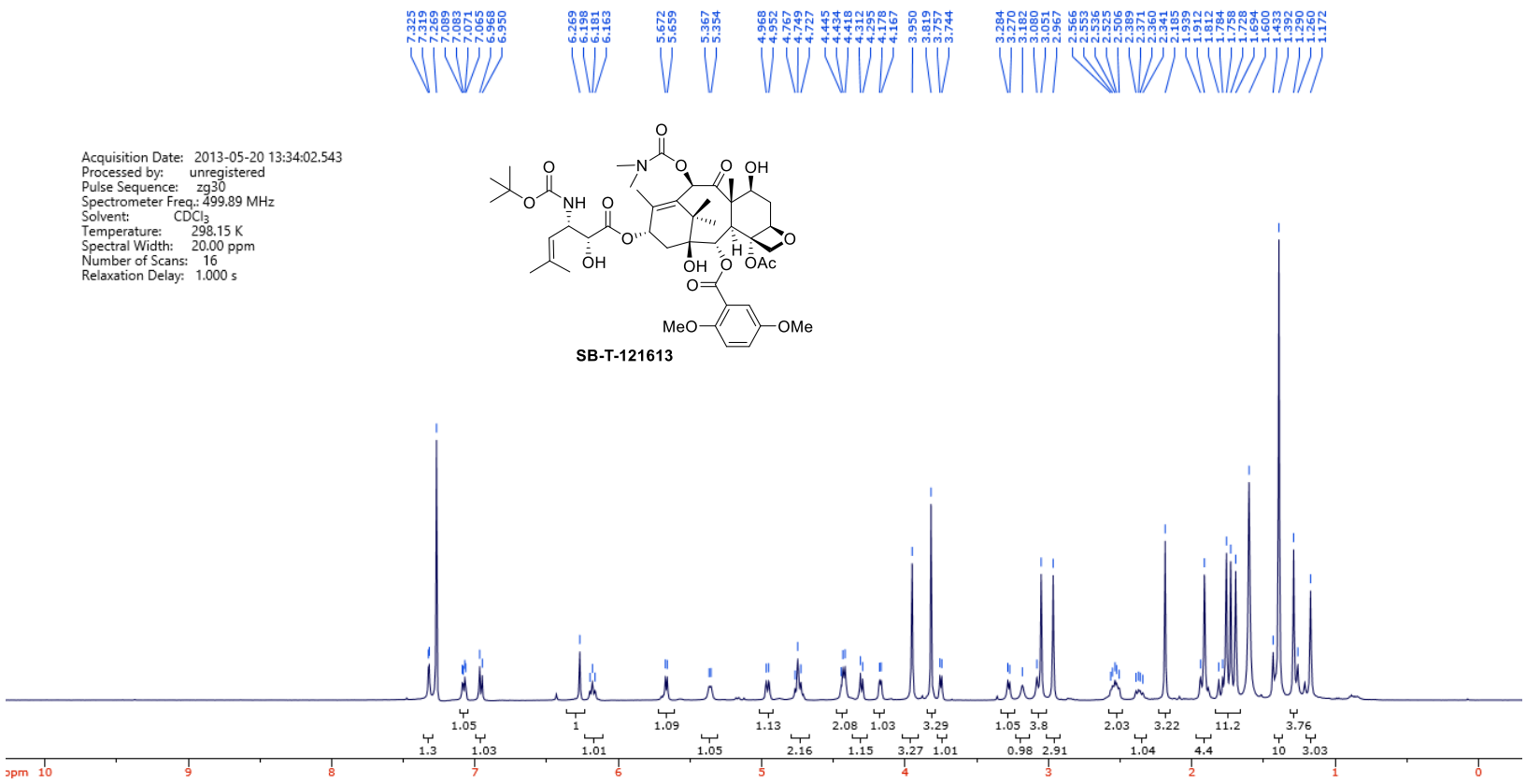
7.325
7.319
7.289
7.089
7.083
7.071
7.065
6.968
6.950
6.269
6.198
6.181
6.163
5.672
5.659
5.367
5.354
4.968
4.952
4.767
4.749
4.727
4.445
4.434
4.418
4.312
4.295
4.178
4.167
3.950
3.819
3.757
3.744
3.284
3.270
3.182
3.100
3.051
2.967
2.566
2.553
2.536
2.525
2.506
2.389
2.371
2.360
2.341
2.185
1.939
1.912
1.812
1.784
1.758
1.728
1.694
1.600
1.433
1.392
1.290
1.250
1.172
Acquisition Date: 2013-05-20 13:34:02.543
Processed by: unregistered
Pulse Sequence: zg30
Spectrometer Freq.: 499.89 MHz
Solvent: CDCl3
Temperature: 298.15 K
Spectral Width: 20.00 ppm
Number of Scans: 16
Relaxation Delay: 1.000 s
SB-T-121613
1.05
1
1.09
1.13
2.08
1.03
3.29
1.05
3.8
2.03
3.22
11.2
3.76
1.3
1.03
1.01
1.05
2.16
1.15
3.27
1.01
0.98
2.91
1.04
4.4
10
3.03
ppm
10
9
8
7
6
5
4
3
2
1
0

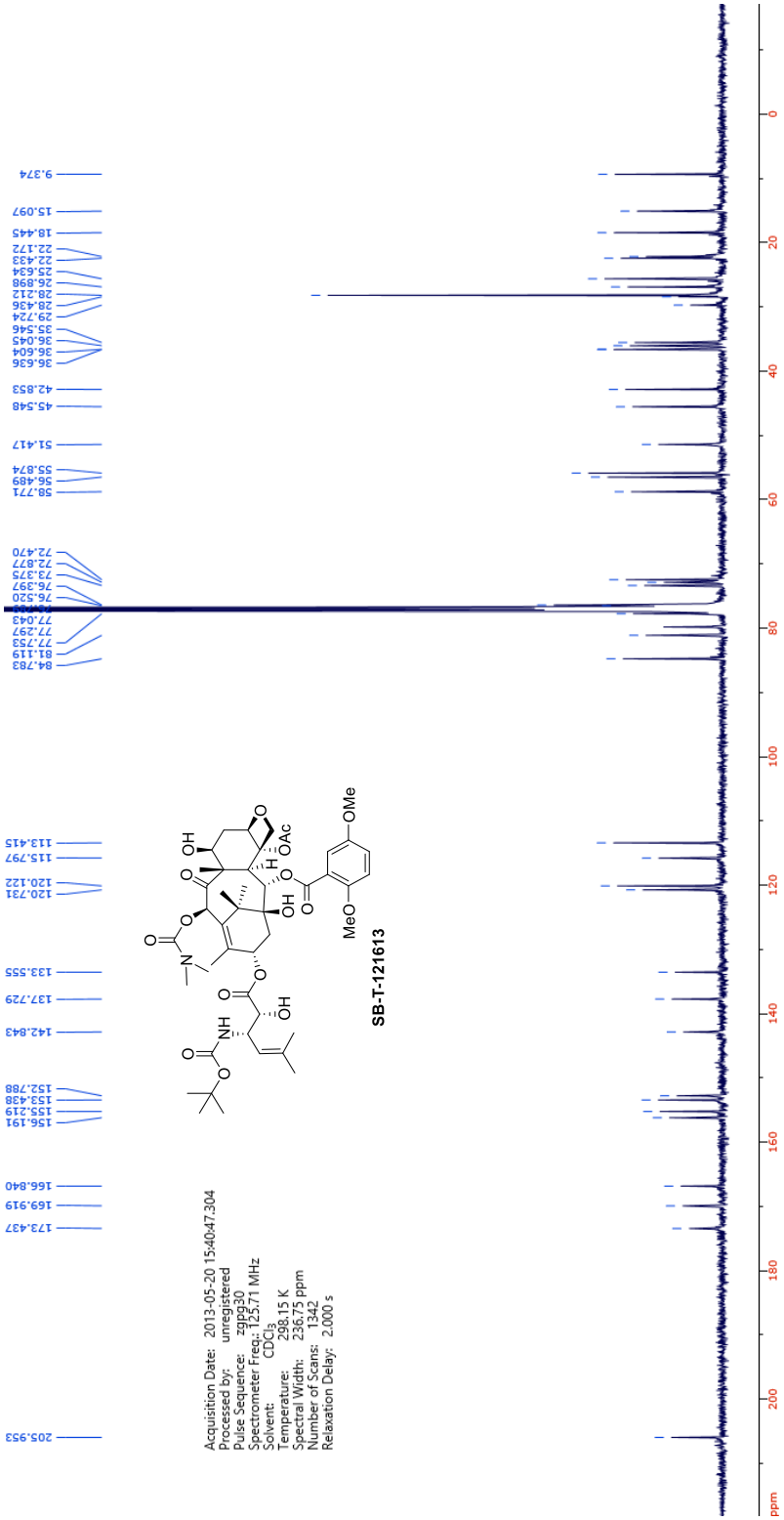
9.374
15.097
18.445
22.172
22.433
25.634
26.898
28.212
28.436
29.724
35.546
36.045
36.604
36.636
42.853
45.548
51.417
55.874
56.489
58.771
72.470
72.877
73.375
76.397
76.520
77.043
77.297
77.753
81.119
84.783
113.415
115.797
120.122
120.731
133.555
137.729
142.843
152.788
153.438
155.219
156.191
166.840
169.919
173.437
205.953
ppm
0
20
40
60
80
100
120
140
160
180
200
SB-T-121613
Acquisition Date: 2013-05-20 15:40:47.304
Processed by: unregistered
Pulse Sequence: zgpg30
Spectrometer Freq.: 125.71 MHz
Solvent: CDCl3
Temperature: 298.15 K
Spectral Width: 236.75 ppm
Number of Scans: 1342
Relaxation Delay: 2.000 s

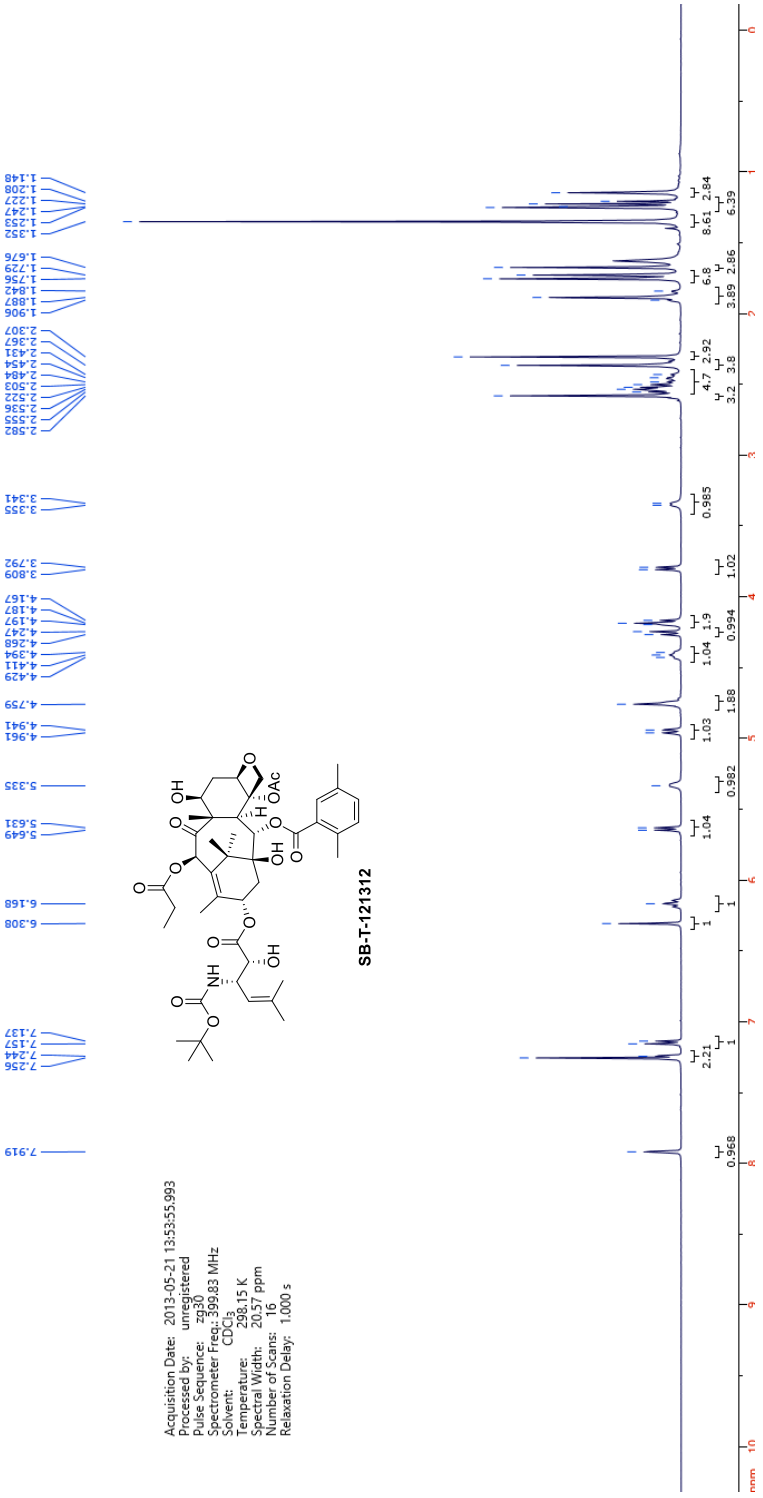
SB-T-121312
Acquisition Date: 2013-05-21 13:53:55.993
Processed by: unregistered
Pulse Sequence: zg30
Spectrometer Freq.: 399.83 MHz
Solvent: CDCl3
Temperature: 298.15 K
Spectral Width: 20.57 ppm
Number of Scans: 16
Relaxation Delay: 1.000 s

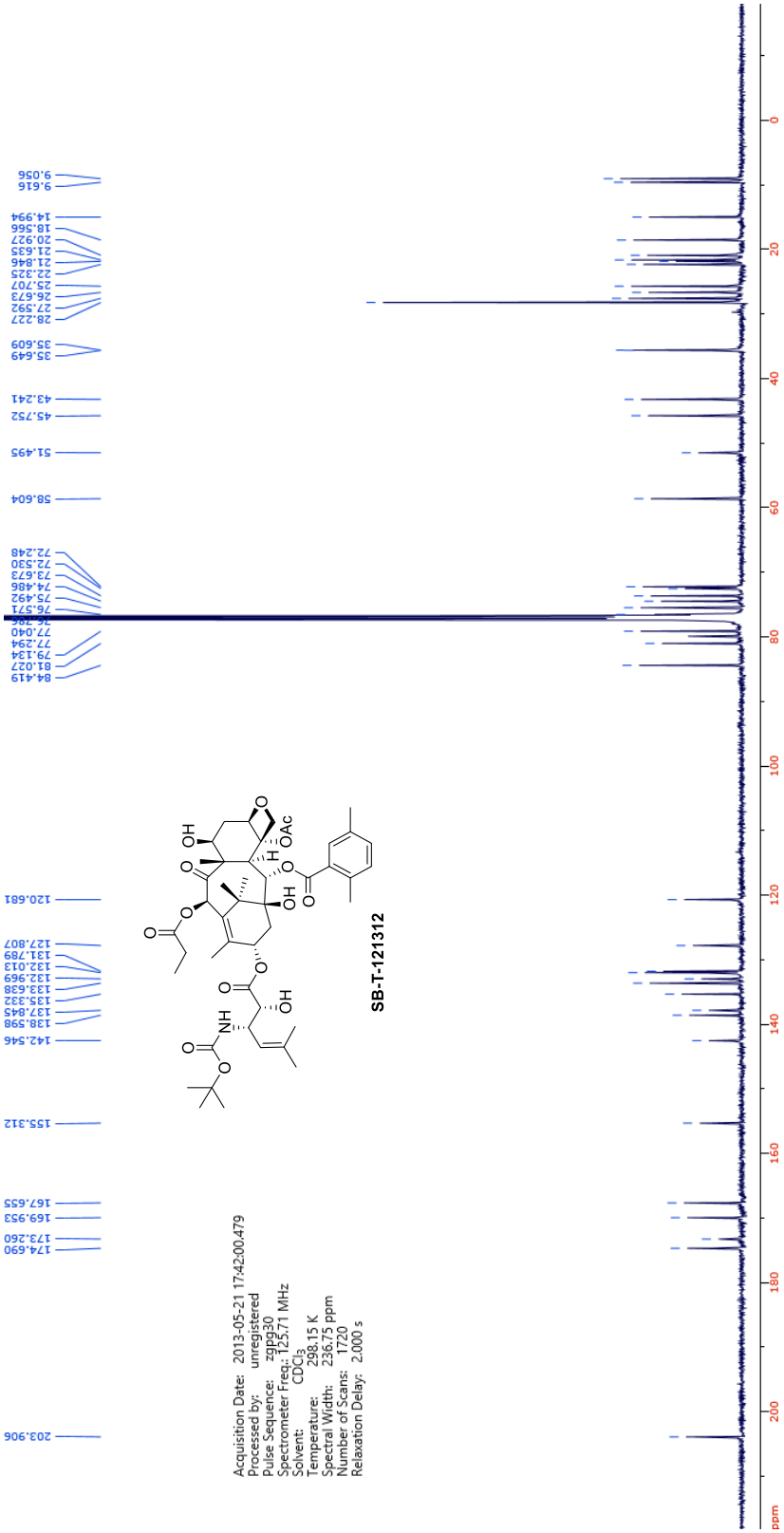
9.056
9.616
14.994
18.566
20.927
21.635
21.846
22.325
25.707
26.673
27.392
28.227
35.609
35.649
43.241
45.752
51.495
58.604
72.248
72.530
73.673
74.486
75.492
76.571
76.796
77.040
77.294
79.134
81.027
84.419
120.681
127.807
131.789
132.013
132.969
133.638
135.332
137.845
138.598
142.546
155.312
167.655
169.953
173.260
174.690
203.906
SB-T-121312
Acquisition Date: 2013-05-21 17:42:00.479
Processed by: unregistered
Pulse Sequence: zgpg30
Spectrometer Freq.: 125.71 MHz
Solvent: CDCl3
Temperature: 298.15 K
Spectral Width: 236.75 ppm
Number of Scans: 1720
Relaxation Delay: 2.000 s
ppm

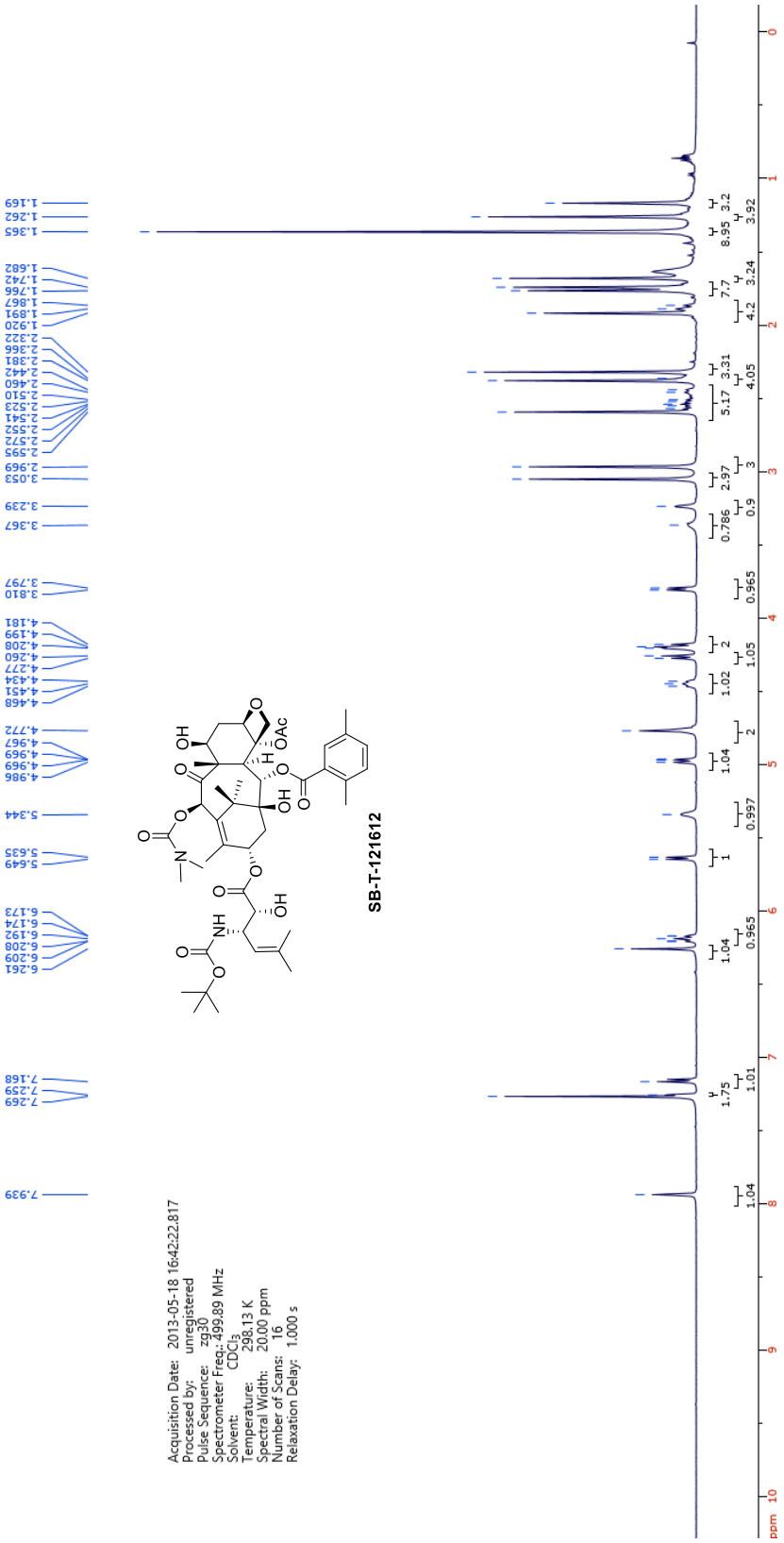
Acquisition Date: 2013-05-18 16:42:22.817
Processed by: unregistered
Pulse Sequence: zg30
Spectrometer Freq.: 499.89 MHz
Solvent: $CDCl_3$
Temperature: 298.13 K
Spectral Width: 20.00 ppm
Number of Scans: 16
Relaxation Delay: 1.000 s
SB-T-121612
ppm

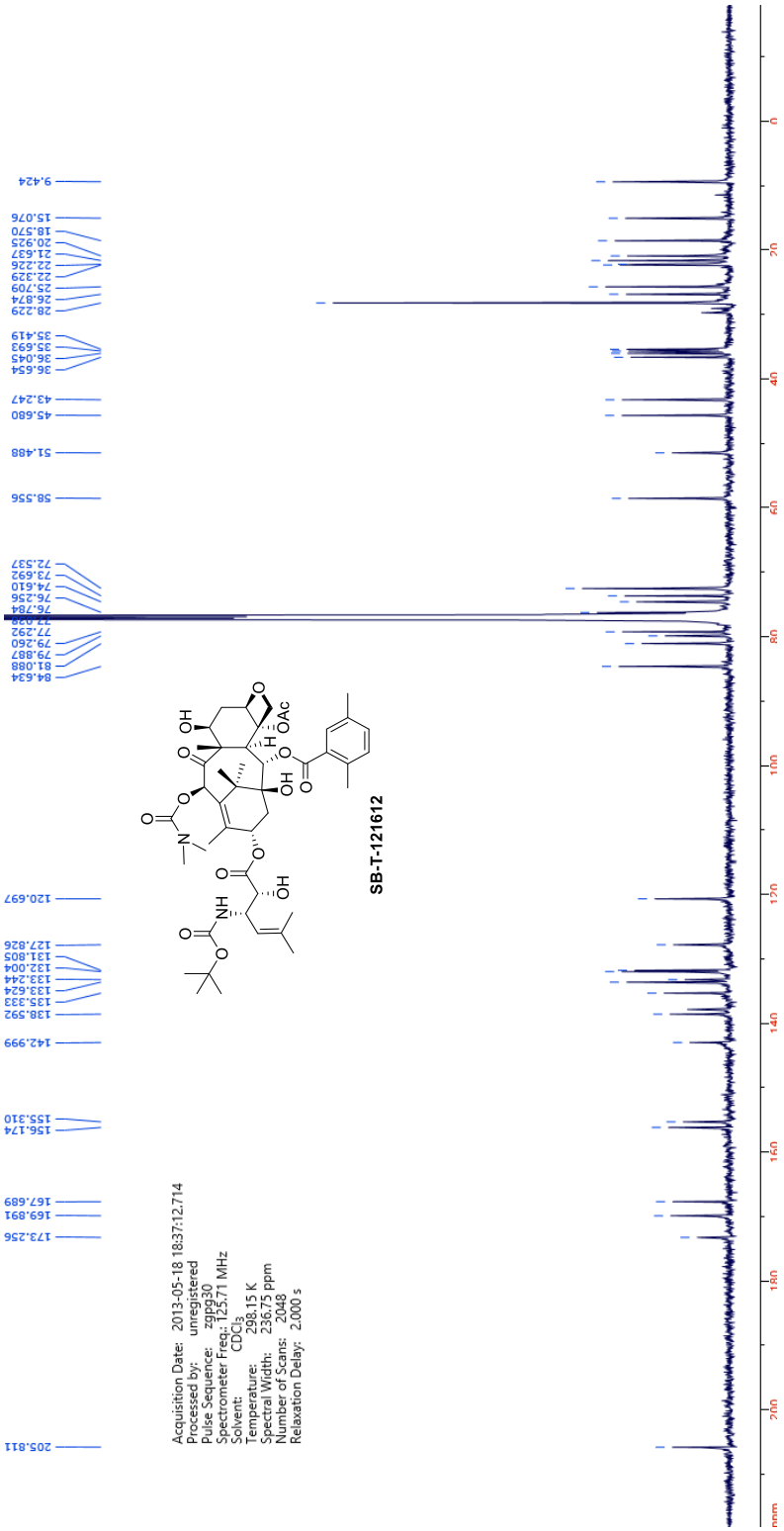
SB-T-I21612
Acquisition Date: 2013-05-18 18:37:12.714
Processed by: unregistered
Pulse Sequence: zgpg30
Spectrometer Freq.: 125.71 MHz
Solvent: CDCl3
Temperature: 298.15 K
Spectral Width: 236.75 ppm
Number of Scans: 2048
Relaxation Delay: 2.000 s
9.424
15.076
18.570
20.925
21.637
22.226
22.329
25.709
26.874
28.229
35.419
36.654
36.045
35.693
43.247
45.680
51.488
58.556
72.537
73.692
74.610
76.256
76.784
77.292
79.260
79.887
81.088
84.634
120.697
127.826
131.805
132.004
133.244
133.624
135.333
138.592
142.999
155.310
156.174
167.689
169.891
173.256
205.811

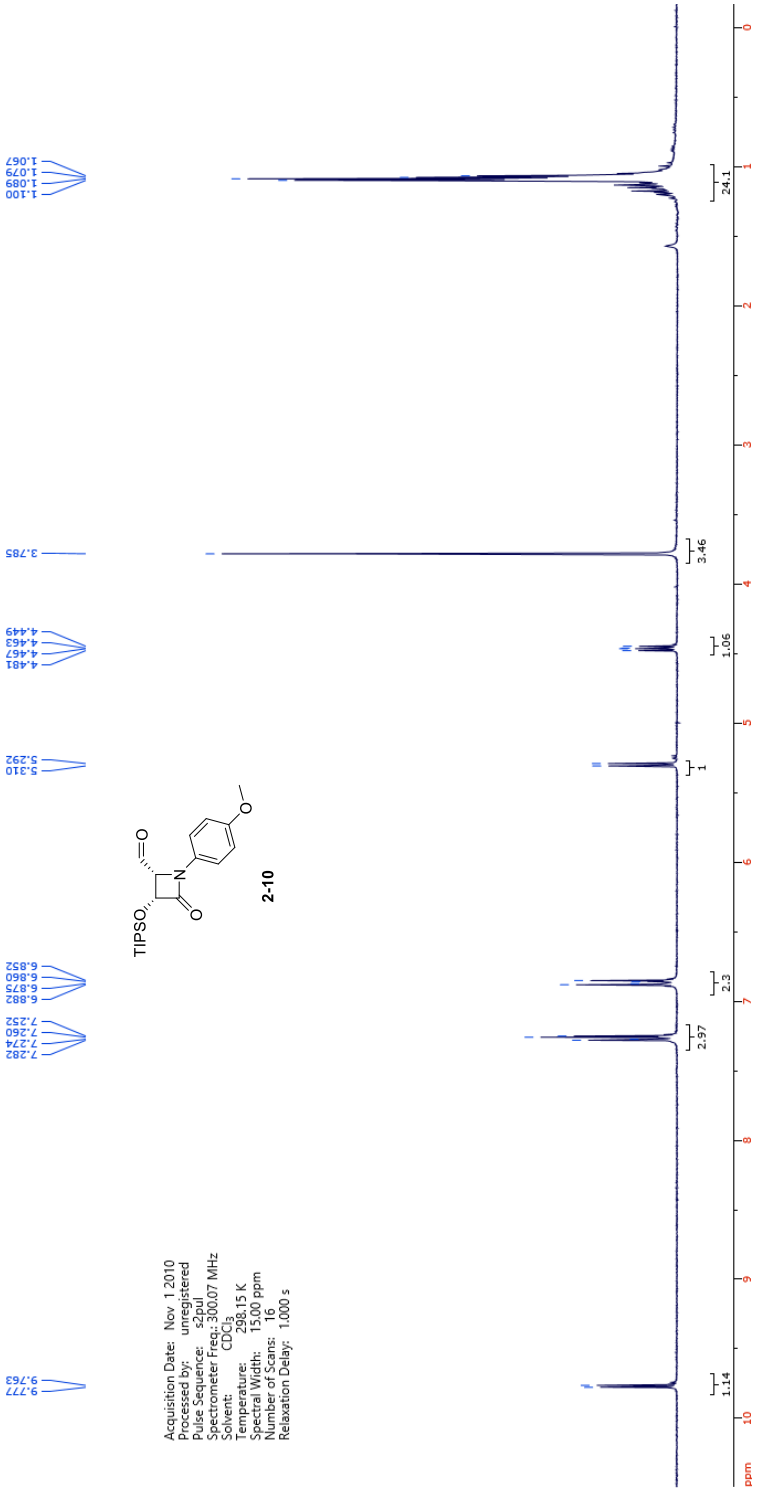
1.067
1.079
1.089
1.100
3.785
4.449
4.467
4.481
5.292
5.310
6.852
6.860
6.875
6.882
7.252
7.260
7.274
7.282
9.763
9.777
TIPSO
O
N
O
O
2-10
Acquisition Date: Nov 1 2010
Processed by: unregistered
Pulse Sequence: s2pul
Spectrometer Freq.: 300.07 MHz
Solvent: CDCl3
Temperature: 298.15 K
Spectral Width: 15.00 ppm
Number of Scans: 16
Relaxation Delay: 1.000 s
24.1
3.46
1.06
1
2.3
2.97
1.14
ppm

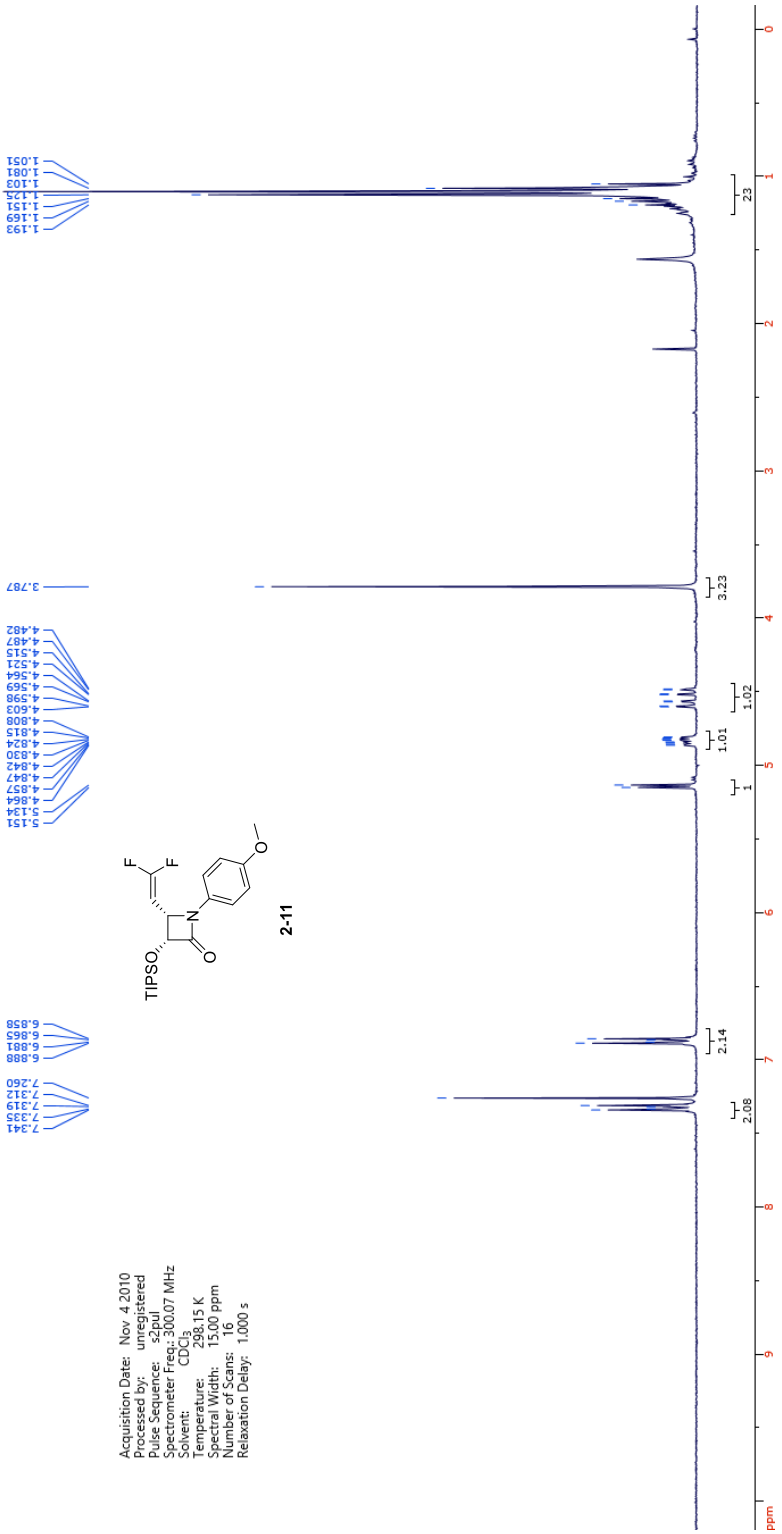
1.051
1.081
1.103
1.125
1.151
1.169
1.193
3.787
4.482
4.487
4.515
4.521
4.564
4.569
4.598
4.603
4.808
4.815
4.824
4.830
4.842
4.847
4.857
4.864
5.134
5.151
6.858
6.865
6.881
6.888
7.260
7.312
7.319
7.335
7.341
TIPSO
F
F
N
O
O
2-11
Acquisition Date: Nov 4 2010
Processed by: unregistered
Pulse Sequence: s2pul
Spectrometer Freq.: 300.07 MHz
Solvent: CDCl3
Temperature: 298.15 K
Spectral Width: 15.00 ppm
Number of Scans: 16
Relaxation Delay: 1.000 s
23
3.23
1.02
1.01
1
2.14
2.08
ppm

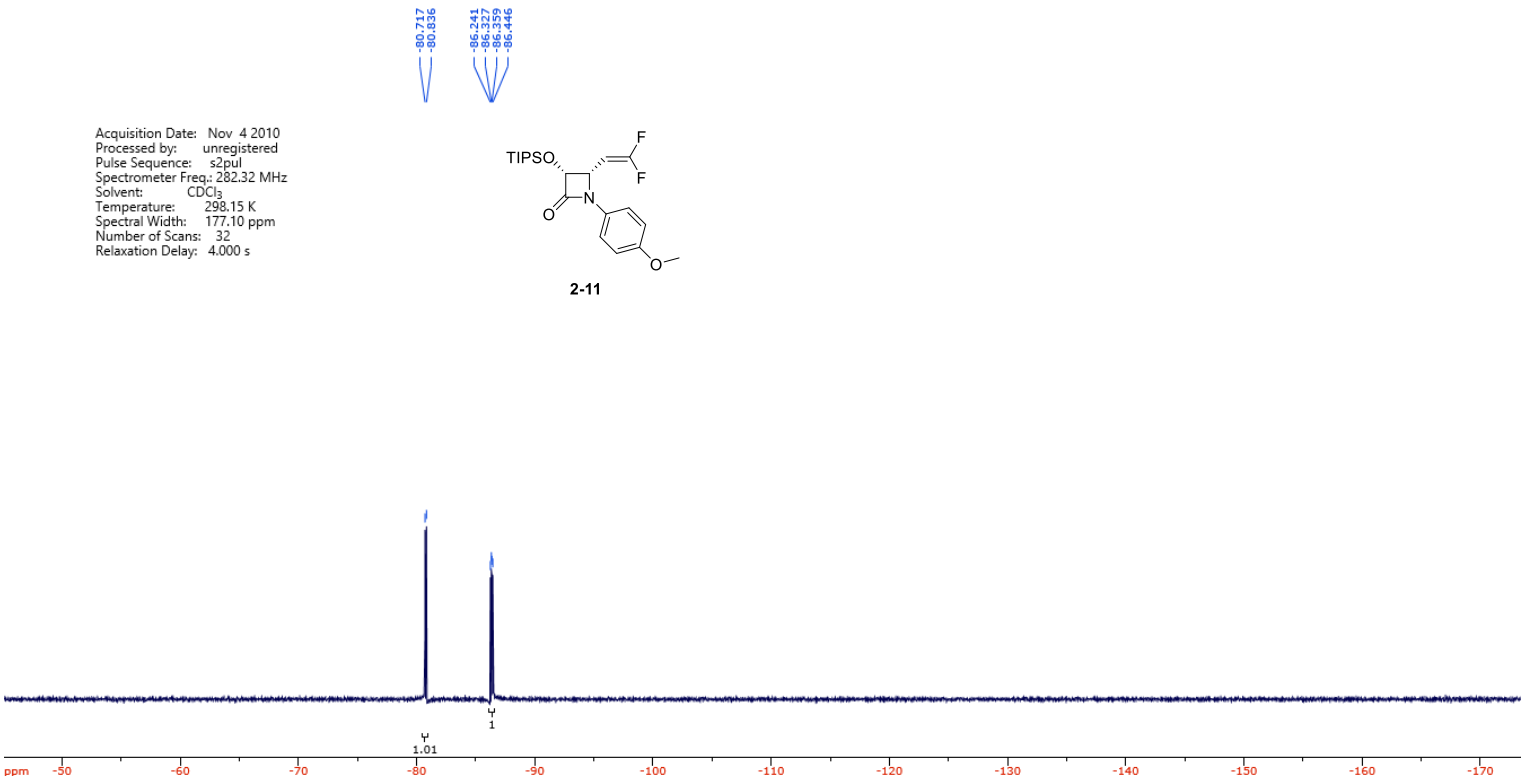
-80.717
-80.836
-86.241
-86.327
-86.359
-86.446
Acquisition Date: Nov 4 2010
Processed by: unregistered
Pulse Sequence: s2pul
Spectrometer Freq.: 282.32 MHz
Solvent: CDCl3
Temperature: 298.15 K
Spectral Width: 177.10 ppm
Number of Scans: 32
Relaxation Delay: 4.000 s
TIPSO
F
F
O
N
O
2-11
1.01
1
ppm
-50
-60
-70
-80
-90
-100
-110
-120
-130
-140
-150
-160
-170

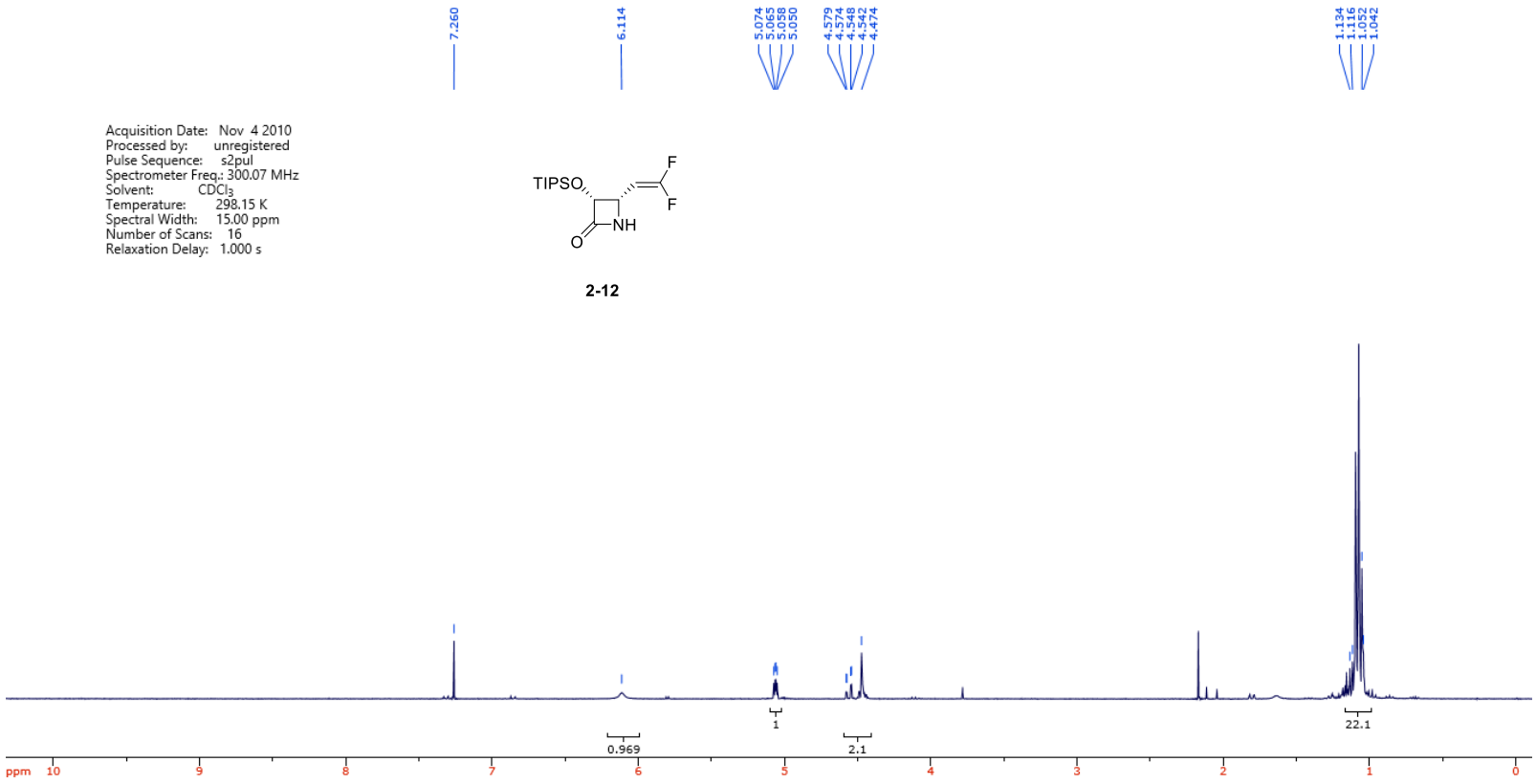
7.260
6.114
5.074
5.065
5.058
5.050
4.579
4.574
4.548
4.542
4.474
1.134
1.116
1.052
1.042
Acquisition Date: Nov 4 2010
Processed by: unregistered
Pulse Sequence: s2pul
Spectrometer Freq.: 300.07 MHz
Solvent: CDCl3
Temperature: 298.15 K
Spectral Width: 15.00 ppm
Number of Scans: 16
Relaxation Delay: 1.000 s
TIPSO
F
F
NH
O
2-12
0.969
1
2.1
22.1
ppm
10
9
8
7
6
5
4
3
2
1
0

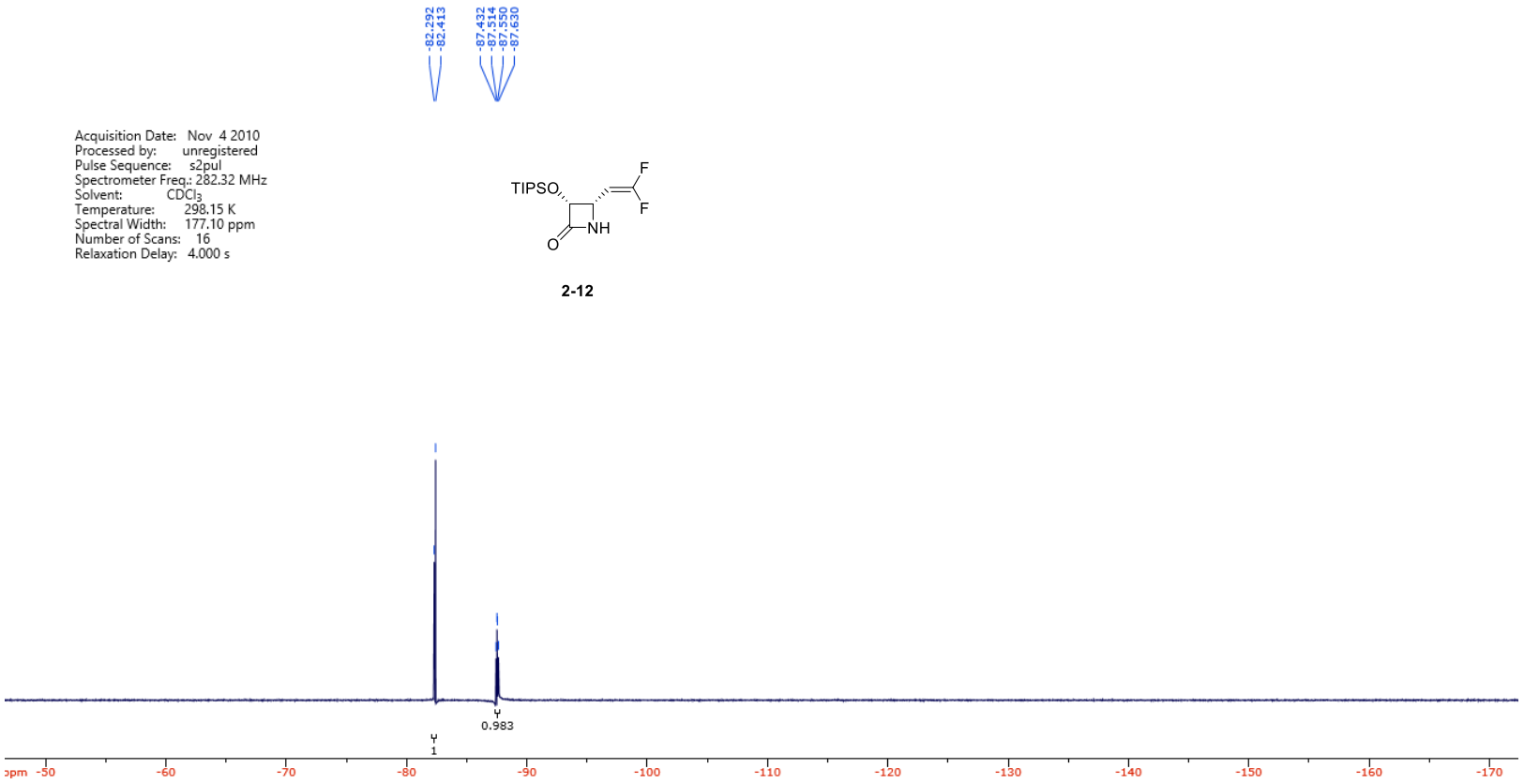
-82.292
-82.413
-87.432
-87.514
-87.550
-87.630
Acquisition Date: Nov 4 2010
Processed by: unregistered
Pulse Sequence: s2pul
Spectrometer Freq.: 282.32 MHz
Solvent: CDCl3
Temperature: 298.15 K
Spectral Width: 177.10 ppm
Number of Scans: 16
Relaxation Delay: 4.000 s
TIPSO
F
F
NH
O
0.983
1
ppm -50 -60 -70 -80 -90 -100 -110 -120 -130 -140 -150 -160 -170

2-12

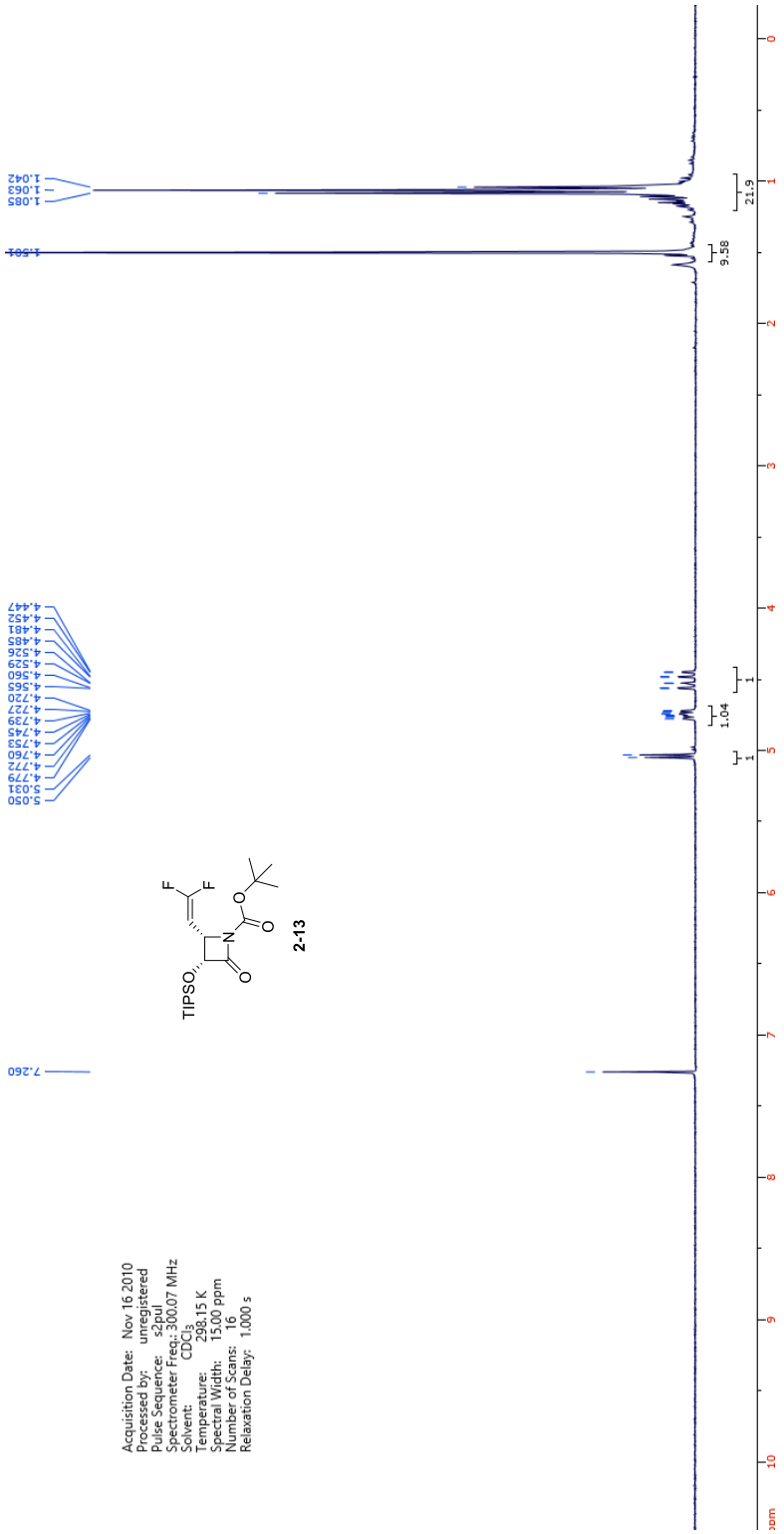
1.042
1.063
1.085
1.801
4.447
4.452
4.481
4.485
4.526
4.529
4.560
4.565
4.720
4.727
4.739
4.745
4.753
4.760
4.772
4.779
5.031
5.050
7.260
21.9
9.58
1.04
1
1
F
F
O
O
N
O
O
TIPSO
2-13
Acquisition Date: Nov 16 2010
Processed by: unregistered
Pulse Sequence: s2pul
Spectrometer Freq.: 300.07 MHz
Solvent: $CDCl_3$
Temperature: 298.15 K
Spectral Width: 15.00 ppm
Number of Scans: 16
Relaxation Delay: 1.000 s

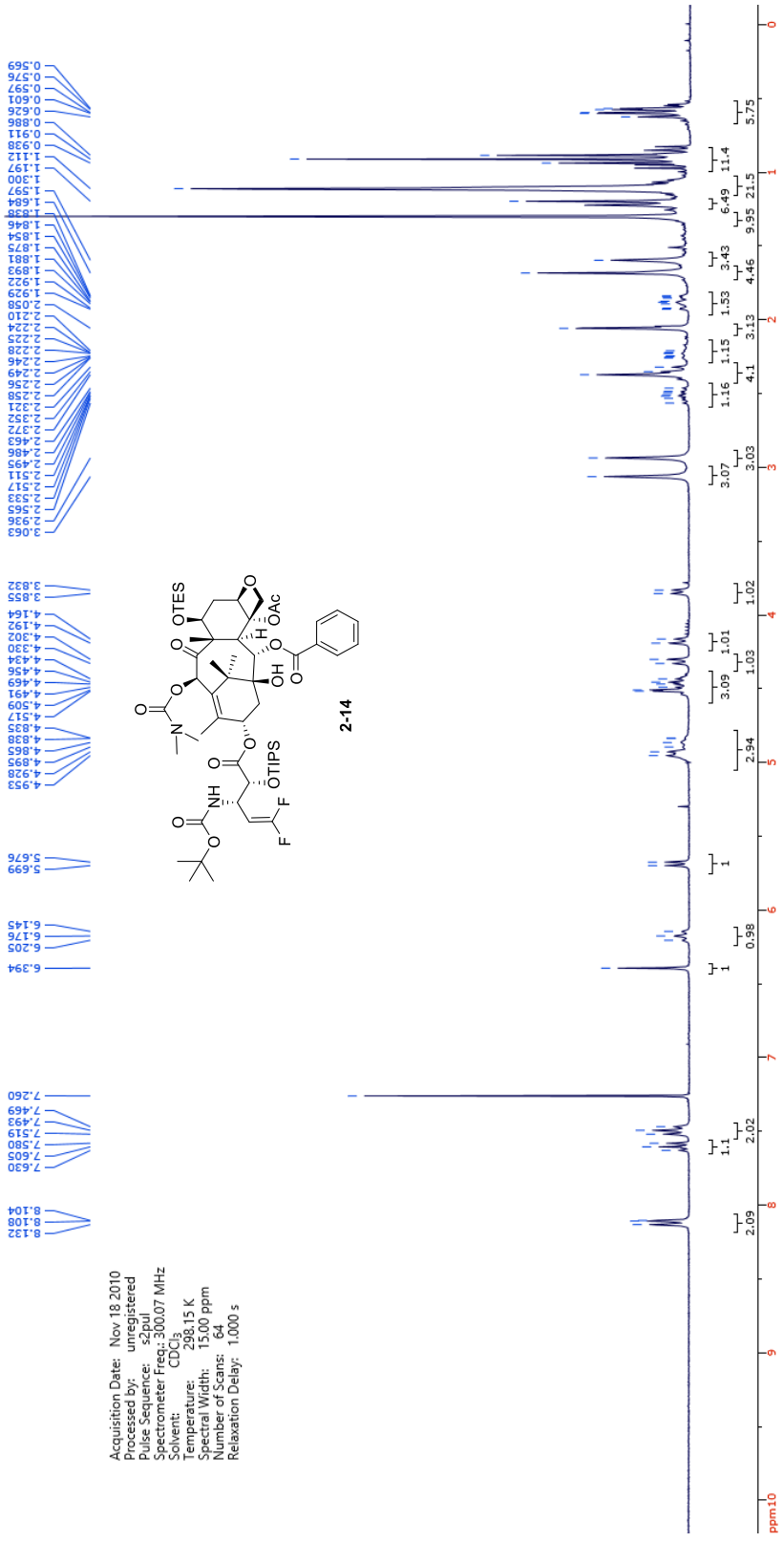
Acquisition Date: Nov 18 2010
Processed by: unregistered
Pulse Sequence: s2pul
Spectrometer Freq.: 300.07 MHz
Solvent: CDCl3
Temperature: 298.15 K
Spectral Width: 15.00 ppm
Number of Scans: 64
Relaxation Delay: 1.000 s
OTES
OAc
OH
OTIPS
NH
F
F
2-14

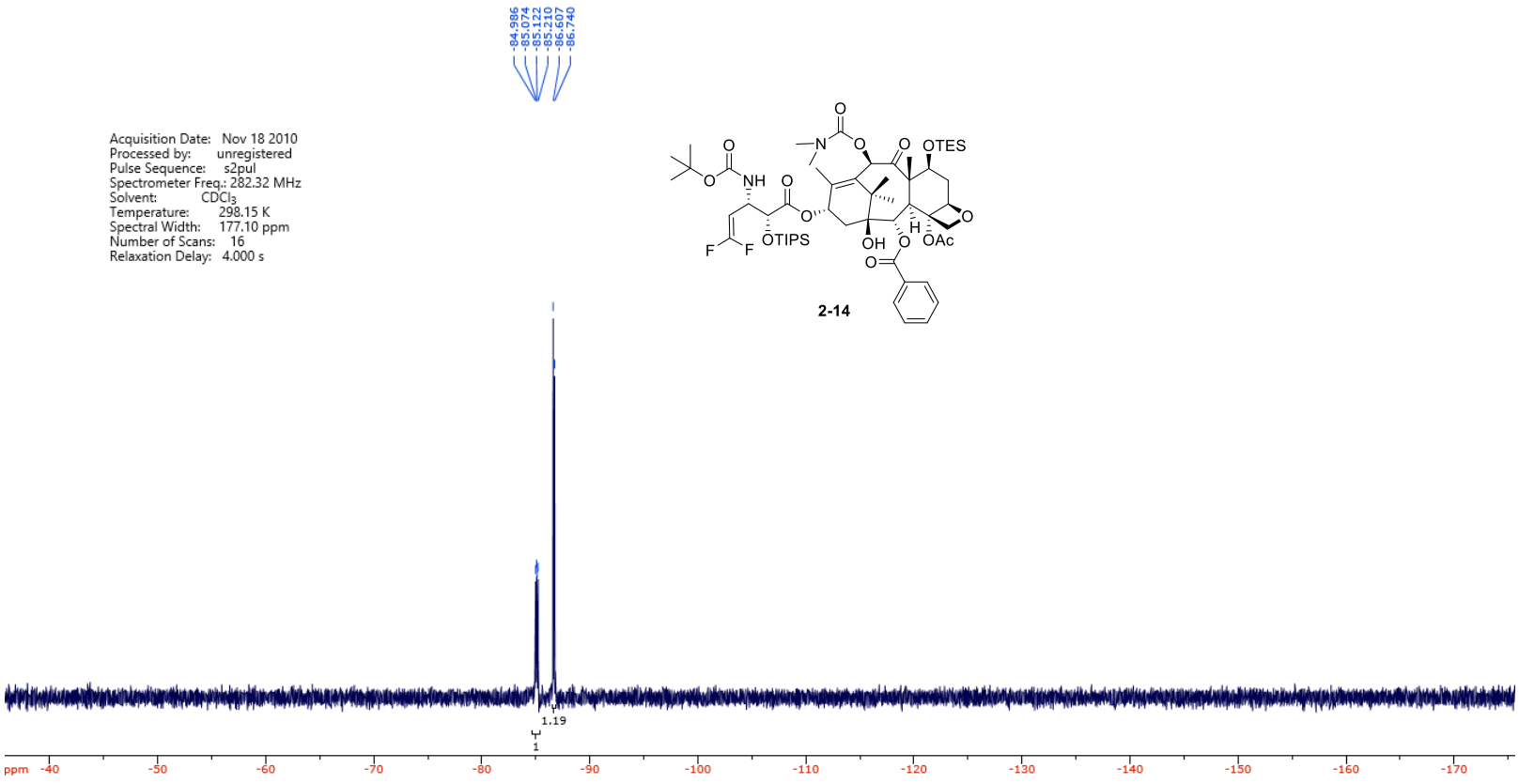
-84.986
-85.074
-85.122
-85.210
-86.607
-86.740
Acquisition Date: Nov 18 2010
Processed by: unregistered
Pulse Sequence: s2pul
Spectrometer Freq.: 282.32 MHz
Solvent: CDCl3
Temperature: 298.15 K
Spectral Width: 177.10 ppm
Number of Scans: 16
Relaxation Delay: 4.000 s
2-14
1.19
ppm -40 -50 -60 -70 -80 -90 -100 -110 -120 -130 -140 -150 -160 -170

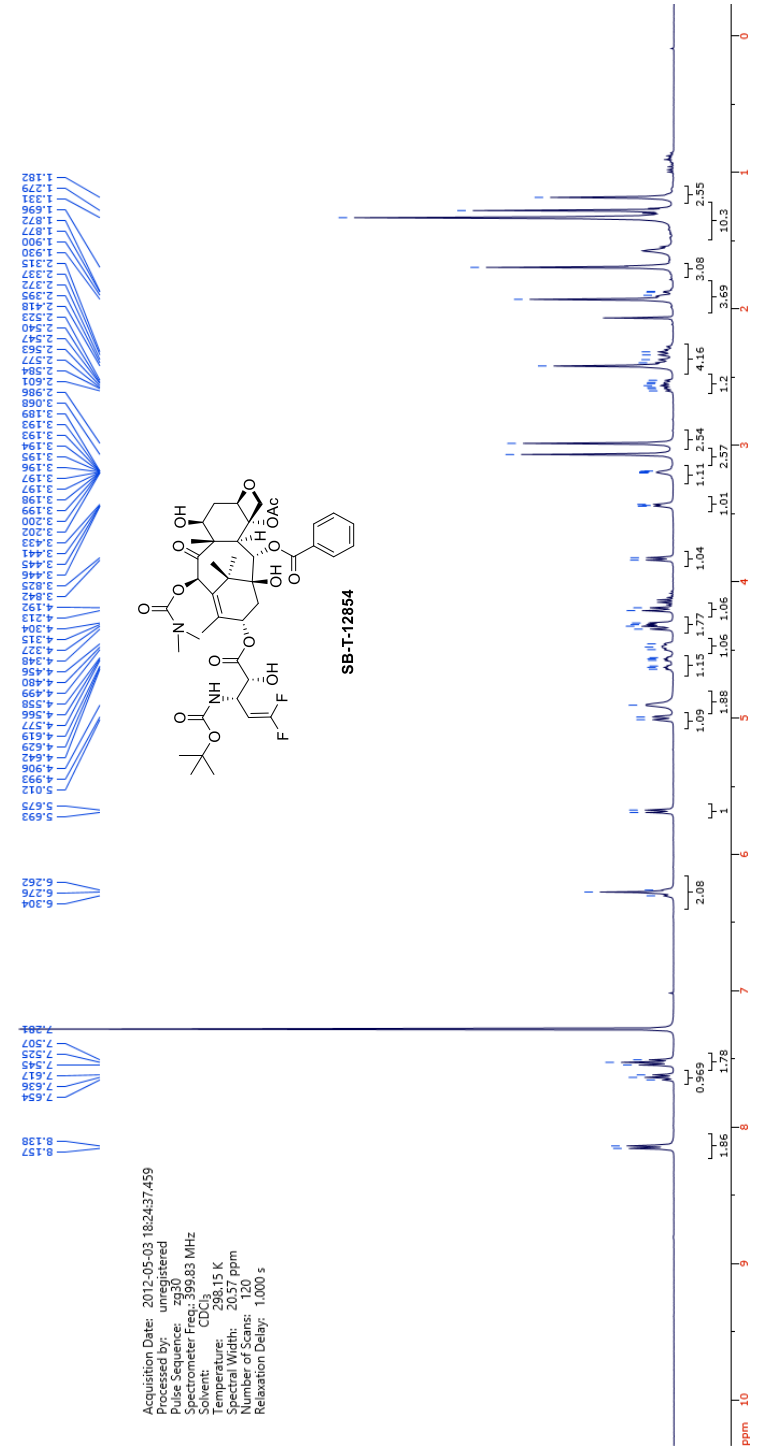
SB-T-12854
Acquisition Date: 2012-05-03 18:24:37.459
Processed by: unregistered
Pulse Sequence: zg30
Spectrometer Freq.: 399.83 MHz
Solvent: $CDCl_3$
Temperature: 298.15 K
Spectral Width: 20.57 ppm
Number of Scans: 120
Relaxation Delay: 1.000 s
ppm

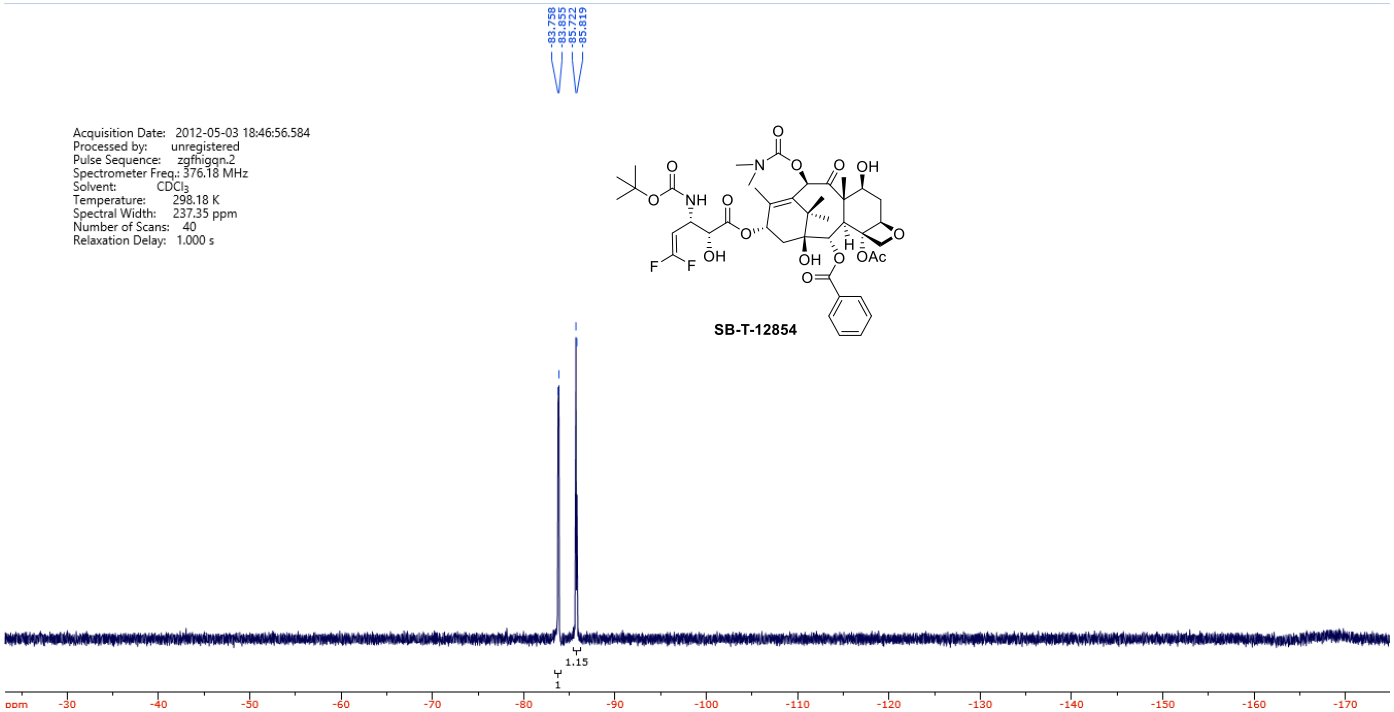
-83.758
-83.855
-85.722
-85.819
Acquisition Date: 2012-05-03 18:46:56.584
Processed by: unregistered
Pulse Sequence: zgfhigqn.2
Spectrometer Freq.: 376.18 MHz
Solvent: CDCl3
Temperature: 298.18 K
Spectral Width: 237.35 ppm
Number of Scans: 40
Relaxation Delay: 1.000 s
SB-T-12854
1.15
1
ppm
-30
-40
-50
-60
-70
-80
-90
-100
-110
-120
-130
-140
-150
-160
-170

Appendix Chapter 3

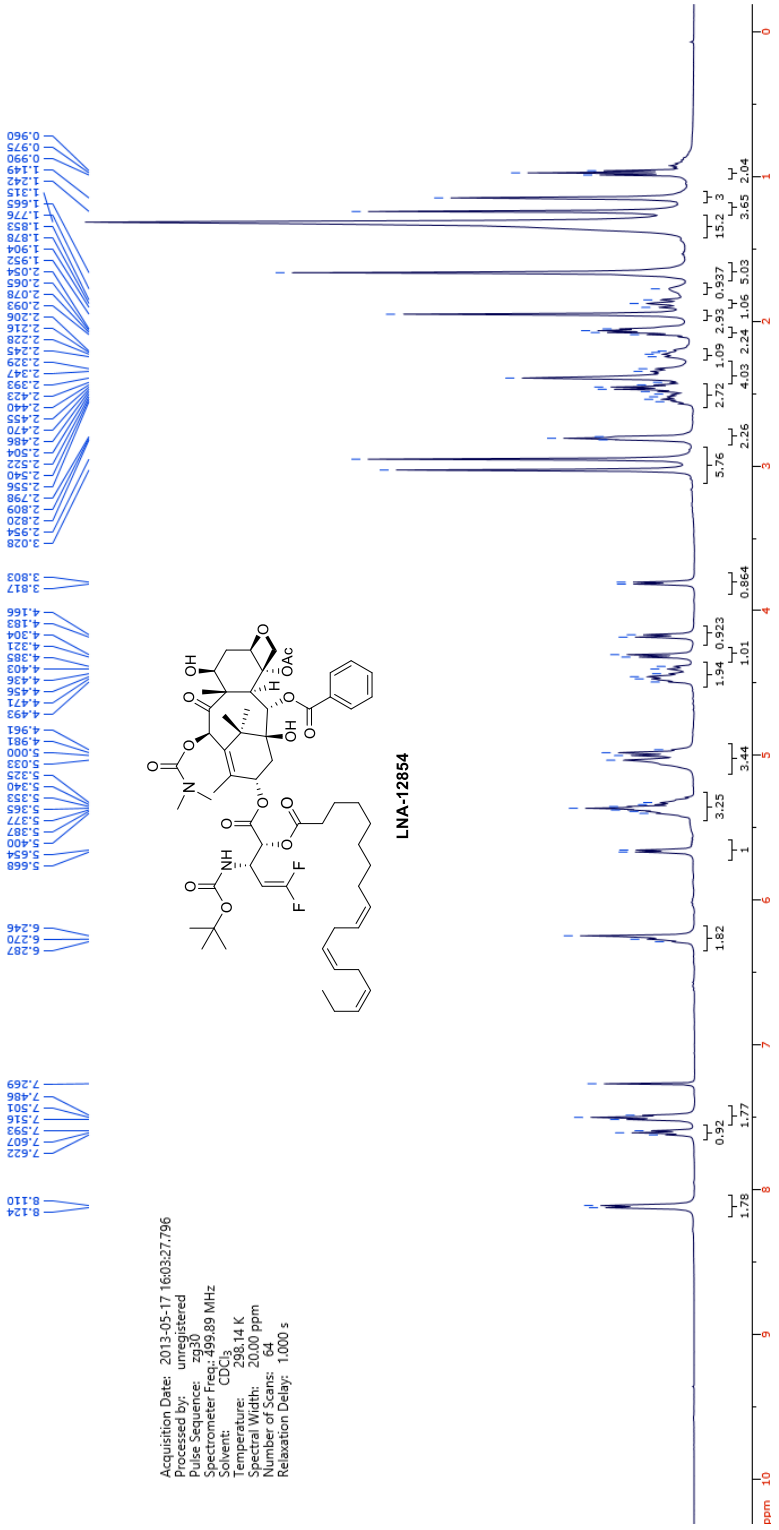
LNA-12854
Acquisition Date: 2013-05-17 16:03:27.796
Processed by: unregistered
Pulse Sequence: zg30
Spectrometer Freq.: 499.89 MHz
Solvent: $CDCl_3$
Temperature: 298.14 K
Spectral Width: 20.00 ppm
Number of Scans: 64
Relaxation Delay: 1.000 s
ppm

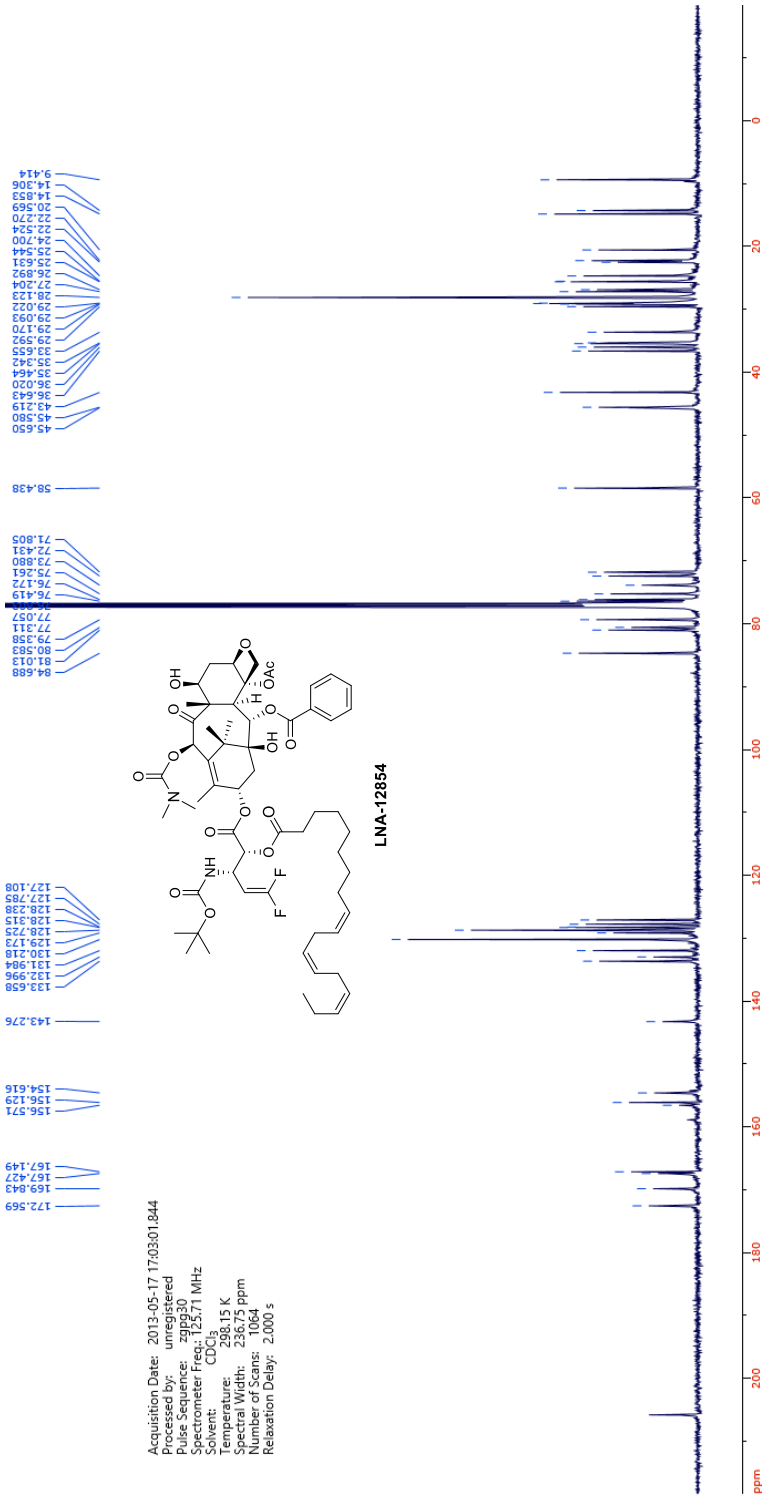
LNA-12854
Acquisition Date: 2013-05-17 17:03:01.844
Processed by: unregistered
Pulse Sequence: zgpg30
Spectrometer Freq.: 125.71 MHz
Solvent: CDCl3
Temperature: 298.15 K
Spectral Width: 236.75 ppm
Number of Scans: 1064
Relaxation Delay: 2.000 s
9.414
14.306
14.853
20.569
22.270
22.524
24.700
25.544
25.631
26.892
27.204
28.122
29.022
29.093
29.170
29.592
33.655
35.342
35.464
36.020
36.643
43.219
45.580
45.650
58.438
71.805
72.431
73.880
75.261
76.172
76.419
77.057
77.311
79.358
80.583
81.013
84.688
127.108
127.785
128.238
128.315
128.725
129.173
130.218
131.904
132.996
133.658
143.276
154.616
156.129
156.571
167.149
167.427
169.043
172.569
ppm

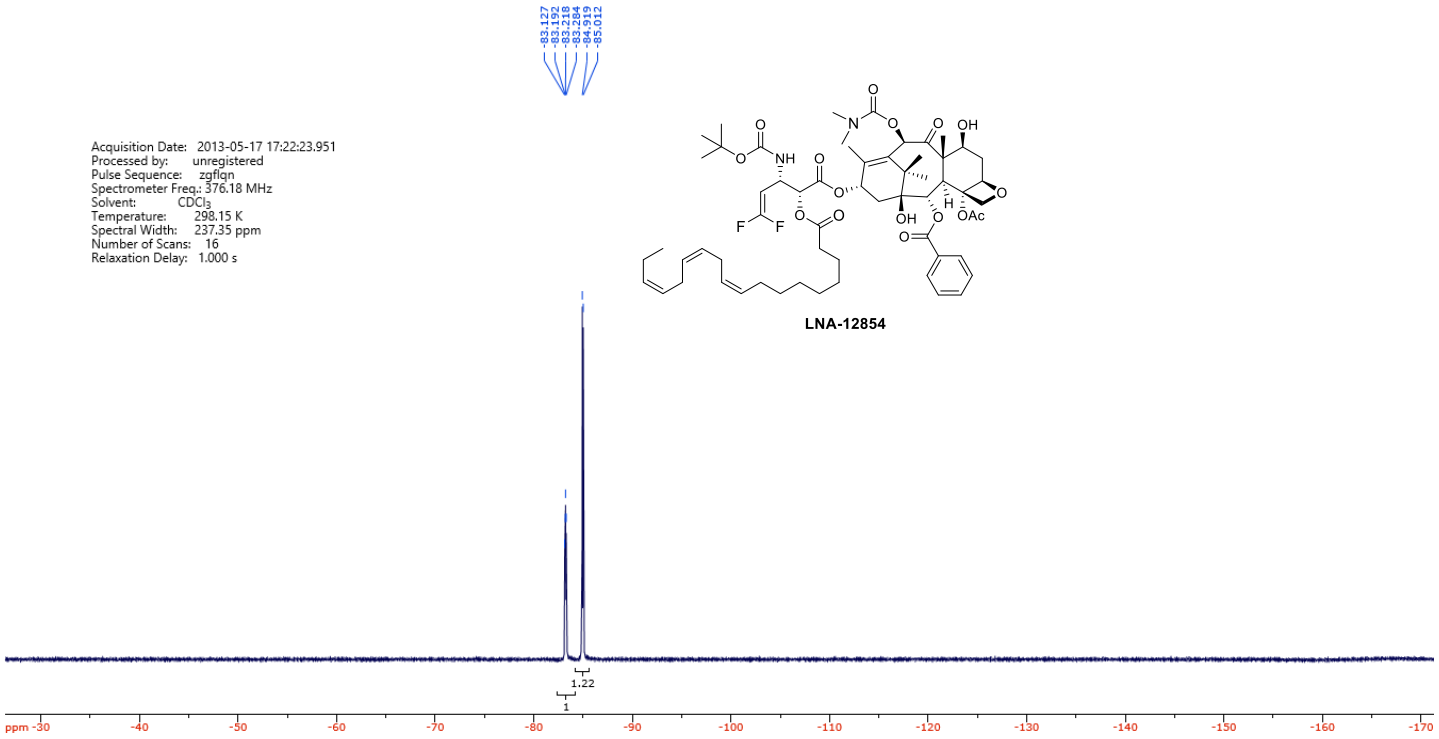
-83.127
-83.192
-83.218
-83.284
-84.919
-85.012
Acquisition Date: 2013-05-17 17:22:23.951
Processed by: unregistered
Pulse Sequence: zgflqn
Spectrometer Freq.: 376.18 MHz
Solvent: CDCl3
Temperature: 298.15 K
Spectral Width: 237.35 ppm
Number of Scans: 16
Relaxation Delay: 1.000 s
LNA-12854
1.22
1
ppm -30
-40
-50
-60
-70
-80
-90
-100
-110
-120
-130
-140
-150
-160
-170

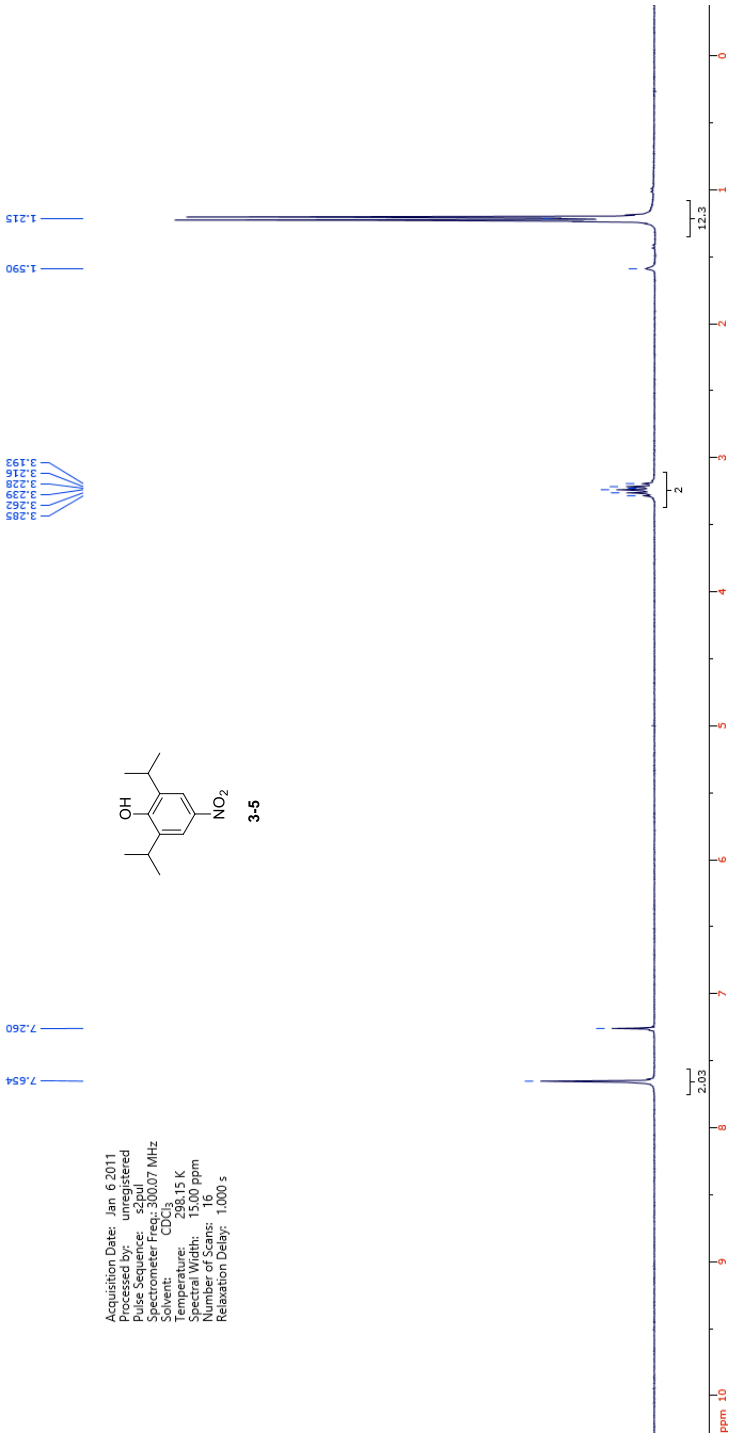
1.215
1.590
3.193
3.216
3.228
3.239
3.262
3.285
7.260
7.654
12.3
2
2.03
OH
NO2
3-5
Acquisition Date: Jan 6 2011
Processed by: unregistered
Pulse Sequence: s2pul
Spectrometer Freq: 300.07 MHz
Solvent: CDCl3
Temperature: 298.15 K
Spectral Width: 15.00 ppm
Number of Scans: 16
Relaxation Delay: 1.000 s
ppm

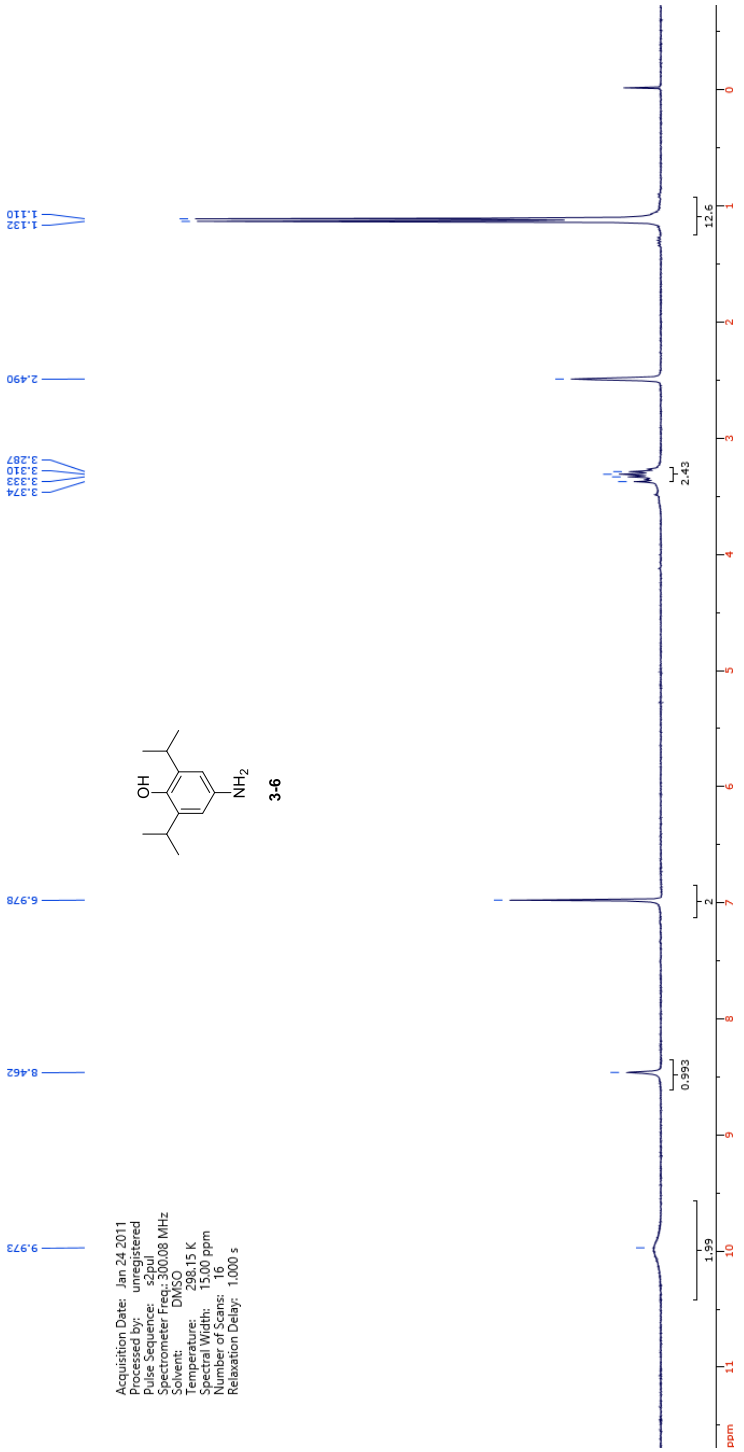
1.110
1.132
2.490
3.287
3.310
3.333
3.374
6.978
8.462
9.973
OH
NH2
3-6
Acquisition Date: Jan 24 2011
Processed by: unregistered
Pulse Sequence: s2pul
Spectrometer Freq.: 300.08 MHz
Solvent: DMSO
Temperature: 298.15 K
Spectral Width: 15.00 ppm
Number of Scans: 16
Relaxation Delay: 1.000 s
12.6
2.43
2
0.993
1.99
ppm

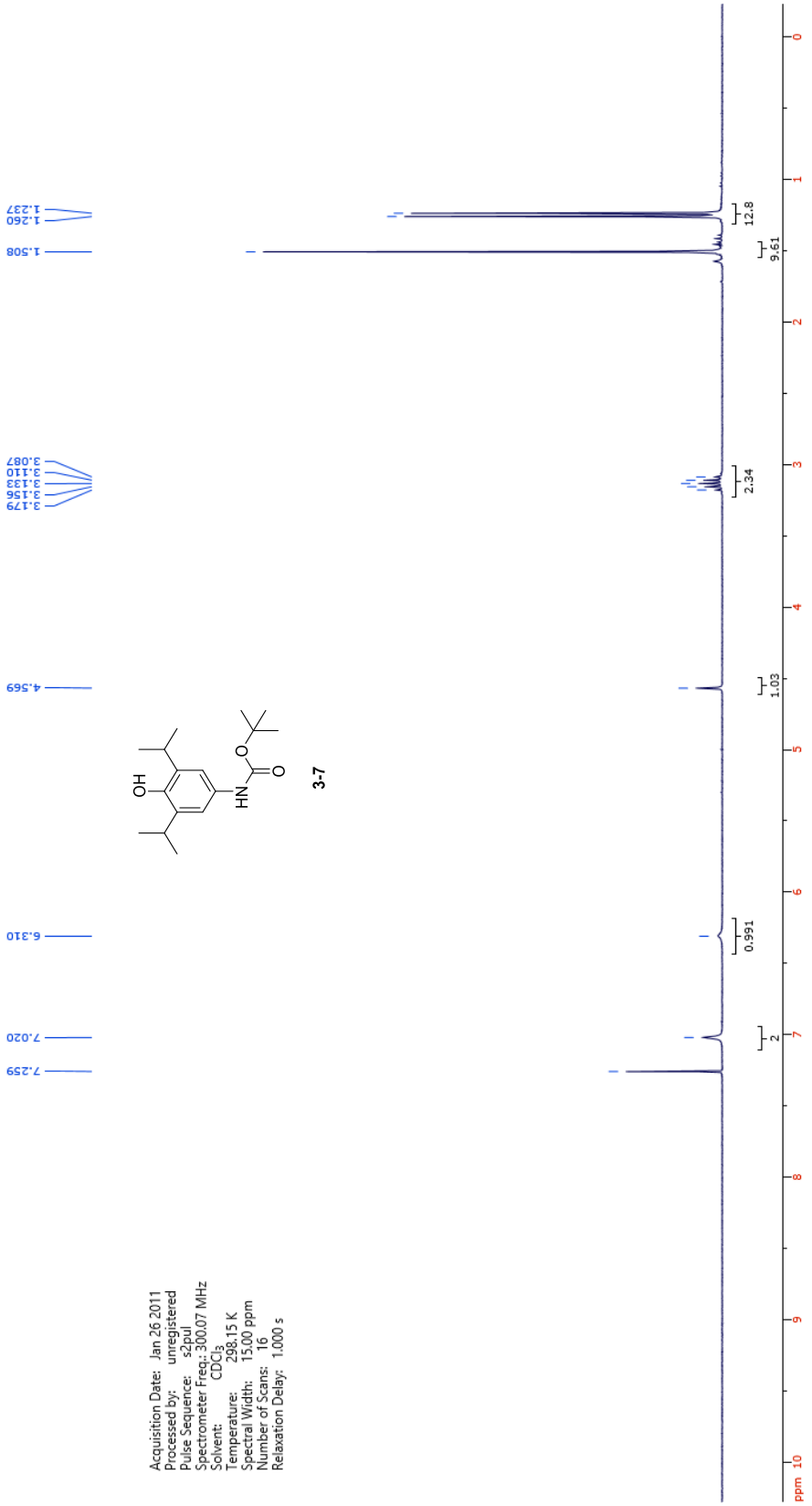
1.237
1.260
1.508
3.087
3.110
3.133
3.156
3.179
4.569
6.310
7.020
7.259
12.8
9.61
2.34
1.03
0.991
2
ppm
Acquisition Date: Jan 26 2011
Processed by: unregistered
Pulse Sequence: s2pul
Spectrometer Freq.: 300.07 MHz
Solvent: CDCl3
Temperature: 298.15 K
Spectral Width: 15.00 ppm
Number of Scans: 16
Relaxation Delay: 1.000 s
OH
HN
O
O
3-7

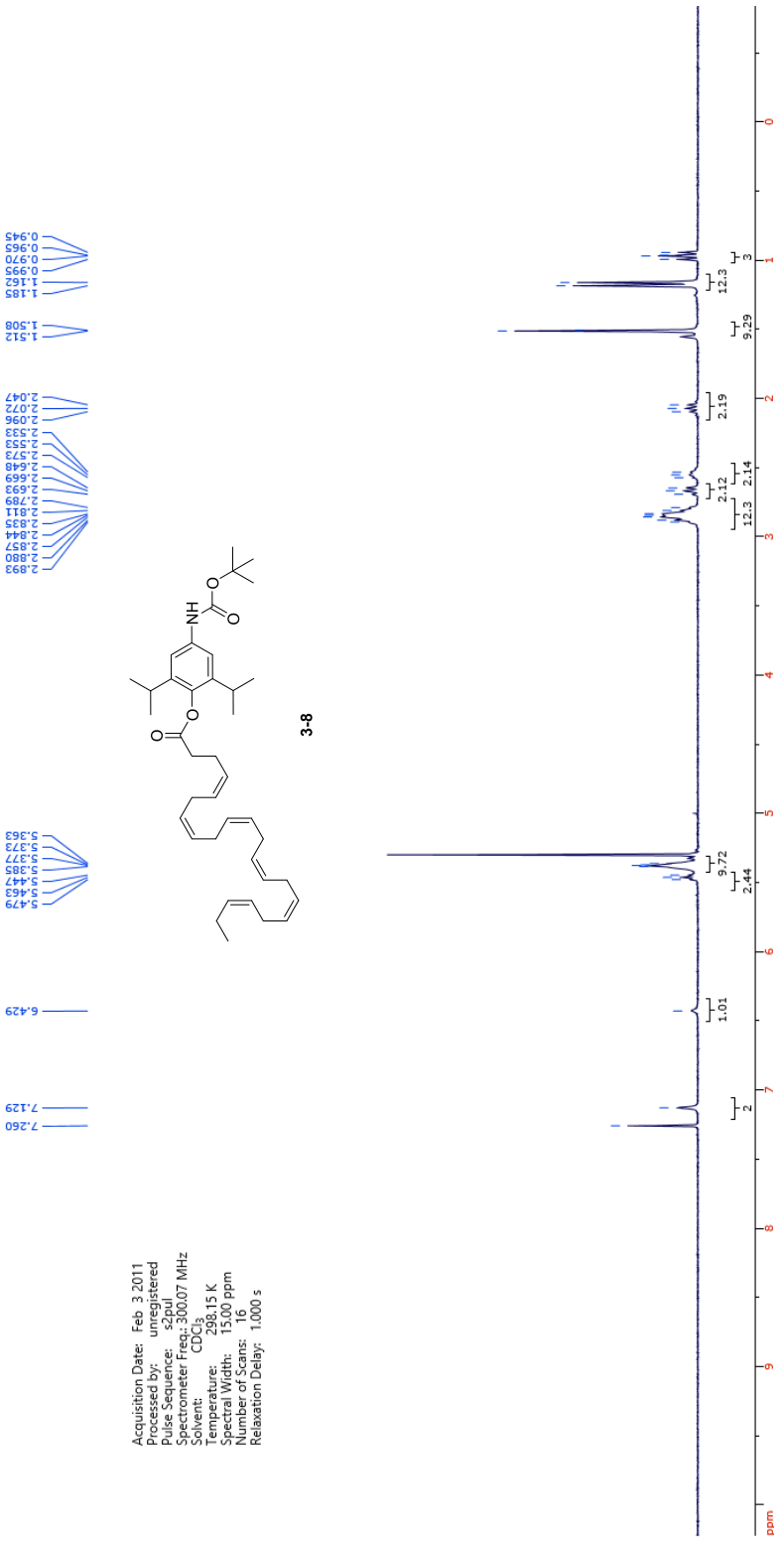
0.945
0.965
0.970
0.995
1.162
1.185
1.508
2.047
2.072
2.096
2.533
2.553
2.573
2.648
2.669
2.693
2.789
2.811
2.835
2.844
2.857
2.880
2.893
5.363
5.373
5.377
5.385
5.447
5.463
5.479
6.429
7.129
7.260
3-8
Acquisition Date: Feb 3 2011
Processed by: unregistered
Pulse Sequence: s2pul
Spectrometer Freq.: 300.07 MHz
Solvent: $CDCl_3$
Temperature: 298.15 K
Spectral Width: 15.00 ppm
Number of Scans: 16
Relaxation Delay: 1.000 s
2
1.01
9.72
2.44
2.12
12.3
2.14
2.19
9.29
12.3
3
ppm

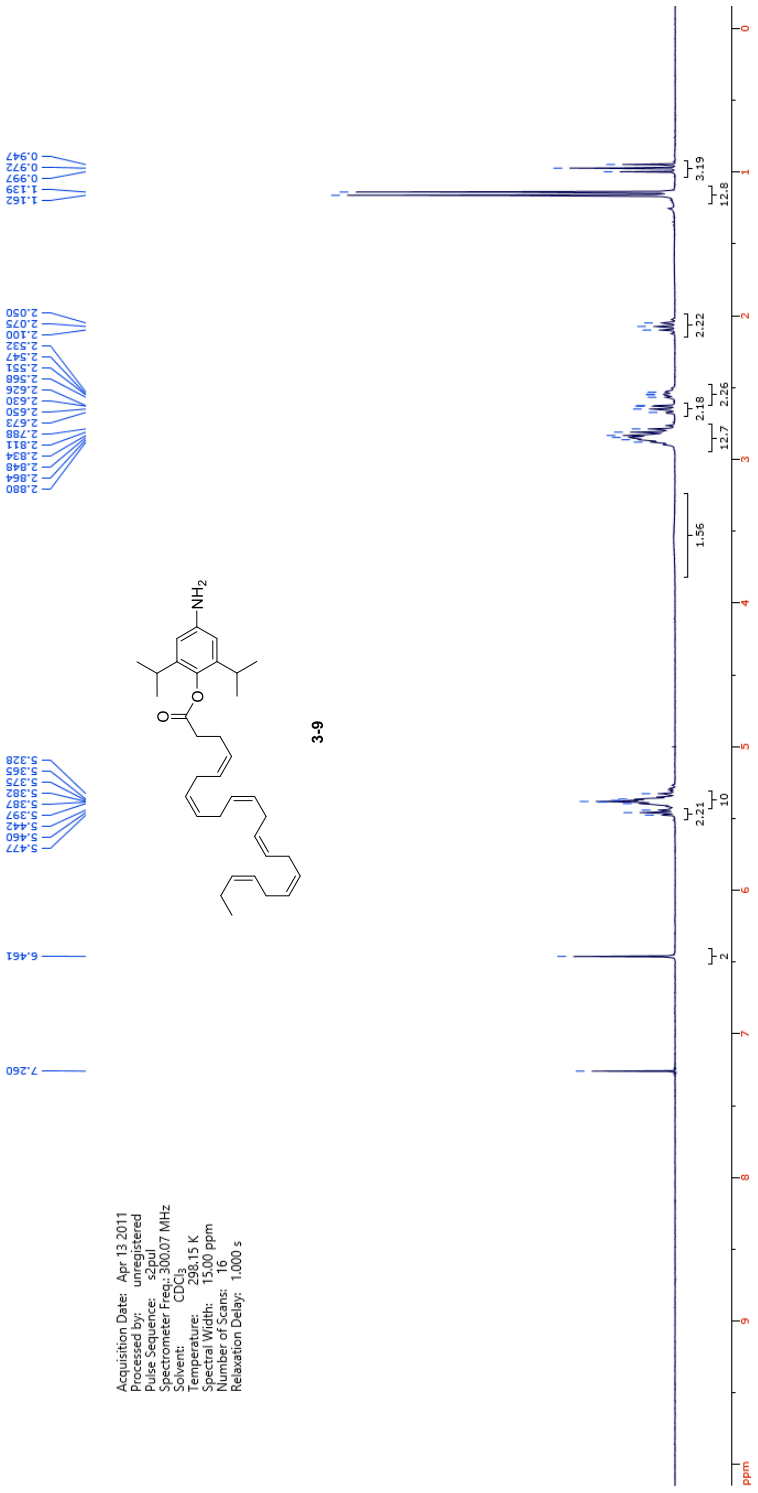
Acquisition Date: Apr 13 2011
Processed by: unregistered
Pulse Sequence: s2pul
Spectrometer Freq.: 300.07 MHz
Solvent: $CDCl_3$
Temperature: 298.15 K
Spectral Width: 15.00 ppm
Number of Scans: 16
Relaxation Delay: 1.000 s
3-9
NH_2
O
O
ppm

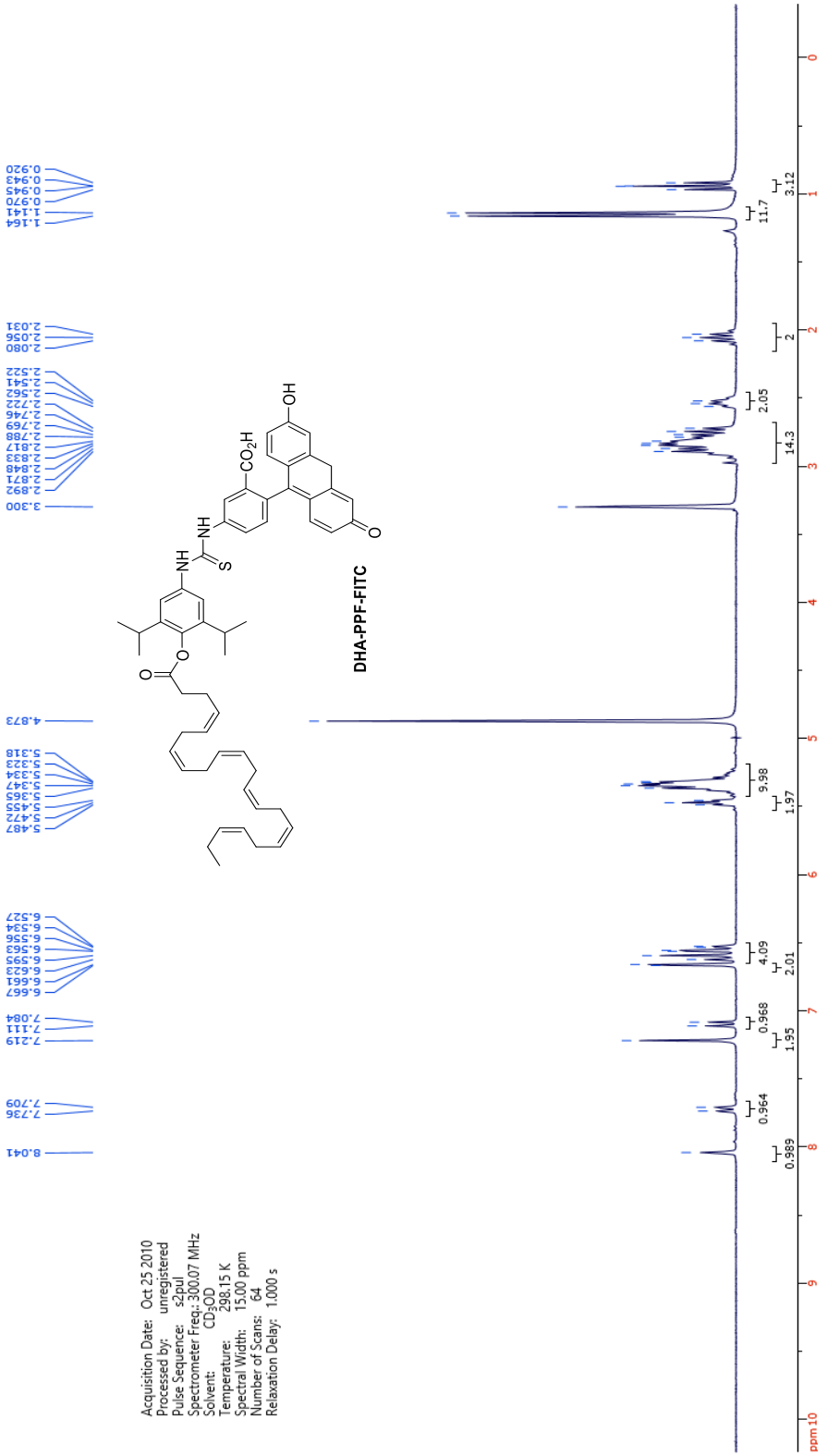
DHA-PPF-FITC
Acquisition Date: Oct 25 2010
Processed by: unregistered
Pulse Sequence: s2pul
Spectrometer Freq.: 300.07 MHz
Solvent: CD3OD
Temperature: 298.15 K
Spectral Width: 15.00 ppm
Number of Scans: 64
Relaxation Delay: 1.000 s
8.041
7.736
7.709
7.219
7.111
7.084
6.667
6.661
6.623
6.595
6.563
6.556
6.534
6.527
5.487
5.472
5.455
5.365
5.347
5.334
5.323
5.318
4.873
3.300
2.892
2.871
2.848
2.833
2.817
2.788
2.769
2.746
2.722
2.562
2.541
2.522
2.080
2.056
2.031
1.164
1.141
0.970
0.945
0.943
0.920
0.989
0.964
1.95
0.968
2.01
4.09
1.97
9.98
2
2.05
14.3
3.12
11.7
ppm

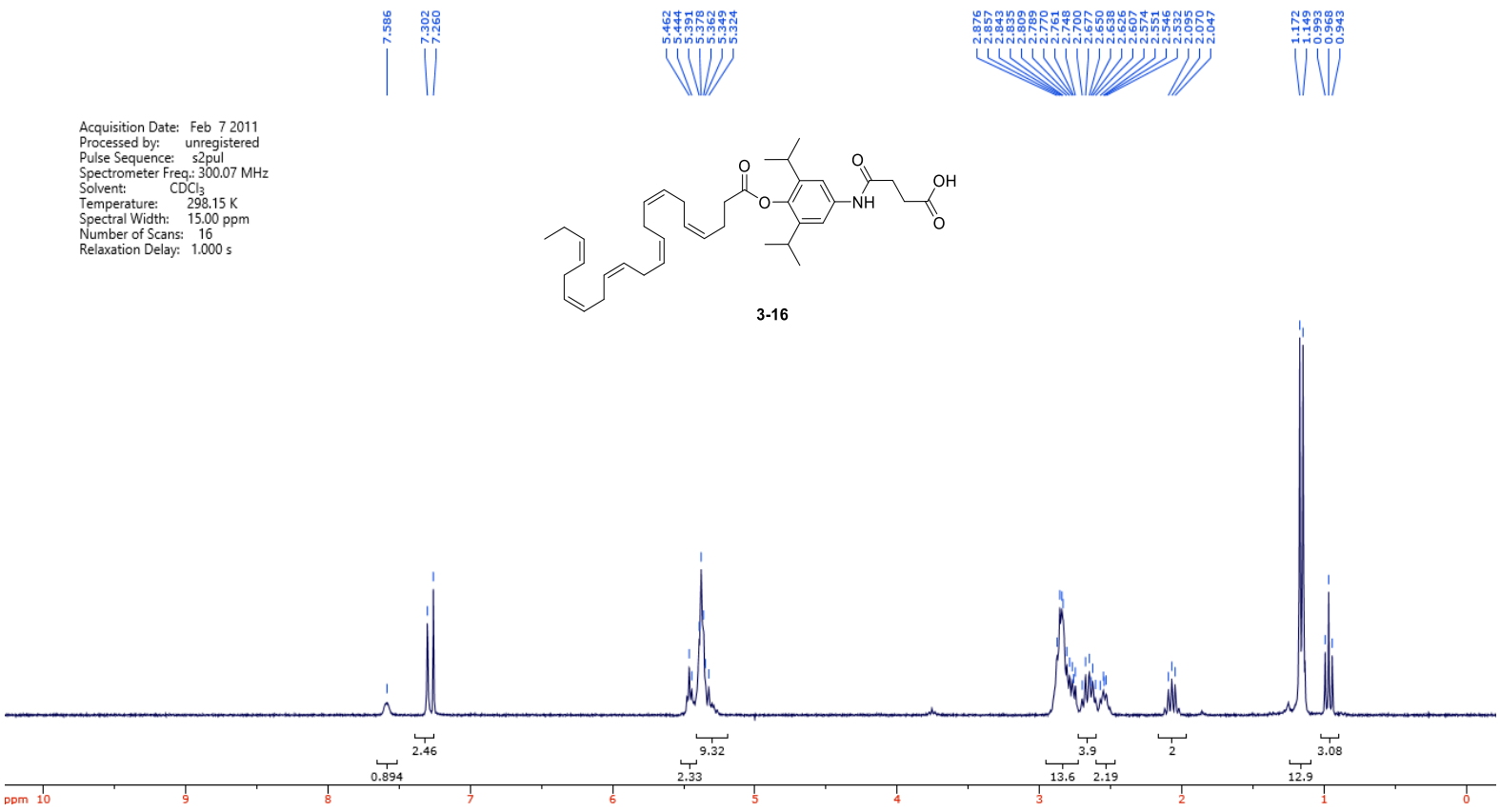
7.586
7.302
7.260
5.462
5.444
5.391
5.378
5.362
5.343
5.324
2.876
2.857
2.843
2.835
2.809
2.789
2.770
2.761
2.748
2.700
2.677
2.650
2.638
2.625
2.607
2.574
2.551
2.546
2.532
2.095
2.075
2.047
1.172
1.145
0.993
0.968
0.943
Acquisition Date: Feb 7 2011
Processed by: unregistered
Pulse Sequence: s2pul
Spectrometer Freq.: 300.07 MHz
Solvent: CDCl3
Temperature: 298.15 K
Spectral Width: 15.00 ppm
Number of Scans: 16
Relaxation Delay: 1.000 s
O
O
NH
OH
O
3-16
0.894
2.46
2.33
9.32
13.6
2.19
3.9
2
12.9
3.08
ppm 10
9
8
7
6
5
4
3
2
1
0

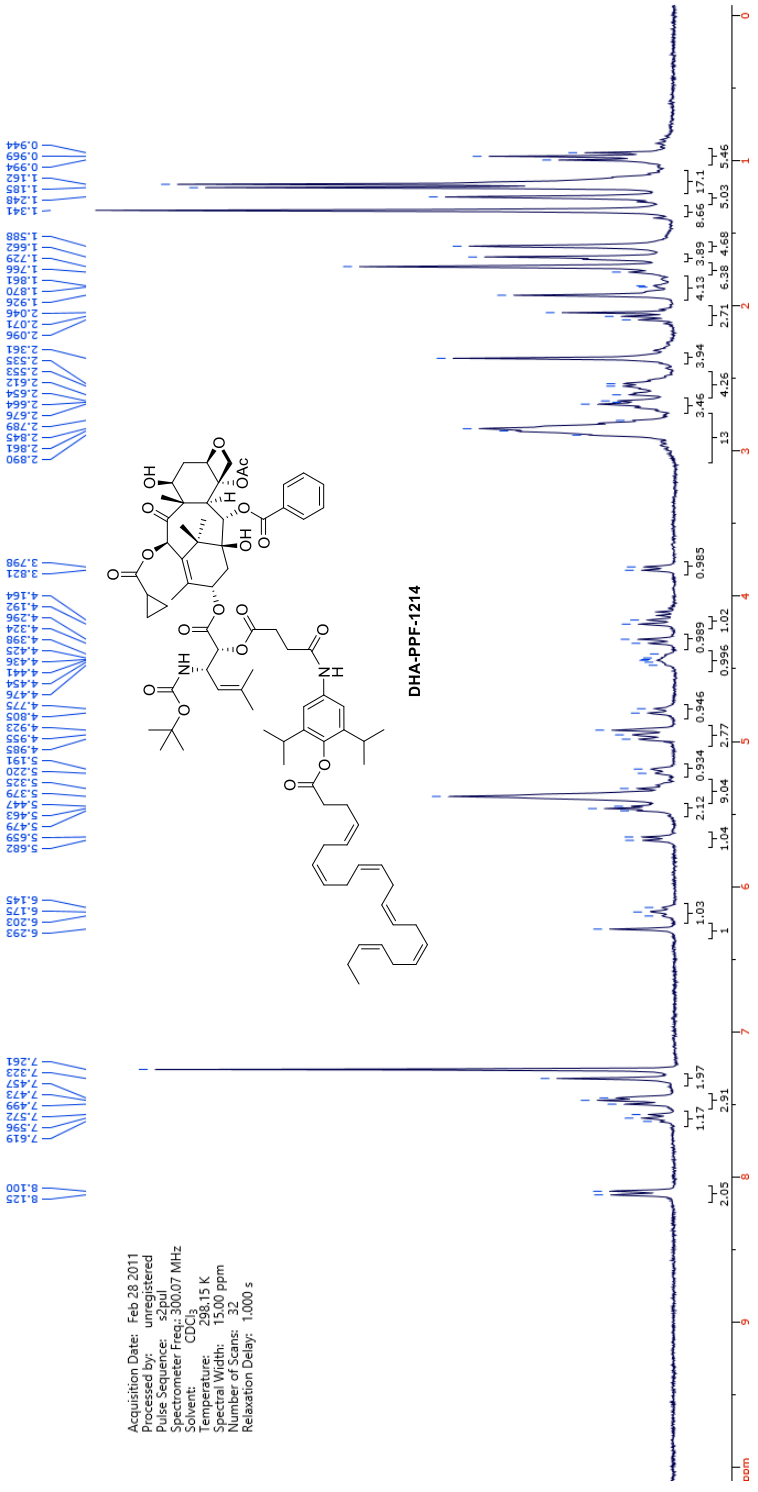
DHA-PPF-1214
Acquisition Date: Feb 28 2011
Processed by: unregistered
Pulse Sequence: s2pul
Spectrometer Freq.: 300.07 MHz
Solvent: CDCl3
Temperature: 298.15 K
Spectral Width: 15.00 ppm
Number of Scans: 32
Relaxation Delay: 1.000 s
ppm

Appendix Chapter 4

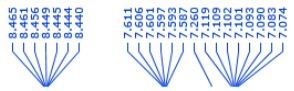

Acquisition Date: Jun 19 2009
Processed by: unregistered
Pulse Sequence: s2pul
Spectrometer Freq.: 300.07 MHz
Solvent: $CDCl_3$
Temperature: 298.15 K
Spectral Width: 15.00 ppm
Number of Scans: 16
Relaxation Delay: 1.000 s

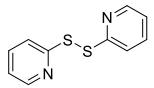

4-1

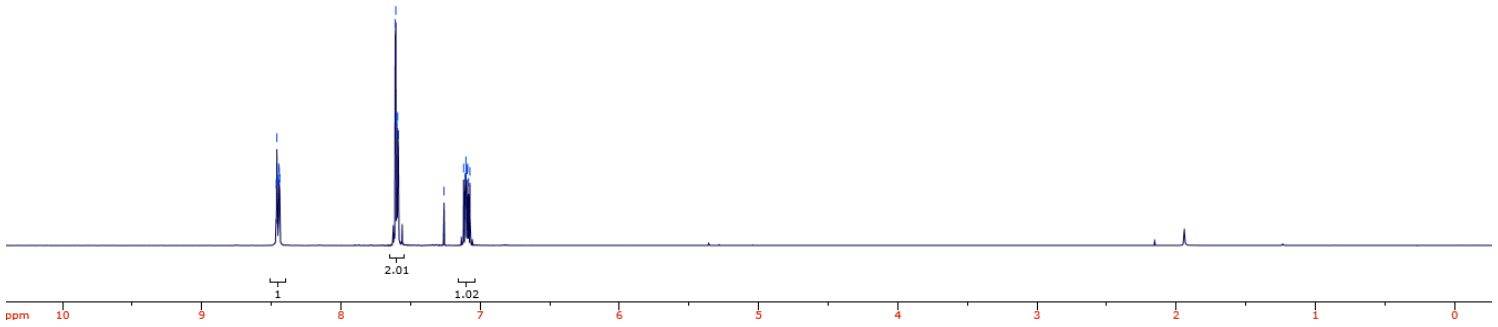

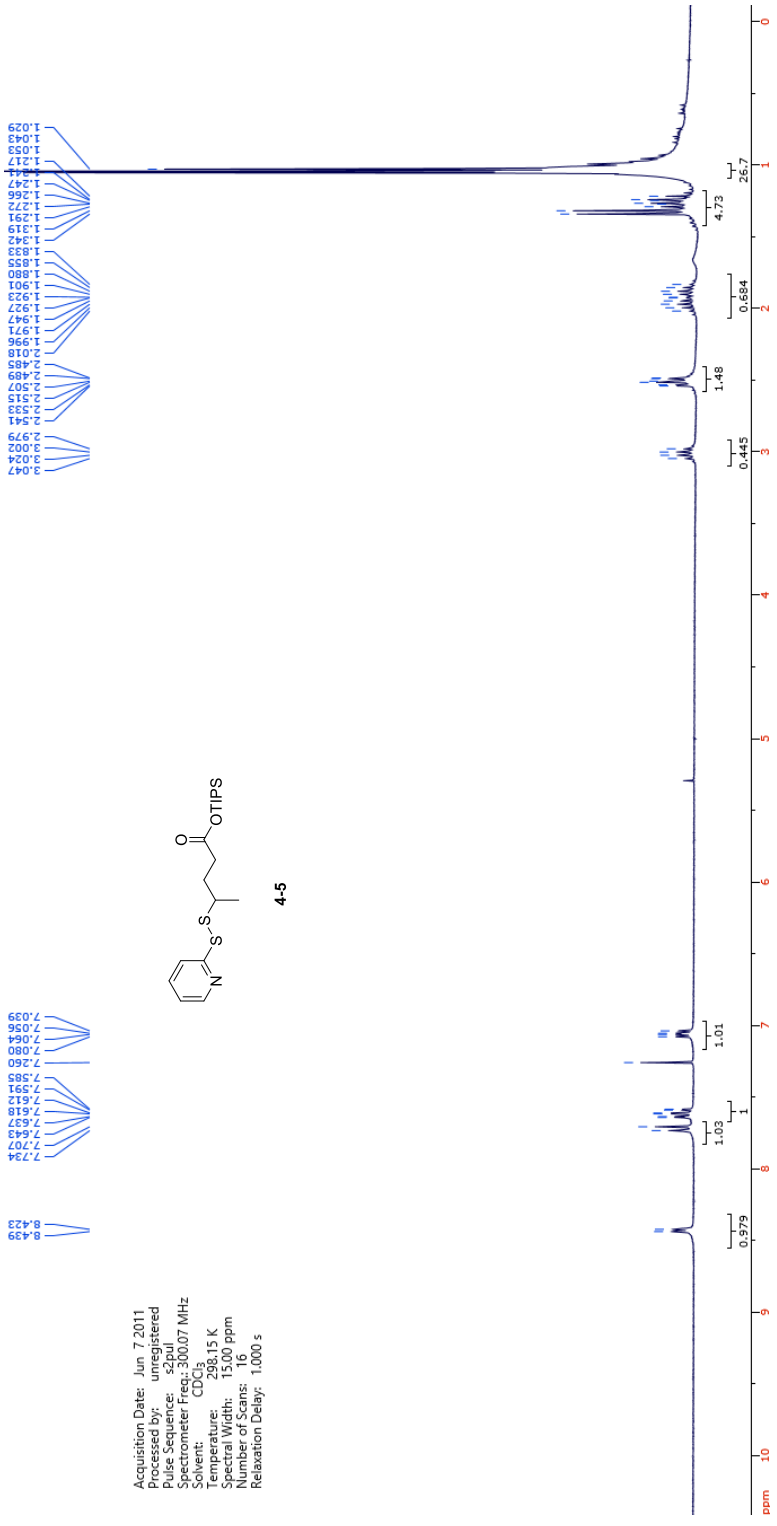
8.439
8.423
7.734
7.707
7.643
7.637
7.618
7.612
7.591
7.585
7.260
7.080
7.064
7.056
7.039
3.047
3.024
3.002
2.979
2.541
2.533
2.515
2.507
2.489
2.485
2.018
1.996
1.971
1.947
1.927
1.923
1.901
1.880
1.855
1.833
1.342
1.319
1.291
1.272
1.266
1.247
1.214
1.217
1.053
1.043
1.029
Acquisition Date: Jun 7 2011
Processed by: unregistered
Pulse Sequence: s2pul
Spectrometer Freq.: 300.07 MHz
Solvent: $CDCl_3$
Temperature: 298.15 K
Spectral Width: 15.00 ppm
Number of Scans: 16
Relaxation Delay: 1.000 s
OTIPS
4-5
0.979
1.03
1
1.01
1.48
0.445
4.73
0.684
26.7
ppm

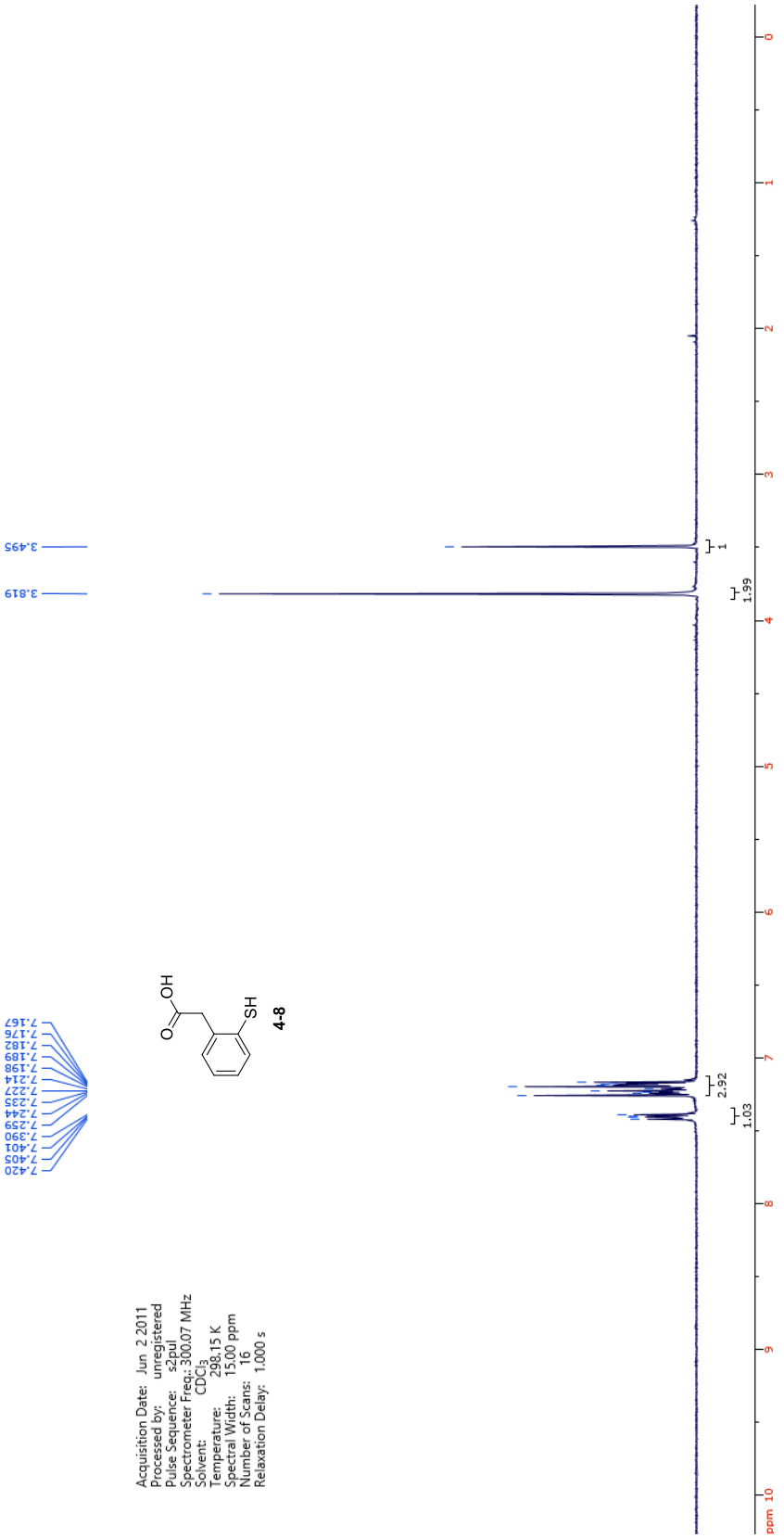
3.495
3.819
7.420
7.405
7.401
7.390
7.259
7.244
7.235
7.227
7.214
7.198
7.189
7.182
7.176
7.167
OH
O
SH
4-8
Acquisition Date: Jun 2 2011
Processed by: unregistered
Pulse Sequence: s2pul
Spectrometer Freq.: 300.07 MHz
Solvent: CDCl3
Temperature: 298.15 K
Spectral Width: 15.00 ppm
Number of Scans: 16
Relaxation Delay: 1.000 s
1
1.99
2.92
1.03
ppm

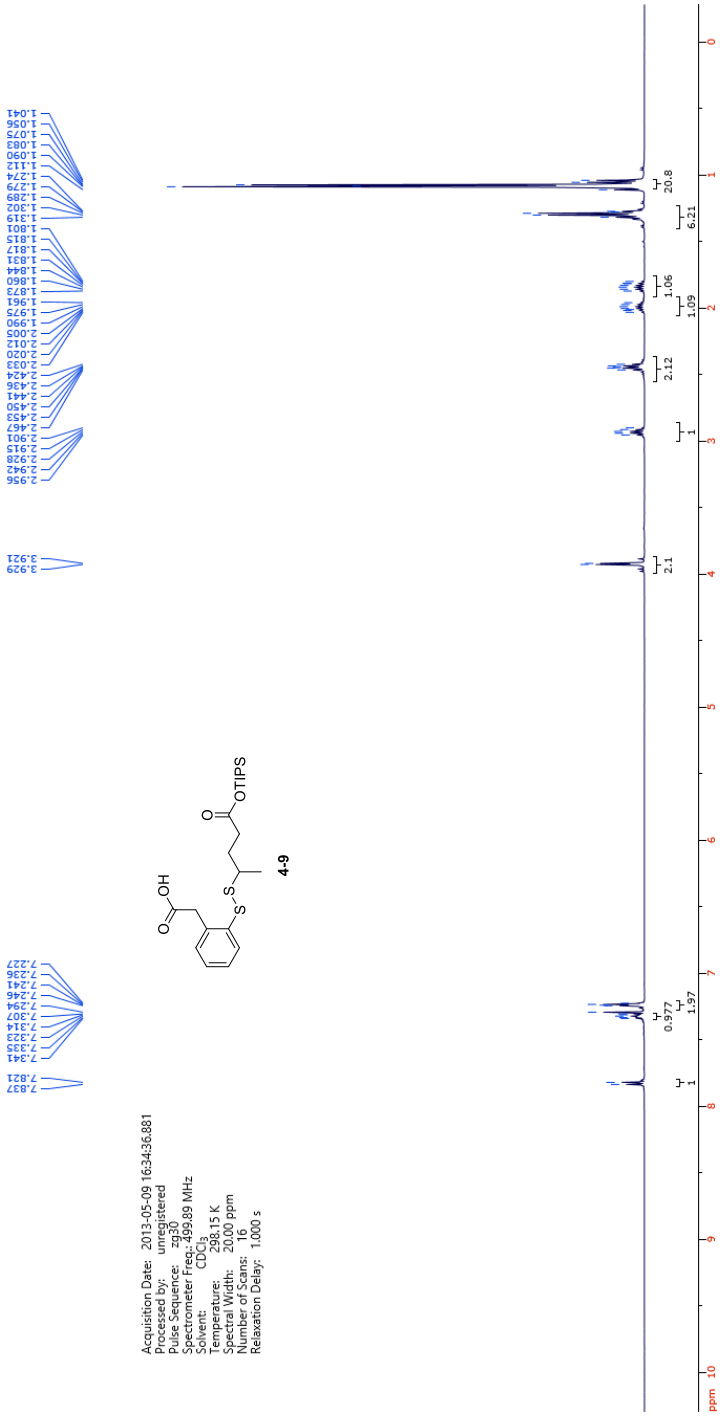
Acquisition Date: 2013-05-09 16:34:36.881
Processed by: unmastered
Pulse Sequence: zg30
Spectrometer Freq.: 499.89 MHz
Solvent: $CDCl_3$
Temperature: 298.15 K
Spectral Width: 20.00 ppm
Number of Scans: 16
Relaxation Delay: 1.000 s
OH
O
S
S
O
O
OTIPS
4-9
ppm

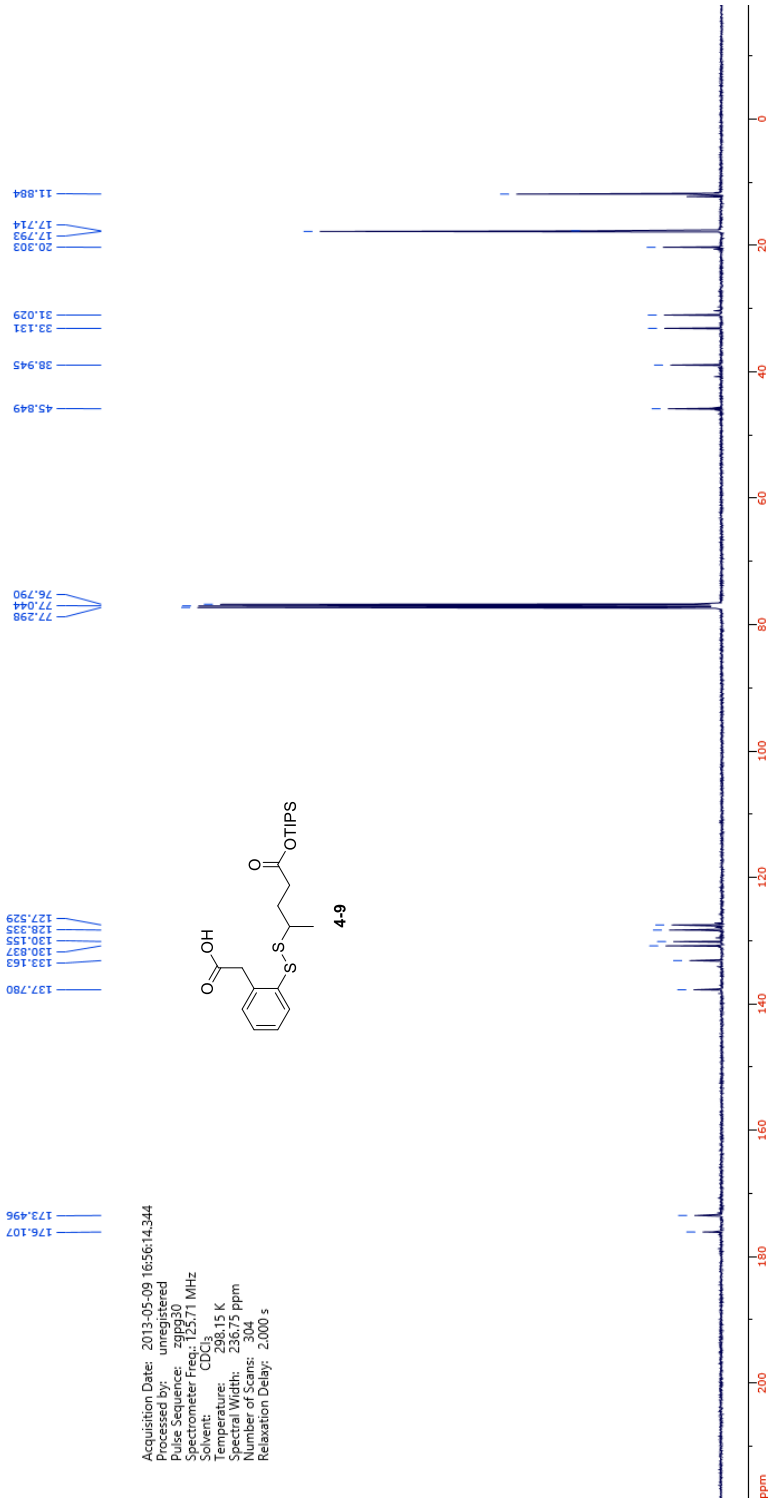
11.884
17.714
17.793
20.303
31.029
33.131
38.945
45.849
76.790
77.044
77.298
127.529
128.335
130.159
130.837
133.163
137.780
173.496
176.107
Acquisition Date: 2013-05-09 16:56:14.344
Processed by: unregistered
Pulse Sequence: zgpg30
Spectrometer Freq.: 125.71 MHz
Solvent: CDCl3
Temperature: 298.15 K
Spectral Width: 236.75 ppm
Number of Scans: 304
Relaxation Delay: 2.000 s
OH
O
S
S
O
O
OTIPS
4-9
ppm

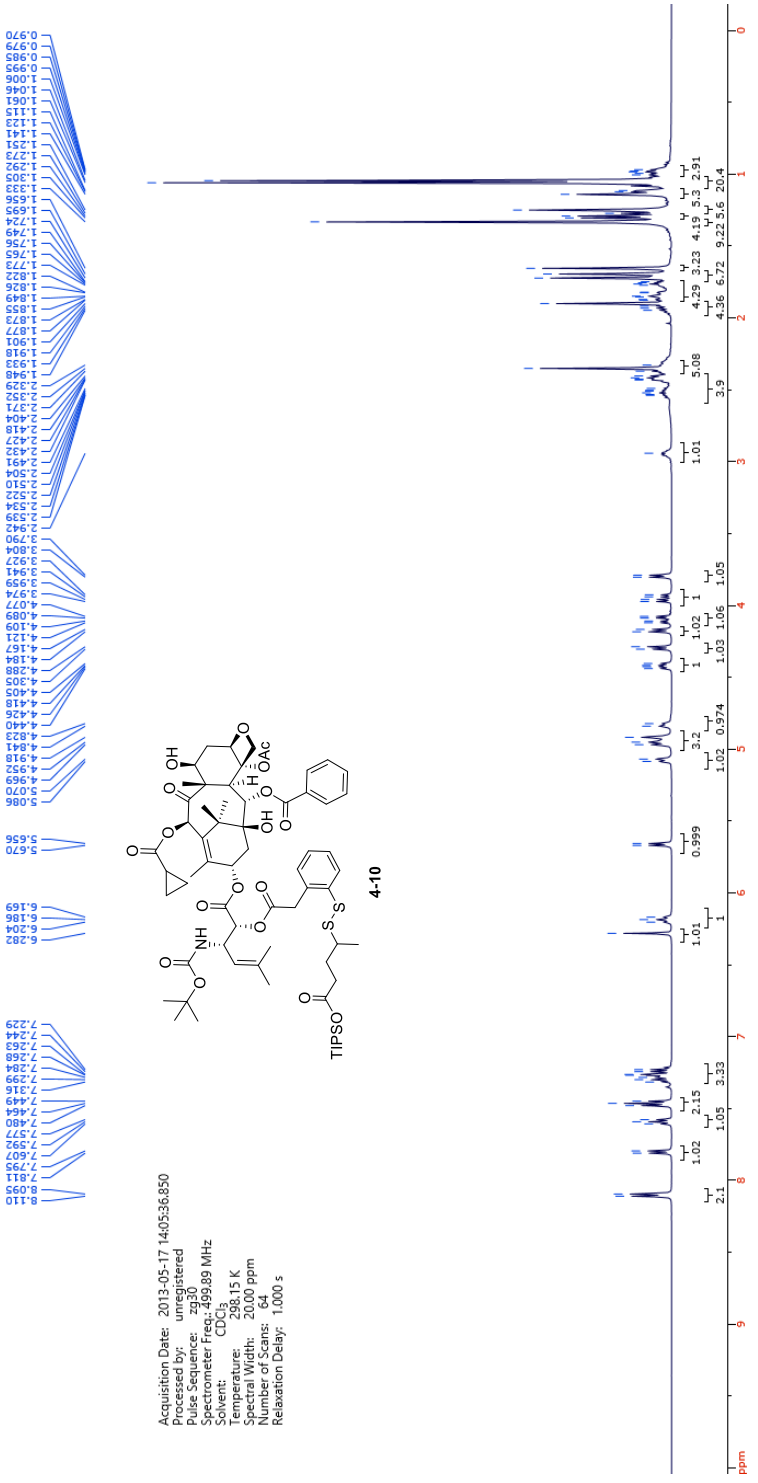
Acquisition Date: 2013-05-17 14:05:36.850
Processed by: unregistered
Pulse Sequence: zg30
Spectrometer Freq.: 499.89 MHz
Solvent: $CDCl_3$
Temperature: 298.15 K
Spectral Width: 20.00 ppm
Number of Scans: 64
Relaxation Delay: 1.000 s
4-10
TIPSO
ppm

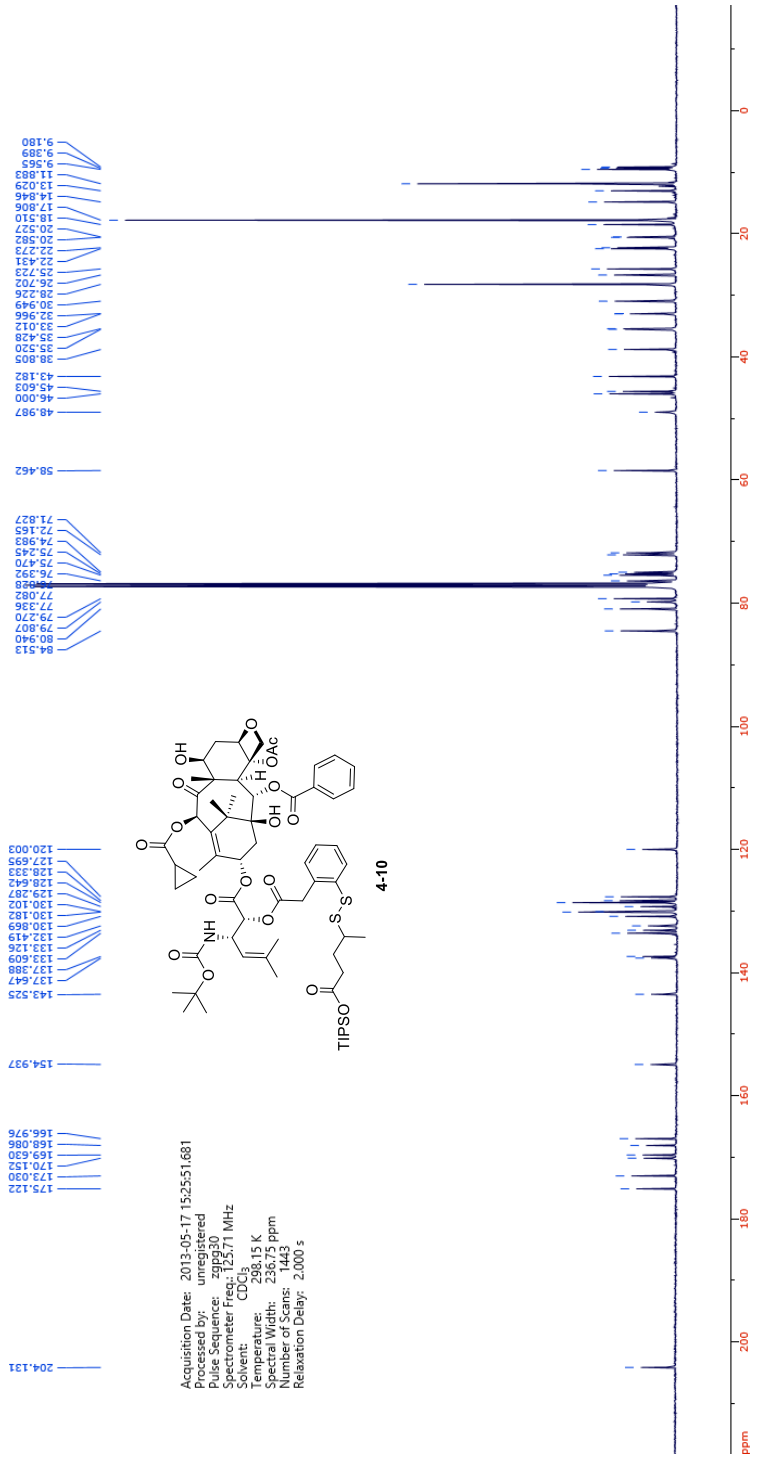
9.180
9.389
9.563
11.883
13.029
14.846
17.806
18.510
20.527
20.582
22.273
22.431
25.723
26.702
28.226
30.949
32.966
33.012
35.428
35.520
38.805
43.182
45.603
46.000
48.987
58.462
71.827
72.165
74.983
75.245
75.470
76.392
77.082
79.270
79.807
80.940
84.513
120.003
127.693
128.333
128.642
129.287
130.102
130.182
130.869
132.419
133.126
133.609
137.388
137.647
143.525
154.937
166.976
168.086
169.630
170.152
173.030
175.122
204.131
Acquisition Date: 2013-05-17 15:25:51.681
Processed by: unregistered
Pulse Sequence: zgpg30
Spectrometer Freq.: 125.71 MHz
Solvent: CDCl3
Temperature: 298.15 K
Spectral Width: 236.75 ppm
Number of Scans: 1443
Relaxation Delay: 2.000 s
4-10
0
20
40
60
80
100
120
140
160
180
200
ppm

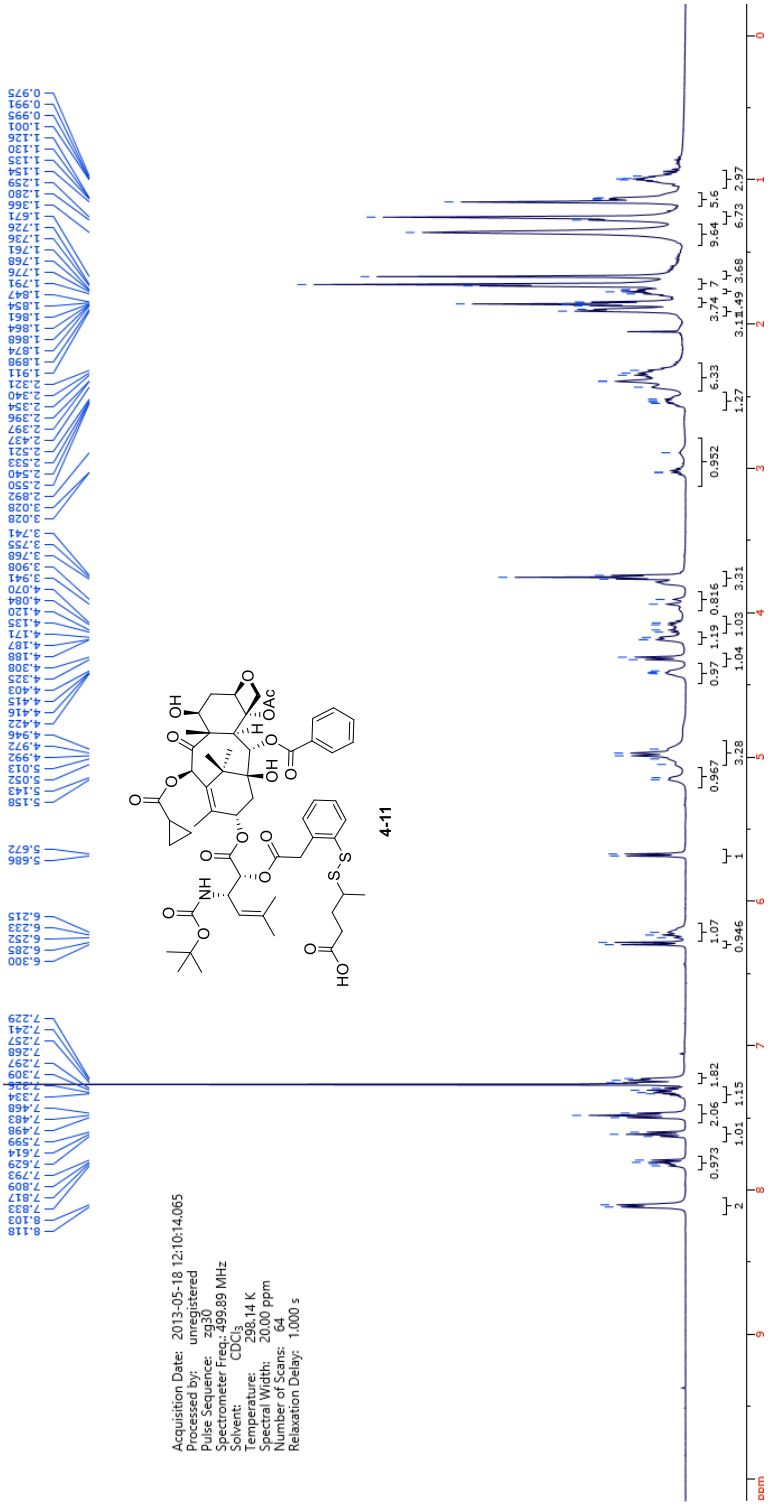
Acquisition Date: 2013-05-18 12:10:14.065
Processed by: unregistered
Pulse Sequence: zg30
Spectrometer Freq.: 499.89 MHz
Solvent: $CDCl_3$
Temperature: 298.14 K
Spectral Width: 20.00 ppm
Number of Scans: 64
Relaxation Delay: 1.000 s
4-11
ppm

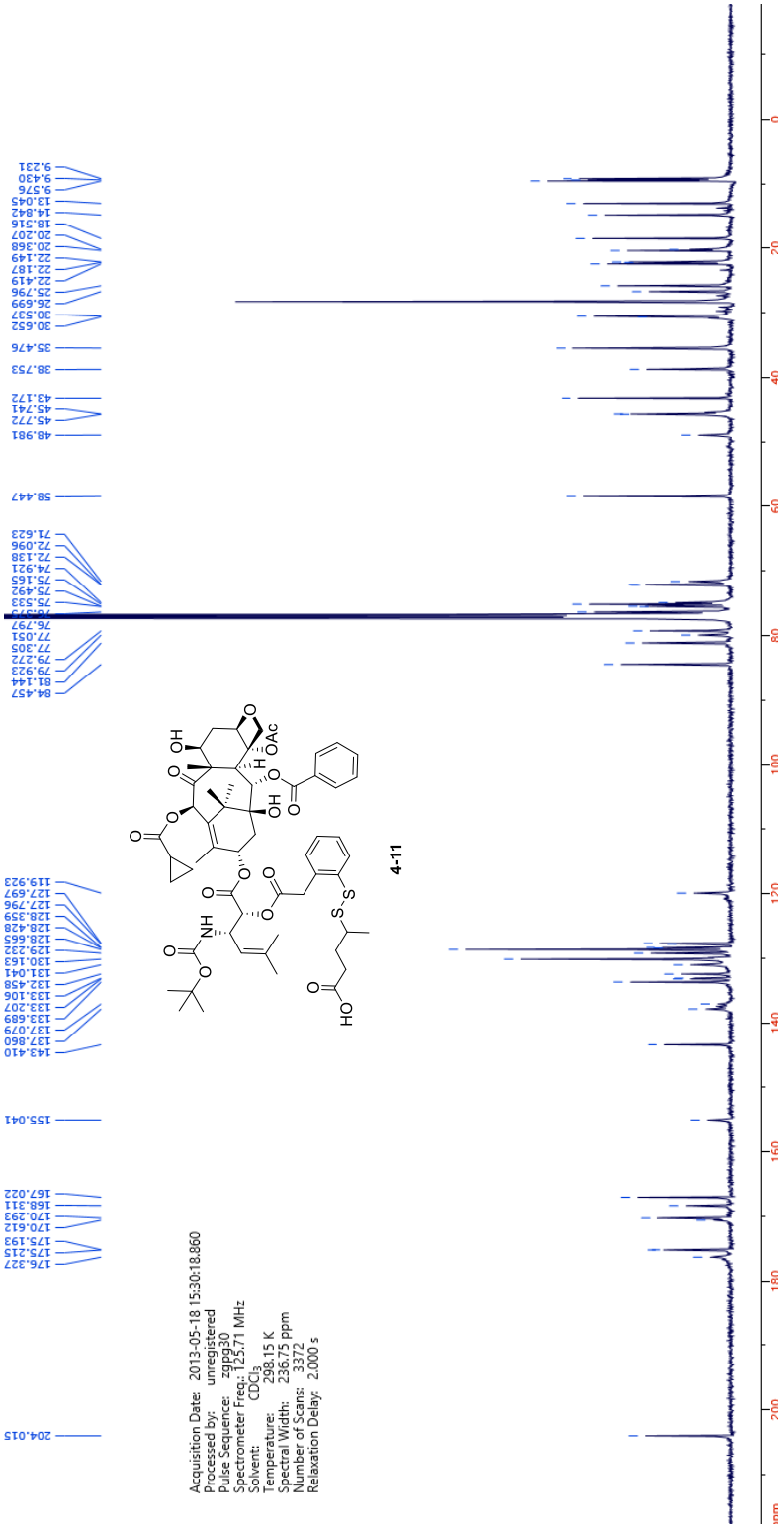
4-11
Acquisition Date: 2013-05-18 15:30:18.860
Processed by: unregistered
Pulse Sequence: zgpg30
Spectrometer Freq.: 125.71 MHz
Solvent: $CDCl_3$
Temperature: 298.15 K
Spectral Width: 236.75 ppm
Number of Scans: 3372
Relaxation Delay: 2.000 s

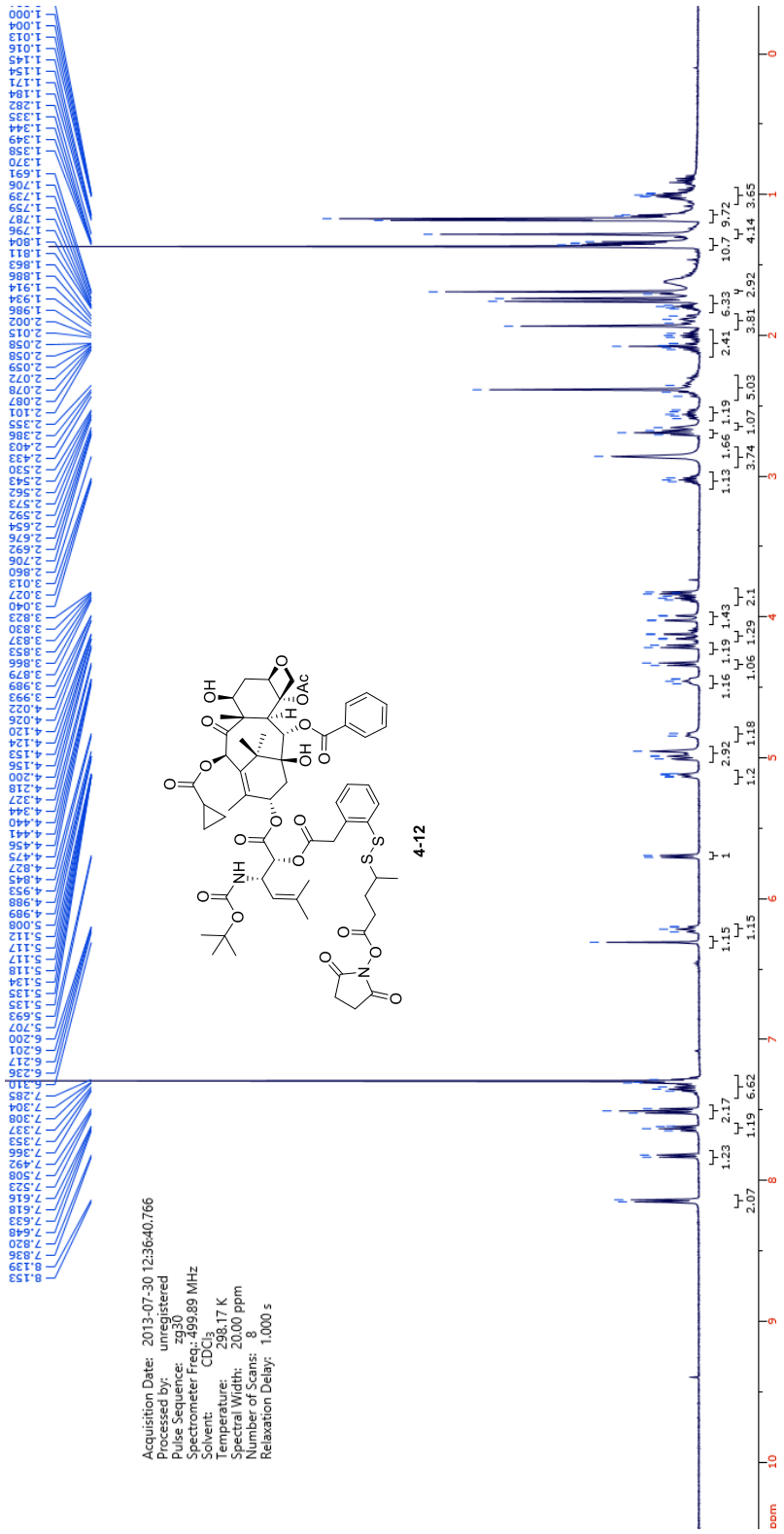
Acquisition Date: 2013-07-30 12:36:40.766
Processed by: unregistered
Pulse Sequence: zg30
Spectrometer Freq.: 499.89 MHz
Solvent: $CDCl_3$
Temperature: 298.17 K
Spectral Width: 20.00 ppm
Number of Scans: 8
Relaxation Delay: 1.000 s
4-12

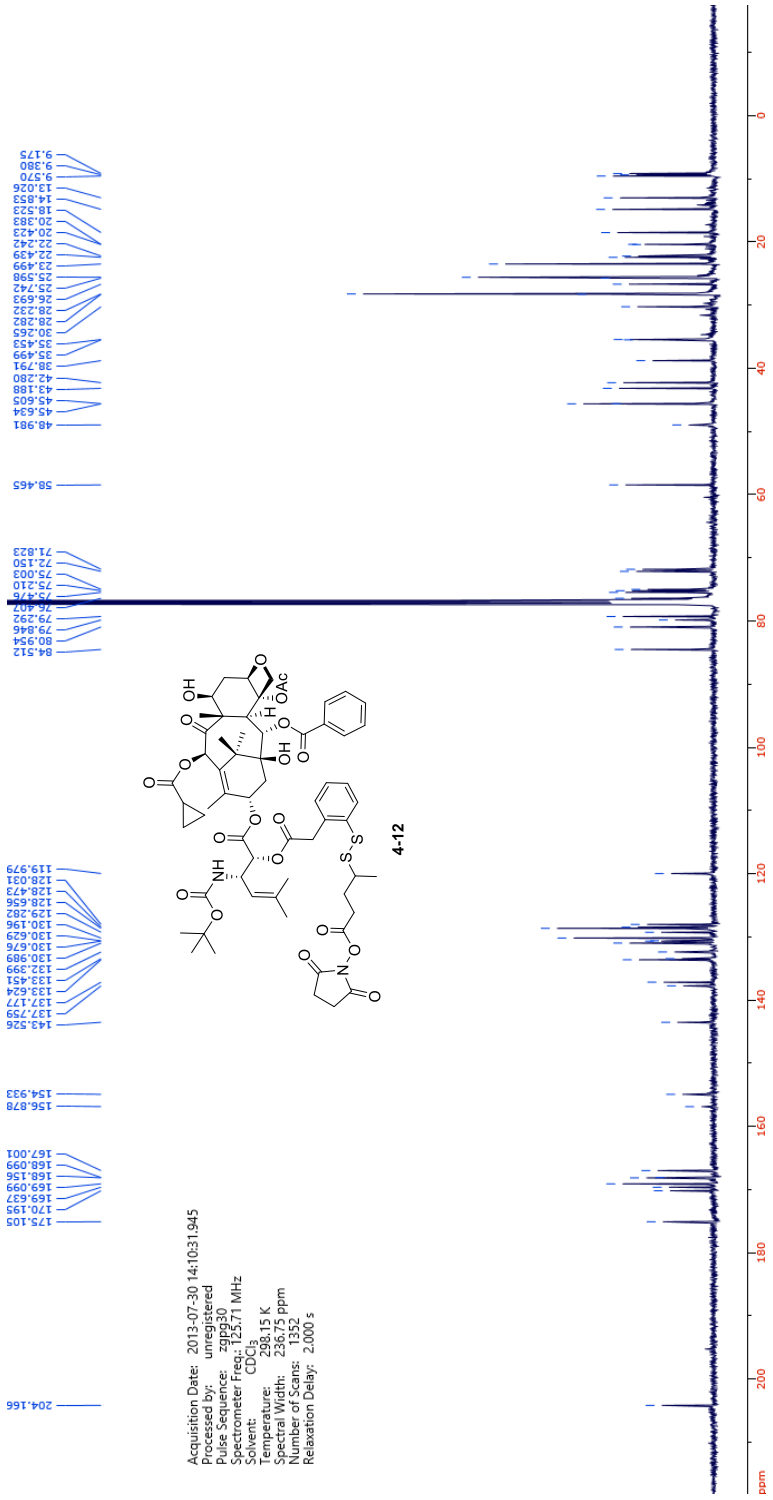
Acquisition Date: 2013-07-30 14:10:31.945
Processed by: unregistered
Pulse Sequence: zgpg30
Spectrometer Freq.: 125.71 MHz
Solvent: $CDCl_3$
Temperature: 298.15 K
Spectral Width: 236.75 ppm
Number of Scans: 1352
Relaxation Delay: 2.000 s
4-12
ppm

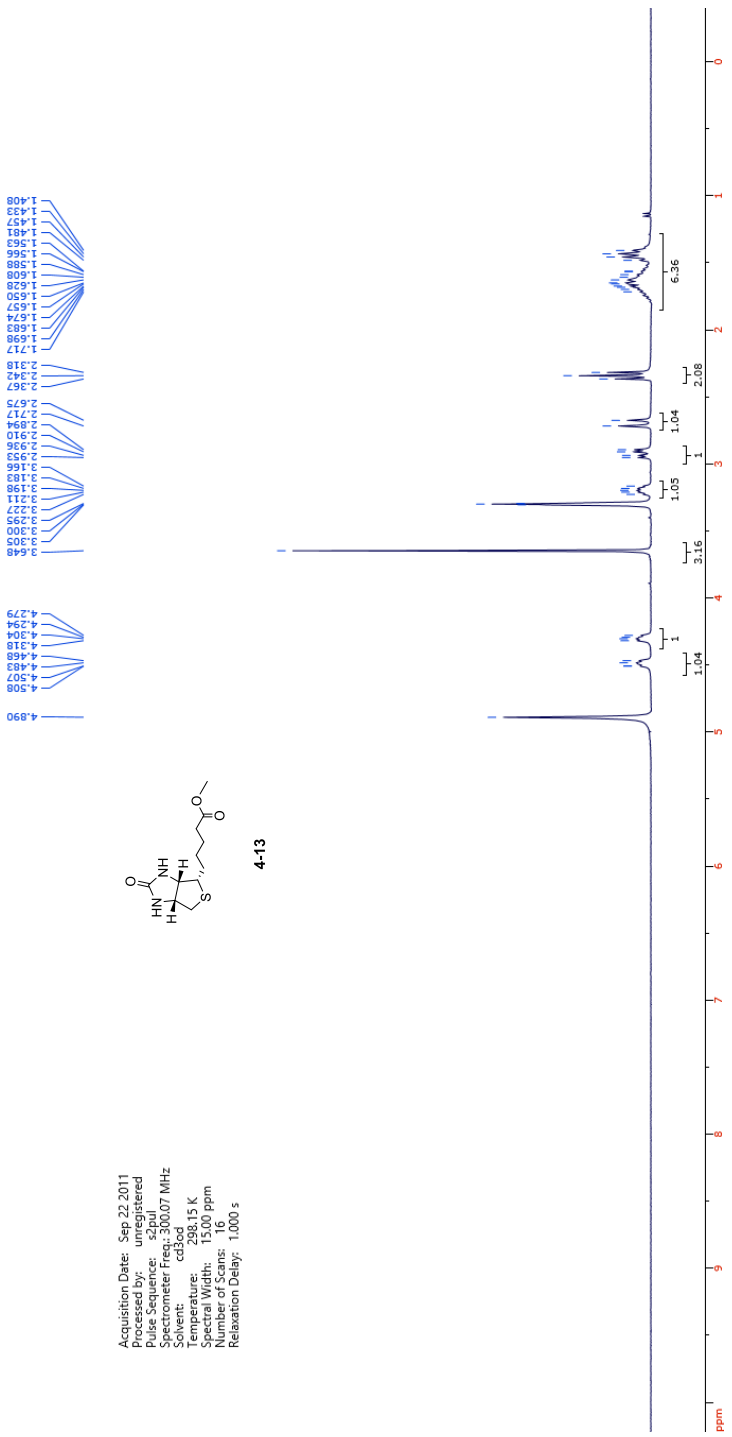
1.408
1.433
1.457
1.481
1.563
1.566
1.588
1.608
1.628
1.650
1.657
1.674
1.683
1.698
1.717
2.318
2.342
2.367
2.675
2.717
2.894
2.910
2.936
2.953
3.166
3.183
3.198
3.211
3.227
3.295
3.300
3.305
3.648
4.279
4.294
4.304
4.318
4.468
4.483
4.507
4.508
4.890
1
1.04
3.16
1.05
1
1.04
2.08
6.36
ppm
Acquisition Date: Sep 22 2011
Processed by: unregistered
Pulse Sequence: s2pul
Spectrometer Freq.: 300.07 MHz
Solvent: cd3od
Temperature: 298.15 K
Spectral Width: 15.00 ppm
Number of Scans: 16
Relaxation Delay: 1.000 s
4-13

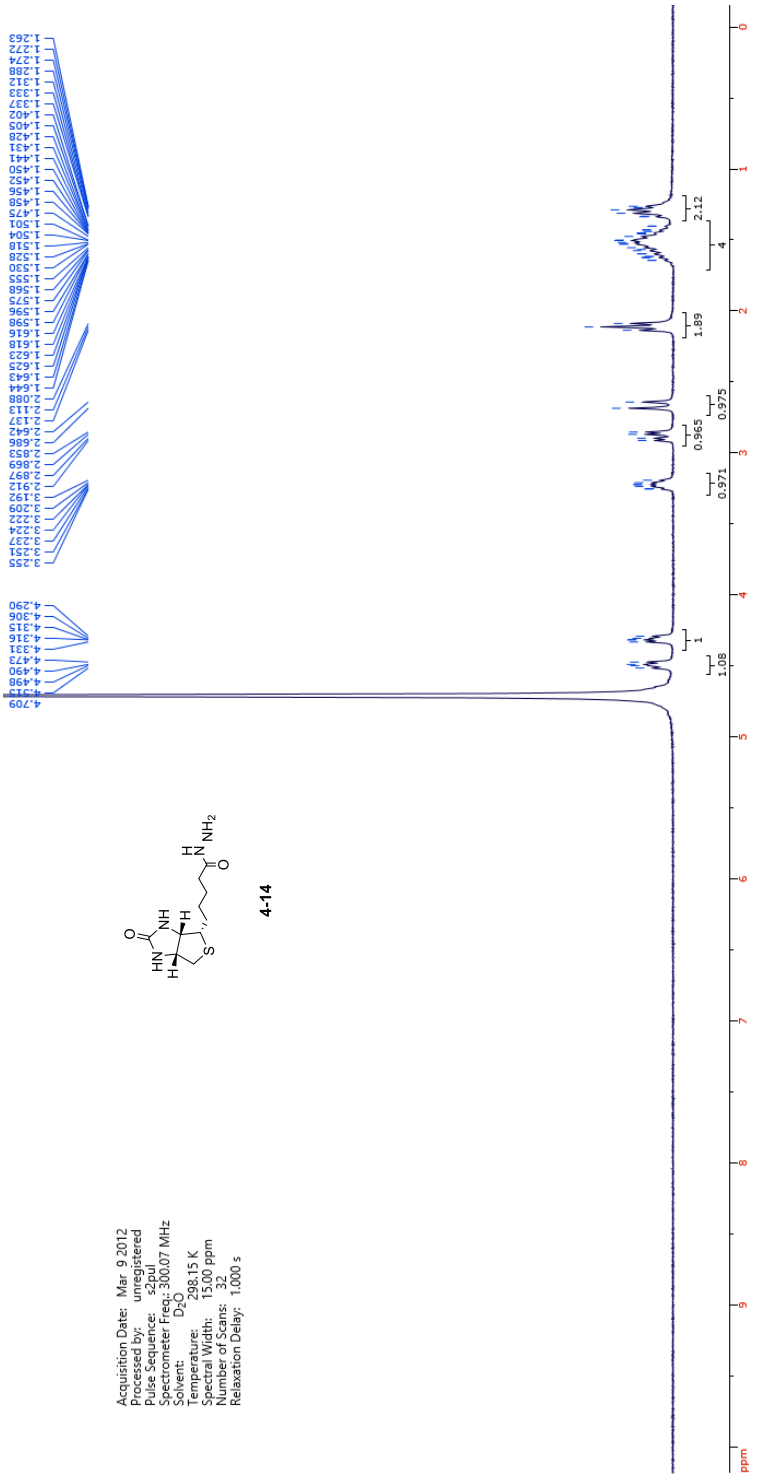
Acquisition Date: Mar 9 2012
Processed by: unregistered
Pulse Sequence: s2pul
Spectrometer Freq.: 300.07 MHz
Solvent: D2O
Temperature: 298.15 K
Spectral Width: 15.00 ppm
Number of Scans: 32
Relaxation Delay: 1.000 s
4-14
ppm

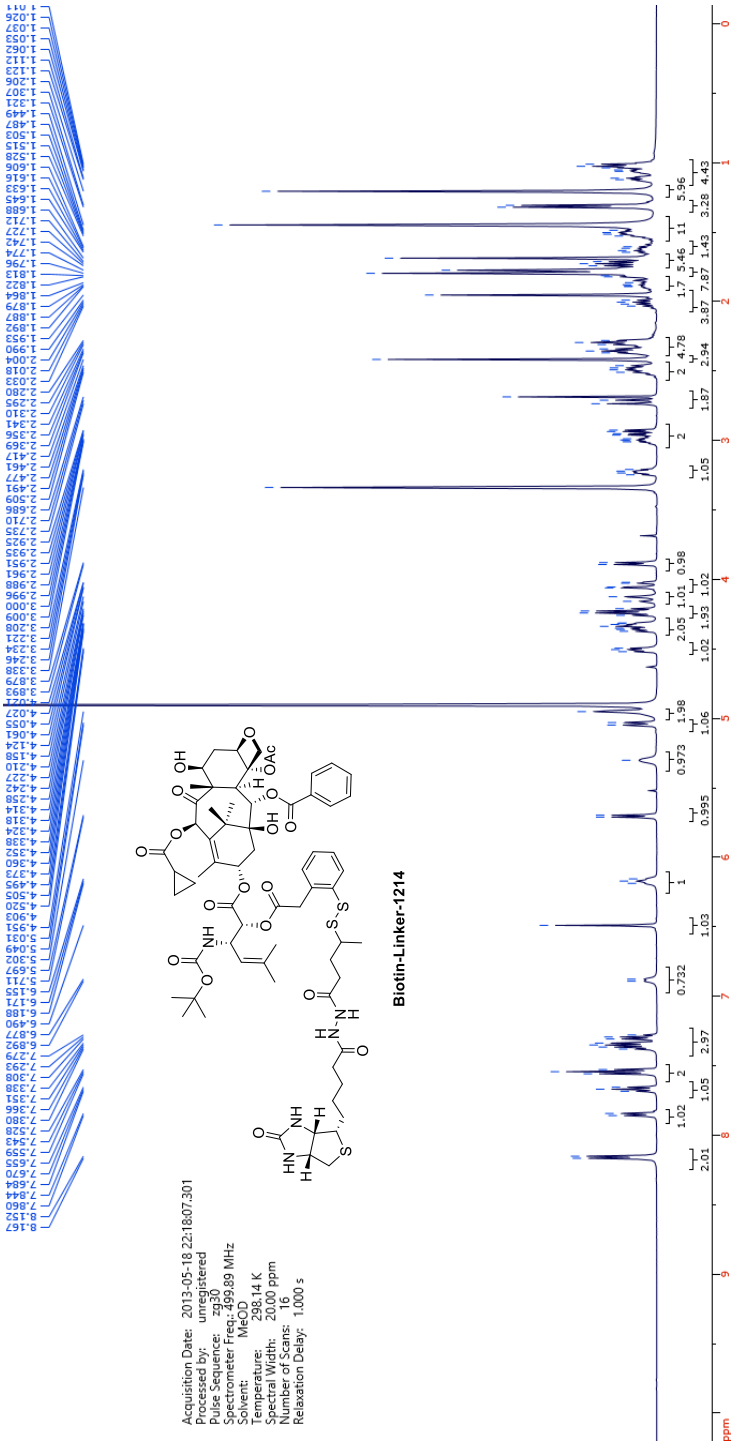
Biotin-Linker-1214
Acquisition Date: 2013-05-18 22:18:07.301
Processed by: unregistered
Pulse Sequence: zg30
Spectrometer Freq.: 499.89 MHz
Solvent: MeOD
Temperature: 298.14 K
Spectral Width: 20.00 ppm
Number of Scans: 16
Relaxation Delay: 1.000 s
ppm

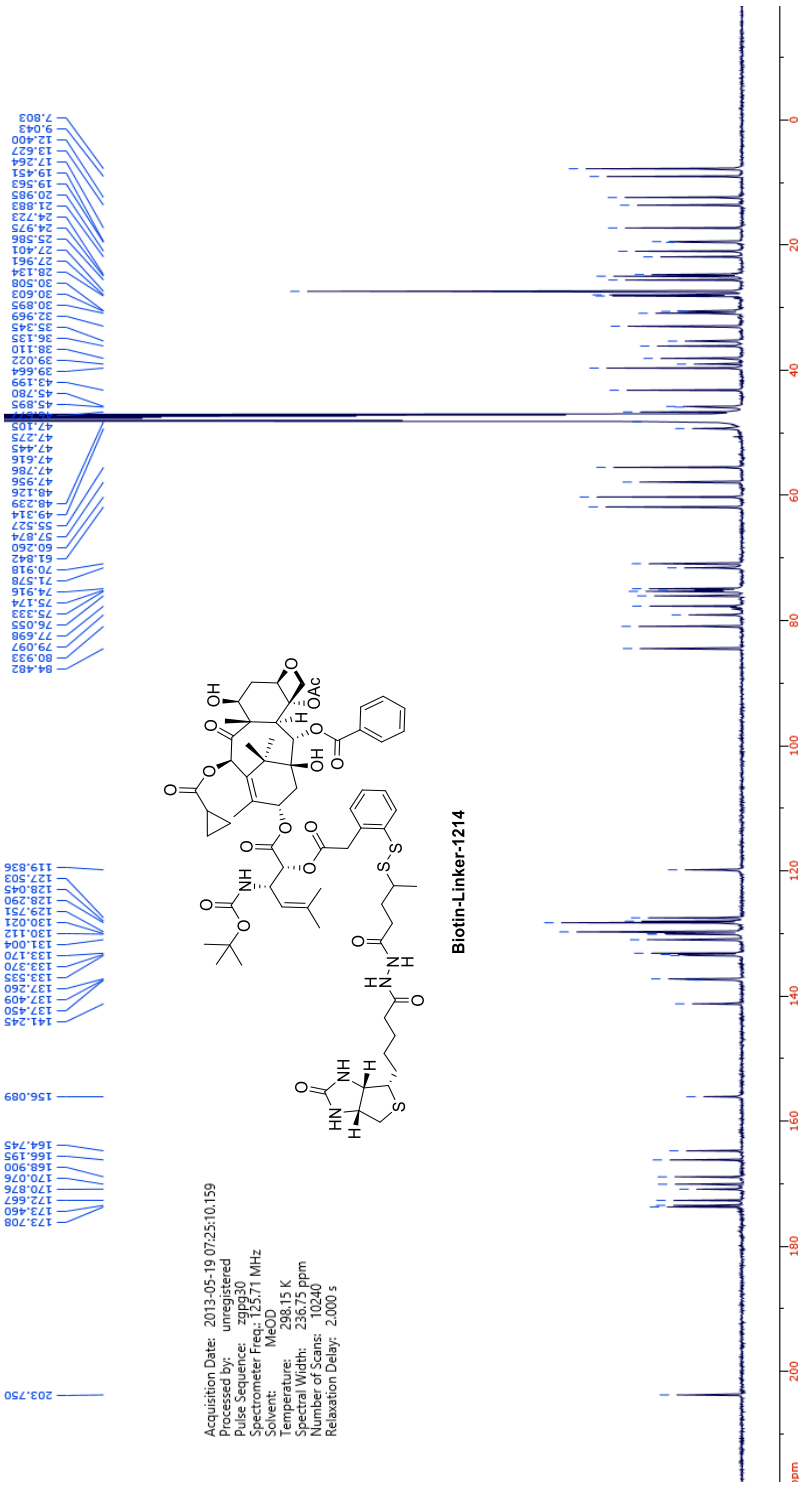
Biotin-Linker-1214
Acquisition Date: 2013-05-19 07:25:10.159
Processed by: unregistered
Pulse Sequence: zgpg30
Spectrometer Freq.: 125.71 MHz
Solvent: MeOD
Temperature: 298.15 K
Spectral Width: 236.73 ppm
Number of Scans: 10240
Relaxation Delay: 2.000 s

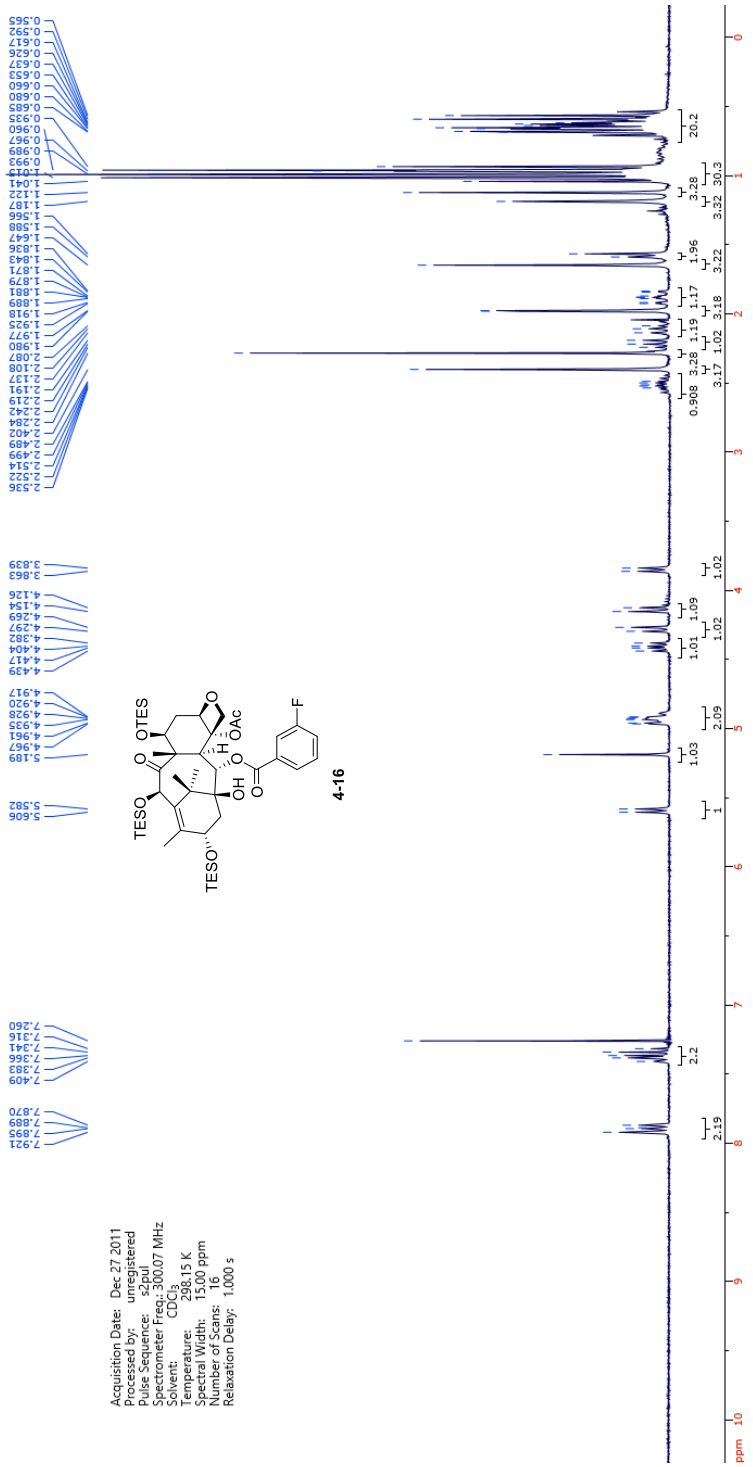
Acquisition Date: Dec 27 2011
Processed by: unregistered
Pulse Sequence: s2pul
Spectrometer Freq.: 300.07 MHz
Solvent: CDCl3
Temperature: 298.15 K
Spectral Width: 15.00 ppm
Number of Scans: 16
Relaxation Delay: 1.000 s
TESO
OTES
OAc
OH
TESO
F
4-16

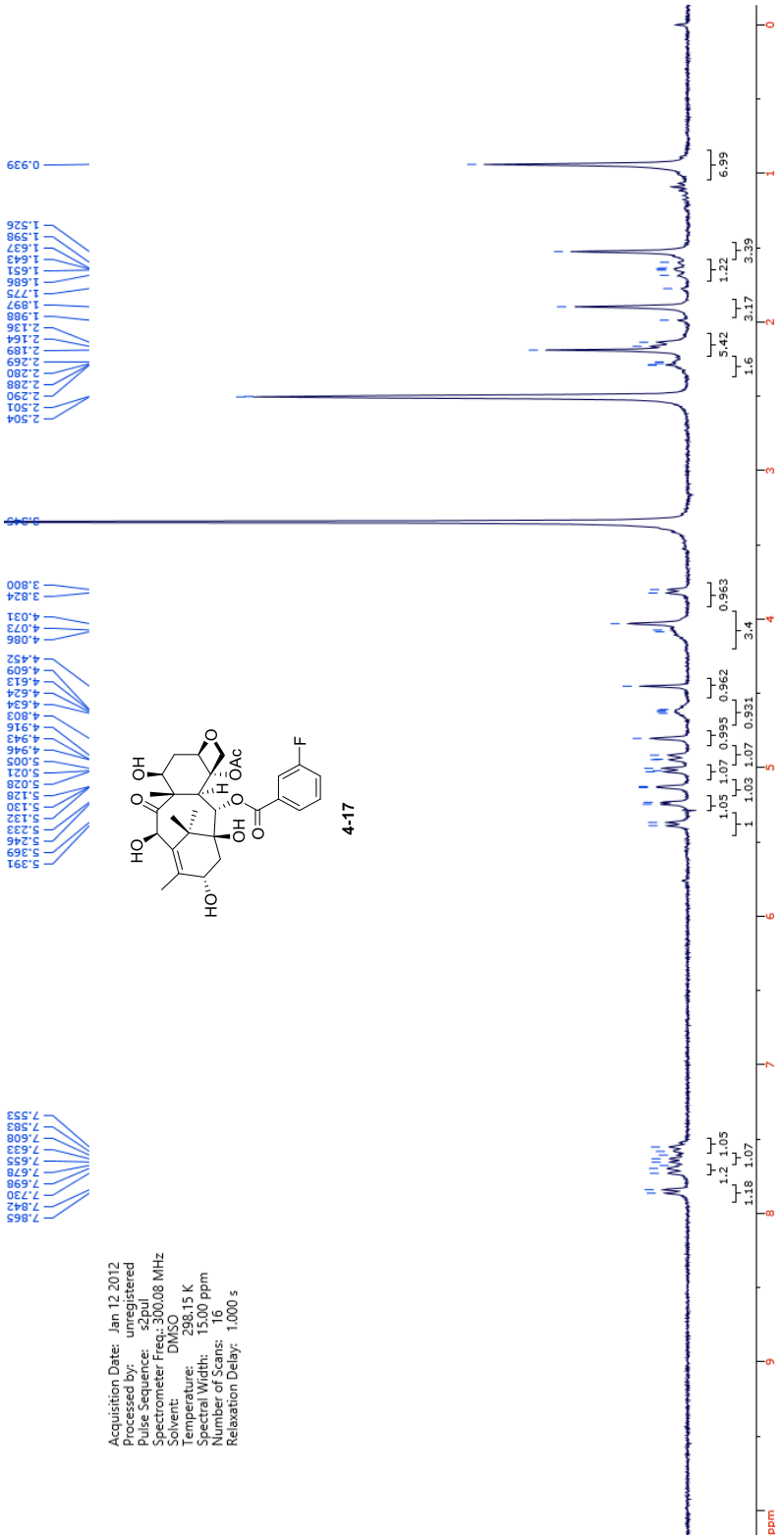
Acquisition Date: Jan 12 2012
Processed by: unregistered
Pulse Sequence: s2pul
Spectrometer Freq.: 300.08 MHz
Solvent: DMSO
Temperature: 298.15 K
Spectral Width: 15.00 ppm
Number of Scans: 16
Relaxation Delay: 1.000 s
4-17
ppm

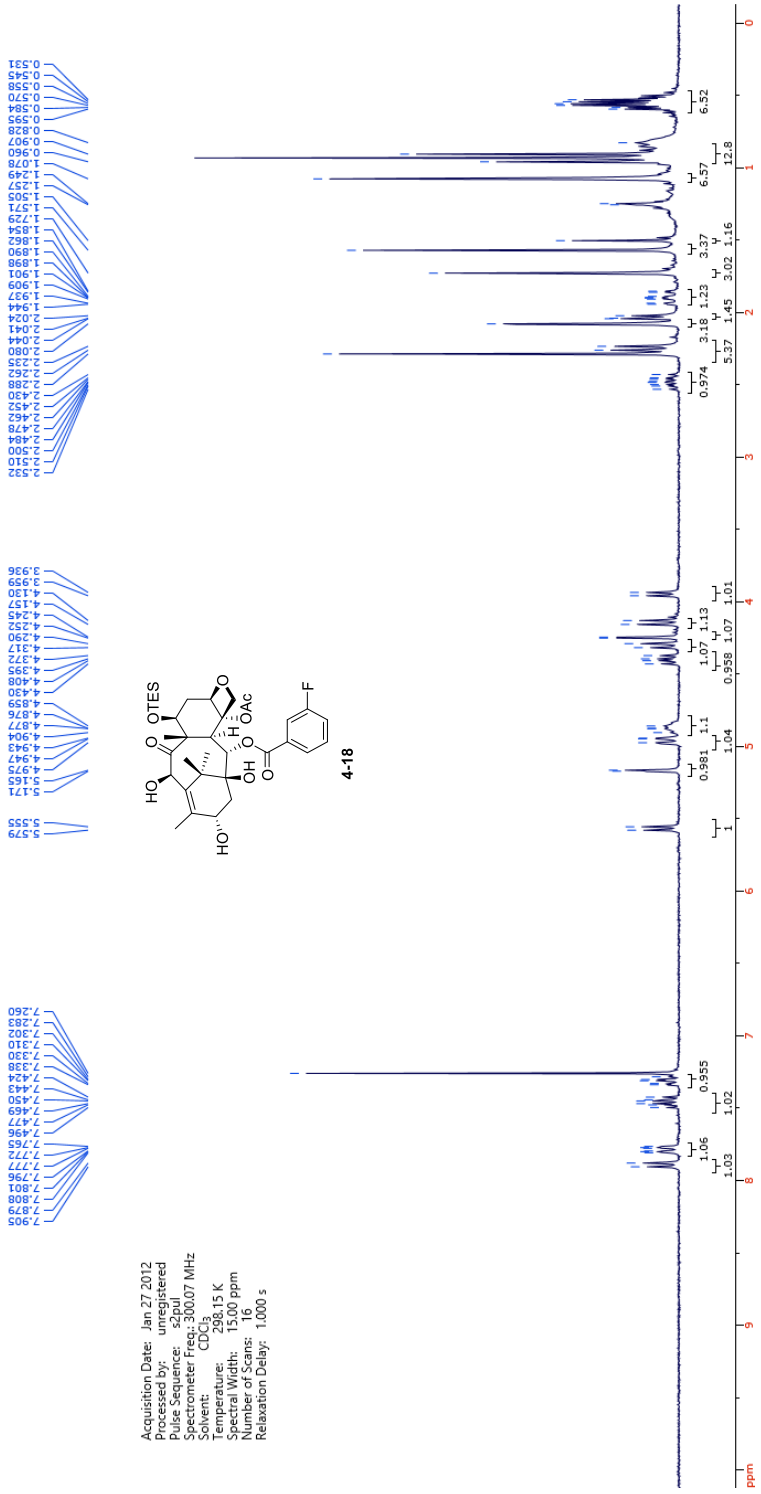
Acquisition Date: Jan 27 2012
Processed by: unregistered
Pulse Sequence: s2pul
Spectrometer Freq.: 300.07 MHz
Solvent: $CDCl_3$
Temperature: 298.15 K
Spectral Width: 15.00 ppm
Number of Scans: 16
Relaxation Delay: 1.000 s
4-18
ppm

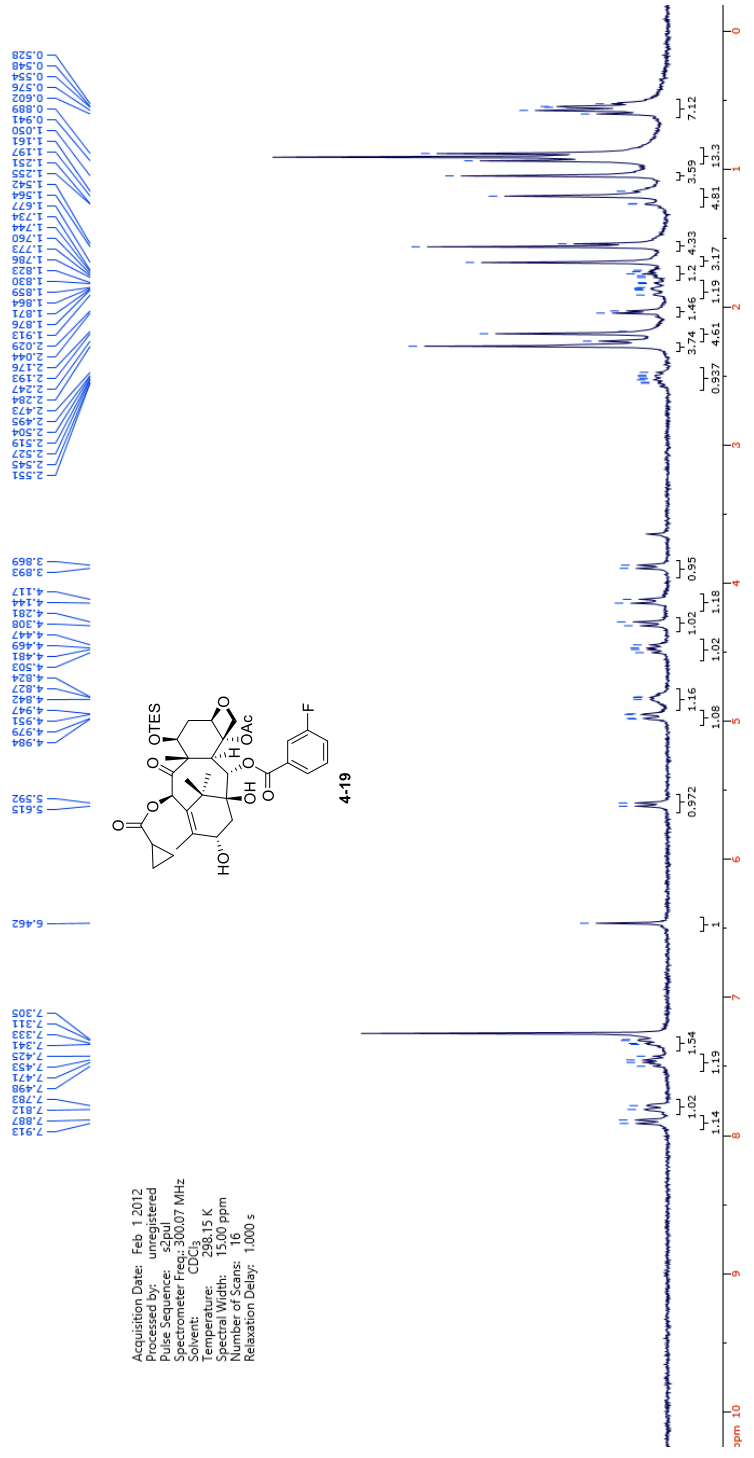
Acquisition Date: Feb 1 2012
Processed by: unregistered
Pulse Sequence: s2pul
Spectrometer Freq.: 300.07 MHz
Solvent: $CDCl_3$
Temperature: 298.15 K
Spectral Width: 15.00 ppm
Number of Scans: 16
Relaxation Delay: 1.000 s
OTES
OAc
OH
HO
F
4-19

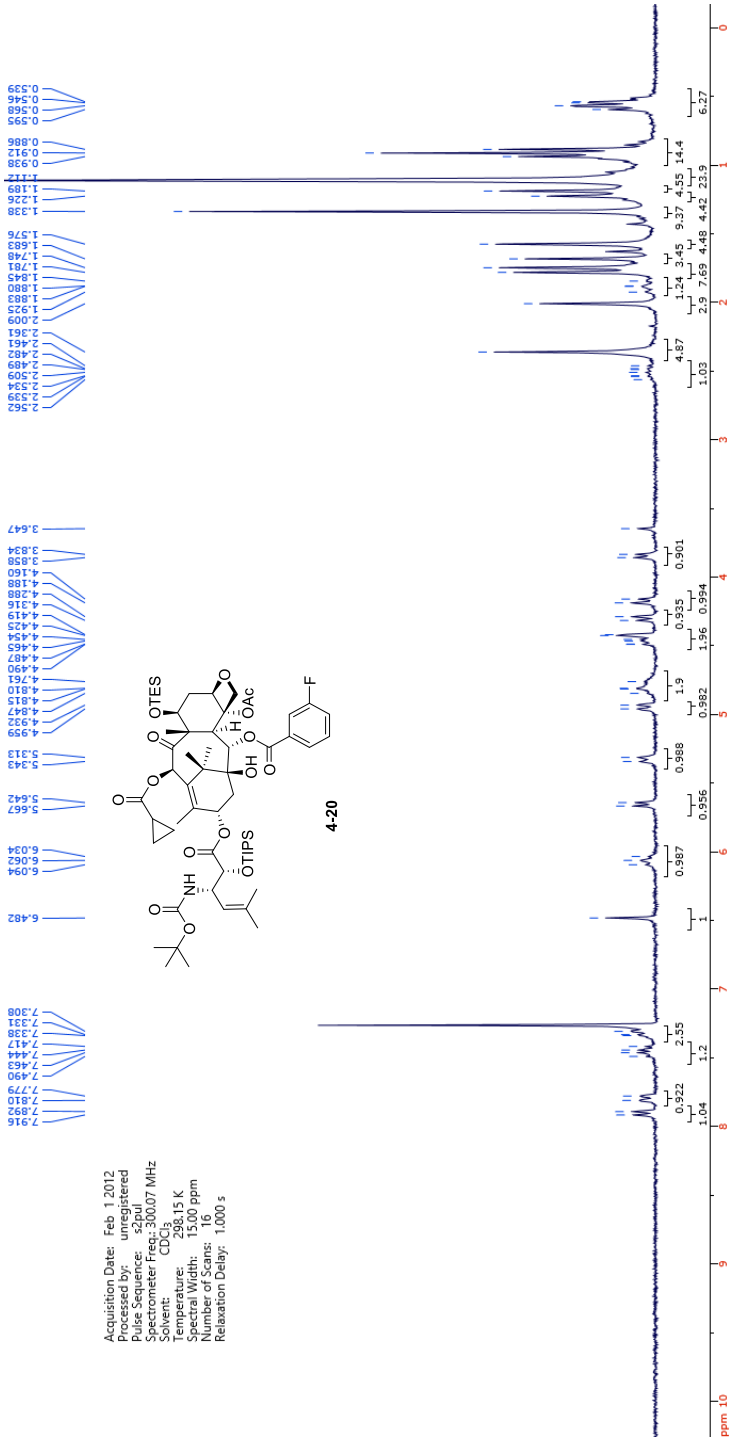
Acquisition Date: Feb 1 2012
Processed by: unregistered
Pulse Sequence: s2pul
Spectrometer Freq.: 300.07 MHz
Solvent: $CDCl_3$
Temperature: 298.15 K
Spectral Width: 15.00 ppm
Number of Scans: 16
Relaxation Delay: 1.000 s
OTES
OAc
OH
ÖTIPS
NH
F
4-20
ppm

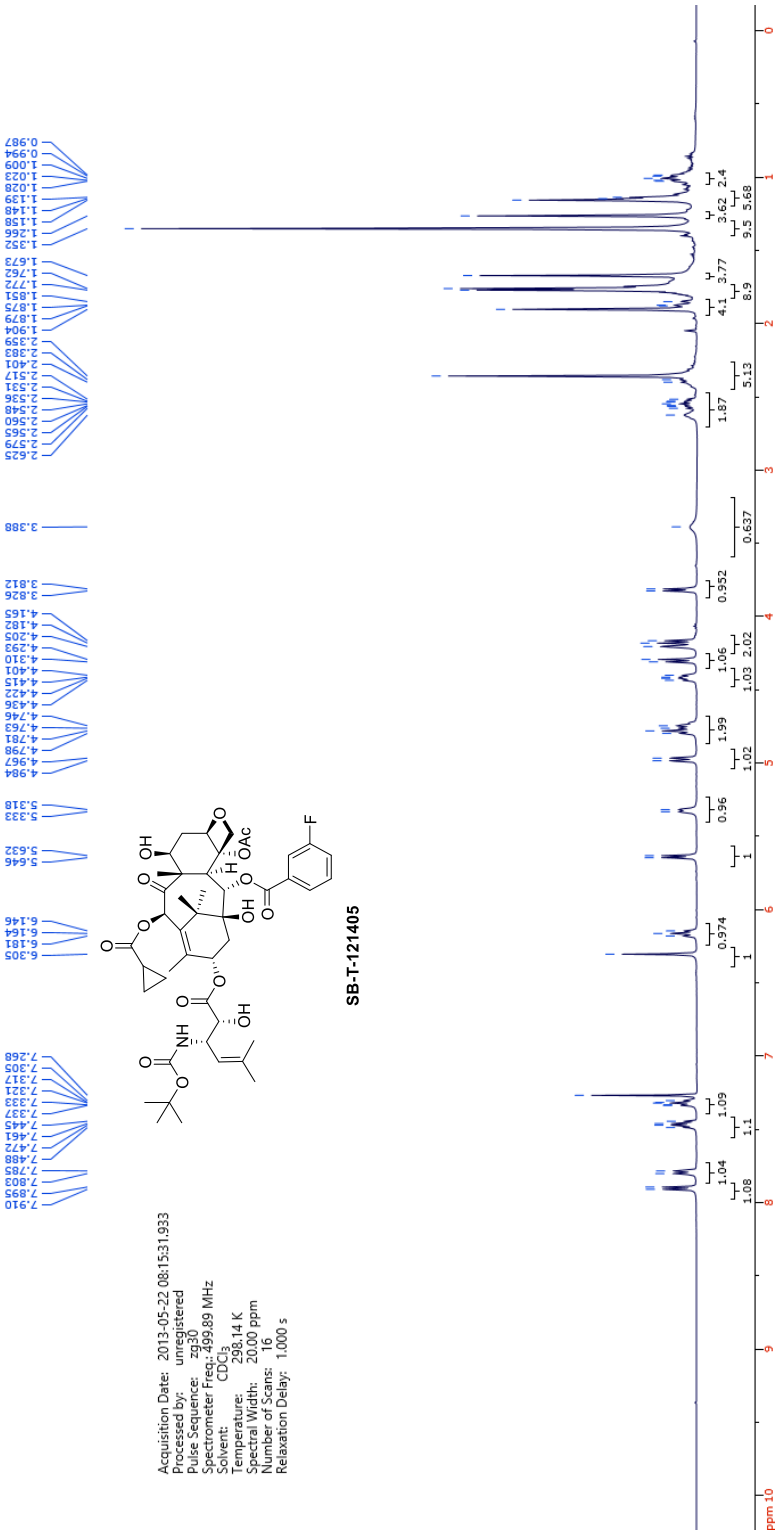
SB-T-121405
Acquisition Date: 2013-05-22 08:15:31.933
Processed by: unregistered
Pulse Sequence: zg30
Spectrometer Freq.: 499.89 MHz
Solvent: $CDCl_3$
Temperature: 298.14 K
Spectral Width: 20.00 ppm
Number of Scans: 16
Relaxation Delay: 1.000 s
ppm 10

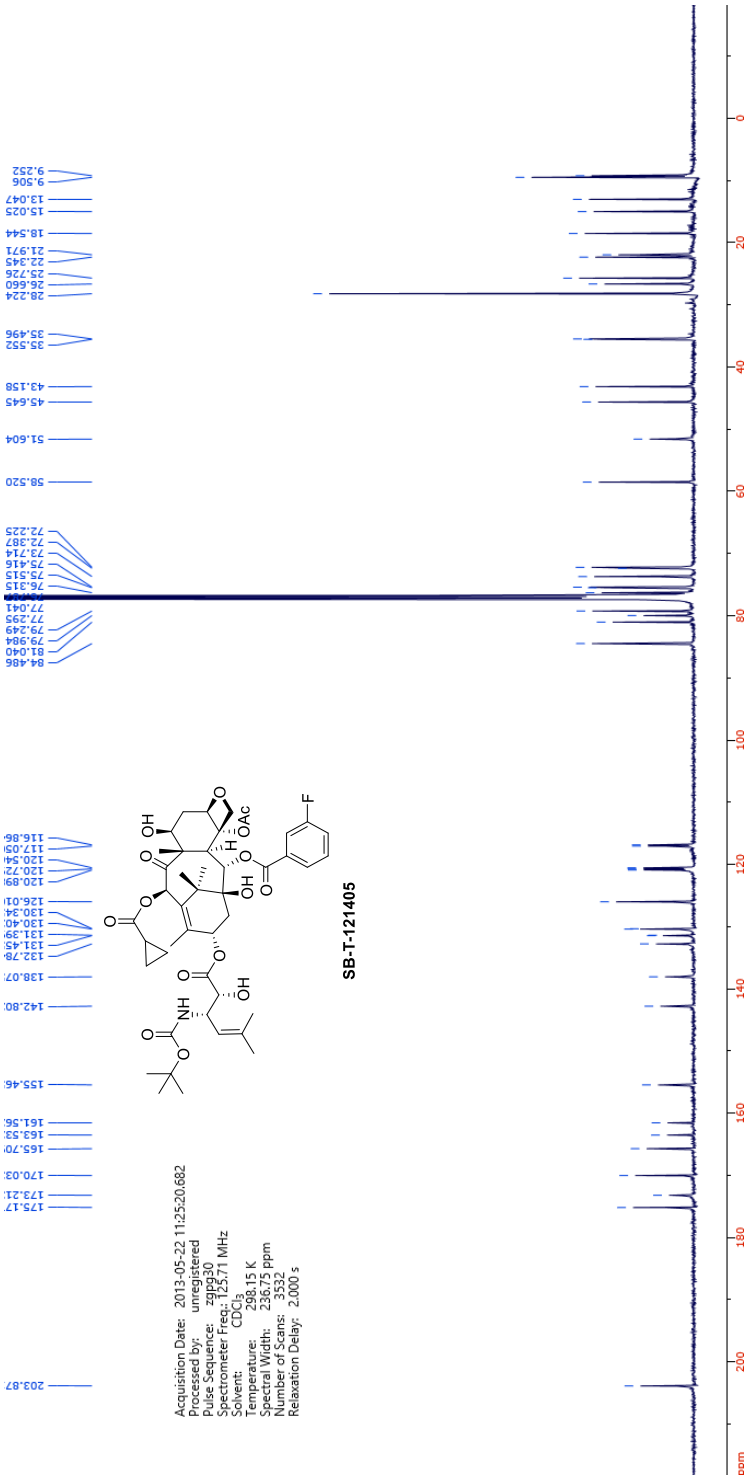
SB-T-121405
Acquisition Date: 2013-05-22 11:25:20.682
Processed by: unregistered
Pulse Sequence: zgpg30
Spectrometer Freq.: 125.71 MHz
Solvent: CDCl3
Temperature: 298.15 K
Spectral Width: 236.75 ppm
Number of Scans: 3532
Relaxation Delay: 2.000 s

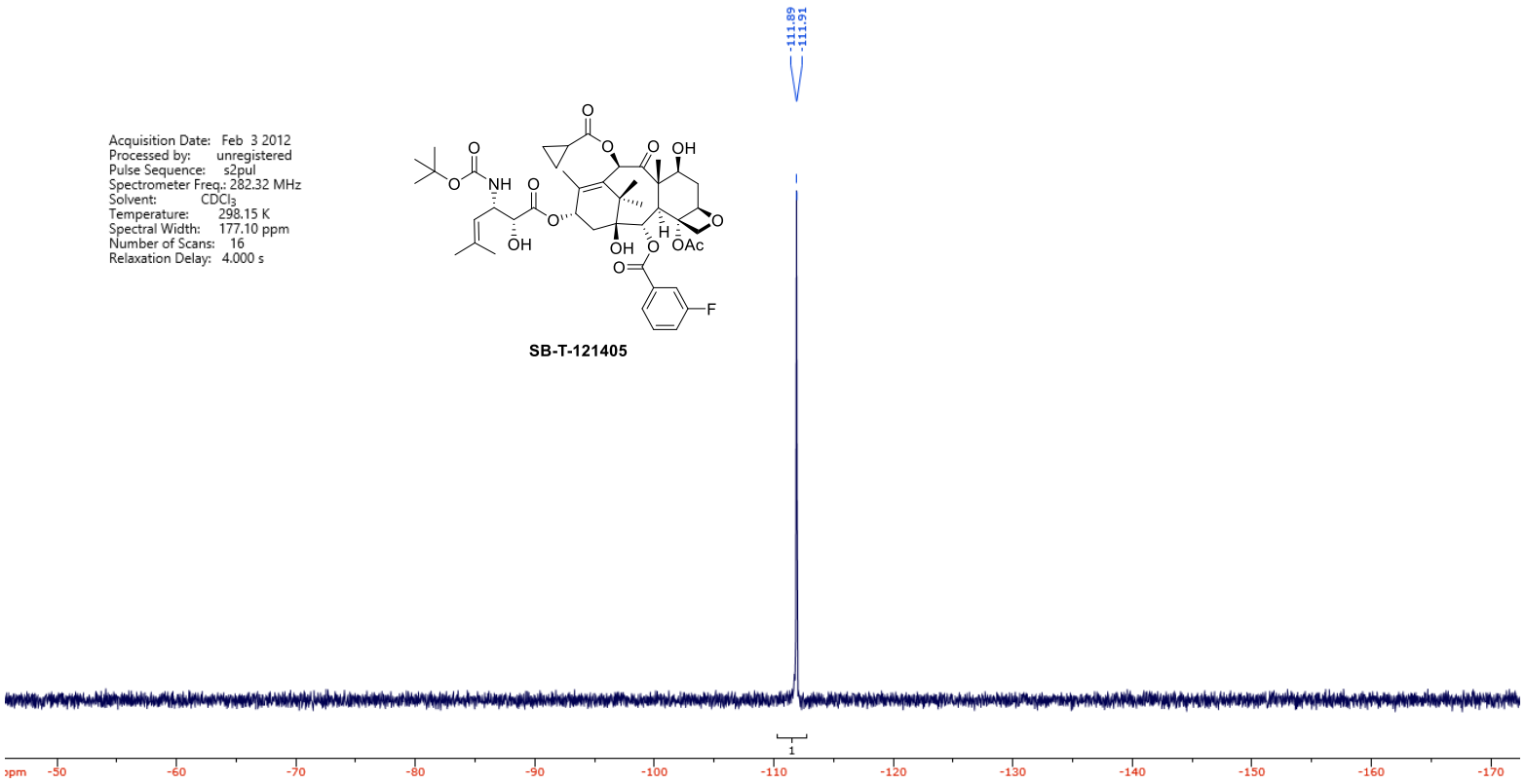
Acquisition Date: Feb 3 2012
Processed by: unregistered
Pulse Sequence: s2pul
Spectrometer Freq.: 282.32 MHz
Solvent: CDCl3
Temperature: 298.15 K
Spectral Width: 177.10 ppm
Number of Scans: 16
Relaxation Delay: 4.000 s
-111.89
-111.91
SB-T-121405
1
-50
-60
-70
-80
-90
-100
-110
-120
-130
-140
-150
-160
-170

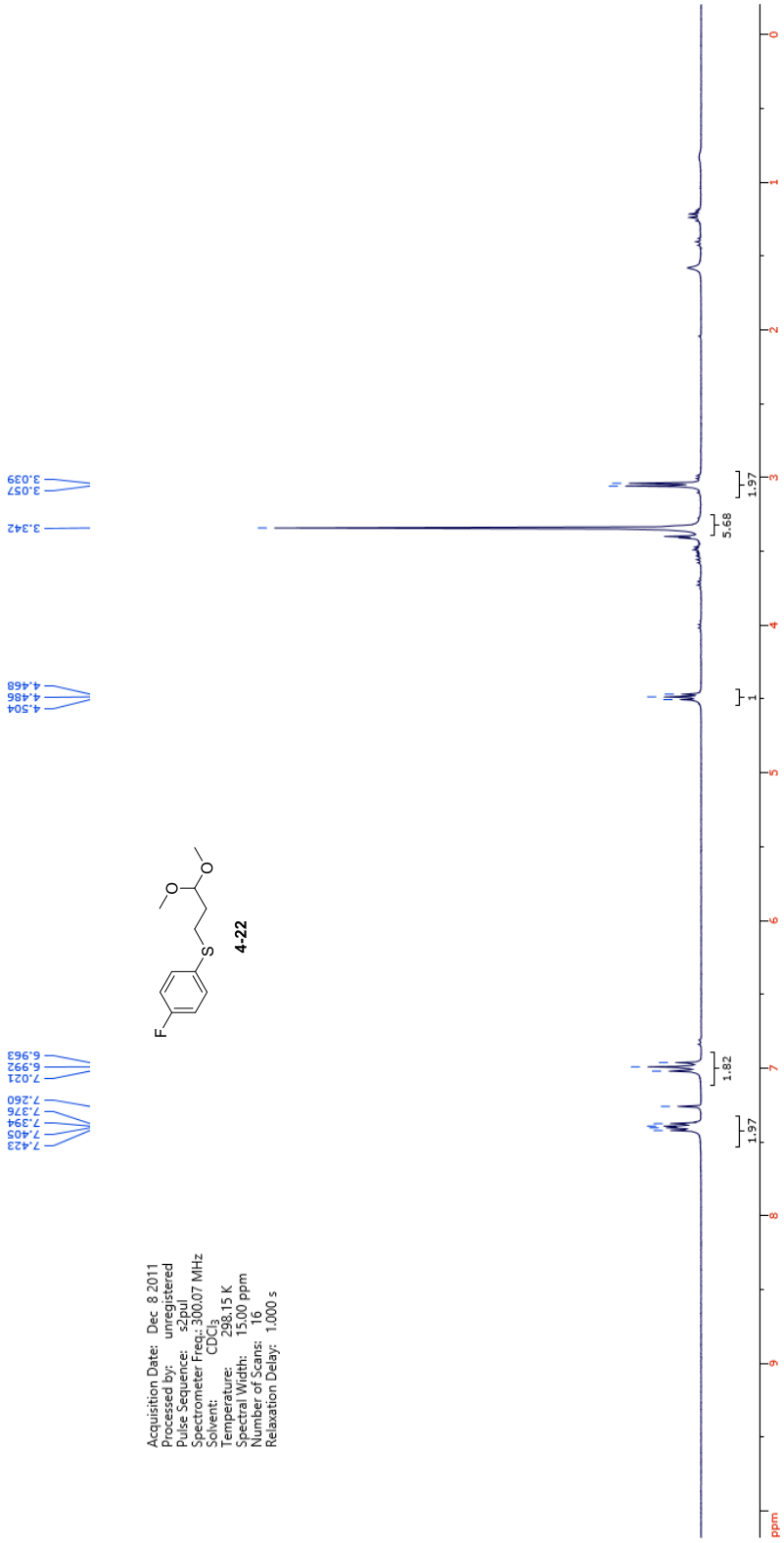
4-22
Acquisition Date: Dec 8 2011
Processed by: unregistered
Pulse Sequence: s2pul
Spectrometer Freq.: 300.07 MHz
Solvent: CDCl3
Temperature: 298.15 K
Spectral Width: 15.00 ppm
Number of Scans: 16
Relaxation Delay: 1.000 s
7.423
7.405
7.394
7.376
7.260
7.021
6.992
6.963
4.504
4.486
4.468
3.342
3.057
3.039
1.97
1.82
1.97
1
5.68
1.97
ppm

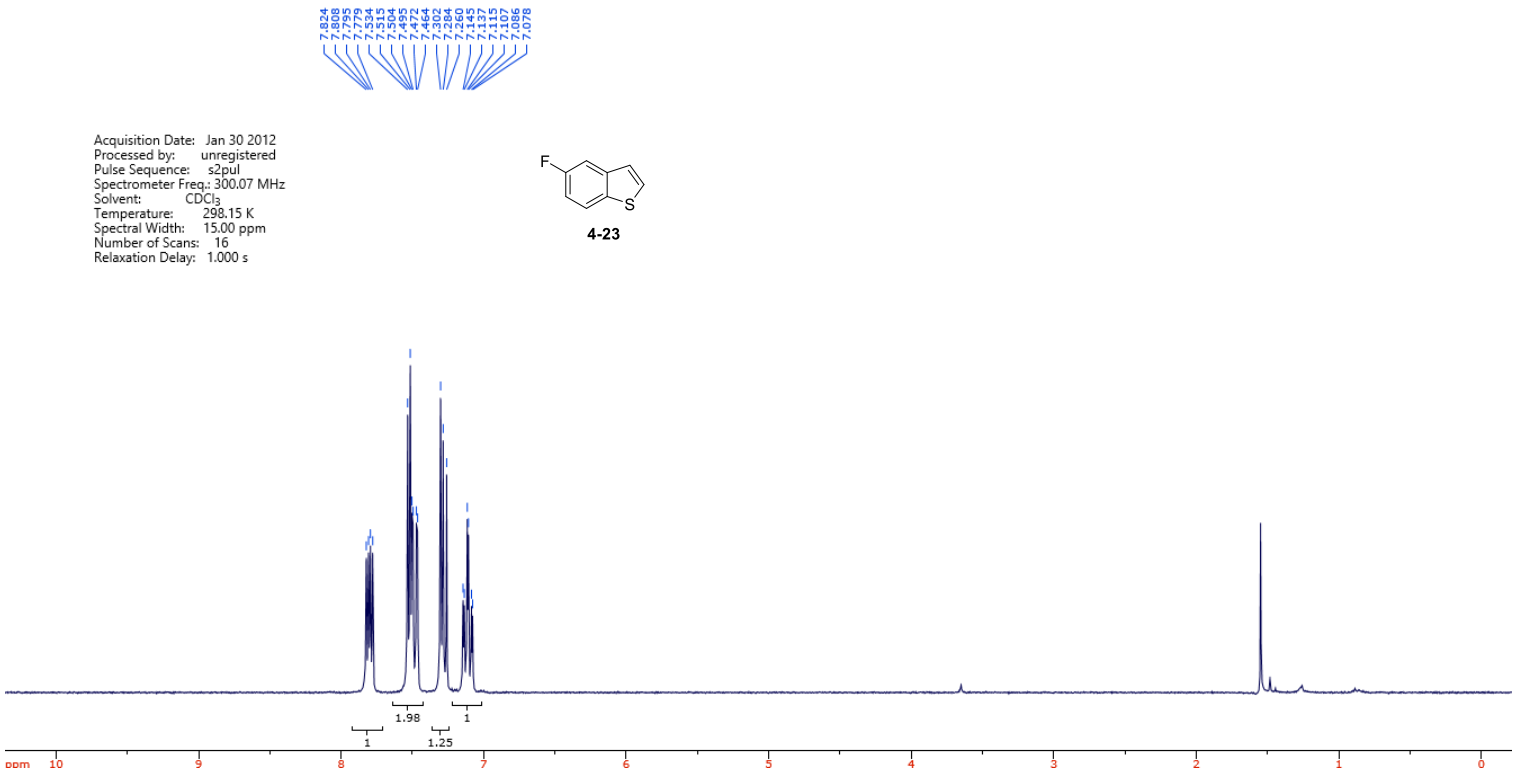
7.824
7.808
7.795
7.779
7.534
7.515
7.504
7.485
7.472
7.464
7.302
7.284
7.260
7.145
7.137
7.115
7.107
7.096
7.078
Acquisition Date: Jan 30 2012
Processed by: unregistered
Pulse Sequence: s2pul
Spectrometer Freq.: 300.07 MHz
Solvent: CDCl3
Temperature: 298.15 K
Spectral Width: 15.00 ppm
Number of Scans: 16
Relaxation Delay: 1.000 s
F
S
4-23
1.98
1
1.25
1
ppm
10
9
8
7
6
5
4
3
2
1
0

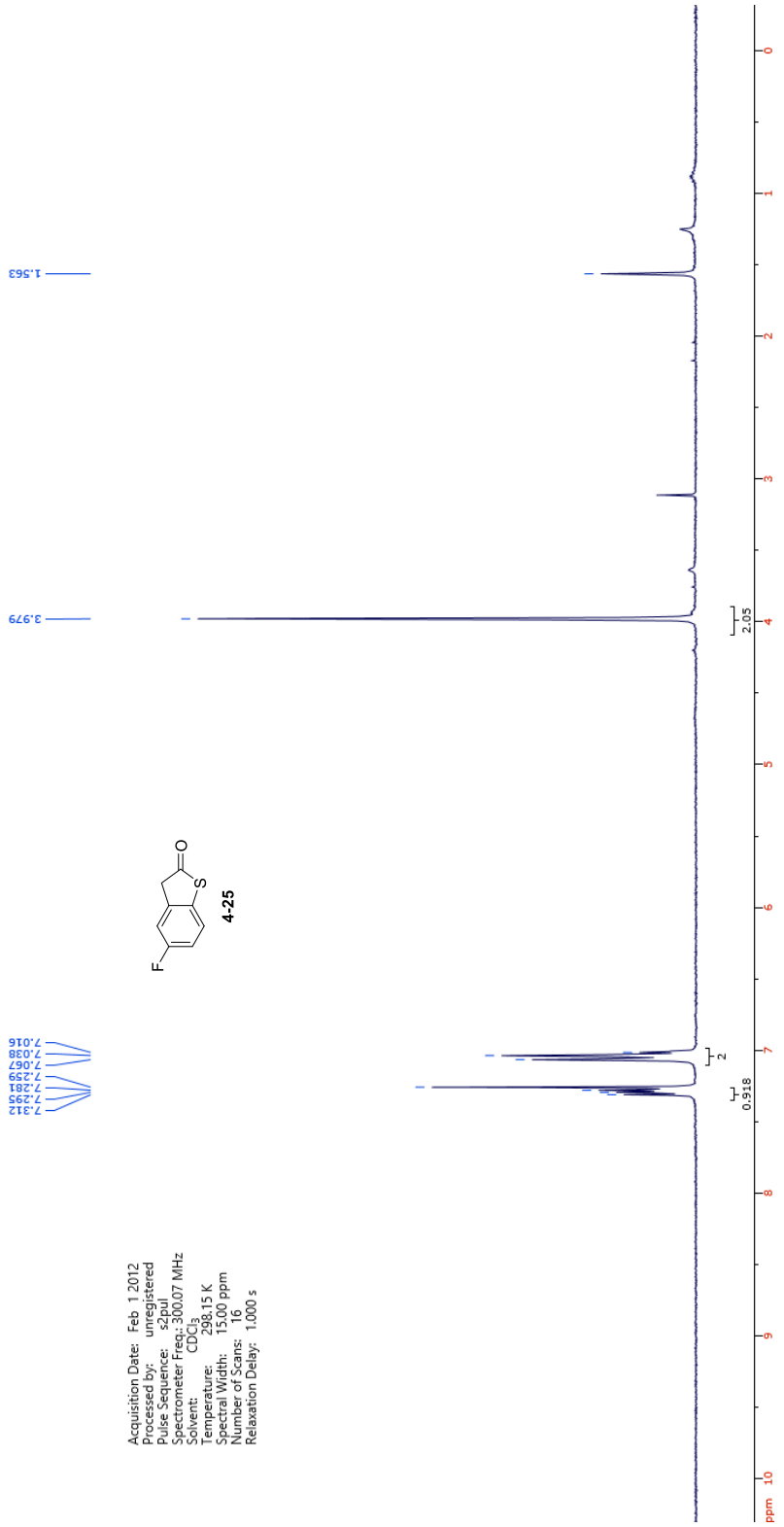
1.563
3.979
7.312
7.295
7.281
7.259
7.067
7.038
7.016
2.05
2
0.918
ppm
4-25
Acquisition Date: Feb 1 2012
Processed by: unregistered
Pulse Sequence: s2pul
Spectrometer Freq.: 300.07 MHz
Solvent: CDCl3
Temperature: 298.15 K
Spectral Width: 15.00 ppm
Number of Scans: 16
Relaxation Delay: 1.000 s

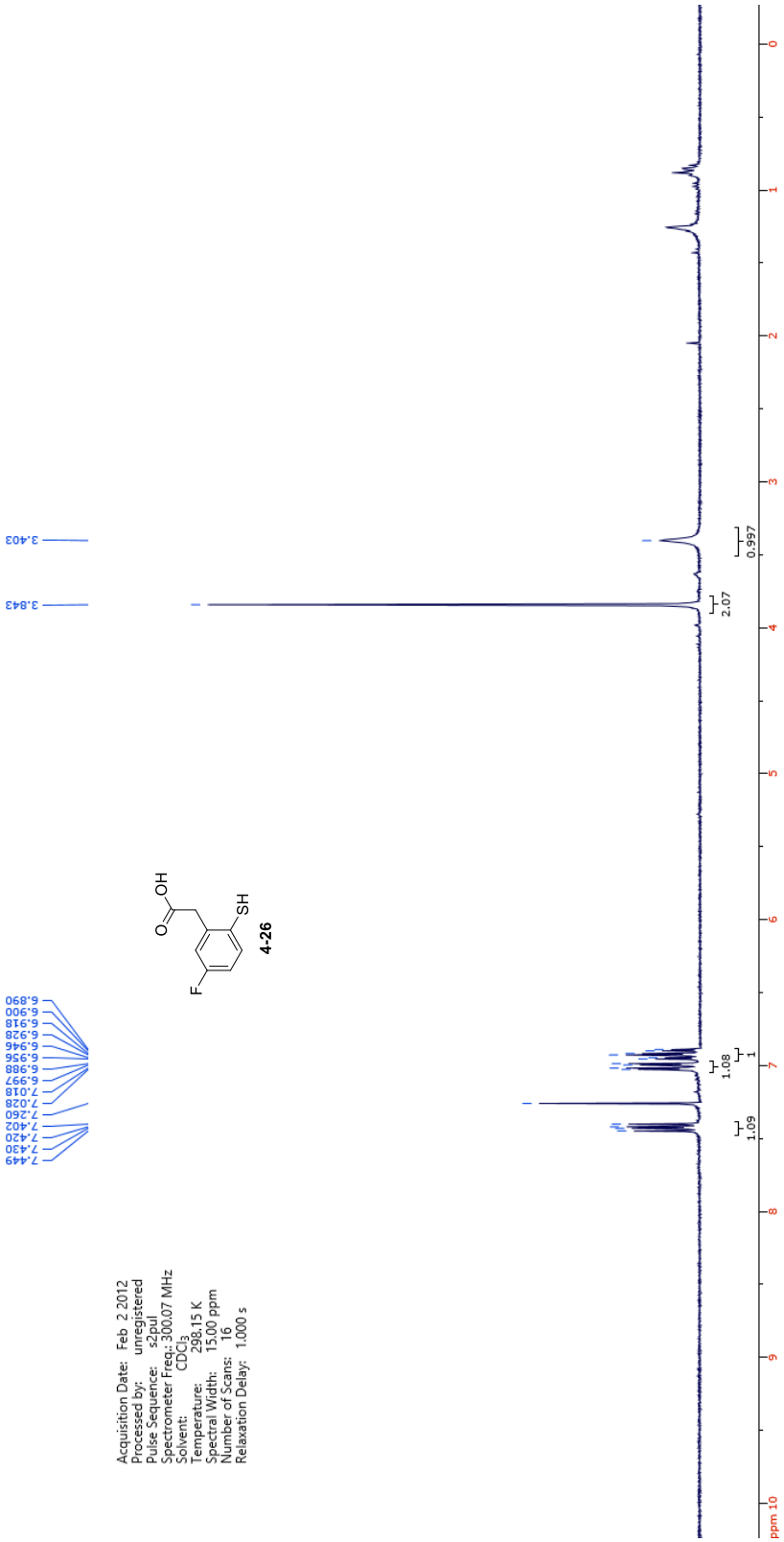
3.403
3.843
6.890
6.900
6.918
6.928
6.946
6.956
6.988
6.997
7.018
7.028
7.260
7.402
7.420
7.430
7.449
OH
O
SH
F
4-26
Acquisition Date: Feb 2 2012
Processed by: unregistered
Pulse Sequence: s2pul
Spectrometer Freq.: 300.07 MHz
Solvent: $CDCl_3$
Temperature: 298.15 K
Spectral Width: 15.00 ppm
Number of Scans: 16
Relaxation Delay: 1.000 s
2.07
0.997
1.08
1
1.09
ppm 10

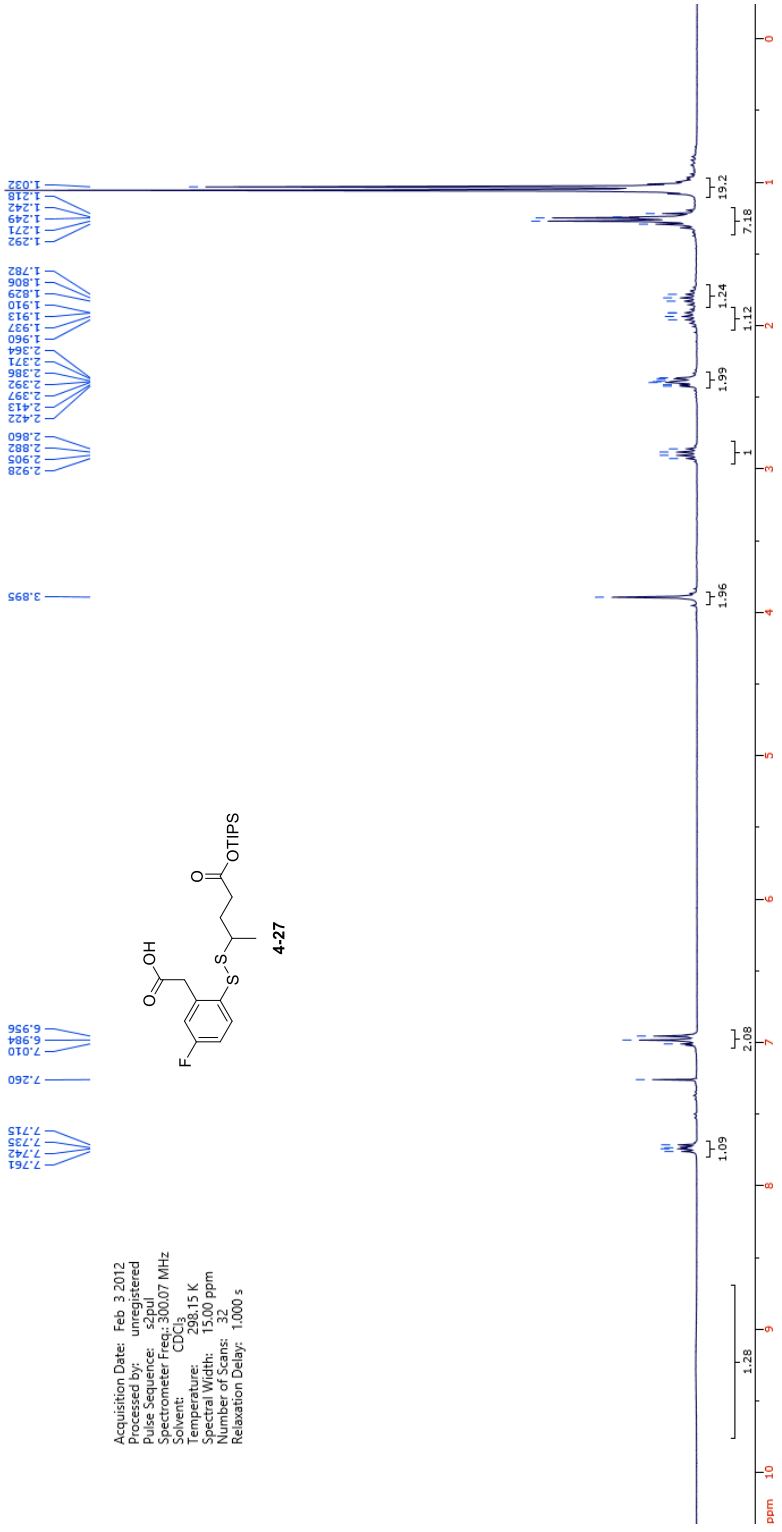
1.052
1.218
1.242
1.249
1.271
1.292
1.782
1.806
1.829
1.910
1.913
1.937
1.960
2.364
2.371
2.386
2.392
2.397
2.413
2.422
2.860
2.882
2.905
2.928
3.895
6.956
6.984
7.010
7.260
7.713
7.735
7.742
7.761
19.2
7.18
1.24
1.12
1.99
1
1.96
2.08
1.09
1.28
ppm
OH
O
S
S
O
OTIPS
F
4-27
Acquisition Date: Feb 3 2012
Processed by: unregistered
Pulse Sequence: s2pul
Spectrometer Freq.: 300.07 MHz
Solvent: CDCl3
Temperature: 298.15 K
Spectral Width: 15.00 ppm
Number of Scans: 32
Relaxation Delay: 1.000 s

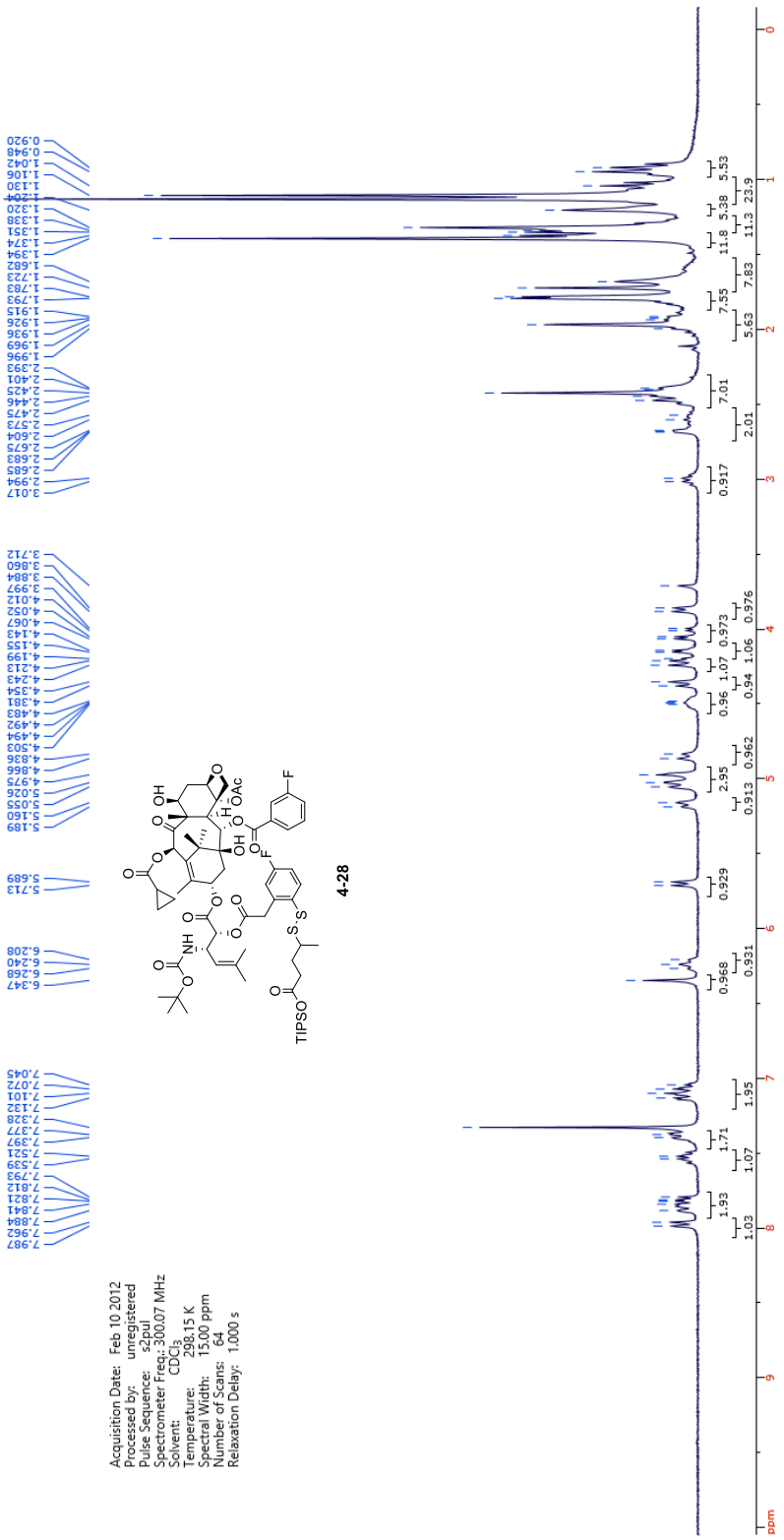
Acquisition Date: Feb 10 2012
Processed by: unregistered
Pulse Sequence: s2pul
Spectrometer Freq.: 300.07 MHz
Solvent: $CDCl_3$
Temperature: 298.15 K
Spectral Width: 15.00 ppm
Number of Scans: 64
Relaxation Delay: 1.000 s
4-28
TIPSO
ppm

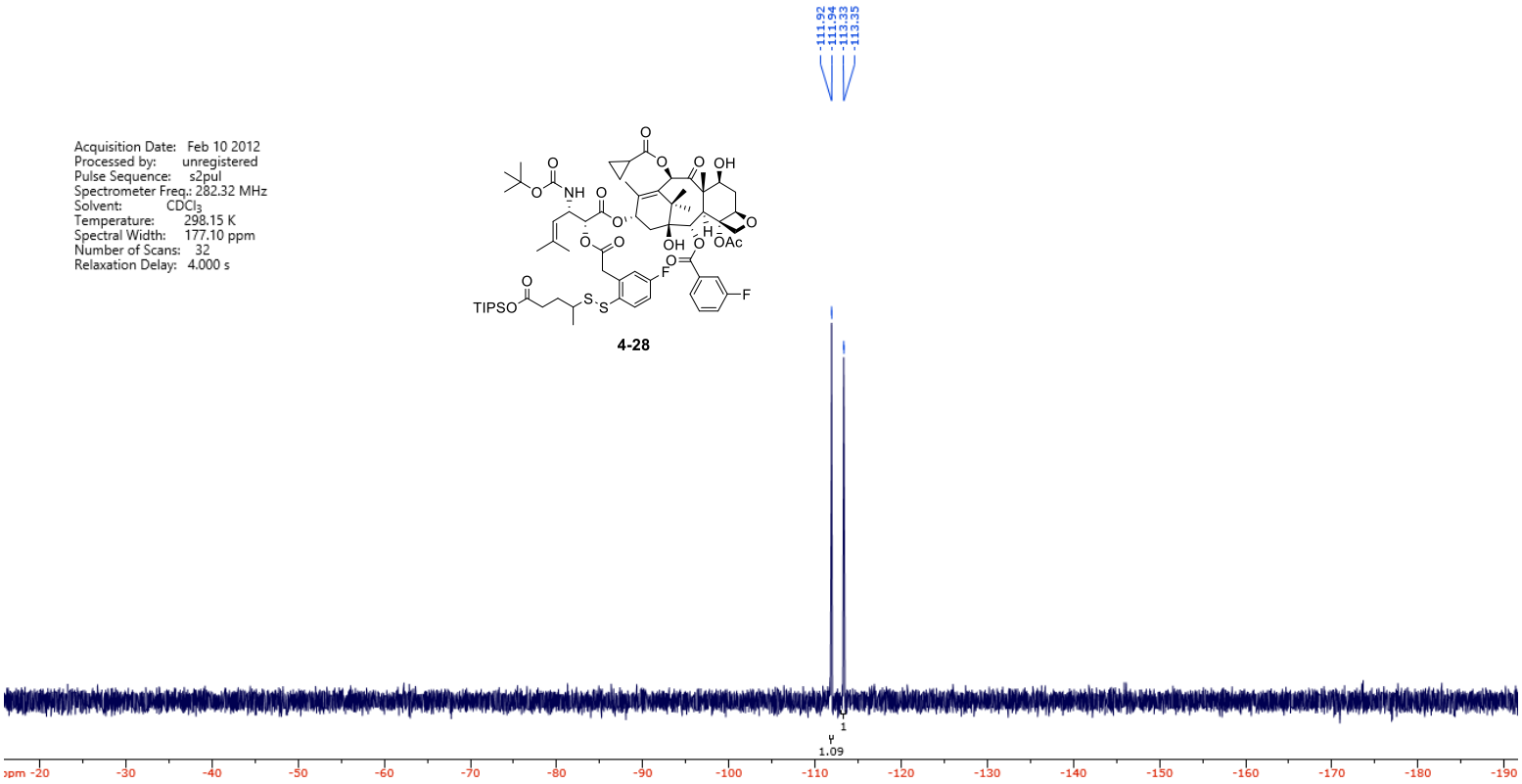
-111.92
-111.94
-113.33
-113.35
Acquisition Date: Feb 10 2012
Processed by: unregistered
Pulse Sequence: s2pul
Spectrometer Freq.: 282.32 MHz
Solvent: CDCl3
Temperature: 298.15 K
Spectral Width: 177.10 ppm
Number of Scans: 32
Relaxation Delay: 4.000 s
TIPSO
NH
OH
OAc
F
F
1.09
ppm -20
-30
-40
-50
-60
-70
-80
-90
-100
-110
-120
-130
-140
-150
-160
-170
-180
-190

4-28

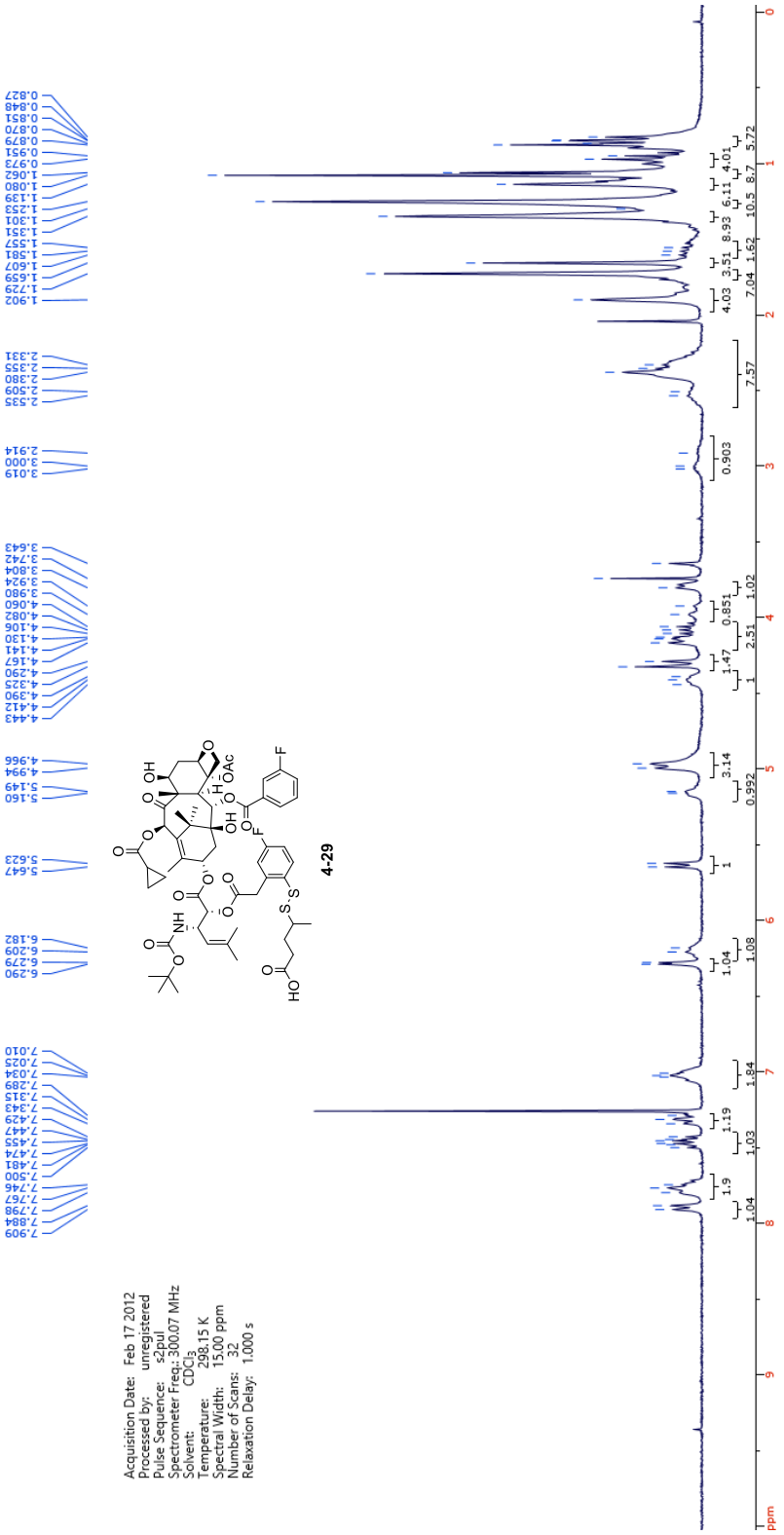
4-29
Acquisition Date: Feb 17 2012
Processed by: unregistered
Pulse Sequence: s2pul
Spectrometer Freq.: 300.07 MHz
Solvent: $CDCl_3$
Temperature: 298.15 K
Spectral Width: 15.00 ppm
Number of Scans: 32
Relaxation Delay: 1.000 s
ppm

Acquisition Date: Feb 17 2012
Processed by: unregistered
Pulse Sequence: s2pul
Spectrometer Freq.: 282.32 MHz
Solvent: $CDCl_3$
Temperature: 298.15 K
Spectral Width: 177.10 ppm
Number of Scans: 32
Relaxation Delay: 4.000 s

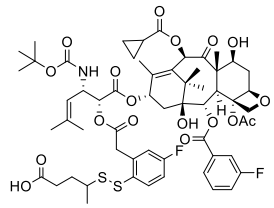

4-29

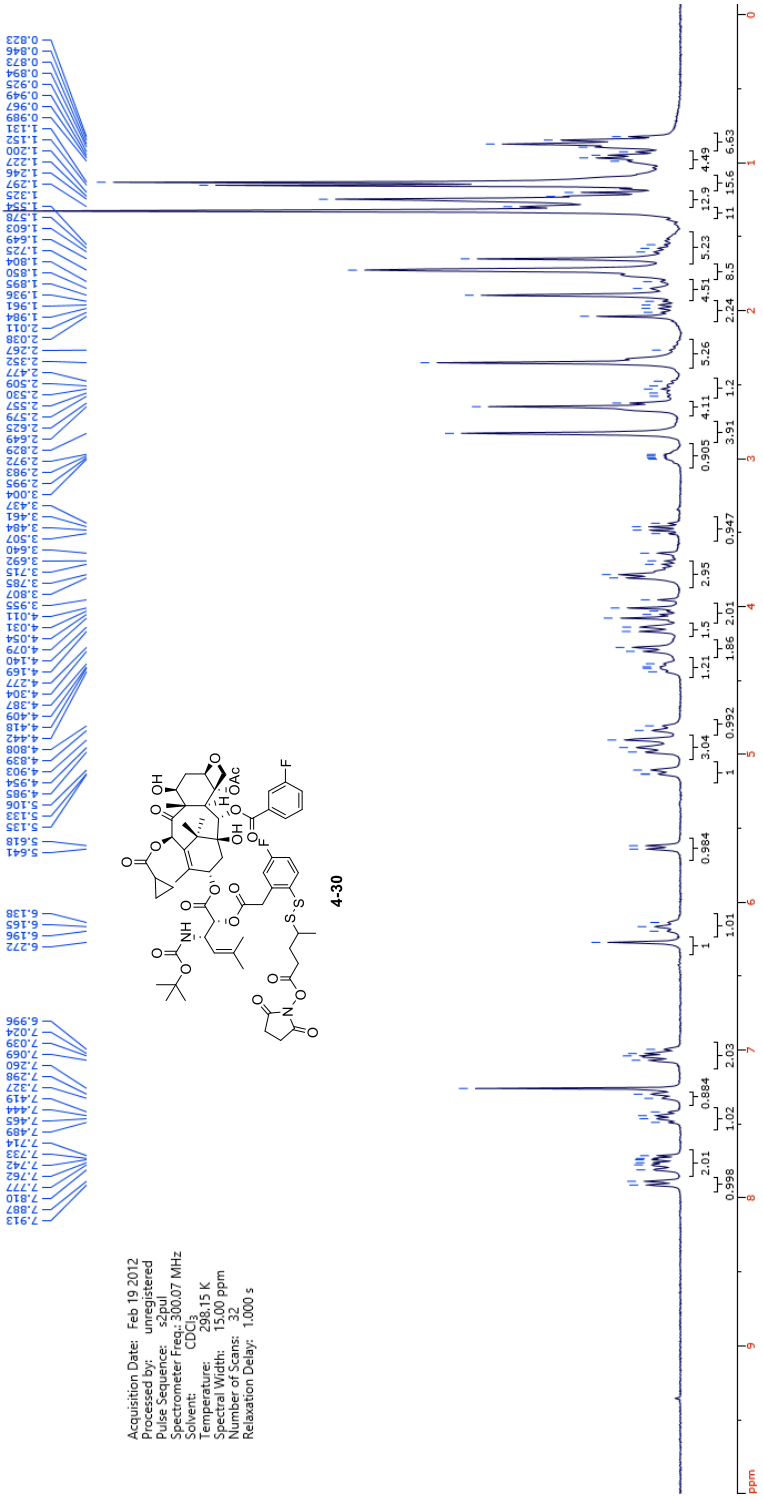
Acquisition Date: Feb 19 2012
Processed by: unregistered
Pulse Sequence: s2pul
Spectrometer Freq.: 300.07 MHz
Solvent: $CDCl_3$
Temperature: 298.15 K
Spectral Width: 15.00 ppm
Number of Scans: 32
Relaxation Delay: 1.000 s
4-30
ppm

Acquisition Date: Feb 19 2012
Processed by: unregistered
Pulse Sequence: s2pul
Spectrometer Freq.: 282.32 MHz
Solvent: $CDCl_3$
Temperature: 298.15 K
Spectral Width: 177.10 ppm
Number of Scans: 32
Relaxation Delay: 4.000 s

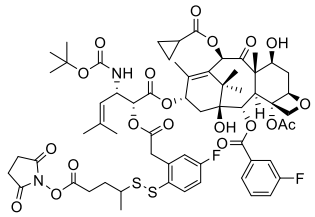

4-30

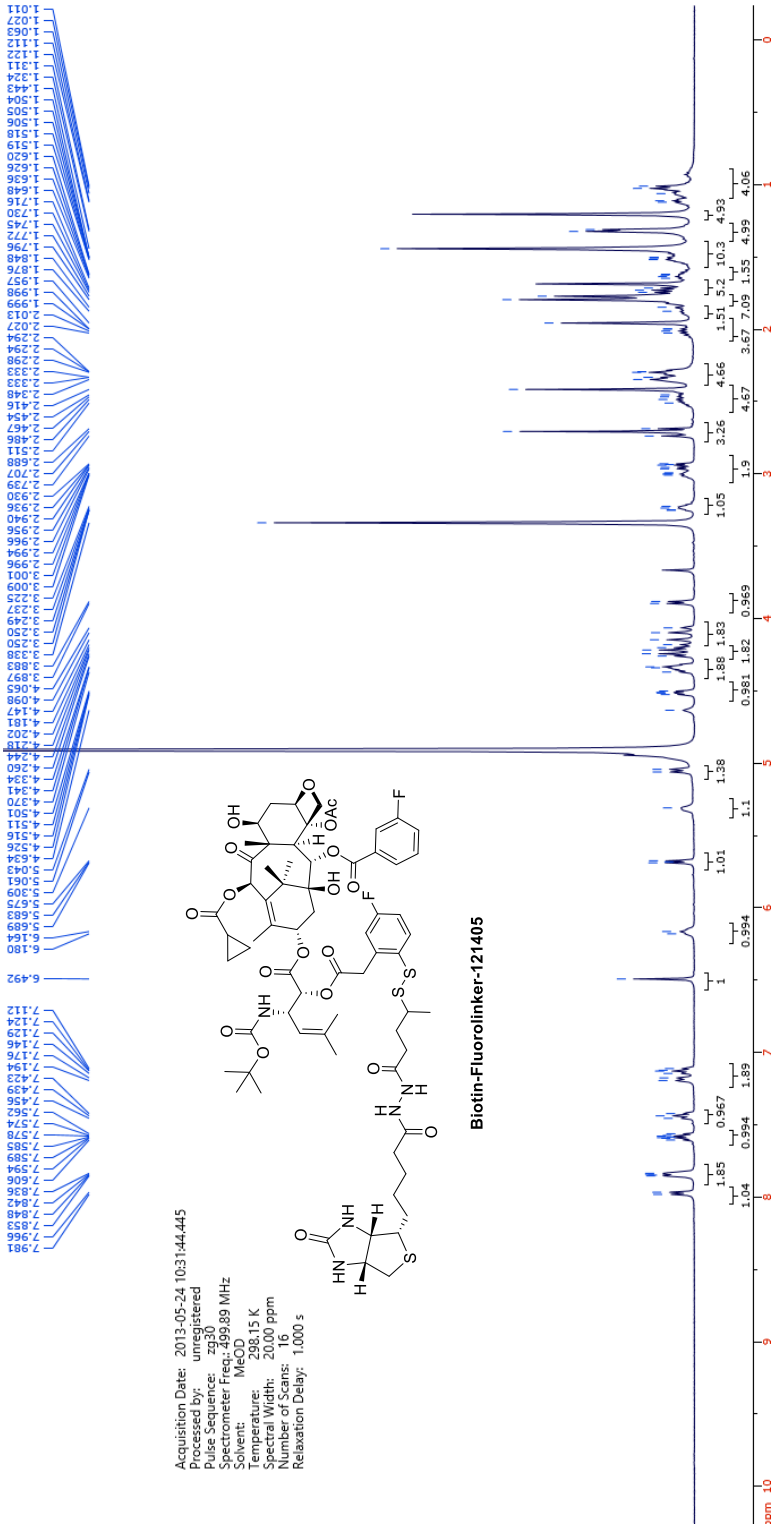
Acquisition Date: 2013-05-24 10:31:44.445
Processed by: unregistered
Pulse Sequence: zg30
Spectrometer Freq.: 499.89 MHz
Solvent: MeOD
Temperature: 298.15 K
Spectral Width: 20.00 ppm
Number of Scans: 16
Relaxation Delay: 1.000 s
Biotin-Fluorolinker-121405

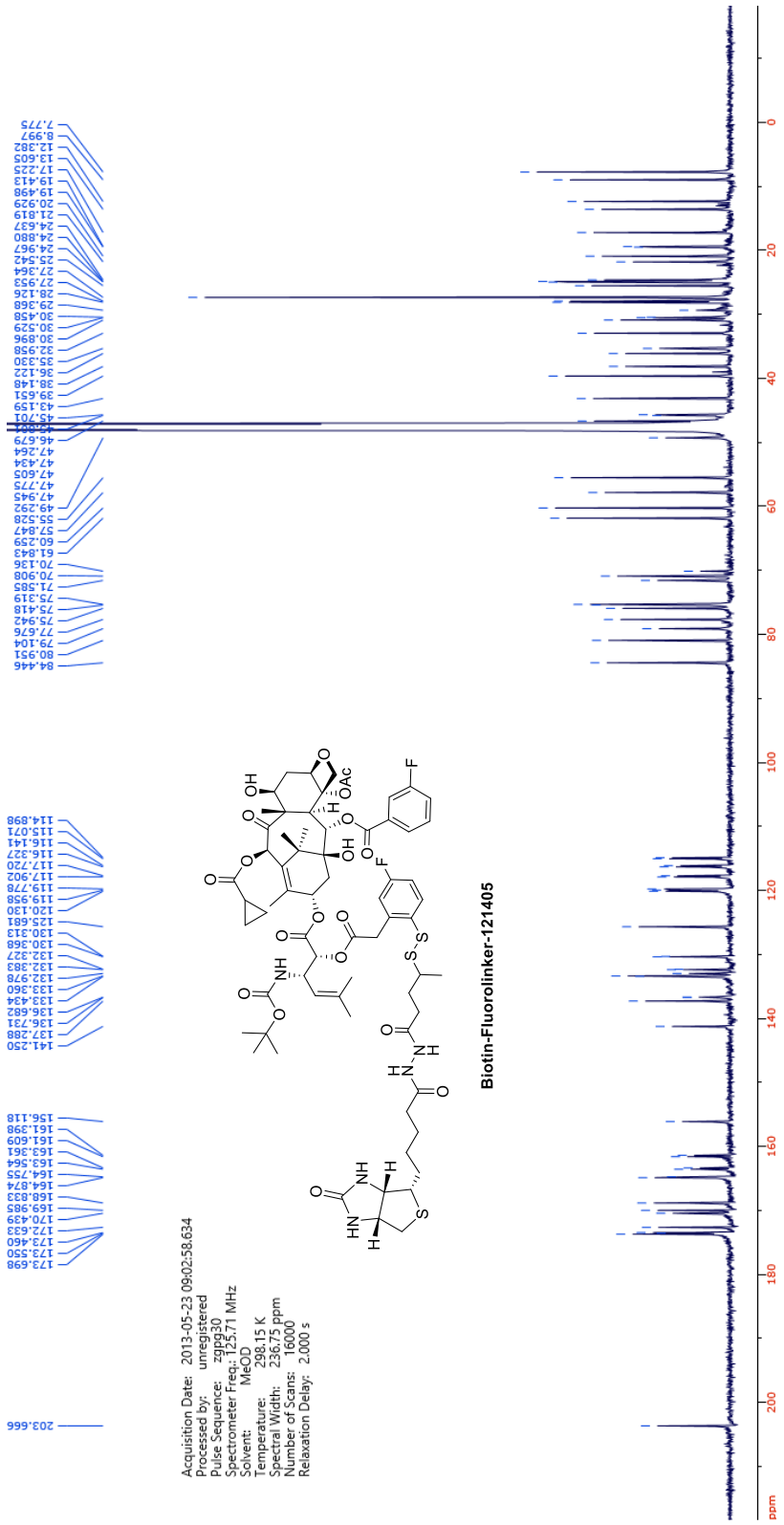
Biotin-Fluorolinker-121405
Acquisition Date: 2013-05-23 09:02:58.634
Processed by: unregistered
Pulse Sequence: zgpg30
Spectrometer Freq.: 125.71 MHz
Solvent: MeOD
Temperature: 298.15 K
Spectral Width: 236.75 ppm
Number of Scans: 16000
Relaxation Delay: 2.000 s
ppm

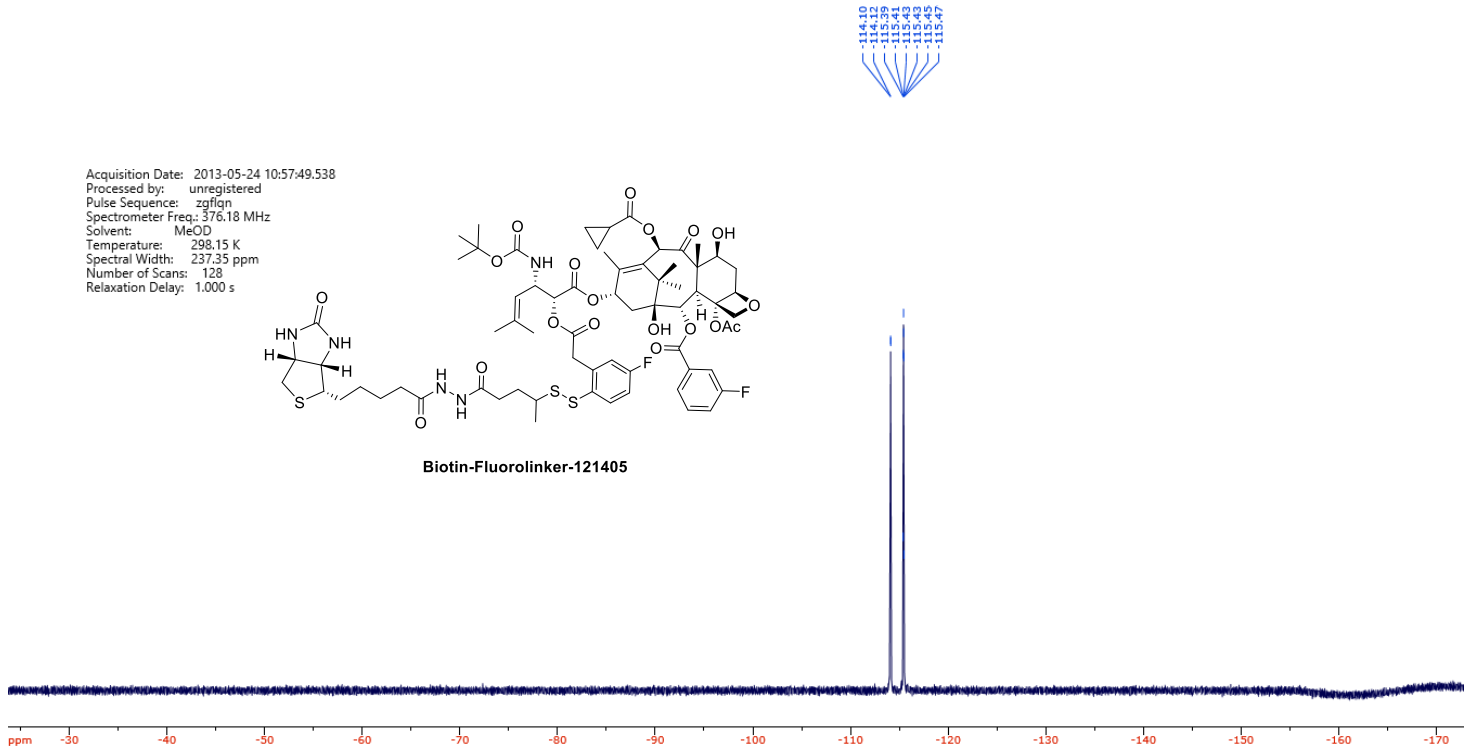

Biotin-Fluorolinker-121405

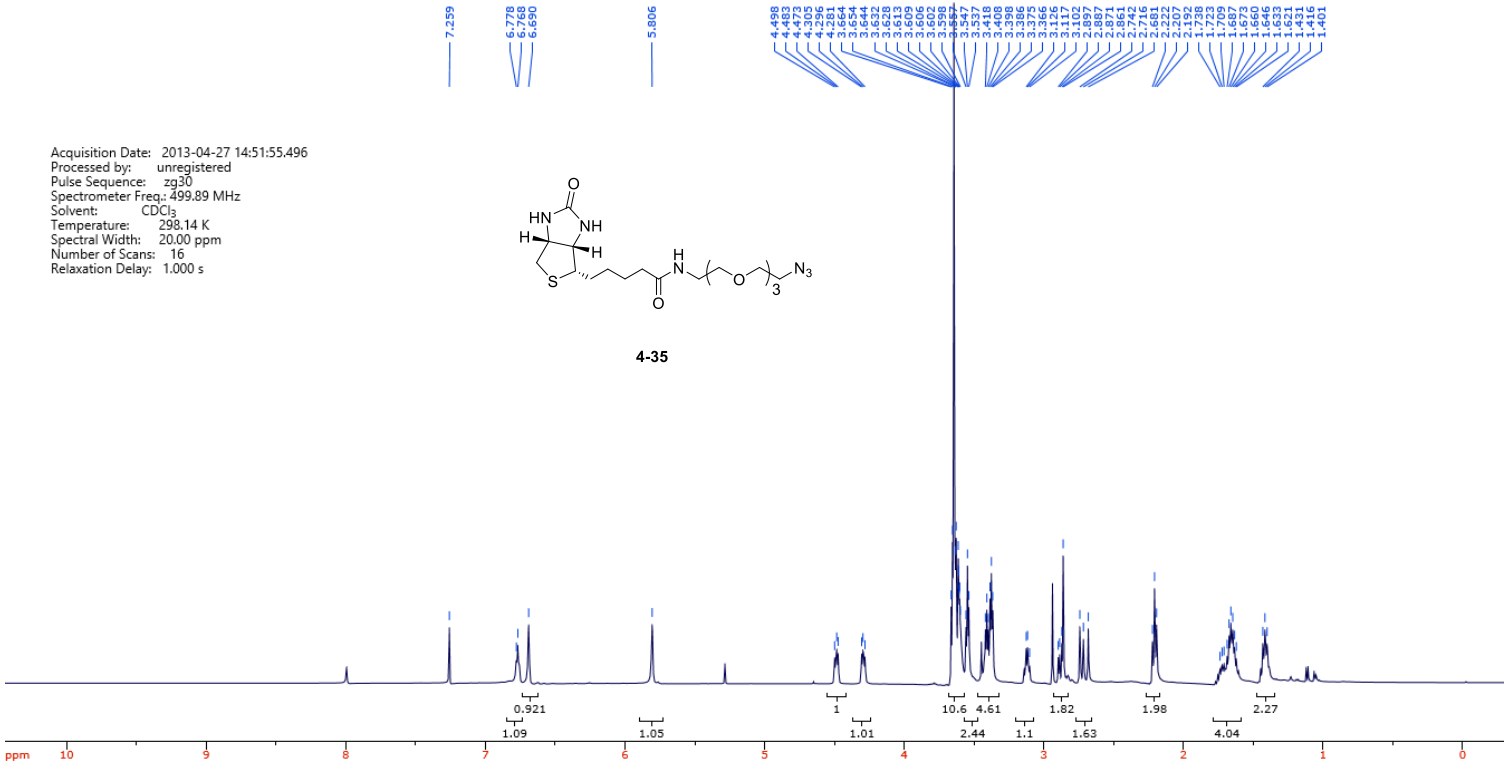
Acquisition Date: 2013-04-27 14:51:55.496
Processed by: unregistered
Pulse Sequence: zg30
Spectrometer Freq.: 499.89 MHz
Solvent: CDCl3
Temperature: 298.14 K
Spectral Width: 20.00 ppm
Number of Scans: 16
Relaxation Delay: 1.000 s
7.259
6.778
6.768
6.690
5.806
4.498
4.483
4.473
4.305
4.296
4.281
3.664
3.654
3.644
3.632
3.628
3.613
3.609
3.606
3.592
3.588
3.547
3.537
3.418
3.408
3.398
3.386
3.375
3.366
3.356
3.117
3.102
2.897
2.887
2.871
2.861
2.742
2.716
2.221
2.207
2.192
1.738
1.723
1.709
1.687
1.673
1.660
1.646
1.633
1.621
1.431
1.416
1.401
0.921
1.09
1.05
1
1.01
10.6
2.44
4.61
1.1
1.82
1.63
1.98
2.27
4.04
ppm
10
9
8
7
6
5
4
3
2
1
0

4-35

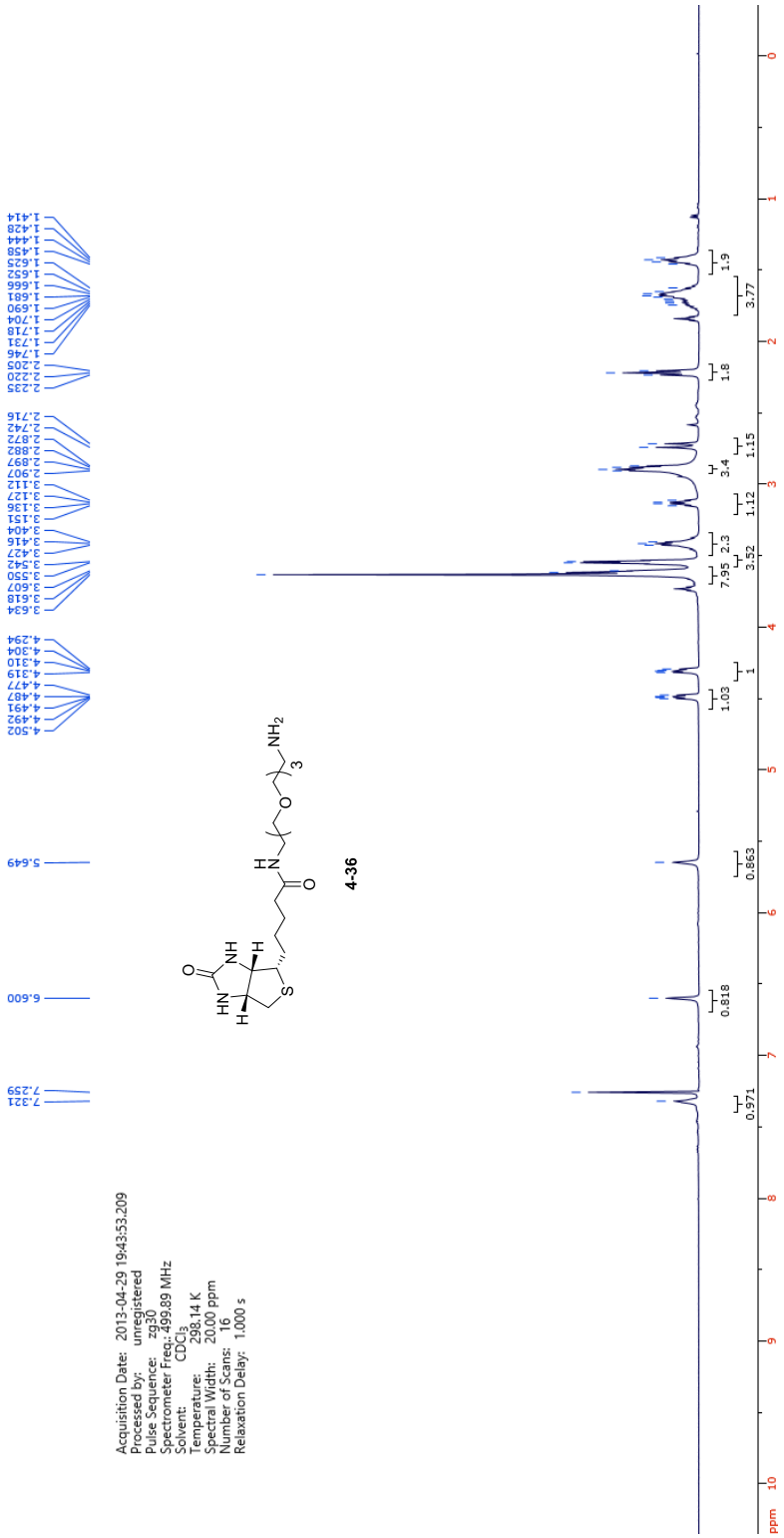
4-36
Acquisition Date: 2013-04-29 19:43:53.209
Processed by: unregistered
Pulse Sequence: zg30
Spectrometer Freq.: 499.89 MHz
Solvent: $CDCl_3$
Temperature: 298.14 K
Spectral Width: 20.00 ppm
Number of Scans: 16
Relaxation Delay: 1.000 s
7.321
7.259
6.600
5.649
4.502
4.492
4.491
4.487
4.477
4.319
4.310
4.304
4.294
3.634
3.618
3.607
3.550
3.542
3.427
3.416
3.404
3.151
3.136
3.127
3.112
2.907
2.897
2.882
2.872
2.742
2.716
2.235
2.220
2.205
1.746
1.731
1.718
1.704
1.690
1.681
1.666
1.652
1.625
1.458
1.444
1.428
1.414
0.971
0.818
1.03
1
0.863
7.95
2.3
3.52
1.12
3.4
1.15
1.8
3.77
1.9
ppm

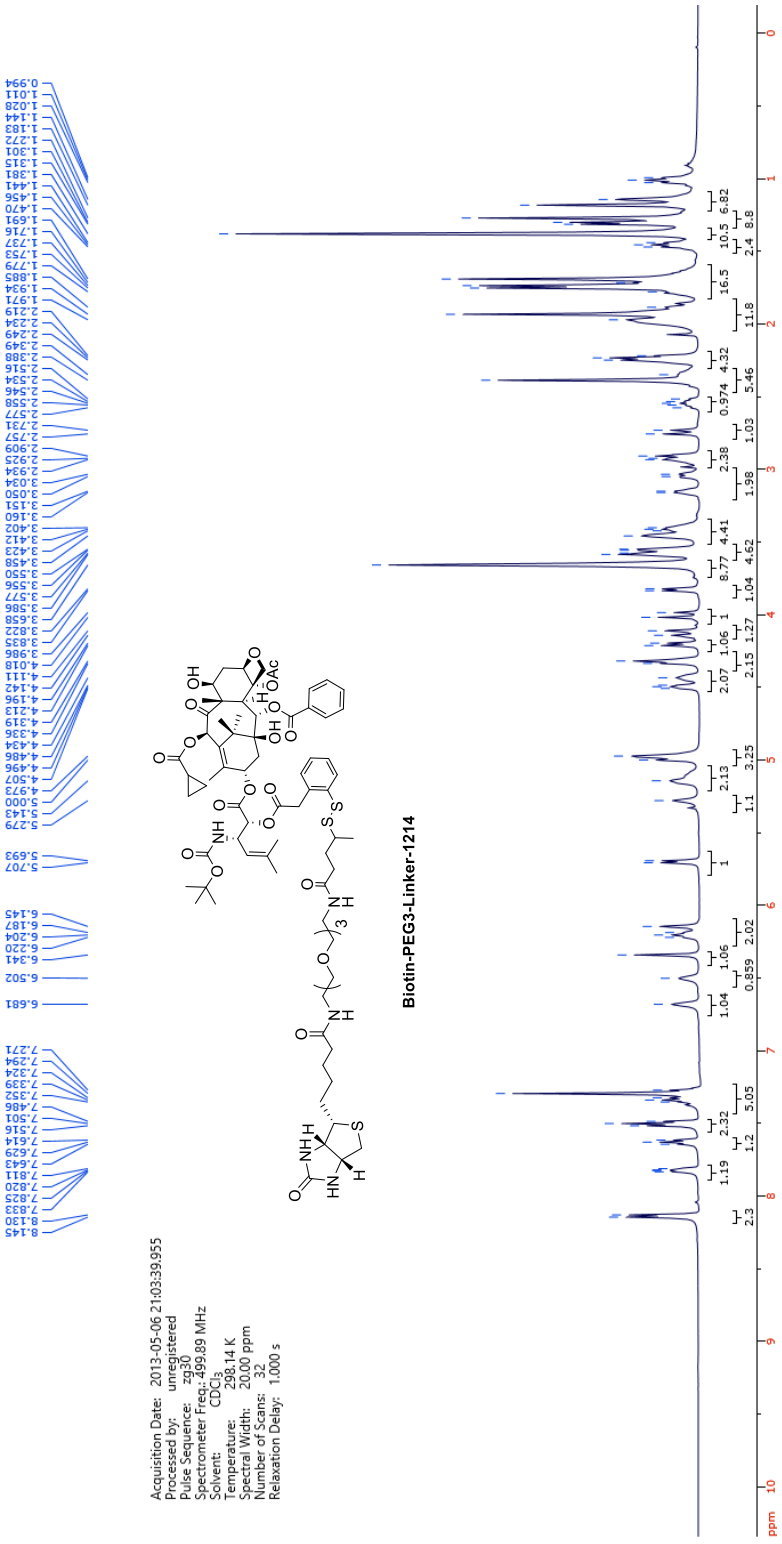
Acquisition Date: 2013-05-06 21:03:39.955
Processed by: unregistered
Pulse Sequence: zg30
Spectrometer Freq.: 499.89 MHz
Solvent: $CDCl_3$
Temperature: 298.14 K
Spectral Width: 20.00 ppm
Number of Scans: 32
Relaxation Delay: 1.000 s
Biotin-PEG3-Linker-1214
ppm

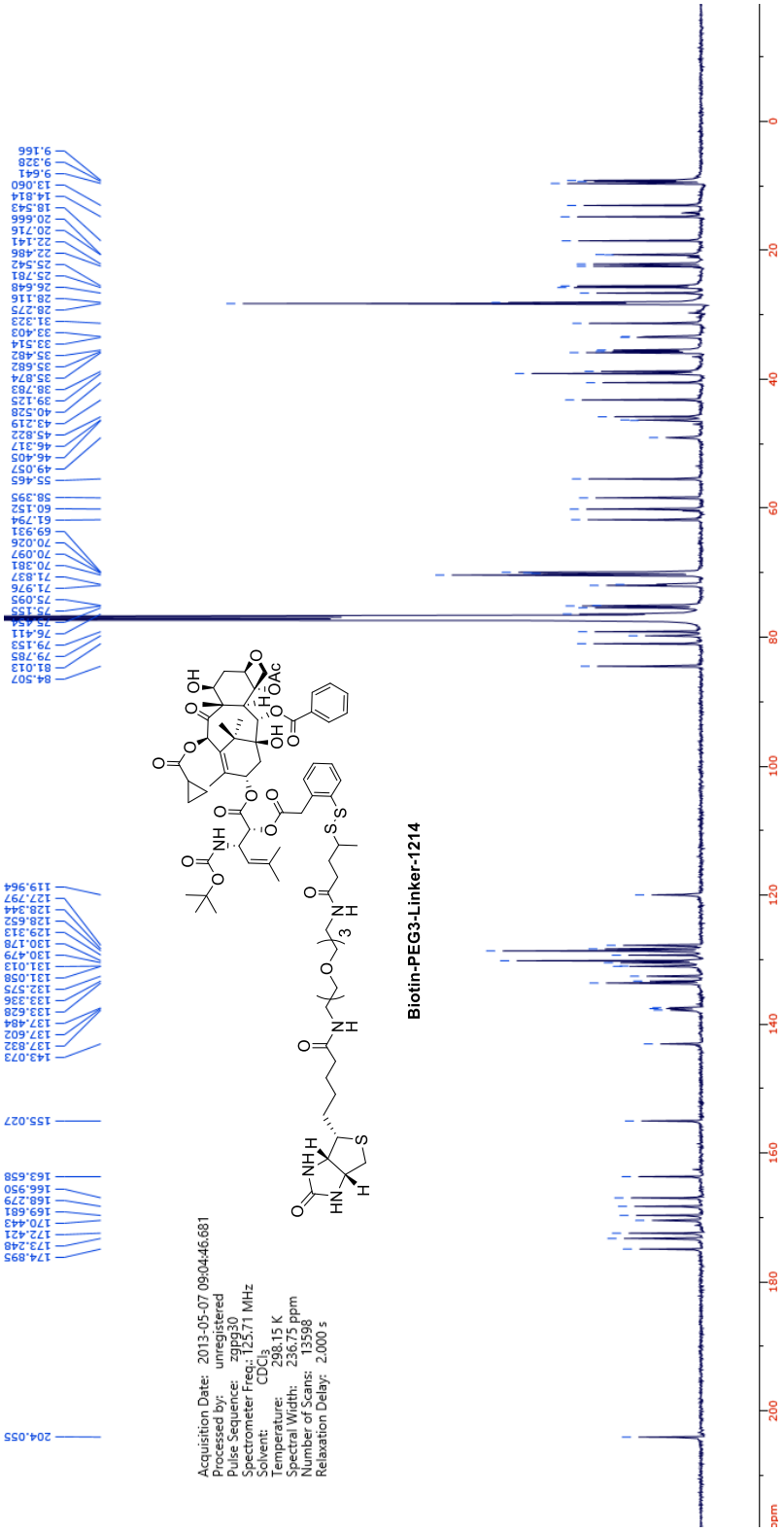
Biotin-PEG3-Linker-1214
Acquisition Date: 2013-05-07 09:04:46.681
Processed by: unregistered
Pulse Sequence: zgpg30
Spectrometer Freq.: 125.71 MHz
Solvent: $CDCl_3$
Temperature: 298.15 K
Spectral Width: 236.75 ppm
Number of Scans: 13598
Relaxation Delay: 2.000 s
9.166
9.328
9.641
13.060
14.814
18.543
20.666
20.716
22.141
22.486
25.542
25.781
26.648
28.116
28.275
31.323
33.403
33.514
35.482
35.682
35.874
38.783
39.125
40.528
43.219
45.822
46.317
46.405
49.057
55.465
58.395
60.152
61.794
69.931
70.026
70.097
70.381
71.837
71.976
75.095
75.135
76.411
79.153
79.785
81.013
84.507
119.964
127.797
128.344
128.652
129.313
130.178
130.479
131.013
131.058
132.575
133.336
133.628
137.484
137.602
137.832
143.073
155.027
163.658
166.950
168.279
169.681
170.443
172.421
173.248
174.895
204.055
0
20
40
60
80
100
120
140
160
180
200
ppm

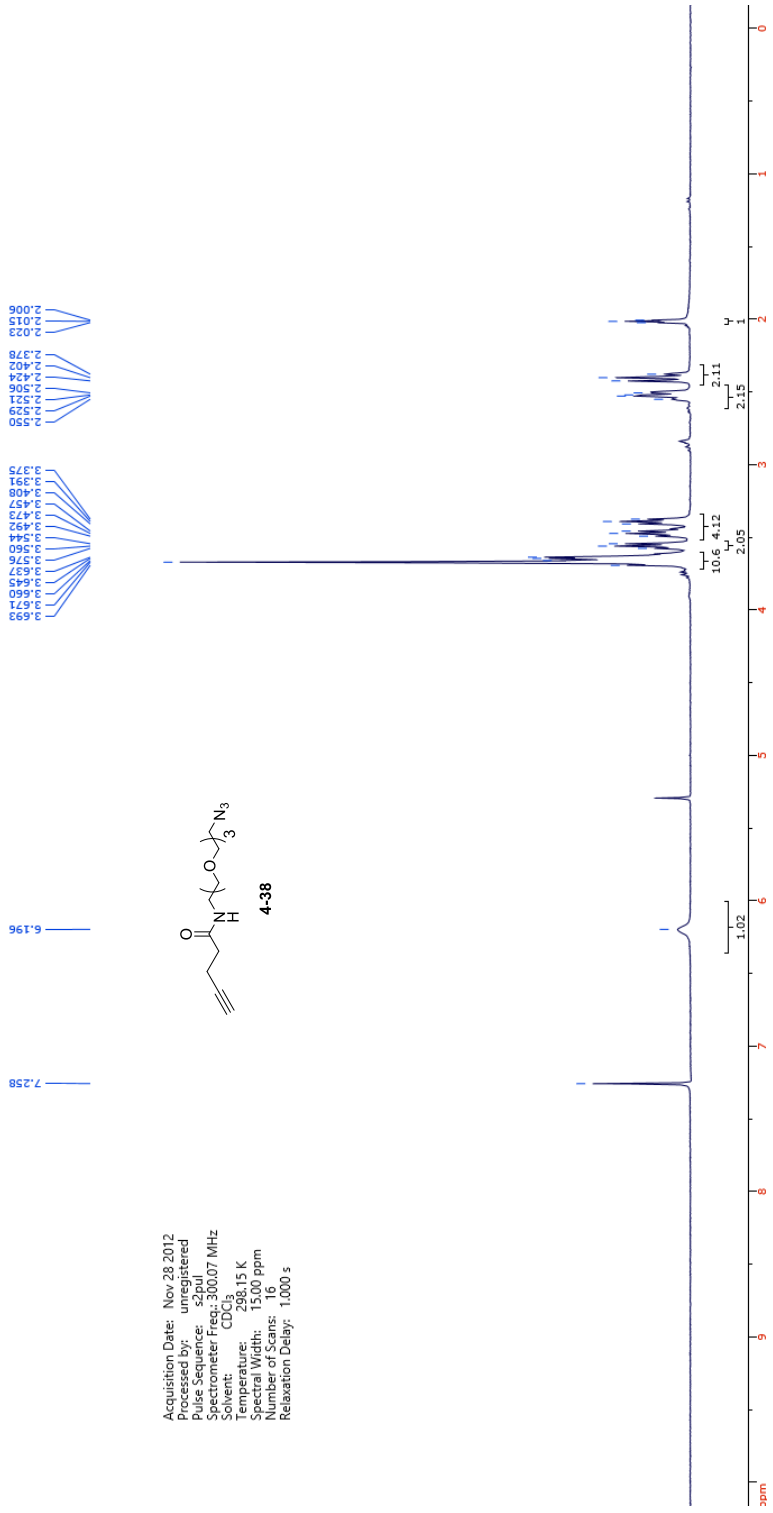
Acquisition Date: Nov 28 2012
Processed by: unregistered
Pulse Sequence: s2pul
Spectrometer Freq.: 300.07 MHz
Solvent: CDCl3
Temperature: 298.15 K
Spectral Width: 15.00 ppm
Number of Scans: 16
Relaxation Delay: 1.000 s
4-38
7.258
6.196
3.693
3.671
3.660
3.645
3.637
3.576
3.560
3.544
3.492
3.473
3.457
3.408
3.391
3.375
2.550
2.529
2.521
2.506
2.424
2.402
2.378
2.023
2.015
2.006
1.02
10.6
4.12
2.05
2.11
2.15
ppm

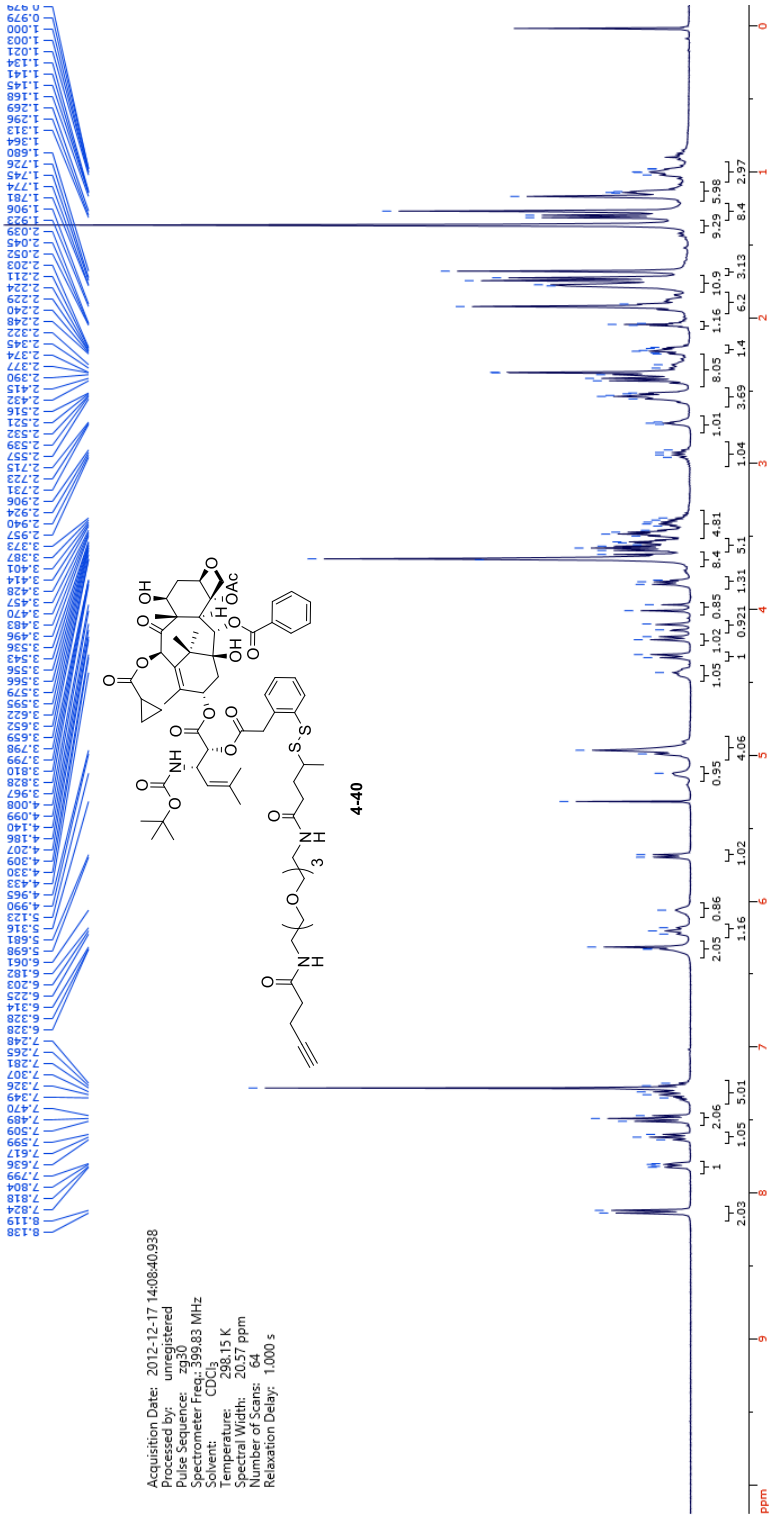
4-40
Acquisition Date: 2012-12-17 14:08:40.938
Processed by: unregistered
Pulse Sequence: zg30
Spectrometer Freq.: 399.83 MHz
Solvent: $CDCl_3$
Temperature: 298.15 K
Spectral Width: 20.57 ppm
Number of Scans: 64
Relaxation Delay: 1.000 s
ppm

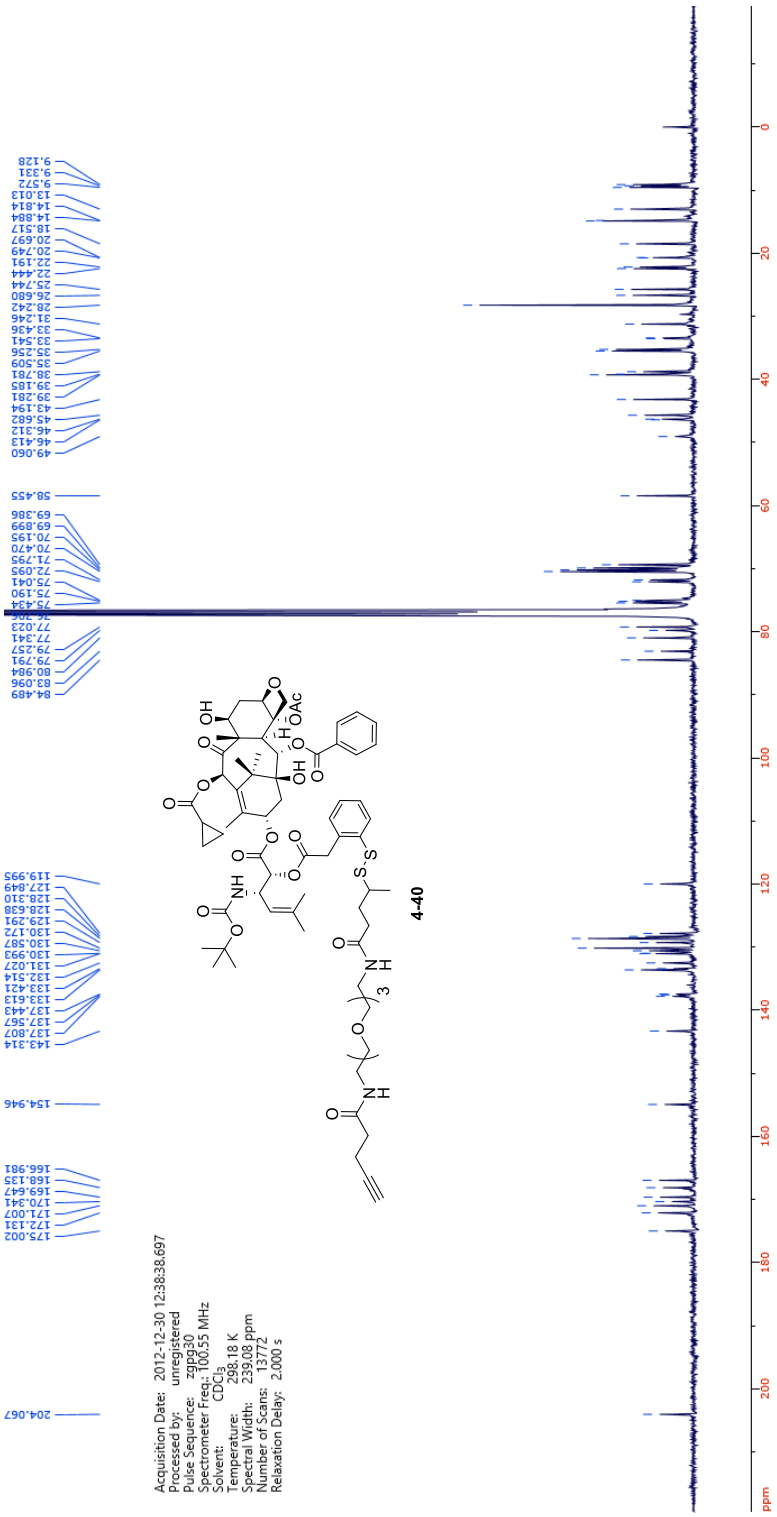
Acquisition Date: 2012-12-30 12:38:38.697
Processed by: unregistered
Pulse Sequence: zgpg30
Spectrometer Freq.: 100.55 MHz
Solvent: CDCl3
Temperature: 298.18 K
Spectral Width: 239.08 ppm
Number of Scans: 13772
Relaxation Delay: 2.000 s
4-40
ppm

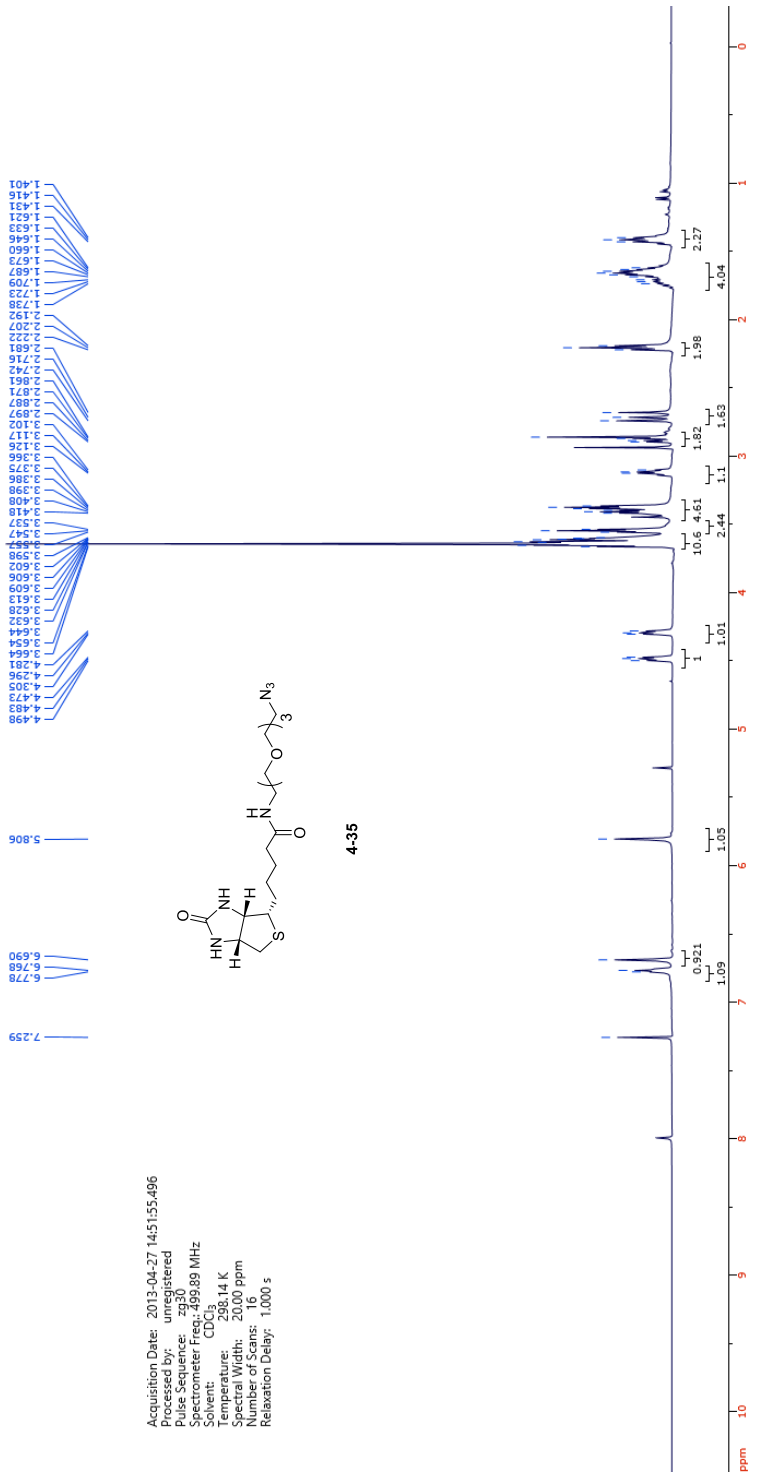
4-35
Acquisition Date: 2013-04-27 14:51:55.496
Processed by: unregistered
Pulse Sequence: zg30
Spectrometer Freq.: 499.89 MHz
Solvent: CDCl3
Temperature: 298.14 K
Spectral Width: 20.00 ppm
Number of Scans: 16
Relaxation Delay: 1.000 s
ppm

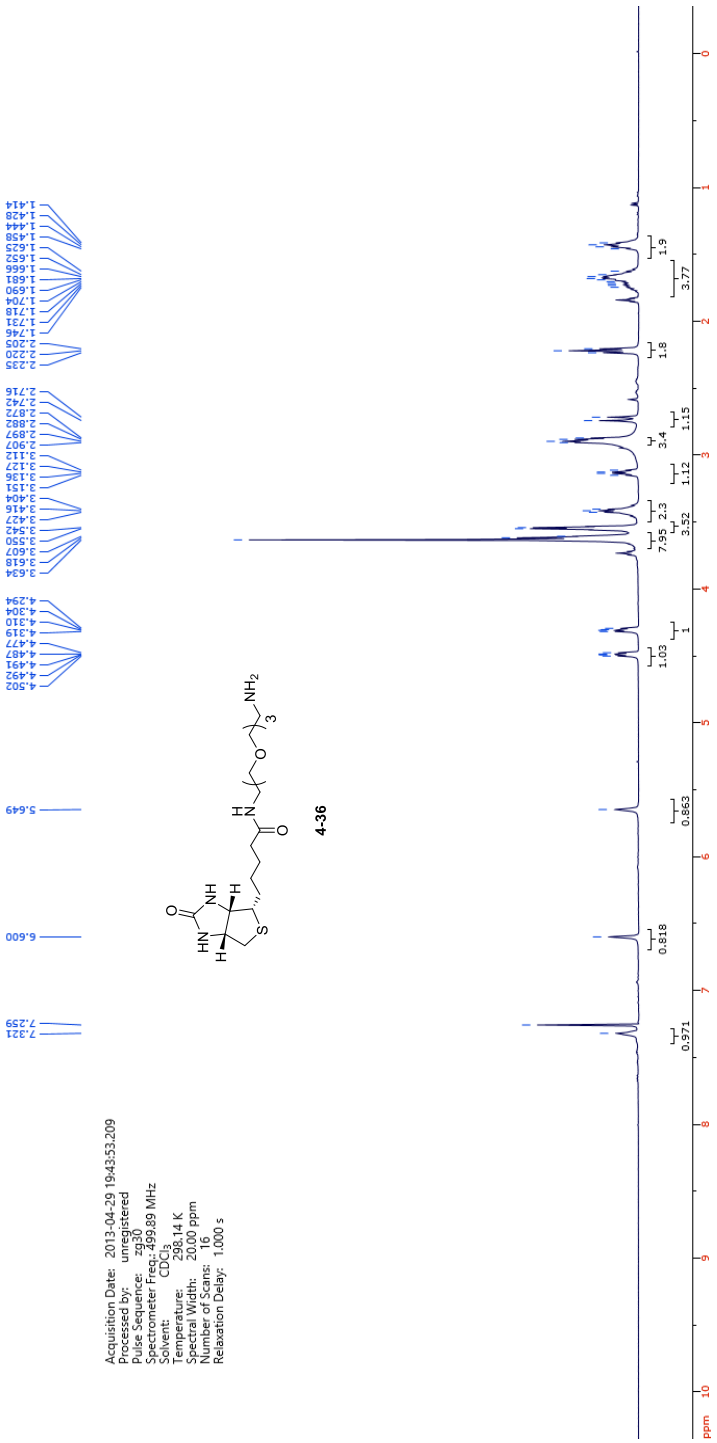
Acquisition Date: 2013-04-29 19:43:53.209
Processed by: unregistered
Pulse Sequence: zg30
Spectrometer Freq.: 499.89 MHz
Solvent: CDCl3
Temperature: 298.14 K
Spectral Width: 20.00 ppm
Number of Scans: 16
Relaxation Delay: 1.000 s
4-36
ppm

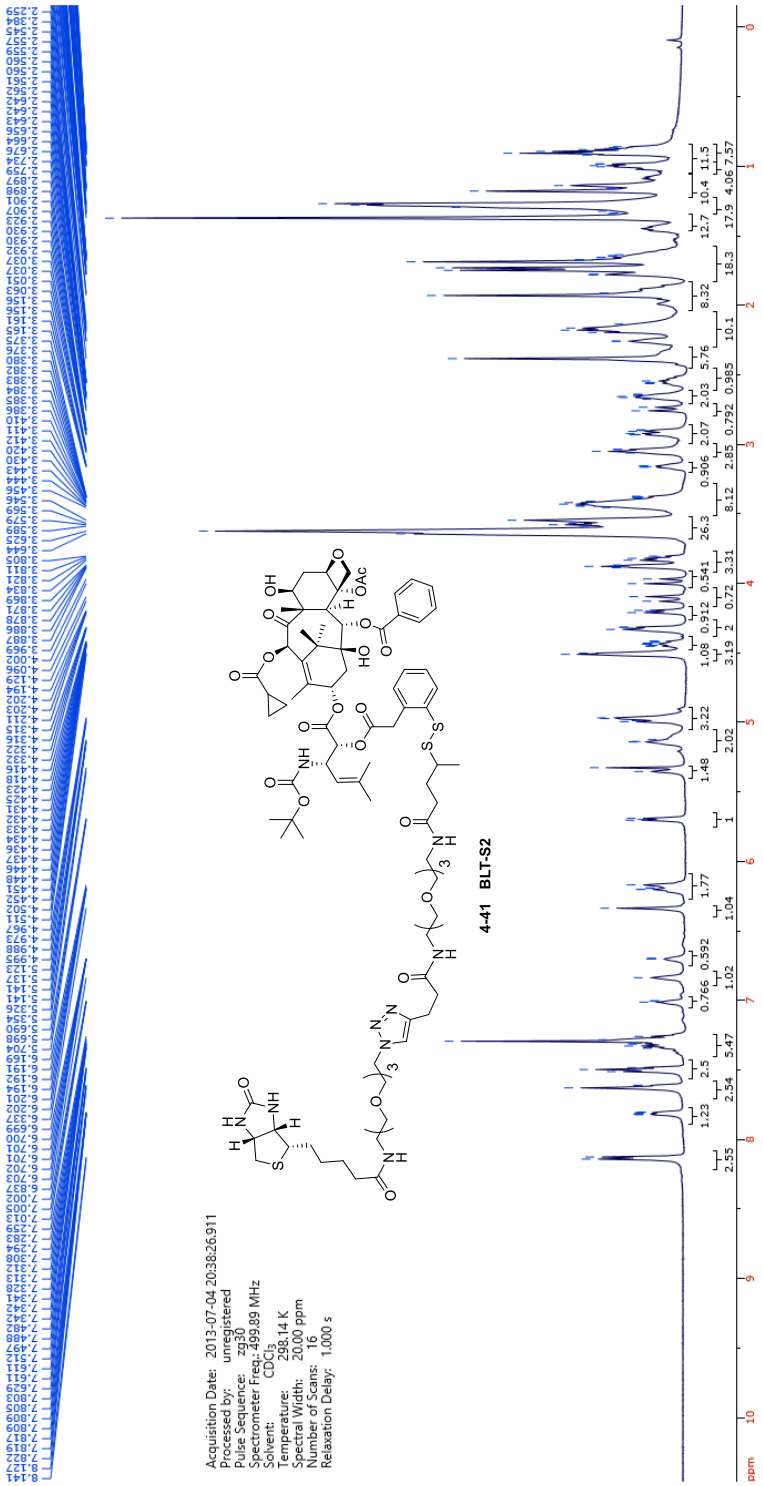
Acquisition Date: 2013-07-04 20:38:26.911
Processed by: unregistered
Pulse Sequence: zg30
Spectrometer Freq.: 499.89 MHz
Solvent: $CDCl_3$
Temperature: 298.14 K
Spectral Width: 20.00 ppm
Number of Scans: 16
Relaxation Delay: 1.000 s
4-41 BLT-S2
ppm

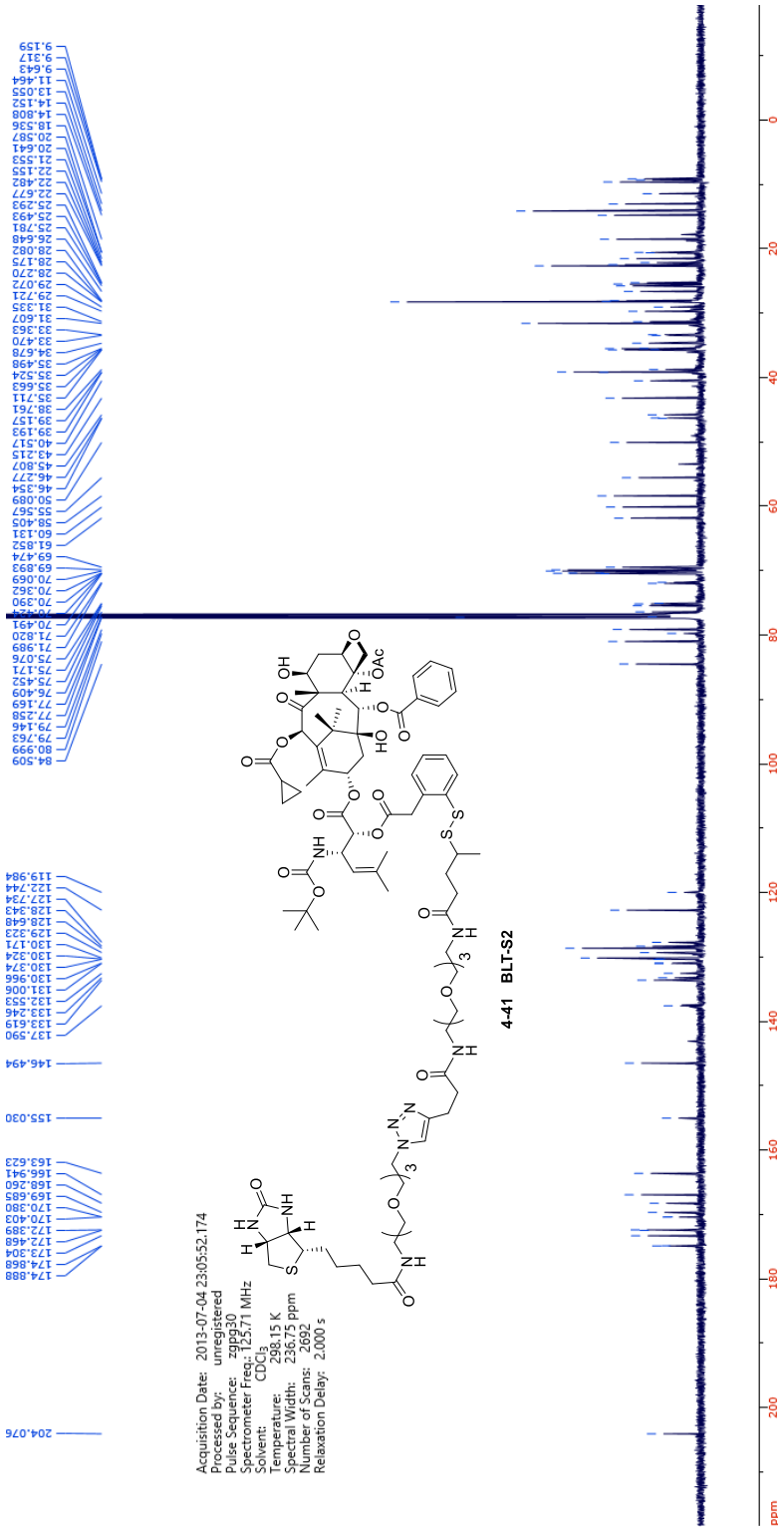
4-41 BLT-S2
Acquisition Date: 2013-07-04 23:05:52.174
Processed by: unregistered
Pulse Sequence: zgpg30
Spectrometer Freq.: 125.71 MHz
Solvent: $CDCl_3$
Temperature: 298.15 K
Spectral Width: 236.75 ppm
Number of Scans: 2692
Relaxation Delay: 2.000 s
ppm

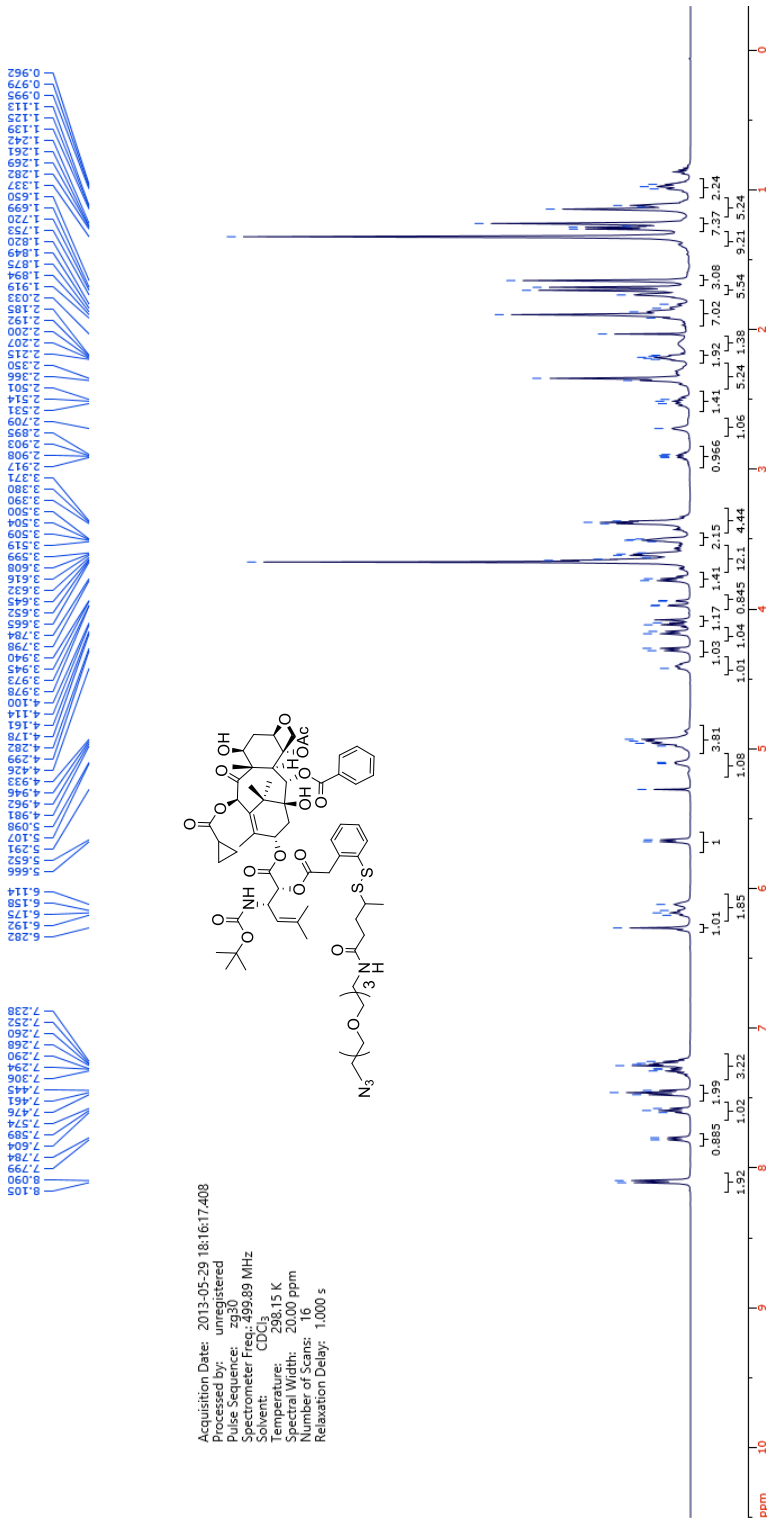
Acquisition Date: 2013-05-29 18:16:17.408
Processed by: unregistered
Pulse Sequence: zg30
Spectrometer Freq.: 499.89 MHz
Solvent: CDCl3
Temperature: 298.15 K
Spectral Width: 20.00 ppm
Number of Scans: 16
Relaxation Delay: 1.000 s
ppm

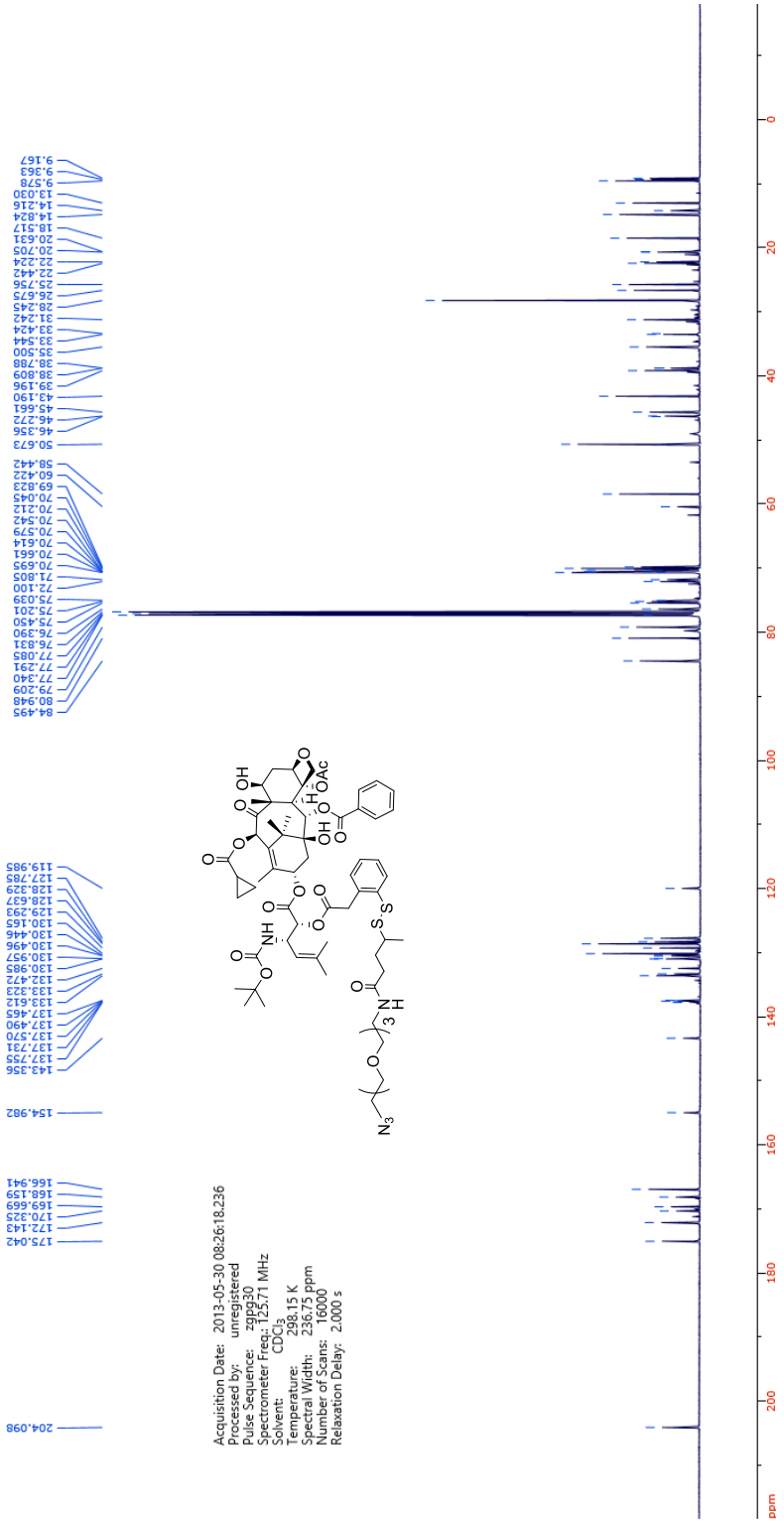
Acquisition Date: 2013-05-30 08:26:18.236
Processed by: unregistered
Pulse Sequence: zgpg30
Spectrometer Freq.: 125.71 MHz
Solvent: CDCl3
Temperature: 298.15 K
Spectral Width: 236.75 ppm
Number of Scans: 16000
Relaxation Delay: 2.000 s
ppm

Appendix Chapter 5

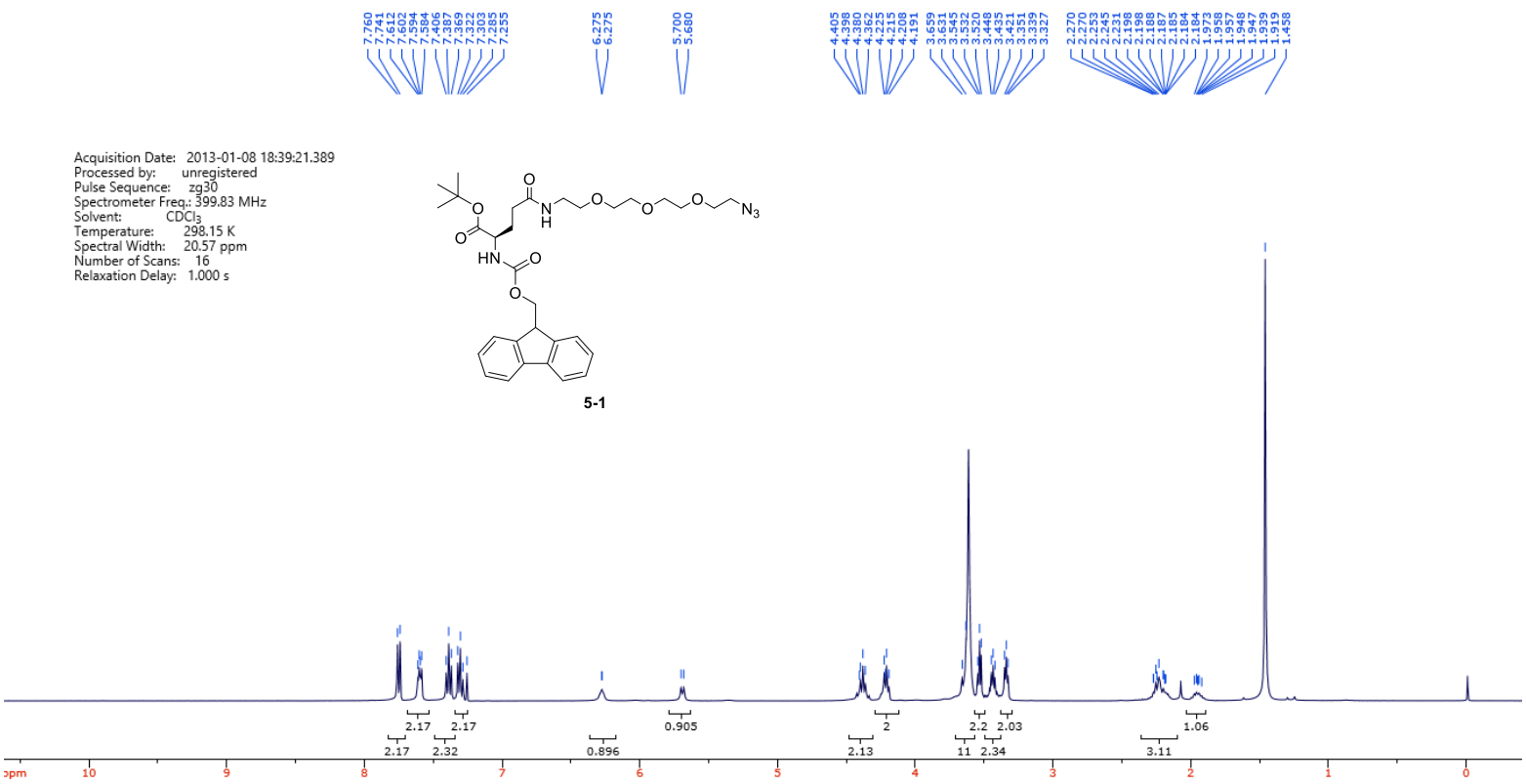
7.760
7.741
7.612
7.602
7.594
7.584
7.406
7.387
7.369
7.322
7.303
7.285
7.255
6.275
6.275
5.700
5.680
4.405
4.398
4.380
4.362
4.225
4.215
4.208
4.191
3.659
3.631
3.545
3.532
3.520
3.448
3.435
3.421
3.351
3.339
3.327
2.270
2.270
2.253
2.245
2.231
2.198
2.198
2.188
2.187
2.185
2.184
2.173
1.958
1.957
1.948
1.947
1.939
1.939
1.458
Acquisition Date: 2013-01-08 18:39:21.389
Processed by: unregistered
Pulse Sequence: zg30
Spectrometer Freq.: 399.83 MHz
Solvent: CDCl3
Temperature: 298.15 K
Spectral Width: 20.57 ppm
Number of Scans: 16
Relaxation Delay: 1.000 s
5-1
2.17
2.17
2.17
2.32
0.896
0.905
2
2.13
2.2
11
2.03
2.34
1.06
3.11
ppm
10
9
8
7
6
5
4
3
2
1
0

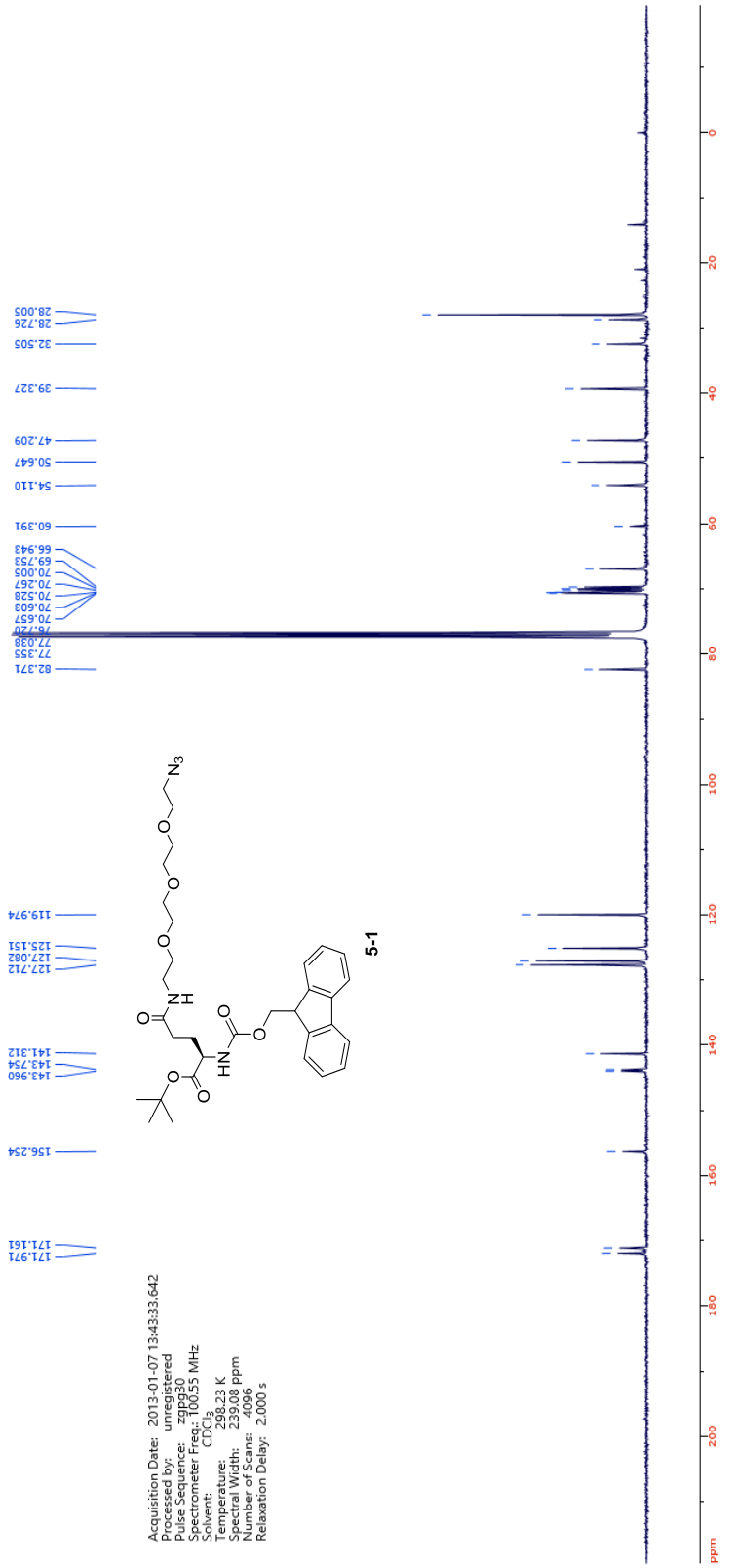
Acquisition Date: 2013-01-07 13:43:33.642
Processed by: unregistered
Pulse Sequence: zgpg30
Spectrometer Freq.: 100.55 MHz
Solvent: $CDCl_3$
Temperature: 298.23 K
Spectral Width: 239.08 ppm
Number of Scans: 4096
Relaxation Delay: 2.000 s
5-1
ppm

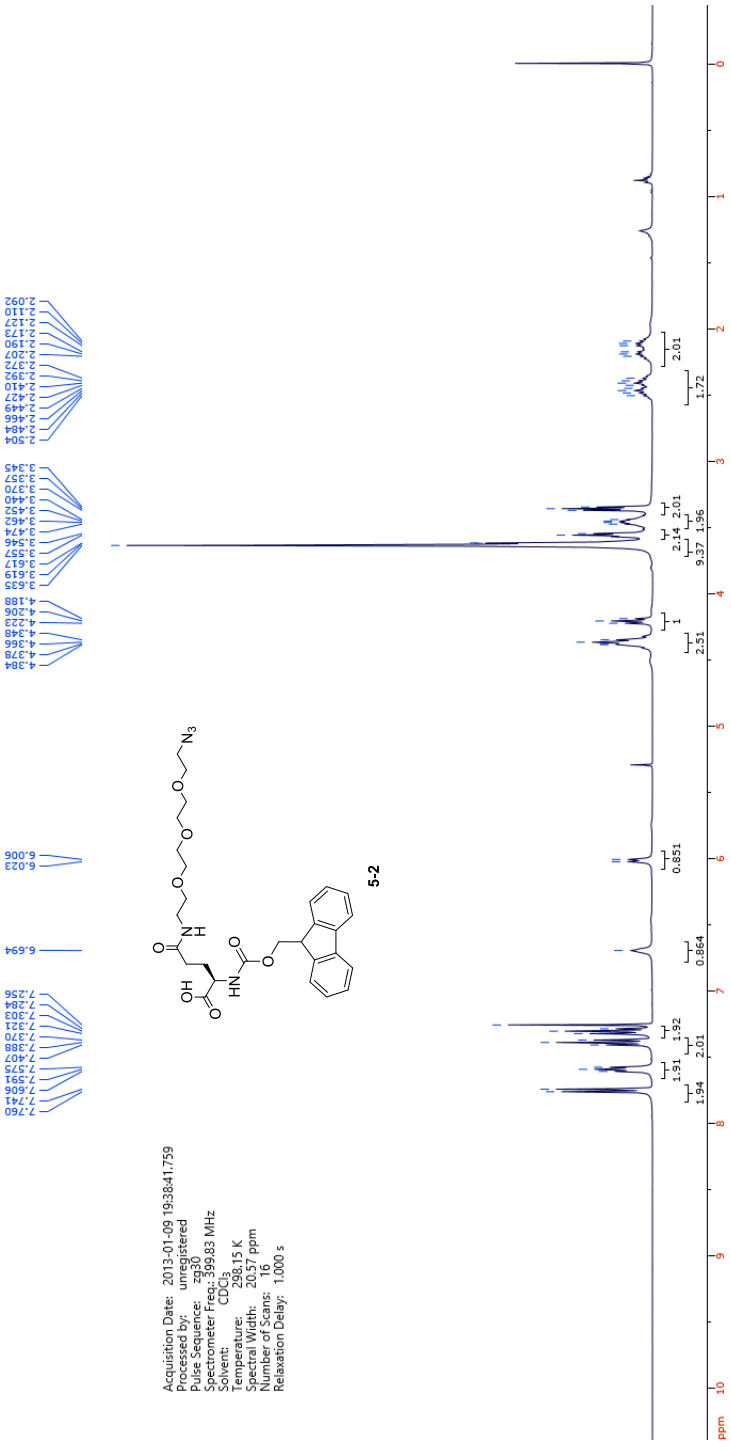
Acquisition Date: 2013-01-09 19:38:41.759
Processed by: unregistered
Pulse Sequence: zg30
Spectrometer Freq.: 399.83 MHz
Solvent: CDCl3
Temperature: 298.15 K
Spectral Width: 20.57 ppm
Number of Scans: 16
Relaxation Delay: 1.000 s
5-2
ppm

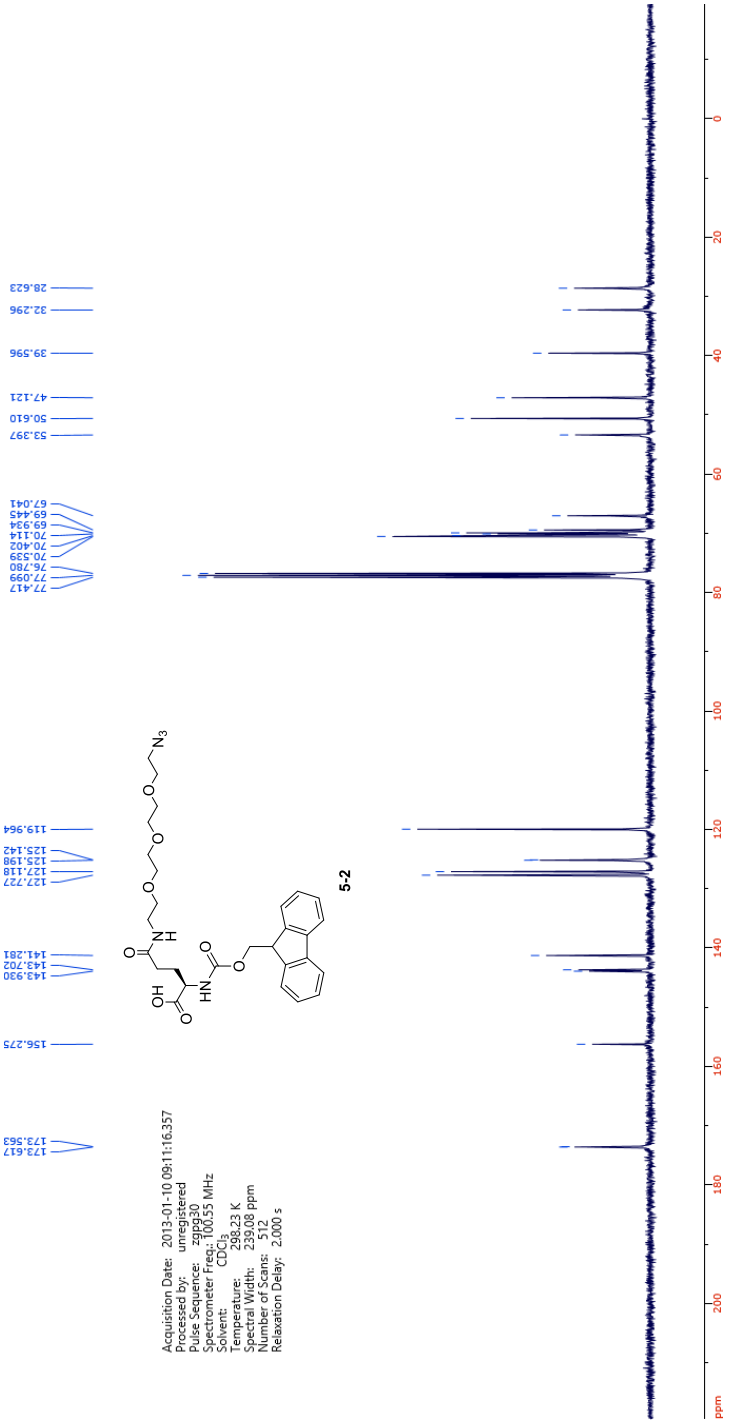
28.623
32.296
39.596
47.121
50.610
53.397
67.041
69.445
69.934
70.114
70.402
70.539
76.780
77.099
77.417
119.964
125.142
125.198
127.118
127.727
141.281
143.702
143.930
156.275
173.563
173.617
5-2
Acquisition Date: 2013-01-10 09:11:16.357
Processed by: unregistered
Pulse Sequence: zgpg30
Spectrometer Freq.: 100.55 MHz
Solvent: CDCl3
Temperature: 298.23 K
Spectral Width: 239.08 ppm
Number of Scans: 512
Relaxation Delay: 2.000 s
ppm

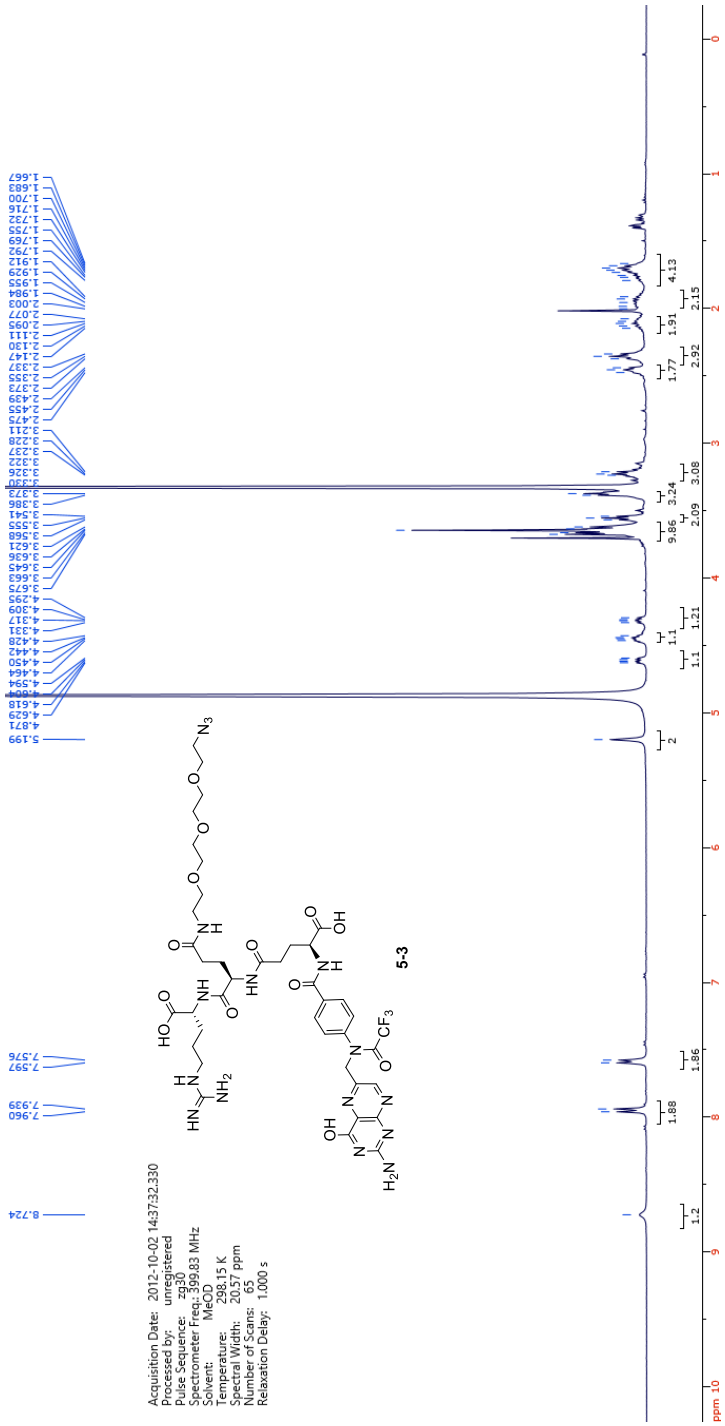
Acquisition Date: 2012-10-02 14:37:32.330
Processed by: unregistered
Pulse Sequence: zg30
Spectrometer Freq.: 399.83 MHz
Solvent: MeOD
Temperature: 298.15 K
Spectral Width: 2037 ppm
Number of Scans: 65
Relaxation Delay: 1.000 s
5-3
ppm

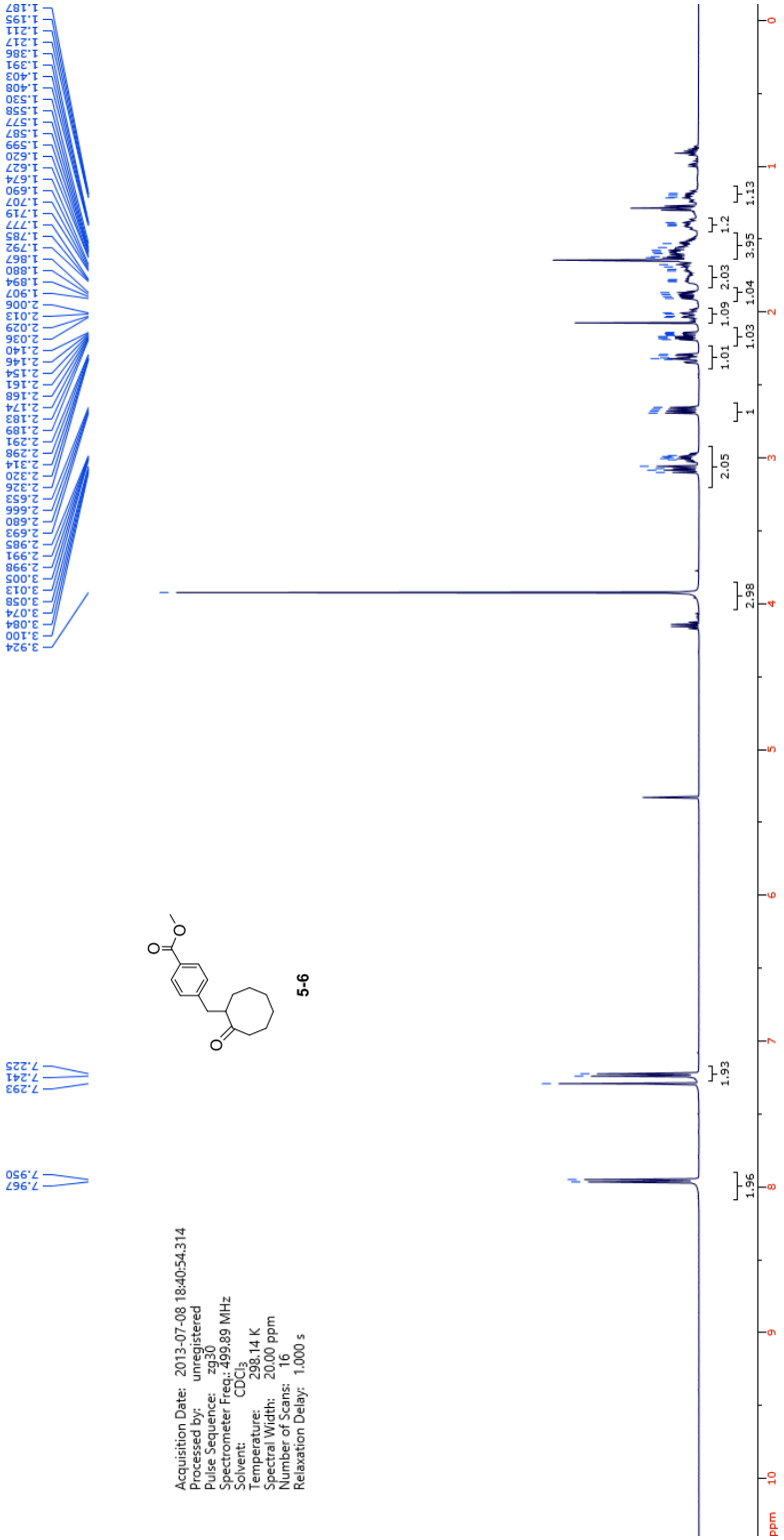
Acquisition Date: 2013-07-08 18:40:54.314
Processed by: unregistered
Pulse Sequence: zg30
Spectrometer Freq.: 499.89 MHz
Solvent: $CDCl_3$
Temperature: 298.14 K
Spectral Width: 20.00 ppm
Number of Scans: 16
Relaxation Delay: 1.000 s
5-6
ppm

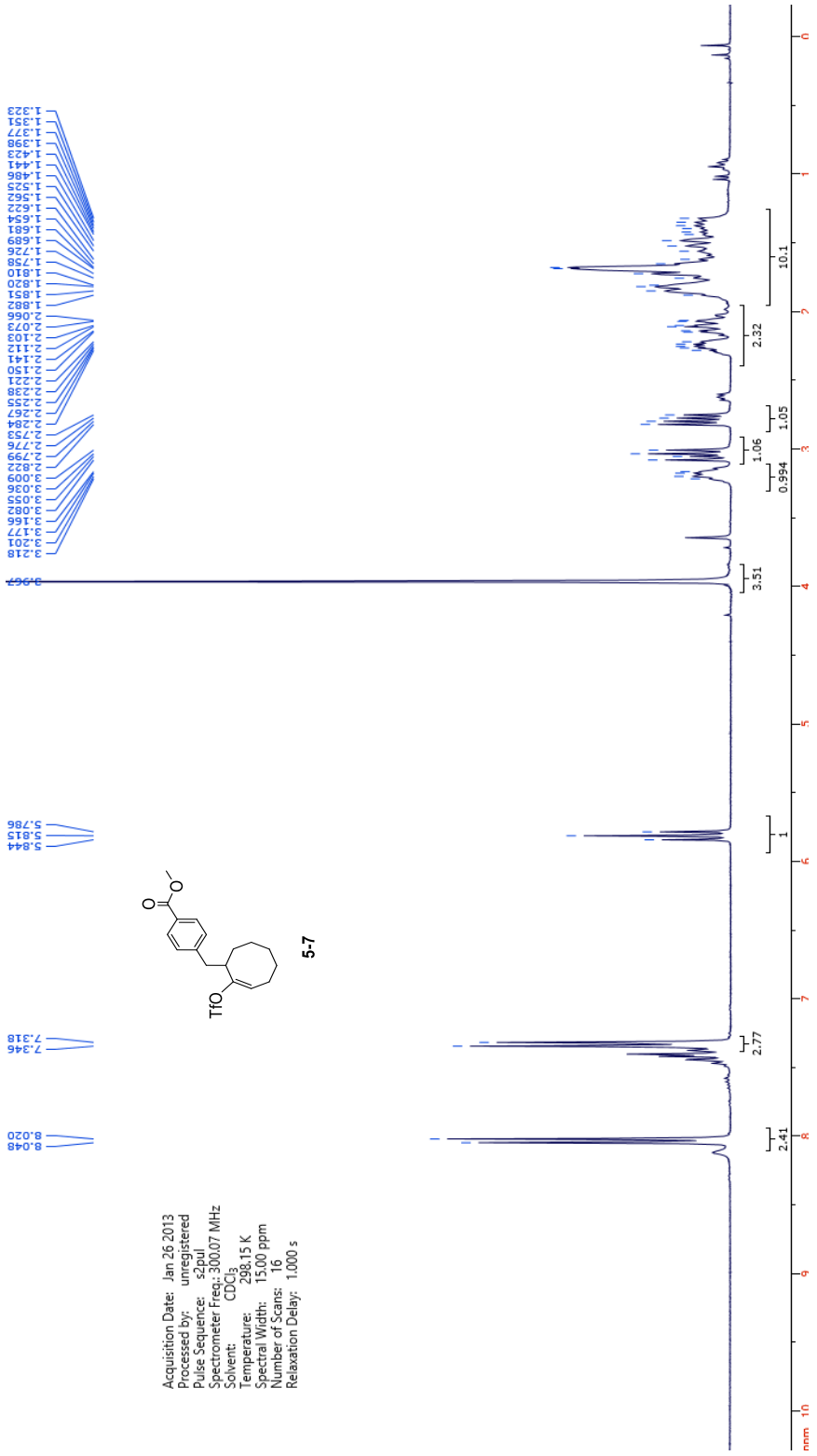
8.048
8.020
7.346
7.318
5.844
5.815
5.786
3.967
3.218
3.201
3.177
3.166
3.082
3.055
3.036
3.009
2.822
2.799
2.776
2.753
2.284
2.267
2.255
2.238
2.221
2.150
2.141
2.112
2.103
2.073
2.066
1.882
1.851
1.820
1.810
1.758
1.726
1.689
1.681
1.654
1.622
1.562
1.525
1.486
1.441
1.423
1.398
1.377
1.351
1.323
2.41
2.77
1
3.51
0.994
1.06
1.05
2.32
10.1
TfO
5-7
Acquisition Date: Jan 26 2013
Processed by: unregistered
Pulse Sequence: s2pul
Spectrometer Freq.: 300.07 MHz
Solvent: CDCl3
Temperature: 298.15 K
Spectral Width: 15.00 ppm
Number of Scans: 16
Relaxation Delay: 1.000 s
ppm

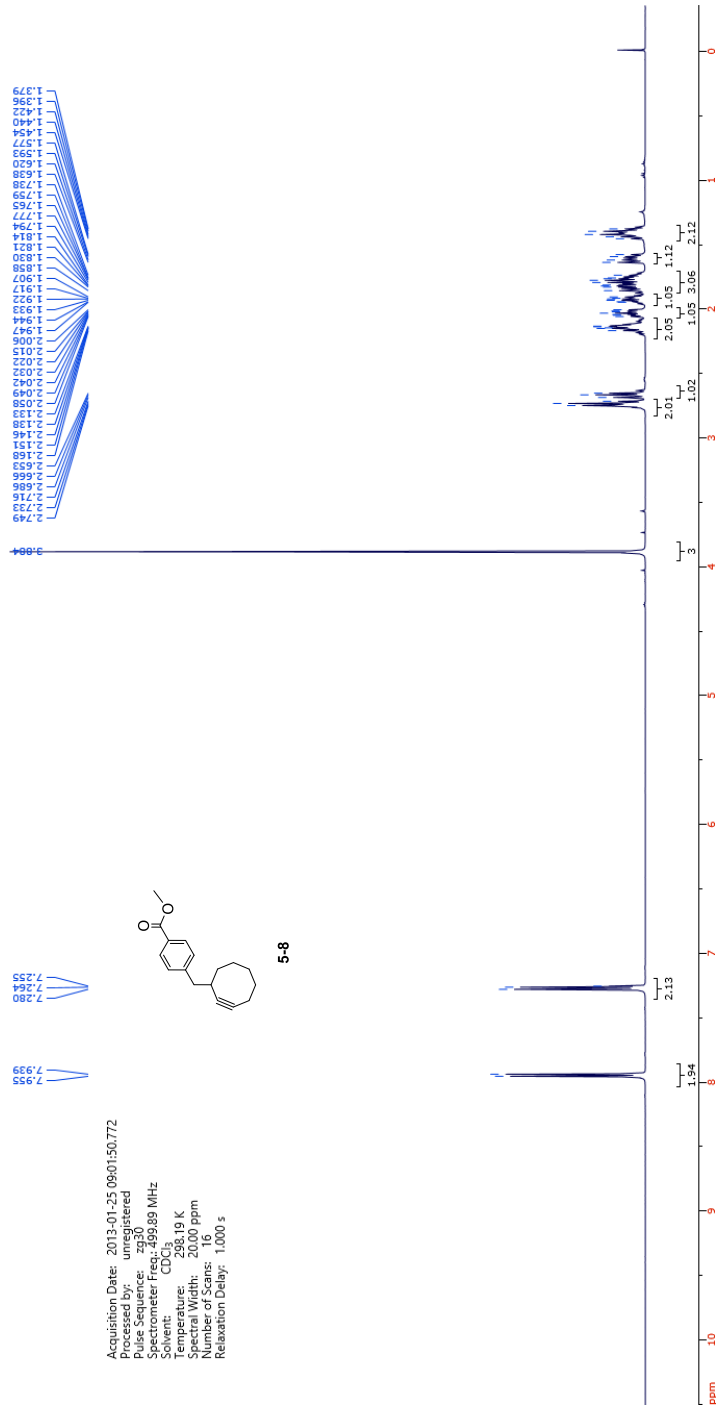
Acquisition Date: 2013-01-25 09:01:50.772
Processed by: unregistered
Pulse Sequence: zg30
Spectrometer Freq.: 499.89 MHz
Solvent: CDCl3
Temperature: 298.19 K
Spectral Width: 20.00 ppm
Number of Scans: 16
Relaxation Delay: 1.000 s
5-8
ppm

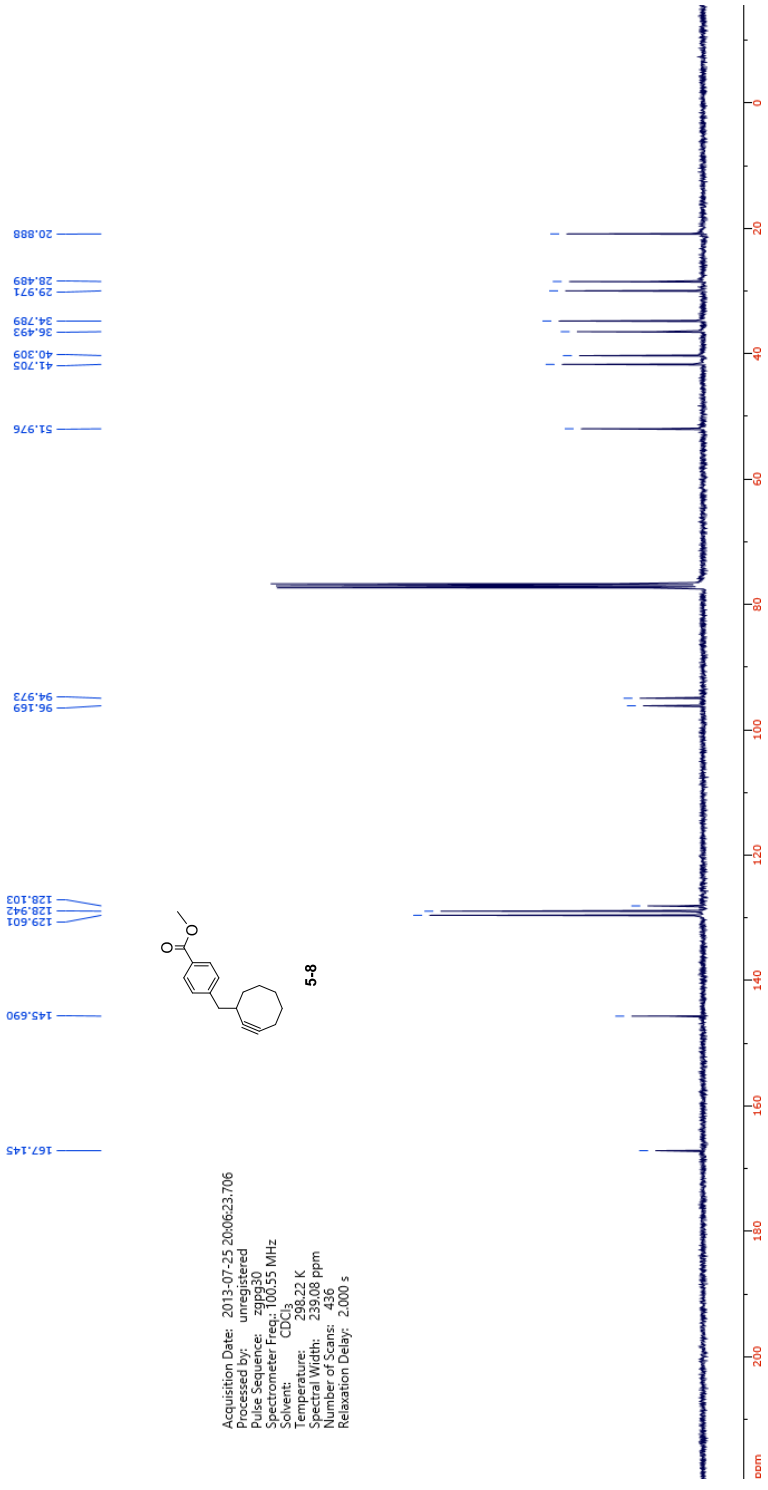
20.888
28.489
29.971
34.789
36.493
40.309
41.705
51.976
94.973
96.169
128.103
128.942
129.601
145.690
167.145
5-8
Acquisition Date: 2013-07-25 20:06:23.706
Processed by: unregistered
Pulse Sequence: zgpg30
Spectrometer Freq.: 100.55 MHz
Solvent: CDCl3
Temperature: 298.22 K
Spectral Width: 239.08 ppm
Number of Scans: 436
Relaxation Delay: 2.000 s
ppm
0
20
40
60
80
100
120
140
160
180
200

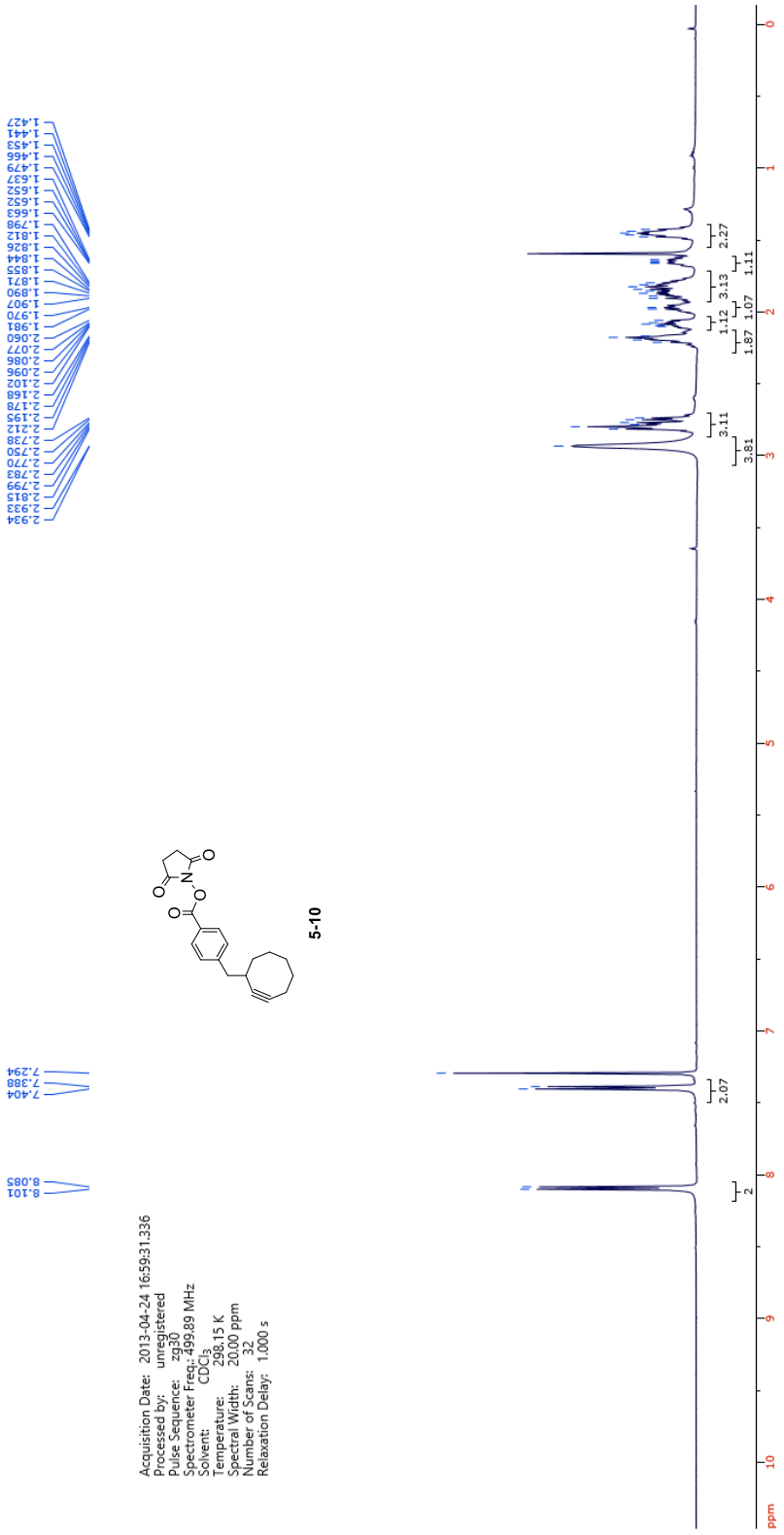
8.101
8.085
7.404
7.388
7.294
2.934
2.933
2.815
2.799
2.783
2.770
2.750
2.738
2.212
2.195
2.178
2.168
2.102
2.096
2.086
2.077
2.060
1.981
1.970
1.907
1.890
1.871
1.855
1.844
1.826
1.812
1.798
1.663
1.652
1.637
1.632
1.479
1.466
1.453
1.441
1.427
5-10
Acquisition Date: 2013-04-24 16:59:31.336
Processed by: unregistered
Pulse Sequence: zg30
Spectrometer Freq.: 499.89 MHz
Solvent: $CDCl_3$
Temperature: 298.15 K
Spectral Width: 20.00 ppm
Number of Scans: 32
Relaxation Delay: 1.000 s
2
2.07
3.81
3.11
1.87
1.12
1.07
3.13
1.11
2.27
ppm

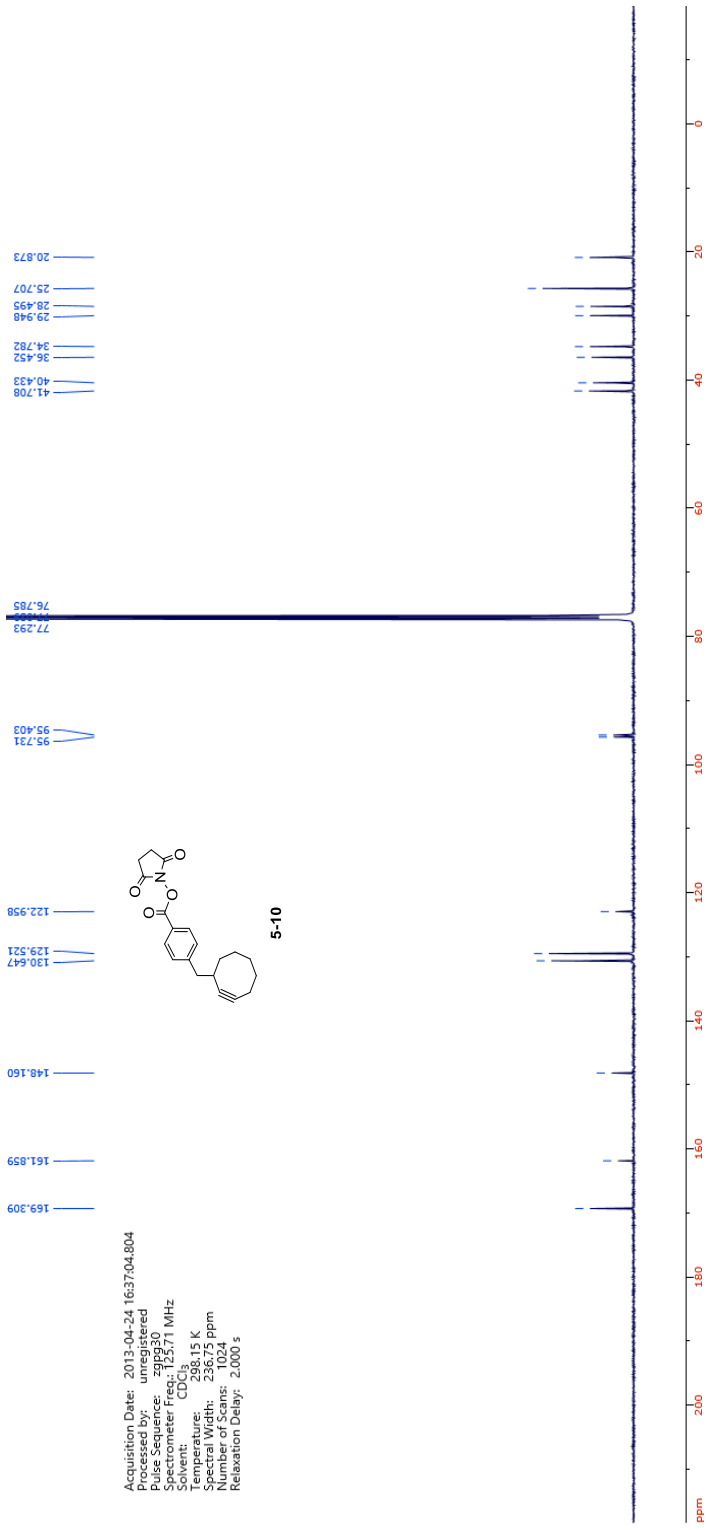
20.873
25.707
28.495
29.948
34.782
36.452
40.433
41.708
76.785
77.293
95.403
95.731
122.958
129.521
130.647
148.160
161.859
169.309
5-10
Acquisition Date: 2013-04-24 16:37:04.804
Processed by: unregistered
Pulse Sequence: zgpg30
Spectrometer Freq.: 125.71 MHz
Solvent: CDCl3
Temperature: 298.15 K
Spectral Width: 236.75 ppm
Number of Scans: 1024
Relaxation Delay: 2.000 s
ppm

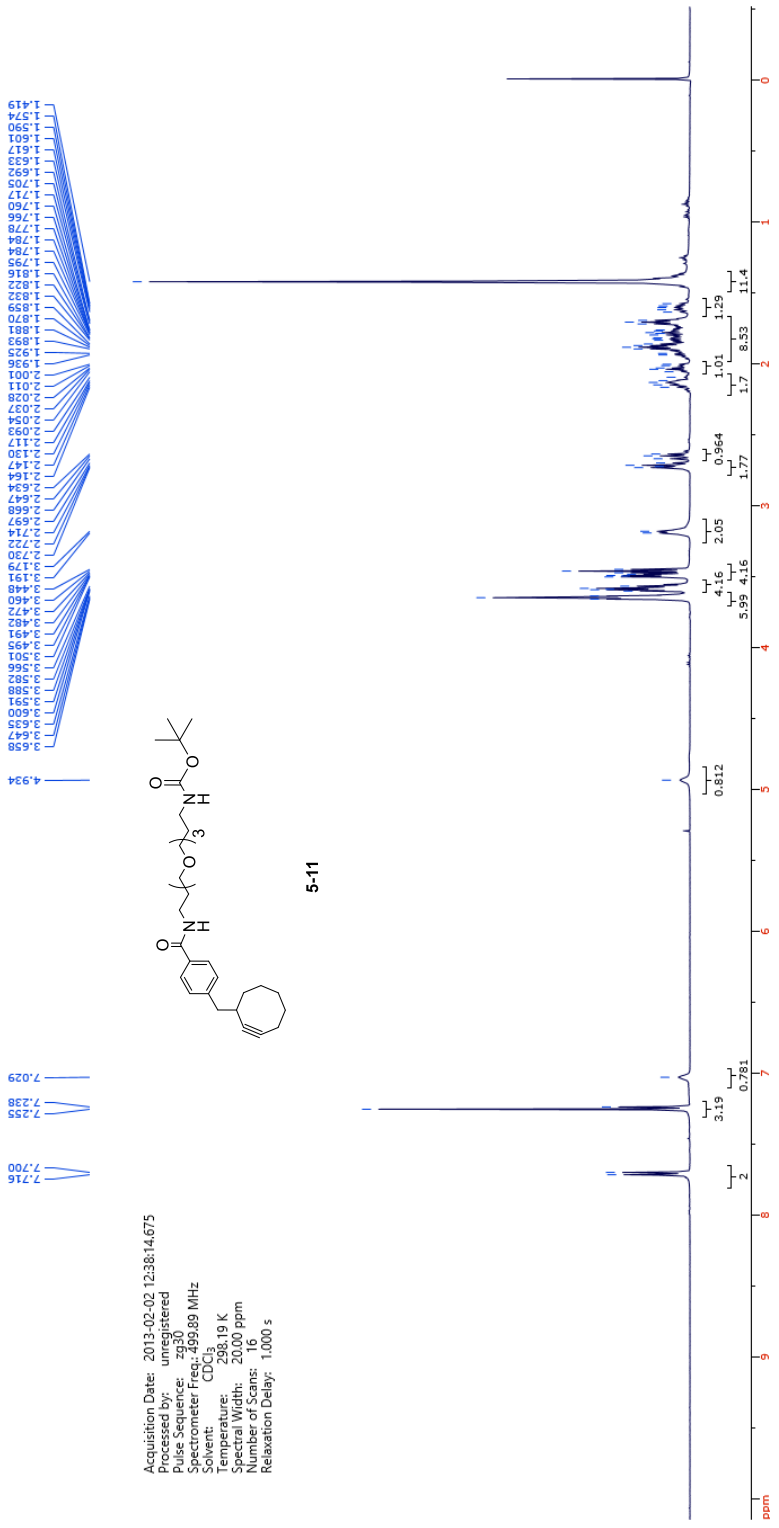
Acquisition Date: 2013-02-02 12:38:14.675
Processed by: unregistered
Pulse Sequence: zg30
Spectrometer Freq.: 499.89 MHz
Solvent: $CDCl_3$
Temperature: 298.19 K
Spectral Width: 20.00 ppm
Number of Scans: 16
Relaxation Delay: 1.000 s
5-11
ppm

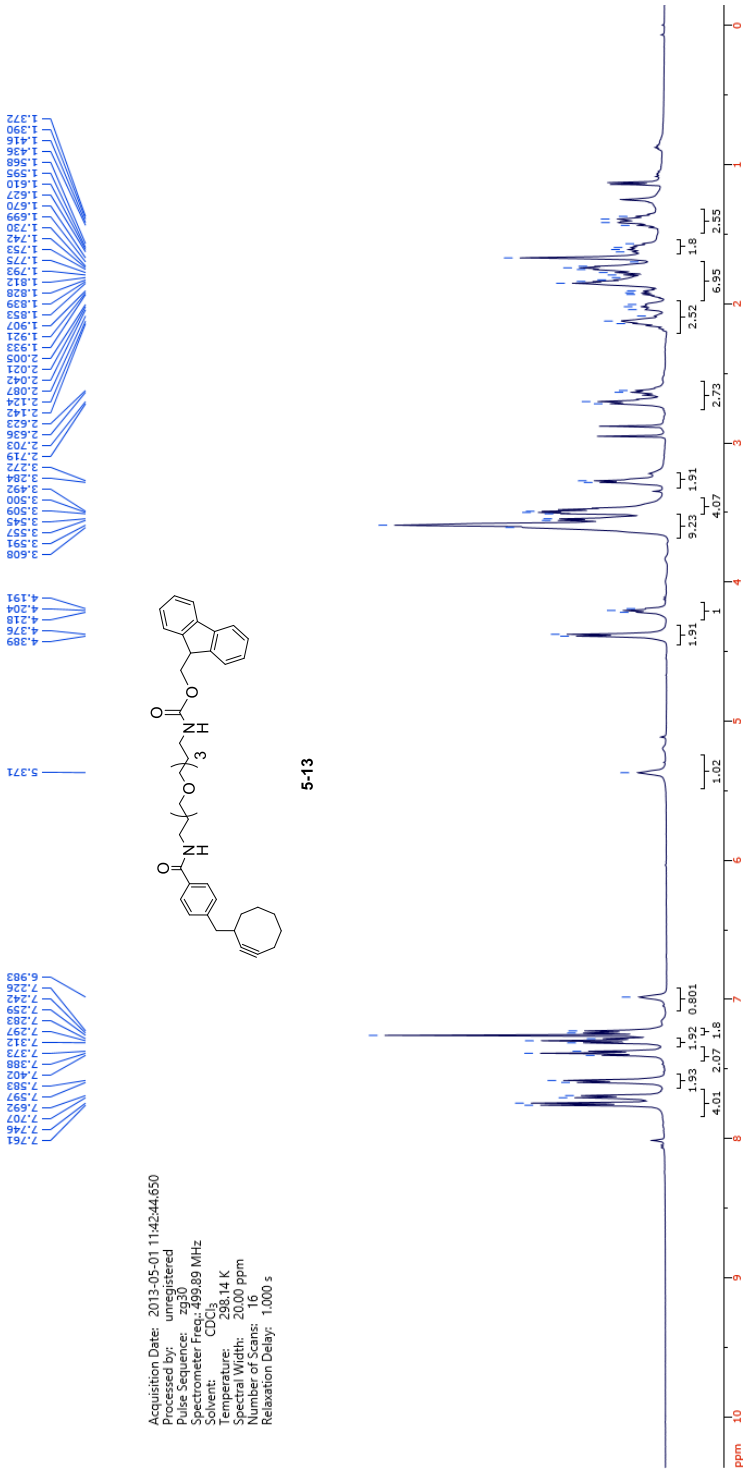
Acquisition Date: 2013-05-01 11:42:44.650
Processed by: unregistered
Pulse Sequence: zg30
Spectrometer Freq.: 499.89 MHz
Solvent: $CDCl_3$
Temperature: 298.14 K
Spectral Width: 20.00 ppm
Number of Scans: 16
Relaxation Delay: 1.000 s
5-13
ppm

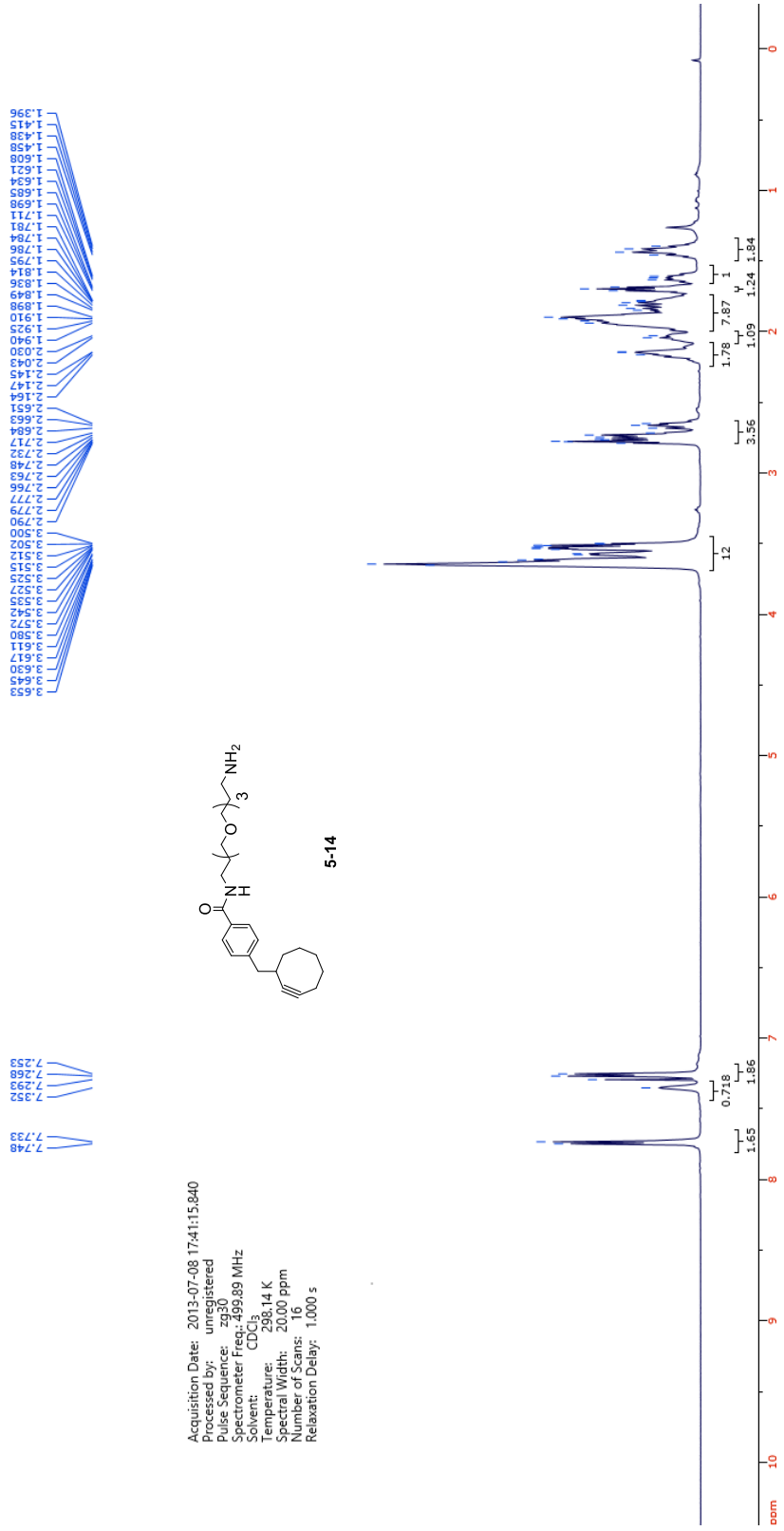
Acquisition Date: 2013-07-08 17:41:15.840
Processed by: unregistered
Pulse Sequence: zg30
Spectrometer Freq.: 499.89 MHz
Solvent: $CDCl_3$
Temperature: 298.14 K
Spectral Width: 20.00 ppm
Number of Scans: 16
Relaxation Delay: 1.000 s
5-14
ppm

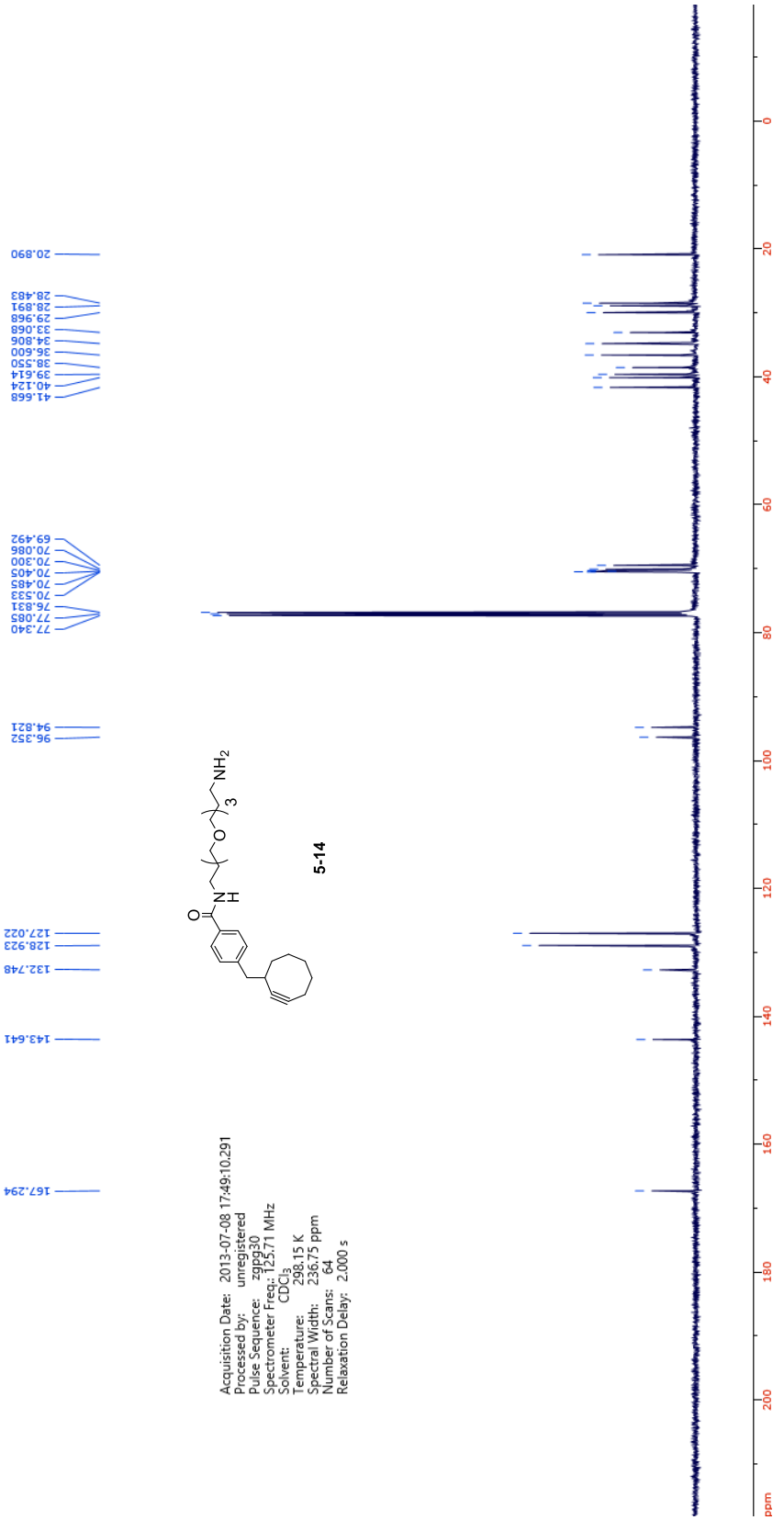
20.890
28.483
28.891
29.968
33.068
34.806
36.600
38.550
39.614
40.124
41.668
69.492
70.086
70.300
70.405
70.485
70.533
76.831
77.085
77.340
94.821
96.352
127.022
128.923
132.748
143.641
167.294
5-14
Acquisition Date: 2013-07-08 17:49:10.291
Processed by: unregistered
Pulse Sequence: zgpg30
Spectrometer Freq.: 125.71 MHz
Solvent: CDCl3
Temperature: 298.15 K
Spectral Width: 236.75 ppm
Number of Scans: 64
Relaxation Delay: 2.000 s
ppm

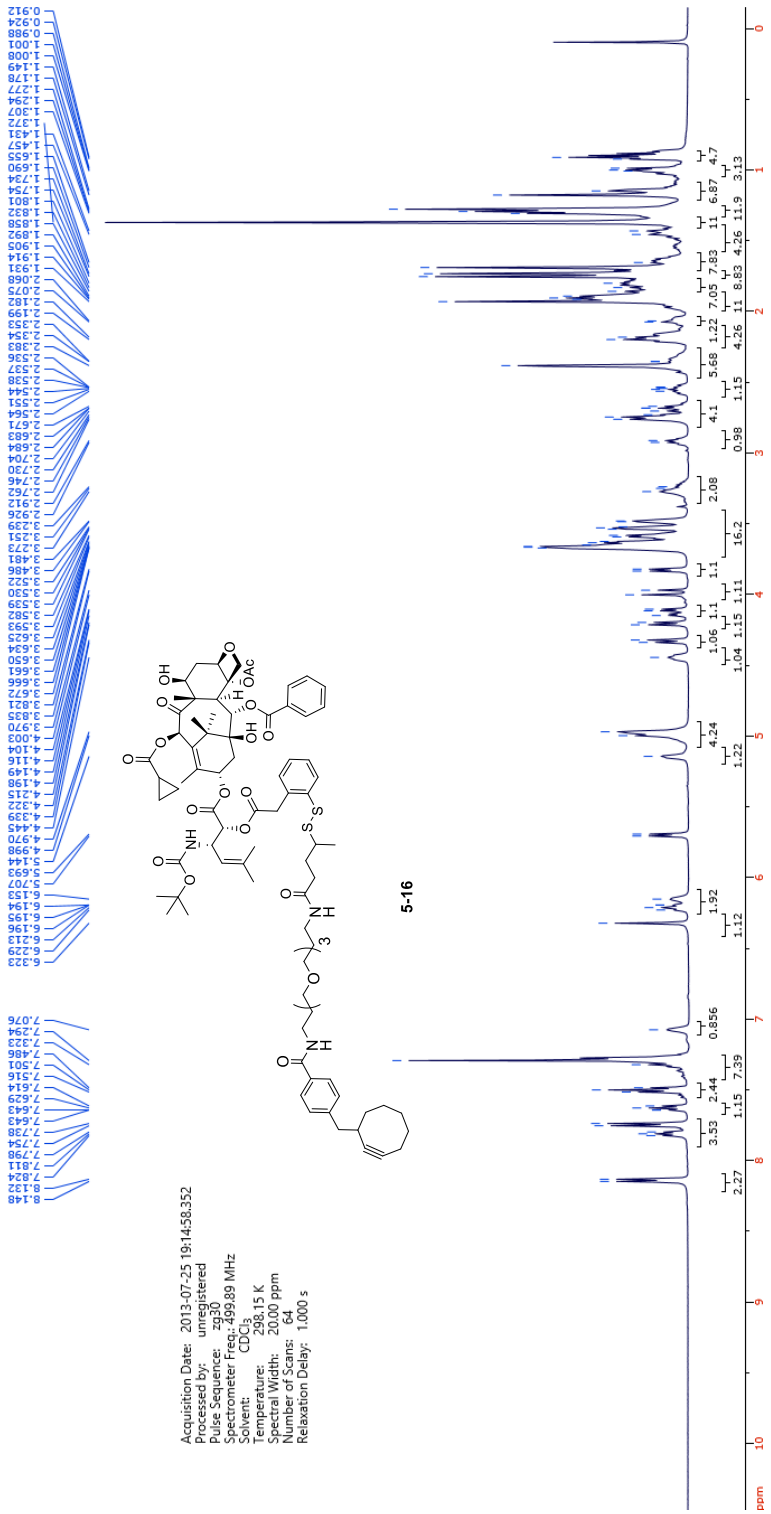
Acquisition Date: 2013-07-25 19:14:58.352
Processed by: unregistered
Pulse Sequence: zg30
Spectrometer Freq.: 499.89 MHz
Solvent: $CDCl_3$
Temperature: 298.15 K
Spectral Width: 20.00 ppm
Number of Scans: 64
Relaxation Delay: 1.000 s
5-16
ppm

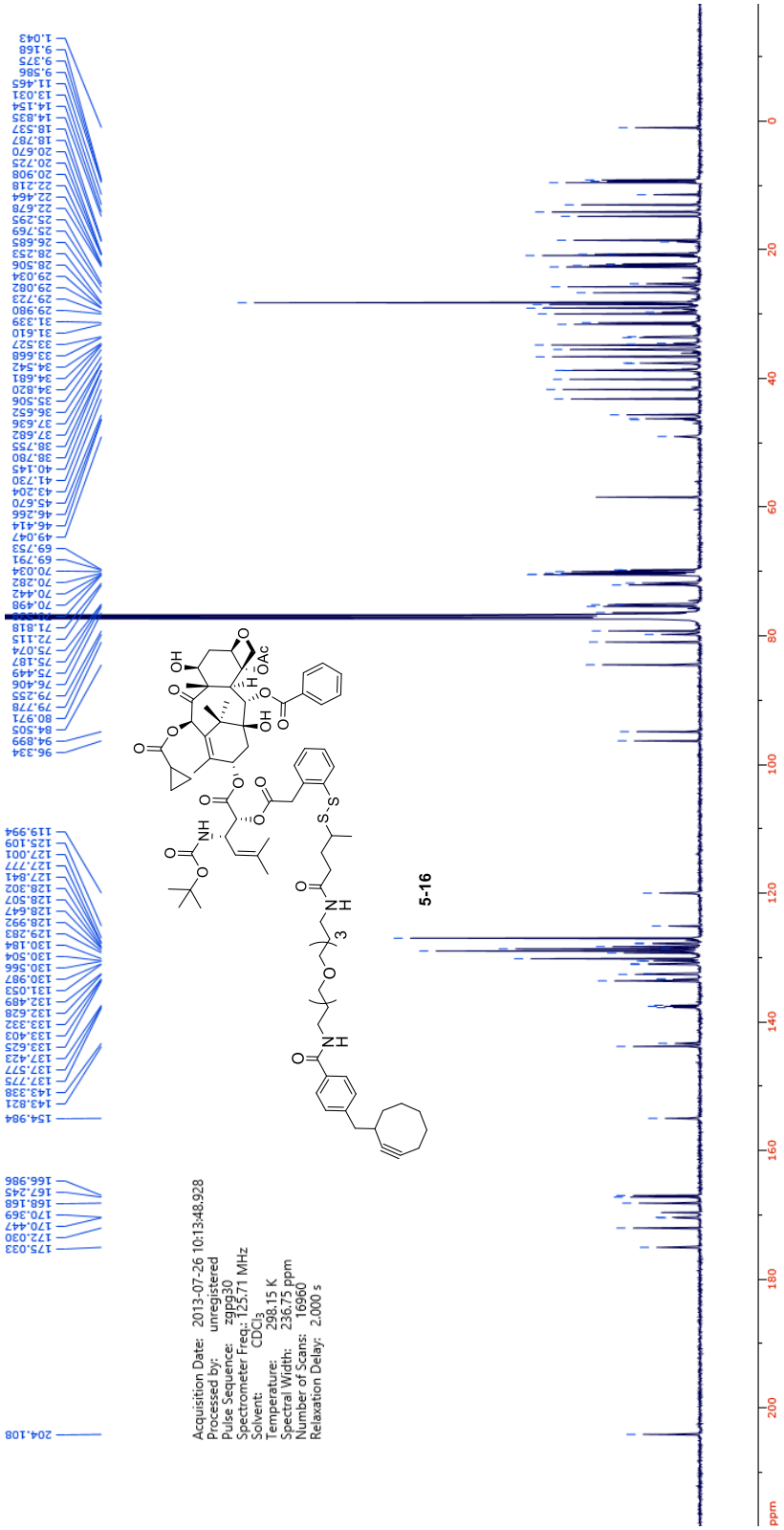
5-16
Acquisition Date: 2013-07-26 10:13:48.928
Processed by: unregistered
Pulse Sequence: zgpg30
Spectrometer Freq.: 125.71 MHz
Solvent: CDCl3
Temperature: 298.15 K
Spectral Width: 236.75 ppm
Number of Scans: 16960
Relaxation Delay: 2.000 s
ppm

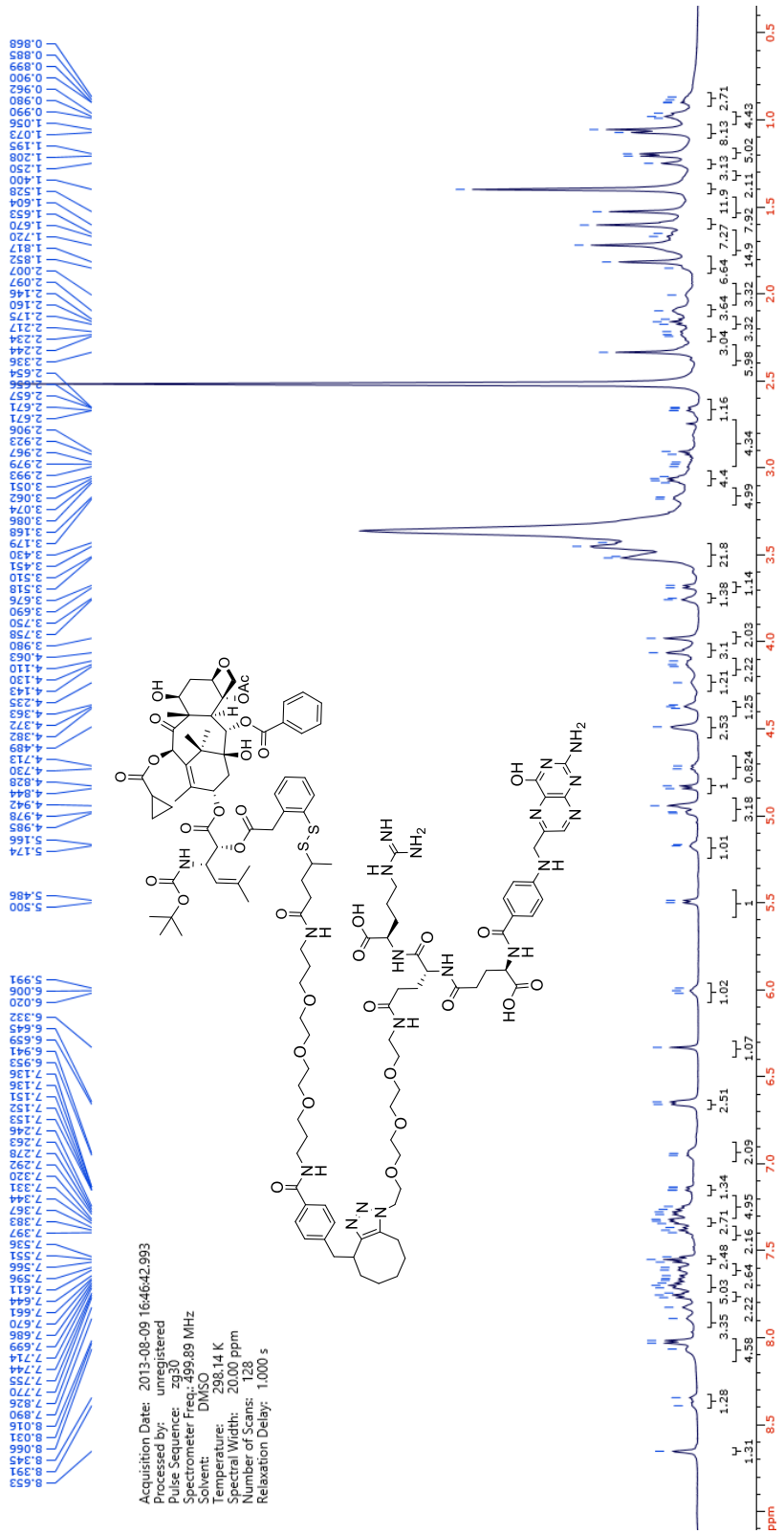
Acquisition Date: 2013-08-09 16:46:42.993
Processed by: unregistered
Pulse Sequence: zg30
Spectrometer Freq.: 499.89 MHz
Solvent: DMSO
Temperature: 298.14 K
Spectral Width: 20.00 ppm
Number of Scans: 128
Relaxation Delay: 1.000 s
ppm

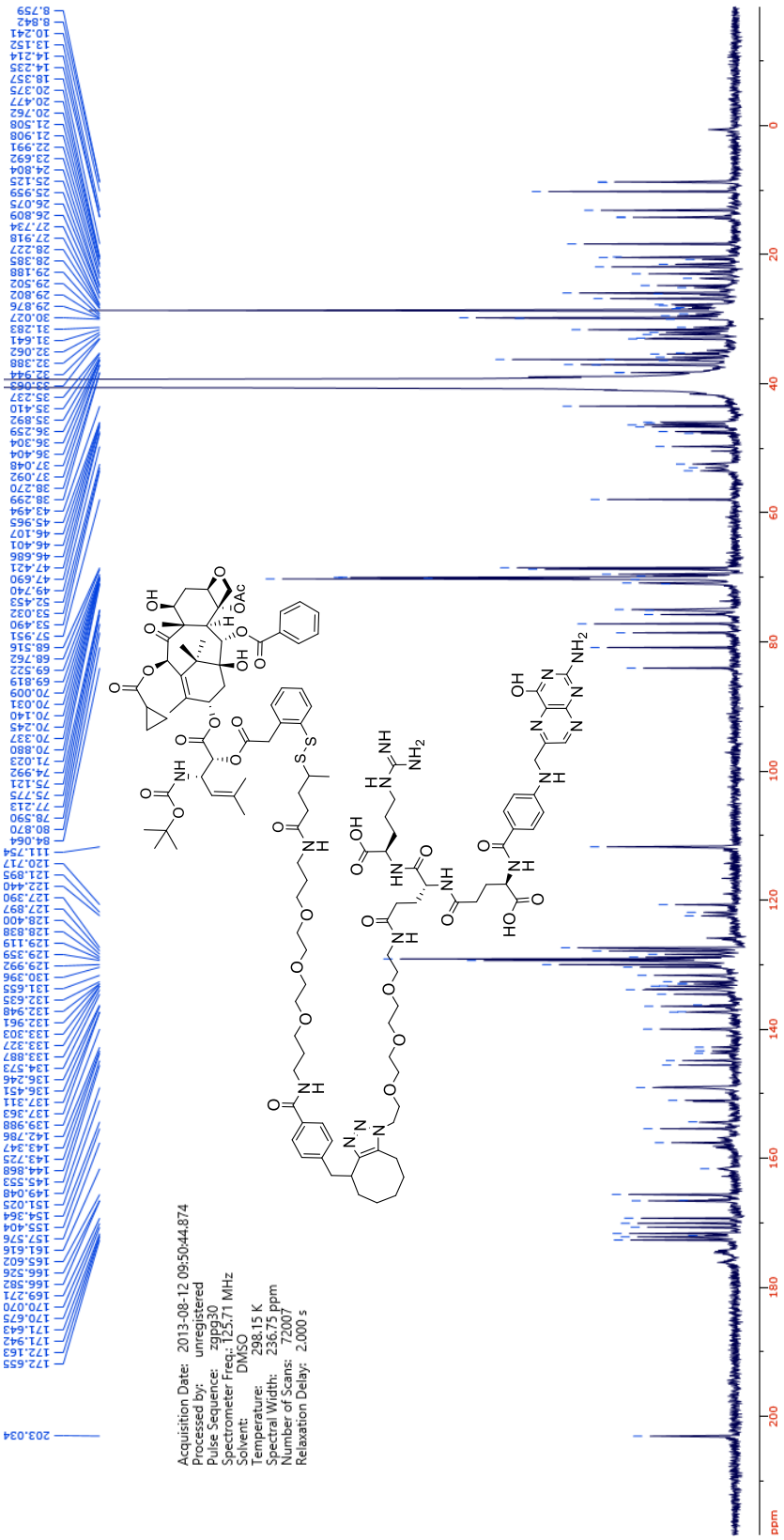
Acquisition Date: 2013-08-12 09:50:44.874
Processed by: unregistered
Pulse Sequence: zgpg30
Spectrometer Freq.: 125.71 MHz
Solvent: DMSO
Temperature: 298.15 K
Spectral Width: 236.75 ppm
Number of Scans: 72007
Relaxation Delay: 2.000 s
ppm

Appendix Chapter 6

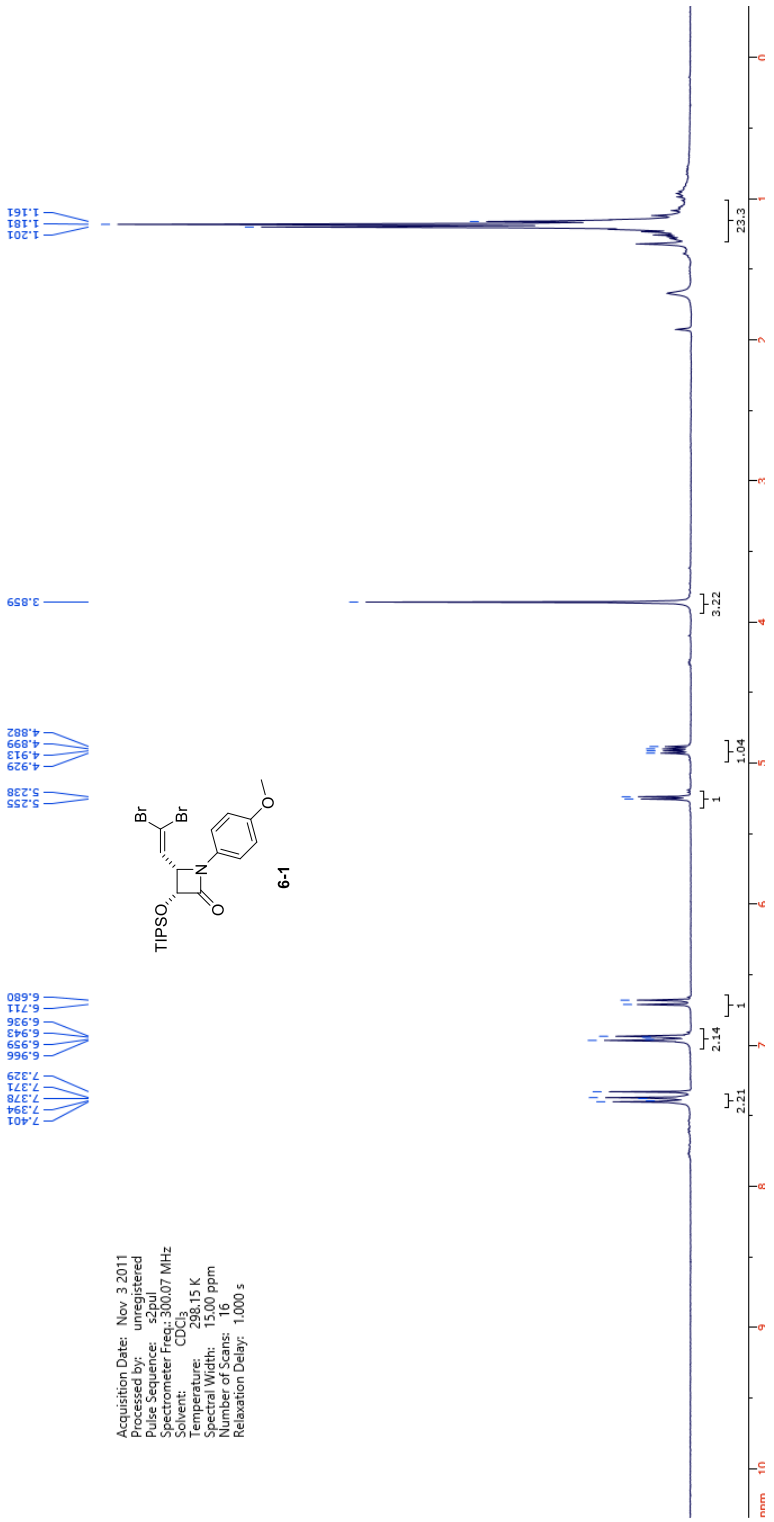
1.201
1.181
1.161
3.859
4.929
4.899
4.913
4.882
5.255
5.238
6.680
6.711
6.936
6.943
6.959
6.966
7.329
7.371
7.378
7.394
7.401
23.3
3.22
1.04
1
1
2.14
2.21
Br
Br
TIPSO
N
O
O
6-1
Acquisition Date: Nov 3 2011
Processed by: unregistered
Pulse Sequence: s2pul
Spectrometer Freq.: 300.07 MHz
Solvent: CDCl3
Temperature: 298.15 K
Spectral Width: 15.00 ppm
Number of Scans: 16
Relaxation Delay: 1.000 s
ppm

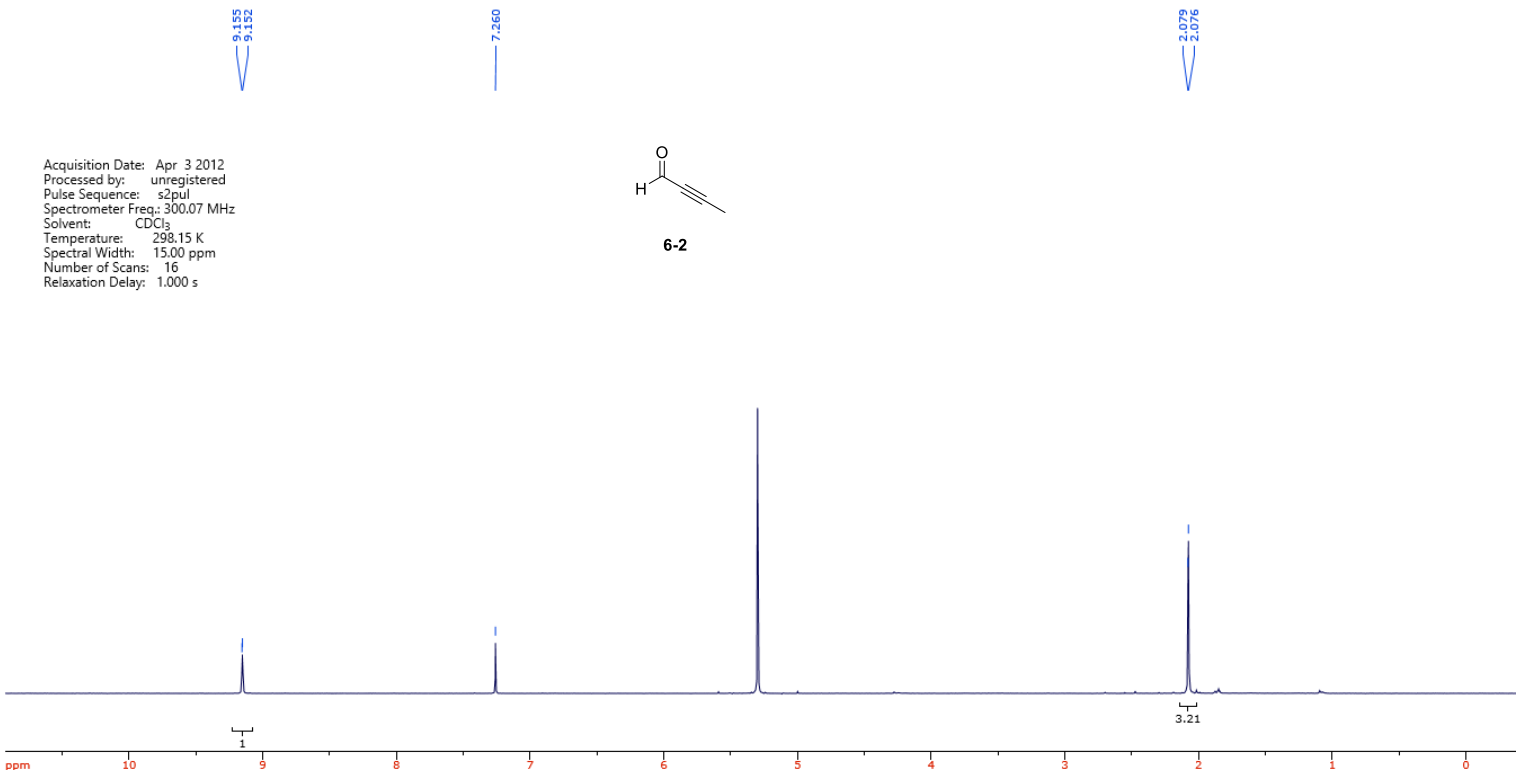
9.155
9.152
7.260
2.079
2.076
Acquisition Date: Apr 3 2012
Processed by: unregistered
Pulse Sequence: s2pul
Spectrometer Freq.: 300.07 MHz
Solvent: CDCl3
Temperature: 298.15 K
Spectral Width: 15.00 ppm
Number of Scans: 16
Relaxation Delay: 1.000 s
O
H
6-2
1
3.21
ppm
10
9
8
7
6
5
4
3
2
1
0

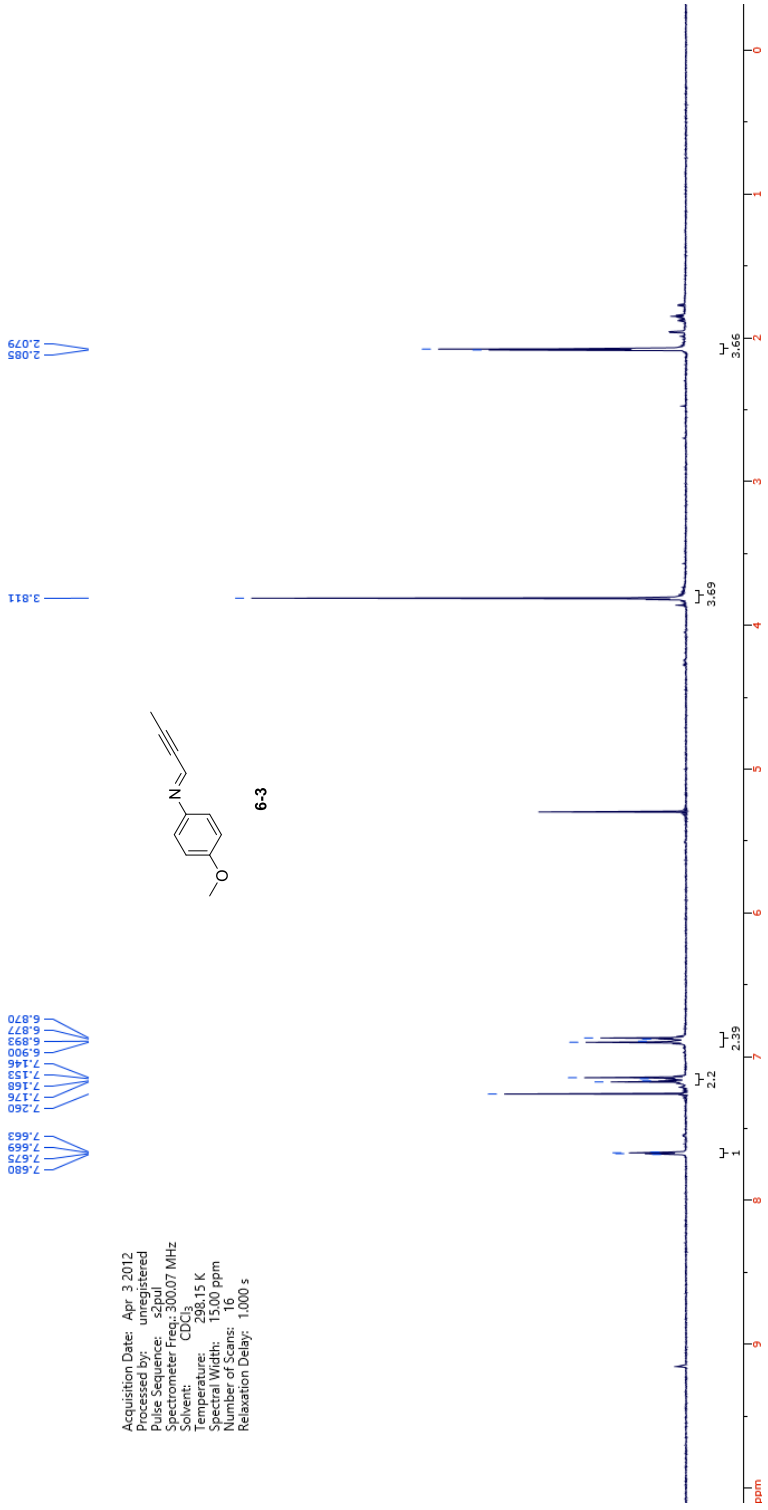
2.085
2.079
3.811
6.870
6.877
6.893
6.900
7.146
7.153
7.168
7.176
7.260
7.663
7.669
7.675
7.680
3.66
3.69
2.39
2.2
1
6-3
Acquisition Date: Apr 3 2012
Processed by: unregistered
Pulse Sequence: s2pul
Spectrometer Freq.: 300.07 MHz
Solvent: CDCl3
Temperature: 298.15 K
Spectral Width: 15.00 ppm
Number of Scans: 16
Relaxation Delay: 1.000 s
ppm

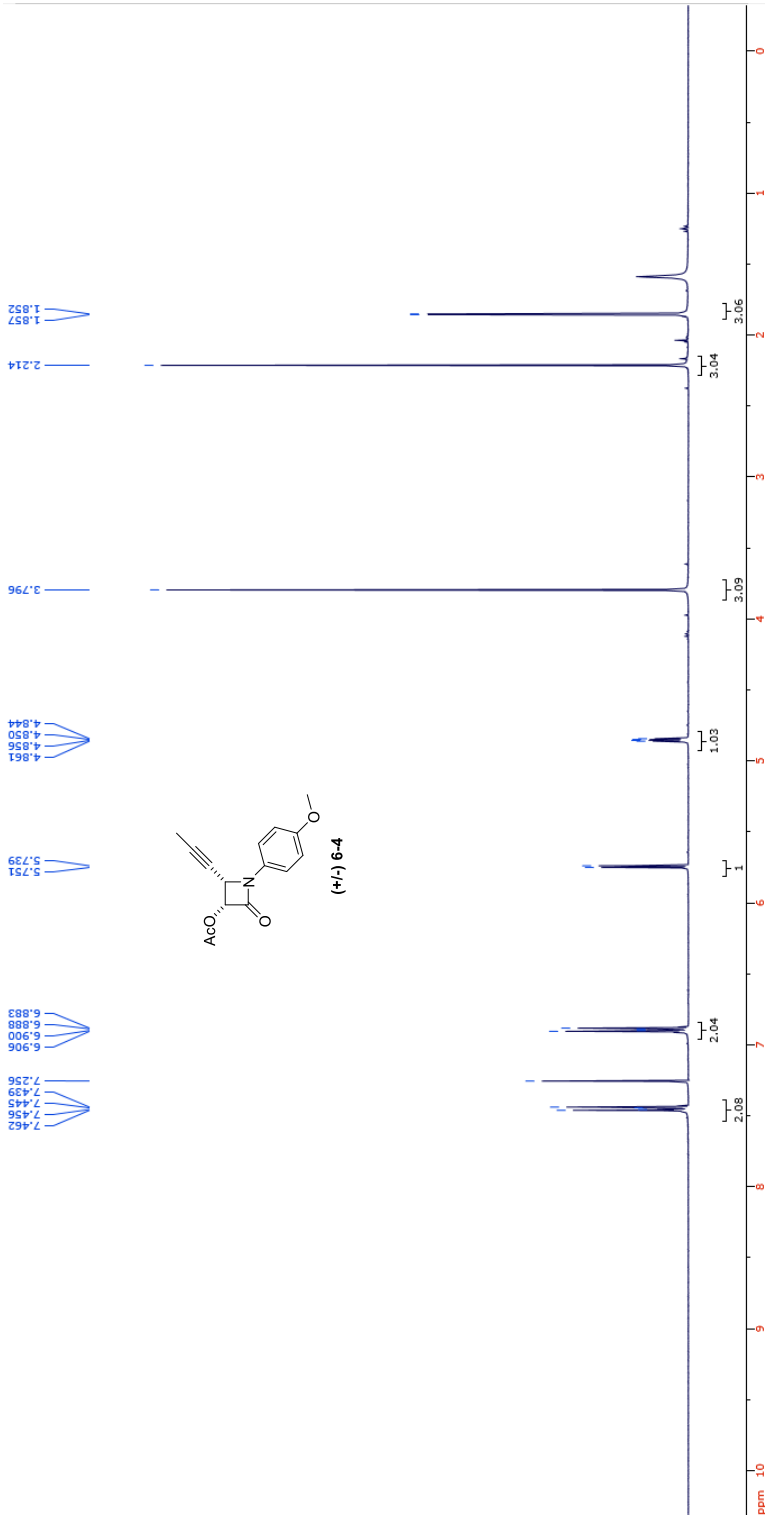
1.852
1.857
2.214
3.796
4.844
4.850
4.856
4.861
5.739
5.751
6.883
6.888
6.900
6.906
7.256
7.439
7.445
7.456
7.462
3.06
3.04
3.09
1.03
1
2.04
2.08
AcO
O
N
O
(+/-) 6-4
ppm

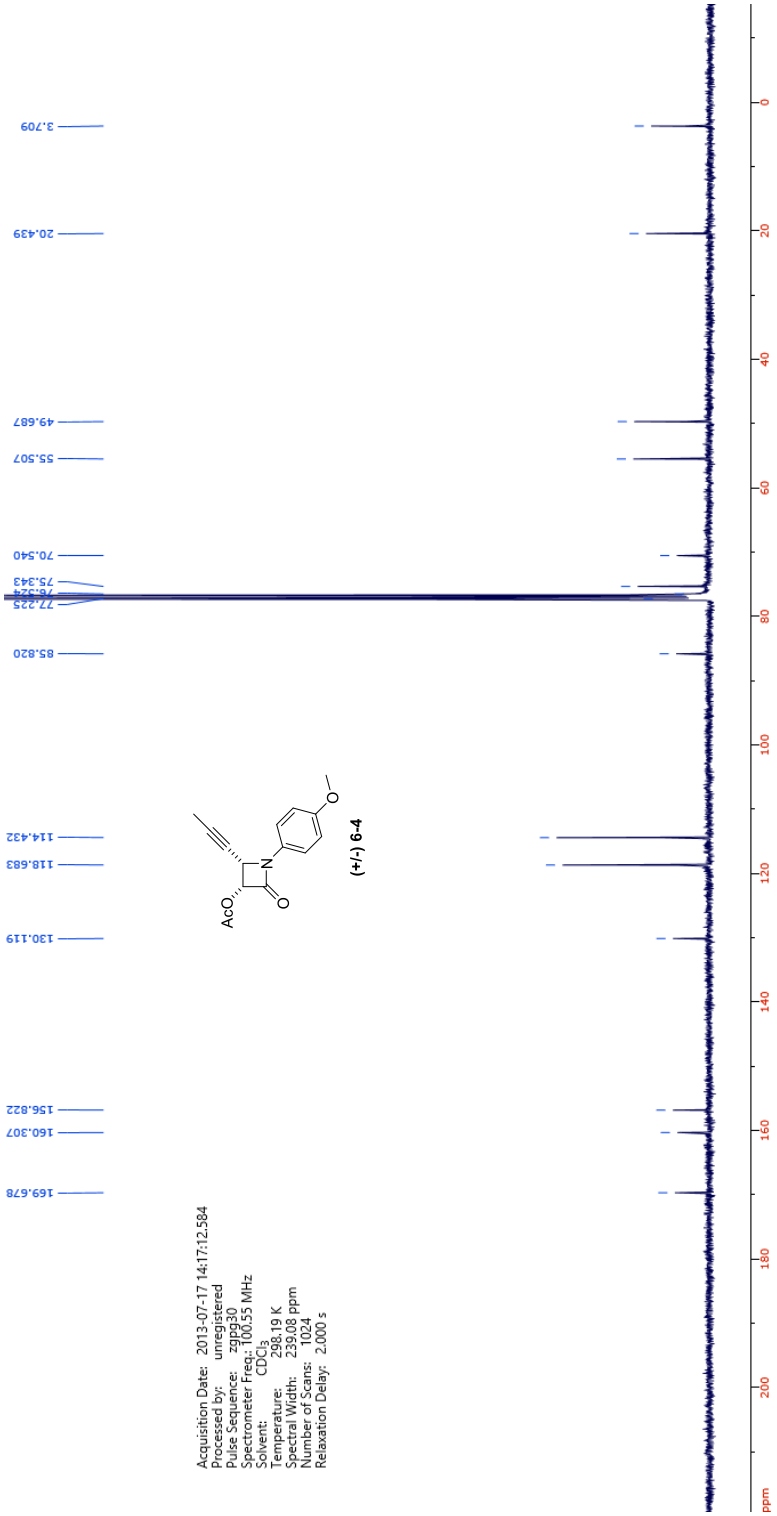
3.709
20.439
49.687
55.507
70.540
75.343
77.225
85.820
114.432
118.683
130.119
156.822
160.307
169.678
AcO
N
O
O
(+/-) 6-4
Acquisition Date: 2013-07-17 14:17:12.584
Processed by: unregistered
Pulse Sequence: zgpg30
Spectrometer Freq.: 100.55 MHz
Solvent: CDCl3
Temperature: 298.19 K
Spectral Width: 239.08 ppm
Number of Scans: 1024
Relaxation Delay: 2.000 s
ppm

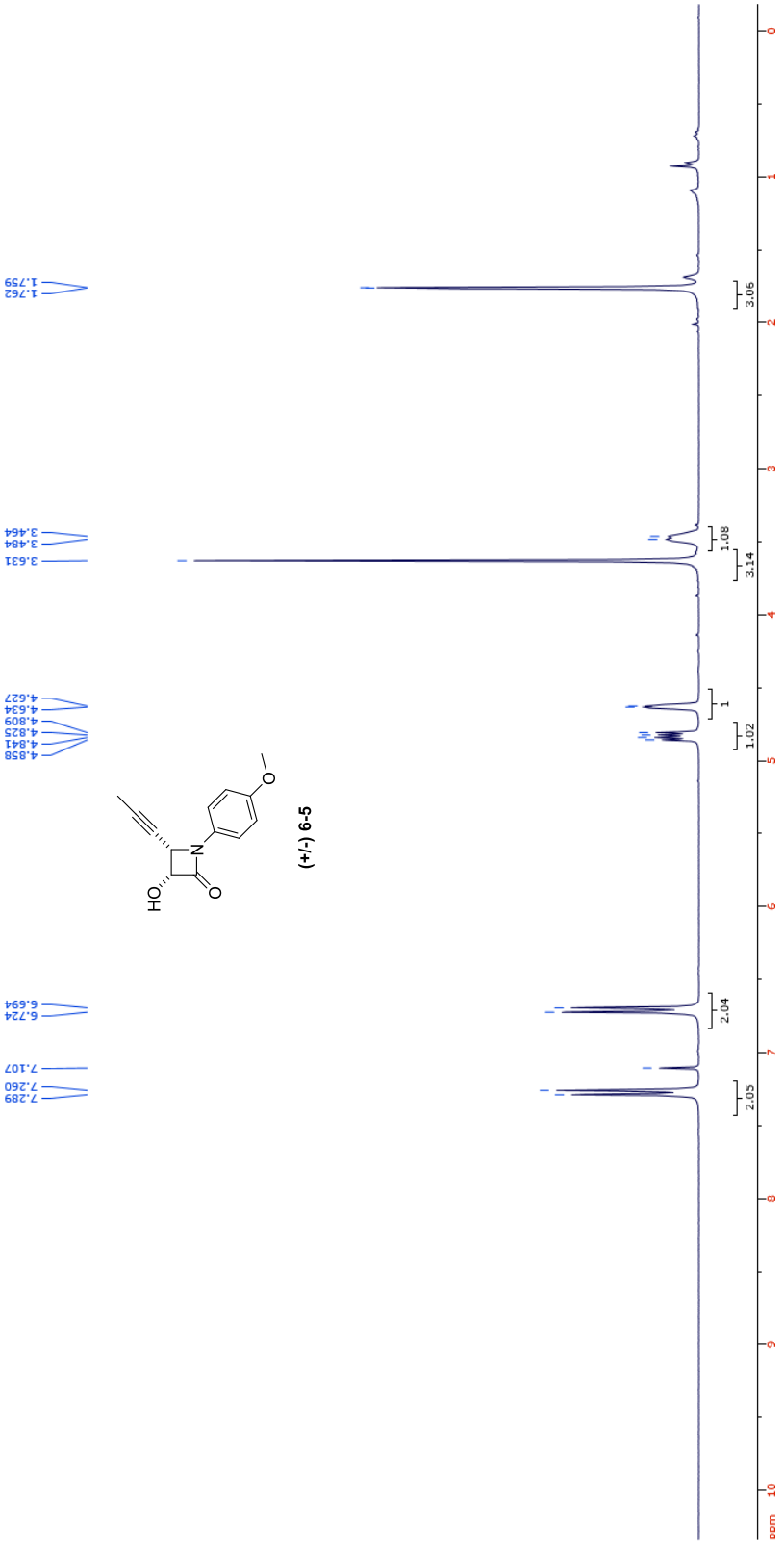
1.759
1.762
3.464
3.484
3.631
4.627
4.634
4.809
4.825
4.841
4.858
6.694
6.724
7.107
7.260
7.289
3.06
1.08
3.14
1
1.02
2.04
2.05
ppm
(+/-) 6-5

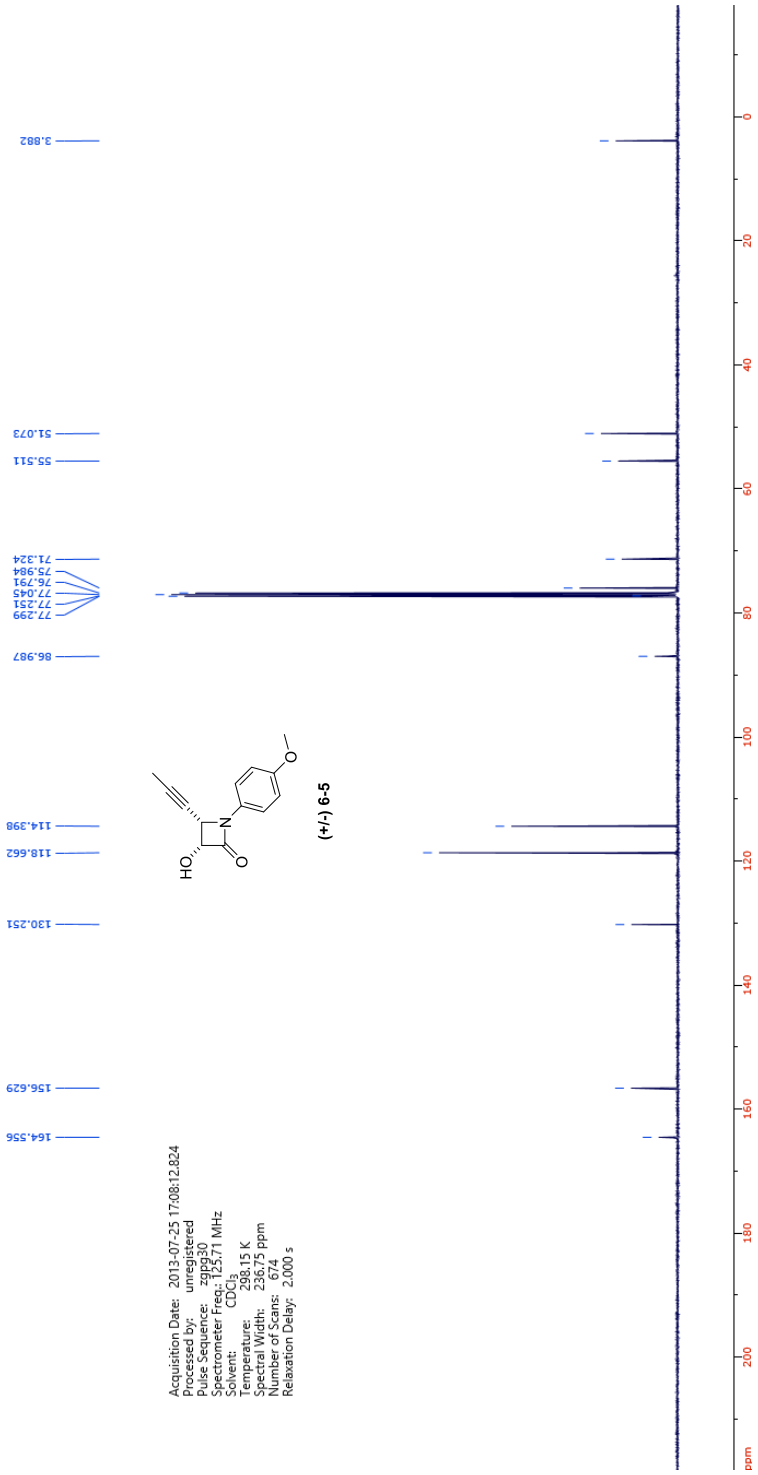
3.882
51.073
55.511
71.324
75.984
76.791
77.043
77.251
77.299
86.987
114.398
118.662
130.251
156.629
164.556
Acquisition Date: 2013-07-25 17:08:12.824
Processed by: unregistered
Pulse Sequence: zgpg30
Spectrometer Freq.: 125.71 MHz
Solvent: CDCl3
Temperature: 298.15 K
Spectral Width: 236.75 ppm
Number of Scans: 674
Relaxation Delay: 2.000 s
HO
N
O
O
(+/-) 6-5
0
20
40
60
80
100
120
140
160
180
200
ppm

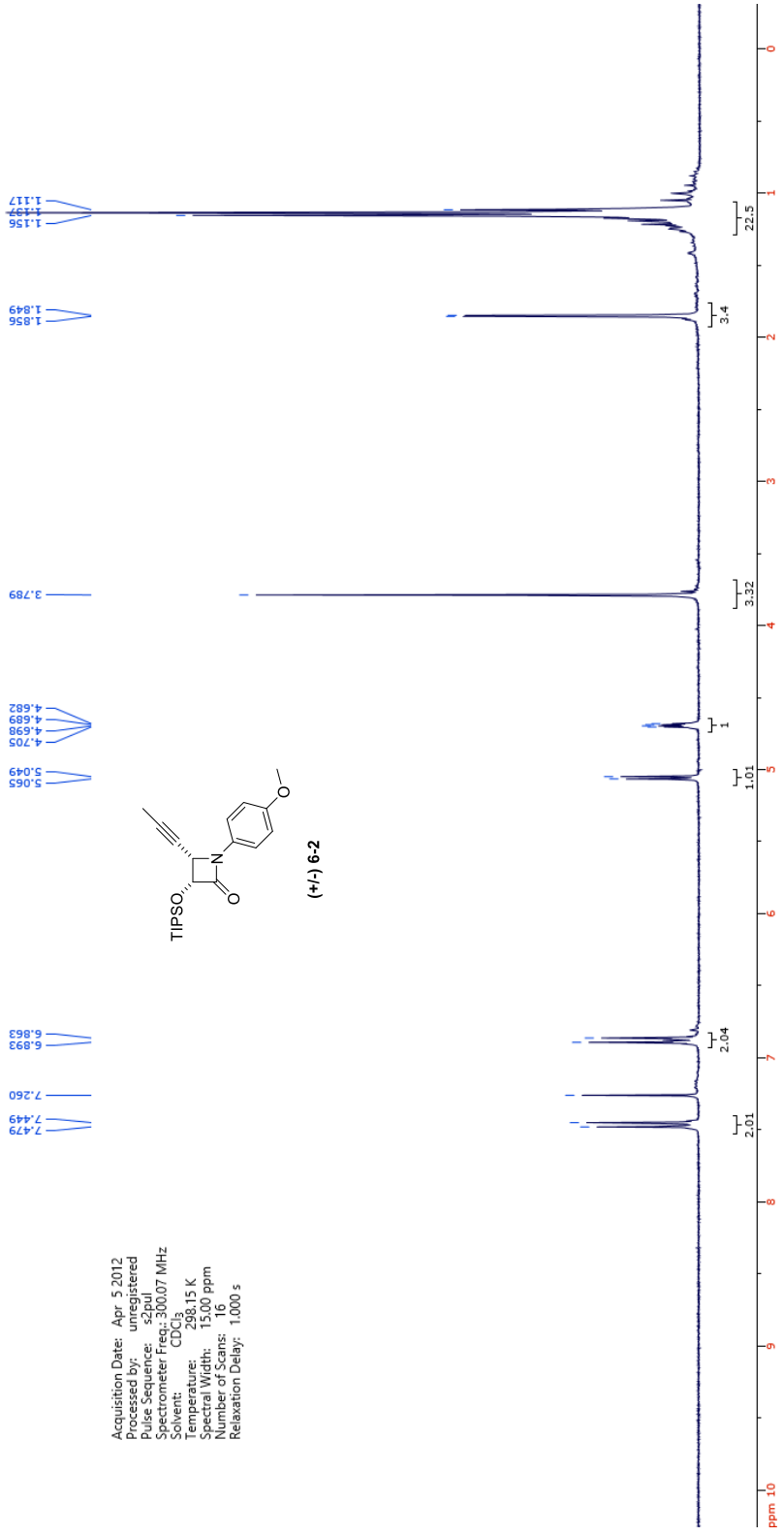
1.117
1.137
1.156
1.849
1.856
3.789
4.682
4.689
4.698
4.705
5.049
5.065
6.863
6.893
7.260
7.449
7.479
22.5
3.4
3.32
1
1.01
2.04
2.01
TIPSO
O
N
O
(+/-) 6-2
Acquisition Date: Apr 5 2012
Processed by: unregistered
Pulse Sequence: s2pul
Spectrometer Freq.: 300.07 MHz
Solvent: $CDCl_3$
Temperature: 298.15 K
Spectral Width: 15.00 ppm
Number of Scans: 16
Relaxation Delay: 1.000 s
ppm 10

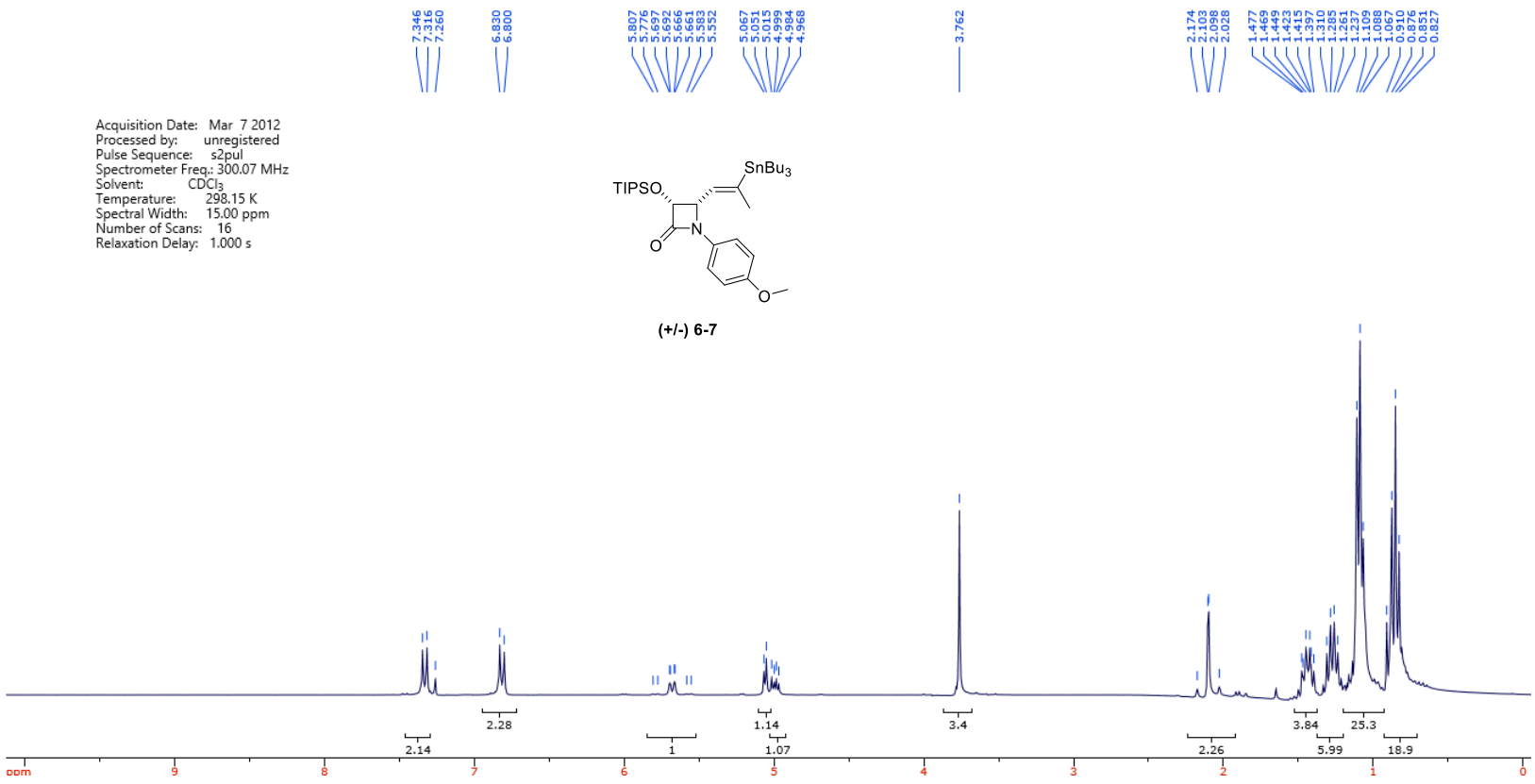
7.346
7.316
7.260
6.830
6.800
5.807
5.776
5.697
5.692
5.666
5.661
5.583
5.552
5.067
5.051
5.015
4.999
4.984
4.968
3.762
2.174
2.103
2.098
2.028
1.477
1.469
1.448
1.423
1.415
1.397
1.310
1.285
1.261
1.237
1.109
1.088
1.067
0.910
0.876
0.851
0.827
Acquisition Date: Mar 7 2012
Processed by: unregistered
Pulse Sequence: s2pul
Spectrometer Freq.: 300.07 MHz
Solvent: CDCl3
Temperature: 298.15 K
Spectral Width: 15.00 ppm
Number of Scans: 16
Relaxation Delay: 1.000 s
TIPSO
SnBu3
O
N
O
(+/-) 6-7
2.14
2.28
1
1.14
1.07
3.4
2.26
3.84
5.99
25.3
18.9
ppm
9
8
7
6
5
4
3
2
1
0

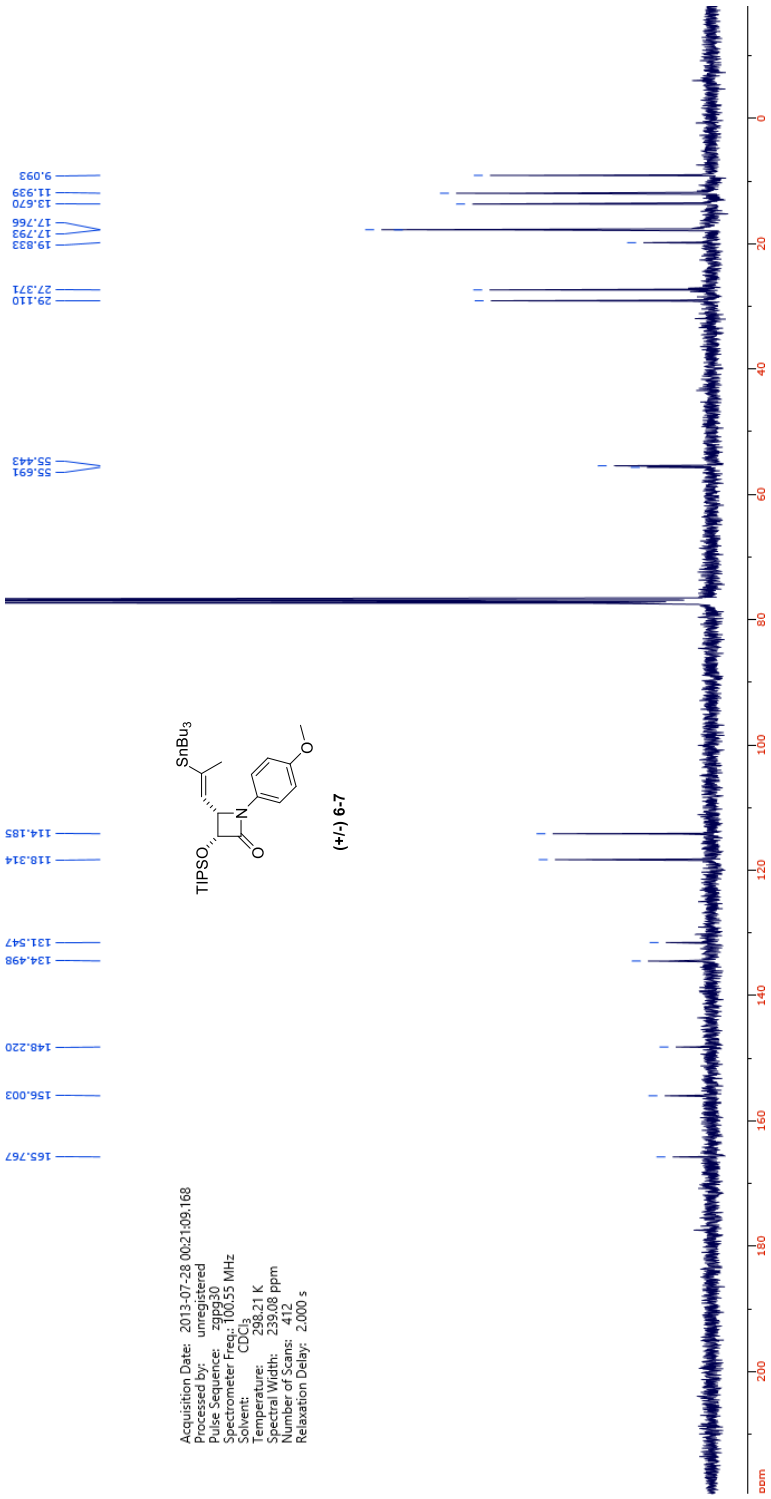
9.093
11.939
13.670
17.766
17.793
19.833
27.371
29.110
55.691
55.443
114.185
118.314
131.547
134.498
148.220
156.003
165.767
SnBu3
TIPSO
O
N
O
(+/-) 6-7
Acquisition Date: 2013-07-28 00:21:09.168
Processed by: unregistered
Pulse Sequence: zgpg30
Spectrometer Freq.: 100.55 MHz
Solvent: CDCl3
Temperature: 298.21 K
Spectral Width: 239.08 ppm
Number of Scans: 412
Relaxation Delay: 2.000 s
0
20
40
60
80
100
120
140
160
180
200
ppm

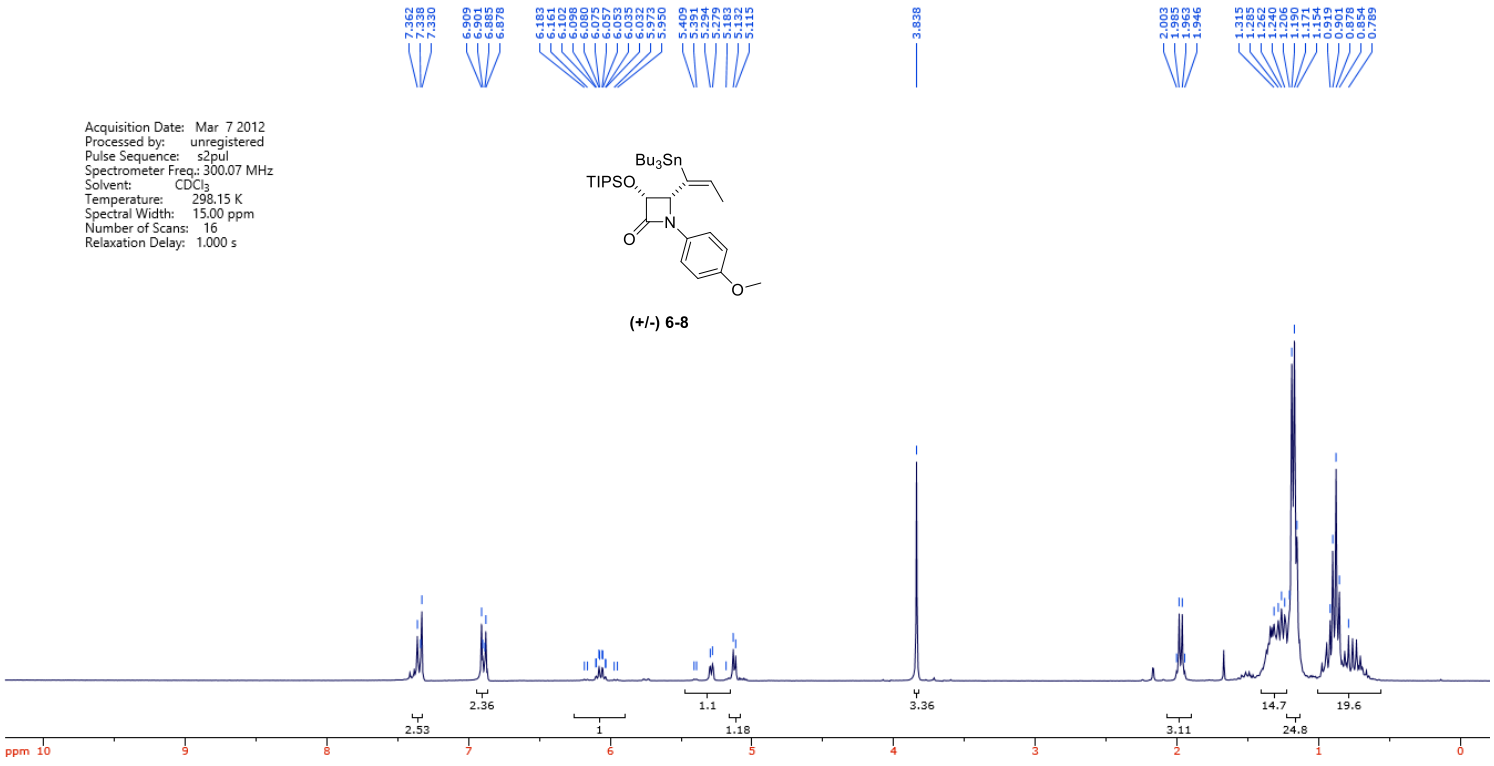
7.362
7.338
7.330
6.909
6.901
6.885
6.878
6.183
6.161
6.102
6.098
6.080
6.075
6.057
6.053
6.035
6.032
5.973
5.950
5.409
5.391
5.294
5.279
5.183
5.172
5.115
3.838
2.003
1.985
1.963
1.946
1.315
1.285
1.262
1.240
1.206
1.190
1.171
1.154
0.919
0.901
0.878
0.854
0.789
Acquisition Date: Mar 7 2012
Processed by: unregistered
Pulse Sequence: s2pul
Spectrometer Freq.: 300.07 MHz
Solvent: CDCl3
Temperature: 298.15 K
Spectral Width: 15.00 ppm
Number of Scans: 16
Relaxation Delay: 1.000 s
Bu3Sn
TIPSO
O
N
O
(+/-) 6-8
2.53
2.36
1
1.1
1.18
3.36
3.11
14.7
24.8
19.6
ppm 10
9
8
7
6
5
4
3
2
1
0

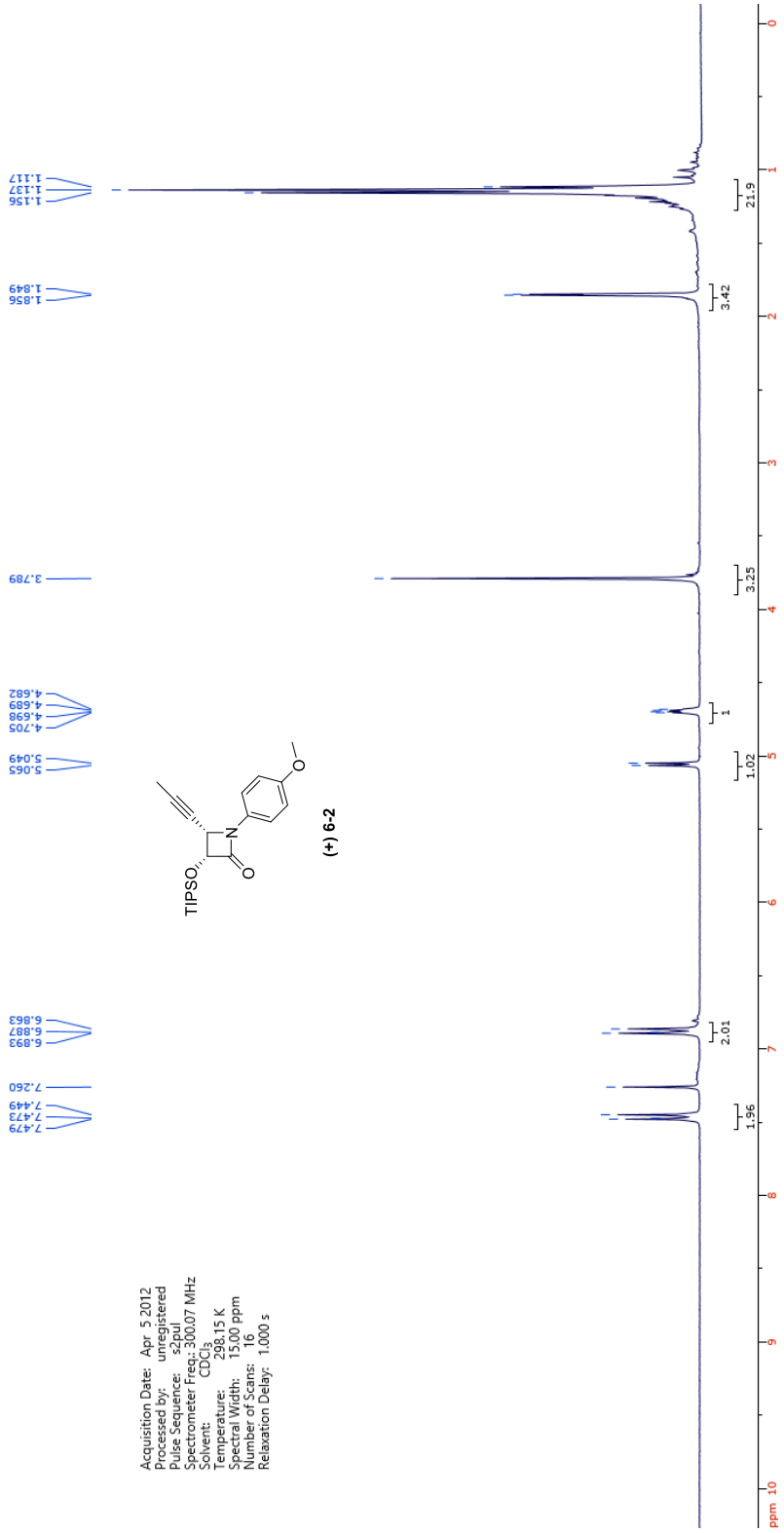
1.117
1.137
1.156
1.849
1.856
3.789
4.682
4.689
4.698
4.705
5.049
5.065
6.863
6.887
6.893
7.260
7.449
7.473
7.479
21.9
3.42
3.25
1
1.02
2.01
1.96
ppm
TIPSO
O
N
O
(+) 6-2
Acquisition Date: Apr 5 2012
Processed by: unregistered
Pulse Sequence: s2pul
Spectrometer Freq.: 300.07 MHz
Solvent: $CDCl_3$
Temperature: 298.15 K
Spectral Width: 15.00 ppm
Number of Scans: 16
Relaxation Delay: 1.000 s

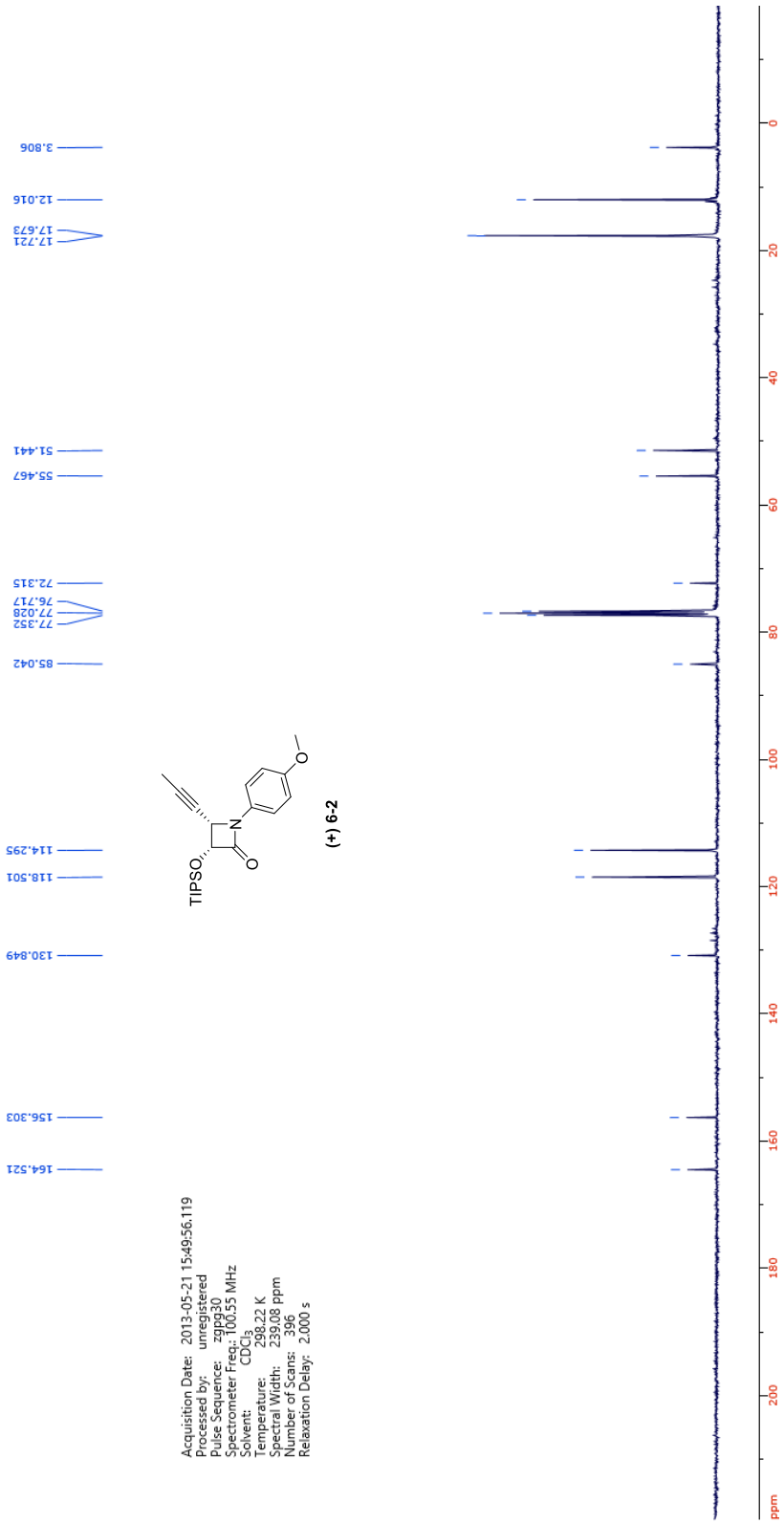
3.806
12.016
17.673
17.721
51.441
55.467
72.315
76.717
77.028
77.352
85.042
114.295
118.501
130.849
156.303
164.521
TIPSO
O
N
O
(+) 6-2
Acquisition Date: 2013-05-21 15:49:56.119
Processed by: unregistered
Pulse Sequence: zgpg30
Spectrometer Freq.: 100.55 MHz
Solvent: CDCl3
Temperature: 298.22 K
Spectral Width: 239.08 ppm
Number of Scans: 396
Relaxation Delay: 2.000 s
ppm
0
20
40
60
80
100
120
140
160
180
200

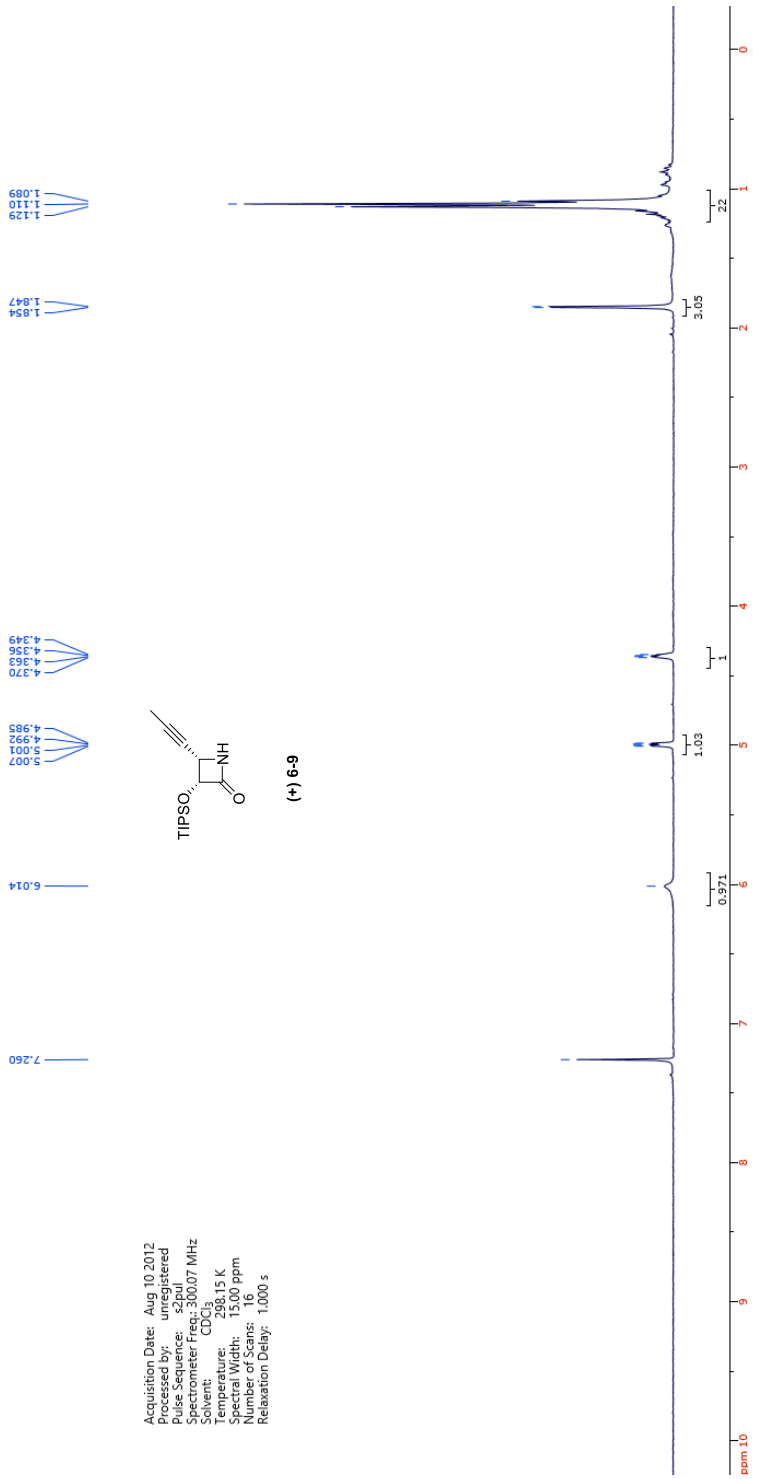
Acquisition Date: Aug 10 2012
Processed by: unregistered
Pulse Sequence: s2pul
Spectrometer Freq.: 300.07 MHz
Solvent: CDCl3
Temperature: 298.15 K
Spectral Width: 15.00 ppm
Number of Scans: 16
Relaxation Delay: 1.000 s
TIPSO
NH
O
(+) 6-9
7.260
6.014
5.007
5.001
4.992
4.985
4.370
4.363
4.356
4.349
1.854
1.847
1.129
1.110
1.089
0.971
1.03
1
3.05
22
ppm

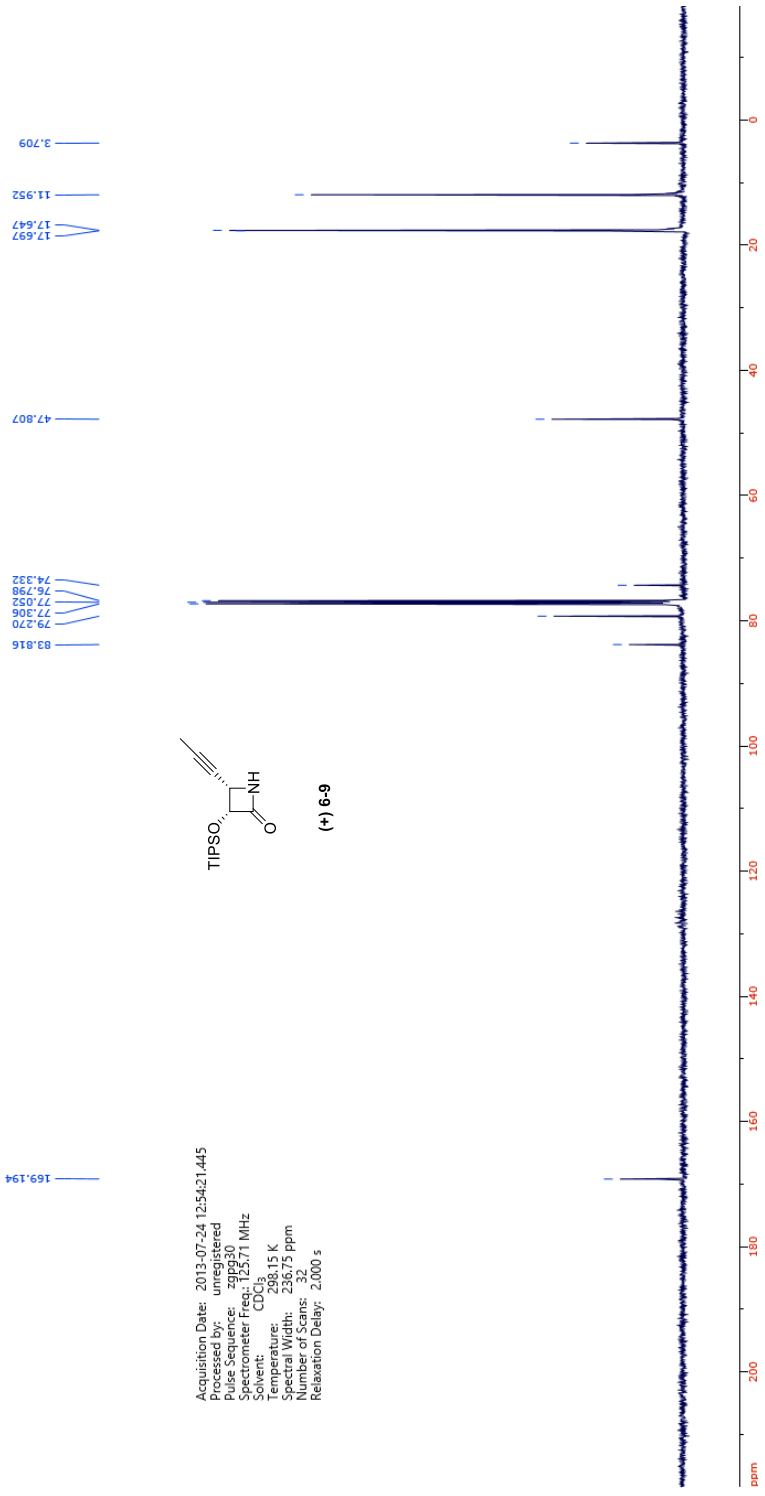
3.709
11.952
17.647
17.697
47.807
74.332
76.798
77.052
77.306
79.270
83.816
169.194
TIPSO
NH
O
(+) 6-9
Acquisition Date: 2013-07-24 12:54:21.445
Processed by: unregistered
Pulse Sequence: zgpg30
Spectrometer Freq.: 125.71 MHz
Solvent: CDCl3
Temperature: 298.15 K
Spectral Width: 236.75 ppm
Number of Scans: 32
Relaxation Delay: 2.000 s
ppm

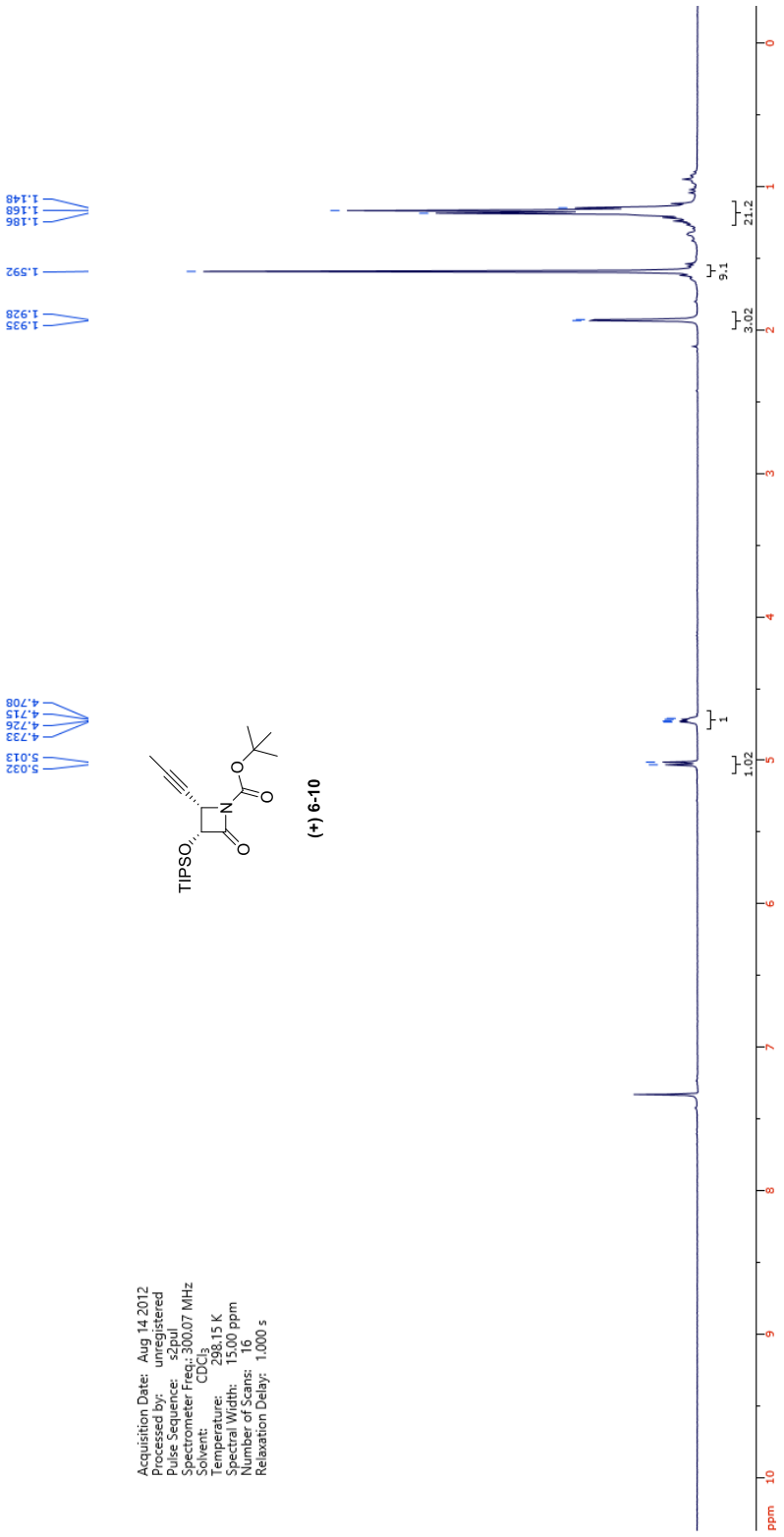
1.448
1.468
1.486
1.592
1.928
1.935
4.708
4.715
4.726
4.733
5.013
5.032
21.2
9.1
3.02
1
1.02
ppm
TIPSO
(+) 6-10
Acquisition Date: Aug 14 2012
Processed by: unregistered
Pulse Sequence: s2pul
Spectrometer Freq.: 300.07 MHz
Solvent: $CDCl_3$
Temperature: 298.15 K
Spectral Width: 15.00 ppm
Number of Scans: 16
Relaxation Delay: 1.000 s

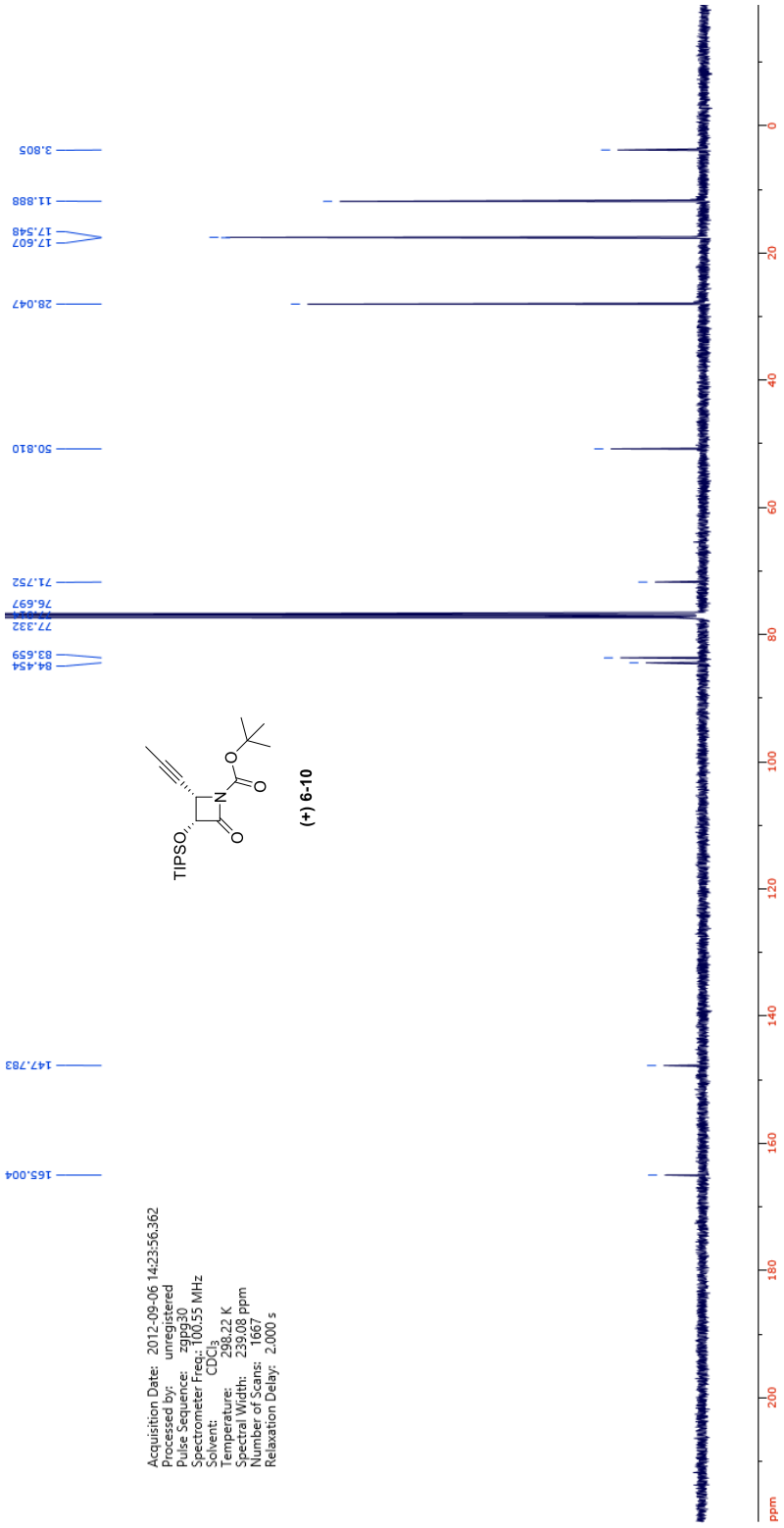
3.805
11.888
17.548
17.607
28.047
50.810
71.752
76.697
77.332
83.659
84.454
147.783
165.004
ppm
0
20
40
60
80
100
120
140
160
180
200
TIPSO
O
N
O
O
O
(+) 6-10
Acquisition Date: 2012-09-06 14:23:56.362
Processed by: unregistered
Pulse Sequence: zgpg30
Spectrometer Freq.: 100.55 MHz
Solvent: CDCl3
Temperature: 298.22 K
Spectral Width: 239.08 ppm
Number of Scans: 1667
Relaxation Delay: 2.000 s

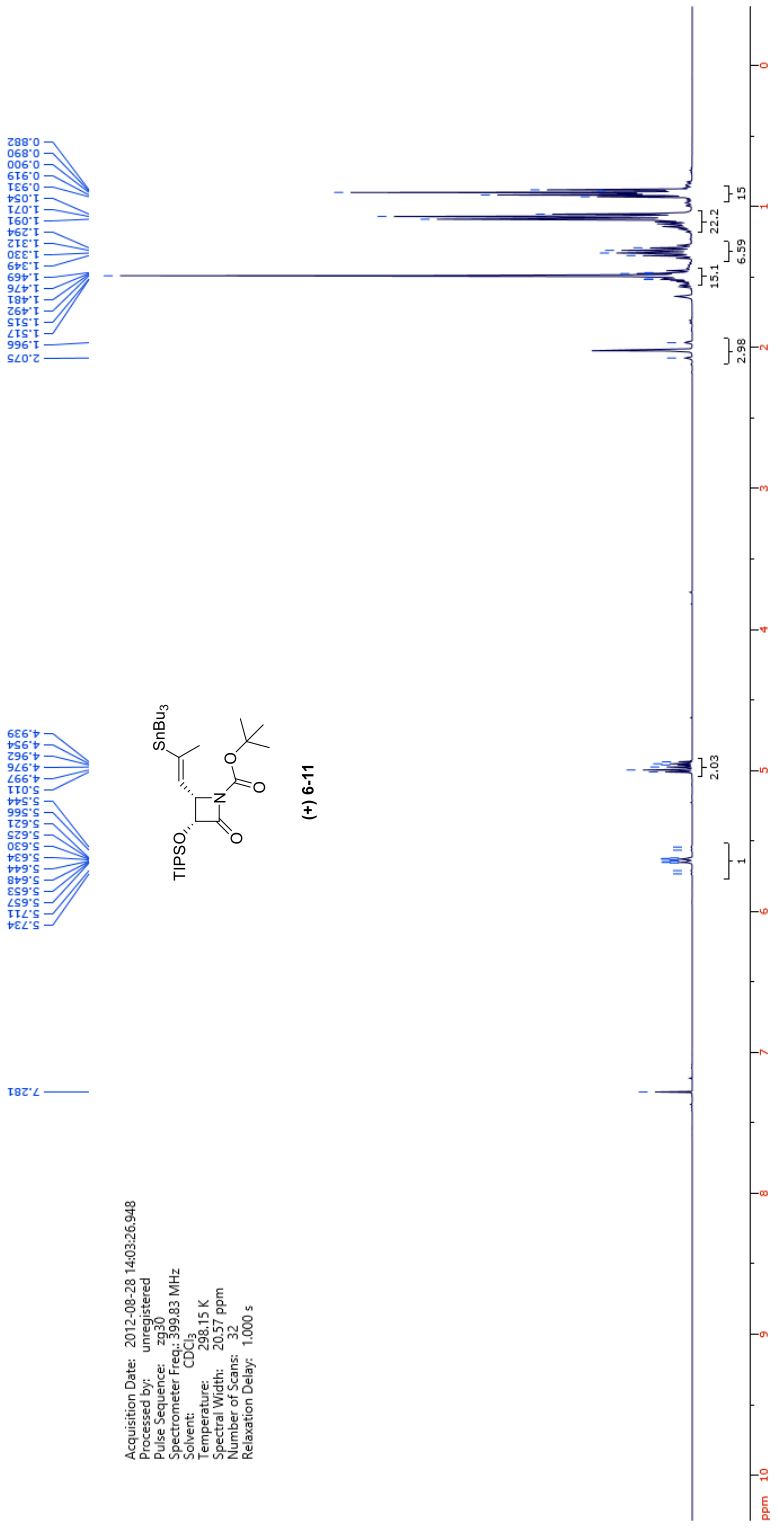
Acquisition Date: 2012-08-28 14:03:26.948
Processed by: unregistered
Pulse Sequence: zg30
Spectrometer Freq.: 399.83 MHz
Solvent: $CDCl_3$
Temperature: 298.15 K
Spectral Width: 20.57 ppm
Number of Scans: 32
Relaxation Delay: 1.000 s
$SnBu_3$
$TIPSO_2S$
N
O
O
O
O
(+) 6-11
7.281
5.734
5.711
5.657
5.653
5.648
5.644
5.634
5.630
5.625
5.621
5.566
5.544
5.011
4.997
4.976
4.962
4.954
4.939
2.075
1.966
1.517
1.515
1.492
1.481
1.476
1.469
1.349
1.330
1.312
1.294
1.091
1.071
1.054
0.931
0.919
0.900
0.890
0.882
1
2.03
2.98
15.1
6.59
22.2
15
ppm

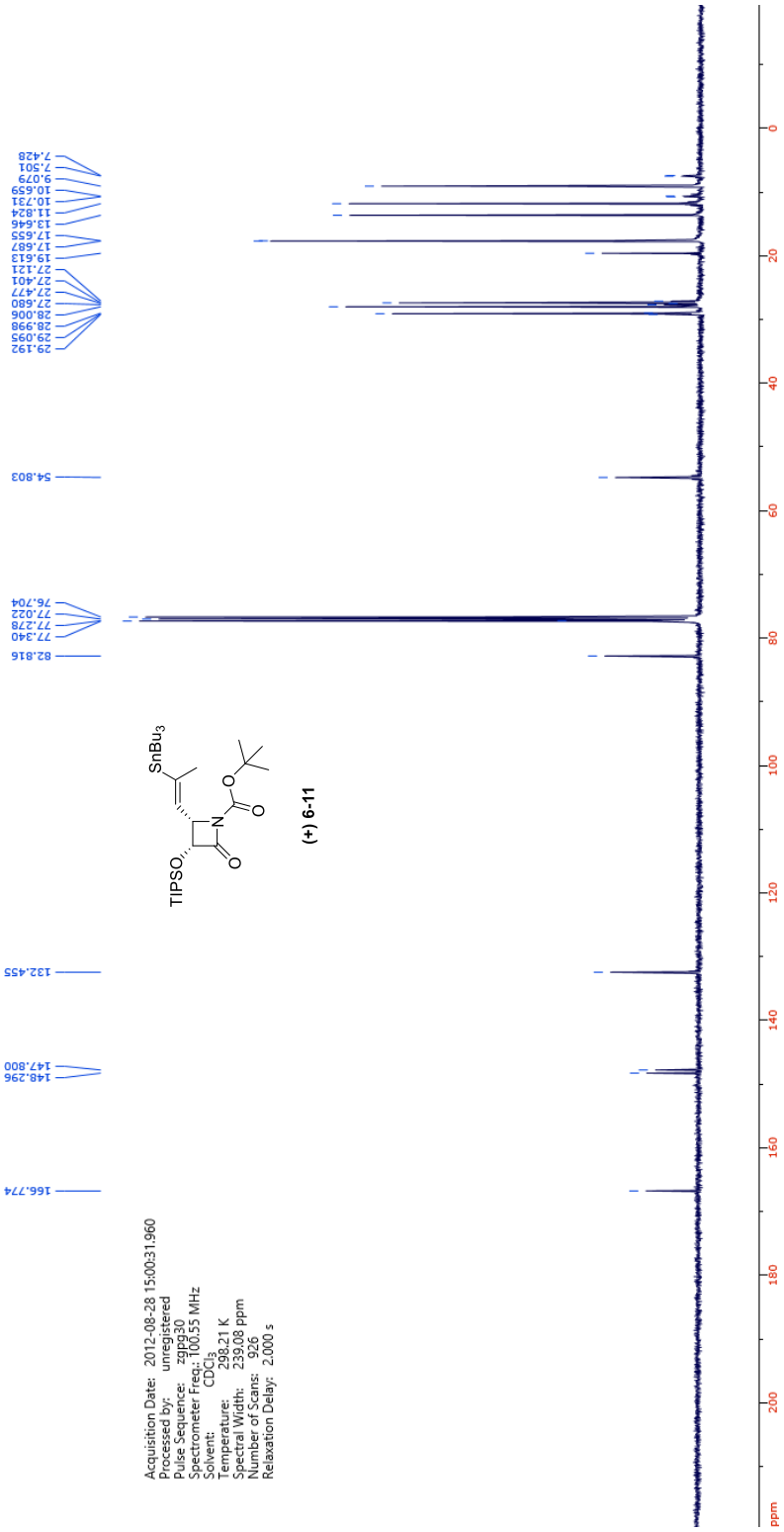
Acquisition Date: 2012-08-28 15:00:31.960
Processed by: unregistered
Pulse Sequence: zgpg30
Spectrometer Freq.: 100.55 MHz
Solvent: CDCl3
Temperature: 298.21 K
Spectral Width: 239.08 ppm
Number of Scans: 926
Relaxation Delay: 2.000 s
SnBu3
TIPSO
(+) 6-11
166.774
148.296
147.800
132.455
82.816
77.340
77.022
76.704
54.803
29.192
29.095
28.998
28.006
27.680
27.477
27.401
27.121
19.613
17.687
17.655
13.646
11.824
10.731
10.659
9.079
7.501
7.428
ppm

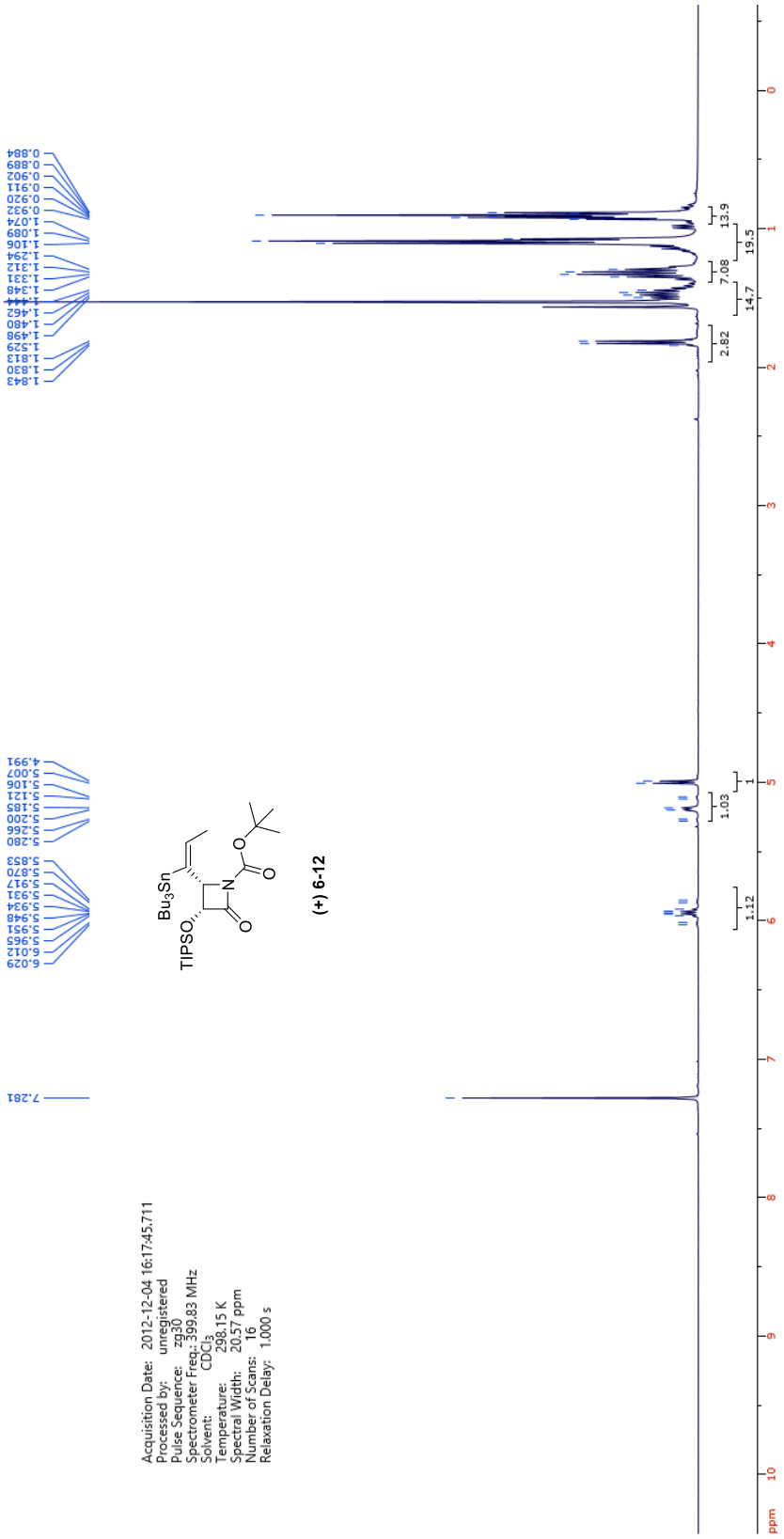
Acquisition Date: 2012-12-04 16:17:45.711
Processed by: unregistered
Pulse Sequence: zg30
Spectrometer Freq.: 399.83 MHz
Solvent: $CDCl_3$
Temperature: 298.15 K
Spectral Width: 20.57 ppm
Number of Scans: 16
Relaxation Delay: 1.000 s
Bu_3Sn
TIPSO
(+) 6-12
ppm

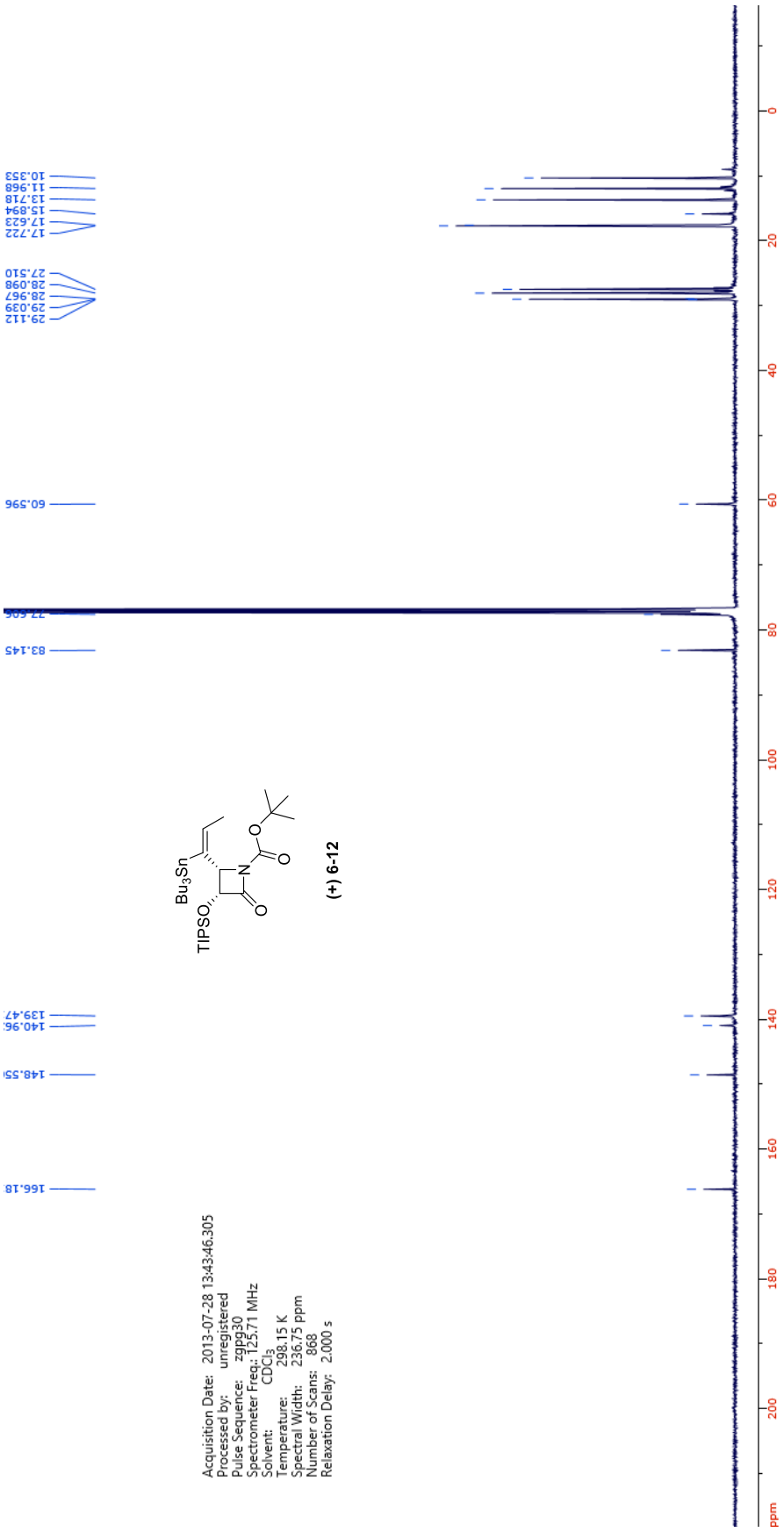
Acquisition Date: 2013-07-28 13:43:46.305
Processed by: unregistered
Pulse Sequence: zgpg30
Spectrometer Freq.: 125.71 MHz
Solvent: CDCl3
Temperature: 298.15 K
Spectral Width: 236.75 ppm
Number of Scans: 868
Relaxation Delay: 2.000 s
Bu3Sn
TIPSO
O
N
O
O
(+) 6-12
166.18
148.55
140.96
139.47
83.145
77.606
60.596
29.112
29.039
28.967
28.098
27.510
17.722
17.623
15.894
13.718
11.968
10.353
ppm
0
20
40
60
80
100
120
140
160
180
200

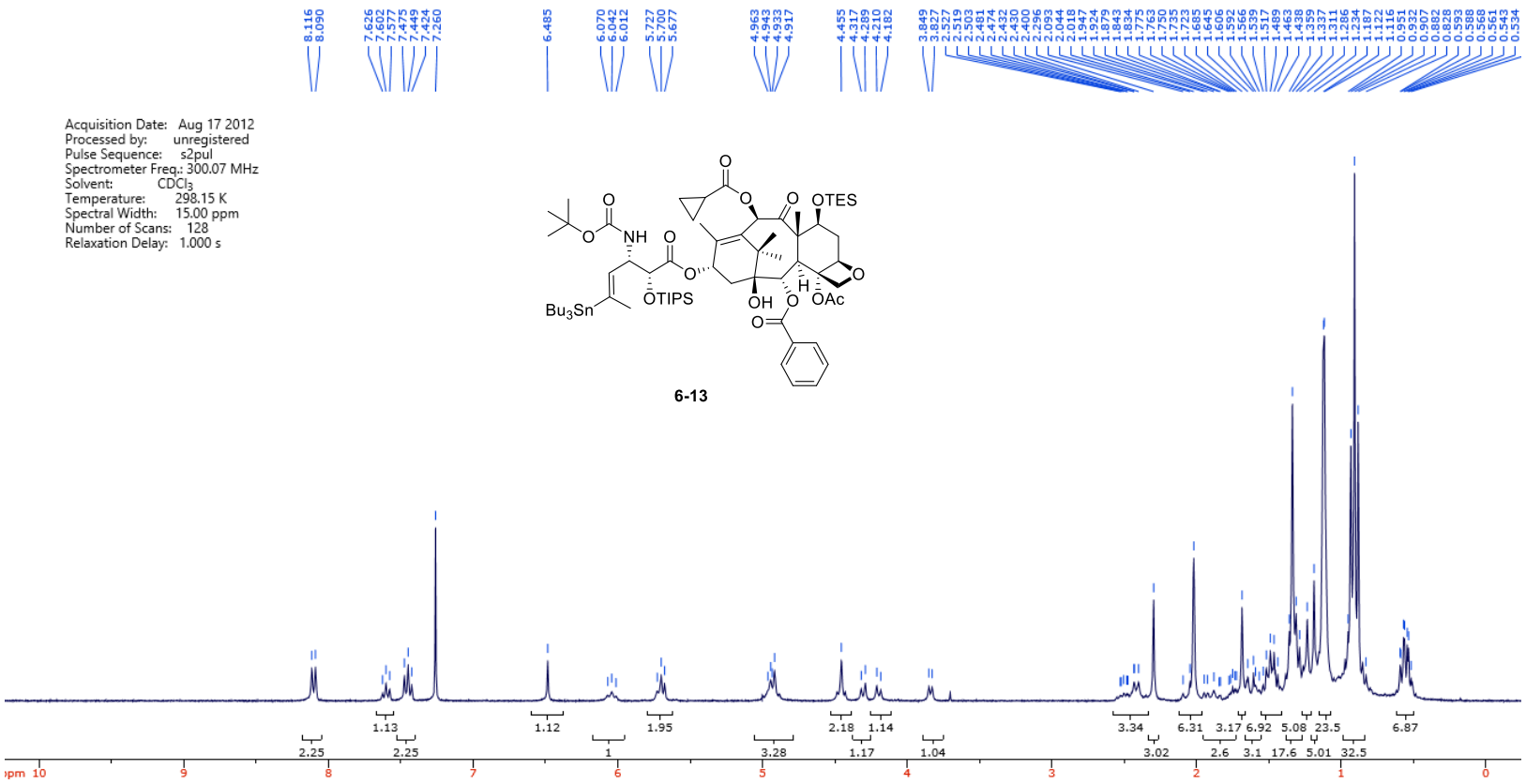
Acquisition Date: Aug 17 2012
Processed by: unregistered
Pulse Sequence: s2pul
Spectrometer Freq.: 300.07 MHz
Solvent: CDCl3
Temperature: 298.15 K
Spectral Width: 15.00 ppm
Number of Scans: 128
Relaxation Delay: 1.000 s
OTES
NH
OTIPS
Bu3Sn
OH
OAc
6-13

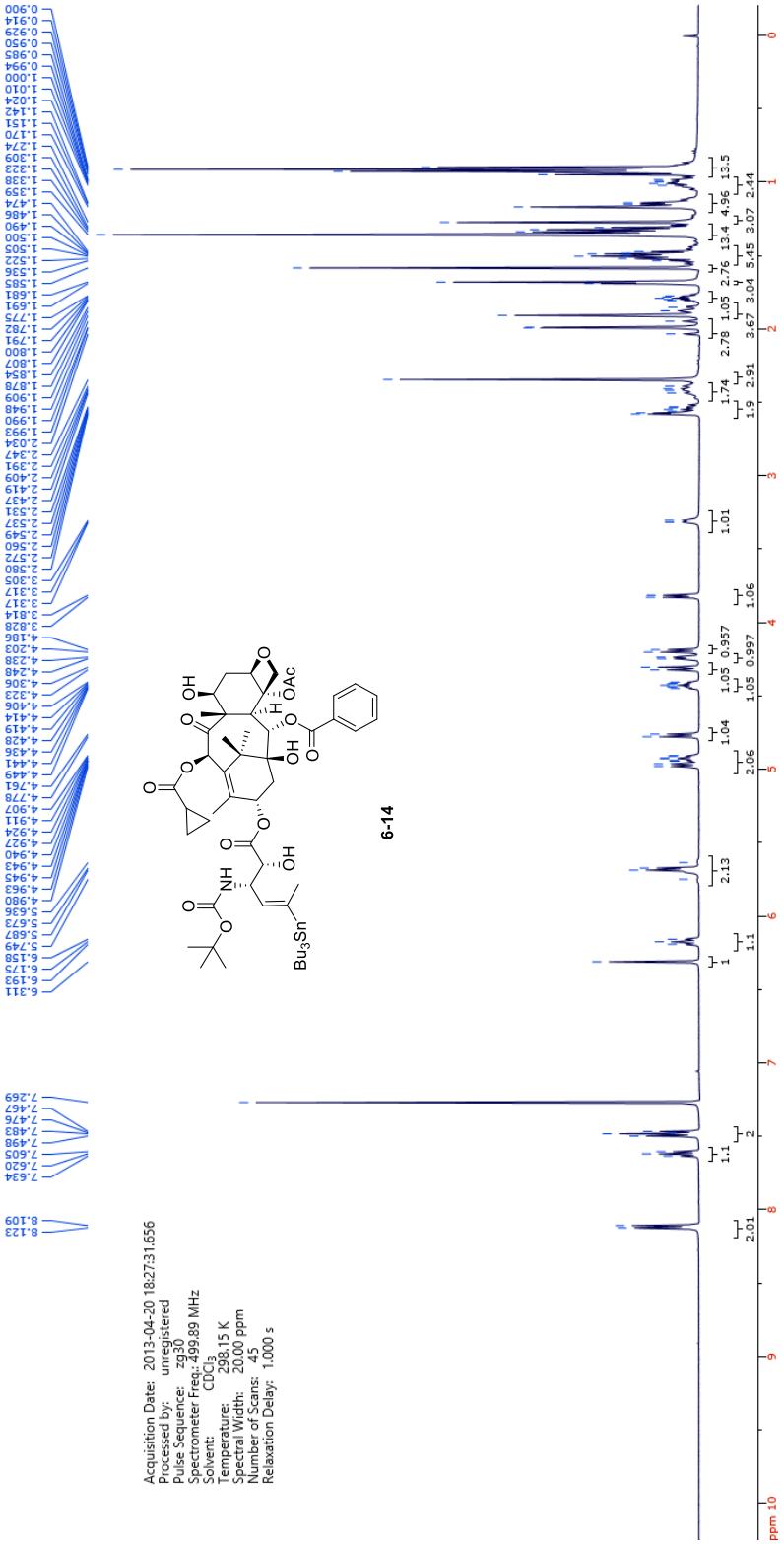
Acquisition Date: 2013-04-20 18:27:31.656
Processed by: unregistered
Pulse Sequence: zg30
Spectrometer Freq.: 499.89 MHz
Solvent: CDCl3
Temperature: 298.15 K
Spectral Width: 20.00 ppm
Number of Scans: 45
Relaxation Delay: 1.000 s
6-14
ppm

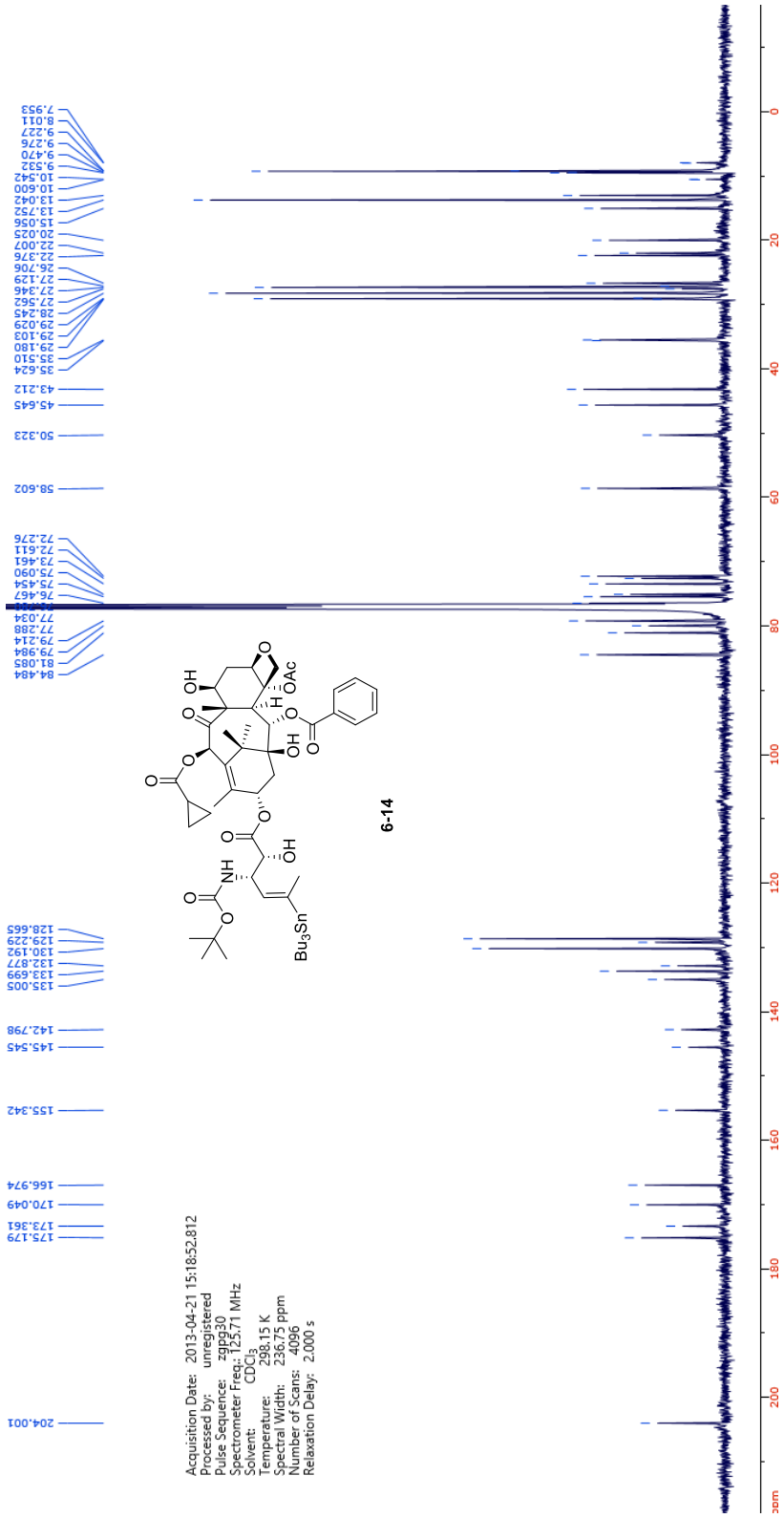
7.953
8.011
9.227
9.276
9.470
9.532
10.542
10.600
13.042
13.752
15.056
20.025
22.007
22.376
26.706
27.129
27.346
27.562
28.245
29.029
29.103
29.180
35.510
35.624
43.212
45.645
50.323
58.602
72.276
72.611
73.461
75.090
75.454
76.467
77.034
77.288
79.214
79.984
81.085
84.484
128.665
129.229
130.192
132.877
133.699
135.005
142.798
145.545
155.342
166.974
170.049
173.361
175.179
204.001
Acquisition Date: 2013-04-21 15:18:52.812
Processed by: unregistered
Pulse Sequence: zgpg30
Spectrometer Freq.: 125.71 MHz
Solvent: $CDCl_3$
Temperature: 298.15 K
Spectral Width: 236.75 ppm
Number of Scans: 4096
Relaxation Delay: 2.000 s
6-14
ppm

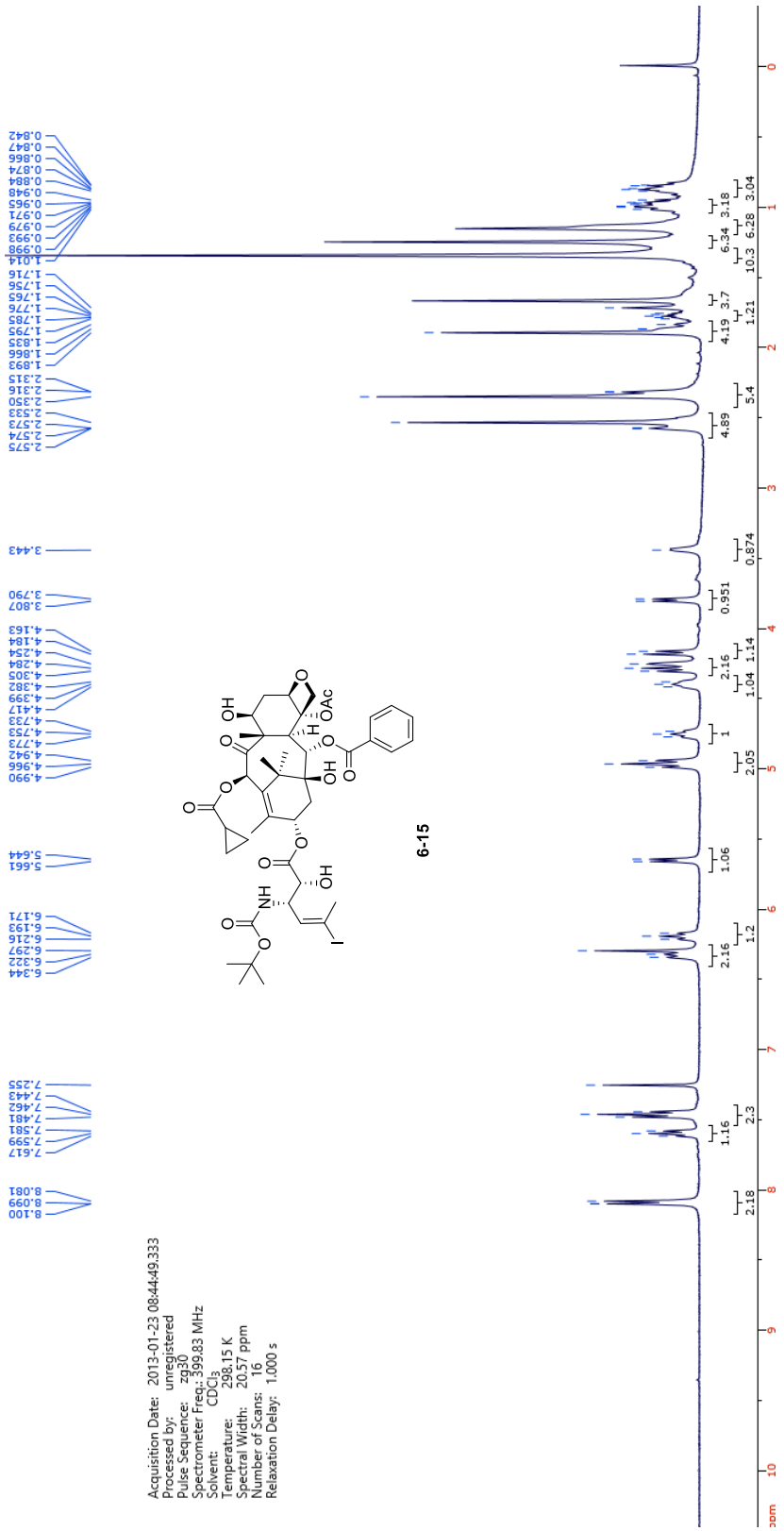
Acquisition Date: 2013-01-23 08:44:49.333
Processed by: unregistered
Pulse Sequence: zg30
Spectrometer Freq.: 399.83 MHz
Solvent: $CDCl_3$
Temperature: 298.15 K
Spectral Width: 20.57 ppm
Number of Scans: 16
Relaxation Delay: 1.000 s
6-15

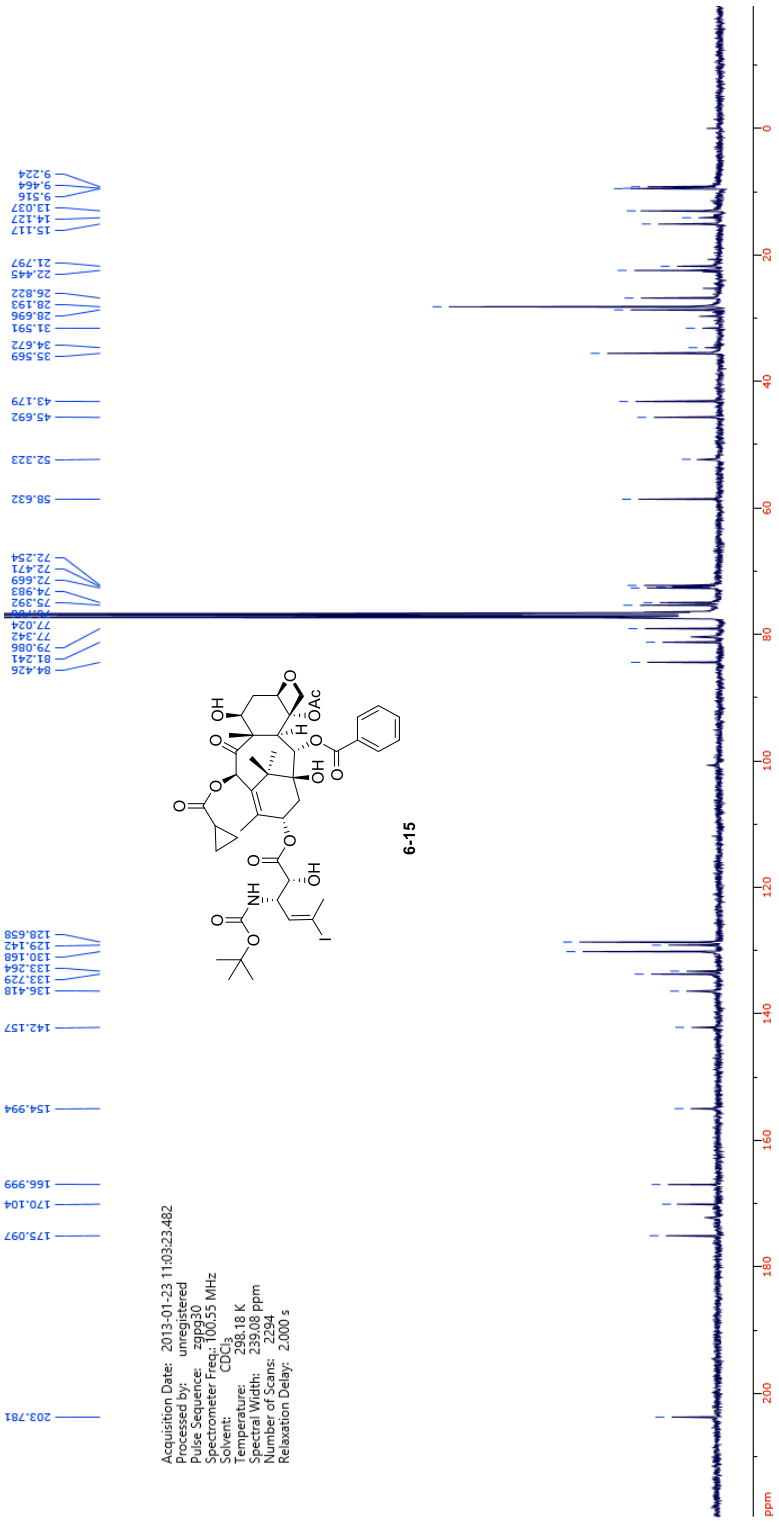
9.224
9.464
9.916
13.037
14.127
15.117
21.797
22.445
26.822
28.193
28.696
31.591
34.672
35.569
43.179
45.692
52.323
58.632
72.254
72.471
72.669
74.983
75.392
77.024
77.342
79.086
81.241
84.426
128.658
129.142
130.168
133.264
133.729
136.418
142.157
154.994
166.999
170.104
175.097
203.781
Acquisition Date: 2013-01-23 11:03:23.482
Processed by: unregistered
Pulse Sequence: zgpg30
Spectrometer Freq.: 100.55 MHz
Solvent: $CDCl_3$
Temperature: 298.18 K
Spectral Width: 239.08 ppm
Number of Scans: 2294
Relaxation Delay: 2.000 s
6-15
ppm

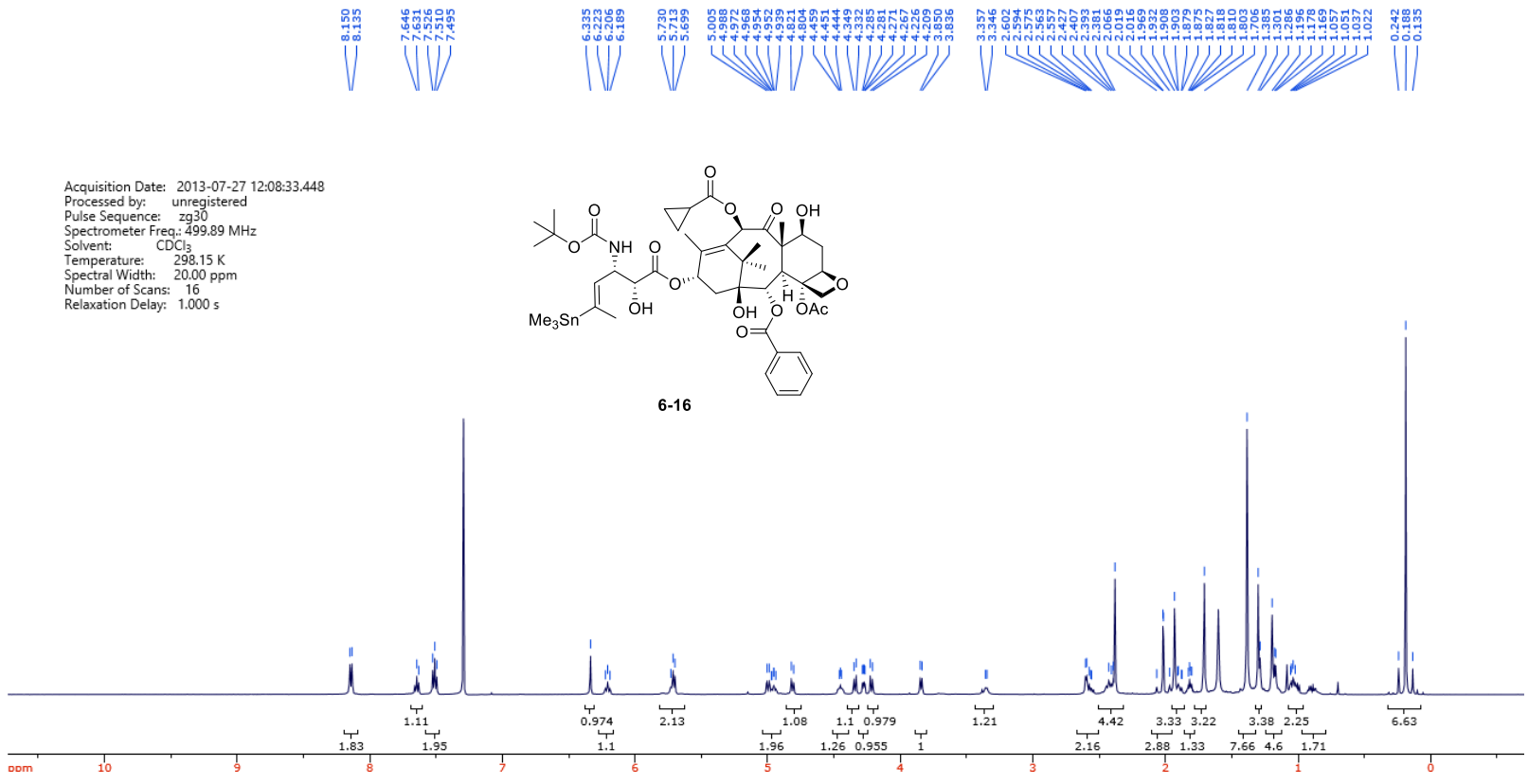
8.150
8.135
7.646
7.631
7.526
7.510
7.495
6.335
6.223
6.066
6.189
5.730
5.713
5.699
5.005
4.988
4.972
4.968
4.954
4.952
4.939
4.821
4.804
4.459
4.451
4.444
4.349
4.332
4.285
4.281
4.271
4.267
4.255
4.209
3.850
3.836
3.357
3.346
2.602
2.594
2.575
2.563
2.557
2.427
2.407
2.393
2.381
2.066
2.019
2.016
1.969
1.932
1.908
1.903
1.879
1.875
1.827
1.818
1.810
1.803
1.706
1.385
1.301
1.286
1.196
1.178
1.169
1.057
1.051
1.037
1.022
0.242
0.188
0.135
Acquisition Date: 2013-07-27 12:08:33.448
Processed by: unregistered
Pulse Sequence: zg30
Spectrometer Freq.: 499.89 MHz
Solvent: CDCl3
Temperature: 298.15 K
Spectral Width: 20.00 ppm
Number of Scans: 16
Relaxation Delay: 1.000 s
Me3Sn
OAc
6-16
1.11
0.974
2.13
1.08
1.1
0.979
1.21
4.42
3.33
3.22
3.38
2.25
6.63
1.83
1.95
1.1
1.96
1.26
0.955
1
2.16
2.88
1.33
7.66
4.6
1.71
ppm
10
9
8
7
6
5
4
3
2
1
0

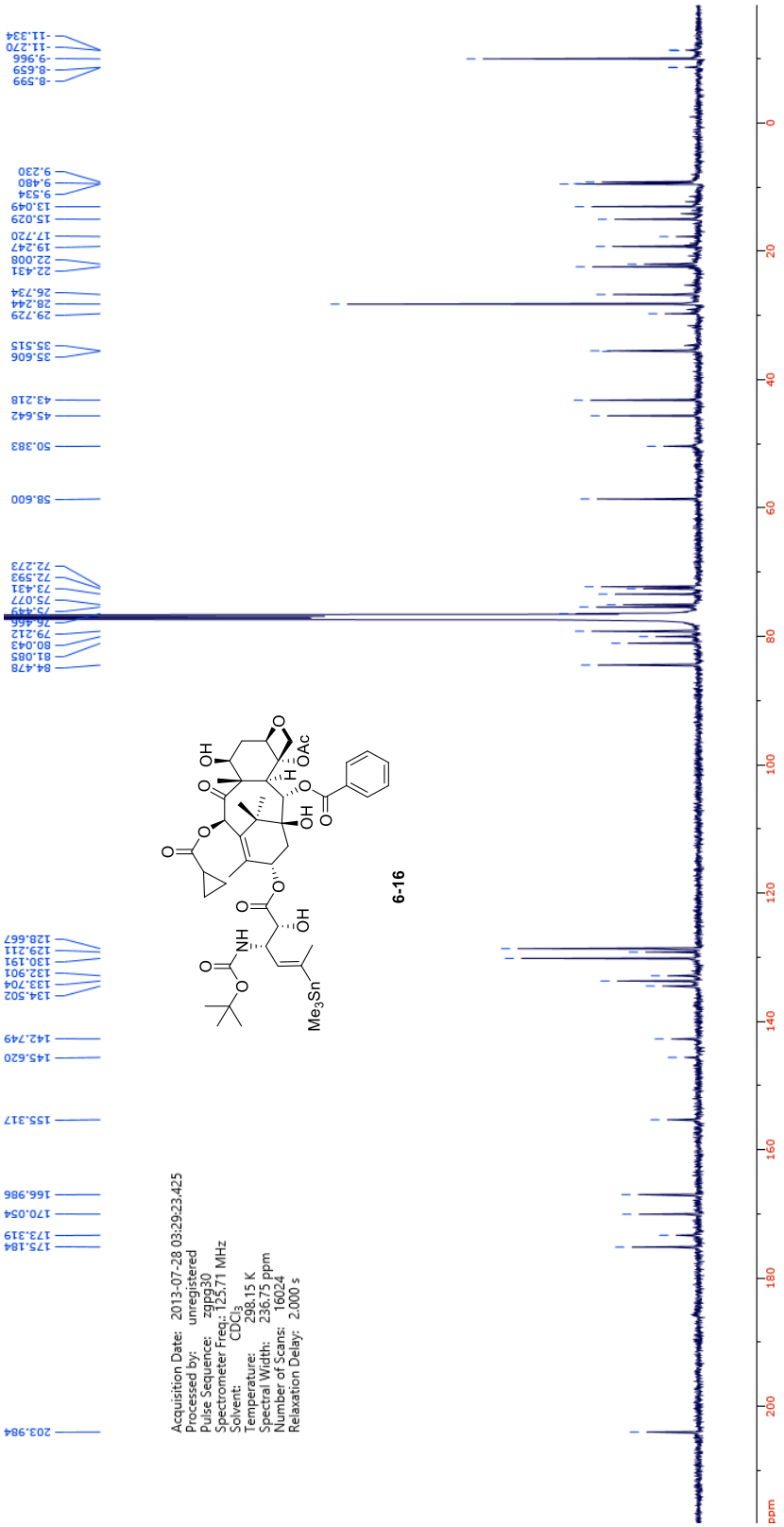
-11.334
-11.270
-9.968
-8.659
-8.599
9.230
9.480
9.534
13.049
15.029
17.720
19.247
22.008
22.431
26.734
28.244
29.729
35.515
35.606
43.218
45.642
50.383
58.600
72.273
72.593
73.431
75.077
75.449
76.466
79.212
80.043
81.085
84.478
128.667
129.211
130.191
132.901
133.704
134.502
142.749
145.620
155.317
166.986
170.054
173.319
175.184
203.984
Acquisition Date: 2013-07-28 03:29:23.425
Processed by: unregistered
Pulse Sequence: zgpg30
Spectrometer Freq.: 125.71 MHz
Solvent: $CDCl_3$
Temperature: 298.15 K
Spectral Width: 236.75 ppm
Number of Scans: 16024
Relaxation Delay: 2.000 s
OH
OAc
H
O
NH
OH
Me_3Sn
ppm

6-16

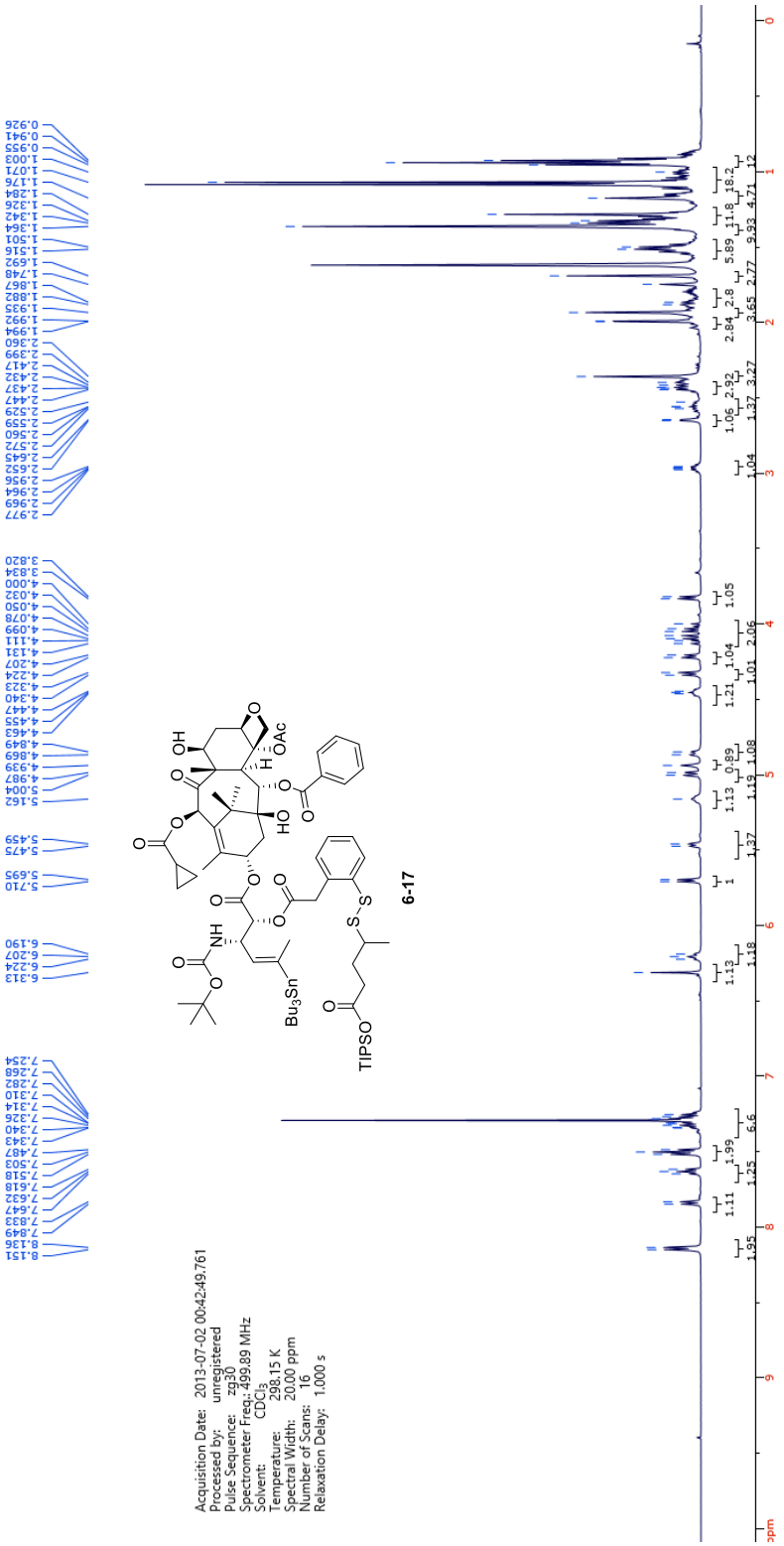
Acquisition Date: 2013-07-02 00:42:49.761
Processed by: unregistered
Pulse Sequence: zg30
Spectrometer Freq.: 499.89 MHz
Solvent: $CDCl_3$
Temperature: 298.15 K
Spectral Width: 20.00 ppm
Number of Scans: 16
Relaxation Delay: 1.000 s
6-17
ppm

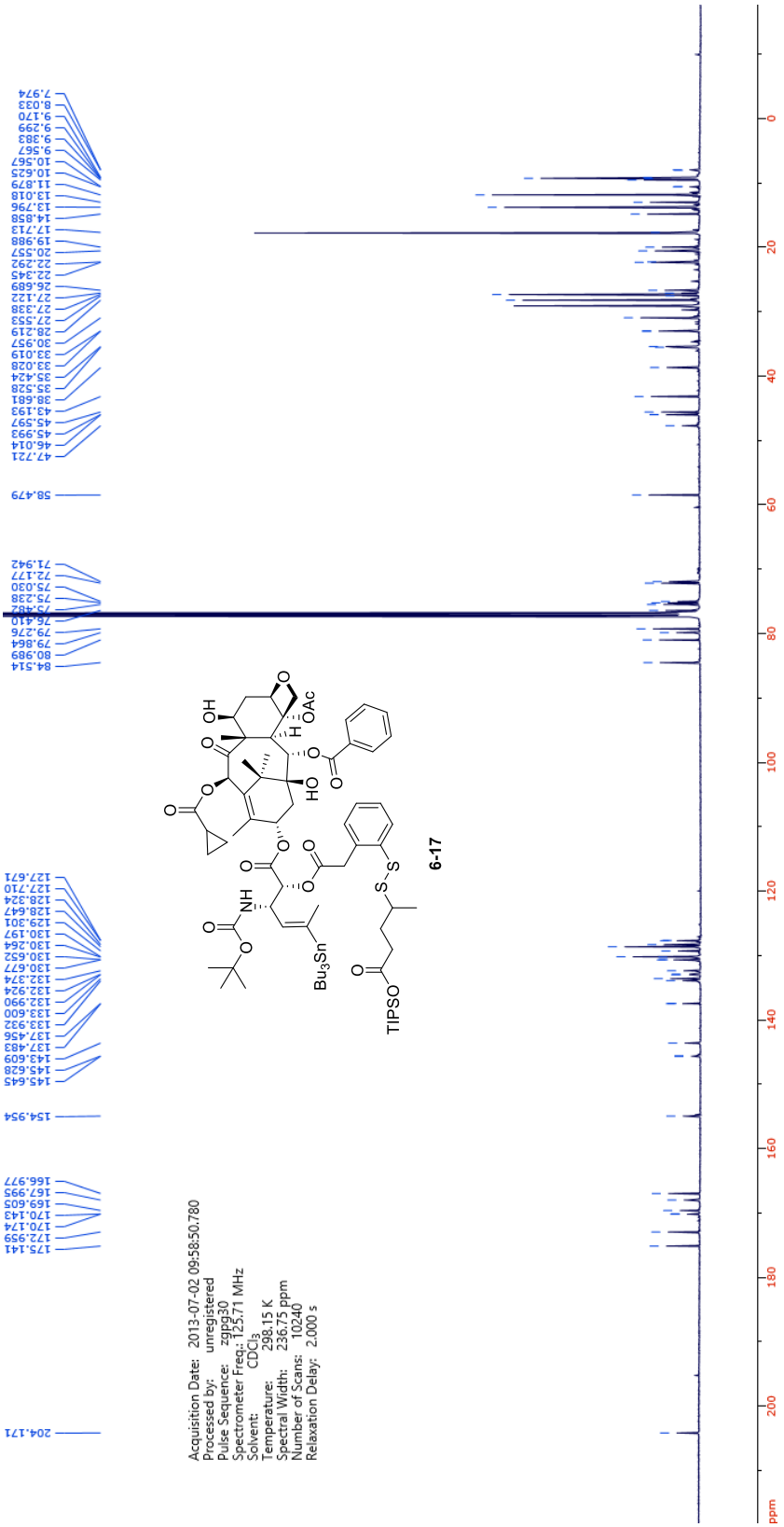
Acquisition Date: 2013-07-02 09:58:50.780
Processed by: unregistered
Pulse Sequence: zgpg30
Spectrometer Freq.: 125.71 MHz
Solvent: $CDCl_3$
Temperature: 298.15 K
Spectral Width: 236.75 ppm
Number of Scans: 10240
Relaxation Delay: 2.000 s
6-17
ppm

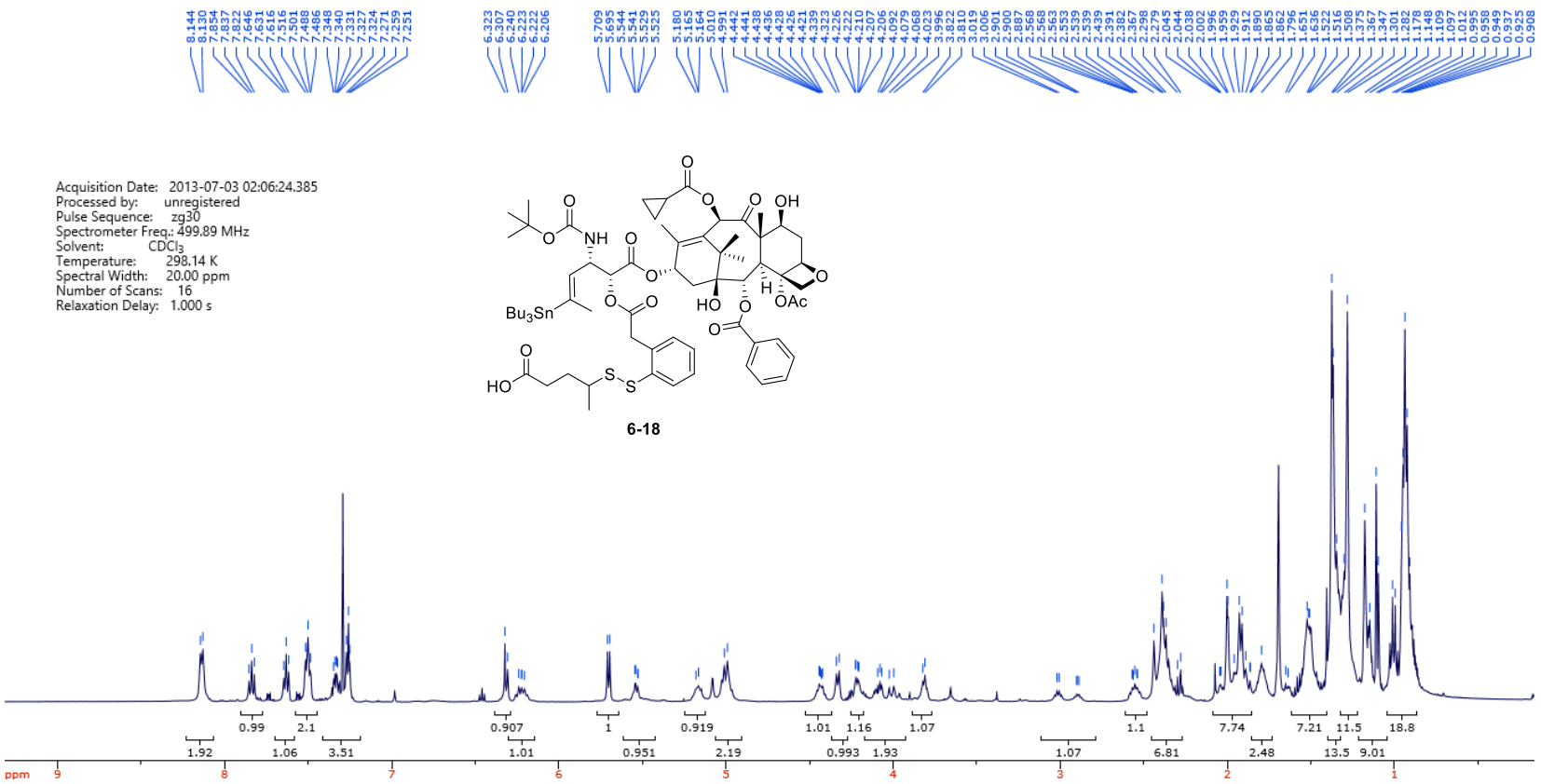
Acquisition Date: 2013-07-03 02:06:24.385
Processed by: unregistered
Pulse Sequence: zg30
Spectrometer Freq.: 499.89 MHz
Solvent: CDCl3
Temperature: 298.14 K
Spectral Width: 20.00 ppm
Number of Scans: 16
Relaxation Delay: 1.000 s
6-18
ppm

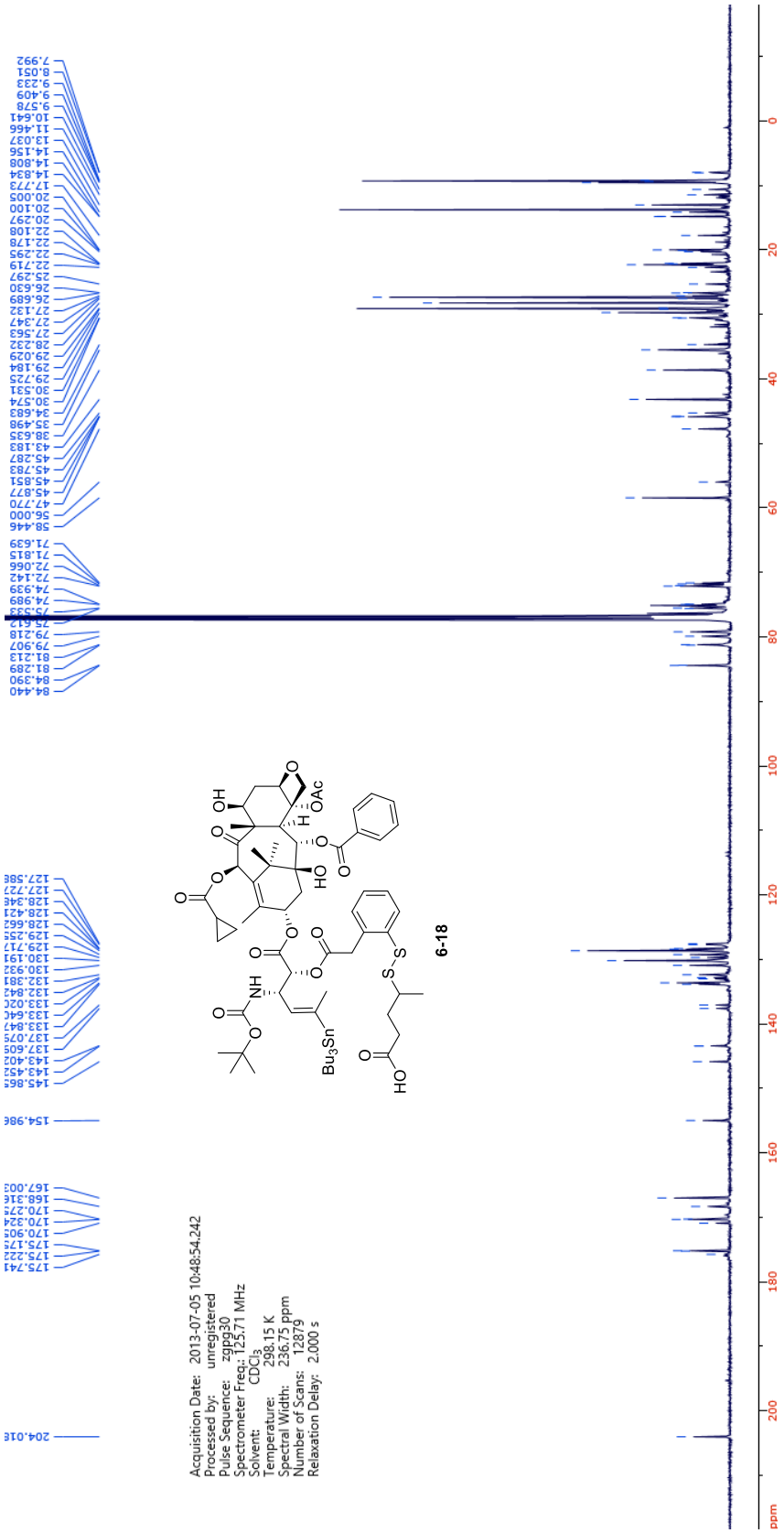
Acquisition Date: 2013-07-05 10:48:54.242
Processed by: unregistered
Pulse Sequence: zgpg30
Spectrometer Freq.: 125.71 MHz
Solvent: $CDCl_3$
Temperature: 298.15 K
Spectral Width: 236.75 ppm
Number of Scans: 12879
Relaxation Delay: 2.000 s
6-18
ppm

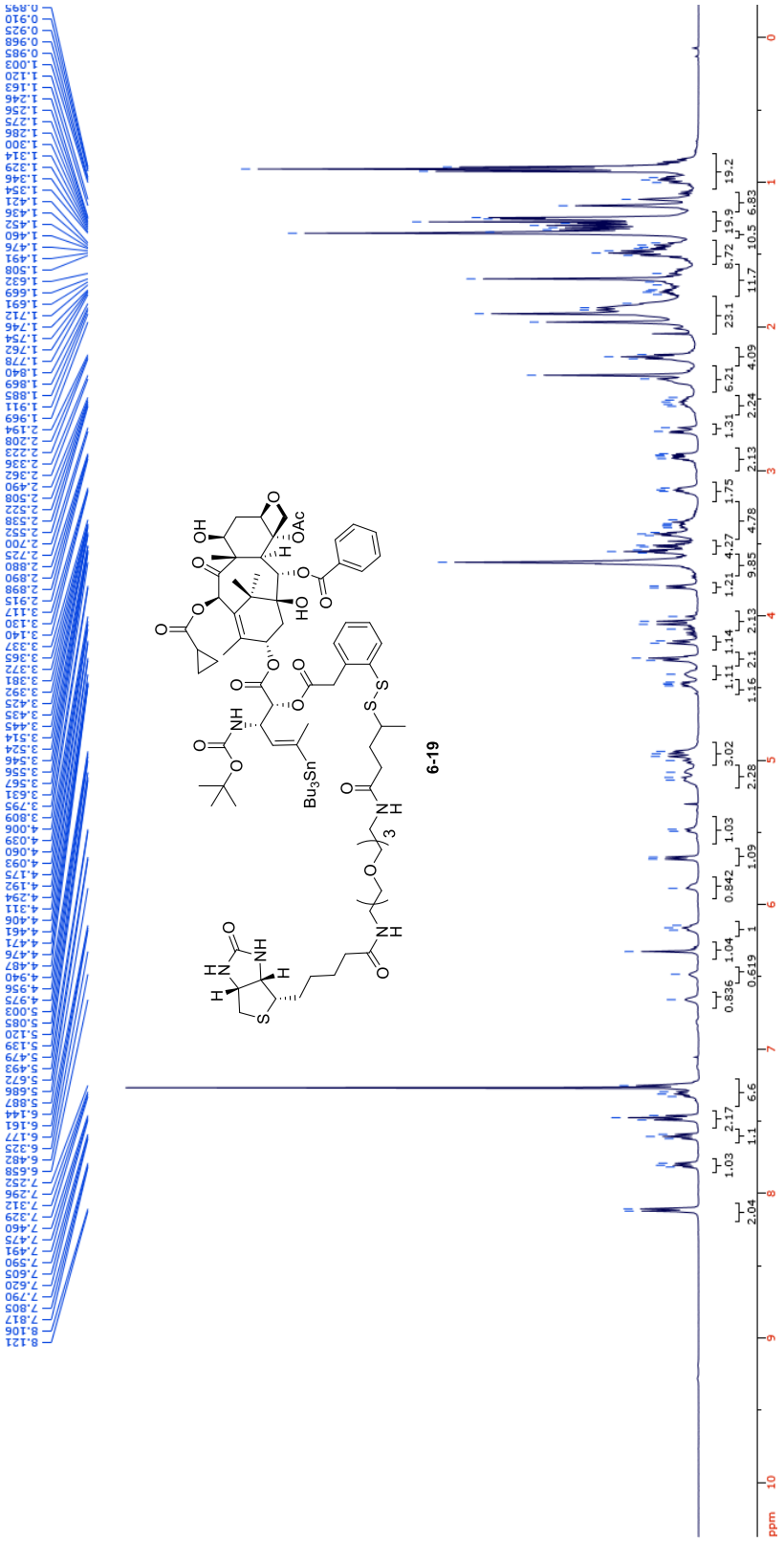
6-19

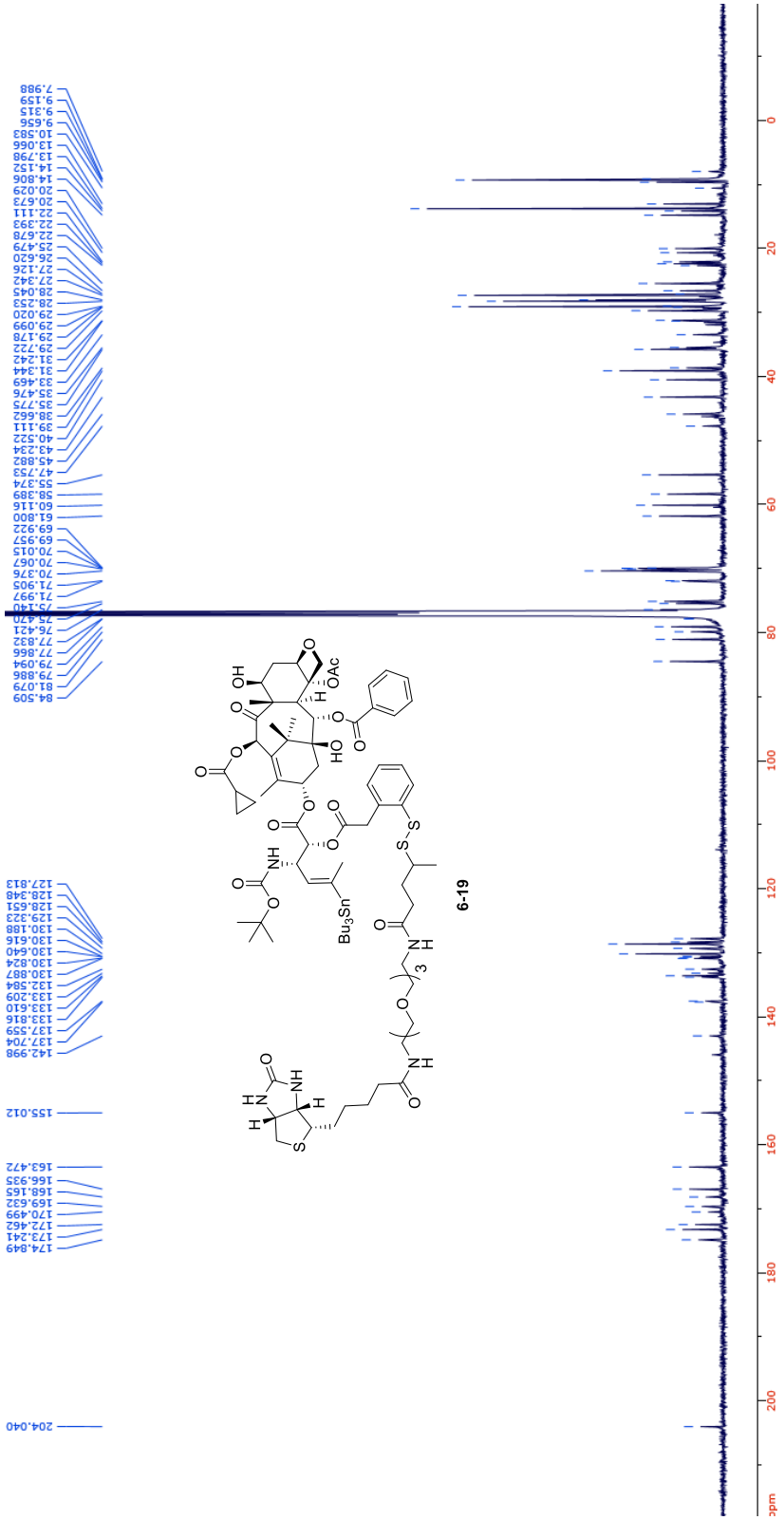
6-19